

NASA CR-132576-2

(NASA-CR-132576-Vol-2) STUDY OF STRUCTURAL
DESIGN CONCEPTS FOR AN ARROW WING SUPERSONIC
TRANSPORT CONFIGURATION, VOLUME 2. TASKS 1
AND 2 Final Report (Boeing Commercial
Airplane Co., Seattle) 667 p HC A99/MF AC1 G3/05 26706

N77-25148

Unclass
26706

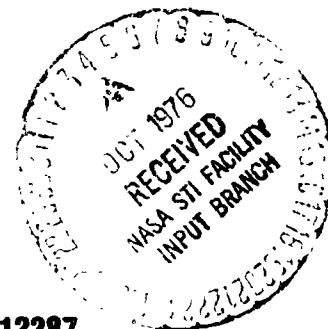
STUDY OF STRUCTURAL DESIGN CONCEPTS FOR AN ARROW WING SUPERSONIC TRANSPORT CONFIGURATION

VOLUME 2

Tasks I and II Final Report

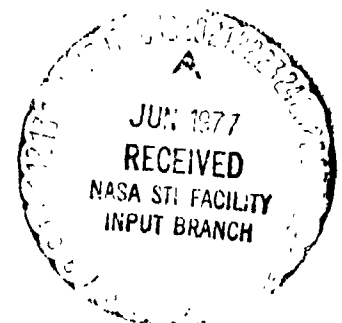
**Boeing Commercial Airplane Company
Preliminary Design Department**

August 1976



prepared under contract NAS1-12287

**for
Langley Research Center
NATIONAL AERONAUTICS AND SPACE ADMINISTRATION
Hampton, Virginia 23665**



SECTION 5

STRUCTURAL ARRANGEMENT AND MATERIAL SELECTION

by

D L. Grande

CONTENTS

	Page
STRUCTURAL ARRANGEMENT AND MATERIAL SELECTION	213
Introduction	213
Structural Arrangement	213
Detail Design of Components	213
Body	214
Wing	215
Empennage	217

FIGURES

No.		Page
5-1	Wing and Body Structural Selection	218
5-2	Centerline Diagram, Wing Structure, 969-512B	219
5-3	Structural Arrangement, Body and Empennage, 969-512B	221
5-4	Body Crown Panel, Titanium Skin Stiffener, 969-512B (Mach 2.7)	223
5-5	Body Side Panel, Titanium Skin Stringer, 969-512B (Mach 2.7)	227
5-6	Body Frame, Sta. 3486.78 (1372.75), 969-512B (Mach 2.7)	229
5-7	Body Frame, Sta. 6642.74 (2615.25), 969-512B (Mach 2.7)	231
5-8	Sinewave Wing Spar, Sta. 5842.64 (2300.25), 969-512B (Mach 2.7)	233
5-9	Sheet-Stiffener Wing Spar, Sta. 7176.14 (2825.25), 969-512B (Mach 2.7) ..	235
5-10	Skin Panel, Forward Wing, 969-512B (Mach 2.7)	237
5-11	Skin Panel, Aft Wing, 969-512B (Mach 2.7)	239

SECTION 5

STRUCTURAL ARRANGEMENT AND MATERIAL SELECTION

INTRODUCTION

The available materials for 1975 use on a Mach 2.7 airplane are reviewed and recommendations are made in Section 3. These materials are then considered in the analysis, evaluation and selection of structural concepts in Section 4. Areas of the Model 969-512B selected for use of the various materials and concepts are illustrated in figure 5-1. The arrangement of the internal structural members and practical design aspects are then considered for application of the selected materials and concepts. Some of the aspects are; how the loads are introduced into the structure, provisions for fastening, fabrication, access and assembly.

STRUCTURAL ARRANGEMENT

The structural arrangement for the 969-512B wing and body developed in Task I are shown in figures 5-2 and 5-3. The wing is of multispar arrangement with a spar spacing of 88.90 cm (35.00 in.). Engines are supported by cantilevered beams attached to the rear spar and backed up by inspar ribs. The rear spar location provides adequate control surface size and space for flight control installation. The location of actuators for flight control and high lift devices is identified.

The body structural arrangement shown in figure 5-3 uses semimonocoque construction with frame spacing of 44.45 cm (17.50 in.) used throughout the body except in the forward area. The wheel well front spar, and spars aft of the wheel well to the rear spar, are continuous through the body structure. Forward of the wheel well the wing spars attach to alternate body frames at the side of the body. The body floor line is on water line 1016 (400.0) except forward of Body Station 2997.84 (1180.25). The lower body lobe structure is continuous, with the main landing gear being stowed in the wing rather than the body. Body floor beams are transverse to the airplane center-line except over the wing carry through structure where they are oriented longitudinally. The body is of double lobe circular cross-section with the floor beam located approximately at the body crease line.

DETAIL DESIGN OF COMPONENTS

Following the development of the structural arrangement, a group of structural details were selected and typical designs developed. These designs are selected from the more critical structural zones of the airframe to show the type of consideration applicable to each of these zones. Three panels are selected from the body, a crown skin panel and a belly skin panel that take primarily axial loads due to body bending, and a side panel including the window belt detail that is critical for shear. Two body frames are shown, one from the forebody, and one from the wing box area.

Wing details include upper and lower skin panels and spar from the heavily loaded main box area and the lightly loaded strake area.

These details have not been subject to stress analysis but have been drawn with dimensions typical for the 969-336C.

BODY

BODY CROWN PANEL

The body crown panel selected for detail design lies in the upper quadrant of the fuselage shell between BS 3531.24 (1390.25) and BS 5086.98 (2002.75). This panel is illustrated in figure 5-4. It is typical of a crown skin that will experience high axial loads due to symmetrical body bending for maneuvers and ground load conditions.

The panel is constructed of titanium skin with riveted titanium "Zee" section stiffeners. The stiffeners are machined, and riveted to chem-milled pads on the skins. Chem-milled pads are also provided around the circumference of the panel to provide for the splice fasteners, and under the frames. Tear straps are provided under each frame.

Longitudinal and circumferential splices are accomplished with internal splice plates. The stiffeners are spliced across frames by the use of machined fittings.

The geometry of the panel varies along the longitudinal axis due to the variation in body cross section. Therefore, the stringer spacing varies from 11.4 cm (4.49 in.) to 13.87 cm (5.46 in.). The frame spacing is 45.2 cm (17.75 in.). Other dimensions on the panel are tabulated on figure 5-4.

BODY SIDE SHEAR PANEL

The side panel selected for detail design is presented in figure 5-5. This panel is located between BS 3531.24 (1390.25) and BS 5086.98 (2002.75) with the window belt running along the center line of the panel. The panel tapers from 55.88 cm (22.0 in.) at the front edge to 45.72 cm (18.0 in.) at the aft edge to accommodate the tapering cross section of the fuselage. This panel takes the high shear flows associated with vertical bending of the body. The installation of the windows requires special design consideration.

The panel consists of a chem-milled titanium skin with machined "Zee" section stringers riveted on. The window cutouts are 20.32 cm (8.0 in.) in diameter, with chem-milled pads around the circumference for reinforcing. Frames are spaced at 44.5 cm (17.5 in.). Tear straps are located under each frame. A machined circular reinforcement frame is riveted around each window cutout. This frame also fastens to the stringers running above and below the window. Longitudinal and circumferential skin splices utilize internal splice plates. The stringer splices use machined fittings.

The small diameter windows are provided to minimize the weight penalty associated with the reinforcement necessary for the cutout, as well as to minimize the heat input from the boundary layer.

BODY FRAME-BS 3486.78 (1372.75)

The frame shown in figure 5-6 is typical of the majority of the frames used in the fuselage. The basic frame is made up of a formed titanium "J" section making up the inner chord and riveted to the titanium outer chord. The outer chord is a formed angle with relief provided for the continuous stringers to pass through. The frame web is chem-milled to provide a pad-up for the inner and outer chords, and the stringer attaching clips. Machined clips are riveted to the frames to provide support to each stringer. A tear strap is provided on the skin running adjacent to the frame outer chord to limit panel rupture from pressurization stress. The frame is spliced along the sides where the bending moment in the frame is relatively low.

BODY FRAME-BS 6642.74 (2615.25)

The frame shown in figure 5-7 is typical of the frames used in the vicinity of the wing carry through structure. The frame is designed to provide for the interaction between the fuselage frame and the wing spars as they deflect under loads.

The inner chord and web are machined from a titanium extrusion having a modified "Tee" cross section. The outer chord is machined from a simple "Tee" titanium extrusion. Each of these sections has the outstanding leg relieved to clear the continuous "Zee" section stringers. The web of the frame is chem-milled to provide pad-ups for the clips supporting the "Zee" stringers.

The "Tee" section forming the outer flange runs completely around the cross section and serves as the tear strap for fail-safe design. The inner flange and web have a secondary flange in the mid-section of the frame to provide bending continuity in the event of failure of either the inner or outer flange. The frame is spliced along the sides where bending moments tend to be low. The splice is made through machined splice plates.

The attachment of the frame to the wing spars, requires special design considerations, since wing deflections induce bending in the body frame. It is necessary to attach the frames to the spars in a manner that will carry bending moment due to frame bending. However, it is desired to minimize any bending moment in the frame due to spar bending. For this reason a fitting is designed, as shown, that provides an offset leg restrained by a short flexible strap. The strap will react loads due to frame bending, but will flex as the wing bends, thus minimizing the transfer of loads.

WING

SINEWAVE WING SPAR

Figure 5-8 shows a spar using a sinewave web configuration. This arrangement is particularly efficient in lightly loaded areas since it effectively combines the shear carrying function of the web and simultaneously the sine waves provide stiffening to the web. This type of web stiffening is not effective however, in areas where cutouts are required, or where significant pressure loads must be reacted. These areas require a more conventional flat web with stiffeners.

The spar web consists of a chem-milled titanium sheet with pad attachments at the ends and along the beam chords. The beam chords are flat plates, electron-beam welded to the web. At the points where cutouts are provided for system runs or fuel tank access, stiffened flat webs are provided. These webs are chem-milled to provide pad-ups under the stiffeners.

SHEET-STIFFENER WING SPAR

The sheet-stiffener spar is used in areas that react higher bending moments or fuel tank pressures, or where a large number of cutouts are required for systems or access to the inner wing. Figure 5-9 shows a sheet-stiffener spar design for the main wing box with typical details for system runs and fuel tank access.

The titanium web is chem-milled to provide pads for end attachments, chord and stiffener attachments, and reinforcing around holes. The chords are machined titanium "Tee" section extrusions riveted to the web. The web stiffeners are extruded angles. The intermittent chordwise intercostals are used to stabilize the lower skin panel.

SKIN PANEL-FORWARD WING

Figure 5-10 shows the design of upper and lower skin panels extending outboard from the side-of-body, between BS 5575.94 (2195.25) and BS 5664.84 (2230.25). These panels are typical of the strake area ahead of the wheel well having relatively low bending moments to react.

The skin panels consist of chem-milled titanium face sheets brazed to titanium honeycomb core using the aluminum braze alloy. The edges of the panels use skin pad-ups for the attachments backed up by dense core. The panels are one spar bay wide with the spanwise splices being made through a flush external splice plate, and a nonflush internal splice plate. The panel attaches to the fuselage through a series of machined fittings.

SKIN PANEL-AFT WING

Figure 5-11 shows an upper and lower skin panel design extending outboard from the fuselage between BS 7087.24 (2790.25) and BS 7176.14 (2825.25). These panels are of interest because they are in the main wing box aft of the wheel well where the bending moments are the highest. The upper skins in this region consist of chem-milled titanium face sheets, aluminum brazed to the titanium core. The panel is one frame bay in width, with a flush splice plate on the exterior surface and a protruding splice plate on the interior surface. The splice across the side-of-body rib is accomplished by the "double plus" rib cap. The edges of the panel have chem-milled pads for the fasteners, backed up by dense honeycomb.

The lower wing panel consists of a machined and welded titanium sheet-stringer panel outboard of the side-of-body rib, and a machined titanium waffle panel on the inboard side. This combination of designs appears to be most efficient for the high tension loads due to wing bending on the outboard side of the rib, and the biaxial stress field for wing

bending combined with fuselage bending on the inboard side of the rib. The panel splice across the side-of-the body rib is accomplished using the rib cap.

EMPENNAGE

The main landing gear consists of a six wheel truck mounted on a single oleo strut. The gear folds forward and up into a well ahead of the main wing box and outboard of the side-of-body rib. The trunnions mount on fittings on the forward side of the main wing box, and the uplock, which supports the gear weight in the retracted position, is located on local beams at about BS 6020(2370).

The wing mounted fin consists of a series of vertical spars attached to the wing main spars, supporting two aft sloping spars. The remainder of the ribs and spars are supported off these elements. The construction consists of riveted titanium ribs and spars supporting aluminum brazed titanium honeycomb skins.

The fin is of multispar design having a sloping front spar, and a series of vertical spars or ribs, with auxiliary ribs supporting the rudder hinge line. The spars and ribs are built up of riveted titanium construction, supporting surfaces of aluminum brazed titanium honeycomb sandwich. The leading edge wedges are aluminum brazed titanium sandwich. The rudder consists of three segments, each having a front and rear titanium spar with intermediate and end ribs supporting aluminum brazed titanium sandwich surfaces. The trailing edge is an aluminum brazed titanium wedge.

The horizontal stabilizer is of multispar construction, supporting aluminum brazed titanium honeycomb sandwich surfaces and leading edge wedges. The elevators are constructed in a manner similar to the rudders.

The aft engine mount is supported by a cantilever beam that extends aft of the rear spar. These beams are extensions of the wing ribs that run forward in the main wing box to distribute the engine loads into the structure. The beam cap loads are distributed into the upper and lower wing surfaces to react the bending moments. The support beams are riveted titanium boxes and are typically designed for stiffness rather than strength.

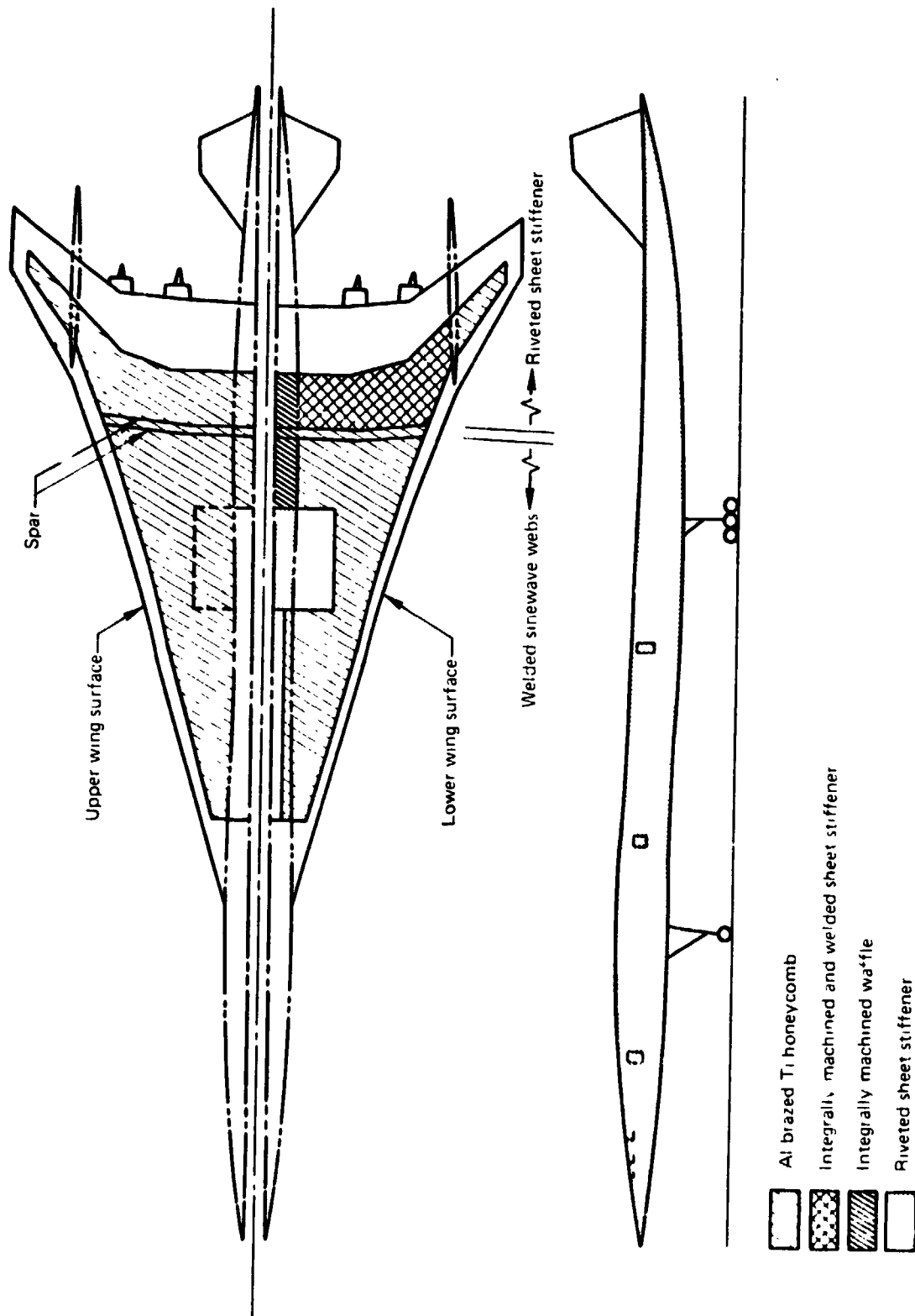
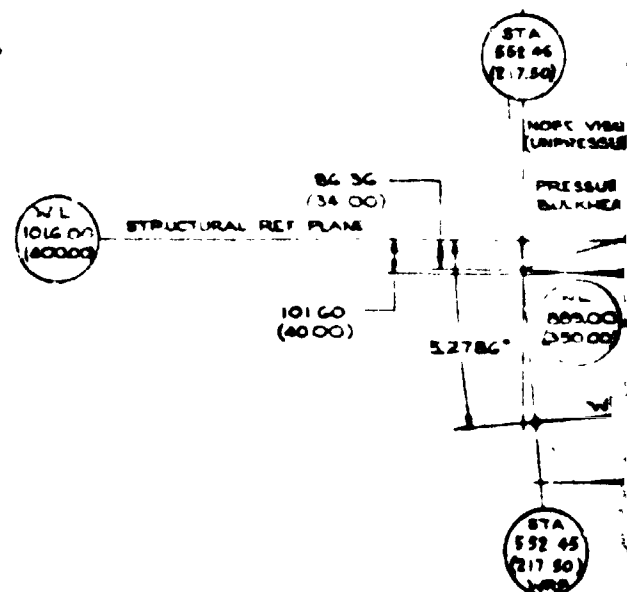
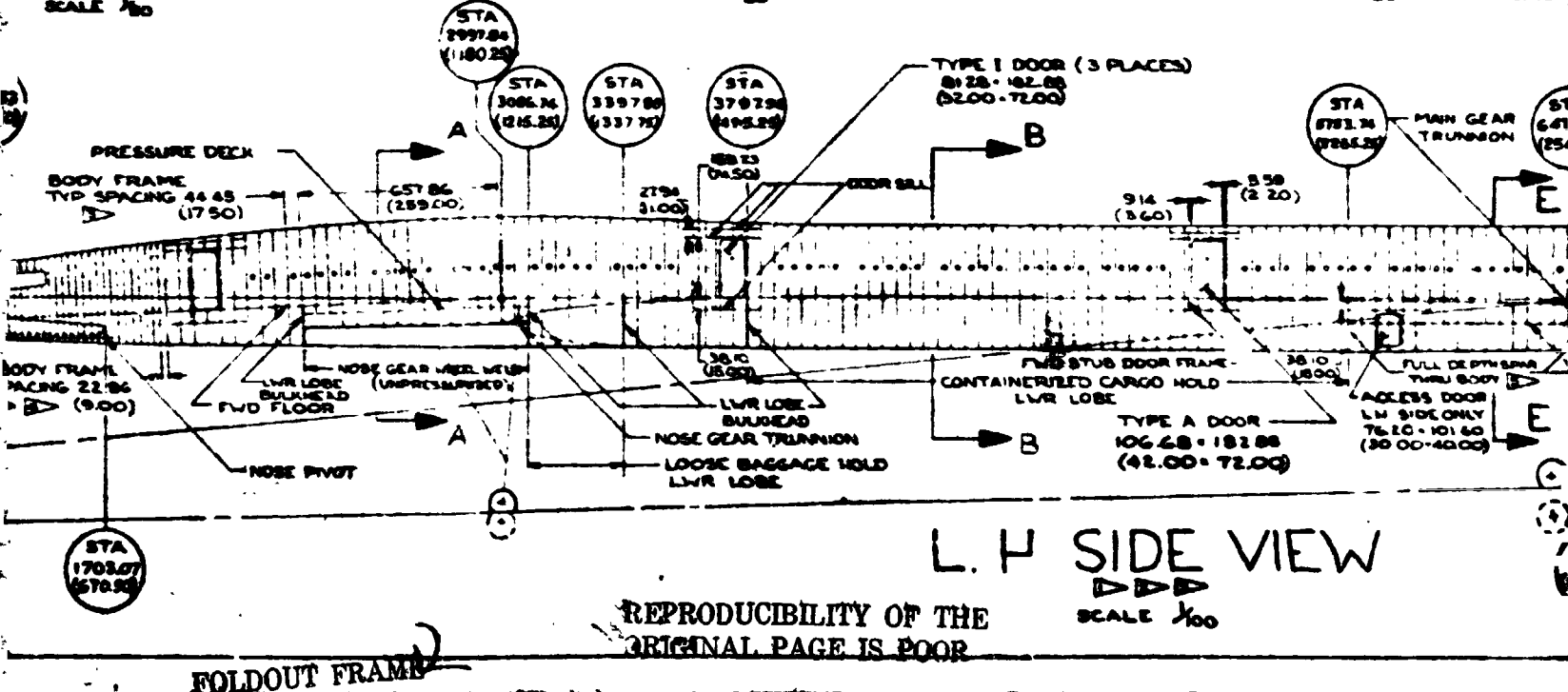
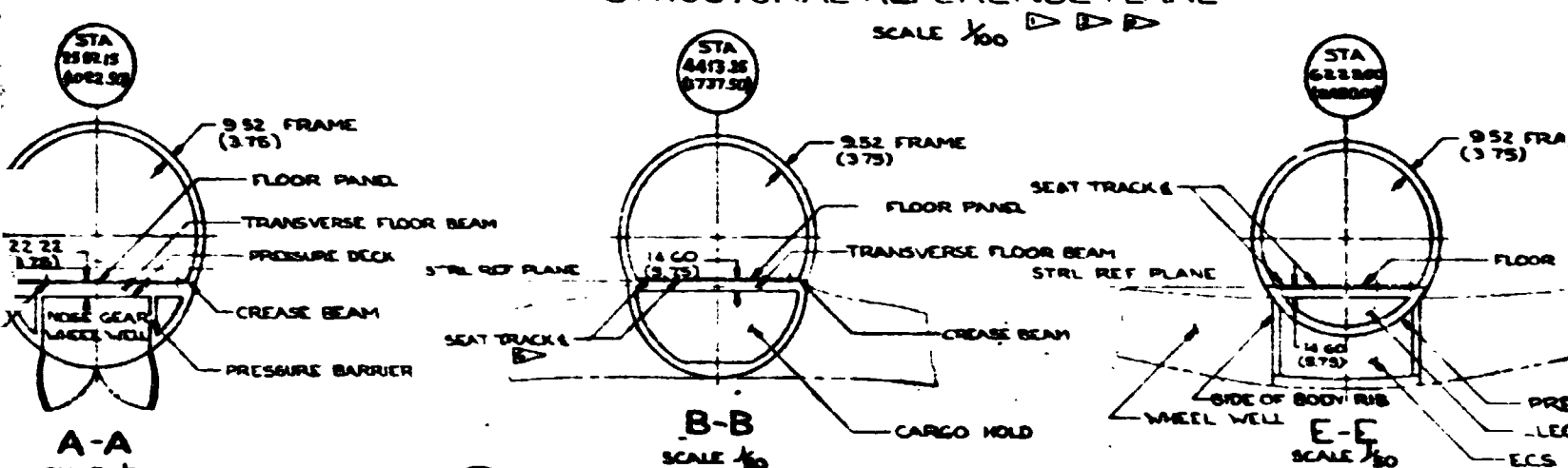
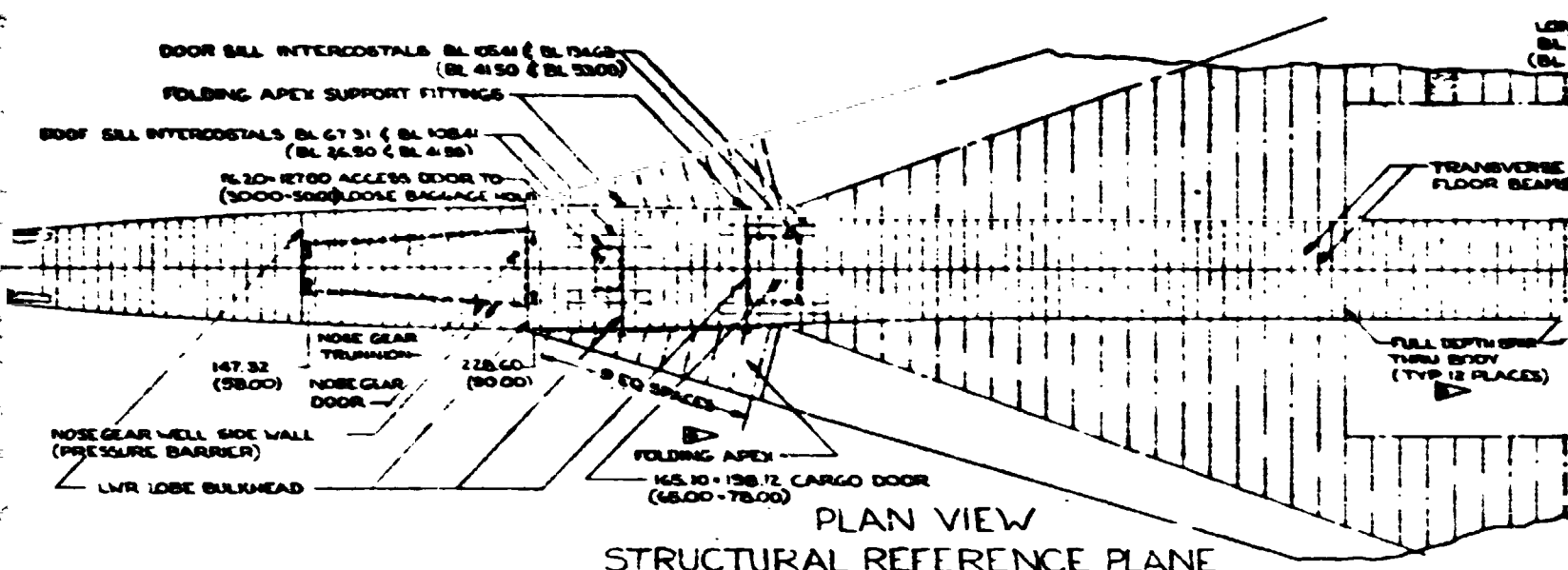


Figure 5-1.—Wing and Body Structural Selection

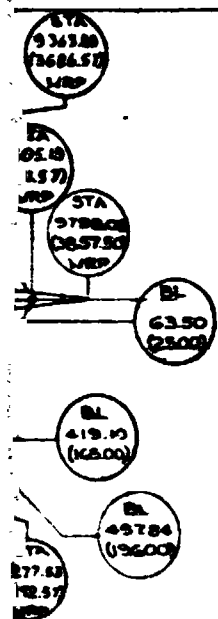
FOLDOUT FRAME





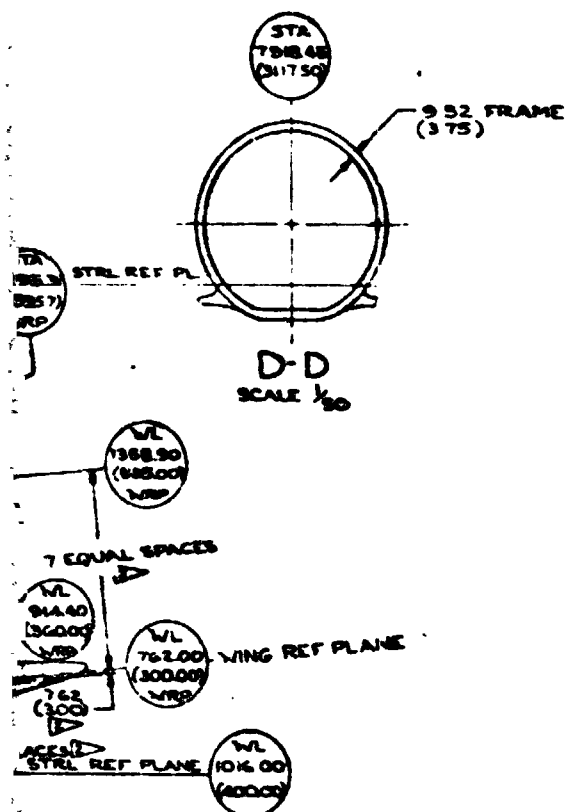
FOLDOUT FRAME

REPRODUCIBILITY OF THE ORIGINAL PAGE IS POOR



SYM	DESCRIPTION	DATE	APPR
A	B ADDED TO TITLE. BODY MOVED AFT. 175. GEAR MOVED AFT ON BODY 175. ALL STA REVISED ACCORDINGLY LOCATION OF FWD LOWER LOBE ACCESS DOORS AND BULK UNCHANGED. REASON FOR CHANGE - TO COMPLY WITH 969-512 B CONFIGURATION PER LB 84980	9-21-73	AWR
B	STA 385780 WAS CHANGED FROM 384000 & STA 3637.67 FROM 3635.97	8-14-73	AWR
C	DELETE FUEL TANK & ADDED LWR LOBE PRESSURE BARRIER BETWEEN WHEEL WELLS. ADDED ACCESS DOOR TO L.H. SIDE OF BODY RID. ADDED VIEW E-E. ADDED FAIRING IN VIEW DD	11-21-73	AWR

D 3689.57 WAS 3621.57



- ▷ DIMENSIONS AND STATION CALLOUTS ARE IN THE STRUCTURAL REF PLANE EXCEPT AS NOTED
- ▷ EMPENNAGE DIMENSIONS ARE IN THE WING REF PLANE OR NORMAL TO IT
- ▷ BODY FRAMES, FLOOR BEAMS, DOORS, ETC. ARE NORMAL TO THE FLOOR
- ▷ STRINGERS ARE NOT REQ'D WITH CLOSE PITCHED FRAMES
- ▷ SEE AWS-122 FOR WING STRUT ARRANGEMENT
- ▷ SEAT TRACKS FORM UPR CHORD OF 4 OUTBD FLOOR BEAMS AND CONTINUE FORE & AFT PARALLEL TO BODY CREASE BEAM OUTER CHORD THROUGHOUT THE PRESSURE CABIN

PRECEDING PAGE BLANK NOT FILED

NOTE BASIC UNIT SYSTEM IS THE INTERNATIONAL S.I. SYSTEM
ENGLISH UNIT SYSTEM EQUIVALENT VALUES ARE SHOWN IN ()

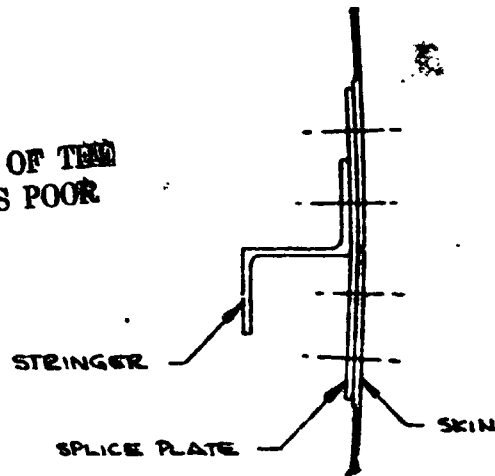
SEE SHEET 1 OR PL FOR LIST OF MATERIAL USAGE AND NOTES	
USED ON	DRAWN R. K. ROBINSON CHECKED
DATE	8-2-73
THE BOEING COMPANY COMMERCIAL AIRPLANE DIVISION RENTON WASH	
STRESS	
GROUP	8-25-73
PROJ	
GROUP 080	
STRUCTURAL ARRANGMENT BODY & EMPENNAGE 969-5128	
CDR IDENT NO 01295	J AWS-123
SCALE NOTED	1/8" = 1"

Figure 5-3

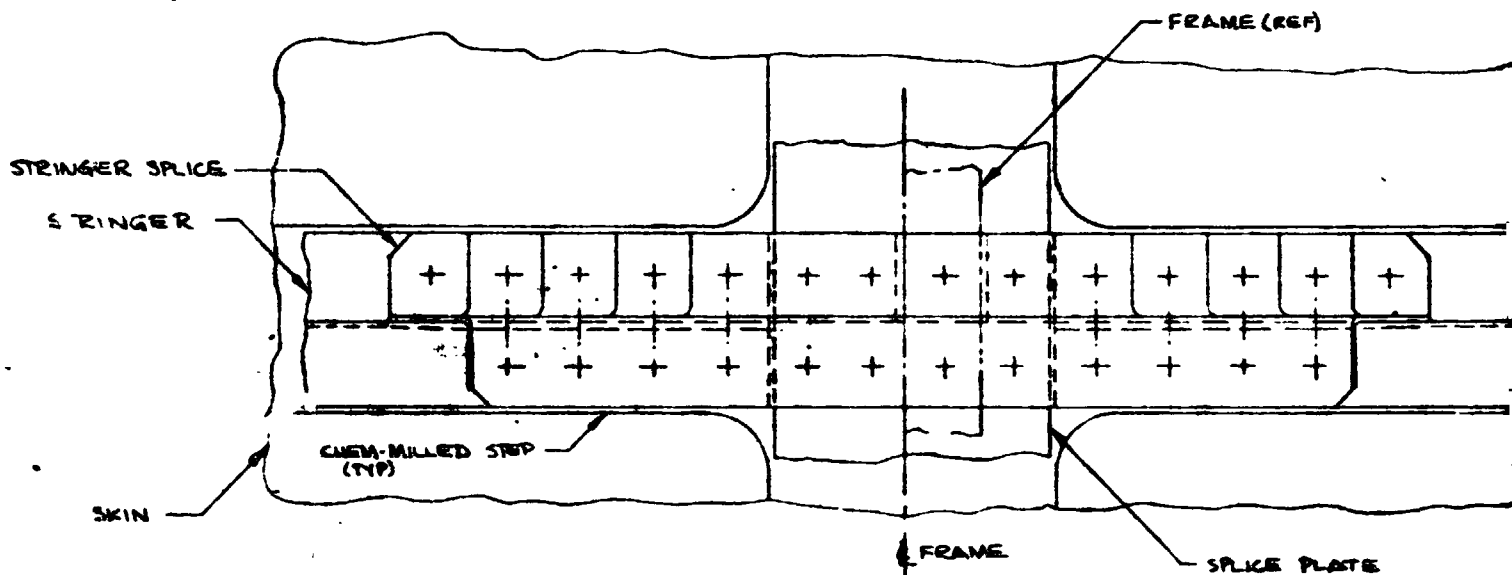
FOLDOUT FRAME 4

FOLDOUT FRAME 1

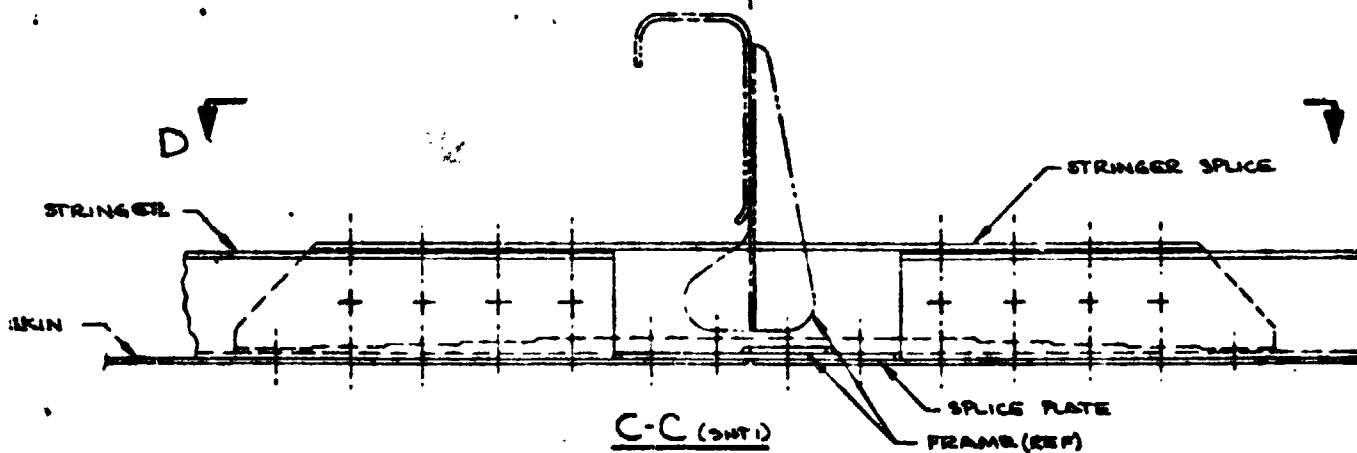
REPRODUCIBILITY OF THE
ORIGINAL PAGE IS POOR



B-B (CONT)

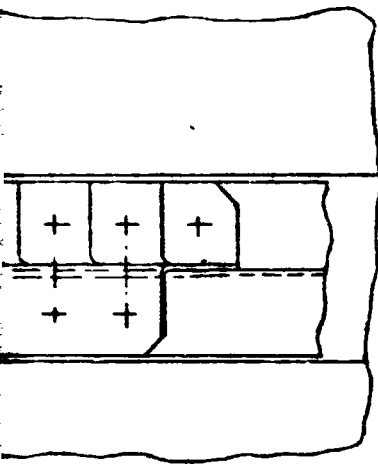


D-D



FOLDOUT FRAME 2

NAME (REF)



SPICE PLATE

STRINGER SPICE

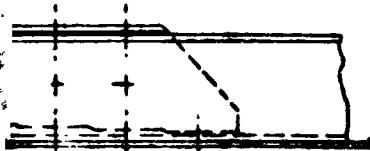


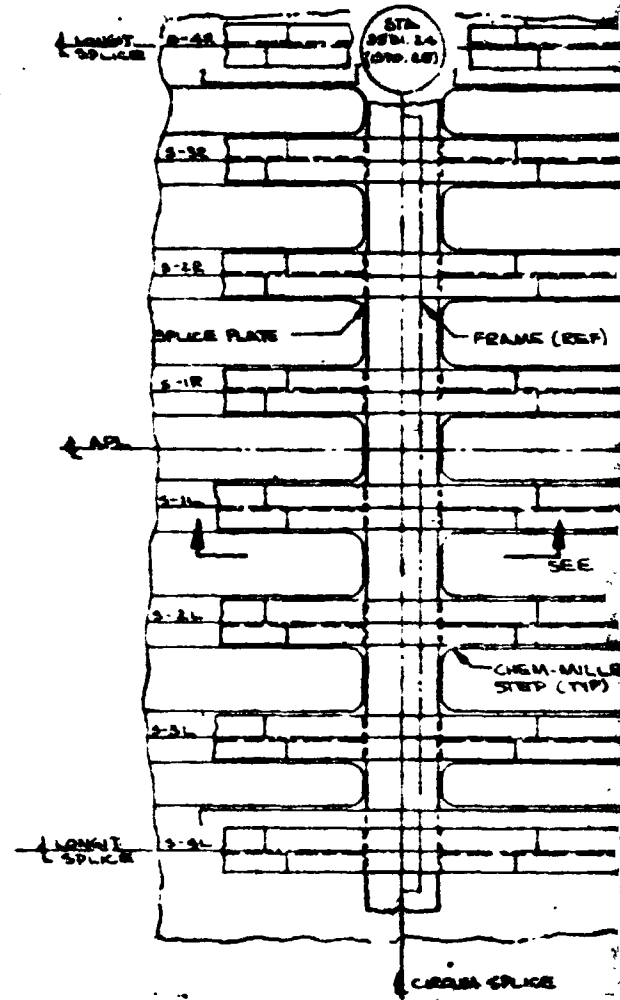
PLATE
(REF)

PRECEEDING PAGE BLANK NOT FILLED

SEE SHEET 1 OR PL FOR LIST OF MATERIAL USAGE AND NOTES			
USED ON	DRAWN <i>S. J. JONES</i>	DATE <i>10-1-73</i>	THE BOEING COMPANY COMMERCIAL AIRPLANE DIVISION, RENTON, WASH.
	CHECKED		BODY CROWN PANEL
SECT NO	STRESS		TITANIUM SKIN/STIFFENER
	ENGR <i>S. J. JONES</i>	DATE <i>10-1-73</i>	969-512B (MACH 2.7)
CHG NO	GROUP		CODE IDENT NO <i>81705</i>
	PROJ		J AWS-130
GROUP CHG			SCALE <i>1 IN = 2 FT</i>

Figure 5-4

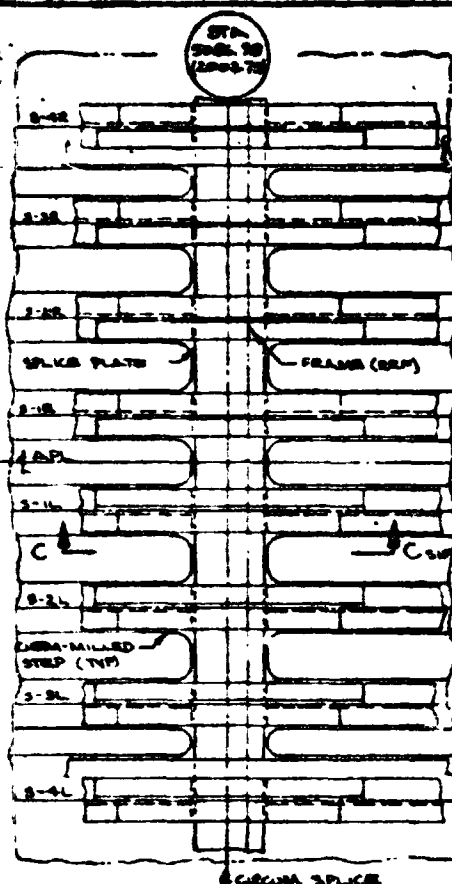
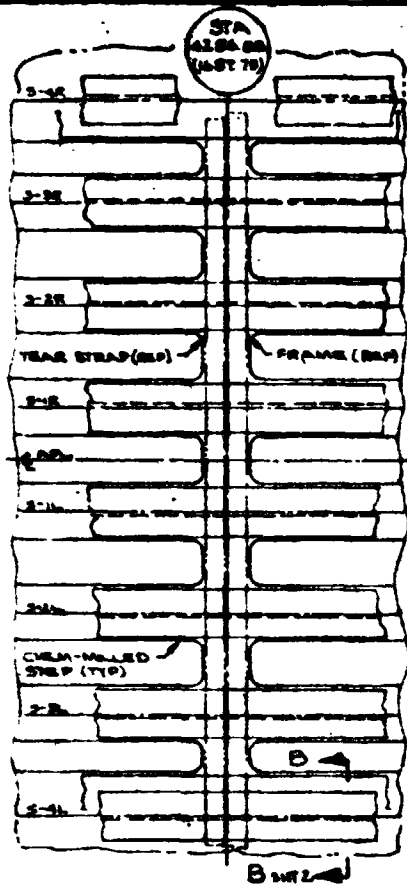
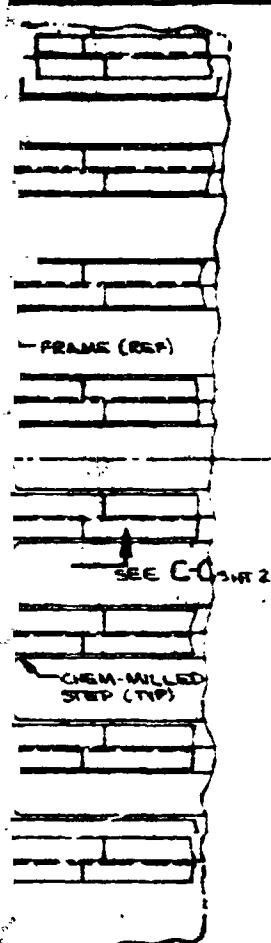
FOLDOUT FRAME *B*



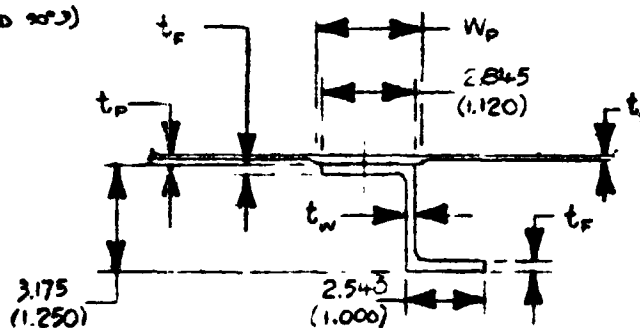
REPRODUCIBILITY OF THE ORIGINAL PAGE IS POOR

STATION	DESCRIPTION	DESIGN COND		
		MACH NUMBER	EQUIV S-VEL / SEC KNOTS	ACTUAL ALTITUDE / 1000 FT
3531.24 (1390.25)	MAX CANARD	.30	169 1250	SEA LEVEL
4286.88 (1607.75)	END OF CRUISE	0.70	227 1444	1923 6310
5086.98 (2002.75)	END OF CRUISE	2.70	227 1441	1923 6310

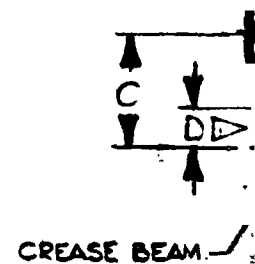
FOLDOUT FRAME



AA (ROTATED 90°)



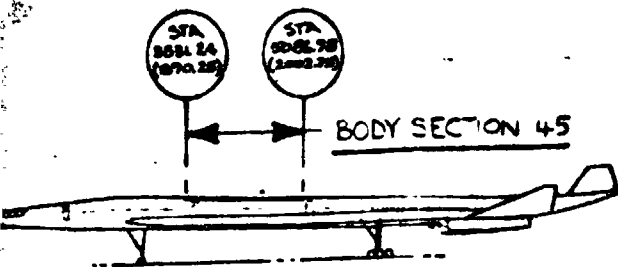
STRINGER CONFIGURATION



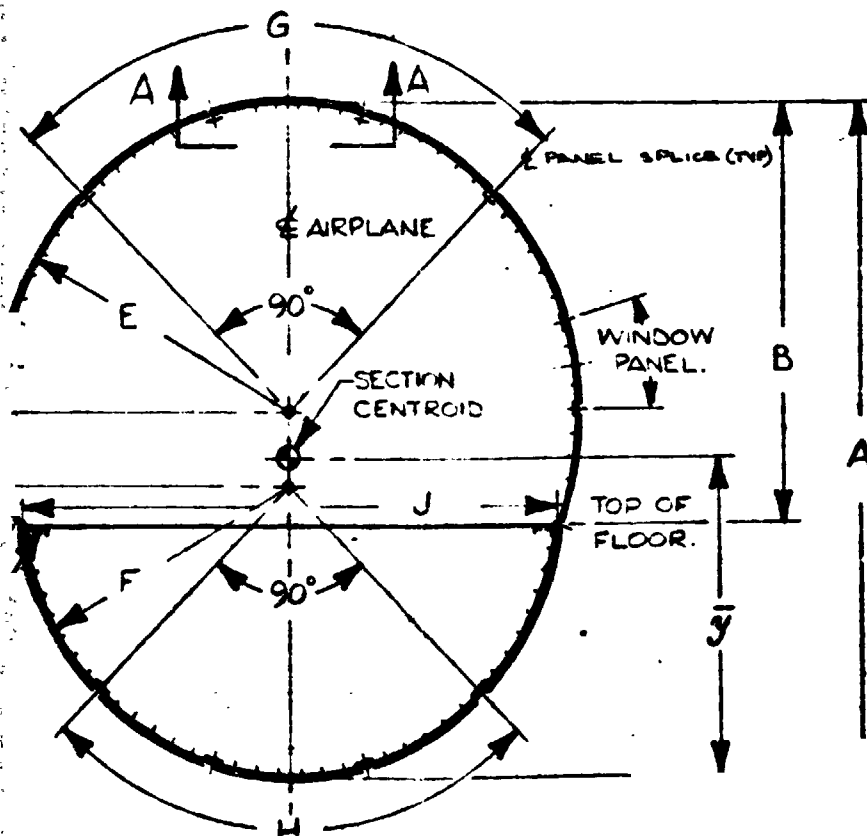
CROWN PANEL

DESIGN CONDITIONS					LOAD										
CH	EQUIV S.E.V.E. 1800	ALTITUDE 100' M (300 FT)	INTER PRESS N.C.M. (25.1)	TEMP ° K (° F)	LOAD FACTOR ULF	VERT B.M. N.C.M. (K.F.N)	VERT S.EAR N.C.M. (K.F.N)	SHELL N.C.M. (K.F.N)	PANEL LOAD N/C.M. (K.BE/N)	PANEL t C.M. (N)	SKIN t _s C.M. (IN)	PAD W _p C.M. (IN.)	PAD t _p C.M. (IN)	WEB t _w C.M. (IN)	FLANGE t _f C.M. (IN.)
	129 (290)	SEA LEVEL	—	ROOM TEMP	2.5 3.0	+23.162 (-750)	+396.0 (-890)	+113.5 (1132)	7570 (323)	.186 (.077)	.094 (.037)	2.710 (1.067)	.37 (.05)	.132 (.060)	.118 (.070)
2	227 (44)	19232 (63100)	74.33 (1.73)	505 (+50)	2.50 7.5	+44321 (-1310)	+413 (-270)	+4886.6 (117.5)	15150 (650)	.246 (.07)	.114 (.045)	2.710 (1.067)	.183 (.072)	.165 (.065)	.191 (.075)
0	227 (44)	19232 (63100)	74.33 (1.73)	505 (+50)	2.50 3.75	+23.162 (-205)	+396.0 (-377)	770.5 (185.0)	1451.3 (340)	.16 (.160)	.160 (.063)	1.175 (1.250)	.163 (.072)	.254 (.100)	.330 (.130)

STA.	A	B
	BODY	FLOC
	DEPTH	2.08
3531.24	40132	351.4
(1590.29)	(15200)	(990)
4184.88	38100	231.1
(1487.75)	(15000)	(910)
5084.98	37842	226.0
(1602.75)	(14900)	(890)



CROWN PANEL LOCATION.



BODY MONOCOQUE PANNELIZATION
(SECTION 45)

▷ (+) ABOVE & (-) BELOW THE FLOOR

SKIN MATL IS T1.6AL-4V COND I

EXTRUDED STRINGER MATL IS T1.6AL-4V COND II

BASIC UNIT SYSTEM IS THE INTERNATIONAL SI SYSTEM
ENGLISH UNIT SYSTEM EQUIVALENT VALUES
ARE SHOWN IN ()

SEE SHEET 1 OF PL FOR LIST OF MATERIAL USAGE AND REVISED

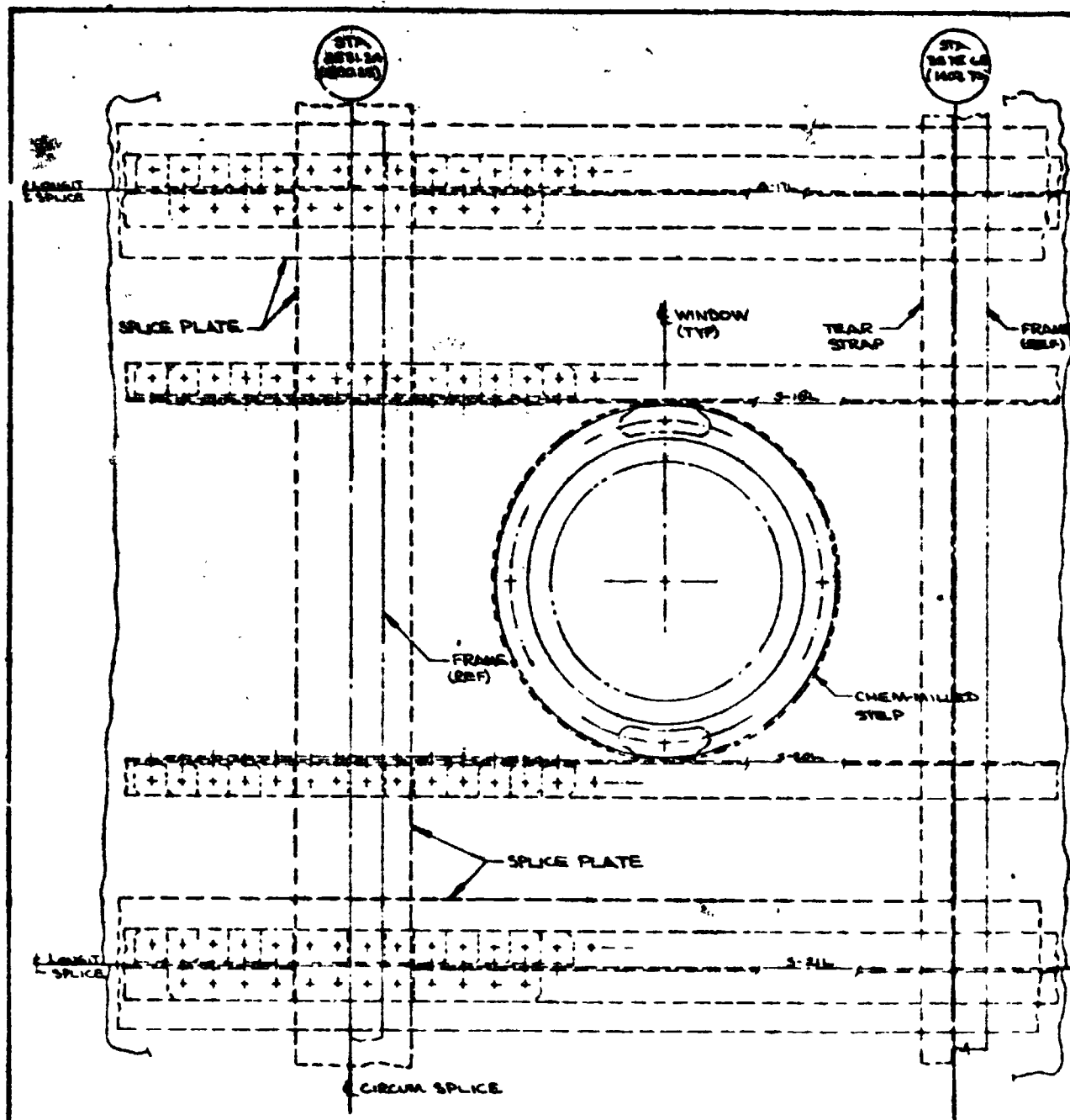
C	D	E	F	G		H		J	\bar{y}
				ARC LENGTH	STIFF. PITCH	ARC LENGTH	STIFF. PITCH	FLOOR WIDTH	
67.31 (26.50)	+21.86 (+9.00)	15.46 (73.00)	17.58 (67.55)	291.24 (114.64)	15.97 (5.59)	169.51 (66.1)	14.20 (5.59)	339.85 (133.80)	189.69 (74.68)
67.31 (26.50)	-2.54 (-1.00)	22.56 (89.00)	14.34 (56.40)	255.25 (100.53)	12.74 (4.99)	233.02 (91.74)	12.24 (4.82)	259.56 (102.52)	177.94 (69.07)
7.12 (28.00)	-19.25 (-7.50)	152.40 (60.00)	136.14 (53.60)	239.44 (94.25)	11.49 (4.49)	213.57 (84.43)	11.25 (4.43)	209.75 (82.90)	157.30 (61.93)

DRAWN CHECKED STRESS ENG GROUP PROJ	DATE 10-1-73 10-1-73 10-1-73 10-1-73 10-1-73	THE BOEING COMPANY COMMERCIAL AIRPLANE DIVISION, RENTON, WASH. BODY CROWN PANEL TITANIUM SKIN/STIFFENER 969-512B (MACH 27) CODE IDENT NO 81285 J AWS-130 STATE
--	---	--

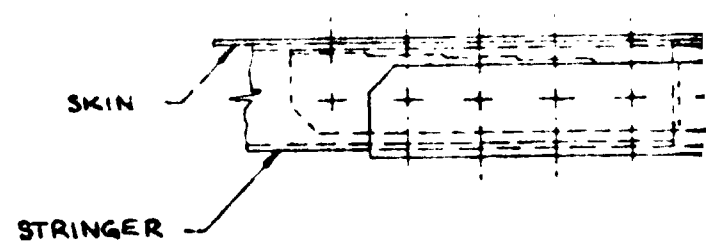
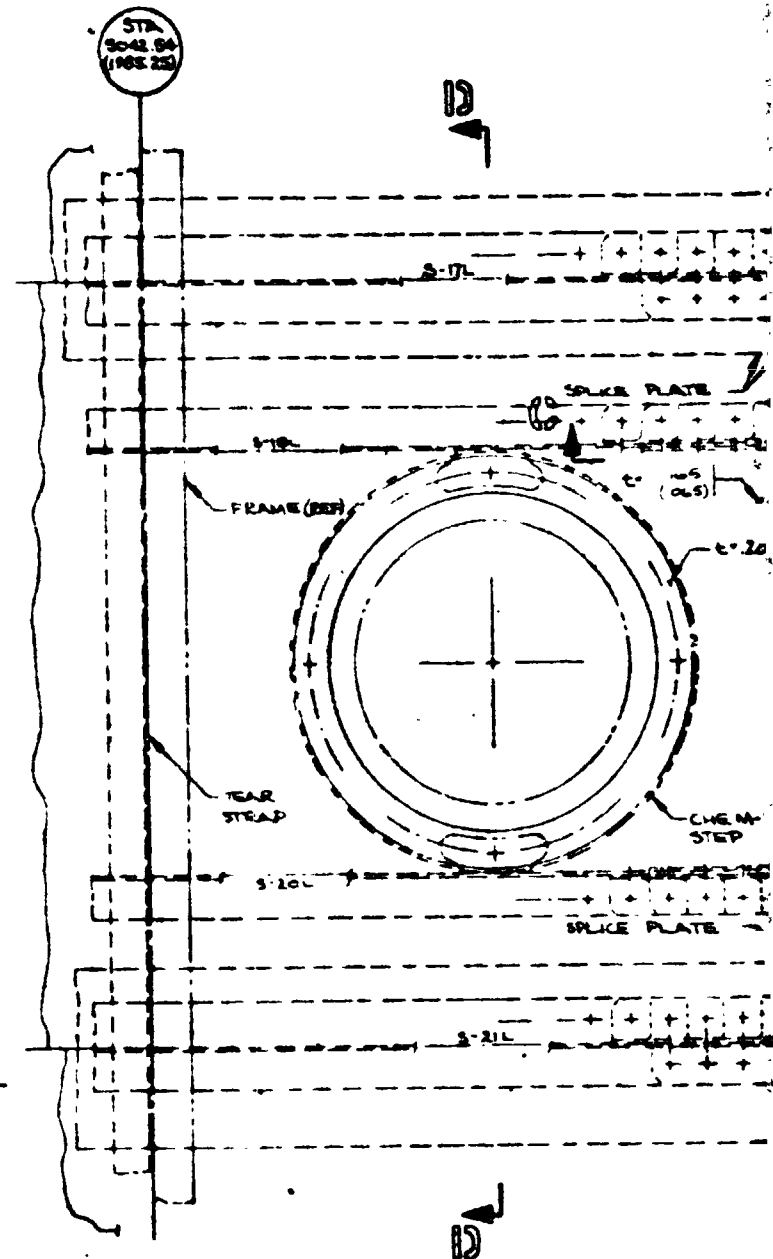
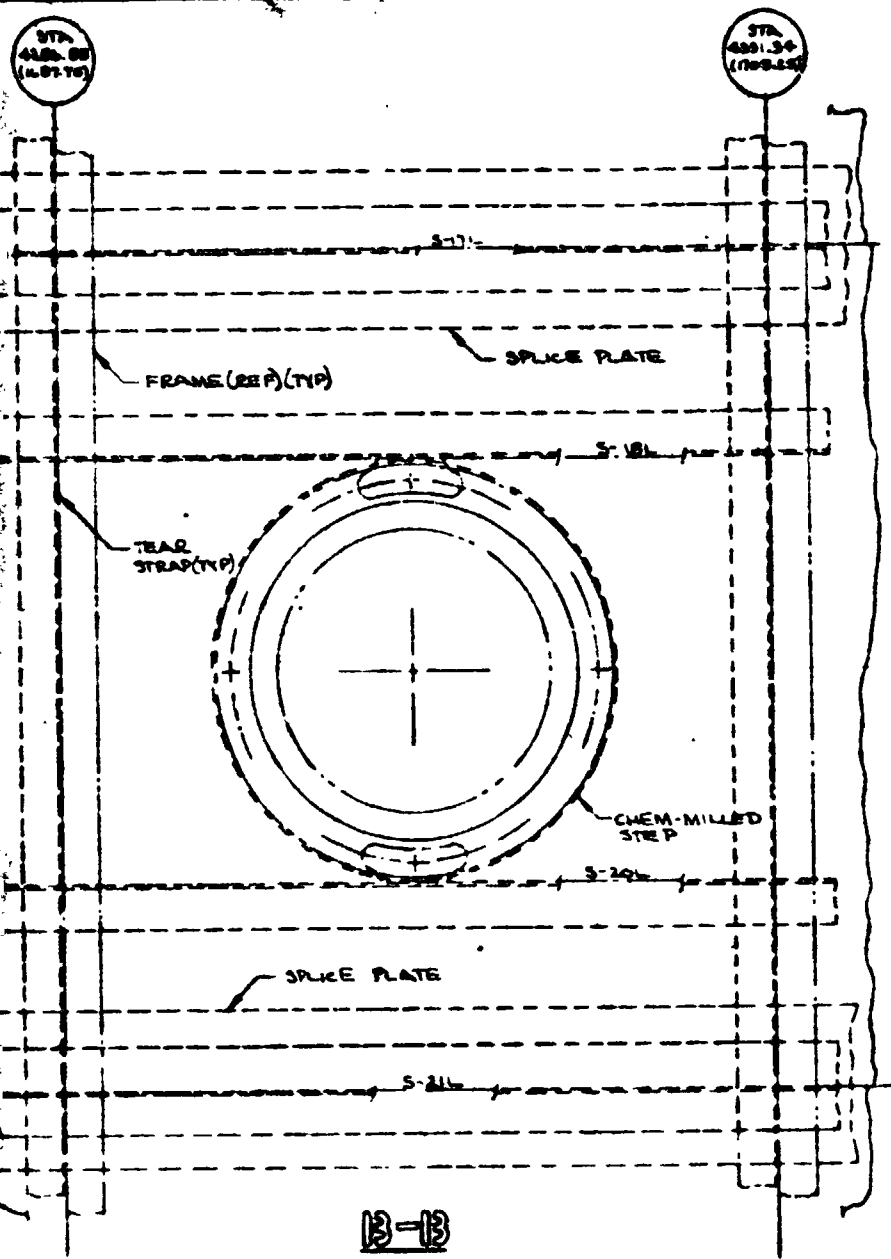
FOLDOUT FRAME

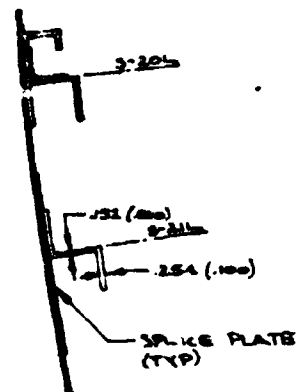
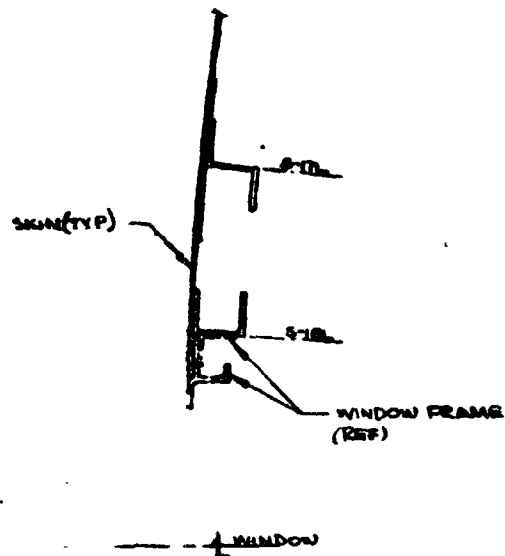
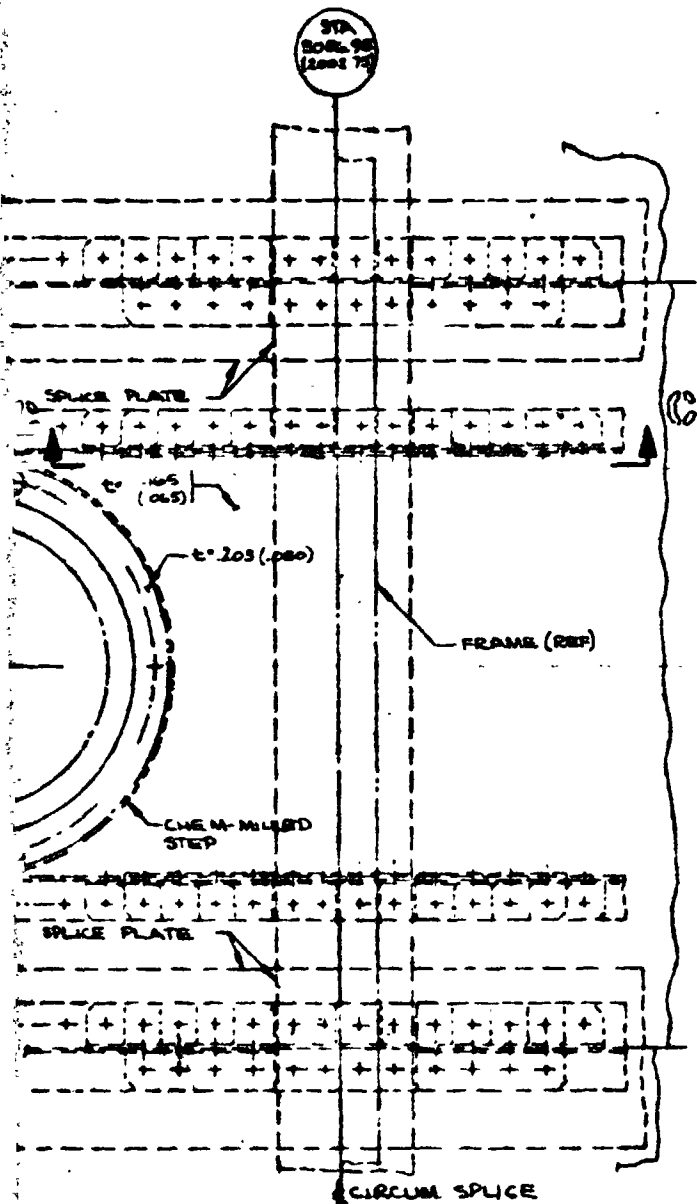
PRECEDING PAGE BLANK NOT FILLED

Figure 5-4 (Continued)

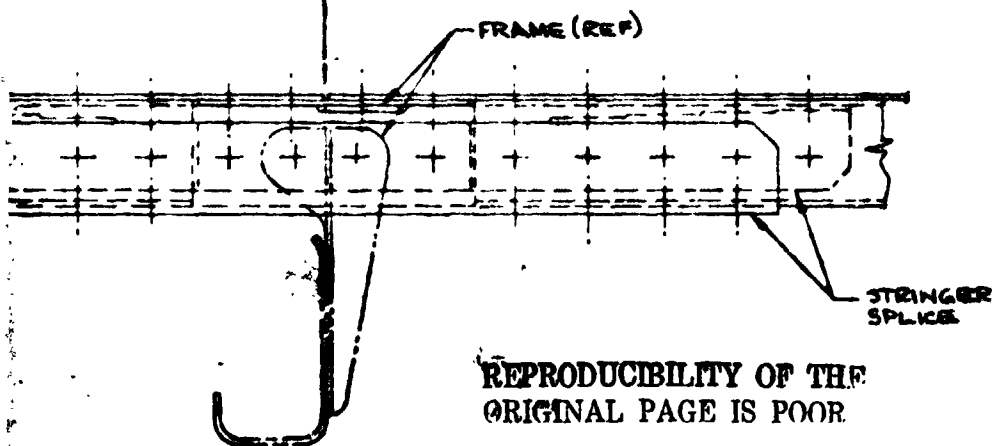


FOLDOUT FRAME





12-12



REPRODUCIBILITY OF THE
ORIGINAL PAGE IS POOR.

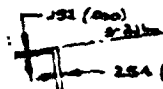
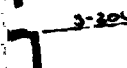
C-C

FOLDOUT FRAME 3



- WINDOW FRAME
(REF)

SHADOW



- SPRING PLATE
(TYP)

2-13

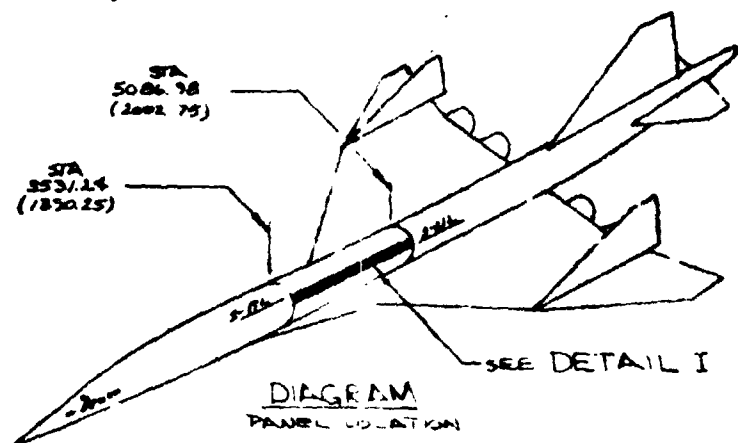
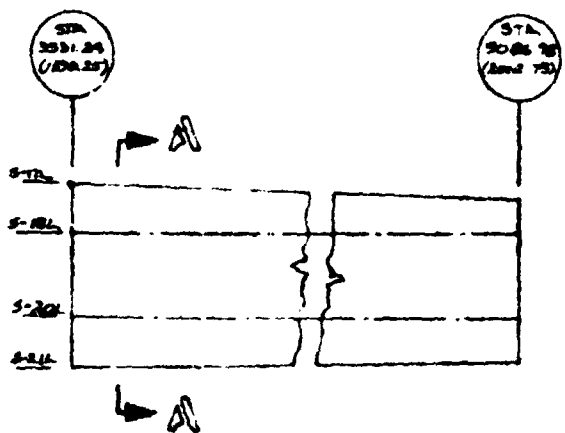


DIAGRAM
PANEL COLLOCATION



A-A

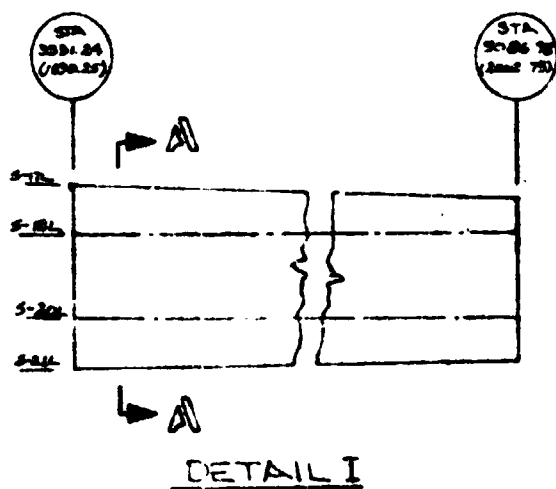
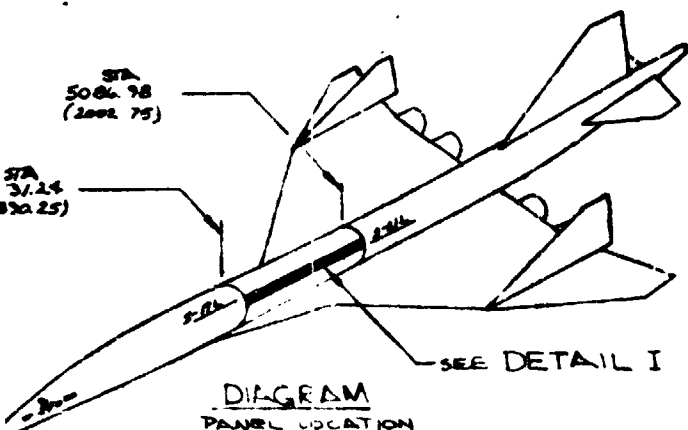


DETAIL I

SKIN
EXTRA
DASH
RENEE
ACRE

FOLDOUT FRAME

U.S. 000
1000
1000
1000



FOLDOUT FRAME 5

SKIN MATL IS TI 6AL-4V COND I

EXTRUDED STIFFENER MATL IS TI 6AL-4V COND II

BASIC UNIT SYSTEM IS THE INTERNATIONAL SI SYSTEM.
ENGLISH UNIT SYSTEM EQUIVALENT VALUES
ARE SHOWN IN ().

FOLDOUT FRAME 4

USED ON		DRAWN	DATE	SEE SHEET 1 OF PL FOR LIST OF MATERIAL USAGE AND NOTES	
		PS AMCHUK	10/12/72	THE BOEING COMPANY	
		CHECKED		COMMERCIAL AIRPLANE DIVISION RENTON WASH	
SHEET NO		STRESS		BODY SIDE PANEL	
CHG NO		ENG. 2 Ruck 10/15/72		TITANIUM SKIN/STRINGER	
GROUP C40		PROJ		969-512B (MACH 2.7)	
				CODE IDENT NO	SIZE
				31205	J AWS-131
				SCALE	SM

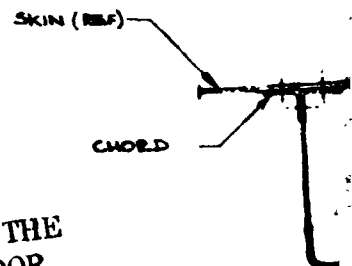
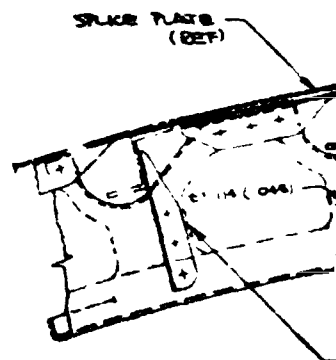
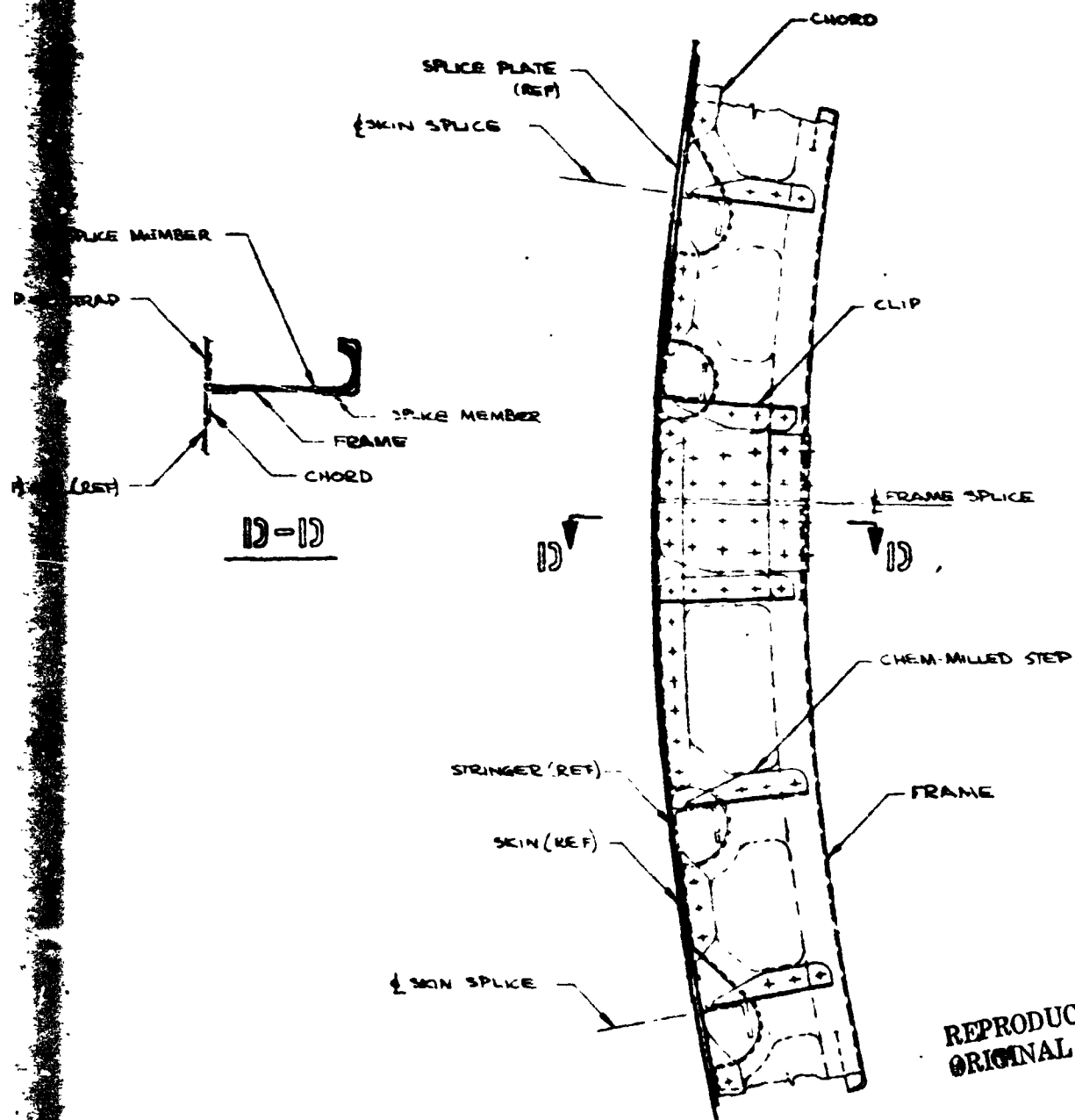
Figure 5-5

SPACE

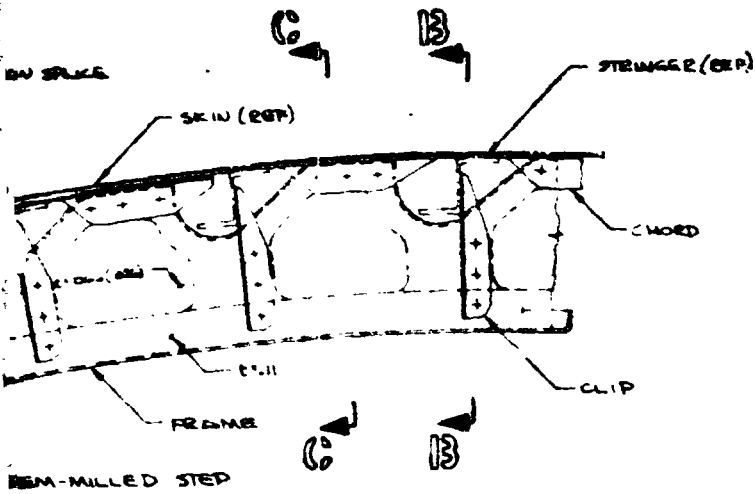
TEAR STRAP

SEAL (REF)

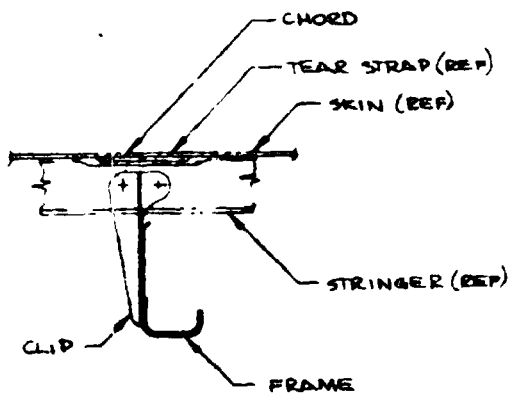
FOLDOUT FRAME



FOLDOUT FRAME



DETAIL 1



B-13

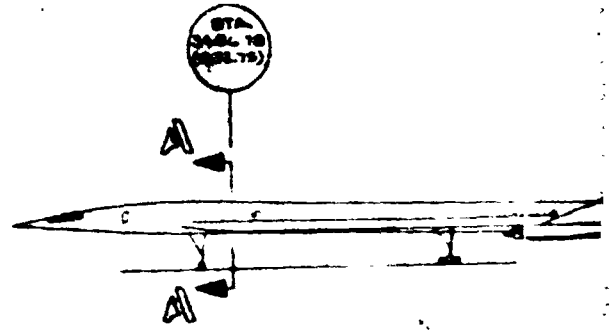
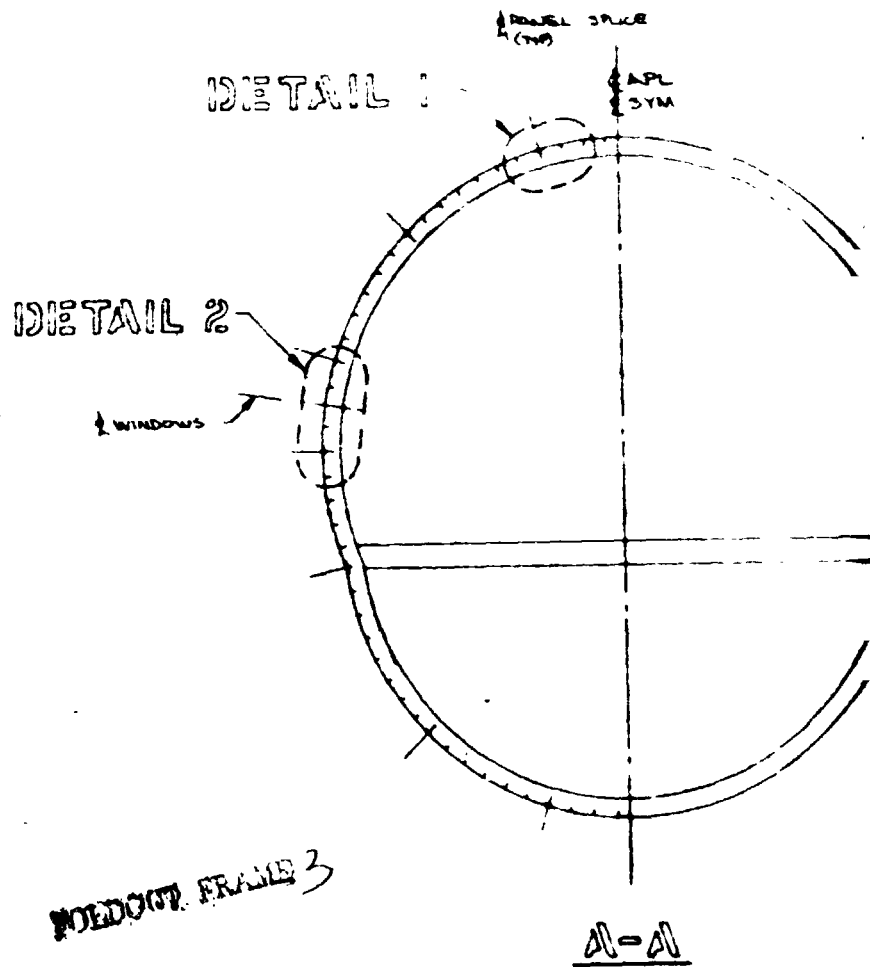


DIAGRAM
FRAME LOCATION



WELDOUT FRAME 3

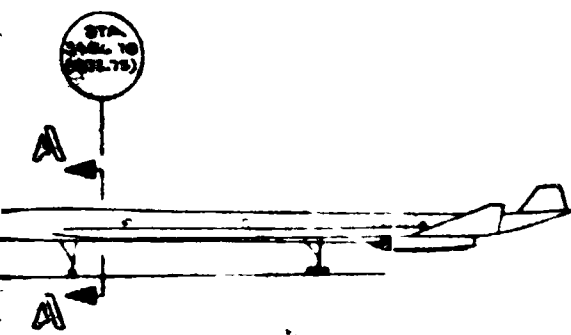
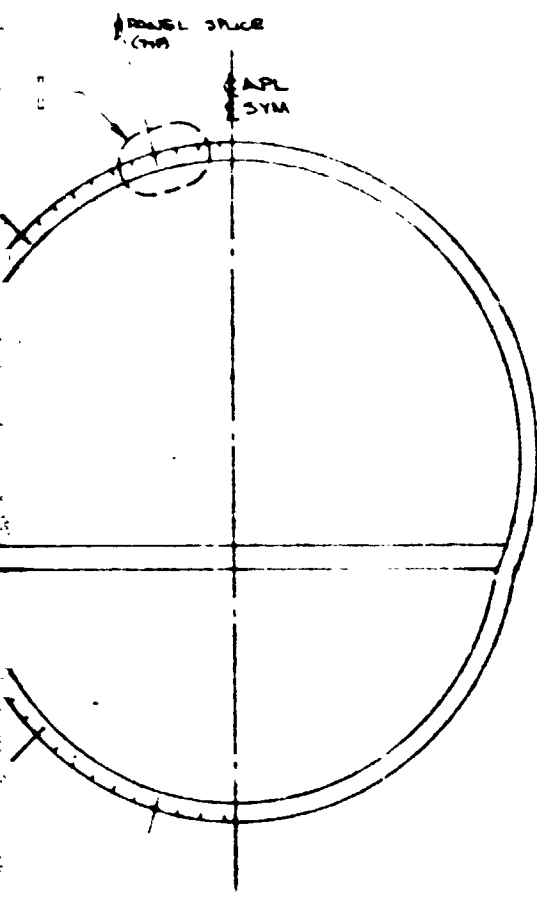


DIAGRAM
FRAME LOCATION



A-A

PREVIOUS PAGE BLANK NOT FOLDOUT

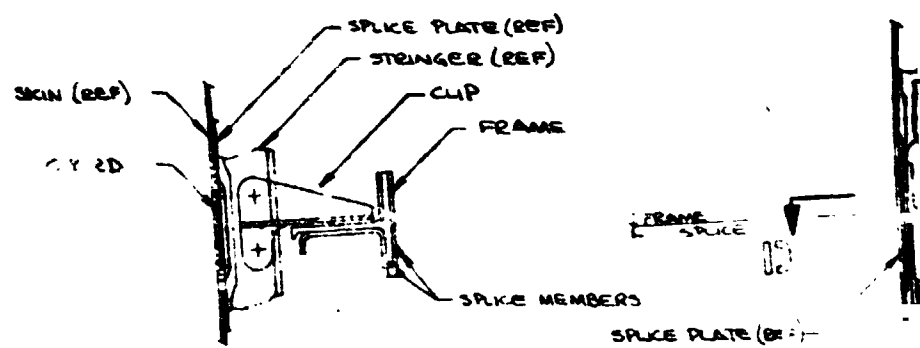
FOLDOUT FRAME

ALL MATERIALS TIGAL-4V COND I

BASIC UNIT SYSTEM IS THE INTERNATIONAL SI SYSTEM
ENGLISH UNIT SYSTEM EQUIVALENT VALUES ARE
SHOWN IN ().

USED ON		DATE	REF. SPEC. FOR LIST OF MATERIAL USAGE AND NOTES	
DRAWN: <i>[Signature]</i>		8-22-77	THE BOEING COMPANY	
CHECKED			COMMERCIAL AIRPLANE DIVISION RENTON WASH	
SECT NO	STRESS		BODY FRAME	
	WOP		STA 3486.78 (1372.75)	
CNO NO	GROUP		962-512B MACH 2.7	
GROUP DEC	PROJ		CODE IDENT NO	81205
			SIZE	J
			SCALE	1/8" = 1"
				AW5-132

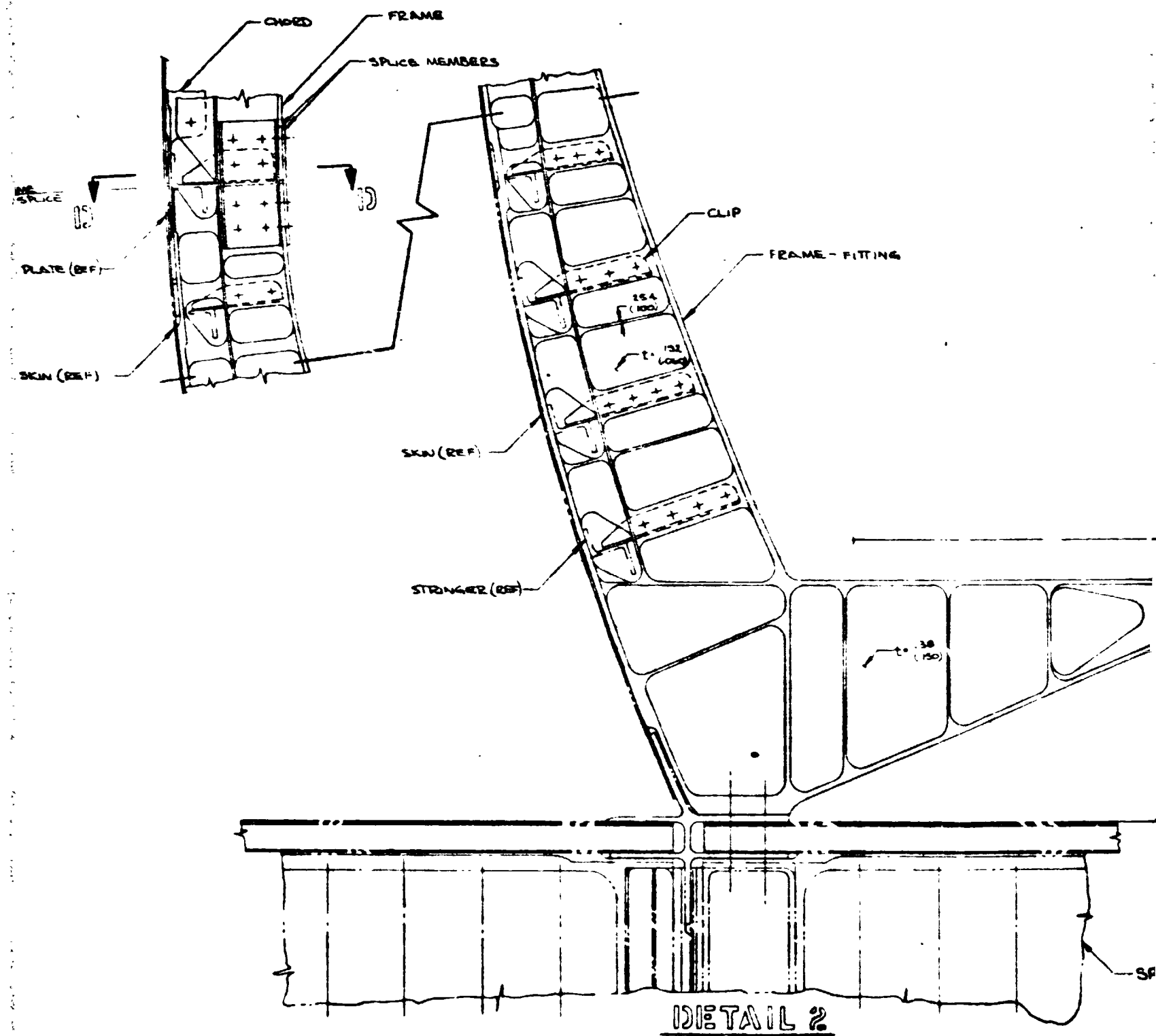
Figure 5-6



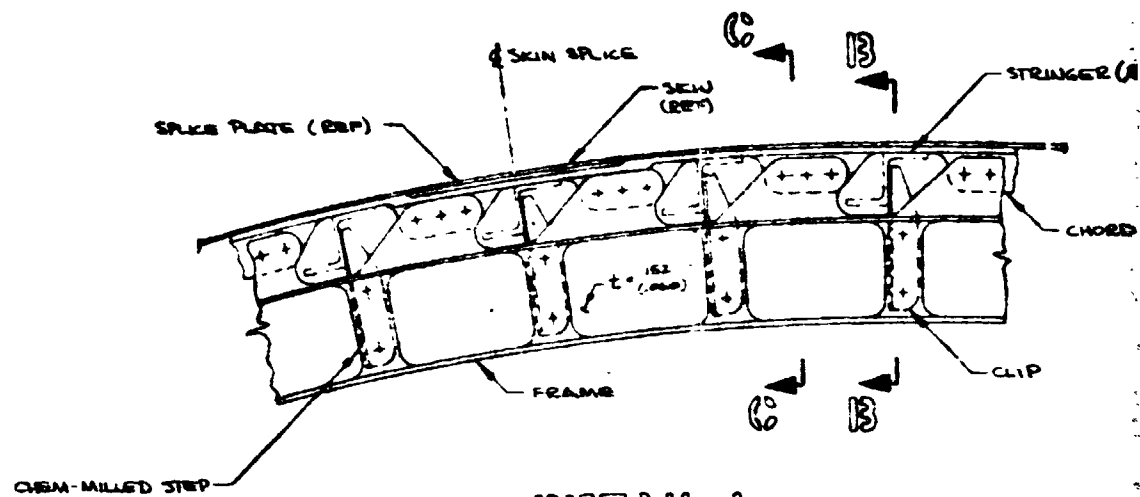
10-10

SKIN (REF)

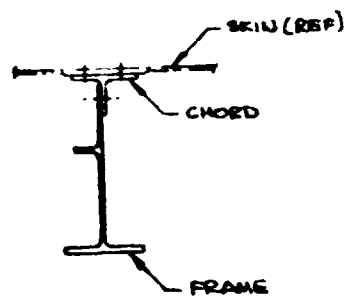
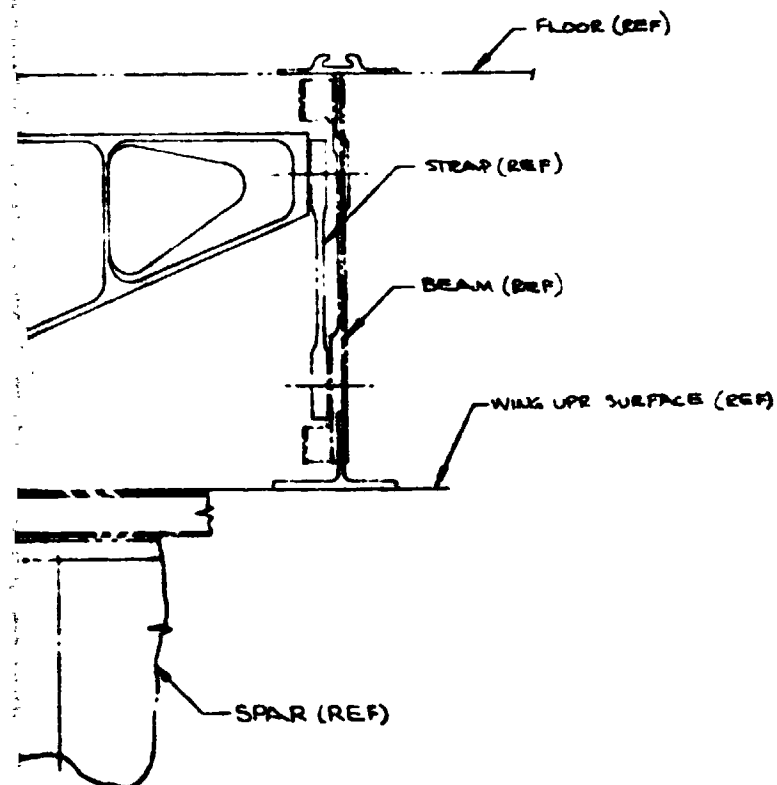
FOLDOUT FRAME



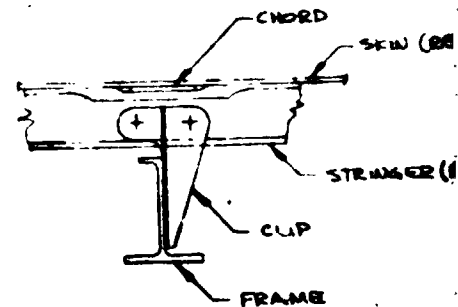
FOLDOUT FRAME 2



DETAIL 1



C-C



B-B

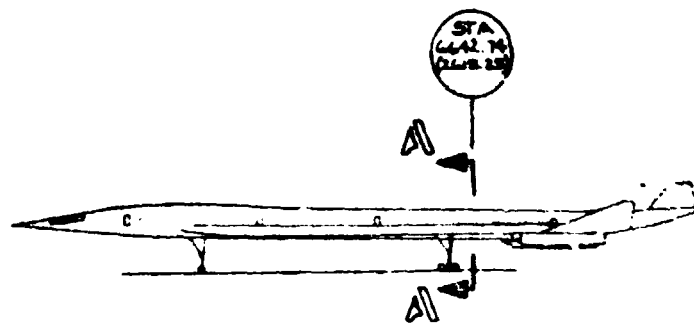
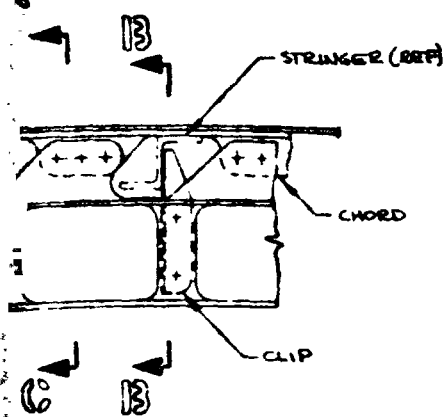
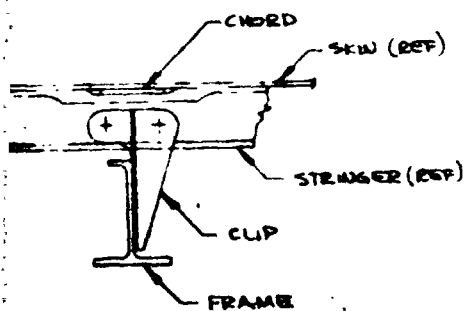
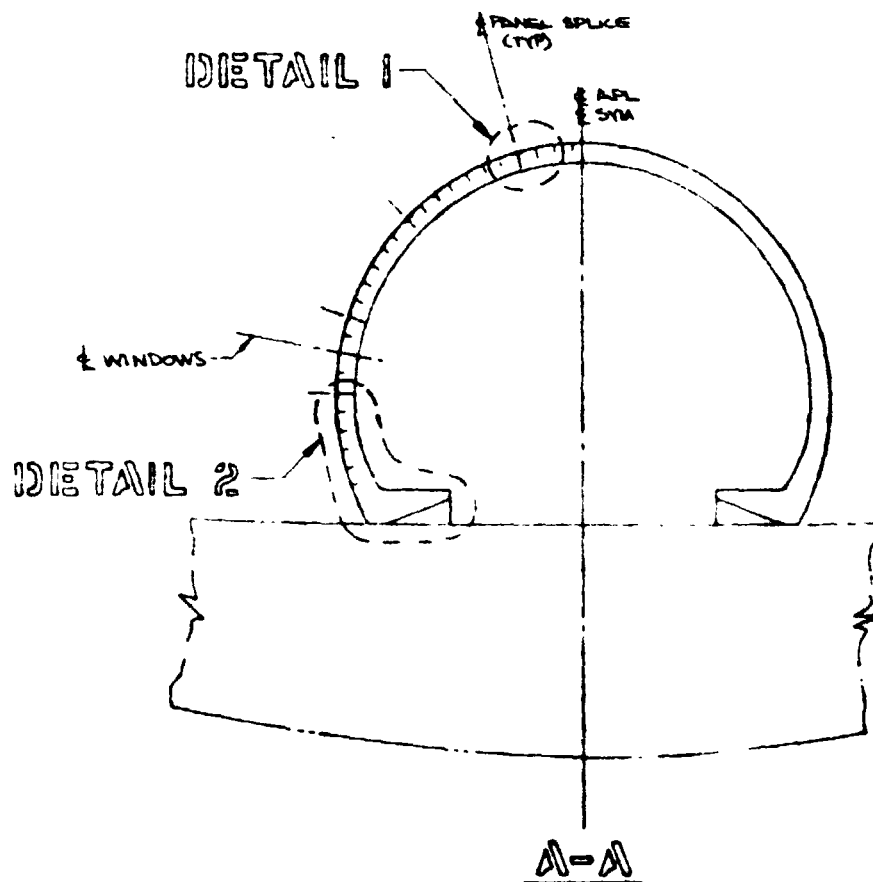


DIAGRAM
FRAME LOCATION



B-B

FOLDOUT FRAME 4

ALL M

BASIC
ENGLISH
SHOWN

USED ON
SECT NO
CHG NO
GROUP OR

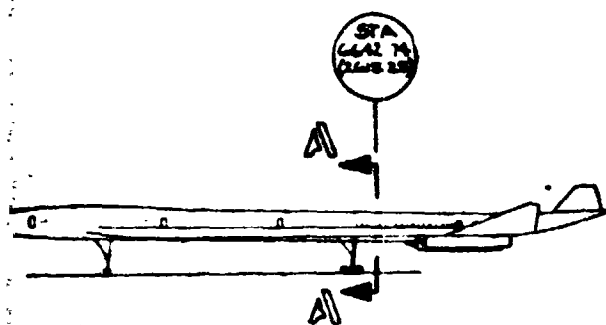
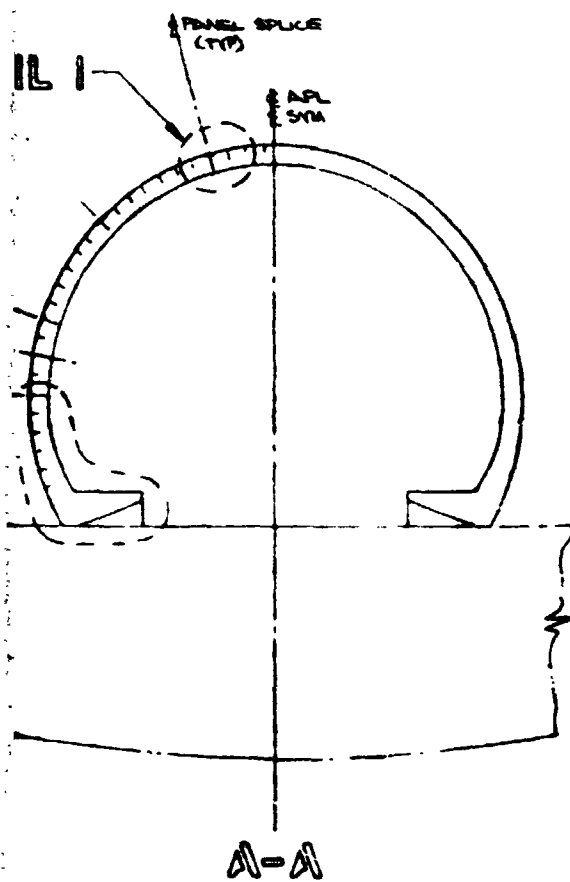


DIAGRAM
FRAME LOCATION



PRECEDING PAGE BLANK NOT FOR FILE

FOLDOUT FRAME **5**

ALL MATERIALS TIGAL-4V COND I

BASIC UNIT SYSTEM IS THE INTERNATIONAL SI SYSTEM
ENGLISH UNIT SYSTEM EQUIVALENT VALUES ARE
SHOWN IN ()

USED ON		DATE	SEE SHEET 1 OF PL FOR LIST OF MATERIAL USAGE AND NOTES	
DRAWN		DATE	THE BOEING COMPANY	
CHECKED		DATE	COMMERCIAL AIRPLANE DIVISION, RENTON, WASH.	
STRESS		DATE	BODY FRAME	
SECT NO	1	0.25.75	STA 6642.74 (2615.25)	
CHG NO			969-512B MACH 2.7	
GROUP			CODE	SIZE
PROJ			IDENT NO	J
GROUP ORG			81205	AWS-133
		SCALE	SH	

Figure 5-7

FRONT 31

LINE

FOLDOUT FRAME |

FRONT SPAR

STIFFENER

SINE WAVE WEB

C-C

13

UPPER WING SKIN
(REF)

SINE WAVE WEB

13-13

CHORD (TYP)

0.00

STIFFENER

SYSTEM HOLES

DETAIL 2

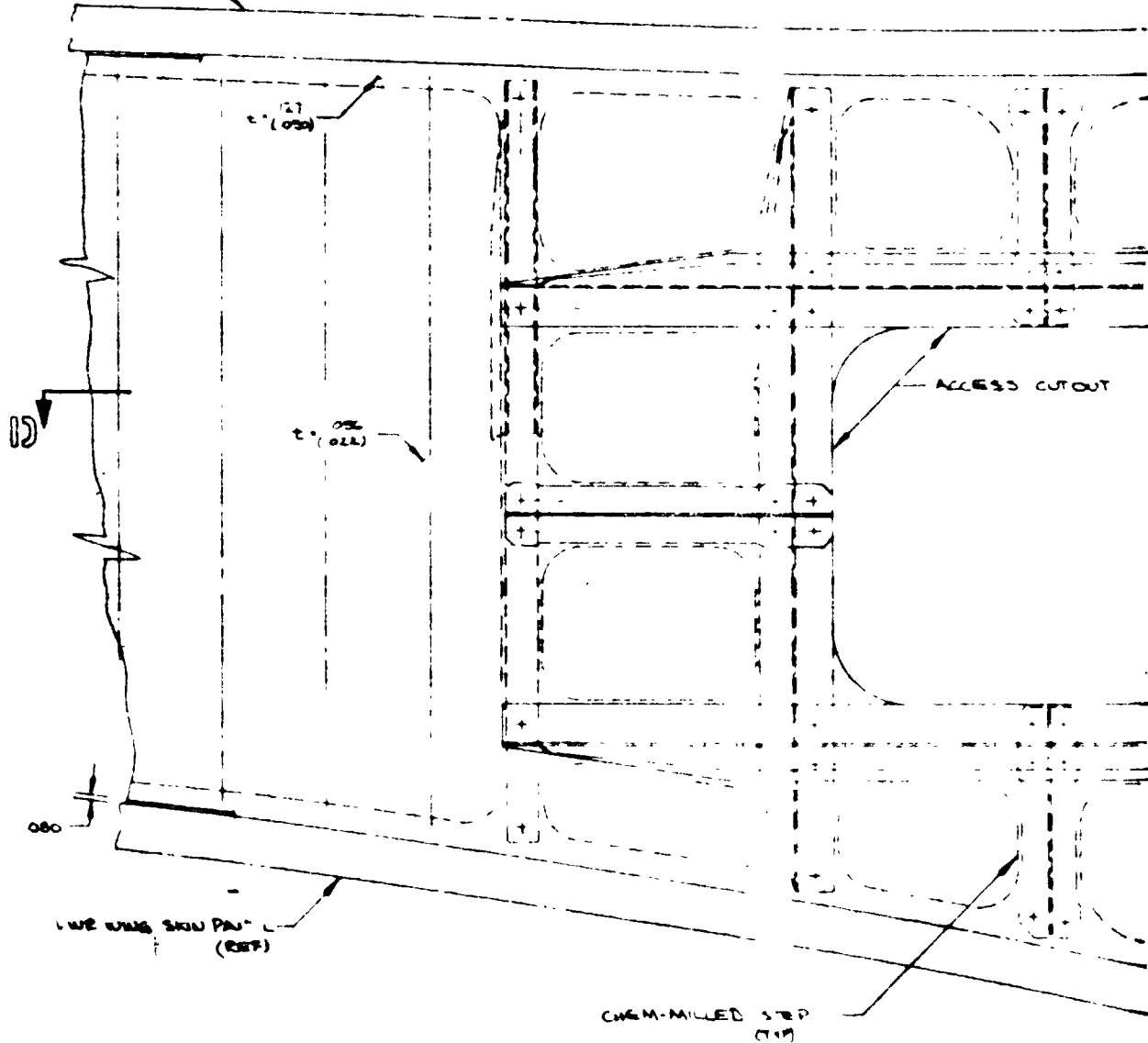
FOLDOUT FRAME 2



10-0

UPR WING SKIN PANEL
(0029)

WING SKIN PANEL



LWR WING SKIN PAN-
(REF)

DETAIL I

FOLDOUT FRAME

STIFFENER (TYP)

10-10

ACCESS CUTOUT

SEE 3-3

t = .076 (0.30)

SIDEW

10

CHORD (TYP)

STIFFENER (TYP)

DETAIL 1

FOLDOUT FRAME 4

SIDEWAVE WEB

SIDEWAVE WEB

12

030

CHORD (TYP)

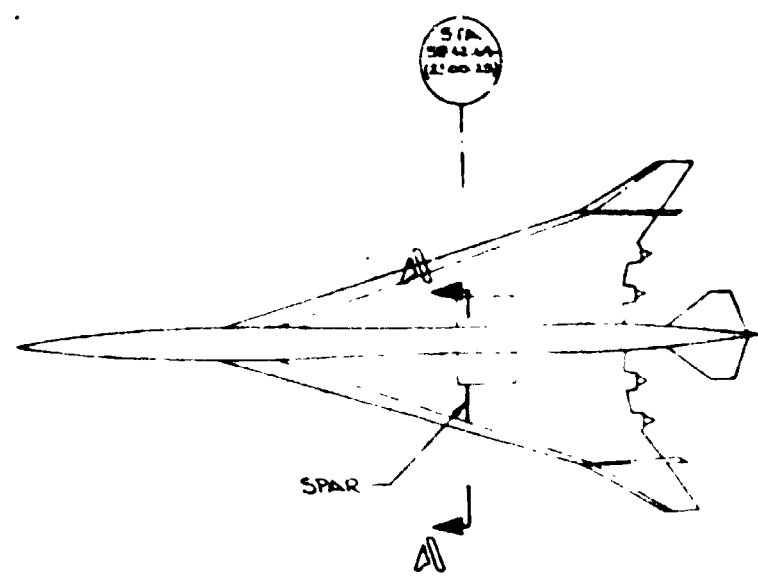
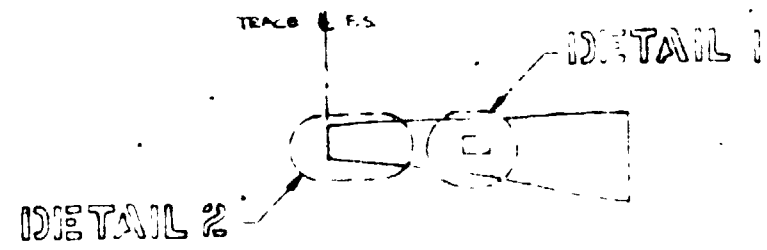


DIAGRAM
SPAR LOCATION



A-A (ROTATE 180°)

ALL PARTS

BASIC UNIT
ENGLISH I
SHOWN

FOLDOUT FRAME

USED ON	01
W. NO.	02
CHG NO.	03
GROUP ORG.	04

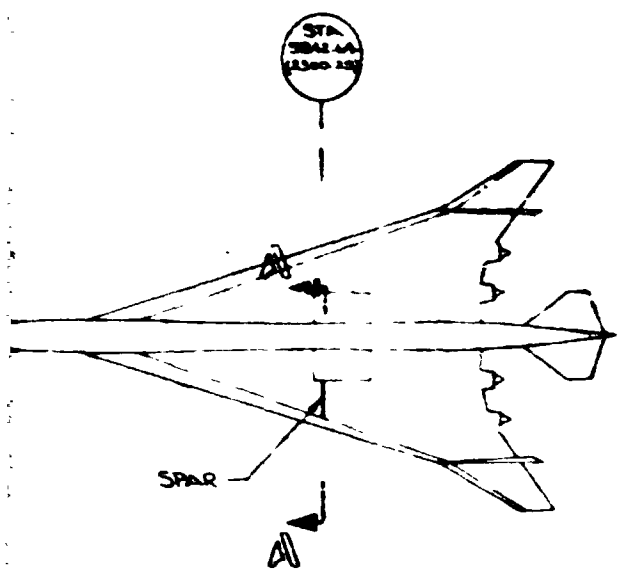
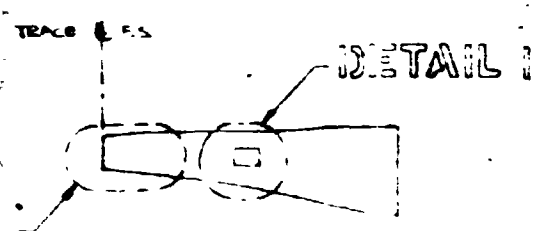


DIAGRAM
SPAR LOCATION

PRECEDING PAGE BLANK NOT FILMED.



A-A (ROTATED 90°)

WING SPAR

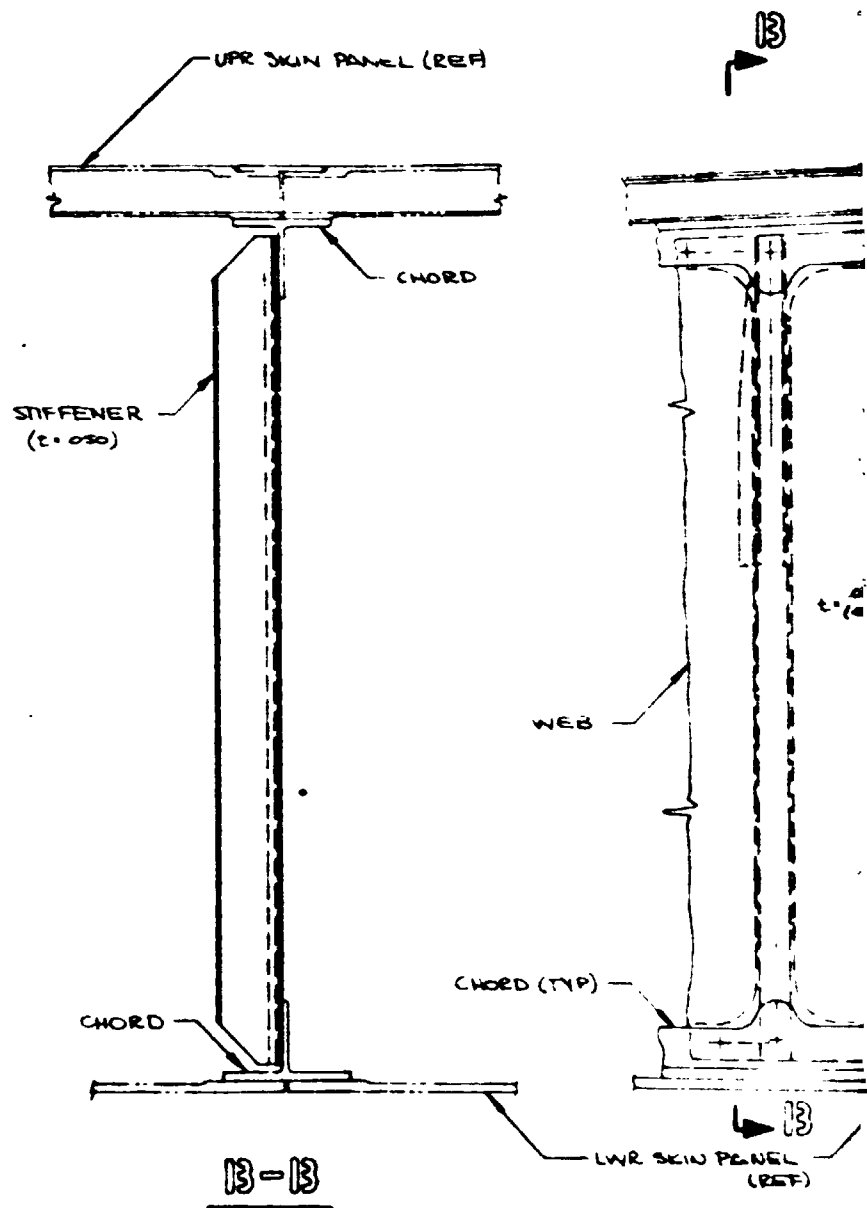
ALL MATERIALS TO GAL-4V COND I

BASIC UNIT SYSTEM IS THE INTERNATIONAL SI SYSTEM
ENGLISH UNIT SYSTEM EQUIVALENT VALUES ARE
SHOWN IN ()

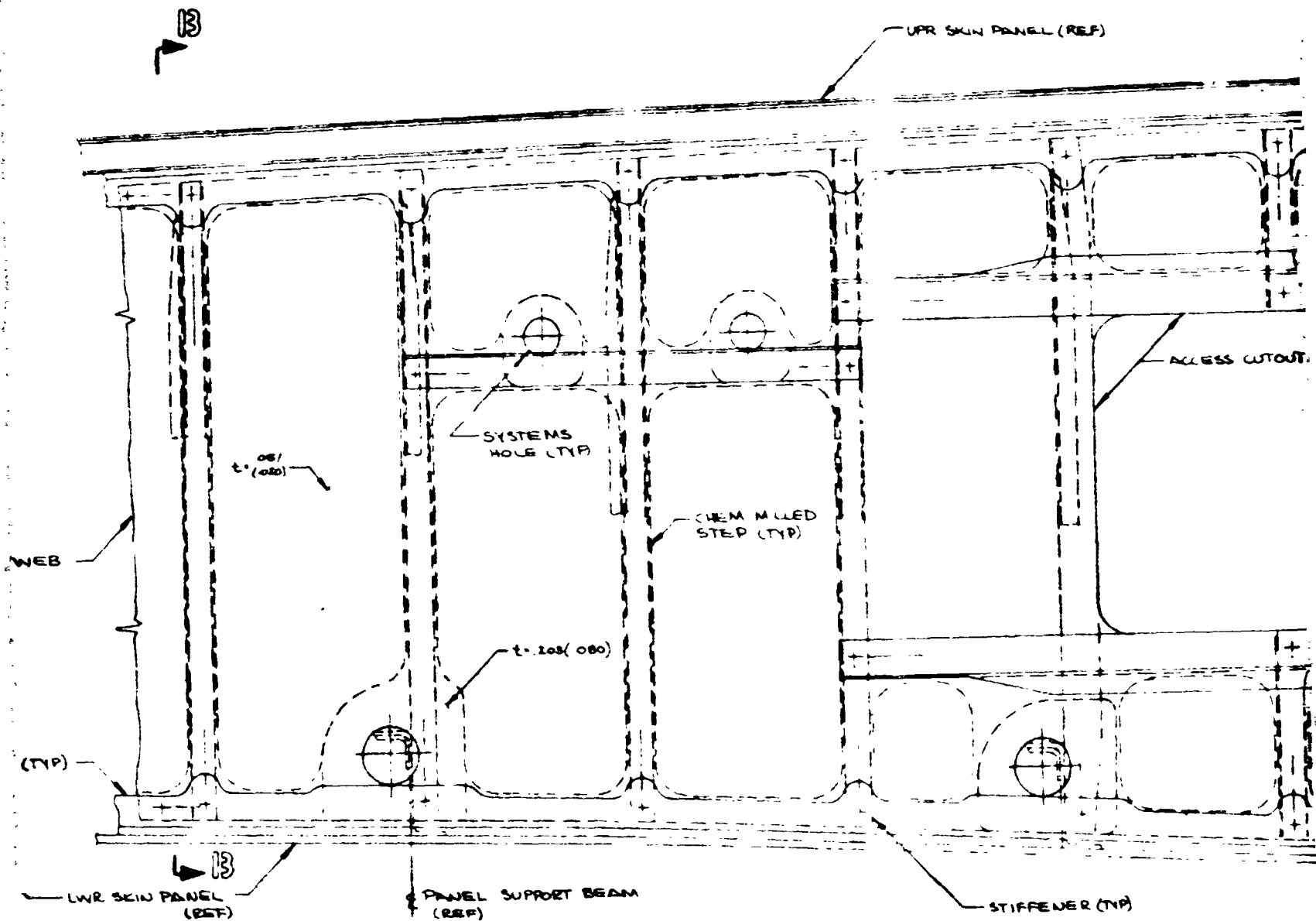
FOLDBOUT FRAME 5

REF SHEET FOR LIST OF MATERIAL USAGE AND NOTES			
USED ON	DESIGN	DATE	THE BOEING COMPANY COMMERCIAL AIRPLANE DIVISION, RENTON, WASH.
	CHECKED		
SECT NO	STRESS		NEWAVE WING SPAR
	ENG		STA 5842 64 (2300 25)
CHG NO	GROUP		9-512 B MACH 27
GROUP ORG	PROJ		LODI IDENT NO 81725
			J AWS-134
			SCALE
			SM

Figure 5-8



FOLDOUT FRAME

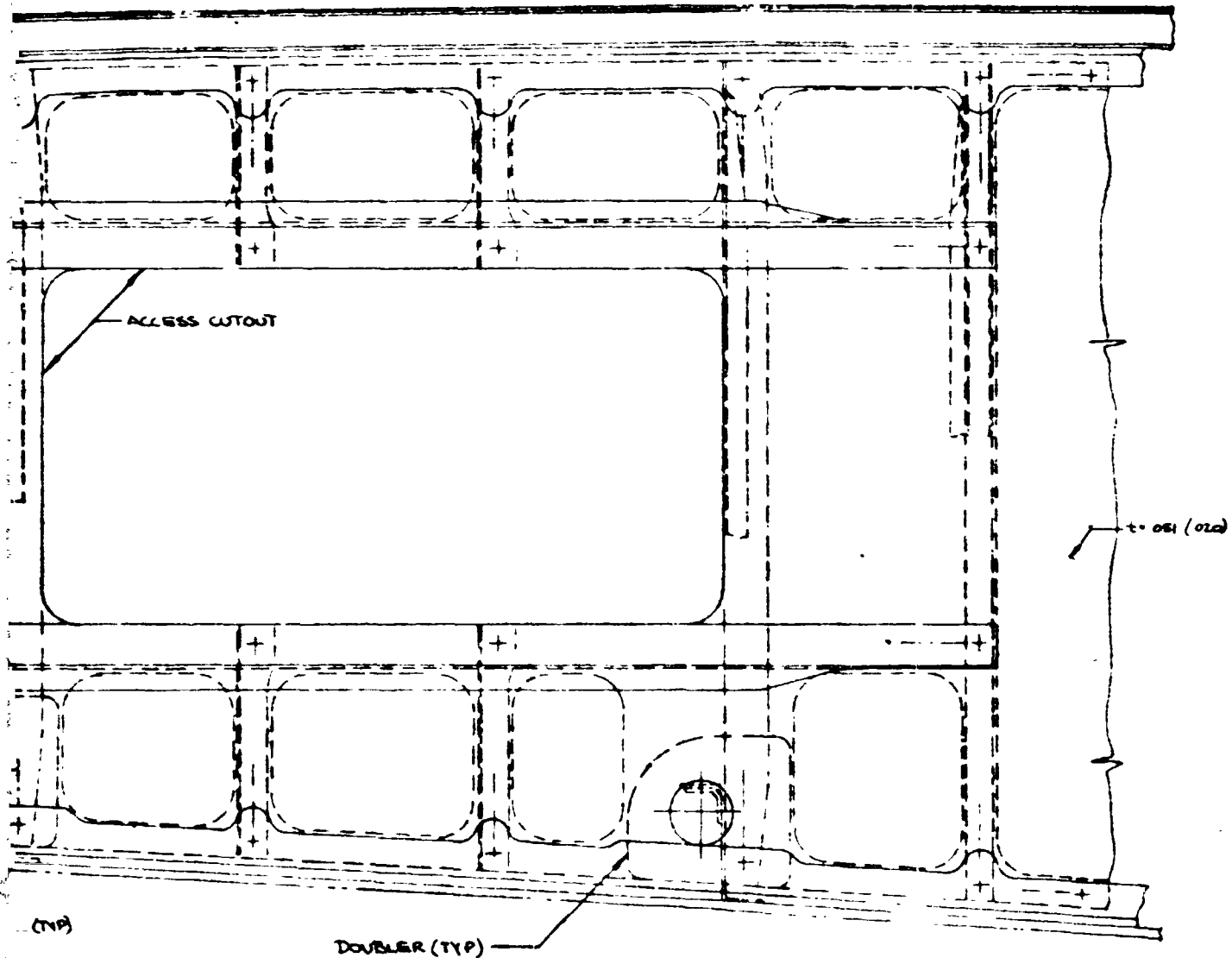


REPRODUCIBILITY OF THE
ORIGINAL PAGE IS POOR

DETAIL 2

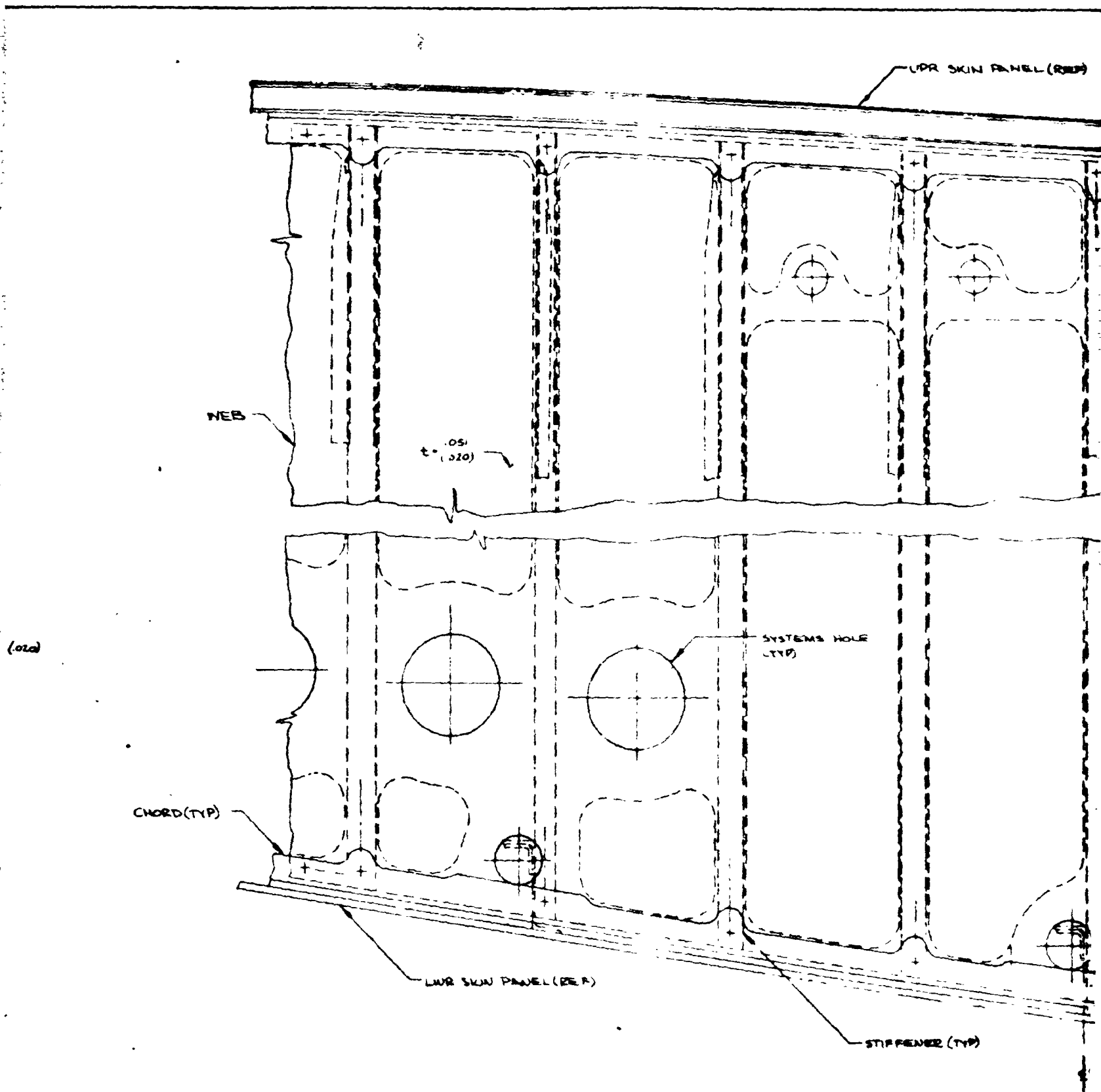
FOLDOUT FRAME 2

REF)



REPRODUCIBILITY OF THE
ORIGINAL PAGE IS POOR

FOLDOUT FRAME 3

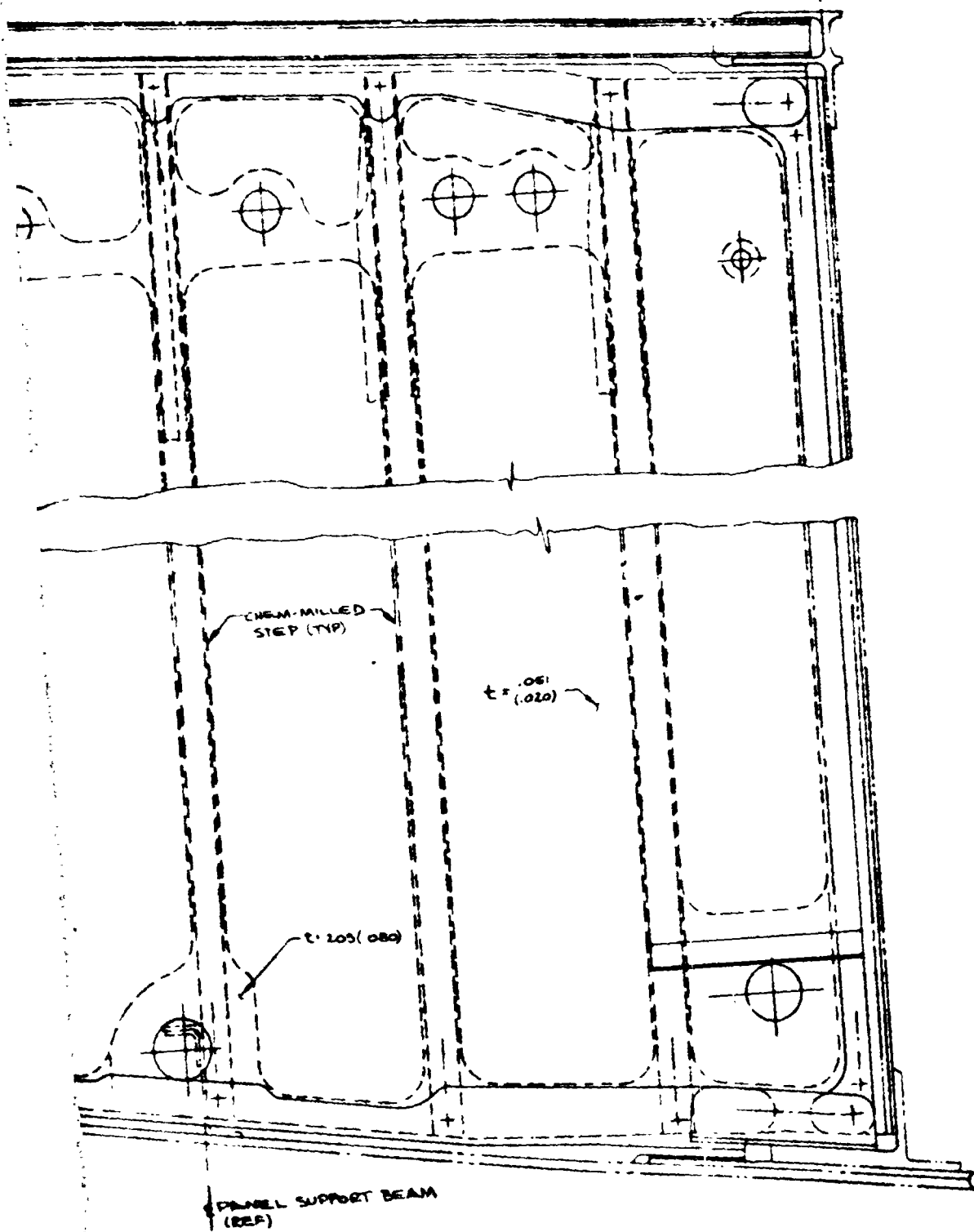


FOLDOUT FRAME 4

DETAIL 1

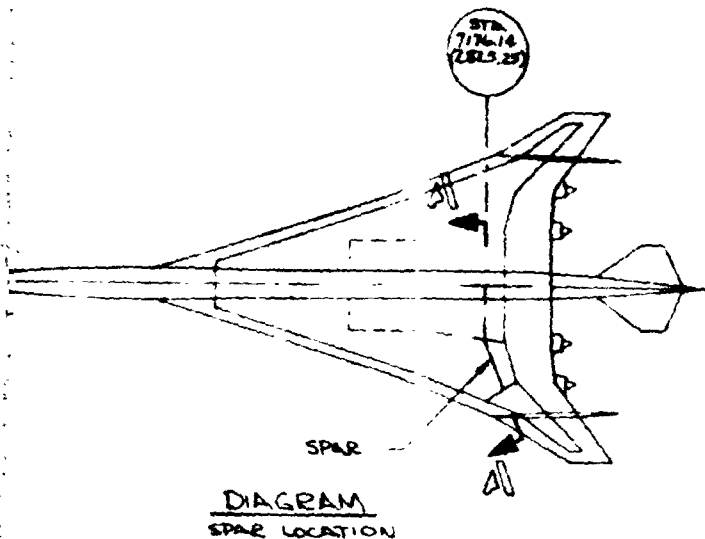
PANEL (REP)

28



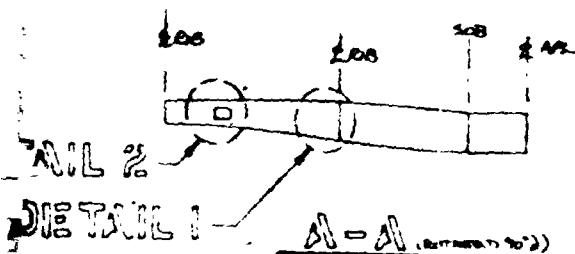
DETAIL
DE

FOLDOUT FRAME



PRECEDING PAGE BLANK NOT FILMED.

REPRODUCIBILITY OF THE
ORIGINAL PAGE IS POOR



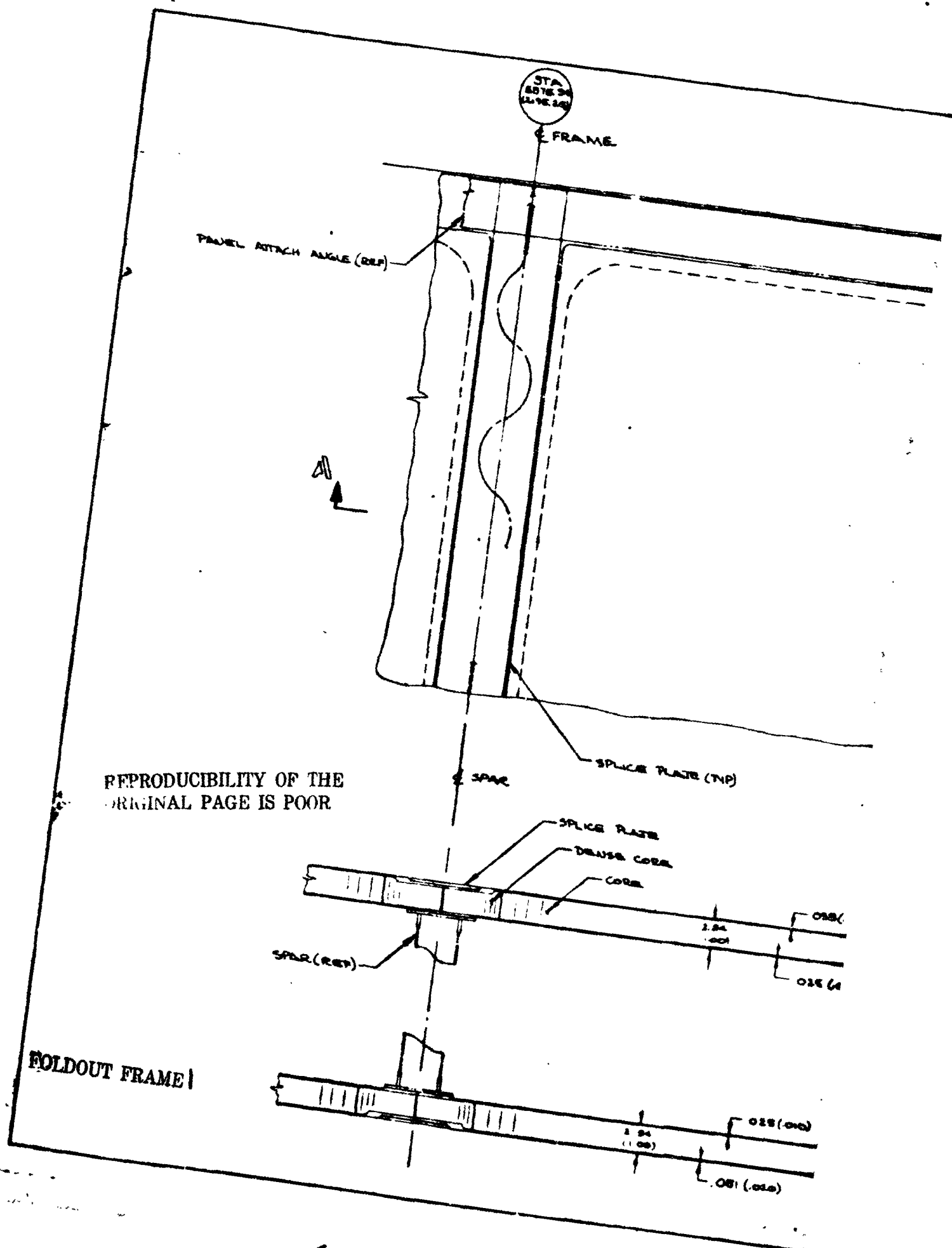
FOLDOUT FRAME 6

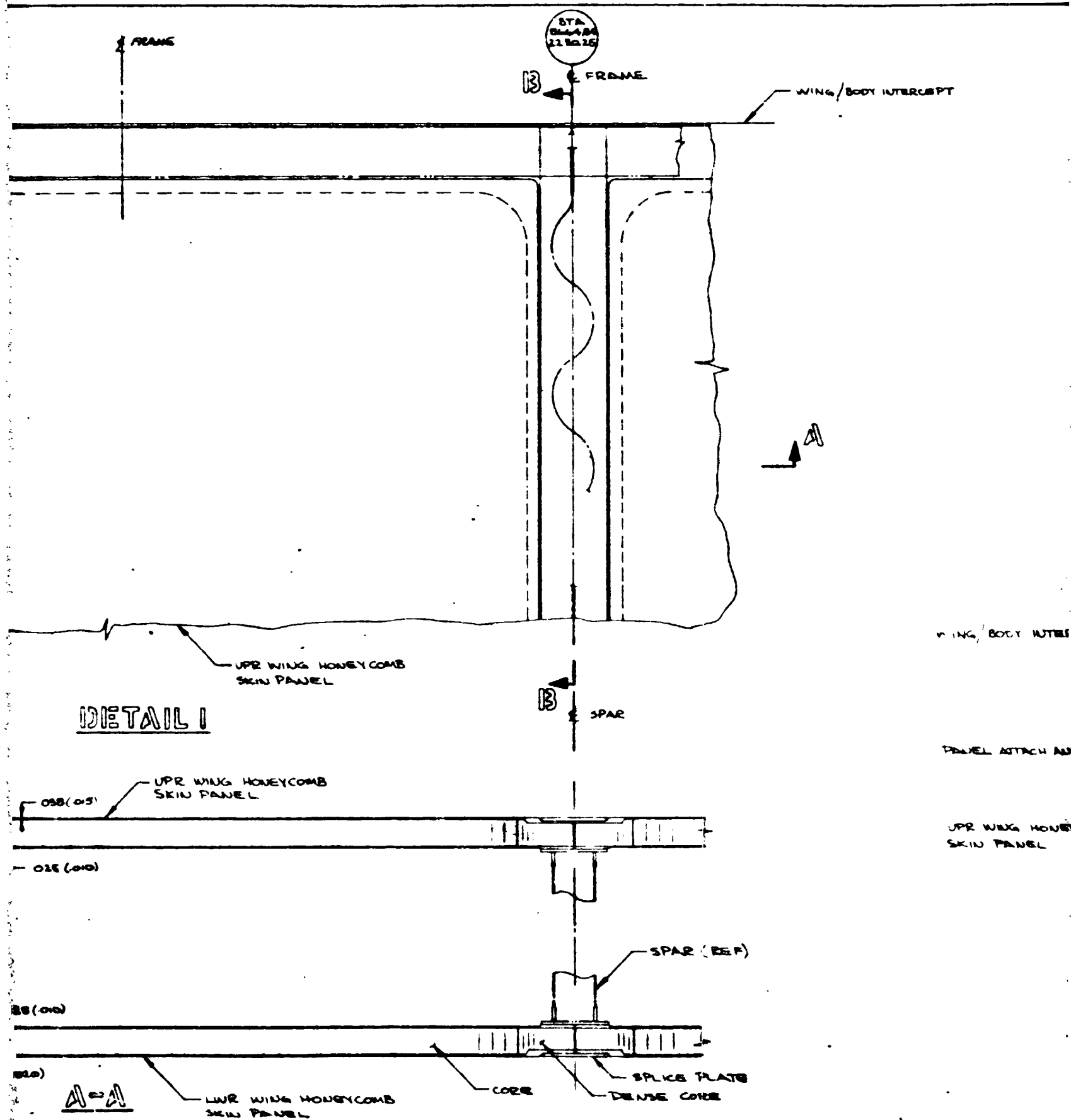
ALL MATERIALS TO GAL-4V COND I

BASIC UNIT SYSTEM IS THE INTERNATIONAL SI SYSTEM.
ENGLISH UNIT SYSTEM EQUIVALENT VALUES ARE
SHOWN IN ().

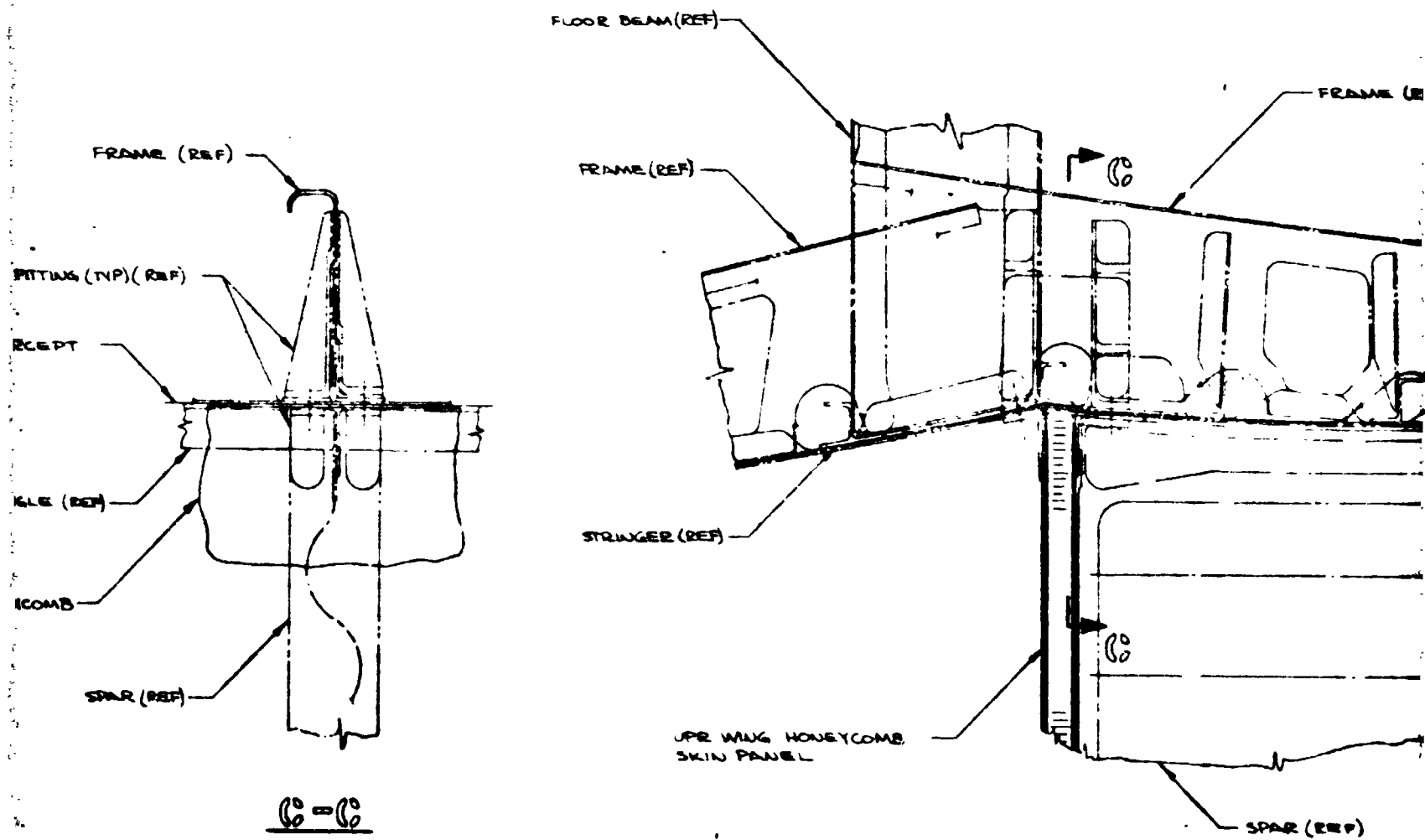
USED ON	DESIGN	CASE	SEE SHEET 1 OF PL FOR LIST OF MATERIAL GRADE AND NOTES	
	CHECKED		THE BOEING COMPANY COMMERCIAL AIRCRAFT DIVISION, RENTON, WASH.	
SECT NO	STRESS		SHEET STIFFENER WING SPAR	
CHG NO	ENG		STA 7176.14 (2825.25)	
GROUP ORG	GROUP		969-528 MACH 27	
	PROJ		CODE IDENT. NO. 81205	
			J AWS-135	
			SCALE 1/8"	

Figure 5-9

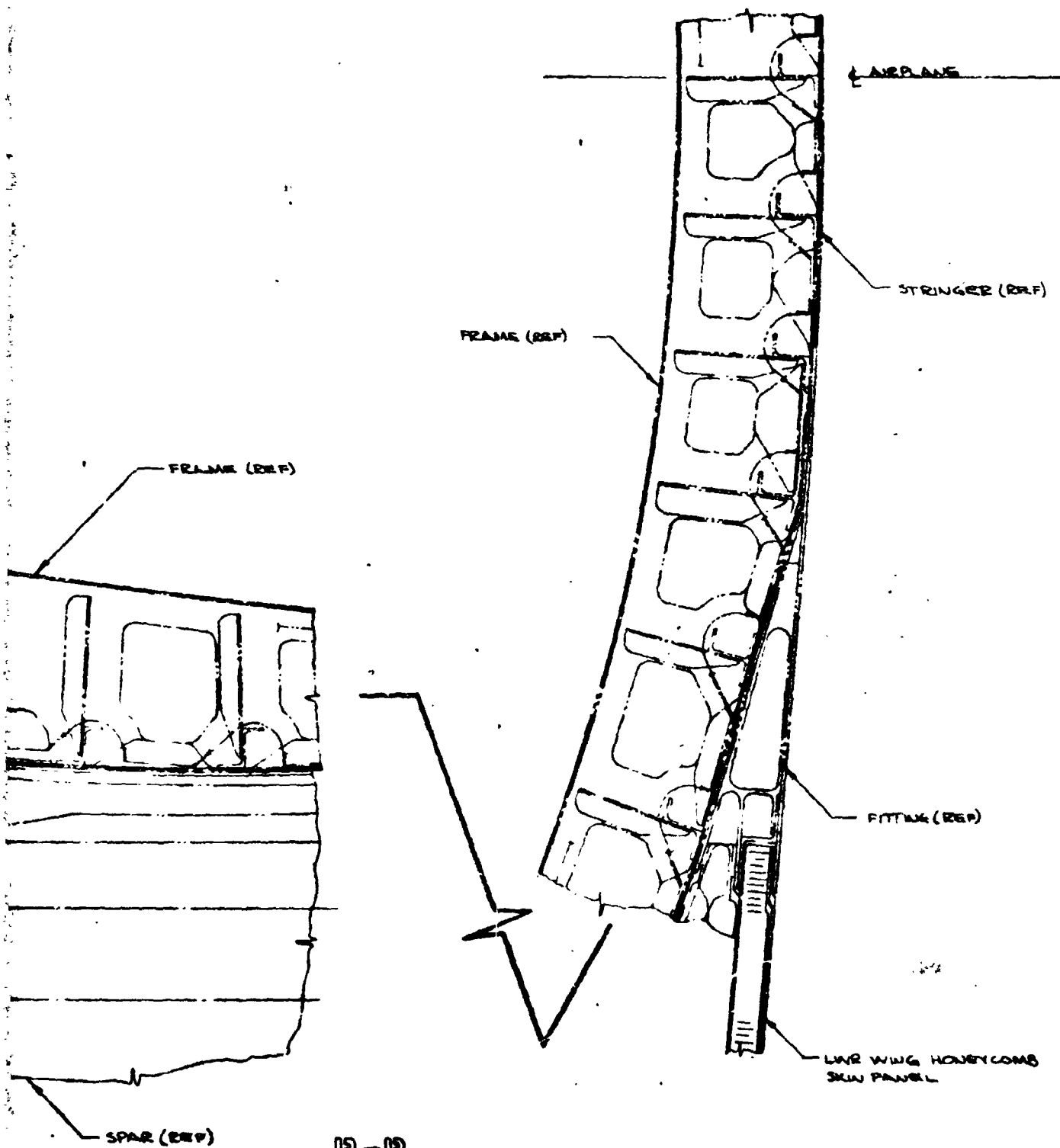




FOLDOUT FRAME 2



FOLDOUT FRAME 3



SEE D127

SKIN PA
(UPR & LWR)

13-13

FOLDOUT FRAME 4

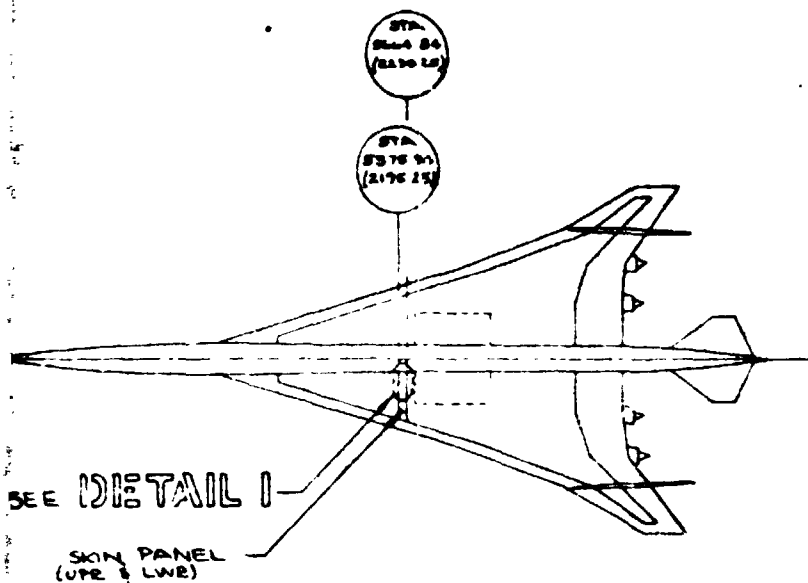


DIAGRAM
SKIN PANEL LOCATION

PRECEDING PAGE BLANK NOT FILMED.

FOLDOUT FRAME 5

MATERIALS:

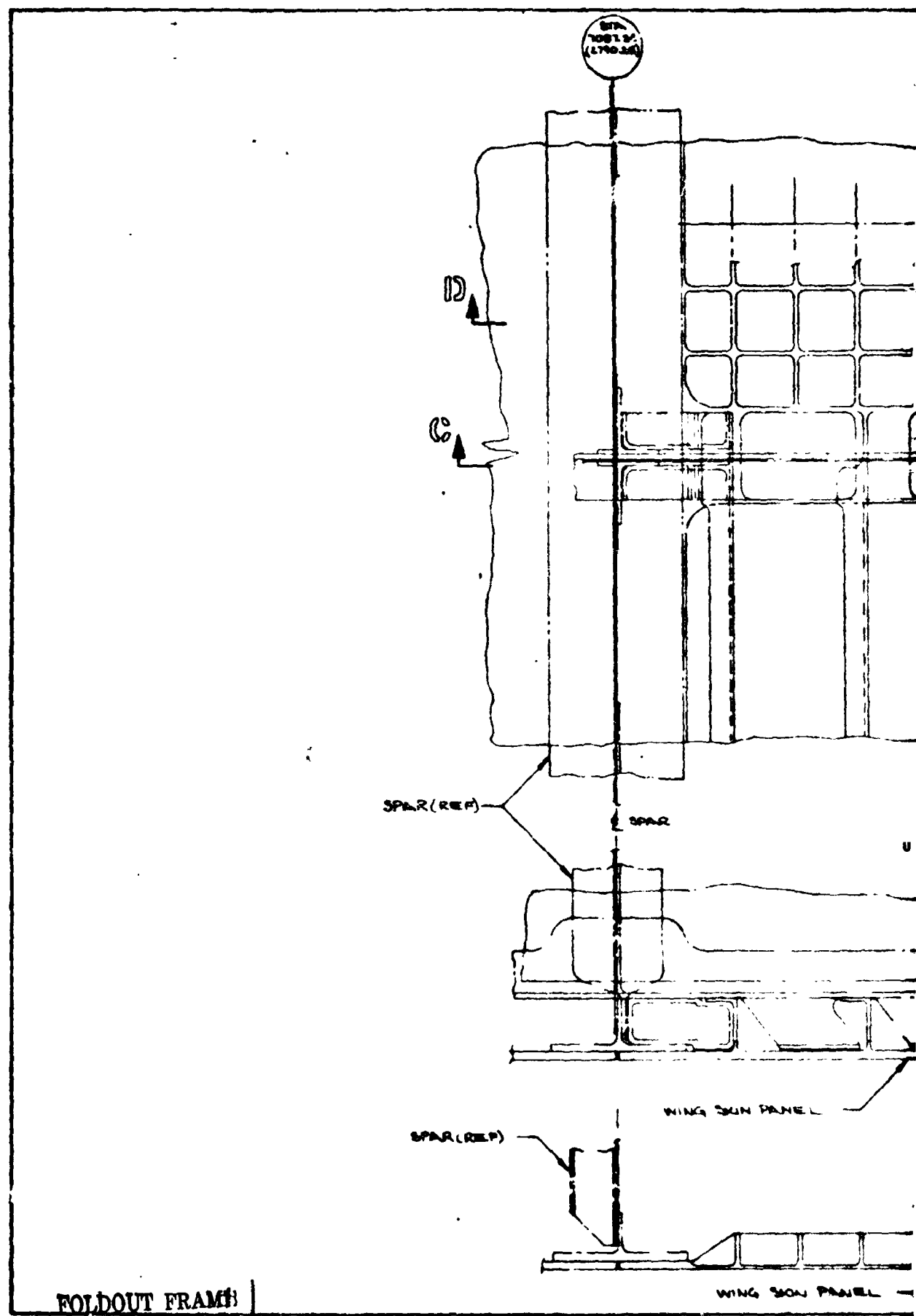
SHEET - TI-6AL-4V COND I
CORE - TI-3AL-2.5V
DENSE CORE - TI-6AL-4V

SKIN PANEL - ALUMINUM DRAZED TITANIUM

BASIC UNIT SYSTEM IS THE INTERNATIONAL SI SYSTEM.
ENGLISH UNIT SYSTEM EQUIVALENT VALUES ARE SHOWN
IN C

SEE SHEET 1 OF PL FOR LIST OF MATERIAL USAGE AND NOTES			
USED ON	DRAWN	DATE	THE BOEING COMPANY COMMERCIAL AIRPLANE DIVISION, RENTON, WASH.
	CHECKED		
SHEET NO	STRESS		SKIN PANEL - FORWARD WING
	INCH		969-5128 MACH 2.7
CHG NO	GROUP		CODE IDENT NO 81705
	PROJ		J AWS-136
GROUP DES			SCALE 1/8"

Figure 5-10



STA-
1087.84
02790.38

FRA
SPAR

WING/BOL
INTERFACES PT

WING SKIN PANEL

A

SPICE PLATE

100-100

WING OR BODY RIB

100-100

WING SKIN PANEL

WING DOUT FRAME 3

STA
1087.24
(2710.38)

FRAME
SPAR

SPAR (REF)

SPLICE PLATE

WING SKIN PANEL

FRAME

SPLICE PLATE

SPAR (REF)

SPLICE PLATE

SPAR

WING SKIN PANEL

CORE

DENSE CORE

SPAR (REF)

DETAIL I

229 (090)

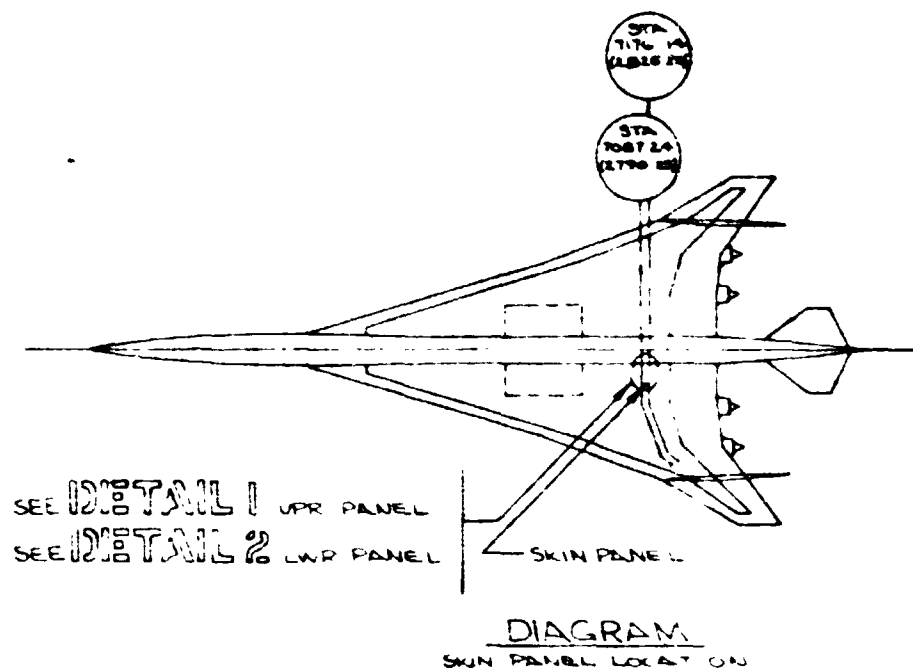
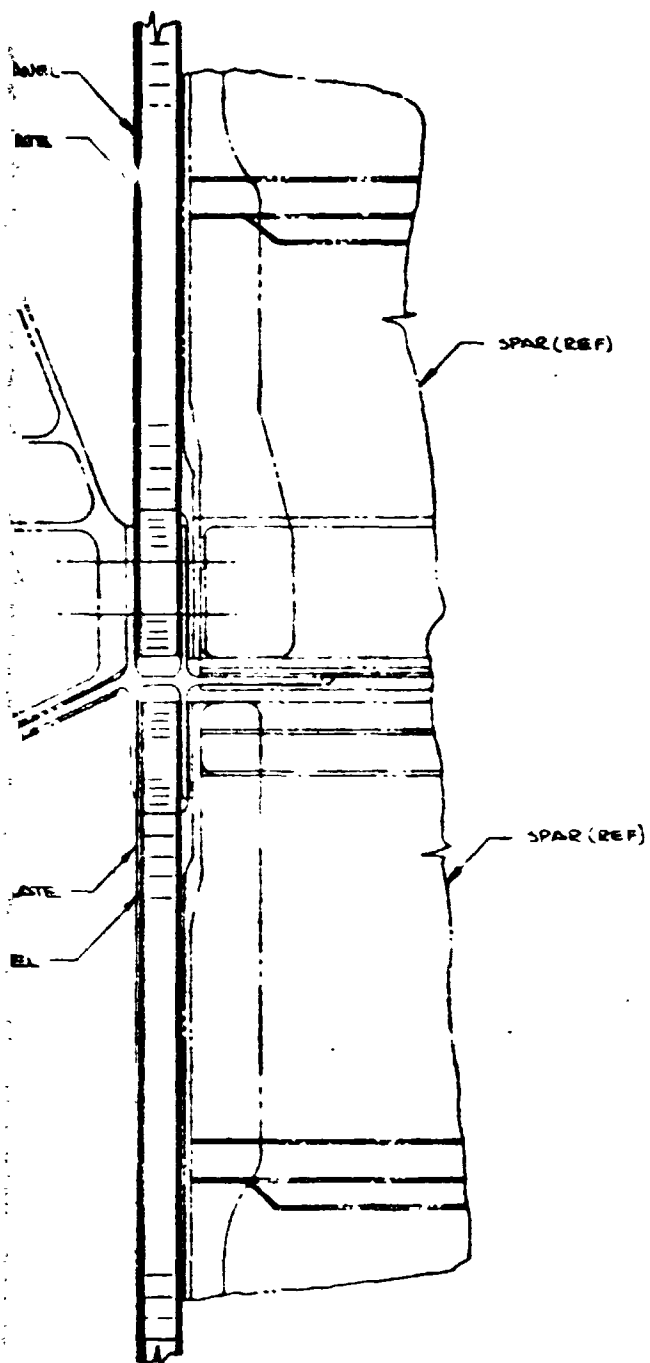
193 (060)

254 (100)

A-A

SPAR (REF)

FOLDOUT FRAME 4



FOLDOUT FRAME 6

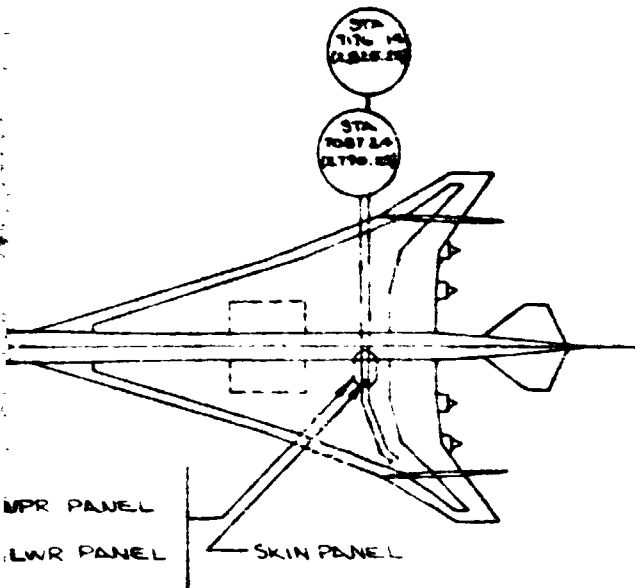


DIAGRAM
SKIN PANEL LOCATION

ALL MATERIALS TIGAL-4V

SKIN PANELS:

UPPER - BRAZED HONEYCOMB

LOWER - INTEGRALLY MACHINED AND WELDED

BASIC UNIT SYSTEM IS THE INTERNATIONAL SI SYSTEM.
ENGLISH UNIT SYSTEM EQUIVALENT VALUES ARE SHOWN
IN ().

FOLDOUT FRAME 7

SEE SHEET 1 OF PL FOR LIST OF MATERIAL, USAGE AND NOTES			
USED ON	DRAWN	DATE	THE BOEING COMPANY
	CHECKED		COMMERCIAL AIRPLANE DIVISION RENTON WASH
SECT NO.	STRESS		SKIN PANEL -
CNS NO.	ENG		AFT WING
GROUP ORG	PROJ		969-512 B MACH 2.7
			CODE IDENT NO 81205
			SIZE J AWS-138
			SCALE
			SN

Figure 5-11

PRECEDING PAGE BLANK NOT FILLED

SECTION 6

DETAILED STRUCTURAL ANALYSIS AND DESIGN

by

D. L. Grande
M. J. Turner

PRECEDING PAGE BLANK NOT FILLED

CONTENTS

	Page
DETAILED STRUCTURAL ANALYSIS AND DESIGN	244
Introduction	244
The Aeroelastic Cycle	244
Basic Structural Model	244
Mass Models	246
Aerodynamic Models	247
The Analysis and Design System	247
FLEXSTAB	249
Flutter Modules	249
Resume of Detailed Analysis and Design Task	249
Flutter Analysis and Design To Satisfy Flutter Criteria	253
REFERENCE	255

TABLES

No.		Page
6-1	A Summary of ATLAS 2.2 Capabilities	256
6-2	Boeing Program to Improve Efficiency and Reliability of Aeroelastic Loads Analysis	257

FIGURES

No.		Page
6-1	Aeroelastic Cycle	258
6-2	Mass Paneling for Flutter	259
6-3	Basic Structural Model	260
6-4	Basic Aerodynamic Model	261
6-5	Aerodynamic Paneling for Loads	262
6-6	ATLAS-An Integrated Structural Analysis and Design System	263
6-7	Wing Cover Element Subsets for Sizing	264
6-8	Effect of Design Changes to Improve Flutter Characteristics	265
6-9	Final Stiffness Design	266
6-10	Arrow Wing Flutter Boundary, 969-512B	267

SECTION 6

DETAILED STRUCTURAL ANALYSIS AND DESIGN

INTRODUCTION

The objective of the present section is to provide a general overview of the analytical and computational procedures that were used in Task II to establish an efficient distribution of structural material to satisfy strength and flutter criteria. This will include a discussion of work flow and interrelations between the various subtasks comprising the aeroelastic cycle for structural design. The computerized system that was used in performing this work will be described. This system was organized around an interim version of the ATLAS Structural Analysis and Design System, interfaced with external programs to obtain capabilities for loads and flutter analysis that had not been incorporated in the ATLAS System. A chronological account of the detailed structural analysis and design work is presented at the end of this section, with comments on problems that were encountered and on related development needs.

THE AEROELASTIC CYCLE

The major subtasks comprising the detailed structural analysis and design task and their relationships to each other are identified in figure 6-1. The task may be visualized as three interconnected discipline-oriented segments with the interconnection being provided by the ATLAS system. On the left of the figure is a group of operations associated with the prediction of steady aeroelastic loads which provide input to the strength design segment shown in the center of the figure. On the right is a group of operations associated with the flutter analysis and design to satisfy flutter criteria. The computer programs performing the various functions are shown in the upper portion of the diagram boxes.

Basic data describing the aircraft (with the exception of structural member sizes) were developed during Task I and the initial six week period of Task II. This information, comprising aircraft geometry, structural arrangement, structural concepts, and structural materials, was then used to develop structural, aerodynamic, and mass models of the aircraft and other input data to initiate the analysis and design cycle.

BASIC STRUCTURAL MODEL

One finite element model of the structure was developed as a common basis for aeroelastic loads, thermal, stress, vibration, and flutter analyses. Consistency of geometric data from design was found to be particularly critical. Geometry of an individual component was generally defined in a convenient local reference frame. Hence, particular care had to be taken in defining coordinate transformations between these local reference systems and the global system that was used in defining the assembled model of the complete structure.

Close coordination between stress, flutter, and loads specialists was required to provide a single basic model from which special purpose models could be derived to satisfy the requirements of each individual discipline. This interdisciplinary coordination is particularly important in the design of large supersonic transport aircraft that tend to be slender and very flexible, thus causing aeroelasticity to be a major design consideration. Dynamic loadings associated with flutter often exhibit distributions that are vastly different from strength-critical loadings. Hence, requirements exist for detailed representation of structural characteristics in different regions of the aircraft to satisfy requirements for stress analysis, strength design, flutter analysis, and stiffness design. Prior experience on the National SST Program provided useful background for modeling the Arrow Wing structure. Initial structural sizing to start the aeroelastic cycle was derived from the 969-336C design study, with appropriate adjustments to reflect the increase in maximum taxi gross weight to 340,194 kg (750,000 lb.). Since program constraints permitted only a single cycle of aeroelastic loads analysis it was considered necessary to develop an initial sizing to match strength requirements reasonably well. Automated resize capability had not been provided in the ATLAS System when the job had to be done. Hence, this initial sizing was performed manually. Availability of automated resize capability will make it possible to employ a crude estimate of the initial size with considerable savings of time and effort on future jobs of this kind. A description of the model and an account of model development and checkout are presented in section 7.

The structural model used in this study is shown in figure 6-2. It contains approximately 2,000 nodes, 4,200 elements, and 8,500 active degrees of freedom. For dynamic analyses, a much smaller number of degrees of freedom are retained (225 for symmetric conditions and 260 for antisymmetric conditions). These retained degrees of freedom, the important freedoms at the nodes at which the mass of the airplane will be lumped, are selected to provide the necessary accuracy of the lower mode shapes and frequencies. The complexity of the model results from (1) the use of one model for both stress and flutter analysis, and (2) the detail requirements for meaningful flutter analysis. For the wing, these requirements include structural modeling of the engine beams (allowing complete c.g. motion of the engines), leading and trailing edge controls, wing secondary structure, landing gear and wheelwell cut-out, major access doors, and wing mounted fins as well as wing primary structure. For the rest of the aircraft, they include a detailed body idealization for wing attachment and a less sophisticated model of the remaining fuselage and the empennage.

The ATLAS stiffness module uses the displacement method of finite element structural analysis to calculate a structural stiffness matrix, displacements due to applied loads, and flexibility matrices. In ATLAS, wing-like structures are modeled with mid-plane nodes having five degrees of freedom. Cover elements, either quadrilateral or triangular, are referenced to the mid-plane nodes for definition of both upper and lower surface properties. Spar properties are defined by an element that includes two caps, not necessarily of the same area, a shear web and two "rigid" posts bounding the vertical edges of the shear web. In the fuselage-wing intersection region, the fuselage is modeled with beam elements representing two "lumped" frames, axial elements for several "lumped" stringers and shear panels for the skin. The forward and aft portions of the fuselage and the empennage were modeled with beam elements. The connection between

the wing structure, modeled with mid-plane nodes, and the carry through structure in the fuselage, modeled with nodes at the wing upper and lower surface locations, was made with stiff beam elements to approximate the distribution of the spar cap loads to the fuselage structure.

The structural model was generated and initial checks made over a period of about 5 months. During this period, a maximum of three people worked on the model. About seventeen manweeks of effort were required to define and size the elements in the body. About eighteen manweeks of effort were involved in formulating the wing model, distributed equally between model definition and sizing. An additional four months were required to connect the wing and fuselage models, correct modeling errors, improve some local modeling details, make an initial flutter check, and resize part of wing structure to increase the flutter speed before strength sizing.

The length of time required for model generation and validation was caused by the small size of the study team, the use of ATLAS for the first time on a model of this size and geometric complexity, and lack of a "body" geometry package in ATLAS. While experience gained from this study and planned improvements in the ATLAS system will probably decrease both the effort and time required to generate and validate a complex structural model, it would appear that model generation should begin as soon as possible in a design study to obtain maximum benefit from an automated design system. The use of the mid-plane nodes in modeling the wing is efficient, but modeling the row of elements adjacent to the fuselage in a conventional manner would probably result in a better model by removing the stiff beam attachment. The planned inclusion in ATLAS of an analytic description of external surface geometry of the fuselage as well as the wing will make the generation of the total model much easier. The automated strength resizing capability (presently available for wing structure only) makes generation of refined element sizes unnecessary because the automated resizing capability will refine crude initial element size estimates in several executions over a period of a few days (compared to nine manweeks of manual effort), and thus cut flow time by allowing use of a less refined initial model. Graphical presentation of stresses on a model would be desirable for model checkout as well as interpretation of final results. Finally, the ability to readily extract and plot portions of the model for study of local problems is essential to correct detail modeling problems that routinely occur in finite element model generation.

MASS MODELS

Since different sets of retained freedoms describing structural deformation were required for aeroelastic loads analysis and for flutter analysis, the numbers and distributions of retained structural freedoms were different in these two analyses. Hence, it was necessary to develop two different mass models. To "lump" the masses at the retained nodes a "cookie cutter" technique was used. For this process the location of the retained node is selected and the boundaries of the space that contributes mass to this node defines a vertical prism ("cookie"). Figure 6-3 shows the retained nodes and panels used for modeling the flutter mass matrix. An external boundary as shown in the figure is required by the "PLOT GRID" ATLAS program.

AERODYNAMIC MODELS

A basic aerodynamic model consists of the loft definition, illustrated in figure 6-4, that is usually produced in the computer. The contours of this loft define the envelope of the airframe that is used for subsequent aerodynamic analyses. This loft is used to produce the geometrical description of the surfaces of the airplane, and the associated slopes for use in the steady state loads analyses, as described later. These panels are illustrated in figure 6-5. A different aerodynamic idealization is used for generating unsteady airloads for the flutter analysis. This requires the geometric definition of the lifting surface planforms, with a specified set of downwash points subsonically, or a Mach box grid for each supersonic Mach number. The magnitude and phase angle of the unsteady pressures at each point on the wing surface are dependent on the frequency and mode shape in which the wing is vibrating. These local pressures are calculated and integrated over the aerodynamic surfaces to yield generalized aerodynamic forces in each degree of freedom for use in the flutter analysis. Section 11 describes the calculation of these air forces in detail.

Although different aerodynamic models of the aircraft were employed for loads and flutter analysis, this did not present a serious problem. Required geometric data were provided as part of the job input data for loads and flutter analyses. These matters are discussed more fully in sections 8 and 11.

THE ANALYSIS AND DESIGN SYSTEM

ATLAS is an integrated structural analysis and design system operational on the Control Data Corporation (CDC) 6600/CYBER computers. It is a modular system of computer codes, controlled by one executive module and with a common data base. The analysis of the Arrow Wing conducted during Task II used a preliminary version of ATLAS designated 2.2. Hence, the system description that follows reports an evolving capability as it existed during Task II of the Arrow Wing study. The ATLAS system's capabilities are broad in scope, supporting analyses in many different but related aeroelastic technologies. Execution of modules is controlled by the user via a concise and powerful technically-oriented language. Input data are written in a problem-oriented language which provides versatile automatic data generating capabilities. Additionally, the various data preprocessors provide capabilities to reduce the amount of input data and flowtime required to define the structural problem. Data postprocessors allow selected data to be extracted, manipulated and displayed to facilitate the evaluation of either input data or analysis results.

The ATLAS problem size limitations for non-substructured stiffness and mass models are:

Number of stiffness nodes	4,095
Number of stiffness elements	32,767
Number of loadcases	4,095
Number of mass nodes	4,095
Number of mass elements	32,767
Number of mass conditions	200

Problems generally become critical for bulk storage or hardware reliability before these limitations are reached. For substructured stiffness and mass models, there are no practical limits to the total problem size.

There are two basic types of modules in the ATLAS system: executive modules and computational modules. There are two executive modules, ATLAS(0,0) and Control. ATLAS(0,0) monitors the job execution. Control, which is generated by the user, performs such functions as selecting the sequence of computations, selecting analysis results to be displayed and handling of execution. In general, the Control module is generated from the control deck at execution time by the precompilers and compilers.

Computational modules are grouped into three types according to their function:

- Preprocessors read, decode, generate and interrogate the input data or load data for a restarted job;
- Processors perform technical, analytical computations in the following disciplines:
 - Stiffness
 - Weights
 - Design
 - Linear matrix algebra
- Postprocessors extract and display input data or analysis results and save data for a later restart of the job

Table 6-1 provides a summary of the capabilities of the ATLAS 2.2 system used during Arrow Wing Task II. The table is divided into three sections representing the Executive, Technical and Pre- and Postprocessor modules.

Data required to define the mathematical model were supplied in the problem deck. These data were read and formatted by the preprocessors and stored in the data base and transmission of data from one module to another was accomplished primarily by the use of named random-access files. Data on a random-access file are organized into matrices which are accessed as a unit. Management of all internal data is automatic. A more extensive description of the system is available in reference 6-1 and the general system architecture is shown in figure 6-6.

As a supplement to the capabilities contained within the ATLAS system, interfaces with the FLEXSTAB system were developed. Symmetrical and antisymmetrical flexibility matrices for use in the FLEXSTAB loads analysis were generated in ATLAS. The external structural influence coefficient program, ESIC, in FLEXSTAB takes these flexibility matrices, nodal geometry for the retained nodes and the mass matrices generated by ATLAS as input data. These data are transmitted on magnetic tape through the ATLAS-FLEXSTAB interface subroutine within ATLAS.

FLEXSTAB

FLEXSTAB is a system of programs developed by Boeing under contract NAS2-5006 to NASA Ames Research Center. It was designed to predict the stability characteristics of flexible airplanes based on the geometry, mass distribution and flexibility of the airframe, using linear aerodynamic and structural theories. Although not principally designed as a loads analysis tool, FLEXSTAB generates sufficient information in the process of performing a stability analysis, that its extension for use in loads analysis was a fairly simple task.

In preparation for the Arrow Wing contract, a Boeing development effort was directed at producing a version of FLEXSTAB that would produce design loads. The changes and additions made to FLEXSTAB during this time are shown in table 6-2. These changes were subsequently incorporated in the NASA version of FLEXSTAB 1.2.

The modifications to FLEXSTAB were carried out with two major purposes in mind—improved program efficiency and improved analytical capability—and table 6-2 identifies in which of these categories the various changes fall.

FLUTTER MODULES

As indicated in figure 6-1, the flutter modules were also linked to the ATLAS system through a tape interface. Modal data, flexibility matrices, and mass matrices were transmitted from ATLAS to the flutter modules. RHO III was used to calculate unsteady aerodynamic loadings caused by motions of lifting surfaces based on the subsonic kernel function approach, utilizing the modal data supplied by ATLAS. These loadings were then used to calculate generalized aerodynamic airforces for use in subsonic flutter analysis. Similar airload calculations for supersonic flutter analysis were obtained from the Mach Box program. Generalized aerodynamic force matrices, together with generalized mass and stiffness matrices from ATLAS, were incorporated in the flutter equations and solved to define the flutter stability envelope by utilization of TV-133. This is a V-g solution program based on the QR algorithm.

RESUME OF DETAILED ANALYSIS AND DESIGN TASK

Detailed analysis and design of the Arrow Wing structure was initiated on September 17, 1973, following completion of configuration development work. The final flutter analysis (following redesign to satisfy flutter criteria) was completed in January 1975. Expenditures during that period totalled 28,000 manhours of engineering effort and approximately \$100,000 for computing. A brief chronological account of this work is presented in the remainder of this section.

PRELIMINARY FLUTTER ANALYSIS AND STIFFNESS RESIZE

Approximately four months were spent in defining the structural model and initial sizing. After initial sizing to modified 969-336C loads, mass and stiffness matrices were calculated for a preliminary flutter analysis. Also, a flexibility matrix was generated for model checkout purposes. As a result of initial assessment of flexibilities and

preliminary vibration mode analyses, it was decided on the basis of previous experience to increase stiffness in three areas prior to initiation of the aeroelastic loads analysis. Spars and covers of the main wing box outboard of the wing mounted fin were doubled, the low speed aileron cover thickness quadrupled to minimize wind-up relative to the inboard location of the actuators and the nacelle support beams were stiffened by a factor of 1.5. Furthermore, the vibration analysis revealed an unacceptable low frequency resonance of the main landing gear in the stowed position. This problem was eliminated by stiffening the uplock beam and modifying the adjacent local structure.

A preliminary subsonic flutter analysis was performed for the following conditions of the structural model:

1. As initially sized to modified 969-336C loads;
2. As revised for static aeroelastic loads analysis;
3. With further increase in engine beam stiffness to 4.5 times the initial value.

The flutter speed with initial sizing was about 300 knots EAS below the design requirement, 504 knots at $M = .90$. Small improvement was achieved from Condition 2. A substantial increase in flutter speed, about 200 knots, was obtained from Condition 3.

The objectives of this preliminary flutter analysis were to provide an early check of the flutter analysis system and to obtain information that should be useful in understanding the flutter characteristics of the strength design and in developing modifications to correct the flutter deficiencies that were expected. The preliminary flutter analysis and stiffness resize were accomplished during a three month period beginning in February 1974.

LOADS ANALYSIS

The selection of loads conditions for analysis was based on the requirements of the Federal Aviation Regulations, Part 25, and the Tentative Airworthiness Standards for Supersonic Transports. Loads analysis experience on the National SST program and on the previous NASA Boeing study of the 969-336C configuration was used as the basis for selecting design conditions.

The lateral gust loads were computed using the approach embodied in the FAR gust load formula, the rudder maneuver loads in compliance with FAR 25.351(a), and the ground handling loads in compliance with FAR 25.471 through 25.509. The landing impact loads, which are critical only for the forward body, were computed on the basis of the acceleration levels obtained in the dynamic analysis of landing impact for the National SST Program.

Prior to the aeroelastic loads analysis, considerable effort went into planning and checkout of the FLEXSTAB analysis. This included the development of the paralling scheme for airload analysis and selection of the freedoms to be retained in the structural model organization and preliminary check runs on the computer. A

structural model with 164 retained nodes and 192 degrees of freedom was selected from the complete structural mathematical model. Close coordination between stress and loads engineers is particularly important at this stage of the analysis to insure that the retained freedom set is sufficiently inclusive, so that all the loads required for stress analysis will be available from the FLEXSTAB run. A component of a load vector acting on a structural node can be obtained from the FLEXSTAB analysis only if the corresponding nodal displacement is one of the retained freedoms.

Aeroelastic loads analysis, utilizing the ATLAS FLEXSTAB System, began in the latter part of April 1974, when revised mass and stiffness matrices, reflecting the preliminary stiffness resize, was obtained from ATLAS. Results from symmetrical flight load analyses were obtained in June and loads due to lateral gusts, rudder maneuvers, ground handling, and landing impact were obtained in July 1974. However, in computing loads and preparing for the stress analysis the following problems were encountered at this time, delaying the automated resize of wing structure by about two months:

1. Lateral wing inertia forces were omitted from antisymmetric flight loads due to the omission of the corresponding retained freedoms.
2. A program addition was required for superposition of symmetric and antisymmetric components to obtain asymmetric load distributions on the half-airplane model.
3. Panel airloads in the wheelwell area were applied at a node without adequate structural backup, requiring redistribution.
4. Allowables data for ATLAS resize modules required additional work.
5. Incompatibility between wing and body displacements was found at the side of the body. Additional stiffness was required in the load transfer members joining wing mid-plane nodes to upper and lower wing nodes.

Results of the loads analysis were transmitted to the ATLAS data bank via the FLEXSTAB ATLAS interface for use in stress analysis and design operations. A detailed account of the loads analysis work is presented in section 8.

STRENGTH DESIGN

The strength design required evaluation of; (1) the stresses due to the various load conditions, (2) the relation between the imposed and allowable stresses (margins of safety), and (3) structural member size changes necessary to obtain the desired value of the margins of safety.

The stability interaction equation used for evaluation of margins of safety in biaxial compression and shear in the honeycomb sandwich wing covers is:

$$R = \left[\frac{R_x}{1 - R_{xy}} \right]^4 + \left[\frac{R_y}{1 - R_{xy}} \right]^4$$

where R_x , R_y , R_{xy} , are the ratios of the actual to allowable inplane load for the axial and shear loads. For strength critical loading conditions, a modified Hill's yield criterion was used. The influence of temperature on elastic moduli and allowable stresses was included in the analysis.

Structural elements were resized using a fully stressed design algorithm to obtain new sizes. Elements in the fuselage were resized by hand and the resizing process for these elements converged in two cycles. Since lumped areas used in model beam elements in the fuselage are composed in part of effective skin areas and these are influenced by buckling, body pressurization and thermal stresses, iterative procedures were employed in resizing these elements. Automated resizing of the fuselage elements was not attempted because of the more difficult problem posed by buckled skins and the smaller structural weight savings expected in the fuselage.

Elements in the wing covers were resized using an automated resizing module with convergence, as measured by total mass change, occurring in three cycles. The resizing module uses the interaction equation given above, and an iterative solution technique. Margins of safety were calculated considering stability, material strength (or allowable stress level), and fail safety for multiple load cases. The loading components included membrane stress resultants due to overall load condition, local pressure loading, thermal and acoustic environment. Elements were grouped in sets as shown in figure 6-7 to allow imposition of common constraints such as minimum face sheet thickness, constant honeycomb core height, and stability data. Constraints between element types, such as maintaining cap areas of at least one-quarter of the area of the largest adjacent panel for fail-safety, were manually imposed between resize cycles. The calculation of allowables, stability allowables in particular, requires considerable effort, but this effort can be expended during the earlier stages of the design, i.e., concurrently with model development.

In this case, a strength analysis of the complete aircraft and automated resizing of the wing elements could be accomplished in an overnight computer run while the manual resizing of fuselage structure required three additional manweeks of effort. Thus, automated strength-resizing capability can reduce total design cycle time, by reducing the time required for one of the sequential tasks (strength-resizing), required in the design cycle.

On completion of the strength resize, new stiffness and mass matrices and a new set of vibration modes were generated in ATLAS. These were then transmitted to the flutter modules via the tape interface for initiation of final flutter analysis and redesign to satisfy flutter criteria.

Stress analysis and redesign for strength are reported in section 10 and a detailed account of the structural thermal analysis is presented in section 9.

FLUTTER ANALYSIS AND DESIGN TO SATISFY FLUTTER CRITERIA

Flutter analysis of the strength designed structure began in mid-November 1974. A generalized coordinate approach was used in formulating the equations of motion for wing flutter analysis, with a truncated set of vibration modes, the first 18, and the relevant rigid-body modes as degrees of freedom. Equations of motion were developed for the half-airplane with appropriate boundary conditions in the plane of symmetry for separate treatment of symmetric and antisymmetric cases. The free-free vibration modes were computed within the ATLAS system, utilizing a reduced finite-element stiffness matrix (with 225 symmetric and 260 antisymmetric freedoms for the half-airplane) and a lumped mass inertia matrix. Subsonic kernel function and supersonic Mach box versions of unsteady lifting surface theory were used in the calculations of generalized aerodynamic forces. A classical V-g solution technique, based on the QR algorithm, was used in solving the complex eigenvalue problem. The flutter analysis is described in detail in section 11. The following paragraphs describe the general approach to the analysis and the major results for the purpose of illustrating to the reader the magnitude of the effort, and the usefulness of the integrated analysis system.

STIFFNESS REDESIGN

The flutter analysis was conducted only for the symmetrical heavy gross weight condition since this is the most critical condition. The analysis showed a very low flutter speed due primarily to the flexibility of the engine support beams, the control surfaces, and the wing mounted fin.

Supplementary calculations, based on energy balance concepts at neutral stability were employed for diagnostic purposes to identify essential degrees of freedom in the critical flutter mode. Essentially, this involves an analysis of the work per cycle contributed by the coupling terms of the aerodynamic force matrix. This information, together with frequency coalescence trends from the flutter solution, provided useful guidance with regard to needed changes in modal frequencies to increase flutter speeds. Engineering judgment, based on experience on the National SST program was used in defining structural design changes to meet flutter criteria. The starting point for stiffness redesign was the strength designed structure; no reductions in areas or member sizes below the values specified for strength, were allowed.

The initial stiffness modification to the strength sized structure consisted of increasing the stiffnesses of nacelle support beams to 4.5 times the initial value, increasing the low speed aileron cover thickness by a factor of 4.0, doubling the spar and wing cover thicknesses outboard of the wing mounted fin, and adding high speed control locks for the low-speed aileron and outboard flaperon. The effect of this change is illustrated as change number 1 in figure 6-8. Subsequently, a number of stiffness design changes were tried to achieve the greatest improvement in flutter speed for the minimum weight. These are also shown in figure 6-8, and are described in detail in section 11. The final stiffness design is change number 9 in figure 6-8, and is defined in detail in figure 6-9. It should be pointed out that the final stiffness modification also includes a change in the wing thickness in the outboard region. The discontinuity in the airfoil shape at the

fin station was removed, and the thickness ratio at the fin station was increased from 2.8% to 3.5%, with the increment decreasing linearly to zero at the wing tip and the outboard nacelle station. A complete analysis of the final configuration was conducted for symmetric and antisymmetric flutter at low and high gross weight conditions for subsonic and supersonic Mach numbers. The results of the final analysis are summarized in figure 6-10.

RESULTS

The mass increment above strength design associated with the final stiffness design changes shown in figure 6-9 and the wingtip thickening is 4640 kg (10,220 lb) per aircraft, including the mass equivalence of the drag increase due to thickening the wing tip. It was concluded that further effort to increase the flutter speed by structural changes based on engineering judgment would produce an unrealistically high weight penalty. Hence, the subsonic dive placard was reduced by 50 knots, imposing a range decrease of 46 km (25 nm) with fixed fuel loading, or an increase of 600 kg (1,300 lb) in fuel loading for constant range. Undoubtedly a significant saving and/or a higher placard could be achieved by utilizing a formal optimization technique. However, that approach could not be implemented within the scope of the arrow wing study.

The advantages gained from using an integrated system for flutter analysis may be determined from a comparison between this recent experience in flutter analysis and redesign to satisfy flutter criteria for an Arrow Wing configuration and similar experience on the National SST program. During the final two or three years of the National SST program, finite element methods of structural analysis and lifting surface aerodynamic theory were being used with a mathematical model of the structure comparable in complexity to the Arrow Wing model. However, the load, mass, stress, resize, vibration, and flutter analysis programs were not combined in an integrated system. Consequently, a great deal of manual data processing was involved in accomplishing a single structural analysis and design cycle. In that environment, approximately 3 to 4 months were required after the external loads were defined to determine strength sizing, develop flexibility and mass matrices, and complete a flutter analysis. Subsequent cycles to evaluate the effect of an extensive change in structural sizing required 4 to 6 weeks to redefine flexibility and mass matrices and conduct a new flutter analysis.

In the present study, approximately 2 weeks were spent in developing and verifying flexibility and mass matrices and conducting the flutter analysis for the critical subsonic condition after the initial structural sizing had been defined. Subsequent cycles to evaluate stiffness changes were accomplished generally within 2 days, including revisions of flexibility and mass matrices and flutter analysis. Analysis of the final configuration symmetric and antisymmetric flutter at high and low gross weights for subsonic and supersonic conditions, was accomplished in two weeks. Three engineers were involved in performing the work in this study, whereas an average of approximately 3 times this number were required to perform comparable work on the National SST program. The computer resources used in performing the Arrow Wing flutter work were also substantially less than required for similar work on the earlier project, even though substructuring was not available in ATLAS.

Evaluation of the flutter analysis and design effort in this study and comparisons with similar efforts in the National SST program, provide the following observations. The primary advantage of the ATLAS system in flutter analysis and design is the reduction in resources and cycle time to perform a flutter analysis. This improved efficiency in flutter analysis makes possible early application of the capability and thus permits stiffness requirements to be imposed earlier in the design cycle which prevents unnecessary strength resizing of stiffness critical structure. The addition of substructuring is desirable to further improve flutter analysis efficiency. Finally, the method of resizing for flutter based on engineering judgment used in this study may be acceptable for a design study such as this, but for actual aircraft design, an automated flutter resizing capability is highly desirable.

REFERENCE

- 6-1 Dreisbach, R. L., *ATLAS-An Integrated Structural Analysis and Design System, User's Manual-Input and Execution Data, (ATLAS 3.0)*, Boeing Commercial Airplane Co., December 1974.

Table 6-1.—A Summary of ATLAS 2.2 Capabilities

Module	Function
ATLAS (0,0) Control	Initializes loading of module overlays, and closes system data files. Defines the sequence of execution of modules.
Aerodynamics	Generates aerodynamic influence coefficients using two-dimensional linearized potential flow theory for general planar surfaces.
Design	Calculates margins of safety, and resizes the structure using a fully-stressed approach.
Airloads	Generates steady-state loads using AIC's from "AERODYNAMICS," mass matrices from "MASS," and flexibility matrix from "STIFFNESS."
Loads	Prepares finite element static and thermal loads.
Mass	Generates finite element mass matrices for primary and secondary structure, fuel, and payload.
Stiffness	Generates the finite element stiffness and stress matrices.
Stress	Calculates the finite element stresses.
Interpolation	Establishes mode shape interpolation functions to be used by the airload generators.
Vibration	Calculates frequencies and mode shapes of a structure undergoing free, undamped vibrations.
Preprocessor	Reads the ATLAS Problem Deck, and loads the restart tape.
Plot	Prepares SC4020, Gerber, and Calcomp plot data.
Report	Prepares printed reports of results generated by technical and utility modules.
Output	Saves all problem data on a checkpoint file to enable subsequent problem restart.

Table 6-2.—Boeing Program to Improve Efficiency and Reliability of Aeroelastic Loads Analysis

	Reason for modification	
	Improved efficiency	Improved capability
Addition of cycling capability for balanced maneuvers or unit solutions For unit solutions on $\alpha, \beta, q, \dot{\theta}, \dot{\phi}, \dot{\psi}, \delta_E, \delta_R, \delta_A, V_{TAS}, \text{THRUST},$ ALTITUDE and ATTITUDE For balanced maneuvers on: $n, q, \dot{\theta}, V_{TAS}, U_{de}, \text{THRUST and ALTITUDE}$	●	●
Added capability to generate rigid and flexible solutions in one computer run	●	
Capability to select the degrees of freedom retained at the structural nodes	●	●
Addition of static gust solution based on the revised gust load formula		●
Addition of the capability to superimpose an externally generated pressure distribution on that computed by SD&SS** (nacelles, for example)		●
Added capability to generate in SD&SS the airloads and the inertia loads at the nodes separately		●
Added capability to specify load factor rather than pitch rate for balanced maneuvers	●	●
Added capability to put user-specified matrices on the SD&SS output tape		●
Print out the equivalent airspeed and C_{N_α} in SD&SS		●
Develop interfaces: ATLAS \rightarrow FLEXSTAB and FLEXSTAB \rightarrow ATLAS	●	
*Develop a program (VAMAT) providing the capability to generate net shear, moment, and torsion along wing, body, and horizontal tail in user-specified cross sections (using SD&SS tape output)		●
*Develop a program (VMTSCM) providing the capability to scan through the loads and select critical loads	●	●
*Develop a plotting program providing plots of shear, moment, and torsion along wing, body, and horizontal tail	●	●

*These programs are not part of the FLEXSTAB program

**Stability derivatives and static stability

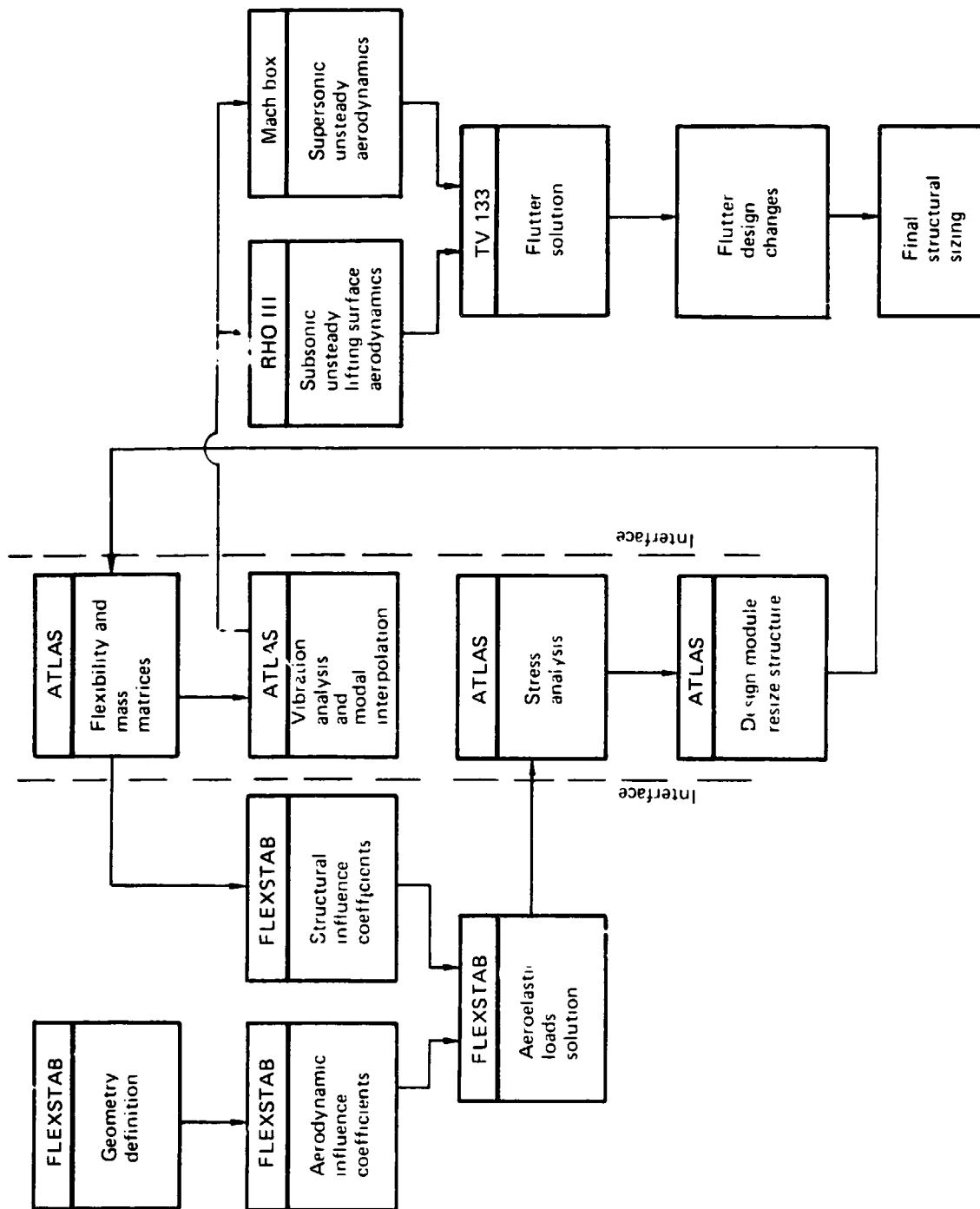


Figure 6-1.—Aeroelastic Cycle

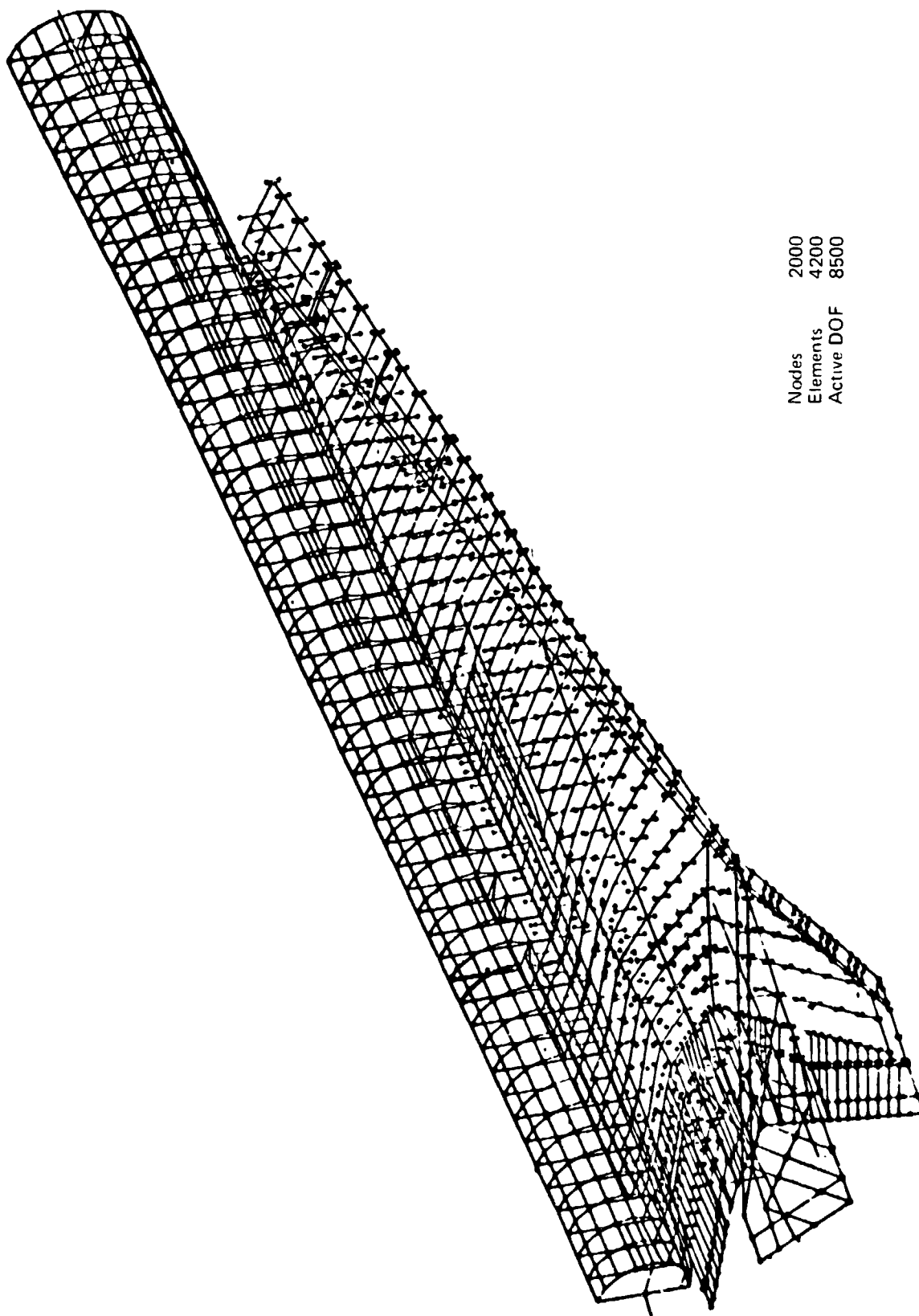


Figure 6-2. --Basic Structural Model

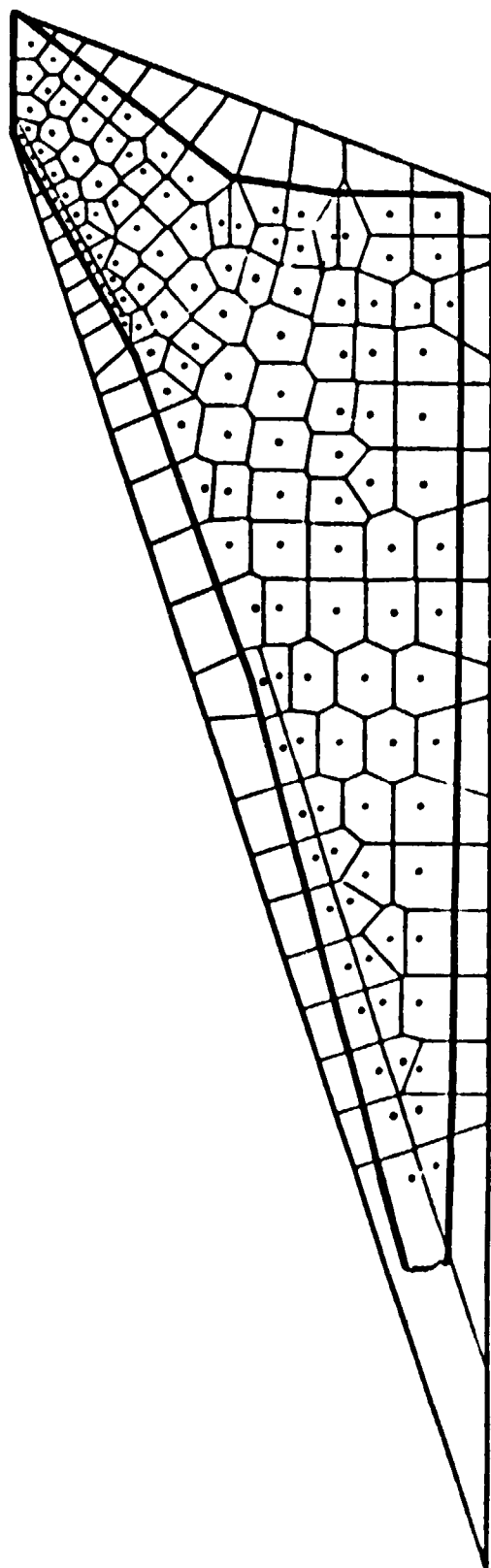


Figure 6-3. -- Mass Paneling for Flutter

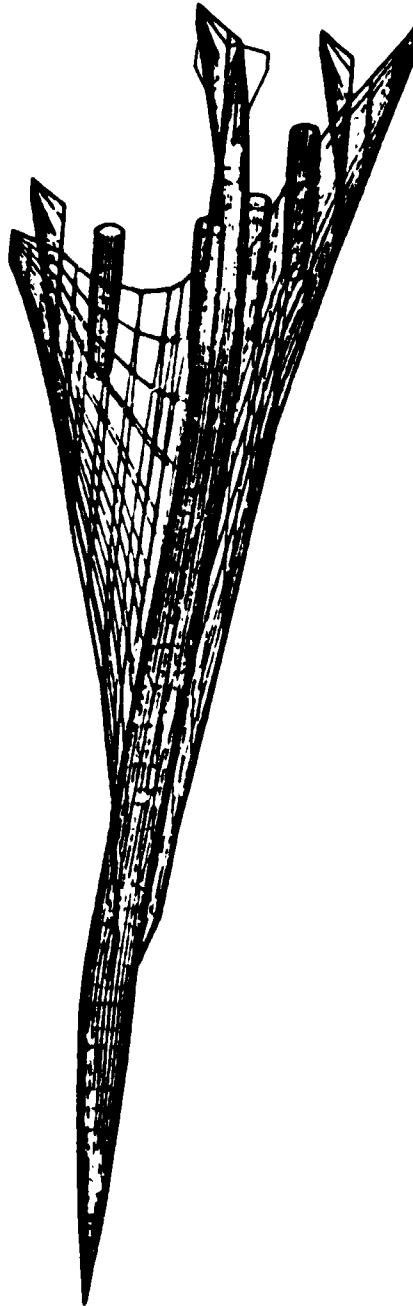


Figure 6-4. —Basic Aerodynamic Model

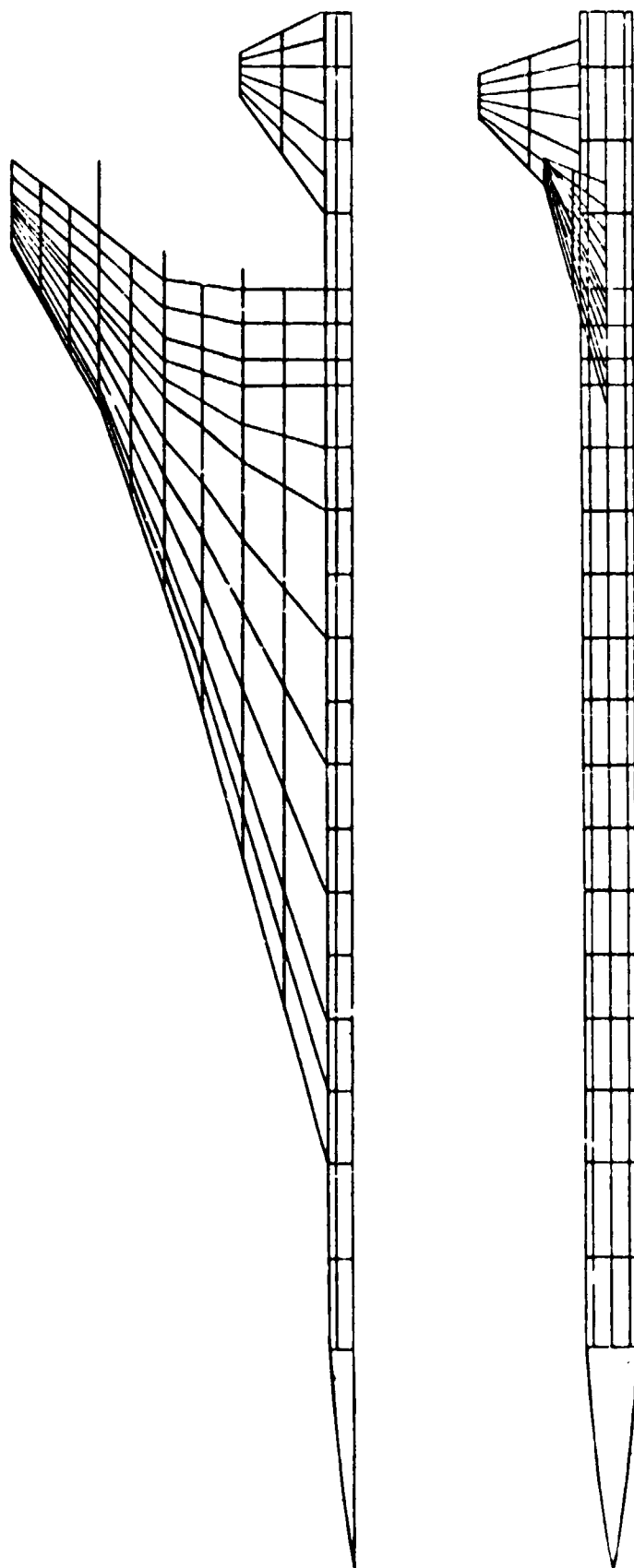


Figure 6-5.—Aerodynamic Paneling for Loads

Version 2.2

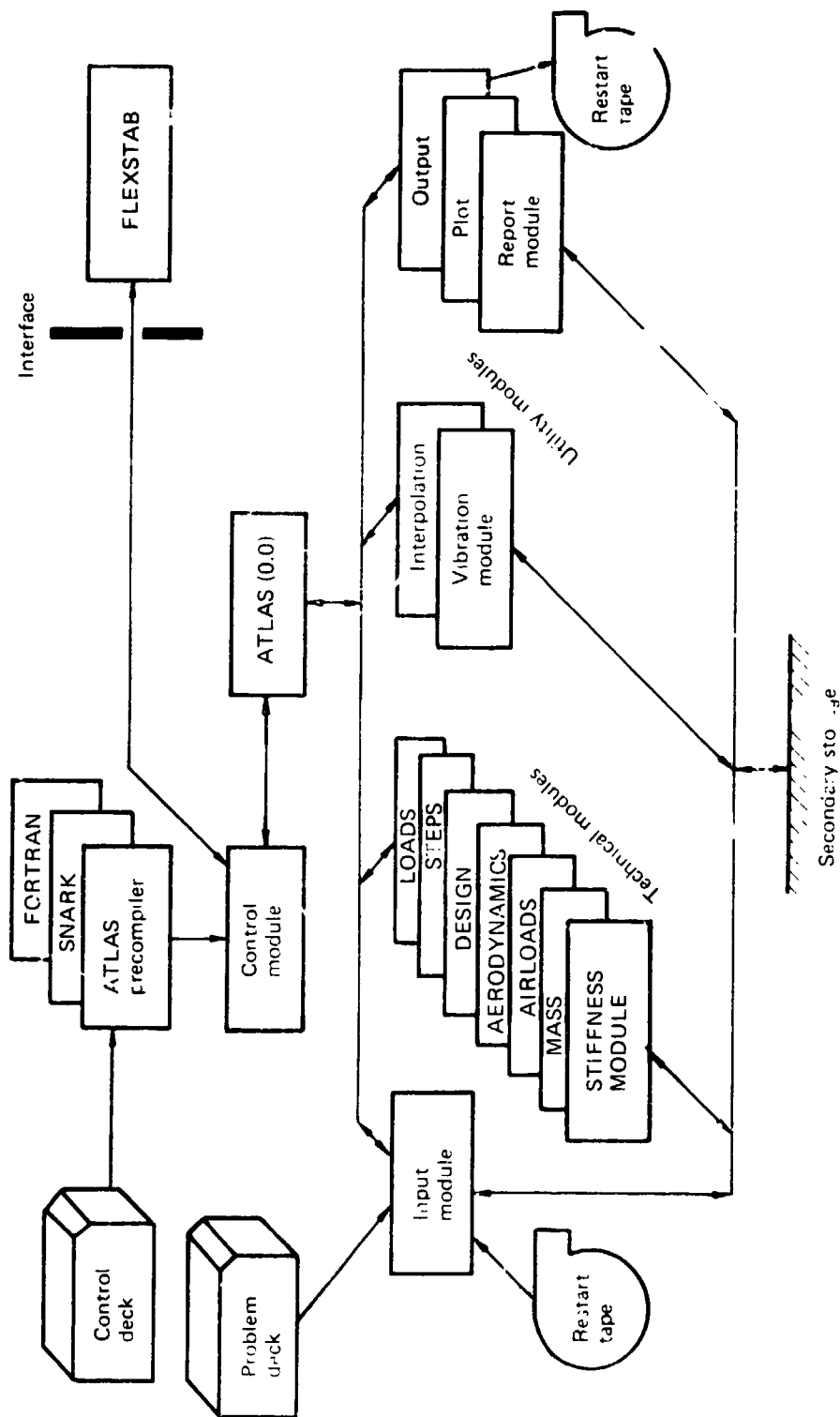


Figure 5-6.—ATLAS—An Integrated Structural Analysis and Design System

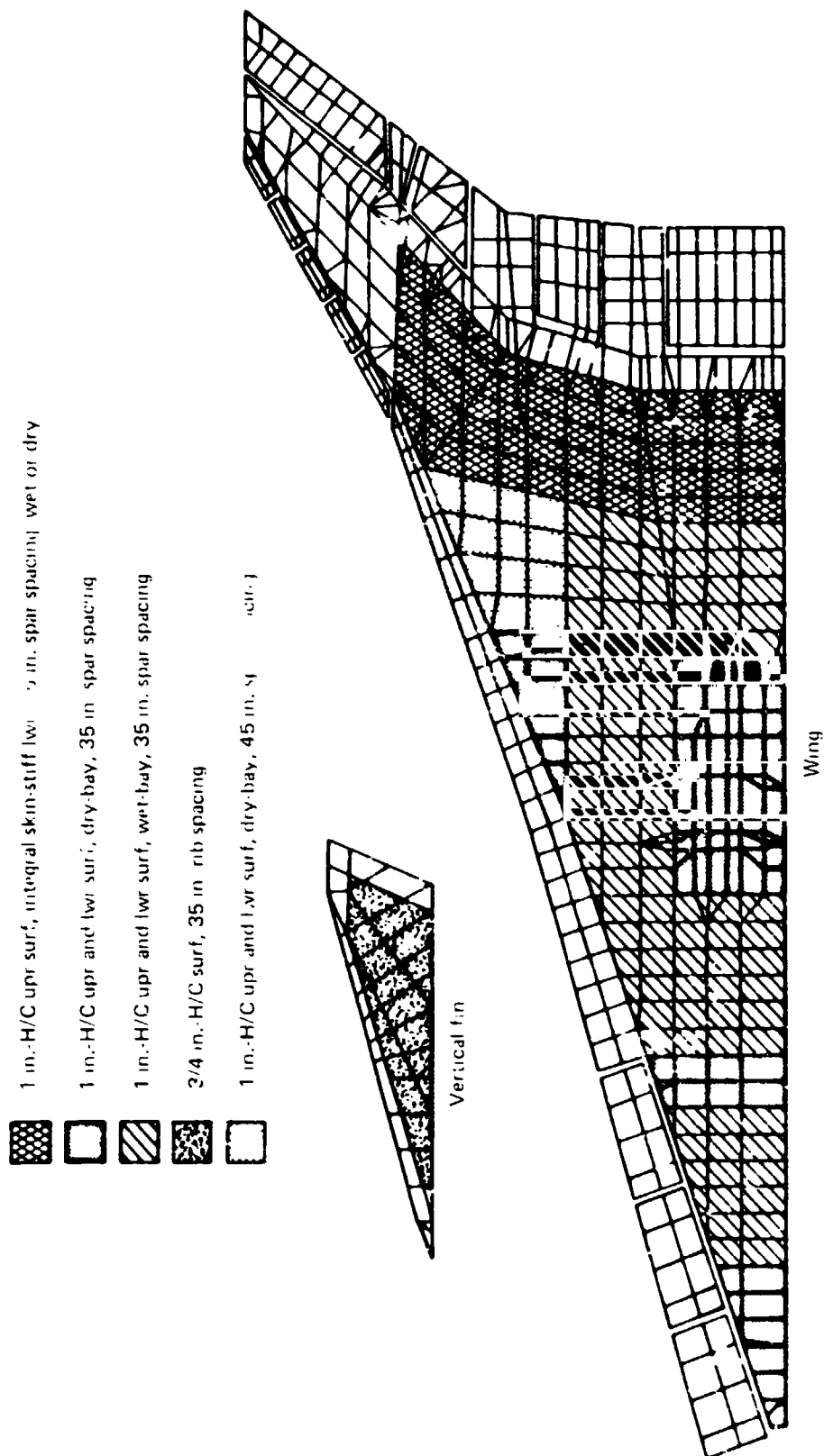


Figure 6-7.—Wing Cover Element Subsets for Sizing

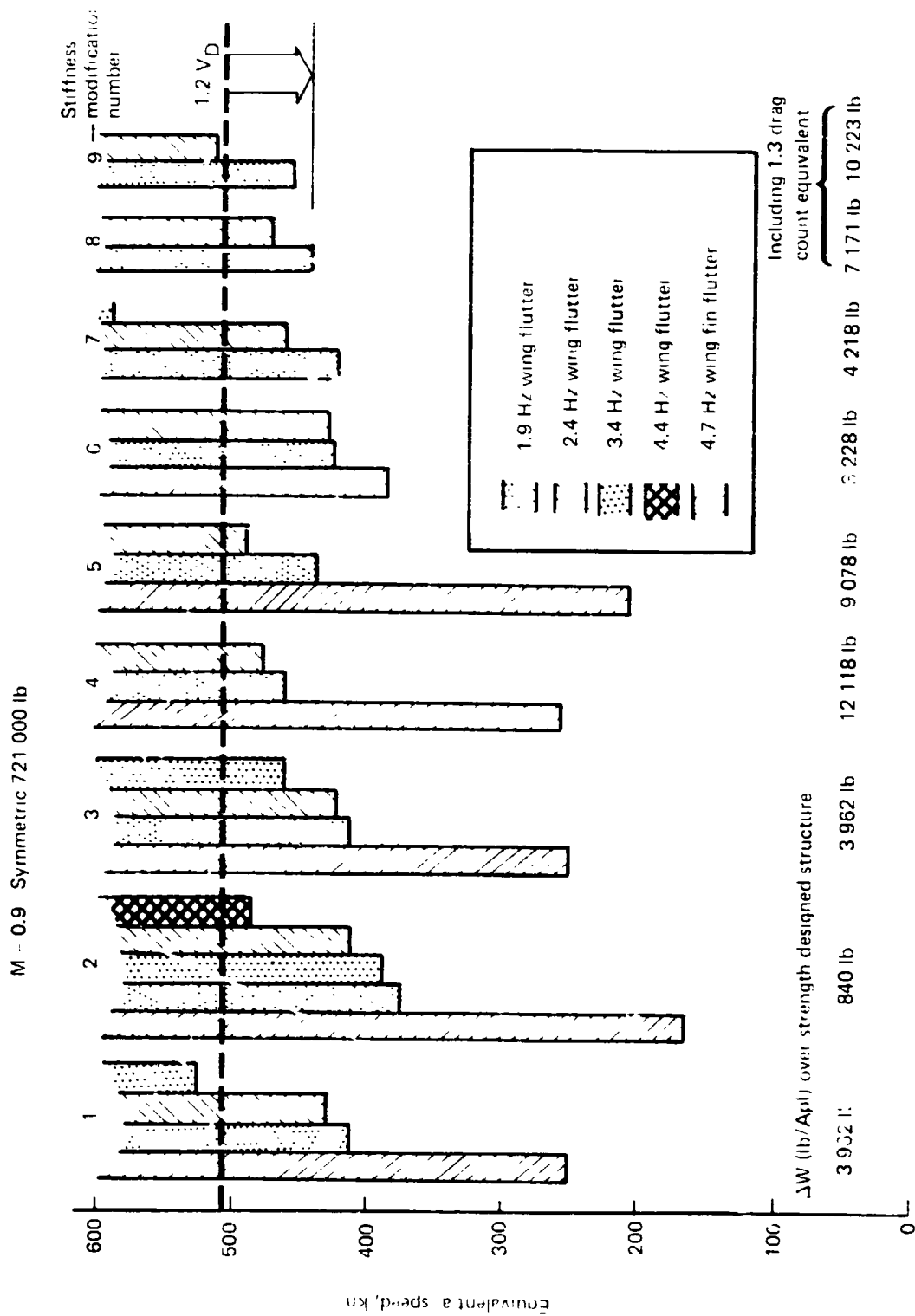


Figure 6-8 — Effect of Design Changes to Improve Flutter Characteristics

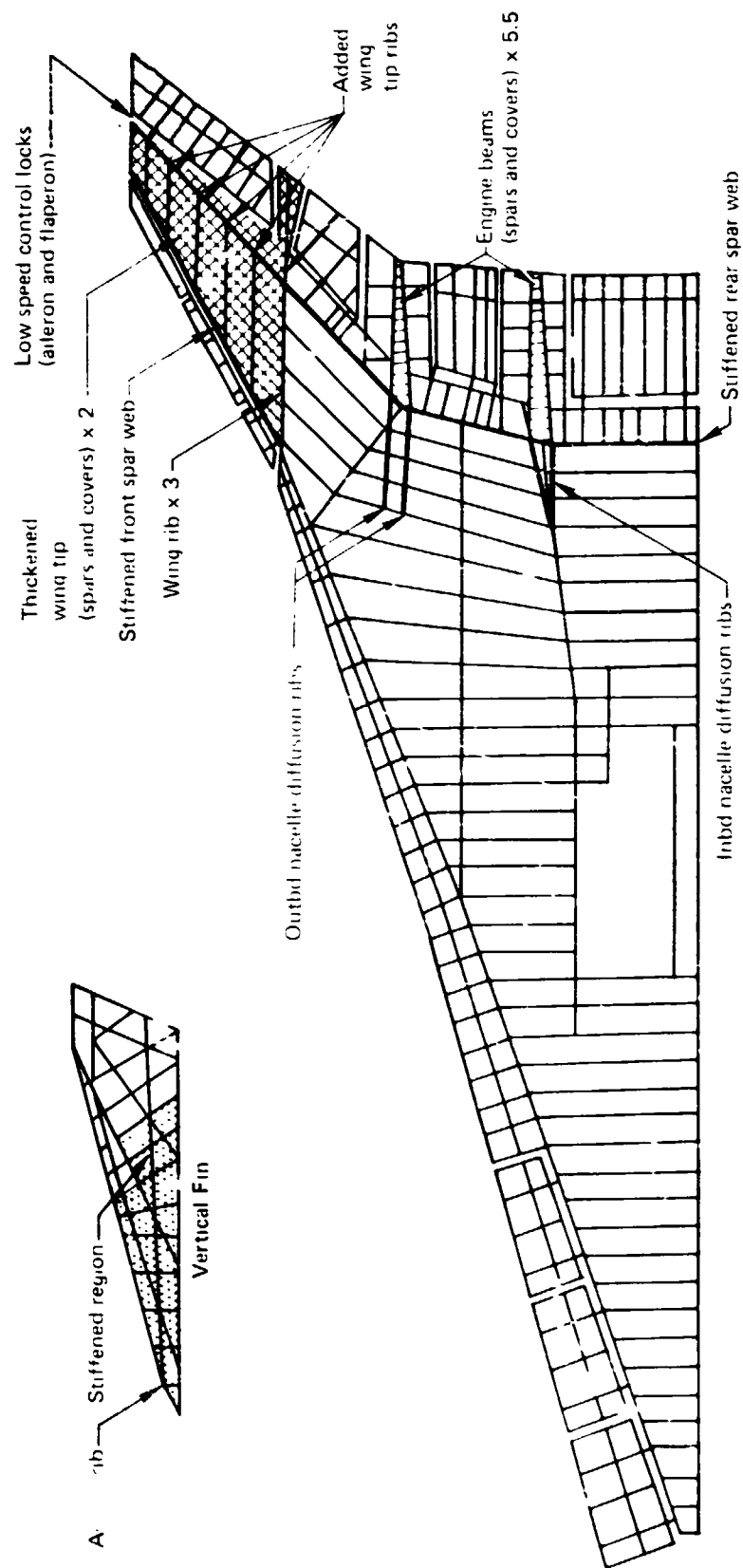


Figure 6-9. — Final Stiffness Design
(Modification 9)

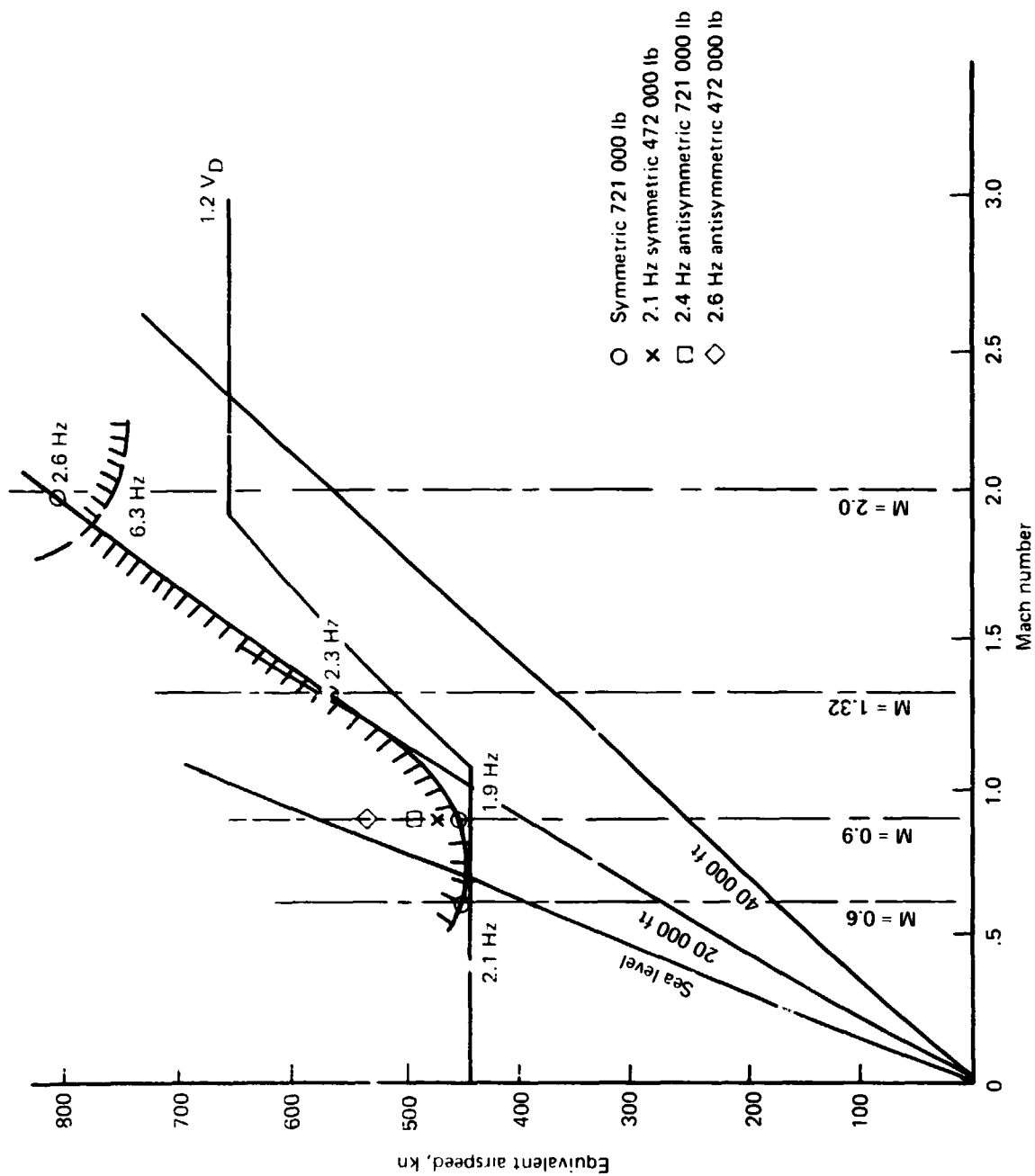


Figure 6-10.—Arrow Wing Flutter Boundary, 969-5128

SECTION 7

STRUCTURAL MODELING

by

J. G. Lelong
C. R. Pratt-Barlow
V. D. Bess
F. D. Flood

~~PRECEDING PAGE BLANK NOT FILMED~~

CONTENTS

	Page
STRUCTURAL MODELING	273
Introduction	273
Geometry and Coordinate Systems	274
Idealization of Wing and Body structure	274
Structural Model Checkout	278
Model Revisions for Aeroelastic Cycle	279
Development Task/Time and Model Utilization	280
Final Definition of Structural Model	280

TABLES

No.	Page
7-1	281

FIGURES

No.	Page
7-1	283
7-2	284
7-3	285
7-4	286
7-5	287
6	288
7	289
7-8	290
7-9	291
7-10	292
7-11	293
7-12	294
7-13	295
7-14	296
7-15	297
7-16	298
7-17	299
7-18	300
7-19	301
7-20	302
7-21	303
7-22	304
7-23	305
7-24	306
7-25	307
7-26	308
7-27	309
7-28	310
7-29	311
7	312

FIGURES (CONCLUDED)

No.		Page
7-31	Region 2 Cover Elements	313
7-32	Region 2 Spar and Beam Elements	314
7-33	Region 3 Cover Elements	315
7-34	Region 3 Spar and Beam Elements	316
7-35	Region 4 Cover Elements	317
7-36	Region 4 Spar and Beam Elements	318
7-37	Wing Fin Cover and G-Plate Elements	319
7-38	Wing Fin Spar and Beam Elements	320
7-39	Body Finite Elements, Wheelwell and Aft	321
7-40	Body Finite Elements Forward of Wheelwell	322

SECTION 7

STRUCTURAL MODELING

INTRODUCTION

One basic finite-element structural model of the Arrow Wing was developed utilizing the ATLAS Program System. This model, developed as the basic source of structural data, satisfies the requirements of loads, stress, and flutter analyses in the aeroelastic cycle. During the national SST program, it was found that a number of details were very influential on the flutter sensitivity of the SST wing. Details such as flexible wing leading and trailing edges, engine mount flexibility, stiffness of control surface actuators, etc., were significant to the flutter evaluation, and this sensitivity was verified by flutter model wind tunnel test. It was, therefore, the flutter requirements that dictated the level of detail in the mathematical model of the Arrow Wing.

Effects of camber changes are particularly important in flutter of thin low aspect ratio wings. Figure 7-1 shows that detailed simulation of flexible leading and trailing edge structure produced a substantial degradation of the calculated flutter speed of the National SST prototype. Flutter boundaries were also very sensitive to nacelle support beam flexibility. Figure 7-2 shows the low flutter speed that existed subsonically for strength-designed nacelle support beams, and the effect of flexibility of the outboard beam. Symmetric flutter could be eliminated by softening this beam. Unfortunately, antisymmetric flutter became critical with softer engine beams and dynamic load problems also proved intractable. Therefore the decision was made to stiffen the nacelle support beams to 32,000 lb./inch outboard and 24,000 lb./inch inboard.

Figure 7-3 shows the requirements imposed on the Arrow Wing Task II structural model, gained from prior experience in the analysis of large, low aspect ratio wings. These requirements include:

- Nacelle support beam flexibility
- Flexible leading and trailing edge control surfaces
- Hinge and actuator flexibility
- Wing secondary structure
- Landing gear and wheelwell cut-out
- Major access doors
- Attachment details for flexible wing mounted fins
- Complete engine c.g. motion
- Detailed wing-body attachment

Some of the above refinements are visible in figure 7-4 which shows the complete structural half-model of the airplane. Figure 7-5 shows detail in the multi-element body and the wing mid-plane. Figure 7-6 shows the wing half-depths added to the wing mid-plane nodes.

GEOMETRY AND COORDINATE SYSTEMS

A well integrated airplane results from a design and configuration process involving a number of engineers, each working in his individual specialty. Each constructs a coordinate system appropriate to the work that is being performed. The integration and consolidation of these various pieces of work to fit into the integrated aeroelastic analysis requires careful definition of the interrelationship between these coordinate systems. To accomplish this consolidation on Arrow Wing, each coordinate system has been related to an ATLAS global coordinate frame. The transformation equations are given in table 7-1, and the various coordinate frames are identified in figure 7-7. A consistent configuration geometry thus prevails from the configuration geometry definition, through aerodynamics performance analysis, design group layout, and structural design to the representation in the finite-element model. The importance of this consistent geometry in any integrated computer analysis cannot be overemphasized. For convenience, a local ATLAS coordinate frame was used for the wing mounted fin. Transformation to the global coordinate frame is accomplished automatically within the ATLAS SYSTEM.

Figure 7-8 shows the wing fin coordinate frame and details of the wing fin and wing mid-plane nodal grids, comprising roughly 50 and 850 mid-plane nodes respectively. The wing idealization closely follows the actual structure, and the nodal grid was designed to include the landing gear cutout and secondary structure contributing leading edge, trailing edge and nacelle attachment flexibility. The wing nodal grid extends to within a half percent of the semi-span and local chords, so that arbitrarily stiff structure can be used to define mode shapes accurately near the planform edges, since the edges have an important influence on unsteady aerodynamic load.

The preparation of input data describing the location of mid-plane nodes and the offsets to the wing upper and lower surfaces was simplified by use of the aerodynamic loft describing the wing for the aerodynamic analysis. The aerodynamics program predicts pressure distributions for a particular definition of airfoil thickness and camber, and wing twist and shear. A special control program was written to calculate the location and surface offsets for each node from this geometric data in the proper format for use in ATLAS and properly decremented for location of cover skin centroids within profile. Thus the structural wing geometry definition is consistent with that used for drag estimates. Further simplification of input data was accomplished by exploiting the ATLAS capability for internally generating "strings" of nodes where a regular pattern exists.

IDEALIZATION OF WING AND BODY STRUCTURE

The structural half-model comprises about 2000 nodes with 4200 flexible elements having a total of 8500 active freedoms. Figures 7-9 and 7-10 present a pictorial

representation of the multi-element body in the vicinity of the wing. Roughly 1100 nodes describe the body and empennage structural geometry. The body model includes the wing side-of-body rib and wing carry-thru structure. Lumping of structural components into an equivalent single component was used to reduce the complexity of the body model. Lumping two frames into an equivalent single frame reduces the size of the model and provides a one-to-one correspondence with wing spars. Lumping three or four stringers into an equivalent single stringer provides a model of the body cross-section that adequately describes overall as well as local structural characteristics. The fuselage finite-element model extends for the length of the wing box as shown in figure 7-6. Forward and aft of this region, the fuselage is idealized as a simple beam, tying into the finite-element portion of the structure as a cantilevered beam. The structure of the horizontal tail surfaces is modeled as a simple network of beams to simulate the flexibility for the aeroelastic loads analysis. The surfaces are treated as rigid in the flutter analysis, with the mass of each surface located at the center of gravity, and attached to the fuselage with a stiff beam.

The wing structure is comprised of ATLAS "SPAR" and "COVER" macro-elements, so-called because the element itself is an assembly of simpler elements. These elements simulate three-dimensional airfoil structures with great versatility, while requiring one-third to one-half the usual finite-element descriptive input data. Figure 7-11 shows an ATLAS "SPAR" element connecting two structural mid-plane nodes, each having three kinematic freedoms. It has neither lateral bending nor torsional stiffness. The web effectiveness in bending can be taken into account using an optional lumping factor. Offset parameters allow the user to ensure the correct location of the spar chords relative to the cover skins. Figure 7-12 shows a triangular ATLAS "COVER" element connecting three structural mid-plane nodes, each with four kinematic freedoms. This element consists of two membranes, possibly orthotropic, that can carry in-plane loads, and can be stiffened uniaxially in one or two orthogonal directions, but have no plate bending stiffness. The ATLAS library also contains a quadrilateral "COVER" element. The membrane on one side of a "COVER" element can have zero thickness. This capability is used for the wheel-well and spoiler cut-outs. However, care had to be taken in the specification of boundary condition data for such "COVER" elements to delete any inactive freedoms of the mid-plane nodes in the boundary condition data for such COVER elements, created by the absence of the plate on one side within neighboring structural idealizations.

Modeling of the fin attachment to the wing required the use of ATLAS "GPLATE" elements with auxiliary offset nodes, figure 7-13. The "GPLATE" element can carry out-of-plane bending in addition to membrane stresses. The plate bending capability of the GPLATE was not used.

The shell-body was entirely modeled using ATLAS "4-NODE SPLATE" elements and "BEAM" elements, figure 7-13. The ATLAS "BEAM" element connects two structural nodes with up to six kinematic freedoms each and has offset elastic axis capability using auxiliary nodes. The offset capability of the beam element was not used in modeling the body; however, it was used in modeling the control surface hinges and the wheel-well in the wing. The "SPLATE" element is a membrane that carries only shear stress.

ATLAS "ROD" elements or "BEAM" elements with degenerate properties were used where appropriate in modeling the landing gear trunnions, spoiler cut-outs, and hinge assemblies.

FUSELAGE LOAD-DISTRIBUTION STRUCTURE

The airloads and inertia loads on the fuselage occur as continuous load distributions on the surface of the body. For the purpose of the analysis, however, these loads are lumped together and applied to nodes along the centerline of the mathematical model. It is therefore necessary to provide auxiliary structures to redistribute those local loads across the frames in a manner that prevents large local stress concentrations and deflections. These auxiliary structures are provided as shown in figures 7-14 and 7-15, and consist of "whiffle-trees" that span three frames. The members are weightless simple beams with bending stiffness in one plane only, and allow the fuselage structure to deflect without affecting the structural properties of the shell.

WING BODY CONNECTION

The wing-body connection involves forty nodes; these are simultaneously wing root chord mid-plane nodes and body frame nodes. Figure 7-16 shows a typical connection node between the wing "SPAR" and "COVER" macro-elements and the "BEAM" and "SPLATE" elements of the body.

NACELLE AND SUPPORT BEAM IDEALIZATION

The nacelle is simulated by a collection of extremely stiff beams, with a node at the nacelle center of gravity. This nacelle assembly is attached in a statically determinate manner to a flexible box beam cantilevered off the wing rear spar. The engine nacelle and support idealization in the structural model is illustrated in figure 7-17. The exploded view also shows the wing trailing edge secondary structure which is attached to the nacelle support beam. As indicated in the figure, vertical shear and pitch loads are reacted at the front and rear nacelle mounts and thrust, roll and yaw loads are reacted at the front mount on the wing rear spar. Roll and yaw loads are reacted by differential shear loads. This simulation of the engine nacelle allows the retention of all six nacelle center of gravity degrees of freedom in the vibration analysis.

WHEELWELL IDEALIZATION

Figure 7-18 shows the idealization of the wheel-well and main landing gear. The main gear load, gear-up, is reacted at two trunnions tied to the wing spar aft of the wheel-well, and at an uplock tied to a lattice of beams reinforcing the upper skin covering the wheel-well. These reinforcing beams have only bending stiffness.

CONTROL SURFACE HINGES AND ACTUATORS

Figure 7-19 shows a typical control surface hinge and actuator idealization. In order to satisfy mid-node connectivity each discrete hinge is idealized by offset beams, A is and

\underline{AB} , which have extensional, and lateral and vertical bending stiffnesses, and are hinged at node \bar{B} to form a ball and socket joint. Each actuator is similarly idealized as an offset beam, \underline{AB} , which has only extensional stiffness.

Control surface hinge line nodes, \bar{B} , are defined by the ATLAS "string generation" routine so that they lie on a straight line. The only constraint to control surface rotation is imposed by the three actuators, \underline{AB} .

Each control surface support idealization requires a dummy beam, AC , with lateral bending stiffness, to prevent rigid body rotation of the hinge assembly about a vertical axis.

WING-MOUNTED FIN IDEALIZATION

The wing mounted fin attachment is shown in figure 7-20. The special handling of SPAR and GPLATE elements in this region, is shown in figure 7-21 and figure 7-22 respectively. The wing-mounted fin mid-plane nodes are defined in a local frame of coordinates $(\bar{O}, \bar{X}, \bar{Y}, \bar{Z})$, except the connecting mid-nodes, which, like all wing mid-nodes, are input in a global frame of coordinates (O, X, Y, Z) . A mid-node i , input in a frame of coordinates (O, X, Y, Z) , local or global, is defined by four quantities.

$$X, Y, Z, \Delta Z$$

X, Y, Z are the cartesian coordinates of the mid-node i in the frame (O, X, Y, Z) . ΔZ is the half depth, associated with mid-node i , oriented along a line parallel to OZ , passing through mid-node i .

Figure 7-21 shows a SPAR element connecting a mid-node N_1 ($\bar{X}_1, \bar{Y}_1, \bar{Z}_1, \Delta Z_1$), input in the local frame of coordinates $(\bar{O}, \bar{X}, \bar{Y}, \bar{Z})$, to a mid-node N_2 ($\bar{X}_2, \bar{Y}_2, \bar{Z}_2, \Delta Z_2$), input in the global frame of coordinates (O, X, Y, Z) . Because the quantities ΔZ_1 and ΔZ_2 have different orientations, the SPAR element looks warped and it would appear that way if it were plotted. However, despite the apparent geometric warping, the element stiffness matrix generated for the SPAR will be correct when the following procedure is used:

The mid-node having a ΔZ with the desired spar orientation must be mentioned first on the SPAR element input card.

"SPAR $N_1 N_2 \dots$ ".

Because mid-node N_1 is mentioned first, a half-depth ΔZ_1 , parallel to \bar{OZ} , will be associated with mid-node N_1 and a half-depth ΔZ_2 , also parallel to \bar{OZ} , will be associated with mid-node N_2 . If we want a half depth ΔZ_2 , we have to use the SPAR offset parameter O_2 (possibly negative) to correct the value to ΔZ_2 , in such a manner that

$$\Delta Z_2 = \Delta Z_2 + O_2$$

as shown in figure 7-21. It was in this manner that fin half-depths were obtained for the fin spars at the connection mid-nodes from the wing half-depths associated with these nodes.

In the COVER element, the direction of the rigid post associated with each node depends on the input frame for that node. COVER elements connecting wing-mounted fin mid-nodes, defined in the local frame of coordinates $(\tilde{O}, \tilde{X}, \tilde{Y}, \tilde{Z})$ and the connection mid-nodes, input in the global frame of coordinates $(\bar{O}, \bar{X}, \bar{Y}, \bar{Z})$ would be completely unrepresentative, because of the completely different orientation of these two frames (see figure 7-21). This difficulty is solved by using GPLAT elements instead of COVER elements. Auxiliary nodes, properly offset from the mid-nodes, must be defined on each side of the wing-mounted fin as shown in figure 7-22.

For all wing nodes input in the global frame of coordinates $(\bar{O}, \bar{X}, \bar{Y}, \bar{Z})$, no global $R\bar{Z}$ stiffnesses are defined, since only SPAR and COVER elements are used. These zero global $R\bar{Z}$ stiffnesses are automatically deleted in ATLAS and need not be deleted in specifying boundary conditions. Similarly, all wing-mounted fin nodes input in the local frame $(\tilde{O}, \tilde{X}, \tilde{Y}, \tilde{Z})$ have no $R\tilde{Z}$ local stiffness; however, these zero local $R\tilde{Z}$ stiffnesses are not automatically deleted and also boundary conditions cannot be imposed in a local frame in ATLAS 2.0. This problem was solved by using a fictitious BEAM element with only lateral bending stiffness, in parallel with each wing-mounted fin SPAR element, thus defining all local $R\tilde{Z}$ stiffnesses.

STRUCTURAL MODEL CHECKOUT

The structural model validation commenced with the checking for keypunch and transcription errors of bulk nodal and element card data, supplemented by the input error diagnostics of the ATLAS program system. Finite-element sizing was verified against structural preliminary sizing. Further confidence in the modeling was gained by uncovering and correcting mislocated nodes, missing or duplicated elements and incorrect element connections, using ATLAS nodal and element geometry plots as shown on figure 7-9. Model validation proceeded in several stages: stress and displacement analysis for symmetric and antisymmetric loading of the body, examination of wing and body details and computer plots of both cantilevered wing and complete airplane flexibility influence coefficients, preliminary vibration analyses, and a stress analysis with preliminary symmetric airplane loads, which uncovered further model deficiencies. All errors were corrected before proceeding with the Task II detailed configuration analyses.

The stress and displacement analyses confirmed that the body load distribution structures did not constrain the body. Good deflection continuity at the connection of the multi-element body to the single beam representation fore and aft was similarly confirmed. The stress analysis also revealed an improper reaction at the hingeline of the low speed aileron, created by a slight nodal misalignment which was undetectable at the scale of the geometry plots.

Large flexibility matrices were calculated and examined using computer plots for one load at a time. Figure 7-23 shows, for the same point load at mid-span near the wing

as shown in figure 7-21. It was in this manner that fin half-depths were obtained for the fin spars at the connection mid-nodes from the wing half-depths associated with these nodes.

In the COVER element, the direction of the rigid post associated with each node depends on the input frame for that node. COVER elements connecting wing-mounted fin mid-nodes, defined in the local frame of coordinates $(\tilde{O}, \tilde{X}, \tilde{Y}, \tilde{Z})$ and the connection mid-nodes, input in the global frame of coordinates $(\bar{O}, \bar{X}, \bar{Y}, \bar{Z})$ would be completely unrepresentative, because of the completely different orientation of these two frames (see figure 7-21). This difficulty is solved by using PLATE elements instead of COVER elements. Auxiliary nodes, properly offset from the mid-nodes, must be defined on each side of the wing-mounted fin as shown in figure 7-22.

For all wing nodes input in the global frame of coordinates $(\bar{O}, \bar{X}, \bar{Y}, \bar{Z})$, no global $R\bar{Z}$ stiffnesses are defined, since only SPAR and COVER elements are used. These zero global $R\bar{Z}$ stiffnesses are automatically deleted in ATLAS and need not be deleted in specifying boundary conditions. Similarly, all wing-mounted fin nodes input in the local frame $(\tilde{O}, \tilde{X}, \tilde{Y}, \tilde{Z})$ have no $R\tilde{Z}$ local stiffness; however, these zero local $R\tilde{Z}$ stiffnesses are not automatically deleted and also boundary conditions cannot be imposed in a local frame in ATLAS 2.0. This problem was solved by using a fictitious BEAM element with only lateral bending stiffness, in parallel with each wing-mounted fin SPAR element, thus defining all local $R\tilde{Z}$ stiffnesses.

STRUCTURAL MODEL CHECKOUT

The structural model validation commenced with the checking for keypunch and transcription errors of bulk nodal and element card data, supplemented by the input error diagnostics of the ATLAS program system. Finite-element sizing was verified against structural preliminary sizing. Further confidence in the modeling was gained by uncovering and correcting mislocated nodes, missing or duplicated elements and incorrect element connections, using ATLAS nodal and element geometry plots as shown on figure 7-9. Model validation proceeded in several stages: stress and displacement analysis for symmetric and antisymmetric loading of the body, examination of wing and body details and computer plots of both cantilevered wing and complete airplane flexibility influence coefficients, preliminary vibration analyses and a stress analysis with preliminary symmetric airplane loads, which uncovered further model deficiencies. All errors were corrected before proceeding with the Task II detail configuration analyses.

The stress and displacement analyses confirmed that the body load distribution structures did not constrain the body. Good deflection continuity at the connection of the multi-element body to the single beam representation fore and aft was similarly confirmed. The stress analysis also revealed an improper reaction at the hingeline of the low speed aileron, created by a slight nodal misalignment which was undetectable at the scale of the geometry plots.

Large flexibility matrices were calculated and examined using computer plots for one load at a time. Figure 7-23 shows, for the same point load at mid-span near the

leading edge, a deflection comparison between the wing cantilevered at the wing-body connection nodes and the complete structure with fore and aft body supports and symmetrically loaded on right and left wings. Figure 7-24 shows another deflection plot for the half-airplane model with fore and aft body supports and symmetric loading: first, for a point load in the mid-body region and secondly, for symmetric loading on right and left horizontal stabilizers. Figures 7-23 and 7-24 are typical of the good deflection continuity that prevails for loading anywhere on the model. Care must be exercised not to apply unusually large loads on the wing planform edge structure. This structure was added to avoid extrapolation of vibration mode shapes when transferring this data from structural to aerodynamic grids.

The deflection checks were also useful in uncovering local soft spots in wing secondary structure. Such unrepresentative localized flexibilities were removed from the model before proceeding further.

Examination of nacelle coupled vibration modes, with the support beam cantilevered at the wing rear spar, revealed the need to decouple side translation and torsion of the support beam by revising the aft mount for the engine as shown in figure 7-17.

The preliminary vibration analysis also revealed a low frequency local resonance of the main gear in the stowed position. This was due to the long load path for the gear uplock on the lattice of beams supporting the wheel-well upper surface. A localized ATLAS model was used to evaluate proposed structural modifications to increase the stiffness at the gear uplock. The modification adopted is shown in figure 7-18 and included addition of a full-depth rib on the inboard edge of the wheel-well, addition of lower honeycomb skin panels inboard of the above rib extending to the side-of-body rib, and an increased bending stiffness of the uplock beam, obtained principally by a depth increase.

Excessive frame local deformation was detected at the side-of-body connection with the wing in the complete model stress analysis. This difficulty was corrected before resizing the structure for strength design. Special consideration in modeling is required at any structural junction containing ATLAS mid-surface nodes. The wing SPAR and COVER elements have rigid end-posts which equate upper and lower skin and spar loads to a statically equivalent set of forces and moments at the wing mid-surface wing-body connection nodes. Body frame BEAM elements from the connection nodes to the upper and lower chords of the side-of-body rib had to be adequately stiffened to essentially restore the statically equivalent loads at the connection nodes to the realistic upper and lower wing skin and spar chord loads.

MODEL REVISIONS FOR AEROELASTIC CYCLE

As a result of the initial assessment of flexibilities and the preliminary vibration analyses it was decided to increase stiffness in three areas prior to initiation of the aeroelastic loads analysis. In the wing tip outboard of the wing-mounted-fin, spars and covers of main box and secondary structure behind the rear spar were doubled. The low speed aileron cover thickness was increased by a factor of 4.0 to minimize wind-up relative to the inboard location of the actuators. Finally, nacelle support beams were

stiffened by a factor of 1.5 to roughly 9000 lb/in., defined at the rear mount location with the beam cantilevered at the wing rear spar. These model revisions for the aeroelastic cycle are shown in figure 7-25.

DEVELOPMENT TASK/TIME AND MODEL UTILIZATION

The structural model and its associated distributed mass model took approximately 63 man-months of effort over a period of 7 months to set-up and check-out, and cost about 80 CDC 6600 computer capacity units, a value of \$12,000. Figure 7-26 shows a breakdown of the tasks and time taken in setting-up the separate wing and body models and in pooling data to form the airplane structural model. Apart from the obvious tasks of preparing node and element data, considerable time was spent in initially sizing structure and in checking the structural model, before any detailed configuration analyses were started. Figure 7-27 summarizes the use of the ATLAS Program System in the technical analysis.

FINAL DEFINITION OF STRUCTURAL MODEL

Following the aeroelastic strength design of the structure, additional stiffness modifications, described in Section 11, were added in satisfying flutter criteria. Figures 7-29 through 7-40 show the nodal connectivity in the model. The wing was separated into four regions plus the fin as defined in figure 7-28, to preserve detail. Figures 7-29 and 7-30 show the cover elements and the spar and beam elements, respectively, in region 1. The body elements and node numbering schemes are shown in figures 7-39 and 7-40.

ENGINE BEAM STIFFENING AND DIFFUSION RIBS

An innovative design concept, which was committed for use on the National SST prototypes, is used for the stiffened engine 27 beams and their diffusion ribs. It comprises a strength designed titanium beam with borsic-aluminum composite added to the chords to achieve the required stiffness level, with consequent weight saving relative to an all titanium beam. For direct correlation, the "flutter option" of the ATLAS design module was used to factor up the element sizing for strength designed titanium beams to obtain stiffened engine beams, so that the sizing is disproportionately large compared with the design concept. It should be noted that engine beam weight was included separately with the mass elements in the ATLAS mass module. The diffusion ribs, which were added later, have, similarly, the stiffness properties of titanium only, but since they are in the wing main box which is weighed in the ATLAS mass module, the lighter weight of the design concept was obtained by using an ATLAS "special material" with 0.612 times the density of titanium, to allow for the correct proportion of the two materials used in the design concept.

Table 7-1.—Coordinate Transformation Equations
(ref. fig. 7-7)

$$\begin{bmatrix} \hat{X} \\ \hat{Y} \\ \hat{Z} \end{bmatrix}_{\text{WRP}} = \begin{bmatrix} -32.83588693 \\ 0. \\ 136.2791756 \end{bmatrix} + \begin{bmatrix} \text{SRP to WRP} \\ 0.9957591293 & 0 & 0.0919986773 \\ 0. & 1. & 0. \\ -0.0919986773 & 0. & 0.9957591293 \end{bmatrix} \begin{bmatrix} \hat{X} \\ \hat{Y} \\ \hat{Z} \end{bmatrix}_{\text{SRP}}$$

$$\begin{bmatrix} \hat{X} \\ \hat{Y} \\ \hat{Z} \end{bmatrix}_{\text{SRP}} = \begin{bmatrix} 45.23413807 \\ 0. \\ -132.6803751 \end{bmatrix} + \begin{bmatrix} \text{WRP to SRP} \\ 0.9957591293 & 0 & -0.0919986773 \\ 0. & 1. & 0. \\ 0.0919986773 & 0. & 0.9957591293 \end{bmatrix} \begin{bmatrix} \hat{X} \\ \hat{Y} \\ \hat{Z} \end{bmatrix}_{\text{WRP}}$$

$$\begin{bmatrix} X \\ Y \\ Z \end{bmatrix}_{\text{WRPZ}} = \begin{bmatrix} -32.83588692 \\ 0. \\ -163.7208244 \end{bmatrix} + \begin{bmatrix} \text{SRP to WRPZ} \\ 0.9957591293 & 0. & 0.0919986773 \\ 0. & 1. & 0. \\ -0.0919986773 & 0. & 0.9957591293 \end{bmatrix} \begin{bmatrix} \hat{X} \\ \hat{Y} \\ \hat{Z} \end{bmatrix}_{\text{SRP}}$$

$$\begin{bmatrix} \hat{X} \\ \hat{Y} \\ \hat{Z} \end{bmatrix}_{\text{SRP}} = \begin{bmatrix} 17.63453488 \\ 0. \\ 166.0473637 \end{bmatrix} + \begin{bmatrix} \text{WRPZ to SRP} \\ 0.9957591293 & 0. & -0.0919986773 \\ 0. & 1. & 0. \\ 0.0919986773 & 0. & 0.9957591293 \end{bmatrix} \begin{bmatrix} X \\ Y \\ Z \end{bmatrix}_{\text{WRPZ}}$$

$$\begin{bmatrix} \hat{X} \\ \hat{Y} \\ \hat{Z} \end{bmatrix}_{\text{GCS}} = \begin{bmatrix} -982.8358869 \\ 0. \\ -296.7208244 \end{bmatrix} + \begin{bmatrix} \text{SRP to GCS} \\ 0.9957591293 & 0. & 0.0919986773 \\ 0. & 1. & 0. \\ -0.0919986773 & 0. & 0.9957591293 \end{bmatrix} \begin{bmatrix} \hat{X} \\ \hat{Y} \\ \hat{Z} \end{bmatrix}_{\text{SRP}}$$

$$\begin{bmatrix} \hat{X} \\ \hat{Y} \\ \hat{Z} \end{bmatrix}_{\text{SRP}} = \begin{bmatrix} 951.3698836 \\ 0. \\ 385.8820709 \end{bmatrix} + \begin{bmatrix} \text{GCS to SRP} \\ 0.9957591293 & 0. & -0.0919986773 \\ 0. & 1. & 0. \\ 0.0919986773 & 0. & 0.9957591293 \end{bmatrix} \begin{bmatrix} \hat{X} \\ \hat{Y} \\ \hat{Z} \end{bmatrix}_{\text{GCS}}$$

Table 7-1.—Concluded

$$\begin{bmatrix} \hat{\bar{X}} \\ \hat{\bar{Y}} \\ \hat{\bar{Z}} \end{bmatrix}_{\text{GCSX}} = \begin{bmatrix} -242.8358866 \\ 0. \\ -296.7208239 \end{bmatrix} + \begin{bmatrix} \text{SRP to GCSX} \\ 0.9957591293 & 0. & 0.0919986773 \\ 0. & 1. & 0. \\ 0.0919986773 & 0. & 0.9957591293 \end{bmatrix} \begin{bmatrix} \bar{X} \\ \bar{Y} \\ \bar{Z} \end{bmatrix}_{\text{SRP}}$$

$$\begin{bmatrix} \bar{X} \\ \bar{Y} \\ \bar{Z} \end{bmatrix}_{\text{SRP}} = \begin{bmatrix} 214.5081277 \\ 0. \\ 317.8030507 \end{bmatrix} + \begin{bmatrix} \text{GCSX to SRP} \\ 0.9957591293 & 0. & -0.0919986773 \\ 0. & 1. & 0. \\ 0.0919986773 & 0. & 0.9957591293 \end{bmatrix} \begin{bmatrix} \hat{\bar{X}} \\ \hat{\bar{Y}} \\ \hat{\bar{Z}} \end{bmatrix}_{\text{GCSX}}$$

$$\begin{bmatrix} \bar{X} \\ \bar{Y} \\ \bar{Z} \end{bmatrix}_{\text{SRPZ}} = \begin{bmatrix} 0. \\ 0. \\ -400. \end{bmatrix} + \begin{bmatrix} \text{SRP to SRPZ} \\ 1. & 0. & 0. \\ 0. & 1. & 0. \\ 0. & 0. & 1. \end{bmatrix} \begin{bmatrix} \bar{X} \\ \bar{Y} \\ \bar{Z} \end{bmatrix}_{\text{SRP}}$$

$$\begin{bmatrix} \bar{X} \\ \bar{Y} \\ \bar{Z} \end{bmatrix}_{\text{SRP}} = \begin{bmatrix} 0. \\ 0. \\ 400. \end{bmatrix} + \begin{bmatrix} \text{SRPZ to SRP} \\ 1. & 0. & 0. \\ 0. & 1. & 0. \\ 0. & 0. & 1. \end{bmatrix} \begin{bmatrix} \bar{X} \\ \bar{Y} \\ \bar{Z} \end{bmatrix}_{\text{SRPZ}}$$

$$\begin{bmatrix} \tilde{\bar{X}} \\ \tilde{\bar{Y}} \\ \tilde{\bar{Z}} \end{bmatrix}_{\text{WMF}} = \begin{bmatrix} -2883.852865 \\ -128.1754691 \\ 690.9844089 \end{bmatrix} + \begin{bmatrix} 0.995152200 & -0.034909240 & 0.091942602 \\ -0.0919986773 & 0. & 0.9957591293 \\ -0.034761194 & -0.999390486 & -0.003211603 \end{bmatrix} \begin{bmatrix} \bar{X} \\ \bar{Y} \\ \bar{Z} \end{bmatrix}_{\text{SRP}}$$

$$\begin{bmatrix} \bar{X} \\ \bar{Y} \\ \bar{Z} \end{bmatrix}_{\text{SRP}} = \begin{bmatrix} 2882.09992 \\ 589.8901324 \\ 394.9999972 \end{bmatrix} + \begin{bmatrix} 0.995152200 & -0.0919986773 & -0.034761194 \\ 0.034909240 & 0. & -0.999390486 \\ 0.091942602 & 0.9957591293 & -0.003211603 \end{bmatrix} \begin{bmatrix} \tilde{\bar{X}} \\ \tilde{\bar{Y}} \\ \tilde{\bar{Z}} \end{bmatrix}_{\text{WMF}}$$

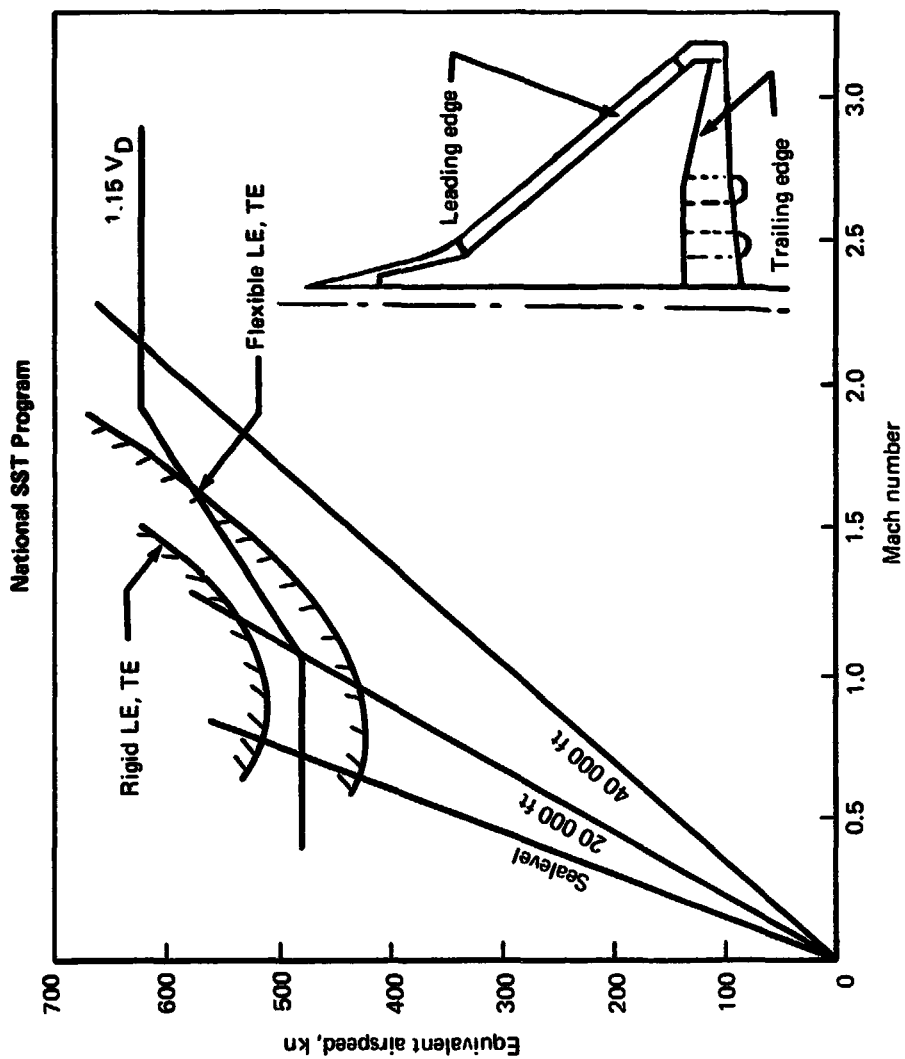


Figure 7-1.—Effect of Flap and Control Surface Flexibility on Flutter

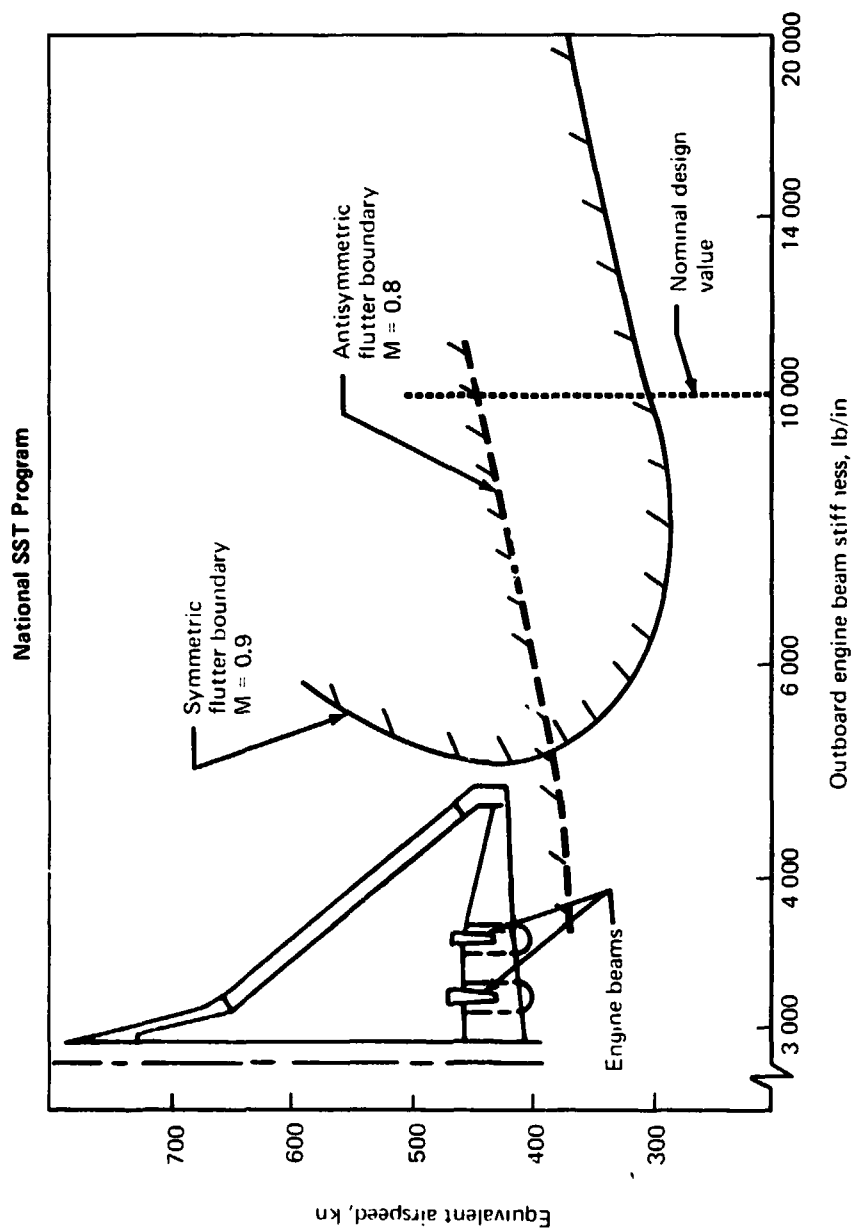
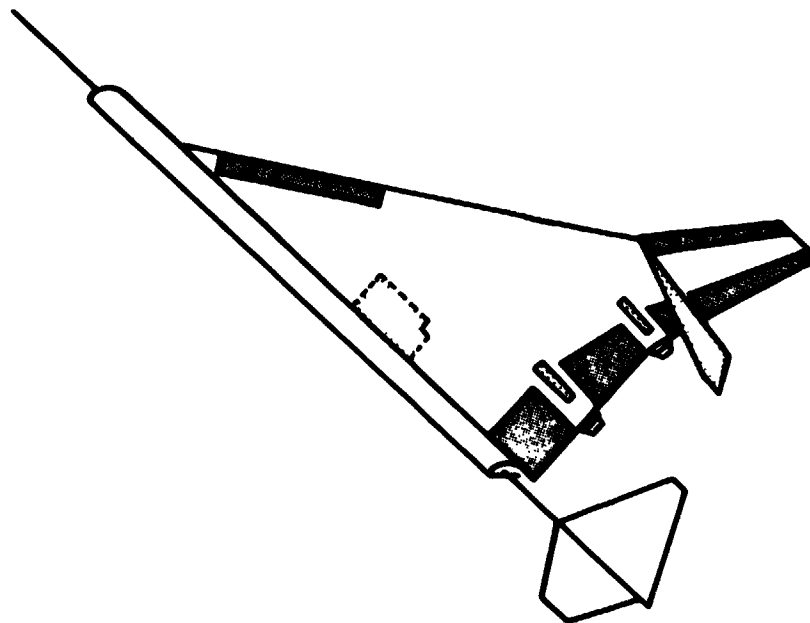


Figure 7-2.—Effect of Engine Support Beam Flexibility on Flutter



- Flexible engine beams
- Flexible LE and TE controls
- All wing secondary structure
- Landing gear and wheelwell cut-out
- Major access doors
- Flexible wing-mounted fins
- Complete cg motion for engines
- Complete airplane model
- Detailed body idealization for wing attachment

Figure 7-3.—Minimum Requirements of Structural Model for Meaningful Flutter Analysis

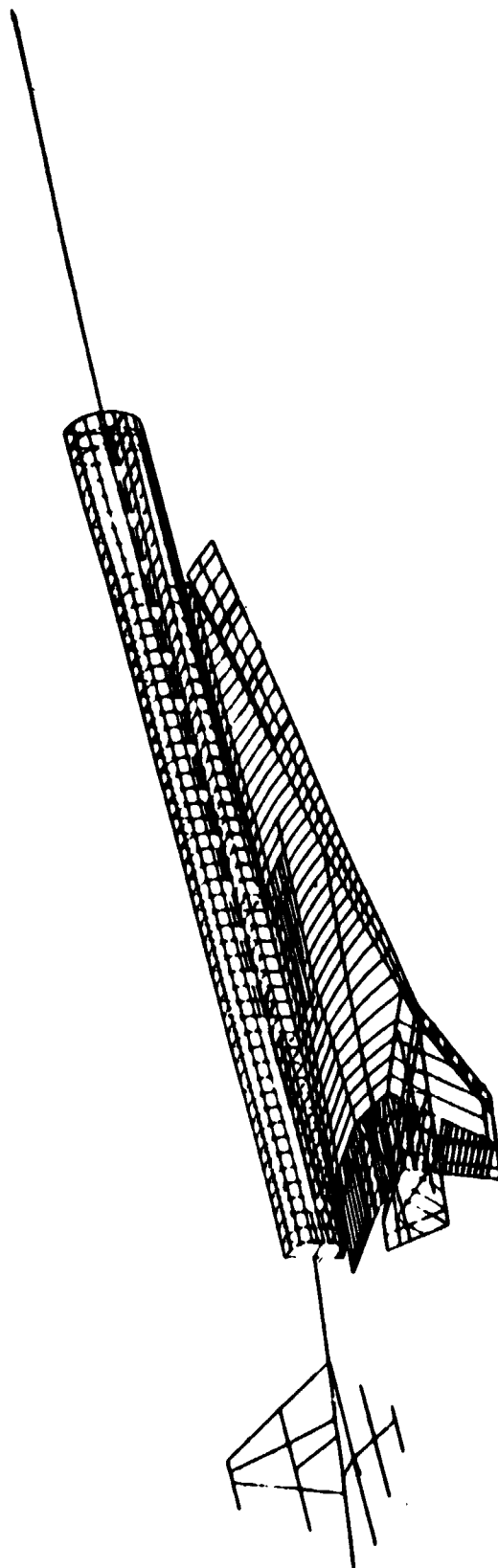


Figure 7-4. —Structural Mathematical Model, 969-512B

Structural Model 980-5128

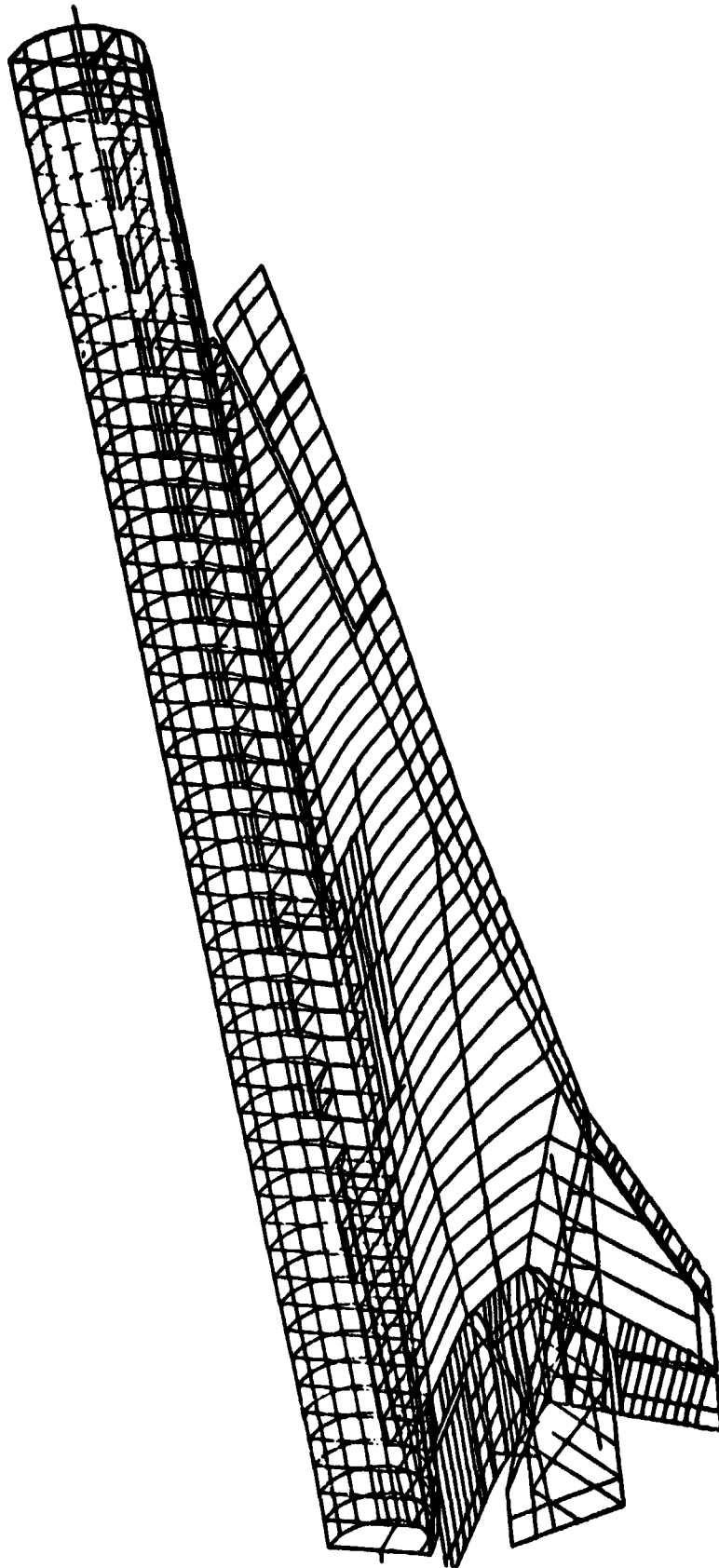


Figure 7-5. —Multielement Body and Wing Midplane

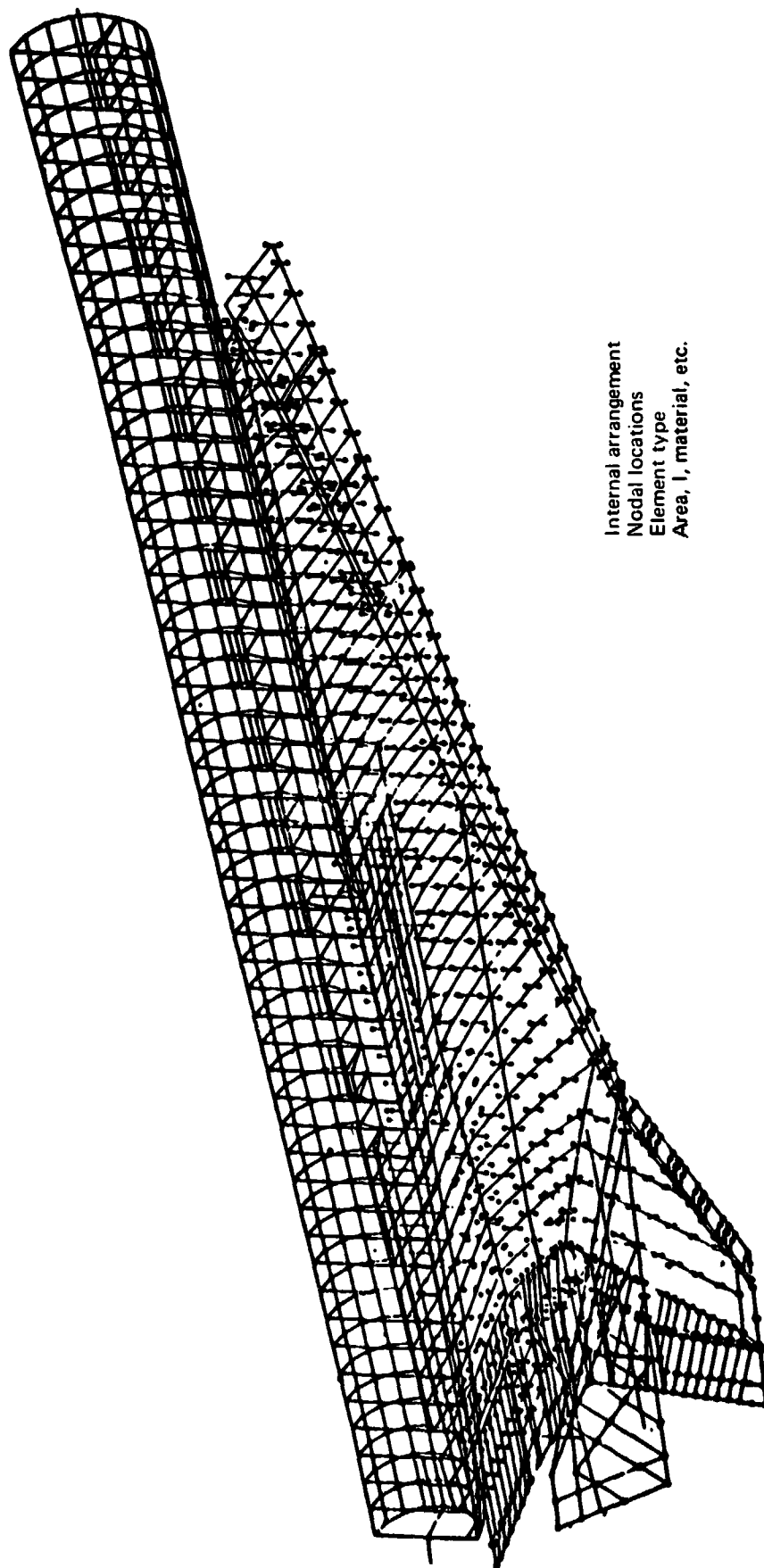


Figure 7-6. — Basic Structural Model

- Airplane reference frame
 - Wing reference plane frame
 - Wing orthomat frame
 - Wing linear aerodynamics programs
 - Structural reference plane frame
 - ATLAS global frame
 - Wing-mounted fin ATLAS local frame
- | | | |
|--|------|--------------|
| $(\bar{O}, \bar{x}, \bar{y}, \bar{z})$ | WRP | (BS, BL, WL) |
| (O, X, Y, Z) | WRPZ | |
| $(\hat{O}, \hat{x}, \hat{y}, \hat{z})$ | GCS | |
| $(\hat{O}, \hat{x}, \hat{y}, \hat{z})$ | GCSX | |
| $(\bar{O}, \bar{x}, \bar{y}, \bar{z})$ | SRPZ | |
| $(\bar{O}, \bar{x}, \bar{y}, \bar{z})$ | SRP | |
| $(\tilde{O}, \tilde{x}, \tilde{y}, \tilde{z})$ | WMF | |

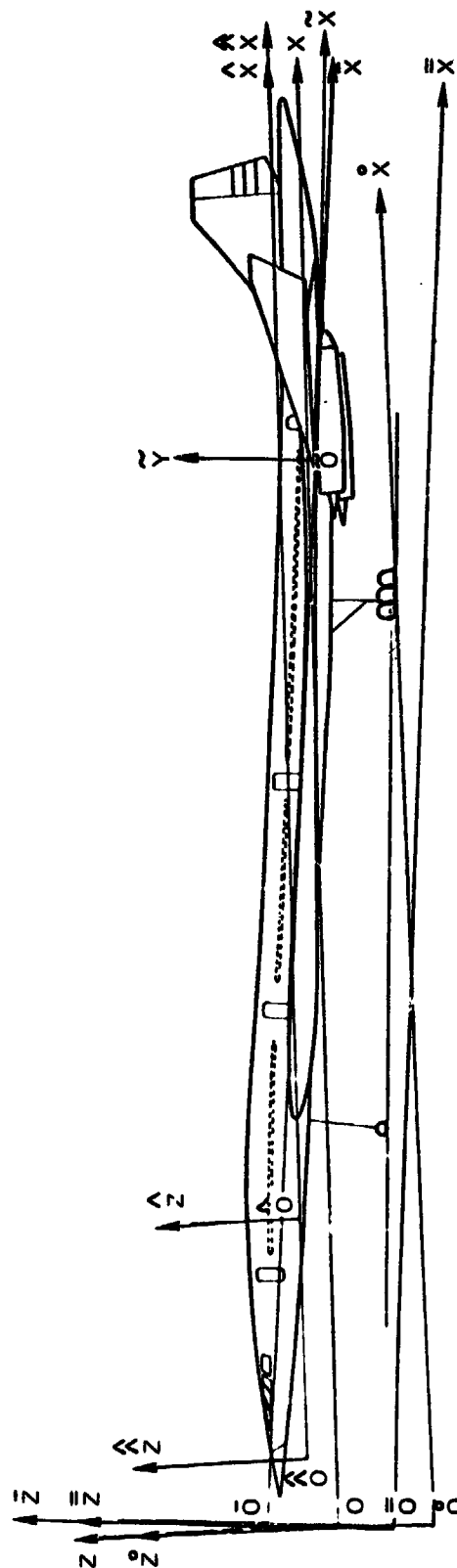


Figure 7-7. Configuration Geometry Equations

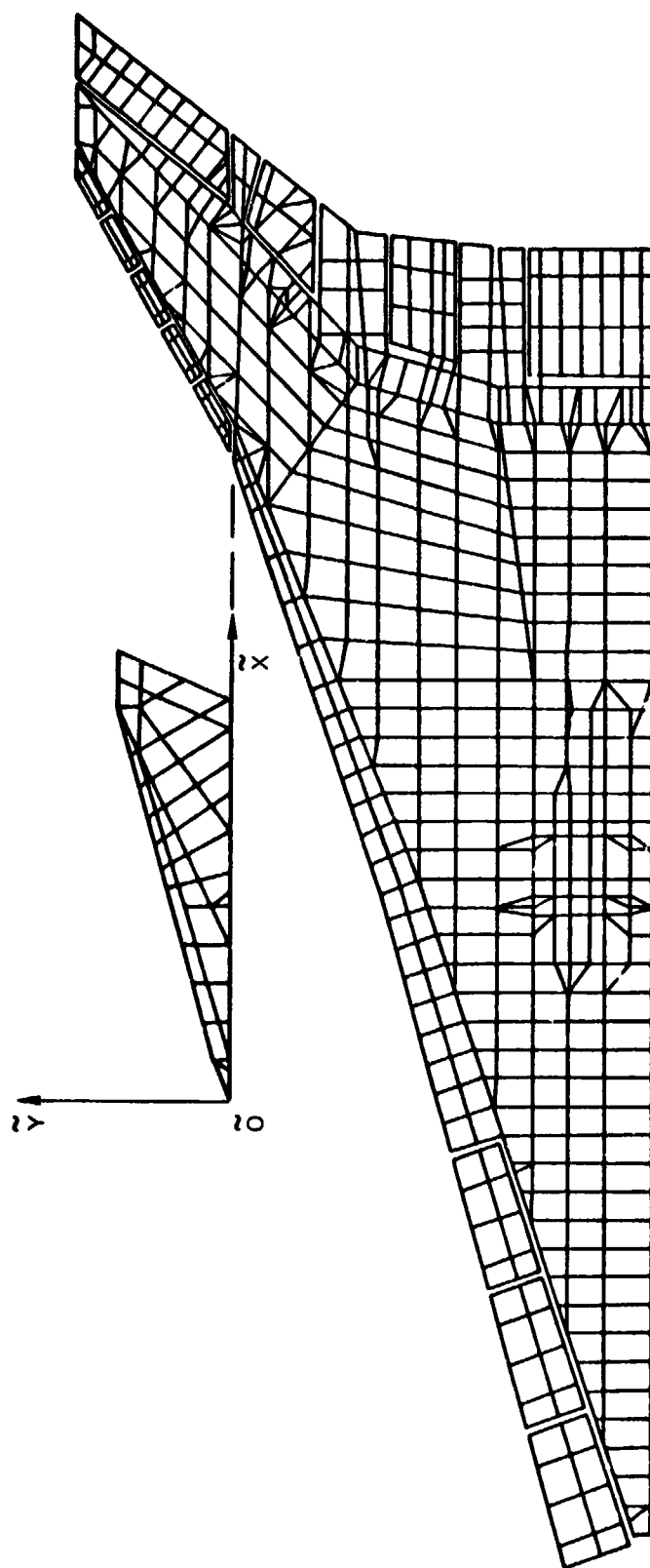


Figure 7-8.—Wing Finite-Element Model, 969-512B

969-5128

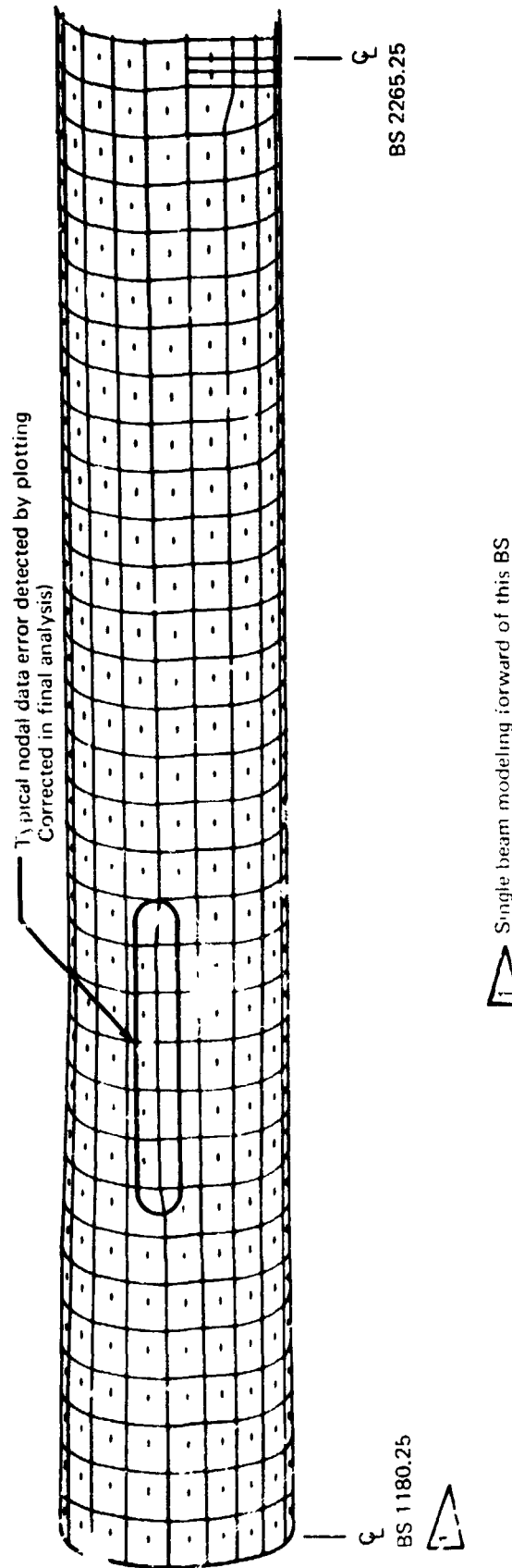


FIGURE 7-9.—Body Finite-Element Model, Forward of Wheelwell

969-5128

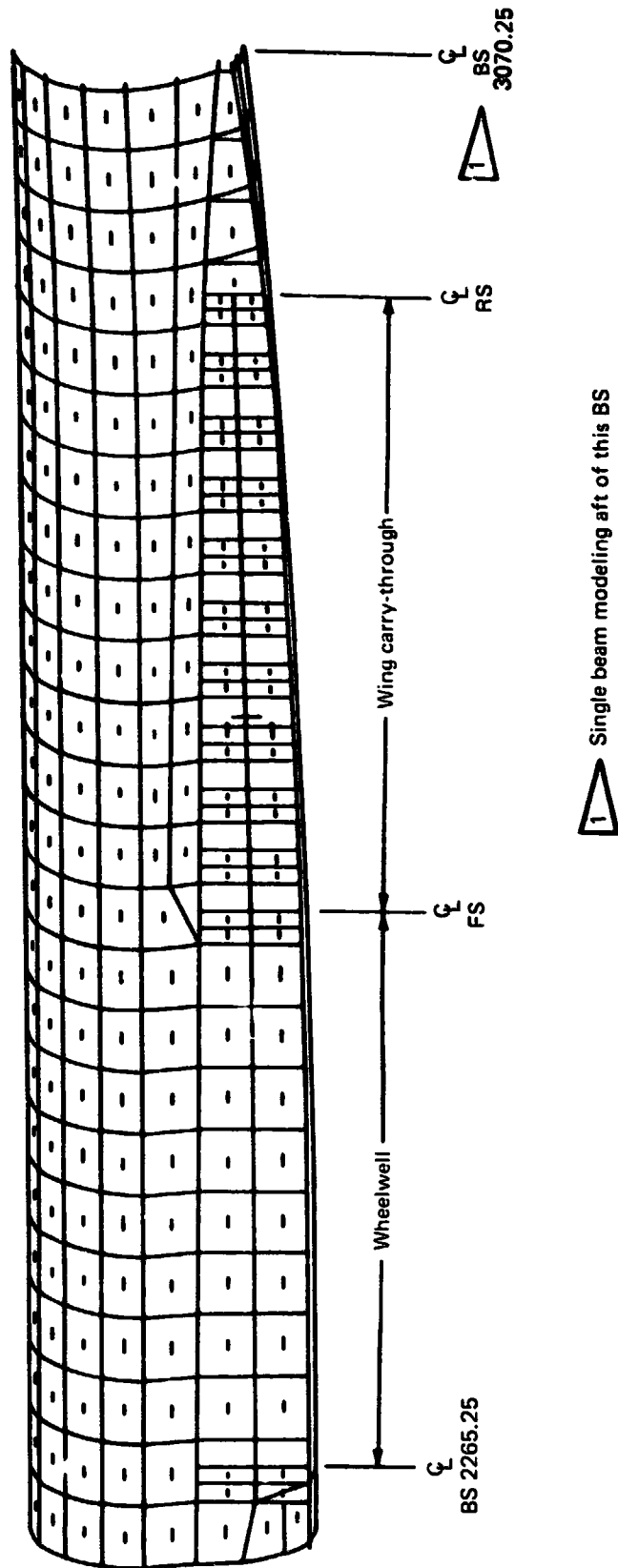


Figure 7-10.—Body Finite-Element Model, Wheelwell and Aft

The diagram illustrates a rectangular spar element with the following components and labels:

- Dimensions and Coordinates:**
 - Z : Vertical axis pointing upwards.
 - X : Horizontal axis pointing to the right.
 - Z_1 : Vertical distance from the bottom edge to the centerline.
 - Z_2 : Vertical distance from the top edge to the centerline.
 - ΔZ_1 : Vertical distance from the bottom edge to the rigid posts.
 - ΔZ_2 : Vertical distance from the top edge to the rigid posts.
- Internal Forces and Moments:**
 - N_1 : Normal force at the bottom edge.
 - N_2 : Normal force at the top edge.
 - $Q(1)U$: Shear force at the bottom edge.
 - $Q(2)L$: Shear force at the top edge.
- Structural Components:**
 - Rigid posts:** Two vertical lines connecting the top and bottom chords.
 - Upr chord:** Upper chord of the spar.
 - Lwr chord:** Lower chord of the spar.
 - Web:** The central vertical section of the spar.
 - Upr skin panel ζ :** The upper skin panel.
 - Lwr skin panel ζ :** The lower skin panel.
- Legend:**
 - Linear depth variation
 - Constant web gage
 - Linear flange-area variation
 - Uniform shear transfer
 - Optional web lumping

Figure 7-11.—Atlas Spar Element

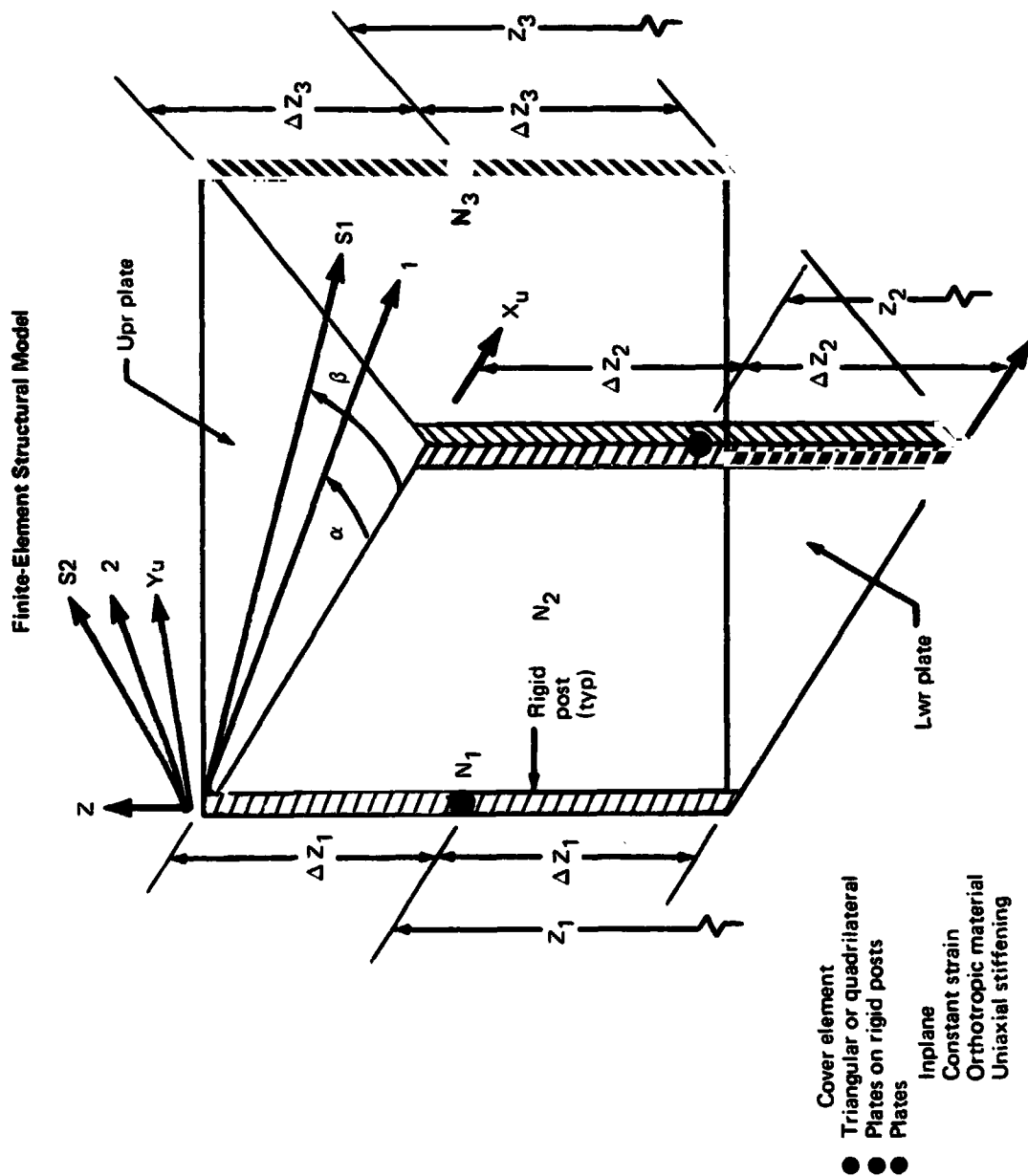


Figure 7-12.—Atlas Cover Element

Finite-Element Structural Model

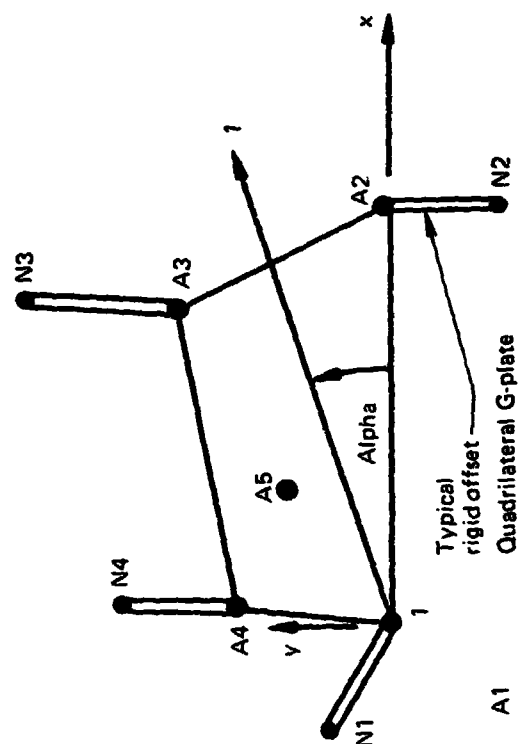
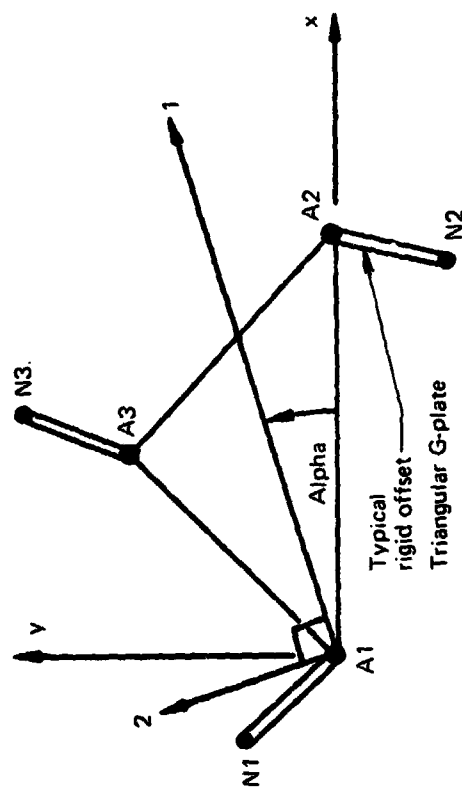
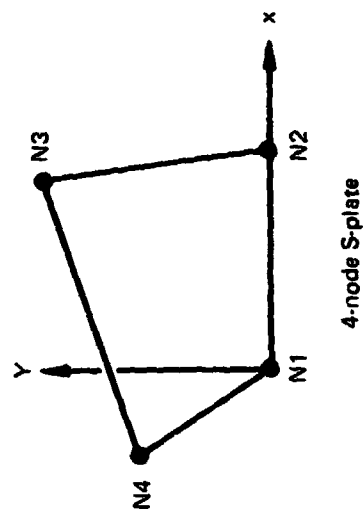
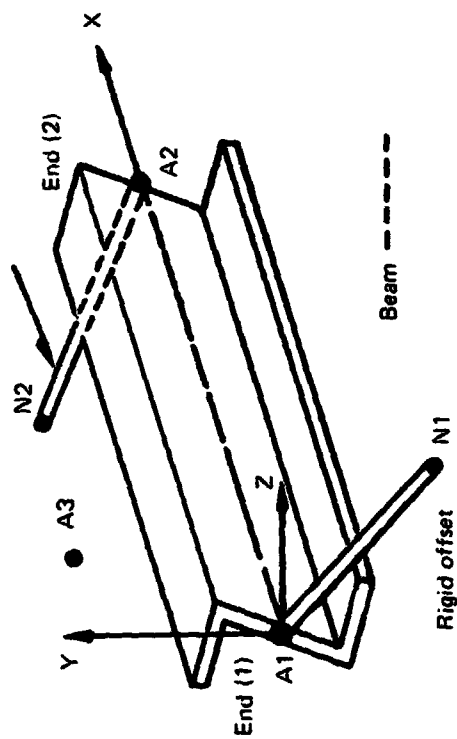


Figure 7-13.—Atlas Structural Elements

Body Finite-Element Model

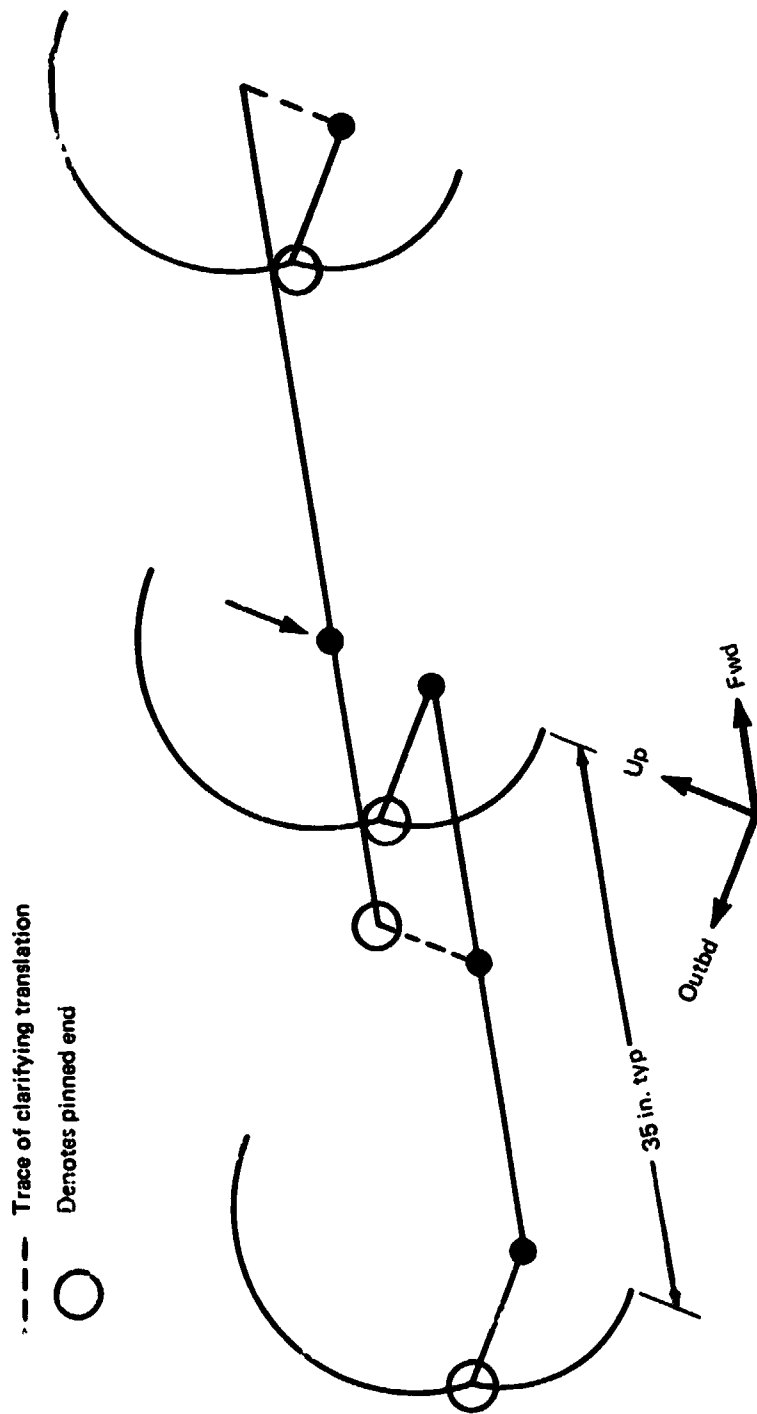


Figure 7-14.— Vertical Load Distribution Structure For Body
(Symmetric Loads and Boundary Conditions)

Body Finite-Element Model

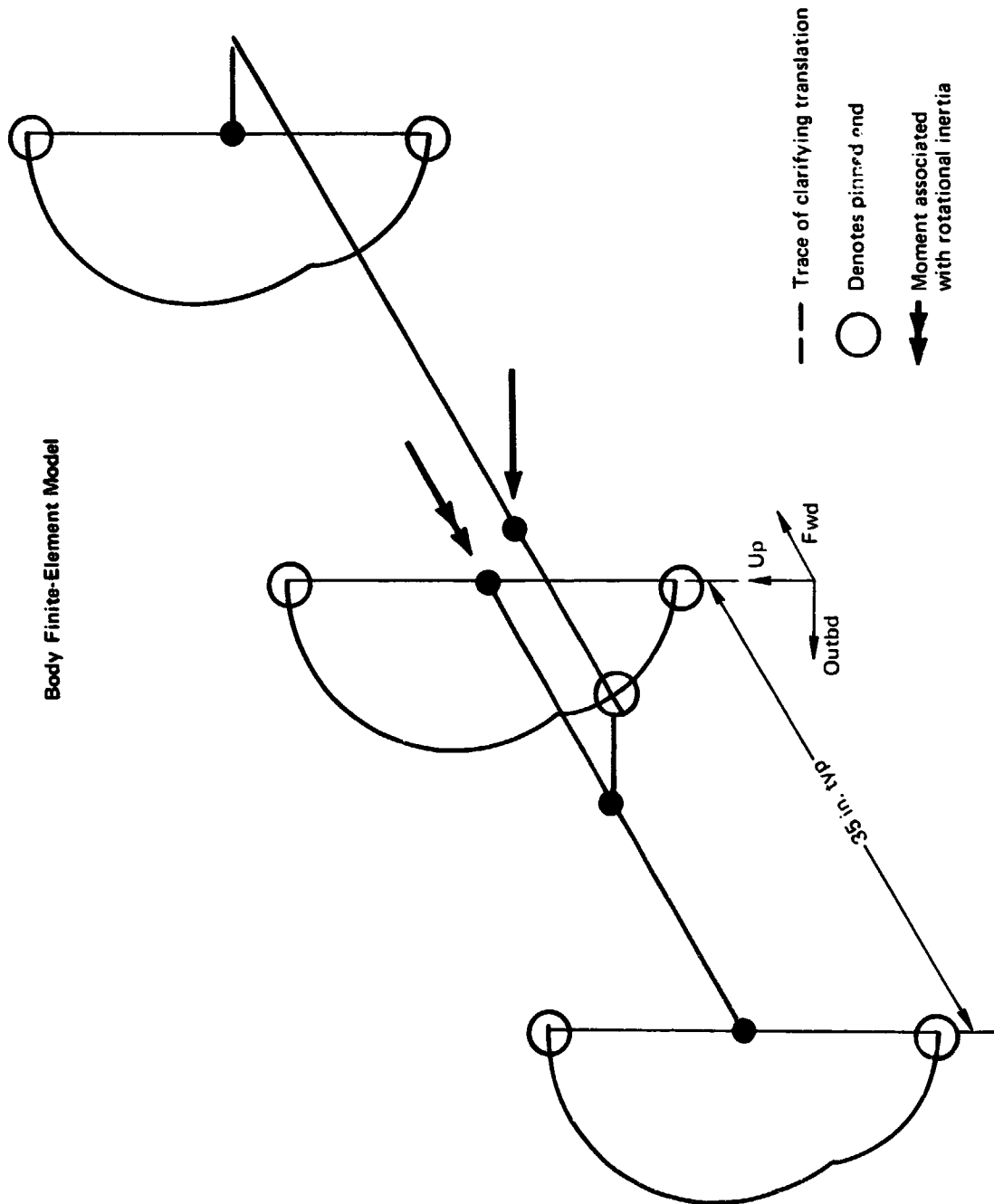


Figure 7-15.—Lateral Load Distribution Structure for Body Antisymmetric Loads and Boundary Conditions)

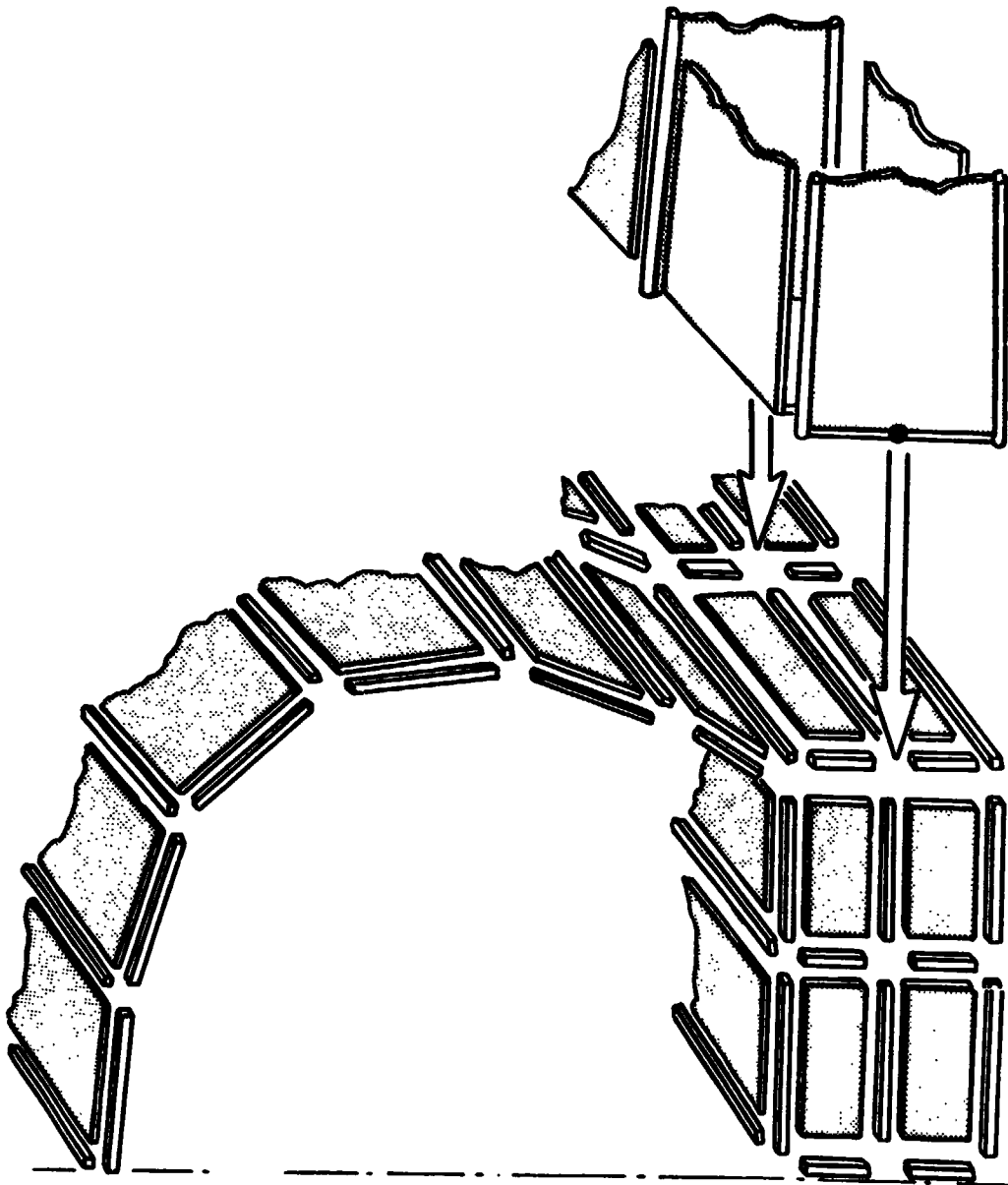


Figure 7-16.—Wing-Body Connection, Finite-Element Model

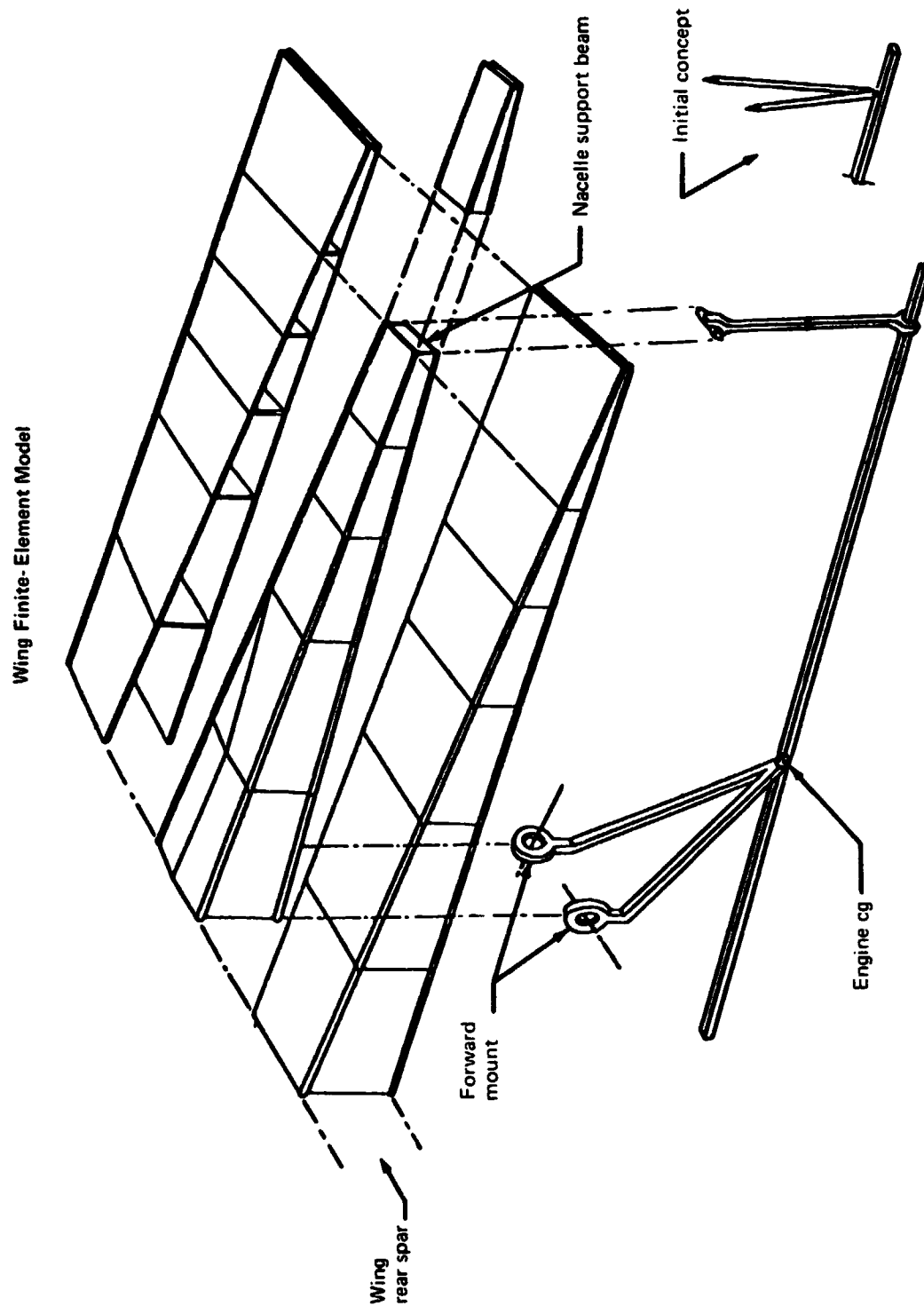


Figure 7-17.—Inboard Nacelle Support Idealization

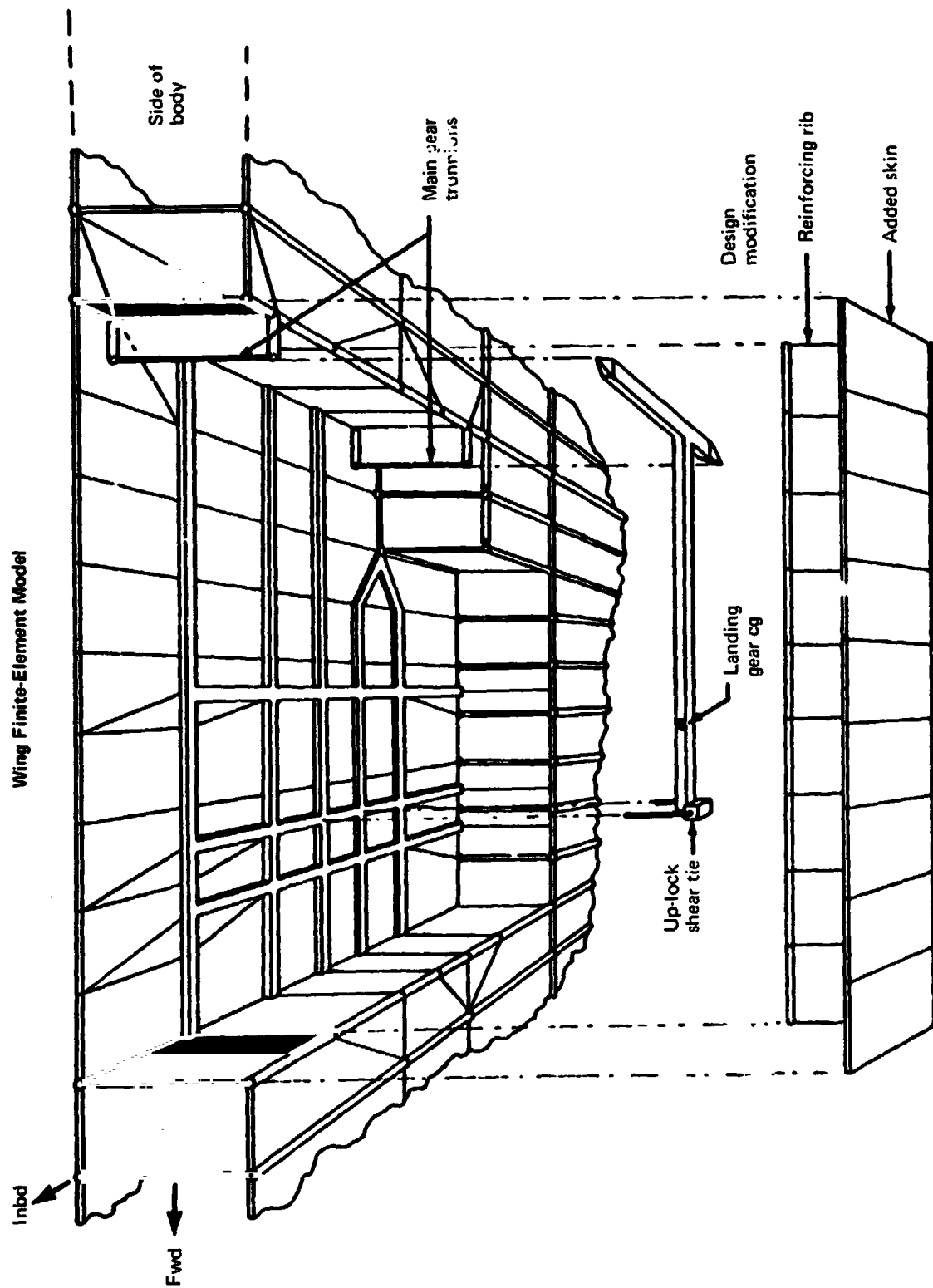


Figure 7-18.—Wheelwell Structural Idealization

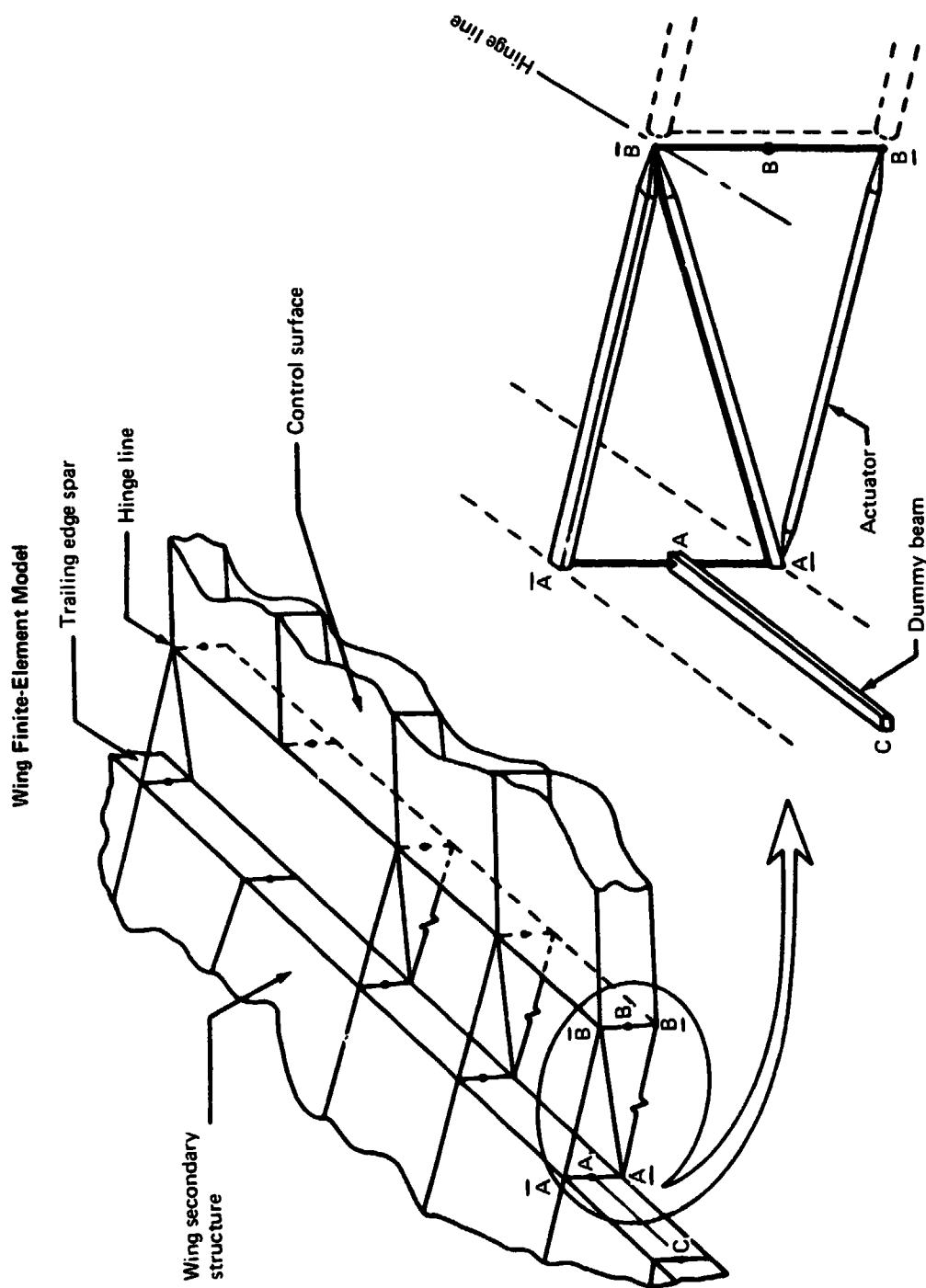


Figure 7-19.—Control Surface Hinge and Actuator Idealization

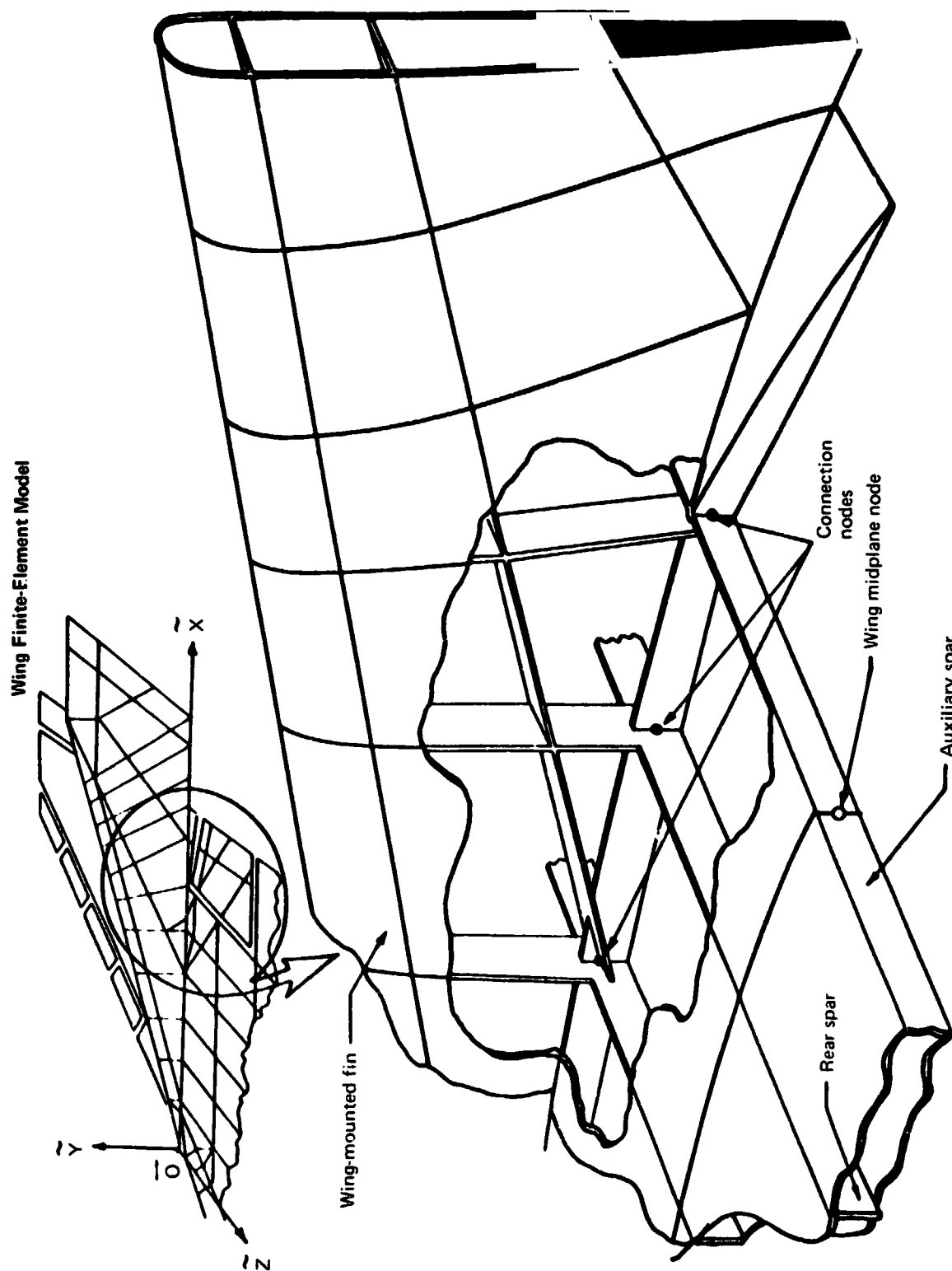
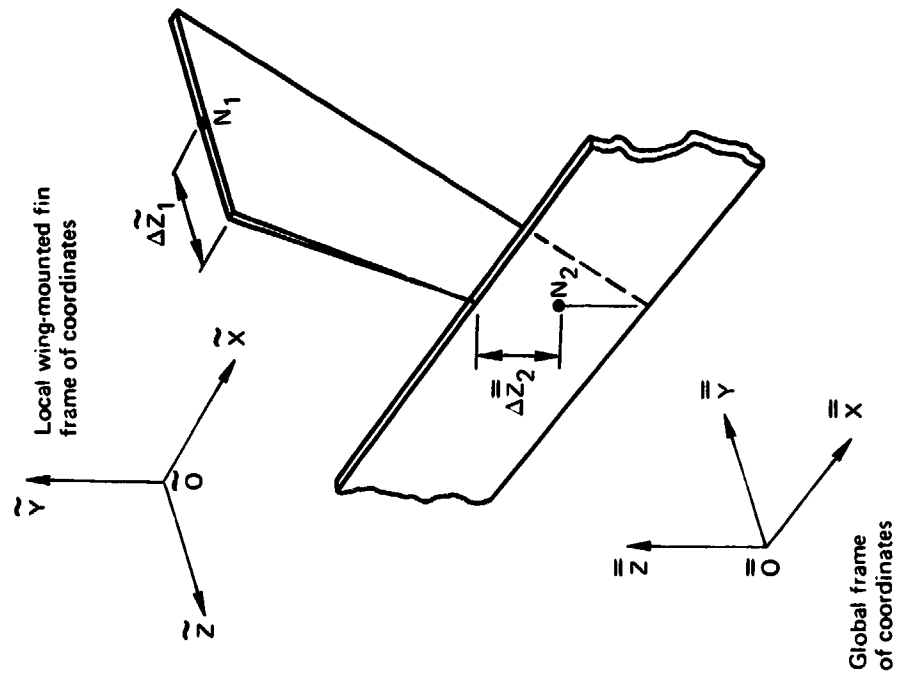


Figure 7-20.—Wing-Mounted Fin Attachment

Apparent Warped Spar Geometry



Spar "N1-N2" Stiffness Element Geometry

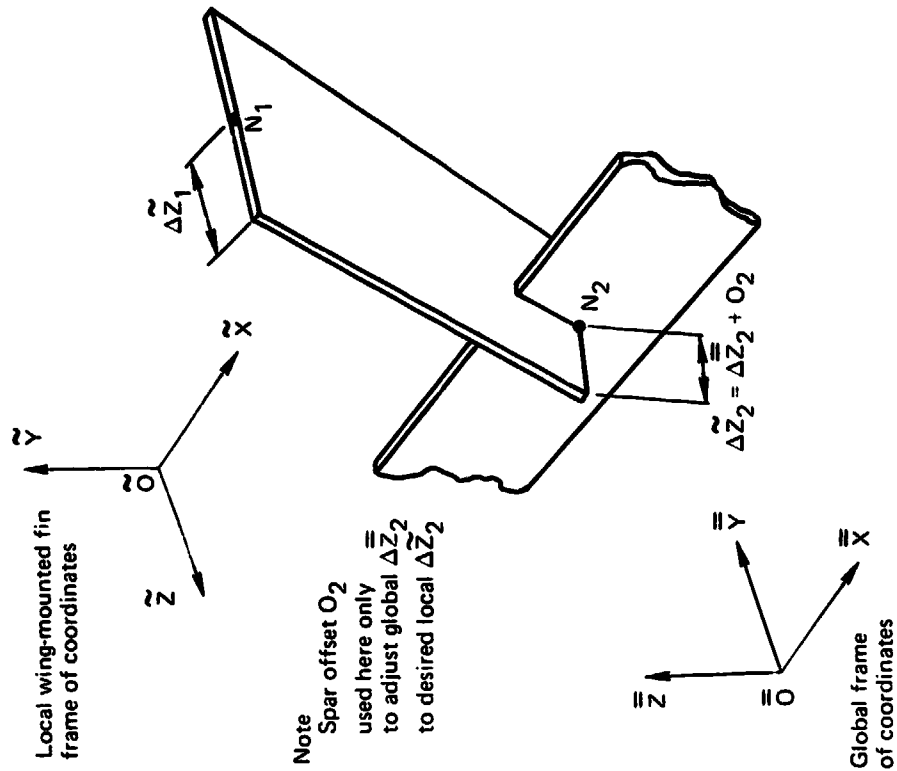


Figure 7-21.—Typical Spar at Wing-Fin Connection
(Zero spar offsets assumed; caps removed for clarity)

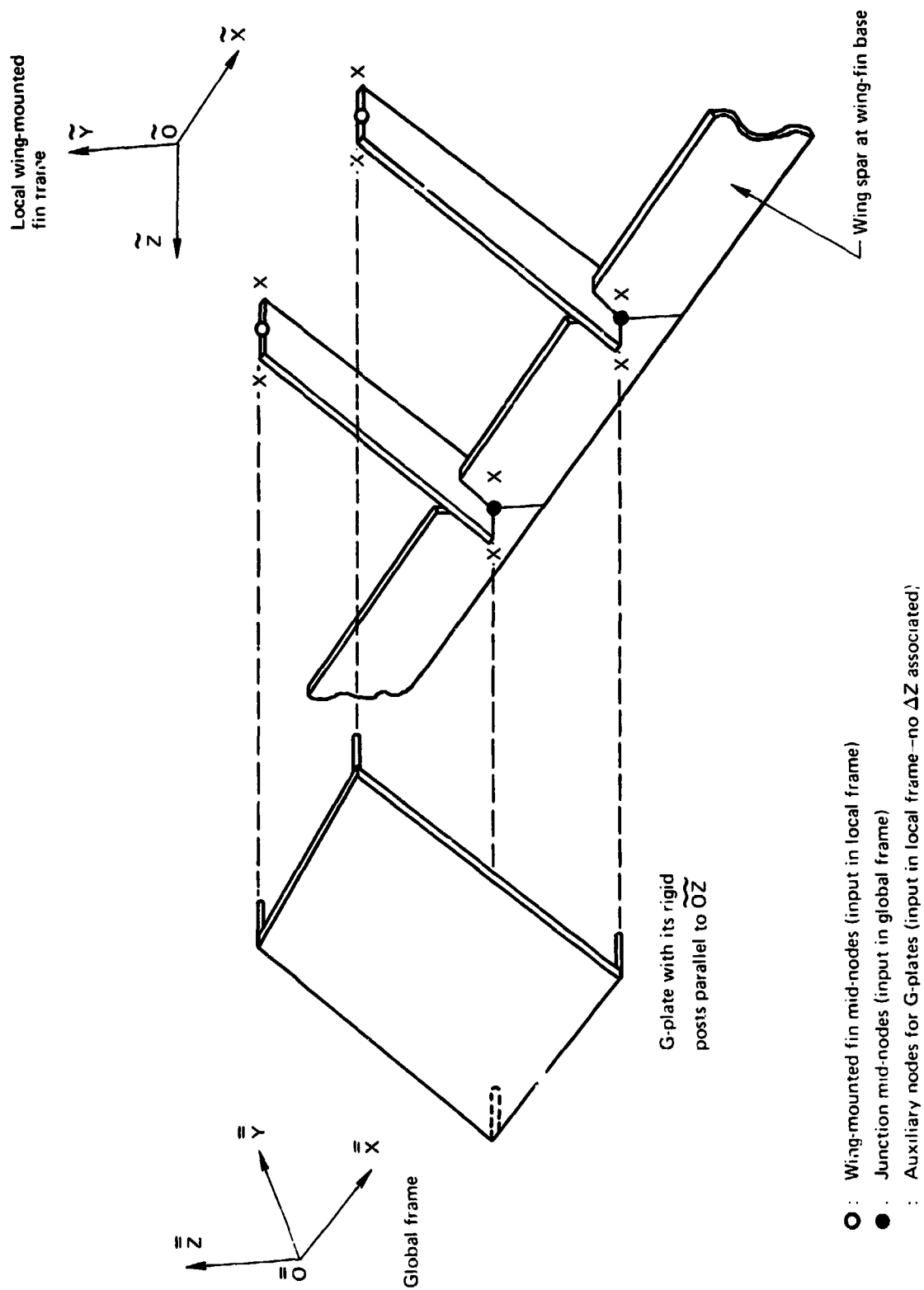


Figure 7-22. — Typical G-Plate at Wing Fin Connection

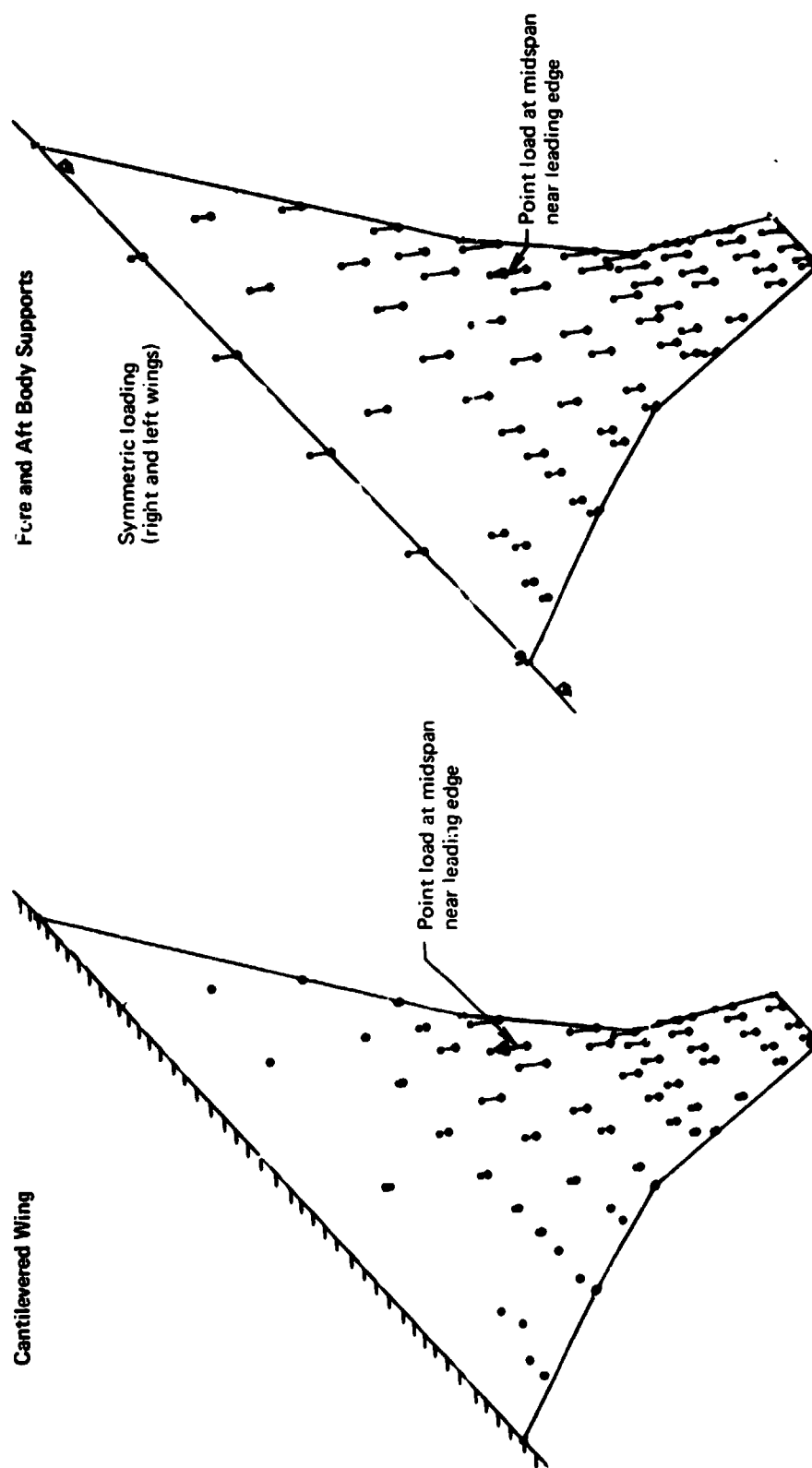


Figure 7-23.—Comparison of Flexibility Influence Coefficients

Fore and Aft Body Supports, Symmetric Loading

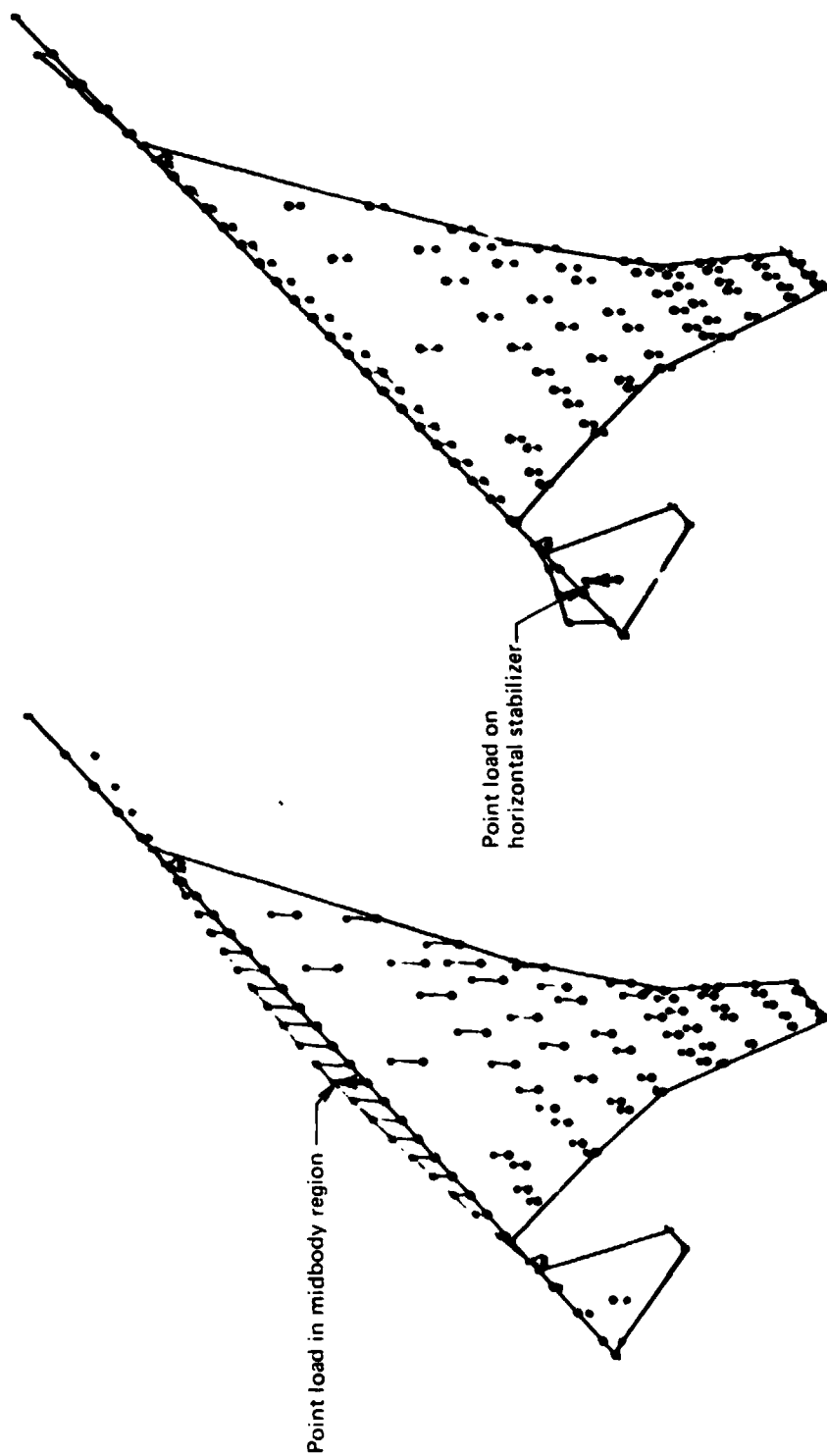


Figure 7.24.—Airplane Flexibility Influence Coefficients

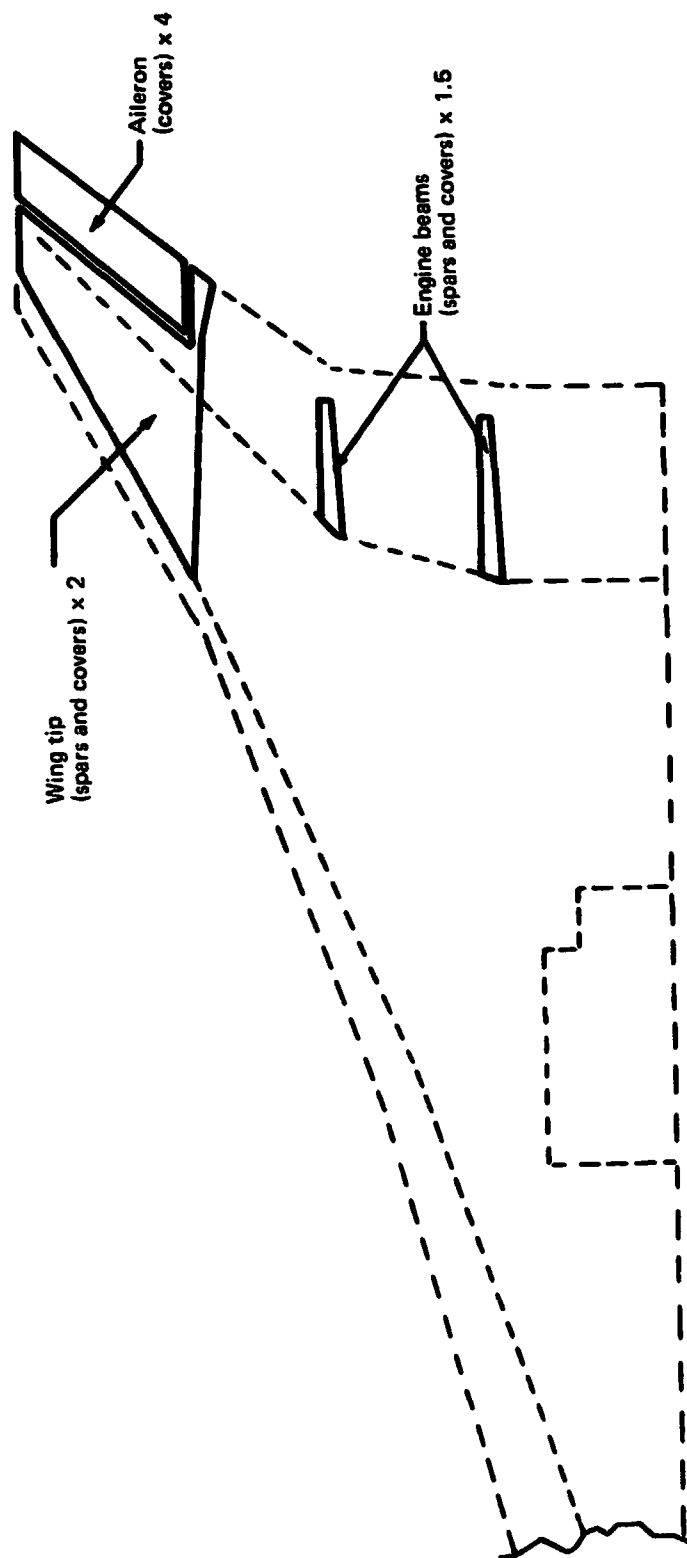
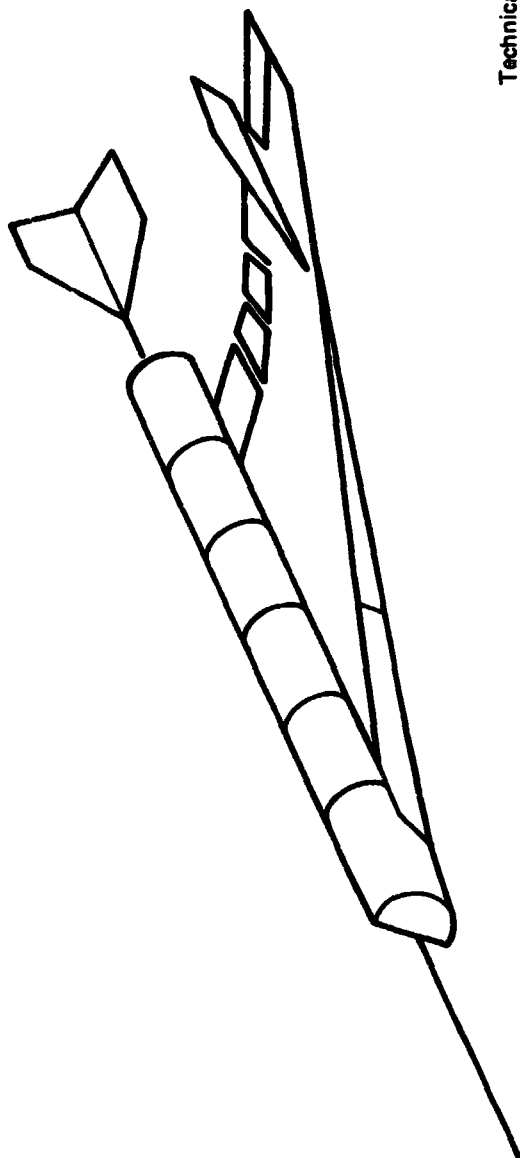


Figure 7-25.—Preliminary Stiffness Resize Prior to Loads Analysis

Figure 7-26.—Structural Model Development, Task/Time



Structural model
Nodes 2000
Elements 4200
Active DOF 8500
Retained DOF 230

Technical analysis	
Module	Purpose
Control	Interface aerodynamic configuration
Stiffness	Flexibility matrix
Control	Invert flexibility and free-up
Control	Modify mass by nonoptimum factors
Mass	Direct mass lumping
Vibration	Eigensolution
Control	Interface flutter solution
Control	Interface FLEXSTAB
Stress	Stress analysis
Design	Fully stressed

Figure 7-27.—Use of ATLAS Program System

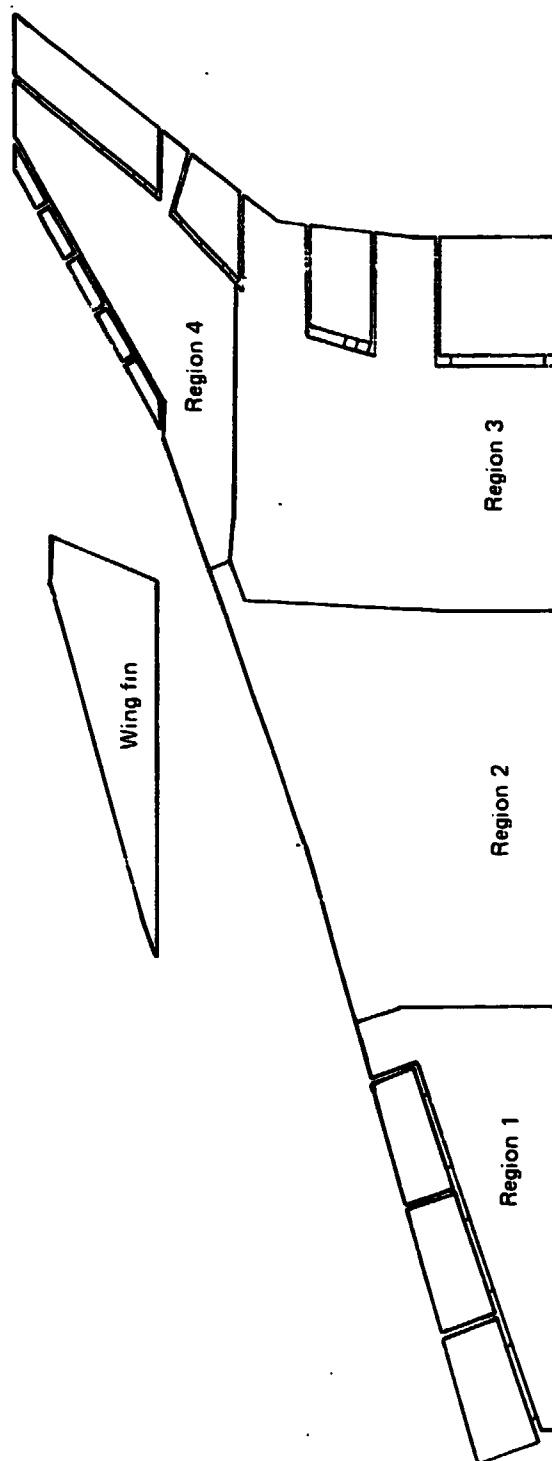


Figure 7-28.—Wing Region Definitions

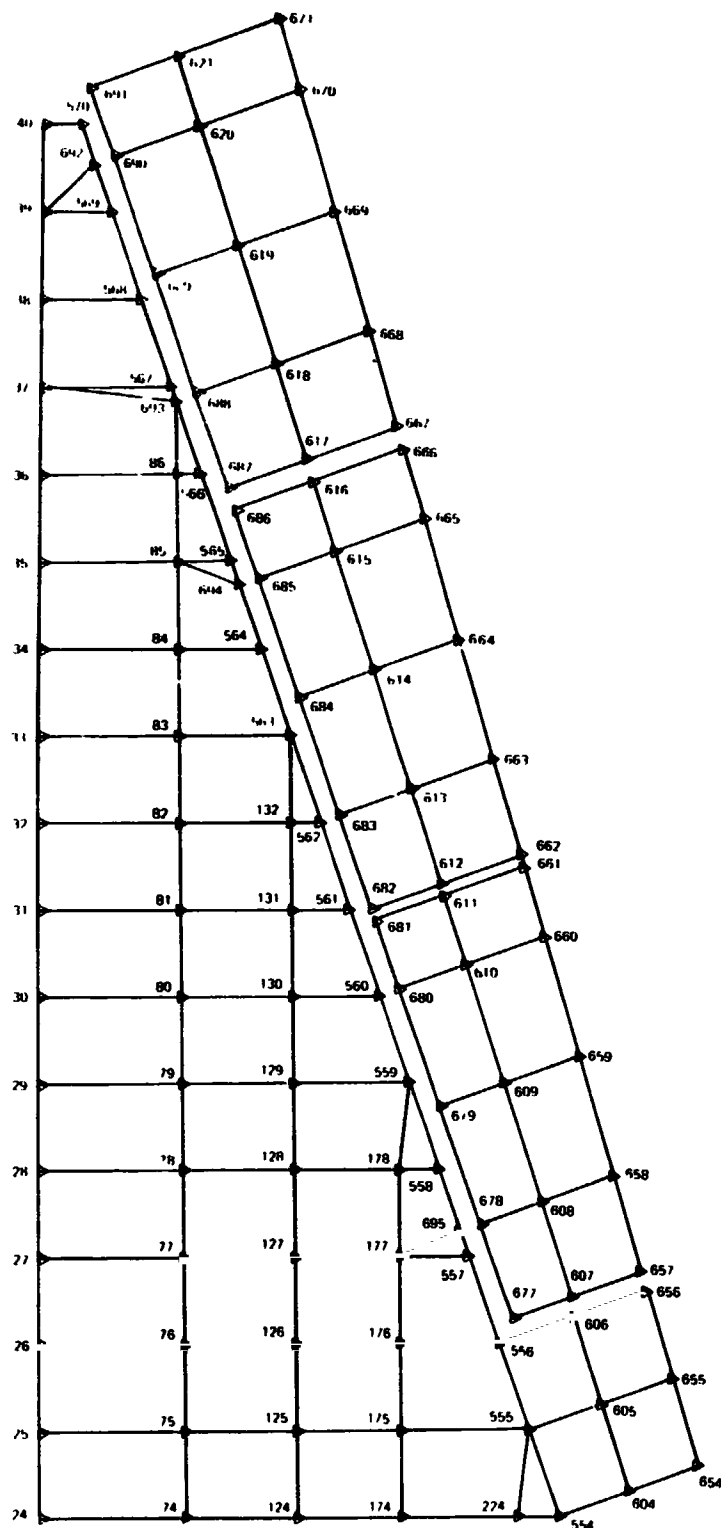
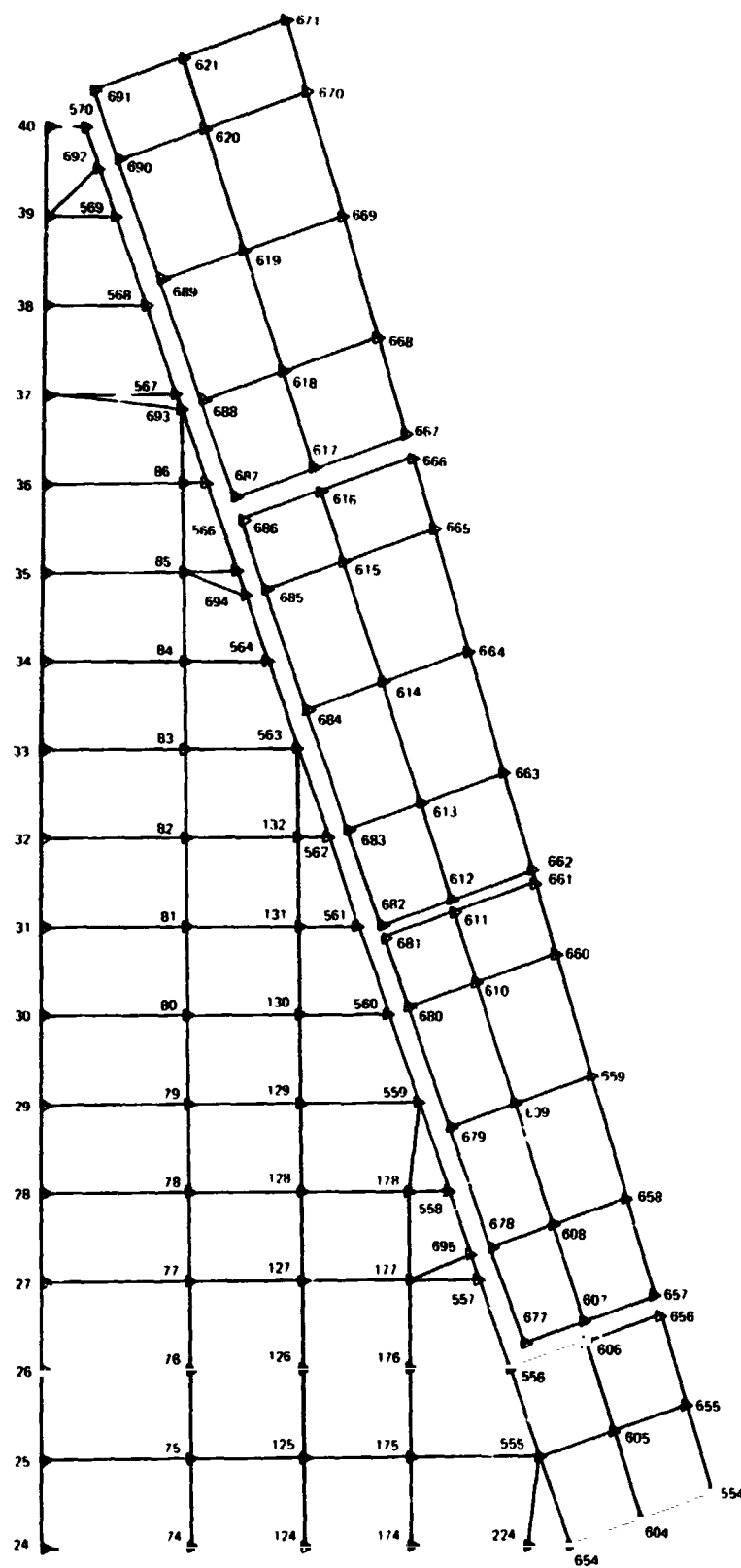


Figure 7-29.—Region 1, Cover Elements



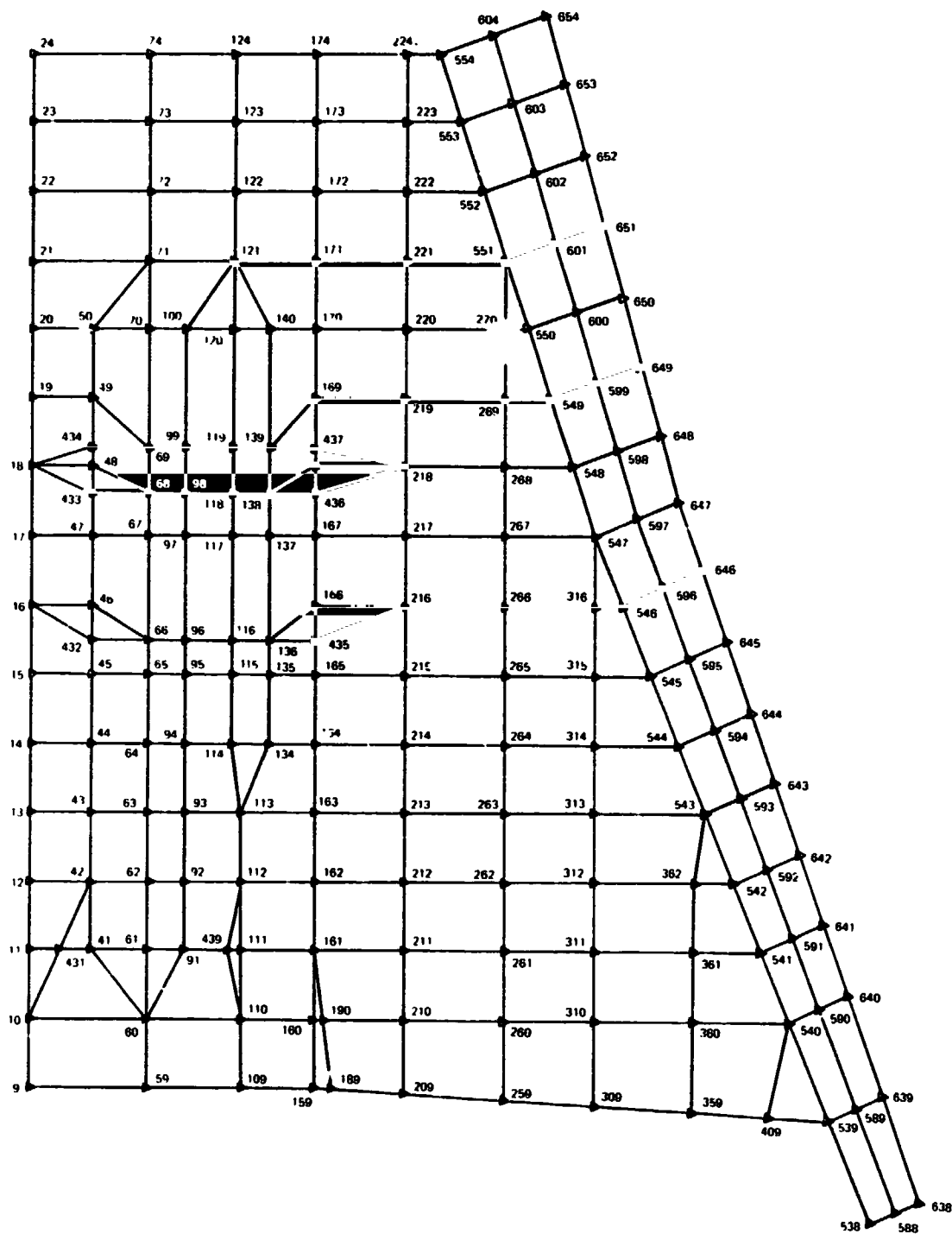


Figure 7-31.—Region 2, Cover Elements

Beam offset nodes in wheel well area not shown
() denotes node out of plane of wing definition

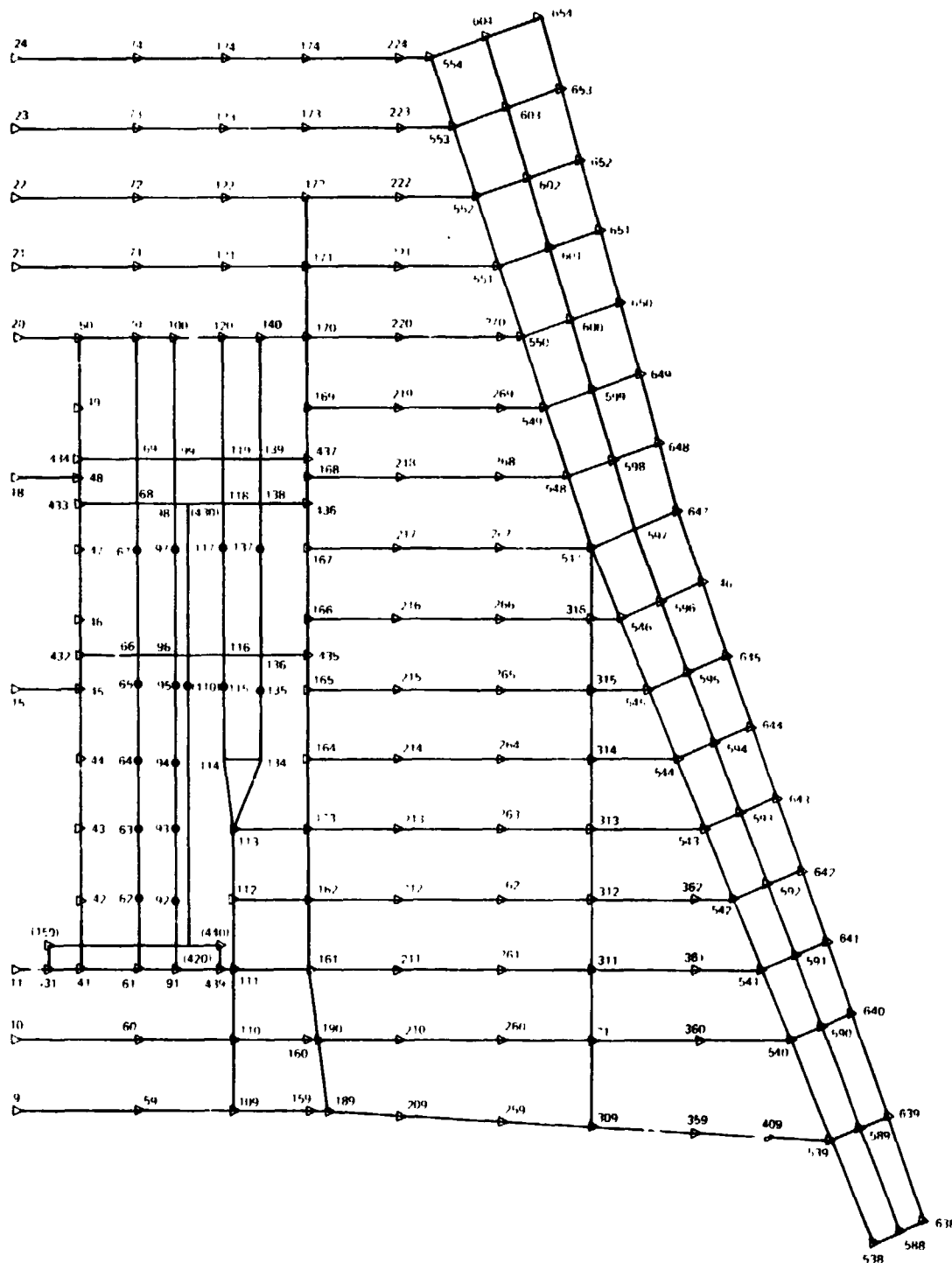


Figure 7-32.--Region 2, Spar and Beam Elements

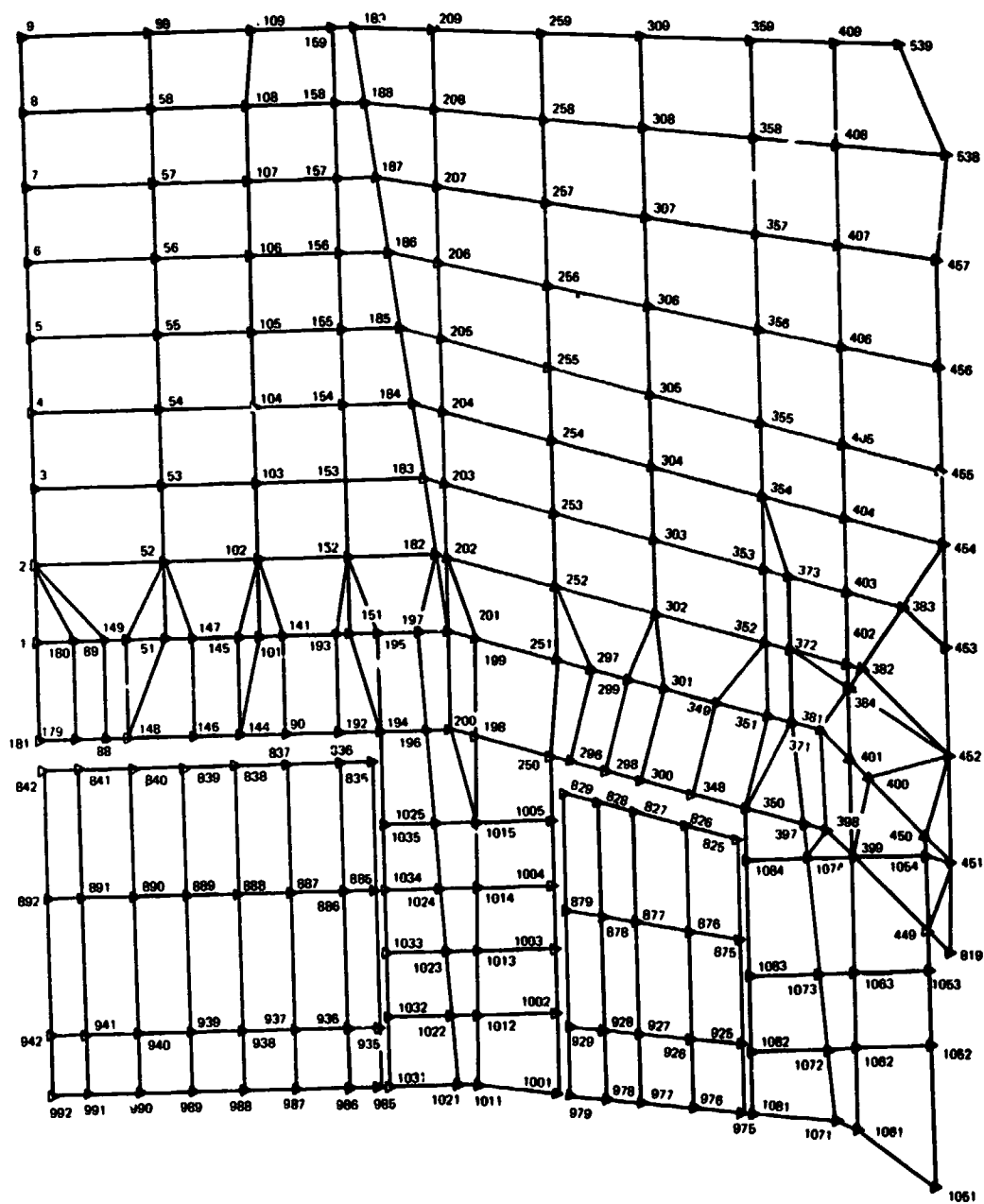


Figure 7-33.—Region 3, Cover Elements

() denotes node out of plane of wing definition

Reference figure 7-19 for detail of control surface hinge and actuator idealization

Node number of \bar{A} = node number of A + 900

Node number of Δ = node number of A + 800 (not shown)

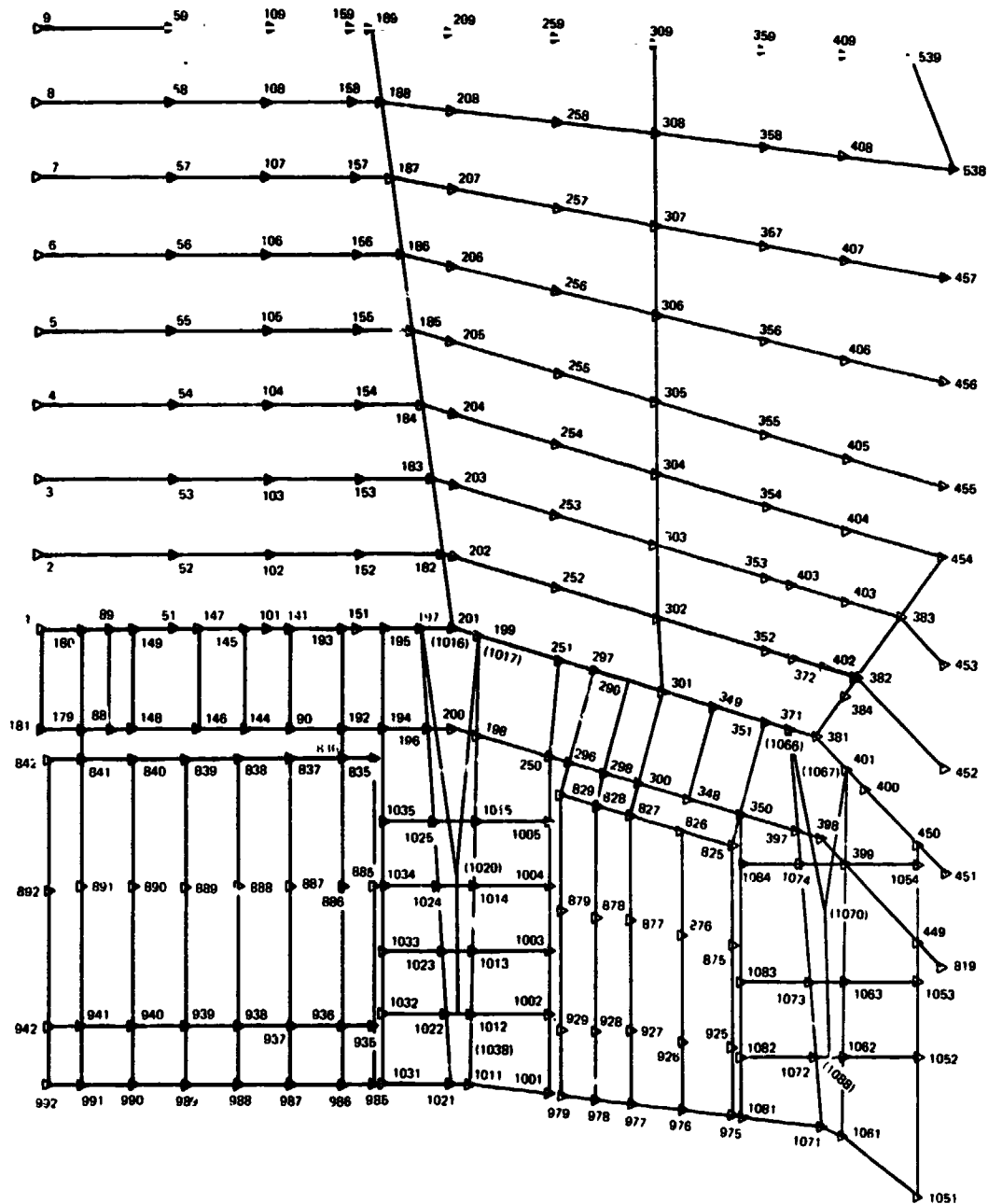


Figure 7-34.—Region 3, Spar and Beam Elements

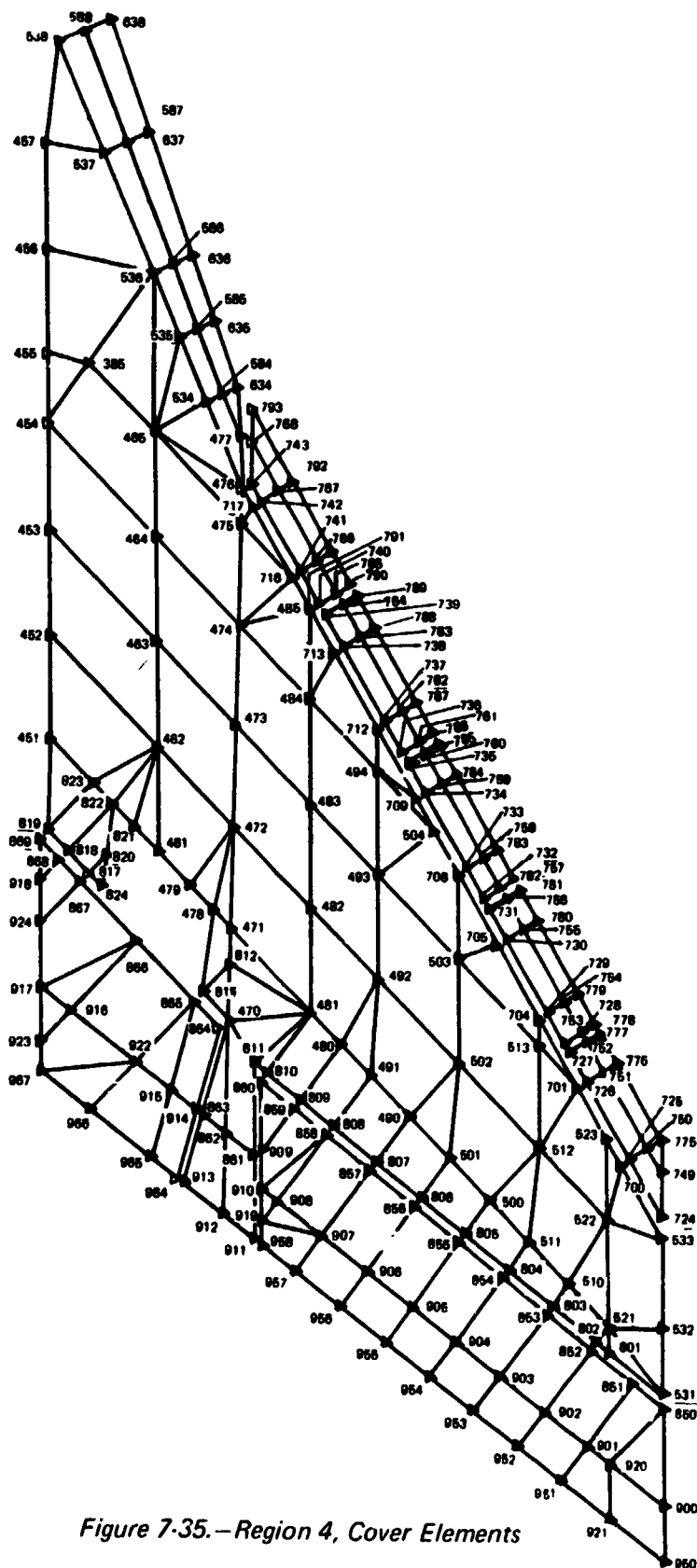
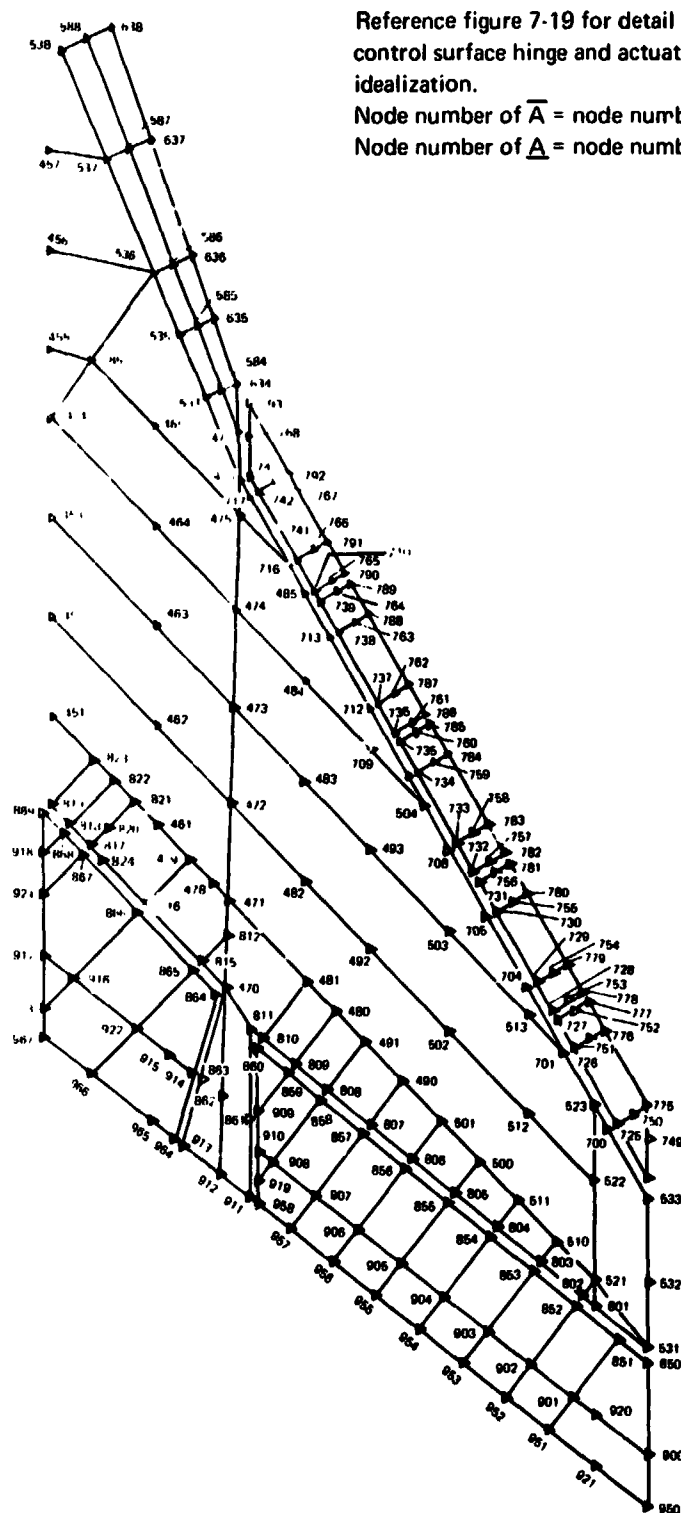


Figure 7-35.—Region 4, Cover Elements



Reference figure 7-19 for detail of control surface hinge and actuator idealization.

Node number of \bar{A} = node number of A + 900

Node number of \underline{A} = node number of A + 800 (not shown)

Figure 7-36.—Region 4, Spar and Beam Elements

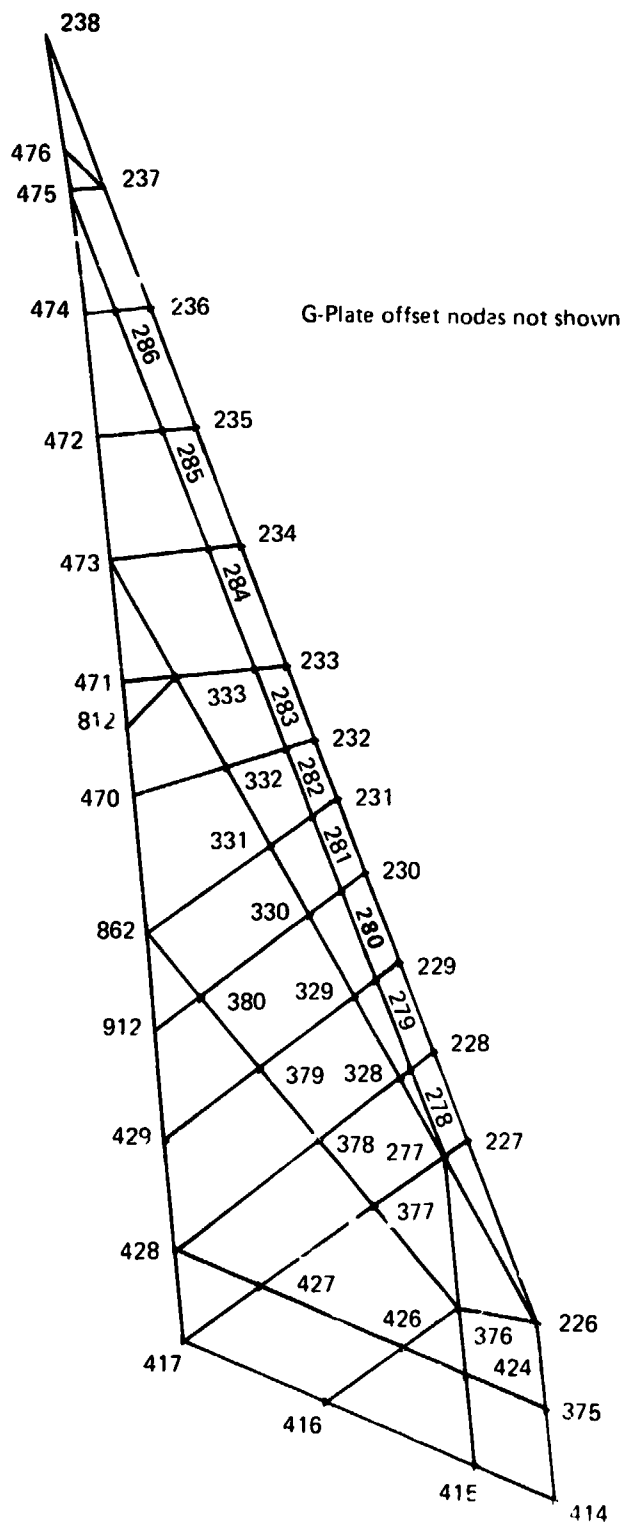


Figure 7-37.—Wing Fin Cover and G-Plate Elements

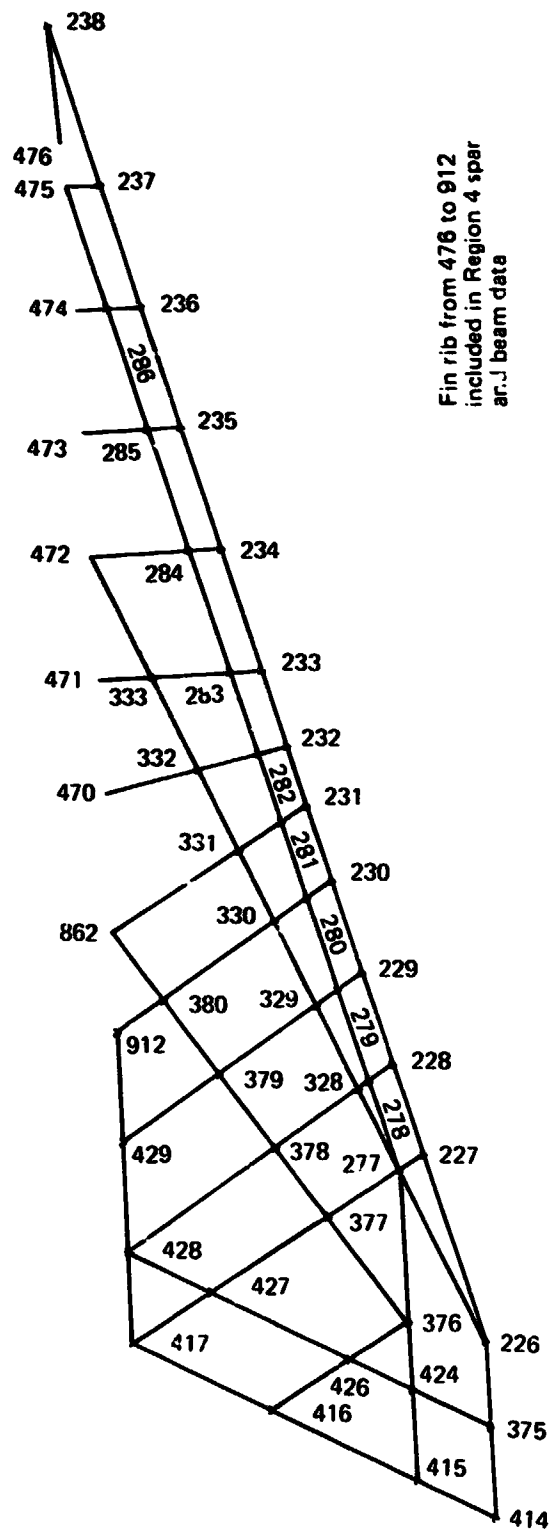


Figure 7-38. —Wing Fin Spar and Beam Elements

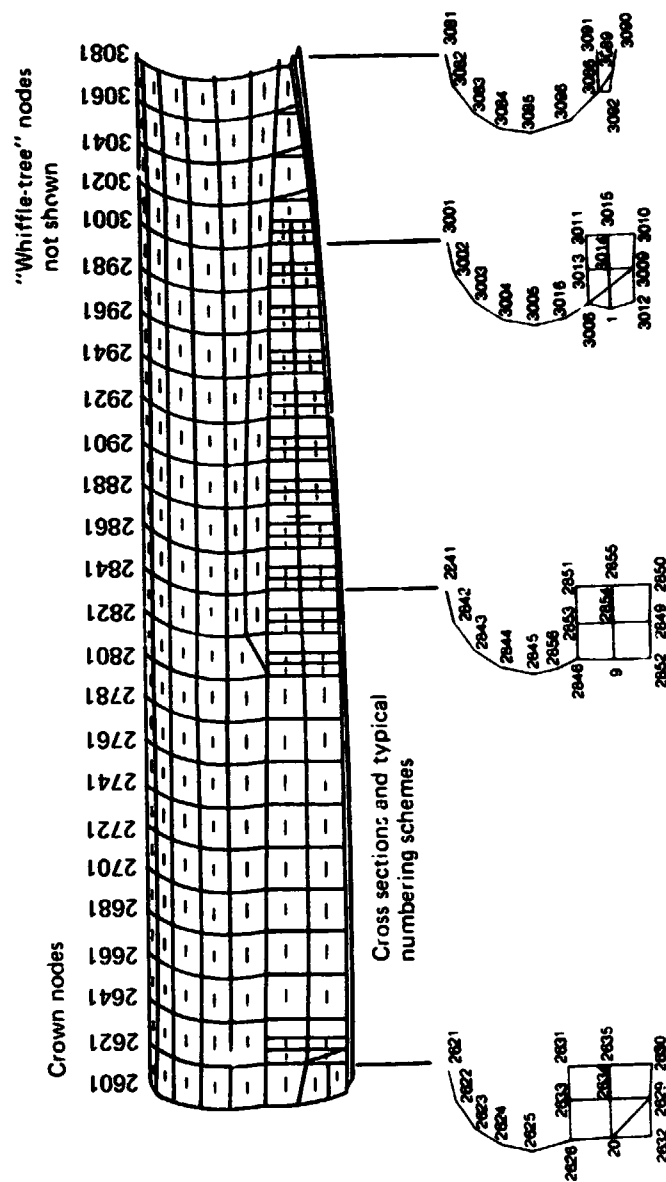


Figure 7-39. —Body Finite Elements, Wheel Well and Aft

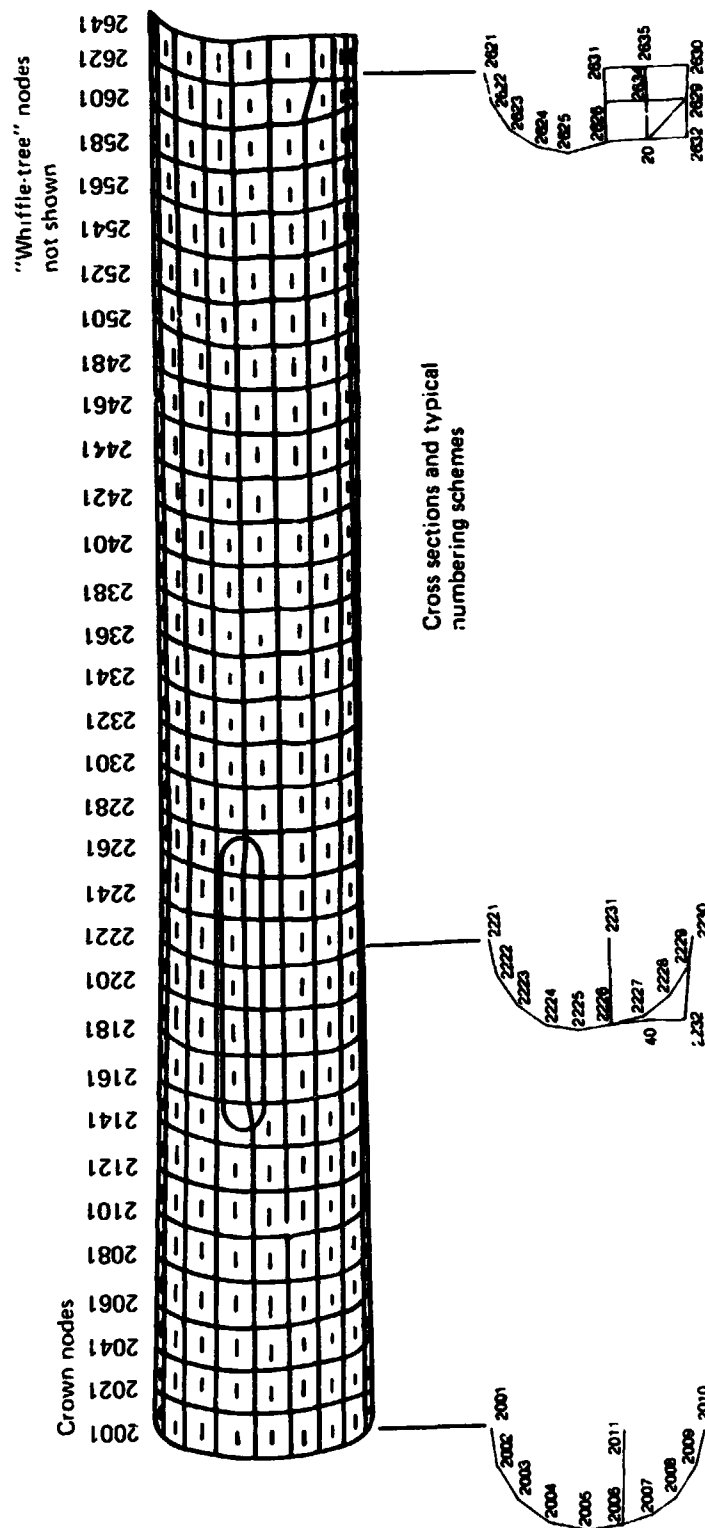


Figure 7.40. —Body Finite Elements Forward of Wheel Well

SECTION 8

LOADS ANALYSIS

by

R. M. Thomas

CONTENTS

	Page
LOADS ANALYSIS	329
Design Loads Analysis	329
Aerodynamic Modeling	330
Structural Modeling	331
Structural Design Placards and Limitations	332
Structural Design Airspeeds	332
Design Gross Weight	333
Flap Deflections	333
Control Surface Deflections	333
Engine Thrust	333
Maneuver and Gust Criteria	334
Landing, Taxi and Ground Handling Loads Criteria	335
Airplane Data	336
Jig Solution	336
Design Load Conditions	336
Critical Load Condition Summary	337
REFERENCES	338

TABLES

8-1	Boeing Program to Improve Efficiency and Reliability of Aeroelastic Loads Analysis	339
8-2	FLEXSTAB Aerodynamic Panel Definition	340
8-3	Design Envelope Points	346
8-4	Flap Placard Speeds	346
8-5	Design Maneuvering Speeds for Positive and Negative Maneuvers	347
8-6	Calculation of Design Speed for Maximum Gust Intensity	348
8-7	Flap Settings for the 969-512B	349
8-8	Geometric Constants	350
8-9	Analysis Conditions	351
8-10	Limit Loads for Ground Handling Conditions	356
8-11	Load Conditions Represented in Loads Matrices	357
8-12	Symmetric Loads Matrix From FLEXSTAB	358
8-13	Anti-Symmetric Loads Matrix From FLEXSTAB	378

FIGURES

8-1	ATLAS-FLEXSTAB Program System	387
8-2	Aerodynamic Paneling for FLEXSTAB	388
8-3	Structural Nodes Retained for Loads Analysis	389
8-4	Retained Degrees of Freedom for Flexibility Matrices	390
8-5	Structural Panels for ESIC	391
8-6	Design Airspeeds, Equivalent Velocity	392
8-7	Design Airspeeds, Mach Number	393
8-8	$C_{L_{Max Dem}}$ Limits	394
8-9	Maximum Flight Weight	395
8-10	969-512B Control Surface Locations	396
8-11	Stabilizer - Elevator Relations, Mechanical Geared Elevator	397
8-12	Deflection Limitations - Outboard Flaperon	398
8-13	Deflection Limitations - Inboard Flaperon	399
8-14	Deflection Limitations - Rudder	400
8-15	Maneuver Envelope at Sea Level	401
8-16	Maneuver Envelope at 10,000 Feet	401
8-17	Maneuver Envelope at 20,000 Feet	402
8-18	Maneuver Envelope at 30,000 Feet	402
8-19	Maneuver Envelope at 40,000 Feet	403
8-20	Maneuver Envelope at 50,000 Feet	403
8-21	Maneuver Envelope at 60,000 Feet	404
8-22	Derived Gust Velocity	405
8-23	2707-300 PPD Limit Vertical Acceleration at Landing Impact	406

FIGURES (Concluded)

8-24	Sign Convention	407
8-25	Geometry & Gear Reactions for Ground Loads	408
8-26	Mid-Cruise Condition for Jig Solution	409
8-27	Jig Shape Deflections	410
8-28	Load Condition Code	411
8-29	Definition of Load Reference Axis	412
8-30	Design Ultimate Shear Force Envelope for the Wing in Symmetrical Flight Conditions	413
8-31	Design Ultimate Bending Moment Envelope for the Wing in Symmetrical Flight Conditions	414
8-32	Design Ultimate Torque Envelope for the Wing in Symmetrical Flight Conditions	415
8-33	Design Ultimate Shear Force Envelope for the Body in Symmetrical Flight Conditions	416
8-34	Design Ultimate Bending Moment Envelope for the Body in Symmetrical Flight Conditions	417
8-35	Forward Body Ultimate Shear Force Caused by Landing Impact	418
8-36	Forward Body Ultimate Bending Moment Caused by Landing Impact	419

Symbols and Abbreviations

$C_{L_{MAX\ dem}}$	Maximum demonstrated lift coefficient
$C_{L_{min}}$	Minimum value of lift coefficient
$C_{N_{\alpha}}$	Slope of normal force coefficient versus angle of attack
D_M	Main gear drag reaction
D_N	Nose gear drag reaction
M_C	Design cruise Mach number
M_D	Design dive Mach number
M_{MO}	Mach number corresponding to the maximum operating speed
n	Normal load factor in a maneuver
n_{gust}	Normal load factor in a gust
q	Dynamic pressure
S_M	Main gear side load
S_N	Nose gear side load
U_{de}	Derived gust velocity
V_A	Design maneuver speed at a positive load factor
V_B	Design speed for maximum gust intensity
V_C	Design cruise speed
V_D	Design dive speed
V_e	Equivalent velocity
V_F	Design flap speed
V_H	Design maneuver speed at a negative load factor
$V_{min\ dem}$	Minimum demonstrated airspeed

Symbols (Concluded)

V_{MO}	Maximum operating speed
V_M	Main gear vertical reaction
V_N	Nose gear vertical reaction
V_{TAS}	True airspeed
α	Angle of attack
β	Angle of sideslip
δ_a	Aileron deflection
δ_e	Elevator deflection
δ_r	Rudder deflection
θ	Pitch angle
ϕ	Roll angle
ψ	Yaw angle
FAR	Federal Aviation Regulations
TAS	Tentative Airworthiness Standards for Supersonic Transports

SECTION 8

LOADS ANALYSIS

DESIGN LOADS ANALYSIS

The analysis of loads for the strength design of the Arrow Wing Supersonic Transport was accomplished with the use of the FLEXSTAB (ref. 8-1) and ATLAS (ref. 8-2) Program Systems.

FLEXSTAB is a system of programs developed by Boeing under contract NAS2-5006 to NASA Ames Research Center. It was designed to predict the stability characteristics of flexible airplanes based on the geometry, mass distribution and flexibility of the airframe, using linear aerodynamic and structural influence coefficient theory. Although not principally designed as a loads analysis tool, FLEXSTAB generates sufficient information in the process of performing a stability analysis, that its extension for use in loads analysis is a fairly simple task. The aerodynamic representation used in the FLEXSTAB system is based on the finite element method developed by Woodward to solve linearized potential flow equations for supersonic and subsonic speeds. This approach uses the vortex lattice analogy for lifting surfaces, and a system of flow singularities on the mean surface for the interference shell in supersonic flow. Slender body theory is used for slender bodies such as the fuselage and nacelle.

In preparation for the Arrow Wing contract, a Boeing development effort was directed at producing a version of FLEXSTAB that would satisfy the needs of the Loads group in analyzing design loads. The changes and additions made to FLEXSTAB during this time are shown in table 8-1. These changes were subsequently incorporated in the official NASA version of FLEXSTAB 1.2.

The modifications to FLEXSTAB were carried out with two major purposes in mind—improved program efficiency and improved analytical capability—and table 8-1 identifies in which of these categories the various changes fall.

ATLAS is a Boeing developed system of technical program modules executed under a user defined control program. In the Arrow Wing loads analysis, the ATLAS stiffness module was used to generate the structural flexibility matrices and the mass module to generate the mass matrices for FLEXSTAB. Figure 8-1 shows a schematic diagram of the ATLAS-FLEXSTAB program system as used in the Arrow Wing loads analysis.

From the point of view of improved program efficiency, the most significant items identified in table 8-1 are the addition of the capability to cycle through multiple load cases, the establishment of tape interfaces between ATLAS and FLEXSTAB for the transmittal of data that are common to both programs, and the capability for the user to retain those structural degrees of freedom in which he is interested, rather than his being forced to retain all translational freedoms at each retained node.

The loads analysis conditions were selected on the basis of the requirements of the Federal Aviation Regulations, Part 25 and the Tentative Airworthiness Standards for Supersonic Transports. Boeing's extensive experience in the loads analysis for the National SST and the previous NASA study for the Boeing Model 969-336C configuration (developed from the NASA SCAT-15F) were used as a basis for selecting potential critical design conditions. Where appropriate, data obtained for these two previous designs were used in this study and are identified where they occur.

AERODYNAMIC MODELING

FLEXSTAB PANELLING SCHEME

The aerodynamic panel scheme used in FLEXSTAB to generate the aerodynamic influence coefficient matrix is shown in figure 8-2 and defined in table 8-2. This model represents 173 panels. The general guidelines adhered to in this particular selection of panels are as follows:

1. The spanwise width of each panel shall be approximately the same.
2. Panels shall be narrow in a chordwise direction in areas of rapidly changing pressure, such as at the wing leading edges.
3. Panel boundaries shall coincide with control surface edges.
4. Adjacent panels shall not be staggered, that is, adjacent panels shall have common corner points.
5. Streamwise panel boundaries on the horizontal tail shall be colinear with panel boundaries on the wing.

Item 5 is only necessary if, as is assumed in this analysis, there is little or no vertical separation between wing and horizontal tail. If the two surfaces are separated vertically by a distance of approximately one half the spanwise width of a wing panel, there is no need for the panel boundaries to be colinear.

Obviously, there are some areas where all of the conditions listed above cannot be satisfied simultaneously. For the aerodynamic model shown in figure 8-2, for example, conditions 1 and 3 cannot both be satisfied. In this case, where a control surface boundary occurs within the boundaries of an aerodynamic panel, the "area ratio" capability of FLEXSTAB must be resorted to. For flaps down conditions, where the camber of an entire panel is changed to represent the flap deflection, the magnitude of the camber change for an aerodynamic panel only partially covered by a control surface, is reduced by the fraction of the total panel area represented by the control surface within that panel. While this is by no means an entirely rigorous solution, studies have shown that it does provide an adequate estimate of the panel loading.

The spoilers and spoiler-slot deflectors cannot be represented theoretically in FLEXSTAB since they involve large angular displacements and flow through the wing

from one surface to the other. In a production program, the influence of spoilers on design loads would be accounted for by superimposing measured pressure data on the basic FLEXSTAB solution, but in the present analysis no such data were available, and the effects of spoilers and spoiler-slot deflectors were ignored.

It has also been found that FLEXSTAB is not capable of an adequate representation of the flow field and resulting pressure distribution caused by underwing nacelles. For the Arrow Wing loads analysis, the interference effects of the nacelles were computed externally and superimposed on the basic FLEXSTAB solution. The calculation of these nacelle pressures is based on the method described in reference 8-3. This consists of assuming that linear theory correctly predicts the perturbation velocities produced by the nacelles but that their longitudinal location requires shifting, the magnitude of this shift being related to the nacelle geometry. Shock waves are inserted and the complete flow field may be calculated including the effects of pressure field reflections.

STRUCTURAL MODELING

STRUCTURAL FLEXIBILITY MATRICES

Symmetrical and asymmetrical flexibility matrices for use in the FLEXSTAB loads analysis were generated in ATLAS. A structural model with 164 retained nodes and 192 degrees of freedom was selected from the complete structural mathematical model. The retained nodes, shown in figure 8-3, were selected to provide adequate accuracy in the definition of the airload distribution over the wing, while minimizing the computing costs. The degrees of freedom retained on each component of the airframe for both symmetrical and asymmetrical flexibility matrices are shown in figure 8-4.

STRUCTURAL DATA IN FLEXSTAB

The External Structural Influence Coefficient (ESIC) program in FLEXSTAB takes the flexibility matrices, nodal geometry of the retained nodes and the mass matrices generated by ATLAS as input data. The transmittal of these data is on magnetic tape and is accomplished by the use of the ATLAS-FLEXSTAB interface subroutine within ATLAS. Structural panels are defined by the analyst, each utilizing three or four of the nodes retained in the generation of the flexibility matrices. The deflections at the corners of these triangular or quadrilateral panels are then used by ESIC to compute the streamwise slope influence coefficients at the aerodynamic centers of the FLEXSTAB aerodynamic panels. The structural panels used in ESIC are shown in figure 8-5.

While ESIC has the ability to extrapolate should an aerodynamic center fall outside the boundaries of a structural panel, the accuracy of such extrapolation is very questionable. As a consequence, care was taken in the Arrow Wing loads analysis to ensure that enough structural nodes were retained on the periphery of the planform that extrapolation by FLEXSTAB was unnecessary. Retention of such extreme nodes, however, can lead to additional problems when it comes to modeling the mass of the structure. In any program such as ATLAS, where the distributed mass is lumped to concentrated masses at the retained nodes, great care must be taken to avoid large

masses being assigned to nodes on the leading or, especially, the trailing edge nodes. Large weights applied to the very thin structure at the trailing edge, for example, give rise to excessively large, and unrealistic, local deformations.

STRUCTURAL DESIGN PLACARDS AND LIMITATIONS

The structural design placards for the Arrow Wing were established in accordance with the requirements of the FAR Part 25 and the Tentative Airworthiness Standards for Supersonic Transports. Where appropriate, recourse was made to the extensive analyses performed for the Boeing 2707-300 National SST in the selection of design parameters.

The structural design airspeeds for the Arrow Wing are shown in figures 8-6 and 8-7, and tables 8-3 through 8-6. The variation of the maximum demonstrated normal force coefficient for use in computing the design maneuvering speed, V_A , is shown in figure 8-8, and the variation of maximum flight weight with altitude in figure 8-9. For negative maneuvers, $C_{L_{MIN}}$ was assumed to be 70% of $C_{L_{MAX DEM}}$.

STRUCTURAL DESIGN AIRSPEEDS

MAXIMUM OPERATING SPEED/MACH NUMBER

The maximum operating speed and Mach number, V_{MO}/M_{MO} , are determined in such a manner as to include all normal operational flight conditions including climb, cruise and descent. The speeds chosen for the Arrow Wing were those determined for the Boeing 2707-300.

DESIGN CRUISING SPEED/MACH NUMBER

The design cruising speed, V_C , is selected to be equal to V_{MO} . Supersonic cruise Mach number is selected as $M_C = 2.7$. The design cruising speeds as selected exceed the requirements of FAR 25.335(a).

DESIGN DIVE SPEED/MACH NUMBER

The design dive speed V_D , is the maximum speed for which the airplane is designed. The design dive speed and Mach number, V_D/M_D , are selected to be the same as those used on the 2707-300, which provided an adequate speed margin between V_C/M_C and V_D/M_D , and met the requirements of TAS [FAR 25.335(b)].

DESIGN MANEUVERING SPEED

The design maneuvering speed, V_A , is the maximum speed at which maneuvers can be performed without regard for structural integrity. This speed is based on the following equation:

$$V_A = V_{MIN DEM} \sqrt{2.5}$$

where $V_{MIN DEM}$ is the minimum demonstrated speed with flaps retracted or a lesser speed based on a rational selection of CL_{MAX} for structural design. This criterion is intended to comply with TAS [FAR 25.335(c)].

DESIGN SPEED FOR MAXIMUM GUST INTENSITY

The design speed for maximum gust intensity, V_B , is established in the subsonic regime in accordance with FAR 25.335(d) and TAS [FAR 25.335(d)]. The V_B concept is not used for supersonic flight where slowdown or gust avoidance may not be operationally feasible.

DESIGN GROSS WEIGHT

The variation of maximum flight weight with altitude is shown in figure 8-9. Other pertinent gross weights are shown below:

Condition	Weight, lb
Maximum flight weight	743,000
Maximum zero fuel weight	407,246
Minimum weight and ballast	346,346
Maximum takeoff weight	748,000
Maximum landing weight	480,000

FLAP DEFLECTIONS

The leading and trailing edge flap deflections for various stages of flight are defined in table 8-7 and the location of these flaps is shown in figure 8-10.

CONTROL SURFACE DEFLECTIONS

The elevator is mechanically geared to the stabilizer for longitudinal control throughout the airplane operational envelope. The deflection relationship between the two surfaces is shown in figure 8-11. All three segments of the rudder are operable for takeoff, climb-out and landing configurations. Deflection of the upper segment to its maximum range is permitted in the climb-out, takeoff and landing configurations but at higher speeds, the upper segment is locked out. Slot-deflector spoilers in combination with the inboard flaperons provide roll control throughout the airplane operating envelope. Low speed roll control is augmented by the outboard flaperon.

Available control surface deflections are shown in figures 8-12 through 8-14.

ENGINE THRUST

The maximum installed thrust for the ATAT-1 engine on the 969-512B are shown below. These data are based on a power setting of 2 (GE4 J6G) on a standard day, except at Mach 2.9 where the maximum power setting is assumed to be 3.2.

Mach No.	Altitude, ft	Installed Thrust Per Engine, lb
0	0	56,767
0.6	5,000	54,028
0.9	25,000	36,000
1.2	35,000	30,600
1.6	40,000	31,421
2.0	45,000	36,329
2.2	45,000	42,751
2.7	60,000	29,336
2.9	60,000	23,040

MANEUVER AND GUST CRITERIA

SYMMETRICAL MANEUVERS

Flight loads for symmetrical balanced maneuvers are established within the maneuvering envelope in accordance with FAR 25.333, 25.337 and 25.345. Except as limited by maximum design lift coefficients, the design limit load factors are as follows:

	Positive Limit Load Factor	Negative Limit Load Factor
All speeds up to V_C	2.5	-1.0
At V_D	2.5	0.0
Flaps Down Conditions	2.0	0.0

The airplane is assumed to be in equilibrium with zero pitching acceleration. The effects of pitching velocity are accounted for in the analysis. The airplane is analyzed for maneuvers at all points on or within the maneuver envelope for both maximum and minimum gross weights at the appropriate altitude.

PITCHING MANEUVERS

The following maneuvers are considered to satisfy the requirements of FAR 25.331(c).

1. **Maximum Stabilizer Displacement**—The airplane is assumed to be flying in a steady level flight attitude at speeds from V_A to V_D and the pitch control is suddenly deflected in an up or down direction at the maximum rate available to a deflection consistent with pilot effort.
2. **Checked Maneuvers**—The airplane is assumed to be subjected to checked maneuvers for balanced conditions at any load factor within the design maneuver envelope and at all speeds between V_A and V_D . The elevators are checked back to a position such that the airplane pitching accelerations meet or exceed the requirements of FAR 25.331(c).

MANEUVER ENVELOPES

Maneuver envelopes for typical altitudes and the maximum flight weight are shown in figures 8-15 through 8-21.

YAWING MANEUVERS

Loads due to yawing maneuvers are established in compliance with FAR 25.351. The following conditions are considered:

1. From a condition of steady level flight at zero sideslip, displace the rudder control to the maximum position as limited by stops, boost capacity or pedal force.
2. With the rudder control displaced as in (1), allow the airplane to yaw to a maximum sideslip angle.
3. With the airplane yawed to the sideslip angle consistent with (2), return the rudder abruptly to neutral.
4. With the airplane yawed to the static sideslip angle consistent with the control displacement in (1), return the rudder control abruptly to the maximum value in the opposite direction.

GUST LOADS

Loads due to both vertical and lateral gust are computed at all speeds and altitudes on and within the flight envelope in compliance with FAR 25.341 and 25.351(b). Use is made of the revised gust load formula in computing airplane load factors due to gusts. The design airspeed for maximum gust intensity, V_B , is not considered at supersonic speeds. The magnitudes of the design gust velocities considered at various design speeds are shown in figure 8-22. These gust velocities are in compliance with FAR 25.341 and TAS [FAR 25.341].

LANDING, TAXI AND GROUND HANDLING LOADS CRITERIA

LANDING IMPACT

Design landing impact loads were determined for the Boeing 2707-300 airplane using a dynamic analysis which included the significant elastic modes of the airframe, rigid body degrees of freedom and a representation of the energy absorption characteristics of the landing gear shock strut and tires. Landing impact loads for the 969-512B Arrow Wing configuration were obtained by applying the load factors obtained for the 2707-300 to the mass distribution of the Arrow Wing. Aerodynamic forces acting during landing impact were neglected. The distribution of fuselage load factors used is shown in figure 8-23.

TAXI AND GROUND HANDLING LOADS

The taxi loads are computed on the assumption that the airplane experiences a 2g acceleration at the center of gravity while taxiing. This requirement meets or exceeds the requirement of FAR 25.235. The ground handling loads are computed in compliance with the requirements of FAR 25.493, 25.495, 25.499, 25.503, 25.507 and 25.509. In all these conditions, the external loads are placed in equilibrium with the linear and angular inertia loads in a rational manner

AIRPLANE DATA

The geometric parameters used in the aeroelastic loads analysis are shown in table 8-8. The sign convention for aerodynamic forces and moments used in FLEXSTAB is shown in figure 8-24 and the definition of geometry and forces for the ground load conditions is shown in figure 8-25.

JIG SOLUTION

The jig-shape represents the stress-free condition for the aircraft structure and corresponds to a state of zero applied loads. The jig-shape is related to an optimum cruise shape of the airplane generally taken at a point midway through the average mission. The desired jig shape is, then, a function of the loads on the airplane at this cruise condition, and the stiffness of the structure. As the design of the airframe progresses through the various design cycles to meet strength and stiffness requirements, the aeroelastic loads and the jig shape are also affected and must be included in the iterative loop.

The analysis of design loads is based on the camber slopes for this jig shape. On the other hand, the performance of the configuration is optimized for a shape corresponding to a particular flight condition—normally, a mid-cruise condition. Before calculating design loads, therefore, the jig shape must be computed from the shape defined for use in the performance calculations.

The jig shape is obtained by calculating the trimmed loads for the mid-cruise design condition, with the airplane treated as a rigid body. The resulting loads are then applied to a flexible airplane and the increments of camber and displacement due to this loading are subtracted from those defined for the design condition to yield the jig shape. The design point at mid-cruise chosen for the Arrow Wing is shown in figure 8-26. The wing and body vertical displacements from the jig shape in the mid-cruise design condition are shown in figure 8-27.

DESIGN LOAD CONDITIONS

Analysis conditions were selected on and within the maneuver envelope to cover the complete range of Mach numbers, design speeds and load factors. Maximum flight weight at the appropriate altitude, and maximum zero fuel weight plus reserve fuel, were considered for all maneuver conditions. In addition, the minimum flight weight, which occurs in the ferry flight configuration, was considered for the gust conditions.

The conditions analyzed comprised the following:

1. Symmetric, balanced maneuvers at maximum flight weight
2. Symmetric, balanced maneuvers at maximum zero fuel weight plus reserve fuel
3. Design vertical gusts at maximum flight weight
4. Design vertical gusts at the ferry flight weight
5. Checked and unchecked elevator maneuvers as specified in FAR 25.331(c)
6. Design lateral gusts at the maximum flight weight
7. Rudder maneuvers as specified in FAR 25.351(a)
8. Landing impact
9. Taxi
10. Ground handling as specified in FAR 25.471 through 25.509.

The analysis conditions considered are listed in tables 8-9 and 8-10 and the critical design condition are shown in table 8-11. A description of the condition number code is shown in figure 8-28. Envelopes of design shear force, bending moment and torsion about the axis shown in figure 8-29 for symmetrical flight conditions are shown in figures 8-30, 8-31 and 8-32 for the wing, and figures 8-33 and 8-34 for the body. Table 8-10 presents the gear loads in the ground conditions and figures 8-35 and 8-36 the forward body shear force and bending moment for landing impact.

CRITICAL LOAD CONDITION SUMMARY

The net loads at the structural nodes retained in the generation of the flexibility matrix are shown in tables 8-12 and 8-13 for those design conditions that were passed on to the ATLAS stress module. These loads are presented in the form of two matrices. The first matrix contains the loads for symmetrical maneuvers and the symmetrical part of the lateral gust and rudder maneuver loads. The second contains the asymmetrical loads in the lateral gust and rudder maneuver conditions.

Each row of these matrices represents the load in a particular direction at a particular retained node and each column corresponds to a particular load condition. The direction of the load and the node at which it is applied is identified in the left hand margin of tables 8-12 and 8-13, and the load cases represented by each column are identified in table 8-11.

REFERENCES

- 8-1 Hink, G. R., et al., *A Method for Predicting the Stability Characteristics of an Elastic Airplane*, NASA CR-114713, October 197
- 8-2 Dreisbach, R. L., *ATLAS-An Integrated Structural Analysis and Design System, User's Manual-Input and Execution Data (ATLAS 3)*, December 1974.
- 8-3 Kane, E. J., and Middleton, W. D., *Considerations of Aerodynamic Interference in Supersonic Airplane Design*, AGARD-CP-71-71, January 1971.

Table 8-1.—Boeing Program to Improve Efficiency and Reliability of Aeroelastic Loads Analysis

	Reason for modification	
	Improved efficiency	Improved capability
<p>Addition of capability to cycle through multiple load cases for balanced maneuvers or unit solutions</p> <p>For unit solutions on $\alpha, \beta, q, \dot{\theta}, \dot{\phi}, \dot{\psi}, \delta_E, \delta_R, \delta_A, V_{TAS}, \text{THRUST},$ ALTITUDE and ATTITUDE</p> <p>For balanced maneuvers on: $n, q, \dot{\theta}, V_{TAS}, U_{de}, \text{THRUST and ALTITUDE}$</p>	●	
Added capability to generate rigid and flexible solutions in one computer run	●	
Capability to select the degrees of freedom retained at the structural nodes	●	●
Addition of the static gust solution based on the revised gust load formula		●
Addition of the capability to superimpose an externally generated pressure distribution on that computed by FLEXSTAB (nacelles, for example)		●
Added capability to generate in FLEXSTAB the airloads and the inertia loads at the nodes separately		●
Added capability to specify load factor rather than pitch rate for balanced maneuvers	●	●
Added capability to put user specified matrices on the FLEXSTAB output tape		●
Print out the equivalent airspeed and C_{N_α} in SD&SS		●
Develop interfaces: ATLAS \rightarrow FLEXSTAB and FLEXSTAB \rightarrow ATLAS	●	
*Develop a program (VAMAT) providing the capability to generate net shear, moment, and torsion along wing, body, and horizontal tail in user-specified cross sections (using FLEXSTAB tape output)		●
*Develop a program (VMTSCM) providing the capability to scan through the loads and select critical loads	●	●
*Develop a plotting program providing plots of shear, moment, and torsion along wing, body, and horizontal tail	●	●

*These programs are not part of the FLEXSTAB program.

Table 8-2.—FLEXSTAB Aerodynamic Panel Definition

Body		24 Panels			
Panel edge	Panel edge	Panel Corner Point Coordinates			
BL inboard, In.	BL outboard, In.	BS inboard LE, In.	BS inboard TE, In.	BS outboard LE, In.	BS outboard TE, In.
0.	8.6560	217.5	336.0180	217.5	336.0180
0.	30.3478	336.0180	514.6620	336.0180	514.6620
0.	48.7175	514.6620	663.2429	514.6620	663.2429
0.	58.3415	663.2429	811.8239	663.2429	811.8239
0.	60.	811.8239	960.4049	811.8239	960.4049
0.	60.	960.4049	1108.9859	960.4049	1108.9859
0.	60.	1108.9859	1257.5668	1108.9859	1257.5668
0.	60.	1257.5668	1406.1478	1257.5668	1406.1478
0.	60.	1406.1478	1554.7288	1406.1478	1554.7288
0.	60.	1554.7288	1703.3098	1554.7288	1703.3098
0.	60.	1703.3098	1851.8907	1703.3098	1851.8907
0.	60.	1851.8907	2000.4717	1851.8907	2000.4717
0.	60.	2000.4717	2149.0527	2000.4717	2149.0527
0.	60.	2149.0527	2297.6337	2149.0527	2297.6337
0.	60.	2297.6337	2446.2146	2297.6337	2446.2146
0.	60.	2446.2146	2594.7956	2446.2146	2594.7956
0.	60.	2594.7956	2743.3766	2594.7956	2743.3766
0.	60.	2743.3766	2891.9576	2743.3766	2891.9576
0.	60.	2891.9576	3040.5385	2891.9576	3040.5385
0.	60.	3040.5385	3189.1195	3040.5385	3189.1195
0.	60.	3189.1195	3337.7005	3189.1195	3337.7005
0.	60.	3337.7005	3486.2815	3337.7005	3486.2815
0.	60.	3486.2815	3634.8624	3486.2815	3634.8624
0.	60.	3634.8624	3783.4434	3634.8624	3783.4434

Inboard nacelle		4 panels			
Panel edge	Panel edge	Panel Corner Point Coordinates			
BL inboard, In.	BL outboard, In.	BS inboard LE, In.	BS inboard TE, In.	BS outboard LE, In.	BS outboard TE, In.
256.9275	257.0725	2745.6249	2872.1471	2745.6249	2872.1471
256.9	257.1	2872.1471	2998.6694	2872.1471	2998.6694
256.9	257.1	2998.6694	3125.1917	2998.6694	3125.1917
256.9196	257.0804	3125.1917	3251.7139	3125.1917	3251.7139

Table 8-2.—Continued

Outboard nacelle

4 panels

Panel edge	Panel edge	Panel Corner Point Coordinates			
BL inboard, In.	BL outboard, In.	BS inboard LE, In.	BS inboard TE, In.	BS outboard LE, In.	BS outboard TE, In.
437.9275	438.0725	2763.4241	2890.2223	2763.4241	2890.2223
437.9	438.1	2890.2223	3017.0206	2890.2223	3017.0206
437.9	438.1	3017.0206	3143.8189	3017.0206	3143.8189
437.9196	438.0725	3143.8189	3270.6171	3143.8189	3270.6171

Fin

12 panels

Panel edge	Panel edge	Panel Corner Point Coordinates			
WL lower, In.	WL upper, In.	BS inboard LE, In.	BS inboard TE, In.	BS outboard LE, In.	BS outboard TE, In.
460.	578.8272	3297.6182	3376.5510	3417.2162	3463.5049
460.	578.8272	3376.5510	3455.4839	3463.5049	3509.7936
460.	578.8272	3455.4839	3534.4168	3509.7936	3556.0824
460.	578.8272	3534.4178	3613.3496	3556.0824	3602.3711
460.	578.8272	3613.3496	3666.6782	3602.3711	3640.9926
460.	578.8272	3666.6782	3720.0069	3640.9926	3679.6142
578.8272	697.6545	3417.2162	3463.5049	3536.8114	3550.4590
578.8272	697.6545	3463.5049	3509.7936	3550.4590	3564.1035
578.8272	697.6545	3509.7936	3556.0824	3564.1035	3577.7480
578.8272	697.6545	3556.0824	3602.3711	3577.7480	3591.3926
578.8272	697.6545	3602.3711	3640.9926	3591.3926	3615.3070
578.8272	697.6545	3640.9926	3679.6142	3615.3070	3639.2215

Table 8-2.—Continued

Wing fin

18 panels

Panel edge	Panel edge	Panel Corner Point Coordinates			
WL lower, In.	WL upper, In.	BS inboard LE, In.	BS inboard TE, In.	BS outboard LE, In.	BS outboard TE, In.
400.	471.5	2883.9991	2921.6515	3134.6796	3155.7906
400.	471.5	2921.6515	2966.0297	3155.7906	3180.5726
400.	471.5	2966.0297	3010.4079	3180.6726	3205.5546
400.	471.5	3010.4079	3054.7861	3205.5546	3230.4366
400.	471.5	3054.7861	3099.1643	3230.4366	3255.3187
400.	471.5	3099.1643	3121.3534	3255.3187	3267.7597
400.	471.5	3121.3534	3143.5425	3267.7597	3280.2007
400.	471.5	3143.5425	3195.3550	3280.2007	3309.8117
400.	471.5	3195.3550	3240.3071	3309.8117	3334.4548
400.	471.5	3240.3071	3284.2592	3334.4548	3359.0979
400.	471.5	3284.2592	3336.1296	3359.0979	3388.1806
400.	471.5	3336.1296	3388.0000	3388.1806	3417.2634
471.5	543.	3134.6796	3180.6726	3385.3602	3395.3156
471.5	543.	3180.6726	3230.4366	3395.3156	3406.0873
471.5	543.	3230.4366	3267.7597	3406.0873	3414.1660
471.5	543.	3267.7597	3309.8117	3414.1660	3423.2684
471.5	543.	3309.8117	3359.0979	3423.2684	3433.9366
471.5	543.	3359.0979	3417.2634	3433.9366	3446.5268

Horizontal tail

12 panels

Panel edge	Panel edge	Panel Corner Point Coordinates			
BL inboard, In.	BL outboard, In.	BS inboard LE, In.	BS inboard TE, In.	BS outboard LE, In.	BS outboard TE, In.
60.	159.	3321.4111	3404.8060	3455.7014	3505.5237
60.	159.	3404.8060	3488.2008	3505.5237	3555.3460
60.	159.	3488.2008	3571.5956	3555.3460	3605.1682
60.	159.	3571.5956	3654.9905	3605.1682	3654.9905
60.	159.	3654.9905	3719.2170	3654.9905	3695.3264
60.	159.	3719.2170	3783.4434	3695.3264	3735.6622
159.	257.	3455.7014	3505.5237	3589.6353	3605.2241
159.	257.	3505.5237	3555.3460	3605.2241	3621.8129
159.	257.	3555.3460	3605.1682	3621.8129	3638.4017
159.	257.	3605.1682	3654.9905	3638.4017	3654.9905
159.	257.	3654.9905	3695.3264	3654.9905	3671.6771
159.	257.	3695.3264	3735.6622	3671.6771	3688.3637

Table 8-2.—Continued

Wing		99 panels			
Panel edge	Panel edge	Panel Corner Point Coordinates			
BL inboard, In.	BL outboard, In.	BS inboard LE, In.	BS inboard TE, In.	BS outboard LE, In.	BS outboard TE, In.
60.	159.	1163.9763	1327.2444	1511.4087	1645.5904
60.	159.	1327.2444	1490.5124	1645.5904	1779.7996
60.	159.	1490.5124	1778.4599	1779.7996	2009.8897
60.	159.	1778.4599	2066.4074	2009.8897	2239.9798
60.	159.	2066.4074	2354.3550	2239.9798	2470.0698
60.	159.	2354.3550	2642.3025	2470.0698	2700.1599
60.	159.	2642.3025	2786.2762	2700.1599	2815.2500
60.	159.	2786.2762	2930.2500	2815.2500	2930.2500
60.	159.	2930.2500	2990.2500	2930.2500	2990.2500
60.	159.	2990.2500	3070.5647	2990.2500	3069.7104
60.	159.	3070.5647	3150.8794	3069.7104	3149.1709
159.	257.	1511.4087	1645.5904	1855.3317	1960.7208
159.	257.	1645.5904	1779.7996	1960.7208	2066.1646
159.	257.	1779.7996	2009.8897	2066.1646	2238.9817
159.	257.	2009.8897	2239.9798	2238.9817	2411.7988
159.	257.	2239.9798	2470.0698	2411.7988	2584.6158
159.	257.	2470.0698	2700.1599	2584.6158	2757.4329
159.	257.	2700.1599	2815.2500	2757.4329	2843.8415
159.	257.	2815.2500	2930.2500	2843.8415	2930.2500
159.	257.	2930.2500	2990.2500	2930.2500	2990.2500
159.	257.	2990.2500	3069.7104	2990.2500	3068.8648
159.	257.	3069.7104	3149.1709	3068.8648	3147.4796
257.	348.	1855.3317	1960.7208	2174.6888	2253.3820
257.	348.	1960.7208	2066.1646	2253.3820	2332.0751
257.	348.	2066.1646	2238.9817	2332.0751	2457.6018
257.	348.	2238.98177	2411.7988	2457.6018	2583.1286
257.	348.	2411.7988	2584.6158	2582.1286	2708.6553
257.	348.	2584.6158	2757.4329	2708.6553	2834.1821
257.	348.	2757.4329	2843.8415	2834.1821	2896.9454
257.	348.	2843.8415	2930.2500	2896.9454	2959.7088
257.	348.	2930.2500	2990.2500	2959.7088	3016.0960
257.	348.	2990.2500	3068.8648	3016.0960	3087.1142
257.	348.	3068.8648	3147.4796	3087.1142	3158.1324
348.	438.	2174.6888	2253.3820	2461.1081	2503.2549
348.	438.	2253.3820	2332.0751	2503.2549	2545.4017
348.	438.	2332.0751	2457.6018	2545.4017	2634.0901
348.	438.	2457.6018	2583.1286	2634.0901	2722.7785
348.	438.	2583.1286	2708.6553	2722.7785	2811.4670
348.	438.	2708.6553	2834.1821	2811.4670	2900.1554
348.	438.	2834.1821	2896.9454	2900.1554	2944.4996
348.	438.	2896.9454	2959.7088	2944.4996	2988.8438
348.	438.	2959.7088	3016.0960	2988.8438	3041.6580
348.	438.	3016.0960	3087.1142	3041.6580	3105.1631
348.	438.	3087.1142	3158.1324	3105.1631	3168.6682

Table 8-2.—Continued

Panel edge	Panel edge	Panel Corner Point Coordinates			
BL inboard, In.	BL outboard, In.	BS inboard LE, In.	BS inboard TE, In.	BS outboard LE, In.	BS outboard TE, In.
438.	514.	2461.1081	2503.2549	2672.7764	2703.2506
438.	514.	2503.2549	2545.4017	2703.2506	2733.7248
438.	514.	2545.4017	2634.0901	2733.7248	2800.3248
438.	514.	2634.0901	2722.7785	2800.2348	2866.7447
438.	514.	2722.7785	2811.4670	2866.7447	2933.2547
438.	514.	2811.4670	2900.1554	2933.2547	2999.7646
438.	514.	2900.1554	2944.4996	2999.7646	3033.0196
438.	514.	2944.4996	2988.8438	3033.0196	3066.2746
438.	514.	2988.8438	3041.5580	3066.2746	3119.0880
438.	514.	3041.6580	3105.1631	3119.0880	3172.8063
438.	514.	3105.1631	3168.6682	3172.8063	3226.5182
514.	589.84	2672.7764	2703.2506	2883.9991	2902.8253
514.	589.84	2703.2506	2733.7248	2902.8253	2921.6515
514.	589.84	2733.7248	2800.2348	2921.6515	2966.0297
514.	589.84	2800.2348	2866.7447	2966.0297	3010.4079
514.	589.84	2866.7447	2933.2547	3010.4079	3054.7861
514.	489.84	2933.2547	2999.7646	3054.7861	3099.1643
514.	589.84	2999.7646	3033.0196	3099.1643	3121.3534
514.	589.84	3033.0196	3066.2746	3121.3534	3143.5425
514.	589.84	3066.2746	3119.0880	3143.5425	3196.3550
514.	589.84	3119.0880	3172.8063	3196.3550	3240.3071
514.	589.84	3172.8063	3226.5182	3240.3071	3284.2465
589.84	658.	2883.9991	2903.8253	3001.8095	3020.7588
589.84	658.	2902.8253	2921.6515	3020.7588	3039.7081
589.84	658.	2921.6515	2966.0297	3039.7081	3073.9289
589.84	658.	2966.0297	3010.4079	3073.9289	3108.1499
589.84	658.	3010.4079	3054.7861	3108.1499	3142.3708
589.84	658.	3054.7861	3099.1643	3142.3708	3176.5917
589.84	658.	3099.1643	3121.3534	3176.5917	3193.7022
589.84	658.	3121.3534	3143.5425	3193.7022	3210.8126
489.84	658.	3143.5425	3202.9365	3210.8126	3256.6125
589.84	658.	3202.9365	3243.5978	3256.6125	3296.3799
589.84	658.	3243.5978	3284.2465	3296.3799	3335.1288
658.	727.	3001.8095	3020.7588	3121.0718	3140.1458
658.	727.	3020.7588	3039.7081	3140.1458	3159.2197
658.	727.	3039.7081	3073.9289	3159.2197	3183.1581
658.	727.	3073.9289	3108.1499	3183.1581	3207.0965
658.	727.	3108.1499	3142.3708	3207.0965	3231.0350
658.	727.	3142.3708	3176.5917	3231.0350	3254.9734
658.	727.	3176.5917	3193.7022	3254.9734	3266.9426
658.	727.	3193.7022	3210.8126	3266.9426	3278.9118
658.	727.	3210.8126	3256.6125	3278.9118	3310.9500

Table 8-2.—Concluded

Panel edge	Panel edge	Panel Corner Point Coordinates			
BL inboard, In.	BL outboard, In.	BS inboard LE, In.	BS inboard TE, In.	BS outboard LE, In.	BS outboard TE, In.
658.	727.	3256.6125	3296.3799	3310.9500	3349.8124
658.	727.	3296.3799	3336.1288	3349.8124	3388.6505
727.	795.	3121.0718	3140.1458	3238.6056	3257.8024
727.	795.	3140.1458	3159.2197	3257.8024	3276.9992
727.	795.	3159.2197	3183.1581	3276.9992	3290.8042
727.	795.	3183.1581	3207.0965	3290.8042	3304.6091
727.	795.	3207.0965	3231.0350	3304.6091	3318.4141
727.	795.	3231.0350	3254.9734	3318.4141	3332.2190
727.	795.	3254.9734	3266.9426	3332.2190	3339.1215
727.	795.	3266.9426	3278.9118	3339.1215	3346.0240
727.	795.	3278.9118	3320.9500	3346.0240	3364.5000
727.	795.	3310.9500	3349.8124	3364.5000	3402.4706
727.	795.	3349.8124	3388.6505	3402.4706	3440.4111

Table 8-3.—Design Envelope Points

	Altitude, ft	V_F , kn	Mach number	Dynamic pressure, psf
Maximum operating speed	0	350	0.53	415
	29 000	350	0.95	415
	46 500	475	1.96	765
	60 000	475	2.70	765
Design dive speed	0	420	0.64	505
	26 000	420	1.07	595
	40 500	545	1.94	1 005
	57 200	545	2.90	1 005

Table 8-4.—Flap Placard Speeds

Weight condition	$V_{MIN DEM}$ KEAS	$V_F = 1.6V_{MIN DEM}$ KEAS	$V_F = 1.8V_{MIN DEM}$ KEAS
Max take-off	170	271	—
Max landing	134	—	240

Table 8-5.—Design Maneuvering Speeds for Positive and Negative Maneuvers

Altitude ft	V _A KEAS	V _H KEAS
0	266	193
10 000	268	198
20 000	275	198
22 500	278	201
25 000	282	201
27 500	288	202
30 000	289	205
32 500	294	206
35 000	300	208
37 500	312	210
40 000	385	214
50 000	516	225
60 000	509	8
70 000	—	371

- Note: 1) Above 40 000 ft $V_A = V_C$
- 2) These airspeeds were obtained from the intersection of the C_{LMAX} and C_{LMIN} curves with the design load factors

Table 8-6.—Calculation of Design Speed for Maximum Gust Intensity

Maximum Flight Weight

Altitude, ft	Gross Weight 10 ³ lb	V _{min dem} , KEAS	n _{gust} at V _C	V _B ¹ min req'd, KEAS	V _B ² min req'd, KEAS	V _B selected, KEAS
0	743	163	1.68	211	200	300
10 000	728	164	1.78	219	207	300
20 000	721	165	1.82	223	216	300
25 000	716.65					
30 000	711.5	166	1.82	224	222	300
35 000	703.35					
40 000	693.5	167	1.92	231	227	300

Minimum Flight Weight

0	376.34	117	2.0	165	146	
10 000	376.34	117	2.17	173	150	
20 000	376.34	117	2.32	179	156	
25 000	376.34	117	2.31	178	157	
30 000	376.34	117	2.34	179	159	
35 000	376.34	118	2.70	194	192	
40 000	376.34	119	2.54	189	148	

¹ $V_B = V_{\text{min dem}} \sqrt{n_g}$

² $V_B = \text{Intersection of } C_{L_{\text{MAX DEM}}} \text{ and gust load factor curve}$

Table 8-7 – Flap Settings for the 969-512B

Flight condition	Trailing edge ¹ deflection, deg Inboard–outboard	Leading edge ¹ deflection, deg Inboard–outboard
Takeoff and landing ² M = 0.3→M = 0.95 M = 0.95→M = 1.20 M > 1.20	20/20/20 0/5/5 0/0/0 0/0/0	30/60 0/20 0/20 0/0

Note: ¹ Deflection angles are perpendicular to the hinge line.

² Flaps Down Configuration. All other configurations are designed to full-flaps-up load factors.

Table 8-8.—Geometric Constants

Wing		
Reference area	9848	ft ²
Aspect ratio	1.78	
LE sweep	74/70.5/60	deg
Root chord	1881.1	in.
Tip chord	204.0	in.
Reference chord	1187.0	in.
Span	1590.0	in.
Wing fin		
Reference area per side	287	ft ²
Aspect ratio	0.493	
LE sweep	74.5	deg
Root chord	510.0	in.
Tip chord	69.0	in.
Reference chord	345.0	in.
Span	143.0	in.
Vertical stabilizer		
Reference area	449	ft ²
Aspect ratio	0.848	
LE sweep	51.0	deg
Root chord	445.0	in.
Tip chord	107.0	in.
Reference chord	311.0	in.
Horizontal stabilizer		
Reference area	600	ft ²
Aspect ratio	1.32	
LE sweep	54.0	deg
Root chord	414.0	in.
Tip chord	102.0	in.
Reference chord	289.0	in.
Span	338.0	in.

Table 8-9.—Analysis Conditions
Balanced Symmetric Maneuvers at Maximum Flight Weight

Condition number *	Airspeed, KEAS	Altitude, ft	Gross weight, 1000 lb
0.4-01-06-07-00E	236	6300	743
0.4-01-06-06-20E	236	6300	743
0.4-01-02-05-00E	275	-2100	743
0.4-01-02-05-20E	275	-2100	743
0.6-01-32-07-1NE	206	31900	732
0.6-01-19-06-25E	274	18900	732
0.6-01-07-03-1NE	350	6700	732
0.6-01-07-03-25E	350	6700	732
0.6-01-03-04-00E	420	-3100	732
0.6-01-03-04-25E	420	-3100	732
0.9-01-46-07-1NE	220	46500	717
0.9-01-34-06-25E	297	33800	717
0.9-01-26-03-1NE	350	26500	717
0.9-01-26-03-25E	350	26500	717
0.9-01-18-04-00E	420	17800	717
0.9-01-18-04-25E	420	17800	717
1.2-01-52-07-1NE	255	52100	703.5
1.2-01-39-06-25E	349	39200	703.5
1.2-01-25-03-1NE	389	34600	703.5
1.2-01-35-03-25E	389	34600	703.5
1.2-01-29-04-00E	445	28800	703.5
1.2-01-29-04-25E	445	28800	703.5
1.6-01-54-07-1NE	327	53700	694
1.6-01-42-06-25E	435	41900	694
1.6-01-41-03-1NE	439	41500	694
1.6-01-41-03-25E	439	41500	694
1.6-01-36-04-00E	503	35600	694
1.6-01-36-04-25E	503	35600	694
2.0-01-58-07-1NE	368	58200	682
2.0-01-48-03-1NE	475	47700	682
2.0-01-48-03-25E	475	47700	682
2.0-01-42-04-00E	545	41900	682
2.0-01-42-04-25E	545	41900	682
2.2-01-61-07-1NE	380	60900	682
2.2-01-52-03-1NE	475	51600	682
2.2-01-52-03-25E	475	51600	682
2.2-01-46-04-00E	545	46000	682
2.2-01-46-04-25E	545	46000	683
2.7-01-67-07-1NE	400	67200	657
2.7-01-60-03-1NE	475	60200	657
2.7-01-60-03-25E	475	60200	657
2.7-01-54-04-00E	545	54200	657
2.7-01-54-04-25E	545	54200	657
2.9-01-57-04-00E	545	57200	657
2.9-01-57-04-25E	545	57200	657

*See figure 8-28 for code description

Table 8-9.—Continued
Balanced Symmetric Maneuvers at Minimum Flight Weight

Condition number *	Airspeed, KEAS	Altitude, ft	Gross weight, 1000 lb
0.4-05-06-07-00E	236	6300	464.9
0.4-05-06-06-20E	236	6300	464.9
0.4-05-02-05-00E	275	-2100	464.9
0.4-05-02-05-20E	275	-2100	464.9
0.6-05-32-07-1NE	206	31900	464.9
0.6-05-19-06-25E	274	18900	464.9
0.6-05-07-03-1NE	350	6700	464.9
0.6-05-07-03-25E	350	6700	464.9
0.6-05-03-04-00E	420	-3100	464.9
0.6-05-03-04-25E	420	-3100	464.9
0.9-05-46-07-1NE	220	46500	464.9
0.9-05-34-06-25E	297	33800	464.9
0.9-05-26-03-1NE	350	26500	464.9
0.9-05-26-03-25E	350	26500	464.9
0.9-05-18-04-00E	420	17800	464.9
0.9-05-18-04-25E	420	17800	464.9
1.2-05-52-07-1NE	255	52100	464.9
1.2-05-39-06-25E	349	39200	464.9
1.2-05-35-03-1NE	389	34600	464.9
1.2-05-35-03-25E	389	34600	464.9
1.2-05-29-04-00E	445	28800	464.9
1.2-05-29-04-25E	445	28800	464.9
1.6-05-54-07-1NE	327	53700	464.9
1.6-05-42-06-25E	435	41900	464.9
1.6-05-41-03-1NE	439	41500	464.9
1.6-05-41-03-25E	439	41500	464.9
1.6-05-36-04-00E	503	35600	464.9
1.6-05-36-04-25E	503	35600	464.9
2.0-05-58-07-1NE	368	58200	464.9
2.0-05-48-03-1NE	475	47700	464.9
2.0-05-48-03-25E	475	47700	464.9
2.0-05-42-04-00E	545	41900	464.9
2.0-05-42-04-25E	545	41900	464.9
2.2-05-61-07-1NE	380	60900	464.9
2.2-05-52-03-1NE	475	51600	464.9
2.2-05-52-03-25E	475	51600	464.9
2.2-05-46-04-00E	545	46000	464.9
2.2-05-46-04-25E	545	46000	464.9
2.7-05-67-07-1NE	400	67200	464.9
2.7-05-60-03-1NE	475	60200	464.9
2.7-05-60-03-25E	475	60200	464.9
2.7-05-54-04-00E	545	54200	464.9
2.7-05-54-04-25E	545	54200	464.9
2.9-05-57-04-00E	545	57200	464.9
2.9-05-57-04-25E	545	57200	464.9

*See figure 8-48 for code description

Table 8-9.—Continued
Vertical Gusts at Maximum Flight Weight

Condition number*	Airspeed, KEAS	Altitude, ft	Gross weight, 1000 lb	Gust velocity ft/sec	Load factor
0.4-01-02-15-01E	275	-2100	743	25	1.253
0.4-01-02-25-01E	275	-2100	743	-25	0.747
0.6-01-15-12-01E	300	14800	732	66	1.873
0.6-01-15-22-01E	300	14800	732	-66	0.127
0.6-01-07-13-01E	350	6700	732	50	1.712
0.6-01-07-23-01E	350	6700	732	-50	0.288
0.6-01-03-14-01E	420	-3100	732	25	1.382
0.6-01-03-24-01E	420	-3100	732	-25	0.618
0.9-01-33-12-01E	300	33400	717	51.9	1.850
0.9-01-33-22-01E	300	33400	717	-51.9	0.150
0.9-01-26-13-01E	350	26500	717	44.6	1.805
0.9-01-26-23-01E	350	26500	717	-44.6	0.196
0.9-01-18-14-01E	420	17800	717	25	1.501
0.9-01-18-24-01E	420	17800	717	-25	0.499
1.2-01-35-13-01E	389	34600	703.5	46.1	1.991
1.2-01-35-23-01E	389	34600	703.5	-46.1	0.009
1.2-01-29-14-01E	445	28800	703.5	21.4	1.499
2.7-02-60-13-01E	475	60200	657	25.1	1.623
2.7-01-60-23-01E	475	60200	657	-25.1	0.377
2.9-01-57-14-01E	545	57200	657	11.2	1.305
2.9-01-57-24-01E	545	57200	657	-11.2	0.695

Vertical Gusts at Ferry Condition Gross Weight

Condition number*	Airspeed, KEAS	Altitude, ft	Gross weight, 1000 lb	Gust velocity, ft/sec	Load factor
0.4-05-02-15-01E	275	-2100	434	25	1.367
0.4-05-02-25-01E	275	-2100	434	-25	0.633
0.6-05-15-12-01E	300	14800	434	66	2.349
0.6-05-15-22-01E	300	14800	434	-66	-0.349
0.6-05-07-13-01E	350	6700	434	50	2.095
0.6-05-07-23-01E	350	6700	434	-50	-0.095
0.6-05-03-14-01E	420	-3100	434	25	1.589
0.6-05-03-24-01E	420	-3100	434	-25	0.411
0.9-05-33-12-01E	300	33400	434	51.9	2.376
0.9-05-33-22-01E	300	33400	434	-51.9	-0.376
0.9-05-26-13-01E	350	26500	434	44.6	2.307
0.9-05-26-23-01E	350	26500	434	-44.6	-0.307
0.9-05-18-14-01E	420	17800	434	25	1.822
0.9-05-18-24-01E	420	17800	434	-25	0.178
1.2-05-35-13-01E	389	34600	434	46.1	2.607
1.2-05-35-23-01E	389	34600	434	-46.1	-0.607
1.2-05-29-14-01E	445	28800	434	21.4	1.814
1.2-05-29-24-01E	445	28800	434	-21.4	0.186
2.7-05-60-13-01E	475	60200	434	25.1	1.976
2.7-05-60-23-01E	475	60200	434	-25.1	0.024
2.9-05-57-14-01E	545	57200	434	11.2	1.480
2.9-05-57-24-01E	545	57200	434	-11.2	0.520

*See figure 8-28 for code description

Table 8-9 .—Concluded

Elevator Maneuvers

Type of condition	Airspeed, KEAS	Altitude ft	Gross weight, 1000 lb	Normal load factor	Elevator angle, deg	Pitch accel, rad/sec ²
Checked maneuver	548	54200	657	2.5	-4.01	0.1779
Checked maneuver	548	54200	657	2.5	17.92	-0.1135
Unchecked maneuver	297	33800	717	1.0	-45.0	0.5733

Rudder Maneuvers

Type of condition	Airspeed, KEAS	Altitude, ft	Gross weight, 1000 lb	Normal load factor	Rudder angle, deg	Sideslip angle, deg
Maximum rudder	236	6300	743	1.0	30.	0.0
Steady sideslip	236	6300	743	1.0	30.	17.9
Cluck-back	236	6300	743	1.0	0	17.9

Lateral Gusts

Condition number *	Airspeed, KEAS	Altitude, ft	Gross weight, 1000 lb	Gust velocity, fps
0.9-01-33-12-01L	300	33400	717	51.9
0.9-01-25-13-01L	350	26500	717	44.6
0.9-01-18-14-01L	420	17800	717	25.0
1.2-01-35-13-01L	389	34600	703.5	46.1
1.2-01-29-14-01L	445	28800	703.5	21.4

*See figure 8-28 for code description

Table 8 9.—Concluded

Body

Body station in structural reference system	Camber slope	Body station in structural reference system	Camber slope
291.7905	-0.0887049	2074.7622	0.0117702
440.3715	-0.0887049	2223.3432	0.0013968
588.9524	-0.0628078	2371.9241	-0.0055198
737.5334	-0.0628078	2520.5051	-0.0158946
886.1144	-0.0354145	2669.0861	-0.0297270
1034.6954	-0.0223736	2817.6671	-0.0331845
1183.2763	-0.0072807	2966.2480	-0.0413400
1331.8573	0.0018681	3114.8290	-0.0648188
1480.4383	0.0018681	3263.4100	-0.0968371
1629.0193	0.0083126	3411.9910	-0.1189804
1777.6002	0.0117709	3560.5719	-0.1404271
1926.1812	0.0086874	3709.1529	-0.1660344

The wing fin camber is constant at $\theta = -0.0322998$ rad.

The horizontal tail camber is constant at $\theta = -0.0923905$ rad.

The nacelles and vertical stabilizer have no camber.

Table 8-10.—Limit Loads for Ground Handling Conditions

All loads are limit

Max ramp weight = 750 000 lb

Body station of c.g. = 2479.16

	Main gear			Main gear			Nose gear			Main gear torque in. lb
	V _M lb	D _M lb	S _M lb	V _M lb	D _M lb	S _M lb	V _N lb	D _N lb	S _N lb	
Static reaction	348 135			348 135			53 730			
Taxi	696 270			696 270			107 460			
2-pt braked roll	375 000	300 000		375 000	300 000					
3-pt braked roll	311 105	248 885		311 105	248 885					
Turning	625 790		3 12.895	70 480		35 240	127 790			
Nose wheel yaw	333 300	266 640	13.840	323 305	-191 475	13 430	53 700		26 865	
Reverse braking	348 135	-191 475		384 135			93 395		27 270	
Pivoting	348 135			348 135			53 730			
Towing	348 135			348 135			53 730			
									F _{Tow} = 112 500	13 407 000

Table 8-11.—Load Conditions Represented in Loads Matrices

Symmetrical Loads

Column number	Condition number*	Condition description
1	0.4-01-02-05-20E	Flaps down maneuver at V_F
2	0.6-01-19-06-25E	Positive maneuver at V_A
3	0.9-01-34-06-25E	Positive maneuver at V_A
4	1.2-01-52-07-1NE	Negative maneuver at V_H
5	1.2-01-39-06-25E	Positive maneuver at V_A
6	2.0-01-48-03-1NE	Negative maneuver at V_C
7	2.7-01-67-07-1NE	Negative maneuver at V_H
8	0.4-05-02-05-20E	Flaps down maneuver at V_F
9	0.6-05-07-03-1NE	Negative maneuver at V_C
10	1.2-05-35-03-1NE	Negative maneuver at V_C
11	0.9-01-34-36-10E	Abrupt elevator maneuver
12		Lateral gust at Mach = 0.9
13		Rudder maneuver no. 1
14		Rudder maneuver no. 2
15		Rudder maneuver no. 3

Asymmetrical Loads

1		Lateral gust at Mach = 0.9
2		Rudder maneuver no. 1
3		Rudder maneuver no. 2
4		Rudder maneuver no. 3

*See figure 8-28 for code description

Table 8-12.— Symmetric Loads Matrix from FLEXSTAB
for the 15 Load Conditions in Table 8-11

Condition number or description (See figure 8-28 for code description)		0.6-01-19-06-25E 2.5-01-67-07-1NE LAT. GUST at M=0.9			0.9-01-34-06-25E 0.4-05-02-05-20E Rudder Man. No. 1			1.2-01-52-07-1NE 0.6-05-07-03-1NE Rudder Man. No. 2			1.2-01-39-06-25E 1.2-05-35-03-1NE Rudder Man. No. 3		
TZ-Node No. (LB)	0.4-01-02-05-20E 2.0-01-48-03-1NE 0.9-01-34-36-10E												
17-3191	-1.1723370E+03 -9.5205620E+02 -5.0697455E+03	-8.1308485E+02 -6.4038298E+02 -6.3670237E+02	-1.0226187E+03 -2.5371457E+03 -6.5641643E+02	-1.308485E+02 -6.4038298E+02 -6.3670237E+02	-1.0226187E+03 -2.5371457E+03 -6.5641643E+02	-1.308485E+02 -6.4038298E+02 -6.3670237E+02	-1.9479580E+02 7.3311995E+02 -6.5641643E+02	-1.206959E+03 2.0297008E+02 -6.5641643E+02					
17-3199	-2.4115516E+03 1.1997236E+03 -5.4834892E+03	-2.7253209E+03 8.4776259E+02 -1.0823065E+03	-2.7468434E+03 -3.1107117E+03 -1.2172020E+03	-2.7253209E+03 8.4776259E+02 -1.0823065E+03	-2.7468434E+03 -3.1107117E+03 -1.2172020E+03	-2.7468434E+03 -3.1107117E+03 -1.2172020E+03	1.3135117E+03 1.6584685E+03 -1.2172020E+03	-2.3177798E+03 2.0605087E+03 -1.2172020E+03					
17-3197	-5.3977681E+03 2.0464728E+03 -9.2873347E+03	-6.6087309E+03 1.9236069E+03 -2.5864580E+03	-6.6929790E+03 -5.8736375E+03 -2.7026532E+03	-6.6087309E+03 1.9236069E+03 -2.5864580E+03	-6.6929790E+03 -5.8736375E+03 -2.7026532E+03	-6.6929790E+03 -5.8736375E+03 -2.7026532E+03	2.1427941E+03 3.2173509E+03 -2.7026532E+03	-6.2360362E+03 2.3990533E+03 -2.7026532E+03					
17-3185	-5.3362884E+03 4.1155843E+03 -7.9621484E+03	-6.7552878E+03 3.2375057E+03 -2.5299450E+03	-5.9353491E+03 -5.4517450E+03 -2.6430734E+03	-6.7552878E+03 3.2375057E+03 -2.5299450E+03	-5.9353491E+03 -5.4517450E+03 -2.6430734E+03	-5.9353491E+03 -5.4517450E+03 -2.6430734E+03	3.3607715E+03 3.3712209E+03 -2.6430734E+03	-6.9518035E+03 4.4665389E+03 -2.6430734E+03					
17-3183	-9.2869627E+03 6.0142503E+03 -1.2713302E+04	-1.1409874E+04 5.5824312E+03 -4.6402318E+03	-1.1827499E+04 -7.4522440E+03 -4.7114338E+03	-1.1409874E+04 5.5824312E+03 -4.6402318E+03	-1.1827499E+04 -7.4522440E+03 -4.7114338E+03	-1.1827499E+04 -7.4522440E+03 -4.7114338E+03	5.3806527E+03 3.3493252E+03 -4.7114338E+03	-1.2363731E+04 4.1115084E+03 -4.7114338E+03					
17-3191	-4.1515383E+03 2.5396564E+03 -5.5313654E+03	-4.4506796E+03 2.5924122E+03 -1.8495327E+03	-4.6320090E+03 -3.0661308E+03 -2.2323565E+03	-4.4506796E+03 2.5924122E+03 -1.8495327E+03	-4.6320090E+03 -3.0661308E+03 -2.2323565E+03	-4.6320090E+03 -3.0661308E+03 -2.2323565E+03	2.3402336E+03 1.3491199E+03 -2.2323565E+03	-4.9355663E+03 1.5030080E+03 -2.2323565E+03					
17-2038	-4.9879172E+03 3.1649469E+03 -6.3865875E+03	-5.0532970E+03 3.2753835E+03 -2.1160173E+03	-5.3144996E+03 -9.6603038E+03 -2.7379500E+03	-5.0532970E+03 3.2753835E+03 -2.1160173E+03	-5.3144996E+03 -9.6603038E+03 -2.7379500E+03	-5.3144996E+03 -9.6603038E+03 -2.7379500E+03	2.4210276E+03 4.4804460E+03 -2.7379500E+03	-5.7639805E+03 4.4365179E+03 -2.7379500E+03					
17-2098	-3.9867385E+03 1.6847693E+03 -5.0335202E+03	-1.9105119E+03 2.2075195E+03 -9.5930486E+02	-2.2629463E+03 -6.0957928E+03 -2.6219062E+03	-1.9105119E+03 2.2075195E+03 -9.5930486E+02	-2.2629463E+03 -6.0957928E+03 -2.6219062E+03	-2.2629463E+03 -6.0957928E+03 -2.6219062E+03	1.3603118E+03 1.3412986E+03 -2.6219062E+03	-2.5065785E+03 1.9403362E+03 -2.6219062E+03					
17-2158	-5.2650522E+03 2.1747789E+03 -5.9352265E+03	-4.8436924E+03 2.4315149E+03 -1.9874369E+03	-5.0538025E+03 -6.6801944E+03 -2.9892882E+03	-4.8436924E+03 2.4315149E+03 -1.9874369E+03	-5.0538025E+03 -6.6801944E+03 -2.9892882E+03	-5.0538025E+03 -6.6801944E+03 -2.9892882E+03	2.1478147E+03 2.3049912E+03 -2.9892882E+03	-5.2385852E+03 2.8180234E+03 -2.9892882E+03					
17-2218	-3.9591689E+03 1.5867808E+03 -4.2547088E+03	-3.4167959E+03 1.7763190E+03 -1.3753887E+03	-3.6157391E+03 -5.3733105E+03 -2.2926124E+03	-3.4167959E+03 1.7763190E+03 -1.3753887E+03	-3.6157391E+03 -5.3733105E+03 -2.2926124E+03	-3.6157391E+03 -5.3733105E+03 -2.2926124E+03	1.6314926E+03 2.4131492E+03 -2.2926124E+03	-3.7767022E+03 2.3580470E+03 -2.2926124E+03					

Table 8-12.—Continued

12-2278	-1.6769023E+03 1.5780188E+03 -3.0399535E+03	-1.6157898E+03 1.3770314E+03 -5.0049416E+02	-1.8679080E+03 -3.8007849E+03 -3.7279867E+02	1.5334251E+03 2.4669792E+03 -9.7279867E+02	-1.7483751E+03 3.0454321E+03 -9.7279867E+02
12-2338	-2.4382496E+03 2.2575231E+03 -3.2059802E+03	-3.6801886E+03 2.1105123E+03 -1.3242174E+03	-3.7942956E+03 -3.8072127E+03 -1.1372911E+03	2.0161462E+03 2.7167280E+03 -1.1372911E+03	-3.7605626E+03 2.9623107E+03 -1.1372911E+03
12-2398	-2.9681163E+03 2.5967845E+03 -2.9961425E+03	-4.4079980E+03 2.4121547E+03 -1.6404568E+03	-4.4984934E+03 -4.1720617E+03 -1.3936599E+03	2.3014073E+03 2.3250806E+03 -1.3936599E+03	-4.4133132E+03 3.1999450E+03 -1.3936599E+03
12-2458	-2.1868298E+03 2.9004330E+03 -2.1093979E+03	-3.9011588E+03 2.5500779E+03 -1.4290919E+03	-3.9860212E+03 -3.7137745E+03 -9.4857149E+02	2.3490489E+03 2.7527393E+03 -9.4857149E+02	-3.7489351E+03 3.6103937E+03 -9.4857149E+02
12-2518	-1.2693524E+03 1.9505312E+03 -1.1655531E+03	-2.7460983E+03 1.7843322E+03 -1.1559764E+03	-2.7745925E+03 -2.7875038E+03 -5.5111715E+02	1.3184233E+03 1.6784298E+03 -5.5111715E+02	-2.7935624E+03 1.8978040E+03 -5.5111715E+02
12-2578	-3.8342046E+03 2.5109657E+03 -1.7887731E+03	-5.5295256E+03 2.5933414E+03 -2.2617234E+03	-5.4972523E+03 -4.8601252E+03 -1.8722949E+03	2.2232111E+03 2.5659146E+03 -1.9722949E+03	-5.5372682E+03 2.4614706E+03 -1.8722949E+03
12-2638	-3.3685953E+03 2.1265601E+03 -9.7431522E+02	-4.9192023E+03 2.2447584E+03 -2.0249603E+03	-4.8565934E+03 -4.4027700E+03 -1.6487725E+03	1.9060697E+03 2.2691458E+03 -1.6487725E+03	-4.9028278E+03 2.0654530E+03 -1.6487725E+03
12-2698	-1.5569127E+03 9.9186750E+02 6.7182351E+02	-3.0967089E+03 1.3261239E+03 -1.3933463E+03	-3.0044038E+03 -3.1619796E+03 -7.068047E+02	8.3638911E+02 1.4771265E+03 -7.068047E+02	-2.7590958E+03 1.1861911E+03 -7.068047E+02
12-2758	-4.4674428E+03 2.2520368E+03 -1.7964772E+02	-6.3987513E+03 2.4229399E+03 -2.6554230E+03	-6.3746852E+03 -5.3251722E+03 -2.1275454E+03	2.2989129E+03 2.6953289E+03 -2.1275454E+03	-6.4236395E+03 2.6191439E+03 -2.1275454E+03
12-2818	-1.1992269E+04 6.076205E+03 -7.7904994E+02	-1.5960512E+04 6.2580823E+03 -6.3935505E+03	-1.5868817E+04 -5.8460391E+03 -5.8174534E+03	6.1923133E+03 3.3150741E+03 -5.3174584E+03	-1.6068791E+04 2.9081221E+03 -5.8174584E+03

Table 8-12.--Continued

72-2878	-1.1025699E+04 5.4152778E+03 8.9511671E+02	-1.5623913E+04 5.8634114E+03 -6.1994083E+03	-1.5024647E+04 -4.4055440E+03 -5.1673221E+03	5.7128940E+03 2.1764784E+03 -5.1673221E+03	-1.5655384E+04 2.0640313E+03 -5.1673221E+03
72-2938	-1.6044670E+04 8.369909E+03 1.4792849E+03	-2.1996432E+04 8.619201E+03 -7.9337872E+03	-1.9637448E+04 -8.3283917E+03 -7.3434923E+03	6.8413573E+03 5.1279091E+03 -7.3434923E+03	-1.7979723E+04 4.1468642E+03 -7.3434923E+03
72-2998	-1.3749709E+03 9.3689583E+02 1.2304814E+03	-5.5199320E+03 1.4183630E+03 -2.1635440E+03	-5.0401098E+03 -1.8941782E+03 2.8551934E+01	1.2704704E+03 1.9573875E+03 2.8551934E+01	-4.5760122E+03 1.0604974E+03 2.8551934E+01
72-3058	2.0564249E+03 -7.4545812E+02 1.1521535E+03	-3.1734817E+03 -1.1550537E+02 -1.2788466E+03	-2.6598103E+03 1.4750935E+03 2.0920310E+03	-2.0172846E+02 6.8434578E+02 2.0920310E+03	-1.9224956E+03 -5.7738043E+02 2.0920310E+03
72-3201	-5.6179270E+02 -1.9687012E+03 6.6687710E+02	-4.5046345E+03 -1.2917685E+03 -2.1519512E+03	-4.3379511E+03 -1.1324152E+03 2.6420726E+02	-5.5044184E+02 6.4563015E+02 2.6420726E+02	-3.7202436E+03 -1.4059646E+03 2.6420726E+02
72-3203	-2.577907E+04 1.8583628E+03 6.5902273E+03	-2.9826677E+04 -4.5351347E+02 -1.2404103E+04	-3.0506661E+04 -5.5725560E+03 -1.3542952E+04	1.1315037E+04 2.1404911E+02 -1.3542952E+04	-3.0879704E+04 -7.0500188E+02 -1.3542952E+04
72-3225	-2.1153884E+04 -2.0497639E+02 -5.6799636E+03	-1.5552189E+04 -4.5988619E+02 -8.2261329E+03	-1.7411847E+04 -1.2533935E+04 -1.3433222E+04	5.2302624E+03 -7.2851809E+02 -1.3433222E+04	-1.7153367E+04 -2.4927964E+03 -1.3433222E+04
72-3208	-8.399450E+03 -2.5693157E+03 -1.5555774E+04	-1.3696181E+03 -1.4936285E+03 -1.9700973E+03	-3.1887201E+03 -1.0497493E+04 -6.6357335E+03	-4.5538257E+02 1.1363143E+03 -6.6357335E+03	-4.3075313E+03 -2.5042307E+03 -6.6357335E+03
72-3212	-5.7217622E+03 1.0963393E+03 -1.6043441E+04	-3.4070324E+02 -3.1648403E+02 -8.2021879E+02	-1.5812634E+03 -7.4457920E+03 -4.6367417E+03	7.3230036E+03 1.3266491E+03 -4.6367417E+03	-2.6606066E+03 1.4107617E+04 -4.6367417E+03
7X-1036	2.5635309E-01 2.2697685E-01 1.2501889E+01	2.8144999E-01 1.2293434E-01 2.8644960E-01	2.613309E-01 5.0734116E-01 2.1081954E-01	1.5748777E-01 8.1466814E-01 2.1081954E-01	2.2690032E-01 4.5823761E-01 2.1081954E-01

Table 8-12.—Continued

TY-1036	5.4303149E-05 1.1396653E-03 2.1923989E-04	-7.6488685E-05 7.973725E-04 1.4168757E-03	-6.7215920E-05 3.3239938E-05 5.1956059E-05	2.4174889E-04 2.1736375E-04 5.1956069E-05	-4.0156905E-04 7.0520410E-04 5.1956069E-05
TZ-1036	-1.37625P3E+04 7.1487218E+03 3.4430129E+02	-1.7254809E+04 7.0886213E+03 -6.7553062E+03	-1.7305008E+04 -1.363327E+04 -6.7919665E+03	7.1336019E+03 7.630776E+03 -6.7919665E+03	-1.7388153E+04 7.2459921E+03 -6.7919665E+03
TX-1037	3.7029374E-01 3.2773741E-01 1.8059086E+01	4.0653443E-01 1.7756987E-01 4.1375600E-01	3.7748564E-01 7.3281808E-01 3.0451378E-01	2.2747985E-01 1.1767300E+00 3.0451378E-01	3.2774131E-01 6.6189152E-01 3.0451378E-01
TY-1037	4.9884386E-07 -9.5089856E-04 2.0139050E-06	-7.0263669E-07 -6.6016102E-04 1.3015210E-07	-6.1743545E-07 3.0535133E-07 4.7728292E-07	-2.0384299E-04 1.7967365E-06 4.7728292E-07	3.3860358E-04 -5.9462926E-04 4.7728292E-07
TZ-1037	-1.9750383E+04 1.0430424E+04 6.5545932E+03	-2.4784155E+04 1.0293650E+04 -9.6187853E+03	-2.4969262E+04 -1.9532969E+04 -9.7046735E+03	1.3378905E+04 1.1278105E+04 -9.7046735E+03	-2.5008326E+04 1.0610520E+04 -9.7046735E+03
TX-1056	2.6077297E-01 2.3079852E-01 1.2717439E+01	2.8630258E-01 1.2505389E-01 2.9138639E-01	2.6584492E-01 5.1608842E-01 2.1445436E-01	1.6020308E-01 8.2871414E-01 2.1445436E-01	2.3081239E-01 4.6613826E-01 2.1445436E-01
TY-1086	2.4250206E-04 -2.3191581E-03 1.3497658E-04	2.1895619E-04 -1.5934578E-03 4.5764793E-05	2.7025367E-04 1.5072414E-04 6.3270466E-05	-8.0360016E-04 -2.2299339E-04 6.3270466E-05	1.5102405E-03 -1.4354307E-03 6.3270466E-05
TZ-1086	-1.3995314E+04 7.2757009E+03 5.6471983E+02	-1.7547379E+04 7.2127897E+03 -6.8668634E+03	-1.7598890E+04 -1.3862741E+04 -6.9053219E+03	7.2592548E+03 7.7714109E+03 -6.9053219E+03	-1.7684147E+04 7.3760339E+03 -6.9053219E+03
TX-1087	3.6584386E-01 3.2377574E-01 1.7842536E+01	4.0168184E-01 1.7545032E-01 4.0881721E-01	3.7297979E-01 7.2407032E-01 3.008786E-01	2.2476454E-01 1.1626840E+00 3.308786E-01	3.2382924E-01 6.5399087E-01 3.008786E-01
TY-1087	1.0702494E-06 1.9369050E-03 5.9573135E-07	9.6586406E-07 1.3206757E-03 2.0195713E-07	1.1926123E-06 6.6520019E-07 2.7921546E-07	6.781991E-04 -9.8412251E-07 2.7921546E-07	-1.2745691E-03 1.2114333E-03 2.7921546E-07

Table 8-12. Continued

17-1087	-1.9509562E+04 1.0310836E+04 6.7620844E+03	-2.4491792E+04 1.0173340E+04 -9.4974242E+03	-2.4566438E+04 -1.292294E+04 -3.5838409E+03	1.0259892E+04 1.155560E+04 -9.5838409E+03	-2.4704719E+04 1.0490491E+04 -9.5838409E+03
17-3199	-3.111325E+00 1.450697E+00 1.2887445E+00	-3.9060300E+03 1.6270128E+03 -1.5123123E+03	-3.9199918E+00 -3.0763478E+00 -1.5273209E+00	1.6413199E+00 1.7908514E+00 -1.5273208E+00	-3.9427142E+00 1.6807450E+00 -1.5273208E+00
17-3206	-1.3895594E+02 7.4115704E+01 7.1972482E+01	-1.7446615E+02 7.2997707E+01 -6.7351431E+01	-1.7446615E+02 -1.319019E+02 -6.3097630E+01	7.3625826E+01 8.0744973E+01 -6.9097659E+01	-1.7618180E+02 7.5553468E+01 -6.8097659E+01
17-3210	-3.77543132E+02 2.0387166E+02 2.4819483E+02	-4.7665889E+02 2.0022394E+02 -1.8329389E+02	-4.7855776E+02 -3.7467012E+02 -1.8561546E+02	2.0227951E+02 2.2130432E+02 -1.8561546E+02	-4.8162210E+02 2.0814171E+02 -1.8561546E+02
17-3214	-4.5469183E+02 2.4227568E+02 2.2771075E+02	-5.7084714E+02 2.3850611E+02 -2.2047974E+02	-5.7297706E+02 -4.492111E+02 -2.228111E+02	2.4073111E+02 2.6370702E+02 -2.2287884E+02	-5.7641903E+02 2.4694838E+02 -2.2287884E+02
17-3215	-8.0093782E+02 4.2824506E+02 4.5177457E+02	-1.0057522E+03 4.2114714E+02 -3.8775076E+02	-1.0096045E+03 -7.9114174E+02 -3.9225502E+02	4.2523956E+02 4.4740599E+02 -3.9225502E+02	-1.0158359E+03 4.3677788E+02 -3.9225502E+02
17-3216	-8.42331197E+02 4.5233652E+02 5.4439835E+02	-1.0579847E+03 4.4429447E+02 -4.0692639E+02	-1.0621855E+03 -8.3166486E+02 -4.1204393E+02	4.4883497E+02 4.7530376E+02 -4.1204380E+02	-1.0689663E+03 4.6177170E+02 -4.1204380E+02
17-3217	-3.4049924E+02 1.8359251E+02 2.4611109E+02	-4.2775621E+02 1.8011401E+02 -1.6416320E+02	-4.2951052E+02 -3.3603999E+02 -1.6637503E+02	1.9203847E+02 2.0162182E+02 -1.6637503E+02	-4.3233556E+02 1.8756983E+02 -1.6637503E+02
17-3218	-1.019217E+02 5.4585263E+01 6.0874916E+01	-1.2798536E+02 5.3654936E+01 -4.9295515E+01	-1.2848285E+02 -1.0364785E+02 -4.9887260E+01	5.4187141E+01 5.7656372E+01 -4.9887260E+01	-1.2928716E+02 5.5694560E+01 -4.9887260E+01
17-3219	-5.9262657E+01 3.1775536E+01 3.6574128E+01	-7.4428697E+01 3.1224106E+01 -2.8681036E+01	-7.4720524E+01 -5.8521260E+01 -2.9001572E+01	3.1537658E+01 3.4754069E+01 -2.9001592E+01	-7.5192023E+01 3.2427836E+01 -2.9001592E+01

Table 8-12.—Continued

TZ-3220	-1.213738E+02	-1.5245122E+02	-1.5305412E+02	6.4650661E+01	-1.5402760E+02
	6.5149738E+01	6.4000229E+01	-1.198484E+02	7.1312233E+01	6.6501783E+01
	7.7319384E+01	-5.8652065E+01	-5.9383289E+01	-5.9383289E+01	-5.9383289E+01
TZ-3221	-1.1816231E+02	-1.4843100E+02	-1.4903029E+02	6.1070748E+01	-1.4999641E+02
	6.3584810E+01	6.2417991E+01	-1.1664154E+02	6.9731342E+01	6.4939133E+01
	8.0997887E+01	-5.7025849E+01	-5.7769149E+01	-5.7769149E+01	-5.7769149E+01
TY-0238	-6.8554455E+00	-8.5964435E+00	-8.6224513E+00	3.5624387E+00	-8.6649544E+00
	3.5719673E+00	3.5387120E+00	-6.7890229E+00	3.8219254E+00	3.6228864E+00
	5.5785940E-01	-3.3601473E+00	-3.3805292E+00	-3.3805292E+00	-3.3805292E+00
TZ-0238	-7.4941695E+02	-7.8422200E+02	-7.3671790E+02	2.4770328E+02	-6.2023294E+02
	1.2773021E+02	2.2287219E+02	-5.6418750E+02	1.7409423E+02	8.4060712E+01
	-2.7304046E+02	-4.1041969E+02	-5.1553276E+02	-5.1553276E+02	-5.1553276E+02
TY-0475	-1.1857737E+02	-1.4871121E+02	-1.4917030E+02	6.1750748E+01	-1.4992712E+02
	6.1941641E+01	6.1321088E+01	-1.1739874E+02	6.441214E+01	6.2861677E+01
	1.5295739E+01	-5.8069402E+01	-5.8432950E+01	-5.8432950E+01	-5.8432950E+01
TZ-0475	-3.3794911E+03	-3.3485784E+03	-3.1357619E+03	9.5854307E+02	-2.5471830E+03
	4.8424053E+02	4.1440165E+02	-2.6303217E+03	6.1390532E+02	1.8451006E+02
	-1.1840262E+03	-1.9286275E+03	-2.4586969E+03	-2.4586969E+03	-2.4586969E+03
TY-0472	-3.2151897E+02	-4.0335576E+02	-4.0467722E+02	1.6826569E+02	-4.0684392E+02
	1.6895935E+02	1.6697922E+02	-3.1813586E+02	1.9199445E+02	1.7168952E+02
	7.7021530E+01	-1.5695567E+02	-1.5819086E+02	-1.5819086E+02	-1.5819086E+02
TZ-0472	-2.8223102E+03	-1.9057458E+03	-1.7151997E+03	-9.8659502E+01	-9.3705214E+02
	-1.0415064E+03	-6.5875856E+02	-2.5389466E+03	-1.2758379E+02	-8.5715379E+02
	-7.5744184E+02	-1.7645357E+03	-2.5132532E+03	-2.5132532E+03	-2.5132532E+03
TY-0852	-2.2394773E+02	-3.5613934E+02	-3.5757429E+02	1.4936945E+02	-3.5959079E+02
	1.5011854E+02	1.4810417E+02	-2.8079178E+02	1.6245336E+02	1.5274315E+02
	9.9974357E+01	-1.3821594E+02	-1.3948226E+02	-1.3948226E+02	-1.3948226E+02
TZ-0862	-1.2842527E+03	-3.7702225E+02	-3.2238178E+02	-6.4654125E+02	-4.7623002E+02
	-7.1831472E+02	9.0800382E+01	-1.3211641E+03	-4.8472388E+02	-1.2541243E+03
	-3.1915319E+02	-1.0789114E+03	-1.5780251E+03	-1.5780251E+03	-1.5780251E+03

Table 8-12.—Continued

TY-0912	-2.2382216E+02 1.1692171E+02 8.5542509E+01	-2.8090877E+02 1.1687769E+02 -1.0886483E+02	-2.9189794E+02 -2.2129899E+02 -1.099001E+02	1.1788229E+02 1.2841798E+02 -1.099001E+02	-2.8350877E+02 1.2063539E+02 -1.099001E+02
TY-0912	-5.9841949E+02 -3.4280441E+03 3.9941011E+02	2.0054245E+02 -9.6045401E+02 9.3593900E+02	4.4275037E+02 -6.5079615E+02 2.3734595E+02	-4.5683694E+02 2.0418276E+02 2.3734595E+02	2.9979781E+03 1.3929040E+02 2.3734595E+02
TY-0428	-1.6853886E+02 8.9544935E+01 7.5484174E+01	-2.1152814E+02 8.8214679E+01 -8.1822751E+01	-2.1229644E+02 -1.5655089E+02 -9.2662960E+01	8.908861E+01 9.7280544E+01 -8.2662960E+01	-2.1354521E+02 9.1209897E+01 -8.2662960E+01
TY-0428	-2.4699272E+02 -2.2203471E+02 3.1561873E+01	-1.1982707E+02 -5.7840872E+02 8.7702966E+02	-1.3202655E+02 -2.2550742E+02 7.3498037E+02	8.0868046E+01 9.2676365E+01 7.3498007E+02	3.6418583E+02 1.5202285E+02 7.0488007E+02
TY-0417	-6.7209335E+01 3.5764770E+01 3.1946382E+01	-8.4374131E+01 3.5220897E+01 -3.2611846E+01	-9.4684591E+01 -6.5418716E+01 -3.2957064E+01	3.5543938E+01 3.9899469E+01 -3.2957064E+01	-8.5188589E+01 3.6443117E+01 -3.2757064E+01
TY-0417	-1.1424833E+02 -4.2826902E+02 7.6811692E+00	-6.5473142E+01 -3.7312731E+02 -1.5946163E+02	-7.3840165E+01 -1.3244534E+02 -2.1366101E+02	2.9993563E+02 4.3956802E+01 -2.1366101E+02	-1.4643639E+02 3.7471886E+02 -2.1366101E+02
TY-0233	-1.5521506E+02 8.1744170E+01 4.2211717E+01	-1.9482842E+02 8.0746494E+01 -7.5742878E+01	-1.3547746E+02 -1.5362476E+02 -7.5366956E+01	8.1384946E+01 8.9169210E+01 -7.5366956E+01	-1.9654007E+02 8.3096601E+01 -7.6366966E+01
TY-0233	1.4486705E+02 -2.4691060E+01 5.2780454E+01	1.5159509E+02 -4.3092607E+01 7.9336730E+01	1.4241225E+02 1.0906102E+02 9.9655754E+01	-4.7882616E+01 -3.3653529E+01 9.3655754E+01	1.1989496E+02 -1.6249469E+01 9.9655754E+01
TY-0281	-1.6033819E+02 8.4446569E+01 5.0781263E+01	-2.0078091E+02 8.3347784E+01 -7.7955763E+01	-2.0146540E+02 -1.5925931E+02 -7.9638843E+01	8.4030538E+01 9.1244470E+01 -7.8638843E+01	-2.0258382E+02 8.5878611E+01 -7.8638843E+01
TY-0291	-1.5130504E+03 2.3284199E+02 -5.6324631E+02	-1.6395966E+03 6.8301286E+02 -8.2073036E+02	-1.5410511E+03 -1.1174936E+03 -1.0151039E+03	5.4668367E+02 3.3388567E+02 -1.0151039E+03	-1.3283655E+03 2.2590766E+02 -1.0151039E+03

Table 8-12. --Continued

TY-0329	-1.683993E+02 8.911908E+01 6.261348E+01	-2.113320E+02 8.789676E+01 -8.192491E+01	-2.120721E+02 -1.565008E+02 -8.269414E+01	8.864660E+01 9.651957E+01 -8.269414E+01	-2.132786E+02 9.069768E+01 -8.269414E+01
TY-0329	-3.4539250E+03 -5.2339843E+02 -1.0120898E+03	-3.018114E+03 -7.305299E+02 -2.1403834E+03	-2.7460185E+03 -2.9894153E+03 -2.7788667E+03	5.0506407E+02 3.4018748E+02 -2.7788667E+03	-1.6403524E+03 -3.134190E+02 -2.7788667E+03
TY-0378	-3.3472250E+02 1.7755898E+02 1.3894483E+02	-4.2013490E+02 1.750849E+02 -1.6266819E+02	-4.2163734E+02 -3.3084113E+02 -1.6427678E+02	1.7654848E+02 1.9264215E+02 -1.6427678E+02	-4.2408242E+02 1.8079327E+02 -1.6427678E+02
TY-0378	-2.1609407E+03 -9.9159324E+02 -5.6649492E+02	-1.9504552E+03 6.8522064E+02 -1.4922509E+03	-1.7195755E+03 -1.7691466E+03 -1.8729155E+03	1.4216782E+02 3.5602683E+02 -1.8729155E+03	-6.9676955E+02 -3.6622133E+02 -1.8729155E+03
TY-0426	-1.8675987E+02 1.0472573E+02 9.4094046E+01	-2.4701322E+02 1.0312290E+02 -9.5466287E+01	-2.4792317E+02 -1.9444229E+02 -9.6480060E+01	1.0407057E+02 1.1391155E+02 -9.6480060E+01	-2.4940050E+02 1.0670957E+02 -9.6480060E+01
TY-0426	-6.4867849E+02 -5.3132620E+02 -1.0491248E+02	-5.2230519E+02 -1.3084757E+01 2.1827655E+02	-4.5335359E+02 -5.4728871E+02 5.4086662E+00	9.2741807E+01 1.2453026E+02 5.4086662E+00	1.6073245E+02 5.2558096E+01 5.4086662E+00
TY-0416	-6.5243800E+01 3.4754228E+01 3.2243886E+01	-8.1907430E+01 3.4214009E+01 -3.1641198E+01	-8.2211414E+01 -6.4466812E+01 -3.1983109E+01	3.4531820E+01 3.7827052E+01 -3.1983109E+01	-8.2704645E+01 3.5419010E+01 -3.1983109E+01
TY-0416	-1.5264597E+02 -7.3596256E+02 -9.7323371E+00	-1.1827022E+02 -1.8017688E+02 -1.4881152E+02	-1.0536905E+02 -1.2901674E+02 -2.2680710E+02	2.3153875E+02 3.4869190E+01 -2.2680710E+02	-1.9700272E+02 3.3532767E+02 -2.2680710E+02
TY-0226	-6.5272561E+01 3.4729423E+01 3.0755166E+01	-8.1941785E+01 3.4200538E+01 -3.1675445E+01	-8.2242660E+01 -6.4506151E+01 -3.2009229E+01	3.4513345E+01 3.7763885E+01 -3.2009229E+01	-8.2731262E+01 3.5383479E+01 -3.2009229E+01
TY-0226	-3.0921260E+02 -2.2355473E+02 -6.8625369E+01	-2.6261549E+02 6.6196349E+01 -1.0269404E+02	-2.2952454E+02 -2.5825867E+02 -1.5755030E+02	1.1343801E+01 5.257977E+01 -1.5755030E+02	2.1039709E+01 -3.3664839E+01 -1.5755030E+02

Table 8-12.—Continued

TV-0375	-5.7276294E+01 3.0516289E+01 2.8482875E+01	-7.1908906E+01 3.0040601E+01 -2.7776363E+01	-7.2176147E+01 -5.6595999E+01 -2.8077469E+01	3.0320195E+01 3.3218361E+01 -2.8077469E+01	-7.2609713E+01 3.1101047E+01 -2.8077469E+01
TZ-0375	3.7397855E+02 2.7039135E+02 8.3000464E+01	3.1762146E+02 -8.0061466E+01 1.2420376E+02	2.7759947E+02 3.1235208E+02 1.9054993E+02	-1.3719810E+01 -6.3784732E+01 1.3054990E+02	-2.5446569E+01 4.0716089E+01 1.9054990E+02
TV-0414	-1.1060539E+01 5.9015727E+00 5.8049617E+00	-1.3887334E+01 5.8071721E+03 -5.3600504E+03	-1.3939597E+01 -1.0927544E+01 -5.4198695E+00	5.9622047E+00 6.4312042E+00 -7.4198695E+00	-1.4024305E+01 6.0165215E+00 -5.4198695E+00
TZ-0414	-1.8970201E-14 1.0121932E-14 9.9562321E-15	-2.3816506E-14 9.960231E-15 -9.1931539E-15	-2.3908145E-14 -1.8742099E-14 -9.2957510E-15	1.3054411E-14 1.1030316E-14 -9.2957510E-15	-2.4053429E-14 1.0319083E-14 -9.2957510E-15
TZ-0040	1.5831699E+04 -9.3349773E+03 1.0060332E+04	3.0597022E+04 -9.2627955E+03 1.1781121E+04	2.8496291E+04 4.7428521E+03 5.7647006E+03	-9.5410620E+03 -4.7469447E+03 5.7647006E+03	2.7520656E+04 -3.7601688E+03 5.7647006E+03
TZ-0034	8.3714453E+02 9.1155473E+02 -2.7330843E+03	-2.3125069E+03 -8.2480844E+02 -2.3047741E+02	-1.9147438E+03 7.0079320E+03 1.0367575E+03	1.9842175E+03 -6.5706841E+02 1.0367575E+03	-7.9481694E+02 6.0171921E+02 1.0367575E+03
TZ-0025	-4.7460310E+03 5.3191593E+03 -1.6876953E+03	-7.0168063E+03 4.7699545E+03 -1.981704E+03	-5.2697094E+03 8.0193597E+02 -2.1341343E+03	2.3442119E+03 5.3084025E+02 -2.1341343E+03	-3.6185640E+03 1.1171978E+03 -2.1341343E+03
TZ-0017	6.3825372E+03 -2.0023605E+03 3.8723765E+03	6.1610865E+03 -1.8134769E+03 2.3193579E+03	4.2273427E+03 3.9961698E+03 3.3489569E+03	-2.7299190E+03 -2.0119643E+03 3.3489569E+03	6.3098929E+03 -1.8991836E+03 3.3489569E+03
TZ-0059	-1.1414798E+04 6.1127807E+03 1.1826651E+03	-1.6129246E+04 6.5264443E+03 -6.4287577E+03	-1.5647666E+04 1.0858163E+03 -5.3776139E+03	5.9704772E+03 -8.4298461E+02 -5.3776139E+03	-1.5771604E+04 -6.3669233E+02 -5.3776139E+03
TZ-0055	-2.9660390E+03 1.1232022E+03 1.2784623E+03	-5.6391115E+03 1.6573503E+03 -2.0444452E+03	-4.3754739E+03 -4.5081471E+02 -1.0712039E+03	9.3396817E+02 1.7523731E+02 -1.0712039E+03	-3.8681736E+03 -2.8263045E+02 -1.0712039E+03

Table 8-12.---Continued

TZ-0001	1.9174384E+03 -4.2197780E+02 7.3981066E+02	-1.6027562E+03 -1.4532639E+02 -6.1939963E+02	-1.1227588E+03 1.3376070E+03 1.0901204E+03	-1.9911058E+02 -7.0280386E+01 1.0901204E+03	-5.9470475E+02 -6.2033038E+02 1.0901204E+03
TZ-0842	3.3376839E+03 -5.1852972E+02 6.6512037E+01	-5.3854823E+01 -4.9810257E+02 -2.8870803E+01	6.1318444E+01 3.1766788E+03 2.5114974E+03	-3.7045595E+02 -1.6912828E+02 2.5114974E+03	3.2646077E+02 -3.4001766E+02 2.5114974E+03
TZ-0892	6.3333381E+03 -9.3470744E+02 2.2114791E+02	5.3966069E+02 -9.6609419E+02 2.5883118E+02	8.2681480E+02 6.0340797E+03 4.5822269E+03	-9.3113945E+02 -4.9899962E+02 4.5822269E+03	1.1102634E+03 -8.9611720E+02 4.5822269E+03
TZ-0992	1.3593119E+03 -7.2169874E+02 1.5769508E+01	3.4936306E+02 -6.7097674E+02 1.2641427E+02	4.9120933E+02 1.2333457E+03 9.0855734E+02	-7.3068470E+02 -3.5785949E+02 9.0855734E+02	7.3706248E+02 -8.6985962E+02 9.0855734E+02
TZ-0671	1.5724491E+04 -2.4515077E+04 1.6117287E+04	5.2457669E+04 -2.3617308E+04 1.1226155E+04	4.8298601E+04 -3.2595651E+03 1.1984991E+03	-1.9417658E+04 -1.2713148E+04 1.1984991E+03	4.5459237E+04 -1.2497158E+04 1.1984991E+03
TZ-0563	-9.2964091E+03 6.9057947E+03 -1.2293300E+04	-2.2561417E+04 4.3031634E+03 -7.2672871E+03	-2.0902845E+04 9.8997339E+03 -2.4335582E+03	9.3333768E+03 2.3488007E+03 -2.4335582E+03	-1.8241072E+04 4.0021815E+03 -2.4335582E+03
TZ-0127	-3.6709185E+03 3.8171275E+03 -4.8463951E+03	-1.2323341E+04 2.9519105E+02 -3.5048261E+03	-1.0834562E+04 1.3111415E+04 -2.9835432E+02	5.9379381E+03 -1.0406157E+03 -2.9835432E+02	-8.2776283E+03 9.3591740E+02 -2.9835432E+02
TZ-0120	-2.4331400E+03 6.2813312E+03 2.2478014E+03	-5.2275416E+03 5.6777079E+03 -9.6768513E+02	-3.1170906E+03 3.7616957E+03 -8.4310198E+02	1.9056252E+03 -2.3272033E+02 -8.4310198E+02	-7.9246156E+02 3.7217007E+02 -8.4310198E+02
TZ-0114	-2.8592153E+04 1.7815532E+04 -1.6874750E+03	-3.9116792E+04 1.7698262E+04 -1.5375203E+04	-3.9083656E+04 -3.0170610E+04 -1.3712234E+04	1.6079721E+04 1.7364440E+04 -1.3712234E+04	-3.9210351E+04 1.7084929E+04 -1.3712234E+04
TZ-0107	-6.6055479E+03 5.1662446E+03 4.8014255E+03	-1.1268496E+04 5.2293983E+03 -4.1603026E+03	-9.6261257E+03 2.8792366E+03 -2.6611370E+03	3.3208746E+03 -1.5204566E+03 -2.6611370E+03	-9.7561347E+03 -8.6975904E+02 -2.6611370E+03

Table 8-12.—Continued

72-0134	-2.3555570E+03 1.0597356E+03 2.7056797E+03	-6.8088345E+03 2.0104549E+03 -2.3705804E+03	-4.6468946E+03 1.0886188E+03 -3.606508E+02	6.1947986E+02 -4.6947297E+02 -3.606508E+02	-3.5579913E+03 -1.2866119E+03 -3.606508E+02
72-0145	3.6822538E+03 -1.2624039E+03 1.4377944E+03	-1.3350991E+01 -6.0945615E+02 -4.6143602E+02	-5.7407045E+02 3.584673E+03 3.0681156E+03	-8.5827156E+02 -3.2831825E+02 3.0681156E+03	6.1796380E+02 -1.2422801E+03 3.0681156E+03
72-0838	8.4515728E+03 -1.4125862E+03 2.5205611E+02	6.5680588E+02 -1.2517730E+03 3.5925211E+02	1.0080892E+03 9.0025244E+03 6.2312548E+03	-1.2085981E+03 -5.5323029E+02 6.2312548E+03	1.5734710E+03 -1.1242817E+03 6.2312548E+03
72-0898	1.3919709E+04 -2.597414E+03 7.7632413E+02	1.9608482E+03 -2.3927021E+03 1.1159622E+03	2.8469383E+03 1.3282650E+04 9.9402733E+03	-2.51244117E+03 -1.2006720E+03 9.9402733E+03	3.1909986E+03 -2.7324186E+03 9.9402733E+03
72-0988	3.2617135E+03 -1.7489849E+03 1.0047578E+02	1.0459921E+03 -1.6467269E+03 4.9920523E+02	1.4389803E+03 2.9694613E+03 2.1671513E+03	-1.3259312E+03 -7.6226340E+02 2.1671513E+03	1.9291654E+03 -2.0182123E+03 2.1671513E+03
72-0651	7.7113482E+03 -1.7003196E+04 7.7143079E+03	2.7408222E+04 -1.6251777E+04 8.7950748E+03	2.5196255E+04 -1.5841072E+03 -9.9956525E+01	-1.1270598E+04 -9.1827497E+03 -9.9956525E+01	2.3521691E+04 -8.8071460E+03 -9.9956525E+01
72-0556	1.2955991E+04 -2.1900270E+03 5.0093696E+03	1.3270063E+04 -1.7126501E+03 5.3715809E+03	1.3089332E+04 9.8736233E+03 5.8825107E+03	-4.1810679E+03 -2.9118110E+03 6.8825107E+03	1.3397674E+04 -1.3848267E+03 6.8825107E+03
72-0221	-4.5839322E+03 9.3759753E+03 -8.0705675E+02	-1.0748243E+04 8.3007364E+03 -1.1710781E+03	-9.1742572E+03 5.8790369E+03 -1.1742323E+03	4.5503225E+03 8.1944285E+02 -1.1742323E+03	-7.5259285E+03 1.8529711E+03 -1.1742323E+03
72-0216	-6.1459221E+03 7.0282648E+03 2.0061616E+03	-9.6505629E+03 6.5931887E+03 -3.3739395E+03	-9.6166818E+03 8.2911659E+03 -2.7703556E+03	5.0542170E+03 -2.9059562E+03 -2.7703556E+03	-8.9878383E+03 -2.3754657E+03 -2.7703556E+03
72-0211	-1.5450787E+04 1.1656586E+04 2.6004906E+03	-2.1650443E+04 1.1025573E+04 -8.1250289E+03	-2.1496139E+04 4.9267850E+03 -7.1535148E+03	9.7179542E+03 -1.2599686E+03 -7.1535188E+03	-2.1790758E+04 -5.0325649E+01 -7.1535188E+03

Table 8-12. -Continued

12-0206	-5.6546644E+02 3.2212855E+03 4.0460758E+03	-2.7298080E+03 2.5400096E+03 -5.8587347E+02	-1.3611781E+03 2.3273262E+03 2.8495814E+02	6.1865472E+02 -5.4291262E+02 2.9495814E+02	-1.3179934E+03 2.3282282E+02 2.8495814E+02
12-0204	-1.0656785E+03 1.8212416E+03 2.2015788E+03	-4.0420117E+03 2.1080917E+03 -1.2175509E+03	-2.5748782E+03 1.0219785E+03 1.5359058E+02	4.9179685E+02 1.2838384E+02 1.5359058E+02	-1.3670089E+03 -3.8998208E+02 1.5359058E+02
12-0201	2.7501335E+03 -1.9104766E+01 1.5495635E+03	-7.7414785E+02 4.4410431E+02 -3.7422460E+03	-1.2573534E+02 2.6544633E+03 2.3651732E+03	-4.2463107E+02 3.5955467E+02 2.3651732E+03	8.4639026E+02 -4.1237102E+02 2.3651732E+03
12-0200	7.0737745E+03 -1.0685358E+03 1.1429550E+03	1.4984107E+03 -7.0081485E+02 1.2897317E+03	2.1266345E+03 6.5359824E+03 5.1616279E+03	-1.3253850E+03 2.7485714E+02 5.1616279E+03	1.7499301E+03 -1.3564352E+03 5.1616279E+03
12-1024	.0522927E+04 -1.2749183E+03 1.8446596E+03	2.8562460E+03 -1.8350442E+03 2.3337180E+03	4.0969230E+03 9.8795270E+03 7.4307675E+03	-2.5454642E+03 5.3219345E+03 7.4307675E+03	3.2234039E+03 -2.7637874E+03 7.4307675E+03
12-1021	2.7865979E+03 -1.4145607E+03 3.9213374E+02	1.0795453E+03 -1.2484971E+03 7.2113306E+02	1.5370815E+03 2.5066972E+03 1.8890805E+03	-1.5907737E+03 -2.7936945E+02 1.8890805E+03	1.8199392E+03 -1.7015548E+03 1.8890805E+03
12-0622	1.6439719E+04 -1.7114018E+04 8.4240057E+03	2.6295474E+04 -1.6267961E+04 8.1932244E+03	2.4417517E+04 7.0536013E+03 6.4172947E+03	-1.1560063E+04 -9.9289426E+03 6.4172947E+03	2.2728052E+04 -9.4825550E+03 6.4172947E+03
12-0547	9.9442850E+03 -4.7353369E+03 6.4682468E+03	1.2483098E+04 -3.8009165E+03 4.1242093E+03	1.1288977E+04 1.0474010E+04 4.5796034E+03	-4.2541539E+03 -6.4591312E+03 4.5796034E+03	1.0443543E+04 -5.5197602E+03 4.5796034E+03
12-0314	-1.2304043E+03 3.4687681E+03 2.6794777E+03	-2.3062711E+03 3.0106379E+03 -7.3732978E+02	-2.5420033E+03 5.2811532E+03 -4.9072839E+02	1.9317312E+03 -1.9354476E+03 -4.9072839E+02	-2.4403977E+03 -1.3862336E+03 -4.9072839E+02
12-0310	-1.9493098E+03 3.4557933E+03 3.4735506E+03	-3.1391724E+03 2.9806889E+03 -8.9195175E+02	-3.1447937E+03 4.4226130E+03 -6.9691363E+02	2.1791019E+03 -1.3736289E+03 -6.9691368E+02	-3.04433184E+03 -6.8477472E+02 -6.9691368E+02

Table 8-12. — Continued

TZ-0307	1.8871406E+03	1.3511440E+03	1.922232E+03	-1.2250616E+02	1.6001642E+03
	1.6069336E+03	1.1279326E+03	2.8653985E+03	-6.5907531E+02	3.7581881E+02
	3.7026560E+03	9.6641308E+02	1.3039307E+03	1.3039307E+03	1.3039307E+03
TZ-0305	1.2357835E+03	4.4075563E+02	1.0575877E+03	-2.1008045E+02	1.3195627E+03
	1.3055707E+03	8.7374301E+02	1.4506370E+03	-1.3555199E+02	2.4635626E+02
	2.2493572E+03	4.7535416E+02	9.8219293E+02	9.5219293E+02	9.8219293E+02
TZ-0303	5.3318232E+02	-1.0780442E+03	-3.8081599E+02	8.5479910E+01	5.1939548E+02
	1.4245286E+03	1.2311225E+03	9.3080608E+02	4.1866823E+02	1.1500755E+02
	1.7486295E+03	-1.0849187E+02	7.8381693E+02	7.9381693E+02	7.8381693E+02
TZ-0299	3.0724331E+03	9.7813535E+02	1.3619650E+03	-6.4096271E+02	1.7309925E+03
	1.6564787E+02	2.1969851E+02	2.3456215E+03	4.797386E+02	-3.3957037E+02
	1.4096326E+03	7.8612737E+02	2.2917692E+03	2.2917692E+03	2.2917692E+03
TZ-0827	5.8109793E+03	2.3184371E+03	3.1006751E+03	-1.2085705E+03	1.8978353E+03
	-5.1841656E+02	-4.1591791E+02	5.2995936E+03	1.0905919E+03	-1.1532292E+03
	1.9593871E+03	2.1460091E+03	4.1753248E+03	4.1753248E+03	4.1753248E+03
TZ-0877	8.5155849E+03	3.7784321E+03	5.1381972E+03	-2.1939198E+03	3.3470086E+03
	-1.2942568E+03	-1.1202892E+03	7.9331545E+03	1.4747859E+03	-2.0717128E+03
	2.8571947E+03	3.4964440E+03	5.5997836E+03	5.5997836E+03	5.9997836E+03
TZ-0977	2.5355433E+03	1.5964574E+03	1.9913163E+03	-1.4647025E+03	2.2116251E+03
	-9.0594423E+02	-7.4792737E+02	2.2673755E+03	-3.1882614E+01	-1.3389293E+03
	5.9059124E+02	1.0619338E+03	1.6944377E+03	1.5944377E+03	1.6944377E+03
TZ-0645	1.6409971E+04	2.2816551E+04	2.1315570E+04	-1.3608239E+04	1.9771559E+04
	-1.6122780E+04	-1.5812895E+04	8.5906979E+03	-9.5159629E+03	-9.3678655E+03
	7.4513431E+03	6.9241890E+03	7.1147330E+03	7.1147330E+03	7.1147330E+03
TZ-0542	1.2421251E+04	1.6448096E+04	1.5589823E+04	-6.4221994E+03	1.4849208E+04
	-7.1393017E+03	-6.4492674E+03	6.9152435E+03	-5.2051084E+03	-4.5627381E+03
	6.6420370E+03	5.7619945E+03	5.7643009E+03	5.7643009E+03	5.7643009E+03
TZ-0360	9.1074715E+03	1.1284505E+04	1.1071548E+04	-3.7122263E+03	1.1059495E+04
	-1.7407555E+03	-2.0897119E+03	5.7070136E+03	-2.5177267E+03	-1.7358861E+03
	5.2522802E+03	4.6115139E+03	4.5859205E+03	4.5859205E+03	4.5859205E+03

Table 8-12. —Continued

TZ-0358	7.4712145E+03 -1.329846E+03 4.2717840E+03	8.7646700E+03 -1.6445848E+03 3.7309159E+03	8.8032822E+03 4.9045656E+03 3.9665346E+03	-2.7289555E+03 -1.9692559E+03 3.9665346E+03	8.5989775E+03 -8.6667971E+02 3.9665346E+03
TZ-0356	5.3702813E+03 -6.7097380E+02 3.0425446E+03	5.7674786E+03 -9.8482741E+02 2.5179040E+03	5.990936E+03 3.5432733E+03 3.0223138E+03	-1.9558837E+03 -1.1964742E+03 3.0223198E+03	5.6332724E+03 -4.2828044E+02 3.0223198E+03
TZ-0373	2.8747590E+03 1.4541072E+01 1.8303696E+03	2.5972998E+03 -2.5315768E+02 1.2264603E+03	2.8685773E+03 1.8440744E+03 1.7682699E+03	-9.4511007E+02 -3.4285926E+02 1.7692699E+03	3.0788520E+03 -2.4390626E+02 1.7682699E+03
TZ-0372	1.7787873E+03 3.4308257E+02 9.9725509E+02	1.2198487E+03 7.6906177E+01 7.1915066E+02	1.4351837E+03 1.2662049E+03 1.2368625E+03	-4.7185735E+02 1.0157471E+02 1.2368625E+03	1.7768288E+03 -1.1964392E+02 1.2368625E+03
TZ-0371	3.6474088E+03 4.2297985E+02 1.6893795E+03	2.2603707E+03 8.9079512E+01 1.6009770E+03	2.7263175E+03 2.9275985E+03 2.5936818E+03	-3.6034943E+02 5.3422161E+02 2.5936818E+03	2.6478896E+03 -4.8227544E+02 2.5936818E+03
TZ-1074	6.0101489E+03 -3.9715057E-01 2.6501641E+03	2.9344171E+03 -3.6336380E+01 2.7941456E+03	3.8898902E+03 5.3746267E+03 4.3486730E+03	-1.3186956E+03 1.5909445E+03 4.3486730E+03	2.6484217E+03 -9.7768762E+02 4.3486730E+03
TZ-1073	5.4140350E+03 -3.464974E+02 2.4063507E+03	2.8133237E+03 -2.2016591E+02 2.7250366E+03	3.7435593E+03 4.9676177E+03 3.8903449E+03	-1.2955738E+03 1.5080059E+03 3.3903449E+03	2.8699408E+03 -8.0769840E+02 3.8903449E+03
TZ-1071	1.6263657E+03 -1.3729509E+02 8.2405394E+02	1.0557880E+03 -6.1469497E+01 9.2578627E+02	1.3375351E+03 1.4243914E+03 1.1818543E+03	-6.2708550E+02 4.9937515E+02 1.1818543E+03	1.6389227E+03 -2.0054457E+02 1.1818543E+03
TZ-0639	1.3660853E+04 -1.3225713E+04 6.1437284E+03	1.8610576E+04 -1.4080760E+04 5.606486E+03	1.7442960E+04 7.4517344E+03 6.1264660E+03	-8.3593970E+03 -8.1941673E+03 6.1264660E+03	1.5942233E+04 -7.9392400E+03 6.1264660E+03
TZ-0535	1.5720248E+04 -1.0112916E+04 7.7670745E+03	2.0777420E+04 -9.4476840E+03 7.1258364E+03	1.9816036E+04 9.1066562E+03 7.4515799E+03	-8.6273893E+03 -7.4069459E+03 7.4515789E+03	1.8495615E+04 -6.4967456E+03 7.4515789E+03

Table 8-12.—Continued

TZ-0456	4.0163603E+03 -2.3057886E+02 2.7225559E+03	4.8016913E+03 -4.7792911E+02 2.0103850E+03	4.7721440E+03 2.2729236E+03 2.1177915E+J3	-1.4819370E+03 -8.2758348E+02 2.1177915E+03	4.5948277E+03 -2.8421099E+02 2.1177915E+03
TZ-0389	4.9683669E+03 -1.9616759E+03 2.7805120E+03	6.7024665E+03 -1.9709246E+03 2.4224237E+03	6.4224496E+03 2.7417264E+03 2.5042730E+03	-2.5663503E+03 -2.3616697E+03 2.5042780E+03	5.6583378E+03 -1.5843191E+03 2.5042780E+03
TZ-0454	8.5283125E+03 -1.6323939E+03 4.6357636E+03	1.0041330E+04 -1.4297947E+03 4.4156005E+03	1.0321893E+04 5.6266355E+03 4.8692024E+03	-3.7017377E+03 -2.1328397E+03 4.3692024E+03	9.9520595E+03 -1.7991026E+03 4.8692024E+03
TZ-0452	6.6060889E+03 -8.2297796E+02 3.7362389E+03	6.3911282E+03 -9.2271556E+02 3.3979823E+03	7.0474049E+03 4.6187742E+03 4.1557967E+03	-2.7761275E+03 -5.3727113E+02 4.1557967E+03	7.0952200E+03 -1.7714046E+03 4.1557967E+03
TZ-0823	2.3873712E+03 9.2269840E+02 2.0643577E+03	1.1764278E+03 5.6248443E+02 1.3809026E+03	1.5930290E+03 1.7719799E+03 1.9739270E+03	-5.0928452E+02 1.2768880E+03 1.9739270E+03	1.0212093E+03 -3.0540029E+01 1.9739270E+03
TZ-0857	5.3412654E+03 3.9693226E+02 2.7654518E+03	2.7674175E+03 2.7508555E+02 2.6668224E+03	3.4771632E+03 4.7387818E+03 3.9651210E+03	-6.6076484E+02 1.7842467E+03 3.9651210E+03	3.3354203E+03 4.4044483E+02 3.9651210E+03
TZ-0916	4.6056673E+03 3.9939579E+02 1.9622751E+03	2.5578633E+03 3.6341341E+02 2.2192342E+03	3.0161538E+03 4.2174255E+03 3.3871627E+03	-4.1874709E+02 1.2742186E+03 3.3871627E+03	3.4039166E+03 7.0943261E+02 3.3871627E+03
TZ-0956	1.3635085E+03 4.2286376E+02 5.2085147E+02	8.6058337E+02 3.4245122E+02 6.4225371E+02	9.1460250E+02 1.2342916E+03 1.0368984E+03	-1.3910908E+02 2.9532564E+02 1.0368984E+03	1.1478283E+03 2.5654918E+02 1.0368984E+03
TZ-0634	7.2952017E+03 -1.0613487E+04 3.7291129E+03	1.4523492E+04 -9.5552067E+03 3.4346625E+03	1.3419706E+04 2.3013555E+03 2.2812349E+03	-8.5320707E+03 -8.5909543E+03 2.2812349E+03	1.1102018E+04 -9.0469597E+03 2.2812349E+03
TZ-0476	1.2299221E+04 -6.7863190E+03 5.9375846E+03	1.5046076E+04 -6.9448068E+03 5.5472918E+03	1.4596717E+04 7.6560843E+03 5.3460360E+03	-5.7805771E+03 -4.6484375E+03 6.3460360E+03	1.3411609E+04 -3.6621261E+03 6.3460360E+03

Table 8-12. -Continued

YZ-0474	6.1616409E+03	6.5259756E+03	6.6767804E+03	-2.1869202E+03	6.4018355E+03
	-1.1373349E+03	-2.0615246E+03	4.1442192E+03	-9.4618485E+02	-7.4120099E+02
	3.3550817E+03	2.9597948E+03	3.5880794E+03	3.5880794E+03	3.5880794E+03
YZ-0473	5.3360775E+03	5.7618754E+03	6.2072947E+03	-2.5799434E+03	6.5609616E+03
	-1.3519705E+03	-1.2087348E+03	3.4974858E+03	-7.4285076E+02	-1.6206774E+03
	3.2942577E+03	2.8159407E+03	3.1243166E+03	3.1243166E+03	3.1243166E+03
YZ-0471	4.6703956E+03	4.5220255E+03	5.0606800E+03	-2.2322860E+03	5.4884475E+03
	-1.8120702E+03	-5.5215049E+02	3.2306855E+03	-1.5898435E+02	-1.4594029E+03
	2.9355284E+03	2.5587234E+03	2.9329592E+03	2.9329592E+03	2.9329592E+03
YZ-0812	2.4157898E+03	1.9303895E+03	2.1692477E+03	-8.2892941E+02	2.2507736E+03
	-4.7240192E+02	-1.1117335E+02	1.9176169E+03	4.0697902E+02	-2.5734618E+02
	1.3981835E+03	1.3033125E+03	1.6544225E+03	1.6544225E+03	1.6544225E+03
YZ-0860	3.3316204E+03	1.9356581E+03	2.2502768E+03	-1.9550194E+02	3.2040884E+03
	-1.0723486E+02	6.6927309E+01	2.8812347E+03	1.0495755E+03	1.1517243E+03
	1.8371716E+03	1.6184176E+03	2.4209444E+03	2.4209444E+03	2.4209444E+03
YZ-0939	2.3303107E+03	1.2113281E+03	1.3035437E+03	7.5688463E+01	2.2415472E+03
	4.8264145E+02	3.4000041E+02	2.0946356E+03	7.0290031E+02	1.0579108E+03
	1.0705695E+03	9.8934113E+02	1.7550697E+03	1.7550697E+03	1.7550697E+03
YZ-0956	7.5930365E+02	4.1646099E+02	3.5969429E+02	-4.0269278E+01	5.8587220E+02
	5.1635803E+02	3.1497667E+02	6.7678139E+02	1.6088177E+02	1.6708781E+02
	2.6610865E+02	2.6182431E+02	6.0687333E+02	6.0687333E+02	6.0687333E+02
YZ-0798	-8.8713322E+02	8.4524380E+03	7.6054654E+03	-7.1921198E+03	5.0479498E+03
	-6.6789872E+03	-2.5196337E+03	-4.1483971E+03	-7.9805349E+03	-9.5802817E+03
	8.7623791E+02	7.6555230E+02	-2.5674479E+03	-2.5674479E+03	-2.5674479E+03
YZ-0712	6.2346761E+03	1.0861570E+04	1.0612496E+04	-5.6438458E+03	9.4216377E+03
	-8.0559932E+03	-5.1138136E+03	2.7951217E+03	-5.3011342E+03	-6.0342566E+03
	3.4092985E+03	3.3191186E+03	2.6018379E+03	2.6018379E+03	2.6018379E+03
YZ-0494	9.1264755E+03	6.5701916E+03	6.8775764E+03	-1.4637389E+03	7.3059772E+03
	-8713042E+03	-3.8173037E+03	7.4179161E+03	2.9352405E+02	1.0273027E+03
	.7023966E+03	3.5136991E+03	5.7875557E+03	5.7875557E+03	5.7875557E+03

Table 8-12. —Continued

TZ-0493	5.4412933E+03 3.9173238E+02 2.8624429E+03	5.2178237E+03 -3.5772680E+03 2.5374944E+03	5.4658643E+03 3.91645.5E+03 3.1907113E+03	-2.0757938E+03 -2.3351324E+02 3.1907113E+03	5.7777986E+03 -3.0075701E+02 3.1907113E+03
TZ-0492	4.2601610E+03 -1.3527737E+03 2.4603192E+03	4.2530272E+03 -2.6082552E+03 2.1286148E+03	4.5810394E+03 3.0063256E+03 2.5035820E+03	-2.1050157E+03 -2.7834995E+02 2.5035820E+03	5.2520896E+03 -8.8113952E+02 2.5035820E+03
TZ-0491	1.7155384E+03 -1.0045765E+03 1.5347783E+03	1.5560255E+03 -7.7122376E+02 8.5739720E+02	1.7277730E+03 1.0891622E+03 1.0616893E+03	-9.4172260E+02 2.7543311E+02 1.0616893E+03	2.6829222E+03 -1.9876596E+02 1.0616893E+03
TZ-0897	1.4053184E+03 -9.1880742E+02 1.1253741E+03	1.3122589E+03 -1.5835470E+02 7.4336610E+02	1.3937840E+03 9.9464412E+02 8.9049403E+02	-5.7798099E+02 3.2915760E+02 8.3049403E+02	2.5742087E+03 1.3940957E+02 8.9049403E+02
TZ-0906	7.3770231E+02 -9.4285833E+01 6.6272626E+02	6.9754546E+02 3.7538684E+02 5.2842042E+02	6.9648313E+02 5.8858497E+02 5.3367870E+02	1.0633191E+02 4.5567322E+02 5.3367870E+02	1.4030599E+03 6.2165855E+02 5.3367870E+02
TZ-0955	3.7387914E+02 1.3403555E+02 3.3844725E+02	3.8701697E+02 2.6541474E+02 3.3466191E+02	3.9837741E+02 3.2056400E+02 2.8368930E+02	1.2885909E+02 2.7920665E+02 2.9368930E+02	6.4954853E+02 3.5314976E+02 2.8368930E+02
TZ-0791	-1.5901763E+03 -1.7955535E+04 1.6671980E+03	1.4440182E+04 -2.4223599E+03 2.0225488E+03	1.3765450E+04 -6.7586850E+03 -4.0343470E+03	-1.2498536E+04 -1.3185177E+04 -4.0343470E+03	1.0484420E+04 -1.8126755E+04 -4.0343470E+03
TZ-0705	6.2611082E+03 1.5999977E+03 1.8927352E+03	2.9961118E+01 -8.3843296E+01 1.5045594E+03	3.8502479E+02 6.5660045E+03 4.8445318E+03	2.5999341E+03 3.4972475E+03 4.8445318E+03	1.5391257E+03 5.0560383E+03 4.8445318E+03
TZ-0513	7.4490959E+03 -9.2574258E+03 3.8763395E+03	1.0820030E+04 -4.1076584E+03 3.9178003E+03	1.0844237E+04 4.1783804E+03 3.7254866E+03	-6.2301713E+03 -3.9459342E+03 3.7254866E+03	1.0219704E+04 -4.6661291E+03 3.7254866E+03
TZ-0512	6.3957607E+03 4.2752748E+02 2.8520040E+03	4.8183925E+03 -3.2796793E+03 2.6089330E+03	4.9989942E+03 5.1063923E+03 4.0561265E+03	-1.7271108E+03 3.1017838E+02 4.0561265E+03	6.1420554E+03 7.2613371E+02 4.0561265E+03

REPRODUCIBILITY OF THE
ORIGINAL PAGE IS POOR

Table 8-12.—Continued

TZ-0511	2.3266652E+03	2.0218874E+03	1.9714226E+03	-8.1069894E+02	3.0695383E+03
	-3.1419105E+02	-2.4415127E+02	1.7210592E+03	1.3740346E+02	3.0151950E+02
	1.3007497E+03	9.9290834E+02	1.137447E+03	1.4379447E+03	1.4379447E+03
TZ-0854	1.4964887E+03	1.3470491E+03	1.2314305E+03	-2.3737859E+02	2.1280416E+03
	-8.2624902E+01	-1.7015571E+03	1.170067E+03	2.3353997E+02	3.9109535E+02
	9.7399755E+02	7.7482844E+02	9.8311748E+02	9.8117484E+02	9.8117484E+02
TZ-0903	8.8893439E+02	7.9955827E+02	7.1936811E+02	5.3903967E+02	1.0658018E+03
	3.8407847E+02	-1.4672425E+02	7.3605323E+02	6.2543555E+02	9.4742174E+02
	7.8663867E+02	6.5241149E+02	6.4163094E+02	6.6163094E+02	6.6163094E+02
TZ-0952	2.9257590E+02	2.6917197E+02	2.4760967E+02	4.3393587E+02	2.6892019E+02
	2.5704102E+02	1.9067836E+02	2.5511826E+02	2.6764951E+02	5.0900528E+02
	2.8949617E+02	2.5466160E+02	2.3018071E+02	2.3018071E+02	2.3018071E+02
TZ-0775	2.2089311E+03	7.7633347E+03	7.6794919E+03	-5.9377527E+02	6.7680904E+03
	-1.0296034E+04	-1.1329922E+03	-3.3858631E+02	-5.1359101E+03	-7.1309752E+03
	1.8036810E+03	1.9561536E+03	2.6736135E+02	2.6736135E+02	2.6736135E+02
TZ-0533	3.1102700E+03	2.0593155E+03	2.1010525E+03	-5.3936101E+02	2.7081246E+03
	5.3475565E+02	-9.4842625E+02	2.5647923E+03	3.0897754E+02	6.6583929E+02
	1.3103401E+03	1.1724034E+03	2.0258205E+03	2.0258205E+03	2.0258205E+03
TZ-0532	8.5853374E+02	5.9913296E+02	5.0954329E+02	-7.1378203E+00	8.4521411E+02
	3.2114641E+02	-1.4303944E+03	6.3542517E+02	1.7947345E+02	5.0467147E+02
	5.5144030E+02	3.1797883E+02	5.6948809E+02	5.6848809E+02	5.6848809E+02
TZ-0531	5.4645170E+02	3.7174516E+02	2.707405E+02	2.3712788E+02	3.6375366E+02
	8.3223121E+02	-1.6314477E+03	4.1227655E+02	3.4223028E+02	4.5853350E+02
	5.0401647E+02	2.6996409E+02	4.0302936E+02	4.0302906E+02	4.0302906E+02
TZ-0900	4.4095410E+02	3.8190450E+02	3.2702749E+02	4.2390943E+02	2.6413587E+02
	8.5783371E+02	-9.3885549E+02	3.8436147E+02	3.1353875E+02	4.3955452E+02
	3.4587801E+02	3.0654527E+02	3.2897850E+02	3.2897850E+02	3.2897350E+02
TZ-0950	1.5791037E+02	1.5070599E+02	1.3780671E+02	2.1760656E+02	1.1718686E+02
	3.2255721E+02	-2.2982611E+02	4.532290E+02	1.1751478E+02	2.0536798E+02
	1.1033483E+02	1.2406345E+02	1.1751478E+02	1.1751478E+02	1.1751478E+02

Table 8-12. — Continued

72-3230	-9.2790384E+03 -1.3389579E+03 -9.5621054E+03	1.4089260E+02 -5.2078720E+02 -1.5899040E+03	-1.1991403E+03 -1.0970952E+04 -7.6126178E+03	-8.8312501E+02 -1.4865815E+03 -7.6126178E+03	-8.8316600E+02 -2.1269544E+03 -7.6126178E+03
72-3231	-7.0299512E+03 -1.03470C2E+03 -7.8542400E+03	-1.0207143E+03 -4.7689574E+02 -1.5260891E+03	-2.2290847E+03 -8.4576724E+03 -5.6184738E+03	-1.6119898E+02 2.9726067E+02 -5.6184738E+03	-2.3408217E+03 -1.2786165E+03 -5.6184738E+03
72-3233	-6.52159P5E+03 4.7546908E+03 -1.5080015E+04	-8.7413559E+02 2.6216788E+03 -6.3760808E+02	-2.1033715E+03 -9.4171237E+03 -5.0465699E+03	3.5629732E+03 3.0722970E+03 -5.0465699E+03	-2.6265398E+03 6.3873825E+03 -5.0465699E+03
72-3234	-2.6932687E+03 5.7347503E+03 -7.0803823E+03	-2.5148346E+02 3.0857386E+03 -1.3998436E+02	-7.6264674E+02 -2.5454186E+03 -2.0794212E+03	3.5443022E+03 1.4999279E+03 -2.0794212E+03	-9.8302832E+02 6.8280694E+03 -2.0794212E+03
72-3235	-1.5299025E+04 -1.4149763E+03 -1.77157P3E+04	3.1662216E+01 -4.1665797E+02 -2.9466568E+03	-2.5047858E+03 -1.8302677E+04 -1.2626993E+04	-1.4211047E+03 -2.2102979E+03 -1.2626993E+04	-2.0668609E+03 -3.6010576E+03 -1.2626993E+04
72-3236	-8.3210567E+03 -1.2510915E+03 -1.1483592E+04	-7.6640685E+02 -4.3239508E+02 -1.7738949E+03	-2.4356996E+03 -1.0334851E+04 -6.8794174E+03	-3.7702009E+02 5.5427552E+02 -6.8794174E+03	-2.6579915E+03 -1.8714272E+03 -6.8794174E+03
72-3238	-8.4841549E+03 5.9797394E+03 -2.5204932E+04	6.1571056E+02 3.3563572E+03 -3.5386816E+01	-1.1862447E+03 -1.1453525E+04 -6.9440400E+03	4.7720436E+03 4.2186490E+03 -6.9440400E+03	-1.8557715E+03 8.9294313E+03 -6.9440400E+03
72-3239	-3.4997958E+03 8.14656C6E+03 -9.732924E+03	-1.2642384E+02 4.4493000E+03 -9.5294365E+01	-8.1216261E+02 -4.6586598E+03 -2.7460004E+03	5.1725660E+03 1.3573025E+03 -2.7460004E+03	-1.0610082E+03 1.0125997E+04 -2.7460004E+03
72-3240	-5.8702173E+03 1.1151032E+01 -8.4702342E+03	-1.3580701E+02 7.7505159E+01 -1.4170942E+03	-1.3891006E+03 -7.1902506E+03 -4.9110210E+03	-5.4233169E+02 -7.1843476E+02 -4.9110210E+03	-1.2662957E+03 -1.5039138E+03 -4.9110210E+03
72-3241	-1.2393234E+03 -4.0273664E+02 -1.6272874E+03	9.9518262E+03 4.0290882E+03 -1.3288525E+02	-2.2943932E+02 -1.6071616E+03 -1.0763957E+03	-7.7902682E+01 2.9737389E+02 -1.0763957E+03	-2.7353837E+02 -3.4243586E+02 -1.0763957E+03

Table 8.12. --Concluded

12-3242	-2.7121759E+03 1.7369330E+03 -9.8202710E+03	5.6465894E+02 1.0720945E+03 2.2498526E+02	-3.6257569E+01 -3.7816454E+03 -2.2717607E+03	1.4502780E+03 1.5695060E+03 -2.2717607E+03	-2.4617862E+02 2.8420715E+03 -2.2717607E+03
12-3243	-7.9505094E+02 2.3573167E+03 -2.0503857E+03	-1.6850777E+01 1.3242679E+03 -2.0902657E+01	-1.7257717E+02 -1.0597839E+03 -6.2764282E+02	1.6498964E+03 4.3304772E+02 -6.2764282E+02	-1.9021620E+02 3.2899372E+03 -6.2764282E+02

Table 8-13.—Antisymmetric Loads Matrix from FLEXSTAB
for the 4 Load Conditions in Table 8-11

TZ-Node No. (LB)	Condition description			
	Lateral gust at M=0.9	Rudder Man. No 1	Rudder Man. No 2	Rudder Man. No 3
TZ-3191	-1.7965876E+03	7.1700537E+02	-2.3117178E+03	-3.0287232E+03
TZ-3189	-1.1965342E+03	7.1137302E+02	-1.0688560E+03	-1.7802290E+03
TZ-3197	-1.1841138E+03	1.0886174E+03	-4.4315271E+02	-1.9317701E+03
TZ-3185	-5.8107511E+02	8.8489613E+02	3.1586421E+02	-5.6903192E+02
TZ-3193	-8.6292874E+02	1.2958245E+03	4.8027151E+02	-8.1555289E+02
TZ-3181	-3.7543174E+02	9.8237185E+02	2.4167397E+02	-3.4069788E+02
TZ-2038	-4.2011525E+02	6.6909608E+02	2.9594774E+02	-3.7314834E+02
TZ-2098	-3.7611202E+02	6.2197468E+02	3.0149953E+02	-3.2049516E+02
TZ-2158	-3.4452614E+02	6.0827736E+02	3.2224598E+02	-2.8603138E+02
TZ-2218	-2.2682532E+02	4.3610074E+02	2.6232547E+02	-1.7377527E+02
TZ-2278	-1.7712077E+02	3.8426845E+02	2.8170598E+02	-1.0256247E+02
TZ-2338	-9.9307766E+01	2.9301278E+02	2.5515584E+02	-3.7856941E+01
TZ-2398	-2.6535712E+01	2.1098724E+02	2.4502134E+02	3.4034696E+01
TZ-2458	5.3136354E+01	1.3066568E+02	2.4882163E+02	1.1815594E+02
TZ-2518	1.1904069E+02	2.9713767E+01	2.0361523E+02	1.7390147E+02
TZ-2578	2.1629734E+02	-7.0482783E+01	2.1378975E+02	2.8427254E+02
TZ-2638	2.8111458E+02	-1.6361781E+02	1.8650853E+02	3.5012634E+02
TZ-2698	3.6490758E+02	-2.9397171E+02	1.8040216E+02	4.7437387E+02
TZ-2758	4.6741053E+02	-3.4639125E+02	1.6035931E+02	5.0675056E+02
TZ-2819	1.0969528E+03	-9.0761526E+02	2.8897275E+02	1.1965980E+03

Table 8-13.—Continued

TZ-1087	-2.1278564E+02	1.0682769E+03	3.6816187E+02	-7.0011508E+02
TZ-3199	-3.2490729E+03	3.8195298E+01	-4.0684832E+03	-4.1066785E+03
TZ-3206	-3.9349715E+03	2.1872654E+03	-2.5266324E+03	-4.7138977E+03
TZ-3210	-1.5105954E+03	1.0614312E+04	9.6037271E+03	-2.0105850E+03
TZ-3214	-4.7819271E+03	7.4235840E+01	-5.6734505E+03	-5.7476863E+03
TZ-3215	-5.1652778E+03	2.3116422E+03	-3.6656528E+03	-5.9772950E+03
TZ-3216	-8.1654396E+02	5.1902333E+03	3.9786631E+03	-1.2115702E+03
TZ-3217	-2.4939196E+02	4.7369750E+03	4.2594978E+03	-4.7747721E+02
TZ-3218	-2.1324170E+02	-3.2065787E+02	-4.7641394E+02	-1.5575607E+02
TZ-3219	-1.8403994E+03	3.2216309E+02	-1.8034989E+03	-2.1256620E+03
TZ-3220	-3.0351799E+02	3.7194020E+03	3.1711289E+03	-5.4827307E+02
TZ-3221	2.3253363E+01	-2.6398073E+02	-2.3968333E+02	2.4297393E+01
TY-0238	1.0013275E-01	-5.0271020E-01	-1.7324976E-01	3.2946044E-01
TY-0238	3.3923026E+02	1.1195948E+02	4.8154536E+02	3.6958588E+02
TY-0475	1.7337270E+00	-8.7040680E+03	-2.9996958E+00	5.7043721E+00
TZ-0475	1.6866701E+03	5.7807403E+02	2.4238871E+03	1.8458131E+03
TY-0472	4.7119611E+00	-2.3656105E+01	-8.1526387E+00	1.5503467E+01
TZ-0472	1.9046099E+03	7.0477614E+02	2.7593356E+03	2.0545594E+03
TY-0862	4.1712443E+00	-2.0941470E+01	-7.2170900E+00	1.3724380E+01
TZ-0862	7.7975988E+02	4.3584029E+02	1.5592251E+03	1.1223848E+03

Table 8-13.—Continued

TY-0912	3.2900761E+00	-1.6517621E+01	-5.6924921E+00	1.0825129E+01
TZ-0912	1.0986082E+03	2.6891623E+01	6.8088936E+01	4.1257313E+01
TY-0428	2.4804313E+00	-1.2452850E+01	-4.2916440E+00	8.1612057E+00
TZ-0428	3.0892770E+02	-2.1378401E+02	-8.3921771E+02	-6.2543369E+02
TY-0417	9.8983376E-01	-4.9696494E+03	-1.7126976E+00	3.2569517E+00
TZ-0417	1.3560570E+02	8.5766677E+01	2.9462924E+02	2.0886257E+02
TY-0233	2.2773048E+00	-1.1433066E+01	-3.9401945E+00	7.4928716E+00
TZ-0233	-8.6201478E+01	5.8282667E-01	-9.3705412E+01	-9.4288239E+01
TY-0291	2.3489222E+00	-1.1792145E+01	-4.0639444E+00	7.7282005E+00
TZ-0291	6.3759698E+02	2.3740759E+02	9.2798450E+02	6.9057692E+02
TY-0329	2.4747094E+00	-1.2424123E+01	-4.2817441E+00	8.1423794E+00
TZ-0329	2.4637733E+03	8.1368159E+02	3.3316814E+03	2.5179998E+03
TY-0378	4.9236704E+00	-2.4718978E+01	-9.5189392E+00	1.6200040E+01
TZ-0378	1.6189467E+03	6.2651021E+02	2.3612593E+03	1.7347480E+03
TY-0426	2.8981279E+00	-1.4549869E+01	-5.0143430E+00	9.5355263E+00
TZ-0426	5.5530089E+02	2.2574447E+01	3.2569458E+01	9.9950107E+00
TY-0416	9.6127440E-01	-4.8260179E+03	-1.6631977E+00	3.1628202E+00
TZ-0416	1.3161024E+02	8.8207493E+01	3.0051512E+02	2.1230763E+02
TY-0226	9.6127440E-01	-4.8260179E+03	-1.6631977E+00	3.1628202E+00
TZ-0226	2.4682358E+02	5.4707714E+01	2.0258518E+02	1.4787746E+02

REPRODUCIBILITY OF THE
ORIGINAL PAGE IS POOR

Table 8-13.—Continued

TY-0375	8.4397604E-01	-4.2371288E+00	-1.4602480E+00	2.7768808E+00
TZ-0375	-3.2071019E+02	-4.0383219E+01	-2.4419032E+02	-2.0380710E+02
TY-0414	1.6307334E-01	-8.1869946E-01	-2.8214961E-01	5.3654985E-01
TZ-0414	-1.8671053E+00	2.1784939E+00	9.2444144E-02	-2.0960497E+00
TZ-0040	-3.3797223E+00	9.8572129E+00	5.7061053E+00	-4.1511076E+00
TZ-0034	-1.5173728E+01	6.8937498E+01	3.5406660E+01	-3.3430838E+01
TZ-0025	-1.7555636E+01	7.1610113E+01	4.8922304E+01	-2.2687809E+01
TZ-0017	-2.1151378E+00	1.6371963E+01	1.6442857E+01	7.0894535E-02
TZ-0009	-2.0619584E+01	1.3291379E+02	4.3326326E+01	-8.9587466E+01
TZ-0005	-4.8427448E+00	4.9581167E+01	1.7514317E+01	-3.2066850E+01
TZ-0001	8.1835642E-01	1.6000449E+01	9.9820008E+00	-6.0194483E+00
TZ-0842	2.4829987E+00	1.9969609E+00	3.4635455E+00	1.4665846E+00
TZ-0592	4.3455252E+00	2.7323206E+00	-3.6046458E+00	-6.3369664E+00
TZ-0992	2.3414793E+00	1.8696634E+00	-6.1575628E+00	-8.0272261E+00
TZ-0671	-4.0621799E+00	1.0674397E+01	2.6604222E+00	-8.0139751E+00
TZ-0563	-9.2943931E+01	4.7910267E+02	1.8619392E+02	-2.9290873E+02
TZ-0127	-9.8666288E+01	5.0516033E+02	2.0802062E+02	-2.9713972E+02
TZ-0120	-7.5081467E+01	3.7513975E+02	1.7867279E+02	-1.9646697E+02
TZ-0114	-1.7307022E+02	8.9944522E+02	3.2774143E+02	-5.7170379E+02
TZ-0107	-6.3335307E+01	4.1178551E+02	1.3888484E+02	-2.7290068E+02

Table 8-13.—Continued

TZ-0134	-2.9461489E+01	2.2444496E+02	8.3138366E+01	-1.4130659E+02
TZ-0145	-3.5661310E+00	7.4273492E+01	4.0046889E+01	-3.4226603E+01
TZ-0839	7.2959995E+00	1.2200977E+01	1.4286909E+01	2.0859318E+00
TZ-0998	1.5004145E+01	7.8175066E+03	-4.6423770E+00	-1.2459884E+01
TZ-0988	8.5403012E+00	1.6765866E+03	-1.0796676E+01	-1.2473263E+01
TZ-0661	-2.2653684E+01	7.8498115E+01	5.5084926E+01	-2.3413189E+01
TZ-0556	-6.4917952E+01	3.3018966E+02	1.5133009E+02	-1.7885958E+02
TZ-0221	-1.3510076E+02	7.2309336E+02	2.9192446E+02	-4.3116890E+02
TZ-0216	-1.2961645E+02	6.3513050E+02	2.5733315E+02	-3.7779735E+02
TZ-0211	-1.7079667E+02	9.1362864E+02	3.3029743E+02	-5.8333122E+02
TZ-0206	-4.5579035E+01	3.3369811E+02	1.2336920E+02	-2.1032891E+02
TZ-0204	-2.9869609E+01	2.4674032E+02	1.0261995E+02	-1.4412047E+02
TZ-0201	-4.4991914E+00	1.1241740E+02	6.2791995E+01	-4.9625405E+01
TZ-0200	1.4454225E+01	2.6528838E+01	2.9636219E+01	3.1073817E+00
TZ-1024	2.7886472E+01	1.1199174E+01	1.4225815E+01	3.0266413E+00
TZ-1021	1.6277604E+01	5.6196986E+03	3.2541449E+00	-2.3655538E+00
TZ-0652	-1.2621558E+01	-1.8475663E+03	5.6603025E+01	5.9450991E+01
TZ-0547	-8.7863051E+01	3.9695037E+02	1.8855693E+02	-2.0839344E+02
TZ-0314	-9.7756660E+01	4.8560221E+02	1.9418179E+02	-2.3142042E+02
TZ-0310	-8.8993610E+01	4.6885894E+02	1.8386291E+02	-2.3499603E+02

Table 8-13.—Continued

TZ-0307	-3.7717830E+01	2.7036383E+02	1.1517843E+02	-1.9518541E+02
TZ-0305	-1.8432450E+01	1.7575419E+02	8.1915261E+01	-9.3838934E+01
TZ-0303	-1.4409651E+01	1.8024611E+02	9.0757323E+01	-8.9488782E+01
TZ-0299	1.0735779E+01	7.6826447E+01	6.2716542E+01	-1.4109906E+01
TZ-0827	2.9425200E+01	2.7597520E+01	4.8138667E+01	2.0541146E+01
TZ-0877	5.3814281E+01	8.4786699E+01	4.7306268E+01	3.8827598E+01
TZ-0977	3.4849270E+01	-2.7575555E+01	2.0347048E+01	2.3104603E+01
TZ-0645	-4.6993626E+00	-3.1944087E+01	5.4903630E+01	8.4747717E+01
TZ-0542	-1.0569011E+01	3.4562414E+01	6.0171935E+01	2.5609521E+01
TZ-0360	-2.7642621E+00	4.6218191E+01	4.9396436E+01	3.1782954E+00
TZ-0358	4.9856572E+00	5.7876460E+01	6.1697493E+01	3.8210331E+00
TZ-0356	8.9948948E+00	6.7772178E+01	6.9761834E+01	1.9896553E+00
TZ-0373	7.8646757E+00	7.3658692E+01	6.4003874E+01	-9.6548179E+00
TZ-0372	1.5230273E+01	4.9211691E+01	5.4379491E+01	5.1678003E+00
TZ-0371	5.2647945E+01	6.3065636E+01	1.0674114E+02	4.3675509E+01
TZ-1074	7.9072495E+01	5.3776901E+01	1.1965410E+02	6.5877199E+01
TZ-1073	8.3899991E+01	2.3374630E+01	8.7949547E+01	6.4574918E+01
TZ-1071	4.9341841E+01	1.4814385E+01	4.5115446E+01	3.0301061E+01
TZ-0639	2.0939408E+00	-1.5599817E-01	8.0153654E+01	8.0309663E+01
TZ-0538	1.1334433E+01	3.0463129E+01	1.1444776E+02	8.3984627E+01

Table 8-13.—Continued

TZ-0456	-8.8879158E+00	8.0180984E+01	5.6211811E+01	-2.3969172E+01
TZ-0385	2.8981710E+01	5.6127302E+01	1.1430002E+02	5.9172717E+01
TZ-0454	1.7409472E+02	1.2345455E+02	3.3281624E+02	2.0936169E+02
TZ-0452	1.8713309E+02	1.5287533E+02	3.4202074E+02	1.9914541E+02
TZ-0823	1.3327678E+02	1.4852791E+02	2.6073911E+02	1.1221120E+02
TZ-0857	1.8183546E+02	1.0091797E+02	2.6919268E+02	1.5827471E+02
TZ-0916	1.7944627E+02	4.7688571E+01	1.9999611E+02	1.5230754E+02
TZ-0966	8.7856265E+01	1.7298172E+01	9.3459671E+01	6.6161499E+01
TZ-0634	-1.0686452E+02	-3.9740617E+01	-8.1989003E+01	-4.2248386E+01
TZ-0476	-1.2045338E+02	6.1656675E-01	-6.0618841E+01	-6.1235408E+01
TZ-0474	-1.0650474E+02	2.9554863E+01	-6.3320146E+01	-9.2875009E+01
TZ-0473	-1.0080889E+02	4.6787919E+01	-5.4552903E+01	-1.0134082E+02
TZ-0471	3.9313444E+01	8.7732212E+01	1.3213815E+02	4.4405941E+01
TZ-0812	-4.4169488E+01	1.4817365E+01	-9.9857506E+00	-2.4803115E+01
TZ-0860	-9.0723788E+00	4.0695499E+01	4.6019999E+01	5.3244998E+00
TZ-0909	-9.4392771E+00	2.3333096E+01	3.7584828E+01	1.4251731E+01
TZ-0958	-1.8021405E+00	9.5815434E+00	2.4515501E+01	1.4933957E+01
TZ-0798	-2.0697153E+02	-7.3850915E+01	-2.4597394E+02	-1.7212303E+02
TZ-0712	-3.3050840E+02	-1.0903135E+02	-4.0747930E+02	-2.9844795E+02
TZ-0494	-2.9917913E+02	-5.9584706E+01	-3.2625133E+02	-2.4666663E+02

Table 8-13.—Continued

TZ-0493	-4.0247356E+02	-7.7163822E+01	-4.5025597E+02	-3.7309215E+02
TZ-0492	-4.1170771E+02	-7.4385569E+01	-4.4233839E+02	-3.6795282E+02
TZ-0491	-3.0177671E+02	-1.5290778E+01	-3.0436848E+02	-2.8907770E+02
TZ-0857	-2.6353376E+02	-3.2459646E+01	-2.5960394E+02	-2.2714419E+02
TZ-0906	-1.5632146E+02	-1.5513821E+01	-1.1528760E+02	-9.9773780E+01
TZ-0955	-7.8071602E+01	-7.9882469E+00	-4.2629909E+01	-3.4641662E+01
TZ-0791	-3.7289042E+02	-1.5164942E+02	-4.0583513E+02	-2.5418571E+02
TZ-0705	-4.6301670E-01	4.0358166E+01	-4.4940198E+00	-4.4852186E+01
TZ-0513	-3.8260574E+02	-7.3547578E+01	-3.0626868E+02	-2.3272110E+02
TZ-0512	-2.5994896E+02	-1.9266568E+01	-2.0098362E+02	-1.9171705E+02
TZ-0511	-1.8070529E+02	-7.7571899E+00	-1.5275898E+02	-1.4500179E+02
TZ-0854	-1.4970913E+02	-7.2809144E+00	-1.1358040E+02	-1.0629949E+02
TZ-0903	-9.9963432E+01	2.8956512E+00	-5.3885371E+01	-5.6781022E+01
TZ-0952	-3.1056314E+01	1.9963789E+00	-1.2383337E+01	-1.4379716E+01
TZ-0775	-2.2144400E+02	-5.8902771E+01	-1.8321633E+02	-1.2441356E+02
TZ-0533	-9.8392166E+01	4.1286453E+00	-5.378647E+01	-5.7914892E+01
TZ-0532	-5.3572030E+01	1.6360043E+01	-3.2148482E+01	-4.8508525E+01
TZ-0531	-4.7505967E+01	1.8414648E+01	-2.3847421E+01	-4.2262069E+01
TZ-0900	-2.7493754E+01	1.4156700E+00	-1.5810464E+01	-1.7226134E+01
TZ-0950	-7.2891262E+00	-1.7182809E+00	-4.7143443E+00	-2.3960634E+00

Table 8-13.—Concluded

TZ-3230	-1.1675573E+03	5.1257343E+02	-9.3656041E+02	-1.3491338E+03
TZ-3231	-9.9183548E+02	9.3024573E+02	-1.2769815E+02	-1.0579439E+03
TZ-3233	-3.3847057E+02	8.8838312E+02	4.4772384E+02	-4.4065929E+02
TZ-3234	-3.9076126E+01	3.1760607E+02	2.1274939E+02	-1.0485668E+02
TZ-3235	-1.8815940E+03	9.4203736E+02	-1.1791028E+03	-2.1211402E+03
TZ-3236	-1.2074282E+03	1.2043423E+03	-3.6849152E+01	-1.2411914E+03
TZ-3238	-3.9519365E+02	1.0152114E+03	4.7391103E+02	-5.4130040E+02
TZ-3239	-5.9699095E+01	3.7016527E+02	2.2304441E+02	-1.4712086E+02
TZ-3240	-7.3685587E+02	4.5531554E+02	-3.1648083E+02	-7.7179637E+02
TZ-3241	-1.6342279E+02	2.0036493E+02	3.2120098E+01	-1.6824483E+02
TZ-3242	-8.0619556E+01	1.8726131E+02	6.1245237E+01	-1.2601607E+02
TZ-3243	-1.8295688E+01	6.9918100E+01	3.0635590E+01	-3.9282511E+01

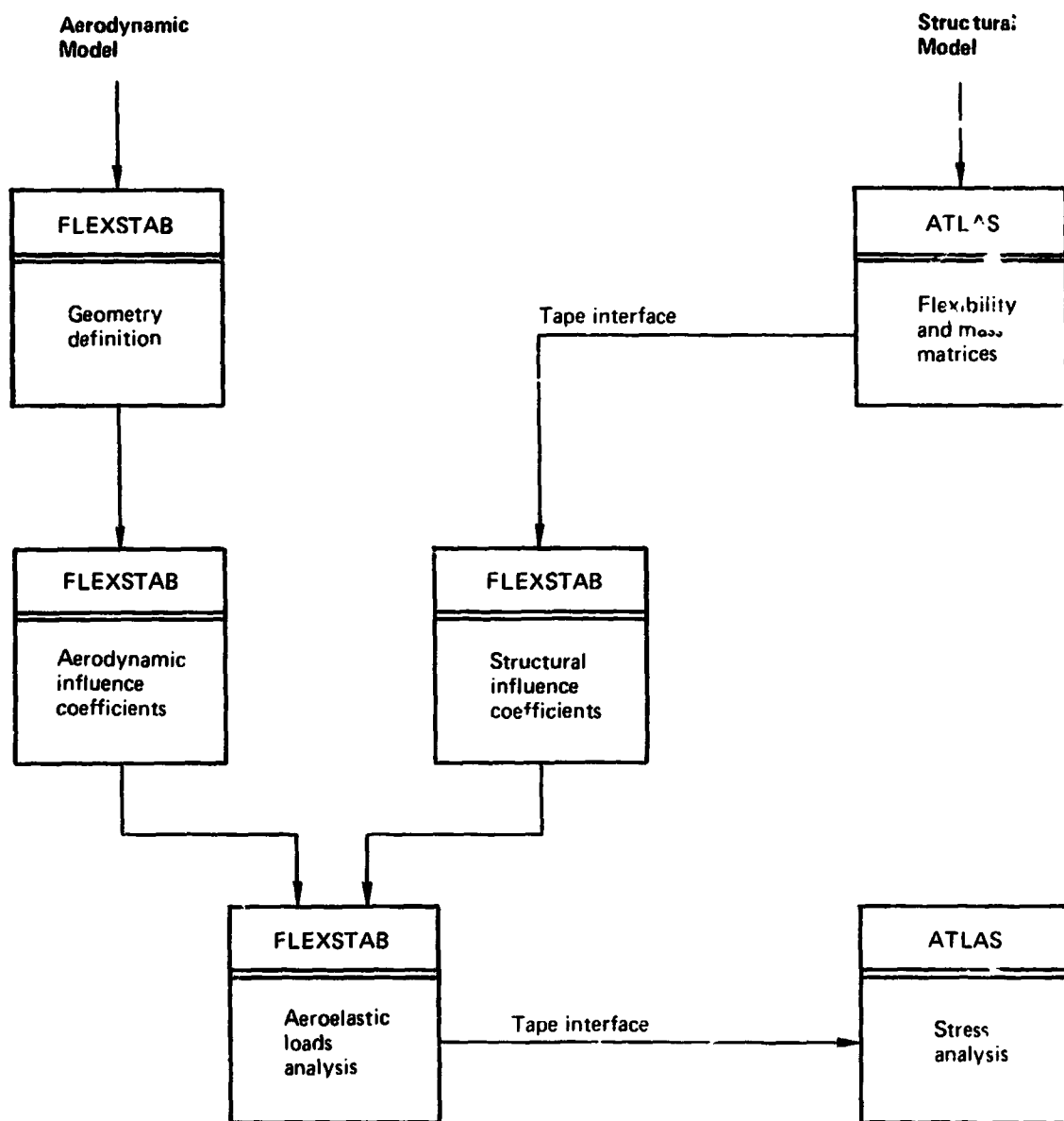


Figure 8-1.—ATLAS-FLEXSTAB Program System

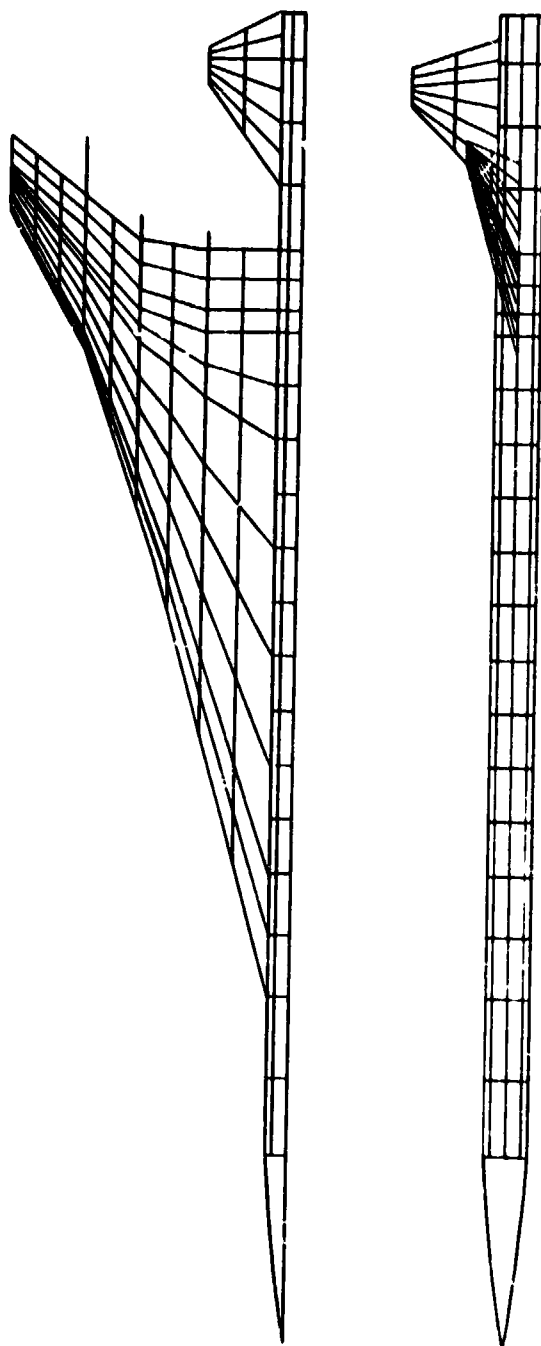


Figure 8-2.—Aerodynamic Paneling for FLEXSTAB

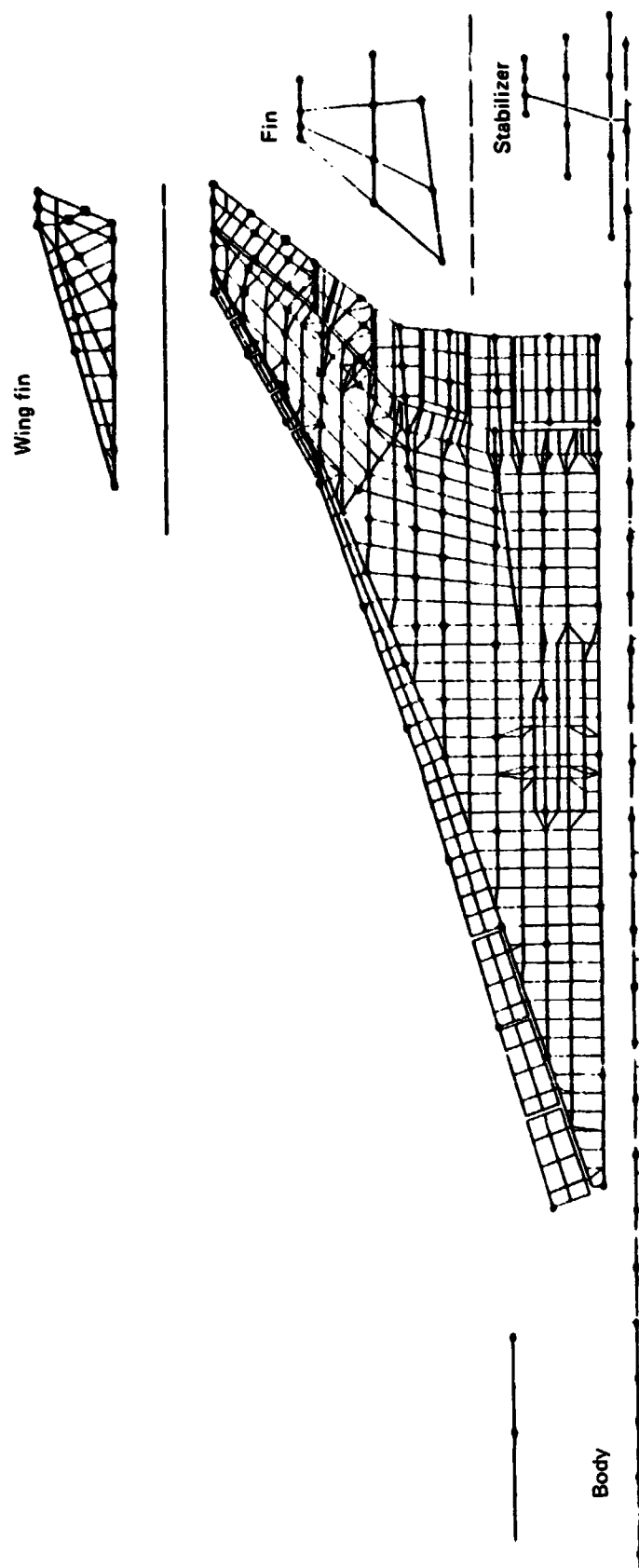
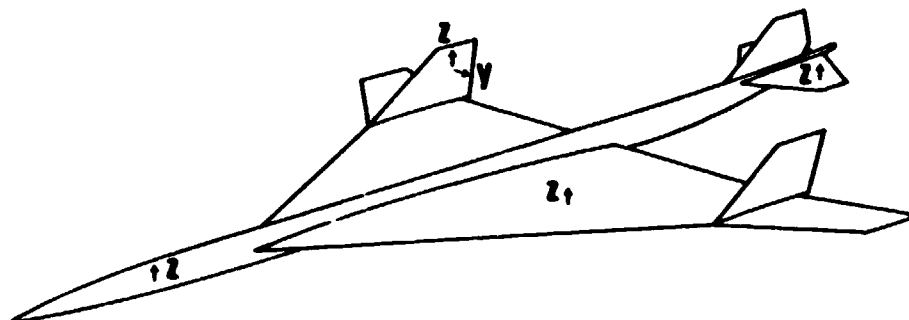
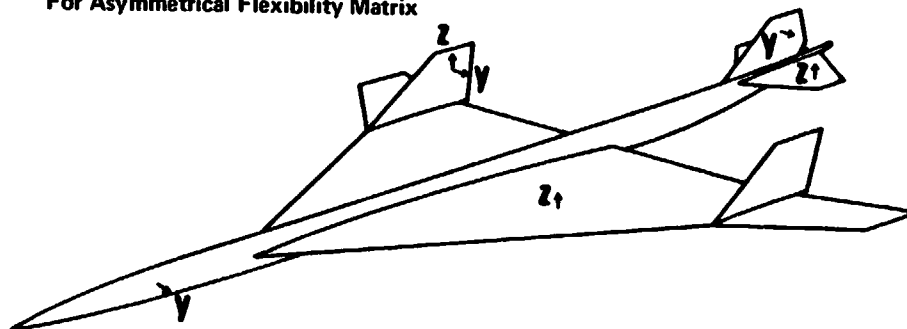


Figure 8-3.—Structural Nodes Retained For Loads Analysis

For Symmetrical Flexibility Matrix



For Asymmetrical Flexibility Matrix



Note: The retained nodes for the nacelles have X, Y, and Z degrees of freedom for both symmetrical and asymmetrical cases

Figure 8-4.—Retained Degrees of Freedom for Flexibility Matrices

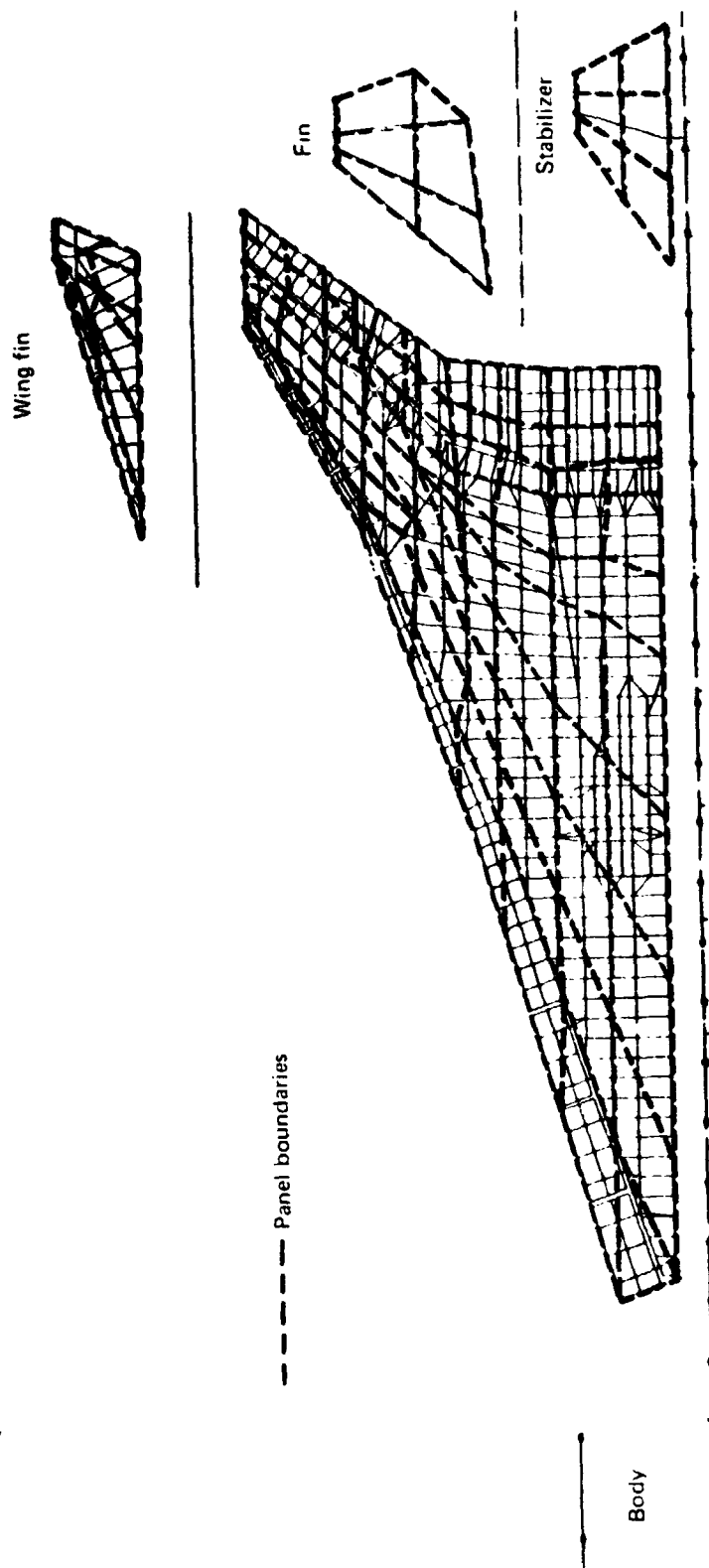


Figure 8-5.—Structural Panels For ESIC

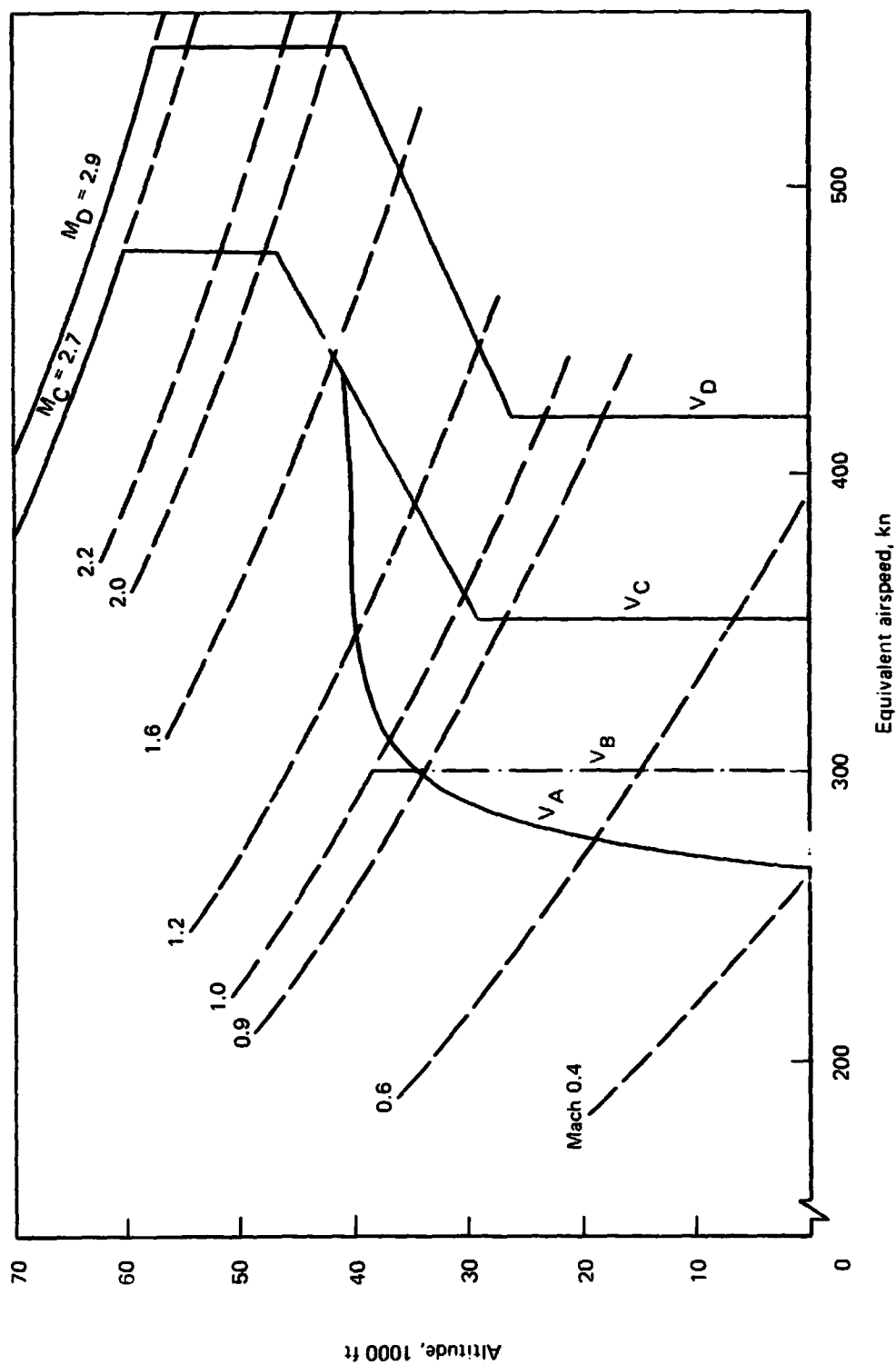


Figure 8-6. — Design Airspeeds, Equivalent Velocity

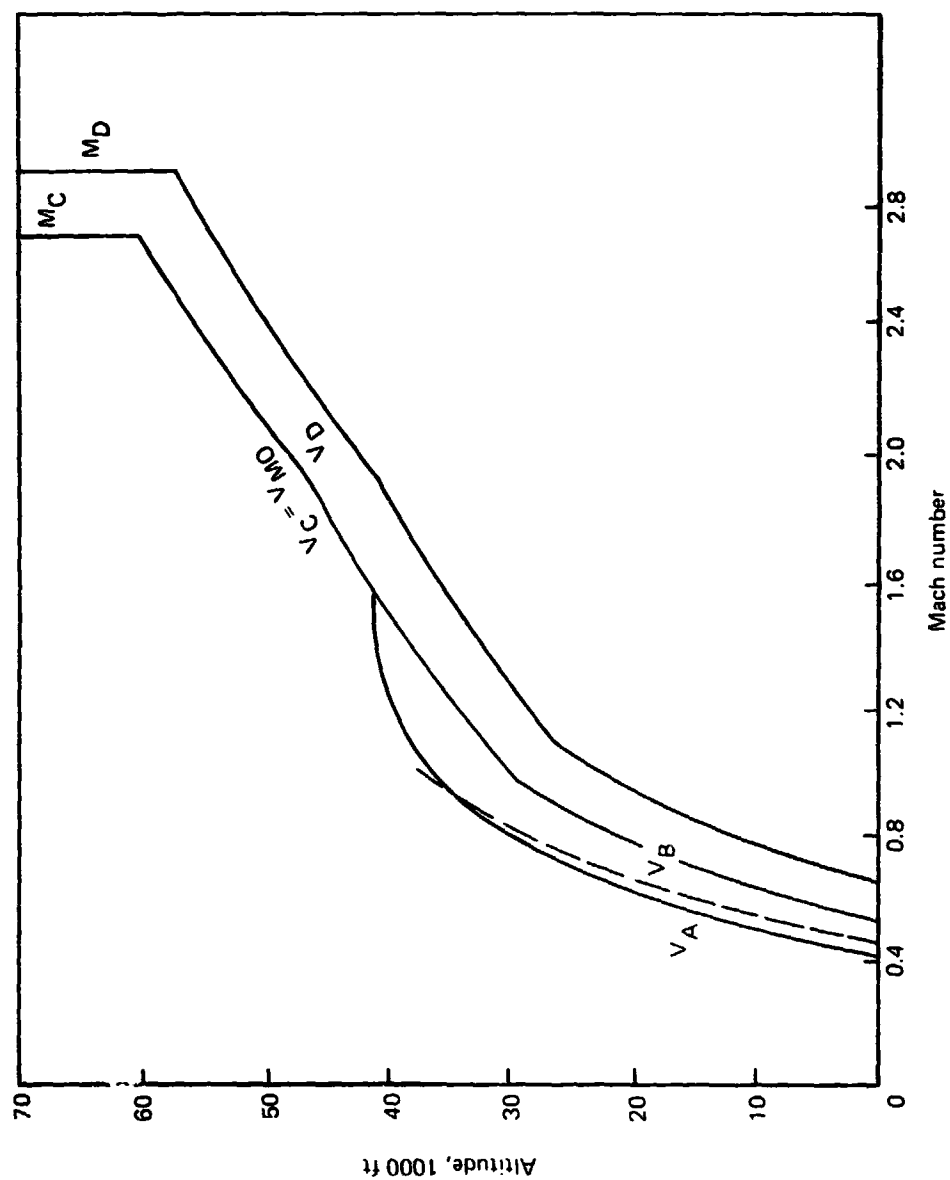


Figure 8-7.—Design Airspeeds, Mach Number

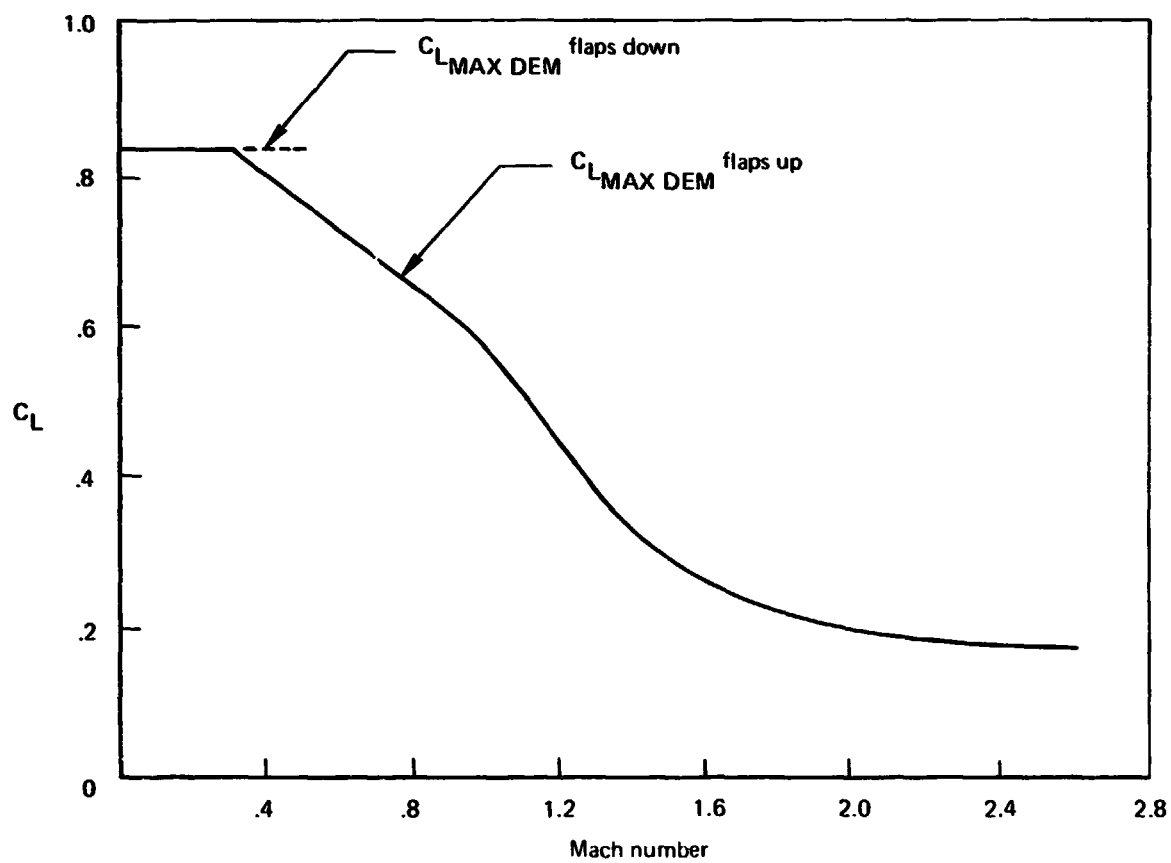


Figure 8-8.— $C_{LMAX DEM}$ Limits

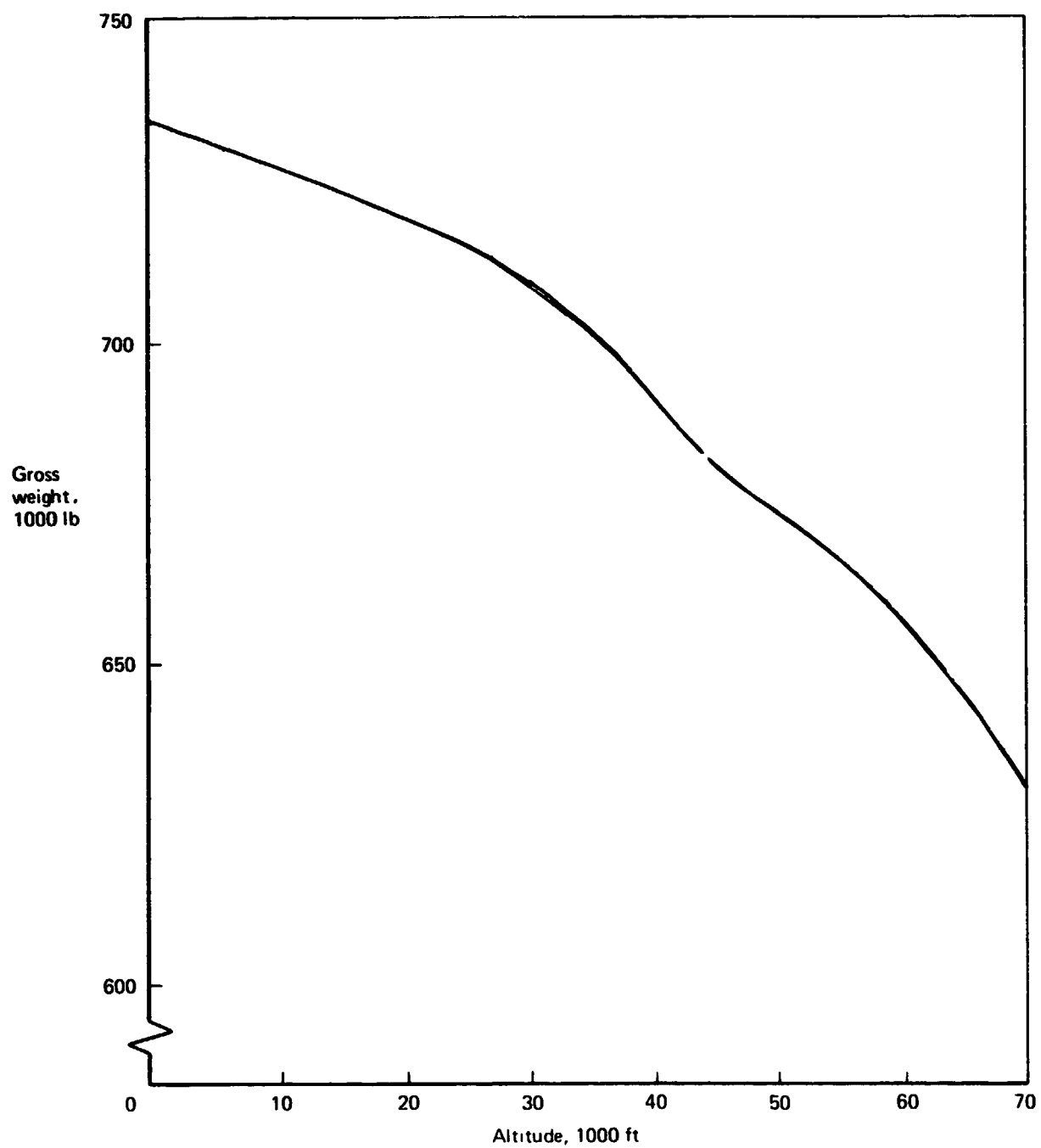


Figure 8-9.—Maximum Flight Weight

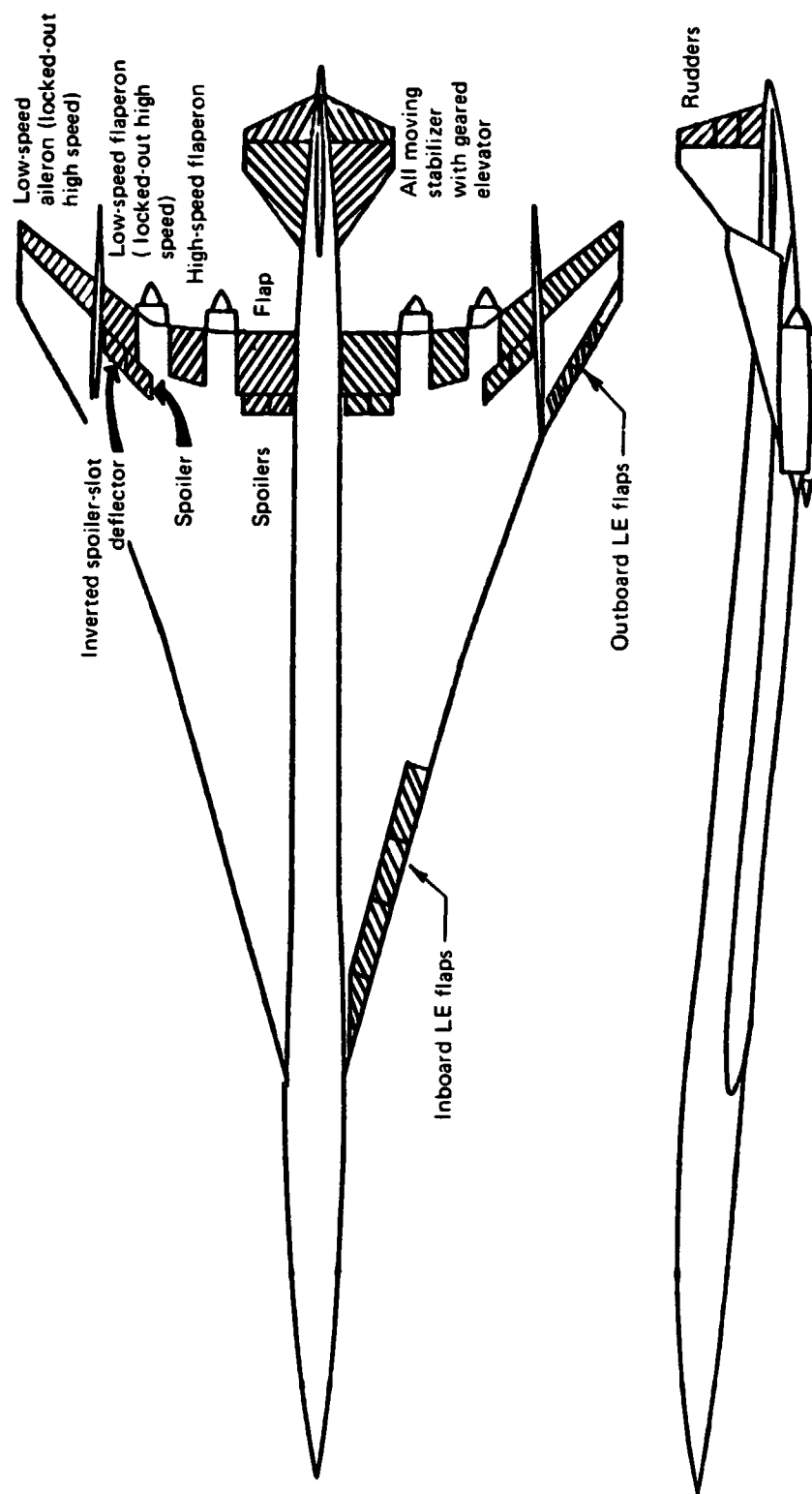


Figure 8-10.—969-512B, Control Surface Locations

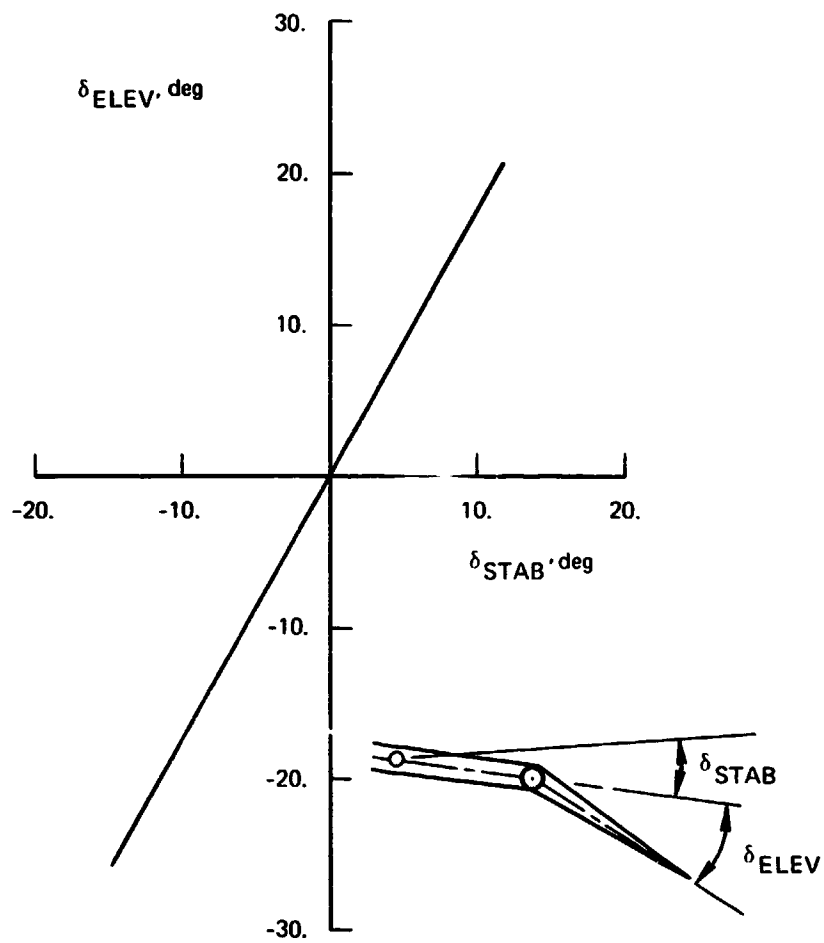


Figure 8-11.—Stabilizer-Elevator Relations Mechanical Geared Elevator

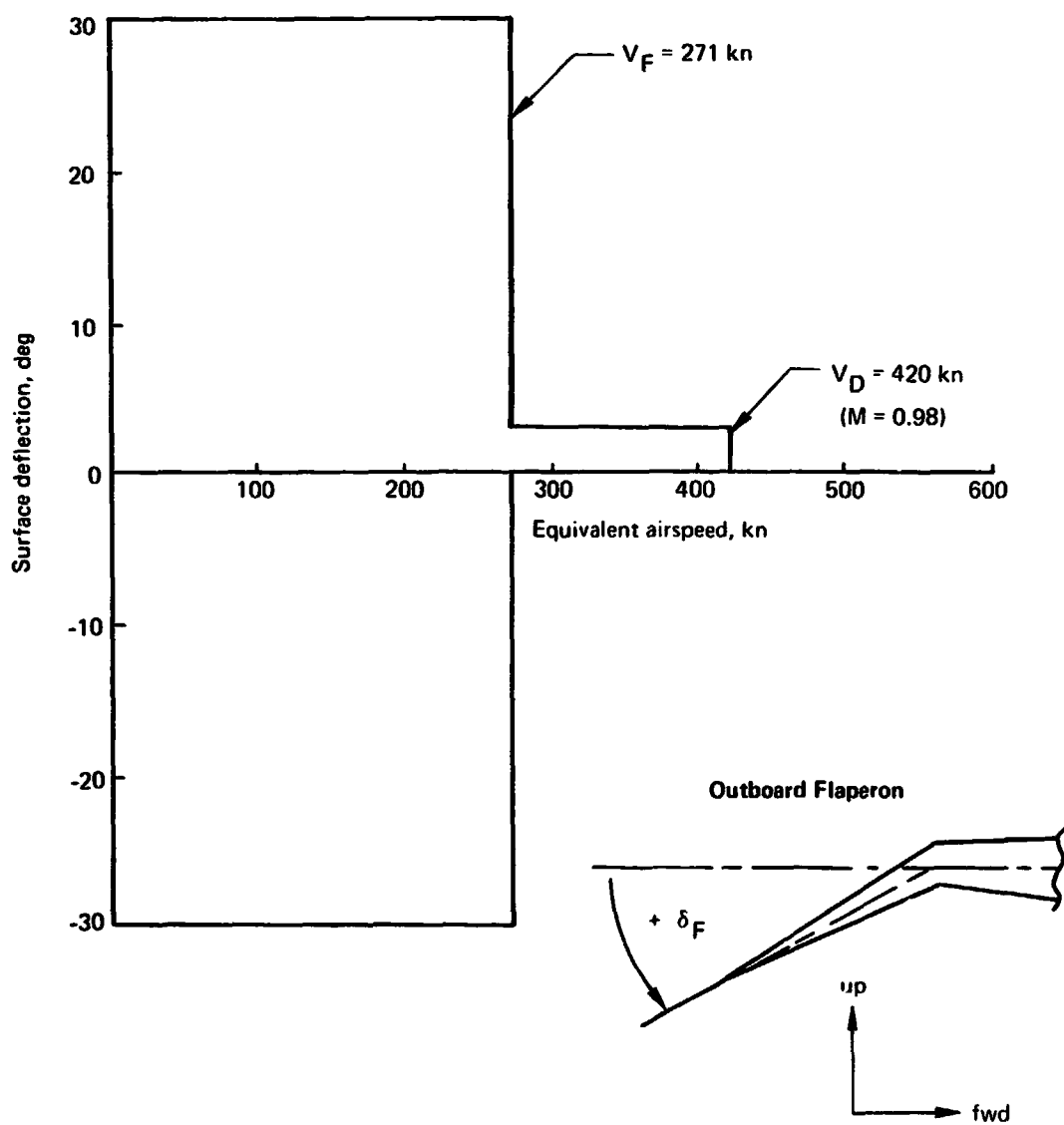


Figure 8-12.—Deflection Limitations—Outboard Flaperon

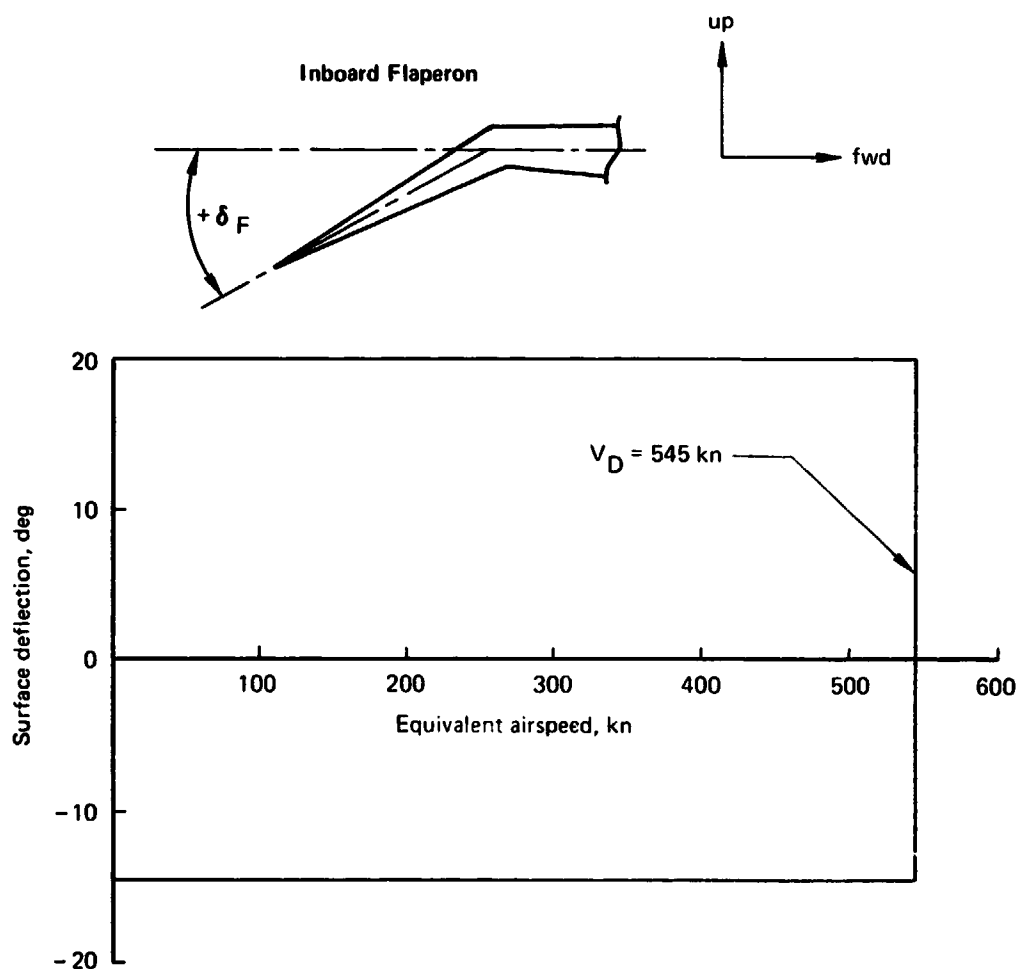


Figure 8-13.—Deflection Limitations—Inboard Flaperon

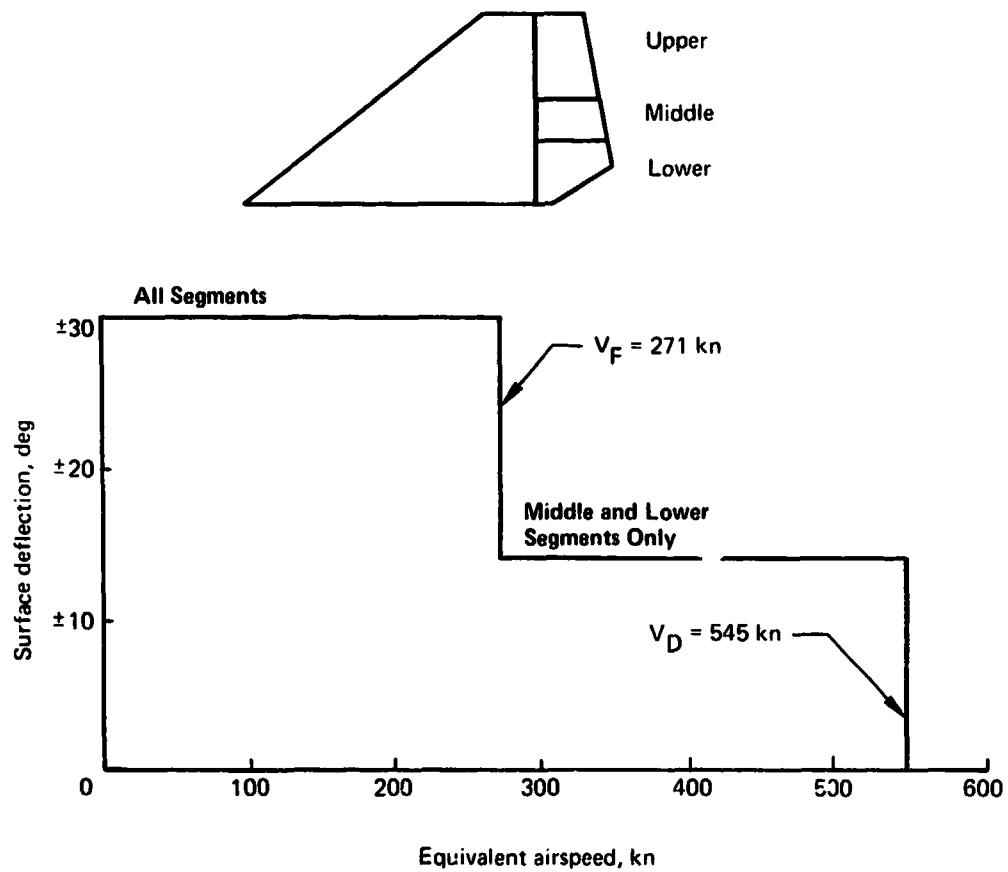


Figure 8-14.—Deflection Limitations—Rudder

V-n diagrams are for the maximum flight weight at the altitudes shown

Sea Level

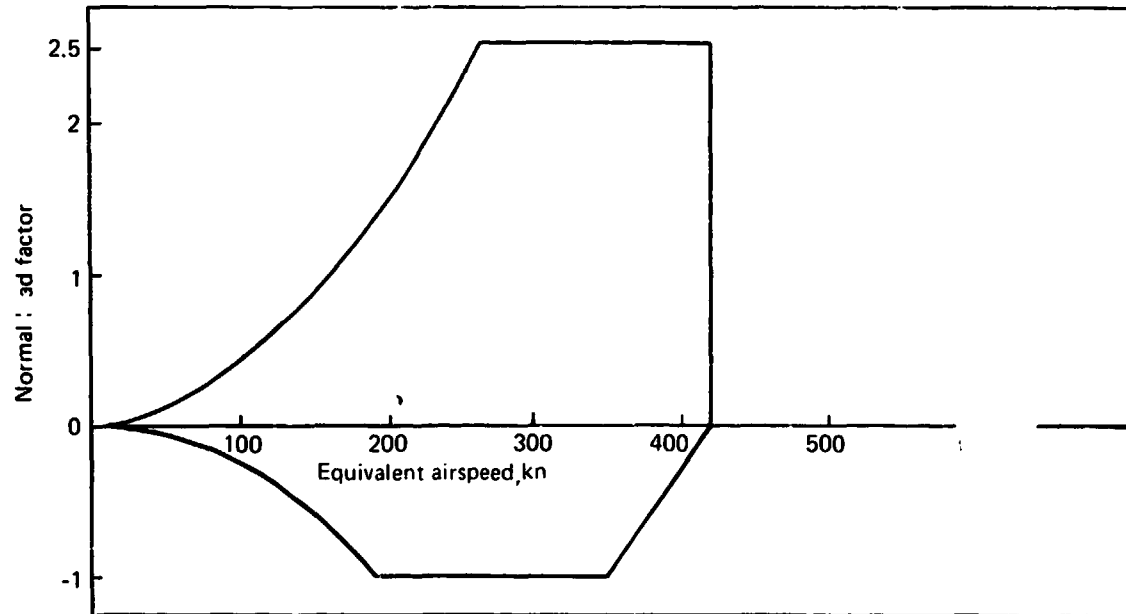


Figure 8-15.—Maneuver Envelope at Sea Level

10 000 ft

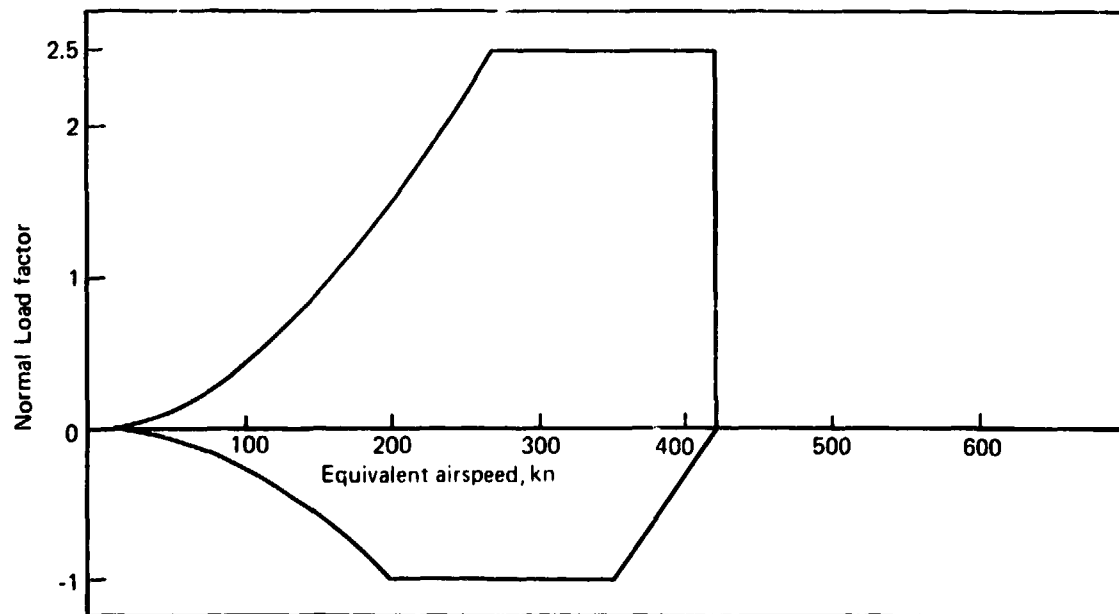


Figure 8-16.—Maneuver Envelope at 10 000 ft

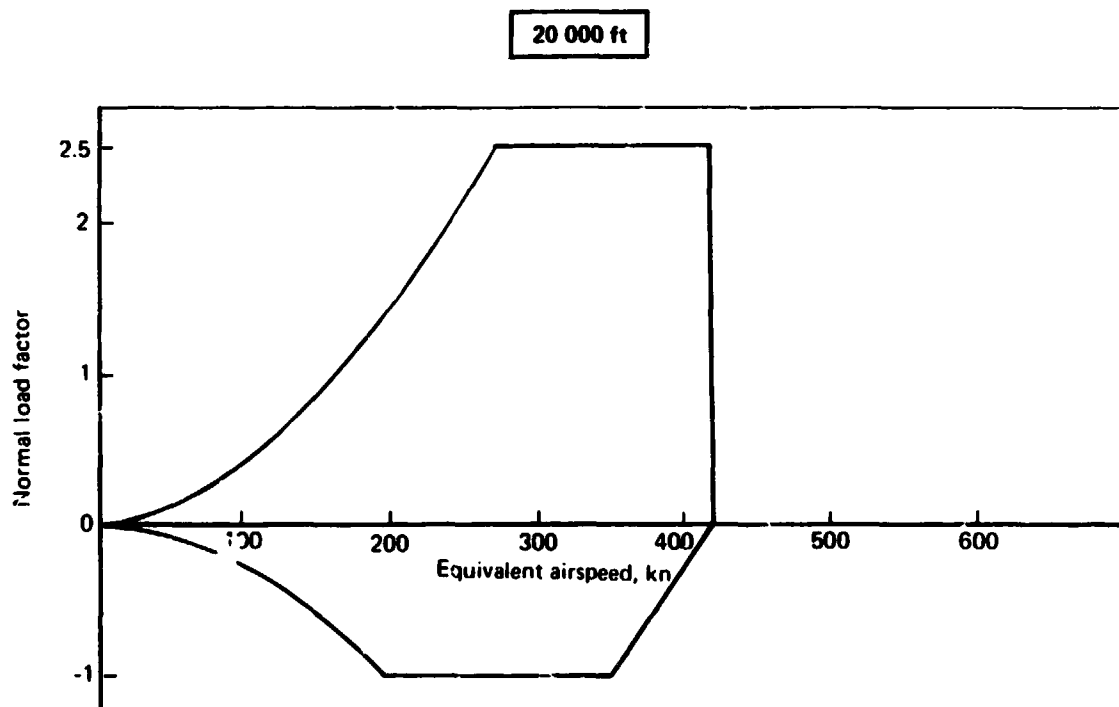


Figure 8-17.—Maneuver Envelope at 20 000 ft

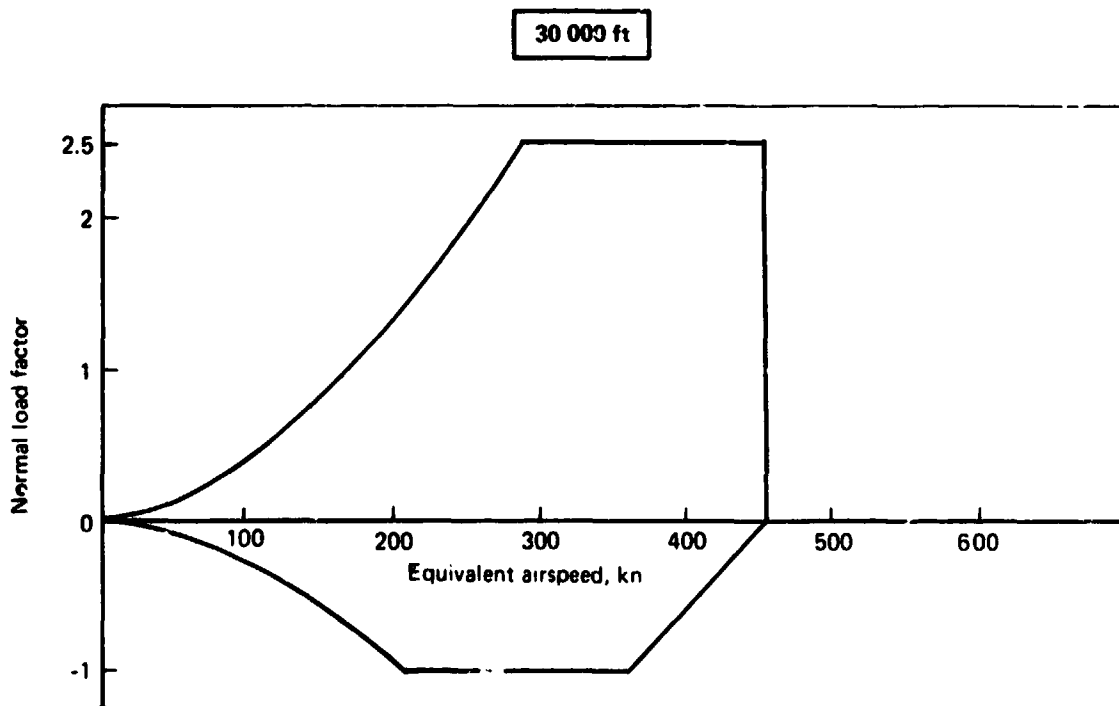


Figure 8-18.—Maneuver Envelope at 30 000 ft

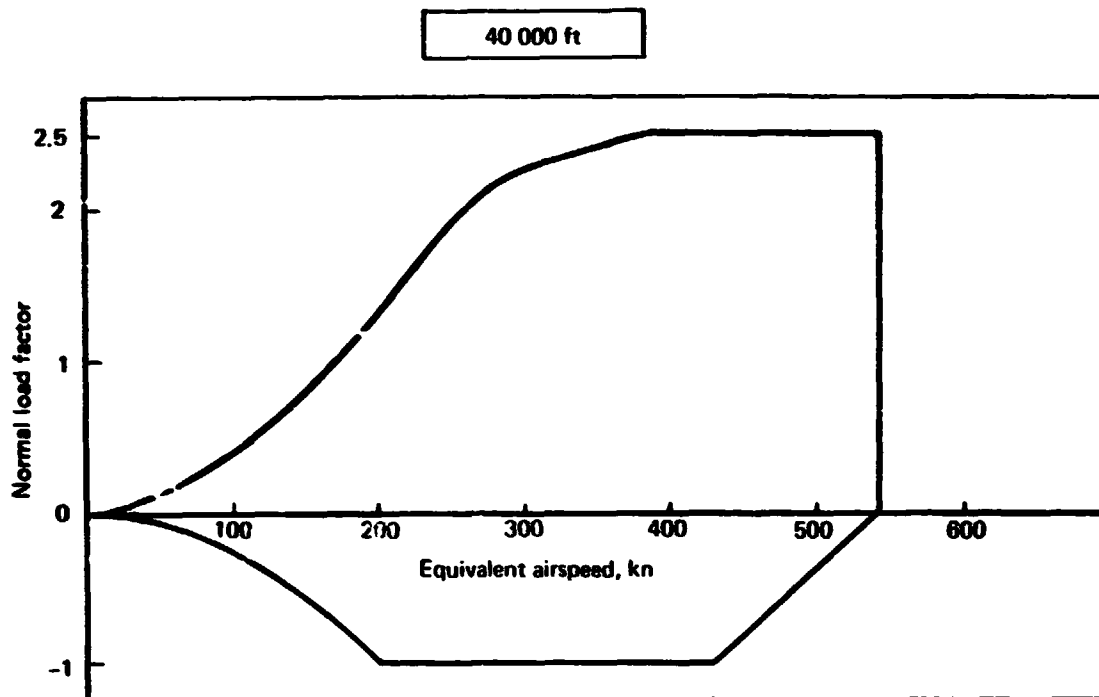


Figure 8-19.—Maneuver Envelope at 40 000 ft

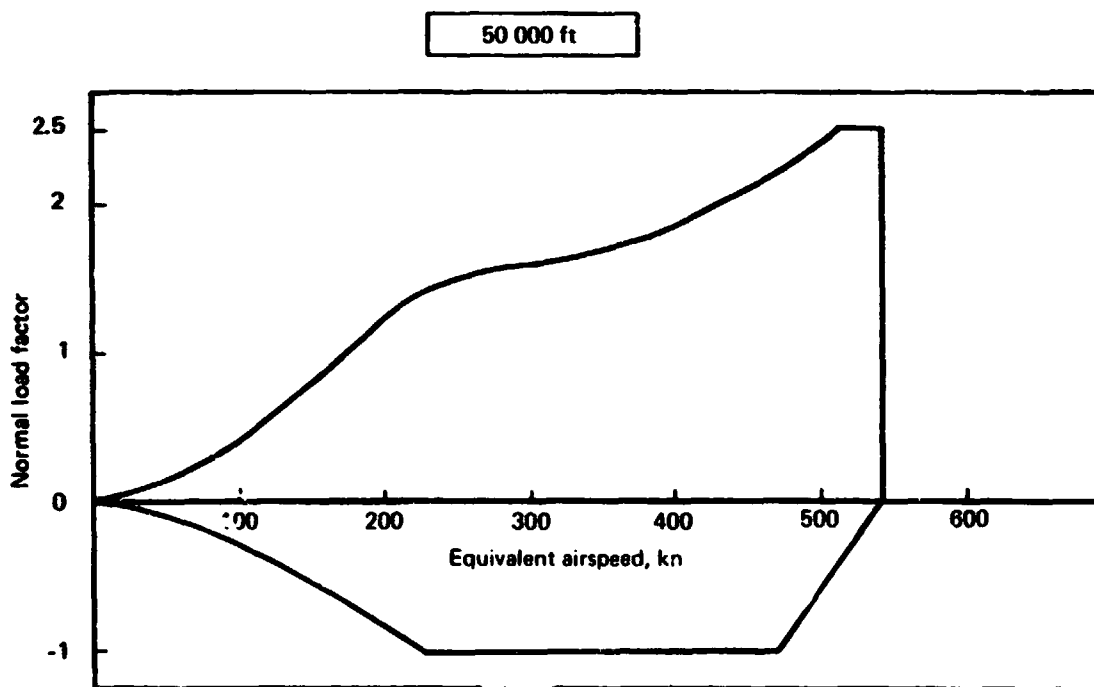


Figure 8-20.—Maneuver Envelope at 50 000 Ft

60 000 ft

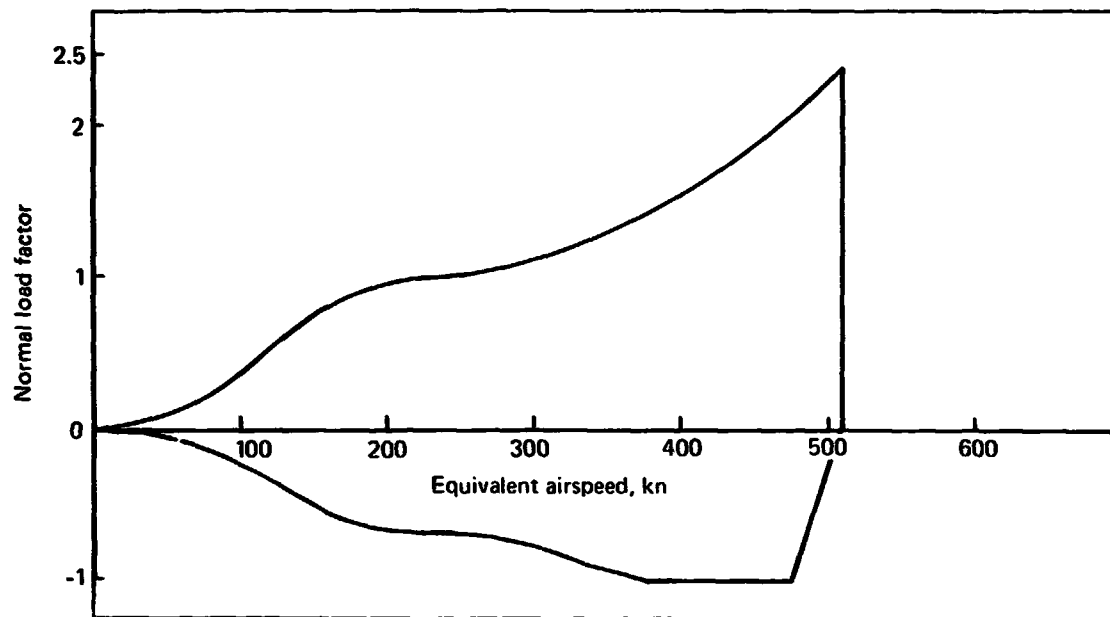


Figure 8-21.—Maneuver Envelope at 60 000 ft

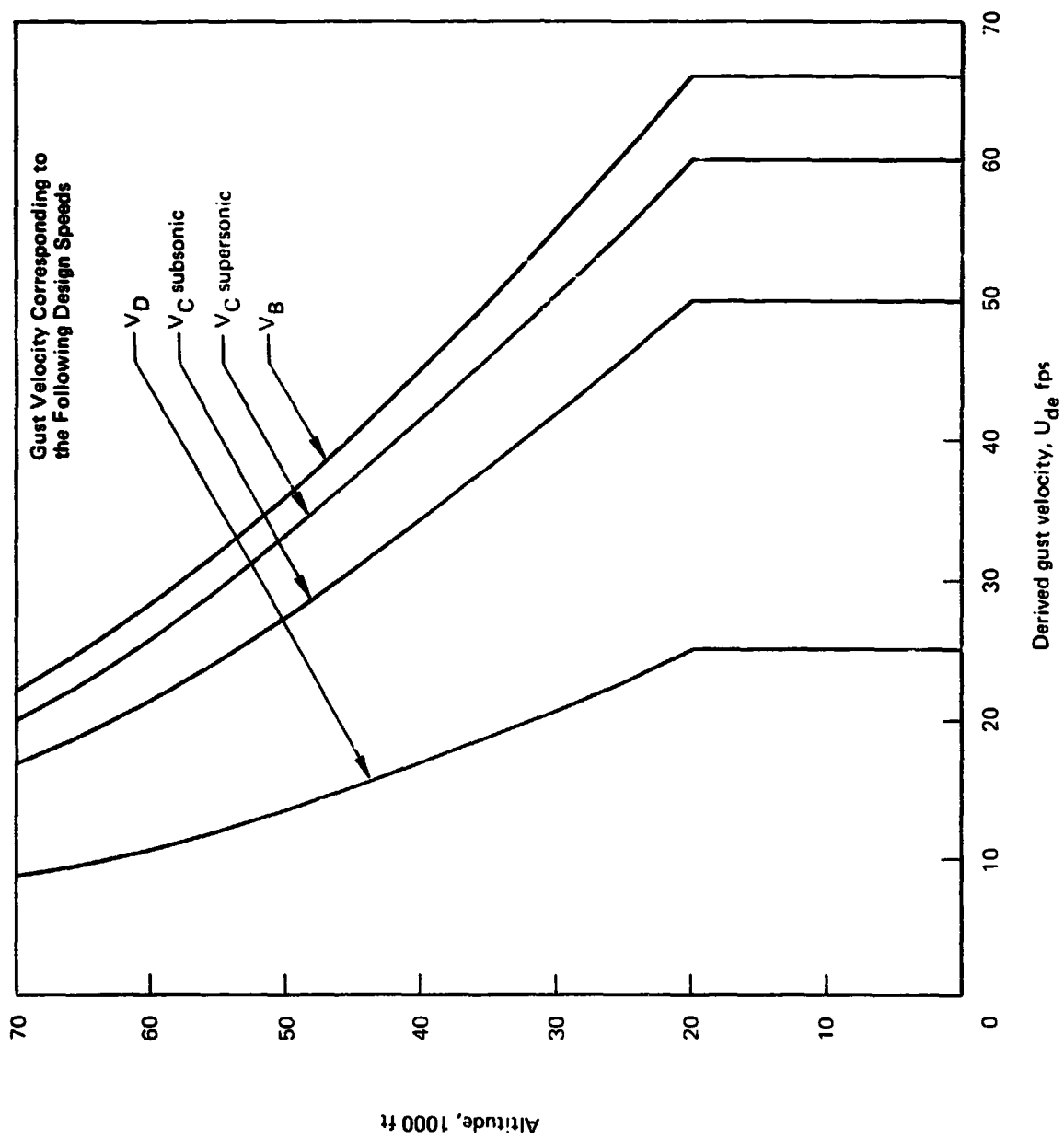


Figure 8-22.—Derived Gust Velocity

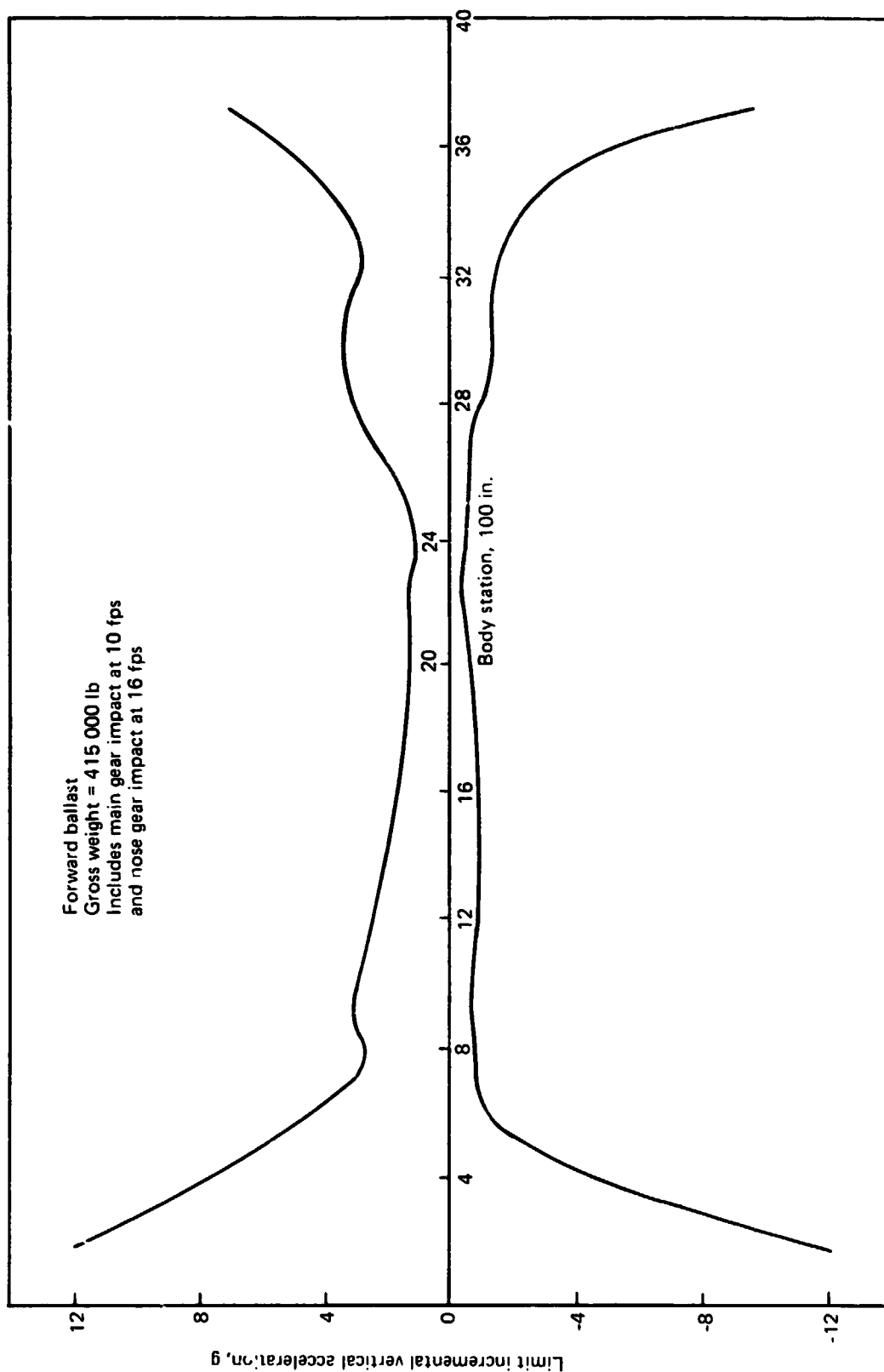


Figure 8-23. -2707-300 PPD Limit Vertical Acceleration at Landing Impact

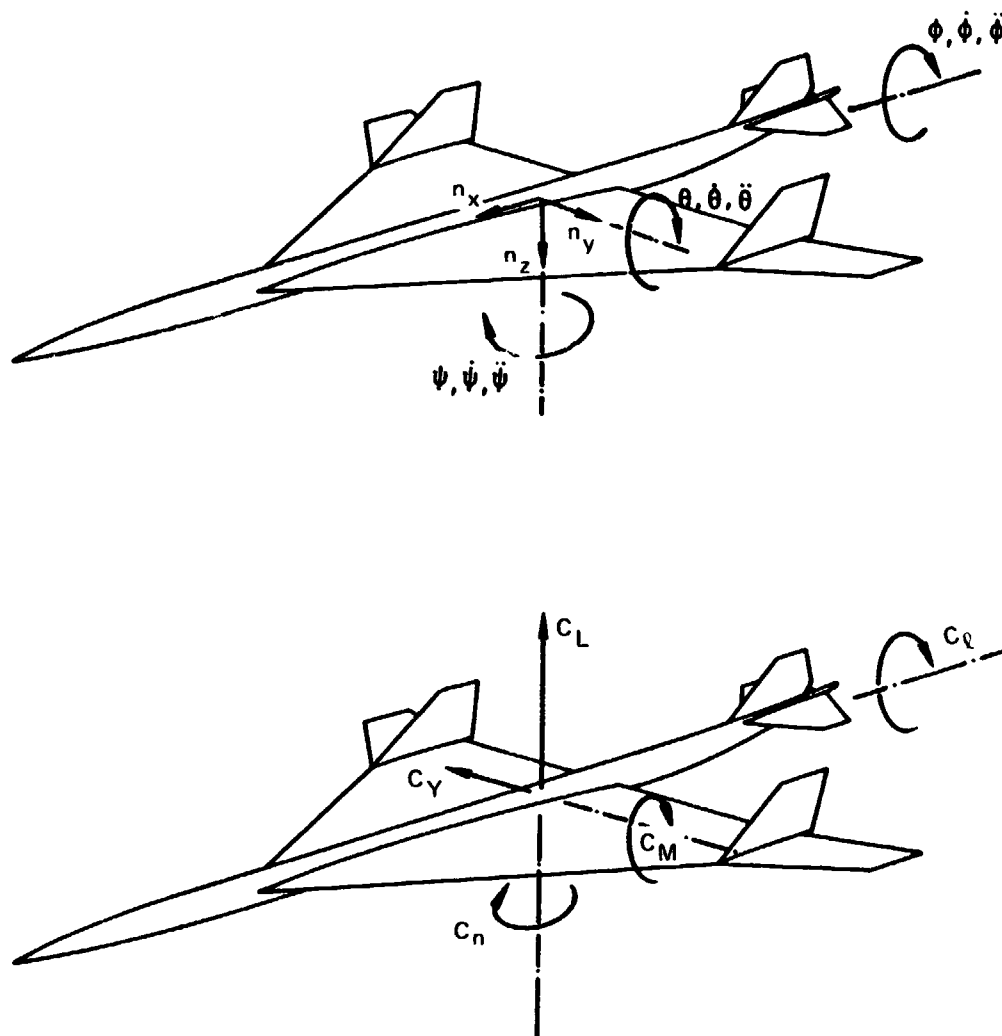


Figure 8-24.—Sign Convention

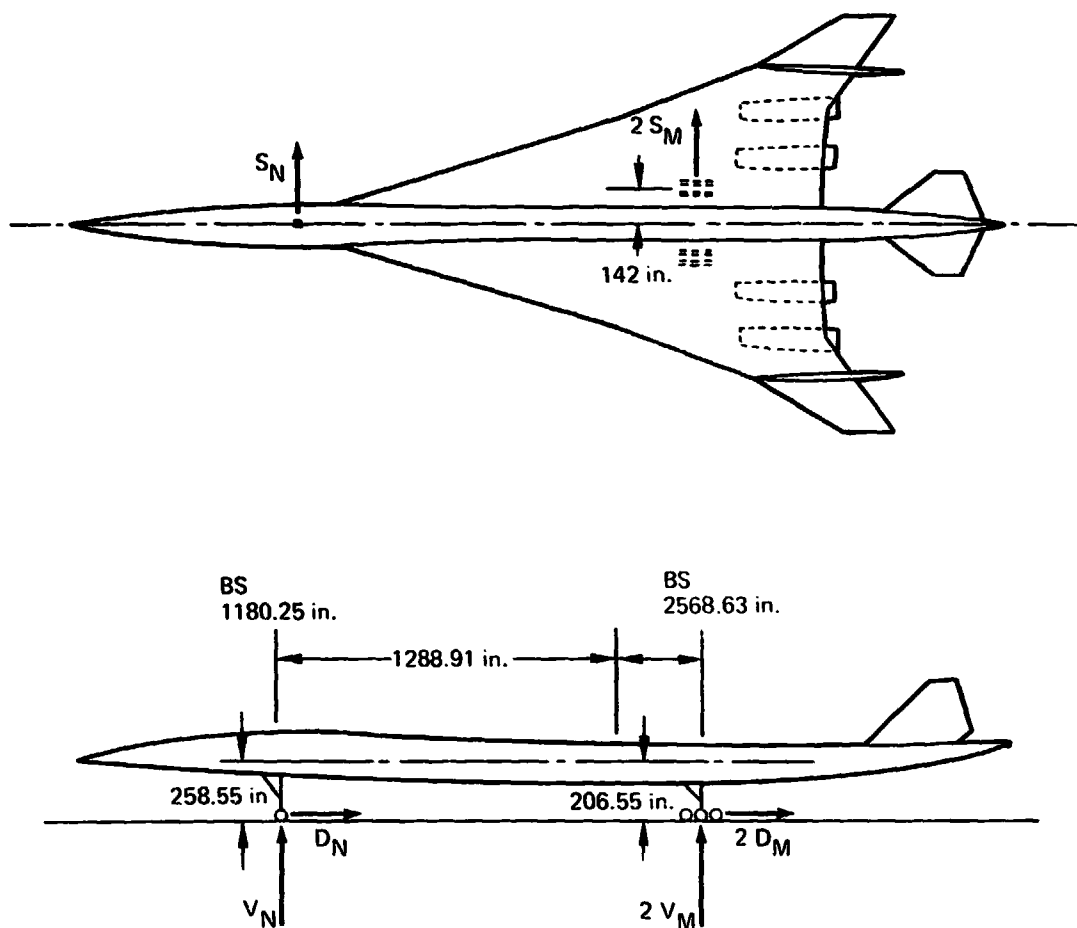


Figure 8-25.—Geometry and Gear Reactions for Ground Loads

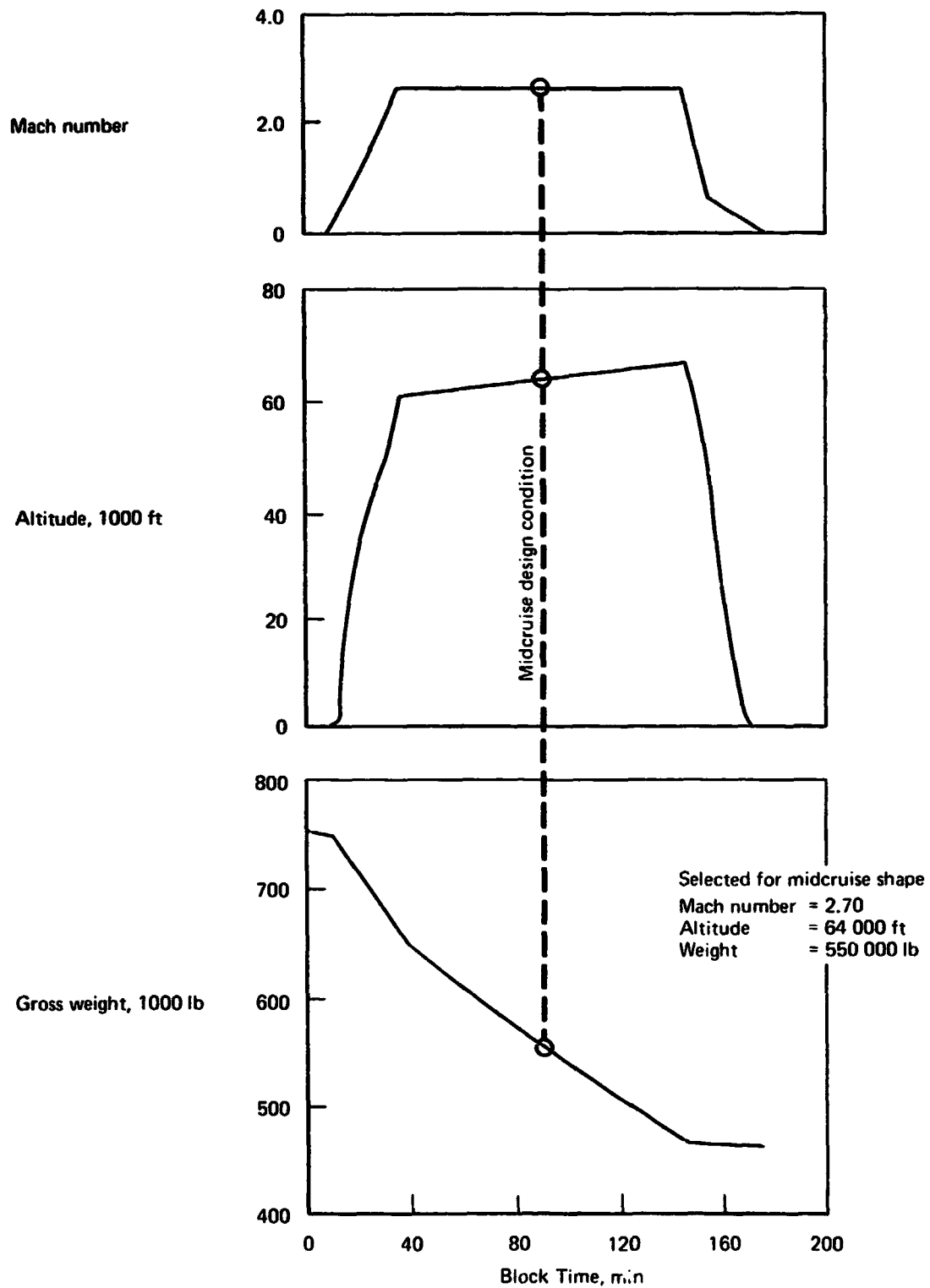


Figure 8-26.—Midcruise Condition For Jig Solution

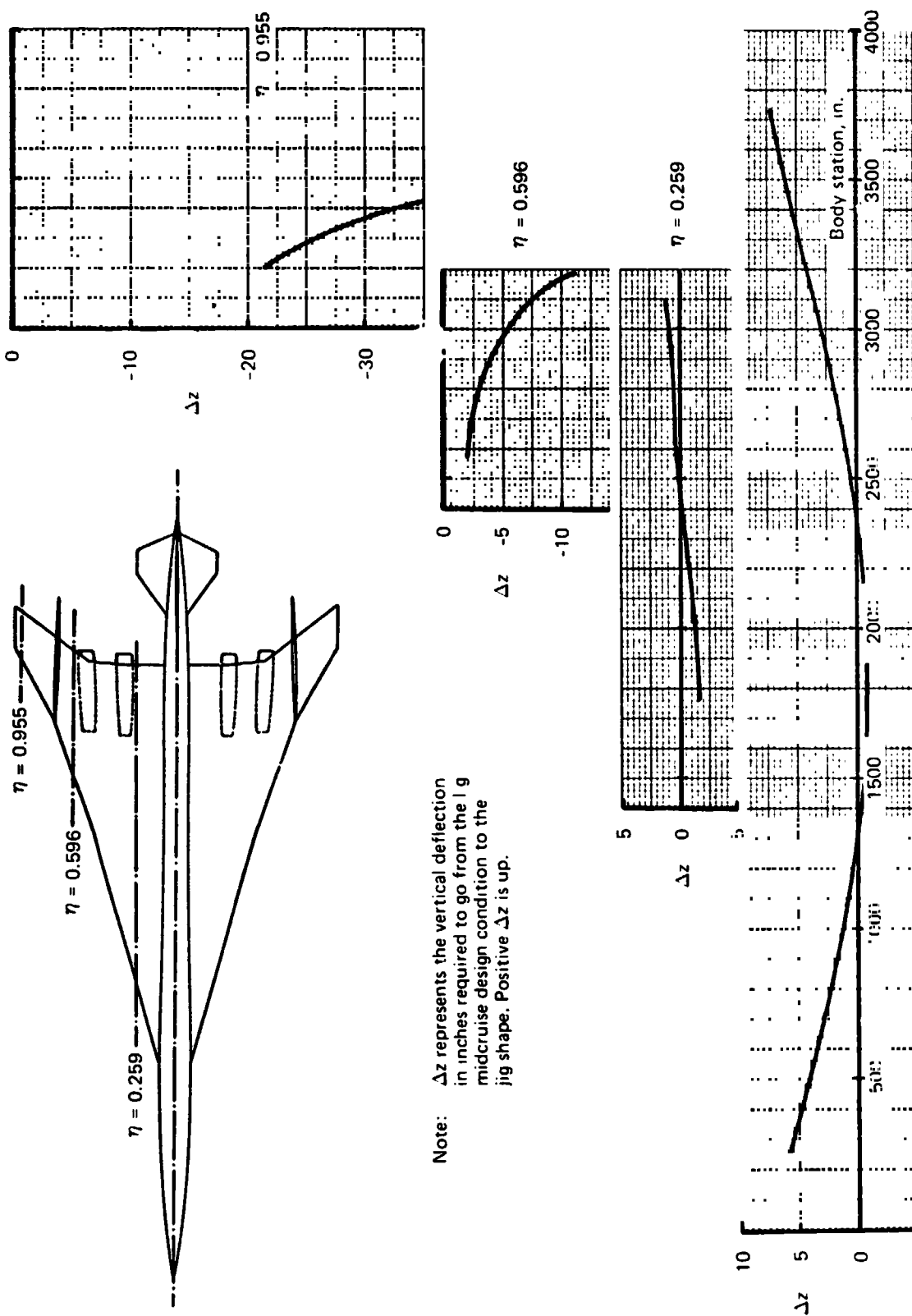


Figure 8-27.—Jig Shape Deflections

MN-WT-AL-TC-NF
 XXX-XX-XX-XX-XXX

MN = Mach number
 WT = Gross weight and c.g. code
 AL = Altitude in ft/1000
 TC = Type of condition code
 NF = Normal load factor/10 and flexibility code (E = elastic, R = rigid)

Gross Weight and Center of Gravity

Code	Gross weight	C.g.
01	MAX FLIGHT WEIGHT	FWD
02	MAX FLIGHT WEIGHT	AFT
03	MAX ZERO FUEL WEIGHT	FWD
04	MAX ZERO FUEL WEIGHT	AFT
05	MIN FLIGHT WEIGHT	FWD
06	MIN FLIGHT WEIGHT	AFT
07	MAX TAKEOFF WEIGHT	FWD
08	MAX TAKEOFF WEIGHT	AFT
09	MAX LANDING WEIGHT	FWD
10	MAX RAMP WEIGHT	AFT
11	MAX RAMP WEIGHT	FWD

Type of Condition

Code	Description	Code	Description
0X	BALANCED MANEUVER	X0	SPECIFIED VE
1X	POSITIVE GUST	X1	DESIGN MANEUVERING SPEED VA
2X	NEGATIVE GUST	X2	DESIGN MAX GUST SPEED VB
3X	ELEVATOR MANEUVER	X3	DESIGN CRUISING SPEED VC
4X	RUDDER MANEUVER	X4	DESIGN DIVE SPEED VD
5X	AILERON MANEUVER	X5	DESIGN FLAP SPEED VF
6X	LANDING	X6	VE FOR CL MAX AT POSITIVE N
7X	GROUND HANDLING	X7	VE FOR CL MAX AT NEGATIVE N

Figure 8-28.—Load Condition Code

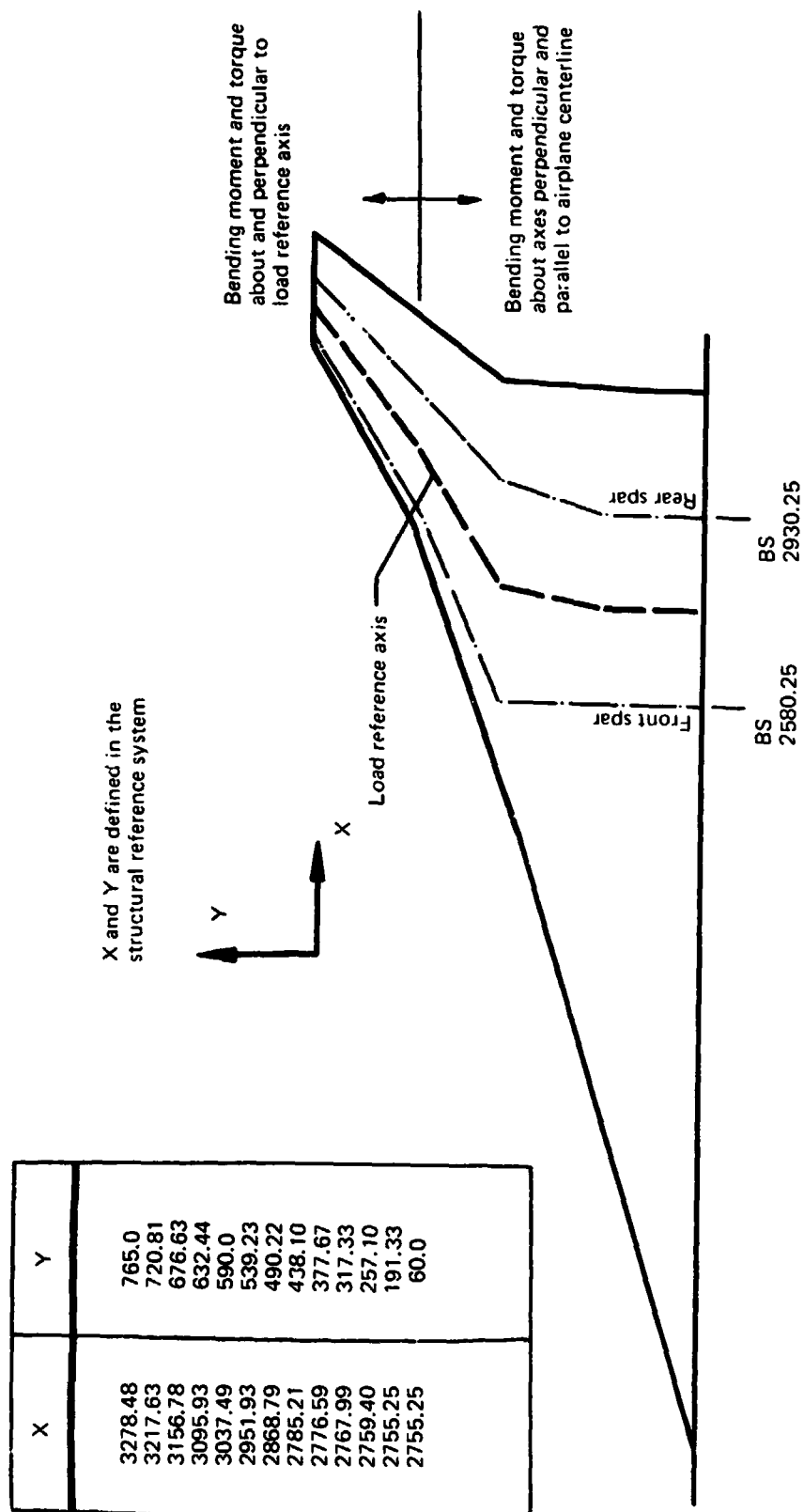
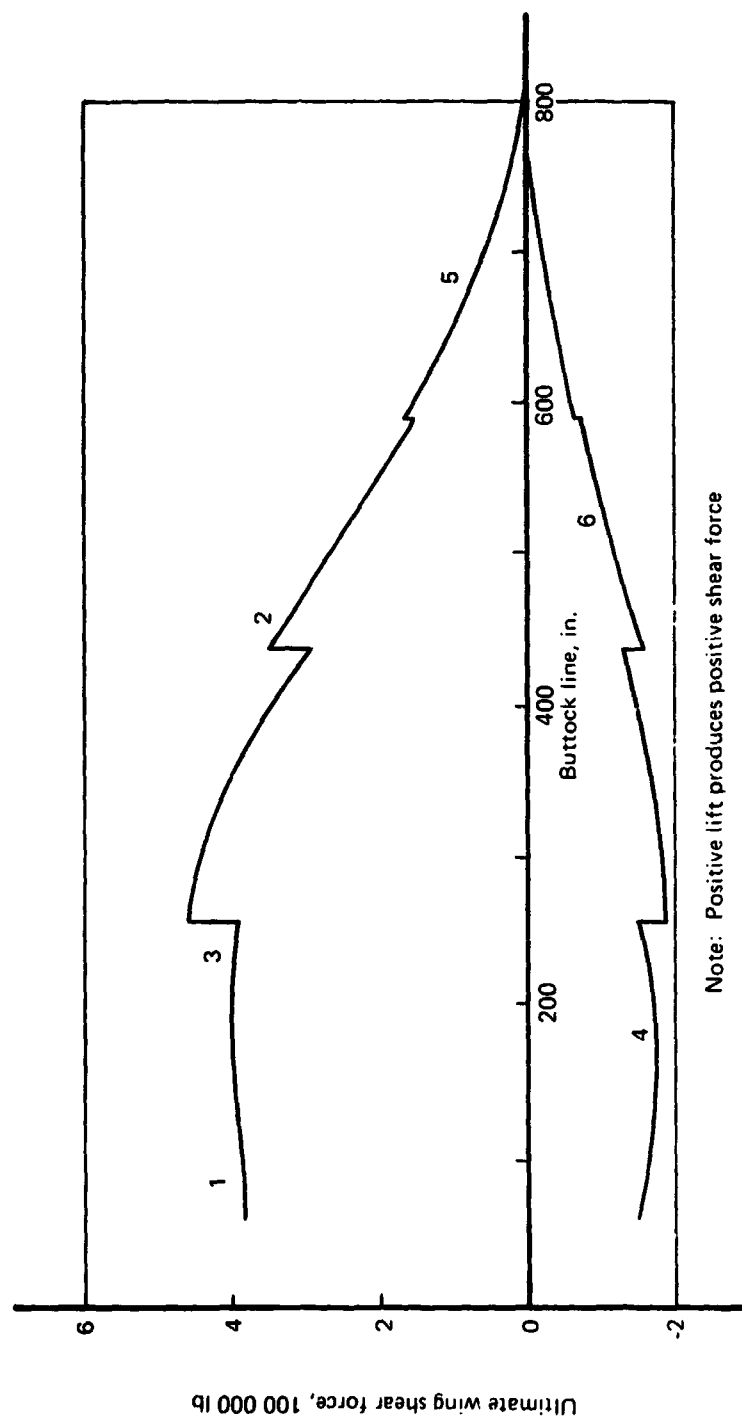


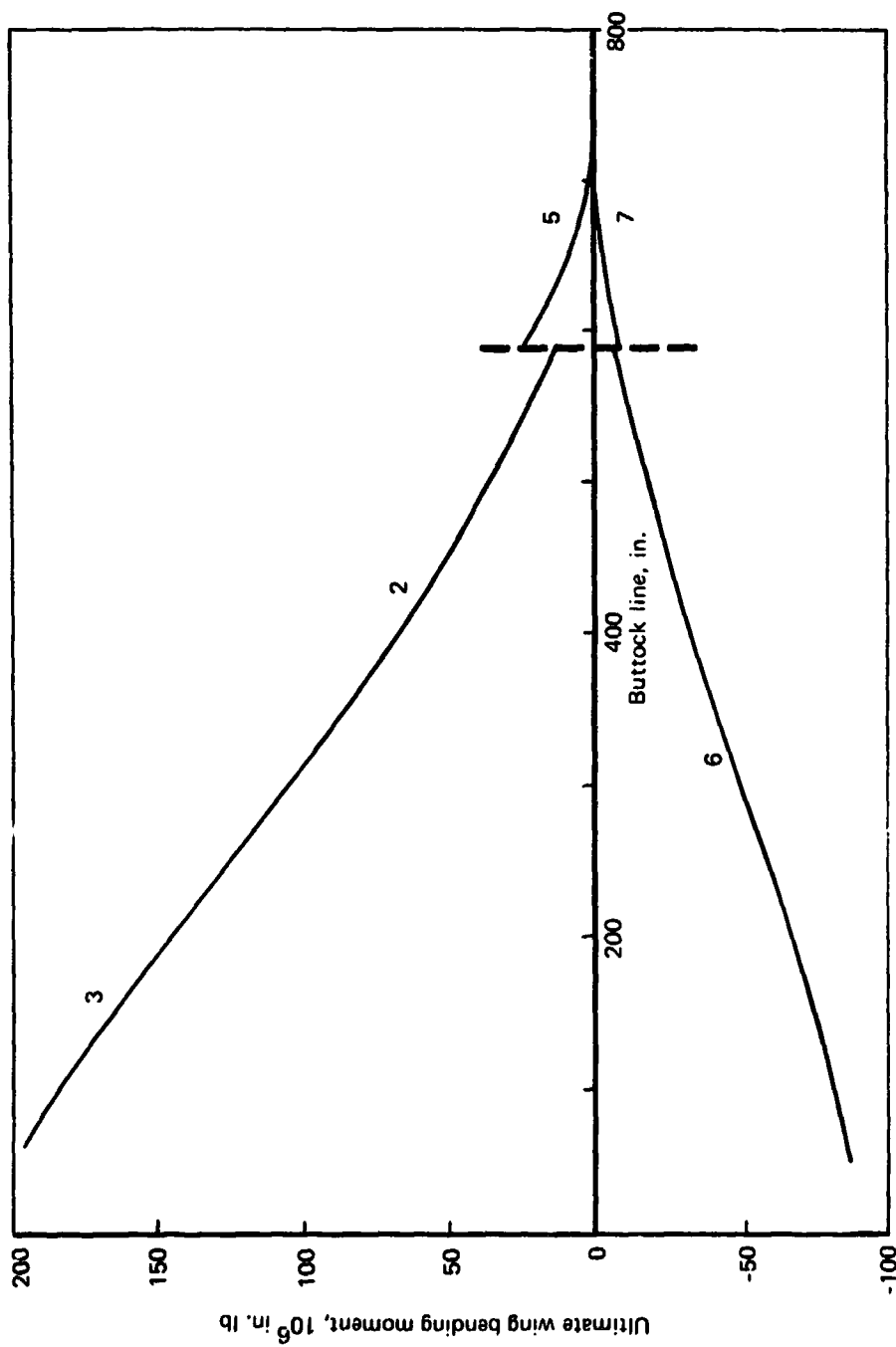
Figure 8-29.—Definition of Load Reference Axis



Note: Positive lift produces positive shear force

The condition numbers shown above correspond to the column numbers in table 8-11.

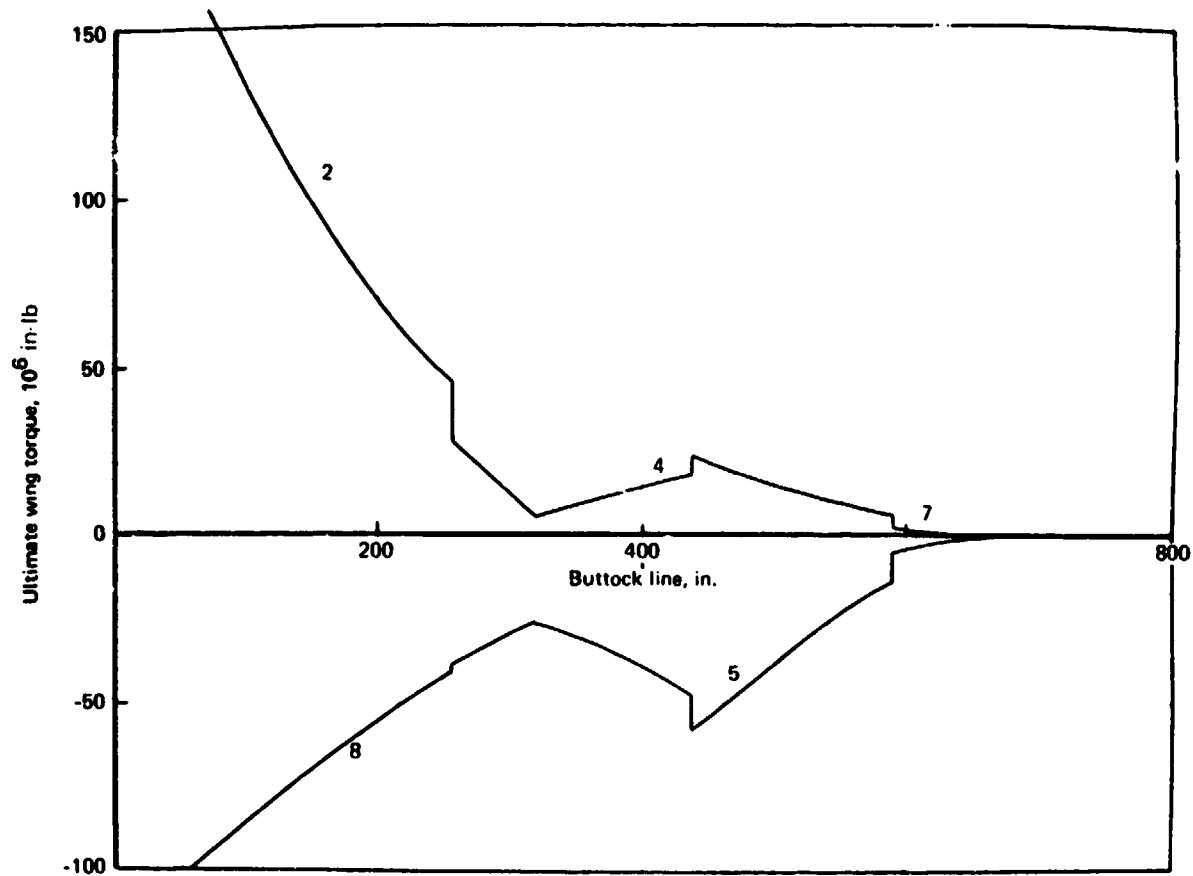
Figure 8-30. — Design Ultimate Shear Force Envelope for the Wing in Symmetrical Flight Conditions



- Notes: 1) Positive shear force produces positive bending moment
 2) The discontinuity in the bending moment is caused by the change in orientation of the load reference axis (see fig. 8-29)

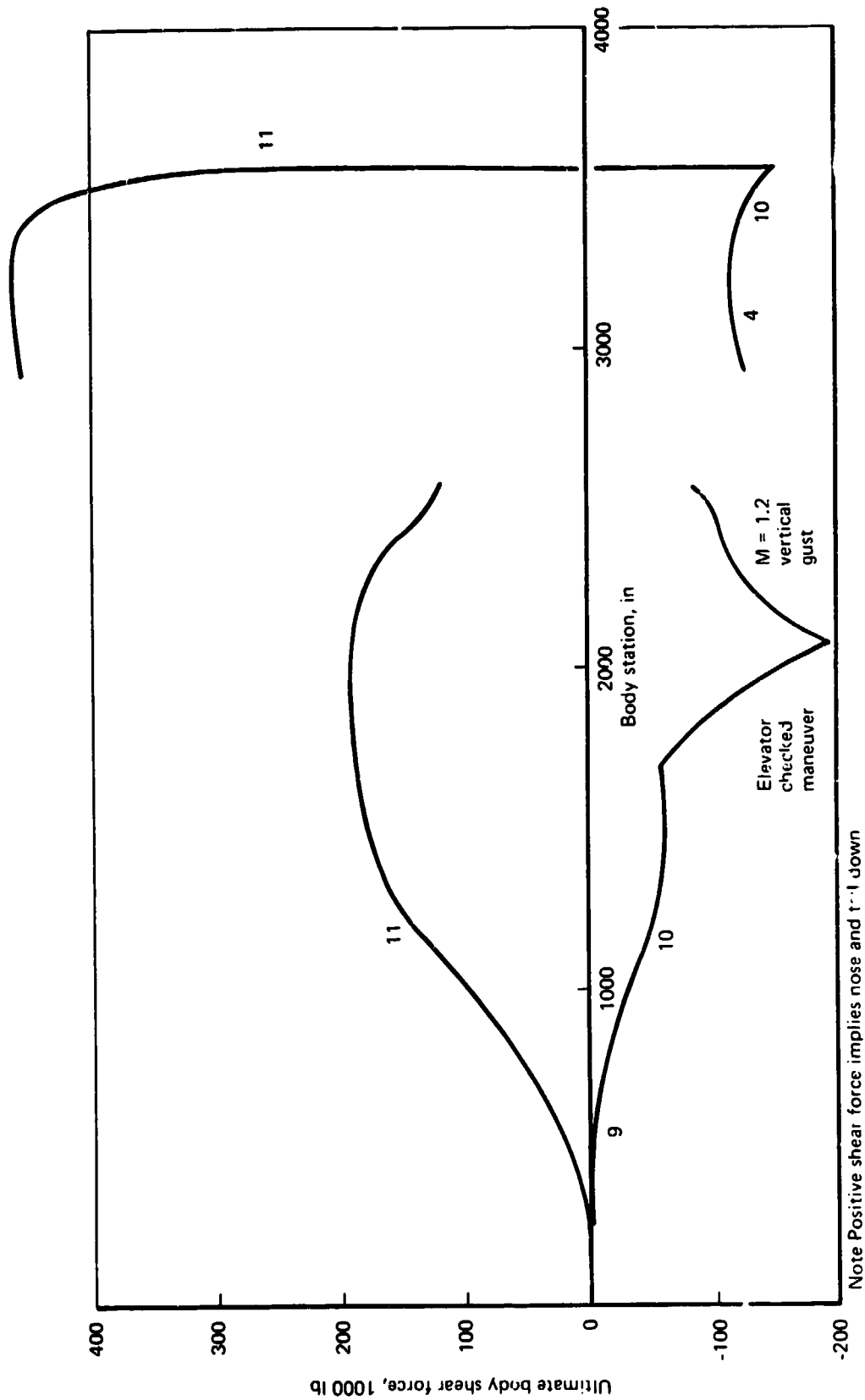
The condition numbers shown above correspond to the column numbers in table 8-11

Figure 8-31.—Design Ultimate Bending Moment Envelope for the Wing in Symmetrical Flight Conditions



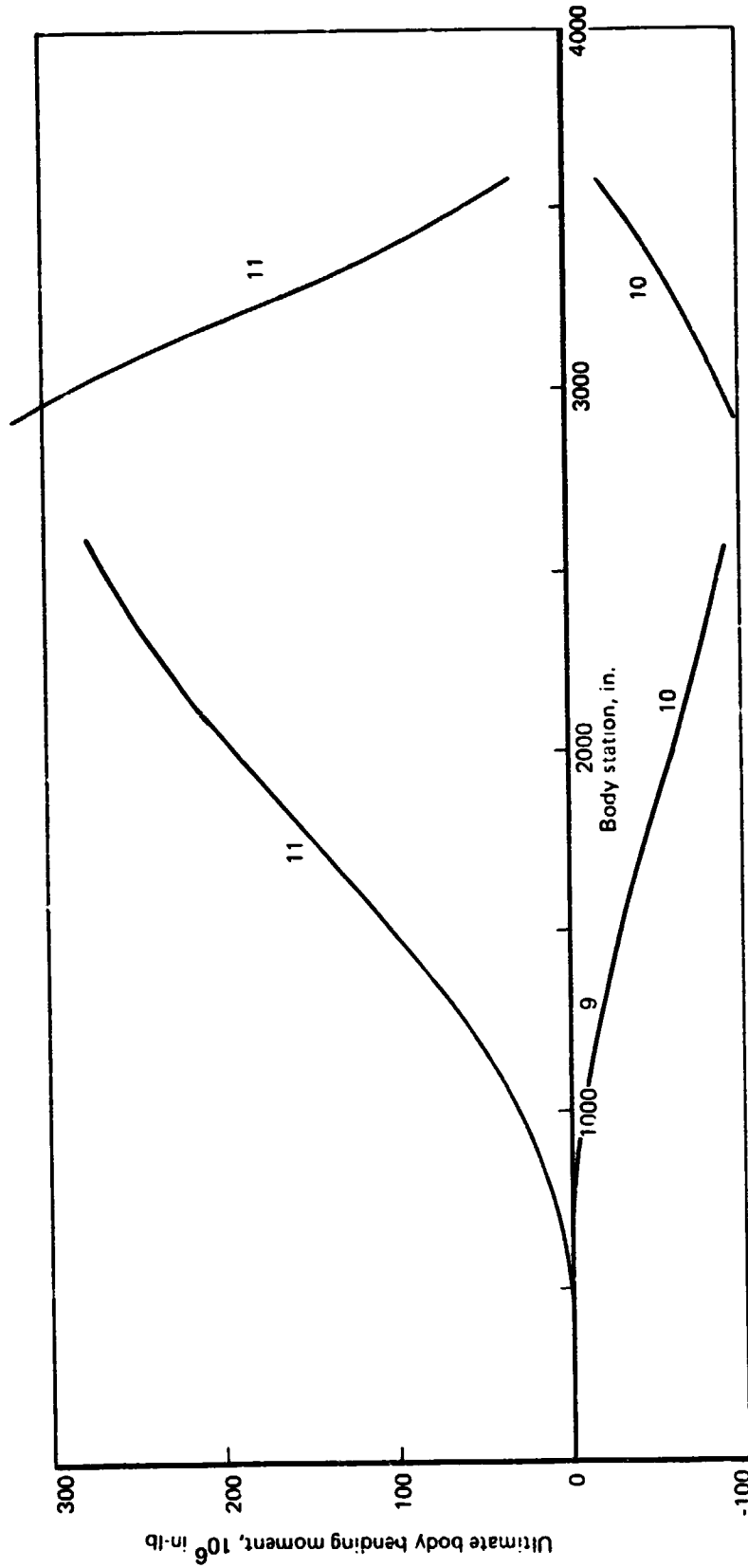
The condition numbers shown above correspond to the column numbers in table 8-11

Figure 8-32.—Design Ultimate Torque Envelope for the Wing in Symmetrical Flight Conditions



The condition numbers shown above correspond to the column numbers in table 8-11

Figure 8-33.—Design Ultimate Shear Force Envelope for the Body in Symmetrical Flight Conditions



Note: Positive bending implies nose and tail down

The condition numbers shown above correspond to the column numbers in table 8-13

Figure 8-34. —Design Ultimate Bending Moment Envelope for the Body in Symmetrical Flight Conditions

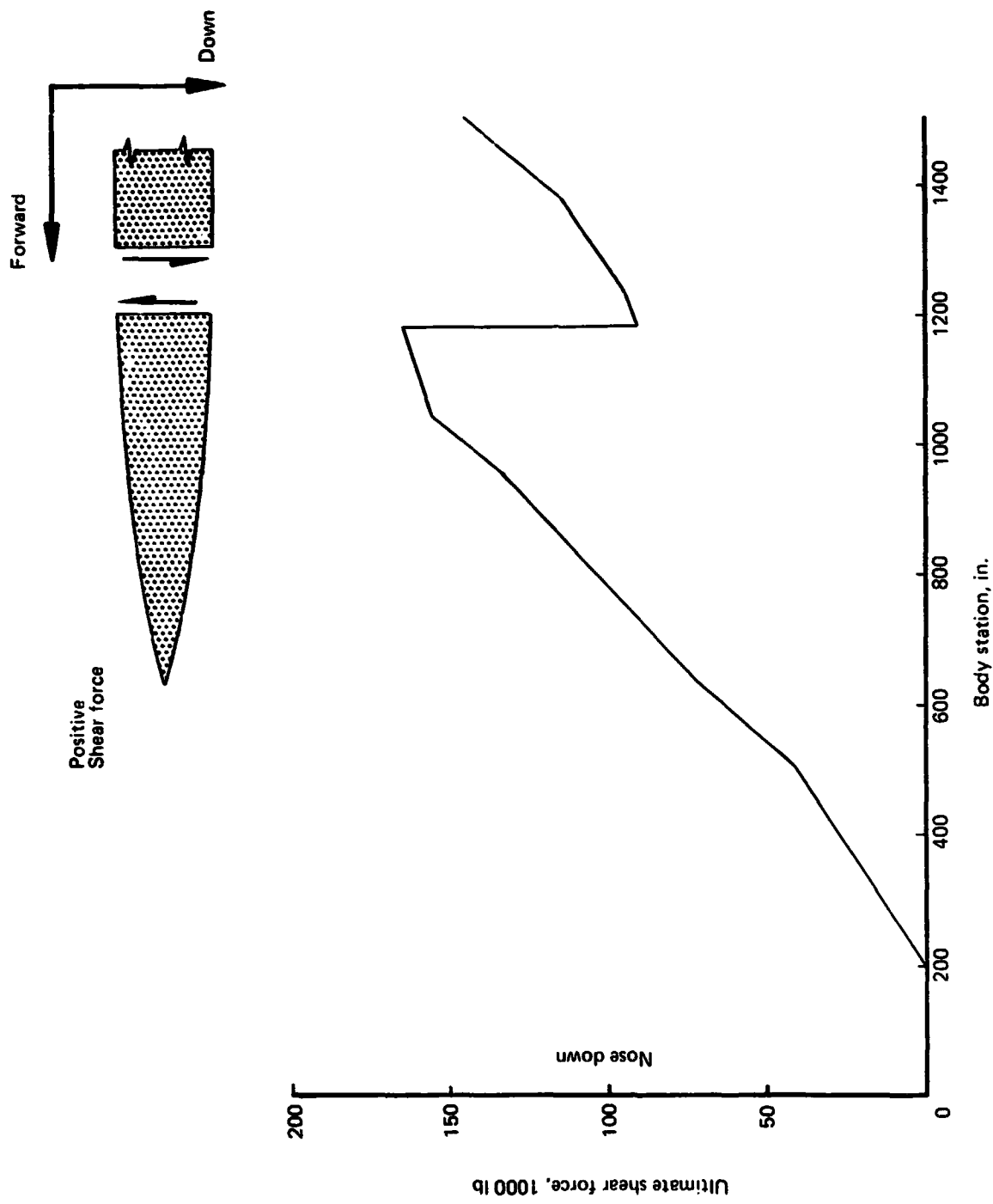


Figure 8-35. — Forward Body Ultimate Shear Force Caused by Landing Impact

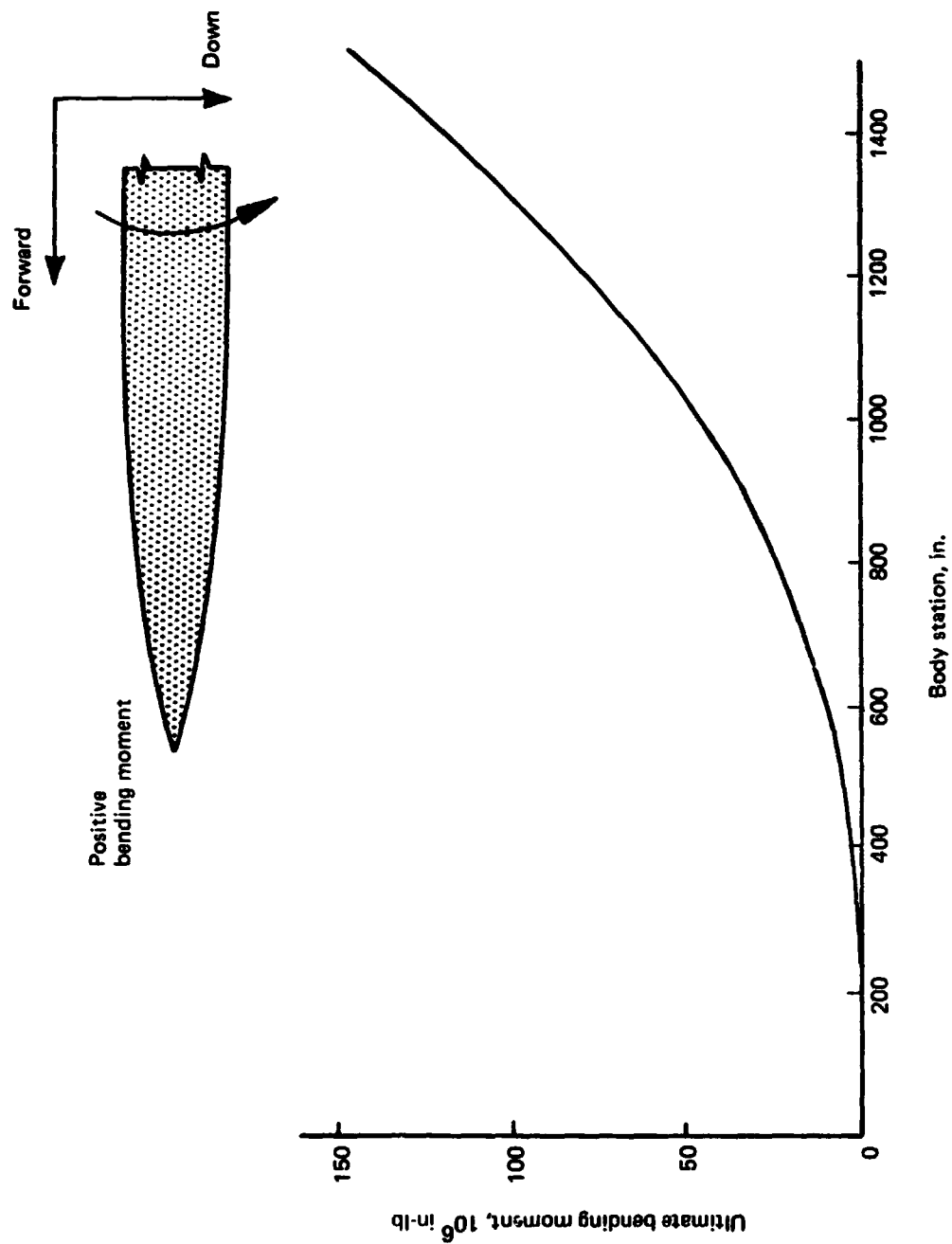


Figure 8-36. — Forward Body Ultimate Bending Moment Caused by Landing Impact

SECTION 9

STRUCTURAL THERMAL ANALYSIS

by

V. Deriugin
B. K. Gulrajani

PRECEDING PAGE BLANK NOT FILLED

CONTENTS

	Page
STRUCTURAL THERMAL ANALYSIS	430
General	430
Aerodynamic Heating	430
Equilibrium Wall Temperature	431
Effects of Angle of Attack, Distance and Sweep	432
Effects of Solar Absorptance and Surface Emittance	433
Transient Thermal Analysis	433
Thermal Stresses	434
Analysis Results	434
REFERENCES	435

TABLES

No.		Page
9-1	Thermal Analysis of Arrow Wing SST Configuration	436
9-2	Management of Fuel in Tank Nos. 1 and 2	437

FIGURES

No.		Page
9-1	Angle of Attack Effect on the Aerodynamic Heat Transfer Coefficient	438
9-2	Angle of Attack Effect on Aircraft Skin Temperature	438
9-3	Solar and Emittance Effects	439
9-4	Arrow Wing SST Configuration - Points for Thermal Analysis	440
9-5	Mission Profile (3340nm)	441
9-6	Fuel Tank Nos. 1 and 2, Fuel Management	442
9-7	Fuel Tank No. 1, Point 249	443
9-8	Fuel Tank No. 1 Temperatures, Point 249, Case 1, T1, T2, T24, T25	444
9-9	Fuel Tank No. 1 Temperatures, Point 249, Case 1, T5, T6, T20, T21	445
9-10	Fuel Tank No. 1 Temperatures, Point 249, Case 1, T8, T10, T12	446
9-11	Fuel Tank No. 1 Temperatures, Point 249, Case 1, T14, T16, T18	447
9-12	Fuel Tank No. 1 Thermal Gradients, Point 249, Case 1, T1-T2, T5-T7, T21-T19, T24-T25	448
9-13	Fuel Tank No. 1 Thermal Gradients, Point 249, Case 1, T7-T8, T8-T10, T8-T13	449
9-14	Fuel Tank No. 1 Thermal Gradients, Point 249, Case 1, T18-T13, T18-T16, T19-T18	450
9-15	Fuel Tank No. 1 Thermal Stresses, Point 249, Case 1, σ_1 , σ_2 , σ_{24} , σ_{25}	451
9-16	Fuel Tank No. 1 Thermal Stresses, Point 249, Case 1, σ_5 , σ_6 , σ_{20} , σ_{21}	452
9-17	Fuel Tank No. 1 Thermal Stresses, Point 249, Case 1, σ_8 , σ_{10} , σ_{12}	453
9-18	Fuel Tank No. 1 Thermal Stresses, Point 249, Case 1, σ_{14} , σ_{18}	454
9-19	Fuel Tank No. 1 Temperatures, Point 249, Case 2, T1, T2, T24, T25	455
9-20	Fuel Tank No. 1 Temperatures, Point 249, Case 2, T5, T6, T20, T21	456
9-21	Fuel Tank No. 1 Temperatures, Point 249, Case 2, T8, T10, T12	457
9-22	Fuel Tank No. 1 Temperatures, Point 249, Case 2, T14, T16, T18	458
9-23	Fuel Tank No. 1 Thermal Gradients, Point 249, Case 2, T1-T2, T5-T7, T21-T19, T24-T25	459
9-24	Fuel Tank No. 1 Thermal Gradients, Point 249, Case 2, T7-T8, T8-T10, T8-T13	460

FIGURES (CONTINUED)

No.		Page
9-25	Fuel Tank No. 1 Thermal Gradients, Point 249, Case 2, T18-T13, T18-T16, T19-T18	461
9-26	Fuel Tank No. 1 Thermal Stresses, Point 249, Case 2, σ_1 , σ_2 , σ_{24} , σ_{25}	462
9-27	Fuel Tank No. 1 Thermal Stresses, Point 249, Case 2, σ_5 , σ_6 , σ_{20} , σ_{21}	463
9-28	Fuel Tank No. 1 Thermal Stresses, Point 249, Case 2, σ_8 , σ_{10} , σ_{12}	464
9-29	Fuel Tank No. 1 Thermal Stresses, Point 249, Case 2, σ_{14} , σ_{16} , σ_{18}	465
9-30	Fuel Tank No. 2, Point 269	466
9-31	Fuel Tank No. 2 Temperatures, Point 269, Case 1, T1, T3, T7, T10	467
9-32	Fuel Tank No. 2 Temperatures, Point 269, Case 1, T11, T13, T17, T20	468
9-33	Fuel Tank No. 2 Thermal Gradients, Point 269, Case 1, T1-T3, T3-T7, T3-T10	469
9-34	Fuel Tank No. 2 Thermal Gradients, Point 269, Case 1, T11-T13, T13-T17, T13-T20	470
9-35	Fuel Tank No. 2 Thermal Stresses, Point 269, Case 1, σ_1 , σ_3 , σ_7 , σ_{10}	471
9-36	Fuel Tank No. 2 Thermal Stresses, Point 269, Case 1, σ_{11} , σ_{13} , σ_{17} , σ_{20}	472
9-37	Fuel Tank No. 2 Temperatures, Point 269, Case 2, T1, T3, T7, T10	473
9-38	Fuel Tank No. 2 Temperatures, Point 269, Case 2, T11, T13, T17, T20	474
9-39	Fuel Tank No. 2 Thermal Gradients, Point 269, Case 2, T1-T3, T3-T7, T3-T7, T3-T10	475
9-40	Fuel Tank No. 2 Thermal Gradients, Point 269, Case 2, T11-T13, T13-T17, T13-T20	476
9-41	Fuel Tank No. 2 Thermal Stresses, Point 269, Case 2, σ_1 , σ_3 , σ_7 , σ_{10}	477
9-42	Fuel Tank No. 2 Thermal Stresses, Point 269, Case 2, σ_{11} , σ_{13} , σ_{17} , σ_{20}	478
9-43	Fuel Tank No. 2 Temperatures, Point 269, Case 3, T1, T3, T7, T10	479
9-44	Fuel Tank No. 2 Temperatures, Point 269, Case 3, T11, T13, T17, T20	480
9-45	Fuel Tank No. 2 Thermal Gradients, Point 269, Case 3, T1-T3, T3-T7, T3-T10	481
9-46	Fuel Tank No. 2 Thermal Gradients, Point 269, Case 3, T11-T13, T13-T17, T13-T20	482
9-47	Fuel Tank No. 2 Thermal Stresses, Point 269, Case 3, σ_1 , σ_3 , σ_7 , σ_{10}	483
9-48	Fuel Tank No. 2 Thermal Stresses, Point 269, Case 3, σ_{11} , σ_{13} , σ_{17} , σ_{20}	484
9-49	Fuel Tank No. 2 Temperatures, Point 269, Case 4, T1, T3, T7, T10	485
9-50	Fuel Tank No. 2 Temperatures, Point 269, Case 4, T11, T13, T17, T20	486

FIGURES (CONTINUED)

No.		Page
9-51	Fuel Tank No. 2 Thermal Gradients, Point 269, Case 4, T1-T3, T3-T7, T3-T10	487
9-52	Fuel Tank No. 2 Thermal Gradients, Point 269, Case 4, T11-T13, T13-T17, T13-T20	488
9-53	Fuel Tank No. 2 Thermal Stresses, Point 269, Case 4, $\sigma_1, \sigma_3, \sigma_7, \sigma_{10}$	489
9-54	Fuel Tank No. 2 Thermal Stresses, Point 269, Case 4, $\sigma_{11}, \sigma_{13},$ σ_{17}, σ_{20}	490
9-55	Intermediate and Rear Spars, Point 431	491
9-56	Wing Spar Temperatures, Point 431, Case 1, Forward, T1, T2, T5, T6	492
9-57	Wing Spar Temperatures, Point 431, Case 1, Forward, T8, T12, T17, T19	493
9-58	Wing Spar Thermal Gradients, Point 431, Case 1, Forward, T5-T7, T7-T12, T7-T13, T19-T17	494
9-59	Wing Spar Thermal Stresses, Point 431, Case 1, Forward, $\sigma_1, \sigma_5, \sigma_8, \sigma_9$	495
9-60	Wing Spar Thermal Stresses, Point 431, Case 1, Forward, $\sigma_{12}, \sigma_{17}, \sigma_{18}, \sigma_{21}$	496
9-61	Wing Spar Temperatures, Point 431, Case 2, Aft, T1, T2, T5, T6	497
9-62	Wing Spar Temperatures, Point 431, Case 2, Aft, T8, T12, T17, T19	498
9-63	Wing Spar Thermal Gradients, Point 431, Case 2, Aft, T5-T7, T7-T12, T7-T13, T19-T17	499
9-64	Wing Spar Thermal Stresses, Point 431, Case 2, Aft, $\sigma_1, \sigma_5, \sigma_8, \sigma_9$	500
9-65	Wing Spar Thermal Stresses, Point 431, Case 2, Aft, $\sigma_{12}, \sigma_{17}, \sigma_{18}, \sigma_{21}$	501
9-66	Wing Panel Dry Bay Area, Point 431	502
9-67	Wing Panel Temperatures, Point 431, Case 1, Forward, T1, T2	503
9-68	Wing Panel Temperatures, Point 431, Case 1, Forward, T3, T4, T5, T6	504
9-69	Wing Panel Thermal Gradients, Point 431, Case 1, Forward, T1-T2, T3-T4, T3-T5, T3-T6	505
9-70	Wing Panel Thermal Stresses, Point 431, Case 1, Forward, $\sigma_3, \sigma_4, \sigma_5, \sigma_6$	506
9-71	Wing Panel Temperatures, Point 431, Case 2, Aft, T1, T2	507
9-72	Wing Panel Temperatures, Point 431, Case 2, Aft, T3, T4, T5, T6	508
9-73	Wing Panel Thermal Gradients, Point 431, Case 2, Aft, T1-T2, T3-T4, T3-T5, T3-T6	509
9-74	Wing Panel Thermal Stresses, Point 431, Case 2, Aft, $\sigma_3, \sigma_4, \sigma_5, \sigma_6$	510
9-75	Body Stringers, Points 5 and 6	511
9-76	Body Stringer Temperatures, Point 5, Case 1, T1, T4, T7, T10	512

FIGURES (CONCLUDED)

No.		Page
9-77	Body Stringer Thermal Gradients, Point 5, Case 1, T1-T3, T3-T5, T3-T7, T3-T10	513
9-78	Body Stringer Thermal Stresses, Point 5, Case 1, $\sigma_1, \sigma_4, \sigma_7, \sigma_{10}$	514
9-79	Body Stringer Temperatures, Point 6, Case 2, T1, T4, T7, T10	515
9-80	Body Stringer Thermal Gradients, Point 6, Case 2 T1-T3, T3-T5, T3-T7, T3-T10	516
9-81	Body Stringer Thermal Stresses, Point 6, Case 2, $\sigma_1, \sigma_4, \sigma_7, \sigma_{10}$	517

Symbols and Abbreviations

A	Area for heat conduction m^2 (ft^2)
A_i	Cross-sectional area of element i, mm^2 (in^2)
c_p	Specific heat, $\frac{J}{Kg\ K} \left(\frac{Btu}{lb. \ ^\circ R} \right)$
E	Modulus of Elasticity, N/m^2 (lb/in^2)
h	Heat transfer coefficient $\frac{W}{m^2\ K} \left(\frac{Btu}{ft.^2\ hr. \ ^\circ R} \right)$
h_l	Heat transfer coefficient for laminar flow $\frac{W}{m^2\ K} \left(\frac{Btu}{ft.^2\ hr. \ ^\circ R} \right)$
h_T	Heat transfer coefficient for turbulent flow, $\frac{W}{m^2\ K} \left(\frac{Btu}{ft.^2\ hr. \ ^\circ R} \right)$
h_δ	Heat transfer coefficient with angle of attack, $\frac{W}{m^2\ K} \left(\frac{Btu}{ft.^2\ hr. \ ^\circ R} \right)$
k	Thermal conductivity, $\frac{W}{m\ K} \left(\frac{Btu}{ft. \ hr. \ ^\circ R} \right)$
Pr	Prandtl number, $\frac{C_p \mu}{K}$
\dot{q}	Heating rate, $\frac{W}{m^2} \left(\frac{Btu}{ft.^2\ sec.} \right)$
\dot{q}_{earth} reflected solar	Earth reflected solar heat flux-earth albedo $30-558 \frac{W}{m^2} \quad \left(0-177 \frac{Btu}{ft.^2\ hr} \right)$

Symbols (Continued)

$q_{\text{earth infrared}}$	Earth radiated infrared heat flux $375 - 409 \frac{\text{W}}{\text{m}^2 \text{K}} \left(66 - 72 \frac{\text{Btu}}{\text{ft}^2 \text{hr}} \right)$
q_{solar}	Solar heat flux $\frac{1386 \text{ W}}{\text{m}^2} \left(\frac{400 \text{ Btu}}{\text{ft}^2 \text{hr.}} \right)$ at 15240 m (50,000 ft) altitude
r	Recovery factor
Re	Local Reynolds number
S^*	Rubesin correction factor (reference 9-2)
T	Temperature, K ($^{\circ}$ R)
T_{aw}	Recovery temperature, or adiabatic wall temperature K ($^{\circ}$ R)
T_w	Wall temperature K ($^{\circ}$ R)
T_{∞}	Free-stream temperature, K ($^{\circ}$ R)
T^*	Reference temperature, K ($^{\circ}$ R)
$T_{w\text{eq}}$	Equilibrium wall temperature, K ($^{\circ}$ R)
ΔT	Final temperature-initial temperature, K ($^{\circ}$ R)
V	Velocity, M/S (ft/sec)
ΔV	Volume of an element, mm^3 (ft^3)
χ	Distance between consecutive nodes, mm (ft)
X	Streamwise distance from leading edge, m (ft)
α	Angle of attack, degrees
α	Coefficient of thermal expansion, $\frac{\text{mm}}{\text{mm K}} \left(\frac{\text{in.}}{\text{in. } ^{\circ}\text{R}} \right)$

Symbols (Concluded)

α_{solar} Material absorptance for solar energy

ϵ Surface emittance

ρ Density

$$\frac{\text{kg}}{\text{m}^3} \left(\frac{\text{lb.}}{\text{in.}^3} \right)$$

σ Stefan-Boltzmann constant,

$$\frac{\text{W}}{\text{m}^2 \text{ K}^4} \left(\frac{\text{Btu}}{\text{ft.}^2 \text{ sec. } ^\circ \text{R}^4} \right)$$

σ_j Stress in component j,

$$\text{N/m}^2 \quad (\text{lb./in.}^2)$$

γ Ratio of specific heats, 1.4 for air

μ Dynamic viscosity,

$$\frac{\text{N s}}{\text{m}^2} \left(\frac{\text{lb. sec.}}{\text{in.}^2} \right)$$

SECTION 9

STRUCTURAL THERMAL ANALYSIS

GENERAL

Structural-thermal analysis of supersonic aircraft, which are subjected to heating effects from several external and internal sources, is required in order to determine temperature gradients which produce thermal stresses, and to establish temperature limits for material selection. Internal heat sinks provided by the structure and the fuel must also be considered in the analysis in order to accurately predict temperature and stress distributions. These are then used in the design and sizing of the structural elements, in the selection of suitable structural materials, and in determining insulation requirements for fuel tanks.

The thermal analysis initially requires the establishment of analysis methods and criteria, a mission profile, a fuel management plan and the determination of the external and the internal environment to predict the heating rates to the various regions of the aircraft. The next phase is the determination of the thermal response of the particular structural cross section yielding the required temperature distributions, gradients and stresses.

The criteria and the analysis methods used in the present analysis are identical to those employed on the National SST Program. In determining the structural temperatures, no factors of safety are applied. However, a factor of safety of 1.25 is applied on thermal strains to account for thermal uncertainties.

The major source of external heating for a commercial supersonic transport is aerodynamic heating. Since solar heating is also a significant source, both were considered in the present analysis. The analysis methods and the analysis results are briefly described in the following paragraphs.

AERODYNAMIC HEATING

The aerodynamic heat transfer rates can be determined from Newton's cooling law which defines a heat transfer coefficient h in the following form:

$$h = \dot{q} / (T_{aw} - T_w) \quad (9-1)$$

where

$$T_{aw} = T_\infty \left(1 + r \frac{\gamma - 1}{2} M_\infty^2 \right) \quad (9-2)$$

represents the temperature of an adiabatic (insulated) wall for the respective environmental conditions and a given free-stream Mach number. The recovery factor, r , is a parameter relating the adiabatic temperature rise across the boundary layer on an

insulated (flat plate) wall to the stagnation temperature rise and is commonly accepted as approximately .85 for laminar and .89 for turbulent flow.

During the preliminary design phase of the National SST, the Boeing Company considered a multitude of methods for determining the heat transfer coefficient. As a result of this study and related test data, it was decided to use Eckert's Reference Temperature (T^*) Method for calculating the aerodynamic heat transfer coefficients (ref. 9-1). This method is used in conjunction with the Reynolds analogy and the Blasius skin friction relationship for laminar flow. A modified Reynolds analogy with the Prandtl-Schlichting-Wieghardt skin friction relationship and a Rubesin correction factor (ref. 9-2) is used for turbulent flow.

The reference temperature is defined by the equation:

$$T^* = .22T_{aw} + .28T_{\infty} + .5 T_w \quad (9-3)$$

The corresponding heat transfer coefficients on a flat plate are given by the following equations:

$$h_L = .332 \frac{k^*}{x} (Pr^*)^{1/3} (Re^*)^{1/2} \quad (\text{laminar}) \quad (9-4)$$

and

$$h_T = \frac{.144 \frac{k^*}{x} (Pr^*) (Re^*) (S^*)}{(\log_{10} Re^*)^{2.45}} \quad (\text{turbulent}) \quad (9-5)$$

where the superscript * indicates that the respective parameter is evaluated at the reference temperature T^*

The flat plate approach is generally considered to be sufficiently accurate for determining heat transfer coefficients on large surfaces on configurations such as the SST, except in specific locations, such as stagnation regions, areas of large curvature and regions of protuberances or discontinuities.

EQUILIBRIUM WALL TEMPERATURE

The wall temperature, used to determine the reference temperature for obtaining the heat transfer coefficient, is computed from radiation equilibrium. The equilibrium wall temperature T_{weq} is defined as the temperature of an insulated thin skin receiving aerodynamic heating and losing heat by radiation, as shown in the following thermal balance equation:

$$h(T_{aw} - T_{weq}) - \sigma \epsilon T_{weq}^4 = 0 \quad (9-6)$$

Many aircraft structural elements which consist of thin metal skins with little thermal capacitance will rapidly reach a steady state temperature, as given by T_{weq} in the

above equation. During the proposal phase of the National SST Program, a digital computer program was written, to solve simultaneously the aerodynamic heating and the equilibrium wall temperature equations, using a CDC 6600 computer (ref. 9-3). The program input consists of flight trajectory (time, altitude, Mach number), flow classification (laminar or turbulent) and the surface emittance. The program has the capability of using the U.S. standard atmosphere of 1962, and the Air Force hot or cold atmospheres. The output of the program is the aerodynamic heat transfer coefficient and the adiabatic wall temperature for discrete intervals on the mission profile.

It should be noted that, in reality, aircraft surfaces are also subjected to solar, earth reflected solar and earth infra-red radiation. Consequently, the real equilibrium wall temperature is given more accurately by the following equations:

$$h(T_{aw} - T_{w_{eq}}) + \dot{q}_{solar} - \sigma \epsilon T_{w_{eq}}^4 = 0 \quad \text{for upper surfaces} \quad (9-7)$$

$$h(T_{aw} - T_{w_{eq}}) + \dot{q}_{earth \text{ reflected solar}} + \dot{q}_{earth \text{ infrared}} - \sigma \epsilon T_{w_{eq}}^4 = 0 \quad \text{for lower surfaces} \quad (9-8)$$

However, the increased accuracy of these equations does not significantly influence the heat transfer coefficient obtained on the basis of the reference temperature. It was therefore decided to use the wall temperature computed from the simpler preceding equation for determining heat transfer coefficients.

EFFECTS OF ANGLE OF ATTACK, DISTANCE AND SWEEP

The aerodynamic heat transfer coefficients are influenced by angle of attack due to changes in the flow field along the upper and lower surfaces of the aircraft. During the design phase of the National SST, these effects were considered (ref. 9-1), and the results are shown in figures 9-1 and 9-2. Figure 9-1 shows that for a moderate angle of attack of 6 degrees, the flat plate heat transfer coefficient increases by about 47% on the lower surface and decreases by about 35% on the upper surface. Figure 9-2 shows, however, that the equilibrium wall temperatures show very small variations for both upper and lower titanium surfaces for angles of attack between 0° and 6°. Consequently, for the temperature ranges and flight regimes considered, the effect of moderate angles of attack on the equilibrium wall temperature can be regarded as negligible. However, this effect may be more significant during transient (ascent and descent) periods when temperatures are relatively low.

Figure 9-2 also shows that the effect of the streamwise distance, aft of the leading edge, on the equilibrium wall temperature is very small. Therefore, the temperatures along the wings and body are also expected to show only small changes.

The effect of the sweep angle on the maximum thermal gradients and the equilibrium wall temperatures is similarly considered negligible.

EFFECTS OF SOLAR ABSORPTANCE AND SURFACE EMITTANCE

The effects of the solar absorptance and the surface emittance on the equilibrium wall temperature are shown in figure 9-3. Although small changes in absorptive and emissive material properties may not significantly affect equilibrium wall temperatures, this may be an area of potential payoff by tailoring such properties in order to improve temperature distributions and thermal control. For the thermal analysis reported in the subsequent paragraphs, the titanium solar absorptance was assumed to be $\alpha_{\text{solar}} = 0.7$, and the surface emittance was assumed to be $\epsilon = 0.2$. It was further assumed that the lower surfaces of the aircraft received 10% of the solar energy reflected from the ground or the oceans (albedo). The radiation to the ground or the ocean was assumed to occur at a ground temperature of 311K (100° F). No separate earth infrared radiation was considered.

TRANSIENT THERMAL ANALYSIS

The externally generated heat flows into the internal equipment and fuel through the wetted aircraft skin surfaces and the adjoining structures, such as the wing spars, ribs, wheel well structure, etc., mostly by conduction and radiation. Due to resistance to the heat flow, there is a certain time lag in the structural temperature response resulting in temperature gradients which may produce instantaneous thermal stresses. The thermal gradient and the temperature-time histories required for the selection and sizing of various structural members were generated using the thermal analyzer CDC 6600 computer program (ref. 9-4). The program is based on a finite difference solution of the heat flow equation using a 3-dimensional nodal network and includes the effects of conduction, convection, radiation, external and internal heat sources, and property variations with time, temperature and direction. The aerodynamic heating program (ref. 9-3) is coupled with the thermal analyzer program (ref. 9-4), providing the required boundary conditions. In addition, the thermal analyzer program has a plotting routine such that temperature and stress time histories can be directly plotted using an SC 4020 plotter.

For transient thermal analyses, selected representative structural members and cross sections, such as a wing spar and upper and lower panel combination, are divided into a suitable number of elements. These elements are then represented by lumped masses (nodes) at the element centroids. The various nodes, which also are represented as capacitors, are connected in a network by means of resistors. This network of capacitors, resistors and, when applicable, radiators, in conjunction with sources, sinks, and the aerodynamic heating boundary conditions are used to calculate the thermal response and the stresses in the structure at the designated nodes.

Analysis has indicated that fuel tank panels should have sufficiently low thermal conductance to prevent fuel boiling at the end of cruise. An aluminum brazed titanium honeycomb sandwich panel was developed during the design of the National SST which had a thermal conductance of $51 \text{ W/m}^2\text{-K}$ ($9.0 \text{ BTU/ft}^2\text{-hr-}^\circ\text{R}$) for a panel 25.4 mm (1 inch) deep. The work on a low conductance sandwich panel has been continued since then, under the Department of Transportation funded SST follow-on contract. By reducing the number of nodes in the honeycomb, panels have been developed with a conductance of

34 W/m²-K(6.0 BTU/ft²-hr-°R), and the required mechanical properties. Attempts were made to develop an aluminum brazed titanium panel with a thermal conductance of 14.2 W/m²-K(2.5 BTU/ft²-hr-°R) (the conductance of an equivalent diffusion bonded panel) with the required mechanical properties (ref. 9-5). However, additional work is required in this area. For the present thermal analysis, a honeycomb panel conductance of 34 W/m²-K(6.0 BTU/ft²-hr-°R) was used.

THERMAL STRESSES

The thermal stresses in the structural members were calculated using a stress subroutine written into the thermal analyzer computer program. The subroutine solves the following equation:

$$\sigma_j = \alpha_j E_j \Delta_j - E_j \frac{\sum_{i=1}^n \alpha_i E_i A_i \Delta T_i}{\sum_{i=1}^n A_i E_i} \quad (9-9)$$

This equation predicts the thermal stress in each of n uniaxial elements. The n elements are assumed to be of equal length at a reference temperature. When subjected to temperature differentials from the reference temperature, the members are constrained against rotation but free to translate to a common length at which the total axial load of the n members is zero.

ANALYSIS RESULTS

The thermal analysis of the Arrow Wing SST configuration was conducted for a number of selected locations as shown in figure 9-4. These locations and structural arrangements are listed in table 9-1.

The aerodynamic heating rates were calculated using a 6190 km (3340 nm) mission profile, as shown in figure 9-5, and the 1962 U.S. standard atmosphere. The flow along the wing and the body is mostly turbulent. Therefore, turbulent heat transfer rates were used in the analysis. Solar heating and radiation to outer space was included in the calculation of the transient skin temperatures. The titanium solar absorptance was assumed to be 0.7, and the emittance to outer space or for internal radiation was assumed to be 0.2.

The thermal conductance of the 25.4mm (1 inch) deep honeycomb panel was assumed as 34 W/m²-K(6.0 BTU/ft²-hr-°R). For the denser honeycomb, at the joint with the spar, a value of 216 W/m²-K(38.0 BTU/ft²-hr-°R) was used.

To determine the effect of fuel on tank structures, the fuel management scheme shown in figure 9-6 and listed in table 9-2, was used in the transient analysis. This fuel management is consistent with the flight performance of the Arrow Wing airplane. The thermal conductance between the structure and the fuel was assumed as 171.0 W/m²-K (30.0 BTU/ft²-hr-°R). It was further assumed that the panel and the spars of tank No.1

were not internally insulated. Insulation with a thermal conductivity of .058 W/m-K (0.4 BTU-in/ft²-hr-°R) was used only for the tank No.2 area which contained integrally stiffened lower panels.

The initial temperature before the aircraft flight was assumed as 288.8 K (60° F). The structural concepts and the results of the transient analysis, including temperature, thermal gradient and thermal stress histories are shown in figures 9-7 through 9-81 for various nodes. The positive values represent tensile stresses and negative values compressive stresses.

REFERENCES

- 9-1 Davis, J. G., *SST Environmental Design Criteria*, Boeing document D6-6800-7, February 1969.
- 9-2 Rubesin, M. W., *A Modified Analogy for the Compressible Turbulent Boundary Layer on a Flat Plate*, NACA TN 2917, 1953.
- 9-3 Wrathal, C. and Hahn, E., *A Digital Program to Determine the Heat Transfer Coefficients and Adiabatic Wall Temperatures by the Reference Temperature Method*, Boeing document D6-7614 TN, January 1964.
- 9-4 Frimanslund, S. K., *Thermal Analyzer - BETA, User's Manual, TES-176*, Boeing document D6-29116 TN-1, June 1969.
- 9-5 Elrod, E. and Lindth, D. V., *Development and Evaluation of Aluminum Brazed, Titanium System*, FAA-SS-73-5-4, Volume IV, Material Properties. Boeing document D6-60277-4, May 1974.

Table 9-1. -Thermal Analysis of Arrow Wing SST Configuration

Configuration	Point	Case	Description	Insulation	Figures
Fuel tank no. 1 (Spar area)	249	1	Tank height = 43.3 in. Upper panel does not touch fuel	None	9-7 through 9-18
		2	Tank height = 35.0 in. Upper panel touches fuel	None	9-19 through 9-29
Fuel tank no. 2 (Stringer area)	269	1	Upper panel touches fuel	0.25 in.	9-30 through 9-36
		2	Upper panel touches fuel	0.50 in.	9-37 through 9-42
		3	Upper panel does not touch fuel	0.25 in.	9-43 through 9-48
		4	Upper panel does not touch fuel	0.50 in.	9-49 through 9-54
Intermediate and rear spars	431	1	Spar fwd of point 431	None	9-55 through 9-60
		2	Spar aft of point 431	None	9-61 through 9-65
Wing panel dry bay area	431	1	Fwd of point 431	None	9-66 through 9-70
		2	Aft of point 431	None	9-71 through 9-74
Body stringers	5	1	Lower crown	None	9-75 through 9-78
	6	2	Upper crown	None	9-79 through 9-81

Table 9-2.—Management of Fuel in Tank Nos. 1 and 2

Time, min	Fuel weight, lb
0	36 732
10	35 661
13	31 766
14	30 928
16	29 548
18	28 201
20	28 366
24	29 804
30	30 690
33	30 562
35	30 499
42	32 828
63	41 025
85	31 265
90	29 091
115	18 754
131	12 476
142	9,961
149	16 216
156	15 969
162	15 714
167	14 844
172	24 999

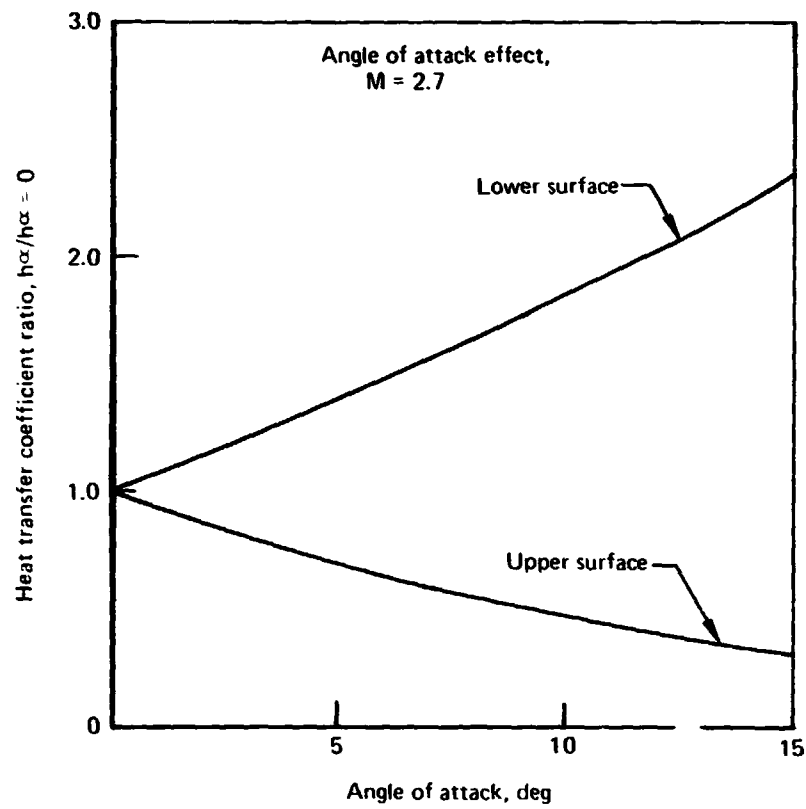


Figure 9-1.-Angle of Attack Effect on Aerodynamic Heat Transfer Coefficient

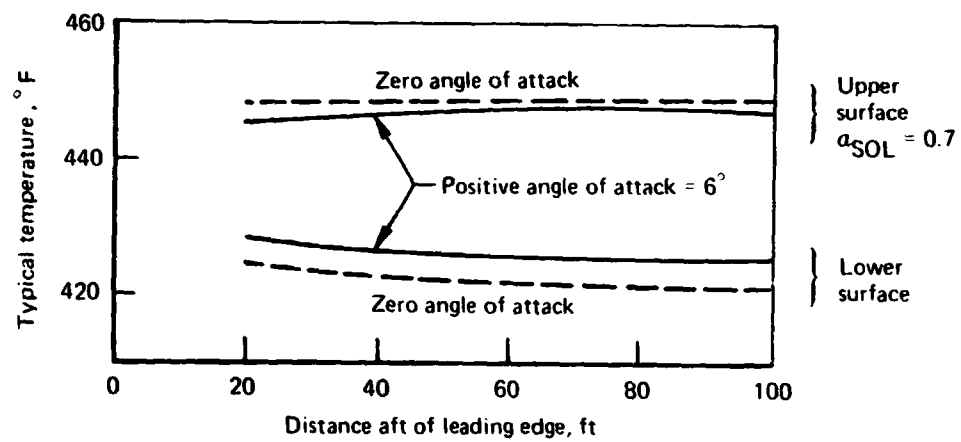


Figure 9-2.-Angle of Attack Effect on Aircraft Skin Temperature

$M_{\infty} = 2.7$
 $X_{LE} = 25 \text{ ft}$
Altitude = 60 000 ft

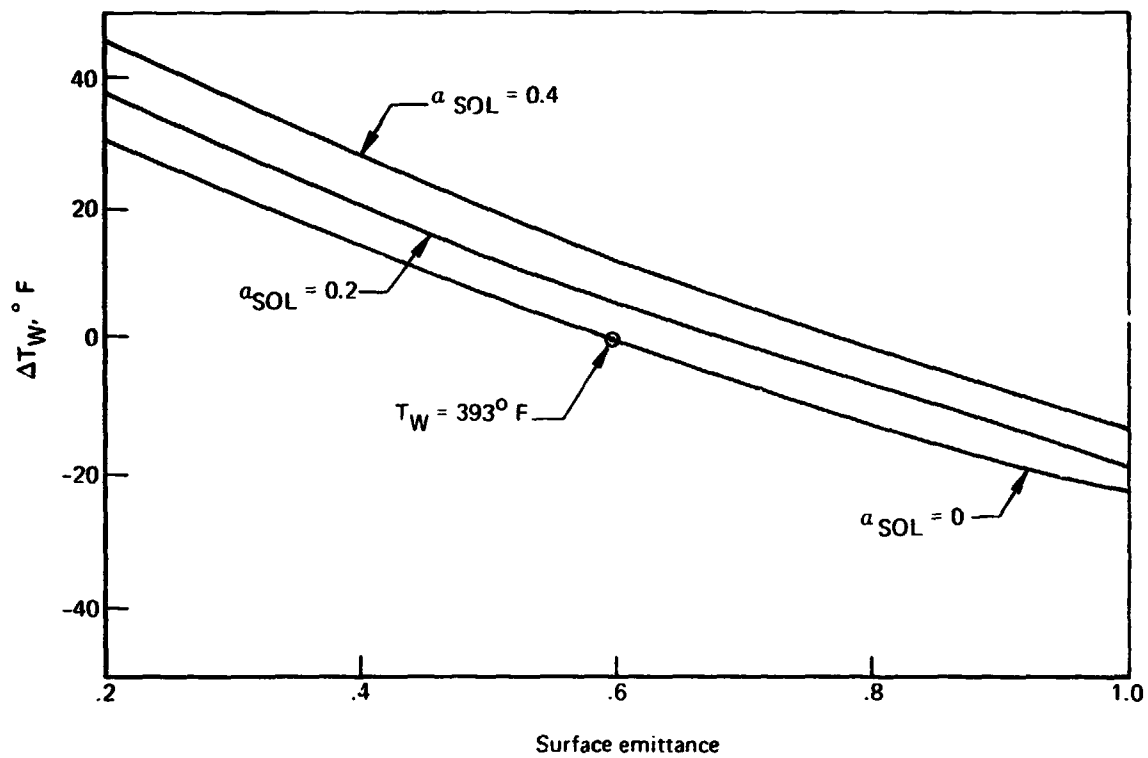
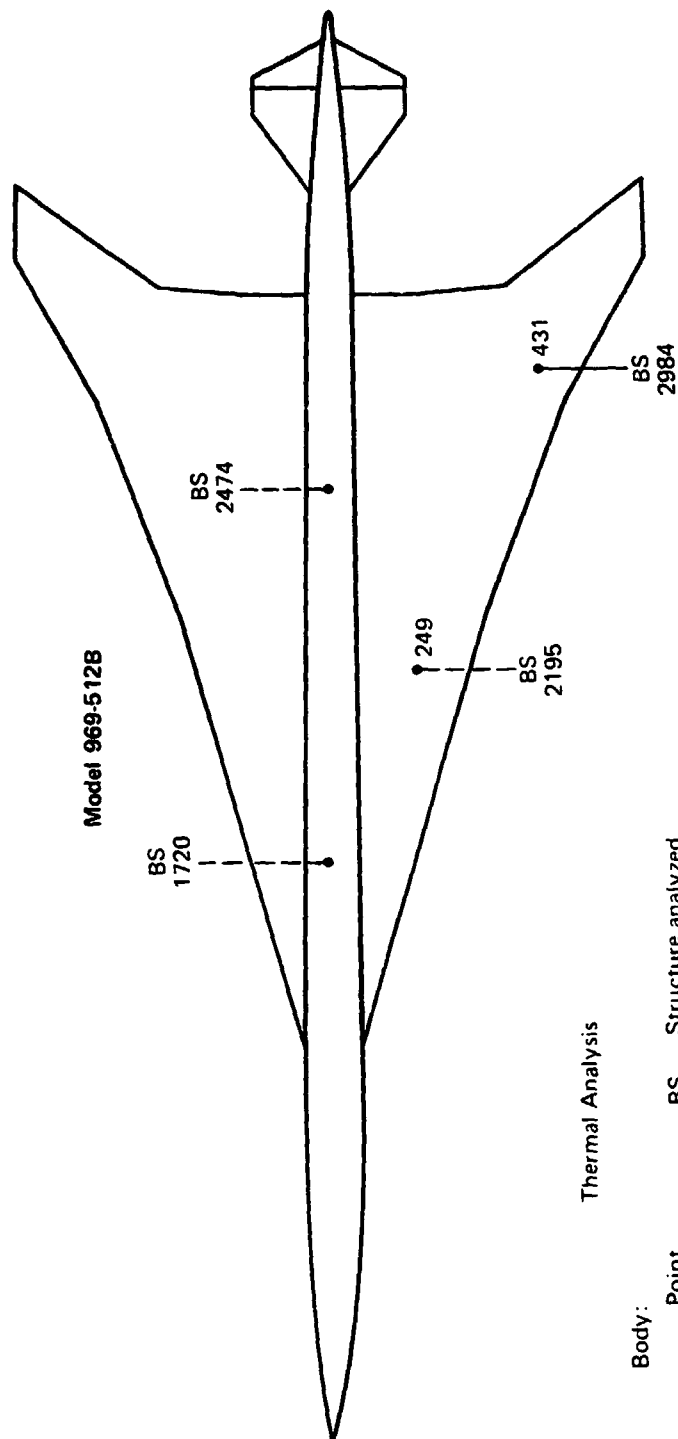


Figure 9-3.-Solar and Emittance Effects



Thermal Analysis

Body:	
Point	BS Structure analyzed
5 (Lower crown)	1720 Body stringer
6 (Upper crown)	2474 Body stringer
Wings:	
Point	BS Structure analyzed
249 (tank I)	2195 (1) panels (2) spar
431 (dry bay)	2984 (1) panels (2) spar

Figure 9-4. -Arrow Wing SST Configuration Points for Thermal Analysis

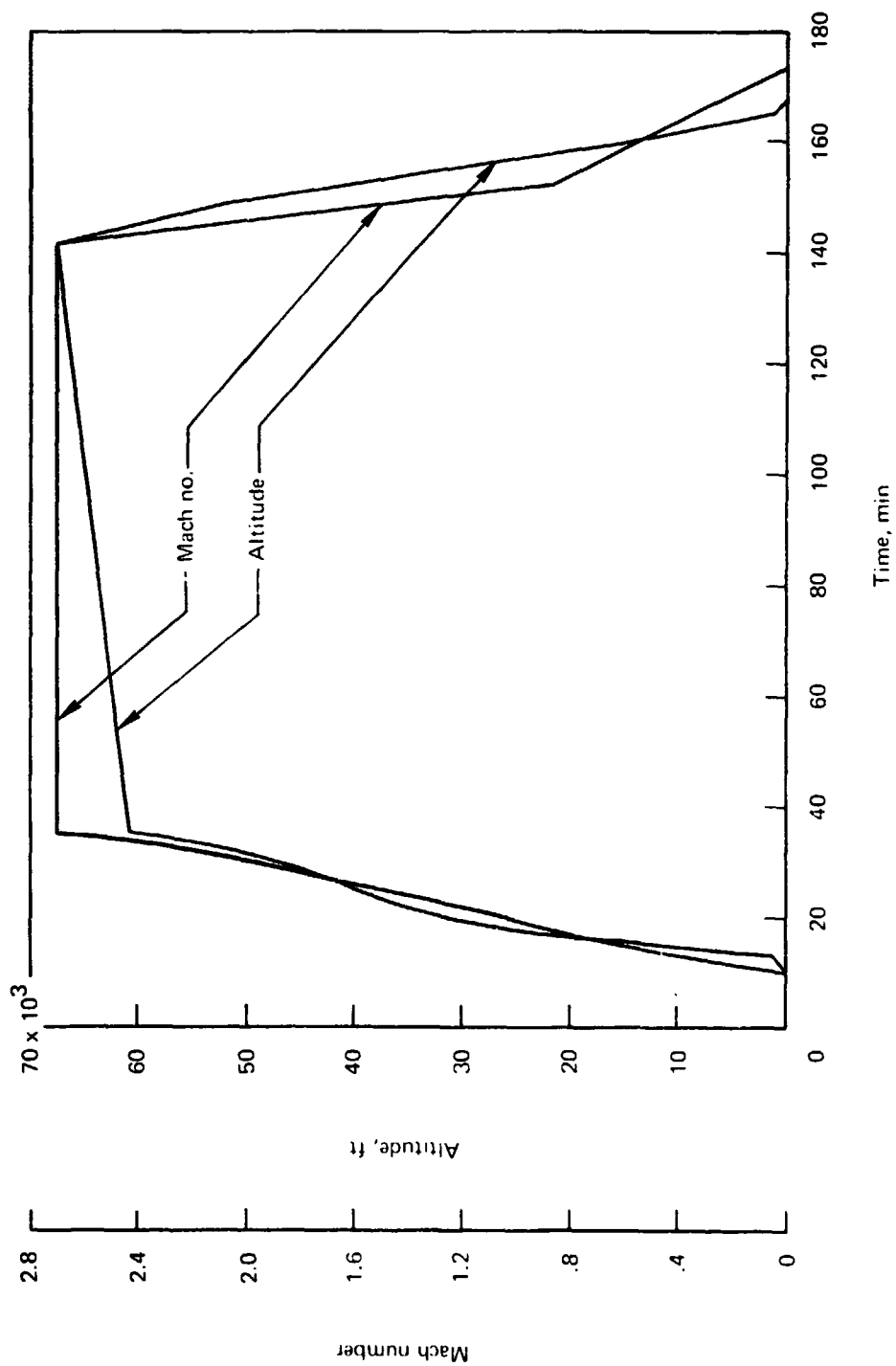


Figure 9-5.-Mission Profile (3340 nmi)

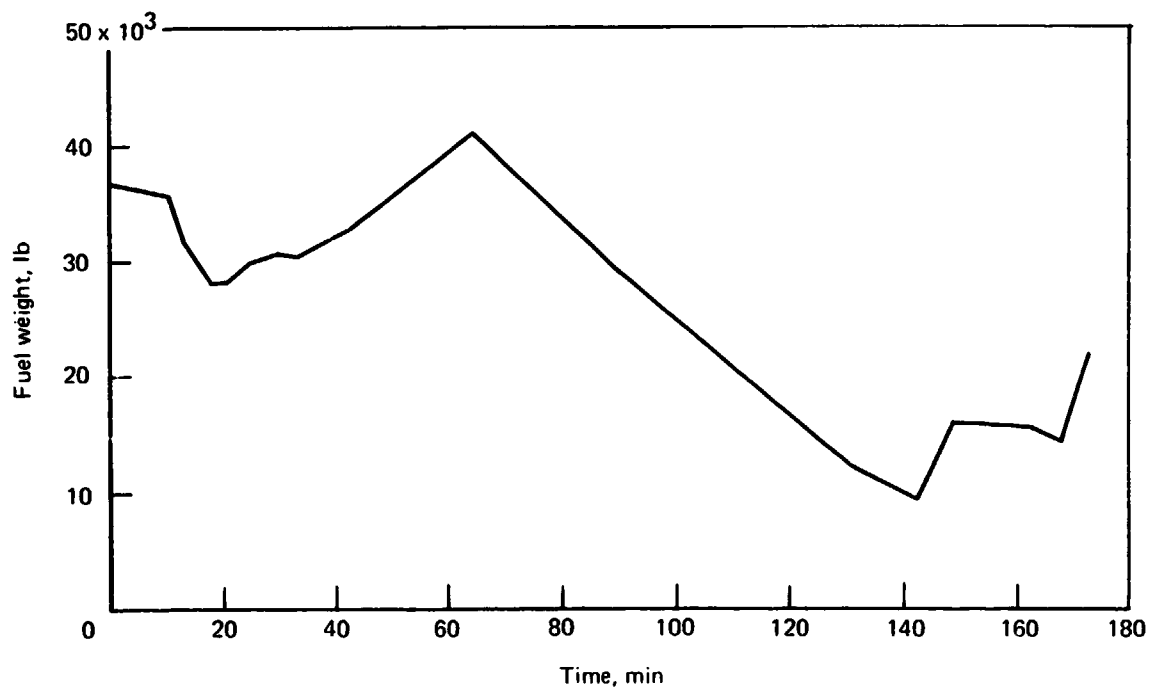


Figure 9-6.—Fuel Tank Nos. 1 and 2, Fuel Management

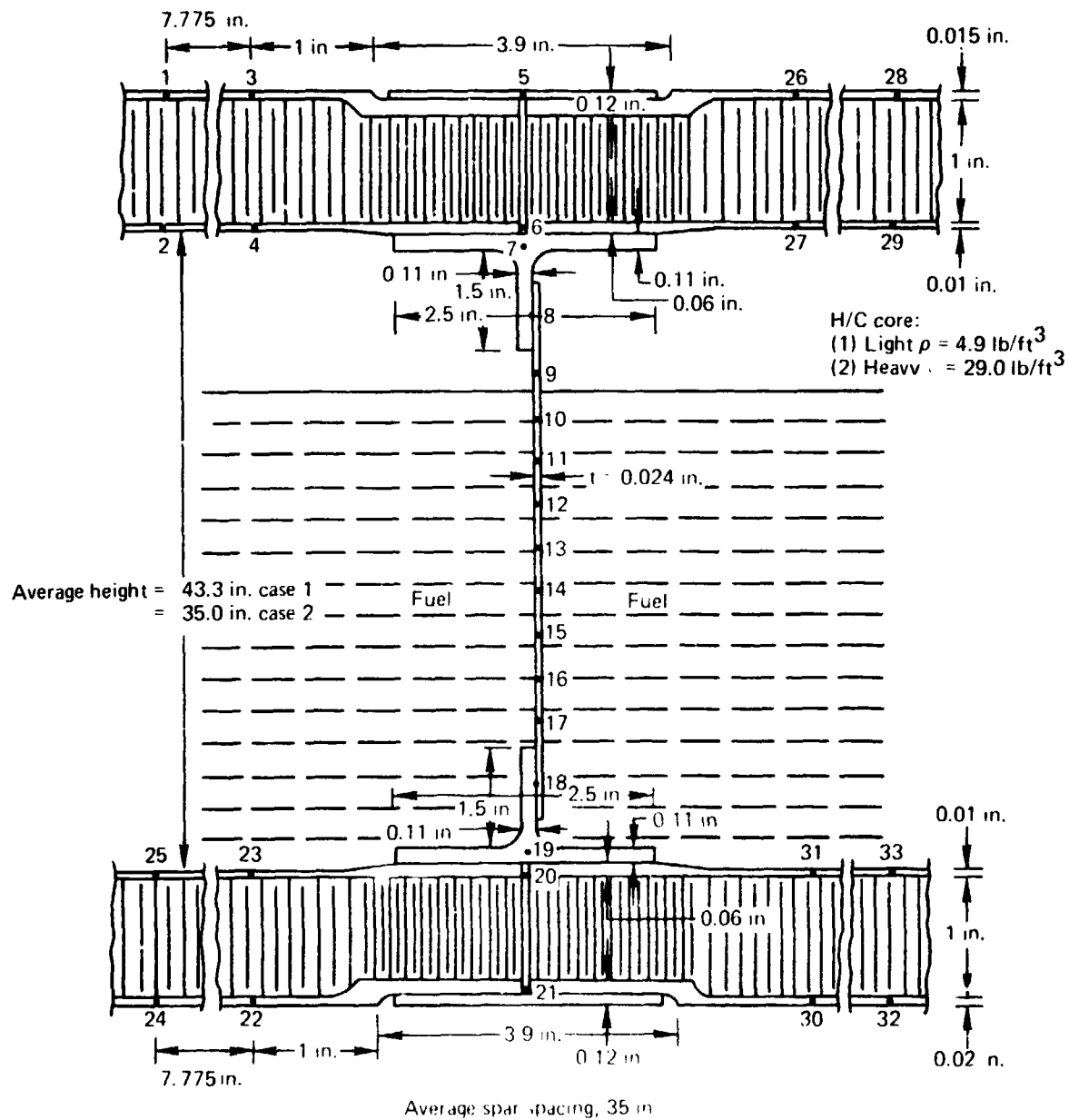


Figure 9-7.-Fuel Tank No. 1, Point 249

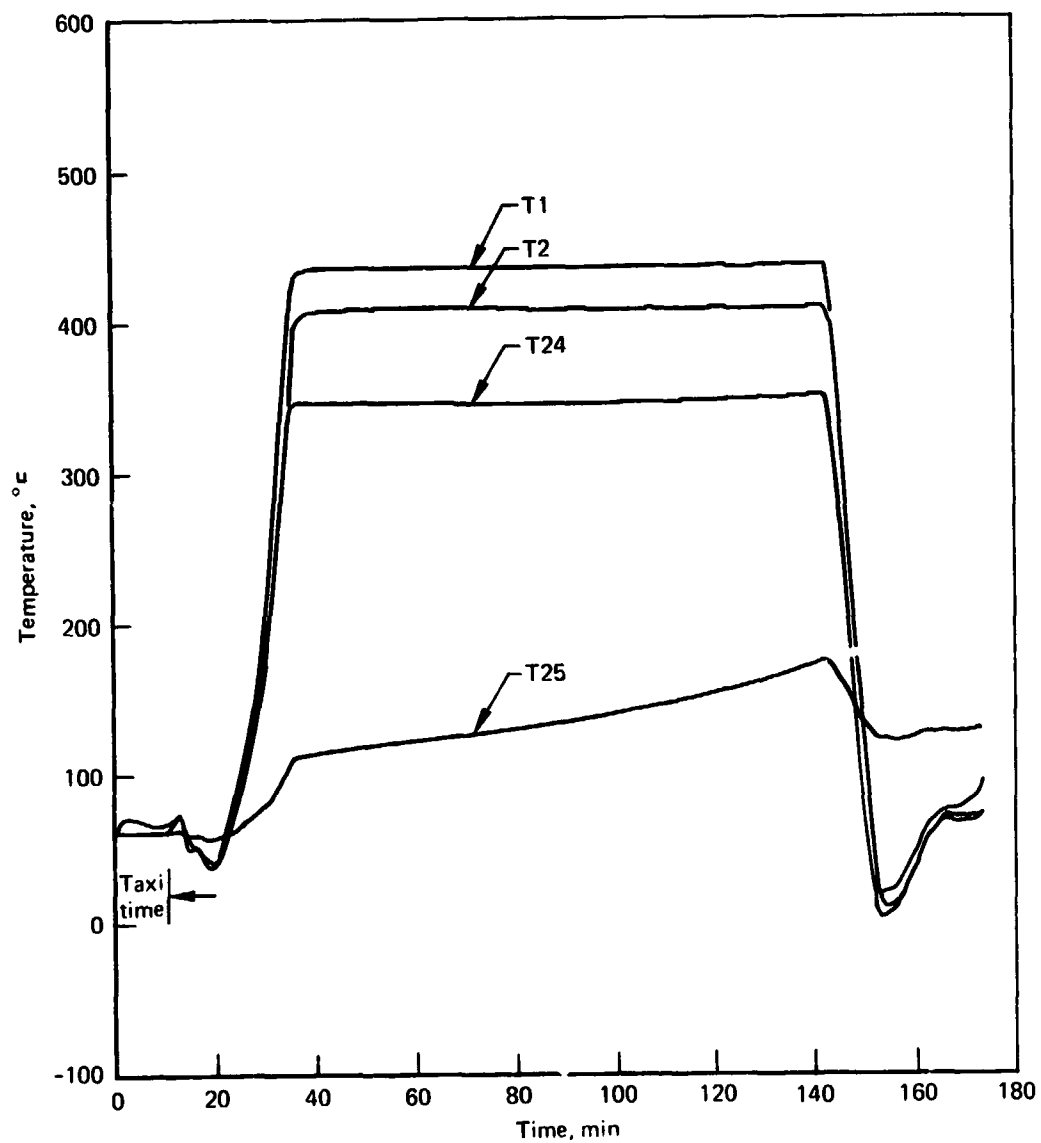


Figure 9-8.-Fuel Tank No. 1 Temperatures, Point 249, Case 1, T1, T2, T24, T25

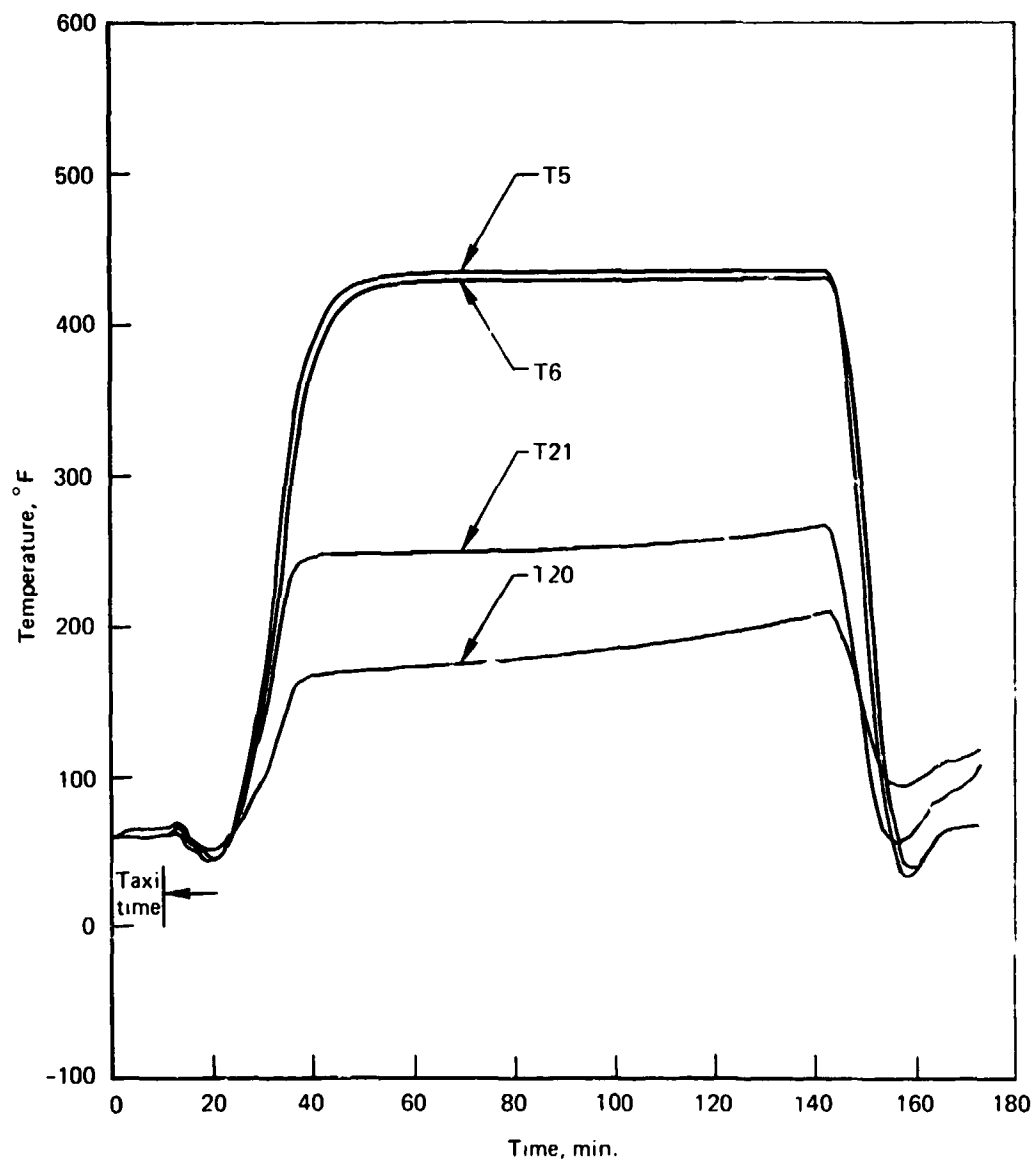


Figure 9-9.-Fuel Tank No. 1 Temperatures, Point 249, Case 1, T5, T6, T20, T21

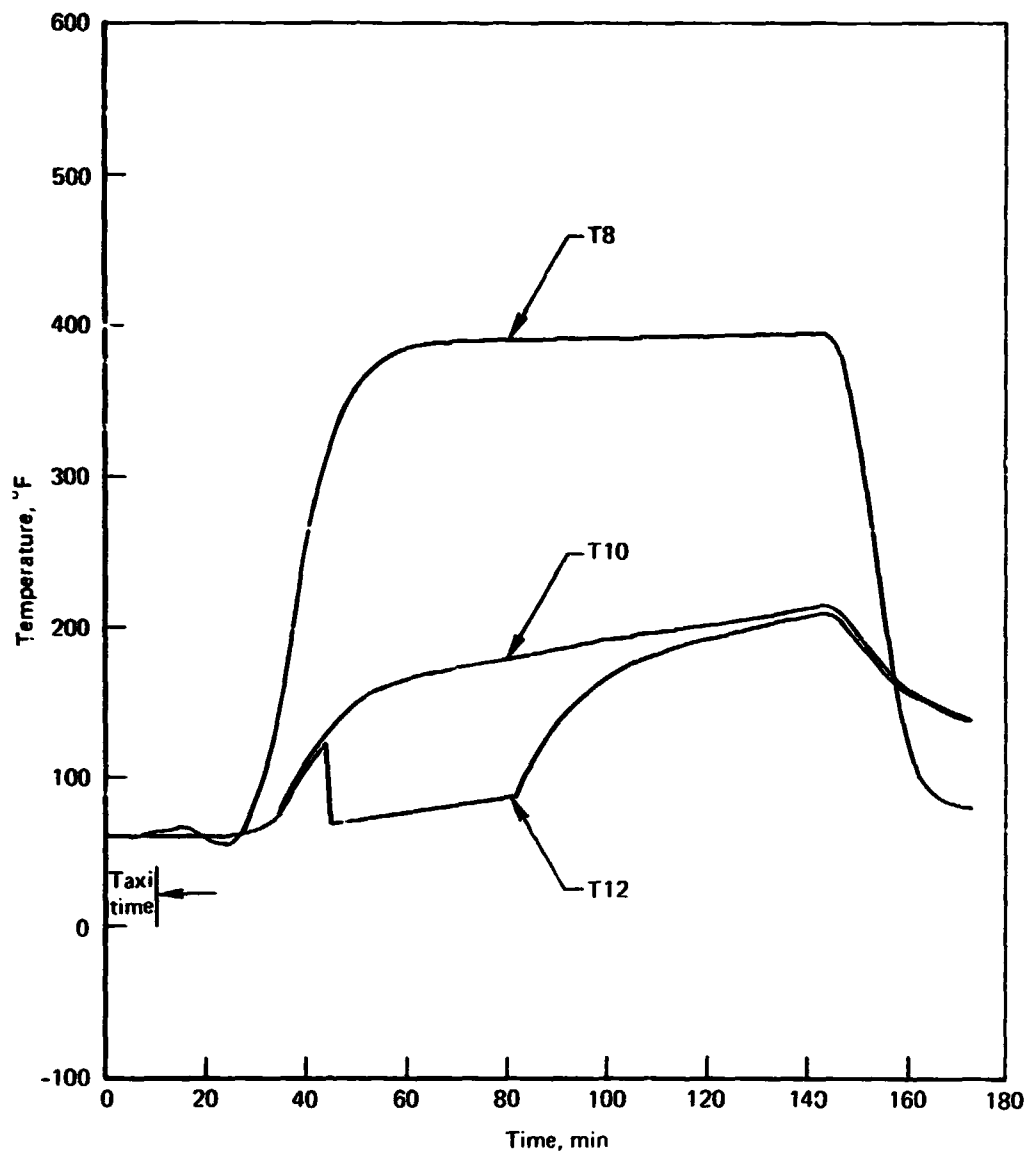


Figure 9-10.-Fuel Tank No. 1 Temperatures, Point 249, Case 1, T8, T10, T12

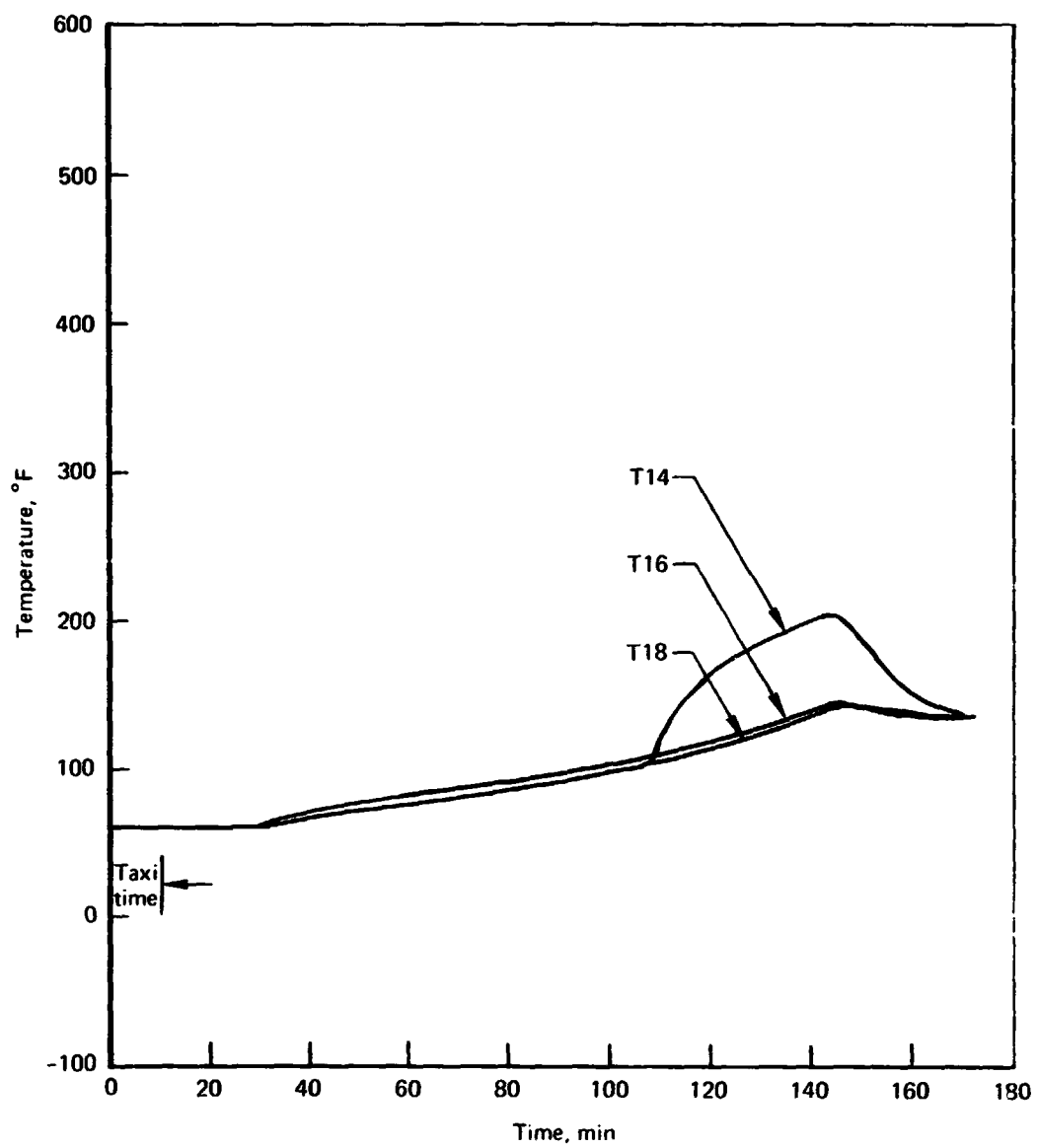


Figure 9-11.-Fuel Tank No. 1 Temperatures, Point 249, Case 1, T14, T16, T18

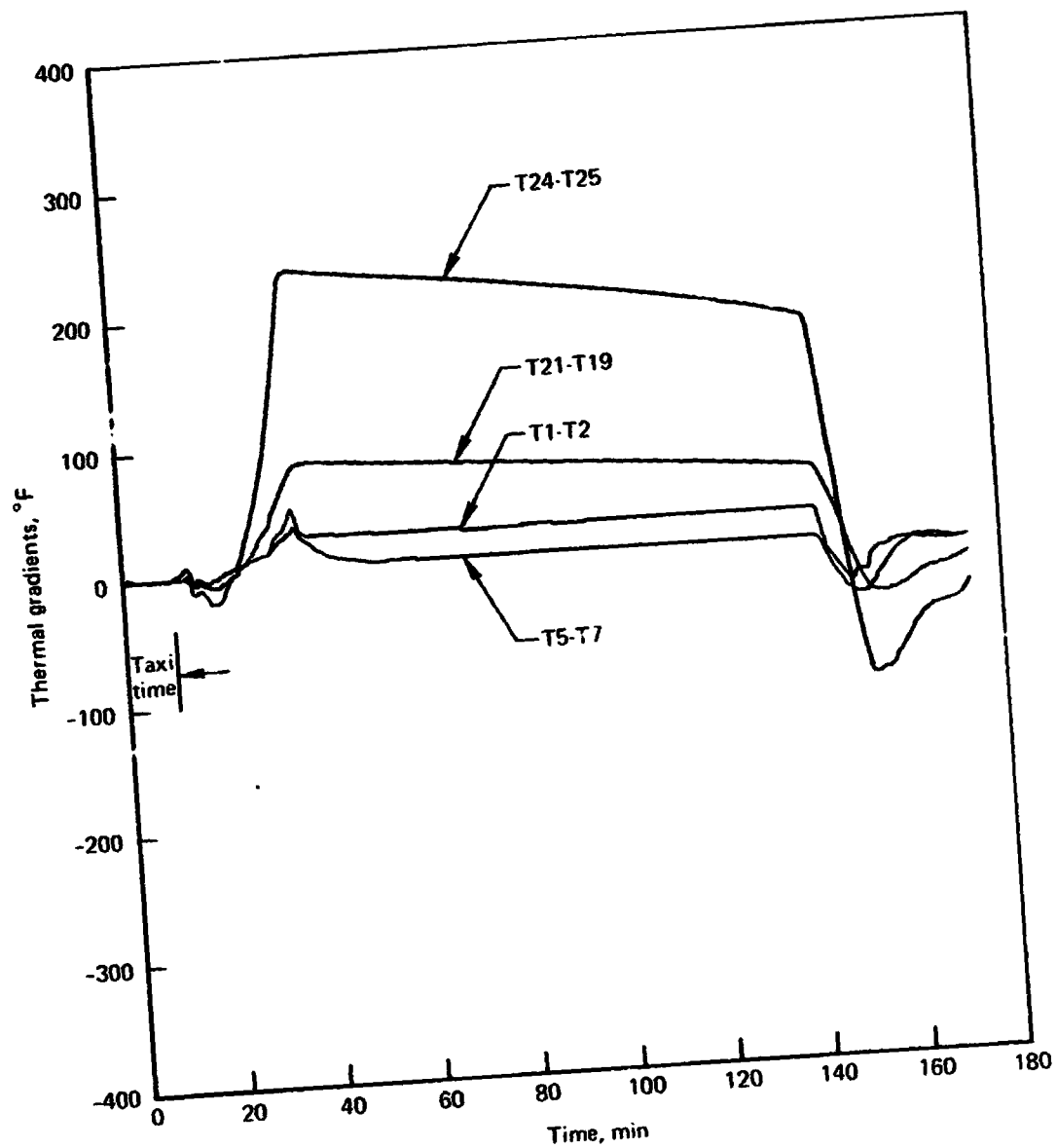


Figure 9-12.-Fuel Tank No. 1 Thermal Gradients, Point 249, Case 1, T1-T2, T5-T7, T21-T19, T24-T25

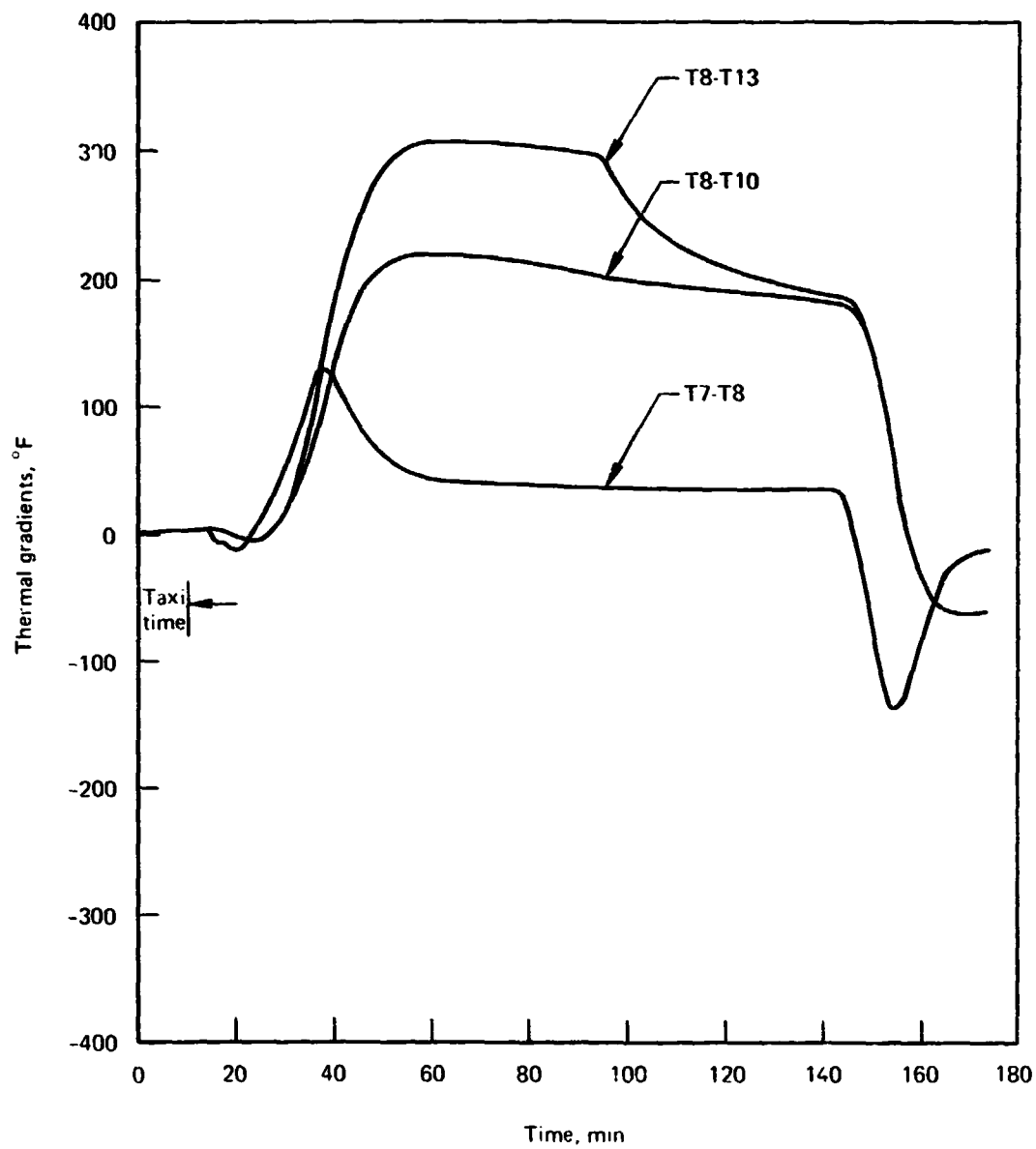


Figure 9-13.-Fuel Tank No. 1 Thermal Gradients. Point 249, Case 1, T7-T8, T8-T10, T8-T13

REPRODUCIBILITY OF THE
ORIGINAL PAGE IS POOR

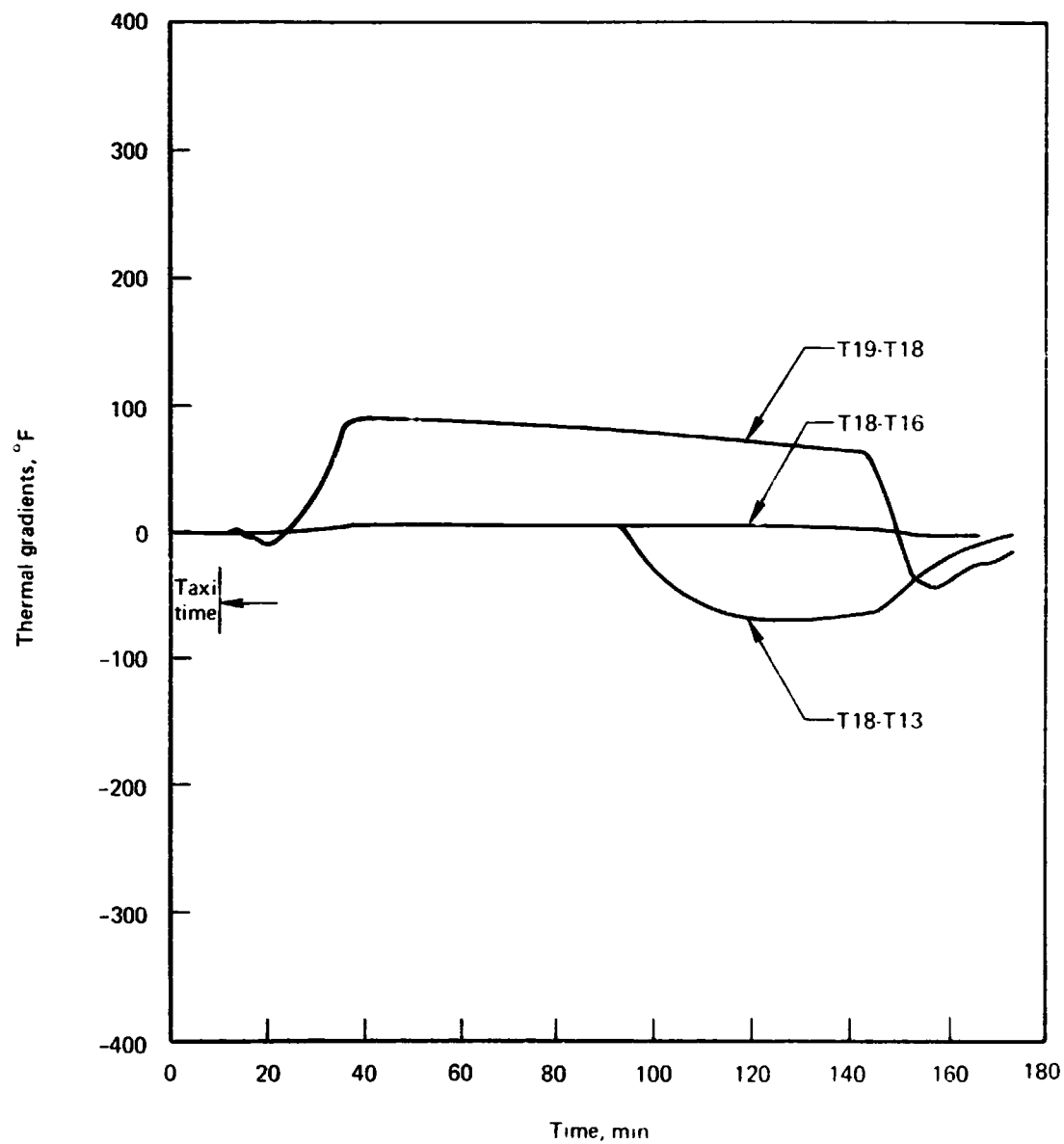


Figure 9-14.-Fuel Tank No. 1 Thermal Gradients, Point 249, Case 1, T18-T13, T18-T16, T19-T18

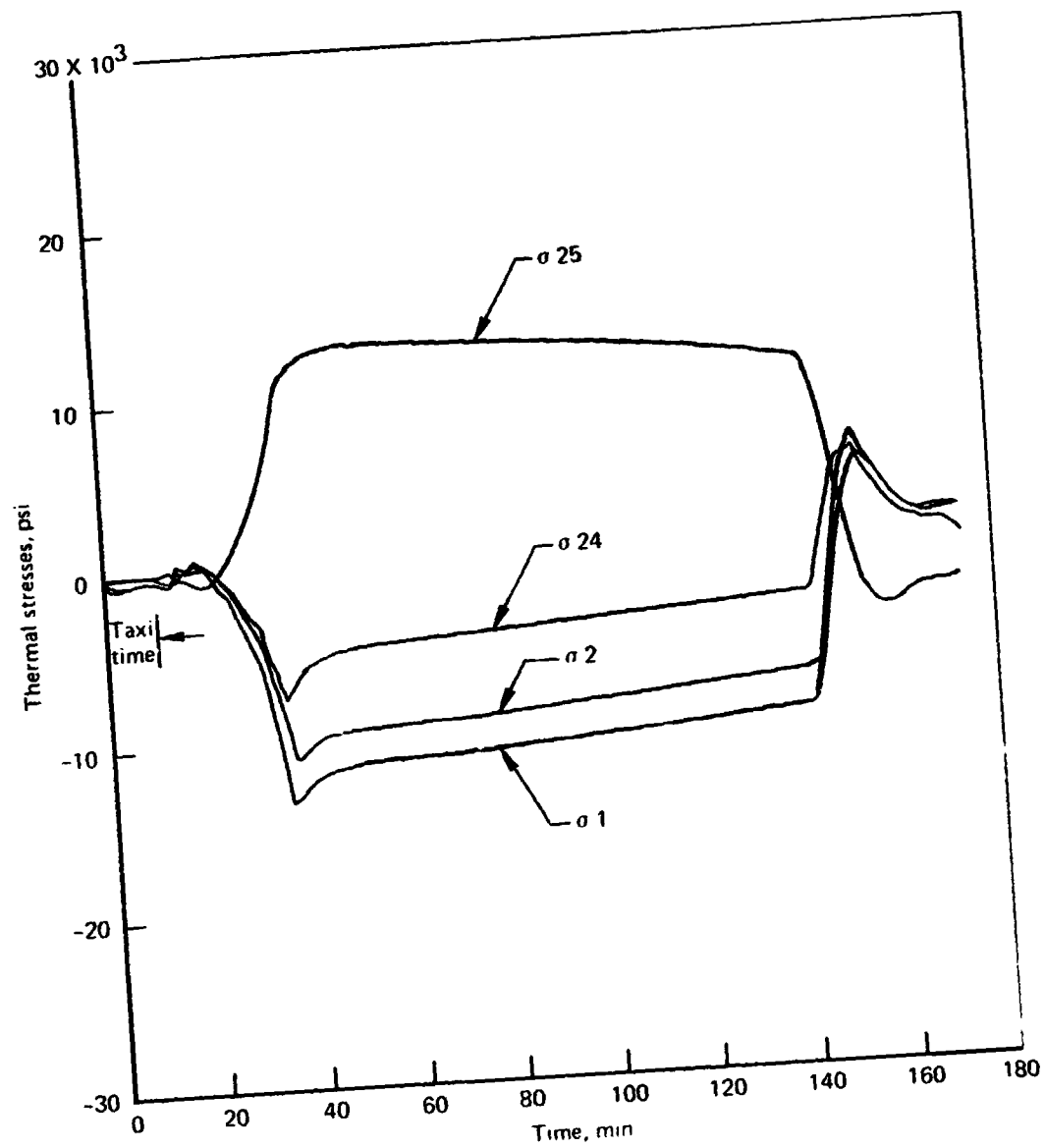


Figure 9-15.-Fuel Tank No. 1 Thermal Stresses, Point 249, Case 1, σ_1 , σ_2 , σ_{24} , σ_{25}

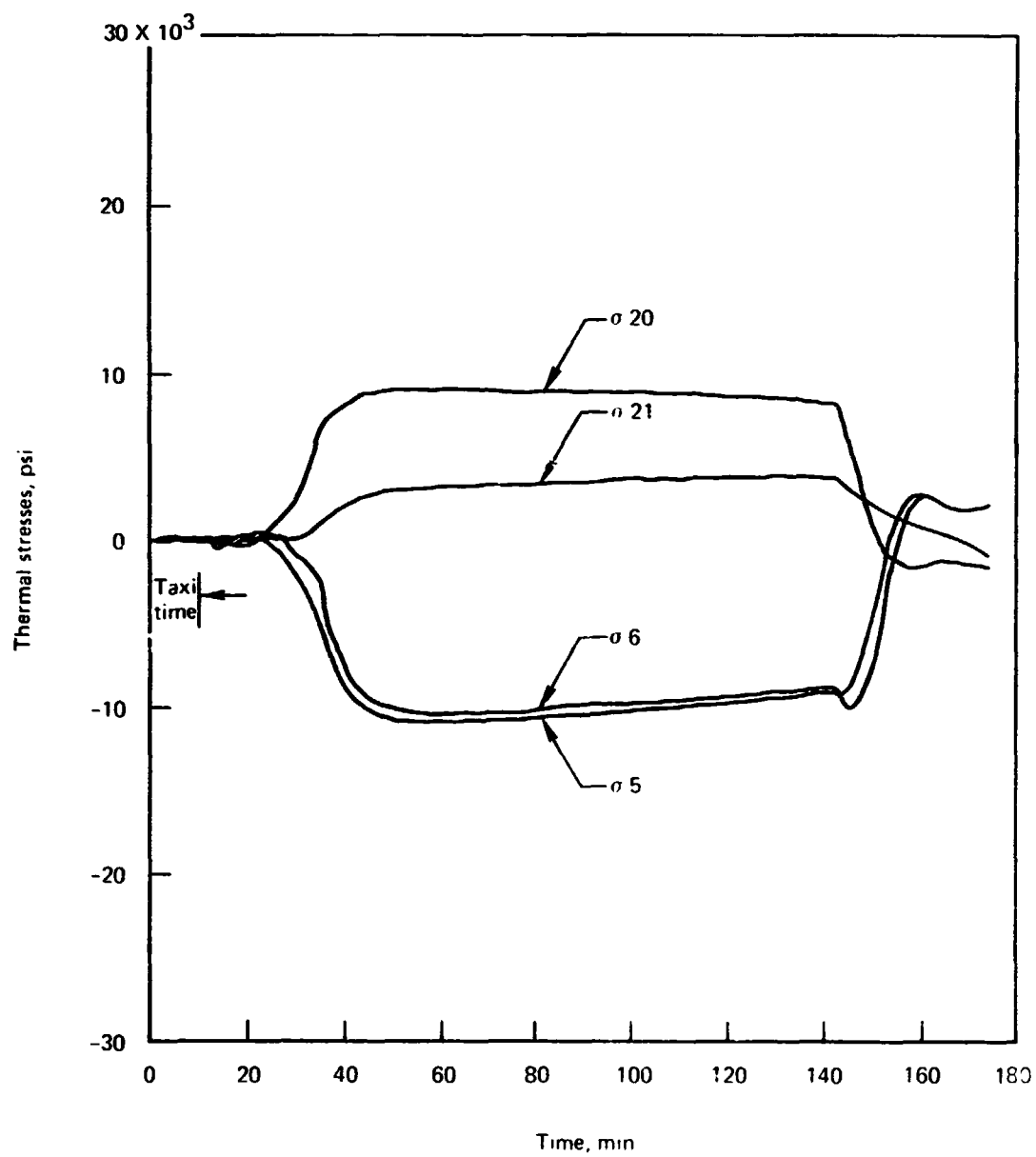


Figure 9-16.-Fuel Tank No. 1 Thermal Stresses. Point 249, Case 1, σ_5 , σ_6 , σ_{20} , σ_{21}

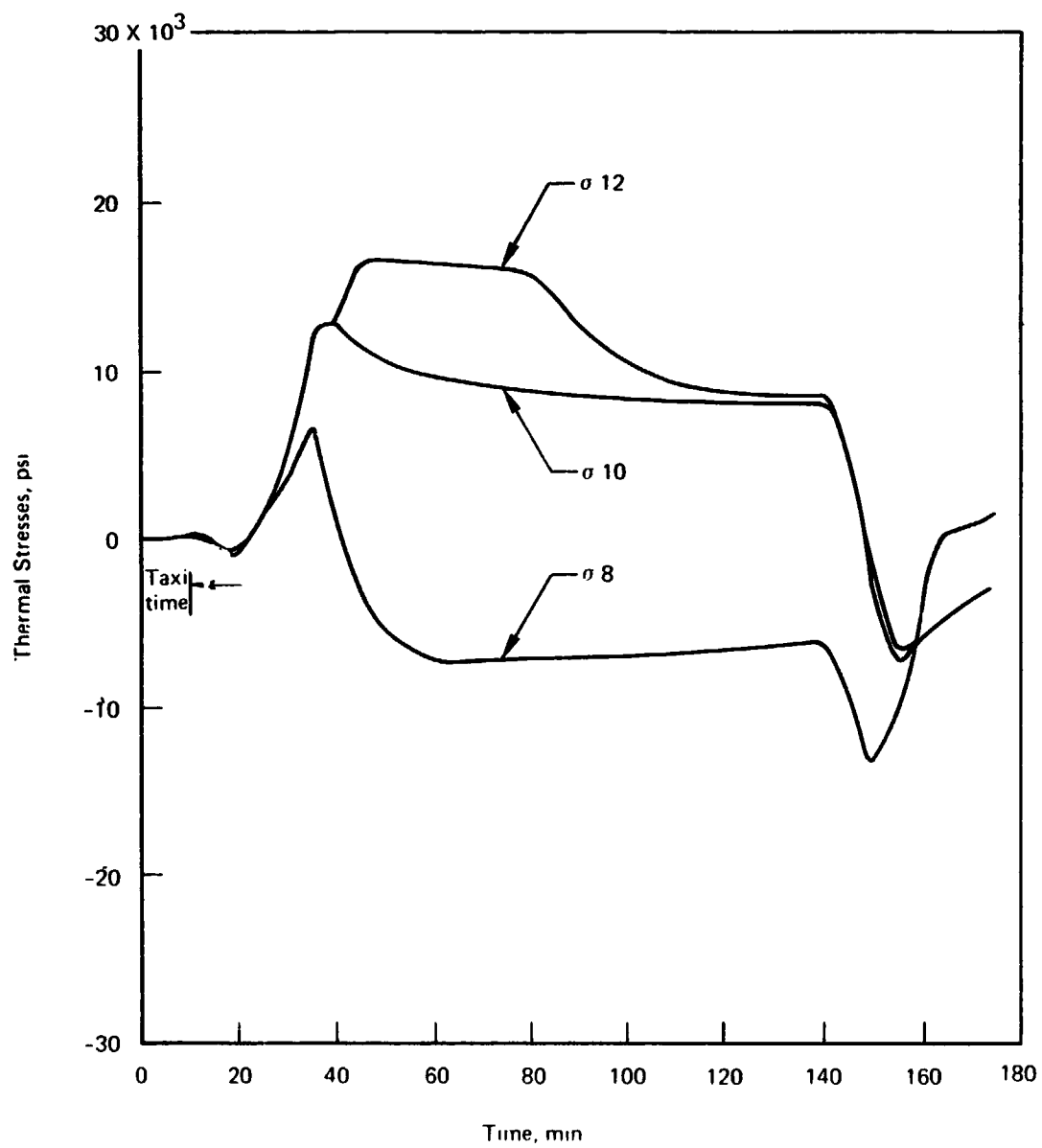


Figure 9-17.-Fuel Tank No. 1 Thermal Stresses, Point 249, Case 1, $\sigma 8$, $\sigma 10$, $\sigma 12$

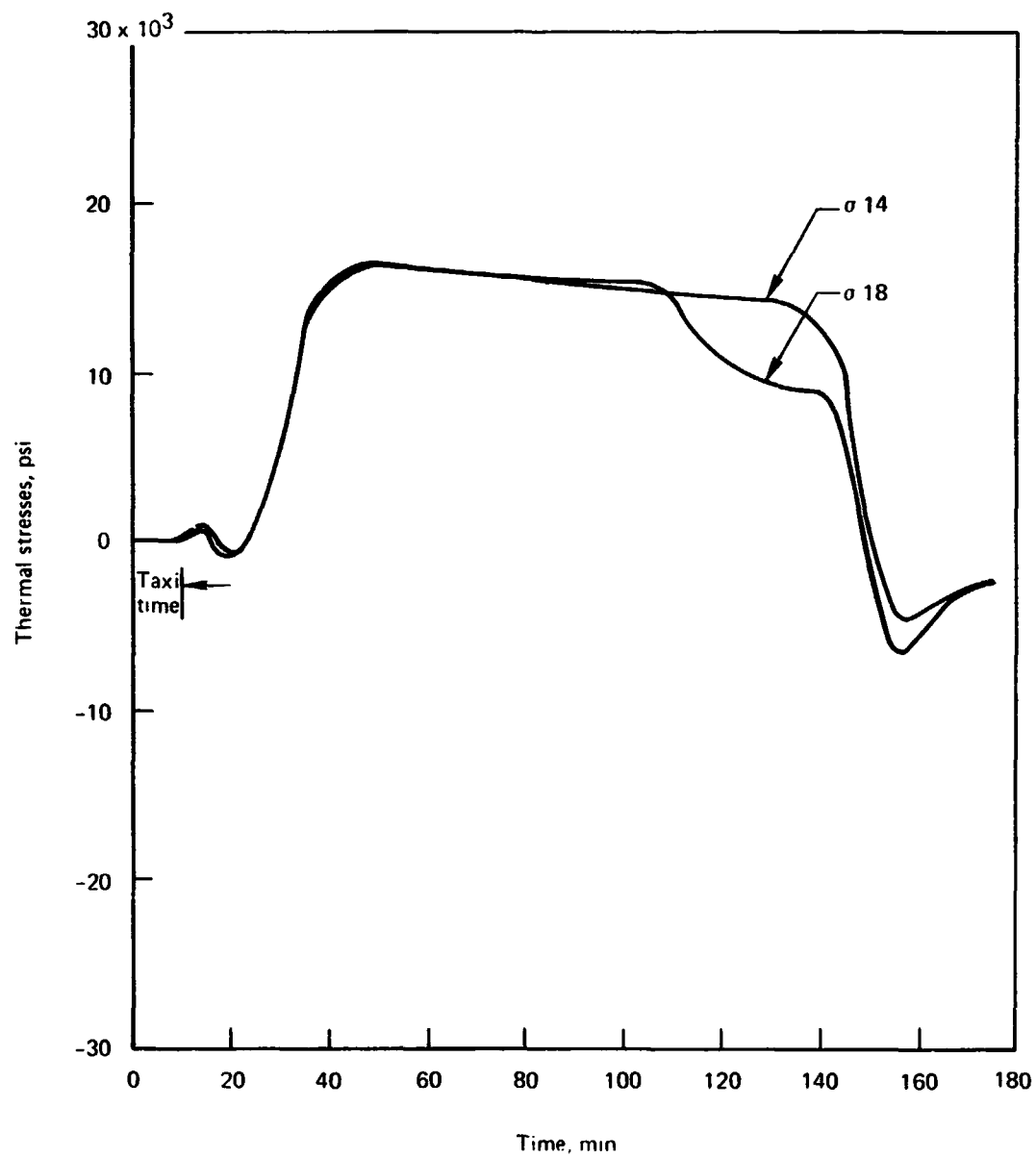


Figure 9-18.—Fuel Tank No. 1 Thermal Stresses, Point 249, Case 1, $\sigma 14$ $\sigma 18$

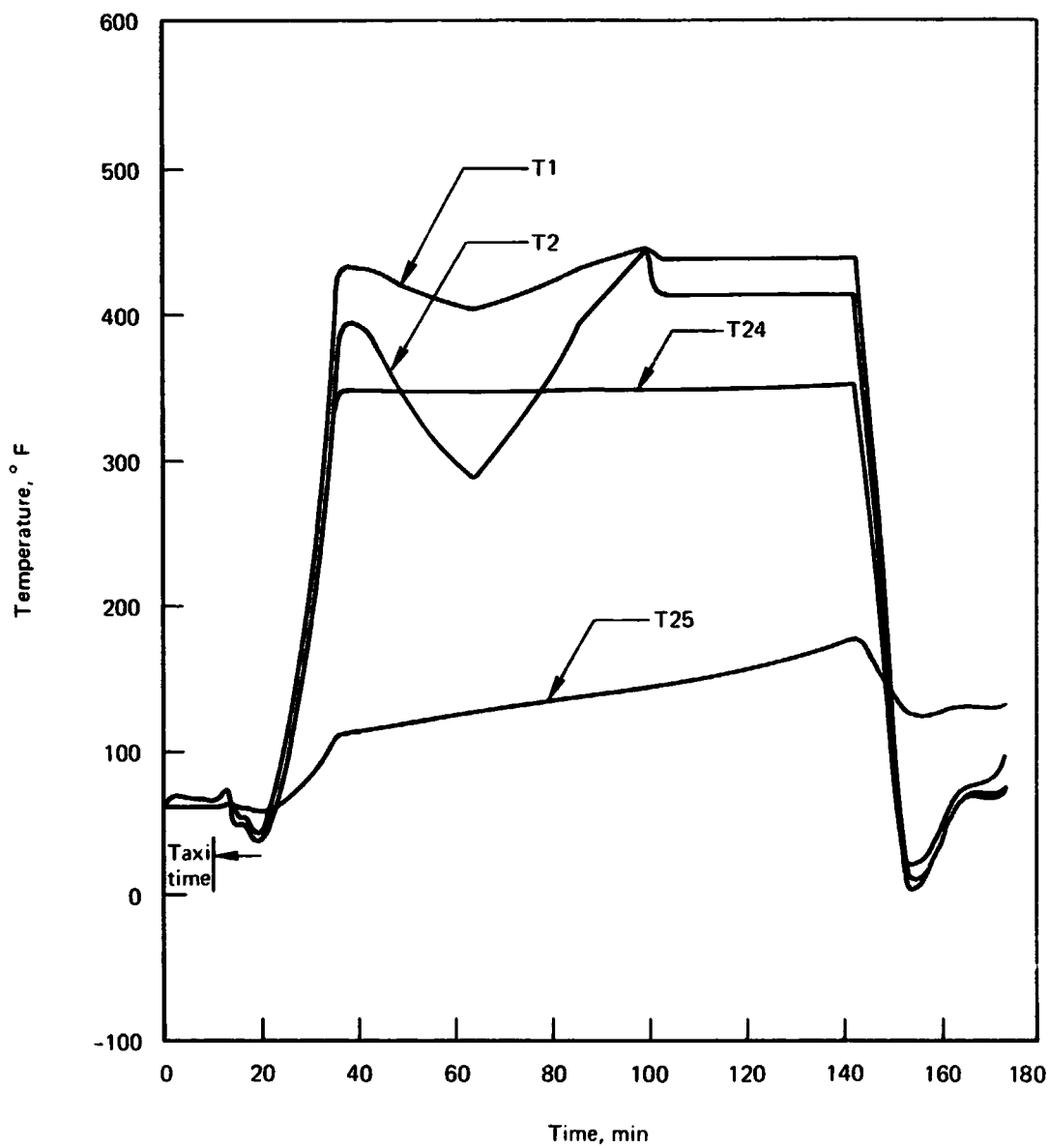


Figure 9-19.-Fuel Tank No. 1 Temperatures, Point 249, Case 2, T1, T2, T24, T25

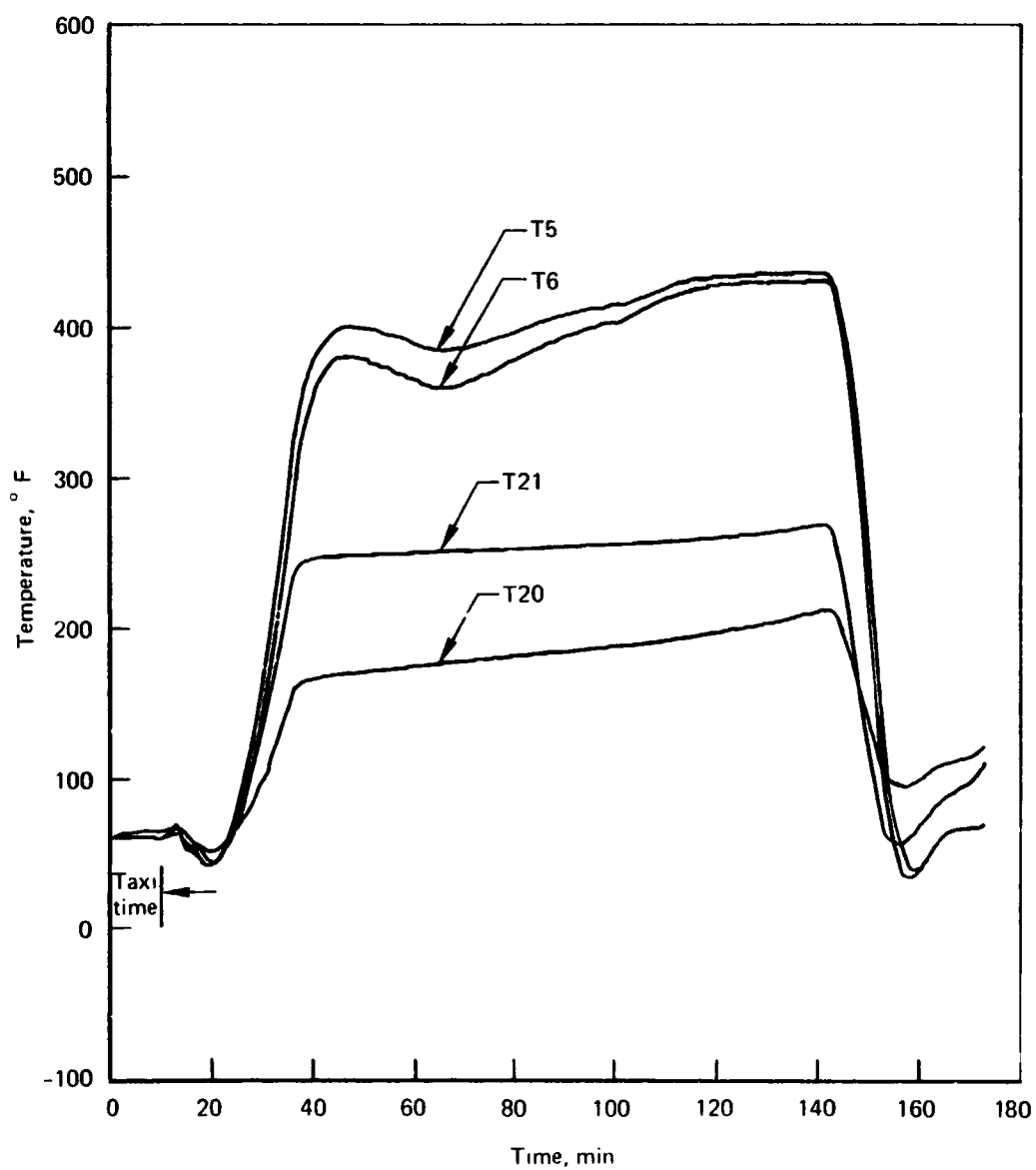


Figure 9-20.-Fuel Tank No. 1 Temperatures, Point 249, Case 2, T5, T6, T20, T21

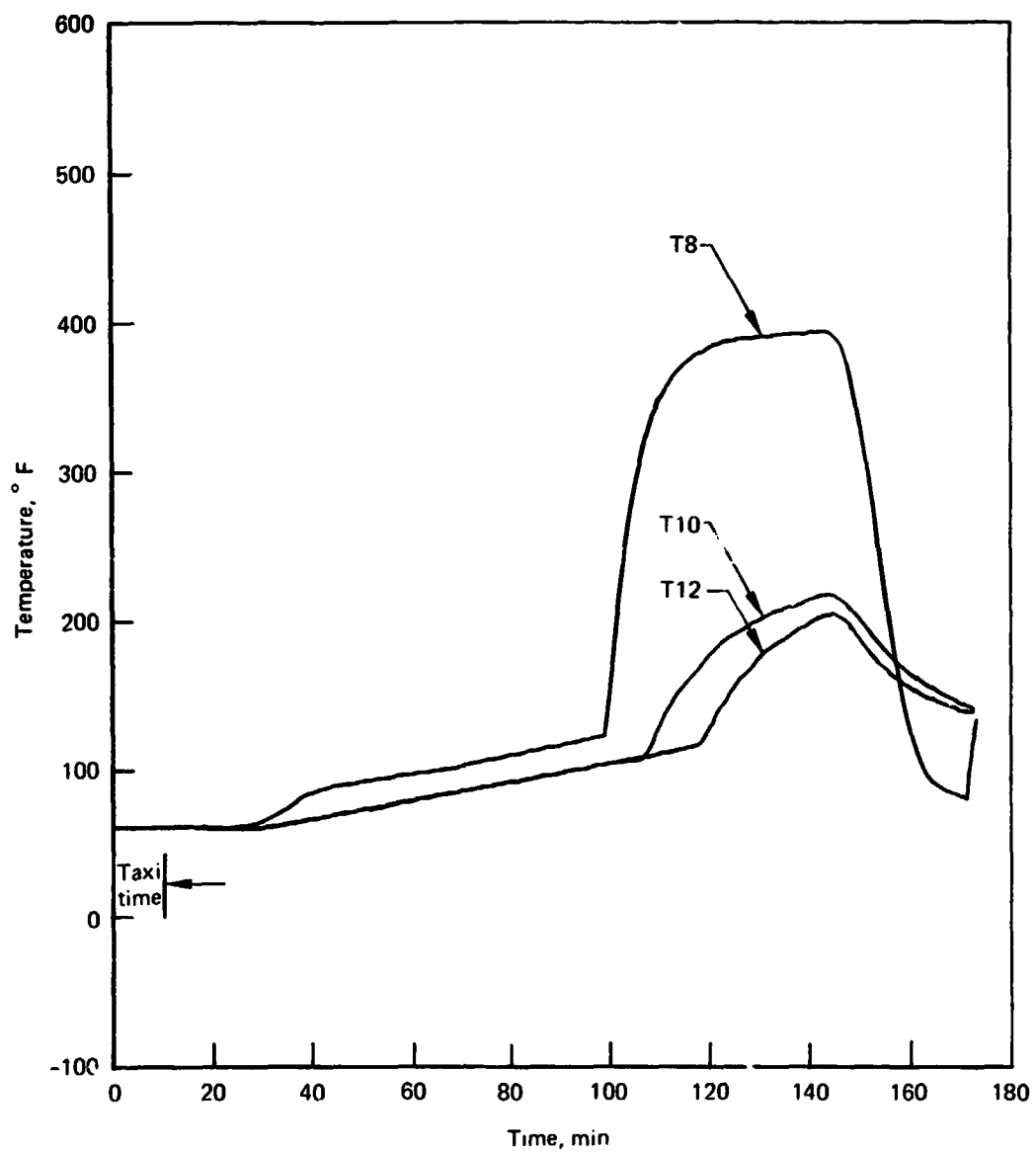


Figure 9-21.-Fuel Tank No. 1 Temperatures, Point 249, Case 2, T8, T10, T12

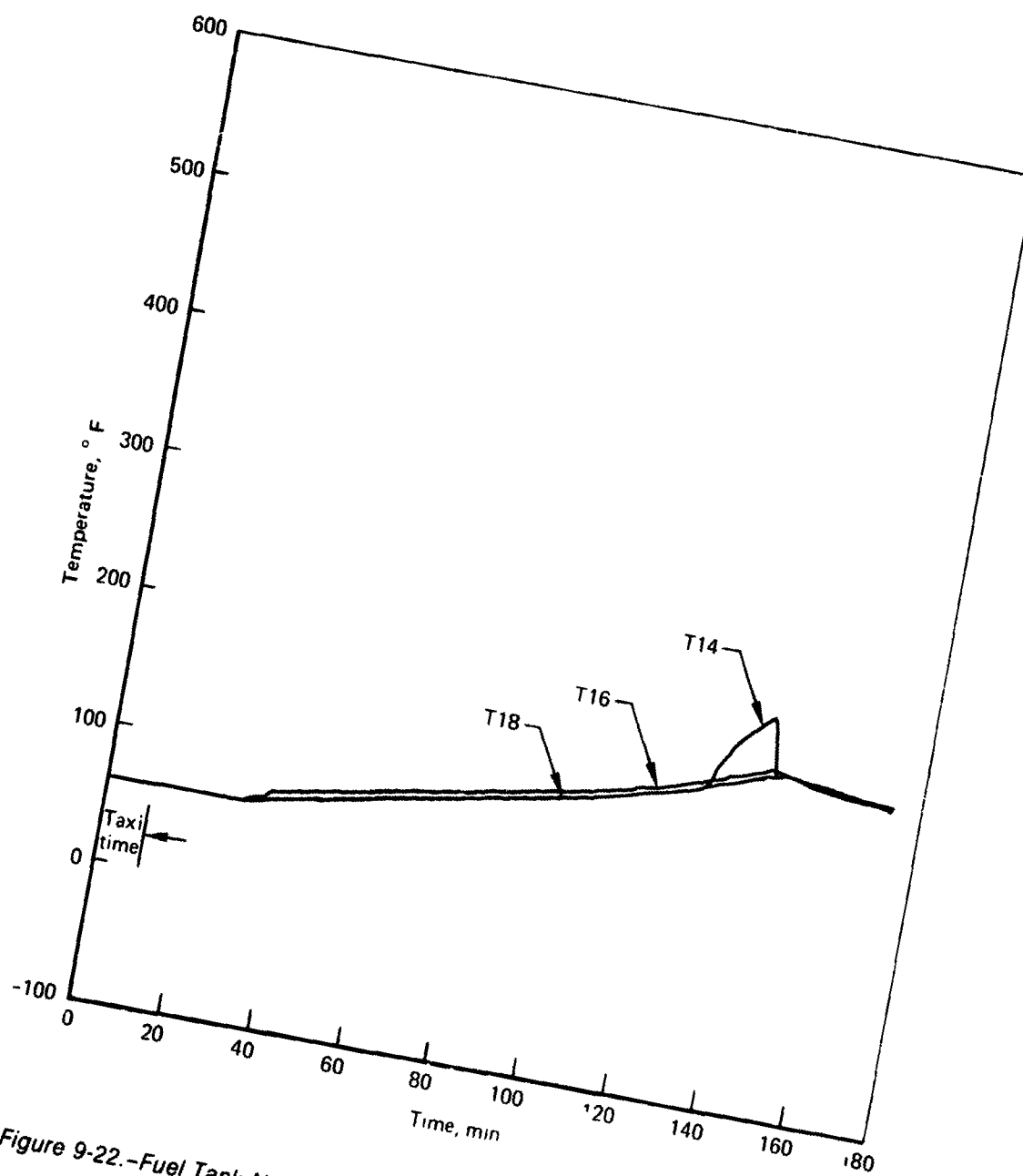


Figure 9-22.-Fuel Tank No. 1 Temperatures, Point 249, Case 2, T14, T16, T18

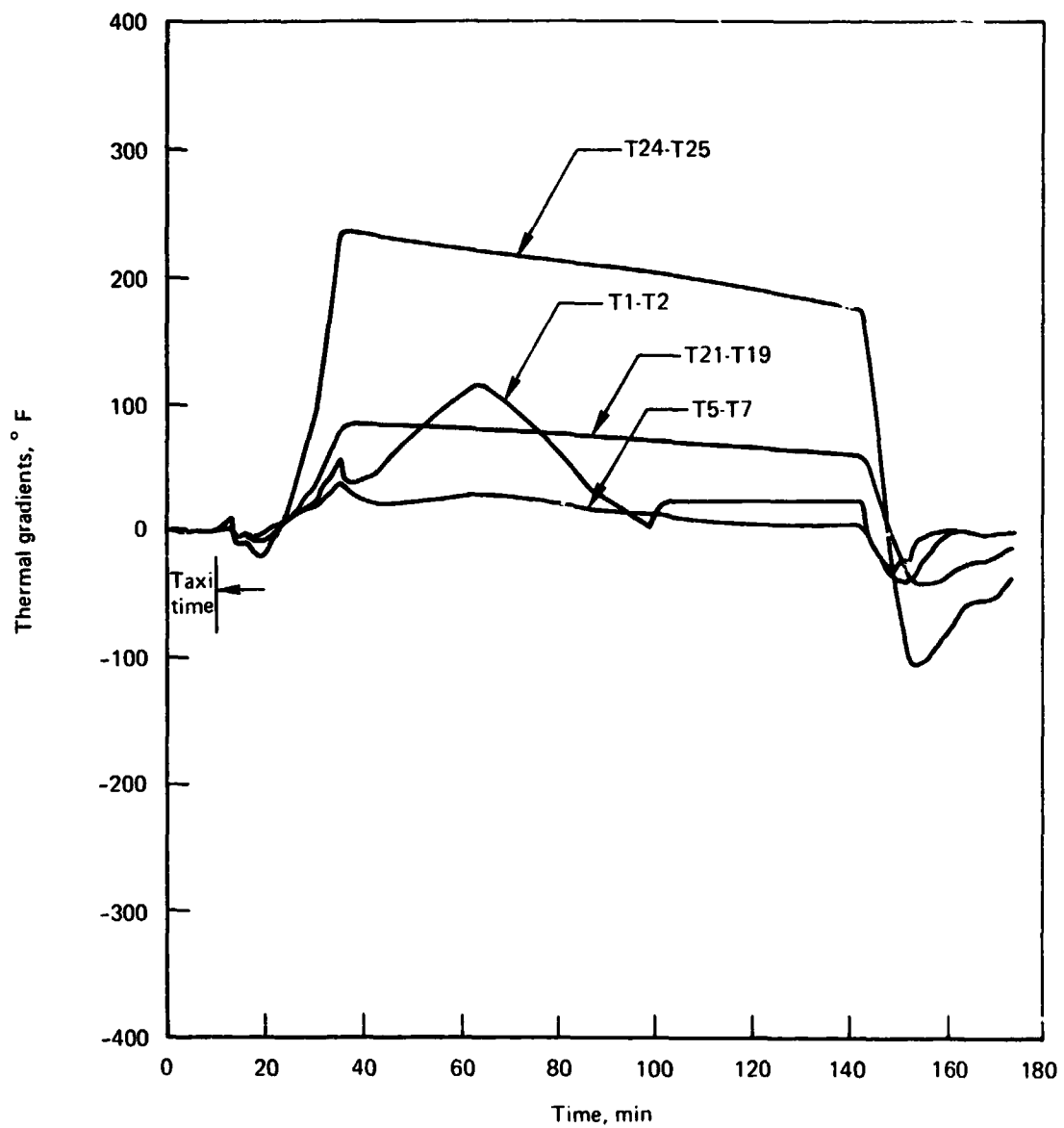


Figure 9-23.-Fuel Tank No. 1 Thermal Gradients, Point 249, Case 2,
T1-T2, T5-T7, T21-T19, T24-T25

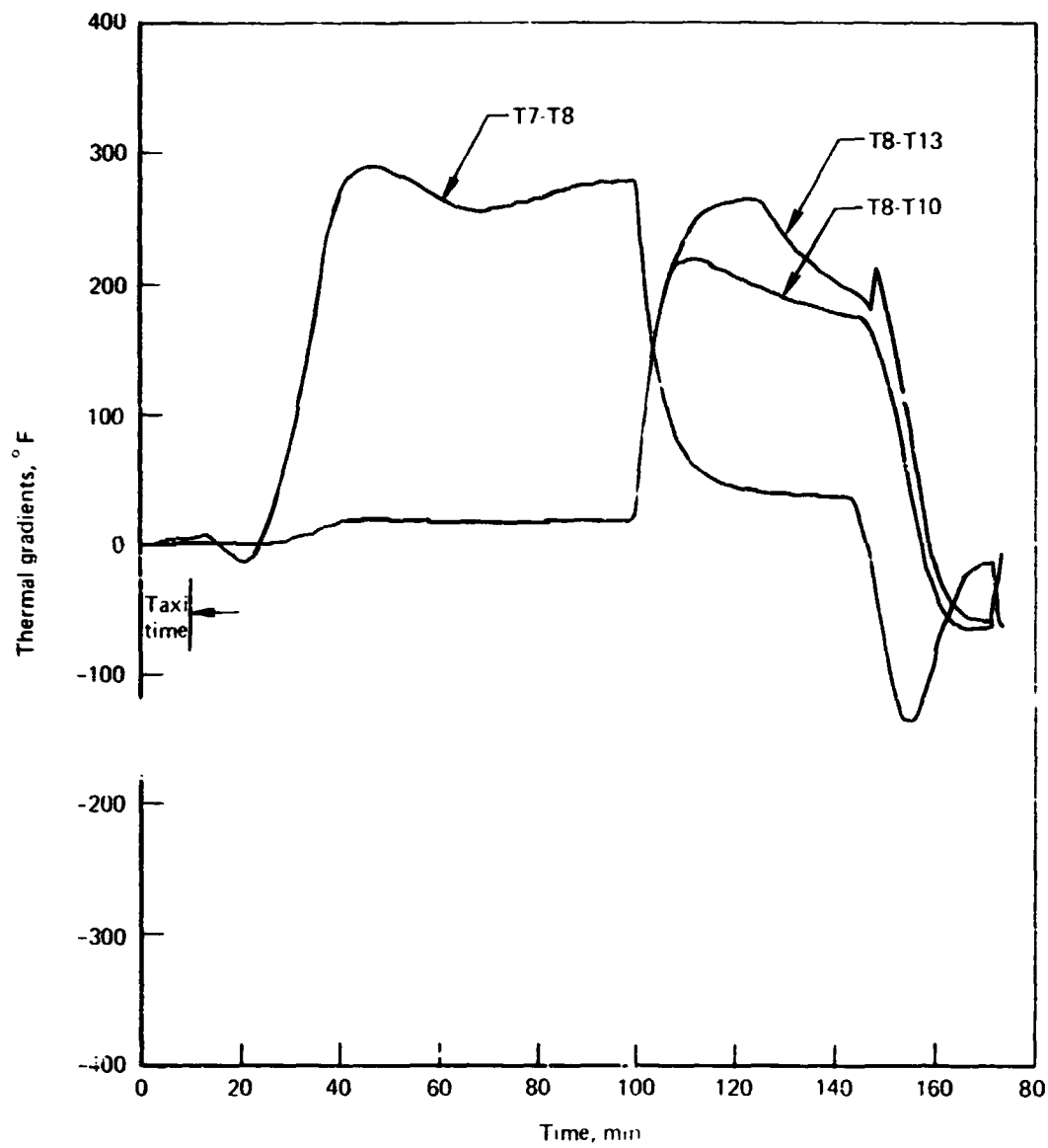


Figure 9-24.-Fuel Tank No. 1 Thermal Gradients, Point 249, Case 2, T7-T8, T8-T10, T8-T13

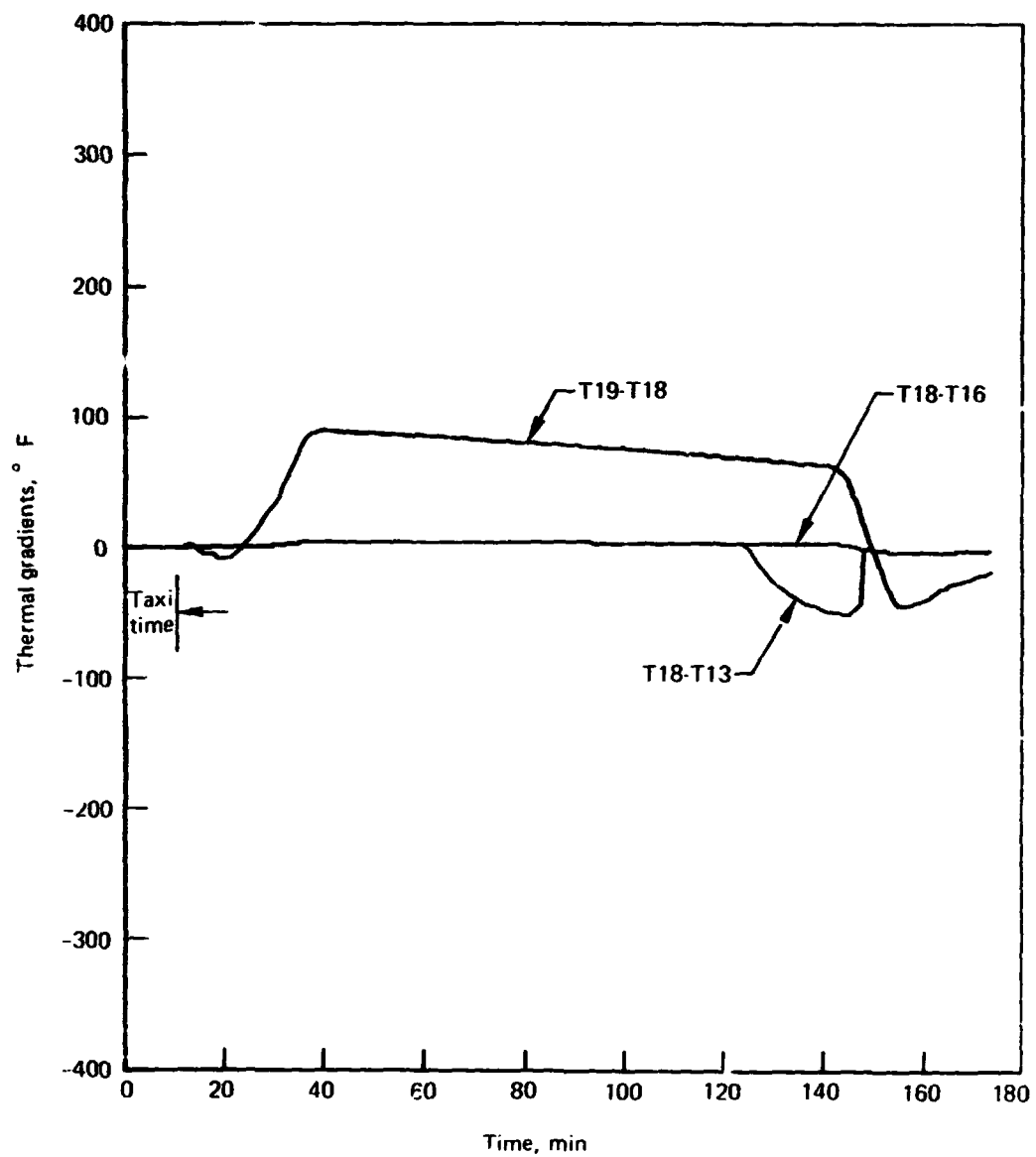


Figure 25.-Fuel Tank No. 1 Thermal Gradients, Point 249, Case 2, T18-T13, T18 T16, T19-T18

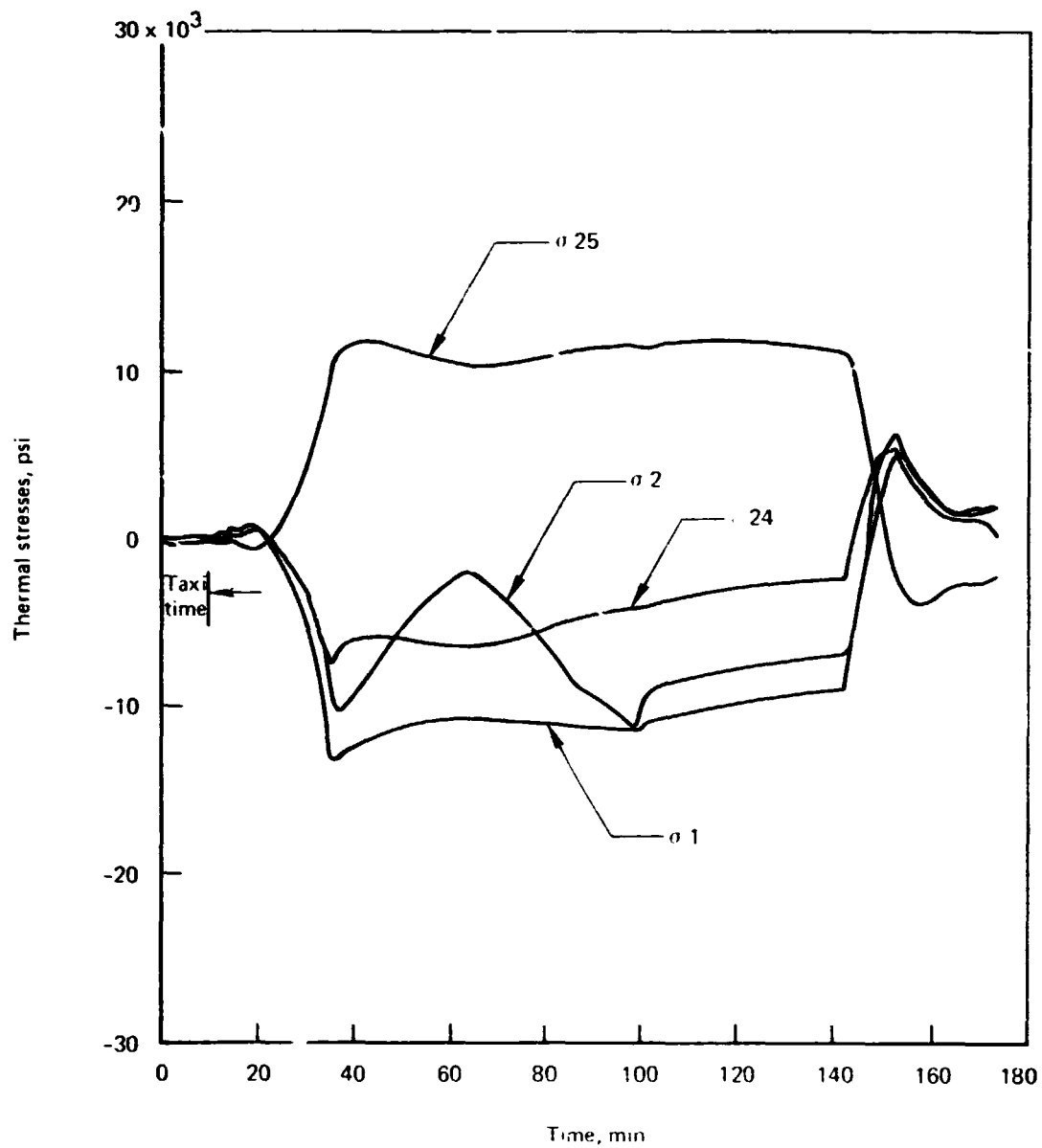


Figure 9-26.—Fuel Tank No. 1 Thermal Stresses, Point 249, Case 2, $\sigma 1$, $\sigma 2$, $\sigma 24$, $\sigma 25$

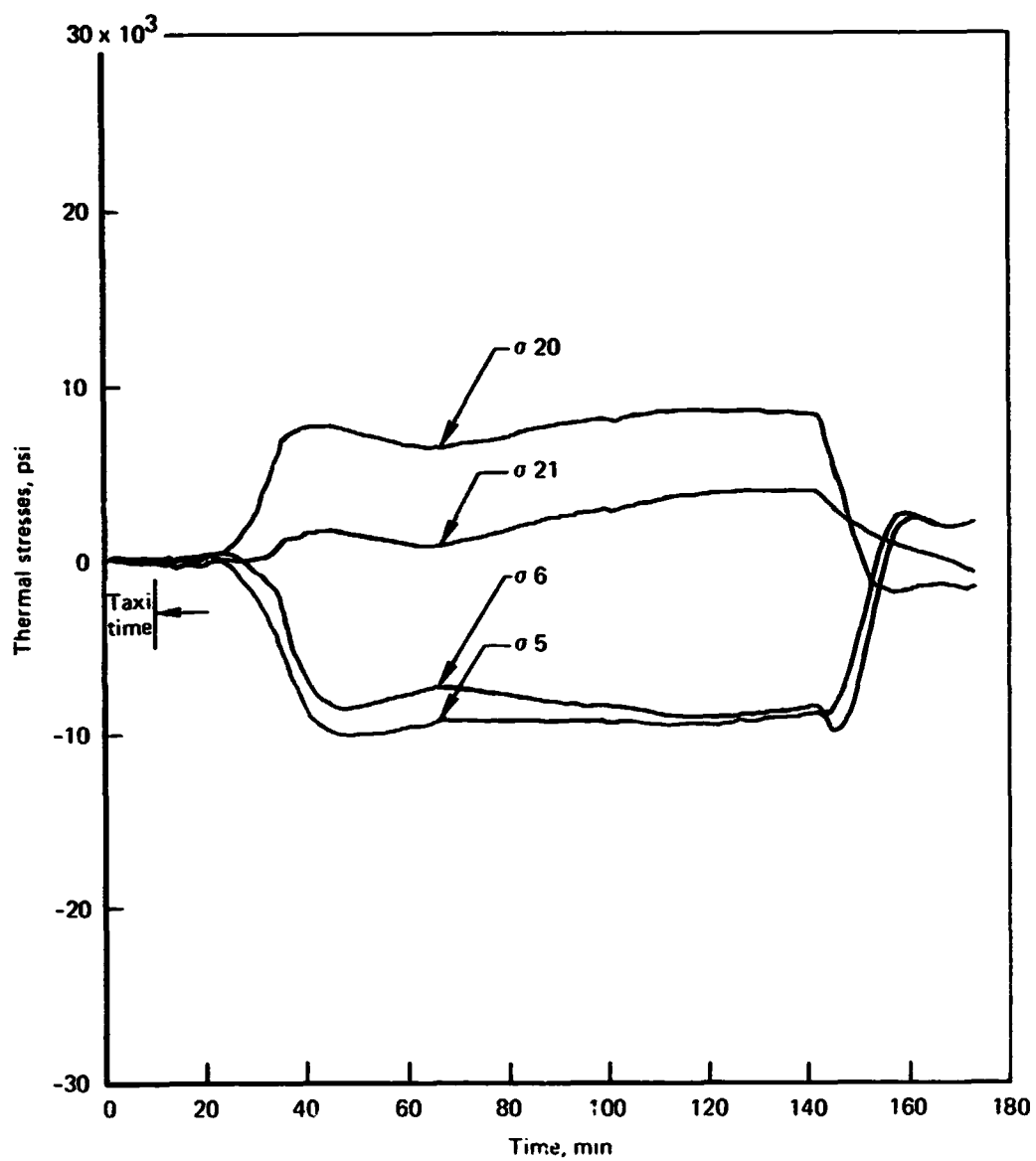


Figure 9-27.-Fuel Tank No. 1 Thermal Stresses, Point 249, Case 2, σ5, σ6, σ20, σ21

PRODUCIBILITY OF THE
ORIGINAL PAGE IS POOR

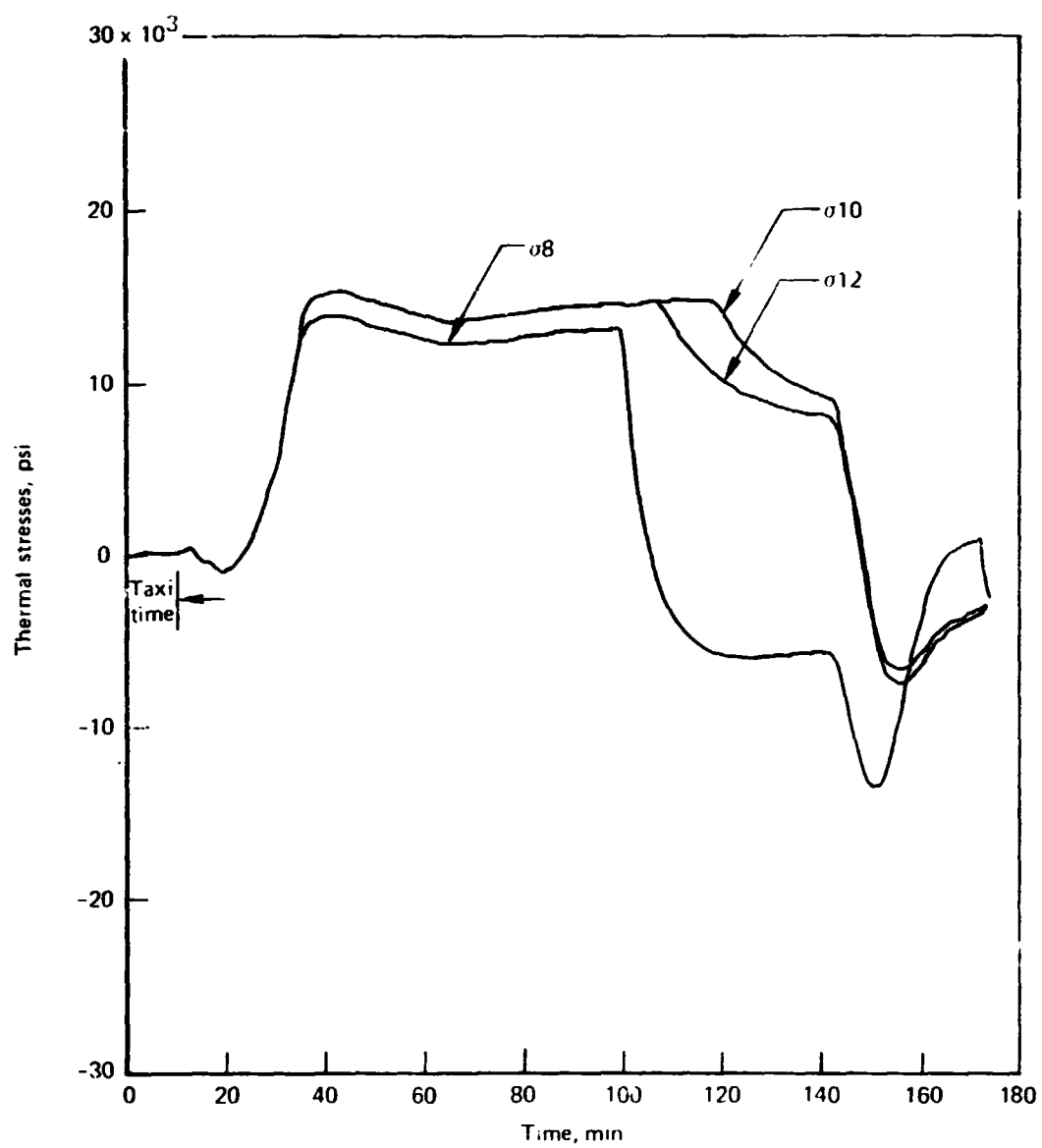


Figure 9-28.—Fuel Tank No. 1 Thermal Stresses, Point 249, Case 2, σ_8 , σ_{10} , σ_{12}

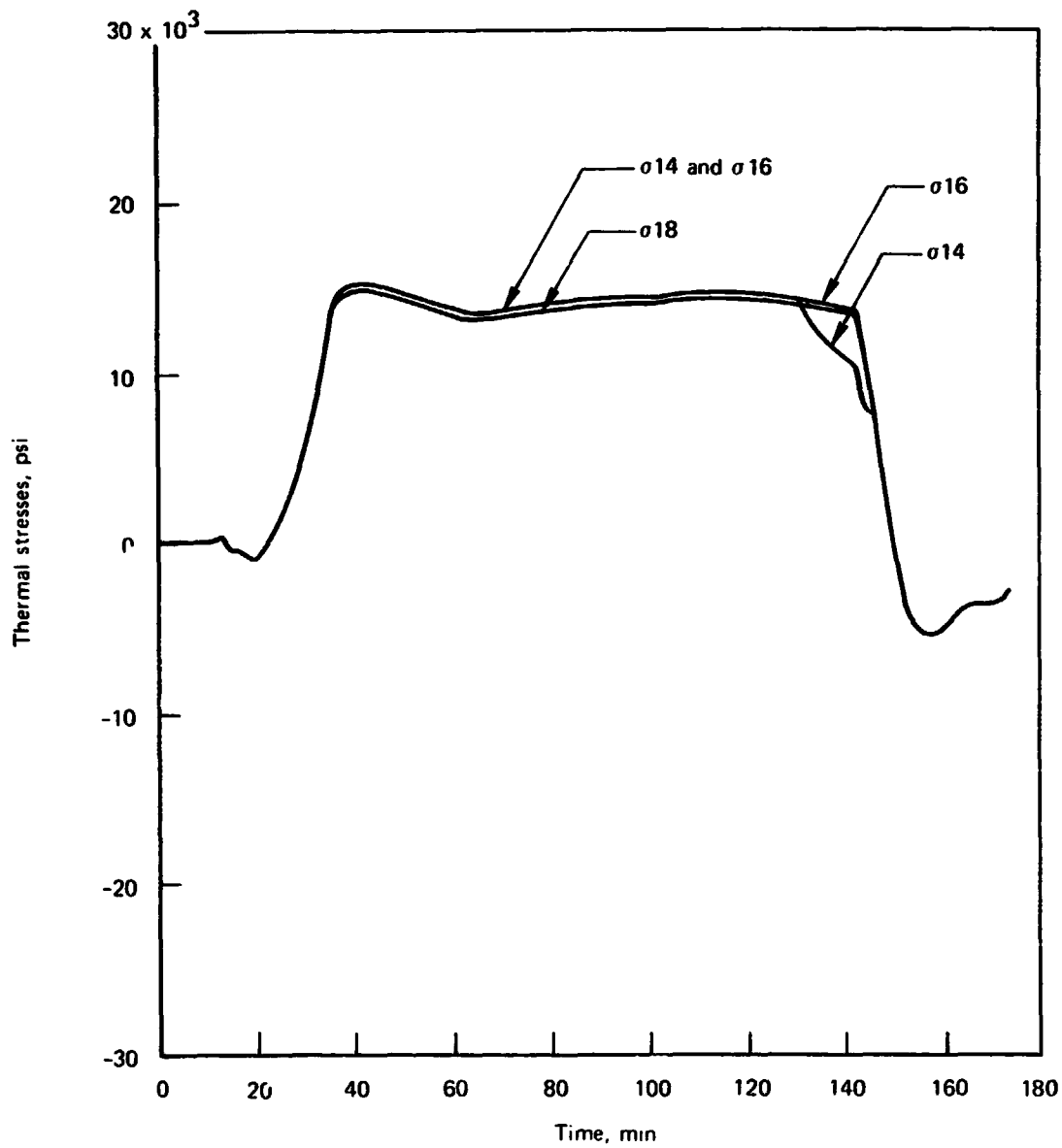


Figure 9-29.-Fuel Tank No. 1 Thermal Stresses, Point 249, Case 2, σ_{14} , σ_{16} , σ_{18}

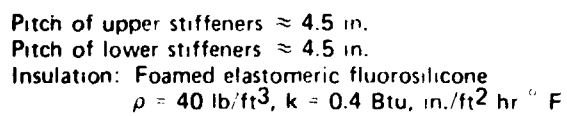


Figure 9-30.—Fuel Tank No. 2, Point 269

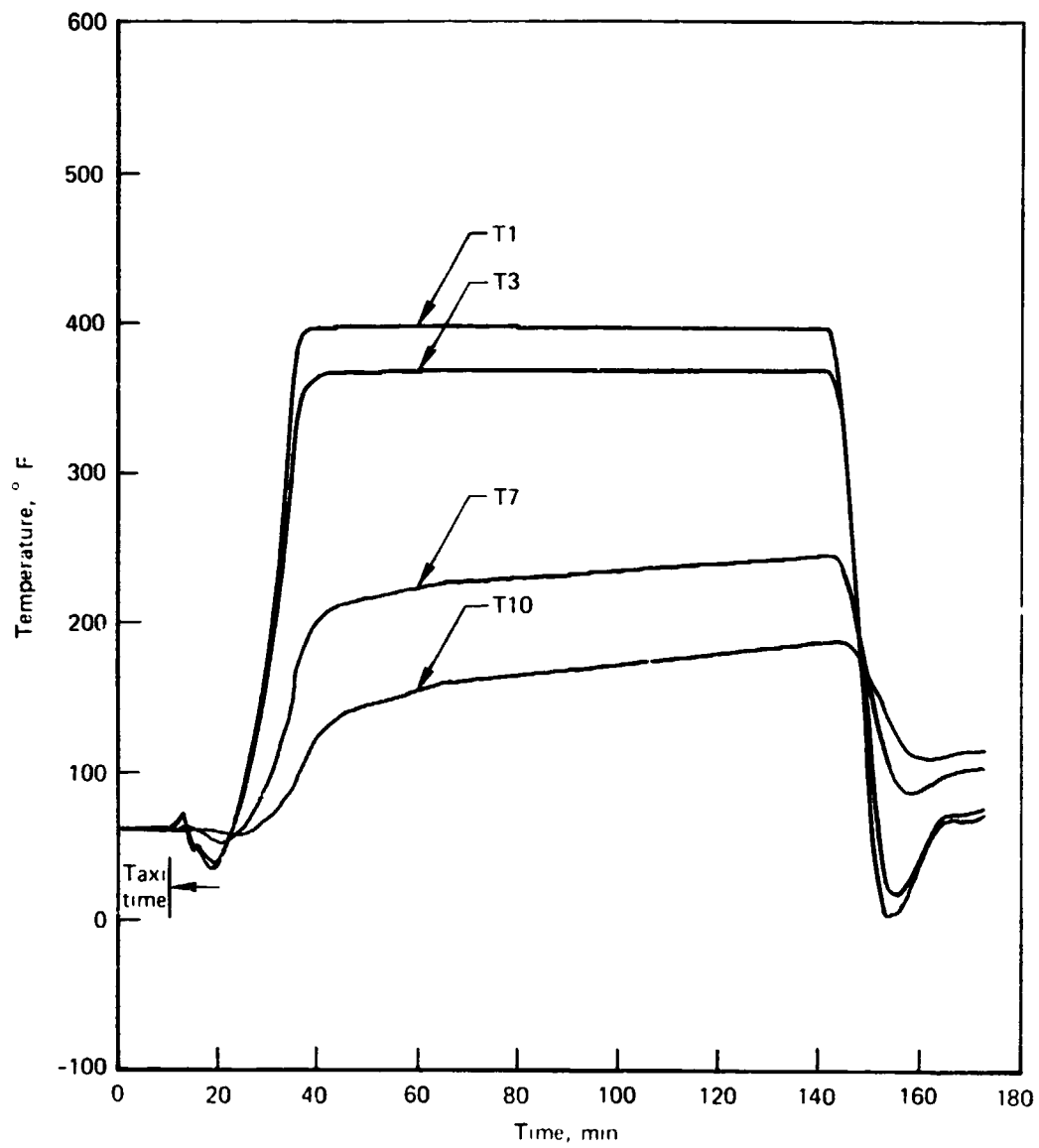


Figure 9-31.-Fuel Tank No. 2 Temperatures, Point 269, Case 1, T1,T3, T7, T10

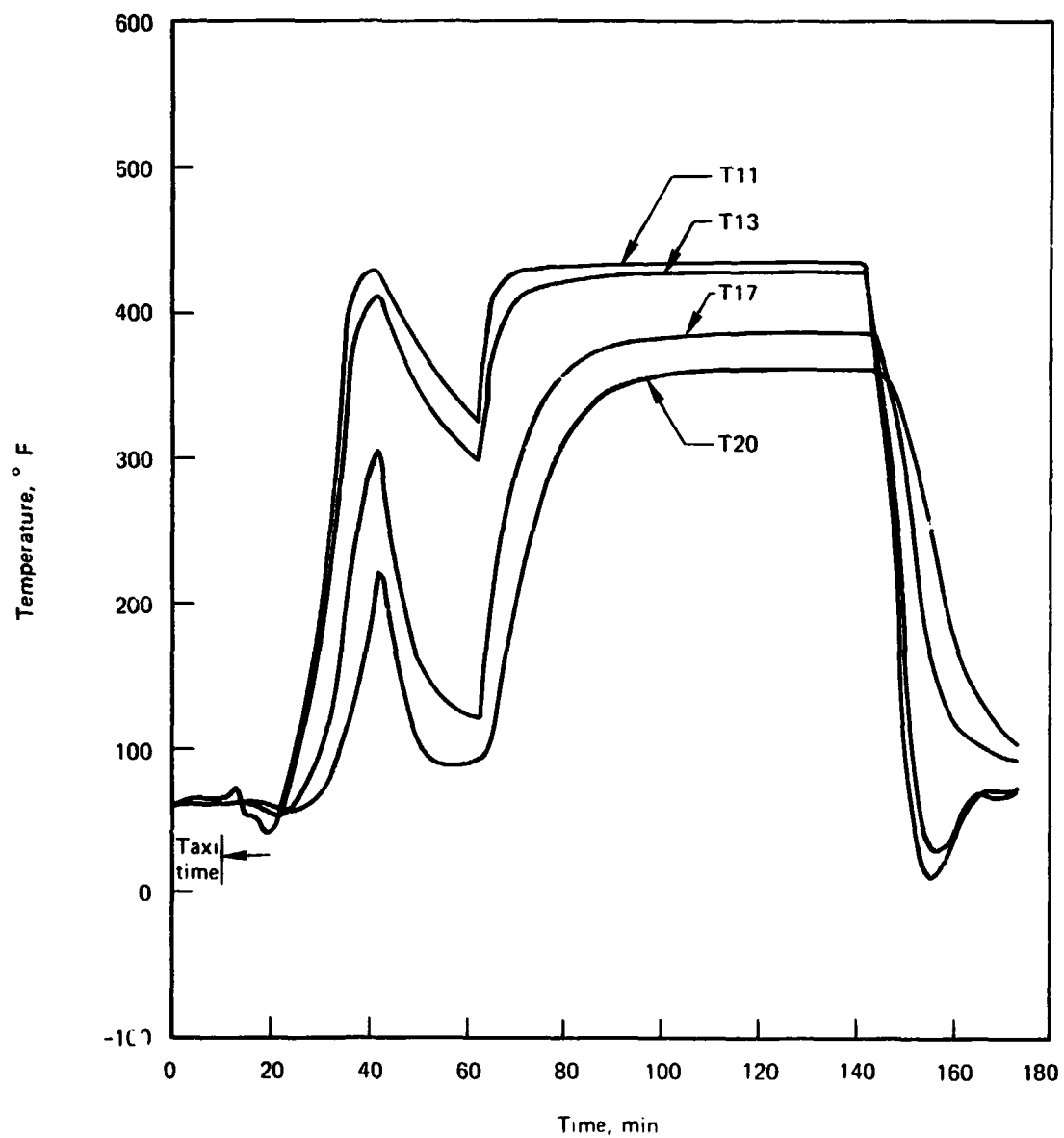


Figure 9-32.-Fuel Tank No. 2 Temperatures, Point 269, Case 1, T11, T13, T17, T20

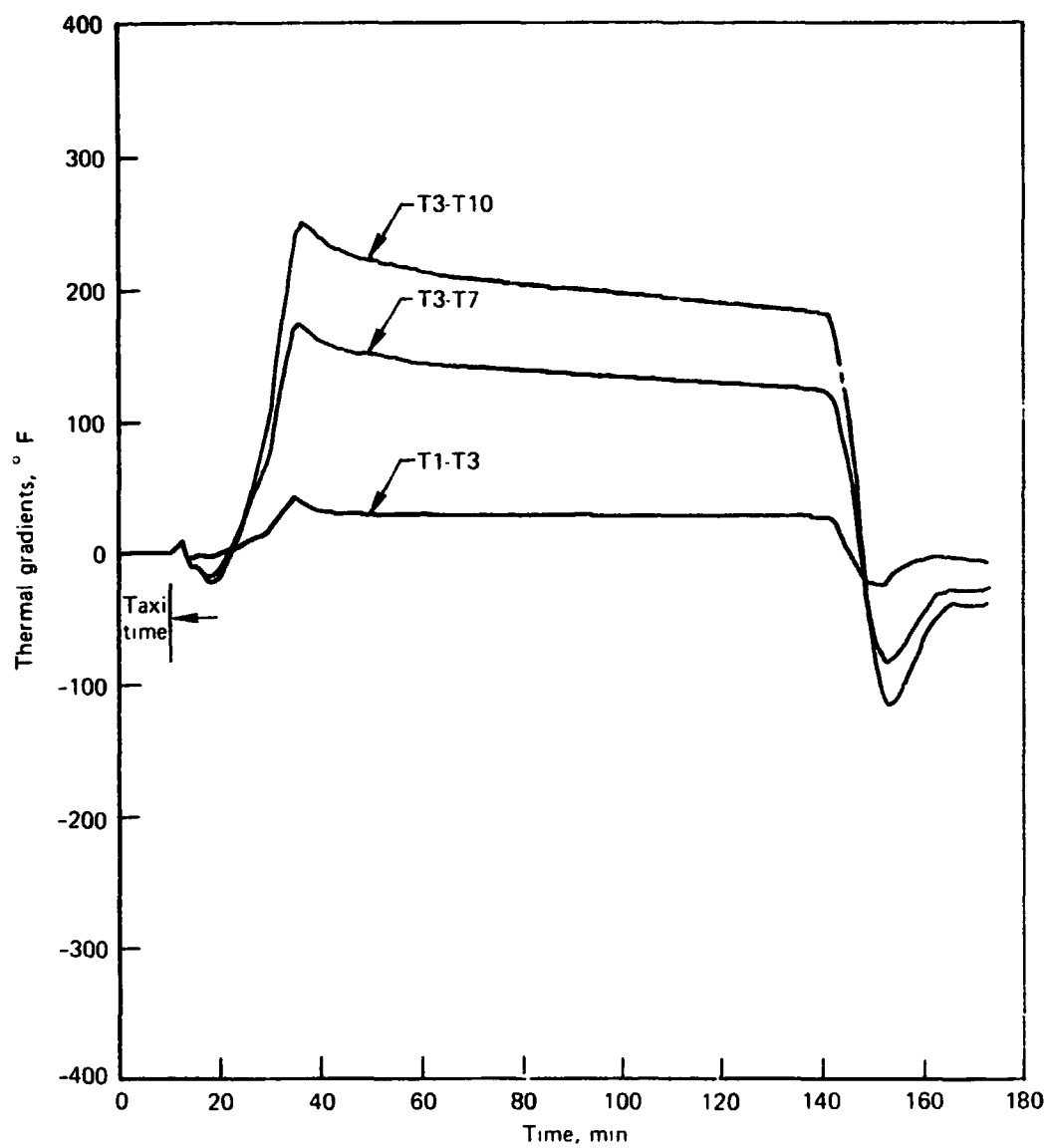


Figure 9-33.-Fuel Tank No. 2 Thermal Gradients. Point 269, Case 1, T1-T3, T3-T7, T3-T10

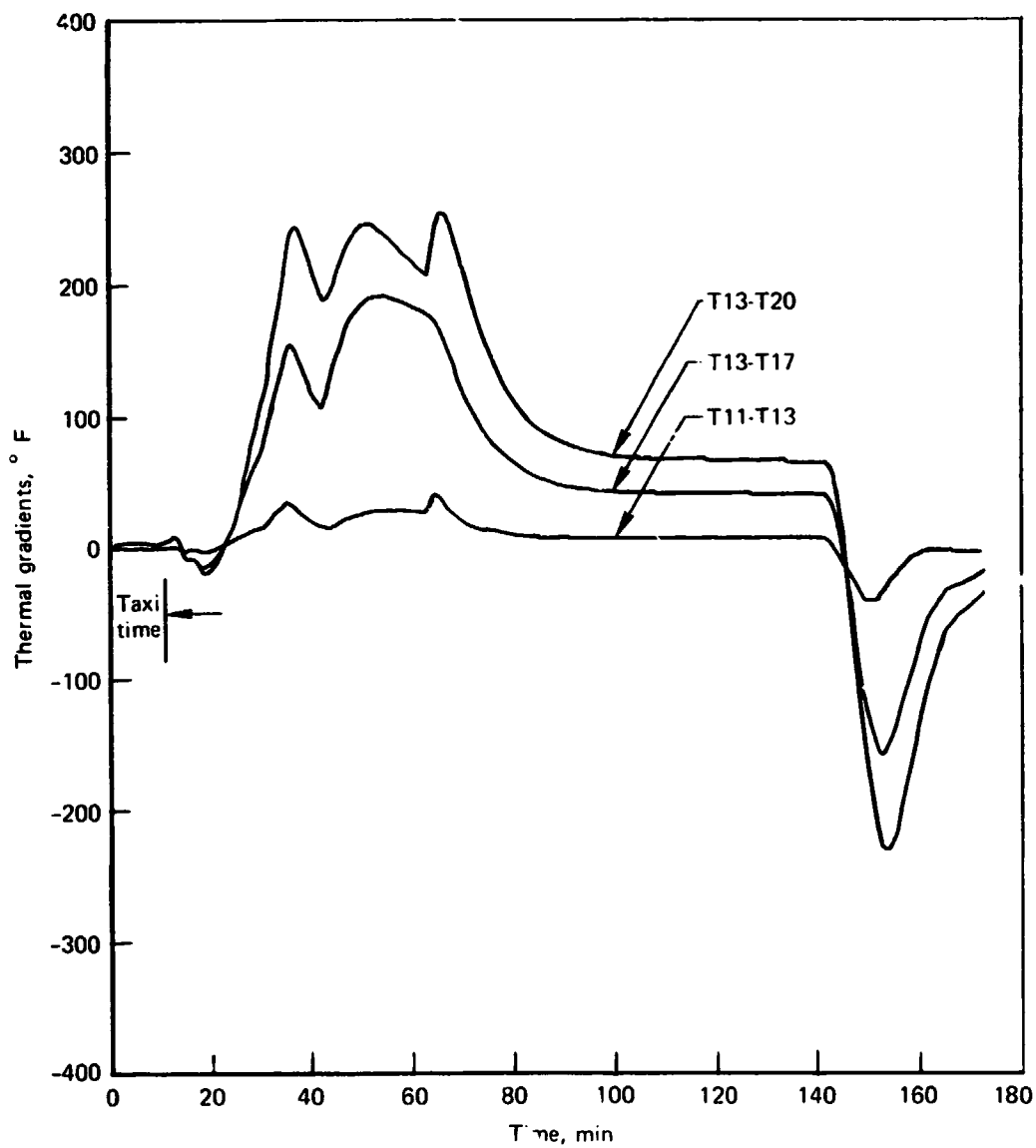


Figure 9-34.-Fuel Tank No. 2 Thermal Gradients, Point 269, Case 1, T11-T13, T13-T17, T13-T20

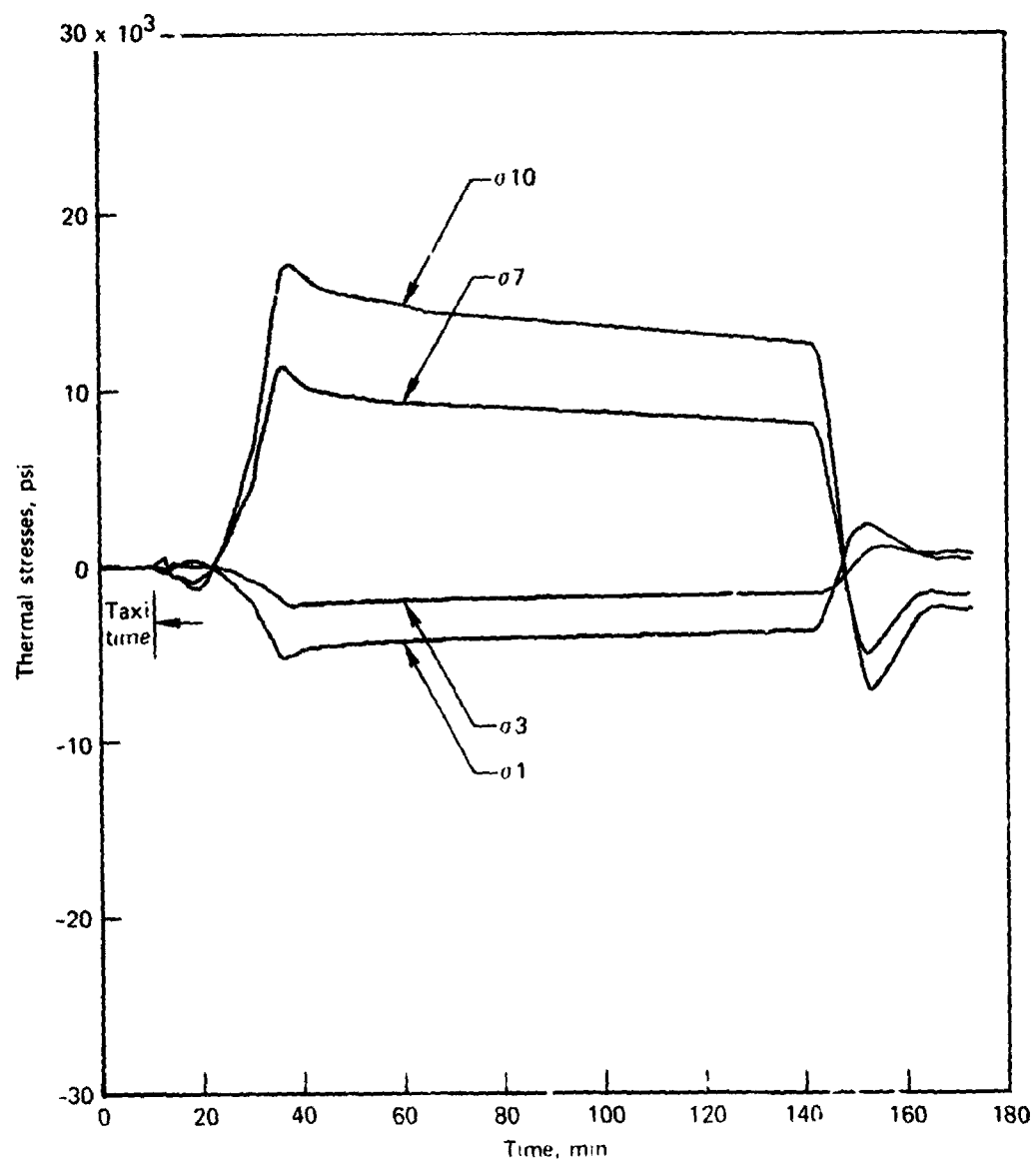


Figure 9-35.-Fuel Tank No. 2 Thermal Stresses, Point 269, Case 1, σ_1 , σ_3 , σ_7 , σ_{10}

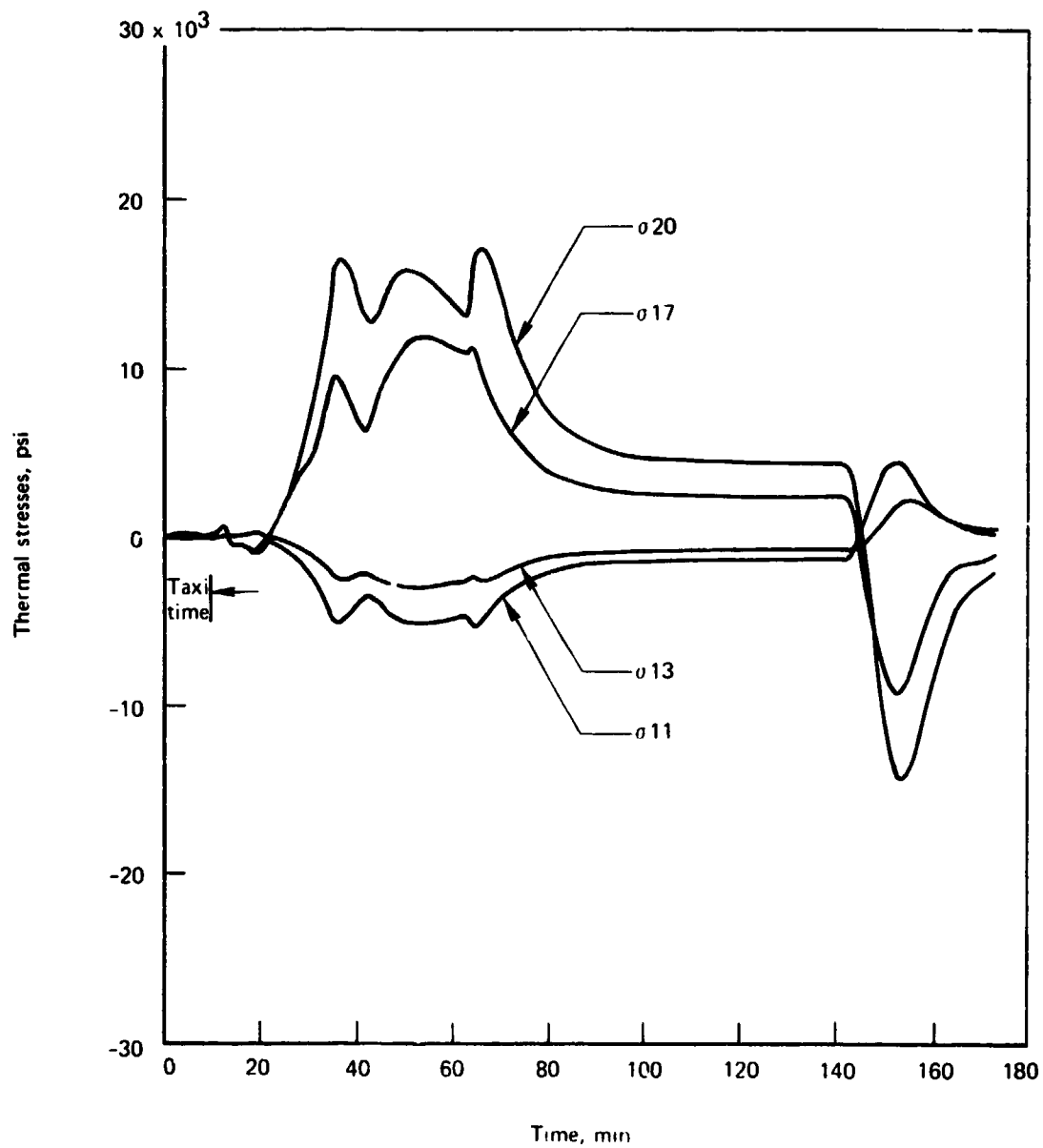


Figure 9-36.-Fuel Tank No. 2 Thermal Stresses, Point #69, Case 1, σ_{11} , σ_{13} , σ_{17} , σ_{20}

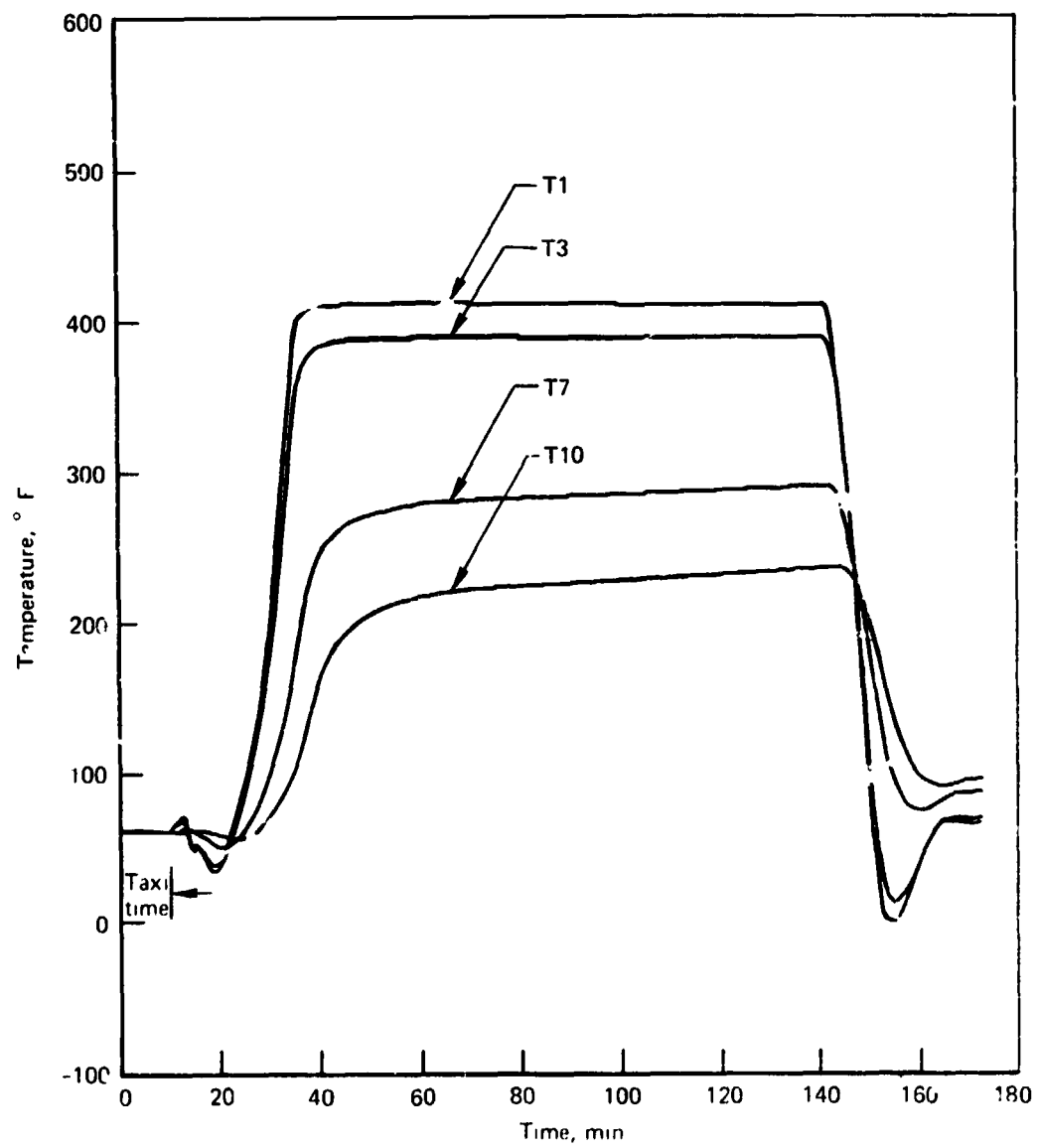


Figure 9-37.—Fuel Tank No. 2 Temperatures, Point 269, Case 2, T1, T3, T7, T10

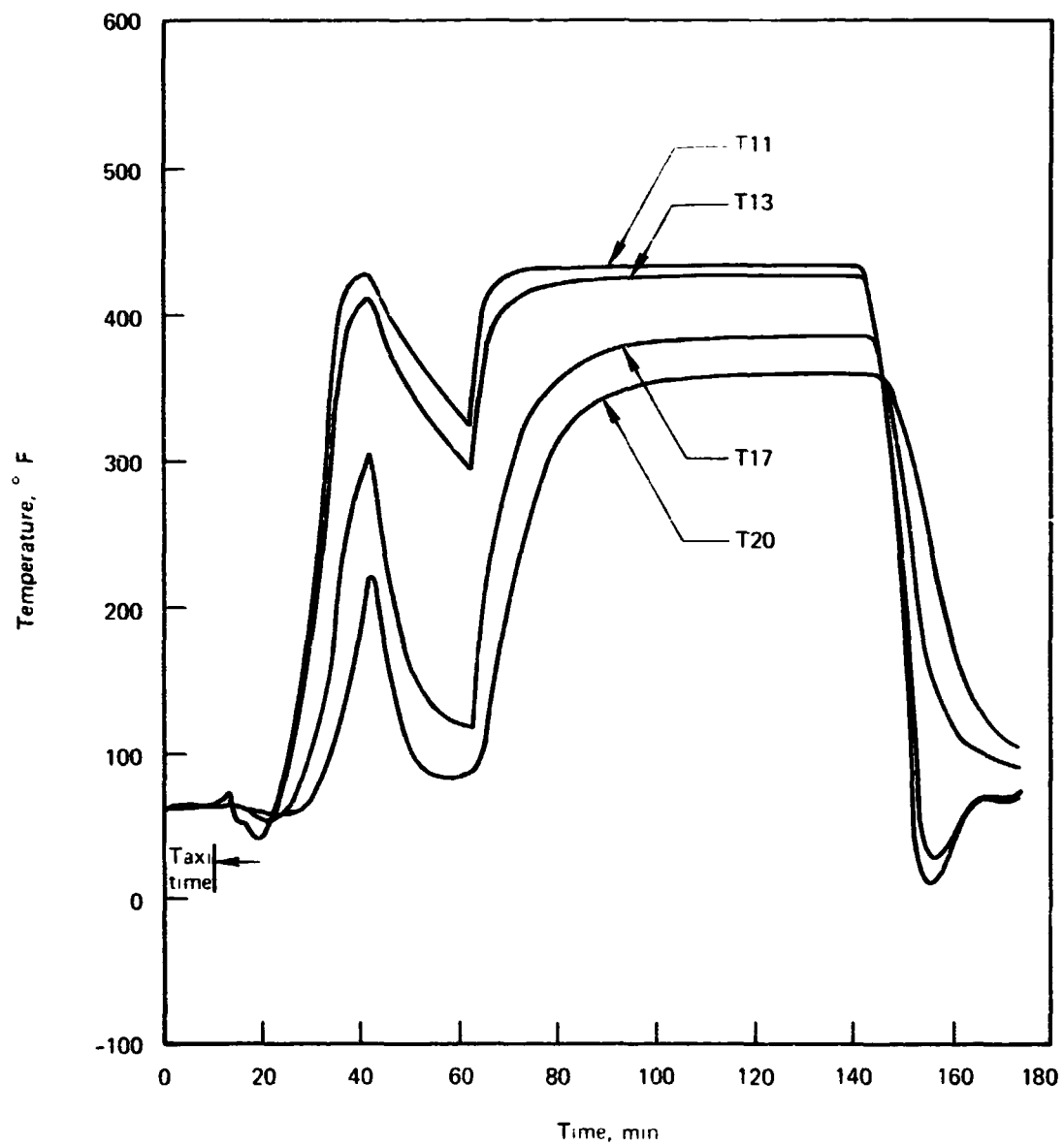


Figure 9-38.-Fuel Tank No. 2 Temperatures, Point 269, Case 2, T11, T13, T17, T20

474

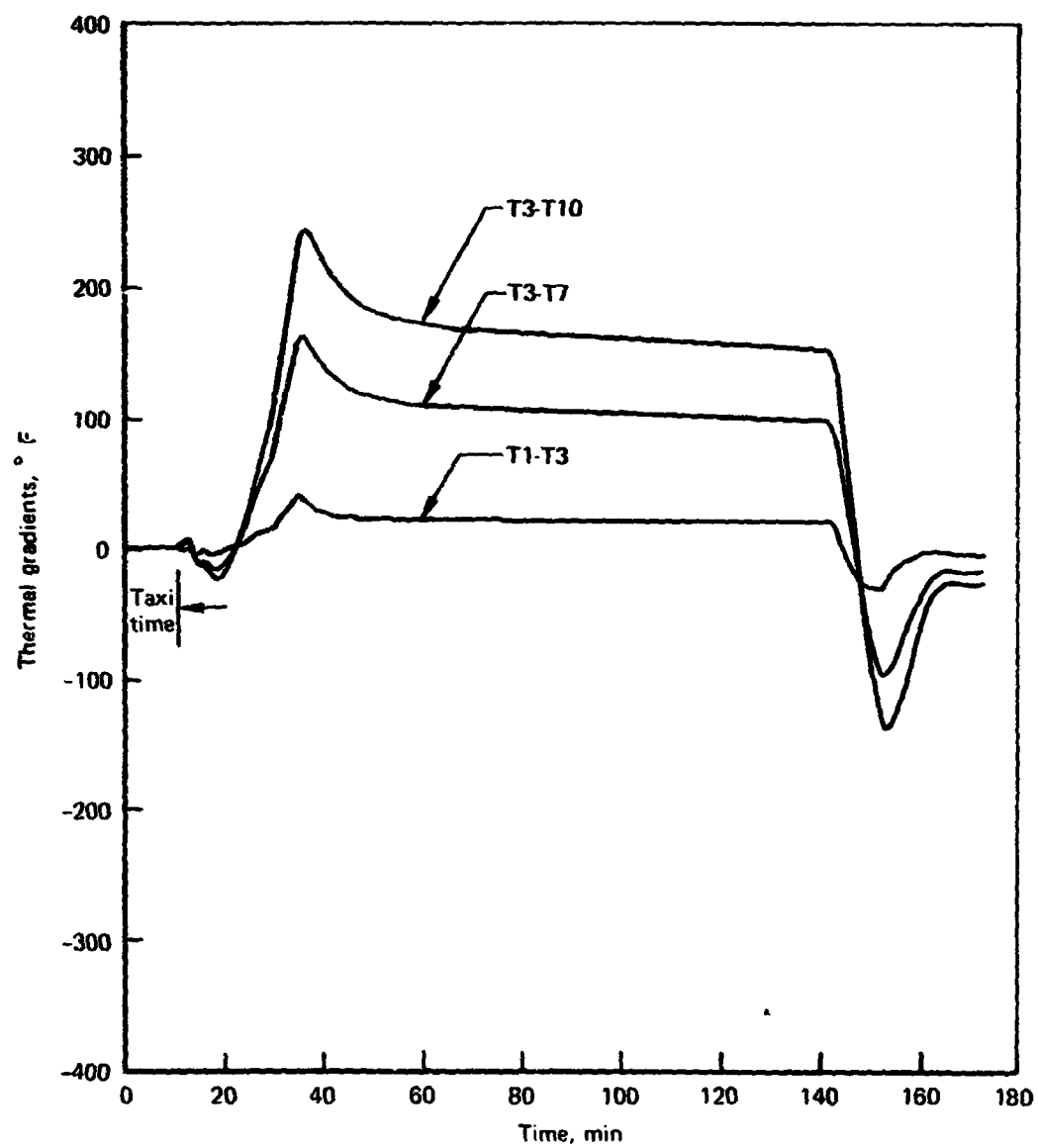


Figure 9-39.-Fuel Tank No. 2 Thermal Gradients, Point 269, Case 2, T1-T3, T3-T7, T3-T10

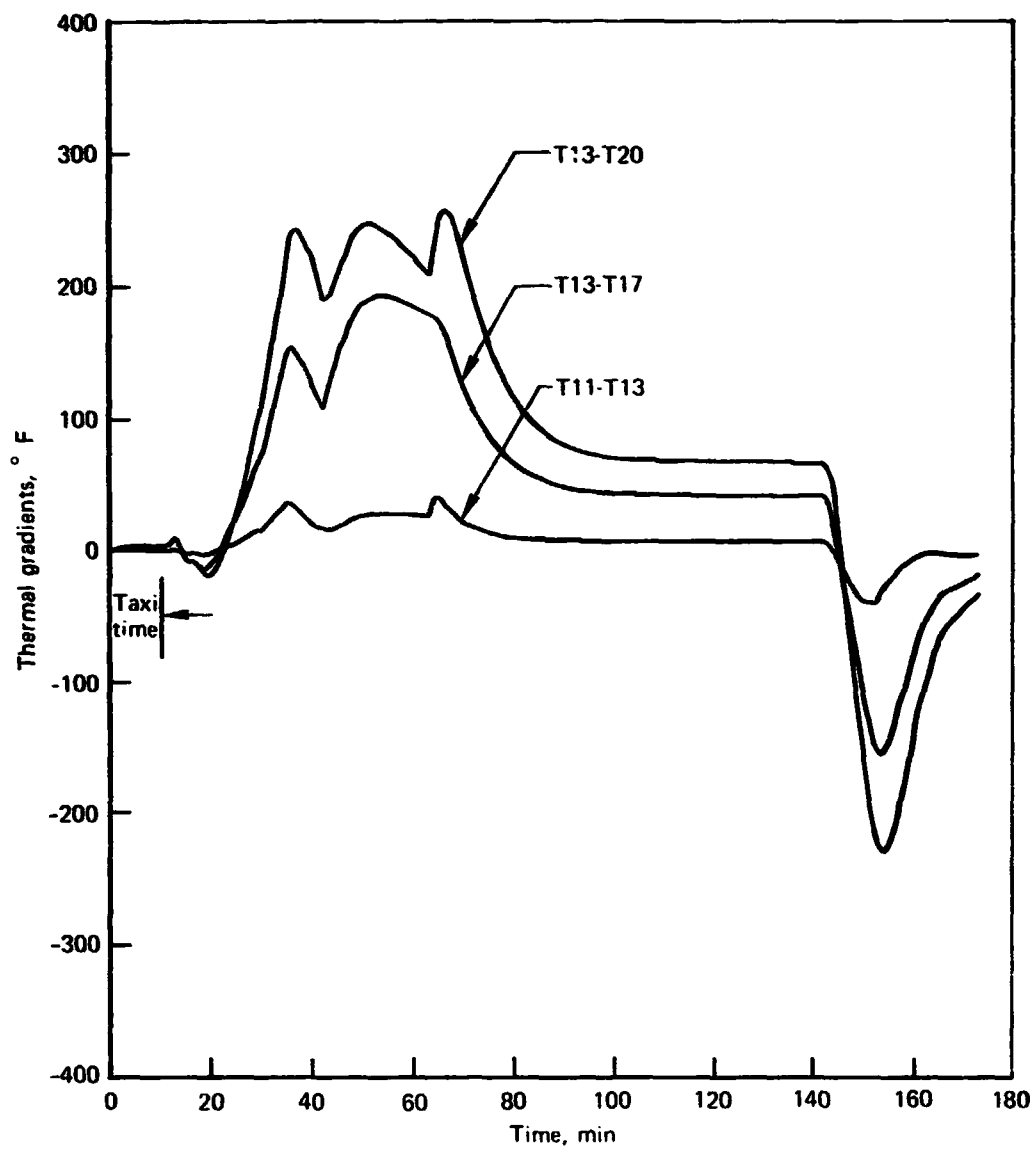


Figure 9-40.-Fuel Tank No. 2 Thermal Gradients, Point 269, Case 2, T11-T13, T13-T17, T13-T20

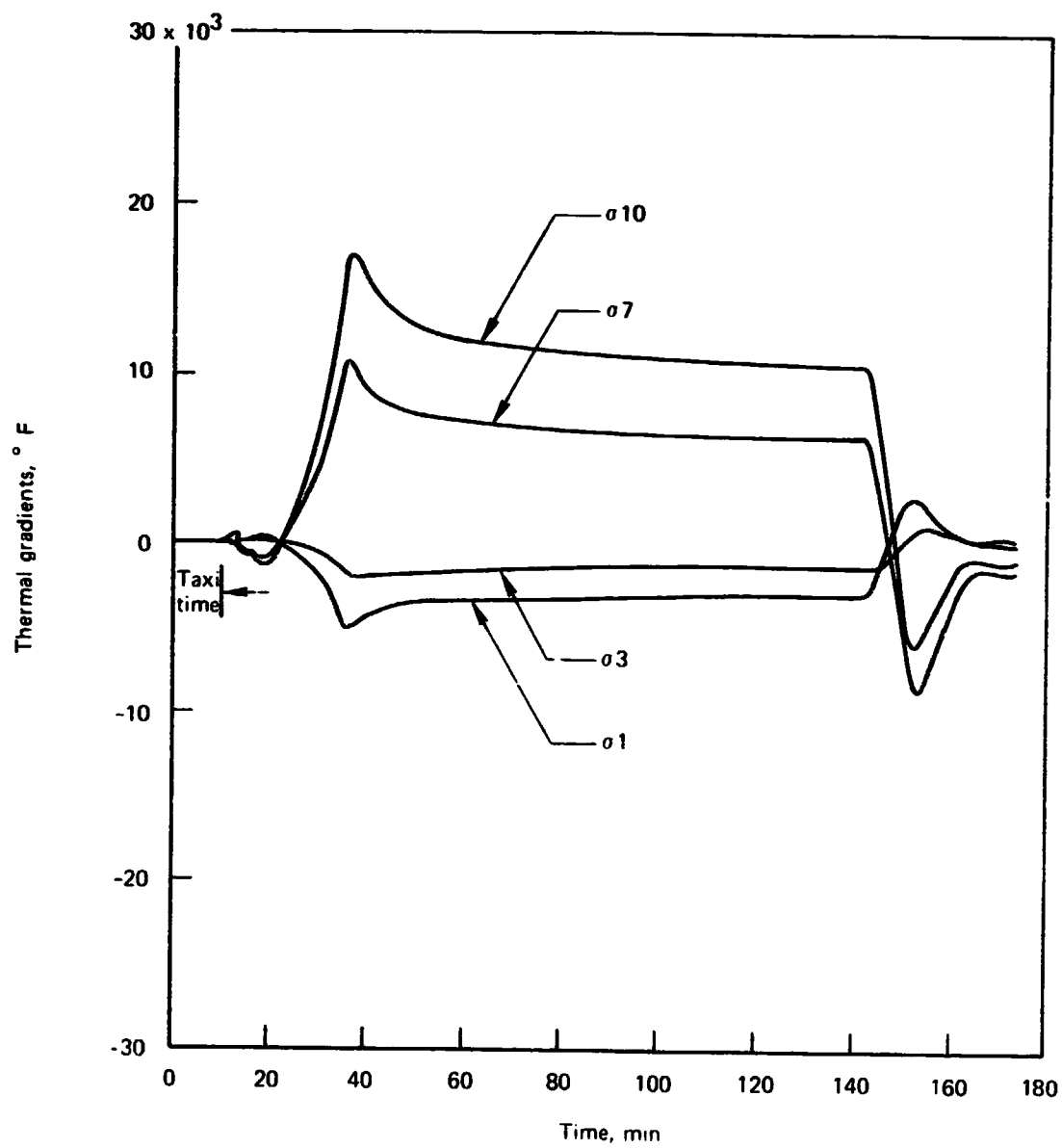


Figure 9-41.-Fuel Tank No. 2 Thermal Stresses, Point 269, Case 2, σ_1 , σ_3 , σ_7 , σ_{10}

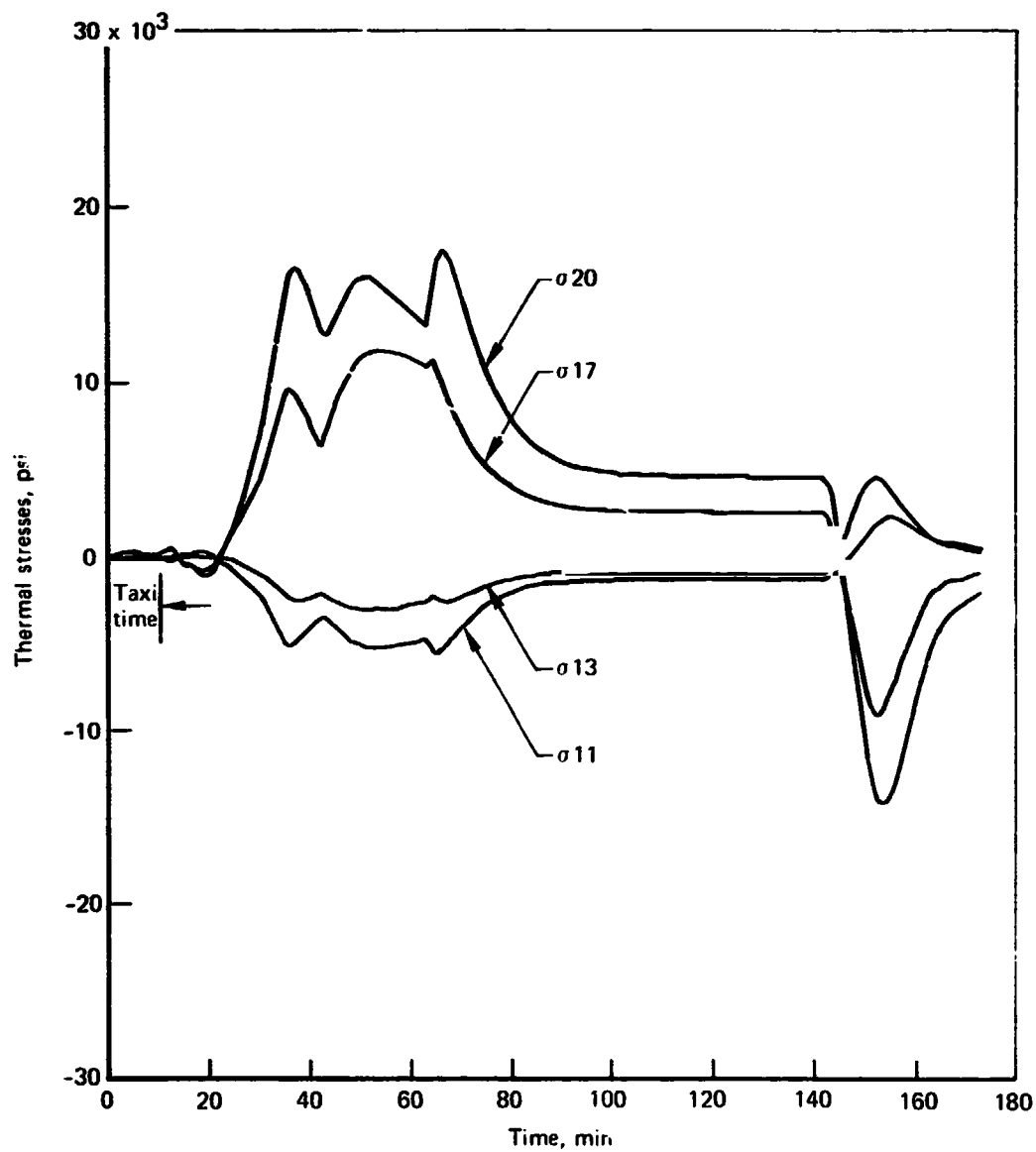


Figure 9-42.-Fuel Tank No. 2 Thermal Stresses, Point 269, Case 2, σ_{11} , σ_{13} , σ_{17} , σ_{20}

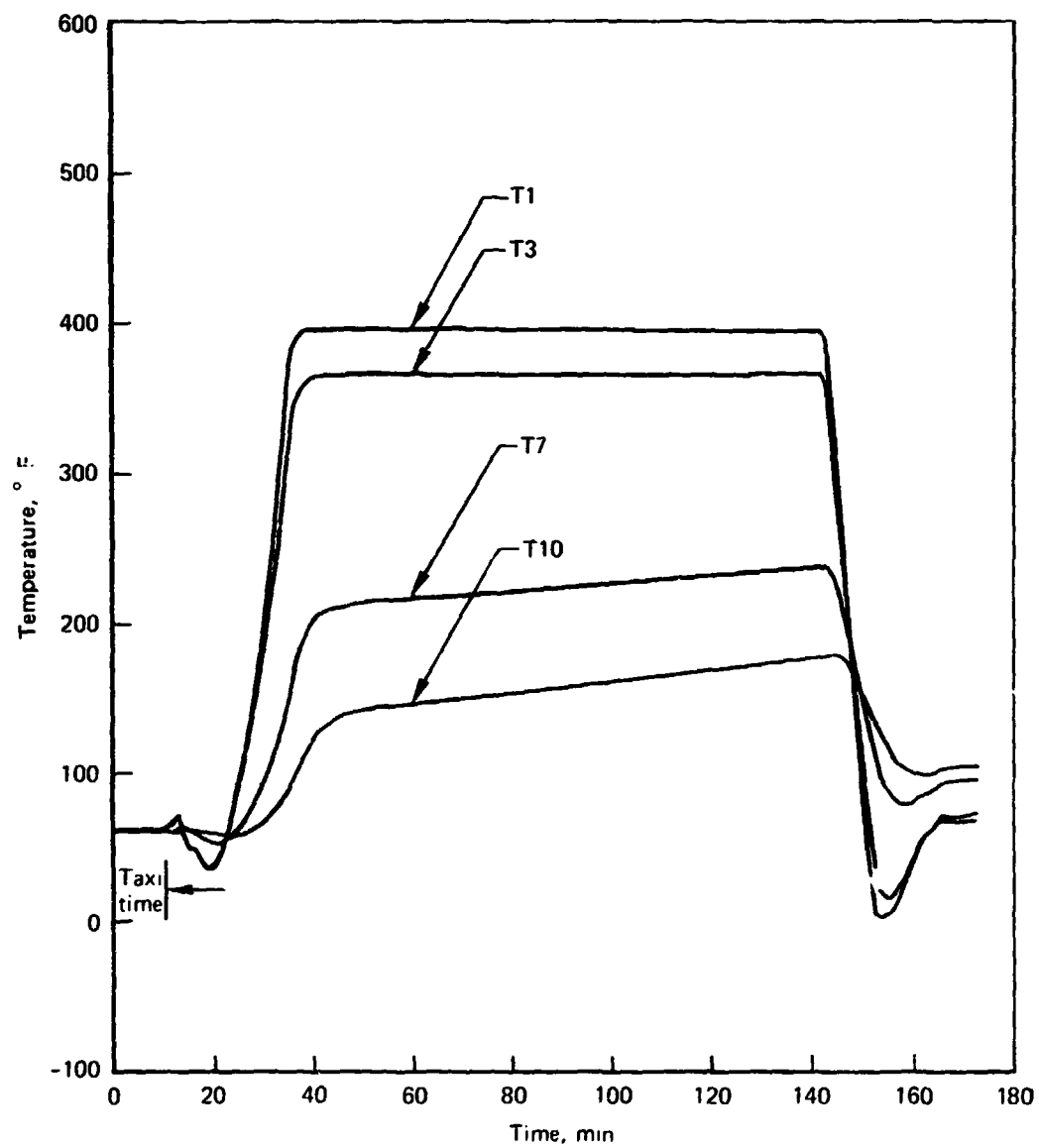


Figure 9-43.-Fuel Tank No. 2 Temperatures, Point 269, Case 3, T1, T3, T7, T10

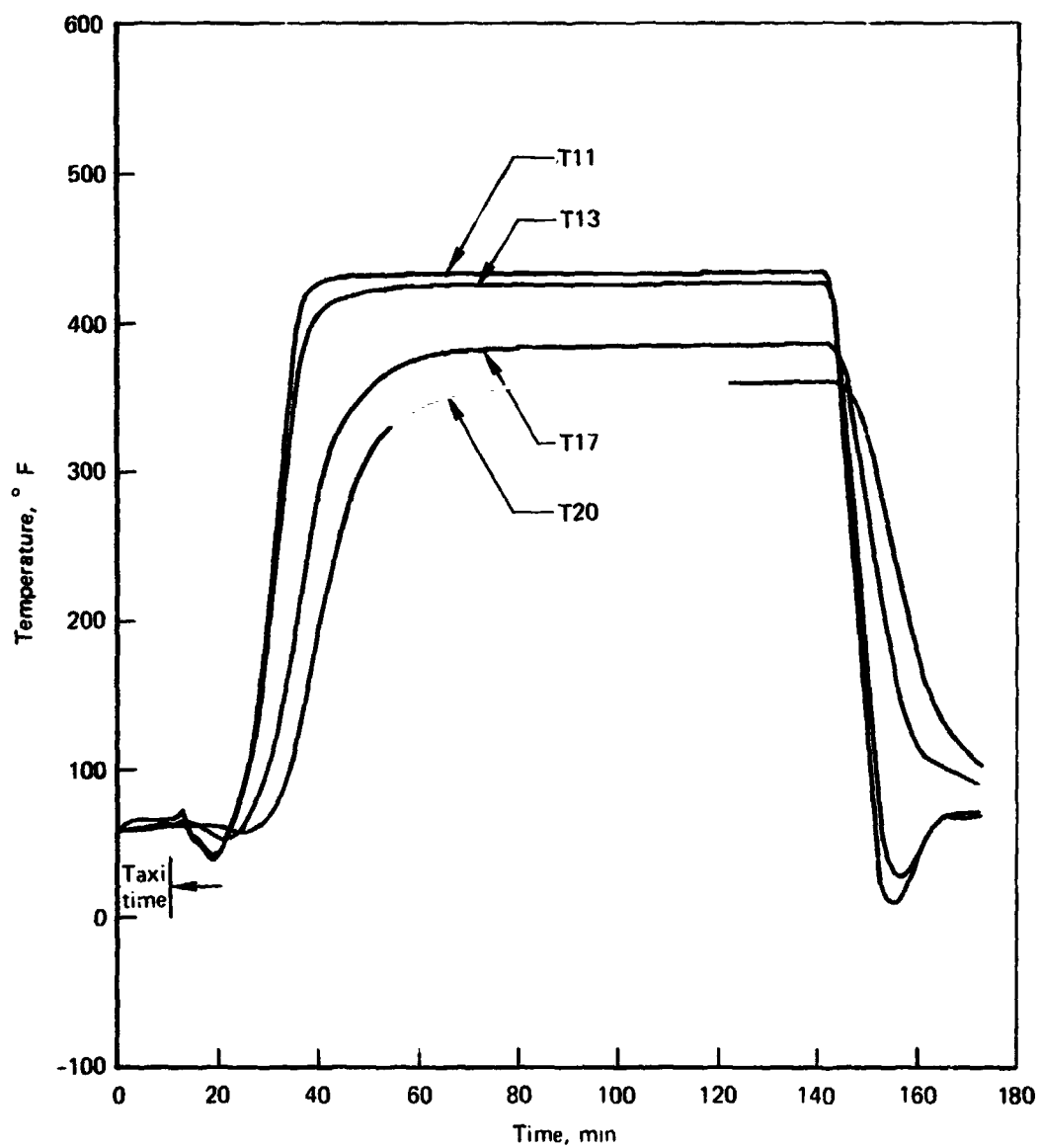


Figure 9-44.—Fuel Tank No. 2 Temperatures, Point 269, Case 3, T11, T13, T17, T20

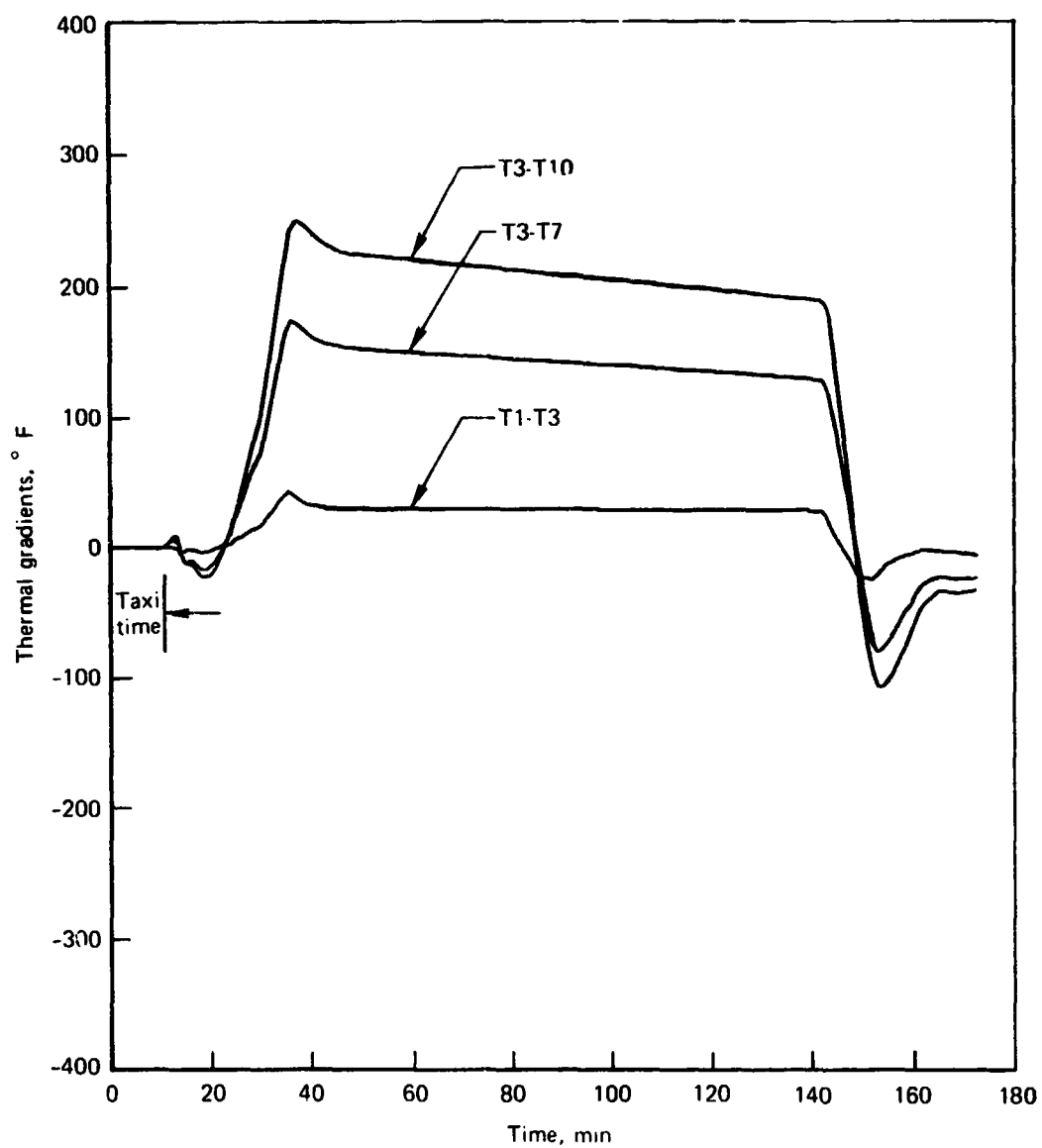


Figure 9-45.-Fuel Tank No. 2 Thermal Gradients, Point 269, Case 3, T1-T3, T3-T7, T3-T10

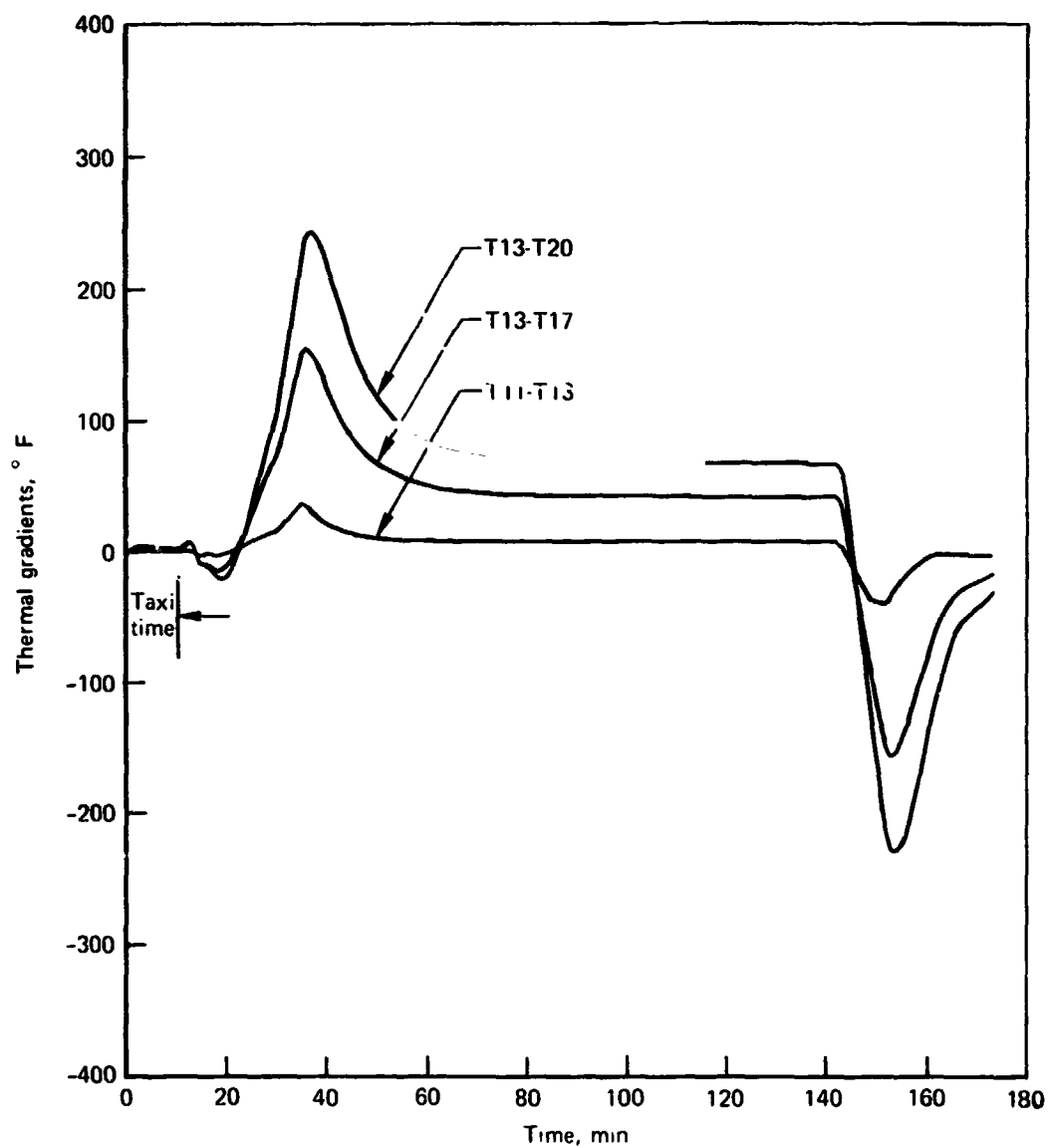


Figure 9-46. -Fuel Tank No. 2 Thermal Gradients, Point 269, Case 3, T11-T13, T13-T17, T13-T20

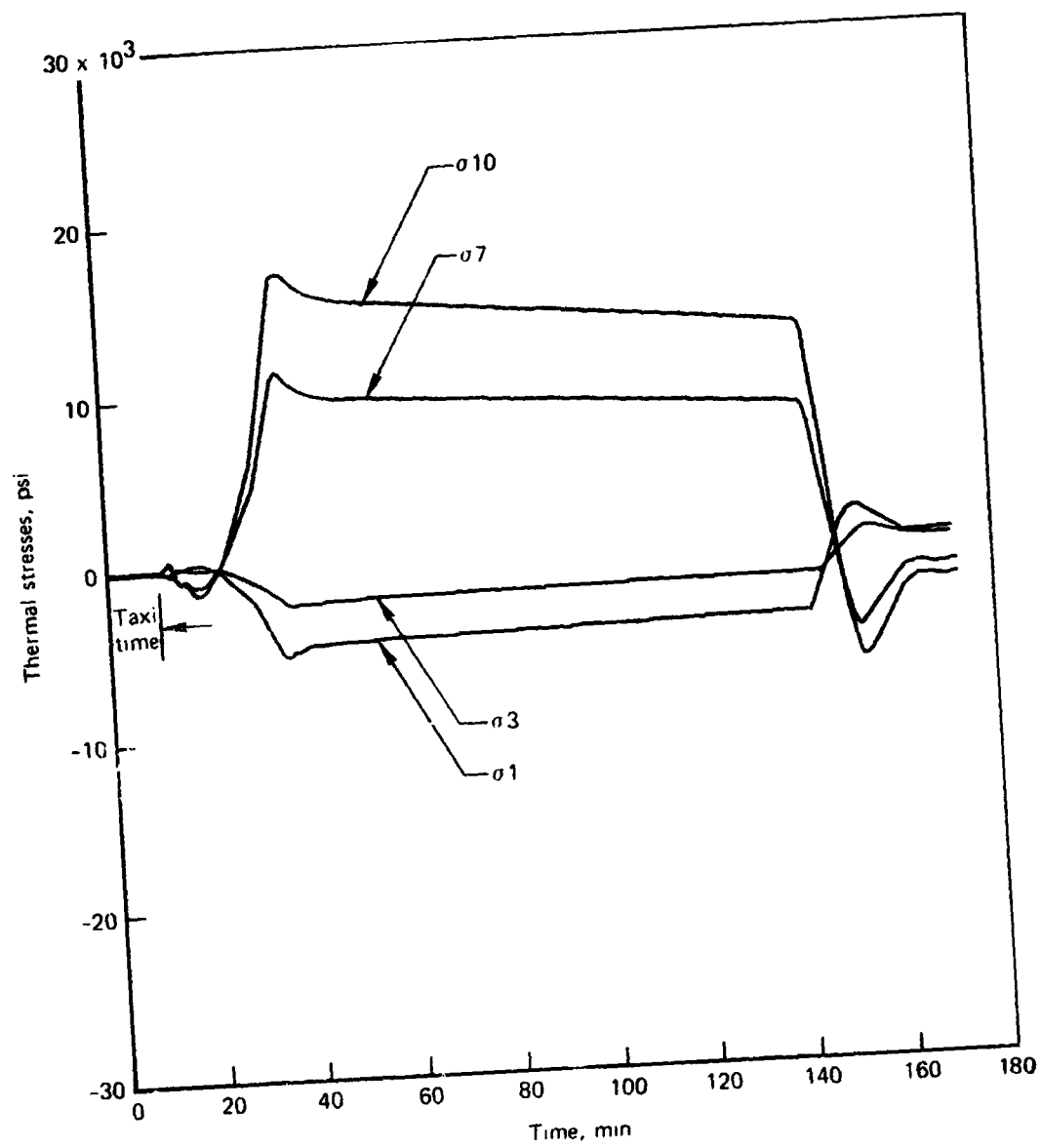


Figure 9-47.-Fuel Tank No. 2 Thermal Stresses, Point 269, Case 3, $\sigma 1$, $\sigma 3$, $\sigma 7$, $\sigma 10$

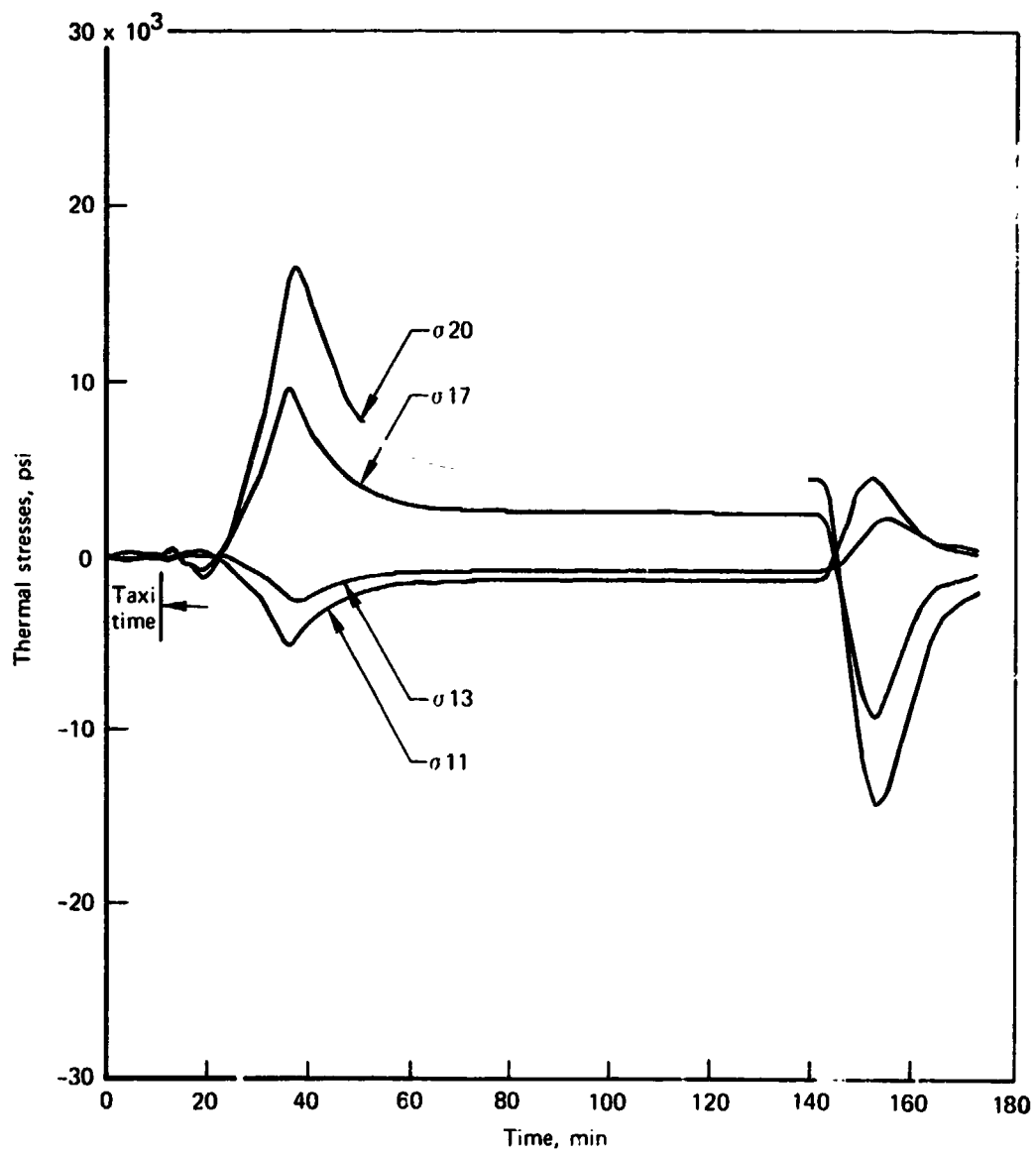


Figure 9-48.—Fuel Tank No. 2 Thermal Stresses, Point 269, Case 3, σ_{11} , σ_{13} , σ_{17} , σ_{20}

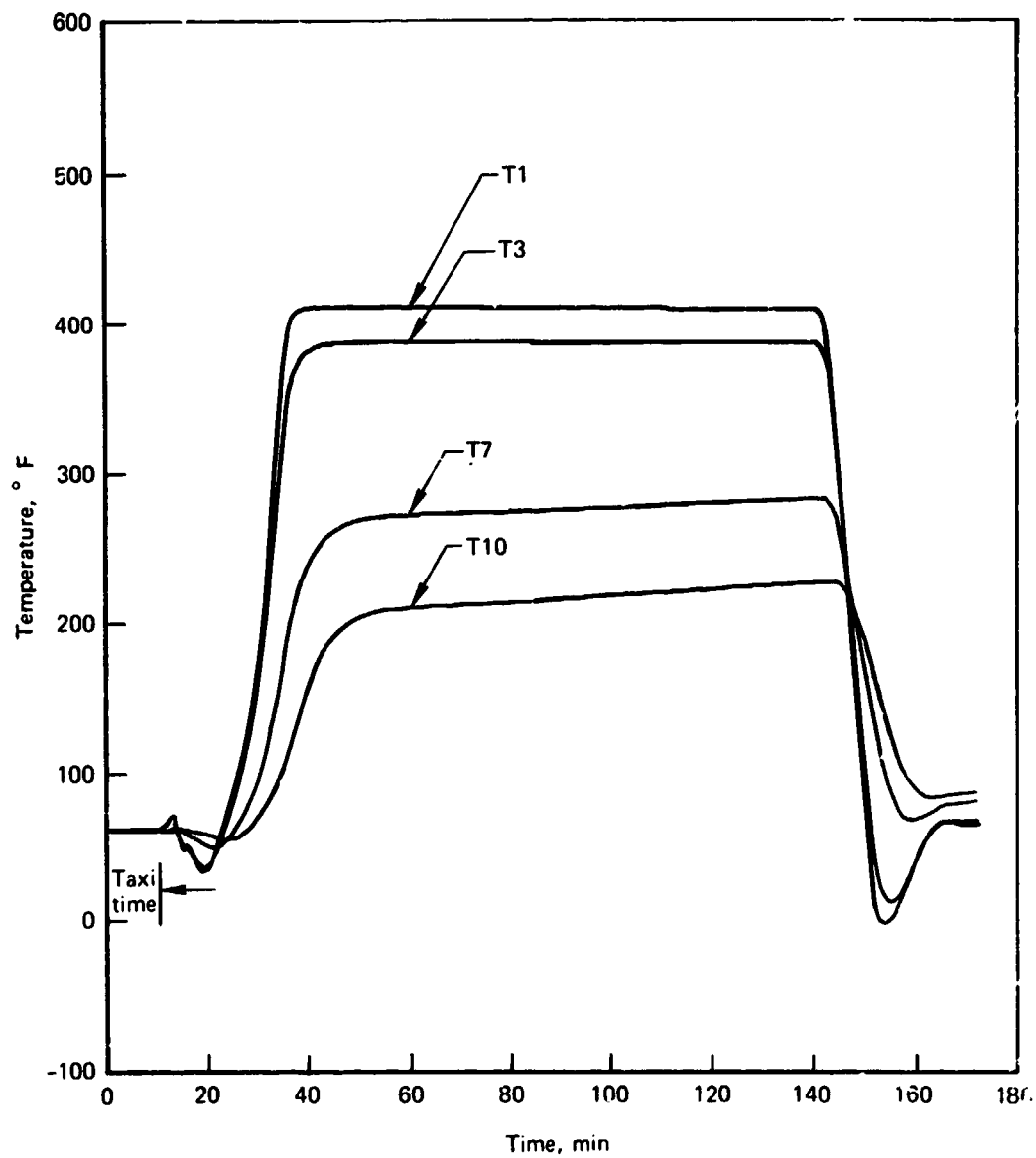


Figure 9-49.-Fuel Tank No. 2 Temperatures, Point 269, Case 4, T1, T3, T7, T10

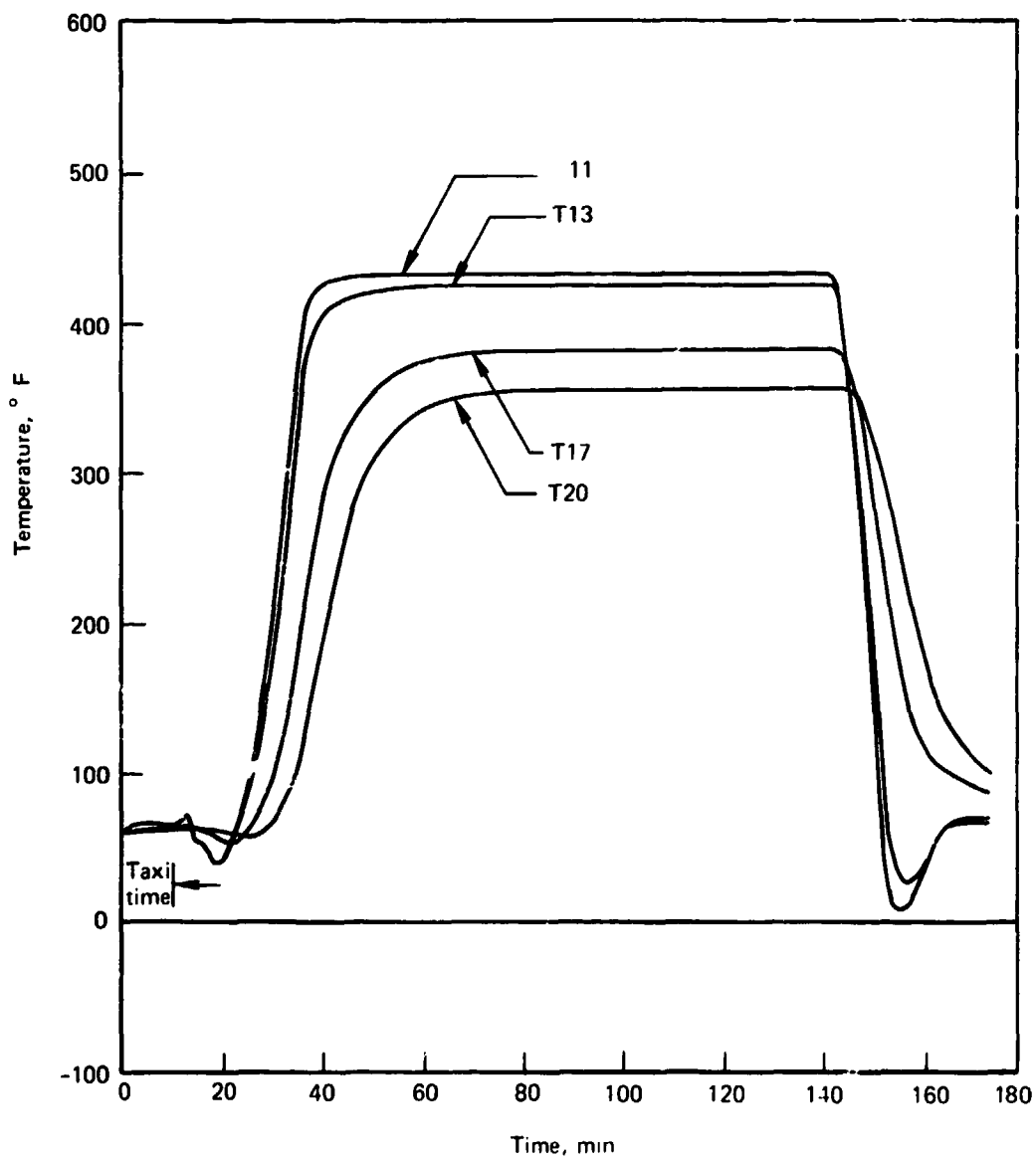


Figure 9-50.-Fuel Tank No. 2 Temperatures, Point 269, Case 4, T11, T13, T17, T20

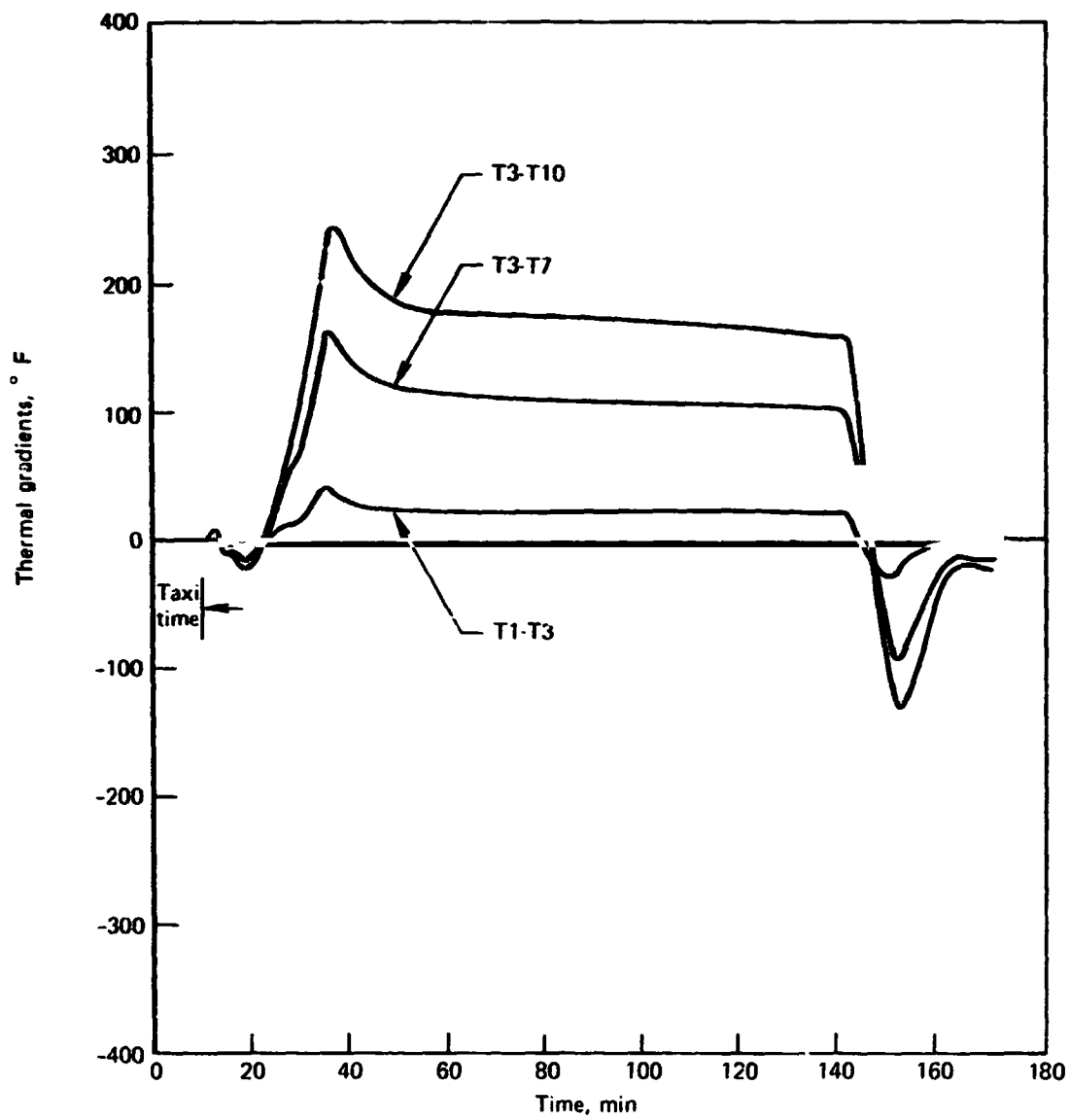


Figure 9-51.-Fuel Tank No. 2 Thermal Gradients, Point 269, Case 4, T1-T3, T3-T7 T3-T10

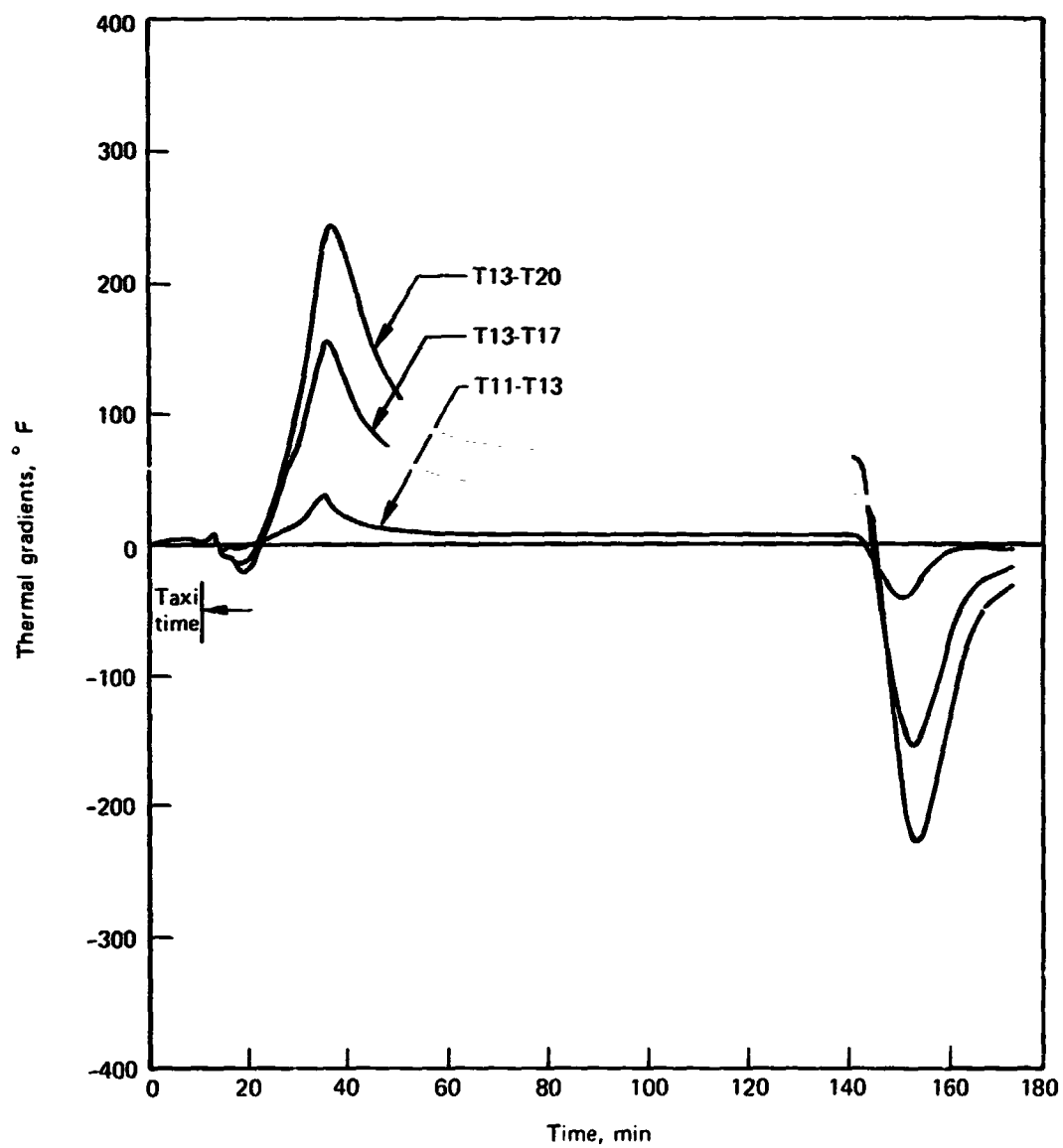


Figure 9-52.-Fuel Tank No. 2 Thermal Gradients, Point 269, Case 4, T11-T13, T13-T17, T13-T20

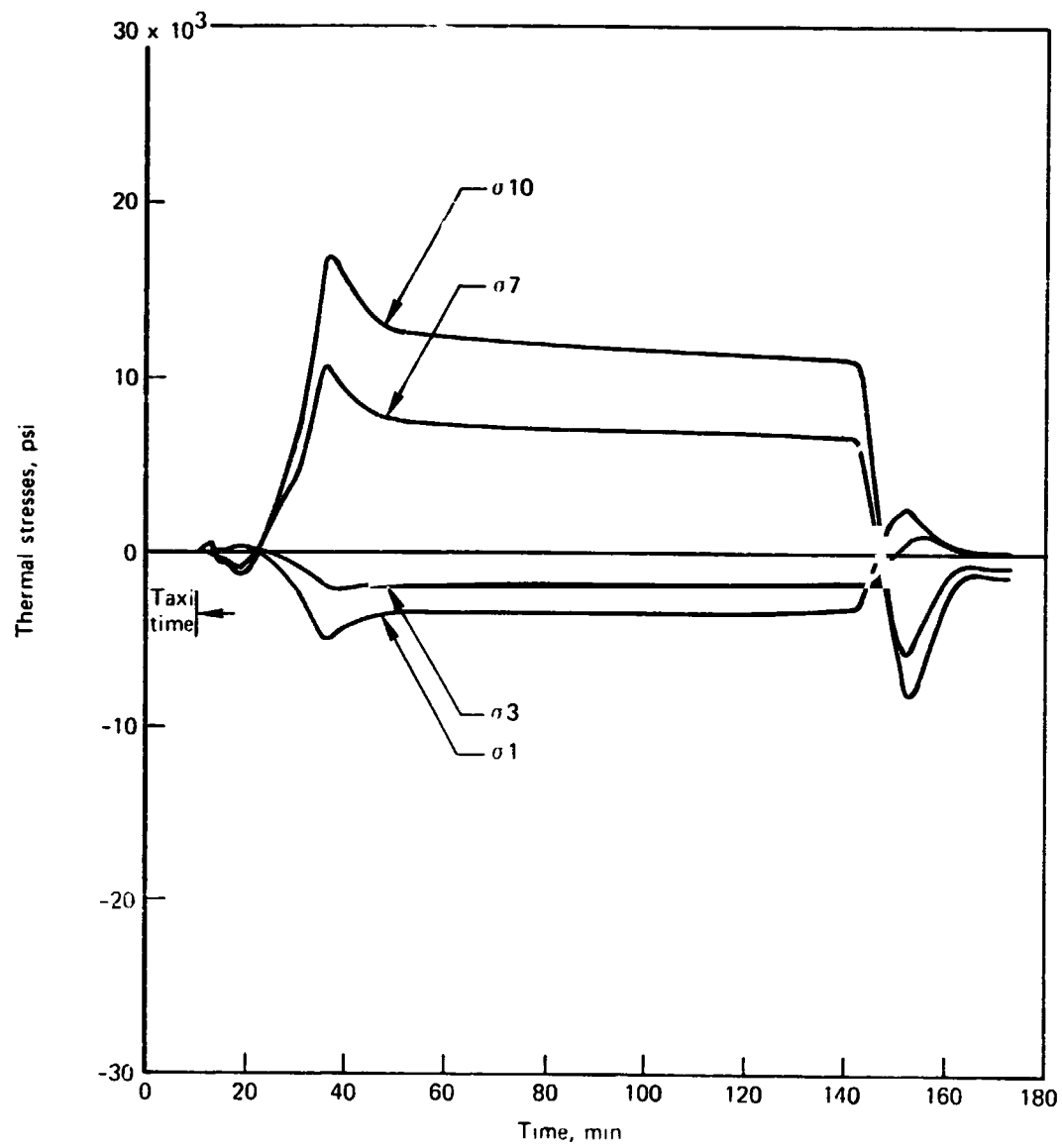


Figure 9-53.-Fuel Tank No. 2 Thermal Stresses, Point 269, Case 4, σ_1 , σ_3 , σ_7 , σ_{10}

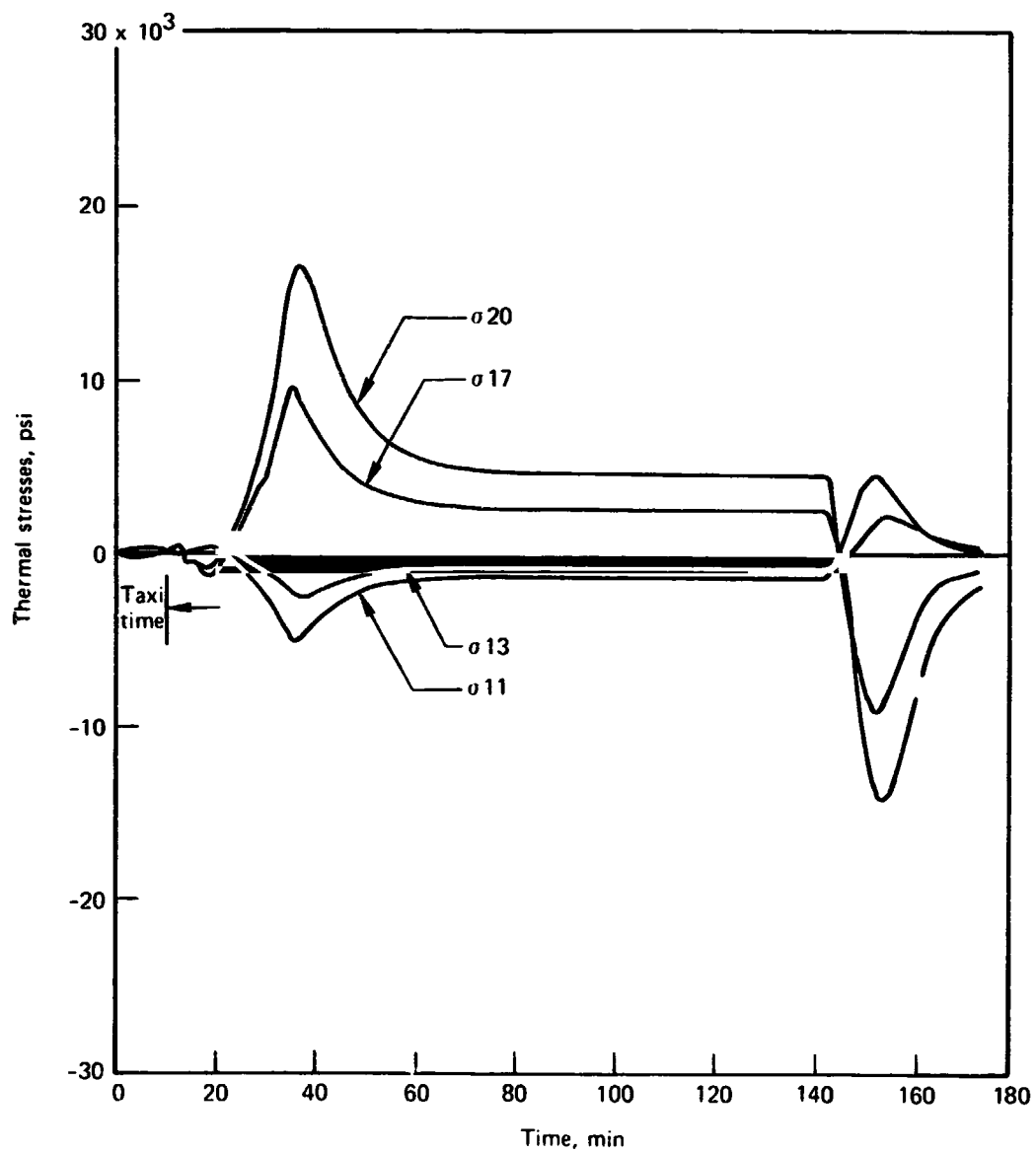
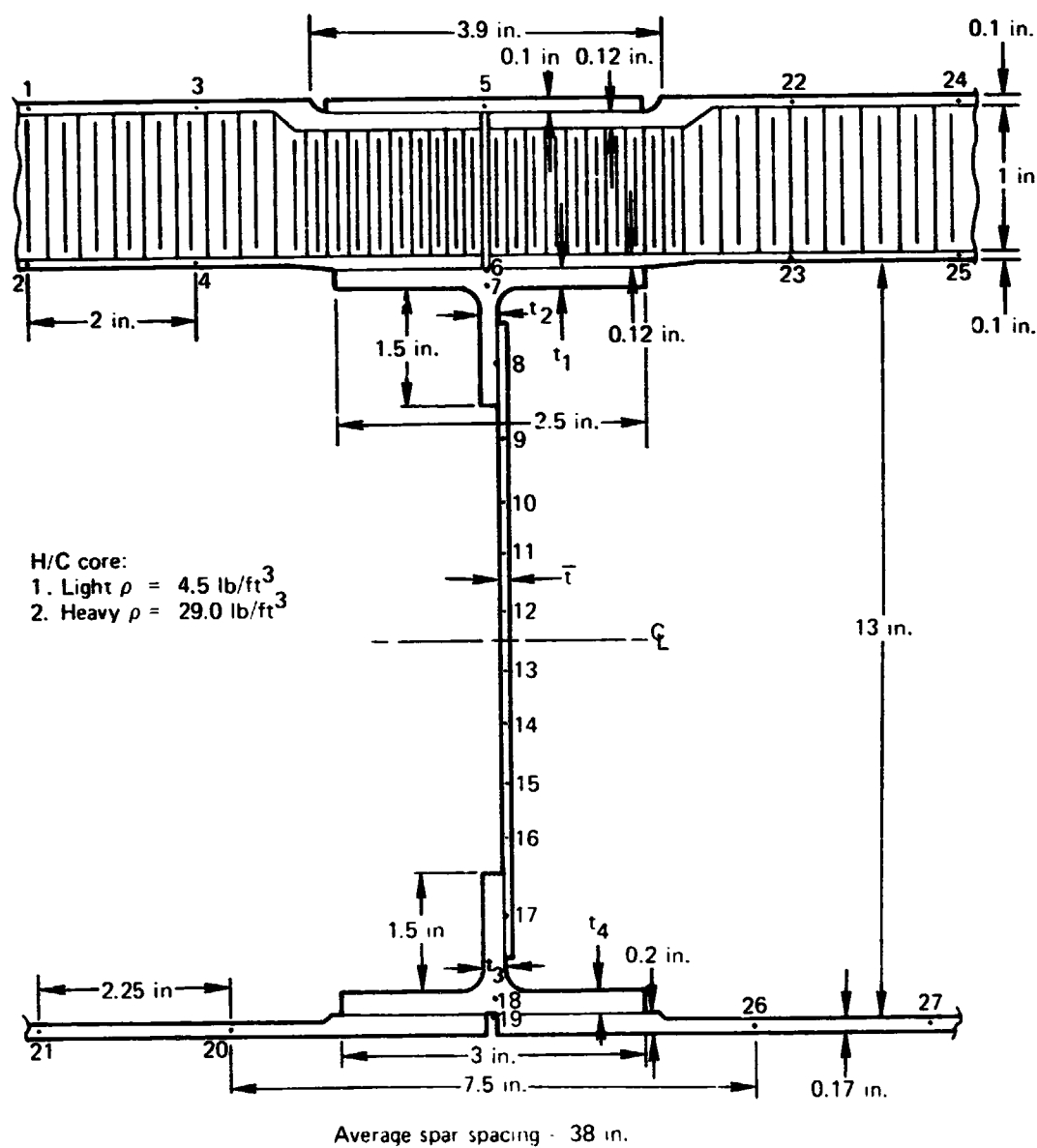


Figure 9-54.-Fuel Tank No. 2 Thermal Stresses, Point 269, Case 4, σ_{11} , σ_{13} , σ_{17} , σ_{20}

REPRODUCIBILITY OF THE
ORIGINAL PAGE IS POOR



Dimension	t1, in.	t2, in.	\bar{t} , in.	t3, in.	t4, in.	Case
Spar fwd of 431	0.277	0.277	0.024	0.225	0.3	1
Spar aft of 431	0.37	0.37	0.15	0.45	0.6	2

Figure 9-55.—Intermediate and Rear Spars, Point 431

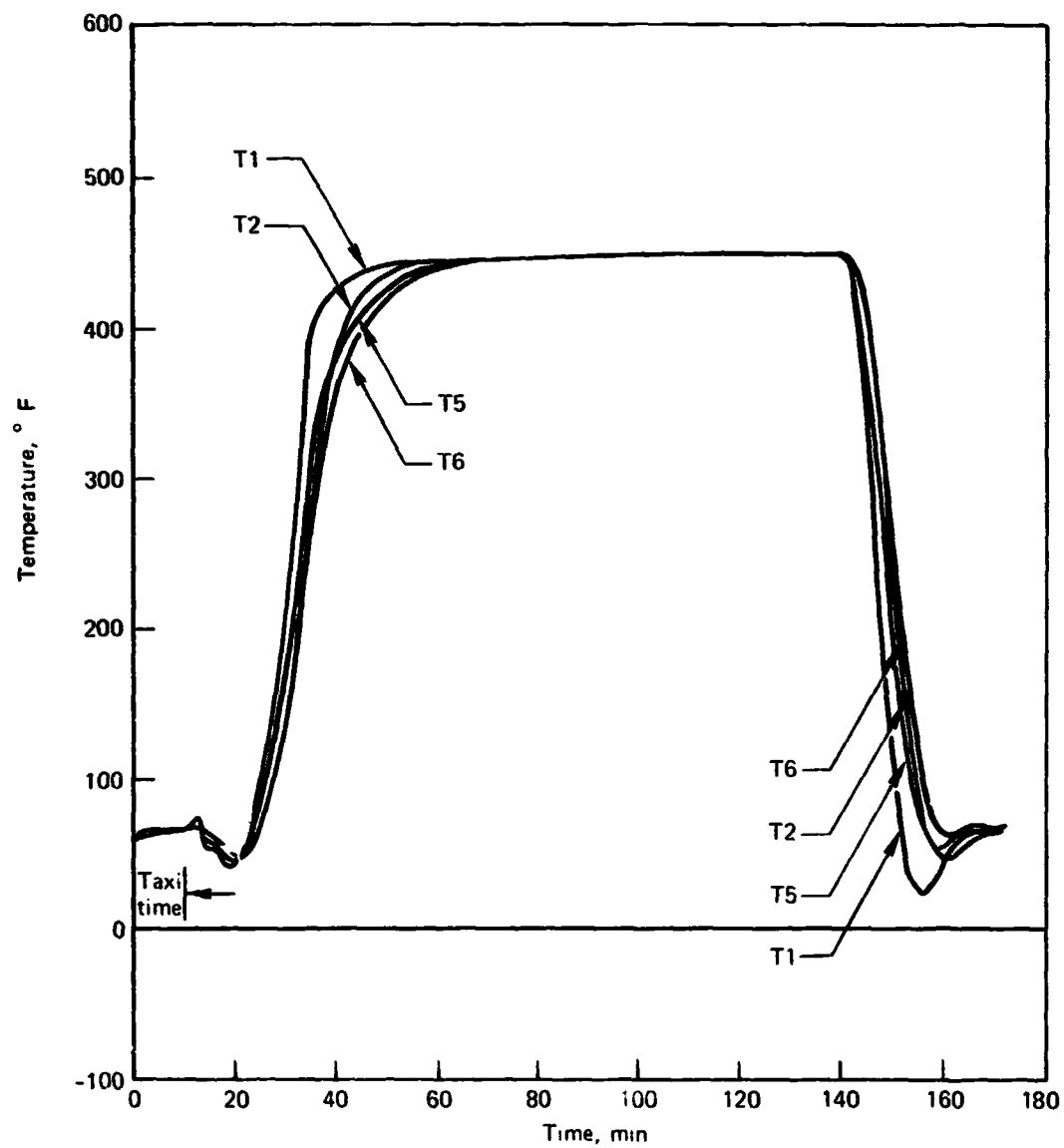


Figure 9-56.-Wing Spar Temperatures, Point 431, Case 1, Forward, T1, T2, T5, T6

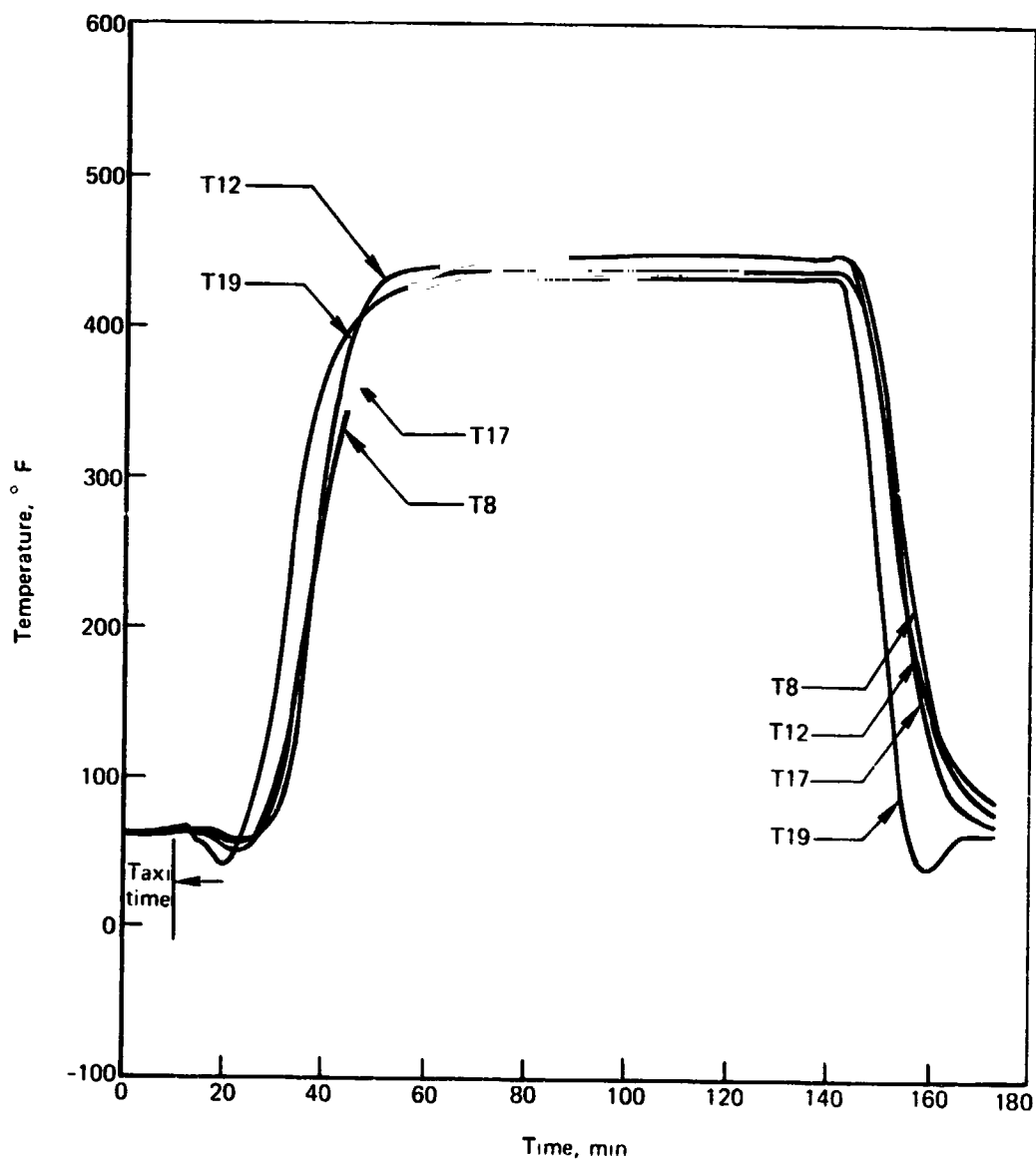


Figure 9-57.-Wing Spar Temperatures, Point 431, Case 1, Forward, T8, T12, T17, T19

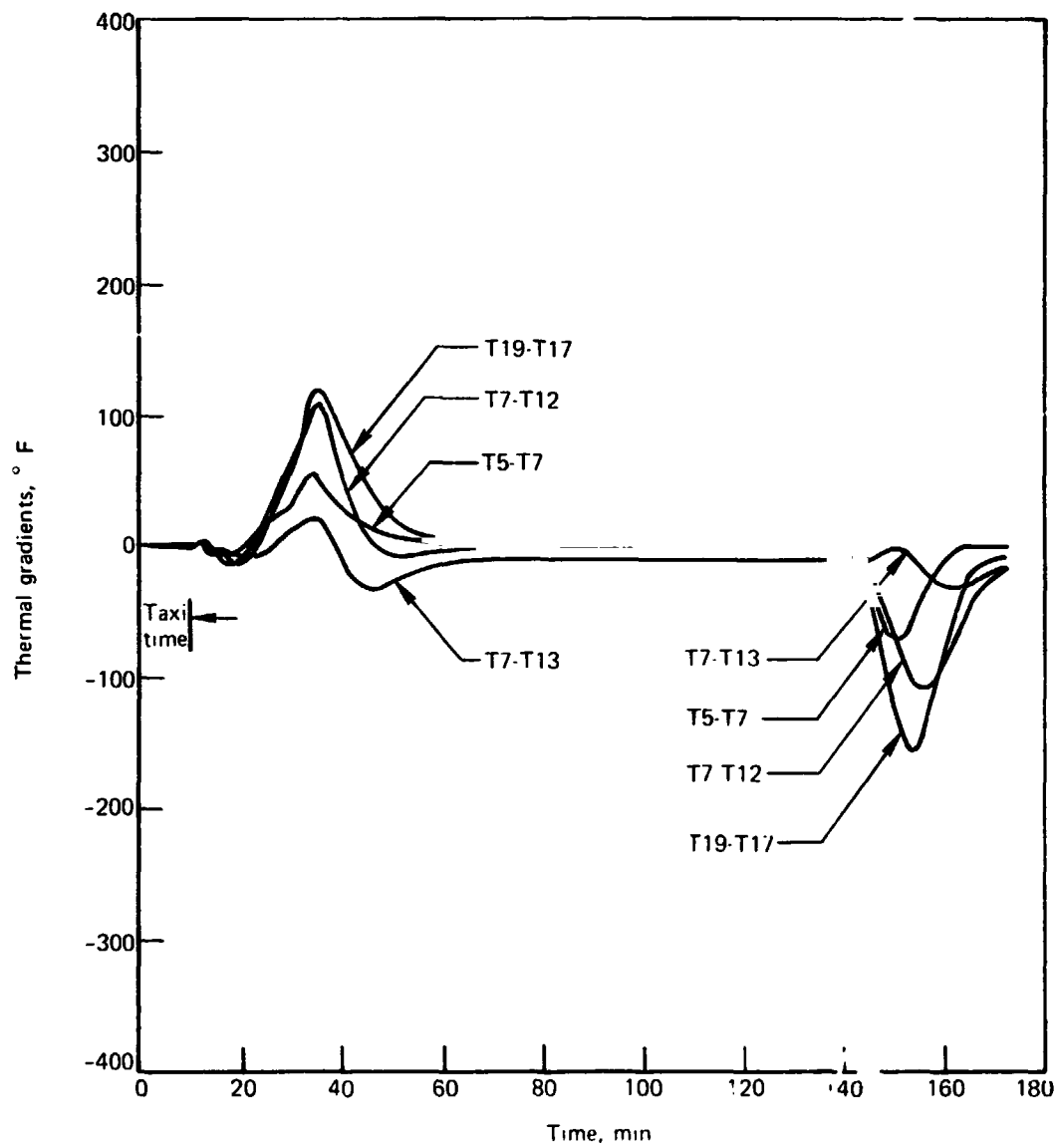


Figure 9-58.—Wing Spar Thermal Gradients, Point 431, Case 1, Forward, T5-T7, T7-T12, T7-T13, T19-T17

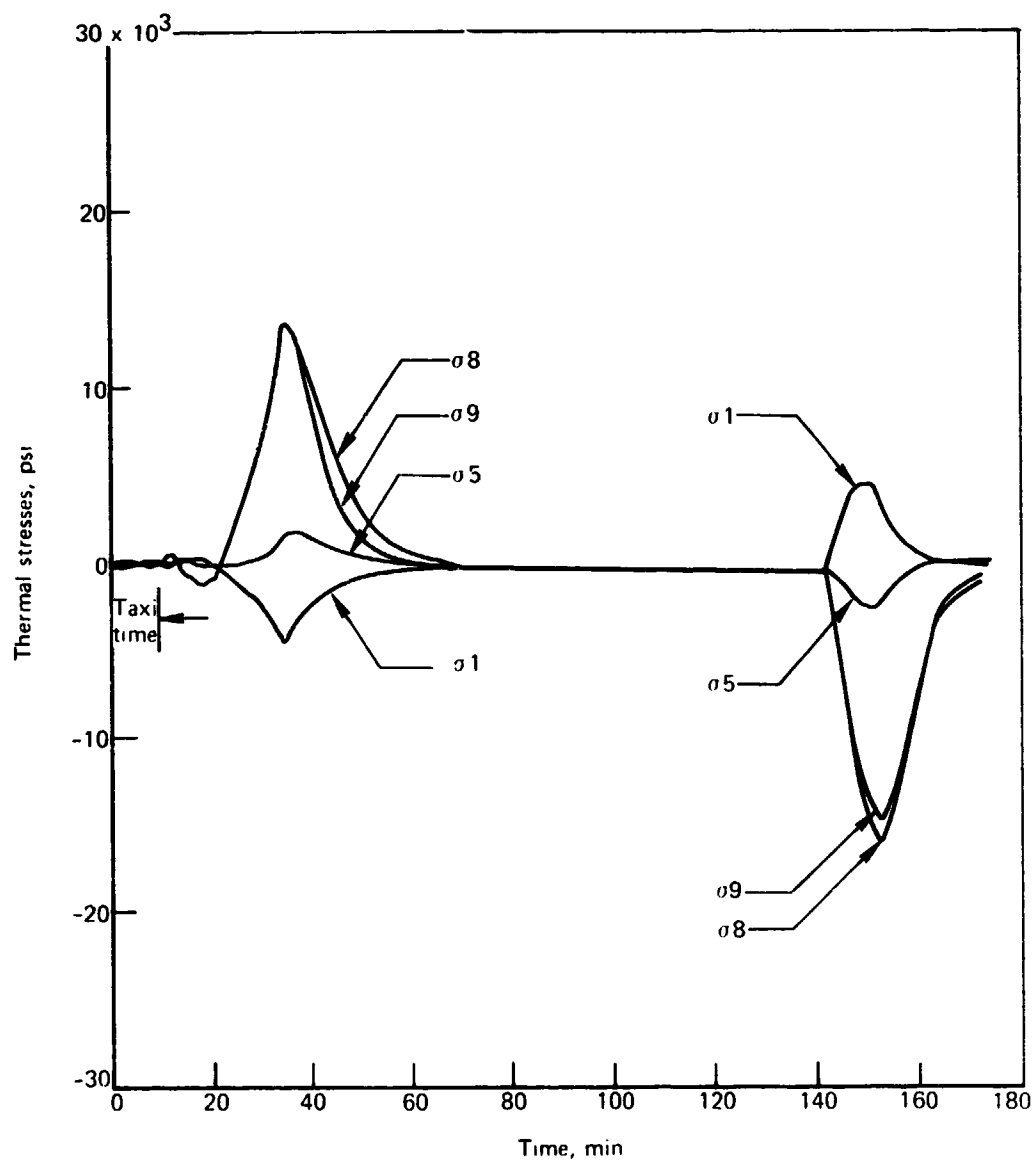


Figure 9-59. - Wing Spar Thermal Stresses, Point 431, Case 1, Forward, σ_1 , σ_5 , σ_8 , σ_9

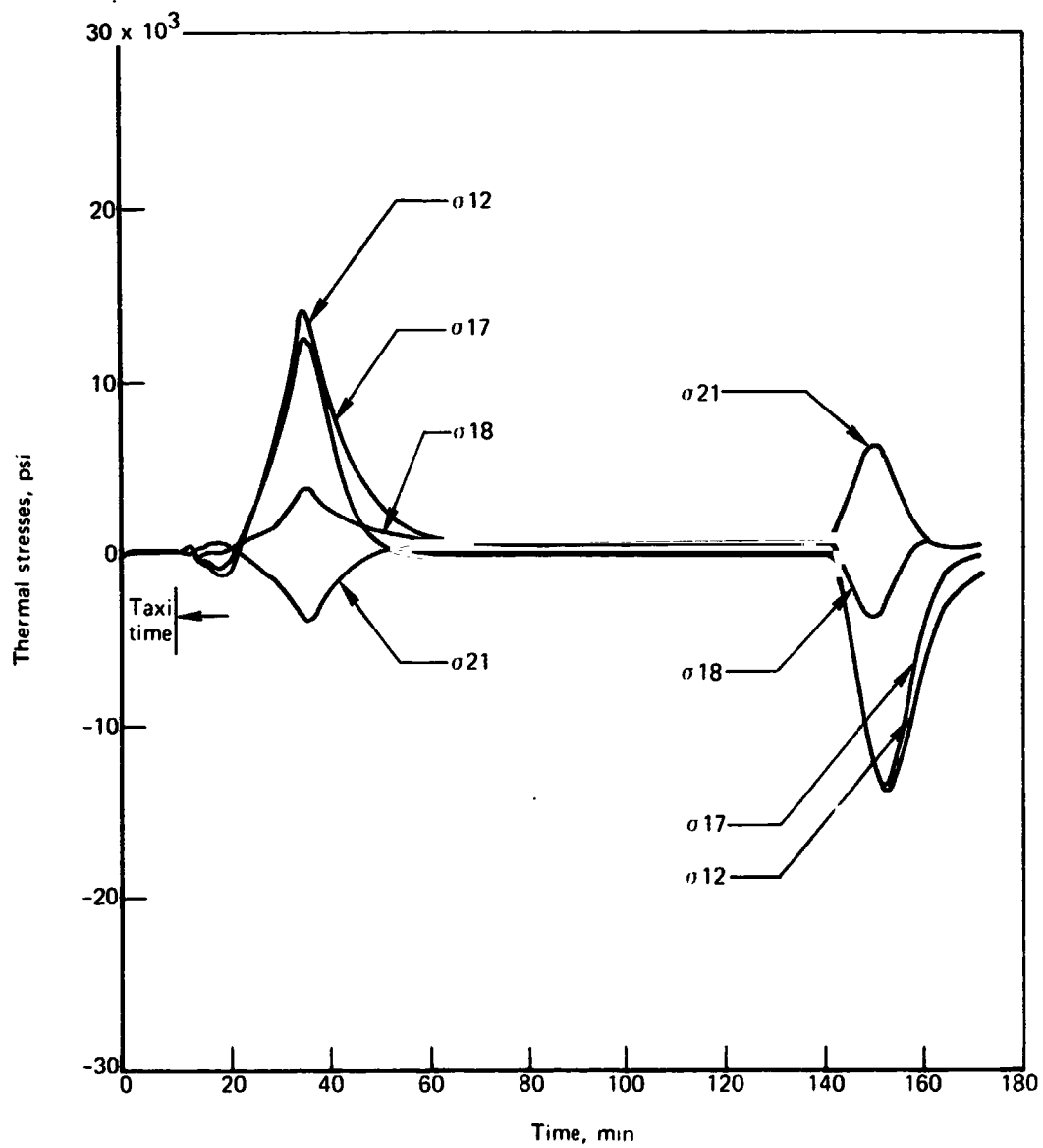


Figure 9-60. -Wing Spar Thermal Stresses, Point 431, Case 1, Forward, σ_{12} , σ_{17} , σ_{18} , σ_{21}

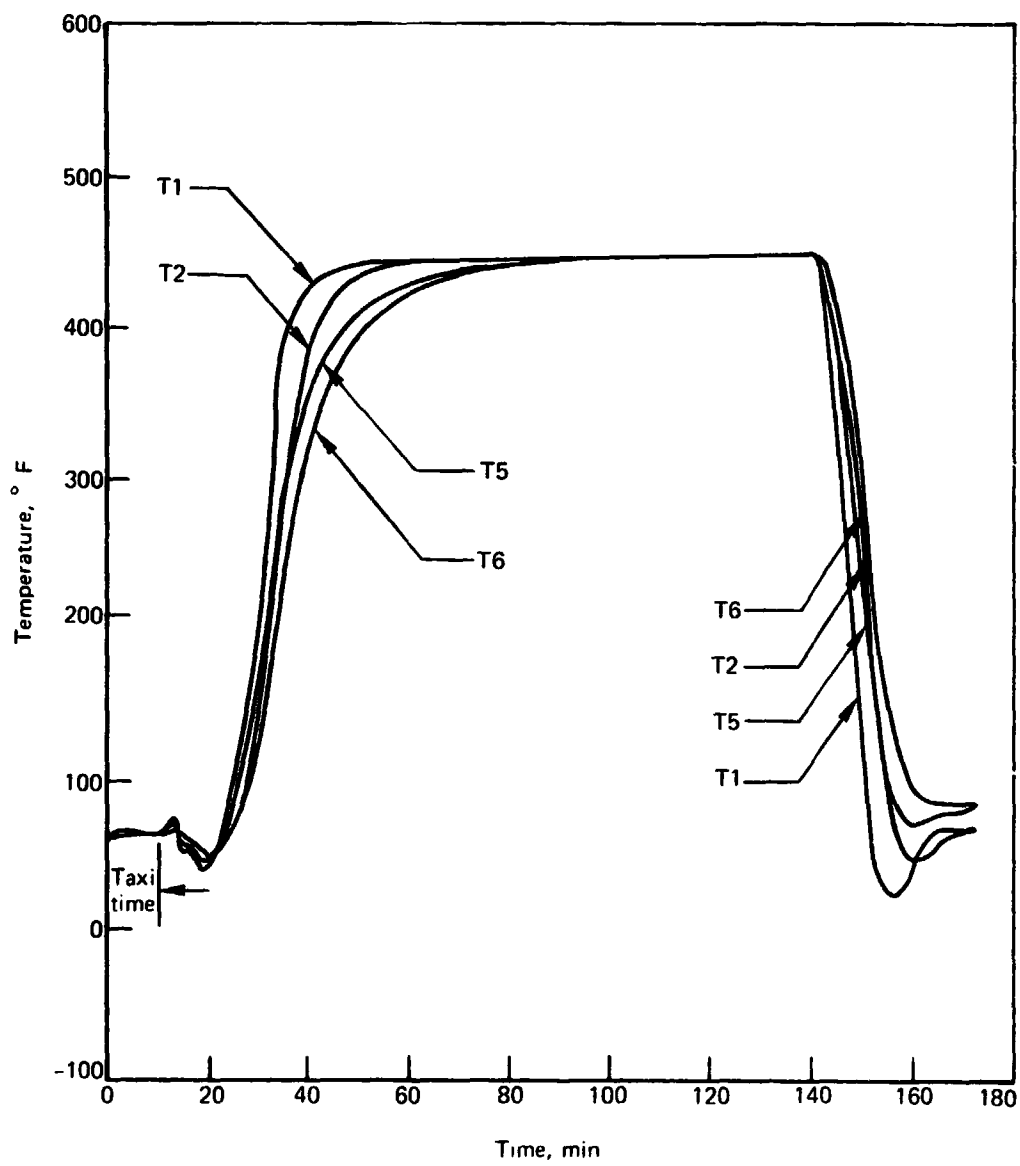


Figure 9-61.—Wing Spar Temperatures, Point 431, Case 2, Aft, T1, T2, T5, T6

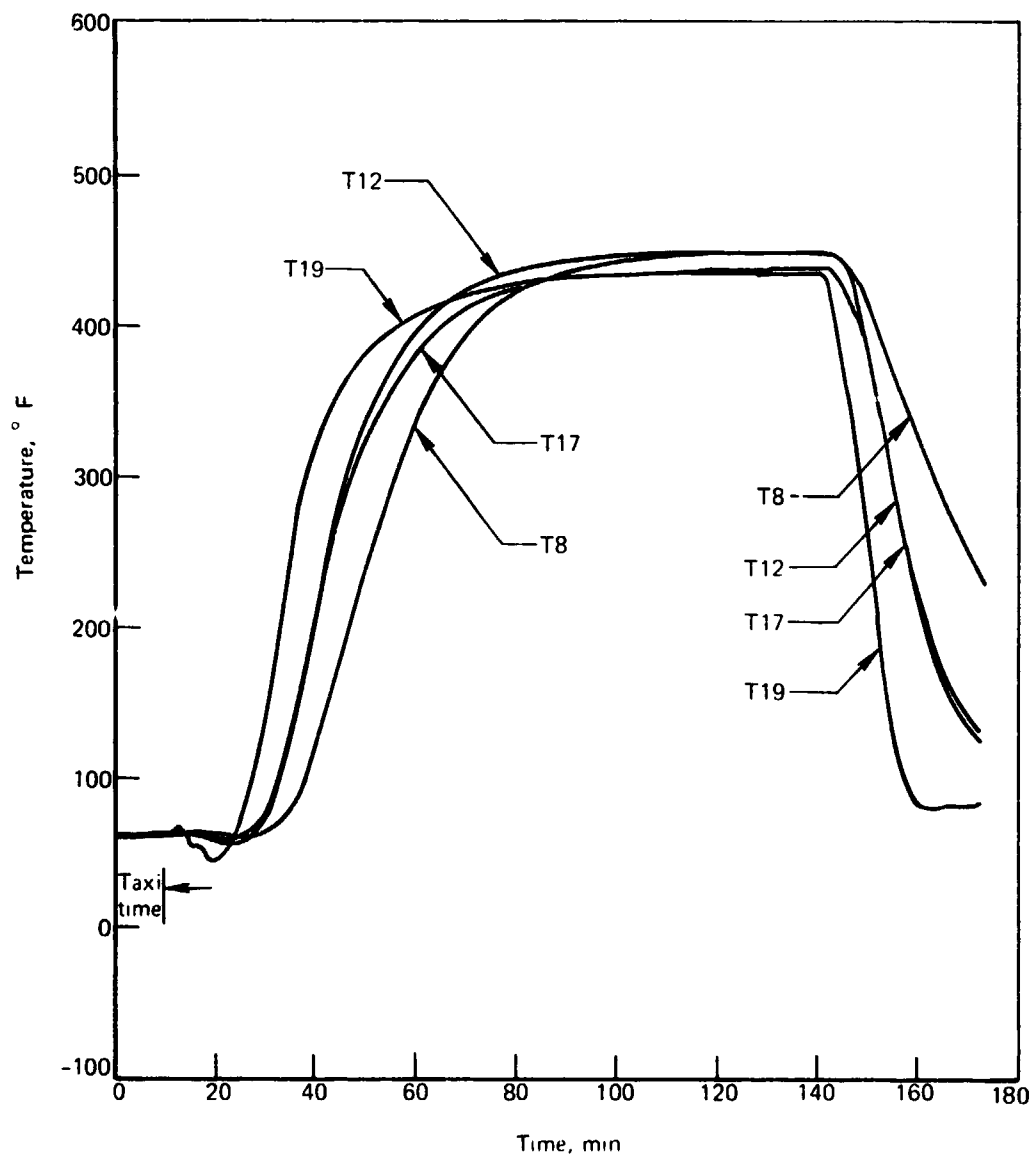


Figure 9-62.—Wing Spar Temperatures, Point 431, Case 2, Aft, T8, T12, T17, T19

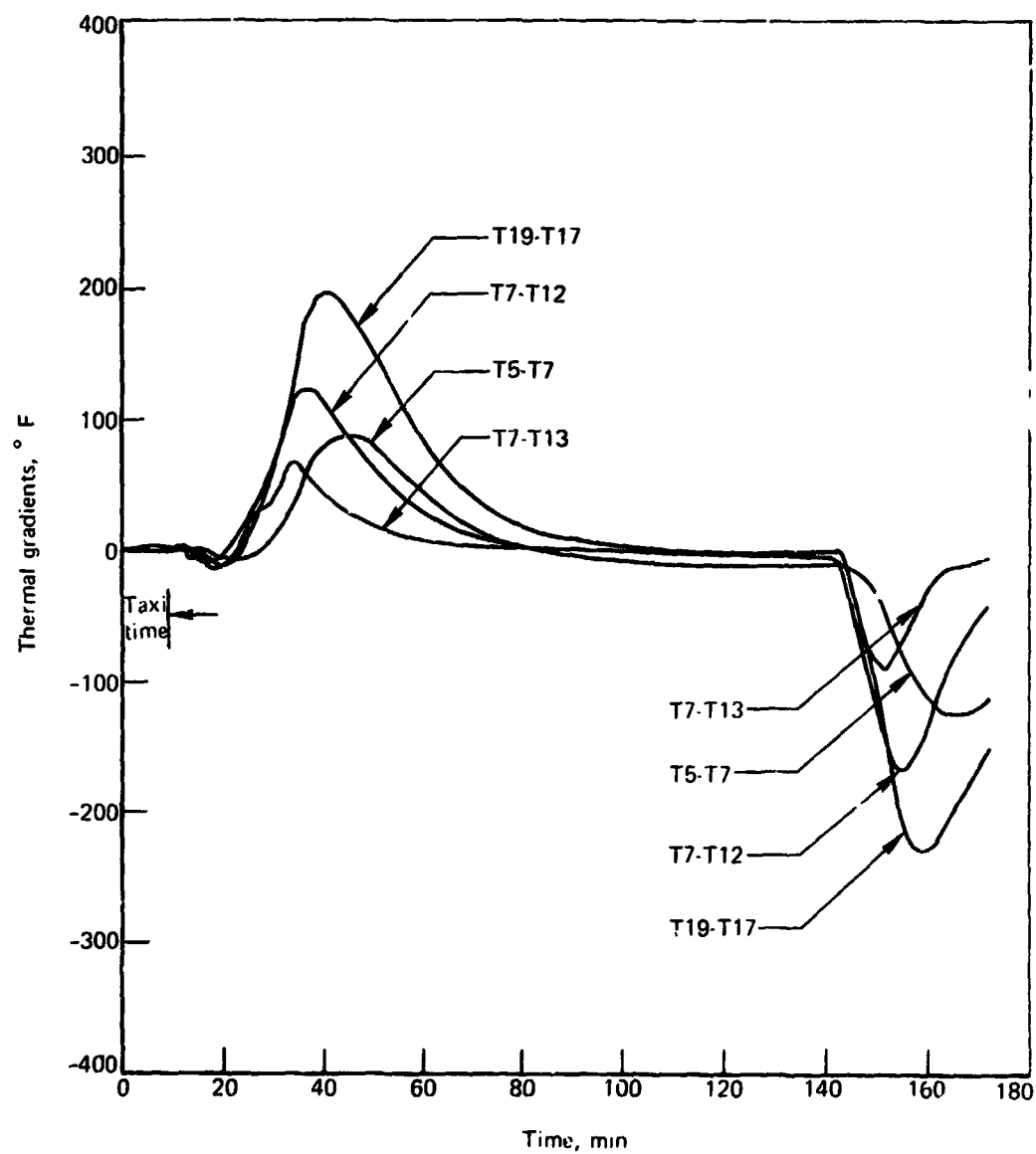


Figure 9-63.—Wing Spar Thermal Gradients, Point 431, Case 2, Aft, T5-T7, T7-T12, T7-T13, T19-T17

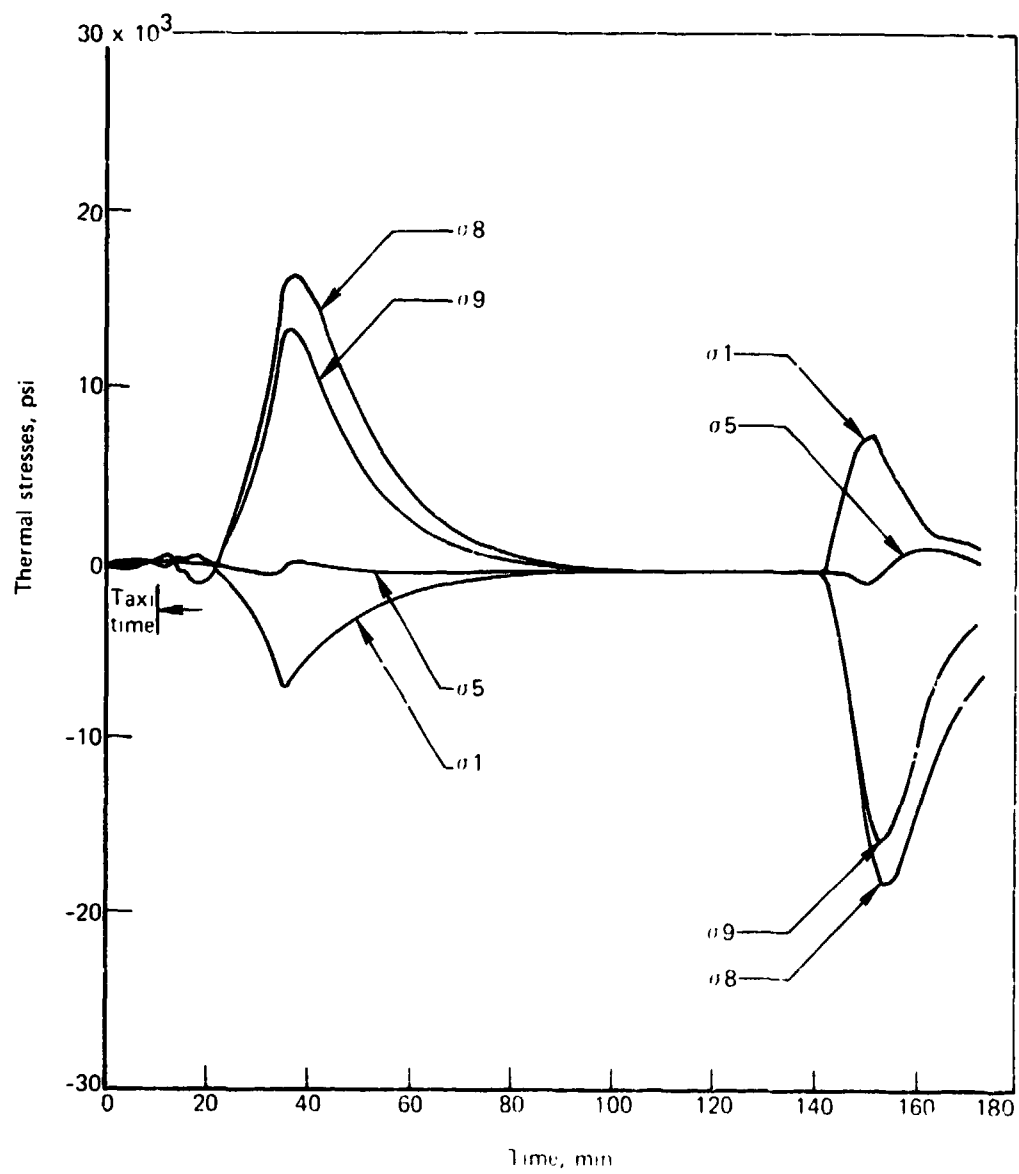


Figure 9-64. - Wing Spar Thermal Stresses, Point 43; Case 2, Aft, σ_1 , σ_5 , σ_8 , σ_9

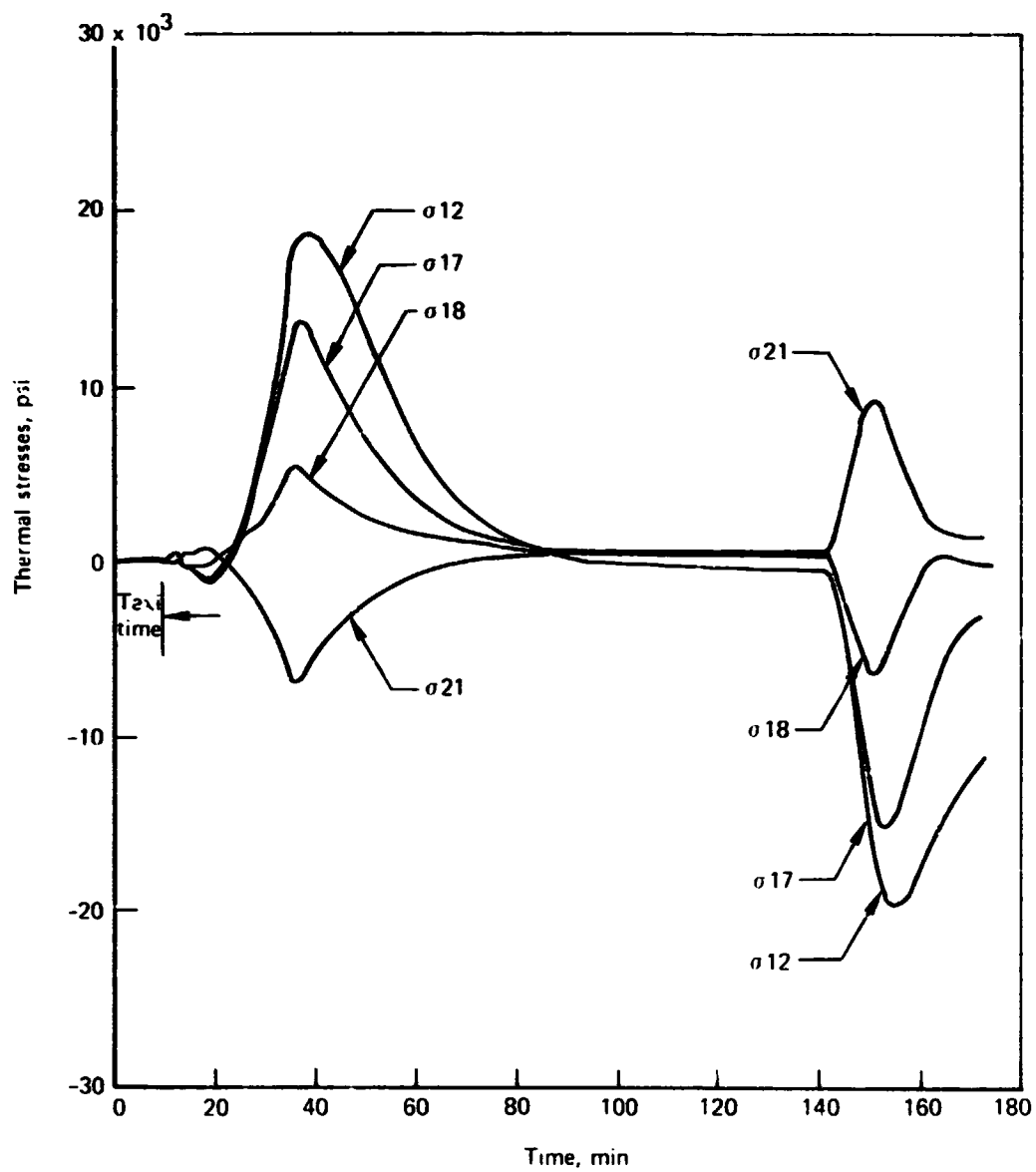
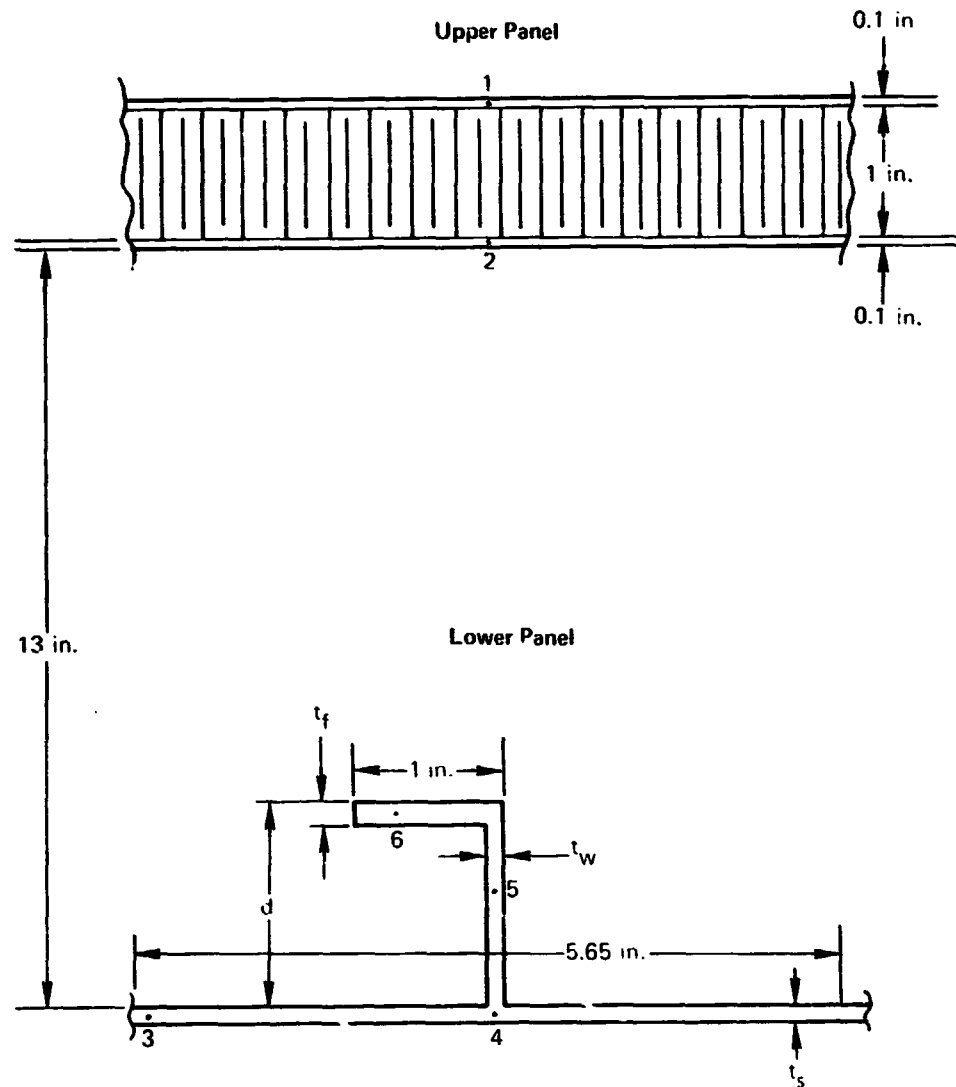


Figure 9-65.—Wing Spar Thermal Stresses, Point 431, Case 2, Aft, σ_{12} , σ_{17} , σ_{18} , σ_{21}

Distance from LE = 320 in.
 Sweep angle = 70°
 Lower panel stiffener pitch = 5.65 in.



Dimension	Case 1 Forward of 431, in.	Case 2 Aft of 431, in.
d	1.5	1.75
t_f	0.095	0.1
t_w	0.06	0.08
t_s	0.116	0.17

Figure 9-66.—Wing Panel Dry Bay Area, Point 431

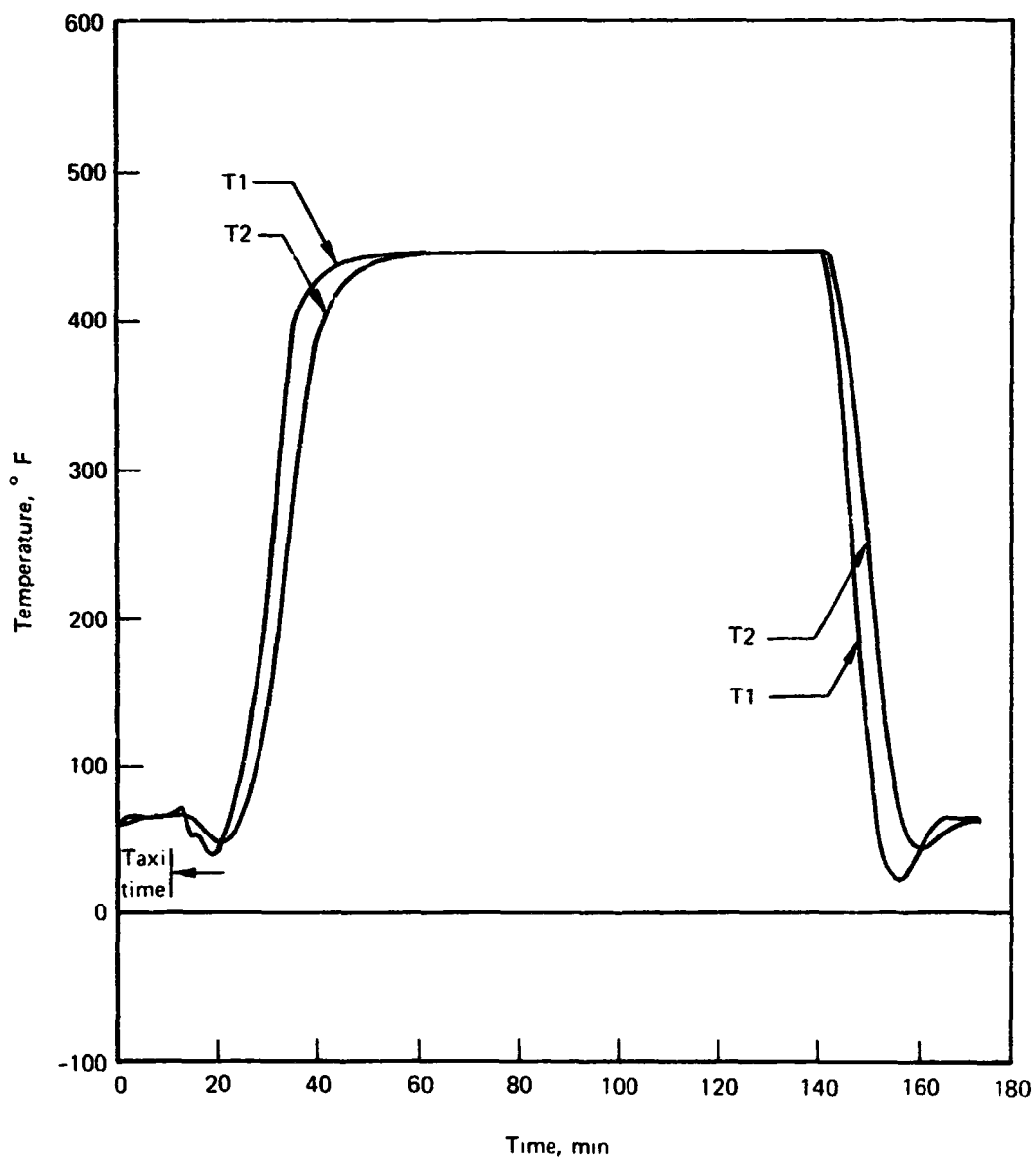


Figure 9-67.—Wing Panel Temperatures, Point 431, Case 1, Forward, T1, T2

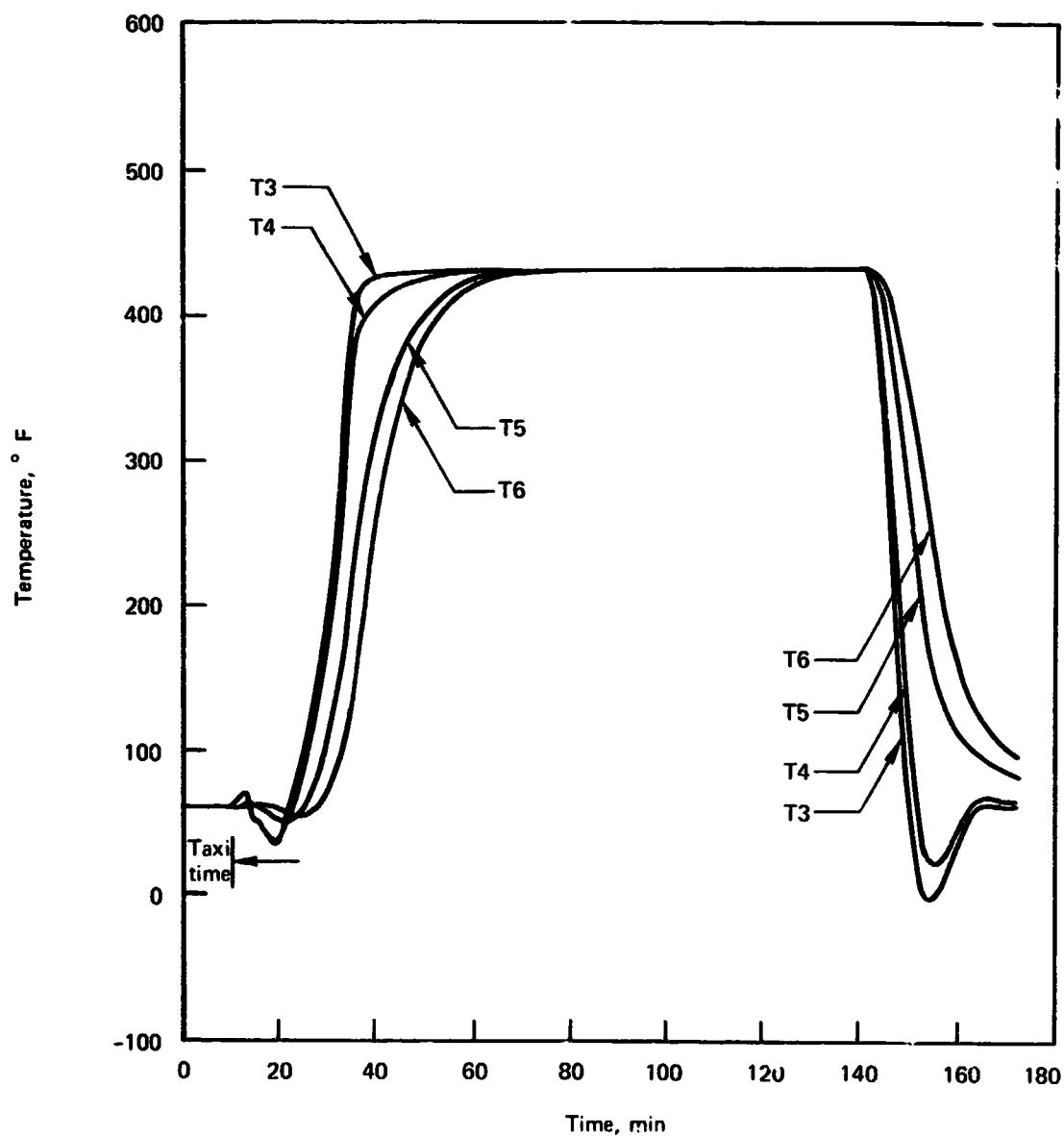


Figure 9-68.—Wing Panel Temperatures, Point 431, Case 1, Forward, T3, T4, T5, T6

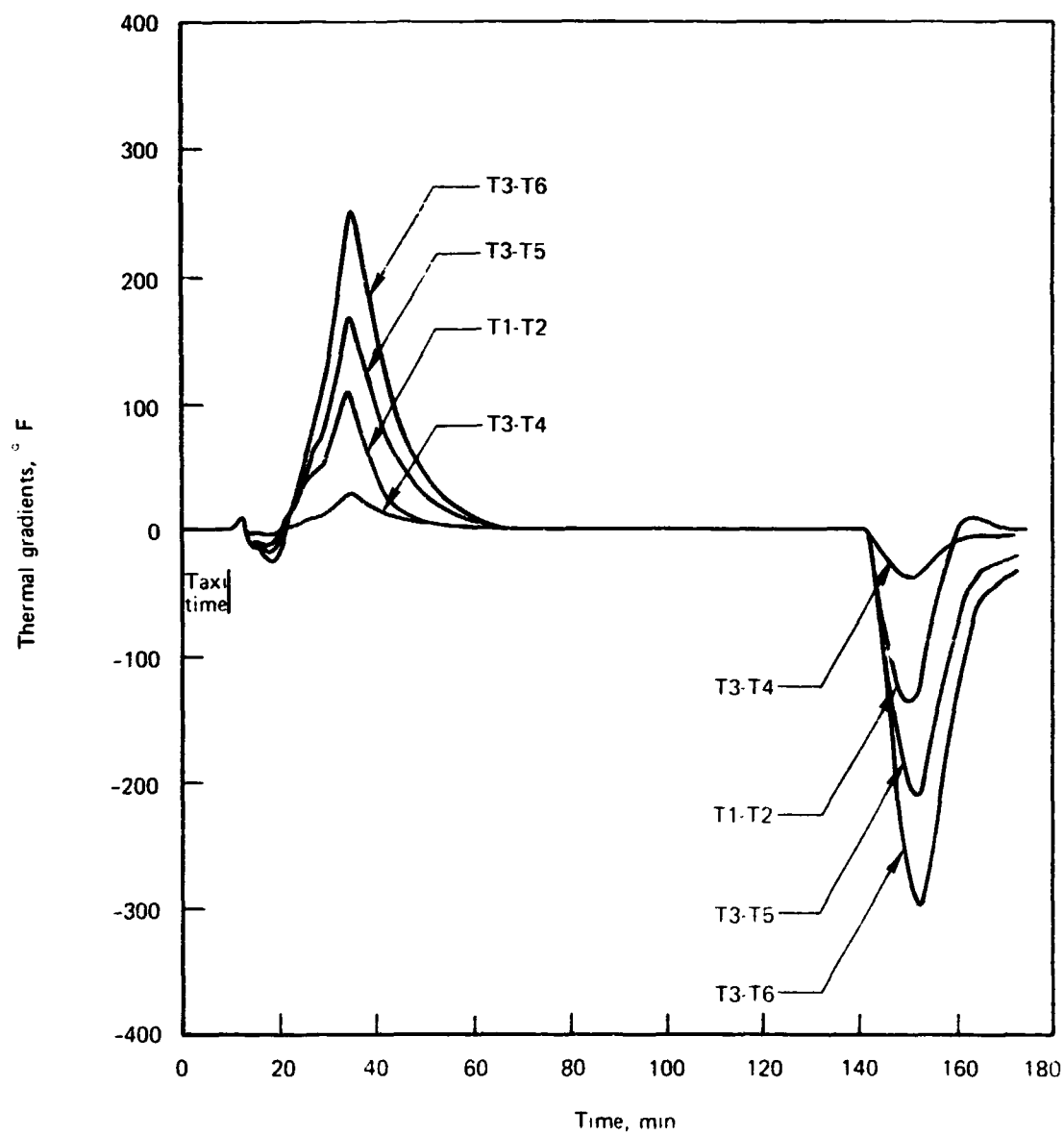


Figure 9-69.—Wing Panel Thermal Gradients, Point 431, Case 1, Forward, T1-T2, T3-T4, T3-T5, T3-T6

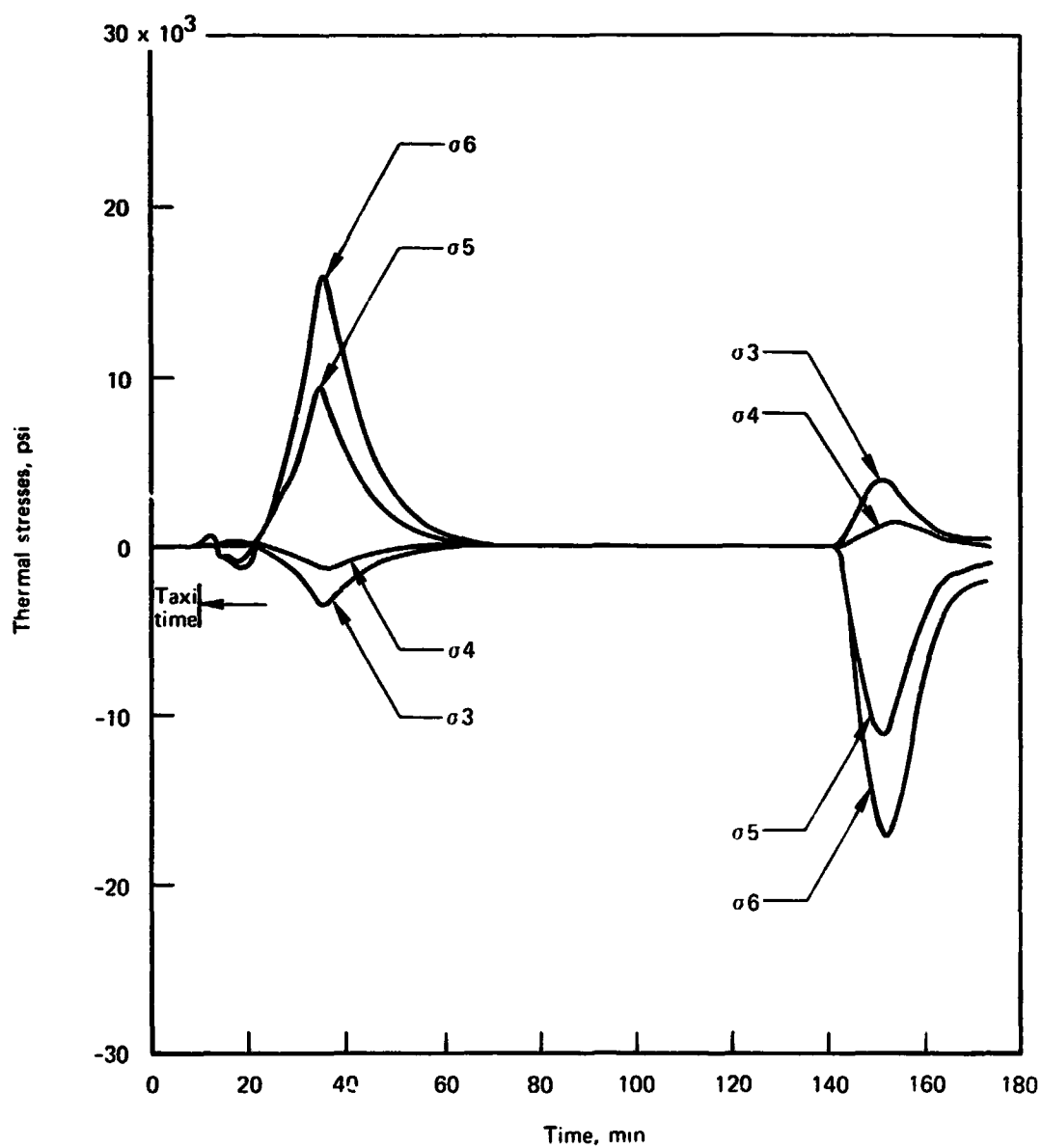


Figure 9-70.—Wing Panel Thermal Stresses, Point 431, Case 1, Forward, σ_3 , σ_4 , σ_5 , σ_6

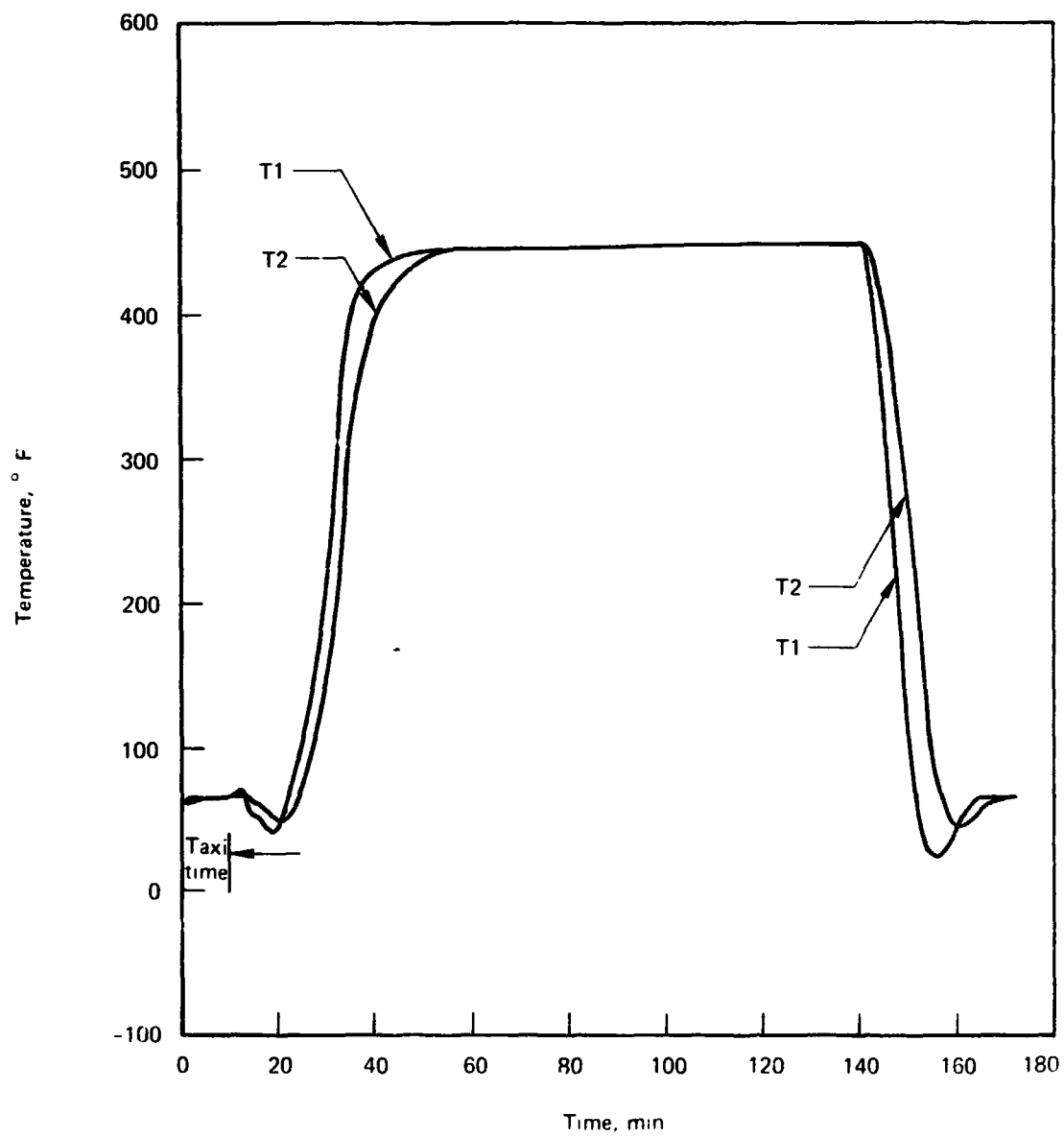


Figure 9-71.—Wing Panel Temperatures, Point 431, Case 2, Aft, T1, T2

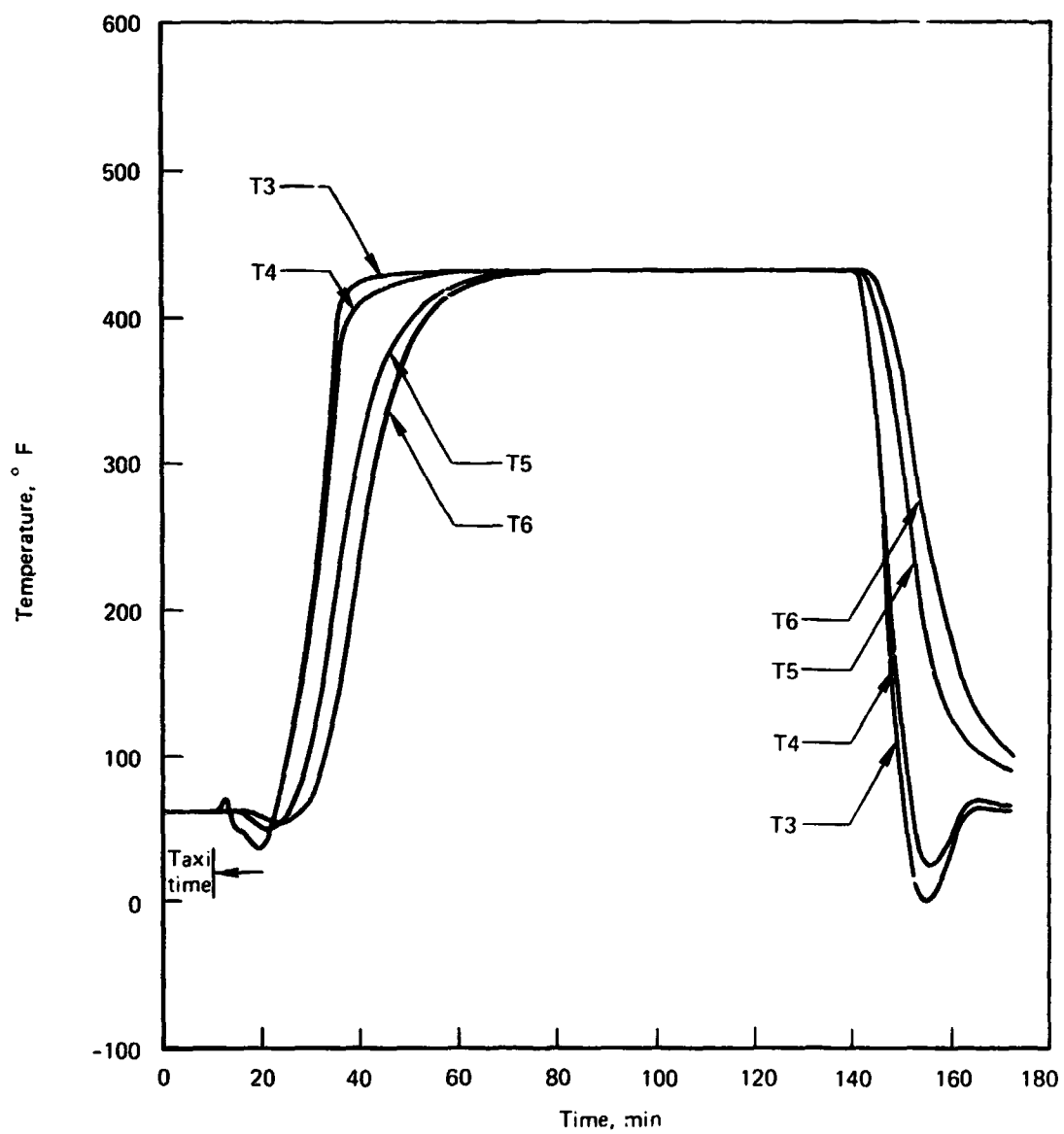


Figure 9-72.—Wing Panel Temperatures, Point 431, Case 2, Aft, T3, T4, T5, T6

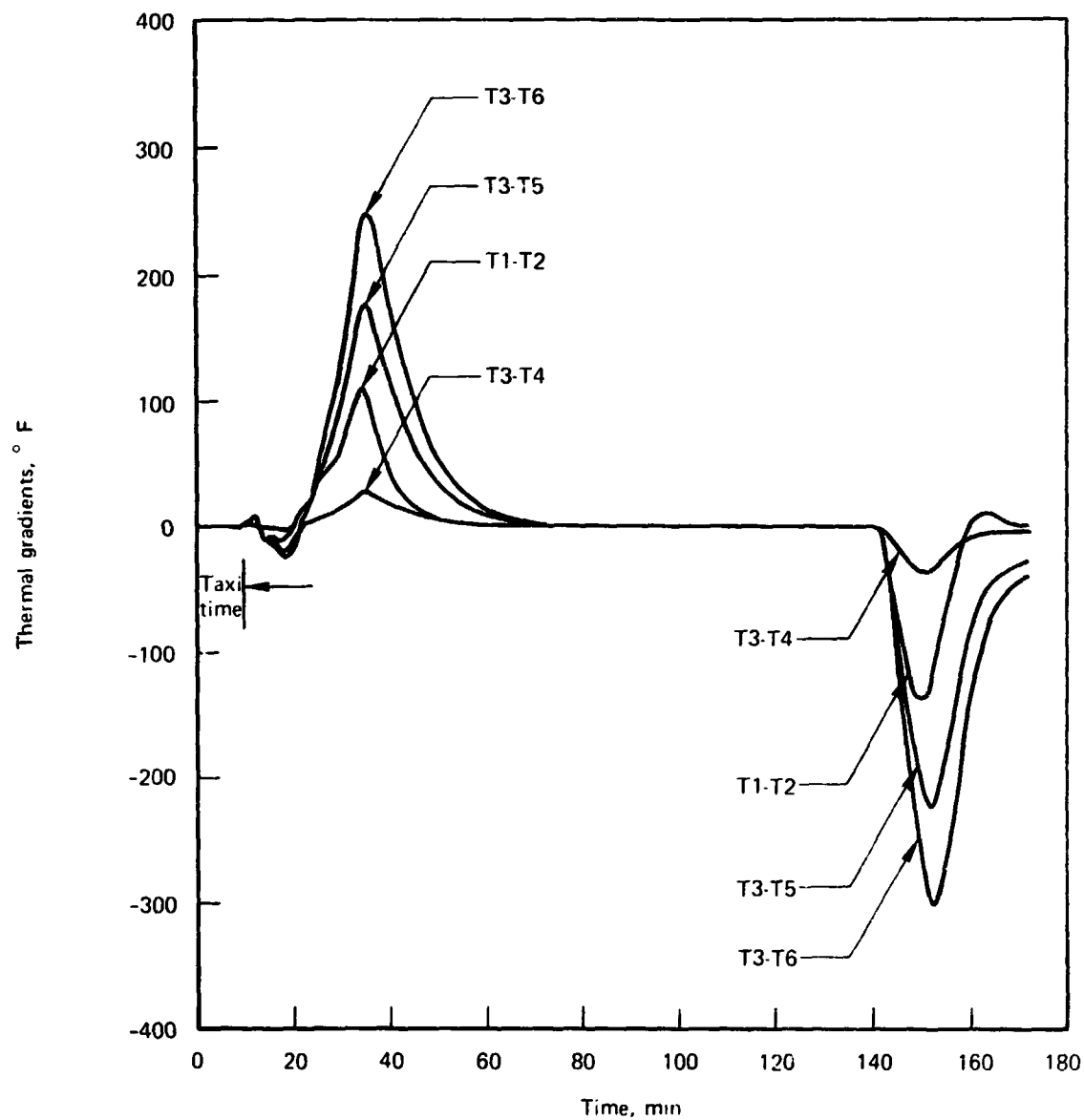


Figure 9-73.—Wing Panel Thermal Gradients, Point 431, Case 2, Aft, T1-T2, T3-T4, T3-T5, T3-T6

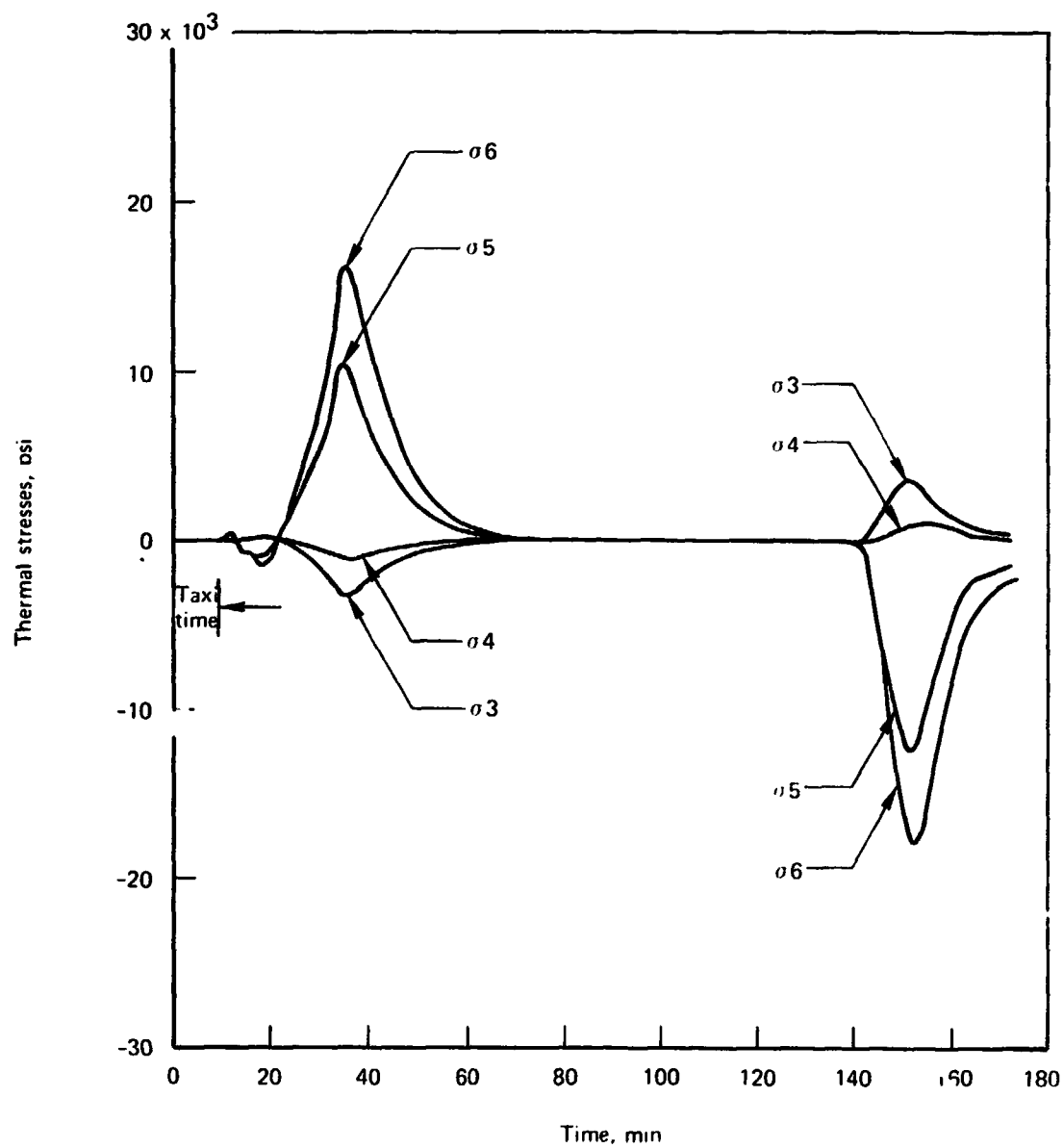
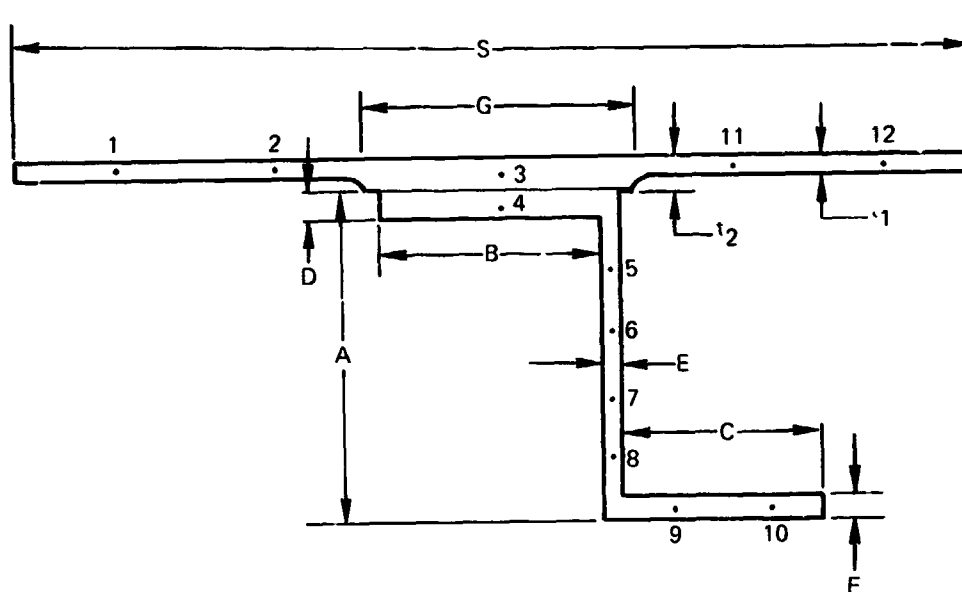


Figure 9-74. -Wing Panel Thermal Stresses, Point 431, Case 2, Aft, σ_3 , σ_4 , σ_5 , σ_6



Case	1	2
Point	5 (lower crown)	6 (upper crown)
Body station	1720.0 in.	2474.0 in.
Dimension	in.	in.
A	1.25	1.25
B	1.08	1.08
C	1.00	1.00
D	0.15	0.12
E	0.06	0.12
F	0.25	0.2
G	1.25	1.25
S	4.4	4.5
t_1	0.05	0.08
t_2	0.072	0.1

Figure 9-75.—Body Stringers, Points 5 and 6

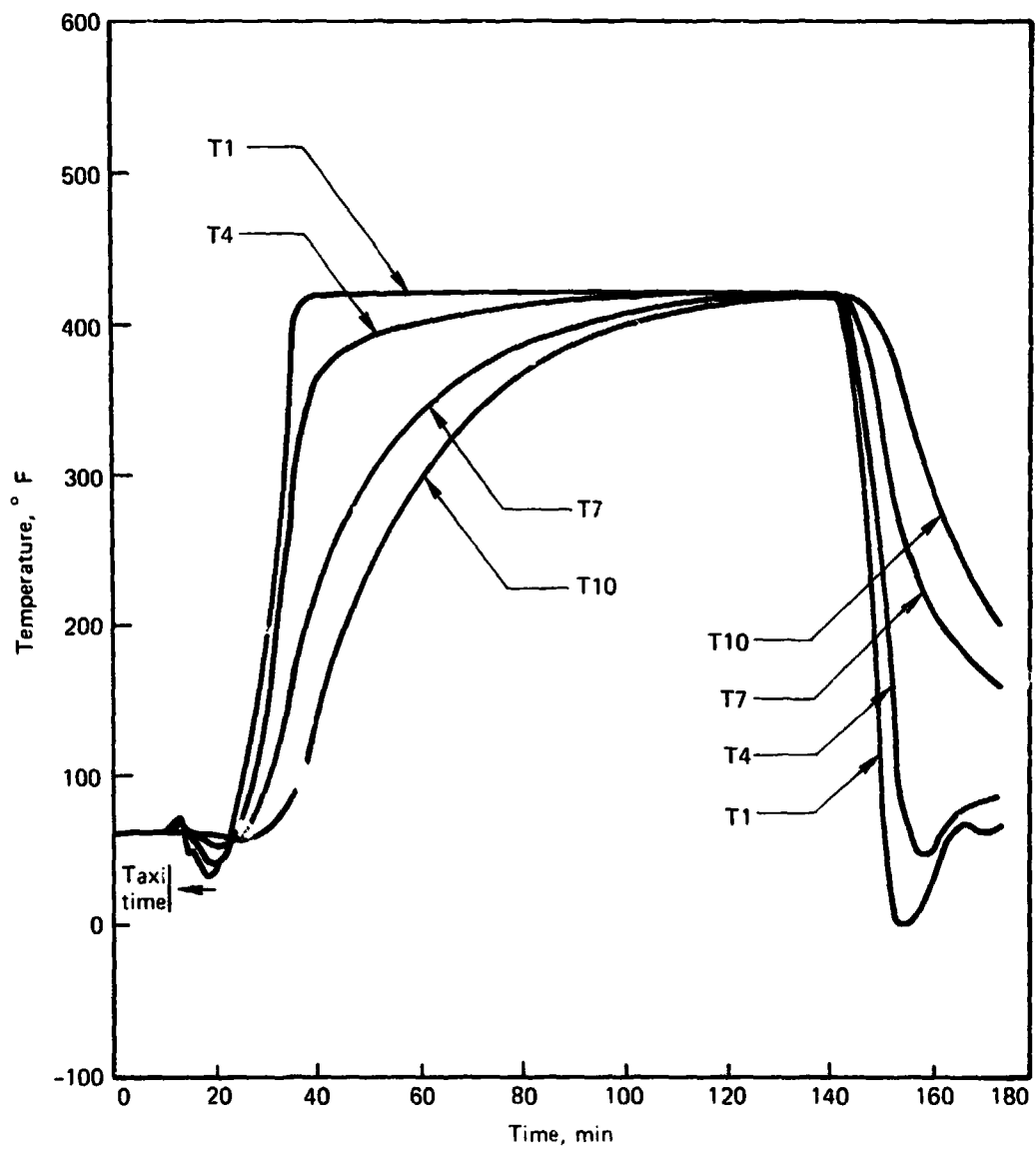


Figure 9-76.—Body Stringer Temperatures, Point 5, Case 1, T1, T4, T7, T10

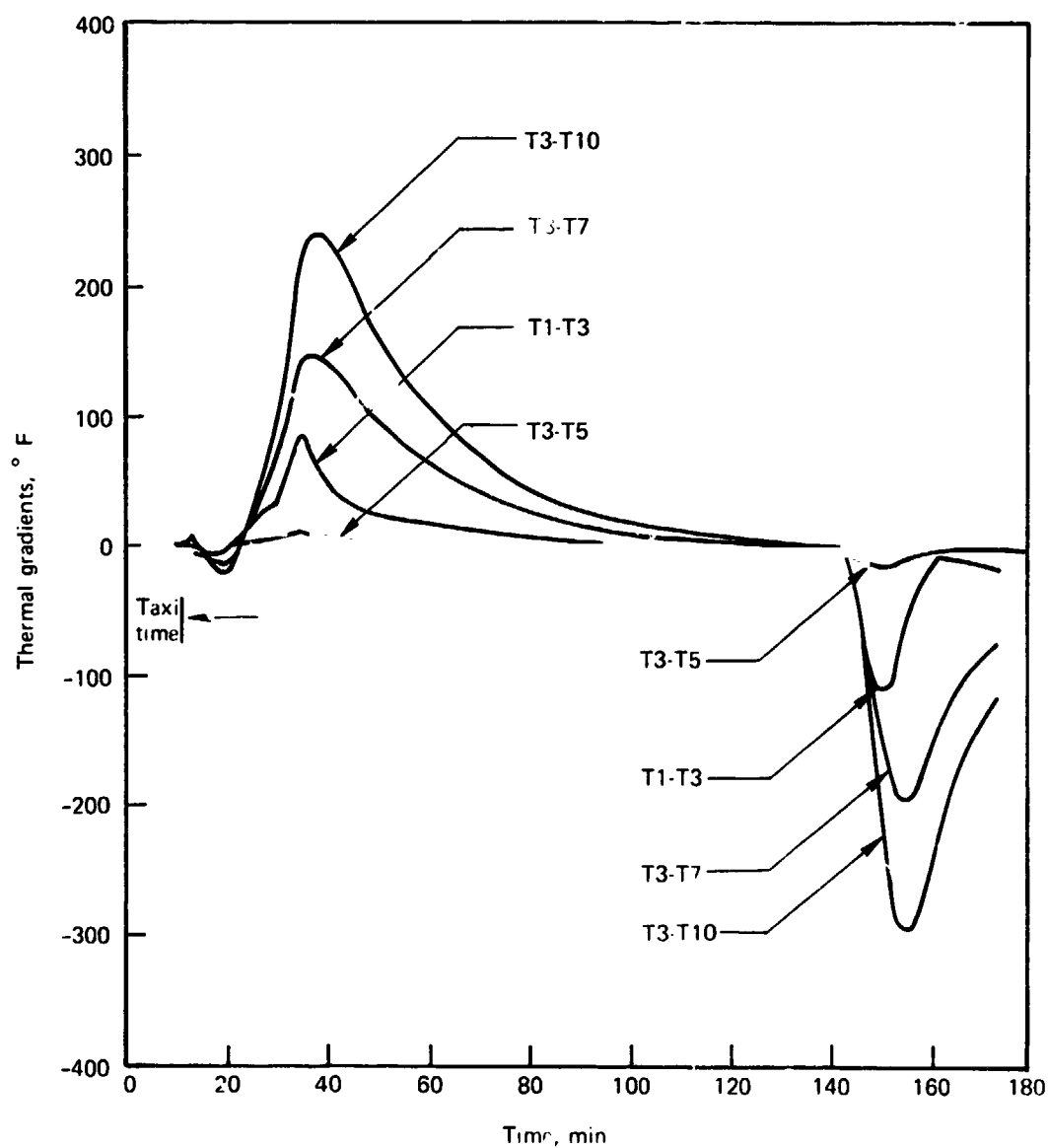


Figure 9-77.—Body Stringer Thermal Gradients, Point 5, Case 1, T1-T3, T3-T5, T3-T7, T3-T10

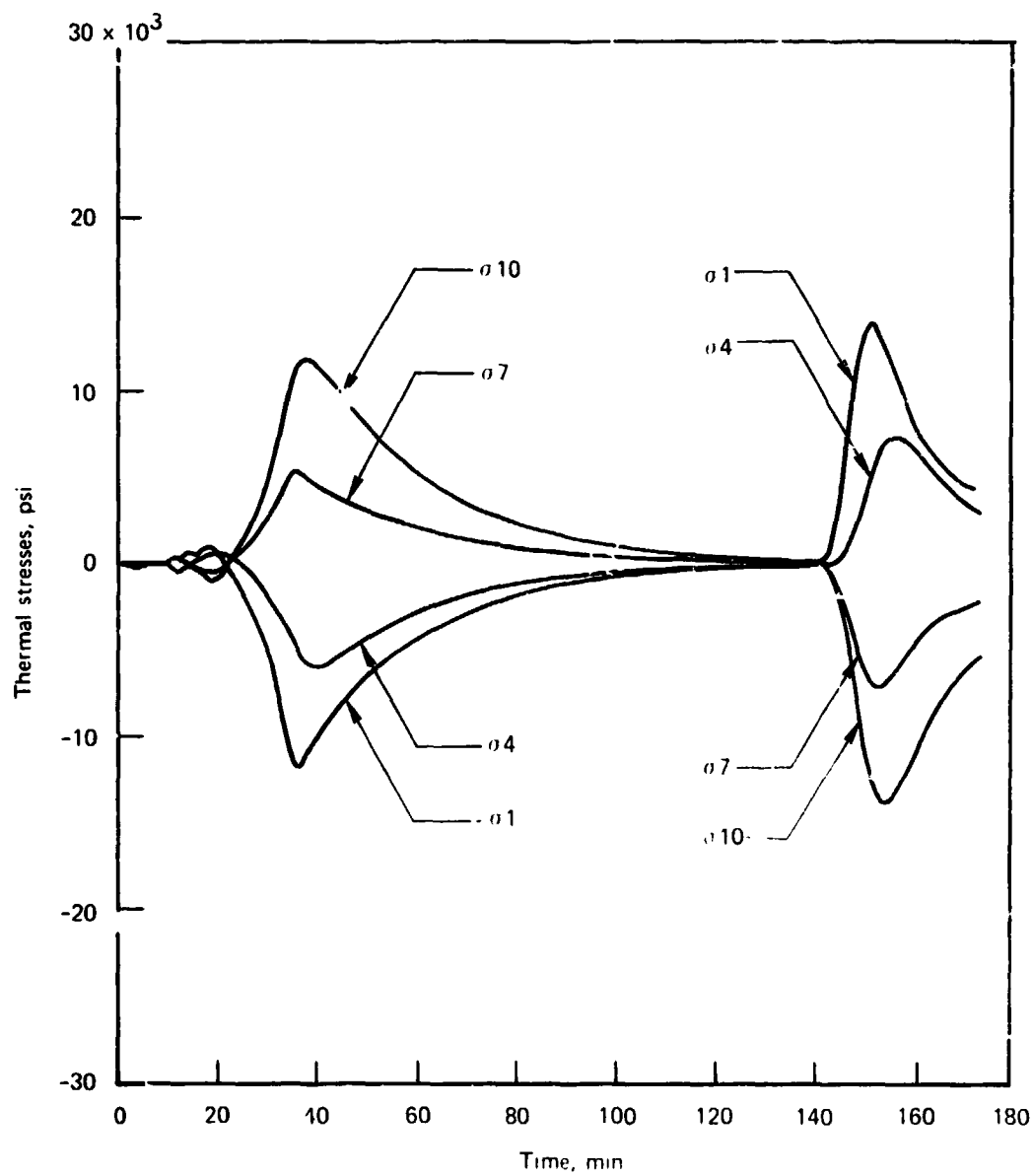


Figure 9-78.—Body Stringer Thermal Stresses, Point 5, Case 1, $\sigma 1$, $\sigma 4$, $\sigma 7$, $\sigma 10$

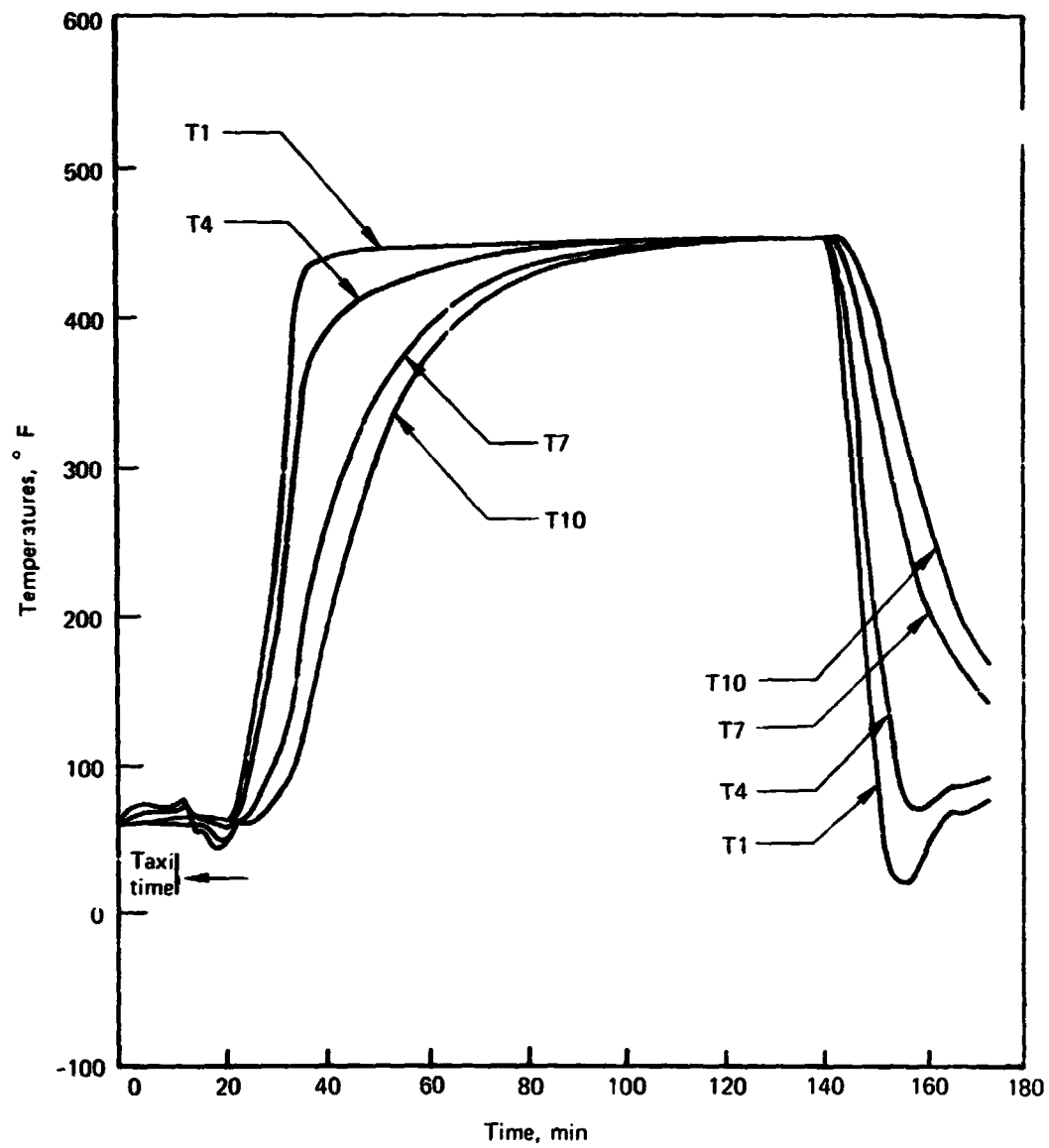


Figure 9-79.—Body Stringer Temperatures, Point 6, Case 2, T1, T4, T7, T10

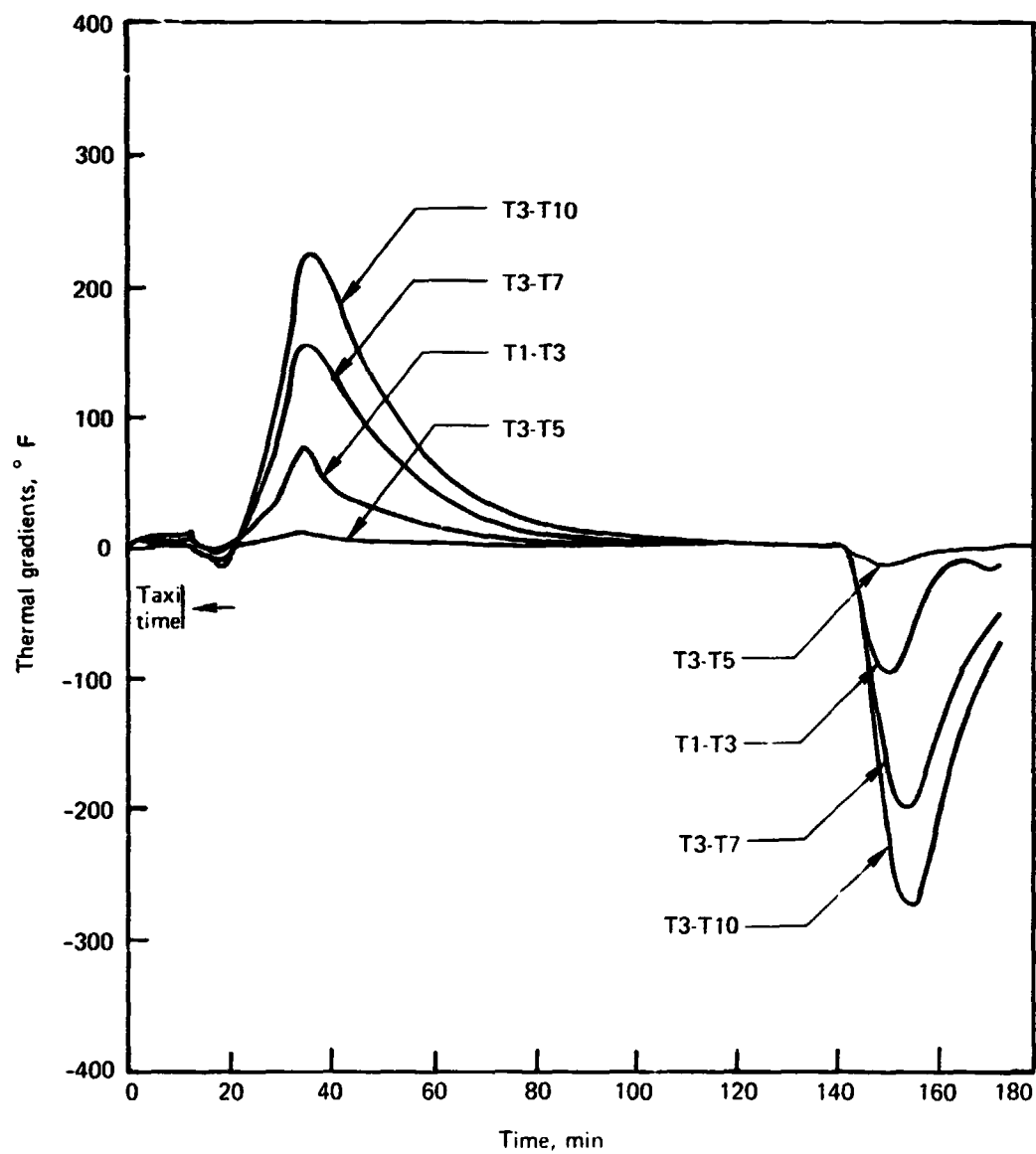


Figure 9-80.—Body Stringer Thermal Gradients, Point 6, Case 2, T1-T3, T3-T5, T3-T7, T3-T10

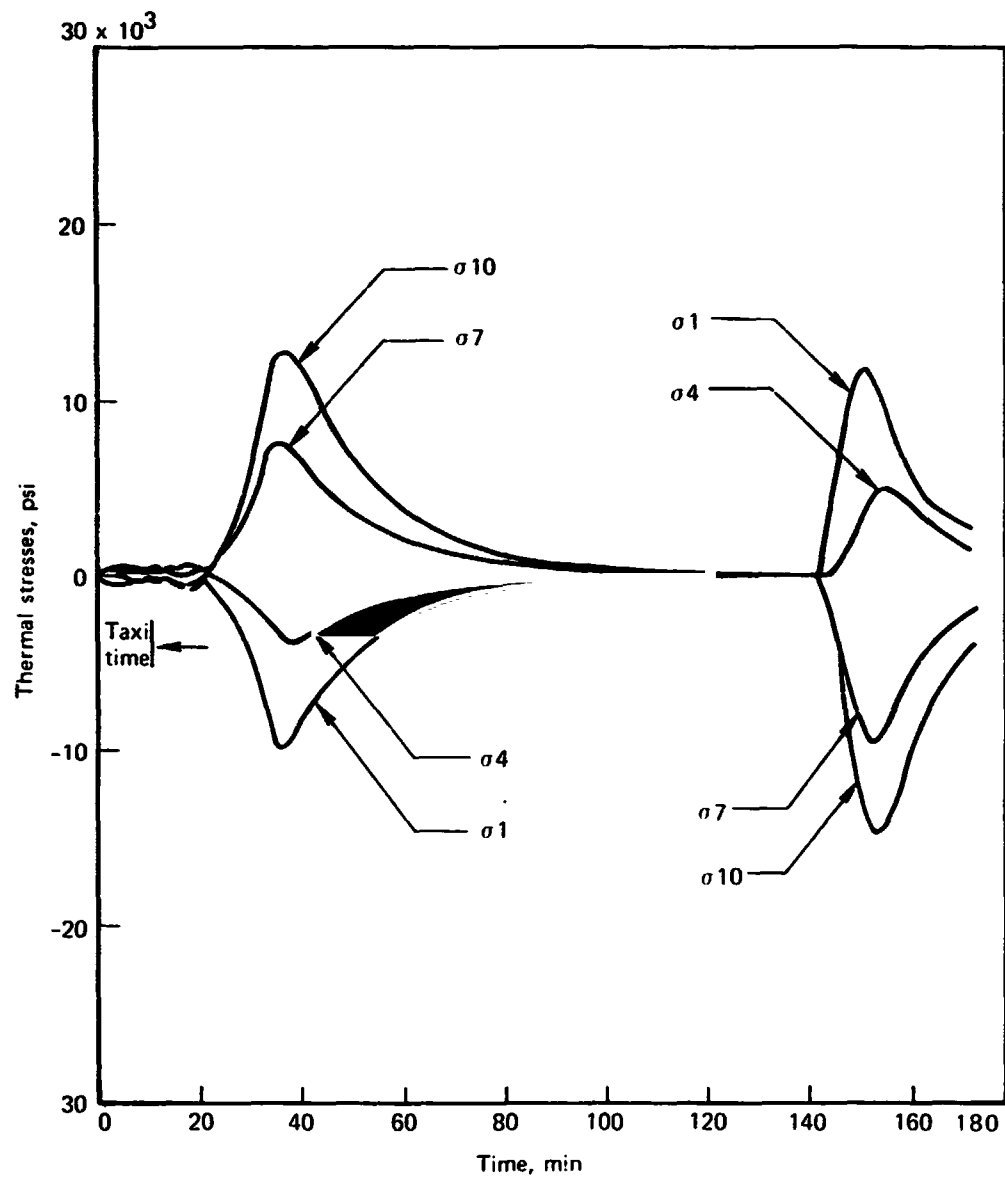


Figure 9-81.—Body Stringer Thermal Stresses, Point 6, Case 2, σ_1 , σ_4 , σ_7 , σ_{10}

SECTION 10

STRESS ANALYSIS

by

**J. M. Hopper
V. D. Bess
F. D. Flood**

CONTENTS

	Page
STRESS ANALYSIS	522
Introduction	522
Resizing Criteria	522
Resize Algorithm	523
Implementation of Design Guidelines	523
Checkout	525
Structural Sizing	525
REFERENCES	526

TABLES

No.		Page
10-1	Element Subset Definition	527
10-2	Design Load Cases	528
10-3	Sources of Sizing Data for Design	530
10-4	Basic Material Tables	531
10-5	Shear Buckling Allowable Stress	532
10-6	Compression Buckling Allowable Stress	533
10-7	Temperature Design Data	534

FIGURES

No.		Page
10-1	Typical Mechanical Properties	535
10-2	Typical Instability Allowables	536
10-3	Wing Structure Regions	537
10-4	Wing Spar Element Subsets	538
10-5	Wing Cover Element Subsets	539
10-6	Internal Loads and Stress Analysis Sequence	540
10-7	Lower Bound Data	541
10-8	Typical Wing Panel Resizing Results	542
10-9	Critical Design Conditions - Upper Surface	543
10-10	Critical Design Conditions - Lower Surface	544
10-11	Effect of Resizing on Theoretical Wing Weight	545
10-12	Effect of Resizing on Wing Spar Theoretical Weight	546
10-13	Effect of Resizing on Wing Panel Theoretical Weight	547

SECTION 10

STRESS ANALYSIS

INTRODUCTION

The arrow-wing structure was sized for strength requirements using the integrated structural analysis and design capabilities of the ATLAS system (ref. 10-1). In preparation for the stress analysis, the mathematical model was defined, checked-out, and loads were generated in the ATLAS format, as described in previous sections. In preparation for the resizing cycles, allowables and sizing limitations were defined. The checkout activities were the most difficult of all to estimate in terms of flow time and manpower, due to lack of experience on models of this size. These estimates were generally low, resulting in budget over-runs and slippage of milestones.

RESIZING CRITERIA

Four sets of criteria were necessary to accomplish the resizing of the structural elements:

1. Mechanical properties of the materials were defined for various temperature ranges for those elements critical in tension;
2. Stability allowables were defined for those elements critical in compression;
3. Those elements that were not to be resized were defined;
4. The constraints on the resizing of elements were defined, such as minimum gauges, fail-safe areas of spar chords, etc.

Sets of allowables were defined based on information of the type shown in figures 10-1 and 10-2. These data provide the mechanical properties of materials and stability allowables for resizing individual elements. Effects of thermal stresses were included by reducing the allowables on each member by an amount appropriate for the thermal stress, rather than superimposing the thermal stress on the basic member stress.

In establishing stability and material allowables to be used for resizing, type of construction, panel size, and thermal environment were considered for wing cover elements. Spar web depth and type of construction, i.e., sine-wave or sheet-stiffener webs, were considered for spar elements.

After selecting the elements to be automatically resized, constraints on the range of sizing were established. Constraints for spar chords included practical design and manufacturing limitations and fail safety. The fail safety criterion required that a spar chord must have a cross-sectional area equal to or greater than twenty five percent of the area of the largest adjacent skin panel. For skin panels the requirements included walking loads, hail and lightning criteria and manufacturing and handling limitations.

Those areas for which an automated resize was not desired were identified and sizing constraints were imposed. The elements aft of the rear spar and forward of the leading edge spar were not included in the elements to be machine resized because they were either minimum gage or were established by criteria other than strength, for example handling requirements. The fuselage elements were not resized because of the problem posed by allowables for buckled skin panels. These elements were manually sized, with convergence occurring in two cycles. Also, elements that were not important in a structural sense but were required for accurate model behavior, such as control surface hinges and the landing gear uplock, were excluded from resizing. Finally the nacelle support elements were excluded from machine sizing because these items were covered by special supplementary design conditions (such as engine seizure), as specified in FAR 25.

The spar webs in the fuel tank areas are critical for fuel pressure loads due to crash load factors and refueling pressures. Since these load conditions were not included in stress analysis and resizing, the spar web weights were adjusted to account for the additional stiffening required.

RESIZE ALGORITHM

The principal concern in establishing the design algorithm was to have the greatest possible accuracy in resizing of structural elements loaded in biaxial compression and shear. The allowable stress-ratio interaction equation used for evaluation of margins of safety is (ref. 10-2)

$$R = \left[\frac{R_x}{1 - R_{xy}^2} \right]^4 + \frac{R_y}{1 - R_{xy}^4}$$

where R_x , R_y and R_{xy} are the ratios of the actual to allowable inplane load for axial and shear loads. For strength critical loading conditions, a modified Hill's yield criterion was used.

The resizing algorithm is a first order approximation, and thus is accurate only for relatively small variations in thickness. A local iteration based on the Newton-Raphson method was developed to assure a converged design after each design cycle and to speed convergence of the fully stressed design. During each resize cycle, it is assumed that the loads on individual elements are not altered as the sizing varies. Successive cycles of stress analysis and design, however, recognize and provide for the redistribution of internal loads as the member sizing varies.

IMPLEMENTATION OF DESIGN GUIDELINES

It was advantageous to group together elements having the same design guidelines to minimize the amount of input data required for the design. In addition to the considerations of element size, construction, and thermal environment previously mentioned, similar element reference frames were required for cover elements. A review of the orientation of cover elements revealed that a few did not conform to the required input data format. After appropriate revisions were made to these element orientations,

elements meeting the commonality criteria were grouped into subsets. An illustration of the common regions of wing structure is given in figure 10-3. A list of subsets used for design inputs is given in table 10-1 and illustrations of the wing spar and wing cover element subsets are given in figures 10-4 and 10-5, respectively.

The most critical design load cases from section 8 were selected and loads were derived for application to the structural nodes for stress analysis. For example, an unsymmetric load case was broken down to its symmetric and antisymmetric components, so that elastic analyses could be performed on the half-airplane model, with appropriate boundary conditions at the airplane plane of symmetry for symmetric and antisymmetric loading conditions. The design load conditions were identified after superposing component deflections and multiplying by the appropriate factors-of-safety to obtain ultimate design load conditions. These superposed deflections then formed the basis for the stress analysis for the selected design conditions. This procedure, starting from the applied external load conditions and proceeding through the stress analysis is illustrated in figure 10-6. Table 10-2 identifies and describes all the design load cases used in the stress analysis.

Material and stability allowables for specific groups of elements were specified with a combination of sizing data (which are referenced to material and stability files) and temperature data (which are referenced to the temperature data files).

In order to define allowables for the upper and lower cover elements accounting for differences in structural concept, thermal stress, or temperature, eleven sets of sizing data were required. These consisted of combinations of eight sets of materials data, five sets of allowable shear buckling tables and four sets of allowable compression buckling tables. Also, separate data sets were specified for upward bending and downward bending because of the different character of the loading in the upper and lower surfaces.

One sizing data set and temperature can be specified for each load case and element. The most convenient method of differentiating between the sizing data sets was to insert a qualifying symbol preceding the temperature callout, as a key to the loading on the structure. This was done by inserting a negative sign in front of the temperature for load cases having the lower surface in compression, with the positive temperature signifying the opposite case having the lower surface in tension. The stress analysis was reviewed to determine the state of stress in each cover element so that the proper sign could be given to the temperature for each subset load condition. The complete tables of sizing data, special materials, shear buckling, compression buckling and temperature information are given in tables 10-3 through 10-7, respectively.

In calculating both material and stability allowables, temperature effects on modulus were considered. However, the stiffness and stress analyses were not executed for different temperatures because the effect on load paths and element loads would have been negligible and the increase in computer costs would have been significant. The effects of thermally induced stresses caused by temperature gradients in the structure were included in the analysis by modifying the allowables used for resizing to account for these stress increments. The flight conditions at which these thermal gradient

effects are significant occur near room temperature. For convenience, these sets of allowables are identified in tables 10-4, 10-5, 10-6 and 10-7 by the use of temperature callouts from 68° to 75° F.

Constraints on the range of sizing were specified by lower bound information at both the element and subset level. For example lower bounds for covers and some spars were set up in subsets because common values were valid for large areas of the wing. Lower bounds for rear spar elements were specified at the element level due to relatively rapid changes in properties of these elements. Typical lower bound information and stringer sizing criteria for the skin-stringer panels are presented in figure 10-7. Fail-safe spar chord lower bounds were checked and updated after each resize cycle.

All wing elements that were not to be automatically resized were put into a subset included in the "Restrain Sizing Data". All of the fuselage members were resized by hand and the revised element data were inserted into the program before each resizing cycle.

CHECKOUT

Checkout of the mathematical model, as described in section 7, concerned itself with accuracy, completeness, and continuity. Checking also confirmed that all design parameters were correctly associated with the proper elements. This was done in part with machine plotting of the design subsets and in part by manual checking of the data listings. With respect to fuselage sizing, the constraint against rigid body translations and rotations of the model was originally provided at the airplane cg, but a check after the initial stress run showed body stresses in the region of the constrained point being affected. The constraint was therefore subsequently revised to a node pair located at the fore and aft extremities of the model so that a slight imbalance would not produce large reactions.

STRUCTURAL SIZING

Typical panel gages are presented in figure 10-8. For each upper and lower surface panel, three sets of gages are shown. Reading from top to bottom, the upper set of values are the upper/lower surface panel gages derived manually from the SCAT-15F and used for initial sizes in the analysis. The middle and lower sets of gages were obtained from successive stress analysis and design cycles.

For lower surface panels of integrally stiffened skin construction, the first value of each line is the area per inch, of skin plus stiffener, while the second value, in parentheses, is the skin gage. For upper and lower surface panels of honeycomb sandwich construction, the single value shown is the sum of the inner and outer face sheet gages.

Figures 10-9 and 10-10 present a summary of the load conditions that were critical for strength sizing of each panel of upper and lower surfaces, respectively. It is also indicated on those figures which of the panels were sized at the minimum gage, and which areas are stiffness critical.

At the end of each design cycle the total theoretical weight of the wing box was calculated and compared to the weight from the previous cycle. Using total mass change between cycles as a measure, convergence was achieved with three stress analysis-design cycles. Figure 10-11, presents the normalized weight of the wing box, Figures 10-12 and 10-13 show the theoretical weights of the wing spar and panel elements, respectively, for successive cycles of redesign.

REFERENCES

- 10-1 *ATLAS An Integrated Structural Analysis and Design System, User's Manual Input and Execution Data*, Document No. D6-25400-0003TN, Boeing Commercial Airplane Company, 1974.
- 10-2 J. H. Johnson, Jr., "Critical Buckling Stresses of Simply Supported Flat Rectangular Plates Under Combined Longitudinal Compression, Transverse Compression and Shear," *Journal of the Aeronautical Sciences*, June 1954, p 41.

Table 10-1—Element Subset Definition

Subset identification	ATLAS element type	Description
E3	Spar	L E Spar, wheel well rib, fin rib
E4	Spar	Spars BS 2790.25, 2755.25, wheel well front spar, inbd engine beam extension, rib BL 352.6
E5	Spar	Spars BS 2895.25, 2860.25, 2825.25
E6	Spar	Spar BS 2580.25, outbd nacelle diffusion rib, inbd nacelle diffusion rib
E9	Spar	Corrugated web spars (120° arc) depth = 35 in.
E11	Spar	Rear Spar, outbd engine beam extension (near RS)
E12	Spar	Rear Spar (outbd), fin rib (near RS), outbd engine beam extension
E13	Spar	Corrugated web spars (120° arc) depth = 20 in.
E14	Spar	Fin spars and ribs
E38	G-plate	Fin root covers
E26	Cover	Honeycomb covers BS 2755.25 to L E
E37	Cover	Fin covers
E28	Cover	Covers rear spar to BS 2755.25 Honeycomb upper skin-stringer lower
E17	Spar	All sheet-stiffener spars
E19	Spar	All spars BS 2230.25 to L E
E21	Spar	Spars BS 2720.25 to BS 2300.25
E25	Spar	All corrugated web spars
E33	Cover	Honeycomb covers (upr and lwr) dry bay 35-in. spar spacing
E34	Cover	Honeycomb covers (upr and lwr) wet bay 35-in. spar spacing
E35	Cover	Honeycomb covers (upr and lwr) dry bay 45-in. spar spacing
E42	Beam S-plate Cover Spar	All elements not to be machine resized.

Table 10-2.—Design Load Cases

Load case (Reference section 8)	Internal load case	Description
Symmetrical		
0.4-01-02-05-20E	FMVF743	Flap down maneuver at V_F $M = 0.4$, 2100-ft alt, $n_z = 3.0$ ult 275 KEAS, 743 000 lb GW
0.6-01-19-06-25E	PMVA732	Positive maneuver at V_C $M = 0.6$, 18 900 ft alt, $n_z = 3.75$ ult 275 KEAS, 732 000 lb GW
0.9-01-34-06-25E	PMVA717	Positive maneuver at V_A $M = 0.9$, 33 800 ft, $n_z = 3.75$ ult 297 KEAS, 717 000 lb GW
1.2-01-52-07-1NE	NMVH704	Negative maneuver at V_H $M = 1.2$, 52 100 ft, $n_z = -1.5$ ult 255 KEAS, 703 500 lb GW
1.2-01-39-06-25E	PMVA704	Positive maneuver at V_A $M = 1.2$, 39 200 ft, $n_z = 3.75$ ult 350 KEAS, 703 500 lb GW
2.0-01-48-03-1NE	NMVC682	Negative maneuver at V_C $M = 2.0$, 47 700 ft, $n_z = -1.5$ ult 475 KEAS, 682 000 lb GW
2.7-01-67-07-1NE	NMVH657	Negative maneuver at V_H $M = 2.7$, 67 100 ft, $n_z = -1.5$ ult 400 KEAS, 657 000 lb GW
0.4-05-02-05-20E	FMVF465	Flap down maneuver at V_F $M = 0.4$, 2100 ft, $n_z = -3.0$ ult 275 KEAS, 464 900 lb GW
0.6-05-07-03-1NE	NMVC465	Negative maneuver at V_C $M = 1.2$, 6700 ft, $n_z = -1.5$ ult 389 KEAS, 464 900 lb GW
0.9-01-34-36-10E	ELEV717	Abrupt elevator deflection $M = 0.9$, 33 800 ft, $n_z = 0.723$ ult 300 KEAS, 717 000 lb GW
TAXI	TAX1N23	TAXI $n_z = 3$ ult c.g. at BS 2479 16, 750 000 lb GW
2-pt braked roll	TWOPTBR	Two point braked roll $n_z = 1.5$ ult, $n_x = 1.2$, c.g. 206.55 in above MLG static ground line
Reverse braking	REVBRAK	Reversed braking, $n_z = 1.5$ ult $n_x = -0.7659$

Table 10-2.-(Concluded)

Load case (Reference section: 8)	Internal load case	Description
Asymmetrical		
Lateral gust at $M = 0.9$	LATGSTR	Lateral gust R. H. S. $M = 0.9$ 33400 ft, $n_y = 0.18$ 300 KEAS, 716 600 lb GW
Rudder maneuver no. 1	LATGSTL	L.H.S
	RUDMN1R	Rudder maneuver R.H.S. $M = 0.4$ 6300 ft, $n_y = 0.135$ ult 350 KEAS, 742 600 lb GW
Rudder maneuver no. 2	RUDMN1L	L.H. S.
	RUDMN2R	Rudder maneuver R.H.S. $M = 0.4$, 6300 ft, $n_y = 0.06$ ult 350 KEAS, 742 600 lb GW
Rudder maneuver no. 3	RUDMN2L	L.H.S
	RUDMN3R	Rudder maneuver R.H.S. $M = 0.4$, 6300 ft, $n_y = 0.195$ ult 350 KEAS, 742 600 lb GW
Turning	RUDMN3L	L.H.S.
	GRTURNR	Ground turn R.H.S. c.g. at BS 2479.16 206.55 in. above MLG static ground line 258.55 in. above NG static ground line $n_y = -0.75$ ult, 750 000 lb GW
Nose wheel yaw	GRTURNL	L.H.S.
	NWYAWR	Nose wheel yaw R.H.S. unsymmetric MLG braking $n_z = 1.5$ ult, $n_x = 0.799$ 750 000 lb GW
	NWYAWL	L.H.S.

Table 10-3.- Sources of Sizing Data for Design

Element subset	Element type	^a Material properties table	^b Compression buckling table	^c Shear buckling table	^d Factor for two-direction compression
E17	Spars	M55		BS55 for Spar webs	
E19	Spars	M52		BS52	
	Spars	M53		BS53	
E25	Spars	M54		BS54	
E33	Covers	M56	BC56	Mat'l FSU ^f	0.65
E34	Covers	M57	BC57	Mat'l FSU	0.65
E28	Covers	M58	BC59	Mat'l FSU	0.65
E35	Covers	M56	BC58	Mat'l FSU	0.385
E37	Covers	M60	Mat'l FCU ₂ ^e	Mat'l FSU	0.468
E38	G-plates	M60	Mat'l FCU ₂ 1 dir. Mat'l FCU ₃ 2 dir.	Mat'l FSU	0.468
Structure (Default)		M56			

^a See table 10-4

^b See table 10-6

^c See table 10-5

^d Compression stability allowables to be used in the local element 2 direction are generated by multiplying the 1 direction allowables in the specified table by the designated factor.

^e FCU —ultimate compression stress

^f FSU —ultimate shear stress

Table 10-4.—Basic Material Allowable Stress

Material	a Temperature, °F	Allowable, ksi				
		FTU _{1,2,3}	FCU ₁	FCU ₂	FCU ₃	FSU
M52	71 ^b	125.1	137.0	137.0	137.0	80.1
	250	107.5	111.5	111.5	111.5	68.8
M53	71	125.1	137.0	137.0	137.0	80.1
	250	107.5	111.5	111.5	111.5	68.8
M54	71	125.1	137.0	137.0	137.0	80.1
	250	107.5	111.5	111.5	111.5	68.8
M55	71	125.1	137.0	137.0	137.0	80.1
	250	107.5	111.5	111.5	111.5	68.8
M56	68	124.8	136.6	139.6	136.6	80.1
	70	123.4	134.2	137.2	134.2	80.1
	71	125.1	137.0	140.0	137.0	80.1
	174	112.9	123.6	126.3	123.6	73.9
	264	103.8	109.3	111.8	109.3	68.8
	373	94.8	95.2	97.3	95.2	63.3
	500	94.8	95.2	97.3	95.2	63.3
M57	-230	94.8	95.2	97.3	95.2	63.3
	-190	103.8	109.3	111.8	109.3	68.8
	-130	112.9	123.6	126.3	123.6	73.9
	-74	125.1	137.0	140.0	137.0	80.1
	-71	125.1	137.0	140.0	137.0	80.1
	70	125.1	137.0	140.0	137.0	80.1
	71	125.1	137.0	140.0	137.0	80.1
	72	125.1	136.6	139.6	136.6	80.1
	373	94.8	95.2	97.3	95.2	63.3
M58	-384	94.8	95.2	97.3	95.2	63.3
	-286	103.8	109.3	111.8	109.3	68.8
	-180	112.9	123.6	126.3	123.6	73.9
	-171	125.1	137.0	140.0	137.0	80.1
	-77	123.4	134.2	137.2	134.2	80.1
	71	125.1	137.0	140.0	137.0	80.1
	75	124.8	136.6	139.6	136.6	80.1
M60	68	124.8	85.5	41.5	41.5	80.1
	69	124.8	85.5	41.5	41.5	80.1
	70	123.4	85.7	41.7	41.7	80.1
	71	125.1	86.0	41.0	42.0	80.1
	174	112.9	81.0	37.3	37.3	73.9
	264	103.8	77.3	34.6	34.6	68.8
	373	94.8	73.4	31.1	31.1	63.3
	500	94.8	73.4	31.1	31.1	63.3

All materials are isotropic with:

$$E = 16.0 \cdot 10^6$$

$$G = 6.2 \cdot 10^6$$

$$\nu = 0.3$$

ATLAS Users Manual (ref. 2) details how specific allowables are used with each element type.

a A negative sign preceding the temperature is used to signify materials data appropriate for load conditions having the lower surface in compression.

b Temperature callouts from 68° to 77° F are used to identify room temperature allowables corrected for stresses induced by thermal gradients.

Table 10-5.—Shear Buckling Allowable Stress

Table	Gage, in.	Shear allowable, ksi							
		^a Temperature, °F	71 ^b	250					
BS52	0.024		11.0	10.0					
	0.12		53.5	52.0					
	0.144		60.0	55.0					
BS53	0.024		12.0	11.5					
	0.072		41.5	40.0					
	0.096		55.0	51.0					
	0.12		61.0	54.5					
	0.144		64.0	57.0					
BS54	0.024		12.0	11.5					
	0.072		58.0	54.0					
	0.096		65.0						
	0.12		67.0						
	0.144		68.0	59.5					
BS55	0.02		46.0	44.0					
	0.14		54.0	52.0					
	0.2		57.0	55.0					
	0.24		58.0	56.0					
BS59	0.02 0.058 0.076 0.101 0.125 0.154 0.3	^a Temperature, °F	-384	-286	-180	-171	-77 ^b	71	75
			11.8	11.8	12.6	13.0	13.0	72.0	72.0
			19.9	20.0	21.3	22.0	22.0	72.0	72.0
			35.3	35.5	37.8	39.0	39.0	72.0	72.0
			51.9	53.7	57.0	59.6	59.6	72.0	72.0
			52.6	59.6	66.7	74.5	74.5	72.0	72.0
								72.0	72.0
								72.0	72.0

^a A negative sign preceding the temperature is used to signify materials data appropriate for load conditions having the lower surface in compression.

^b Temperature callouts from 68° to 77° F are used to identify sets of room temperature allowables corrected for stresses induced by thermal gradients.

Table 10-6.- Compression Buckling Allowable Stress

Table	Gage, in.	Compression allowable, ksi							
BC56	0.02 0.04 0.06 0.08	^a Temperature, °F	68 ^b	70	71	174	264	373	
			93.6	91.2	94.0	91.5	86.8	82.5	
			122.6	120.8	123.0	110.6	97.9	85.9	
			122.6	120.8	123.0	110.6	97.9	85.9	
			123.6	121.8	124.0	111.1	97.9	85.9	
BC57	0.02 0.04 0.06 0.08	^a Temperature, °F	-230	-190	-130	-74	-71 ^b	71	72
			89.2	90.7	92.8	88.0	94.0	94.0	93.6
			93.8	102.6	112.0	118.5	123.0	123.0	122.6
			93.8	102.6	112.0	118.5	123.0	123.0	122.6
			93.8	102.6	113.0	119.5	124.0	124.0	123.6
BC58	0.02 0.04 0.3	^a Temperature, °F	68 ^b	69	70	71	174	264	373
			93.6	93.8	91.2	94.0	91.5	86.8	77.9
			94.6	94.8	92.2	95.0	94.1	88.9	77.9
			102.6	102.8	100.8	103.0	98.1	88.9	77.9
BC59	0.02 0.04 0.058 0.06 0.08 0.101 0.125 0.166 0.223 0.265	^a Temperature, °F	-384	-286	-180	-171	-77 ^b	71	75
								94.0	93.6
								123.0	122.6
			2.79	4.0	6.5	9.0	9.0		
								123.0	122.6
								124.0	123.6
			16.3	17.6	21.1	24.0	24.0		
			27.2	28.6	32.7	36.0	36.0		
			51.6	53.1	58.9	63.0	63.0		
			93.2	95.0	103.5	109.0	109.0		
			103.2	105.0	114.2	120.0	120.0		

a A negative sign preceding the temperature is used to signify materials data appropriate for load conditions having the lower surface in compression.

b Temperature callouts from 68° to 77° F are used to identify sets of room temperature allowables corrected for stresses induced by thermal gradients.

REPRODUCIBILITY OF THE
ORIGINAL PAGE IS POOR

Table 10- Temperature Design Data

Load case ^a	^b Temperature, °F	Element subsets affected
TWOPTBR	71 ^c	E17, E19, E21, E25 spars
REVBRAIL		E33, E35, E37 covers, E38 g-plate
GRTURNR	- 71	E34 covers
GRTURNL	- 171	E28 covers
NWHYAWR		
NWHYAWL		
TAXINZ3		
LATGSTR	71	Whole structure
PMVA704	71	
LATGSTL	71	
ELEV717	71	
RUDMN1R	71	
RUDMN1L	71	
RUDMN2R	71	
RUDMN2L	71	
RUDMN3R	71	
RUDMN3L	71	
FMVF743	71	
PMVA732	71	
PMVA717	71	
NMVH704	250	E17, E19, E21, E25 spars
	264	E33, E35, E37 covers; E38 g-plates
	- 190	E34 covers
	- 286	E28 covers
NMVC682	250	E17, E19, E21, E25 spars
	174	E33, E35, E37 covers, E38 g-plates
	-130	E34 covers
	-180	E28 covers
NMVH657	250	E17, E19, E21, E25 spars
	373	E33, E35, E37 covers, E38 g-plates
	- 230	E34 covers
	384	E28 covers
FMVF465	71	E17, E19, E21, E25 spars
	68	E33, E35, E37 covers, E38 g-plates
	72	E34 covers
	75	E28 covers
NMVC465	71	E17, E19, E21, E25 spars
	70	E33, E35, E37 covers, E38 g-plates
	- 74	E34 covers
	- 77	E28 covers

a See table 10-2 for definition of load cases.

b A negative sign preceding the temperature is used to signify materials data appropriate for load conditions having the lower surface in compression.

c Temperature callouts from 68° to 77° F are used to identify sets of room temperature allowables corrected for stresses induced by thermal gradients.

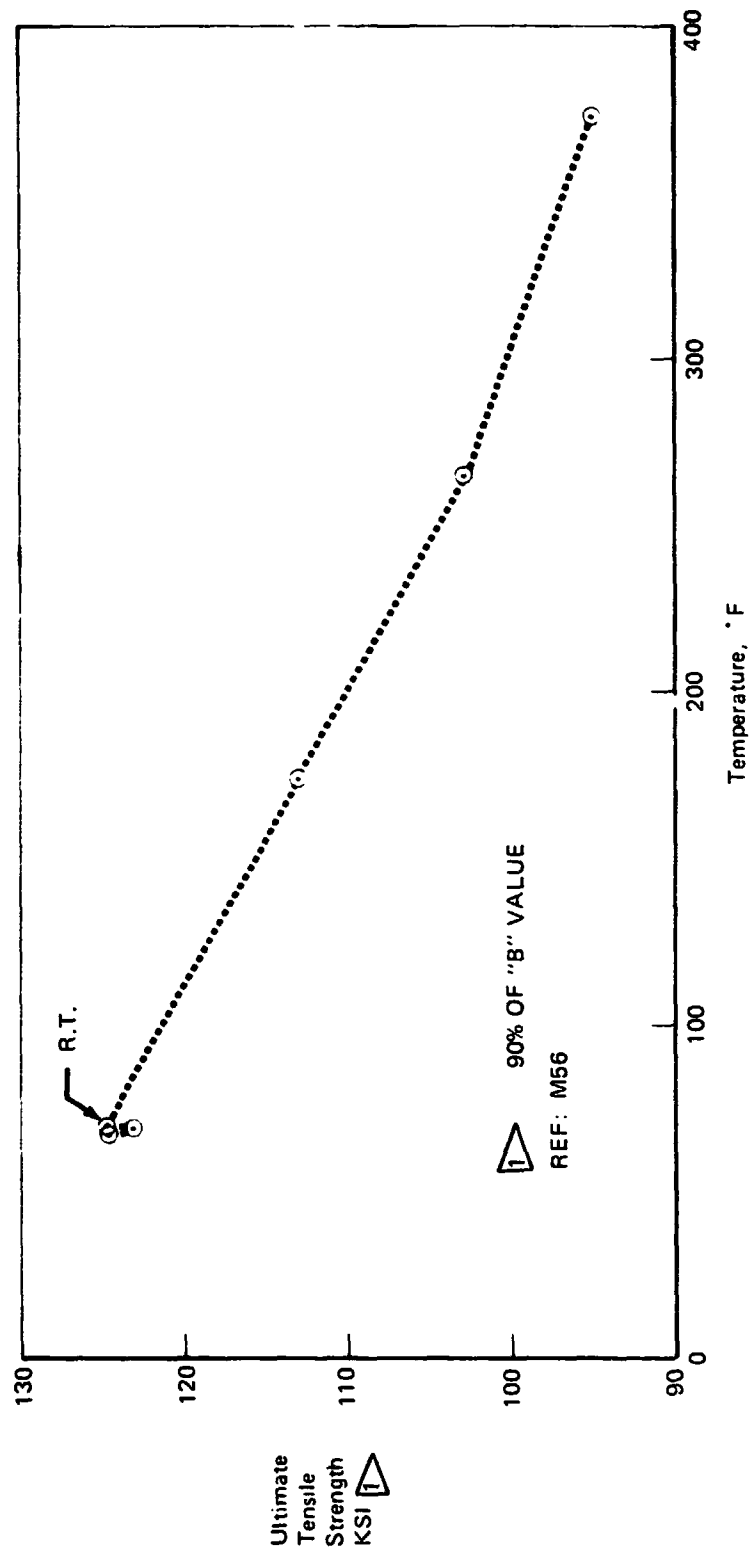
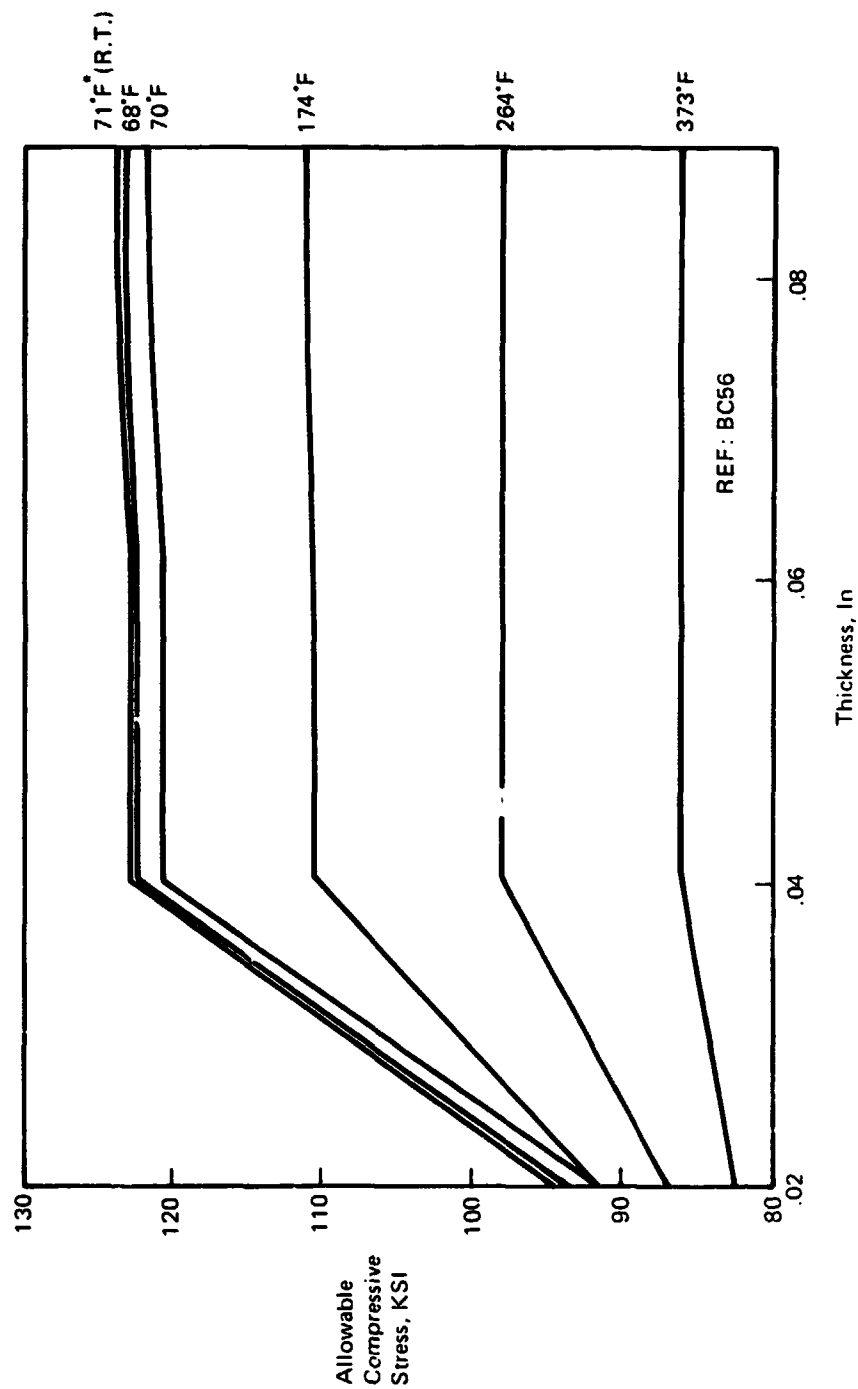


Figure 10-1.- Typical Mechanical Properties
(Including thermal stress decrements)
Ti-6Al-4V, condition 1



*See note b, table 10-6, for explanation of room temperature allowable data.

Figure 10-2.—Typical Instability Allowables
(Including thermal stress decrements)
Ti-6Al-4V, condition 1

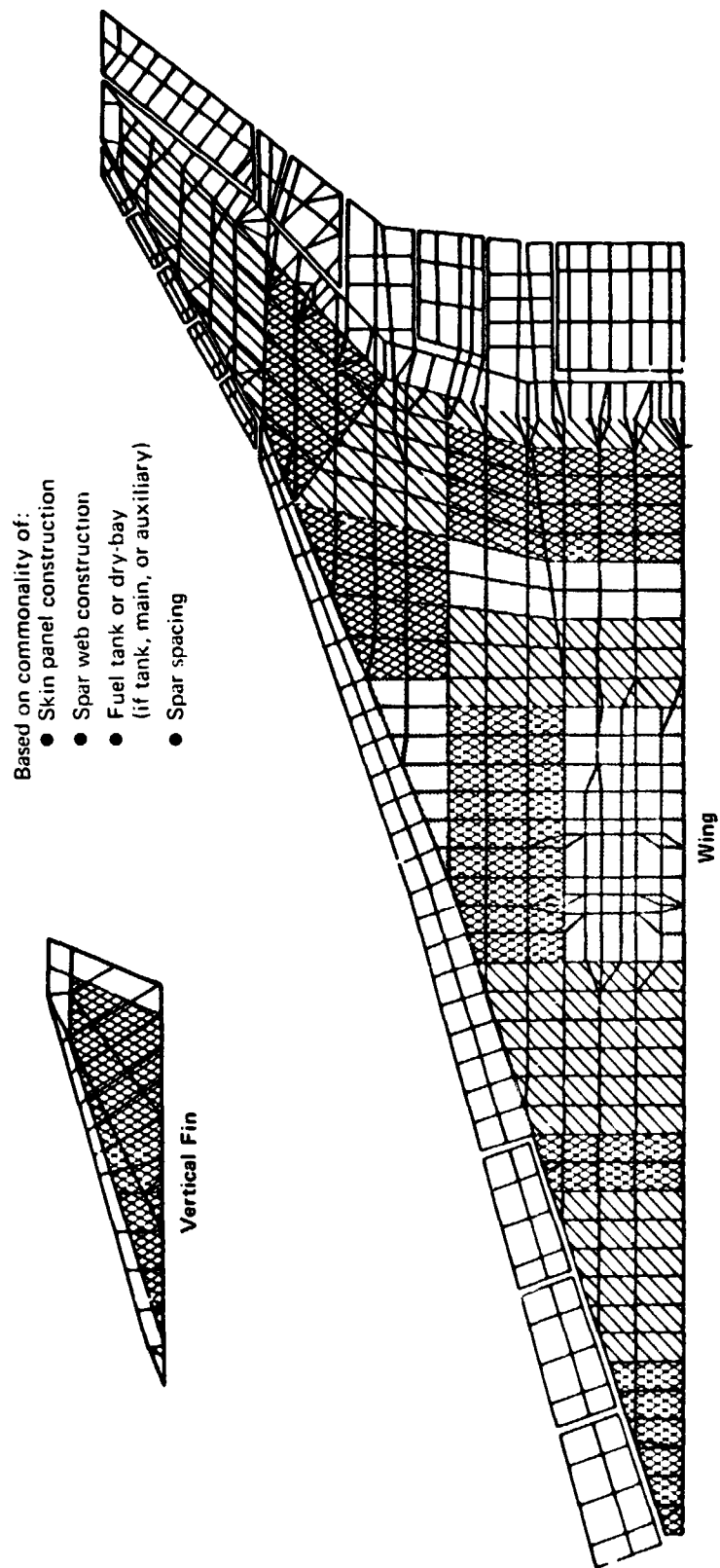


Figure 10-3. — Wing Structure Regions

Subsets
 E3, E4, E5, E6, E11, E12, E17
 E25, E19
 E9, E21, E25
 E13, E14, E25

Plane sheet-stiffened web
 Corrugated web (120° arc), depth = 45 in.
 Corrugated web (120° arc), depth = 35 in.
 Corrugated web (120° arc), depth = 20 in.

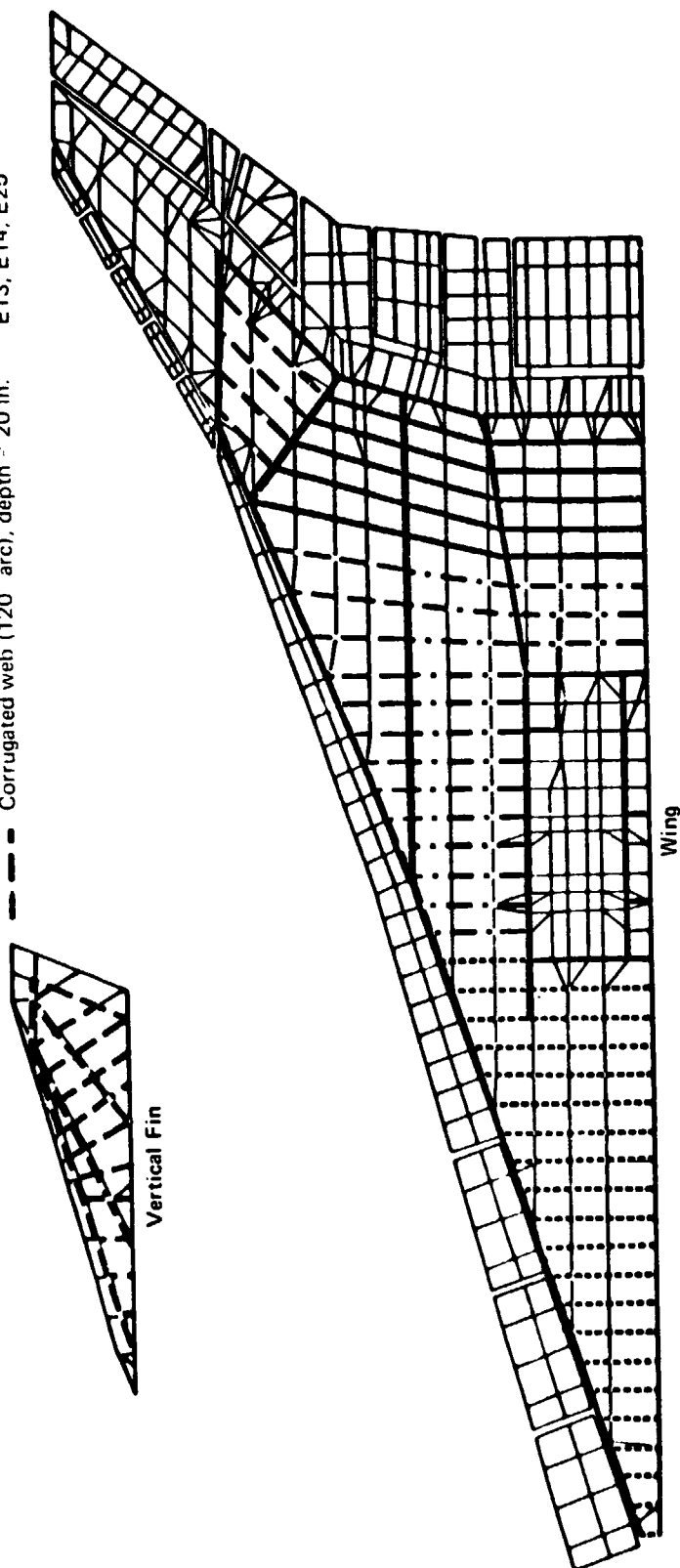


Figure 10-4.—Wing Spar Element Subsets

Subsets

E28
E26, E33
E26, E34
E38, E37
E26, E35

- 1-in. honeycomb upper surface, integral skin-stiffener lower, 35-in. spar spacing, wet or dry
- 1-in. honeycomb upper and lower surface, dry-bay, 35-in. spar spacing
- 1-in. honeycomb upper and lower surface, wet-bay, 35-in. spar spacing
- 3/4 in. honeycomb surfaces, 35-in. rib spacing
- 1-in. honeycomb upper and lower surface, dry-bay, 45-in. spar spacing

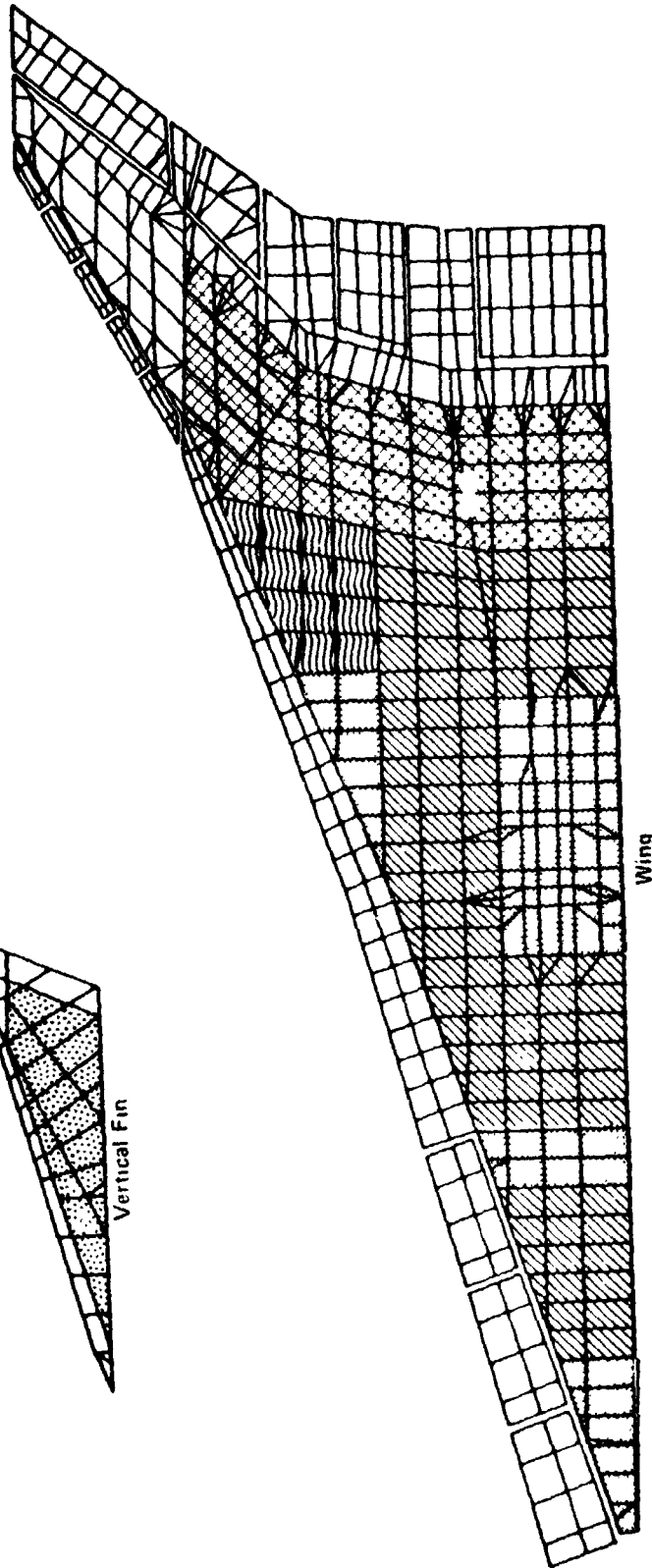
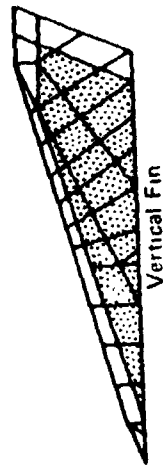


Figure 10-5.—Wing Cover Element Subsets

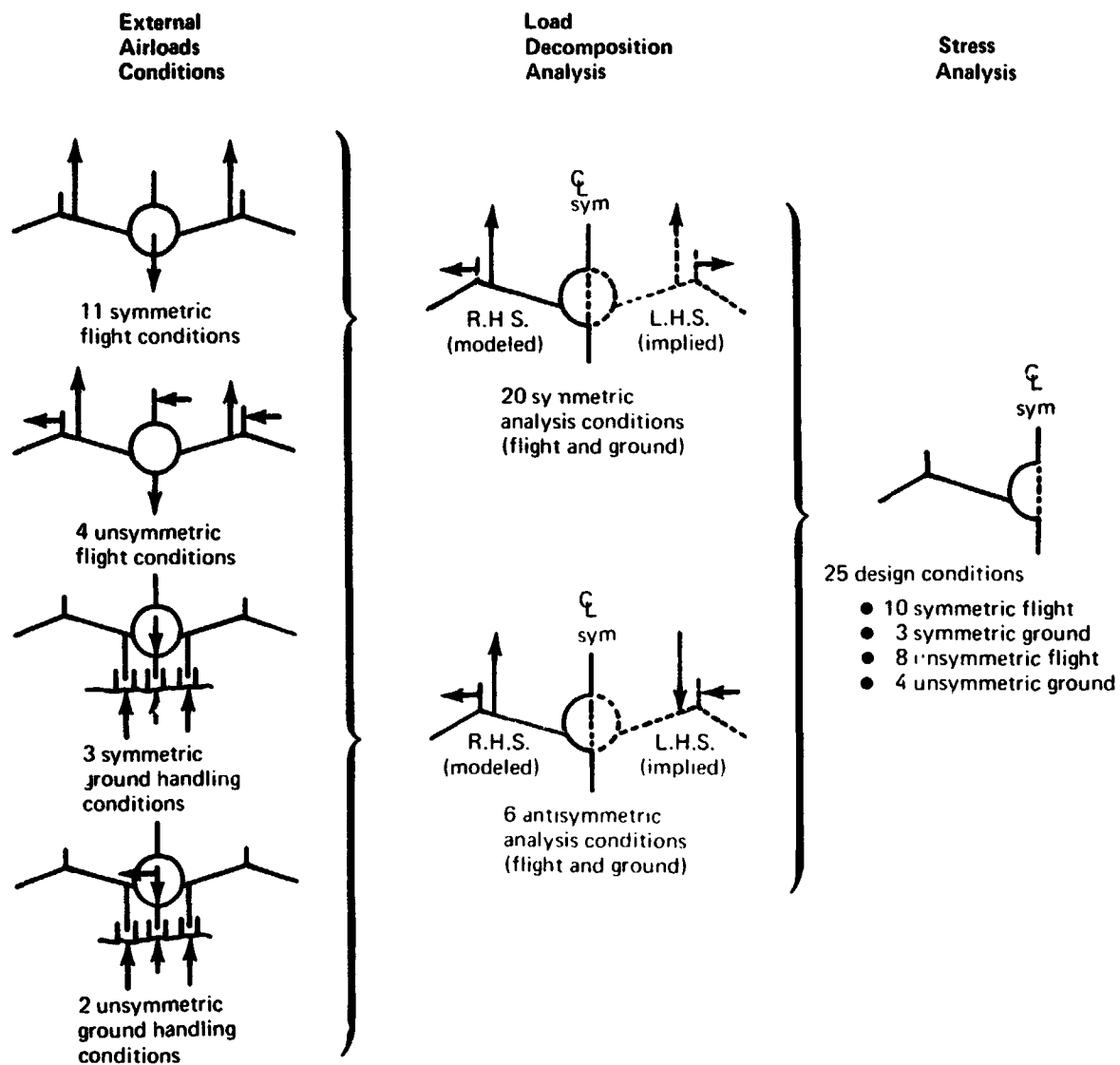


Figure 10-6.—Internal Loads and Stress Analysis Sequence

Design cycle	Honeycomb panel face sheet		Integral skin-stiffener panel		Corrugated or sheet-stiffener spar	
	Inner thickness, in.	Outer thickness, in.	Skin thickness, in.	Stiffener-to-skin area ratio	Web gage, in.	Chord area, in ²
1	0.010 ↓	0.020 (lower surface) 0.015 (upper surface and fin) ↓	0.058 ↓	0.20	0.020 ⚠ ↓	As initially sized
2				2.41t-0.016		0.25 of area of larger adjacent skin panel
				Cycle 2 value		Cycle 2 value

⚠ 0.020 except for corrugated webs in fuel tanks which are designed by 6-g crash or refueling overpressure.

Figure 10-7. Element Lower Bound Constraints



- 1 - PMVA732
- 2 - TAXINZ3
- 3 - NWHYAWR
- 4 - TWOPTBR
- 5 - PMVA717
- 6 - GRTURNR
- 7 - PMVA704
- 8 - REVBRK
- 9 - FMVF743

• See table 10-2 for load condition definition

Note
M denotes minimum gage.
For minimum gage panels,
the critical design condition
shown would des gn without
the constraint.

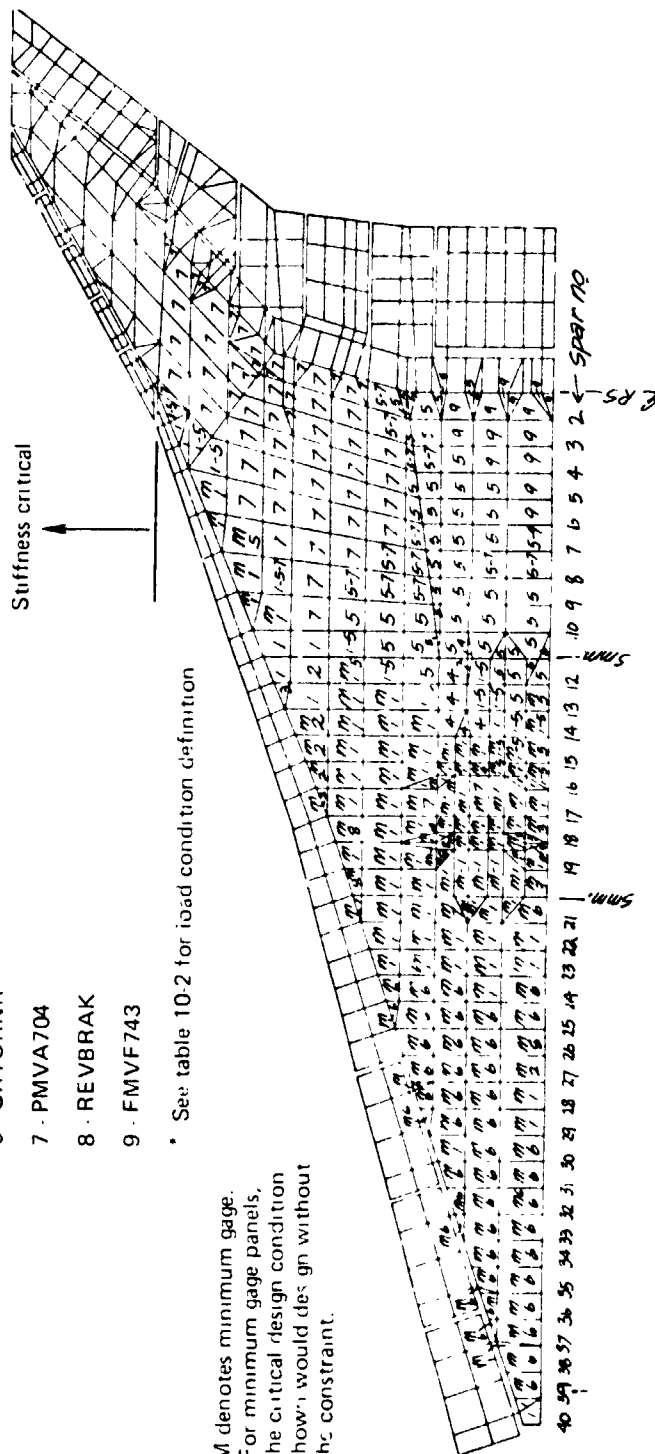


Figure 10-9. Critical Design Conditions
Upper Surface

- *1 - PMVA732
- 2 - TAXINZ3
- 3 - NWHYAWR
- 4 - TWOPTBR
- 5 - PMVA717
- 6 - GRTURNR
- 7 - PMVA704
- 8 - REVBRK
- 9 - FMVF743
- 10 - ELEV717
- 11 - FMVF465
- 12 - NMVH657
- 13 - NMVC682
- 14 - NMVH704

*See table 10-2 for load condition definition

Not: M denotes minimum gage.
F for minimum gage panels.
the critical design condition
shown would design without
the constraint.

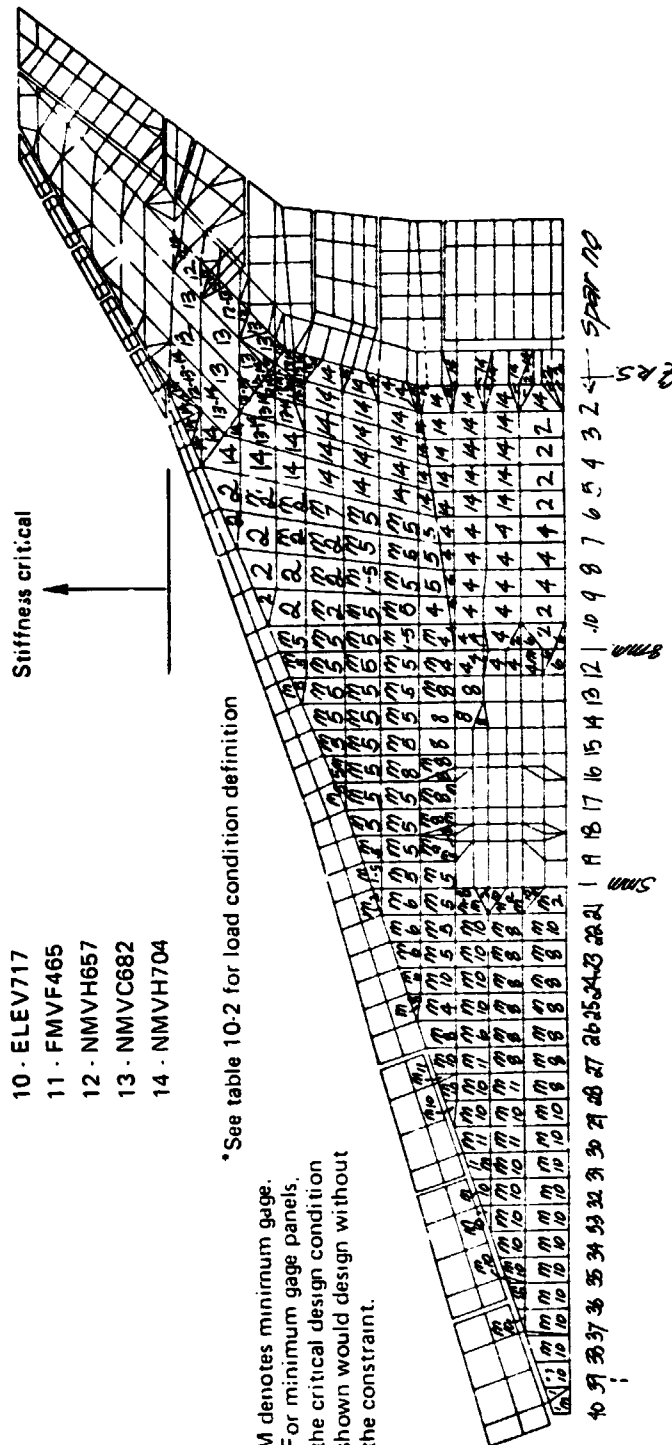


Figure 10-10.—Critical Design Conditions
Lower Surface

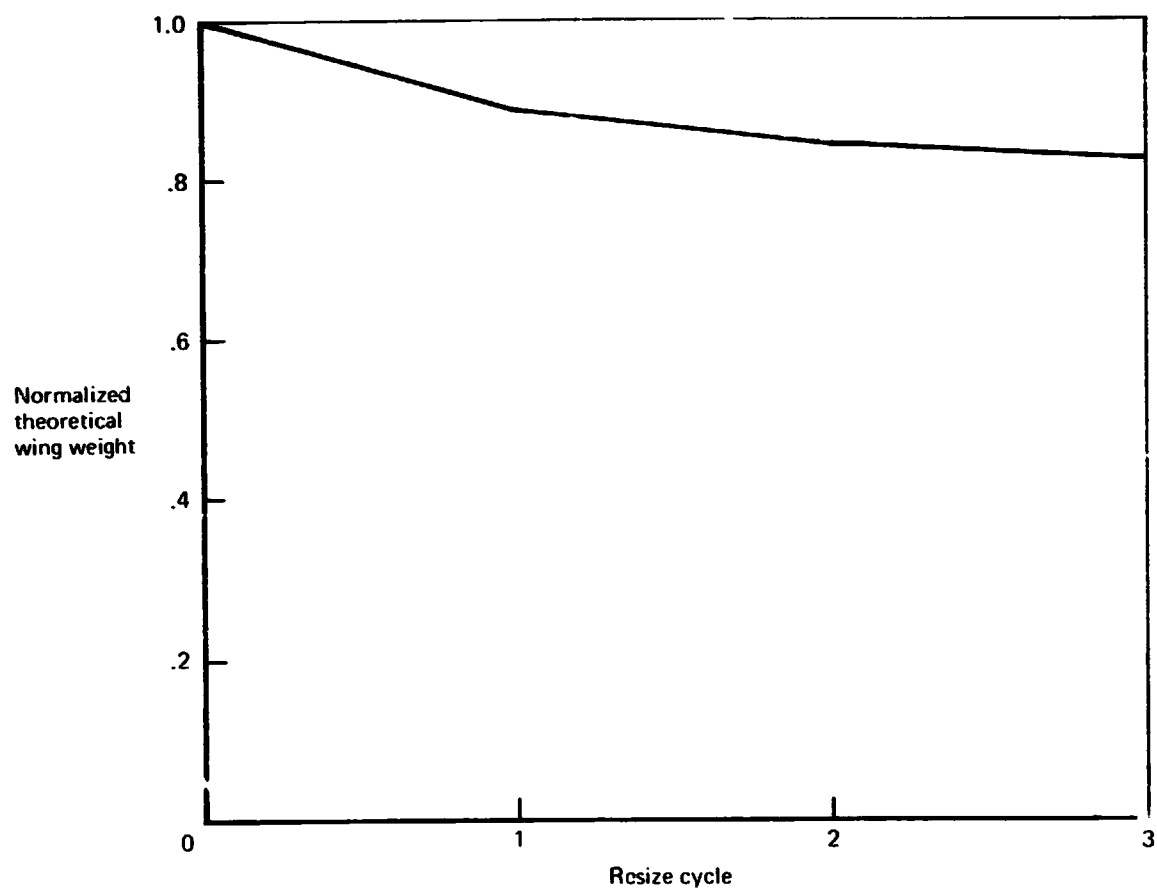


Figure .0-11.—Effect of Resizing on Theoretical Wing Weight

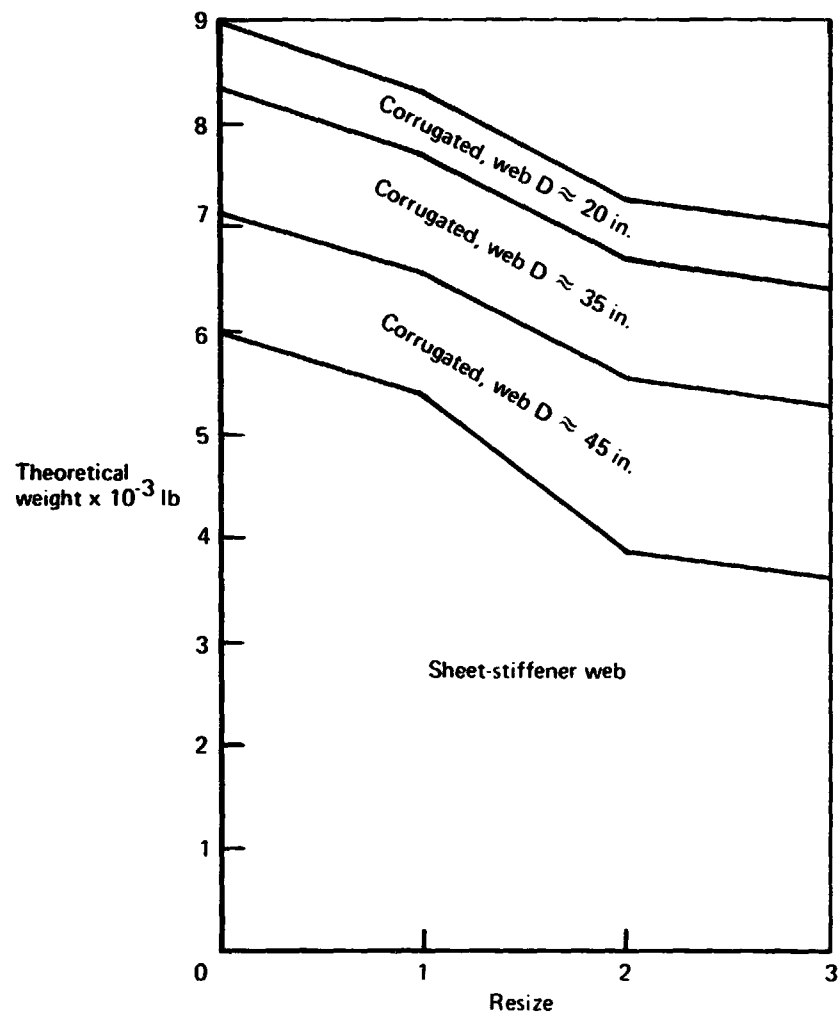


Figure 10-12.—Effect of Resizing on Wing Spar Theoretical Weight

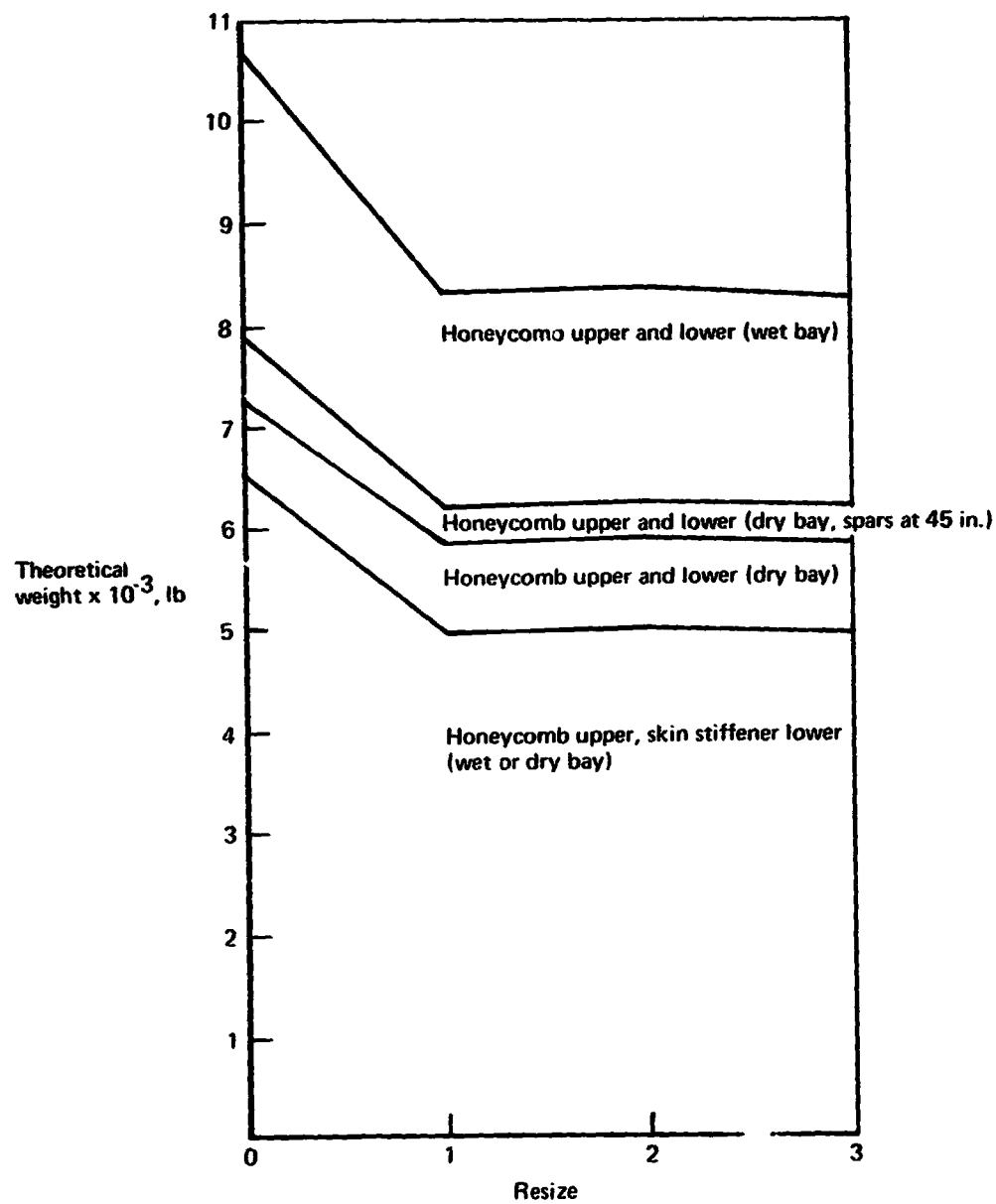


Figure 10-13.—Effect of Resizing on Wing Panel Theoretical Weight

SECTION 11

FLUTTER ANALYSIS

by

C. R. Pratt-Barlow
F. G. Hyland
J. G. Lelong

INTENDING PAGE

✓K NOT FILMED

CONTENTS

	Page
FLUTTER ANALYSIS	554
Flutter Analysis Summary	554
Retained Freedoms and Vibration Analysis	556
Mode Shape Interpolation to Aerodynamic Grids	559
Preliminary Flutter Appraisal	560
Configuration Flutter Sensitivity	562
Final Flutter Analysis and Stiffness Redesign	563
Flutter Boundary-Titanium Structure (1975 Technology)	565

TABLES

No.		Page
11-1	Retained Freedoms-Symmetric Vibration Modes	566
11-2	Retained Freedoms-Antisymmetric Vibration Modes	571
11-3	Atlas 3 BC Data Stages-Flutter Analysis	577
11-4	Atlas 3 Data Details for Vibration Mode Rigid In-Plane Motion	581
11-5	Airplane Vibration Mode Frequencies-Final Stiffness Design	584
11-6	Airplane Vibration Mode Shapes-Final Stiffness Design	585
11-7	Preliminary Symmetric Vibration Mode Frequencies	663
11-8	Preliminary Symmetric Wing Flutter Results	664
11-9	Energy Balance-Preliminary Low Frequency Symmetric Flutter	665
11-10	Strength Resized Wing Flutter With Initial Stiffness Constraints	666

FIGURES

No.		Page
11-1	Arrow Wing Flutter Boundary, 969-512B	667
11-2	Effect of Structural Changes on Critical Symmetric Flutter (1.9 Hz)	668
11-3	Final Stiffness Design Modification 9	669
11-4	Flutter Analysis Procedure	670
11-5	Wing Mass Paneling for Flutter	671
11-6	Wing Retained Nodes and Mode Interpolation Beam Splines	672
11-7	Wing Edge Nodes for Vibration Modes Shapes	673
11-8	Freedoms for Rigid In-Plane Motion of Vibration Modes	674
11-9	Airplane Vibration Mode 1-Final Stiffness Design	675
11-10	Airplane Vibration Mode 2-Final Stiffness Design	676
11-11	Airplane Vibration Mode 3-Final Stiffness Design	677
11-12	Airplane Vibration Mode 4-Final Stiffness Design	678
11-13	Airplane Vibration Mode 5-Final Stiffness Design	679
11-14	Airplane Vibration Mode 6-Final Stiffness Design	680
11-15	Airplane Vibration Mode 7-Final Stiffness Design	681
11-16	Airplane Vibration Mode 8-Final Stiffness Design	682
11-17	Airplane Vibration Mode 9-Final Stiffness Design	683
11-18	Airplane Vibration Mode 10-Final Stiffness Design	684
11-19	Airplane Vibration Mode 11-Final Stiffness Design	685
11-20	Airplane Vibration Mode 12-Final Stiffness Design	686
11-21	Airplane Vibration Mode 13-Final Stiffness Design	687
11-22	Airplane Vibration Mode 14-Final Stiffness Design	688
11-23	Airplane Vibration Mode 15-Final Stiffness Design	689
11-24	Airplane Vibration Mode 16-Final Stiffness Design	690

FIGURES (CONCLUDED)

No.		Page
11-25	Airplane Vibration Mode 17-Final Stiffness Design	691
11-26	Airplane Vibration Mode 18-Final Stiffness Design	692
11-27	Typical Surface Spline Interpolation	693
11-28	Rho III Downwash Collocation Points ..	694
11-29	Mach-Box Pattern-M = 1.32	695
11-30	Mach-Box Pattern-M = 2.0	696
11-31	Preliminary Flutter Speeds	697
11-32a	Effect of Nacelle Beam Stiffening on Modal Coupling	698
11-32b	Effect of Nacelle Beam Stiffening on Modal Coupling	699
11-32c	Effect of Nacelle Beam Stiffening on Modal Coupling	700
11-33	Flutter Sensitivity to Engine Beam Stiffness	701
11-34	Flutter Sensitivity to Airload and Structural Components	702
11-35	Effect of Control Locks on a Vibration Mode	703
11-36	Low Frequency Flutter Mechanism	704
11-37	Generalized Force Loops and Energy Balance	705
11-38	Energy Flux and Energy Compatibility	706
11-39	Stiffness Design Modification 1	707
11-40	Stiffness Design Modification 2	708
11-41	Stiffness Design Modification 3	709
11-42	Stiffness Design Modification 4	710
11-43	Stiffness Design Modification 5	711
11-44	Stiffness Design Modification 6	712
11-45	Stiffness Design Modification 7	713
11-46	Stiffness Design Modification 8	714
11-47	Effect of Stiffness Design Changes on Flutter Speed	715

Symbols and Abbreviations

BC	Boundary condition
EAS	Equivalent airspeed
F	Generalized force component
Hz	Hertz
k, kip	One thousand pounds
kn	Knots
KPI	One thousand pounds per inch
q	Generalized coordinate displacement
γ	Vector displacement
RHO III	Subsonic Kernel Function unsteady aerodynamic program
R_x, R_y, R_z	Rotations about the x, y, z axes
T_s, T_y, T_z	Translations along the x, y, z axes
V_D	Design dive speed
V-g	Velocity-added damping flutter solution
θ	Vector angle

SECTION 11

FLUTTER ANALYSIS

FLUTTER ANALYSIS SUMMARY

Sufficient detail as determined from experience on the National SST, was included in the structural model to yield realistic analytical wing flutter results, as explained at the start of Section 7, and displayed in figures 7-1 and 7-2. There were two phases to accomplishing the flutter analyses.

A preliminary flutter analysis phase followed the structural flexibility and airplane vibration mode calculations which validated the complex Arrow Wing mathematical model. It was performed for the symmetric, high gross weight condition at $M=0.9$ since this was the most critical condition from previous studies. The following states of the structural model were analyzed:

1. As initially sized to modified 969-336C loads and with strength design engine beams.
2. As revised for FLEXSTAB static aeroelastic analysis with doubled wing tip stiffness, quadrupled low speed aileron cover gage and engine beams stiffened to 1.5 times the strength design value.
3. With an additional increase in engine beam stiffness to 4.5 times the strength design value.

This preliminary flutter analysis checked the soundness of the flutter analysis procedure, provided early insight into characteristics of the Arrow Wing flutter modes and allowed a limited study of the influence on wing symmetric flutter of airplane components such as the flexible wing fin, flexibly mounted engine nacelles and the unsteady airloads of the horizontal tail and the wing fin. The flutter speed with initial sizing was more than 300 knots EAS below the $M=0.9$ design requirement. Little improvement was achieved from the preliminary stiffness resize for FLEXSTAB, but with engine beams stiffened further, the flutter speed was only about 100 knots EAS below the $M=0.9$ design requirement. This in fact bettered the bare wing flutter speed (minus wing fins and nacelles) for state (2) above.

The final flutter analysis phase followed completion of the automated strength resize of wing primary structure. Before proceeding, however, some overriding stiffness requirements were imposed on the structural model, because the preliminary flutter analysis had indicated that the strength design would have a low flutter speed. These modifications comprised the stiffened wing tip and low-speed aileron that had been adopted prior to the FLEXSTAB aeroelastic loads analysis, and engine beams stiffened to 4.5 times the strength design value. In addition locks for high speed flight were incorporated on the low-speed aileron and outboard flaperon. With these stiffness

constraints, the effect of strength resizing was only a slight decrease in flutter speed from the preliminary result with stiffened engine beams, state (3) above.

As the analysis proceeded, a systematic set of further stiffness design modifications, based on engineering judgement, were made to remove the wing flutter deficiency. No reduction in gages or member sizes below the values specified for strength were allowed. This analytical work to satisfy flutter criteria was first confined to the symmetric, high gross weight condition at $M = 0.9$. It was finally concluded that further efforts to increase the flutter speed of the critical 1.9-Hz wing flutter mode, via structural changes based on engineering judgement, would produce an unrealistically high weight penalty. Hence it was proposed that the subsonic dive placard be reduced by 50 knots EAS to achieve flutter clearance. Undoubtedly a substantially higher placard could be achieved without additional weight increment, by utilizing formal optimization techniques. This approach could be easily justified on an aircraft development program. The reduced placard would impose a range decrease of 25 nautical miles with fixed fuel loading, or an increase of 1297 lbs. in fuel loading for constant range.

The structure with the latest stiffness design modifications was then analysed for symmetric flutter at low gross weight and for antisymmetric flutter at both high and low gross weights and $M = 0.9$. This confirmed that the symmetric, high gross weight condition is critical. Flutter analyses were then conducted for that condition at other Mach numbers. The resulting flutter boundary for the 969-512B configuration with titanium structure (1975 technology) appears in figure 11-1. Budget limitations prevented determination of the flutter boundaries over the Mach number range for the conditions not critical at $M = 0.9$. Figure 11-2 shows, in terms of flutter speed ratio relative to the original goal of 504 knots EAS, the sensitivity, to configuration features and structural changes, of the critical 1.9 Hz, symmetric, high gross weight, wing flutter mode at $M = 0.9$.

The stiffness design modifications to provide flutter clearance are summarized in figure 11-3. The penalty associated with this Task II stiffness design is equivalent to 10,223 lbs per aircraft including 2953 lbs weight equivalent of a 1.3 drag count increase for thickening the wing tip.

FLUTTER ANALYSIS PROCEDURE

Figure 11-4 is a flow chart showing the integrated flutter analysis procedure. Flutter results were obtainable in a single computer run starting with the complex ATLAS stiffness and mass models, incorporating stiffness or mass modifications, progressing through generation of reduced stiffness and mass distribution matrices, solution for airplane vibration modes, interfacing to the generation of unsteady airforces for all lifting surfaces and finally, solution of the flutter equations and interpretation of the flutter mechanism. In order to accomplish this degree of analysis integration, two things were necessary. First, user control deck procedures were developed, both to enhance the ATLAS 2 system as shown in figure 11-4, and to interface with Boeing Flutter Library programs. Secondly, that interfacing was facilitated by the versatile applications monitor of the CDC 6600 CYBER computer system.

A generalized coordinate approach was used in formulating the flutter equations, with a truncated set of airplane vibration modes, the first eighteen symmetric or seventeen antisymmetric, together with the relevant rigid airplane degrees of freedom for symmetric and antisymmetric cases. The vibration mode shapes were interpolated from structural to aerodynamic grids. Subsonic kernel-function and supersonic Mach box versions of unsteady lifting surface theory were used to calculate generalized airforces. The Q-R algorithm was used to solve the complex eigenvalue flutter problem. Standard Atmosphere constant altitude classical V-g flutter solutions were cross-plotted to match the Mach number of the unsteady airforces and this result was confirmed by an automated flutter solution routine based on the Nyquist criterion. The generalized force loops of the flutter mode, showing the dynamical freedom interaction created by the unsteady airforces, and the associated energy balance at neutral stability were then obtained.

The stiffness modifications which were made in meeting flutter criteria were based on engineering judgment. These judgments were aided by interpretation of the flutter mechanism energy compatibility, which highlighted the vibration modes important to the flutter mechanism. Frequency coupling on the V-g solution frequency-speed plots showed which of these modes required stiffening. Inspection for high strain regions in those mode shapes allowed effective stiffening to be achieved for controlling frequency coupling. This process would have been much more effective if distributions of strain energy density for mode shapes were available from ATLAS. Indeed, it is recommended that future development plans for ATLAS include such calculations, not only for vibration mode shapes but for mode shapes with phase lags, such as flutter modes or dynamic response vectors.

RETAINED FREEDOMS AND VIBRATION ANALYSIS

CHOICE OF RETAINED FREEDOMS

The following considerations affected the choice of retained freedoms for the vibration analyses which provided the free rigid airplane and the elastic airplane generalized coordinates used in the flutter analyses:

1. Maximum commonality between a half-model 225 reduced freedom symmetric case (table 11-1) and 260 reduced freedom antisymmetric case (table 11-2), constrained by a CDC 6600/CYBER core size limitation on the maximum number of freedoms in the ATLAS 2 vibration module.
2. An adequate number of judiciously spaced wing vertical translation freedoms, to provide representative distributed mass from the consequent mass-lumping mosaic, figure 11-5, of the ATLAS automated paneling algorithm, without any unduly large lumped masses promoting local resonances.
3. Correct loading from major localized masses, such as the landing gear
4. Full six degree-of-freedom motion for the underslung engines to feed their inertia loads into the wing correctly.

5. Provision for a sufficient number of "beam splines," figure 11-6, for interpolating vibration mode shapes from the structural grid to unsteady aerodynamic grids.
6. A sufficient distribution of points around the wing planform edges, figure 11-7, to minimize extrapolation of vibration mode shapes in transferring this data from structural to unsteady aerodynamic grids.
7. Adequate distribution sampling of only first order body deflections, namely vertical translation freedoms for the symmetric case and side translation and torsional freedoms for the antisymmetric case.
8. Including dominant inertia loading at the centers of gravity of the rigid horizontal and vertical tails: that is, from vertical translation and pitch in the symmetric case, and side translation, yaw and roll in the antisymmetric case, with the addition of horizontal tail vertical and fore-and-aft translations antisymmetrically.
9. Incorporation of the kinetic energy from wing fin and wing inplane motions.

NACELLE FORE-AND-AFT MOTION

Since fore-and-aft freedoms of the half-model were retained only for the nacelles (with the exception discussed in the next paragraph,) and the free rigid airplane fore-and-aft freedom is unimportant in a flutter analysis, this latter freedom was suppressed in the symmetric case via a fore-and-aft support on a body centerline node near the airplane cg. This expedient was used to obtain correct phasing of fore-and-aft motion for the two nacelles in the half-model rather than lumping the rest of the half-airplane mass at its cg and retaining its fore-and-aft freedom to balance the fore-and-aft inertia loads of both nacelles. One or the other of these procedures must be applied, otherwise the ATLAS vibration module, unable to sense the half-model of a bilaterally symmetric system from the dynamic matrix, would put the fore-and-aft motion of the half-model nacelle masses into antiphase in every vibration mode, disturbing the true dynamic coupling. Again, were all the fore-and-aft freedoms of the half-model retained, the problem would not arise, but this was impossible for the analysis at hand because of matrix size limitations.

WING FIN AND WING IN-PLANE MOTIONS

Interaction of the in-plane wing fin inertia loads with the wing also demanded special attention to stay within matrix size limitations. This interaction is represented in the analysis by lumping the fin in-plane translational and rotational inertias at a single node located at its cg. However, this duplicates the wing fin mass, which is distributed for lateral distortion and localized for in-plane motions, and therefore necessitates special treatment to avoid an error in the airplane total mass matrix from the ATLAS mass module. The same condition exists in the antisymmetric case for the wing mass as well; that is, it is distributed for vertical deflections and localized at its cg for in-plane motions. Correct overall inertia balance would not exist without this treatment because the retained distributed freedoms are judiciously chosen and deliberately incomplete in order to stay within matrix size limitations. To state it another way, the wing and wing

fin are considered flexible for out-of-plane motions and rigid for in-plane motions, to obtain correct dynamic simulation while economizing on the required number of retained freedoms. It should be noted that the in-plane torque loads were displaced to nodes where such loads could be carried.

The ATLAS 3 total mass matrix is used in decoupling the rigid airplane freedoms that emerge from the vibration module. The error from the above duplicated mass that would otherwise arise in the ATLAS 3 total mass matrix is avoided using "dummy BC Data," Stages 3 and 5 of table 11-3, together with compatible concentrated mass data cards for the ATLAS mass module where "dummy inertias" equal to the weight are used to represent the localized weight that is duplicating a set of distributed weights. The "dummy BC Data Stages" have "dummy rotation freedoms," corresponding to the "dummy inertias," at the same row/column matrix location as the translation freedoms in reduced stiffness BC Data Stages 4 and 6, for the duplicating localized masses. This is currently the best way in the ATLAS program system, of excluding from the total mass matrix a specialized mass needed only for the vibration model. Figure 11-8 and table 11-4 summarize the procedure used for incorporating rigid in-plane motions. It is recommended that future versions of ATLAS allow such duplicating masses to be excluded from the total mass matrix more directly.

RIGID AIRPLANE ANTISYMMETRIC ROTATION MODES

The lack of an adequate mode interpolation routine in the early stages of development of the ATLAS 3 system forced the use of ATLAS 2 for determining vibration modes. It was not possible, using the free-free stiffness matrix option of the ATLAS 2 vibration module, to decouple rigid airplane freedoms for roll and yaw in the antisymmetric case. Thus, these freedoms appear as dominantly roll and dominantly yaw of the rigid airplane. A much improved "beam-spline" mode interpolation routine has since been developed for ATLAS 3 to transfer vibration mode data from structural to unsteady aerodynamic grids so that ATLAS 3 boundary condition data matching that used in ATLAS 2 has been incorporated in the "Data Tape" supplied to NASA during Task II. Rigid airplane roll and yaw freedoms can be decoupled in ATLAS 3.

Table 11-3 shows the ATLAS 3 BC Data Stages 4 and 6 which match, respectively, the symmetric and antisymmetric retained freedoms that appear in tables 11-1 and 11-2, respectively. Whereas these ATLAS 3 BC Data Stages 4 and 6 are pertinent to direct free-free stiffness matrices, this procedure was not available in the stiffness module of ATLAS 2 and those matrices were obtained via a user control deck procedure after first obtaining corresponding flexibility matrices for the airplane on fore-and-aft body supports. In either event, the ATLAS mass module Condition Data sets up new matrices matching the free-free stiffness matrices, for use when solving for vibration. The body support freedoms used for this contract are located at the end of the free-free set.

AIRPLANE VIBRATION MODES

Vibration mode frequencies for the Arrow Wing with final stiffness modifications appear in table 11-5, the corresponding mode shapes in table 11-6 and mode shapes for

the symmetric, high gross weight case in figures 11-9 through 11-26. Symmetric and antisymmetric cases were analyzed for light and heavy airplane gross weight conditions.

MODE SHAPE INTERPOLATION TO AERODYNAMIC GRIDS

The accuracy with which the mode shapes generated in a vibration analysis and definition structural grid are interpolated to obtain deflections and chordwise slopes at the grid points required by unsteady aerodynamics programs is critical for the accuracy of a flutter analysis. The complication of camber bending of a low-aspect ratio wing, over and above the spanwise deflections, puts further special demands on the mode interpolation process. The sensitivity of the unsteady aerodynamics to such camber bending and the fact that some of the required unsteady aerodynamics grid points need to be very close to the planform edges necessitates some combination of careful extrapolation of mode shapes and modeling of structure as close to the edges of the planform as possible. This somewhat arbitrarily stiff edge structure must not be overloaded in the vibration modes (nor, for that matter, in the static aeroelastic analysis). It should be recalled that only vertical translation displacements were retained at the wing structural grid and both such displacements and consistent chordwise slopes must be retained at the unsteady aerodynamics grid points.

Two mode interpolation programs are available in the ATLAS 2 Boeing Flutter Library program system which was used for the Arrow Wing flutter analysis and they will be described briefly in a discussion of the procedure adopted for mode interpolation.

NASA SURFACE SPLINE INTERPOLATION PROGRAM

This program is contained in the Boeing Flutter Library RHO III subsonic lifting surface unsteady airforces program. It is also available in stand-alone form for use with the Mach Box supersonic unsteady airforces program. It forces a simply supported flexible plate of infinite extent through all the input structural grid points. Examination of the output displacement shape shows serious errors as the edge is approached for wing regions with discontinuous displacements, such as the vicinity of the nacelles. The errors detectable in such regions are symptomatic of a serious shortcoming in the nature of surface spline interpolation. This shortcoming can affect the accuracy of the interpolated chordwise slopes around the edges of the entire lifting surface planform. It is occasioned by the fact that the interpolation plate deflections degenerate to a mean plane much too close to the edge structure grid points used to define the vibration modes of a lifting surface. This effect can even reverse the algebraic sign of the local slope near the edge, completely invalidating any mode shape extrapolation in such regions. Figure 11-27(a), with seven input points per chord shows such edge slope sign reversal at the nacelle stations, despite precautions taken to minimize errors by modeling structure close to the planform edges. Figure 11-27(b), with nine input points per chord, shows the improvement in surface spline edge slope output in the vicinity of the nacelles with added input points off the edge of the planform in the chordwise direction. These added input points, and indeed all the input points to the surface spline interpolation subroutine of Rho III were obtained by first processing the vibration mode data at the structural grid using the other mode

interpolation program in the ATLAS 2/Boeing Flutter Library system, the Beam-Spline Interpolation Module of ATLAS 2. In order to minimize surface spline interpolation errors, its input points, other than points off the planform, were made to coincide with the non-uniformly distributed seven downwash points on each of nine downwash chords used in Rho III for the wing as shown in figure 11-28. The other lifting surfaces shown were treated similarly.

ATLAS 2 BEAM-SPLINE INTERPOLATION MODULE

Rather than surface interpolation, this program contains a matrix scheme using two-way beam-splines for transferring modal data from structural to aerodynamic grids. It requires a set of beams, which can coincide with existing structure, running in a more or less spanwise direction. With mode displacement input points treated as "supports," the desired output chords become secondary beam-splines which must intersect two or more input beams or their extrapolation at the wing tip. The input beam-splines should pass through as regular a pattern of the retained structural nodes as possible, to improve numerical conditioning during the interpolation process. Figure 11-6 shows the wing and wing-fin beam-spline patterns used. These surfaces and the slab tail surfaces, which are not shown, required only two input beam-splines each. The wing input beam-spline pattern comprises 141 wing retained nodes and 18 body retained nodes. Based on geometry alone, this program forms an interpolation transformation between a set of input and output points, which can be used for any set of mode shapes. Chordwise extrapolation is achieved using the interpolation function for the secondary splines. Limited "beam-spline" extrapolation to points 8.65% semichord beyond the leading and trailing edges was used for the extra off-planform input points required to control the surface spline interpolation in Rho III, as discussed previously. Modal interpolation for the Mach Box patterns in figures 11-29 and 11-30, comprising roughly 200 boxes each, was accomplished using the beam-spline program directly.

PRELIMINARY FLUTTER APPRAISAL

This first phase of the flutter analysis considered only one airplane condition but it was conducted in as much depth as the final phase. It was preliminary only in the sense that it was performed immediately after the complex structural model with initial sizing had been set up and validated. Wing flutter considerations, from experience gained on the National SST program for realistic flutter results, dictated the considerable and essential detail incorporated in the structural model as discussed in Section 7. Unsteady airforces were generated using the Rho III subsonic kernel function program, which has been validated extensively by comparing analytical flutter results against flutter model tests. Flutter solutions were obtained which matched the Mach number of the unsteady airforces. The preliminary flutter analysis was confined to the symmetric, high gross weight condition, which was judged likely to be the critical case, and to a high subsonic Mach number, $M = 0.9$. Supersonic flutter analysis, using a refined Mach box unsteady airforce program, was deferred until the subsonic flutter boundary was determined. The downwash collocation points used on all surfaces for subsonic unsteady airforces are shown in figure 11-28. Downwash chords were carefully located to sample structural distortion as well as possible. Airplane plunge and pitch and the first eighteen

symmetric airplane vibration modes were used as generalized coordinates in setting up the flutter equations. The results of the preliminary flutter analysis are shown in figure 11-31 and table 11-8.

FLUTTER WITH INITIAL STRUCTURAL SIZING

The flutter speed with initial sizing of the structural model was 180 knots EAS at a frequency of 1.9-Hz, more than 300 knots EAS below the design requirement at $M = 0.9$. An appraisal of the flutter mode showed large amplitude nacelle motion as well as large energy inputs from excessive wing tip distortion and wind-up of the low speed aileron relative to the inboard location of its actuator. These high flexibilities were also very apparent in the flexibility influence coefficients and the vibration mode shapes.

FLUTTER WITH PRELIMINARY STIFFNESS RESIZE

As a result of the initial assessment of flexibilities and preliminary vibration analysis, it was decided to stiffen structure in three areas before initiating the FLEXSTAB aeroelastic loads analysis:

1. In the wing tip outboard of the wing-fin, spars and covers of main box and secondary structure behind the rear spar were doubled.
2. The low speed aileron covers were quadrupled to minimize wind-up relative to the inboard location of its actuators.
3. The strength designed nacelle support beams were stiffened by a factor of 1.5 to roughly 9,000 lb/in, defined at the rear mount location with the beam cantilevered at the wing rear spar.

Little improvement in flutter speed of the critical low frequency mode was obtained with this preliminary stiffness resize; it rose to 217 knots EAS, still nearly 300 knots EAS below the $M = 0.9$ design requirement. However, the flutter speed of non-critical overtone flutter modes did rise appropriately with the stiffened wing tip, as can be seen for this condition in table 11-8.

FLUTTER WITH STIFF ENGINE BEAMS

Experience from the National SST program indicated that the critical low frequency flutter mode would not be controlled without further stiffening of the engine beams which are cantilevered off the wing rear spar. The engine beams were therefore stiffened by a factor of 4.5 over the strength design value to roughly 27,000 lb/in, defined at the rear mount location with the beam cantilevered at the wing rear spar. The flutter speed of the critical low frequency flutter mode rose dramatically to 412 knots EAS, roughly 100 knots EAS below the 1.2 V_D design requirement at $M = 0.9$ and better than the bare wing flutter speed as shown in figure 11-31. The stiffened engine beams were responsible for a dramatic change in modes 5, 6 and 7 as illustrated in figure 11-32. Other mode shapes were practically unaffected. Frequencies are tabulated in table 11-7. It is the decoupling of the outboard nacelle resonance from

mode 5 that is mainly responsible for the improved flutter speed with stiff engine beams.

It must be noted that the "flutter option" of the ATLAS design module was used to factor up initial element sizing in achieving both the preliminary stiffness resize and the stiff engine beam condition. This results in sharp sizing discontinuities between neighboring finite elements and finite elements for the engine beams with stiffnesses which cannot be achieved with the original titanium beam concept. That problem was overcome on the National SST Program by addition of Borsic/Aluminum composite reinforcement to the engine beam chords. In the ATLAS analysis, the engine beam weight, being outside the wing main box, was included separately with the mass elements in the ATLAS mass module.

CONFIGURATION FLUTTER SENSITIVITY

EFFECT OF ENGINE MOUNTING ON WING FLUTTER SPEED

The preliminary wing flutter analysis with initially sized structure showed significant effects of engine support flexibility on wing flutter speed, figure 11-33. With soft engine beams (vertical stiffness at rear engine mount of about 6 kips/in) vertical motions of the outboard engines are relatively large at the wing flutter frequency. If the trailing edge of the wing is attached to the nacelle, changes in airload distribution induced by trailing edge motion (analogous to the displacement of a flap, driven by engine inertia) have a destabilizing effect on wing flutter. If the trailing edge structure could be detached from the nacelles, the wing flutter speed would be relatively insensitive to engine support flexibility. However, that is very difficult to achieve with present engine locations. With relatively stiff engine beams (approximately 27 kips/in) the flutter speed is insensitive to the attachment of trailing edge structure to the nacelle.

FLUTTER INFLUENCE OF AIRPLANE COMPONENTS

A limited sensitivity study was conducted to evaluate the influence of airplane components on symmetric wing flutter for the preliminary stiffness resize condition with strength designed engine beams stiffened by a factor of 1.5. ATLAS user control deck and mass module "Condition Data" capability was exploited to set up in a single computer run the vibration modes for four different airplane "configurations" approximately, replacing the actual weights of "missing" components with 1 lb weights. The "configurations" were:

1. Airplane without wing fins and nacelles (bare wing)
2. Airplane with wing fins but without nacelles.
3. Airplane with wing fins and inboard nacelles but without outboard nacelles.
4. Complete airplane.

Only wing unsteady airforces were used in flutter analyses for the first three "configurations," while the effects of adding first horizontal tail and then wing fin unsteady airforces were investigated for the complete airplane. Figure 11-34 shows the

influence of the selected airplane components on wing symmetric flutter and points up the highly destabilizing influence of the outboard nacelles, the small favorable effect of tail damping, and the relatively decoupled effect of the wing fins. The effect of removed inboard nacelles while outboard nacelles are attached was not investigated. These results were obtained for a constant altitude of 20000 ft. with unsteady aerodynamics for $M = 0.9$.

FINAL FLUTTER ANALYSIS AND STIFFNESS REDESIGN

Following the automated resize of wing primary structure, and prior to the final flutter analysis, some overriding stiffness requirements were imposed on the strength designed structural model. These constraints included locks for high speed flight on the low-speed aileron and outboard flap, the stiffened wing tip and low speed aileron that had been adopted prior to the FLEXSTAB aeroelastic loads analysis, and engine beams stiffened to 4.5 times the strength design value. With these stiffness constraints the effect of strength resizing was only a slight decrease in flutter speed to 0.817 of the speed requirement at $M = 0.9$, compared with a flutter speed ratio of 0.865 prior to the strength resize, with the same stiffness constraints except for the control locks.

The relative effectiveness of stiffening the wing tip and adding the control locks was investigated and is summarized in table 11-10. The control locks are effective in raising the flutter speeds of overtone flutter modes, whereas wing tip stiffening is also effective for the fundamental 1.9 Hz wing flutter mode. Figure 11-35 shows the typical vibration mode shape amplitude attenuation of low-speed aileron and outboard flap deflections which result from incorporating control locks.

No reduction in gages or member sizes, below the values specified for strength, were allowed in defining further structural design changes to meet flutter criteria. Engineering judgement, based on experience with similar vibration and flutter modes encountered on the National SST Program was used in defining these stiffness design modifications and these judgements were aided by diagnosis of the individual flutter mechanisms encountered, as discussed below.

TECHNICAL APPROACH FOR STIFFNESS REDESIGN

It was not possible to readily interface ATLAS 2 with the flutter optimization system developed during the SST Technology Follow-On Program (Contract DOT-FA72WA-2893). Thus stiffness redesign efforts during this contract were based on engineering judgment and stiffness design iteration. These judgments were supplemented by diagnostic studies to identify the essential degrees of freedom and to characterize the energy transfer process, as discussed in the following paragraphs.

The first indication of the freedoms important to the flutter mechanism is obtained from the larger components of the flutter vector. An examination of the frequency coupling trend for the principal component modes, from the branching behavior in the speed-frequency plane, figure 11-36, can indicate any dominant binary (two degrees of freedom) couplings with the frequency of a "torsion type" mode dropping to near coalescence with a climbing frequency of a "bending type" mode. These observations are confirmed by a lagging phase for the "torsion type" mode evident in the flutter

vector. The energy absorbing and damping modes involved in flutter of slender delta wings exhibit considerable airfoil camber bending, evident in figure 11-36, in addition to torsion and bending deflections. More than two freedoms, and often up to six or seven, are significantly involved in the flutter mechanism. However, considerable understanding can be gained from focusing attention on the dominant binary or low order dynamical system. This is systematically uncovered by studying the equilibrium polygons of generalized forces and the implicit energy balance of the fluttering system at neutral stability as shown in figure 11-37 and table 11-9. The energy extraction process is exhibited by integrating the work done by the generalized forces over one cycle of the flutter oscillation. Only the aerodynamic forces contribute to this process which is dominated by the aerodynamic stiffness coupling and the direct aerodynamic damping terms for the dynamic freedoms essential to the flutter mechanism. It is also possible to detect energy flux relationships between the essential freedoms from the energy balance results and to form an energy compatibility or net energy equation highlighting the energy sources and energy sinks of the flutter mechanism, as shown in figure 11-38 and table 11-9.

The involved load phasing of unsteady aerodynamic loads complicates the flutter redesign process. Frequency separation of the dominant binary freedoms is usually necessary and this must occur despite phase and magnitude shifts in the unsteady airloads which accompany structural stiffness or mass distribution changes calculated to accomplish this. In spite of these complications, stiffening in high strain regions of the "torsion type" mode shapes was found quite effective for stiffness redesign in this study. This process is aimed at a more uniform strain energy density distribution for such mode shapes.

STIFFNESS REDESIGN

Stiffness modifications 1 to 3 were discussed at the start of this section and appear in figures 11-39 to 11-41. Figures 11-42 to 11-46 show five of the six additional stiffness modifications that were investigated in arriving at the final stiffness design for Task II. The final set of stiffness modifications to the strength design appears in figure 11-3 as Stiffness Modification 9. Flutter results for the Task II stiffness design cycles are summarized in figure 11-47.

Stiffness Modifications 4 or 5 incurred unduly large weight penalties for small flutter speed gains. They comprised, respectively, overall doubling of the stiffness of all wing spars and ribs, or stiffening spars and covers of the wing tip by a factor of 3.0 and just inboard of the wing fin by a factor of 1.5.

Stiffness Modification 6 restored the low speed aileron cover thickness to the initial value, thereby raising the flutter speed slightly by removing an adverse mass balance effect on the wing, while the control locks inhibit wind-up of the unstiffened control. Simultaneously, a 4.7 Hz wing fin flutter mode, which appeared as a result of reductions in member sizes at the root of the fin and other local changes in fin attachment structure during strength resize, was much improved by reverting to the original attachment, stiffening the wing rib below the wing fin by a factor of 3.0 and stiffening the fin root region.

Light diffusion rib structure for the outboard nacelle support beam was added in Stiffness Modification 7 and the auxiliary trailing edge spar from the wing root to the outboard nacelle was stiffened to about the same level as the rear spar. A streamwise rib near the wing fin root was added simultaneously and this raised the wing fin flutter speed satisfactorily above $1.2 V_D$. Stiffness Modification 8 comprised the addition to Modification 7 of a graded local increase in wing depth in the tip region. The airfoil discontinuity at the wing fin station was first removed and the maximum thickness ratio was then increased from 2.8 percent to 3.5 percent at the fin station with the increment decreasing linearly to zero at the wing tip and at the outboard nacelle station.

Finally, for Stiffness Modification 9, the stiffened auxiliary trailing edge spar was restored to initial sizing, while stiff diffusion rib structure was added for both outboard and inboard nacelle support beams. The thickened wing tip was retained and four streamwise ribs were added in the wing tip region. The front spar web at the wing tip and the entire rear spar web were thickened to equal the average local cover skin gage. Lastly, nacelle support beams were stiffened to 5.5 times the strength design value.

FLUTTER BOUNDARY-TITANIUM STRUCTURE (1975 TECHNOLOGY)

Figure 11-47 shows that the improved wing flutter speed achieved with Stiffness Modification 9 did not clear the original $1.2 V_D$ flutter placard. It was concluded that further efforts to increase flutter speed of the critical 1.9 Hz wing flutter mode, via structural changes based on engineering judgement, would produce an unrealistically high weight penalty. Hence it was proposed that the subsonic dive placard be reduced by 50 knots EAS to achieve flutter clearance. Undoubtedly a substantially higher placard could be achieved without additional weight increment, by utilizing formal optimization techniques. This approach could be easily justified on an aircraft development program. The reduced placard would impose a range decrease of 25 nautical miles with fixed fuel loading, or an increase of 1297 lbs. in fuel loading for constant range.

The structure with the latest stiffness design modifications was then analysed for symmetric flutter at low gross weight and antisymmetric flutter for both high and low gross weights at $M = 0.9$. This confirmed that the symmetric, high gross weight condition is critical. Flutter analyses were then conducted for that condition at other Mach numbers. The resulting flutter boundary for the 969-512B configuration with titanium structure (1975 technology) appears in figure 11-1. Budget limitations prevented determination of the flutter boundaries over the Mach number range for the conditions not critical at $M = 0.9$. Figure 11-2 shows, in terms of flutter speed ratio relative to the original goal of 504 knots EAS, the sensitivity, to configuration features and structural changes, of the critical 1.9 Hz, symmetric, high gross weight, wing flutter mode at $M = 0.9$.

The stiffness design modifications to provide flutter clearance are summarized in figure 11-3. The penalty associated with this Task II stiffness design is equivalent to 10,223 lbs per aircraft including 2341 lbs weight equivalent of a 1.3 drag count increase for thickening the wing tip.

Table 11-1.—Retained Freedoms—Symmetric Vibration Modes

CUMULATIVE COUNT	USER NODE	FREEDOM CODE	AIRPLANE COMPONENT
1	1020	TX	INBD NACELLE C.G.
2	1020	TY	
3	1020	TZ	
4	1020	RX	
5	1020	RY	
6	1020	RZ	
7	1070	TX	OUTBD NACELLE C.G.
8	1070	TY	
9	1070	TZ	
10	1070	RX	
11	1070	RY	
12	1070	RZ	
13	670	TZ	WING
14	663	TZ	
15	652	TZ	
16	644	TZ	
17	637	TZ	
18	792	TZ	
19	784	TZ	
20	779	TZ	
21	775	TZ	
22	620	TZ	
23	618	TZ	
24	615	TZ	
25	613	TZ	
26	610	TZ	
27	608	TZ	
28	605	TZ	
29	603	TZ	
30	600	TZ	
31	597	TZ	
32	692	TZ	
33	693	TZ	
34	694	TZ	
35	562	TZ	
36	560	TZ	
37	695	TZ	
38	555	TZ	
39	553	TZ	
40	550	TZ	
41	547	TZ	
42	544	TZ	
43	541	TZ	
44	539	TZ	
45	537	TZ	
	536	TZ	
	534	TZ	
48	476	TZ	
49	716	TZ	
50	713	TZ	
51	712	TZ	

Table 11-1.--(Continued)

CUMULATIVE COUNT	USER NODE	FREEDOM CODE	AIRPLANE COMPONENT
52	709	TZ	WING
53	708	TZ	
54	705	TZ	
55	704	TZ	
56	701	TZ	
57	700	TZ	
58	533	TZ	
59	85	TZ	
60	82	TZ	
61	79	TZ	
62	129	TZ	
63	76	TZ	
64	176	TZ	
65	73	TZ	
66	173	TZ	
67	50	TZ	
68	120	TZ	
69	220	TZ	
70	67	TZ	
71	167	TZ	
72	267	TZ	
73	44	TZ	
74	114	TZ	
75	214	TZ	
76	314	TZ	
77	41	TZ	
78	111	TZ	
79	211	TZ	
80	311	TZ	
81	58	TZ	
82	158	TZ	
83	209	TZ	
84	309	TZ	
85	409	TZ	
86	207	TZ	
87	307	TZ	
88	407	TZ	
89	55	TZ	
90	155	TZ	
91	205	TZ	
92	305	TZ	
93	405	TZ	
94	385	TZ	
95	454	TZ	
96	464	TZ	
97	474	TZ	
98	484	TZ	
99	493	TZ	
100	502	TZ	
101	512	TZ	
102	522	TZ	

Table 11-1.—(Continued)

CUMULATIVE COUNT	USER NODE	FREEDOM CODE	AIRPLANE COMPONENT
103	52	TZ	WING
104	152	TZ	
105	262	TZ	
106	301	TZ	
107	382	TZ	
108	452	TZ	
109	462	TZ	
110	482	TZ	
111	492	TZ	
112	179	TZ	
113	146	TZ	
114	192	TZ	
115	200	TZ	
116	298	TZ	
117	350	TZ	
118	398	TZ	
119	819	TZ	
120	816	TZ	
121	470	TZ	
122	810	TZ	
123	808	TZ	
124	806	TZ	
125	804	TZ	
126	803	TZ	
127	901	TZ	
128	531	TZ	
129	890	TZ	
130	887	TZ	WING
131	940	TZ	
132	937	TZ	
133	1023	TZ	
134	878	TZ	
135	876	TZ	
136	928	TZ	
137	926	TZ	
138	1063	TZ	
139	916	TZ	
140	915	TZ	
141	908	TZ	
142	906	TZ	
143	904	TZ	
144	902	TZ	
145	920	TZ	
146	900	TZ	
147	1021	TZ	
148	1061	TZ	
149	965	TZ	
150	957	TZ	
151	954	TZ	
152	951	TZ	
153	950	TZ	

Table 11-1.-(Continued)

CUMULATIVE COUNT	USER NODE	FREEDOM CODE	AIRPLANE COMPONENT
154	767	TZ	WING
155	766	TZ	
156	763	TZ	
157	762	TZ	
158	759	TZ	
159	758	TZ	
160	755	TZ	
161	754	TZ	
162	751	TZ	
163	750	TZ	WING FIN
164	237	TY	
165	235	TY	
166	232	TY	
167	229	TY	
168	227	TY	
169	226	TY	
170	475	TY	
171	285	TY	
172	282	TY	
173	472	TY	
174	332	TY	
175	329	TY	
176	277	TY	
177	862	TY	
178	379	TY	
179	377	TY	
180	376	TY	
181	375	TY	
182	428	TY	
183	427	TY	
184	426	TY	
185	424	TY	
186	417	TY	
187	416	TY	
188	415	TY	
189	414	TY	
190	374	TZ	C.G.
191	374	TX	
192	4	RY	PITCH INERT 1A LOAD
193	3191	TZ	FWD STICK BODY
194	3189	TZ	
195	3187	TZ	
196	3185	TZ	
197	3181	TZ	BODY SHELL
198	2038	TZ	
199	2098	TZ	
200	2158	TZ	
201	2218	TZ	
202	2278	TZ	
203	2338	TZ	
204	2398	TZ	

Table 11-1.—(Concluded)

CUMULATIVE COUNT	USER NODE	FREEDOM CODE	AIRPLANE COMPONENT
205	2458	TZ	BODY SHELL
206	2518	TZ	
207	2578	TZ	
208	2638	TZ	
209	2698	TZ	
210	2758	TZ	
211	2818	TZ	
212	2878	TZ	
213	2938	TZ	
214	2998	TZ	
215	3058	TZ	
216	3201	TZ	AFT STICK BODY
217	3205	TZ	
218	3208	TZ	
219	3212	TZ	
220	3250	RY	HORIZONTAL TAIL
221	3250	TZ	C.G.
222	3225	TZ	VERTICAL TAIL
223	3225	RY	C.G.
224	3183	TZ	FWD STICK BODY
225	3203	TZ	AFT STICK BODY

USED AS SUPPORTS
IN ATLAS 2.

Table 11-2.—Retained Freedoms—Antisymmetric Vibration Modes

CUMULATIVE COUNT	USER NODE	FREEDOM CODE	AIRPLANE COMPONENT
1	1020	TX	INBD NACELLE C.G.
2	1020	TY	
3	1020	TZ	
4	1020	RX	
5	1020	RY	
6	1020	RZ	
7	1070	TX	OUTBD NACELLE C.G.
8	1070	TY	
9	1070	TZ	
10	1070	RX	
11	1070	RY	
12	1070	RZ	
13	670	TZ	WING
14	663	TZ	
15	652	TZ	
16	644	TZ	
17	637	TZ	
18	792	TZ	
19	784	TZ	
20	779	TZ	
21	775	TZ	
22	620	TZ	
23	618	TZ	
24	615	TZ	
25	613	TZ	
26	610	TZ	
27	608	TZ	
28	605	TZ	
29	603	TZ	
30	600	TZ	
31	597	TZ	
32	652	TZ	
33	632	TZ	
34	611	TZ	
35	562	TZ	
36	550	TZ	
37	695	TZ	
38	555	TZ	
39	553	TZ	
40	550	TZ	
41	547	TZ	
42	544	TZ	
43	541	TZ	
44	539	TZ	
45	537	TZ	
46	536	TZ	
47	534	TZ	
48	476	TZ	
49	716	TZ	
50	713	TZ	
51	712	TZ	

Table 11-2.--(Continued)

CUMULATIVE COUNT	USER NODE	FREEDOM CODE	AIRPLANE COMPONENT
52	709	TZ	
53	708	TZ	
54	705	TZ	
55	704	TZ	
56	701	TZ	
57	700	TZ	
58	533	TZ	
59	85	TZ	
60	82	TZ	
61	79	TZ	
62	129	TZ	
63	76	TZ	
64	176	TZ	
65	73	TZ	
66	173	TZ	
67	50	TZ	
68	120	TZ	
69	220	TZ	
70	67	TZ	
71	167	TZ	
72	267	TZ	
73	44	TZ	
74	114	TZ	
75	214	TZ	
76	314	TZ	
77	41	TZ	
78	111	TZ	
79	211	TZ	
80	311	TZ	
81	58	TZ	
82	158	TZ	
83	209	TZ	
84	309	TZ	
85	409	TZ	
86	207	TZ	
87	307	TZ	
88	407	TZ	
89	55	TZ	
90	155	TZ	
91	205	TZ	
92	305	TZ	
93	405	TZ	
94	385	TZ	
95	444	TZ	
96	464	TZ	
97	474	TZ	
98	484	TZ	
99	493	TZ	
100	502	TZ	
101	512	TZ	
102	522	TZ	

WILL

Table 11-2.-(Continued)

CUMULATIVE COUNT	USER NODE	FREEDOM CODE	AIRPLANE COMPONENT
103	52	TZ	
104	152	TZ	
105	202	TZ	
106	302	TZ	
107	382	TZ	
108	452	TZ	
109	462	TZ	
110	482	TZ	
111	492	TZ	
112	179	TZ	
113	146	TZ	
114	192	TZ	
115	200	TZ	
116	298	TZ	
117	350	TZ	
118	398	TZ	
119	819	TZ	
120	816	TZ	
121	470	TZ	
122	810	TZ	
123	808	TZ	
124	806	TZ	
125	804	TZ	
126	803	TZ	WING
127	801	TZ	
128	531	TZ	
129	890	TZ	
130	887	TZ	
131	940	TZ	
132	937	TZ	
133	1023	TZ	
134	878	TZ	
135	876	TZ	
136	928	TZ	
137	926	TZ	
138	1063	TZ	
139	916	TZ	
140	915	TZ	
141	908	TZ	
142	906	TZ	
143	904	TZ	
144	902	TZ	
145	920	TZ	
146	900	TZ	
147	1021	TZ	
148	1061	TZ	
149	965	TZ	
150	957	TZ	
151	954	TZ	
152	951	TZ	
153	956	TZ	

Table 11-2.-(Continued)

CUMULATIVE COUNT	USER NODE	FREEDOM CODE	AIRPLANE COMPONENT
154	767	TZ	WING
155	766	TZ	
156	763	TZ	
157	762	TZ	
158	759	TZ	
159	758	TZ	
160	755	TZ	
161	754	TZ	
162	751	TZ	
163	750	TZ	
164	237	TY	WING FIN
165	235	TY	
166	232	TY	
167	229	TY	
168	227	TY	
169	226	TY	
170	475	TY	
171	285	TY	
172	282	TY	
173	472	TY	
174	332	TY	
175	329	TY	
176	277	TY	
177	862	TY	
178	379	TY	
179	377	TY	
180	376	TY	
181	375	TY	
182	428	TY	
183	427	TY	
184	426	TY	
185	424	TY	
186	417	TY	
187	416	TY	
188	415	TY	
189	414	TY	
190	374	TZ	C.G.
191	374	TX	
192	471	RY	WING C.G.
193	165	TY	
194	165	TX	
195	3101	RZ	WING YAW INERTIA LOAD
196	3191	RX	FWD STICK BODY
197	3189	RX	
198	3187	RX	
199	3185	RX	
200	2181	RX	
201	3191	TY	
202	3189	TY	
203	3187	TY	
204	3185	TY	
205	3181	TY	

Table 11-2.—(Continued)

CUMULATIVE COUNT	USER NODE	FREEDOM CODE	AIRPLANE COMPONENT
206	2039	RX	BODY SHELL
207	2099	RX	
208	2159	RX	
209	2219	RX	
210	2279	RX	
211	2339	RX	
212	2399	RX	
213	2459	RX	
214	2519	RX	
215	2579	RX	
216	2639	RX	
217	2699	RX	
218	2759	RX	
219	2819	RX	
220	2879	RX	
221	2939	RX	
222	2999	RX	
223	3059	RX	
224	2037	TY	
225	2097	TY	
226	2157	TY	
227	2217	TY	
228	2277	TY	
229	2337	TY	
230	2397	TY	
231	2457	TY	
232	2517	TY	
233	2577	TY	
234	2637	TY	
235	2697	TY	
236	2757	TY	
237	2817	TY	
238	2877	TY	
239	2937	TY	
240	2997	TY	
241	3057	TY	
242	3201	RX	AFT STICK BODY
243	3205	RX	
244	3208	RX	
245	3212	RX	
246	3201	TY	
247	3205	TY	
248	3208	TY	
249	3212	TY	
250	3250	RX	HORIZONTAL TAIL C.G.
251	3250	RZ	
252	3250	TX	
253	3250	TY	
254	3250	TZ	

Table 11-2.-(Concluded)

CUMULATIVE COUNT	USER NODE	FREEDOM CODE	AIRPLANE COMPONENT
255	3225	RX	<div style="display: flex; align-items: center;"> <div style="margin-right: 10px;"> ↑ ↓ </div> VERTICAL TAIL C.G. </div>
256	3225	RZ	
257	3225	TY	
258	3183	TY	<div style="display: flex; align-items: center;"> <div style="margin-right: 10px;"> FWD STICK BODY AFT STICK BODY </div> } </div>
259	3203	TY	
260	3203	RX	

USED AS SUPPORTS
IN ATLAS 2

Table 11-3.-ATLAS 3 BC Data Stages-Flutter Analysis

DUMMY BC DATA - SYMMETRIC (MASS)

SET 1 STAGE 3 /
RETAIN ALL FOR 1020 /
RETAIN ALL FOR 1070 /

RETAIN TZ FOR	670	663	652	644	677	792	784	779	775	620
	618	615	613	610	608	605	603	600	597	693
	694	562	560	695	555	553	550	547	544	539
	537	536	534	476	716	713	712	709	708	704
	701	700	533	85	82	79	129	76	176	73
	50	120	220	67	167	267	44	114	214	314
	111	211	311	58	158	209	309	409	207	307
	55	155	205	305	405	385	454	464	474	484
	502	512	522	52	152	202	302	382	452	462
	492	179	146	192	200	298	350	398	819	816
	810	808	806	804	803	801	531	890	887	940
	1023	878	876	928	926	1063	916	915	908	906
	902	920	900	1021	1061	965	957	954	951	950
	766	763	762	759	758	755	754	751	750	/
RETAIN TY FOR	237	235	232	229	227	226	475	285	282	472
	332	329	277	862	379	377	376	375	428	427
	424	417	416	415	414	/				426

RETAIN RZ RX FOR 374 /

RETAIN RY FOR 471 /

RETAIN TZ FOR 3181 3189 3187 3185 3181 2038 2098 2158 2218
2278 2338 2398 2458 2518 2578 2638 2698 2758 2818
2878 2938 2998 3058 3201 3205 3208 3212 /

RETAIN RY TZ FOR 3250 /

RETAIN TZ RY FOR 3225 /

RETAIN TZ FOR 3183 3203 /

Table 11-3.-(Continued)

BC DATA-SYMMETRIC (STIFFNESS)

SET 1 STAGE 4 /
 SUPPORT ASYM IN SURFACE 2 THROUGH 2001 /
 SUPPORT TX FOR 3183 /
 SUPPORT RX RZ FOR 150 440 /
 SUPPORT RZ FOR 825 827 828 829 865 866 867 868 869 852
 854 856 858 859 860 197 371 401 1012 1022 1062
 1072 41 TO 50 61 TO 70 91 TO 97 99 100 115 TO 117
 119 120 123 TO 140 432 TO 437 /
 SUPPORT TY FOR 62 TO 65 67 92 TO 95 115 117 135 137 /
 RETAIN ALL FOR 1020 /
 RETAIN ALL FOR 1070 /
 RETAIN TZ FOR 670 663 652 644 637 792 784 779 775 620
 618 615 613 610 608 605 603 600 597 692 693
 594 562 560 695 555 553 550 547 544 541 539
 537 536 534 476 716 713 712 709 708 705 704
 701 700 533 85 82 79 129 76 176 73 173
 50 120 220 67 167 267 44 114 214 314 41
 111 211 311 58 158 209 309 409 207 307 407
 55 155 205 305 405 385 454 464 474 484 493
 502 512 522 52 152 202 302 382 452 462 482
 492 179 146 192 200 298 350 398 819 816 470
 810 808 806 804 803 801 531 890 887 940 937
 1023 878 876 928 926 1063 916 915 908 906 904
 902 920 900 1021 1061 965 957 954 951 950 768
 766 763 762 759 758 755 754 751 750 /
 RETAIN TY FOR 237 235 232 229 227 226 475 285 282 472
 332 329 277 862 379 377 376 375 428 427 426
 424 417 417 415 414 /
 RETAIN TZ TX FOR 374 /
 RETAIN RY FOR 471 /
 RETAIN TZ FOR 3191 3189 3187 3185 3181 2038 2098 2158 2218
 2278 2338 2398 2458 2518 2578 2638 2698 2758 2818
 2878 2838 2998 3058 3201 3205 3208 3212 /
 RETAIN RY TZ FOR 3250 /
 RETAIN TZ RY FOR 3225 /
 RETAIN TZ FOR 3183 3203 /

Table 11-3.-(Continued)

DUMMY BC DATA-ANTISYMMETRIC (MASS)

SET 1 STAGE 5 /

RETAIN ALL FOR 1020 /

RETAIN ALL FOR 1070 /

RETAIN TZ FOR	670	663	652	644	677	792	784	779	775	620
618	615	613	610	608	605	603	600	597	692	693
694	562	560	695	555	553	550	547	544	541	539
537	536	534	476	716	713	712	709	708	705	704
701	700	533	85	82	79	129	76	176	73	173
50	120	220	67	167	267	44	114	214	314	41
111	211	311	58	158	209	309	409	207	307	407
55	155	205	305	405	385	454	464	474	484	493
502	512	522	52	152	202	302	382	452	462	482
492	179	146	192	200	298	350	398	819	816	470
810	808	806	804	803	801	531	890	887	940	937
1023	878	876	928	926	1063	916	915	908	906	904
902	920	900	1021	1061	965	957	954	951	950	767
766	763	762	759	758	755	754	751	750	/	
RETAIN TY FOR	237	235	232	229	227	226	475	285	282	472
332	329	277	862	379	377	376	375	428	427	426
424	417	416	415	414	/					

RETAIN RZ RX FOR 374 /

RETAIN RY FOR 471 /

RETAIN RY RX FOR 165 /

RETAIN RZ FOR 3101 /

RETAIN RX FOR 3191 3189 3187 3185 3181 /

RETAIN TY FOR 3191 3189 3187 3185 3181 /

RETAIN RX FOR 2039 2099 2159 2219 2279 2339 2399

2459 2519 2579 2539 2699 2759 2819 2879 2939

2999 3059 /

RETAIN TY FOR 2037 2097 2157 2217 2277 2337 2397

2457 2517 2577 2637 2697 2757 2817 2877 2937

2997 3057 /

RETAIN RX FOR 3201 3205 3208 3212 /

RETAIN TY FOR 3201 3205 3208 3212 /

RETAIN RX RZ TX TY TZ FOR 3250 /

RETAIN RX TZ TY FOR 3225 /

RETAIN TY FOR 3183 3203 /

RETAIN RX FOR 3203 /

Table 11-3.-(Concluded)

BC DATA - ANTISYMMETRIC (STIFFNESS)

SET 1 STAGE 6 /									
SUPPORT SYMM IN SURFACE 2 THROUGH 2001 /									
SUPPORT RX RZ FOR 150 440 /									
SUPPORT RZ FOR 825 827 828 829 865 866 867 868 869 852									
854 856 858 859 860 197 199 371 401 1012 1022 1062 1072									
41 TO 59 61 TO 70 91 TO 97 99 100 115 TO 117 119 120									
135 TO 140 432 TO 437 /									
SUPPORT TY FOR 62 TO 65			67	92 TO 95	97	115	117	135	137 /
RETAIN ALL FOR 1020 /									
RETAIN ALL FOR 1070 /									
RETAIN TZ FOR	670	663	652	644	677	792	784	779	775 620
618	615	613	610	608	605	603	600	597	692 693
694	562	560	695	555	553	550	547	544	541 539
537	536	534	476	716	713	712	709	708	705 704
701	700	533	85	82	79	129	76	176	73 173
50	120	220	67	167	267	44	114	214	314 41
111	211	311	58	158	209	309	409	207	307 407
55	155	205	305	405	385	454	464	474	484 493
502	512	522	52	152	202	302	382	452	462 482
492	179	146	192	200	298	350	398	819	816 470
810	808	806	804	803	801	531	890	887	940 937
1023	878	876	928	926	1063	916	915	908	906 904
902	920	900	1021	1061	965	957	954	951	950 767
766	763	762	759	758	755	754	751	750	/
RETAIN TY FOR	237	235	232	229	227	226	475	285	282 472
332	329	277	862	379	377	376	375	428	427 426
424	417	416	415	414	/				
RETAIN TZ TX FOR 374 /									
RETAIN RY FOR 471 /									
RETAIN TY TX FOR 165									
RETAIN RZ FOR 3101 /									
RETAIN RX FOR	3191	3189	3187	3185	3181 /				
RETAIN TX FOR	3191	3189	3187	3185	3181 /				
RETAIN RX FOR	2039	2099	2159	2219	2279	2339	2399		
2459	2519	2579	2639	2699	2759	2819	2879	2939	
2999	3059	/							
RETAIN TY FOR	2037	2097	2157	2217	2277	2337	2397		
2457	2517	2577	2637	2697	2757	2817	2877	2937	
2997	3057	/							
RETAIN RX FOR	3201	3205	3208	3212	/				
RETAIN TY FOR	3201	3205	3208	3212	/				
RETAIN RX RZ TX TY TZ FOR 3250 /									
RETAIN RX RZ TY FOR 3225 /									
RETAIN TY FOR 3183 3203 /									
RETAIN RX FOR 3203 /									

Table 11-4. ATLAS 3 Data Details for Vibration Mode Rigid In-Plane Motion

BC DATA DETAILS

BEGIN BC DATA /

...

SET 1 STAGE 3 / DUMMY BC DATA SYMM (MASS)

...

RETAIN RZ RX FOR 374 /
RETAIN RY FOR 471 /

...

SET 1 STAGE 4 / SYMM (STIFFNESS)

...

RETAIN TZ TX FOR 374 /
RETAIN RY FOR 471 /

...

SET 1 STAGE 5 / DUMMY BC DATA ANTISYM (MASS)

...

RETAIN RZ RX FOR 374 /
RETAIN RY FOR 471 /
RETAIN RY RX FOR 165 /
RETAIN RZ FOR 3101 /

...

SET 1 STAGE 6 / ANTISYM (STIFFNESS)

...

RETAIN TZ TX FOR 374 /
RETAIN RY FOR 471 /
RETAIN TY TX FOR 165 /
RETAIN RZ FOR 3101 /

...

END BC DATA

MASS DATA DETAILS

END MASS DATA /

Table 11-4.-(Concluded)

USER DECK DETAILS

BEGIN CONTROL MATRIX PROGRAM ...

BC DATA STAGE

EXECUTE MERGE (STIFFNESS, STAGE = 4, K11 = 11, K12 = 22)
 EXECUTE CHOLESKI (DEFO, K11, FK12, K12)
 EXECUTE MULTIPLY (KREDS4 = [K22 - FK12(T) * FK12])

EXECUTE MERGE (STIFFNESS, STAGE = 6, A11 = 11, A12 = 12, A22 = 22)
 EXECUTE CHOLESKI (DEFO, A11, FA12, A12)
 EXECUTE MULTIPLY (KREDA6 = [A22 - FA12 (T) * F A12])

EXECUTE MASS (....)

Condition number (see MASS DATA)

PRINT OUTPUT (MASS, STATEMENT, SUMMARY, MDC = MDC00*A)

BC data stage
 Mass condition BC data stage
 Mass condition BC data stage
 BC data stage

EXECUTE VIBRATION (([KREDS4 - LAM44SH * MDC004A] * V44SH = 0), NFREQS = 20, ... STAGF = 4)
 EXECUTE VIBRATION (([KREDS4 - LAM54SL * MDC005A] * V54SL = 0), NFREQS = 20, ... STAGE = 4)
 EXECUTE VIBRATION (([KREDA6 - LAM66AH * MDC006A] * V66AH = 0), NFREQS = 20, ... STAGE = 6)
 EXECUTE VIBRATION (([KREDA6 - LAM76AL * MDC007A] * V76AL = 0), NFREQS = 20, ... STAGE = 6)

END CONTROL MATRIX PROGRAM

Table 11-5.—Airplane Vibration Mode Frequencies—Final Stiffness Design

Mode	Symmetric		Antisymmetric	
	High gross weight Frequency, Hz	Low gross weight Frequency, Hz	High gross weight Frequency, Hz	Low gross weight Frequency, Hz
1	0.974	1.084	0.717	0.944
2	1.183	1.232	1.213	1.577
3	2.177	2.271	2.132	2.203
4	2.427	2.741	2.313	2.531
5	2.792	2.801	2.583	2.687
6	2.999	3.010	2.810	2.820
7	3.370	3.508	2.998	3.011
8	3.626	3.628	3.045	3.520
9	3.806	3.817	3.652	3.714
10	3.997	4.424	3.862	3.951
11	4.410	4.762	4.048	4.696
12	4.678	5.807	4.468	6.038
13	6.216	6.655	5.731	6.472
14	6.354	7.246	6.033	6.594
15	6.748	8.281	6.260	6.760
16	7.214	8.754	6.511	7.242
17	8.026	8.873	6.819	8.244
18	8.623	9.293		

Table 11-6.—Airplane Vibration Mode Shapes,* Final Stiffness Design

SYMMETRIC CASES. HIGH GROSS WEIGHT

ROW	MODE 1	MODE 2	MODE 3	MODE 4	MODE 5	MODE 6	MODE 7	MODE 8
1	.0000	.1737	.0519	.0135	-.0595	-.1244	.0061	.1403
2	.0000	-.0000	.0109	.0177	.0159	.0635	-.0106	-.2207
3	1.0000	-.2837	.0781	-.0396	-.1998	-.3007	.0039	.3129
4	.0000	.0000	.0003	.0005	-.0002	.0003	-.0002	-.0031
5	.0000	.0005	-.0005	.0001	.0007	.0022	-.0000	-.0024
6	.0000	-.0000	-.0000	.0000	.0001	.0003	-.0000	-.0005
7	.0000	.1923	.0632	.0408	-.0444	-.1357	.0025	-.0965
8	.0000	.0000	.0178	.0279	.0733	.1758	-.0075	.0917
9	1.0000	-.2917	.2208	.1497	-.1452	-.2565	-.0245	-.2624
10	.0000	.0000	.0006	.0009	.0010	.0029	-.0001	.0016
11	.0000	.0005	-.0009	-.0005	.0003	.0025	.0001	.0022
12	.0000	-.0000	.0000	.0000	.0001	.0003	-.0000	.0001
13	1.0000	.4461	-.0167	.0277	.1772	-.2086	-.0088	.0183
14	1.0000	.3146	-.1065	.0613	.1556	-.1622	-.0060	.0097
15	1.0000	.1405	-.1553	.0574	.0272	.0413	.0019	-.0161
16	1.0000	.0026	-.1297	.0117	-.0923	.2168	.0019	-.0419
17	1.0000	-.1454	.0208	.0836	-.1358	.2368	-.0213	-.0508
18	1.0000	-.2257	.1937	.2166	-.0564	.2387	-.0472	-.0220
19	1.0000	-.2930	.4050	.4195	.1554	.3872	-.0739	.1284
20	1.0000	-.3434	.5826	.5991	.3805	.5805	-.1074	.3388
21	1.0000	-.3774	.7091	.7300	.5593	.7451	-.1383	.5254
22	1.0000	.4391	-.0212	.0293	.1759	-.2063	-.0087	.0180
23	1.0000	.3923	-.0369	.0437	.1728	-.1959	-.0078	.0154
24	1.0000	.3557	-.021	.0532	.1669	-.1832	-.0070	.0130
25	1.0000	.3088	-.0083	.0615	.1522	-.1575	-.0058	.0092
26	1.0000	.2743	-.1244	.0652	.1347	-.1291	-.0045	.0055
27	1.0000	.2275	-.1402	.0660	.1023	-.0793	-.0024	-.0004
28	1.0000	.1878	-.1490	.0633	.0699	-.0285	-.0004	-.0056
29	1.0000	.1532	-.1527	.0589	.0401	.0176	.0012	-.0123
30	1.0000	.1014	-.1532	.0496	-.0067	.0906	.0031	-.0218
31	1.0000	.0504	-.1456	.0389	-.0516	.1575	.0036	-.0312
32	1.0000	.4319	-.0258	.0310	.1745	-.2038	-.0084	.0176
33	1.0000	.3854	-.0609	.0451	.1709	-.1928	-.0076	.0150
34	1.0000	.3491	-.0847	.0537	.1636	-.1783	-.0068	.0125
35	1.0000	.3026	-.1101	.0616	.1485	-.1523	-.0055	.0087
36	1.0000	.2684	-.1250	.0646	.1301	-.1235	-.0043	.0051
37	1.0000	.2219	-.1399	.0651	.0980	-.0746	-.0022	-.0005
38	1.0000	.1828	-.1477	.0622	.0666	-.0266	-.0004	-.0062

*Elastic modes start at "mode 3."

TABLE 11-6 AIRPLANE VIBRATION MODE SHAPES* , FINAL STIFFNESS DESIGN

SYMMETRIC , HIGH GROSS WEIGHT

ROW	MODE 1	MODE 2	MODE 3	MODE 4	MODE 5	MODE 6	MODE 7	MODE 8
39	1.0000	.1486	-.1513	.0577	.0374	.0185	.0012	-.0116
40	1.0000	.0972	-.1514	.0482	-.0084	.0895	.0031	-.0207
41	1.0000	.0459	-.1433	.0370	-.0525	.1548	.0037	-.0297
42	1.0000	-.0055	-.1244	.0280	-.0903	.2028	.0021	-.0374
43	1.0000	-.0568	-.0918	.0272	-.1188	.2284	-.0023	-.0440
44	1.0000	-.0983	-.0509	.0395	-.1333	.2287	-.0082	-.0479
45	1.0000	-.1501	.0222	.0780	-.1339	.2133	-.0196	-.0502
46	1.0000	-.1775	.0719	.1110	-.1236	.2019	-.0272	-.0489
47	1.0000	-.2073	.1351	.1589	-.0987	.1931	-.0363	-.0464
48	1.0000	-.2273	.1834	.1989	-.0689	.1979	-.0425	-.0359
49	1.0000	-.2476	.2421	.2530	-.0201	.2240	-.0487	-.0104
50	1.0000	-.2652	.2960	.3040	.0303	.2553	-.0544	.0207
51	1.0000	-.2821	.3502	.3565	.0862	.2944	-.0608	.0603
52	1.0000	-.2987	.4047	.4099	.1460	.3391	-.0678	.1066
53	1.0000	-.3156	.4625	.4675	.2141	.3938	-.0766	.1647
54	1.0000	-.3321	.5207	.5264	.2878	.4567	-.0872	.2331
55	1.0000	-.3491	.5820	.5890	.3698	.5293	-.1000	.3138
56	1.0000	-.3649	.6407	.6495	.4513	.6033	-.1136	.3974
57	1.0000	-.3830	.7088	.7203	.5498	.6247	-.1310	.5022
58	1.0000	-.3999	.7728	.7871	.6440	.7826	-.1479	.6039
59	1.0000	.3540	-.0815	.0525	.1643	-.1800	-.0069	.0128
60	1.0000	.3026	-.1093	.0611	.1478	-.1519	-.0056	.0088
61	1.0000	.2513	-.1290	.0643	.1181	-.1074	-.0037	.0037
62	1.0000	.2513	-.1300	.0649	.1196	-.1084	-.0037	.0035
63	1.0000	.1999	-.1402	.0622	.0793	-.0538	-.0015	-.0014
64	1.0000	.1999	-.1433	.0633	.0809	-.0510	-.0013	-.0027
65	1.0000	.1486	-.1446	.0560	.0402	-.0016	.0006	-.0057
66	1.0000	.1486	-.1481	.0570	.0397	.0077	.0009	-.0087
67	1.0000	.0972	-.1400	.0449	.0013	.0418	.0023	-.0068
68	1.0000	.0972	-.1432	.0454	-.0011	.0552	.0026	-.0105
69	1.0000	.0972	-.1485	.0469	-.0050	.0765	.0030	-.0168
70	1.0000	.0459	-.1323	.0320	-.0308	.0807	.0037	-.0089
71	1.0000	.0459	-.1372	.0320	-.0381	.1112	.0039	-.0168
72	1.0000	.0459	-.1418	.0356	-.0483	.1433	.0039	-.0263
73	1.0000	-.0055	-.1157	.0149	-.0511	.0922	.0041	-.0046
74	1.0000	-.0055	-.1193	.0159	-.0599	.1180	.0045	-.0114
75	1.0000	-.0055	-.1218	.0192	-.0707	.1490	.0039	-.0209
76	1.0000	-.0055	-.1237	.0250	-.0841	.1861	.0027	-.0324

*Elastic modes start at "mode 3."

TABLE 11-6 AIRPLANE VIBRATION MODE SHAPES*, FINAL STIFFNESS DESIGN

SYMMETRIC, HIGH GROSS WEIGHT

ROW	MODE 1	MODE 2	MODE 3	MODE 4	MODE 5	MODE 6	MODE 7	MODE 8
77	1.0000	-.0568	-.0974	-.0035	-.0673	.1028	.0046	-.0016
78	1.0000	-.0568	-.0975	-.0007	-.0745	.1200	.0040	-.0080
79	1.0000	-.0568	-.0970	.0049	-.0872	.1472	.0030	-.0176
80	1.0000	-.0568	-.0948	.0156	-.1042	.1879	.0005	-.0318
81	1.0000	-.1082	-.0747	-.0224	-.0779	.1042	.0044	.0013
82	1.0000	-.1082	-.0705	-.0142	-.0897	.1174	.0029	-.0088
83	1.0000	-.0921	-.0773	-.0041	-.0958	.1374	.0021	-.0142
84	1.0000	-.0949	-.0676	.0120	-.1141	.1719	-.0016	-.0308
85	1.0000	-.0974	-.0557	.0318	-.1286	.2123	-.0063	-.0439
86	1.0000	-.1277	-.0547	-.0128	-.1003	.1144	.0012	-.0142
97	1.0000	-.1361	-.0326	.0114	-.1205	.1327	-.0041	-.0283
88	1.0000	-.1437	-.0046	.0449	-.1313	.1672	-.0115	-.0431
89	1.0000	-.1595	-.0482	-.0444	-.0763	.0850	.0041	.0063
90	1.0000	-.1595	-.0395	-.0312	-.0927	.0828	.0023	-.0063
91	1.0000	-.1622	-.0305	-.0213	-.1026	.0787	.0007	-.0129
92	1.0000	-.1761	.0064	.0141	-.1269	.0707	-.0058	-.0252
93	1.0000	-.1889	.0506	.0615	-.1324	.1015	-.0155	-.0391
94	1.0000	-.1984	.0939	.1113	-.1189	.1427	-.0253	-.0500
95	1.0000	-.2120	.1081	.1113	-.1172	.0978	-.0235	-.0560
96	1.0000	-.2382	.1842	.1826	-.0746	.1231	-.0337	-.0526
97	1.0000	-.2585	.2512	.2489	-.0202	.1685	-.0426	-.0257
98	1.0000	-.2757	.3131	.3124	.0417	.2270	-.0515	.0179
99	1.0000	-.3158	.4346	.4260	.1687	.2961	-.0625	.1059
100	1.0000	-.3595	.5790	.5675	.3466	.4263	-.0846	.2631
101	1.0000	-.3792	.6650	.6621	.4731	.5660	-.1005	.4020
102	1.0000	-.3956	.7386	.7436	.5858	.6936	-.1327	.5301
103	1.0000	-.2109	-.0190	-.0676	-.0652	.0445	.0038	.0268
104	1.0000	-.2109	-.0037	-.0468	-.0960	.0098	.0024	.0308
105	1.0000	-.2115	.0104	-.0283	-.1144	-.0099	.0001	.0193
106	1.0000	-.2255	.0628	.0259	-.1392	-.0427	-.0076	-.0311
107	1.0000	-.2392	.1342	.1078	-.1215	-.0069	-.0197	-.0799
108	1.0000	-.2599	.1971	.1672	-.0875	.0033	-.0255	-.0904
109	1.0000	-.2861	.2876	.2578	-.0108	.0606	-.0327	-.0594
110	1.0000	-.3236	.4306	.4075	.1500	.2160	-.0510	.0575
111	1.0000	-.3398	.4962	.4776	.2329	.3030	-.0641	.1460
112	1.0000	-.2507	-.0027	-.0933	-.0374	.0338	.0042	.0310
113	1.0000	-.2507	.0052	-.0833	-.0626	-.0022	.0042	.0552
114	1.0000	-.2507	.0238	-.0606	-.1085	-.0723	.0034	.0961

*Elastic modes start at "mode 3."

TABLE 11-6 AIRPLANE VIBRATION MODE SHAPES*, FINAL STIFFNESS DESIGN

SYMMETRIC, HIGH GROSS WEIGHT

ROW	MODE 1	MODE 2	MODE 3	MODE 4	MODE 5	MODE 6	MODE 7	MODE 8
115	1.0000	-.2507	.0446	-.0341	-.1384	-.1165	.0008	.0954
116	1.0000	-.2610	.0920	.0169	-.1567	-.1578	-.0062	-.0051
117	1.0000	-.2703	.1487	.0818	-.1560	-.1819	-.0156	-.1301
118	1.0000	-.2758	.1869	.1277	-.1302	-.1470	-.0205	-.1520
119	1.0000	-.3050	.2899	.2309	-.0485	-.0967	-.0228	-.1435
120	1.0000	-.3289	.3823	.3278	.0569	.0032	-.0249	-.0630
121	1.0000	-.3490	.4619	.4121	.1535	.1003	-.0326	.0218
122	1.0000	-.3613	.5081	.4601	.2125	.1542	-.0410	.0759
123	1.0000	-.3737	.5663	.5257	.2962	.2539	-.0576	.1665
124	1.0000	-.3902	.6468	.6171	.4178	.4006	-.0832	.3040
125	1.0000	-.4067	.7292	.7115	.5484	.5594	-.1120	.4572
126	1.0000	-.4150	.7710	.7596	.6161	.6422	-.1273	.5382
127	1.0000	-.4256	.8245	.8210	.7028	.7482	-.1468	.6420
128	1.0000	-.4360	.8767	.8810	.7868	.8509	-.1656	.7418
129	1.0000	-.2866	.0226	-.1038	-.0477	-.0212	.0046	.0661
130	1.0000	-.2866	.0416	-.0813	-.1019	-.1077	.0044	.1250
131	1.0000	-.3183	.0409	-.1194	-.0457	-.0544	.0050	.0882
132	1.0000	-.3183	.0613	-.0945	-.1056	-.1525	.0050	.1572
133	1.0000	-.3012	.0903	-.0459	-.2057	-.3399	.0045	.3406
134	1.0000	-.2938	.1321	.0258	-.1735	-.2758	-.0076	-.0123
135	1.0000	-.2977	.1674	.0682	-.1811	-.2990	-.0142	-.1158
136	1.0000	-.3200	.1676	.0371	-.1990	-.3802	-.0097	-.0338
137	1.0000	-.3224	.2012	.0791	-.2009	-.3992	-.0164	-.1389
138	1.0000	-.3086	.2570	.1763	-.1332	-.2833	-.0261	-.2799
139	1.0000	-.3467	.3986	.3226	.0489	-.1008	-.0133	-.1101
140	1.0000	-.3650	.4795	.4118	.1505	.0141	-.0178	-.0201
141	1.0000	-.3909	.5893	.5314	.3050	.1826	-.0472	.1442
142	1.0000	-.4071	.6711	.6253	.4335	.3387	-.0751	.2933
143	1.0000	-.4233	.7547	.7217	.5702	.5065	-.1060	.4578
144	1.0000	-.4395	.8401	.8211	.7161	.6866	-.1403	.6396
145	1.0000	-.4516	.9064	.8991	.8383	.8376	-.1704	.8000
146	1.0000	-.4616	.9604	.9620	.9330	.9545	-.1930	.9201
147	1.0000	-.3318	.1238	-.0506	-.2804	-.5511	.0084	.6098
148	1.0000	-.3443	.3287	.2197	-.1681	-.5253	-.0345	-.5148
149	1.0000	-.3808	.5133	.4353	.1767	-.0193	-.0109	-.0268
150	1.0000	-.4069	.6409	.5810	.3731	.2271	-.0562	.2078
151	1.0000	-.4312	.7666	.7264	.5800	.4806	-.1030	.4571
152	1.0000	-.4554	.8979	.8802	.8146	.7707	-.1597	.7588

*Elastic modes start at "mode 3."

TABLE 11-6 AIRPLANE VIBRATION MODE SHAPES* , FINAL STIFFNESS DESIGN

SYMMETRIC , HIGH GROSS WEIGHT

ROW	MODE 1	MODE 2	MODE 3	MODE 4	MODE 5	MODE 6	MODE 7	MODE 8
153	1.0000	-.4741	1.0000	1.0000	1.0000	1.0000	-.2051	1.0000
154	1.0000	-.2277	.1840	.2140	-.0578	.2259	-.0460	-.0255
155	1.0000	-.2440	.2416	.2581	-.0169	.2498	-.0514	-.0022
156	1.0000	-.2616	.2958	.3096	.0347	.2833	-.0575	.0312
157	1.0000	-.2785	.3503	.3625	.0916	.3242	-.0643	.0720
158	1.0000	-.2950	.4049	.4161	.1521	.3703	-.0718	.1207
159	1.0000	-.3120	.4627	.4738	.2207	.4258	-.0809	.1798
160	1.0000	-.3285	.5210	.5328	.2946	.4895	-.0918	.2489
161	1.0000	-.3454	.5824	.5956	.3767	.5625	-.1048	.3300
162	1.0000	-.3613	.6409	.6558	.4577	.6362	-.1184	.4129
163	1.0000	-.3794	.7090	.7266	.5560	.7275	-.1357	.5173
164	.0000	-.0000	-.0116	-.0164	.0112	.0098	.0010	.0011
165	.0000	-.0000	-.0310	-.0451	-.0064	-.0382	.0077	-.0241
166	.0000	-.0000	-.0626	-.0923	-.0551	-.1452	.0317	-.1166
167	.0000	.0000	-.0859	-.1285	-.0944	-.2523	.0739	-.2503
168	.0000	.0000	-.1050	-.1588	-.1285	-.3509	.1140	-.3844
169	.0000	.0000	-.1252	-.1910	-.1660	-.4620	.1608	-.5427
170	.0000	-.0000	-.0037	-.0048	.0201	.0327	-.0018	.0098
171	.0000	-.0000	-.0223	-.0323	.0058	-.0100	.0031	-.0082
172	.0000	-.0000	-.0536	-.0791	-.0391	-.1137	.0276	-.0964
173	.0000	-.0000	-.0058	-.0083	.0352	.0000	-.0010	.0189
174	.0000	-.0000	-.0353	-.0522	-.0067	-.0400	.0191	-.0553
175	.0000	-.0000	-.0709	-.1063	-.0653	-.1944	.0643	-.2071
176	.0000	.0000	-.0973	-.1474	-.1136	-.3211	.1091	-.3623
177	.0000	-.0000	-.0053	-.0081	.0558	.0701	.0005	.0330
178	.0000	-.0000	-.0392	-.0595	-.0030	-.0720	.0438	-.1156
179	.0000	-.0000	-.0740	-.1130	-.0684	-.2310	.0940	-.2950
180	.0000	.0000	-.1003	-.1535	-.1184	-.3569	.1355	-.4439
181	.0000	.0000	-.1271	-.1950	-.1699	-.4872	.1786	-.5991
182	.0000	-.0000	-.0091	-.0158	.0570	.0350	.0374	-.0637
183	.0000	-.0000	-.0359	-.0565	.0059	-.0814	.0683	-.1805
184	.0000	-.0000	-.0814	-.1257	-.0818	-.2841	.1236	-.3902
185	.0000	.0000	-.1017	-.1564	-.1209	-.3743	.1481	-.4832
186	.0000	-.0000	-.0103	-.0186	.0561	.0202	.0501	-.1008
187	.0000	-.0000	-.0559	-.0878	-.0319	-.1838	.1064	-.3138
188	.0000	.0000	-.1036	-.1604	-.1246	-.3990	.1657	-.5387
189	.0000	.0000	-.1292	-.1993	-.1744	-.5152	.1979	-.6611
190	1.0000	-.3808	.5596	.5023	.2565	.1115	.6982	.0177

*Elastic modes start at "mode 3."

TABLE 11-6 AIRPLANE VIBRATION MODE SHAPES* , FINAL STIFFNESS DESIGN

SYMMETRIC , HIGH GROSS WEIGHT

ROW	MODE 1	MODE 2	MODE 3	MODE 4	MODE 5	MODE 6	MODE 7	MODE 8
191	.0000	.2306	-.0160	.0014	-.0525	.0097	1.0000	-.0546
192	.0000	.0005	-.0012	-.0010	-.0011	.0001	-.0000	-.0005
193	1.0000	1.0000	.7508	-.3721	-.4192	.5987	-.0058	-.0604
194	1.0000	.9140	.6119	-.2959	-.2785	.3905	-.0053	-.0362
195	1.0000	.8419	.4981	-.2340	-.1681	.2293	-.0051	-.0179
196	1.0000	.7719	.3921	-.1772	-.0724	.0930	-.0051	-.0033
197	1.0000	.6517	.2252	-.0902	.0571	-.0801	-.0062	.0132
198	1.0000	.6107	.1690	-.0615	.0964	-.1268	-.0075	.0166
199	1.0000	.5594	.1065	-.0306	.1316	-.1664	-.0084	.0188
200	1.0000	.5080	.0483	-.0026	.1575	-.1933	-.0088	.0196
201	1.0000	.4567	-.0035	.0213	.1718	-.2041	-.0087	.0186
202	1.0000	.4053	-.0463	.0393	.1728	-.1979	-.0080	.0161
203	1.0000	.3540	-.0809	.0521	.1626	-.1777	-.0068	.0126
204	1.0000	.3026	-.1081	.0602	.1429	-.1457	-.0053	.0083
205	1.0000	.2513	-.1274	.0633	.1136	-.1029	-.0035	.0036
206	1.0000	.1999	-.1387	.0615	.0775	-.0537	-.0015	-.0009
207	1.0000	.1486	-.1425	.0552	.0393	-.0049	.0004	-.0043
208	1.0000	.0972	-.1391	.0448	.0033	.0369	.0021	-.0059
209	1.0000	.0459	-.1293	.0311	-.0264	.0670	.0032	-.0053
210	1.0000	-.0055	-.1150	.0147	-.0501	.0879	.0041	-.0033
211	1.0000	-.0569	-.0971	-.0041	-.0656	.0985	.0046	-.0000
212	1.0000	-.1002	-.0757	-.0252	-.0712	.0963	.0048	.0051
213	1.0000	-.1595	-.0509	-.0487	-.0658	.0818	.0046	.0120
214	1.0000	-.2109	-.0245	-.0745	-.0482	.0598	.0042	.0197
215	1.0000	-.2622	.0010	-.1046	-.0151	.0431	.0042	.0197
216	1.0000	-.3211	.0313	-.1463	.0400	.0268	.0040	.0085
217	1.0000	-.4609	.1080	-.2580	.2611	-.0273	.0056	-.0378
218	1.0000	-.5324	.1496	-.3227	.4028	-.0616	.0072	-.0737
219	1.0000	-.6105	.1955	-.3948	.5648	-.1007	.0092	-.1159
220	.0000	.0005	-.0003	.0005	-.0010	.0003	-.0000	.0003
221	1.0000	-.5647	.1689	-.3536	.4750	-.0788	.0082	-.0931
222	1.0000	-.5243	.1506	-.3242	.4058	-.0623	.0072	-.0744
223	.0000	.0005	-.0003	.0004	-.0010	.0002	-.0000	.0003
224	1.0000	.7013	.2916	-.1243	.0092	-.0182	-.0056	.0078
225	1.0000	-.3928	.0696	-.2003	.1443	.0015	.0045	-.0103

*Elastic modes start at "mode 3."

TABLE 11-6 AIRPLANE VIBRATION MODE SHAPES*, FINAL STIFFNESS DESIGN

SYMMETRIC, HIGH GROSS WEIGHT

ROW	MODE 9	MODE 10	MODE 11	MODE 12	MODE 13	MODE 14	MODE 15	MODE 16
1	.0177	.0002	-.0016	-.0821	.0213	-.2365	-.1446	-.0158
2	-.1603	.0002	.3761	-.1473	-.0219	-.1330	-.0280	.0021
3	-.0437	.0017	.1252	-.1370	.0072	-.0399	.0233	.0217
4	-.0027	-.0000	.0061	-.0030	.0001	-.0023	-.0005	.0002
5	-.0001	-.0000	-.0006	.0021	-.0001	.0017	.0002	-.0003
6	-.0002	.0000	.0004	.0001	-.0001	.0001	.0001	-.0000
7	.1084	-.0047	-.0096	.0348	-.0112	-.2380	-.1839	-.0004
8	-.1731	.0239	-.1499	-.2492	-.1360	-.2609	-.0589	.0388
9	-.0346	.0003	-.1263	-.0783	-.0153	.0080	.0105	-.0023
10	-.0035	.0004	-.0029	-.0047	-.0018	-.0038	-.0007	.0005
11	-.0019	.0000	.0003	.0002	.0008	.0021	.0009	-.0007
12	-.0002	.0000	-.0002	-.0004	-.0003	-.0006	-.0002	.0002
13	-.1032	.0015	-.0043	.2354	-.0005	.0114	.0608	.1419
14	-.0349	.0006	.0030	-.0544	-.0095	.2723	-.0244	.1614
15	.0831	-.0017	-.0037	-.3030	.0318	-.1545	.1522	-.2328
16	.0122	-.0042	-.0563	-.0725	.1360	-.5198	.1783	.2901
17	-.3200	-.0096	-.1749	.0329	.2396	.1776	-.1747	.0527
18	-.4052	-.0136	-.2365	-.0944	.2523	.3613	-.3417	-.3310
19	-.2430	-.0154	-.1284	-.0296	.2169	.2956	-.3594	-.3916
20	-.0189	-.0233	.0679	.1457	.1873	.2138	-.4689	-.3376
21	.1801	-.0301	.2582	.3273	.1664	.1389	-.6290	-.2253
22	-.1002	.0015	-.0040	.2251	-.0007	.0169	.0572	.1390
23	-.0792	.0012	-.0017	.1302	-.0037	.1105	.0296	.1627
24	-.0603	.0009	.0004	.0486	-.0064	.1872	.0051	.1728
25	-.0324	.0006	.0031	-.0579	-.0094	.2659	-.0245	.1539
26	-.0074	.0003	.0049	-.1366	-.0098	.2786	-.0335	.0790
27	.0274	-.0003	.0060	-.2184	-.0060	.2115	-.0127	-.0639
28	.0560	-.0008	.0042	-.2697	.0047	.0802	.0429	-.1817
29	.0740	-.0013	.0003	-.2869	.0189	-.0611	.1018	-.2257
30	.0868	-.0022	-.0108	-.2670	.0501	-.3055	.1996	-.1657
31	.0699	-.0030	-.0282	-.1846	.0877	-.4828	.2350	.0453
32	-.0971	.0014	-.0038	.2143	-.0010	.0228	.0533	.1358
33	-.0760	.0011	-.0015	.1197	-.0039	.1147	.0263	.1578
34	-.0571	.0009	.0005	.0419	-.0063	.1831	.0041	.1633
35	-.0297	.0006	.0032	-.0615	-.0092	.2584	-.0245	.1454
36	-.0060	.0002	.0048	-.1318	-.0096	.2651	-.0337	.0754
37	.0273	-.0002	.0059	-.2085	-.0062	.2012	-.0158	-.0582
38	.0536	-.0007	.0046	-.2535	.0026	.0859	.0296	-.1657

*Elastic modes start at "mode 3."

TABLE 11-6 AIRPLANE VIBRATION MODE SHAPES* , FINAL STIFFNESS DESIGN

SYMMETRIC , HIGH GROSS WEIGHT

DOF	MODE 9	MODE 10	MODE 11	MODE 12	MODE 13	MODE 14	MODE 15	MODE 16
39	.0723	-.0012	.0012	-.2738	.0155	-.0485	.0852	-.2231
40	.0852	-.0020	-.0092	-.2526	.0448	-.2884	.1829	-.1663
41	.0687	-.0028	-.0259	-.1690	.0809	-.4628	.2177	.0483
42	.0143	-.0036	-.0483	-.0497	.1160	-.4618	.1498	.2676
43	-.0744	-.0048	-.0777	.0496	.1521	-.3068	.0248	.3605
44	-.1659	-.0063	-.1091	.0809	.1830	-.1058	-.0627	.2942
45	-.2927	-.0086	-.1597	.0400	.2172	.1663	-.1562	.0570
46	-.3518	-.0100	-.1894	-.0123	.2294	.2799	-.2009	-.1006
47	-.3789	-.0116	-.2148	-.0627	.2343	.3317	-.2618	-.2297
48	-.3757	-.0117	-.2207	-.0872	.2280	.3381	-.2858	-.2924
49	-.3460	-.0108	-.2081	-.0902	.2180	.3236	-.2821	-.3213
50	-.3079	-.0100	-.1866	-.0813	.2071	.3041	-.2733	-.3351
51	-.2612	-.0099	-.1555	-.0614	.1959	.2823	-.2677	-.3414
52	-.2080	-.0102	-.1165	-.0324	.1849	.2593	-.2678	-.3414
53	-.1433	-.0114	-.0644	.0106	.1737	.2331	-.2793	-.3316
54	-.0696	-.0136	-.0003	.0676	.1635	.2057	-.3107	-.3130
55	.0170	-.0168	.0789	.1405	.1521	.1725	-.3584	-.2753
56	.1069	-.0199	.1636	.2204	.1412	.1377	-.4198	-.2251
57	.2200	-.0238	.2731	.3255	.1282	.0927	-.5192	-.1468
58	.3313	-.0272	.3820	.4307	.1150	.0466	-.6022	-.0570
59	-.0597	.0009	.0002	.0539	-.0059	.1702	.0080	.1603
60	-.0310	.0006	.0030	-.0535	-.0091	.2515	-.0231	.1509
61	.0021	.0001	.0053	-.1430	-.0102	.2531	-.0423	.0527
62	.0038	.0001	.0055	-.1555	-.0100	.2633	-.0409	.0482
63	.0310	-.0002	.0065	-.1817	-.0089	.1698	-.0349	-.0616
64	.0387	-.0004	.0061	-.2202	-.0050	.1594	-.0104	-.1042
65	.0548	-.0006	.0072	-.1982	-.0077	.0779	-.0262	-.1633
66	.0657	-.0009	.0048	-.2477	.0028	.0230	.0270	-.2271
67	.0598	-.0005	.0082	-.1287	-.0116	-.0015	-.0369	-.1158
68	.0687	-.0008	.0043	-.1633	.0017	-.0809	.0185	-.1398
69	.0930	-.0016	-.0031	-.2296	.0274	-.2210	.1346	-.1736
70	.0646	-.0006	.0067	-.0786	-.0093	-.0835	-.0277	-.0863
71	.0704	-.0012	-.0036	-.1094	.0201	-.2399	.0627	-.0386
72	.0749	-.0024	-.0191	-.1648	.0662	-.4404	.2142	.0182
73	.0511	.0001	.0117	.0095	-.0249	-.0433	-.0679	-.0449
74	.0562	-.0006	.0029	.0019	-.0039	-.1552	-.0321	.0101
75	.0476	-.0014	-.0134	-.0167	.0364	-.2960	.0351	.1232
76	.0264	-.0029	-.0373	-.0409	.0922	-.4219	.1160	.2337

*Elastic modes start at "mode 3."

TABLE 11-6 AIRPLANE VIBRATION MODE SHAPES*, FINAL STIFFNESS DESIGN

SYMMETRIC, HIGH GROSS WEIGHT

ROW	MODE 9	MODE 10	MODE 11	MODE 12	MODE 13	MODE 14	MODE 15	MODE 16
77	.0413	.0006	.0151	.0791	-.0349	-.0330	-.0788	-.0185
78	.0326	.0000	.0050	.0784	-.0132	-.0868	-.0624	.0385
79	.0144	-.0009	-.0125	.0600	.0239	-.1655	-.0468	.1474
80	-.0272	-.0028	-.0450	.0678	.0901	-.2524	-.0059	.2815
81	.0248	.0011	.0179	.1482	-.0438	.0057	-.0899	.0022
82	.0003	.0001	.0022	.1477	-.0116	-.0086	-.0778	.0610
83	-.0097	-.0007	-.0116	.1335	.0161	-.0625	-.0772	.1276
84	-.0680	-.0028	-.0493	.1176	.0865	-.0995	-.0592	.2336
85	-.1368	-.0053	-.0923	.0909	.1572	-.1132	-.0571	.2889
86	-.0300	-.0006	-.0080	.1612	.0086	.0345	-.0641	.0766
87	-.1070	-.0028	-.0488	.1201	.0800	.0627	-.0597	.1181
88	-.1974	-.0055	-.1040	.0854	.1520	.1029	-.0954	.1119
89	.0098	.0018	.0251	.1977	-.0583	.0779	-.0613	-.0168
90	-.0181	.0003	.0109	.1910	-.0243	.0999	-.0398	.0172
91	-.0412	-.0006	-.0004	.1754	.0005	.1141	-.0252	.0310
92	-.1289	-.0027	-.0390	.1105	.0719	.1695	-.0128	.0256
93	-.2464	-.0048	-.1032	.0301	.1429	.2612	-.0352	-.0558
94	-.3157	-.0070	-.1643	-.0248	.1853	.2949	-.1248	-.1223
95	-.2815	-.0047	-.1468	-.0309	.1520	.2650	-.0708	-.1120
96	-.2968	-.0054	-.1767	-.0721	.1663	.2765	-.1294	-.1995
97	-.2860	-.0058	-.1799	-.0845	.1704	.2702	-.1679	-.2534
98	-.2588	-.0065	-.1623	-.0737	.1736	.2638	-.1933	-.2839
99	-.1180	-.0036	-.0683	-.0121	.1261	.1845	-.1186	-.2437
100	.0875	-.0053	.1002	.1250	.0778	.0964	-.1157	-.1342
101	.1991	-.0131	.2201	.2522	.0843	.0598	-.2817	-.0939
102	.3049	-.0202	.3359	.3725	.0899	.0326	-.4509	-.0390
103	.0043	.0027	.0336	.1952	-.0695	.1136	-.0053	-.0380
104	-.0210	.0007	.0263	.1716	-.0335	.1441	.0175	-.0144
105	-.0478	-.0005	.0291	.1341	-.0065	.1497	.0288	-.0016
106	-.1195	-.0024	-.0105	.0535	.0524	.2026	.0156	-.0218
107	-.2092	.0000	-.1177	-.0496	.0806	.2017	.0327	-.0706
108	-.2063	.0024	-.1416	-.0851	.0774	.1823	.0414	-.1010
109	-.1683	.0052	-.1342	-.0889	.0729	.1553	.0643	-.1288
110	-.0643	.0044	-.0517	-.0200	.0706	.1211	.0493	-.1479
111	-.0042	.0010	.0060	.0349	.0732	.1076	-.0037	-.1503
112	.0102	.0030	.0358	.1856	-.0762	.1058	.0098	-.0423
113	.0049	.0026	.0349	.1723	-.0660	.1223	.0238	-.0397
114	-.0134	.0013	.0396	.1234	-.0378	.1363	.0475	-.0220

*Elastic modes start at "mode 3."

TABLE 11-6 AIRPLANE VIBRATION MODE SHAPES*, FINAL STIFFNESS DESIGN

SYMMETRIC, HIGH GROSS WEIGHT

ROW	MODE 9	MODE 10	MODE 11	MODE 12	MODE 13	MODE 14	MODE 15	MODE 16
115	-.0462	.0001	.0593	.0597	-.0082	.1264	.0558	-.0092
116	-.0820	-.0017	.0380	.0147	.0210	.1661	.0965	-.0245
117	-.0952	-.0021	-.0479	-.0231	.0333	.1704	.0958	-.0411
118	-.1219	.0027	-.1088	-.0812	.0154	.1110	.0825	-.0374
119	-.0863	.0146	-.1320	-.1298	-.0266	.0202	.2077	-.0128
120	-.0136	.0216	-.0724	-.0845	-.0316	.0106	.3421	.0021
121	.0557	.0201	-.0090	-.0286	-.0335	-.0038	.3529	.0096
122	.1125	.0202	.0417	.0176	-.0385	-.0229	.3465	.0328
123	.1727	.0134	.1094	.0862	-.0310	-.0335	.2602	.0458
124	.2687	.0044	.2202	.2061	-.0173	-.0503	.0918	.0800
125	.3797	-.0051	.3506	.3468	-.0009	-.0709	-.1326	.1351
126	.4395	-.0101	.4216	.4237	.0077	-.0828	-.2607	.1706
127	.5163	-.0164	.5126	.5225	.0189	-.0980	-.4269	.2161
128	.5390	-.0226	.5987	.6159	.0302	-.1112	-.5838	.2533
129	.0035	.0033	.0572	.1794	-.0846	.385	.0499	-.0707
130	-.0114	.0023	.0715	.1264	-.0622	.1543	.0803	-.0573
131	.0015	.0038	.0770	.1807	-.0980	.1604	.0801	-.0949
132	-.0137	.0029	.0976	.1203	-.0764	.1759	.1147	-.0838
133	-.0376	.0021	.1343	-.1547	.0014	-.0411	.0380	.0158
134	-.0536	-.0011	.0457	-.0382	-.0021	.1509	.1658	-.0372
135	-.0564	-.0019	-.0098	-.0567	.0029	.1634	.1914	-.0526
136	-.0305	-.0008	.0480	-.0853	-.0222	.1494	.2563	-.0562
137	-.0341	-.0017	-.0082	-.1018	-.0165	.1636	.2832	-.0724
138	-.0208	.0039	-.1422	-.1173	-.0460	-.0427	.0376	.0075
139	.0782	.0338	-.0423	-.0900	-.1076	-.0760	.5969	.1165
140	.1372	.0381	.0169	-.0376	-.1007	-.0796	.6420	.1217
141	.2671	.0258	.1521	.0971	-.1017	-.1222	.4765	.1732
142	.3746	.0154	.2770	.2299	-.0908	-.1465	.3041	.2353
143	.4967	.0049	.4221	.3869	-.0756	-.1739	.0566	.3203
144	.6381	-.0060	.5926	.5727	-.0598	-.2111	-.2643	.4577
145	.7744	-.0146	.7584	.7539	-.0515	-.2590	-.5873	.6567
146	.8712	-.0215	.8755	.8816	-.0424	-.2878	-.8125	.7697
147	-.0357	.0041	.2105	-.3970	.0249	-.2595	-.0171	.0607
148	.1661	-.0012	-.1768	-.1143	-.1159	-.2655	-.1163	.0844
149	.2201	.0519	.0537	-.0318	-.1609	-.1502	1.0000	.2410
150	.3645	.0261	.2337	.1663	-.1306	-.1769	.5022	.2662
151	.5514	.0097	.4550	.4046	-.1112	-.2226	.1496	.4073
152	.7985	-.0075	.7548	.7320	-.0912	-.3009	-.4262	.7196

*Elastic modes start at "mode 3."

TABLE 11-6 AIRPLANE VIBRATION MODE SHAPES* , FINAL STIFFNESS DESIGN

SYMMETRIC , HIGH GROSS WEIGHT

ROW	MODE 9	MODE 10	MODE 11	MODE 12	MODE 13	MODE 14	MODE 15	MODE 16
153	1.0000	-.0208	1.0000	1.0000	-.0768	-.3687	-.9069	1.0000
154	-.3933	-.0129	-.2305	-.0925	.2432	.3524	-.3220	-.3198
155	-.3695	-.0124	-.2194	-.0935	.2360	.3423	-.3254	-.3465
156	-.3313	-.0122	-.1968	-.0829	.2263	.3249	-.3231	-.3636
157	-.2840	-.0126	-.1641	-.0609	.2159	.3045	-.3226	-.3717
158	-.2307	-.0136	-.1243	-.0306	.2057	.2829	-.3272	-.3740
159	-.1661	-.0153	-.0717	.0133	.1951	.2579	-.3429	-.3668
160	-.0927	-.0179	-.0074	.0706	.1855	.2314	-.3776	-.3505
161	-.0063	-.0210	.0718	.1439	.1750	.1993	-.4302	-.3158
162	.0820	-.0242	.1549	.2223	.1651	.1663	-.4944	-.2716
163	.1942	-.0279	.2636	.3267	.1530	.1227	-.5877	-.1978
164	.0116	.0022	.0074	.0068	-.0241	-.0223	-.0044	-.0024
165	.0396	.0049	.0163	.0031	-.0663	-.0728	.0921	.0628
166	.0732	.0503	.0058	-.0203	-.0909	-.1124	.2660	.1325
167	.2110	.2434	.0978	.1205	.1001	.0626	.1774	.0807
168	.3643	.4613	.2088	.2942	.3399	.2894	.0048	-.0135
169	.5529	.7325	.3502	.5176	.6522	.5885	-.2549	-.1530
170	-.0023	.0012	-.0001	.0032	-.0119	-.0111	-.0339	-.0236
171	.0257	-.0012	.0103	.0003	-.0593	-.0668	.0563	.0423
172	.0708	.0492	.0122	-.0078	-.0766	-.0991	.2203	.1139
173	.0194	.0053	.0153	.0165	-.0313	-.0450	-.0045	.0078
174	.0651	.0462	.0245	.0166	-.0482	-.0724	.1279	.0755
175	.1988	.2252	.1020	.1295	.1027	.0637	.1171	.0598
176	.3586	.4529	.2117	.3000	.3429	.2917	-.0305	-.0262
177	.0472	.0114	.0372	.0379	-.0477	-.0778	.0256	.0441
178	.1726	.1866	.1109	.1484	.1084	.0664	-.0129	.0143
179	.3400	.4256	.2193	.3158	.3495	.2959	-.1350	-.0631
180	.4866	.6371	.3189	.4716	.5758	.5144	-.2793	-.1499
181	.6406	.8601	.4243	.6369	.8174	.7484	-.4381	-.2456
182	.2134	.2417	.1760	.2563	.2267	.1752	-.2694	-.0895
183	.3035	.3713	.2264	.3328	.3470	.2895	-.2918	-.1155
184	.4733	.6175	.3266	.4870	.5849	.5216	-.3703	-.1828
185	.5481	.7260	.3705	.5545	.6894	.6235	-.4024	-.2116
186	.2744	.3281	.2271	.3376	.3357	.2757	-.3845	-.1446
187	.4499	.5827	.3326	.5004	.5859	.5198	-.4816	-.2206
188	.6347	.8516	.4435	.6718	.8510	.7796	-.5803	-.3013
189	.7364	1.0000	.5053	.7676	1.0000	.9262	-.6426	-.3502
190	.1197	.0145	.0732	-.0061	-.1145	-.0153	.4937	.1313

*Elastic modes start at "mode 3."

REPRODUCIBILITY OF THE
ORIGINAL PAGE IS POOR

TABLE 11-6 AIRPLANE VIBRATION MODE SHAPES* , FINAL STIFFNESS DESIGN

SYMMETRIC , HIGH GROSS WEIGHT

ROW	MODE 9	MODE 10	MODE 11	MODE 12	MODE 13	MODE 14	MODE 15	MODE 16
191	-.1741	-.0294	-.0334	.0043	.0780	.0746	-.3897	-.0890
192	-.0021	-.0001	-.0012	-.0006	.0011	.0015	-.0033	-.0018
193	.2478	-.0014	.0265	-.9537	-.0274	1.0000	.0103	.3924
194	.1334	-.0006	.0139	-.4664	-.0130	.4430	.0126	.1136
195	.0480	.0001	.0048	-.1147	-.0029	.0571	.0162	-.0624
196	-.0197	.0006	-.0020	.1466	.0040	-.2052	.0227	-.1589
197	-.0941	.0013	-.0081	.3841	.0088	-.3720	.0451	-.1639
198	-.1112	.0015	-.0085	.4093	.0081	-.3320	.0704	-.1021
199	-.1195	.0017	-.0081	.3962	.0063	-.2560	.0828	-.0287
200	-.1179	.0017	-.0069	.3464	.0038	-.1541	.0800	.0472
201	-.1059	.0015	-.0049	.2623	.0006	-.0345	.0646	.1118
202	-.0852	.0013	-.0025	.1611	-.0026	.0734	.0385	.1466
203	-.0589	.0009	.0001	.0555	-.0055	.1597	.0094	.1489
204	-.0295	.0005	.0027	-.0437	-.0080	.2139	-.0170	.1166
205	.0007	.0002	.0048	-.1202	-.0093	.2139	-.0344	.0439
206	.0274	-.0002	.0064	-.1596	-.0099	.1626	-.0402	-.0400
207	.0471	-.0004	.0076	-.1610	-.0109	.0894	-.0417	-.0995
208	.0561	-.0003	.0089	-.1210	-.0142	.0233	-.0475	-.1045
209	.0560	-.0001	.0108	-.0589	-.0206	-.0115	-.0611	-.0830
210	.0507	.0003	.0136	.0120	-.0293	-.0252	-.0741	-.0545
211	.0424	.0008	.0171	.0792	-.0394	-.0190	-.0813	-.0309
212	.0321	.0014	.0222	.1359	-.0521	.0126	-.0776	-.0239
213	.0212	.0022	.0281	.1741	-.0649	.0547	-.0542	-.0307
214	.0140	.0028	.0316	.1851	-.0724	.0853	-.0170	-.0407
215	.0110	.0028	.0316	.1825	-.0742	.1011	.0152	-.0508
216	.0104	.0021	.0252	.1536	-.0666	.1051	.0539	-.0618
217	.0201	-.0020	-.0125	-.0475	.0050	-.0213	.0168	-.0253
218	.0313	-.0055	-.0447	-.2234	.0716	-.1596	-.0715	.0285
219	.0449	-.0097	-.0836	-.4367	.1536	-.3333	-.1926	.1013
220	-.0001	.0000	.0003	.0014	-.0005	.0012	.0009	-.0005
221	.0379	-.0075	-.0630	-.3242	.1108	-.2446	-.1348	.0656
222	.0314	-.0056	-.0453	-.2264	.0726	-.1614	-.0717	.0288
223	-.0001	.0000	.0002	.0013	-.0005	.0010	.0007	-.0004
224	-.0697	.0010	-.0064	.3168	.0079	-.3428	.0345	-.1819
225	.0129	.0005	.0107	.0777	-.0407	.0665	.0577	-.0541

*Elastic modes start at "mode 3."

TABLE 11-6 AIRPLANE VIBRATION MODE SHAPES , FINAL STIFFNESS DESIGN

SYMMETRIC , HIGH GROSS WEIGHT

ROW	MODE 17	MODE 18	MODE 19	MODE 20
1	-.0296	-.0171	.1149	.2441
2	.0001	-.0061	.0066	.0102
3	.0062	.0052	-.0308	-.0481
4	-.0002	-.0000	.0003	.0003
5	-.0001	.0002	.0003	.0023
6	.0000	.0000	-.0001	.0001
7	-.0099	-.0167	.1070	.2880
8	.0215	.0063	.0048	.0129
9	.0226	.0202	-.0204	-.0491
10	.0001	.0003	.0005	.0013
11	-.0006	.0002	.0006	.0022
12	.0001	.0000	-.0001	-.0005
13	.0260	-.0071	-.2376	.0232
14	.0175	-.0121	.0309	.1589
15	.0573	.0136	.0839	.2322
16	.0946	-.0168	.2068	.0870
17	.0384	-.0069	.3072	-.0632
18	.0972	-.0757	-.1799	-.0625
19	.0796	-.1469	-.3566	-.1475
20	.1562	-.1299	-.4468	-.2272
21	.2957	-.0388	-.4452	-.2755
22	.0251	-.0070	-.2270	.0248
23	.0243	-.0102	-.1721	.0799
24	.0222	-.0120	-.1012	.1214
25	.0163	-.0116	.0290	.1480
26	.0088	-.0055	.1435	.0961
27	.0042	.0059	.2083	.0137
28	.0161	.0138	.1853	.0302
29	.0354	.0150	.1193	.1174
30	.0782	.0058	-.0187	.3399
31	.1038	-.0099	-.0226	.3579
32	.0241	-.0070	-.2151	.0265
33	.0232	-.0099	-.1603	.0784
34	.0207	-.0112	-.0963	.1100
35	.0149	-.0109	.0264	.1356
36	.0068	-.0053	.1261	.0793
37	.0016	.0053	.1857	-.0013
38	.0097	.0128	.1708	-.0016

TABLE 11-6 AIRPLANE VIBRATION MODE SHAPES , FINAL STIFFNESS DESIGN

SYMMETRIC , HIGH GROSS WEIGHT

ROW	MODE 17	MODE 18	MODE 19	MODE 20
39	.0264	.0154	.1140	.0608
40	.0694	.0059	-.0403	.3097
41	.0952	-.0104	-.0458	.3303
42	.0738	-.0157	.1683	.0133
43	.0406	-.0089	.3962	-.1982
44	.0245	-.0015	.4533	-.1849
45	.0307	-.0036	.2929	-.0496
46	.0463	-.0153	.1232	.0055
47	.0711	-.0417	-.0443	-.0120
48	.0786	-.0625	-.1427	-.0341
49	.0676	-.0859	-.1957	-.0545
50	.0549	-.1058	-.2323	-.0711
51	.0451	-.1230	-.2652	-.0885
52	.0405	-.1363	-.2957	-.1067
53	.0461	-.1421	-.3233	-.1269
54	.0682	-.1375	-.3505	-.1513
55	.1083	-.1152	-.3615	-.1729
56	.1632	-.0781	-.3580	-.1911
57	.2484	-.0130	-.3311	-.2065
58	.3403	.0648	-.2809	-.2116
59	.0208	-.0108	-.1080	.1005
60	.0148	-.0114	.0052	.1332
61	-.0014	-.0032	.1396	.0176
62	.0009	-.0030	.1673	.0362
63	-.0147	.0059	.1184	-.1039
64	-.0034	.0091	.1740	-.0565
65	-.0270	.0140	.0840	-.2335
66	-.0045	.0185	.1301	-.1538
67	-.0339	.0070	-.0556	-.1536
68	-.0106	.0071	-.0793	-.0619
69	.0426	.0084	-.0996	.2209
70	-.0319	.0024	-.1300	-.1305
71	.0116	-.0036	-.1464	-.0086
72	.0912	-.0118	-.1486	.4075
73	-.0426	.0001	-.1030	-.1165
74	-.0308	-.0053	-.1484	-.1792
75	.0047	-.0124	-.0832	-.2154
76	.0566	-.0155	.1021	-.0496

TABLE 11-6 AIRPLANE VIBRATION MODE SHAPES , FINAL STIFFNESS DESIGN

SYMMETRIC , HIGH GROSS WEIGHT

ROW	MODE 17	MODE 18	MODE 19	MODE 20
77	-.0425	-.0024	-.1075	-.0791
78	-.0358	-.0033	-.0696	-.1189
79	-.0274	-.0052	.0338	-.2301
80	.0070	-.0068	.2501	-.2409
81	-.0414	-.0026	-.0885	.0043
82	-.0396	.0029	-.0025	-.0174
83	-.0397	.0028	.0750	-.1135
84	-.0152	.0039	.2817	-.1658
85	.0144	.0003	.4201	-.1869
86	-.0245	.0106	.0650	.0581
87	-.0211	.0161	.2074	.0365
88	.0026	.0097	.2899	-.0084
89	-.0176	-.0002	-.0523	.2420
90	-.0229	.0129	.0093	.2429
91	-.0228	.0191	.0466	.2109
92	-.0202	.0268	.1226	.1740
93	-.0054	.0207	.1064	.1401
94	.0241	-.0046	.0628	.0673
95	.0087	.0034	.0482	.0908
96	.0198	-.0362	-.0523	.0368
97	.0227	-.0698	-.1290	-.0073
98	.0207	-.0991	-.1897	-.0412
99	-.0212	-.1159	-.1907	-.0420
100	.0038	-.0775	-.1533	-.0423
101	.1213	-.0252	-.1939	-.1001
102	.2456	.0443	-.2101	-.1490
103	.0202	-.0032	-.0129	.2436
104	.0052	.0153	.0042	.2786
105	-.0053	.0238	.0130	.2143
106	-.0173	.0352	.0464	.1902
107	-.0152	.0233	.0347	.1142
108	-.0343	-.0019	.0144	.0985
109	-.0730	-.0456	-.0070	.0815
110	-.0927	-.0932	-.0647	.0363
111	-.0669	-.0974	-.1051	.0054
112	.0392	-.0130	.0189	.1438
113	.0317	-.0027	.0036	.1772
114	.0181	.0142	-.0127	.2161

TABLE 11-6 AIRPLANE VIBRATION MODE SHAPES , FINAL STIFFNESS DESIGN

SYMMETRIC , HIGH GROSS WEIGHT

ROW	MODE 17	MODE 18	MODE 19	MODE 20
115	.0045	.0233	-.0123	.1617
116	-.0088	.0412	-.0179	.1711
117	-.0056	.0435	-.0260	.0965
118	-.0149	.0306	-.0026	.0636
119	-.1145	-.0109	.0746	.1124
120	-.2147	-.053	.1361	.1683
121	-.2295	-.0713	.1252	.1478
122	-.2245	-.0655	.1371	.1554
123	-.1714	-.0477	.1165	.1331
124	-.0564	.0040	.0893	.0890
125	.1076	.0890	.0681	.0297
126	.2045	.1432	.0632	-.0029
127	.3304	.2134	.0563	-.0460
128	.4462	.2737	.0392	-.0908
129	.0690	-.0120	.0351	.4903
130	.0574	.0078	.0004	.6250
131	.0990	-.0152	.0527	.8043
132	.0891	.0058	.0114	1.0000
133	.0120	.0053	-.0439	-.0577
134	.0001	.0738	-.1387	.2807
135	.0061	.0980	-.2112	.3505
136	.0103	.1258	-.3190	.5079
137	.0166	.1523	-.3993	.5938
138	.0116	.0172	-.0266	-.0608
139	-.3402	-.0431	.3028	.3042
140	-.3841	-.0743	.3151	.2982
141	-.2675	-.0218	.2839	.2408
142	-.1406	.0519	.2975	.2183
143	.0519	.1692	.3160	.1703
144	.3234	.3607	.4004	.1232
145	.6319	.6230	.6081	.1208
146	.8329	.7781	.7041	.1010
147	.0108	-.0199	-.0586	-.3361
148	.0906	-.0026	-.0746	-.3162
149	-.6066	-.1020	.6032	.5733
150	-.2563	.0255	.3777	.2883
151	.0228	.2057	.4339	.2382
152	.5482	.6243	.7166	.2016

TABLE 11-6 AIRPLANE VIBRATION MODE SHAPES , FINAL STIFFNESS DESIGN

SYMMETRIC , HIGH GROSS WEIGHT

ROW	MODE 17	MODE 18	MODE 19	MODE 20
153	1.0000	1.0000	1.0000	.1875
154	.0900	-.0726	-.1708	-.0539
155	.0843	-.0921	-.2202	-.0733
156	.0750	-.1124	-.2631	-.0932
157	.0682	-.1295	-.3003	-.1128
158	.0659	-.1432	-.3353	-.1332
159	.0736	-.1497	-.3679	-.1560
160	.0970	-.1460	-.3996	-.1828
161	.1394	-.1247	-.4171	-.2083
162	.1939	-.0917	-.4237	-.2314
163	.2793	-.0298	-.4056	-.2516
164	.0062	-.0060	-.0127	-.0250
165	-.0307	.0081	.0601	.0121
166	-.1212	.0085	.1859	.0880
167	-.0933	.0139	.1715	.1101
168	-.0248	.0202	.0928	.1059
169	.0934	.0282	-.0456	.0816
170	.0157	-.0139	-.0355	-.0411
171	-.0163	.0010	.0305	-.0111
172	-.1003	.0051	.1571	.0673
173	.0033	-.0151	-.0086	-.0420
174	-.0583	-.0073	.0982	.0251
175	-.0640	.0071	.1269	.0693
176	-.0076	.0164	.0655	.0809
177	-.0097	-.0155	.0261	-.0425
178	-.0008	-.0078	.0289	-.0203
179	.0438	.0043	-.0165	.0040
180	.1010	.0161	-.0845	.0202
181	.1645	.0295	-.1613	.0400
182	.1179	-.0277	-.1479	-.1643
183	.1215	-.0163	-.1419	-.1220
184	.1457	.0062	-.1562	-.0454
185	.1551	.0165	-.1631	-.0086
186	.1679	-.0304	-.2175	-.2031
187	.2011	-.0082	-.2466	-.1358
188	.2336	.0175	-.2716	-.0492
189	.2556	.0322	-.2927	-.0015
190	-.2216	-.0479	.1212	-.0469

TABLE 11-6 AIRPLANE VIBRATION MODE SHAPES , FINAL STIFFNESS DESIGN

SYMMETRIC , HIGH GROSS WEIGHT

POW	MODE 17	MODE 18	MODE 19	MODE 20
101	.2014	.0430	-.1161	-.0205
192	.0016	-.0001	-.0021	-.0014
193	.0526	-.0223	-.3386	.1213
194	.0141	-.0040	-.0576	-.0010
195	-.0095	.0071	.0997	-.0720
196	-.0214	.0128	.1572	-.1063
197	-.0182	.0131	.0760	-.1203
198	-.0064	.0106	-.0471	-.1381
199	.0053	.0063	-.1490	-.1220
200	.0156	.0007	-.2132	-.0705
201	.0224	-.0047	-.2257	-.0060
202	.0234	-.0084	-.1838	.0524
203	.0193	-.0007	-.1051	.0828
204	.0104	-.0080	-.0099	.0692
205	-.0032	-.0024	.0665	-.0078
206	-.0173	.0040	.0754	-.1029
207	-.0292	.0080	.0330	-.1695
208	-.0370	.0069	-.0370	-.1672
209	-.0430	.0041	-.0801	-.1484
210	-.0456	.0009	-.1054	-.1147
211	-.0429	-.0021	-.1107	-.0659
212	-.0320	-.0044	-.0947	.0128
213	-.0088	-.0073	-.0594	.0973
214	.0207	-.0116	-.0086	.1097
215	.0406	-.0189	.0531	.0798
216	.0842	-.0294	.1436	-.0128
217	.0422	-.0170	.1157	-.0483
218	-.0487	.0102	-.0409	.0284
219	-.1756	.0491	-.2790	.1562
220	.0009	-.0003	.0018	-.0010
221	-.1150	.0306	-.1697	.1021
222	-.0488	.0102	-.0389	.0260
223	.0007	-.0002	.0012	-.0006
224	-.0224	.0141	.1288	-.1184
225	.0844	-.0293	.1698	-.0566

TABLE 11-6 AIRPLANE VIBRATION MODE SHAPES* , FINAL STIFFNESS DESIGN

SYMMETRIC , LOW GROSS WEIGHT

ROW	MODE 1	MODE 2	MODE 3	MODE 4	MODE 5	MODE 6	MODE 7	MODE 8
1	.0000	.1714	.0377	.0071	-.0720	-.1251	-.0076	.1493
2	.0000	-.0000	.0132	.0209	.0276	.0750	-.0033	-.2266
3	1.0000	-.2661	.0093	-.0644	-.2333	-.0822	.0010	.3008
4	.0000	.0000	.0004	.0006	-.0001	.0007	-.0001	-.0031
5	.0000	.0005	-.0003	.0004	.0011	.0018	.0001	-.0025
6	.0000	-.0000	-.0000	.0000	.0002	.0002	.0000	-.0005
7	.0000	.1798	.0542	.0420	-.0607	-.2202	-.0274	-.0661
8	.0000	-.0000	.0213	.0318	.0973	.2230	.0214	.0607
9	1.0000	-.2740	.1685	.1457	-.1773	-.1807	-.0501	-.2366
10	.0000	-.0000	.0007	.0010	.0014	.0040	.0004	.0011
11	.0000	.0005	-.0008	-.0003	.0008	.0038	.0006	.0017
12	.0000	-.0000	.0000	.0000	.0001	.0003	.0000	.0001
13	1.0000	.4536	-.0596	.1178	.0989	-.3516	-.0532	.0406
14	1.0000	.3240	-.1119	.1961	.0845	-.2202	-.0325	.0191
15	1.0000	.1523	-.1400	.1992	.0362	.0732	.0109	-.0218
16	1.0000	.0162	-.1219	.1430	-.0056	.3109	.0403	-.0602
17	1.0000	-.1297	.0026	.1486	-.0376	.4980	.0428	-.1016
18	1.0000	-.2089	.1677	.2594	.0162	.4985	.0147	-.0759
19	1.0000	-.2753	.3837	.4515	.2103	.4983	-.0180	.0813
20	1.0000	-.3250	.5688	.6255	.4273	.5420	-.0533	.2960
21	1.0000	-.3586	.7018	.7535	.6030	.5931	-.0842	.4851
22	1.0000	.4468	-.0622	.1217	.0982	-.3460	-.0522	.0397
23	1.0000	.4006	-.0833	.1554	.0958	-.3113	-.0466	.0335
24	1.0000	.3645	-.0980	.1774	.0917	-.2740	-.0407	.0274
25	1.0000	.3183	-.1130	.1968	.0831	-.2125	-.0313	.0181
26	1.0000	.2842	-.1224	.2067	.0752	-.1604	-.0234	.0105
27	1.0000	.2380	-.1317	.2118	.0626	-.0831	-.0119	-.0002
28	1.0000	.1989	-.1368	.2091	.0507	-.0134	-.0016	-.0097
29	1.0000	.1648	-.1388	.2016	.0400	.0464	.0071	-.0177
30	1.0000	.1137	-.1385	.1844	.0238	.1358	.0196	-.0301
31	1.0000	.0634	-.1332	.1623	.0083	.2204	.0305	-.0430
32	1.0000	.4397	-.0649	.1257	.0974	-.3401	-.0512	.0388
33	1.0000	.3938	-.0857	.1586	.0948	-.3045	-.0455	.0325
34	1.0000	.3580	-.0996	.1789	.0903	-.2656	-.0394	.0262
35	1.0000	.3122	-.1141	.1974	.0816	-.2042	-.0301	.0170
36	1.0000	.2784	-.1227	.2059	.0734	-.1524	-.0223	.0096
37	1.0000	.2325	-.1316	.2103	.0608	-.0762	-.0109	-.0009
38	1.0000	.1940	-.1362	.2069	.0490	-.0090	-.0010	-.0099

*Elastic modes start at "mode 3."

TABLE 11-6 AIRPLANE VIBRATION MODE SHAPES*, FINAL STIFFNESS DESIGN

SYMMETRIC , LOW GROSS WEIGHT

ROW	MODE 1	MODE 2	MODE 3	MODE 4	MODE 5	MODE 6	MODE 7	MODE 8
39	1.0000	.1602	-.1381	.1993	.0383	.0501	.0077	-.0178
40	1.0000	.1096	-.1376	.1815	.0223	.1369	.0198	-.0296
41	1.0000	.0589	-.1320	.1586	.0070	.2190	.0304	-.0419
42	1.0000	.0083	-.1192	.1354	-.0078	.2980	.0390	-.0562
43	1.0000	-.0424	-.0951	.1187	-.0224	.3710	.0444	-.0720
44	1.0000	-.0832	-.0618	.1177	-.0346	.4188	.0453	-.0847
45	1.0000	-.1344	.0020	.1395	-.0425	.4619	.0399	-.0975
46	1.0000	-.1614	.0477	.1641	-.0399	.4710	.0334	-.0997
47	1.0000	-.1908	.1078	.2034	-.0257	.4590	.0219	-.0967
48	1.0000	-.2105	.1550	.2383	-.0035	.4471	.0133	-.0845
49	1.0000	-.2305	.2142	.2895	.0388	.4376	.0045	-.0566
50	1.0000	-.2479	.2690	.3365	.0839	.4311	-.0035	-.0232
51	1.0000	-.2646	.3247	.3864	.1352	.4290	-.0116	.0185
52	1.0000	-.2809	.3808	.4374	.1909	.4304	-.0202	.0666
53	1.0000	-.2976	.4406	.4928	.2555	.4373	-.0302	.1264
54	1.0000	-.3139	.5013	.5498	.3265	.4507	-.0415	.1963
55	1.0000	-.3306	.5655	.6108	.4062	.4694	-.0546	.2784
56	1.0000	-.3462	.6270	.6698	.4860	.4908	-.0684	.3634
57	1.0000	-.3641	.6988	.7392	.5831	.5197	-.0857	.4696
58	1.0000	-.3807	.7663	.8047	.6761	.5479	-.1026	.5728
59	1.0000	.3628	-.0977	.1762	.0909	-.2710	-.0403	.0271
60	1.0000	.3122	-.1136	.1964	.0813	-.2038	-.0300	.0170
61	1.0000	.2615	-.1250	.2062	.0682	-.1258	-.0184	.0062
62	1.0000	.2615	-.1256	.2071	.0686	-.1257	-.0183	.0061
63	1.0000	.2109	-.1321	.2059	.0531	-.0444	-.0063	-.0044
64	1.0000	.2109	-.1337	.2081	.0541	-.0412	-.0057	-.0053
65	1.0000	.1602	-.1348	.1959	.0366	.0354	.0056	-.0140
66	1.0000	.1602	-.1364	.1977	.0377	.0425	.0066	-.0159
67	1.0000	.1096	-.1327	.1757	.0190	.1030	.0156	-.0205
68	1.0000	.1096	-.1341	.1767	.0202	.1120	.0167	-.0228
69	1.0000	.1096	-.1363	.1791	.0217	.1261	.0185	-.0267
70	1.0000	.0589	-.1286	.1509	.0048	.1606	.0241	-.0264
71	1.0000	.0589	-.1305	.1508	.0069	.1797	.0261	-.0316
72	1.0000	.0589	-.1314	.1559	.0070	.2043	.0287	-.0380
73	1.0000	.0083	-.1199	.1164	-.0079	.1895	.0283	-.0261
74	1.0000	.0083	-.1214	.1187	-.0075	.2121	.0312	-.0321
75	1.0000	.0083	-.1207	.1226	-.0070	.2341	.0328	-.0389
76	1.0000	.0083	-.1198	.1309	-.0075	.2755	.0368	-.0502

*Elastic modes start at "mode 3."

TABLE 11-6 AIRPLANE VIBRATION MODE SHAPES*, FINAL STIFFNESS DESIGN

SYMMETRIC , LOW GROSS WEIGHT

ROW	MODE 1	MODE 2	MODE 3	MODE 4	MODE 5	MODE 6	MODE 7	MODE 8
77	1.0000	-.0424	-.1100	.0788	-.0182	.2116	.0315	-.0256
78	1.0000	-.0424	-.1087	.0823	-.0186	.2277	.0329	-.0315
79	1.0000	-.0424	-.1060	.0895	-.0202	.2549	.0350	-.0404
80	1.0000	-.0424	-.1007	.1034	-.0220	.3084	.0393	-.0560
81	1.0000	-.0930	-.0973	.0385	-.0268	.2220	.0320	-.0248
82	1.0000	-.0930	-.0918	.0484	-.0315	.2431	.0340	-.0351
83	1.0000	-.0772	-.0938	.0666	-.0298	.2614	.0354	-.0418
84	1.0000	-.0799	-.0819	.0851	-.0343	.3172	.0389	-.0500
85	1.0000	-.0824	-.0675	.1085	-.0351	.3891	.0434	-.0779
86	1.0000	-.1123	-.0796	.0425	-.0408	.2551	.0341	-.0418
87	1.0000	-.1205	-.0567	.0674	-.0514	.3056	.0356	-.0598
88	1.0000	-.1281	-.0268	.1034	-.0514	.3773	.0373	-.0814
89	1.0000	-.1437	-.0833	-.0080	-.0328	.2109	.0316	-.0207
90	1.0000	-.1437	-.0735	.0074	-.0451	.2220	.0313	-.0333
91	1.0000	-.1463	-.0642	.0176	-.0536	.2282	.0306	-.0400
92	1.0000	-.1600	-.0275	.0521	-.0746	.2578	.0284	-.0552
93	1.0000	-.1726	.0179	.1010	-.0726	.3343	.0286	-.0780
94	1.0000	-.1870	.0639	.1533	-.0529	.3920	.0254	-.0940
95	1.0000	-.1954	.0745	.1460	-.0637	.3278	.0190	-.0935
96	1.0000	-.2213	.1511	.2133	-.0269	.3328	.0078	-.0891
97	1.0000	-.2413	.2199	.2775	.0245	.3479	-.0007	-.0621
98	1.0000	-.2582	.2843	.3399	.0850	.3714	-.0083	-.0191
99	1.0000	-.2978	.4078	.4455	.1967	.3304	-.0281	.0777
100	1.0000	-.3409	.5570	.5802	.3626	.3244	-.0565	.2426
101	1.0000	-.3603	.6491	.6756	.4931	.4011	-.0762	.3789
102	1.0000	-.3765	.7280	.7580	.6098	.4715	-.0948	.5046
103	1.0000	-.1943	-.0678	-.0586	-.0384	.1695	.0266	.0016
104	1.0000	-.1943	-.0513	-.0346	-.0703	.1563	.0241	.0068
105	1.0000	-.1950	-.0361	-.0138	-.0886	.1404	.0212	-.0033
106	1.0000	-.2088	.0171	.0412	-.1161	.1386	.0119	-.0509
107	1.0000	-.2223	.0928	.1273	-.0949	.1836	.0043	-.1023
108	1.0000	-.2427	.1563	.1836	-.0679	.1653	-.0050	-.1090
109	1.0000	-.2685	.2496	.2718	.0033	.1650	-.0142	-.0754
110	1.0000	-.3055	.3996	.4200	.1623	.2194	-.0297	.0507
111	1.0000	-.3215	.4689	.4899	.2463	.2607	-.0402	.1277
112	1.0000	-.2335	-.0621	-.1070	-.0236	.1395	.0233	.0093
113	1.0000	-.2335	-.0540	-.0954	-.0514	.1212	.0216	.0340
114	1.0000	-.2335	-.0349	-.0696	-.1033	.0823	.0171	.0766

*Elastic modes start at "mode 3."

TABLE 11-6 AIRPLANE VIBRATION MODE SHAPES* , FINAL STIFFNESS DESIGN

SYMMETRIC , LOW GROSS WEIGHT

ROW	MODE 1	MODE 2	MODE 3	MODE 4	MODE 5	MODE 6	MODE 7	MODE 8
115	1.0000	-.2335	-.0128	-.0398	-.1369	.0580	.0119	.0781
116	1.0000	-.2437	.0359	.0129	-.1611	.0141	-.0018	-.0142
117	1.0000	-.2529	.0958	.0813	-.1665	-.0359	-.0198	-.1278
118	1.0000	-.2583	.1372	.1302	-.1386	-.0137	-.0227	-.1506
119	1.0000	-.2871	.2434	.2306	-.0656	-.0364	-.0295	-.1373
120	1.0000	-.3107	.3404	.3266	.0383	-.0138	-.0303	-.0575
121	1.0000	-.3306	.4242	.4104	.1350	.0205	-.0359	.0262
122	1.0000	-.3427	.4727	.4575	.1928	.0357	-.0442	.0810
123	1.0000	-.3549	.5354	.5245	.2808	.0974	-.0559	.1685
124	1.0000	-.3712	.6223	.6181	.4092	.1898	-.0743	.3014
125	1.0000	-.3875	.7117	.7151	.5476	.2915	-.0052	.4497
126	1.0000	-.3956	.7571	.7645	.6195	.3448	-.1063	.5282
127	1.0000	-.4060	.8151	.8276	.7116	.4132	-.1206	.6288
128	1.0000	-.4163	.8719	.8892	.8007	.4795	-.1343	.7255
129	1.0000	-.2689	-.0464	-.1359	-.0479	.0968	.0193	.0460
130	1.0000	-.2689	-.0273	-.1104	-.1103	.0483	.0144	.1065
131	1.0000	-.3003	-.0369	-.1675	-.0572	.0664	.0165	.0694
132	1.0000	-.3003	-.0164	-.1405	-.1270	.0106	.0111	.1401
133	1.0000	-.2834	.0165	-.0801	-.2490	-.1187	-.0024	.3306
134	1.0000	-.2761	.0677	.0060	-.2096	-.1153	-.0195	-.0085
135	1.0000	-.2799	.1055	.0515	-.2171	-.1596	-.0335	-.1024
136	1.0000	-.3019	.0967	.0050	-.2533	-.2308	-.0363	-.0178
137	1.0000	-.3043	.1332	.0508	-.2591	-.2709	-.0498	-.1136
138	1.0000	-.2907	.2028	.1668	-.1760	-.2300	-.0586	-.2482
139	1.0000	-.3283	.3510	.3103	.0055	-.1746	-.0398	-.0868
140	1.0000	-.3464	.4373	.4007	.1105	-.1229	-.0384	-.0006
141	1.0000	-.3718	.5543	.5209	.2690	-.0343	-.0621	.1608
142	1.0000	-.3878	.6430	.6174	.4051	.0648	-.0823	.3052
143	1.0000	-.4038	.7339	.7166	.5505	.1732	-.1048	.4646
144	1.0000	-.4198	.8272	.8191	.7061	.2901	-.1302	.6412
145	1.0000	-.4317	.8999	.8998	.8367	.3872	-.1533	.7979
146	1.0000	-.4416	.9589	.9648	.9377	.4628	-.1703	.9148
147	1.0000	-.3136	.0386	-.1033	-.3624	-.2755	-.0138	.6050
148	1.0000	-.3259	.2679	.1951	-.2631	-.5940	-.1177	-.4306
149	1.0000	-.3619	.4694	.4178	.1215	-.2163	-.0436	.0037
150	1.0000	-.3877	.6074	.5674	.3313	-.0465	-.0750	.2299
151	1.0000	-.4116	.7443	.7172	.5513	.1164	-.1093	.4707
152	1.0000	-.4355	.8881	.8761	.8019	.3040	-.1521	.7647

* Elastic modes start at "mode 3."

TABLE 11-6 AIRPLANE VIBRATION MODE SHAPES* , FINAL STIFFNESS DESIGN

SYMMETRIC , LOW GROSS WEIGHT

PCW	MODE 1	MODE 2	MODE 3	MODE 4	MODE 5	MODE 6	MODE 7	MODE 8
153	1.0000	-.4539	1.0000	1.0000	1.0000	.4519	-.1866	1.0000
154	1.0000	-.2109	.1672	.2553	.0119	.4797	.0136	-.0773
155	1.0000	-.2269	.2173	.2564	.0478	.4753	.0065	-.0525
156	1.0000	-.2443	.2174	.3449	.0943	.4714	-.0016	-.0171
157	1.0000	-.2610	.3264	.3952	.1469	.4712	-.0100	.0265
158	1.0000	-.2773	.3827	.4466	.2035	.4744	-.0188	.0761
159	1.0000	-.2940	.4427	.5021	.2686	.4826	-.0290	.1369
160	1.0000	-.3103	.5034	.5593	.3400	.4970	-.0405	.2074
161	1.0000	-.3270	.5676	.6204	.4199	.5165	-.0538	.2898
162	1.0000	-.3427	.6291	.6792	.4992	.5382	-.0675	.3739
163	1.0000	-.3605	.7008	.7485	.5961	.5674	-.0847	.4797
164	.0000	.0000	-.0129	-.0189	.0106	.0026	.0012	.0005
165	.0000	.0000	-.0354	-.0518	-.0147	-.0567	.0010	-.0188
166	.0000	.0000	-.0725	-.1058	-.0783	-.1874	.0109	-.0995
167	.0000	.0000	-.1004	-.1478	-.1338	-.3663	.0339	-.2159
168	.0000	.0000	-.1235	-.1830	-.1832	-.5393	.0551	-.3326
169	.0000	.0000	-.1478	-.2205	-.2379	-.7401	.0800	-.4705
170	.0000	-.0000	-.0037	-.0056	.0230	.0294	.0016	.0065
171	.0000	.0000	-.0253	-.0373	.0015	-.0235	.0001	-.0061
172	.0000	.0000	-.0620	-.0909	-.0583	-.1556	.0102	-.0822
173	.0000	-.0000	-.0059	-.0102	.0382	.0301	.0022	.0159
174	.0000	.0000	-.0404	-.0604	-.0176	-.0906	.0089	-.0470
175	.0000	.0000	-.0826	-.1227	-.0974	-.3037	.0311	-.1784
176	.0000	.0000	-.1143	-.1701	-.1644	-.5072	.0537	-.3135
177	.0000	-.0000	-.0050	-.0107	.0595	.0335	.0038	.0301
178	.0000	.0000	-.0452	-.0696	-.0204	-.1711	.0250	-.0990
179	.0000	.0000	-.0869	-.1311	-.1078	-.4096	.0493	-.2551
180	.0000	.0000	-.1183	-.1778	-.1761	-.6042	.0694	-.3846
181	.0000	.0000	-.1504	-.2255	-.2466	-.8065	.0904	-.5197
182	.0000	-.0000	-.0099	-.0206	.0530	-.0868	.0279	-.0542
183	.0000	.0000	-.0419	-.0672	-.0142	-.2450	.0414	-.1557
184	.0000	.0000	-.0961	-.1462	-.1302	-.5261	.0660	-.3380
185	.0000	.0000	-.1202	-.1814	-.1819	-.6508	.0769	-.4189
186	.0000	-.0000	-.0116	-.0241	.0490	-.1313	.0357	-.0865
187	.0000	.0000	-.0659	-.1034	-.0674	-.4161	.0609	-.2717
188	.0000	.0000	-.1228	-.1864	-.1902	-.7164	.0873	-.4673
189	.0000	.0000	-.1532	-.2309	-.2563	-.8792	.1017	-.5738
190	1.0000	-.3619	.5234	.4944	.2219	-.8201	.6751	.0083

*Elastic modes start at "mode 3."

TABLE 11-6 AIRPLANE VIBRATION MODE SHAPES* , FINAL STIFFNESS DESIGN

SYMMETRIC , LOW GROSS WEIGHT

ROW	MODE 1	MODE 2	MODE 3	MODE 4	MODE 5	MODE 6	MODE 7	MODE 8
191	.0000	.2274	-.0159	.0256	-.0187	-.9638	1.0000	-.0979
192	.0000	.0005	-.0012	-.0008	-.0008	.0017	.0002	-.0007
193	1.0000	1.0000	.4133	-.8083	-.1900	1.0000	.1178	-.1329
194	1.0000	.9152	.3267	-.6317	-.1217	.6195	.0703	-.0794
195	1.0000	.8441	.2559	-.4882	-.0682	.3289	.0340	-.0390
196	1.0000	.7750	.1902	-.3564	-.0219	.0891	.0040	-.0066
197	1.0000	.6565	.0873	-.1551	.0411	-.1984	-.0328	.0298
198	1.0000	.6160	.0529	-.0886	.0607	-.2688	-.0428	.0374
199	1.0000	.5654	.0147	-.0170	.0778	-.3221	-.0500	.0422
200	1.0000	.5147	-.0205	.0478	.0901	-.3508	-.0536	.0437
201	1.0000	.4641	-.0516	.1030	.0965	-.3499	-.0530	.0412
202	1.0000	.4134	-.0771	.1451	.0962	-.3207	-.0481	.0353
203	1.0000	.3628	-.0974	.1755	.0906	-.2693	-.0400	.0269
204	1.0000	.3122	-.1132	.1955	.0808	-.2021	-.0298	.0169
205	1.0000	.2615	-.1245	.2051	.1677	-.1250	-.0193	.0063
206	1.0000	.2109	-.1313	.2046	.0523	-.0448	-.0063	-.0040
207	1.0000	.1602	-.1338	.1946	.0357	.0323	.0051	-.0130
208	1.0000	.1096	-.1322	.1755	.0193	.0986	.0149	-.0197
209	1.0000	.0589	-.1271	.1487	.0045	.1491	.0223	-.0235
210	1.0000	.0083	-.1196	.1160	-.0083	.1863	.0279	-.0250
211	1.0000	-.0424	-.1102	.0780	-.0181	.2080	.0312	-.0243
212	1.0000	-.0930	-.0991	.0349	-.0245	.2128	.0321	-.0207
213	1.0000	-.1437	-.0865	-.0135	-.0266	.1997	.0305	-.0139
214	1.0000	-.1943	-.0734	-.0670	-.0224	.1705	.0269	-.0042
215	1.0000	-.2450	-.0621	-.1268	-.0057	.1327	.0222	-.0004
216	1.0000	-.3030	-.0501	-.2076	.0333	.0699	.0141	-.0041
217	1.0000	-.4409	-.0214	-.4229	.1641	-.1609	-.0138	-.0207
218	1.0000	-.5115	-.0067	-.5470	.2540	-.3232	-.0330	-.0350
219	1.0000	-.5885	.0094	-.6852	.3573	-.5114	-.0553	-.0519
220	.0000	.0005	-.0001	.0009	-.0007	.0012	.0001	.0001
221	1.0000	-.5433	-.0000	-.6063	.3003	-.4082	-.0430	-.0429
222	1.0000	-.5133	-.0063	-.5499	.2559	-.3265	-.0334	-.0353
223	.0000	.0005	-.0001	.0009	-.0006	.0011	.0001	.0001
224	1.0000	.7054	.1281	-.2341	.0178	-.0989	-.0199	.0177
225	1.0000	-.3737	-.0353	-.3121	.0909	-.0312	.0017	-.0102

* Elastic modes start at "mode 3."

TABLE 11-6 AIRPLANE VIBRATION MODE SHAPES* , FINAL STIFFNESS DESIGN

SYMMETRIC , LOW GROSS WEIGHT

ROW	MODE 9	MODE 10	MODE 11	MODE 12	MODE 13	MODE 14	MODE 15	MODE 16
1	-.0143	.0013	.0047	-.0414	.0498	.3327	-.0083	-.0163
2	-.1624	.0002	.3533	-.0650	-.0143	.0666	.0030	-.0058
3	-.0682	.0027	.1240	-.0323	.0145	-.0423	.0024	.0058
4	-.0029	-.0000	.0058	-.0010	.0005	.0014	-.0001	-.0000
5	.0004	-.0000	-.0007	.0008	-.0007	-.0004	-.0000	.0001
6	-.0002	.0000	.0004	-.0000	-.0002	-.0002	.0000	.0000
7	.0818	-.0051	-.0054	-.0396	-.0191	.3799	.0163	-.0174
8	-.1697	.0258	-.1589	-.1846	-.1198	.1073	.0273	.0056
9	-.0401	.0010	-.1252	-.0226	.0055	-.0430	.0183	.0200
10	-.0034	.0004	-.0030	-.0028	-.0012	.0015	.0002	.0002
11	-.0015	.0000	.0003	.0011	.0010	-.0012	-.0006	.0002
12	-.0002	.0000	-.0002	-.0003	-.0003	.0003	.0001	.0000
13	-.0989	.0024	-.0053	.0455	-.0200	-.3332	.0427	.0039
14	-.0180	.0005	.0020	-.0499	.0885	-.3333	.0449	-.0052
15	.0838	-.0020	.0056	-.0970	.1151	.1485	-.0333	-.0021
16	.0417	-.0033	-.0272	.0288	.0815	.4594	-.0564	.0234
17	-.2369	-.0067	-.1561	.2456	.2919	.3668	.0378	.0077
18	-.3407	-.0094	-.2264	.2585	.4139	.3714	.1384	-.0839
19	-.2061	-.0150	-.1211	.2226	.3636	.3860	.1293	-.1594
20	-.0038	-.0235	.0732	.2123	.2681	.5130	.2148	-.1462
21	.1810	-.0328	.2624	.2143	.1719	.6909	.3617	-.0585
22	-.0956	.0023	-.0050	.0420	-.0165	-.3276	.0421	.0036
23	-.0700	.0017	-.0026	.0080	.0250	-.3608	.0491	.0003
24	-.0470	.0012	-.0006	-.0193	.0563	-.3628	.0500	-.0024
25	-.0154	.0004	.0021	-.0509	.0885	-.3217	.0431	-.0051
26	.0092	-.0001	.0042	-.0724	.1077	-.2633	.0320	-.0067
27	.0412	-.0008	.0066	-.0944	.1227	-.1495	.0124	-.0075
28	.0644	-.0014	.0075	-.1026	.1236	-.0208	-.0086	-.0064
29	.0785	-.0018	.0067	-.0993	.1157	.0918	-.0251	-.0038
30	.0880	-.0023	.0026	-.0774	.0945	.2503	-.0452	.0027
31	.0785	-.0027	-.0069	-.0355	.0743	.3678	-.0550	.0116
32	-.0920	.0022	-.0047	.0384	-.0128	-.3213	.0414	.0032
33	-.0664	.0016	-.0023	.0046	.0281	-.3528	.0480	-.0001
34	-.0436	.0011	-.0003	-.0213	.0573	-.3503	.0480	-.0024
35	-.0125	.0004	.0023	-.0520	.0884	-.3084	.0410	-.0050
36	.0109	-.0002	.0042	-.0713	.1049	-.2501	.0308	-.0063
37	.0418	-.0009	.0066	-.0919	.1183	-.1393	.0114	-.0071
38	.0639	-.0014	.0074	-.0994	.1184	-.0198	-.0080	-.0060

*Elastic modes start at "mode 3."

TABLE 11-6 AIRPLANE VIBRATION MODE SHAPES* , FINAL STIFFNESS DESIGN

SYMMETRIC , LOW GROSS WEIGHT

ROW	MODE 9	MODE 10	MODE 11	MODE 12	MODE 13	MODE 14	MODE 15	MODE 16
39	.0784	-.0018	.0070	-.0971	.1108	.0921	-.0247	-.0038
40	.0877	-.0022	.0032	-.0753	.0878	.2447	-.0438	.0024
41	.0784	-.0026	-.0058	-.0342	.0661	.3550	-.0526	.0108
42	.0449	-.0030	-.0229	.0251	.0642	.4244	-.0519	.0208
43	-.0189	-.0037	-.0512	.0989	.0957	.4374	-.0386	.0290
44	-.0949	-.0047	-.0852	.1620	.1543	.4065	-.0162	.0287
45	-.2140	-.0060	-.1426	.2266	.2599	.3327	.0307	.0100
46	-.2758	-.0068	-.1761	.2448	.3184	.2954	.0625	-.0114
47	-.3112	-.0081	-.2042	.2463	.3625	.3062	.1002	-.0450
48	-.3152	-.0081	-.2116	.2361	.3727	.3081	.1135	-.0693
49	-.2935	-.0073	-.1998	.2226	.3667	.2985	.1045	-.0940
50	-.2626	-.0069	-.1789	.2098	.3533	.2889	.0927	-.1145
51	-.2231	-.0072	-.1484	.1985	.3351	.2849	.0839	-.1322
52	-.1769	-.0081	-.1100	.1890	.3134	.2882	.0803	-.1462
53	-.1195	-.0100	-.0585	.1814	.2856	.3046	.0875	-.1527
54	-.0530	-.0131	.0050	.1774	.2537	.3421	.1121	-.1492
55	.0264	-.0173	.0835	.1747	.2125	.3975	.1547	-.1281
56	.1095	-.0215	.1677	.1737	.1679	.4672	.2122	-.0922
57	.2150	-.0268	.2766	.1742	.1090	.5683	.3004	-.0285
58	.3193	-.0316	.3850	.1747	.0481	.6710	.3943	.0484
59	-.0469	.0012	-.0006	-.0175	.0529	-.3496	.0478	-.0020
60	-.0134	.0004	.0022	-.0498	.0854	-.3042	.0403	-.0046
61	.0194	-.0004	.0048	-.0739	.1037	-.2128	.0249	-.0060
62	.0206	-.0004	.0049	-.0764	.1069	-.2139	.0249	-.0063
63	.0487	-.0010	.0070	-.0880	.1069	-.0955	.0056	-.0060
64	.0529	-.0011	.0073	-.0950	.1163	-.0855	.0028	-.0066
65	.0717	-.0015	.0084	-.0894	.0932	.0371	-.0147	-.0046
66	.0761	-.0017	.0080	-.0956	.1044	.0655	-.0206	-.0046
67	.0829	-.0017	.0094	-.0723	.0541	.1344	-.0251	-.0019
68	.0854	-.0018	.0082	-.0743	.0619	.1664	-.0309	-.0010
69	.0878	-.0020	.0057	-.0763	.0765	.2148	-.0393	.0008
70	.0910	-.0020	.0089	-.0548	.0226	.2206	-.0351	.0005
71	.0869	-.0019	.0047	-.0479	.0312	.2569	-.0389	.0034
72	.0819	-.0023	-.0018	-.0400	.0537	.3210	-.0482	.0082
73	.0849	-.0015	.0106	-.0308	-.0223	.2077	-.0264	.0004
74	.0875	-.0020	.0064	-.0254	-.0152	.2800	-.0381	.0041
75	.0729	-.0020	-.0019	-.0109	.0069	.2998	-.0387	.0086
76	.0548	-.0026	-.0155	.0123	.0444	.3810	-.0476	.0167

*Elastic modes start at "mode 3."

TABLE 11-6 AIRPLANE VIBRATION MODE SHAPES* , FINAL STIFFNESS DESIGN

SYMMETRIC , LOW GROSS WEIGHT

ROW	MODE 9	MODE 10	MODE 11	MODE 12	MODE 13	MODE 14	MODE 15	MODE 16
77	.0788	-.0012	.0119	-.0089	-.0610	.1978	-.0204	.0004
78	.0703	-.0014	.0058	.0019	-.0465	.2233	-.0242	.0043
79	.0543	-.0018	-.0047	.0203	-.0204	.2648	-.0292	.0104
80	.0208	-.0026	-.0262	.0571	.0334	.3447	-.0352	.0202
81	.0661	-.0008	.0121	.0153	-.0928	.1621	-.0116	.0008
82	.0464	-.0013	.0013	.0364	-.0632	.1762	-.0164	.0086
83	.0383	-.0017	-.0070	.0427	-.0348	.2190	-.0221	.0123
84	-.0096	-.0027	-.0345	.0879	.0342	.2845	-.0244	.0220
85	-.0695	-.0040	-.0705	.1407	.1198	.3760	-.0201	.0231
86	.0217	-.0016	-.0074	.0632	-.0468	.1520	-.0157	.0155
87	-.0458	-.0027	-.0405	.1154	.0429	.1833	-.0152	.0248
88	-.1276	-.0041	-.0903	.1717	.1513	.2578	.0013	.0227
89	.0540	-.0002	.0157	.0348	-.1306	.0831	.0022	-.0000
90	.0308	-.0012	.0055	.0601	-.0921	.0683	-.0063	.0126
91	.0009	-.0017	-.0031	.0765	-.0604	.0575	-.0102	.0192
92	-.0733	-.0025	-.0357	.1240	.0488	.0492	-.0145	.0285
93	-.1844	-.0031	-.0970	.1799	.1793	.0587	-.0010	.0225
94	-.2510	-.0042	-.1555	.2066	.2656	.1626	.0370	-.0039
95	-.2253	-.0022	-.1404	.1744	.2210	.0924	.0173	.0034
96	-.2477	-.0025	-.1700	.1772	.2699	.1335	.0377	-.0393
97	-.2432	-.0029	-.1733	.1747	.2906	.1733	.0473	-.0750
98	-.2212	-.0038	-.1557	.1759	.2905	.2032	.0502	-.1008
99	-.0997	-.0024	-.0634	.1301	.2140	.1335	.0021	-.1212
100	.0852	-.0064	.1032	.0958	.0942	.1461	.0230	-.0822
101	.1908	-.0157	.2228	.1185	.0625	.3278	.1520	-.0338
102	.2916	-.0241	.3384	.1406	.0279	.5109	.2906	.0320
103	.0432	.0008	.0225	.0366	-.1578	-.0195	.0192	-.0059
104	.0180	-.0007	.0187	.0585	-.1071	-.0468	.0056	.0117
105	-.0102	-.0014	.0239	.0684	-.0637	-.0597	-.0038	.0213
106	-.0823	-.0021	-.0113	.1014	.0404	-.0963	-.0198	.0336
107	-.1718	.0018	-.1148	.1006	.1242	-.0648	-.0170	.0230
108	-.1762	.0045	-.1389	.0851	.1388	-.0708	-.0352	-.0021
109	-.1471	.0070	-.1009	.0719	.1425	-.0808	-.0732	-.0450
110	-.0550	.0052	-.0483	.0715	.1266	-.0433	-.0880	-.0932
111	-.0002	.0010	.0092	.0797	.1161	.0199	-.0568	-.0991
112	.0438	.0012	.0250	.0308	-.1738	-.0569	.0319	-.0170
113	.0350	.0010	.0253	.0355	-.1576	-.0832	.0250	-.0071
114	.0106	.0003	.0327	.0415	-.1081	-.1179	.0126	.0097

*Elastic modes start at "mode 3."

TABLE 11-6 AIRPLANE VIBRATION MODE SHAPES*, FINAL STIFFNESS DESIGN

SYMMETRIC , LOW GROSS WEIGHT

ROW	MODE 9	MODE 10	MODE 11	MODE 12	MODE 13	MODE 14	MODE 15	MODE 16
115	-.0283	-.0003	.0541	.0424	-.0513	-.1170	-.0002	.0202
116	-.0661	-.0015	.0342	.0578	.0070	-.1736	-.0176	.0384
117	-.0815	-.0014	-.0486	.0577	.0475	-.1810	-.0162	.0418
118	-.1097	.0039	-.1092	.0226	.0446	-.1435	-.0235	.0300
119	-.0855	.0159	-.1321	-.0403	.0044	-.2421	-.1320	-.0066
120	-.0186	.0221	-.0716	-.0431	-.0164	-.3622	-.2420	-.0450
121	.0445	.0198	-.0082	-.0398	-.0344	-.3627	-.2569	-.0624
122	.09	.0193	.0425	-.0401	-.0573	-.3470	-.2519	-.0565
123	.1537	.0117	.1099	-.0235	-.0682	-.2470	-.1919	-.0406
124	.2457	.0014	.2206	.0062	-.0876	-.0599	-.0650	.0074
125	.3532	-.0096	.3512	.0423	-.1133	.1829	.1133	.0877
126	.4114	-.0154	.4223	.0619	-.1287	.3200	.2180	.1393
127	.4860	-.0228	.5135	.0872	-.1483	.4974	.3530	.2062
128	.5566	-.0300	.5997	.1118	-.1650	.6652	.4796	.2630
129	.0309	.0016	.0451	.0325	-.1994	-.1510	.0509	-.0214
130	.0066	.0012	.0615	.0335	-.1583	-.2043	.0398	-.0029
131	.0243	.0021	.0631	.0309	-.2313	-.2257	.0708	-.0295
132	-.0020	.0018	.0857	.0290	-.1905	-.2885	.0610	-.0105
133	-.0691	.0031	.1328	-.0418	.0095	-.0762	.0052	.0051
134	-.0572	-.0008	.0407	.0213	-.0099	-.3038	-.0196	.0686
135	-.0614	-.0014	-.0131	.0217	.0108	-.3463	-.0192	.0923
136	-.0506	-.0004	.0420	-.0089	-.0239	-.4585	-.0240	.1174
137	-.0550	-.0010	-.0125	-.0071	-.0028	-.5022	-.0236	.1433
138	-.0352	.0047	-.1422	-.0646	-.0237	-.0751	.0046	.0174
139	.0577	.0336	-.0431	-.1239	-.1341	-.6262	-.3930	-.0271
140	.1142	.0372	.0173	-.1131	-.1400	-.6549	-.4395	-.0565
141	.2348	.0233	.1513	-.0972	-.1854	-.4683	-.3116	-.0077
142	.3381	.0114	.2759	-.0678	-.2169	-.2734	-.1743	.0630
143	.4569	-.0008	.4212	-.0302	-.2532	-.0062	.0319	.1759
144	.5958	-.0136	.5921	.0128	-.3042	.3321	.3177	.3626
145	.7310	-.0242	.7585	.0484	-.3722	.6667	.6344	.6224
146	.8263	-.0324	.8758	.0763	-.4123	.9020	.8435	.7747
147	-.1178	.0068	.2147	-.1333	.0977	.0487	.0073	-.0147
148	.1133	-.0015	-.1741	-.1657	-.1128	.1340	.0994	-.0017
149	.1965	.0503	.0536	-.1775	-.2404	-.9901	-.6936	-.0717
150	.3237	.0224	.2320	-.1184	-.2575	-.4842	-.3072	.0418
151	.5054	.0035	.4533	-.0650	-.3193	-.0991	-.0025	.2163
152	.7495	-.0171	.7540	.0038	-.4293	.5017	.5347	.6287

*Elastic modes start at "mode 3."

TABLE 11-6 AIRPLANE VIBRATION MODE SHAPES* , FINAL STIFFNESS DESIGN

SYMMETRIC , LOW GROSS WEIGHT

ROW	MODE 9	MODE 10	MODE 11	MODE 12	MODE 13	MODE 14	MODE 15	MODE 16
153	.9490	-.0332	1.0000	.0583	-.5251	1.0000	1.0000	1.0000
154	-.3307	-.0090	-.2209	.2497	.3993	.3485	.1292	-.0804
155	-.3132	-.0087	-.2104	.2402	.3958	.3468	.1258	-.1012
156	-.2822	-.0088	-.1884	.2291	.3840	.3433	.1182	-.1224
157	-.2420	-.0098	-.1564	.2192	.3666	.3442	.1128	-.1403
158	-.1959	-.0113	-.1172	.2108	.3460	.3516	.1121	-.1548
159	-.1386	-.0137	-.0653	.2042	.3192	.3719	.1218	-.1622
160	-.0723	-.0172	-.0017	.2009	.2883	.4125	.1482	-.1598
161	.0068	-.0213	.0769	.1991	.2486	.4725	.1937	-.1309
162	.0883	-.0256	.1594	.1990	.2067	.5445	.2515	-.1084
163	.1930	-.0307	.2675	.2003	.1498	.6482	.3404	-.0480
164	.0110	.0019	.0052	-.0181	-.0345	.0021	.0057	-.0060
165	.0343	.0043	.0122	-.0601	-.1012	-.0978	-.0428	.0113
166	.0718	.0498	.0078	-.0940	-.1455	-.2704	-.1514	.0177
167	.2606	.2430	.1424	.0950	.0443	-.1617	-.1129	.0210
168	.4735	.4610	.3028	.3345	.2924	.0311	-.0244	.0221
169	.7375	.7323	.5064	.6475	.6215	.3139	.1137	.0216
170	-.0011	.0011	-.0018	-.0070	-.0134	.0354	.0187	-.0147
171	.0208	-.0017	.0056	-.0532	-.0867	-.0590	-.0244	.0031
172	.0714	.0487	.0149	-.0779	-.1271	-.2205	-.1257	.0130
173	.0201	.0049	.0131	-.0243	-.0497	.0741	.0020	-.0143
174	.0655	.0457	.0282	-.0456	-.0900	-.1197	-.0741	.0030
175	.2467	.2248	.1438	.1010	.0510	-.0963	-.0776	.0125
176	.4672	.4525	.3044	.3394	.2979	.0690	-.0036	.0171
177	.0482	.0107	.0351	-.0378	-.0853	-.0050	-.0156	-.0129
178	.2171	.1860	.1465	.1142	.0660	.0441	-.0016	-.0061
179	.4466	.4251	.3078	.3516	.3117	.1809	.0591	.0019
180	.6494	.6368	.4549	.5757	.5476	.3375	.1327	.0022
181	.8629	.8600	.6107	.8149	.8007	.5087	.2155	.0168
182	.2918	.2409	.2271	.2442	.2007	.3236	.1436	-.0337
183	.4037	.3707	.3056	.3584	.3194	.3493	.1511	-.0232
184	.6351	.6171	.4599	.5895	.5631	.4345	.1865	-.0038
185	.7371	.7258	.5276	.6909	.6700	.4695	.2006	.0052
186	.3682	.3273	.2984	.3531	.3138	.4496	.2063	-.0372
187	.6380	.5822	.4600	.5968	.5712	.5536	.2527	-.0215
188	.8607	.8514	.6302	.8548	.8450	.6592	.2992	.0003
189	1.0000	1.0000	.7248	1.0000	1.0000	.7248	.3297	.0125
190	.1153	.0129	.0672	-.1080	-.1671	-.6018	-.2720	-.0356

*Elastic modes start at "mode 3."

TABLE 11-6 AIRPLANE VIBRATION MODE SHAPES* , FINAL STIFFNESS DESIGN

SYMMETRIC , LOW GROSS WEIGHT

ROW	MODE 9	MODE 10	MODE 11	MODE 12	MODE 13	MODE 14	MODE 15	MODE 16
171	-.1304	-.0285	-.0344	.0865	.1131	.4282	.2387	.0332
192	-.0018	-.0001	-.0012	.0011	.0019	.0032	.0020	-.0002
193	.2860	-.0050	.0243	-.2745	.3461	-.8809	.1086	-.000
194	.1523	-.0025	.0125	-.1227	.1458	-.3151	.0280	.0007
195	.0534	-.0006	.0039	-.0154	.0068	.0501	-.0221	.0017
196	-.0236	.0008	-.0025	.0611	-.0883	.2595	-.0486	.0027
197	-.1040	.0024	-.0085	.1225	-.1532	.2804	-.0479	.0048
198	-.1199	.0028	-.0092	.1248	-.1461	.1410	-.0302	.0074
199	-.1255	.0030	-.0089	.1134	-.1221	-.0122	-.0085	.0082
200	-.1201	.0029	-.0078	.0900	-.0844	-.1580	.0144	.0072
201	-.1073	.0025	-.0059	.0565	-.0369	-.2786	.0340	.0047
202	-.0777	.0019	-.0034	.0194	.0102	-.3387	.0449	.0014
203	-.0468	.0012	-.0006	-.0166	.0512	-.3417	.0462	-.0018
204	-.0137	.0004	.0021	-.0480	.0824	-.2953	.0387	-.0042
205	.0184	-.0003	.0047	-.0711	.0995	-.2075	.0242	-.0055
206	.0465	-.0010	.0068	-.0833	.1003	-.0944	.0062	-.0053
207	.0681	-.0014	.0084	-.0832	.0842	.0231	-.0110	-.0040
208	.0810	-.0016	.0095	-.0715	.0534	.1174	-.0225	-.0021
209	.0857	-.0016	.0106	-.0532	.0160	.1733	-.0265	-.0008
210	.0850	-.0014	.0117	-.0319	-.0249	.1976	-.0211	-.0001
211	.0801	-.0011	.0131	-.0109	-.0641	.1906	-.0193	-.0005
212	.0721	-.0006	.0155	.0070	-.1013	.1505	-.0088	-.0025
213	.0613	.0002	.0187	.0204	-.1350	.0805	.0059	-.0067
214	.0513	.0008	.0213	.0275	-.1600	.0019	.0217	-.0135
215	.0438	.0010	.0215	.0312	-.1728	-.0604	.0367	-.0229
216	.0348	.0007	.0171	.0304	-.1659	-.1236	.0527	-.0358
217	.0071	-.0016	-.0080	-.0094	-.0051	-.0191	.0251	-.0210
218	-.0103	-.0037	-.0295	-.0501	.1576	.1730	-.0262	.0121
219	-.0305	-.0062	-.0553	-.1006	.3609	.4301	-.0970	.0595
220	.0001	.0000	.0002	.0003	-.0014	-.0018	.0005	-.0003
221	-.0193	-.0048	-.0416	-.0746	.2561	.3053	-.0628	.0370
222	-.0107	-.0037	-.0298	-.0507	.1598	.1742	-.0263	.0120
223	.0001	.0000	.0002	.0003	-.0012	-.0014	.0004	-.0003
224	-.0786	.0019	-.0068	.1072	-.1402	.3158	-.0538	.0039
225	.0217	-.0001	.0074	.0174	-.1119	-.1168	.0503	-.0359

*Elastic modes start at "mode 3."

REPRODUCIBILITY OF THE
ORIGINAL PAGE IS POOR

TABLE 11-6 AIRPLANE VIBRATION MODE SHAPES , FINAL STIFFNESS DESIGN

SYMMETRIC , LOW GROSS WEIGHT

ROW	MODE 17	MODE 18	MODE 19	MODE 20
1	-.0615	.1013	.0078	-.0001
2	-.0083	.0044	.0005	-.0017
3	-.0110	-.0364	-.0032	.0063
4	-.0002	.0002	-.0001	-.0000
5	-.0005	.0003	.0003	.0004
6	.0000	-.0001	.0001	.0001
7	-.1155	.0723	.0217	.0162
8	-.0177	-.0063	.0060	-.0031
9	.0462	.0023	-.0155	.0108
10	-.0002	.0004	.0001	.0002
11	.0002	.0000	.0001	.0003
12	-.0000	-.0002	-.0000	-.0001
13	-.2071	-.0101	.0026	-.0449
14	-.0509	.0450	.0073	.0274
15	.2507	-.0031	-.0531	-.0154
16	-.1210	-.0090	-.1374	-.1892
17	-.1832	.0775	-.1206	-.0727
18	.0427	-.0302	.0053	.0116
19	.0287	-.1599	.0904	-.0165
20	.0342	-.2536	.1474	-.0464
21	.0903	-.2603	.1445	-.0487
22	-.1995	-.0082	.0027	-.0423
23	-.1792	.0154	.0061	-.0219
24	-.1344	.0316	.0077	-.0003
25	-.0457	.0433	.0070	.0269
26	.0427	.0446	.0031	.0441
27	.1646	.0354	-.0078	.0534
28	.2363	.0185	-.0242	.0361
29	.2487	.0030	-.0399	.0062
30	.1838	-.0183	-.0665	-.0594
31	.0465	-.0247	-.0946	-.1257
32	-.1908	-.0062	.0029	-.0393
33	-.1602	.0165	.0060	-.0192
34	-.1254	.0303	.0073	.0003
35	-.0400	.0412	.0067	.0261
36	.0374	.0414	.0035	.0409
37	.1515	.0324	-.0063	.0495
38	.2181	.0171	-.0202	.0358

TABLE 11-6 AIRPLANE VIBRATION MODE SHAPES , FINAL STIFFNESS DESIGN

SYMMETRIC , LOW GROSS WEIGHT

ROW	MODE 17	MODE 18	MODE 19	MODE 20
39	.2383	.0012	-.0352	.0084
40	.1710	-.0200	-.0596	-.0552
41	.0368	-.0258	-.0852	-.1172
42	-.1177	-.0119	-.1167	-.1674
43	-.2417	.0198	-.1438	-.1833
44	-.2703	.0525	-.1464	-.1533
45	-.1783	.0737	-.1104	-.0678
46	-.0792	.0619	-.0715	-.0167
47	.0000	.0218	-.0298	.0071
48	.0370	-.0125	-.0006	.0147
49	.0400	-.0430	.0205	.0113
50	.0335	-.0708	.0391	.0050
51	.0235	-.1008	.0585	-.0034
52	.0133	-.1316	.0785	-.0131
53	.0055	-.1627	.0982	-.0236
54	.0050	-.1929	.1167	-.0337
55	.0143	-.2107	.1265	-.0406
56	.0340	-.2144	.1263	-.0428
57	.0724	-.1961	.1100	-.0377
58	.1193	-.1555	.0785	-.0253
59	-.1318	.0278	.0071	-.0029
60	-.0460	.0383	.0068	.0230
61	.0502	.0354	.0042	.0402
62	.0621	.0375	.0028	.0428
63	.1326	.0220	.0002	.0451
64	.1776	.0244	-.0085	.0473
65	.1744	-.0002	-.0039	.0325
66	.2263	.0005	-.0202	.0251
67	.1017	-.0204	.0037	.0067
68	.1245	-.0229	-.0116	-.0094
69	.1587	-.0232	-.0402	-.0374
70	.0548	-.0371	.0021	-.0211
71	.0447	-.0322	-.0261	-.0519
72	.0426	-.0292	-.0646	-.0952
73	-.0197	-.0316	.0144	-.0161
74	-.0433	-.0451	-.0059	-.0605
75	-.0554	-.0290	-.0361	-.0730
76	-.0945	-.0180	-.0891	-.1370

TABLE 11-6 AIRPLANE VIBRATION MODE SHAPES , FINAL STIFFNESS DESIGN

SYMMETRIC , LOW GROSS WEIGHT

ROW	MODE 17	MODE 18	MODE 19	MODE 20
77	-.0697	-.0296	.0197	-.0176
78	-.0971	-.0261	.0034	-.0357
79	-.1182	-.0189	-.0241	-.0648
80	-.1760	-.0011	-.0803	-.1208
81	-.1110	-.0213	.0229	-.0135
82	-.1347	-.0122	.0049	-.0247
83	-.1460	-.0089	-.0144	-.0457
84	-.1901	.0154	-.0665	-.0886
85	-.2571	.0426	-.1284	-.1415
86	-.1580	.0016	-.0034	-.0202
87	-.1801	.0350	-.0454	-.0380
88	-.1957	.0631	-.0885	-.0626
89	-.1379	-.0102	.0340	.0081
90	-.1487	-.0016	.0229	.0129
91	-.1425	.0076	.0123	.0135
92	-.1122	.007	-.0204	.0119
93	-.0449	.005	-.0418	.0217
94	-.0260	.003	-.0456	.0124
95	-.0045	.001	-.0342	.0212
96	.0210	.021	-.0126	.0211
97	.0255	-.0141	.0109	.0150
98	.0190	-.0556	.0350	.0056
99	-.0176	-.0894	.0609	-.0111
100	-.0294	-.0995	.0693	-.0241
101	.0178	-.1228	.0759	-.0275
102	.0779	-.1222	.0660	-.0227
103	-.0949	-.0042	.0374	.0288
104	-.1035	-.0051	.0376	.0461
105	-.0860	-.0014	.0288	.0444
106	-.0218	.0471	.0067	.0368
107	.0352	.0716	-.0157	.0295
108	.0350	.0664	-.0153	.0306
109	.0005	.0411	-.0057	.0227
110	-.0470	-.0282	.0313	-.0035
111	-.0484	-.0628	.0509	-.0142
112	-.0473	.0101	.0318	.0469
113	-.0570	-.0025	.0405	.0607
114	-.0602	-.0183	.0520	.0997

TABLE 11-6 AIRPLANE VIBRATION MODE SHAPES , FINAL STIFFNESS DESIGN

SYMMETRIC , LOW GROSS WEIGHT

PCW	MODE 17	MODE 18	MODE 19	MODE 20
115	-.0397	-.0126	.0345	.0518
116	.0545	.0365	.0607	.0073
117	.1135	.0566	.0429	-.0064
118	.0757	.0511	.0002	.0223
119	-.0027	.0726	-.0238	.0310
120	-.0788	.0804	-.0210	.0183
121	-.1063	.0503	-.0053	.0015
122	-.1169	.0482	-.0018	-.0033
123	-.1048	.0338	.0048	-.0070
124	-.0604	.0244	.0033	-.0077
125	.0185	.0322	-.0145	.0019
126	.0607	.0453	-.0312	.0112
127	.1368	.0624	-.0532	.0233
128	.1956	.0681	-.0665	.0312
129	-.0703	.0058	.1440	.4227
130	-.0871	-.0239	.1909	.5664
131	-.0881	.0046	.2482	.7797
132	-.1102	-.0308	.3180	1.0000
133	.0089	-.0420	.0044	.0158
134	.3247	.1133	.3189	-.2386
135	.5398	.1964	.5124	-.4604
136	.7607	.2602	.7761	-.6949
137	1.0000	.3544	1.0000	-.9521
138	.0546	-.0008	-.0125	.0094
139	-.1378	.1621	-.0512	.0299
140	-.1901	.1363	-.0378	.0071
141	-.1526	.1116	-.0312	-.0008
142	-.1026	.1323	-.0510	.0062
143	-.0015	.1784	-.0961	.0286
144	.1736	.3125	-.2110	.0892
145	.4101	.5792	-.4217	.1999
146	.5520	.7142	-.5321	.2583
147	.0323	-.0704	-.0534	-.0516
148	-.0001	-.1119	-.0422	-.0185
149	-.3547	.2753	-.0830	.0109
150	-.1557	.1622	-.0590	.0058
151	-.0128	.2474	-.1343	.0409
152	.3651	.6271	-.4407	.2016

TABLE 11-6 AIRPLANE VIBRATION MODE SHAPES , FINAL STIFFNESS DESIGN

SYMMETRIC , LOW GROSS WEIGHT

ROW	MODE 17	MODE 18	MODE 19	MODE 20
153	.7075	1.0000	-.7378	.3586
154	.0413	-.0259	.0046	.0126
155	.0454	-.0538	.0238	.0097
156	.0408	-.0848	.0442	.0032
157	.0323	-.1169	.0650	-.0055
158	.0233	-.1500	.0863	-.0153
159	.0166	-.1838	.1077	-.0261
160	.0167	-.2169	.1280	-.0368
161	.0272	-.2387	.1401	-.0444
162	.0463	-.2495	.1445	-.0482
163	.0841	-.2381	.1326	-.0449
164	-.0000	-.0093	.0011	-.0047
165	-.0206	.0207	-.0155	-.0034
166	-.0678	.0795	-.0478	.0019
167	-.0505	.0929	-.0492	.0115
168	-.0018	.0829	-.0340	.0250
169	.0780	.0541	-.0041	.0436
170	.0029	-.0201	.0052	-.0066
171	-.0157	.0037	-.0082	-.0069
172	-.0616	.0639	-.0407	-.0011
173	-.0188	-.0213	.0013	-.0136
174	-.0489	.0319	-.0262	-.0071
175	-.0456	.0617	-.0363	.0028
176	.0017	.0637	-.0260	.0196
177	-.0452	-.0211	-.0046	-.0222
178	-.0344	-.0071	-.0077	-.0164
179	.0109	.0046	-.0015	.0025
180	.0681	.0092	.0106	.0247
181	.1338	.0155	.0241	.0512
182	-.0023	-.1202	.0424	-.0451
183	.0198	-.0915	.0368	-.0279
184	.0776	-.0415	.0319	.0105
185	.1030	-.0171	.0289	.0284
186	.0215	-.1530	.0603	-.0487
187	.0848	-.1106	.0597	-.0112
188	.1562	-.0547	.0562	.0353
189	.2010	-.0246	.0560	.0633
190	-.0931	-.0035	-.0268	-.0243

TABLE 11-6 AIRPLANE VIBRATION MODE SHAPES , FINAL STIFFNESS DESIGN

SYMMETRIC , LOW GROSS WEIGHT

ROW	MODE 17	MODE 18	MODE 19	MODE 20
191	.0793	-.0143	.0171	.0142
192	.0011	-.0006	.0002	.0001
193	-.3581	.0070	.0073	-.0729
194	-.0432	-.0037	-.0001	-.0043
195	.1333	-.0109	-.0043	.0309
196	.2010	-.0167	-.0062	.0395
197	.1364	-.0294	-.0067	.0132
198	.0395	-.0469	-.0077	-.0182
199	-.0570	-.0509	-.0065	-.0411
200	-.1395	-.0396	-.0032	-.0516
201	-.1833	-.0185	.0008	-.0462
202	-.1776	.0060	.0045	-.0281
203	-.1271	.0253	.0066	-.0037
204	-.0468	.0345	.0066	.0201
205	.0393	.0318	.0052	.0361
206	.1051	.0187	.0034	.0394
207	.1275	-.0007	.0032	.0291
208	.0965	-.0182	.0065	.0117
209	.0421	-.0280	.0122	-.0018
210	-.0175	-.0321	.0182	-.0109
211	-.0659	-.0301	.0230	-.0137
212	-.0936	-.0228	.0274	-.0083
213	-.0938	-.0111	.0285	.0014
214	-.0647	.0033	.0236	.0082
215	-.0208	.0252	.0103	.0050
216	.0560	.0582	-.0190	-.0166
217	.0648	.0519	-.0263	-.0215
218	-.0289	-.0039	.0055	.0012
219	-.1767	-.0930	.0582	.0399
220	.0011	.0007	-.0004	-.0003
221	-.1111	-.0525	.0352	.0231
222	-.0270	-.0027	.0046	.0003
223	.0007	.0004	-.0003	-.0002
224	.1816	-.0237	-.0067	.0277
225	.0383	.0689	-.0322	-.0253

TABLE 11-6 AIRPLANE VIBRATION MODE SHAPES*, FINAL STIFFNESS DESIGN

ANTISYMMETRIC CASES HIGH GROSS WEIGHT

ROW	MODE 1	MODE 2	MODE 3	MODE 4	MODE 5	MODE 6	MODE 7	MODE 8
1	.0000	.1251	.0279	.0982	.0116	-.0620	.0463	.0596
2	1.0000	-.3044	-.0153	-.2288	-.0047	.0608	-.2267	-.0836
3	.0000	-.0979	.3203	-.0054	.0222	-.2261	-.1840	.1222
4	.0000	-.0004	.0013	-.0002	.0001	.0001	-.0015	-.0008
5	.0000	.0000	-.0000	-.0000	-.0003	.0010	.0007	-.0012
6	.0000	-.0005	-.0001	-.0004	-.0000	.0002	-.0003	-.0002
7	.0000	.2140	.0478	.1663	.0343	-.0532	.1319	.0928
8	1.0000	-.3058	-.0393	-.2351	.0094	.1225	-.1675	-.1339
9	.0000	-.1674	.5478	-.0179	.1488	-.1422	-.1216	.1201
10	.0000	-.0004	.0013	-.0002	.0004	.0014	-.0004	-.0021
11	.0000	.0000	.0000	.0000	-.0010	.0006	-.0001	-.0019
12	.0000	-.0005	-.0001	-.0004	.0000	.0002	-.0003	-.0002
13	.0000	-.0645	.2111	.0048	-.1182	.0841	.0907	.1870
14	.0000	-.0943	.3087	-.0002	-.1761	.1131	.1803	.2434
15	.0000	-.1338	.4378	-.0164	-.2343	.1087	.2076	.1289
16	.0000	-.1682	.5505	-.0149	-.2287	.0389	.1004	-.0917
17	.0000	-.2101	.6874	-.0147	-.0919	-.0379	-.0836	-.2381
18	.0000	-.2365	.7739	-.0267	.0804	.0205	-.0620	-.2312
19	.0000	-.2672	.8742	-.0401	.3055	.2208	.1352	-.2219
20	.0000	-.2901	.9494	-.0506	.5019	.4367	.3604	-.2414
21	.0000	-.3056	1.0000	-.0580	.6443	.6088	.5424	-.2578
22	.0000	-.0485	.1587	.0041	-.0886	.0629	.0672	.1393
23	.0000	-.0602	.1970	.0028	-.1103	.0740	.0990	.1667
24	.0000	-.0693	.2269	.0015	-.1281	.0836	.1255	.1861
25	.0000	-.0810	.2652	-.0001	-.1510	.0966	.1550	.2081
26	.0000	-.0897	.2934	-.0019	-.1672	.1033	.1733	.2097
27	.0000	-.1014	.3317	-.0052	-.1873	.1082	.1902	.1963
28	.0000	-.1105	.3617	-.0096	-.2006	.1063	.1946	.1660
29	.0000	-.1191	.3897	-.0133	-.2109	.1024	.1929	.1350
30	.0000	-.1320	.4318	-.0174	-.2215	.0890	.1772	.0704
31	.0000	-.1446	.4732	-.0176	-.2230	.0660	.1436	-.0074
32	.0000	-.0318	.1041	.0033	-.0577	.0408	.0429	.0897
33	.0000	-.0444	.1452	.0023	-.0809	.0535	.0739	.1206
34	.0000	-.0542	.1773	.0015	-.0996	.0645	.0976	.1443
35	.0000	-.0667	.2184	.0001	-.1240	.0788	.1277	.1702
36	.0000	-.0760	.2486	-.0014	-.1412	.0869	.1459	.1773
37	.0000	-.0885	.2897	-.0044	-.1629	.0934	.1645	.1690
38	.0000	-.0991	.3242	-.0082	-.1791	.0945	.1730	.1477

*Elastic modes start at "mode 4."

TABLE 11-6 AIRPLANE VIBRATION MODE SHAPES* , FINAL STIFFNESS DESIGN

ANTISYMMETRIC , HIGH GROSS WEIGHT

ROW	MODE 1	MODE 2	MODE 3	MODE 4	MODE 5	MODE 6	MODE 7	MODE 8
39	.0000	-.1083	.3545	-.0119	-.1912	.0922	.1741	.1205
40	.0000	-.1222	.3998	-.0160	-.2044	.0812	.1623	.0617
41	.0000	-.1361	.4452	-.0160	-.2084	.0601	.1318	-.0118
42	.0000	-.1532	.5011	-.0122	-.2042	.0314	.0849	-.0873
43	.0000	-.1702	.5571	-.0087	-.1839	-.0002	.0235	-.1539
44	.0000	-.1840	.6022	-.0090	-.1506	-.0244	-.0280	-.1912
45	.0000	-.2013	.6587	-.0139	-.0837	-.0419	-.0828	-.2172
46	.0000	-.2104	.6885	-.0177	-.0362	-.0403	-.0988	-.2198
47	.0000	-.2203	.7210	-.0220	.0256	-.0231	-.0917	-.2114
48	.0000	-.2270	.7427	-.0252	.0747	.0020	-.0721	-.2040
49	.0000	-.2362	.7730	-.0290	.1356	.0472	-.0302	-.1993
50	.0000	-.2443	.7992	-.0325	.1925	.0945	.0157	-.1959
51	.0000	-.2520	.8245	-.0359	.2506	.1475	.0683	-.1944
52	.0000	-.2595	.8491	-.0393	.3096	.2043	.1257	-.1941
53	.0000	-.2672	.8744	-.0428	.3728	.2695	.1926	-.1959
54	.0000	-.2747	.8990	-.0463	.4372	.3401	.2662	-.2000
55	.0000	-.2825	.9242	-.0499	.5056	.4188	.3490	-.2059
56	.0000	-.2897	.9479	-.0533	.5715	.4972	.4319	-.2127
57	.0000	-.2979	.9749	-.0573	.6485	.5919	.5325	-.2219
58	.0000	-.3056	1.0000	-.0610	.7211	.6826	.6289	-.2308
59	.0000	-.0444	.1452	.0016	-.0812	.0524	.0788	.1178
60	.0000	-.0444	.1452	.0007	-.0819	.0519	.0847	.1144
61	.0000	-.0444	.1452	-.0002	-.0815	.0493	.0840	.1011
62	.0000	-.0621	.2032	-.0012	-.1150	.0697	.1190	.1401
63	.0000	-.0444	.1452	-.0015	-.0796	.0436	.0773	.0776
64	.0000	-.0787	.2576	-.0046	-.1434	.0791	.1421	.1346
65	.0000	-.0444	.1452	-.0036	-.0772	.0374	.0695	.0538
66	.0000	-.0787	.2576	-.0078	-.1390	.0678	.1278	.0925
67	.0000	-.0328	.1073	-.0045	-.0526	.0195	.0390	.0176
68	.0000	-.0617	.2020	-.0082	-.1017	.0391	.0792	.0315
69	.0000	-.0972	.3182	-.0127	-.1632	.0654	.1311	.0508
70	.0000	-.0444	.1452	-.0245	-.0733	.0105	.1189	.0163
71	.0000	-.0787	.2576	-.0064	-.1214	.0353	.0767	-.0050
72	.0000	-.1176	.3847	-.0139	-.1818	.0538	.1174	-.0084
73	.0000	-.0328	.1073	-.0021	-.0423	.0060	.0160	-.0090
74	.0000	-.0617	.2020	.0021	-.0846	.0137	.0284	-.0433
75	.0000	-.0972	.3182	-.0044	-.1315	.0208	.0546	-.0501
76	.0000	-.1361	.4452	-.0100	-.1827	.0285	.0771	-.0751

*Elastic modes start at "mode 4."

TABLE 11-6 AIRPLANE VIBRATION MODE SHAPES*, FINAL STIFFNESS DESIGN

ANTISYMMETRIC, HIGH GROSS WEIGHT

ROW	MODE 1	MODE 2	MODE 3	MODE 4	MODE 5	MODE 6	MODE 7	MODE 8
77	.0000	-.0328	.1073	.0022	-.0366	-.0007	.0035	-.0180
78	.0000	-.0637	.2083	.0023	-.0719	-.0009	.0085	-.0416
79	.0000	-.0972	.3182	.0006	-.1096	-.0016	.0146	-.0717
80	.0000	-.1361	.4452	-.0040	-.1504	-.0016	.0206	-.1134
81	.0000	-.0444	.1452	.0008	-.0403	-.0119	-.0105	-.0321
82	.0000	-.0787	.2576	.0004	-.0695	-.0210	-.0185	-.0611
83	.0000	-.0972	.3182	.0005	-.0926	-.0181	-.0172	-.0795
84	.0000	-.1361	.4452	-.0032	-.1222	-.0236	-.0184	-.1250
85	.0000	-.1717	.5619	-.0075	-.1442	-.0246	-.0247	-.1725
86	.0000	-.0972	.3182	-.0015	-.0741	-.0358	-.0367	-.0776
87	.0000	-.1361	.4452	-.0053	-.0873	-.0490	-.0572	-.1194
88	.0000	-.1717	.5619	-.0098	-.0883	-.0495	-.0717	-.1666
89	.0000	-.0444	.1452	-.0015	-.0300	-.0254	-.0272	-.0313
90	.0000	-.0787	.2576	-.0027	-.0493	-.0446	-.0471	-.0547
91	.0000	-.0972	.3182	-.0038	-.0558	-.0555	-.0592	-.0664
92	.0000	-.1361	.4452	-.0079	-.0510	-.0761	-.0898	-.0934
93	.0000	-.1717	.5619	-.0136	-.0324	-.0737	-.1111	-.1393
94	.0000	-.1981	.6483	-.0181	-.0043	-.0510	-.1057	-.1744
95	.0000	-.1901	.6221	-.0181	.0161	-.0594	-.1085	-.1393
96	.0000	-.2104	.6885	-.0236	.0866	-.0179	-.0769	-.1444
97	.0000	-.2261	.7399	-.0284	.1523	.0364	-.0301	-.1534
98	.0000	-.2394	.7834	-.0328	.2153	.0984	.0246	-.1655
99	.0000	-.2520	.8245	-.0399	.3491	.2147	.1482	-.1437
100	.0000	-.2672	.8744	-.0482	.5109	.3814	.3256	-.1353
101	.0000	-.2825	.9242	-.0537	.6049	.5078	.4541	-.1673
102	.0000	-.2952	.9659	-.0584	.6859	.6202	.5693	-.1941
103	.0000	-.0444	.1452	-.0025	-.0211	-.0405	-.0450	-.0214
104	.0000	-.0787	.2576	-.0044	-.0282	-.0770	-.0755	-.0246
105	.0000	-.0972	.3182	-.0057	-.0261	-.0929	-.0930	-.0255
106	.0000	-.1361	.4452	-.0104	.0008	-.1143	-.1215	-.0299
107	.0000	-.1741	.5696	-.0178	.0533	-.0844	-.1198	-.0618
108	.0000	-.1901	.6221	-.0223	.1125	-.0517	-.0934	-.0563
109	.0000	-.2104	.6885	-.0286	.2029	.0243	-.0237	-.0604
110	.0000	-.2394	.7834	-.0385	.3519	.1849	.1298	-.0891
111	.0000	-.2520	.8245	-.0428	.4215	.2678	.2115	-.1079
112	.0000	-.0270	.0884	-.0019	-.0120	-.0268	-.0315	-.0114
113	.0000	-.0492	.1610	-.0028	-.0159	-.0601	-.0608	-.0061
114	.0000	-.0762	.2494	-.0041	-.0112	-.1109	-.0994	-.0159

*Elastic modes start at "mode 4."

TABLE 11-6 AIRPLANE VIBRATION MODE SHAPES* , FINAL STIFFNESS DESIGN

ANTISYMMETRIC , HIGH GROSS WEIGHT

ROW	MODE 1	MODE 2	MODE 3	MODE 4	MODE 5	MODE 6	MODE 7	MODE 8
115	.0000	-.0972	.3182	-.0062	-.0015	-.1395	-.1276	.0276
116	.0000	-.1259	.4119	-.0102	.0311	-.1552	-.1478	.0404
117	.0000	-.1517	.4965	-.0143	.0781	-.1488	-.1421	.0559
118	.0000	-.1669	.5461	-.0184	.1124	-.1150	-.1278	.0393
119	.0000	-.1895	.6200	-.0264	.2160	-.0341	-.0627	.0422
120	.0000	-.2080	.6806	-.0331	.3128	.0711	.0359	.0260
121	.0000	-.2236	.7317	-.0385	.3968	.1674	.1303	.0076
122	.0000	-.2308	.7553	-.0414	.4472	.2248	.1885	.0013
123	.0000	-.2432	.7957	-.0453	.5092	.3099	.2733	-.0259
124	.0000	-.2598	.8500	-.0507	.5950	.4335	.3972	-.0659
125	.0000	-.2763	.9042	-.0561	.6856	.5660	.5308	-.1092
126	.0000	-.2846	.9313	-.0589	.7313	.6347	.6003	-.1317
127	.0000	-.2952	.9659	-.0624	.7897	.7225	.6893	-.1606
128	.0000	-.3056	1.0000	-.0658	.8467	.8077	.7754	-.1887
129	.0000	-.0369	.1206	-.0030	-.0064	-.0572	-.0549	.0085
130	.0000	-.0664	.2172	-.0042	-.0009	-.1197	-.1062	.0364
131	.0000	-.0367	.1206	-.0036	-.0009	-.0708	-.0650	.0230
132	.0000	-.0664	.2172	-.0047	.0072	-.1394	-.1216	.0568
133	.0000	-.0951	.3113	-.0054	.0317	-.2421	-.1950	.1431
134	.0000	-.1243	.4066	-.0108	.0692	-.1962	-.1735	.1108
135	.0000	-.1405	.4596	-.0133	.0993	-.1947	-.1709	.1265
136	.0000	-.1243	.4066	-.0116	.1029	-.2320	-.1907	.1732
137	.0000	-.1405	.4596	-.0140	.1315	-.2290	-.1932	.1865
138	.0000	-.1713	.5604	-.0202	.1854	-.1357	-.1180	.1437
139	.0000	-.1936	.6336	-.0322	.3396	.0460	.0278	.1061
140	.0000	-.2125	.6954	-.0385	.4234	.1504	.1232	.0761
141	.0000	-.2325	.7608	-.0455	.5423	.3045	.2802	.0388
142	.0000	-.2493	.8156	-.0508	.6311	.4349	.4121	-.0036
143	.0000	-.2660	.8705	-.0563	.7224	.5734	.5528	-.0495
144	.0000	-.2828	.9253	-.0619	.8166	.7211	.7038	-.0982
145	.0000	-.2952	.9659	-.0661	.8910	.8441	.8314	-.1376
146	.0000	-.3056	1.0000	-.0696	.9509	.9397	.9295	-.1688
147	.0000	-.0967	.3164	-.0042	.0551	-.3430	-.2588	.2518
148	.0000	-.1710	.5594	-.0188	.2626	-.1962	-.1092	.3204
149	.0000	-.2088	.6833	-.0398	.4653	.1668	.1460	.1207
150	.0000	-.2359	.7720	-.0482	.6020	.3668	.3493	.0479
151	.0000	-.2611	.8544	-.0564	.7396	.5764	.5627	-.0208
152	.0000	-.2863	.9367	-.0648	.8859	.8132	.8068	-.0978

*Elastic modes start at "mode 4."

TABLE 11-6 AIRPLANE VIBRATION MODE SHAPES* , FINAL STIFFNESS DESIGN

ANTISYMMETRIC , HIGH GROSS WEIGHT

ROW	MODE 1	MODE 2	MODE 3	MODE 4	MODE 5	MODE 6	MODE 7	MODE 8
153	.0000	-.3056	1.0000	-.0714	1.0000	1.0000	1.0000	-.1583
154	.0000	-.2338	.7650	-.0264	.0824	.0168	-.0630	-.2213
155	.0000	-.2412	.7893	-.0296	.1320	.0549	-.0278	-.2188
156	.0000	-.2492	.8155	-.0330	.1892	.1035	.0194	-.2165
157	.0000	-.2570	.8408	-.0364	.2478	.1575	.0734	-.2156
158	.0000	-.2645	.8654	-.0398	.3069	.2150	.1319	-.2160
159	.0000	-.2722	.8906	-.0433	.3702	.2806	.1994	-.2183
160	.0000	-.2797	.9153	-.0468	.4348	.3515	.2735	-.2227
161	.0000	-.2874	.9405	-.0504	.5032	.4304	.3564	-.2289
162	.0000	-.2947	.9642	-.0538	.5689	.5083	.4387	-.2359
163	.0000	-.3029	.9912	-.0578	.6458	.6029	.5389	-.2452
164	1.0000	-.2309	-.0836	-.1810	-.0126	.0300	-.1107	-.0178
165	1.0000	-.2629	-.1381	-.2137	-.0268	.0115	-.1592	.0117
166	1.0000	-.3048	-.2095	-.2577	-.0544	-.0370	-.2592	.0672
167	1.0000	-.3345	-.2602	-.2937	-.0750	-.0707	-.3921	.1281
168	1.0000	-.3584	-.3009	-.3240	-.0922	-.0984	-.5222	.1852
169	1.0000	-.3828	-.3424	-.3562	-.1105	-.1279	-.6733	.2499
170	1.0000	-.2368	-.0663	-.1824	-.0070	.0420	-.1097	-.0320
171	1.0000	-.2685	-.1216	-.2150	-.0199	.0266	-.1471	-.0044
172	1.0000	-.3108	-.1953	-.2599	-.0464	-.0181	-.2447	.0515
173	1.0000	-.3011	-.1007	-.2358	-.0055	.0650	-.1371	-.0337
174	1.0000	-.3233	-.1662	-.2643	-.0299	.0202	-.2150	.0195
175	1.0000	-.3478	-.2390	-.2996	-.0611	-.0370	-.3616	.0995
176	1.0000	-.3650	.2898	-.3269	-.0850	-.0810	-.5067	.1704
177	1.0000	-.3672	-.1324	-.2903	-.0011	.0940	-.1600	-.0377
178	1.0000	-.3760	-.1943	-.3121	-.0317	.0342	-.2970	.0390
179	1.0000	-.3849	-.2567	-.3356	-.0635	-.0287	-.4595	.1258
180	1.0000	-.3916	-.3030	-.3537	-.0876	-.0766	-.5924	.1952
181	1.0000	-.3979	-.3499	-.3719	-.1122	-.1260	-.7301	.2671
182	1.0000	-.4234	-.1588	-.3432	-.0033	.1108	-.2799	-.0101
183	1.0000	-.4175	-.2026	-.3496	-.0281	.0572	-.3788	.0514
184	1.0000	-.4077	-.2761	-.3608	-.0701	-.0341	-.5550	.1592
185	1.0000	-.4034	-.3089	-.3658	-.0888	-.0748	-.6330	.2071
186	1.0000	-.4394	-.1663	-.3588	-.0043	.1149	-.3222	.0007
187	1.0000	-.4296	-.2398	-.3703	-.0464	.0237	-.5015	.1093
188	1.0000	-.4193	-.3163	-.3822	-.0905	-.0726	-.6876	.2240
189	1.0000	-.4139	-.3579	-.3885	-.1141	-.1243	-.7914	.2860
190	.0000	-.2227	.7287	-.0356	.5133	.2555	.4389	.1281

*Elastic modes start at "mode 4."

TABLE 11-6 AIRPLANE VIBRATION MODE SHAPES* , FINAL STIFFNESS DESIGN

ANTISYMMETRIC , HIGH GROSS WEIGHT

ROW	MODE 1	MODE 2	MODE 3	MODE 4	MODE 5	MODE 6	MODE 7	MODE 8
191	.0000	.2847	.0636	.2326	-.0495	-.0450	.4364	.0610
192	.0000	.0000	.0000	.0001	-.0014	-.0009	-.0011	-.0008
193	1.0000	.0046	.0144	.0055	-.0055	-.0096	.0070	-.0073
194	.0000	.1006	.0225	.0777	.0002	-.0119	.0590	-.0019
195	.0000	-.0005	-.0001	.0019	.0000	-.0000	.0000	-.0000
196	.0000	-.0004	.0013	.0000	-.0007	.0005	.0004	.0014
197	.0000	-.0004	.0013	.0000	-.0007	.0005	.0004	.0014
198	.0000	-.0004	.0013	.0000	-.0007	.0005	.0004	.0014
199	.0000	-.0004	.0013	.0000	-.0007	.0005	.0005	.0013
200	.0000	-.0004	.0013	.0000	-.0007	.0005	.0005	.0013
201	1.0000	1.0000	.2420	1.0000	-.0364	.4236	-.8454	1.0000
202	1.0000	.9160	.2139	.8840	-.0233	.2887	-.5579	.6403
203	1.0000	.8454	.1905	.7888	-.0128	.1836	-.3352	.3664
204	1.0000	.7769	.1678	.7001	-.0029	.0938	-.1476	.1420
205	1.0000	.6591	.1295	.5603	.0127	-.0225	.0890	-.1192
206	.0000	-.0004	.0013	.0000	-.0007	.0005	.0005	.0013
207	.0000	-.0004	.0013	-.0000	-.0007	.0005	.0006	.0012
208	.0000	-.0004	.0013	-.0000	-.0007	.0005	.0006	.0012
209	.0000	-.0004	.0013	-.0000	-.0007	.0005	.0006	.0012
210	.0000	-.0004	.0013	-.0000	-.0007	.0005	.0005	.0012
211	.0000	-.0004	.0013	.0000	-.0007	.0005	.0004	.0011
212	.0000	-.0004	.0013	.0000	-.0007	.0004	.0004	.0010
213	.0000	-.0004	.0013	.0000	-.0006	.0004	.0004	.0008
214	.0000	-.0004	.0013	.0001	-.0006	.0003	.0004	.0007
215	.0000	-.0004	.0013	.0001	-.0006	.0003	.0003	.0005
216	.0000	-.0004	.0013	.0002	-.0005	.0002	.0003	.0003
217	.0000	-.0004	.0013	.0002	-.0005	.0001	.0002	.0002
218	.0000	-.0004	.0013	.0000	-.0005	.0000	.0002	.0000
219	.0000	-.0004	.0013	-.0002	-.0004	.0000	.0001	-.0001
220	.0000	-.0004	.0013	-.0002	-.0004	-.0000	-.0000	-.0002
221	.0000	-.0004	.0013	-.0001	-.0004	-.0001	-.0002	-.0003
222	.0000	-.0004	.0013	-.0001	-.0004	-.0000	-.0004	-.0005
223	.0000	-.0004	.0013	-.0000	-.0003	-.0001	-.0005	-.0007
224	1.0000	.6180	.1196	.5172	.0159	-.0472	.1398	-.1612
225	1.0000	.5662	.1080	.4656	.0191	-.0694	.1839	-.1862
226	1.0000	.5144	.0965	.4151	.0216	-.0846	.2113	-.1937
227	1.0000	.4626	.0849	.3660	.0231	-.0919	.2207	-.1849
228	1.0000	.4108	.0733	.3194	.0231	-.0905	.2109	-.1642

*Elastic modes start at "mode 4."

TABLE 11-6 AIRPLANE VIBRATION MODE SHAPES* , FINAL STIFFNESS DESIGN

ANTISYMMETRIC , HIGH GROSS WEIGHT

ROW	MODE 1	MODE 2	MODE 3	MODE 4	MODE 5	MODE 6	MODE 7	MODE 8
229	1.0000	.3590	.0618	.2746	.0220	-.0832	.1891	-.1376
230	1.0000	.3072	.0502	.2307	.0200	-.0726	.1615	-.1104
231	1.0000	.2554	.0386	.1873	.0173	-.0605	.1317	-.0857
232	1.0000	.2036	.0271	.1437	.0142	-.0481	.1015	-.0651
233	1.0000	.1518	.0155	.1000	.0109	-.0350	.0720	-.0480
234	1.0000	.1000	.0039	.0559	.0078	-.0246	.0429	-.0364
235	1.0000	.0483	-.0076	.0104	.0052	-.0146	.0156	-.0269
236	1.0000	-.0035	-.0192	-.0190	.0034	-.0070	-.0060	-.0205
237	1.0000	-.0600	-.0156	-.0295	-.0030	-.0008	.0263	-.0172
238	1.0000	-.1141	-.0196	-.0752	-.0047	.0042	-.0540	-.0154
239	1.0000	-.1651	-.0337	-.1182	-.0019	.0080	-.0808	-.0118
240	1.0000	-.2161	-.0478	-.1615	-.0004	.0112	-.1015	-.0070
241	1.0000	-.2609	-.0821	-.2083	.0044	.0113	-.0900	.0057
242	.0000	-.0004	.0013	-.0000	-.0003	-.0001	-.0006	-.0000
243	.0000	-.0004	.0013	-.0000	-.0003	-.0001	-.0007	-.0012
244	.0000	-.0004	.0013	-.0000	-.0003	-.0001	-.0007	-.0012
245	.0000	-.0004	.0013	-.0000	-.0003	-.0001	-.0007	-.0012
246	1.0000	-.3111	-.1254	-.2680	.0100	.0053	-.0408	.0383
247	1.0000	-.4389	-.2001	-.4325	.0163	-.0336	.2086	.2207
248	1.0000	-.5044	-.2383	-.5236	.0202	-.0702	.3077	.3851
249	1.0000	-.5756	-.2805	-.6250	.0249	-.1079	.6259	.5900
250	.0000	-.0004	.0013	-.0000	-.0003	-.0001	-.0007	-.0013
251	.0000	-.0005	-.0001	-.0006	-.0000	-.0003	.0014	.0011
252	.0000	.0360	.0080	.0467	.0009	.0183	-.0976	-.0823
253	1.0000	-.5360	-.2487	-.5658	.0203	-.0865	.4881	.4628
254	.0000	-.0282	.0922	-.0031	-.0247	-.0043	-.0518	-.0011
255	.0000	-.0004	.0013	-.0000	-.0003	-.0001	-.0007	-.0012
256	.0000	-.0005	-.0001	-.0006	-.0000	-.0002	.0012	.0010
257	1.0000	-.4680	-.3636	-.5216	.0535	-.0584	.6900	.5065
258	1.0000	.7079	.1448	.6158	.0068	.0189	.0057	-.0324
259	1.0000	-.3768	-.1633	-.3496	.0129	-.0131	.0647	.1072
260	.0000	-.0004	.0013	-.0001	-.0003	-.0001	-.0006	-.0011

*Elastic modes start at "mode 4."

TABLE 11-6 AIRPLANE VIBRATION MODE SHAPES , FINAL STIFFNESS DESIGN

ANTISYMMETRIC , HIGH GROSS WEIGHT

ROW	MODE 9	MODE 10	MODE 11	MODE 12	MODE 13	MODE 14	MODE 15	MODE 16
1	-.0049	-.0949	.1178	.0013	.0039	.0021	-.0636	-.0224
2	.0228	.0003	-.0626	-.0287	.1551	.1119	-.1197	.0085
3	.0085	-.2491	.2587	-.0069	.0620	.0245	-.0586	.0141
4	.0002	.0022	-.0018	-.0005	.0025	.0025	-.0023	.0001
5	-.0000	.0017	-.0026	.0000	-.0003	-.0000	.0012	.0005
6	.0000	.0004	-.0003	-.0000	.0001	.0001	-.0001	.0001
7	-.0133	.1349	.0131	.0006	.0076	-.0326	-.0437	.0319
8	.0145	-.1052	.0680	.0131	-.1614	.0369	-.2266	.0789
9	-.0099	.2393	-.1012	.0023	-.0882	-.0038	-.0355	-.0178
10	.0001	-.0024	-.0005	.0002	-.0029	.0015	.0038	.0011
11	.0001	-.0030	-.0009	-.0000	.0001	.0009	.0013	-.0007
12	.0000	-.0001	.0001	.0000	-.0002	.0000	-.0005	.0002
13	-.0067	.0795	.2255	-.0128	-.0627	.0956	.1933	.1469
14	-.0127	.1146	.3481	-.0180	-.0900	.1473	.2290	.1458
15	-.0114	.0828	.2074	-.0014	.0093	-.0044	-.1548	-.2026
16	-.0023	-.0389	-.1652	.0140	.0652	-.1035	-.1494	.0189
17	-.0022	-.1660	-.4519	.0006	-.0567	.0714	.2371	-.1538
18	-.0271	-.1880	-.4287	-.0095	-.1395	.1424	.2609	-.4545
19	-.0761	-.2464	-.2414	-.0114	-.0674	.1042	.2294	-.4682
20	-.1385	-.3500	-.0238	-.0178	.0784	.0326	.2427	-.3713
21	-.1941	-.4468	.1598	-.0231	.2234	-.0349	.2717	-.2330
22	-.0050	.0527	.1684	-.0096	-.0469	.0717	.1447	.1116
23	-.0071	.0679	.2135	-.0120	-.0592	.0937	.1757	.1335
24	-.0089	.0818	.2528	-.0137	-.0685	.1111	.1915	.1387
25	-.0104	.0981	.2980	-.0155	-.0772	.1270	.1969	.1266
26	-.0111	.1052	.3129	-.0149	-.0736	.1217	.1573	.0685
27	-.0125	.1062	.3049	-.0120	-.0574	.0944	.0676	-.0361
28	-.0119	.0964	.2642	-.0075	-.0325	.0519	-.0354	-.1299
29	-.0110	.0835	.2168	-.0033	-.0105	.0142	-.1103	-.1754
30	-.0087	.0533	.1142	.0038	.0254	-.0455	-.2002	-.1807
31	-.0055	.0116	-.0165	.0100	.0533	-.0893	-.2159	-.0962
32	-.0032	.0341	.1091	-.0062	-.0304	.0469	.0930	.0746
33	-.0053	.0498	.1562	-.0087	-.0433	.0692	.1282	.0989
34	-.0070	.0632	.1956	-.0107	-.0533	.0946	.1505	.1111
35	-.0090	.0803	.2440	-.0127	-.0634	.1045	.1624	.1059
36	-.0101	.0884	.2634	-.0126	-.0624	.1037	.1359	.0626
37	-.0108	.0913	.2619	-.0103	-.0489	.0805	.0572	-.0311
38	-.0106	.0855	.2346	-.0067	-.0291	.0465	-.0294	-.1129

TABLE 11-6 AIRPLANE VIBRATION MODE SHAPES , FINAL STIFFNESS DESIGN

ANTISYMMETRIC , HIGH GROSS WEIGHT

ROW	MODE 9	MODE 10	MODE 11	MODE 12	MODE 13	MODE 14	MODE 15	MODE 16
39	-.0099	.0748	.1939	-.0028	-.0085	.0114	-.1030	-.1630
40	-.0079	.0479	.1009	.0038	.0252	-.0447	-.1902	-.1688
41	-.0049	.0086	-.0226	.0097	.0518	-.0865	-.2046	-.0830
42	-.0017	-.0375	-.1560	.0128	.0596	-.0937	-.1289	.0337
43	.0709	-.0837	-.2776	.0121	.0439	-.0631	-.0014	.0885
44	.0015	-.1170	-.3547	.0083	.0119	-.0147	.1107	.0417
45	-.0017	-.1499	-.4183	.0009	-.0509	.0642	.2207	-.1289
46	-.0061	-.1611	-.4321	-.0035	-.0891	.1036	.2496	-.2487
47	-.0148	-.1601	-.4236	-.0070	-.1197	.1254	.2511	-.3565
48	-.0225	-.1594	-.3998	-.0081	-.1310	.1316	.2387	-.4040
49	-.0330	-.1644	-.3581	-.0074	-.1251	.1281	.2232	-.4214
50	-.0437	-.1729	-.3122	-.0068	-.1114	.1203	.2098	-.4741
51	-.0561	-.1871	-.2604	-.0066	-.0900	.1089	.1995	-.4183
52	-.0699	-.2056	-.2039	-.0068	-.0621	.0946	.1926	-.4058
53	-.0860	-.2316	-.1384	-.0078	-.0240	.0756	.1898	-.3822
54	-.1070	-.2648	-.0666	-.0095	.0236	.0524	.1933	-.3495
55	-.1307	-.3055	.0152	-.0120	.0830	.0235	.2008	-.2978
56	-.1554	-.3483	.0986	-.0146	.1472	-.0071	.2115	-.2353
57	-.1866	-.4027	.2018	-.0175	.2308	-.0463	.2278	-.1447
58	-.2169	-.4553	.3025	-.0201	.3142	-.0850	.2441	-.0454
59	-.0056	.0511	.1586	-.0087	-.0435	.0707	.1247	.0944
60	-.0060	.0535	.1637	-.0087	-.0439	.0730	.1184	.0854
61	-.0058	.0507	.1514	-.0073	-.0362	.0604	.0808	.0391
62	-.0082	.0713	.2113	-.0099	-.0489	.0813	.1013	.0399
63	-.0049	.0416	.1197	-.0045	-.0212	.0349	.0229	-.0173
64	-.0090	.0753	.2122	-.0074	-.0343	.0561	.0161	-.0596
65	-.0040	.0318	.0859	-.0019	-.0069	.0104	-.0276	-.0607
66	-.0074	.0569	.1496	-.0026	-.0088	.0126	-.0707	-.1292
67	-.0018	.0125	.0297	.0004	.0038	-.0068	-.0311	-.0222
68	-.0037	.0244	.0537	.0015	.0108	-.0187	-.0826	-.0655
69	-.0064	.0403	.0859	.0031	.0207	-.0365	-.1615	-.1473
70	-.0062	.0029	-.0218	.0033	.0158	-.0197	-.0726	-.0482
71	-.0026	.0089	-.0041	.0055	.0300	-.0481	-.1218	-.0330
72	-.0044	.0101	-.0144	.0089	.0485	-.0811	-.2014	-.0838
73	-.0002	-.0022	-.0119	.0015	.0093	-.0124	-.0115	.0189
74	.0009	-.0004	-.0221	.0044	.0242	-.0451	-.0457	.0399
75	-.0007	-.0169	-.0823	.0085	.0420	-.0648	-.0977	.0526
76	-.0014	-.0305	-.1320	.0116	.0554	-.0869	-.1236	.0415

TABLE 11-6 AIRPLANE VIBRATION MODE SHAPES , FINAL STIFFNESS DESIGN

ANTISYMMETRIC , HIGH GROSS WEIGHT

ROW	MODE 9	MODE 10	MODE 11	MODE 12	MODE 13	MODE 14	MODE 15	MODE 16
77	.0006	-.0081	-.0276	.0018	.0096	-.0131	-.0005	.0351
78	.0010	-.0186	-.0669	.0042	.0209	-.0289	-.0087	.0662
79	.0013	-.0347	-.1230	.0073	.0336	-.0469	-.0140	.1059
80	.0012	-.0589	-.2024	.0102	.0421	-.0595	-.0118	.1114
81	.0016	-.0176	-.0517	.0021	.0117	-.0123	.0249	.0643
82	.0025	-.0338	-.1061	.0039	.0186	-.0104	.0460	.0973
83	.0025	-.0431	-.1407	.0058	.0253	-.0301	.0412	.1184
84	.0026	-.0719	-.2292	.0077	.0259	-.0304	.0662	.1108
85	.0018	-.1036	-.3137	.0085	.0174	-.0212	.0953	.0660
86	.0035	-.0459	-.1405	.0037	.0168	-.0122	.0817	.1030
87	.0026	-.0771	-.2291	.0039	.0065	.0049	.1271	.0640
88	.0015	-.1103	-.3253	.0031	-.0188	.0312	.1721	-.0198
89	.0026	-.0200	-.0477	.0010	.0089	-.0046	.0521	.0689
90	.0041	-.0340	-.0978	.0016	.0131	-.0042	.0904	.0949
91	.0047	-.0429	-.1250	.0016	.0123	.0001	.1291	.0908
92	.0045	-.0717	-.2018	.0003	-.0047	.0299	.1504	.0180
93	.0018	-.1084	-.2989	-.0020	-.0477	.0775	.1969	-.1178
94	-.0050	-.1286	-.3642	-.0032	-.0872	.1020	.2146	-.2272
95	-.0042	-.0986	-.3148	-.0023	-.0833	.0943	.1817	-.1871
96	-.0158	-.1006	-.3152	-.0031	-.1072	.1070	.1784	-.2802
97	-.0285	-.1166	-.2932	-.0034	-.1107	.1004	.1727	-.3318
98	-.0430	-.1438	-.2593	-.0038	-.0976	.1058	.1741	-.3629
99	-.0690	-.1583	-.1105	-.0011	-.0327	.0674	.1312	-.2830
100	-.1143	-.2160	.0905	-.0021	.0003	.0029	.1132	-.1366
101	-.1559	-.3073	.1905	-.0085	.1845	-.0361	.1561	-.0862
102	-.1944	-.3903	.2835	-.0142	.2754	-.0738	.1982	-.0244
103	.0036	-.0285	-.0071	.0003	.0076	-.0035	.0518	.0635
104	.0053	-.0515	-.0348	-.0004	.0139	.0006	.0902	.0848
105	.0058	-.0534	-.0604	-.0017	.0183	.0120	.0970	.0699
106	.0045	-.0370	-.1336	-.0032	-.0036	.0400	.1246	-.0067
107	-.0019	-.0258	-.2162	-.0001	-.0782	.0740	.1031	-.1029
108	-.0087	-.0083	-.2064	.0024	-.0972	.0788	.0792	-.1385
109	-.0220	-.0166	-.1627	.0056	-.0907	.0750	.0600	-.1647
110	-.0568	-.0910	-.0532	.0058	-.0269	.0512	.0666	-.1694
111	-.0796	-.1411	.0054	.0030	.0176	.0333	.0826	-.1635
112	.0025	-.0185	.0136	-.0000	.0042	-.0027	.0258	.0410
113	.0042	-.0464	.0270	-.0000	.0083	-.0046	.0482	.0654
114	.0059	-.0890	.0474	-.0012	.0172	-.0002	.0644	.0719

TABLE 11-6 AIRPLANE VIBRATION MODE SHAPES , FINAL STIFFNESS DESIGN

ANTISYMMETRIC , HIGH GROSS WEIGHT

ROW	MODE 9	MODE 10	MODE 11	MODE 12	MODE 13	MODE 14	MODE 15	MODE 16
115	.0069	-.0974	.0395	-.0039	.0289	.0173	.0584	.0521
116	.0054	-.0206	-.0307	-.0058	.0145	.0344	.0711	.0082
117	-.0006	.0852	-.1052	-.0031	-.0367	.0317	.0655	-.0416
118	-.0039	.0980	-.1274	.0017	-.0831	.0422	.0154	-.0453
119	-.0103	.1163	-.0724	.0131	-.1038	.0447	-.0659	-.0131
120	-.0223	.0724	.0086	.0203	-.0560	.0360	-.0665	.0104
121	-.0406	.0206	.0788	.0194	-.0073	.0186	-.0566	.0263
122	-.0582	-.0070	.1336	.0200	.0321	.0032	-.0512	.0570
123	-.0834	-.0716	.1870	.0141	.0848	-.0191	-.0228	.0744
124	-.1248	-.1687	.2707	.0067	.1723	-.0539	.0267	.1133
125	-.1711	-.2761	.3656	-.0010	.2762	-.0945	.0872	.1710
126	-.1956	-.3326	.4164	-.0050	.3329	-.1166	.1202	.2068
127	-.2270	-.4051	.4814	-.0101	.4056	-.1450	.1627	.2525
128	-.2572	-.4752	.5432	-.0151	.4743	-.1717	.2036	.2910
129	.0037	-.0453	.0450	-.0013	.0136	.0024	.0284	.0644
130	.0063	-.1005	.0885	-.0028	.0267	.0062	.0455	.0854
131	.0042	-.0582	.0700	-.0023	.0204	.0069	.0225	.0791
132	.0071	-.1198	.1255	-.0043	.0361	.0119	.0361	.1014
133	.0088	-.2625	.2990	-.0074	.0643	.0239	-.0704	.0112
134	.0046	.0192	.0422	-.0068	.0102	.0268	.0273	.0079
135	.0005	.1097	-.0143	-.0055	-.0230	.0221	.0256	-.0212
136	.0036	.0665	.0962	-.0079	.0034	.0203	-.0091	.0052
137	-.0005	.1573	.0362	-.0065	-.0299	.0158	-.0091	-.0243
138	-.0115	.2720	-.0713	.0050	-.1067	-.0058	-.0873	.0010
139	-.0118	.1689	.1045	.0312	-.0416	.0130	-.1558	.1541
140	-.0260	.1071	.1697	.0359	.0074	.0061	-.1402	.1630
141	-.0755	.0004	.2873	.0253	.1102	-.0435	-.1027	.2273
142	-.1206	-.1044	.3790	.0166	.2084	-.0844	-.0509	.2923
143	-.1703	-.2193	.4816	.0080	.3238	-.1307	.0140	.3764
144	-.2252	-.3448	.5987	-.0006	.4602	-.1853	.0890	.5034
145	-.2736	-.4523	.7090	-.0073	.5931	-.2397	.1578	.6783
146	-.3100	-.5343	.7883	-.0127	.6868	-.2775	.2084	.7804
147	.0105	-.4545	.5603	-.0105	.1045	.0316	-.2150	-.0369
148	-.0239	.5751	-.0100	.0060	-.1174	-.1044	-.2011	.0643
149	-.0224	.1571	.2586	.0488	.0311	-.0086	-.2131	.3024
150	-.0942	-.0181	.3794	.0258	.1701	-.0757	-.1160	.3337
151	-.1696	-.1916	.5362	.0124	.3455	-.1476	-.0214	.4730
152	-.2607	-.3966	.7377	-.0011	.5856	-.2452	.1057	.7526

TABLE 11-6 AIRPLANE VIBRATION MODE SHAPES , FINAL STIFFNESS DESIGN

ANTISYMMETRIC , HIGH GROSS WEIGHT

ROW	MODE 9	MODE 10	MODE 11	MODE 12	MODE 13	MODE 14	MODE 15	MODE 16
153	-.3335	-.5593	.9012	-.0114	.7821	-.3253	.2081	1.0000
154	-.0262	-.1782	-.4160	-.0089	-.1364	.1386	.2521	-.4384
155	-.0352	-.1849	-.3822	-.0087	-.1310	.1358	.2414	-.4552
156	-.0465	-.1957	-.3364	-.0086	-.1165	.1277	.2302	-.4609
157	-.0595	-.2118	-.2844	-.0090	-.0939	.1156	.2218	-.4567
158	-.0739	-.2321	-.2282	-.0098	-.0655	.1008	.2165	-.4463
159	-.0914	-.2592	-.1631	-.0112	-.0272	.0314	.2150	-.4251
160	-.1119	-.2933	-.0917	-.0133	.0205	.0580	.2194	-.3945
161	-.1358	-.3344	.0101	-.0158	.0800	.0294	.2280	-.3456
162	-.1604	-.3770	.0720	-.0183	.1430	-.0004	.2394	-.2886
163	-.1915	-.4313	.1746	-.0212	.2260	-.0389	.2563	-.2021
164	.0104	.0221	.0800	-.0002	-.0022	-.0384	.0011	.0050
165	.0198	.0630	.1149	.0015	-.0022	-.0560	-.0462	.0826
166	.0550	.1785	.1733	.0451	.0033	-.0271	-.0069	.1570
167	.1173	.3726	.3511	.2384	.1926	.1715	.0678	.0697
168	.1780	.5716	.5434	.4573	.4165	.4041	.3264	-.0676
169	.2495	.8086	.7775	.7299	.7002	.6987	.6404	-.2624
170	.0075	.0067	.0669	-.0009	-.0062	-.0331	.0121	-.0220
171	.0142	.0413	.1000	-.0044	-.0082	-.0572	-.0395	.0598
172	.0495	.1561	.1699	.0443	.0107	-.0253	-.0779	.1346
173	.0098	.0106	.0996	.0025	.0038	-.0452	-.0088	.0149
174	.0381	.1100	.1617	.0421	.0248	-.0221	-.0402	.0887
175	.1039	.3226	.3347	.2207	.1890	.1551	.0983	.0474
176	.1712	.5462	.5356	.4491	.4159	.3968	.3337	-.0812
177	.0123	.0116	.1374	.0052	.0209	-.0568	-.0251	.0553
178	.0755	.2164	.2996	.1831	.1813	.1204	.1206	-.0012
179	.1504	.4685	.5108	.4226	.4119	.3725	.3531	-.1205
180	.2126	.6796	.6932	.6349	.6214	.6003	.5745	-.2465
181	.2774	.9000	.8842	.8588	.8432	.8419	.8112	-.3838
182	.0691	.1777	.3490	.2398	.2787	.1855	.2621	-.1286
183	.1145	.3344	.4628	.3694	.3948	.3214	.3711	-.1745
184	.1762	.6180	.6750	.6159	.6213	.5836	.5943	-.2818
185	.2323	.7437	.7685	.7245	.7208	.6992	.6919	-.3282
186	.0890	.2399	.4253	.3269	.3754	.2791	.3732	-.2030
187	.1723	.5289	.6442	.5819	.6119	.5511	.6093	-.3209
188	.2600	.8339	.8741	.8513	.8614	.8397	.8591	-.4452
189	.3077	1.0000	1.0000	1.0000	1.0000	1.0000	1.0000	-.5200
190	.6878	.0127	.1894	.0103	.0351	-.0511	-.1237	.1541

TABLE 11-6 AIRPLANE VIBRATION MODE SHAPES , FINAL STIFFNESS DESIGN

ANTISYMMETRIC , HIGH GROSS WEIGHT

ROW	MODE 9	MODE 10	MODE 11	MODE 12	MODE 13	MODE 14	MODE 15	MODE 16
191	1.0000	-.1099	-.1818	-.0290	-.0226	.0012	.1029	-.1164
192	.0001	-.0006	-.0022	-.0001	-.0008	.0006	.0012	-.0023
193	.0001	.0050	.0318	-.0010	-.0031	-.0163	.0413	.0026
194	-.0044	-.0005	-.0095	.0001	-.0021	.0163	-.0040	.0003
195	-.0000	-.0000	-.0000	.0000	.0000	.0000	-.0000	-.0000
196	-.0000	.0003	.0012	-.0001	-.0004	.0005	.0014	.0011
197	-.0000	.0003	.0012	-.0001	-.0004	.0005	.0014	.0011
198	-.0000	.0002	.0012	-.0001	-.0004	.0005	.0014	.0011
199	-.0000	.0003	.0012	-.0001	-.0004	.0005	.0014	.0010
200	-.0000	.0003	.0012	-.0001	-.0004	.0005	.0014	.0010
201	.0154	-.2381	-.4670	.0052	.0308	-.0649	.0274	-.0251
202	.0073	-.1485	-.2986	.0037	.0177	-.0246	-.0055	-.0084
203	.0010	-.0821	-.1749	.0027	.0085	.0050	-.0308	.0026
204	-.0045	-.0309	-.0818	.0021	.0024	.0281	-.0534	.0090
205	-.0120	.0185	-.0012	.0026	-.0005	.0547	-.0919	.0108
206	-.0000	.0004	.0012	-.0001	-.0004	.0005	.0013	.0010
207	-.0000	.0004	.0012	-.0001	-.0004	.0005	.0013	.0010
208	-.0000	.0004	.0012	-.0001	-.0004	.0005	.0013	.0009
209	-.0000	.0003	.0011	-.0001	-.0003	.0005	.0013	.0008
210	-.0000	.0003	.0011	-.0001	-.0003	.0004	.0012	.0007
211	-.0000	.0003	.0011	-.0001	-.0003	.0004	.0010	.0006
212	-.0000	.0003	.0010	-.0001	-.0002	.0003	.0008	.0005
213	-.0000	.0003	.0009	-.0000	-.0002	.0003	.0006	.0004
214	-.0000	.0002	.0007	-.0000	-.0002	.0002	.0005	.0003
215	-.0000	.0002	.0006	-.0000	-.0001	.0002	.0003	.0003
216	-.0000	.0001	.0004	-.0000	-.0001	.0001	.0002	.0003
217	-.0000	.0001	.0003	-.0000	-.0000	.0000	.0002	.0004
218	-.0000	.0000	.0002	-.0000	.0000	.0000	.0001	.0004
219	.0000	.0000	.0001	.0000	.0000	-.0000	.0001	.0005
220	.0000	-.0000	.0001	.0000	.0000	-.0000	.0002	.0006
221	.0000	.0000	.0002	.0000	.0000	-.0000	.0002	.0007
222	.0000	.0000	.0003	-.0000	.0000	-.0000	.0002	.0008
223	.0001	.0001	.0005	-.0000	.0000	-.0001	.0003	.0009
224	-.0140	.0227	.0018	.0030	.0002	.0605	-.1018	.0108
225	-.0160	.0204	-.0093	.0037	.0024	.0638	-.1105	.0090
226	-.0170	.0149	-.0239	.0042	.0047	.0615	-.1098	.0054
227	-.0160	.0076	-.0385	.0044	.0066	.0544	-.0995	.0011
228	-.0158	.0014	-.0466	.0041	.0071	.0449	-.0811	-.0006

TABLE 11-6 AIRPLANE VIBRATION MODE SHAPES , FINAL STIFFNESS DESIGN

ANTISYMMETRIC , HIGH GROSS WEIGHT

ROW	MODE 9	MODE 10	MODE 11	MODE 12	MODE 13	MODE 14	MODE 15	MODE 16
229	-.0139	-.0027	-.0473	.0036	.0064	.0349	-.0587	-.0005
230	-.0118	-.0047	-.0419	.0028	.0050	.0253	-.0371	-.0017
231	-.0095	-.0050	-.0332	.0022	.0039	.0152	-.0216	-.0075
232	.0072	-.0042	-.0230	.0017	.0036	.0045	-.0132	-.0168
233	-.0049	-.0027	-.0129	.0013	.0038	-.0058	-.0091	-.0247
234	-.0027	-.0012	-.0036	.0010	.0038	-.0146	-.0040	-.0258
235	-.0006	.0005	.0048	.0007	.0034	-.0212	.0024	-.0240
236	.0011	.0019	.0112	.0004	.0026	-.0255	.0088	-.0219
237	.0029	.0035	.0184	.0001	.0023	-.0283	.0147	-.0154
238	.0048	.0047	.0261	-.0003	.0014	-.0300	.0207	-.0135
239	.0066	.0058	.0341	-.0007	-.0000	-.0308	.0245	-.0204
240	.0081	.0067	.0436	-.0011	-.0007	-.0335	.0268	-.0257
241	.0078	.0077	.0444	-.0015	-.0022	-.0386	.0353	-.0503
242	.0001	.0002	.0007	-.0000	.0000	-.0002	.0005	.0009
243	.0001	.0003	.0011	-.0000	-.0000	-.0003	.0007	.0010
244	.0001	.0003	.0011	-.0000	-.0000	-.0003	.0008	.0011
245	.0001	.0003	.0011	-.0000	-.0000	-.0003	.0008	.0011
246	.0048	.0023	.0254	-.0016	-.0034	-.0399	.0422	-.0808
247	-.0155	-.0654	-.1544	.0020	.0040	.0030	.0028	-.0460
248	-.0337	-.1348	-.3381	.0066	.0044	.0590	-.0706	.0514
249	-.0565	-.2237	-.5733	.0127	.0292	.1350	-.1738	.2068
250	.0001	.0003	.0012	-.0000	-.0000	-.0003	.0000	.0013
251	-.0001	-.0005	-.0014	.0000	.0001	.0004	-.0006	.0012
252	.0094	.0376	.0967	-.0026	-.0064	-.0318	.0398	-.0806
253	-.0426	-.1698	-.4288	.0089	.0206	.0887	-.1088	.1223
254	.0078	.0233	.0857	-.0018	-.0012	-.0229	.0606	.0908
255	.0001	.0003	.0011	-.0000	-.0000	-.0003	.0008	.0011
256	-.0001	-.0005	-.0012	.0000	.0001	.0004	-.0004	.0008
257	-.0442	-.1656	-.4507	.0088	.0162	.0876	-.1448	-.0577
258	-.0092	.0043	-.0219	.0022	-.0004	.0455	-.0763	.0110
259	-.0030	-.0207	-.0361	-.0006	-.0017	-.0284	.0380	-.0835
260	.0001	.0003	.0010	-.0000	-.0000	-.0002	.0006	.0000

TABLE 11-6 AIRPLANE VIBRATION MODE SHAPES , FINAL STIFFNESS DESIGN

ANTISYMMETRIC , HIGH GROSS WEIGHT

ROW	MODE 17	MODE 18	MODE 19	MODE 20
1	.1171	-.1310	-.0163	-.0163
2	.0879	-.0448	-.0061	-.0040
3	-.0227	.0026	.0037	.0064
4	.0045	-.0017	.0004	-.0001
5	.0001	.0017	.0005	.0002
6	-.0003	.0003	.0000	.0000
7	.2008	-.1469	-.0315	-.0004
8	.0988	-.0667	-.0201	.0177
9	-.0293	.0013	-.0188	.0156
10	.0051	-.0013	.0005	.0002
11	.0003	.0019	.0010	-.0001
12	-.0001	-.0003	-.0002	.0001
13	-.1731	-.2595	-.0269	-.0426
14	-.3187	-.2699	.0271	-.0133
15	.0795	.3173	.0071	.0347
16	-.0259	-.2560	-.0117	-.0390
17	-.0136	-.3052	-.1208	-.0050
18	.1755	-.3700	-.3337	-.0317
19	.2118	-.4070	-.3605	-.0769
20	.1815	-.4995	-.4550	-.0258
21	.1315	-.6210	-.5900	.0922
22	-.1353	-.1950	-.0213	-.0324
23	-.1692	-.2421	-.0074	-.0315
24	-.2198	-.2556	.0079	-.0244
25	-.2725	-.2328	.0241	-.0113
26	-.2547	-.1154	.0317	.0088
27	-.1558	.0858	.0302	.0318
28	-.0281	.2436	.0212	.0418
29	.0509	.2963	.0114	.0380
30	.1012	.2291	-.0044	.0128
31	.0539	.0005	-.0136	-.0214
32	-.0959	-.1274	-.0152	-.0217
33	-.1274	-.1779	-.0040	-.0225
34	-.1676	-.2036	.0061	-.0198
35	-.2221	-.1940	.0208	-.0092
36	-.2130	-.1052	.0266	.0063
37	-.1286	.0754	.0256	.0272
38	-.0242	.2150	.0187	.0372

TABLE 11-6 AIRPLANE VIBRATION MODE SHAPES , FINAL STIFFNESS DESIGN

ANTISYMMETRIC , HIGH GROSS WEIGHT

ROW	MODE 17	MODE 18	MODE 19	MODE 20
39	.0554	.2810	.0099	.0360
40	.1004	.2158	-.0044	.0116
41	.0433	-.0138	-.0127	-.0223
42	-.0376	-.2461	-.0082	-.0354
43	-.1028	-.3600	-.0072	-.0263
44	-.0980	-.3470	-.0281	-.0127
45	-.0199	-.2681	-.1010	-.0026
46	.0449	-.2407	-.1620	-.0055
47	.1113	-.2815	-.2436	-.0166
48	.1487	-.3029	-.2795	-.0284
49	.1681	-.3072	-.2818	-.0471
50	.1783	-.3058	-.2759	-.0632
51	.1830	-.3058	-.2714	-.0757
52	.1935	-.3093	-.2711	-.0832
53	.1780	-.3204	-.2799	-.0814
54	.1678	-.3468	-.3064	-.0664
55	.1486	-.3828	-.3456	-.0330
56	.1250	-.4280	-.3961	.0140
57	.0905	-.4928	-.4703	.0000
58	.0523	-.5561	-.5444	.1786
59	-.1351	-.1713	.0036	-.0177
60	-.1573	-.1565	.0148	-.0093
61	-.1211	-.0575	.0171	.0058
62	-.1671	-.0590	.0238	.0103
63	-.0347	.0539	.0089	.0138
64	-.0660	.1297	.0192	.0293
65	.0385	.1356	.0015	.0185
66	.0586	.2504	.0071	.0341
67	.0419	.0687	-.0041	.0023
68	.0677	.1002	-.0028	.0058
69	.1051	.2006	-.0033	.0124
70	.0695	.1153	.0811	.0041
71	.0057	.0024	-.0003	-.0073
72	.0378	-.0037	-.0128	-.0239
73	.0097	-.0037	-.0039	-.0021
74	.0828	-.0483	-.0112	-.0135
75	-.0621	-.1521	.0005	-.0217
76	-.0436	-.2243	-.0052	-.0329

TABLE 11-6 AIRPLANE VIBRATION MODE SHAPES , FINAL STIFFNESS DESIGN

ANTISYMMETRIC , HIGH GROSS WEIGHT

ROW	MODE 17	MODE 18	MODE 19	MODE 20
77	-.0114	-.0121	-.0008	-.0009
78	-.0407	-.0559	.0040	-.0031
79	-.0803	-.1483	.0099	-.0090
80	-.1007	-.2701	.0068	-.0183
81	-.0161	-.0001	.0117	.0063
82	-.0443	-.0230	.0226	.0094
83	-.0748	-.0906	.0222	.0049
84	-.1002	-.2038	.0150	-.0013
85	-.1025	-.3129	-.0137	-.0100
86	-.0482	.0050	.0359	.0177
87	-.0668	-.0594	.0251	.0152
88	-.0546	-.1650	-.0263	.0067
89	.0080	.0822	.0281	.0197
90	-.0156	.1134	.0482	.0237
91	-.0276	.1158	.0527	.0297
92	-.0471	.0801	.0423	.0228
93	-.0180	.0269	-.0098	.0089
94	.0390	-.1101	-.1035	-.0043
95	.0274	-.0359	-.0591	-.0035
96	.0964	-.1216	-.1287	-.0291
97	.1273	-.1808	-.1713	-.0506
98	.1518	-.2199	-.1981	-.0694
99	.1281	-.1435	-.1224	-.0891
100	.0711	-.1250	-.1037	-.0459
101	.0573	-.2693	-.2517	.0356
102	.0381	-.4123	-.4019	.1310
103	.0590	.1446	.0182	.0225
104	.0138	.1965	.0475	.0343
105	-.0170	.1829	.0561	.0325
106	-.0516	.1777	.0621	.0232
107	.0013	.0928	.0254	.0027
108	.0322	.0748	.0289	-.0239
109	.0593	.0671	.0514	-.0663
110	.0740	.0299	.0428	-.0990
111	.0762	-.0231	-.0041	-.0892
112	.0640	.0900	-.0015	.0101
113	.0532	.1550	.0125	.0207
114	.0005	.1990	.0377	.0309

TABLE 11-6 AIRPLANE VIBRATION MODE SHAPES , FINAL STIFFNESS DESIGN

ANTISYMMETRIC , HIGH GROSS WEIGHT

ROW	MODE 17	MODE 18	MODE 19	MODE 20
115	-.0209	.1803	.0485	.0290
116	-.0586	.2144	.0698	.0268
117	-.0755	.1771	.0497	.0159
118	-.0200	.1286	.0513	.0069
119	.0242	.2127	.1892	-.0562
120	.0010	.3372	.3253	-.1176
121	-.0144	.3426	.3380	-.1311
122	-.0249	.3408	.3390	-.1229
123	-.0300	.2636	.2645	-.0891
124	-.0402	.1162	.1160	-.0099
125	-.0559	-.0774	-.0844	.1080
126	-.0661	-.1869	-.1992	.1706
127	-.0792	-.3290	-.3485	.2724
128	-.0894	-.4647	-.4898	.3555
129	.0707	.1755	.0141	.0253
130	.0275	.2611	.0425	.0420
131	.0860	.2331	.0216	.0355
132	.0415	.3292	.0522	.0543
133	-.0247	.0143	.0021	.0064
134	-.1011	.2973	.0911	.0400
135	-.1377	.3202	.0907	.0466
136	-.1500	.4189	.1244	.0613
137	-.1979	.4449	.1248	.0689
138	-.0100	.0146	.0045	.0087
139	-.0640	.6030	.5772	-.1540
140	-.0764	.6369	.6260	-.1869
141	-.0972	.4921	.4815	-.1046
142	-.1205	.3487	.3345	-.0070
143	-.1493	.1416	.1160	.1411
144	-.1926	-.1210	-.1696	.3615
145	-.2505	-.3708	-.4539	.6342
146	-.2967	-.5510	-.6536	.8037
147	-.0256	-.2317	-.0582	-.0241
148	-.0323	-.2565	-.1489	.0307
149	-.1440	1.0000	1.0000	-.2817
150	-.1423	.5379	.5207	-.0667
151	-.1919	.2482	.2140	.1548
152	-.2962	-.2071	-.2950	.6054

TABLE 11-6 AIRPLANE VIBRATION MODE SHAPES , FINAL STIFFNESS DESIGN

ANTISYMMETRIC , HIGH GROSS WEIGHT

ROW	MODE 17	MODE 18	MODE 19	MODE 20
153	-.3898	-.5827	-.7197	1.0000
154	.1676	-.3468	-.3151	-.0318
155	.1852	-.3561	-.3232	-.0460
156	.1964	-.3606	-.3241	-.0610
157	.2011	-.3651	-.3247	-.0723
158	.2019	-.3727	-.3291	-.0792
159	.1970	-.3879	-.3424	-.0770
160	.1874	-.4175	-.3724	-.0619
161	.1700	-.4587	-.4167	-.0284
162	.1493	-.5078	-.4708	.0169
163	.1172	-.5764	-.5493	.0922
164	-.1288	.0208	-.0283	.0009
165	-.2052	.1292	.0623	-.0010
166	-.2566	.3006	.2323	-.0336
167	-.0714	.1954	.1793	-.0246
168	.1953	-.0014	.0498	-.0023
169	.5627	-.2947	-.1522	.0330
170	-.1145	-.0150	-.0572	-.0015
171	-.1969	.0891	.0262	-.0006
172	-.2470	.2534	.1886	-.0280
173	-.1850	.0196	-.0313	-.0037
174	-.2271	.1578	.1002	-.0173
175	-.0823	.1347	.1168	-.0171
176	.1915	-.0372	.0139	.0022
177	-.2592	.0545	-.0033	-.0055
178	-.1042	.0034	-.0157	-.0010
179	.1755	-.1427	-.0932	.0153
180	.4575	-.3117	-.1938	.0359
181	.7658	-.4974	-.3052	.0587
182	-.0226	-.2650	-.2583	.0310
183	.1295	-.2994	-.2569	.0347
184	.4487	-.4040	-.2863	.0475
185	.5916	-.4477	-.2966	.0528
186	.0853	-.3909	-.3562	.0457
187	.4211	-.5156	-.4024	.0614
188	.7879	-.6445	-.4451	.0775
189	1.0000	-.7246	-.4755	.0878
190	-.2354	.4387	.3904	-.1136

TABLE 11-6 AIRPLANE VIBRATION MODE SHAPES , FINAL STIFFNESS DESIGN

ANTISYMMETRIC , HIGH GROSS WEIGHT

ROW	MODE 17	MODE 18	MODE 19	MODE 20
191	.1010	-.3676	-.3432	.1012
192	.0010	-.0034	-.0033	.0005
193	.0753	.0295	-.0177	-.0060
194	.2069	-.0400	.0299	.0005
195	.0000	.0000	.0000	-.0000
196	.0008	-.0022	-.0002	-.0004
197	.0008	-.0022	-.0002	-.0004
198	.0007	-.0021	-.0002	-.0004
199	.0007	-.0021	-.0002	-.0004
200	.0006	-.0020	-.0002	-.0004
201	.7043	-.1053	.2050	.0563
202	.1365	-.0232	.0513	.0140
203	-.2399	.0289	-.0436	-.0113
204	-.4820	.0593	-.0922	-.0228
205	-.6732	.0708	-.0866	-.0157
206	.0006	-.0020	-.0002	-.0004
207	.0006	-.0020	-.0002	-.0004
208	.0009	-.0019	-.0002	-.0004
209	.0014	-.0017	-.0002	-.0003
210	.0011	-.0014	-.0003	-.0003
211	.0004	-.0010	-.0004	-.0003
212	-.0001	-.0006	-.0004	-.0003
213	-.0004	-.0003	-.0004	-.0002
214	-.0004	-.0001	-.0004	-.0002
215	-.0003	.0002	-.0004	-.0001
216	.0000	.0004	-.0004	-.0001
217	.0004	.0005	-.0003	-.0001
218	.0010	.0006	-.0003	-.0000
219	.0015	.0007	-.0004	-.0000
220	.0021	.0010	-.0005	-.0000
221	.0026	.0013	-.0007	-.0000
222	.0030	.0017	-.0009	-.0000
223	.0037	.0019	-.0010	-.0000
224	-.6726	.0588	-.0601	-.0068
225	-.6013	.0345	-.0099	.0089
226	-.4490	.0064	.0412	.0229
227	-.2507	-.0208	.0837	.0329
228	-.0756	-.0425	.1051	.0354

TAB E 11-6 AIRPLANE VIBRATION MODE SHAPES , FINAL STIFFNESS DESIGN

ANTISYMMETRIC , HIGH GROSS WEIGHT

POW	MODE 17	MODE 18	MODE 19	MODE 20
229	.0550	-.0573	.1091	.0326
230	.1391	-.0611	.1016	.0277
231	.1813	-.0495	.0863	.0225
232	.1883	-.0295	.0668	.0171
233	.1638	-.0143	.0471	.0114
234	.1118	-.0137	.0298	.0053
235	.042	-.0221	.0177	.0009
236	-.0258	-.0351	.0132	-.0008
237	-.0762	-.0362	.0096	-.0005
238	-.1328	-.0306	.0101	.0022
239	-.1895	-.0254	.0156	.0054
240	-.2254	-.0218	.0206	.0073
241	-.2382	-.0768	.0575	.0098
242	.0048	.0020	-.0010	-.0000
243	.0069	.0022	-.0012	-.0001
244	.0080	.0025	-.0014	-.0001
245	.0082	.0025	-.0014	-.0001
246	-.2232	-.1598	.1121	.0128
247	-.0644	-.1298	.1005	.0104
248	-.0211	.0923	-.0490	-.0017
249	.0475	.4656	-.3052	-.0226
250	.0099	.0031	-.0018	-.0001
251	.0015	.0028	-.0019	-.0002
252	-.1059	-.1926	.1291	.0103
253	.7552	.2624	-.1638	-.0110
254	.6788	.2137	-.1188	-.0079
255	.0079	.0024	-.0013	-.0001
256	.0011	.0019	-.0012	-.0001
257	-.7960	-.1593	.0911	.0076
258	-.6223	.0719	-.1006	-.0220
259	-.1219	-.1925	.1384	.0138
260	.0061	.0020	-.0011	-.0001

TABLE 11-6 AIRPLANE VIBRATION MODE SHAPES*, FINAL STIFFNESS DESIGN

ANTISYMMETRIC , LOW GROSS WEIGHT

ROW	MODE 1	MODE 2	MODE 3	MODE 4	MODE 5	MODE 6	MODE 7	MODE 8
1	.0000	-.0044	.1252	.0798	.0088	-.1241	.0254	.0365
2	1.0000	.0654	-.2953	-.1914	-.0255	.1743	.1162	-.1963
3	.0000	.3203	.0058	-.0036	-.0618	-.2905	.2496	-.0382
4	.0000	.0013	.0000	-.0002	-.0002	.0008	.0007	-.0015
5	.0000	.0000	-.0000	-.0000	-.0002	.0017	-.0017	.0001
6	.0000	.0000	-.0005	-.0003	-.0000	.0005	.0001	-.0003
7	.0000	-.0075	.2142	.1334	.0396	-.1513	-.0032	.0802
8	1.0000	.0434	-.3038	-.1974	.0002	.2529	.0191	-.1781
9	.0000	.5478	.0099	-.0236	.0389	-.2013	.2156	-.0259
10	.0000	.0013	.0000	-.0003	.0003	.0026	-.0014	-.0013
11	.0000	.0000	-.0000	.0000	-.0010	.0015	-.0020	-.0003
12	.0000	.0000	-.0005	-.0003	.0000	.0004	.0001	-.0003
13	.0000	.2111	.0038	.0149	-.1329	.1374	-.1225	.2546
14	.0000	.3087	.0056	.0100	-.1930	.1596	-.2196	.3364
15	.0000	.4378	.0079	-.0102	-.2604	.1766	-.3211	.3219
16	.0000	.5505	.0099	-.0061	-.2820	.1407	-.3346	.1858
17	.0000	.6874	.0124	-.0080	-.2081	.0921	-.2512	.0014
18	.0000	.7739	.0140	-.0311	-.0534	.1328	-.2159	-.0441
19	.0000	.8742	.0158	-.0583	.1849	.3137	-.3154	-.0177
20	.0000	.9494	.0171	-.0807	.4042	.5181	-.4601	.0228
21	.0000	1.0000	.0181	-.0966	.5674	.6845	-.5857	.0560
22	.0000	.1587	.0029	.0119	-.0996	.0993	-.0916	.1897
23	.0000	.1970	.0036	.0109	-.1232	.1115	-.1264	.2300
24	.0000	.2269	.0041	.0099	-.1417	.1211	-.1550	.2564
25	.0000	.2652	.0048	.0087	-.1655	.1359	-.1885	.2873
26	.0000	.2934	.0053	.0068	-.1827	.1452	-.2148	.3017
27	.0000	.3317	.0060	.0031	-.2054	.1564	-.2493	.3146
28	.0000	.3617	.0065	-.0025	-.2209	.1602	-.2721	.3100
29	.0000	.3897	.0070	-.0071	-.2338	.1620	-.2884	.3016
30	.0000	.4318	.0078	-.0122	-.2493	.1583	-.3056	.2716
31	.0000	.4732	.0085	-.0115	-.2592	.1467	-.3130	.2263
32	.0000	.1041	.0019	.0087	-.0651	.0647	-.0596	.1222
33	.0000	.1452	.0026	.0084	-.0904	.0801	-.0941	.1668
34	.0000	.1773	.0032	.0081	-.1103	.0934	-.1206	.1989
35	.0000	.2184	.0039	.0073	-.1358	.1105	-.1548	.2346
36	.0000	.2486	.0045	.0061	-.1543	.1221	-.1807	.2544
37	.0000	.2897	.0052	.0029	-.1788	.1174	-.2165	.2722
38	.0000	.3242	.0059	-.0011	-.1976	.1428	-.2427	.2763

*Elastic modes start at "mode 4."

TABLE 11-6 AIRPLANE VIBRATION MODE SHAPES* , FINAL STIFFNESS DESIGN

ANTISYMMETRIC , LOW GROSS WEIGHT

ROW	MODE 1	MODE 2	MODE 3	MODE 4	MODE 5	MODE 6	MODE 7	MODE 8
39	.0000	.3545	.0064	-.0062	-.2122	.1464	-.2615	.2720
40	.0000	.3998	.0072	-.0111	-.2301	.1452	-.2816	.2478
41	.0000	.4452	.0080	-.0101	-.2426	.1359	-.2919	.2076
42	.0000	.5011	.0090	-.0036	-.2537	.1234	-.2980	.1617
43	.0000	.5571	.0101	.0021	-.2536	.1078	-.2886	.1057
44	.0000	.6022	.0109	.0011	-.2391	.0917	-.2667	.0589
45	.0000	.6587	.0119	-.0076	-.1955	.0772	-.2264	.0010
46	.0000	.6885	.0124	-.0145	-.1582	.0757	-.2031	-.0240
47	.0000	.7210	.0130	-.0227	-.1032	.0838	-.1846	-.0381
48	.0000	.7427	.0134	-.0290	-.0556	.1018	-.1803	-.0428
49	.0000	.7730	.0140	-.0367	.0063	.1404	-.1541	-.0401
50	.0000	.7992	.0144	-.0437	.0658	.1820	-.2134	-.0346
51	.0000	.8245	.0149	-.0507	.1279	.2298	-.2397	-.0268
52	.0000	.8491	.0153	-.0576	.1917	.2818	-.2709	-.0176
53	.0000	.8744	.0158	-.0650	.2612	.3424	-.3106	-.0060
54	.0000	.8990	.0162	-.0724	.3331	.4093	-.3576	.0073
55	.0000	.9242	.0167	-.0801	.4105	.4844	-.4126	.0226
56	.0000	.9479	.0171	-.0874	.4856	.5598	-.4690	.0379
57	.0000	.9749	.0176	-.0960	.5744	.6516	-.5389	.0564
58	.0000	1.0000	.0181	-.1041	.6584	.7396	-.6061	.0741
59	.0000	.1452	.0026	.0073	-.0901	.0763	-.0973	.1626
60	.0000	.1452	.0026	.0058	-.0897	.0722	-.1015	.1547
61	.0000	.1452	.0026	.0044	-.0890	.0688	-.1034	.1436
62	.0000	.2032	.0037	.0049	-.1254	.0975	-.1474	.2019
63	.0000	.1452	.0026	.0024	-.0882	.0649	-.1052	.1298
64	.0000	.2576	.0047	.0016	-.1580	.1167	-.1928	.2308
65	.0000	.1452	.0026	-.0007	-.0862	.0595	-.1039	.1124
66	.0000	.2576	.0047	-.0033	-.1543	.1068	-.1897	.2003
67	.0000	.1073	.0019	-.0034	-.0605	.0368	-.0711	.0640
68	.0000	.2020	.0036	-.0058	-.1154	.0714	-.1395	.1228
69	.0000	.3182	.0057	-.0087	-.1832	.1155	-.2240	.1970
70	.0000	.1452	.0026	-.0339	-.0909	.0078	-.1452	.1236
71	.0000	.2576	.0047	-.0014	-.1406	.0784	-.1681	.1186
72	.0000	.3847	.0069	-.0085	-.2097	.1178	-.2515	.1795
73	.0000	.1073	.0019	-.0001	-.0535	.0246	-.0568	.0364
74	.0000	.2020	.0036	.0093	-.1048	.0533	-.1200	.0435
75	.0000	.3182	.0057	.0029	-.1610	.0770	-.1833	.1014
76	.0000	.4452	.0080	-.0018	-.2255	.1089	-.2626	.1440

*Elastic modes start at "mode 4."

TABLE 11-6 AIRPLANE VIBRATION MODE SHAPES*, FINAL STIFFNESS DESIGN

ANTISYMMETRIC , LOW GROSS WEIGHT

ROW	MODE 1	MODE 2	MODE 3	MODE 4	MODE 5	MODE 6	MODE 7	MODE 8
77	.0000	.1073	.0019	.0063	-.0496	.0182	-.0476	.0226
78	.0000	.2083	.0038	.0092	-.0965	.0362	-.0968	.0427
79	.0000	.3182	.0057	.0097	-.1469	.0557	-.1523	.0649
80	.0000	.4452	.0080	.0062	-.2040	.0813	-.2226	.0880
81	.0000	.1452	.0026	.0049	-.0610	.0122	-.0502	.0151
82	.0000	.2576	.0047	.0072	-.1065	.0221	-.0912	.0261
83	.0000	.3182	.0057	.0091	-.1357	.0378	-.1272	.0411
84	.0000	.4452	.0080	.0064	-.1845	.0570	-.1855	.0519
85	.0000	.5619	.0101	.0026	-.2258	.0819	-.2453	.0584
86	.0000	.3182	.0057	.0054	-.1236	.0149	-.0975	.0192
87	.0000	.4452	.0080	.0022	-.1598	.0230	-.1351	.0169
88	.0000	.5619	.0101	-.0027	-.1822	.0456	-.1797	.0110
89	.0000	.1452	.0026	.0012	-.0547	-.0050	-.0300	-.0004
90	.0000	.2576	.0047	.0019	-.0935	-.0096	-.0523	.0015
91	.0000	.3182	.0057	.0015	-.1110	-.0137	-.0609	.0007
92	.0000	.4452	.0080	-.0030	-.1320	-.0212	-.0713	-.0083
93	.0000	.5619	.0101	-.0103	-.1367	.0035	-.1027	-.0251
94	.0000	.6483	.0117	-.0168	-.1223	.0411	-.1396	-.0329
95	.0000	.6221	.0112	-.0179	-.0987	.0146	-.0943	-.0359
96	.0000	.6885	.0124	-.0279	-.0356	.0536	-.1096	-.0397
97	.0000	.7399	.0134	-.0369	.0284	.1074	-.1413	-.0373
98	.0000	.7834	.0141	-.0452	.0929	.1703	-.1843	-.0310
99	.0000	.8245	.0149	-.0604	.2390	.2663	-.2250	-.0100
100	.0000	.8744	.0158	-.0785	.4206	.4156	-.3181	.0232
101	.0000	.9242	.0167	-.0897	.5269	.5475	-.4301	.0453
102	.0000	.9659	.0174	-.0992	.6195	.6652	-.5311	.0651
103	.0000	.1452	.0026	-.0005	-.0493	-.0270	-.0006	-.0176
104	.0000	.2576	.0047	-.0012	-.0791	-.0609	.0081	-.0171
105	.0000	.3182	.0057	-.0023	-.0895	-.0753	.0170	-.0189
106	.0000	.4452	.0080	-.0085	-.0886	-.0948	.0330	-.0269
107	.0000	.5696	.0103	-.0196	-.0561	-.0495	.0073	-.0417
108	.0000	.6221	.0112	-.0277	-.0019	-.0226	.0046	-.0427
109	.0000	.6885	.0124	-.0397	.0882	.0495	-.0354	-.0337
110	.0000	.7834	.0141	-.0589	.2458	.2121	-.1529	-.0094
111	.0000	.8245	.0149	-.0676	.3215	.2976	-.2207	.0040
112	.0000	.0884	.0016	-.0009	-.0297	-.0198	.0062	-.0174
113	.0000	.1610	.0029	-.0008	-.0498	-.0555	.0278	-.0234
114	.0000	.2444	.0045	-.0016	-.0666	-.1181	.0732	-.0251

*Elastic modes start at "mode 4."

TABLE 11-6 AIRPLANE VIBRATION MODE SHAPES* , FINAL STIFFNESS DESIGN

ANTISYMMETRIC , LOW GROSS WEIGHT

ROW	MODE 1	MODE 2	MODE 3	MODE 4	MODE 5	MODE 6	MODE 7	MODE 8
115	.0000	.3182	.0057	-.0040	-.0729	-.1519	.1047	-.0308
116	.0000	.4119	.0074	-.0097	-.0593	-.1732	.1356	-.0368
117	.0000	.4065	.0090	-.0164	-.0260	-.1749	.1524	-.0340
118	.0000	.5461	.0099	-.0231	.0035	-.1333	.1325	-.0420
119	.0000	.6200	.0112	-.0379	.1061	-.0563	.1084	-.0402
120	.0000	.6806	.0123	-.0507	.2091	.0504	.0348	-.0220
121	.0000	.7317	.0132	-.0614	.2996	.1486	-.0408	-.0035
122	.0000	.7553	.0136	-.0674	.3554	.2049	-.0811	.0063
123	.0000	.7957	.0144	-.0751	.4242	.2964	-.1618	.0207
124	.0000	.8500	.0153	-.0857	.5217	.4298	-.2804	.0414
125	.0000	.9042	.0163	-.0966	.6239	.5732	-.4090	.0637
126	.0000	.9313	.0168	-.1022	.6762	.6476	-.4760	.0753
127	.0000	.9659	.0174	-.1092	.7432	.7427	-.5619	.0902
128	.0000	1.0000	.0181	-.1162	.8084	.8350	-.6450	.1046
129	.0000	.1206	.0022	-.0023	-.0341	-.0607	.0427	-.0210
130	.0000	.2172	.0039	-.0026	-.0535	-.1382	.1045	-.0298
131	.0000	.1206	.0022	-.0033	-.0311	-.0821	.0662	-.0233
132	.0000	.2172	.0039	-.0037	-.0489	-.1689	.1390	-.0342
133	.0000	.3113	.0056	-.0040	-.0537	-.3186	.2817	-.0425
134	.0000	.4066	.0073	-.0121	-.0269	-.2518	.2375	-.0442
135	.0000	.4596	.0083	-.0162	-.0054	-.2577	.2549	-.0414
136	.0000	.4066	.0073	-.0144	.0013	-.3203	.3278	-.0506
137	.0000	.4596	.0083	-.0184	.0216	-.3233	.3417	-.0476
138	.0000	.5604	.0101	-.0283	.0739	-.2072	.2469	-.0317
139	.0000	.6336	.0114	-.0511	.2423	-.0126	.1323	-.0192
140	.0000	.6954	.0126	-.0628	.3317	.1005	.0440	-.0023
141	.0000	.7608	.0137	-.0770	.4646	.01	-.0907	.0253
142	.0000	.8156	.0147	-.0878	.5655	.010	-.2175	.0478
143	.0000	.8705	.0157	-.0988	.6704	.5513	-.3537	.0717
144	.0000	.9253	.0167	-.1101	.7800	.7117	-.4990	.0973
145	.0000	.9659	.0174	-.1188	.8687	.8451	-.6224	.1192
146	.0000	1.0000	.0181	-.1260	.9389	.9488	-.7171	.1359
147	.0000	.3164	.0057	-.0029	-.0449	-.4790	.4445	-.0481
148	.0000	.5594	.0101	-.0293	.1492	-.3586	.4324	.0007
149	.0000	.6833	.0123	-.0666	.3801	.0951	.0836	.0032
150	.0000	.7720	.0139	-.0832	.5337	.3133	-.1208	.0388
151	.0000	.8544	.0154	-.0998	.6922	.5404	-.3268	.0754
152	.0000	.9367	.0169	-.1171	.8648	.7973	-.5623	.1172

*Elastic modes start at "mode 4."

TABLE 11-6 AIRPLANE VIBRATION MODE SHAPES* , FINAL STIFFNESS DESIGN

ANTISYMMETRIC , LOW GROSS WEIGHT

ROW	MODE 1	MODE 2	MODE 3	MODE 4	MODE 5	MODE 6	MODE 7	MODE 8
153	.0000	1.0000	.0181	-.1306	1.0000	1.0000	-.7484	.1503
154	.0000	.7650	.0138	-.0309	-.0501	.1242	-.2040	-.0436
155	.0000	.7893	.0143	-.0371	.0005	.1575	-.2176	-.0412
156	.0000	.8155	.0147	-.0441	.0605	.2007	-.2390	-.0354
157	.0000	.8408	.0152	-.0511	.1232	.2496	-.2670	-.0273
158	.0000	.8654	.0156	-.0581	.1872	.3025	-.2597	-.0177
159	.0000	.8906	.0161	-.0654	.2569	.3636	-.3404	-.0059
160	.0000	.9153	.0165	-.0728	.3290	.4308	-.3881	.0075
161	.0000	.9405	.0170	-.0805	.4064	.5062	-.4434	.0227
162	.0000	.9642	.0174	-.0878	.4813	.5813	-.4995	.0378
163	.0000	.9912	.0179	-.0964	.5699	.6730	-.5693	.0561
164	1.0000	-.0157	-.2474	-.1473	-.0155	.0794	.0765	-.0888
165	1.0000	-.0585	-.2938	-.1720	-.0257	.0596	.1387	-.1018
166	1.0000	-.1144	-.3545	-.2058	-.0527	.0096	.2737	-.1383
167	1.0000	-.1547	-.3976	-.2364	-.0736	-.0123	.4559	-.2176
168	1.0000	-.1860	-.4322	-.2632	-.0915	-.0261	.6354	-.3026
169	1.0000	-.2186	-.4676	-.2922	-.1109	-.0380	.8443	-.4052
170	1.0000	.0018	-.2477	-.1491	-.0116	.0979	.0571	-.0895
171	1.0000	-.0418	-.2941	-.1737	-.0198	.0812	.1134	-.1005
172	1.0000	-.0998	-.3559	-.2083	-.0446	.0353	.2478	-.1372
173	1.0000	-.0145	-.3181	-.1920	-.0058	.1392	.0787	-.1076
174	1.0000	-.0698	-.3586	-.2133	-.0281	.0877	.1945	-.1347
175	1.0000	-.1313	-.4037	-.2422	-.0589	.0325	.4037	-.2107
176	1.0000	-.1742	-.4351	-.2661	-.0839	-.0029	.6087	-.2994
177	1.0000	-.0279	-.3894	-.2361	.0034	.1889	.0950	-.1247
178	1.0000	-.0831	-.4164	-.2543	-.0279	.1272	.2930	-.1962
179	1.0000	-.1387	-.4436	-.2746	-.0612	.0668	.5276	-.2891
180	1.0000	-.1800	-.4638	-.2906	-.0868	.0227	.7196	-.3687
181	1.0000	-.2219	-.4840	-.3069	-.1129	-.0227	.9189	-.4516
182	1.0000	-.0388	-.4498	-.2830	.0021	.2407	.2409	-.2198
183	1.0000	-.0807	-.4576	-.2882	-.0239	.1806	.3898	-.2694
184	1.0000	-.1512	-.4708	-.2976	-.0684	.0795	.6550	-.3612
185	1.0000	-.1825	-.4767	-.3018	-.0881	.0343	.7725	-.4016
186	1.0000	-.0418	-.4670	-.2970	.0013	.2564	.2939	-.2539
187	1.0000	-.1123	-.4802	-.3068	-.0433	.1562	.5632	-.3486
188	1.0000	-.1860	-.4940	-.3169	-.0901	.0500	.8465	-.4477
189	1.0000	-.2254	-.5013	-.3224	-.1152	-.0069	1.0000	-.5017
190	.0000	.7287	.0132	-.0618	.4393	.1429	-.3017	.5313

*Elastic modes start at "mode 4."

TABLE 11-6 AIRPLANE VIBRATION MODE SHAPES* , FINAL STIFFNESS DESIGN

ANTISYMMETRIC , LOW GROSS WEIGHT

ROW	MODE 1	MODE 2	MODE 3	MODE 4	MODE 5	MODE 6	MODE 7	MODE 8
191	.0000	-.0100	.2849	.1977	-.0351	-.1797	-.5259	.7838
192	.0000	.0000	-.0000	.0001	-.0016	-.0004	-.0004	-.0002
193	1.0000	.0181	.0021	-.0002	-.0116	-.0193	-.0119	-.0180
194	.0000	-.0035	.1007	.0621	.0025	-.0360	-.0428	.0205
195	.0000	.0000	-.0005	.0030	.0000	-.0000	-.0000	.0000
196	.0000	.0013	.0000	.0001	-.0008	.0009	-.0006	.0019
197	.0000	.0013	.0000	.0001	-.0008	.0009	-.0006	.0019
198	.0000	.0013	.0000	.0001	-.0008	.0009	-.0006	.0019
199	.0000	.0013	.0000	.0001	-.0008	.0009	-.0006	.0018
200	.0000	.0013	.0000	.0001	-.0008	.0009	-.0006	.0018
201	1.0000	-.0120	1.0000	1.0000	-.0404	.8657	.9214	1.0000
202	1.0000	-.0178	.9130	.8622	-.0248	.5787	.5907	.6348
203	1.0000	-.0223	.8401	.7503	-.0123	.3555	.3374	.3587
204	1.0000	-.0268	.7693	.6479	-.0007	.1655	.1283	.1355
205	1.0000	-.0338	.6478	.4933	.0169	-.0798	-.1216	-.1144
206	.0000	.0013	.0000	.0001	-.0008	.0008	-.0007	.0018
207	.0000	.0013	.0000	.0000	-.0008	.0007	-.0007	.0017
208	.0000	.0013	.0000	.0000	-.0008	.0007	-.0007	.0017
209	.0000	.0013	.0000	.0000	-.0008	.0007	-.0007	.0018
210	.0000	.0013	.0000	.0000	-.0008	.0008	-.0006	.0017
211	.0000	.0013	.0000	.0001	-.0008	.0008	-.0006	.0016
212	.0000	.0013	.0000	.0001	-.0008	.0008	-.0006	.0014
213	.0000	.0013	.0000	.0001	-.0007	.0007	-.0006	.0013
214	.0000	.0013	.0000	.0002	-.0007	.0006	-.0007	.0011
215	.0000	.0013	.0000	.0002	-.0007	.0005	-.0007	.0009
216	.0000	.0013	.0000	.0003	-.0007	.0004	-.0006	.0008
217	.0000	.0013	.0000	.0003	-.0006	.0003	-.0006	.0006
218	.0000	.0013	.0000	.0001	-.0006	.0003	-.0006	.0005
219	.0000	.0013	.0000	-.0002	-.0006	.0002	-.0006	.0003
220	.0000	.0013	.0000	-.0002	-.0006	.0002	-.0005	.0001
221	.0000	.0013	.0000	-.0002	-.0006	.0002	-.0004	-.0002
222	.0000	.0013	.0000	-.0001	-.0006	.0003	-.0003	-.0004
223	.0000	.0013	.0000	-.0000	-.0006	.0003	-.0003	-.0008
224	1.0000	-.0320	.6064	.4486	.0202	-.1320	-.1693	-.1485
225	1.0000	-.0311	.5545	.3967	.0233	-.1784	-.2047	-.1620
226	1.0000	-.0293	.5027	.3468	.0255	-.2089	-.2216	-.1597
227	1.0000	-.0275	.4508	.2995	.0266	-.2221	-.2199	-.1441
228	1.0000	-.0257	.3990	.2566	.0260	-.2161	-.2019	-.1222

*Elastic modes start at "mode 4."

TABLE 11-6 AIRPLANE VIBRATION MODE SHAPES* , FINAL STIFFNESS DESIGN

ANTISYMMETRIC , LOW GROSS WEIGHT

ROW	MODE 1	MODE 2	MODE 3	MODE 4	MODE 5	MODE 6	MODE 7	MODE 8
229	1.0000	-.0238	.3472	.2168	.0241	-.1975	-.1746	-.0993
230	1.0000	-.0220	.2953	.1788	.0214	-.1723	-.1440	-.0785
231	1.0000	-.0202	.2435	.1415	.0181	-.1441	-.1137	-.0617
232	1.0000	-.0184	.1917	.1042	.0144	-.1149	-.0855	-.0494
233	1.0000	-.0165	.1398	.0666	.0105	-.0865	-.0597	-.0419
234	1.0000	-.0147	.0880	.0286	.0070	-.0594	-.0355	-.0383
235	1.0000	-.0129	.0361	-.0119	.0038	-.0349	-.0137	-.0377
236	1.0000	-.0111	-.0157	-.0281	.0014	-.0158	.0038	-.0391
237	1.0000	.0059	-.0673	-.0160	-.0075	.0027	.0125	-.0391
238	1.0000	.0153	-.1190	-.0567	-.0118	.0206	.0312	-.0491
239	1.0000	.0146	-.1708	-.0937	-.0103	.0339	.0547	-.0589
240	1.0000	.0139	-.2227	-.1312	-.0097	.0449	.0744	-.0662
241	1.0000	-.0070	-.2750	-.1752	-.0012	.0384	.0794	-.0538
242	.0000	.0013	.0000	-.0000	-.0006	.0003	-.0003	-.0011
243	.0000	.0013	.0000	-.0000	-.0006	.0003	-.0004	-.0015
244	.0000	.0013	.0000	-.0000	-.0006	.0003	-.0004	-.0016
245	.0000	.0013	.0000	-.0000	-.0006	.0003	-.0004	-.0016
246	1.0000	-.0350	-.3349	-.2357	.0109	.0096	.0680	-.0018
247	1.0000	-.0732	-.4768	-.4166	.0330	-.1432	-.0193	.3301
248	1.0000	-.0928	-.5495	-.5211	.0476	-.2570	-.0792	.6287
249	1.0000	-.1146	-.6288	-.6387	.0646	-.3935	-.1521	.9999
250	.0000	.0013	.0000	-.0000	-.0006	.0003	-.0004	-.0017
251	.0000	.0000	-.0005	-.0007	.0000	-.0008	-.0005	.0022
252	.0000	-.0013	.0360	.0539	-.0026	.0595	.0364	-.1549
253	1.0000	-.0948	-.5821	-.5698	.0514	-.3117	-.1114	.7726
254	.0000	.0922	.0017	-.0017	-.0424	.0220	-.0271	-.1191
255	.0000	.0013	.0000	-.0000	-.0006	.0003	-.0004	-.0016
256	.0000	.0000	-.0005	-.0007	.0000	-.0008	-.0005	.0019
257	1.0000	-.2176	-.5536	-.5212	.1045	-.2879	-.0445	.7870
258	1.0000	-.0314	.6979	.5534	.0103	.0074	-.0364	-.0339
259	1.0000	-.0542	-.4077	-.3237	.0209	-.0557	.0299	.1245
260	.0000	.0013	.0000	-.0000	-.0006	.0002	-.0004	-.0014

*Elastic modes start at "mode 4."

TABLE 11-6 AIRPLANE VIBRATION MODE SHAPES , FINAL STIFFNESS DESIGN

ANTISYMMETRIC , LOW GROSS WEIGHT

ROW	MODE 9	MODE 10	MODE 11	MODE 12	MODE 13	MODE 14	MODE 15	MODE 16
1	-.0068	.1695	.0126	-.0043	-.0045	-.1338	-.0365	.0467
2	.0485	-.2256	-.0174	-.0506	.0765	-.3436	-.0074	.0200
3	.0185	.4388	.0082	-.0207	.0227	-.0994	.0153	-.0010
4	.0004	-.0033	-.0005	-.0007	.0016	-.0089	-.0005	.0006
5	-.0001	-.0033	-.0002	.0002	.0000	.0022	.0006	-.0005
6	.0001	-.0006	-.0000	-.0000	.0001	-.0003	.0001	-.0001
7	-.0151	-.1683	.0232	-.0109	-.0146	-.0727	.0037	.0807
8	.0286	.1791	-.0103	.0401	-.0645	-.4780	.0396	.0502
9	.0043	-.3292	-.0121	.0183	-.0349	-.0507	-.0069	.0101
10	.0000	.0029	-.0005	.0009	-.0008	-.0114	.0001	.0008
11	-.0001	.0032	-.0005	.0002	.0005	.0012	-.0003	-.0012
12	.0000	.0002	-.0000	.0001	-.0001	-.0010	.0001	.0002
13	-.0277	-.0413	.0660	-.0288	-.0316	-.3247	-.2055	-.1092
14	-.0417	-.0003	.0933	-.0391	-.0414	-.4771	-.2195	-.1012
15	-.0473	-.0805	.0900	-.0330	-.0309	-.3615	.0200	.0365
16	-.0389	-.0645	.0251	-.0006	.0067	.1150	.2025	.1151
17	-.0327	-.0084	-.0919	.0507	.0426	.4688	-.0694	.1367
18	-.0534	.0355	-.1224	.0616	.0296	.3608	-.3665	.2506
19	-.1069	.1708	-.0831	.0327	.0344	.3262	-.4091	.2613
20	-.1791	.3865	-.0313	-.0176	.0575	.4582	-.3357	.3683
21	-.2439	.5714	.0157	-.0638	.0845	.6303	-.2106	.5328
22	-.0207	-.0309	.0492	-.0215	-.0235	.0038	-.1537	-.0827
23	-.0266	-.0396	.0608	-.0262	-.0283	.0000	-.1796	-.0915
24	-.0309	-.0466	.0695	-.0295	-.0315	-.3553	-.1868	-.0910
25	-.0357	-.0550	.0796	-.0333	-.0352	-.4058	-.1854	-.0853
26	-.0387	-.0610	.0854	-.0351	-.0366	-.4324	-.1643	-.0701
27	-.0421	-.0684	.0911	-.0365	-.0372	-.4502	-.1221	-.0428
28	-.0432	-.0719	.0896	-.0347	-.0344	-.4151	-.0602	-.0072
29	-.0435	-.0736	.0855	-.0320	-.0306	-.3629	-.0066	.0211
30	-.0422	-.0729	.0723	-.0246	-.0214	-.2389	.0787	.0608
31	-.0394	-.0683	.0512	-.0140	-.0087	-.0742	.1494	.0887
32	-.0134	-.0200	.0318	-.0138	-.0151	-.1595	-.0994	-.0548
33	-.0155	-.0291	.0442	-.0189	-.0204	-.2253	-.1291	-.0660
34	-.0240	-.0360	.0536	-.0227	-.0243	-.2736	-.1440	-.0703
35	-.0292	-.0449	.0647	-.0270	-.0285	-.3286	-.1435	-.0680
36	-.0326	-.0512	.0716	-.0294	-.0306	-.3602	-.1375	-.0588
37	-.0365	-.0591	.0785	-.0314	-.0319	-.3849	-.1024	-.0356
38	-.0385	-.0640	.0796	-.0309	-.0305	-.3676	-.0533	-.0067

TABLE 11-6 AIRPLANE VIBRATION MODE SHAPES , FINAL STIFFNESS DESIGN

ANTISYMMETRIC , LOW GROSS WEIGHT

ROW	MODE 9	MODE 10	MODE 11	MODE 12	MODE 13	MODE 14	MODE 15	MODE 16
39	-.0393	-.0665	.0770	-.0288	-.0274	-.3249	-.0029	.0205
40	-.0387	-.0669	.0657	-.0223	-.0192	-.2140	.0766	.0576
41	-.0365	-.0633	.0465	-.0124	-.0074	-.0609	.1429	.0831
42	-.0343	-.0572	.0210	.0001	.0069	.1121	.1854	.0999
43	-.0315	-.0460	-.0118	.0154	.0223	.2787	.1771	.1052
44	-.0296	-.0329	-.0428	.0290	.0328	.3961	.1113	.1056
45	-.0297	-.0122	-.0841	.0468	.0395	.4386	-.0523	.1181
46	-.0320	-.0006	-.1030	.0546	.0379	.4162	-.1639	.1381
47	-.0388	.0044	-.1129	.0581	.0313	.3729	-.2700	.1855
48	-.0455	.0146	-.1128	.0580	.0265	.3284	-.3216	.2052
49	-.0559	.0379	-.1048	.0548	.0250	.2918	-.3464	.2004
50	-.0671	.0667	-.0946	.0495	.0250	.2674	-.3569	.1913
51	-.0806	.1043	-.0827	.0419	.0267	.2561	-.3504	.1852
52	-.0960	.1487	-.0693	.0323	.0299	.2570	-.3552	.1848
53	-.1154	.2051	-.0536	.0193	.0353	.2758	-.3401	.1959
54	-.1386	.2722	-.0363	.0033	.0429	.3163	-.3154	.2267
55	-.1661	.3518	-.0161	-.0167	.0529	.3766	-.2712	.2754
56	-.1949	.4345	.0050	-.0376	.0644	.4483	-.2152	.3391
57	-.2312	.5383	.0319	-.0641	.0800	.5481	-.1300	.4342
58	-.2666	.6391	.0587	-.0899	.0959	.6485	-.0367	.5327
59	-.0196	-.0293	.0436	-.0185	-.0198	-.2229	-.1190	-.0588
60	-.0193	-.0292	.0423	-.0177	-.0186	-.2136	-.0984	-.0456
61	-.0185	-.0288	.0400	-.0164	-.0169	-.1971	-.0718	-.0305
62	-.0261	-.0412	.0569	-.0232	-.0240	-.2824	-.0995	-.0412
63	-.0175	-.0281	.0370	-.0147	-.0148	-.1760	-.0420	-.0142
64	.0315	-.0517	.0669	-.0264	-.0265	-.3213	-.0684	-.0196
65	-.0159	-.0264	.0319	-.0121	-.0116	-.1360	-.0065	.0042
66	-.0288	-.0484	.0571	-.0215	-.0206	-.2452	-.0050	.0130
67	-.0097	-.0165	.0173	-.0061	-.0052	-.0554	.0174	.0113
68	-.0190	-.0329	.0332	-.0114	-.0098	-.1090	.0374	.0267
69	-.0306	-.0534	.0530	-.0181	-.0156	-.1758	.0623	.0464
70	-.0228	-.0335	.0179	-.0044	-.0022	-.0476	.0234	.0427
71	-.0205	-.0376	.0288	-.0080	-.0050	-.0543	.0831	.0455
72	-.0313	-.0550	.0413	-.0113	-.0069	-.0625	.1235	.0705
73	-.0066	-.0113	.0076	-.0018	-.0003	.0052	.0330	.0105
74	-.0098	-.0243	.0164	-.0041	-.0021	.0445	.0922	.0449
75	-.0205	-.0369	.0177	-.0021	.0023	.0412	.1190	.0536
76	-.0301	-.0511	.0208	-.0009	.0051	.0864	.1649	.0844

TABLE 11-6 AIRPLANE VIBRATION MODE SHAPES , FINAL STIFFNESS DESIGN

ANTISYMMETRIC , LOW GROSS WEIGHT

ROW	MODE 9	MODE 10	MODE 11	MODE 12	MODE 13	MODE 14	MODE 15	MODE 16
77	-.0048	-.0084	.0032	-.0000	.0019	.0311	.0388	.0077
78	-.0098	-.0177	.0044	.0011	.0047	.0686	.0777	.0203
79	-.0158	-.0274	.0036	.0035	.0086	.1173	.1170	.0378
80	-.0239	-.0382	-.0024	.0088	.0152	.1956	.1536	.0688
81	-.0044	-.0069	-.0011	.0020	.0054	.0734	.0552	.0026
82	-.0085	-.0146	-.0054	.0054	.0108	.1420	.0910	.0061
83	-.0125	-.0213	-.0056	.0069	.0126	.1646	.1098	.0203
84	-.0193	-.0285	-.0178	.0148	.0200	.2554	.1275	.0477
85	-.0268	-.0329	-.0350	.0249	.0295	.3503	.1221	.0899
86	-.0088	-.0149	-.0130	.0092	.0161	.2031	.1032	-.0027
87	-.0138	-.0168	-.0319	.0194	.0258	.2939	.0890	.0136
88	-.0213	-.0194	-.0566	.0330	.0332	.3734	.0335	.0603
89	-.0015	-.0003	-.0045	.0028	.0073	.1058	.0635	-.0146
90	-.0034	-.0073	-.0114	.0064	.0142	.1898	.0960	-.0276
91	-.0044	-.0093	-.0169	.0091	.0181	.2295	.1009	-.0326
92	-.0074	-.0060	-.0386	.0197	.0280	.2870	.0545	-.0313
93	-.0140	-.0023	-.0709	.0372	.0348	.3235	-.0510	-.0069
94	-.0245	-.0067	-.0914	.0496	.0318	.3280	-.1460	.0715
95	-.0190	-.0153	-.0804	.0453	.0261	.2624	-.1195	.0283
96	-.0312	-.0172	-.0861	.0499	.0206	.2289	-.2133	.0762
97	-.0457	.0099	-.0845	.0493	.0187	.2057	-.2699	.1066
98	-.0628	.0550	-.0786	.0447	.0213	.2073	-.3061	.1248
99	-.0893	.1329	-.0399	.0233	.0252	.1576	-.2500	.0611
100	-.1395	.2817	.0127	-.0167	.0419	.2089	-.1271	.0707
101	-.1903	.4252	.0356	-.0473	.0628	.3676	-.0803	.2295
102	-.2371	.5574	.0577	-.0764	.0834	.5250	-.0202	.3947
103	.0025	.0297	-.0019	.0009	.0055	.1035	.0707	-.0224
104	.0025	.0458	-.0088	.0026	.0132	.1838	.0949	-.0475
105	.0028	.0384	-.0153	.0033	.0202	.1902	.0875	-.0564
106	.0013	-.0114	-.0344	.0129	.0256	.2152	.0330	-.0751
107	-.0066	-.0600	-.0569	.0367	.0113	.1156	-.0549	-.0481
108	-.0125	-.0769	-.0550	.0418	.0041	.0492	-.0952	-.0571
109	-.0272	-.0501	-.0439	.0409	.0033	.0029	-.1310	-.0842
110	-.0693	.0796	-.0185	.0226	.0165	.0360	-.1500	-.0795
111	-.0972	.1607	-.0060	.0078	.0260	.0950	-.1490	-.0331
112	.0029	.0283	.0011	-.0006	.0020	.0504	.0448	-.0104
113	.049	.0692	.0005	-.0007	.0044	.1033	.0734	-.0292
114	.0073	.1336	-.0024	-.0020	.0103	.1434	.0859	-.0535

TABLE 11-6 AIRPLANE VIBRATION MODE SHAPES , FINAL STIFFNESS DESIGN

ANTISYMMETRIC , LOW GROSS WEIGHT

ROW	MODE 9	MODE 10	MODE 11	MODE 12	MODE 13	MODE 14	MODE 15	MODE 16
115	.0095	.1434	-.0087	-.0043	.0202	.1145	.0692	-.0585
116	.0106	.0203	-.0204	.0004	.0223	.1172	.0390	-.0914
117	.0065	-.1429	-.0278	.0132	.0038	.1100	-.0023	-.0925
118	.0031	-.1677	-.0317	.0272	-.0118	-.0240	-.0180	-.0697
119	-.0013	-.1660	-.0136	.0383	-.0237	-.2294	-.0092	-.1875
120	-.0168	-.0814	.0102	.0334	-.0088	-.2390	.0063	-.3212
121	-.0399	.0068	.0266	.0191	.0019	-.1969	.0158	-.3342
122	-.0581	.0607	.0415	.0088	.0104	-.1651	.0416	-.3286
123	-.0920	.1559	.0515	-.0106	.0220	-.0682	.0575	-.2504
124	-.1434	.3003	.0693	-.0398	.0429	.0988	.0960	-.0923
125	-.2008	.4610	.0908	-.0729	.0684	.3034	.1552	.1237
126	-.2311	.5459	.1027	-.0907	.0824	.4162	.1924	.2486
127	-.2659	.6547	.1178	-.1135	.1004	.5616	.2401	.4106
128	-.3073	.7595	.1320	-.1353	.1175	.6997	.2800	.5624
129	.0057	.0775	.0018	-.0037	.0062	.0506	.0716	-.0358
130	.0103	.1686	.0008	-.0069	.0126	.0944	.0998	-.0695
131	.0076	.1062	.0032	-.0065	.0086	.0313	.0876	-.0517
132	.0132	.2113	.0028	-.0109	.0158	.0680	.1174	-.0892
133	.0212	.4754	.0117	-.0234	.0212	-.1206	.0119	-.0053
134	.0178	.0095	-.0103	-.0056	.0116	.0441	.0401	-.1336
135	.0156	-.1267	-.0146	.0018	-.0014	.0493	.0209	-.1495
136	.0240	-.0195	-.0025	-.0102	.0014	-.0145	.0441	-.1955
137	.0216	-.1578	-.0072	-.0026	-.0114	-.0062	.0251	-.2129
138	.0066	-.3540	-.0053	.0209	-.0471	-.1651	-.0003	-.0067
139	.0044	-.1528	.0447	.0316	-.0193	-.4106	.1289	-.5429
140	-.0151	-.0541	.0630	.0254	-.0024	-.3781	.1325	-.5916
141	-.0755	.1150	.0871	-.0036	.0164	-.2158	.1903	-.4334
142	-.1314	.2712	.1069	-.0470	.0389	-.0325	.2559	-.2689
143	-.1920	.4436	.1308	-.0839	.0668	.1942	.3433	-.0264
144	-.2606	.6337	.1599	-.1257	.1003	.4657	.4788	.2978
145	-.3199	.8005	.1900	-.1648	.1327	.7253	.6678	.6382
146	-.3645	.9259	.2105	-.1930	.1557	.9109	.7776	.8699
147	.0307	.8406	.0320	-.0426	.0242	-.3826	-.0573	.0755
148	.0102	-.6975	.0371	.0009	-.0973	.2317	.0267	.1669
149	-.0053	-.0746	.0960	.0266	-.0037	-.5404	.2537	-.9303
150	-.0956	.1734	.1132	-.0320	.0243	-.1972	.2874	-.4472
151	-.1888	.4343	.1496	-.0888	.0659	.1402	.4317	-.1009
152	-.3007	.7488	.2026	-.1608	.1244	.6132	.7325	.4961

TABLE 11-6 AIRPLANE VIBRATION MODE SHAPES , FINAL STIFFNESS DESIGN

ANTISYMMETRIC , LOW GROSS WEIGHT

ROW	MODE 9	MODE 10	MODE 11	MODE 12	MODE 13	MODE 14	MODE 15	MODE 16
153	-.3859	1.0000	.2465	-.2190	.1724	1.0000	1.0000	1.0000
154	-.0512	.0295	-.1186	.0602	.0284	.3467	-.3528	.2345
155	-.0605	.0515	-.1124	.0572	.0274	.3211	-.3755	.2360
156	-.0725	.0829	-.1027	.0513	.0277	.3022	-.3888	.2325
157	-.0869	.1227	-.0911	.0429	.0296	.2962	-.3926	.2310
158	-.1031	.1688	-.0783	.0326	.0328	.3019	-.3902	.2344
159	-.1231	.2264	-.0630	.0191	.0381	.3241	-.3772	.2492
160	-.1467	.2943	-.0460	.0026	.0457	.3672	-.3545	.2827
161	-.1746	.3743	-.0259	-.0173	.0559	.4296	-.3132	.3358
162	-.2032	.4563	-.0053	-.0378	.0673	.5014	-.2628	.4013
163	-.2395	.5598	.0214	-.0639	.0830	.6011	-.1827	.4985
164	.0229	.0180	.0154	-.0086	-.0192	.1519	.0180	-.0051
165	.0387	-.0136	.0259	-.0119	-.0293	.0848	.0888	-.0862
166	.0903	-.1164	.0724	.0331	-.0122	-.0705	.1546	-.2398
167	.1830	-.2551	.2628	.2283	.1817	-.0145	.0785	-.1672
168	.2750	-.3932	.4762	.4498	.4099	.0915	-.0450	-.0185
169	.3839	-.5554	.7407	.7262	.6991	.2470	-.2221	.2082
170	.0183	.0303	.0108	-.0070	-.0177	.1678	-.0064	.0188
171	.0305	.0061	.0173	-.0162	-.0322	.1057	.0671	-.0562
172	.0825	-.0922	.0707	.0321	-.0073	-.0306	.1352	-.2011
173	.0240	.0421	.0205	-.0079	-.0190	.1541	.0280	-.0085
174	.0663	-.0428	.0663	.0296	.0019	.0492	.0951	-.1230
175	.1639	-.2051	.2448	.2095	.1721	.0408	.0591	-.1158
176	.2653	-.3676	.4678	.4410	.4062	.1224	-.0569	.0118
177	.0296	.0594	.0335	-.0078	-.0168	.1499	.0663	-.0368
178	.1231	-.0993	.2066	.1694	.1518	.1583	.0169	-.0049
179	.2356	-.2896	.4408	.4127	.3927	.2143	-.0911	.1015
180	.3294	-.4467	.6472	.6287	.6111	.2842	-.2068	.2298
181	.4271	-.6104	.8645	.8567	.8424	.3603	-.3335	.3695
182	.1165	-.0309	.2605	.2239	.2342	.3657	-.0950	.2148
183	.1840	-.1577	.3875	.3564	.3597	.3566	-.1375	.2354
184	.3059	-.3843	.6278	.6093	.6032	.3620	-.2379	.3071
185	.3599	-.4849	.7337	.7195	.7104	.3625	-.2813	.3366
186	.1473	-.0663	.3451	.3115	.3296	.4450	-.1614	.3141
187	.2718	-.2961	.5935	.5722	.5830	.4611	-.2717	.4025
188	.4027	-.5390	.8556	.8478	.8510	.4734	-.3894	.4930
189	.4740	-.6711	1.0000	1.0000	1.0000	.4832	-.4593	.5505
190	.7063	.0995	.0451	-.0118	-.0151	-.2019	.1298	-.3912

TABLE 11-6 AIRPLANE VIBRATION MODE SHAPES , FINAL STIFFNESS DESIGN

ANTISYMMETRIC , LOW GROSS WEIGHT

ROW	MODE 9	MODE 10	MODE 11	MODE 12	MODE 13	MODE 14	MODE 15	MODE 16
191	1.0000	.0907	-.0622	-.0149	-.0012	.2503	-.0929	.3329
192	.0000	-.0002	-.0007	.0002	.0000	.0019	-.0019	.0028
193	.0016	.0082	.0092	-.0055	-.0099	.1385	-.0013	-.0062
194	-.0078	-.0070	-.0001	.0011	.0028	-.0548	-.0089	.0125
195	-.0000	-.0000	-.0000	.0000	.0000	-.0000	.0000	.0000
196	-.0002	-.0002	.0004	-.0002	-.0002	-.0017	-.0015	-.0007
197	-.0002	-.0002	.0004	-.0002	-.0002	-.0017	-.0015	-.0007
198	-.0002	-.0002	.0004	-.0002	-.0002	-.0017	-.0015	-.0007
199	-.0002	-.0002	.0004	-.0002	-.0002	-.0017	-.0015	-.0007
200	-.0002	-.0002	.0004	-.0002	-.0002	-.0017	-.0015	-.0007
201	-.0281	.0834	-.0432	.0126	.0109	.3483	.1035	.1237
202	-.0207	.0492	-.0269	.0090	.0090	.1168	.0321	.0267
203	-.0155	.0236	-.0153	.0066	.0080	-.0475	-.0134	-.0347
204	-.0119	.0033	-.0073	.0054	.0082	-.1665	-.0379	-.0689
205	-.0104	-.0186	-.0031	.0068	.0123	-.2826	-.0380	-.0794
206	-.0002	-.0002	.0004	-.0002	-.0002	-.0017	-.0015	-.0007
207	-.0002	-.0002	.0004	-.0002	-.0002	-.0018	-.0015	-.0007
208	-.0002	-.0002	.0004	-.0002	-.0002	-.0017	-.0014	-.0006
209	-.0002	-.0002	.0004	-.0002	-.0002	-.0014	-.0013	-.0005
210	-.0002	-.0002	.0004	-.0002	-.0002	-.0013	-.0012	-.0005
211	-.0002	-.0002	.0004	-.0002	-.0002	-.0013	-.0010	-.0005
212	-.0001	-.0002	.0003	-.0001	-.0002	-.0013	-.0009	-.0005
213	-.0001	-.0002	.0003	-.0001	-.0001	-.0013	-.0007	-.0004
214	-.0001	-.0002	.0003	-.0001	-.0001	-.0012	-.0005	-.0004
215	-.0001	-.0002	.0002	-.0001	-.0001	-.0010	-.0003	-.0003
216	-.0001	-.0001	.0002	-.0001	-.0001	-.0008	-.0001	-.0002
217	-.0001	-.0001	.0002	-.0001	-.0000	-.0006	.0001	-.0001
218	-.0001	-.0001	.0001	-.0000	-.0000	-.0004	.0003	.0000
219	-.0000	-.0001	.0001	-.0000	-.0000	-.0002	.0004	.0001
220	-.0000	-.0000	.0001	-.0000	-.0000	-.0001	.0006	.0002
221	.0000	.0000	.0001	-.0000	-.0000	-.0001	.0007	.0002
222	.0001	.0000	.0001	-.0000	-.0000	-.0001	.0009	.0003
223	.0001	.0001	.0001	-.0000	-.0000	.0003	.0010	.0003
224	-.0119	-.0220	-.0040	.0080	.0144	-.2971	-.0287	-.0709
225	-.0145	-.0234	-.0066	.0099	.0173	-.2896	-.0090	-.0488
226	-.0166	-.0227	-.0092	.0112	.0190	-.2516	.0126	-.0192
227	-.0177	-.0200	-.0113	.0117	.0192	-.1895	.0317	.0118
228	-.0173	-.0160	-.0118	.0110	.0174	-.1221	.0406	.0325

TABLE 11-6 AIRPLANE VIBRATION MODE SHAPES , FINAL STIFFNESS DESIGN

ANTISYMMETRIC , LOW GROSS WEIGHT

ROW	MODE 9	MODE 10	MODE 11	MODE 12	MODE 13	MODE 14	MODE 15	MODE 16
229	-.0157	-.0116	-.0109	.0095	.0144	-.0586	.0411	.0429
230	-.0134	-.0074	-.0091	.0075	.0107	-.0033	.0370	.0461
231	-.0107	-.0035	-.0066	.0053	.0067	.0421	.0307	.0437
232	-.0077	-.0003	-.0037	.0030	.0028	.0751	.0239	.0379
233	-.0040	.0024	-.0010	.0009	-.0009	.1029	.0183	.0304
234	-.0012	.0050	.0013	-.0008	-.0039	.1266	.0125	.0215
235	.0020	.0071	.0030	-.0023	-.0065	.1464	.0063	.0123
236	.0049	.0087	.0042	-.0033	-.0084	.1622	.0004	.0045
237	.0069	.0094	.0062	-.0044	-.0100	.1707	.0006	-.0013
238	.0106	.0124	.0067	-.0052	-.0112	.1839	-.0002	-.0087
239	.0145	.0165	.0064	-.0036	-.0122	.1976	-.0052	-.0170
240	.0177	.0209	.0070	-.0064	-.0138	.2137	-.0086	-.0231
241	.0171	.0201	.0074	-.0073	-.0162	.2533	-.0316	-.0245
242	.0001	.0001	.0001	-.0001	-.0001	.0608	.0010	.0004
243	.0002	.0001	.0002	-.0001	-.0001	.0013	.0012	.0007
244	.0002	.0001	.0002	-.0001	-.0001	.0015	.0013	.0008
245	.0002	.0001	.0002	-.0001	-.0001	.0015	.0014	.0008
246	.0101	.0159	.0064	-.0071	-.0169	.2806	-.0626	-.0227
247	-.0413	.0020	-.0096	.0047	.0039	.0821	-.0427	-.0070
248	-.0878	-.0082	-.0292	.0194	.0309	-.2374	.0393	-.0013
249	-.1462	-.0205	-.0549	.0391	.0074	-.6889	.1245	.0084
250	.0002	.0001	.0002	-.0001	-.0001	.0017	.0017	.0010
251	-.0003	-.0001	-.0001	.0001	.0002	-.0027	.0011	.0002
252	.0246	.0047	.0101	-.0080	-.0155	.1913	-.0739	-.0119
253	-.1107	-.0127	-.0388	.0270	.0453	-.4156	.1035	.0076
254	.0161	.0079	.0137	-.0076	-.0094	.1204	.1141	.0697
255	.0002	.0001	.0002	-.0001	-.0001	.0015	.0013	.0008
256	-.0003	-.0001	-.0001	.0001	.0002	-.0022	.0007	.0001
257	-.1093	-.0186	-.0468	.0291	.0426	-.3808	-.0945	-.0786
258	-.0102	-.0116	-.0035	.0057	.0100	-.2469	-.0433	-.0810
259	-.0093	.0078	.0018	-.0038	-.0113	.2417	-.0693	-.0128
260	.0002	.0001	.0002	-.0001	-.0001	.0011	.0011	.0006

TABLE 11-6 AIRPLANE VIBRATION MODE SHAPES , FINAL STIFFNESS DESIGN

ANTISYMMETRIC , LOW GROSS WEIGHT

ROW	MODE 17	MODE 18	MODE 19	MODE 20
1	-.0031	-.0274	-.0120	-.0507
2	-.0050	-.0101	-.0034	-.0067
3	.0200	.0072	.0036	-.0054
4	-.0003	-.0008	.0003	-.0018
5	-.0005	.0002	.0003	-.0000
6	.0000	.0001	.0000	.0003
7	-.0204	-.0213	-.0037	-.1055
8	.0191	.0089	.0098	-.0169
9	.0132	.0201	.0185	.0302
10	-.0003	-.0006	.0007	-.0018
11	-.0008	-.0003	.0003	.0002
12	.0003	.0001	-.0000	.0001
13	-.3521	.0488	.076	-.0836
14	-.2706	.1113	.0758	.1401
15	.3347	-.1119	-.0467	.2343
16	.5129	-.0294	-.0744	-.2470
17	.1195	.0146	-.0251	-.2196
18	-.1620	.0011	-.0703	.0743
19	-.2219	-.0388	-.1396	.1315
20	-.1685	.0213	-.1239	.1711
21	-.0524	.1467	-.0339	.1973
22	-.2641	.0379	.0573	-.0668
23	-.2974	.0307	.0702	-.0309
24	-.2795	.0208	.0712	.0344
25	-.2299	.0089	.0644	.1176
26	-.1392	-.0045	.0480	.1963
27	.0066	-.0231	.0202	.2798
28	.1562	-.0382	-.0111	.2869
29	.2627	-.0458	-.0337	.2468
30	.3940	-.0485	-.0602	.1153
31	.4645	-.0409	-.0717	-.0589
32	-.1715	.0263	.0376	-.0484
33	-.2143	.0214	.0515	-.0218
34	-.2207	.0161	.0560	.0186
35	-.1858	.0062	.0521	.0922
36	-.1227	-.0034	.0410	.1549
37	.0069	-.0201	.0167	.2341
38	.1354	-.0335	-.0094	.2513

TABLE 11-6 AIRPLANE VIBRATION MODE SHAPES , FINAL STIFFNESS DESIGN

ANTISYMMETRIC , LOW GROSS WEIGHT

ROW	MODE 17	MODE 18	MODE 19	MODE 20
39	.2416	-.0418	-.0316	.2216
40	.3656	-.0447	-.0561	.0988
41	.4320	-.0372	-.0663	-.0626
42	.4544	-.0250	-.0650	-.2260
43	.4142	-.0062	-.0515	-.3351
44	.3147	.0047	-.0356	-.3395
45	.1149	.0144	-.0205	-.2091
46	-.0043	.0138	-.0219	-.0906
47	-.0967	.0087	-.0408	.0093
48	-.1445	-.0005	-.0578	.0620
49	-.1722	-.0186	-.0799	.0815
50	-.1890	-.0346	-.0992	.0909
51	-.1995	-.0467	-.1163	.0981
52	-.2038	-.0535	-.1298	.1048
53	-.1980	-.0503	-.1360	.1122
54	-.1810	-.0327	-.1319	.1233
55	-.1450	.0034	-.1103	.1330
56	-.0954	.0540	-.0738	.1417
57	-.0171	.1342	-.0094	.1495
58	.0716	.2230	.0678	.1517
59	-.1978	.0144	.0473	.0057
60	-.1347	.0048	.0365	.0472
61	-.0685	-.0028	.0219	.0791
62	-.0767	-.0055	.0278	.1293
63	.0030	-.0098	.0063	.1013
64	.0528	-.0224	.0045	.2109
65	.0714	-.0147	-.0098	.0839
66	.1681	-.0308	-.0225	.1754
67	.0604	-.0088	-.0107	.0163
68	.1512	-.0212	-.0247	.0415
69	.2817	-.0366	-.0446	.0797
70	.2492	-.0564	-.0035	-.0669
71	.2368	-.0220	-.0345	-.0195
72	.3701	-.0325	-.0564	-.0452
73	.0496	-.0015	-.0085	-.0246
74	.1314	-.0165	-.0204	-.0841
75	.2612	-.0147	-.0361	-.1036
76	.3918	-.0220	-.0556	-.1835

TABLE 11-6 AIRPLANE VIBRATION MODE SHAPES , FINAL STIFFNESS DESIGN

ANTISYMMETRIC , LOW GROSS WEIGHT

ROW	MODE 17	MODE 18	MODE 19	MODE 20
77	.0440	.0018	-.0063	-.0333
78	.1122	.0005	-.0138	-.0747
79	.1952	-.0015	-.0229	-.1334
80	.3079	-.0051	-.0365	-.2311
81	.0412	.0058	-.0017	-.0524
82	.0877	.0092	-.0026	-.0990
83	.1412	.0071	-.0102	-.1345
84	.2736	.0062	-.0186	-.2215
85	.2998	.0049	-.0316	-.3160
86	.0868	.0144	.0050	-.1202
87	.1220	.0154	.0039	-.1701
88	.1380	.0149	-.0068	-.2121
89	.0037	.0117	.0101	-.0465
90	.0222	.0192	.0179	-.0747
91	.0295	.0216	.0213	-.0829
92	.0343	.0195	.0236	-.0855
93	-.0104	.0133	.0183	-.0444
94	-.0417	.0082	-.0061	-.0313
95	-.0484	.0044	.0037	-.0100
96	-.1079	-.0148	-.0328	.0313
97	-.1463	-.0324	-.0647	.0552
98	-.1735	-.0479	-.0933	.0715
99	-.1634	-.0733	-.1113	.0572
100	-.0881	-.0329	-.0753	.0422
101	-.0243	.0590	-.0231	.0777
102	.0534	.1638	.0465	.1092
103	-.0526	.0155	.0145	-.0104
104	-.0370	.0255	.0281	-.0226
105	-.0194	.0260	.0325	-.0244
106	-.0205	.0206	.0378	.0052
107	-.0445	.0015	.0264	.0220
108	-.0727	-.0259	.0022	.0219
109	-.1051	-.0695	-.0415	.0059
110	-.1261	-.0989	-.0904	.0020
111	-.1205	-.0843	-.0950	.0160
112	-.0591	.0091	.0070	.0074
113	-.0716	.0196	.0164	.0114
114	-.0549	.0292	.0288	.0167

TABLE 11-6 AIRPLANE VIBRATION MODE SHAPES , FINAL STIFFNESS DESIGN

ANTISYMMETRIC , LOW GROSS WEIGHT

ROW	MODE 17	MODE 18	MODE 19	MODE 20
115	-.0321	.0255	.0323	.0119
116	-.0356	.0251	.0468	.0811
117	-.0312	.0244	.0445	.1159
118	-.0316	.0039	.0337	.0565
119	-.0523	-.0771	-.0061	-.0326
120	-.0740	-.1463	-.0517	-.0832
121	-.0730	-.1580	-.0719	-.0877
122	-.0571	-.1501	-.0667	-.0961
123	-.0309	-.1103	-.0492	-.0830
124	.0295	-.0208	.0024	-.0543
125	.1190	.1100	.0879	-.0141
126	.1754	.1885	.1424	.0086
127	.2471	.2903	.2131	.0385
128	.3097	.3824	.2738	.0690
129	-.0965	.0229	.0261	.0465
130	-.1018	.0390	.0450	.0675
131	-.1306	.0321	.0400	.0829
132	-.1410	.0502	.0620	.1132
133	.0093	.0086	.0048	.0147
134	-.0577	.0424	.0817	.3463
135	-.0621	.0548	.1041	.5461
136	-.0874	.0690	.1373	.7765
137	-.0923	.0826	.1621	1.0000
138	.0100	.0081	.0174	.0288
139	-.0452	-.2058	-.0433	-.1653
140	-.0539	-.2395	-.0774	-.1894
141	.0178	-.1467	-.0257	-.1614
142	.1016	-.0401	.0476	-.1450
143	.2223	.1203	.1653	-.1104
144	.4054	.3540	.3580	-.0722
145	.6443	.6349	.6221	-.0578
146	.7884	.8123	.7782	-.0379
147	.0855	-.0160	-.0356	-.0236
148	.1073	.0467	-.0127	-.0188
149	-.0485	-.3665	-.1091	-.3619
150	.0910	-.1149	.0201	-.1422
151	.2695	.1231	.2005	-.1570
152	.6575	.5920	.6218	-.1141

TABLE 11-6 AIRPLANE VIBRATION MODE SHAPES , FINAL STIFFNESS DESIGN

ANTISYMMETRIC , LOW GROSS WEIGHT

ROW	MODE 17	MODE 18	MODE 19	MODE 20
153	1.0000	1.0000	1.0000	-.0866
154	-.1580	-.0007	-.0674	.0716
155	-.1818	-.0139	-.0856	.0905
156	-.1998	-.0281	-.1053	.1033
157	-.2104	-.0384	-.1223	.1129
158	-.2156	-.0440	-.1362	.1221
159	-.2109	-.0399	-.1430	.1321
160	-.1949	-.0218	-.1398	.1452
161	-.1603	.0150	-.1192	.1578
162	-.1151	.0635	-.0867	.1699
163	-.0400	.1424	-.0253	.1808
164	.0074	.0274	-.0218	.0634
165	.0497	.0218	-.0116	.0451
166	.0766	-.0240	-.0143	-.0083
167	.0312	-.0312	.0038	-.0387
168	-.0422	-.0281	.0304	-.0665
169	-.1474	-.0172	.0673	-.0968
170	-.0026	.0276	-.0294	.0707
171	.0423	.0264	-.0189	.0586
172	.0723	-.0142	-.0176	.0050
173	.0332	.0301	-.0353	.0732
174	.0630	.0052	-.0247	.0316
175	.0331	-.0146	-.0047	-.0122
176	-.0419	-.0186	.0257	-.0508
177	.0730	.0333	-.0410	.0719
178	.0366	.0208	-.0231	.0450
179	-.0394	.0102	.0106	-.0017
180	-.1197	.0049	.0458	-.0471
181	-.2084	-.0008	.0852	-.0994
182	.0123	.0735	-.0408	.1257
183	-.0201	.0568	-.0167	.0817
184	-.1193	.0292	.0339	-.0062
185	-.1594	.0162	.0567	-.0471
186	-.0180	.0867	-.0363	.1374
187	-.1131	.0619	.0150	.0529
188	-.2181	.0322	.0736	-.0491
189	-.2797	.0161	.1078	-.1083
190	.0319	-.1263	-.0634	-.0604

TABLE 11-6 AIRPLANE VIBRATION MODE SHAPES , FINAL STIFFNESS DESIGN

ANTISYMMETRIC , LOW GROSS WEIGHT

ROW	MODE 17	MODE 18	MODE 19	MODE 20
191	.0050	.1218	.0506	.0645
192	-.0006	.0007	-.0000	.0011
193	-.0864	.0067	-.0058	-.0145
194	-.0412	-.0222	.0114	-.0446
195	-.0000	-.0000	.0000	-.0000
196	-.0036	.0003	.0007	-.0022
197	-.0036	.0003	.0007	-.0022
198	-.0035	.0003	.0007	-.0022
199	-.0035	.0003	.0007	-.0022
200	-.0034	.0003	.0007	-.0021
201	-.0023	-.1886	.0548	.1779
202	.0230	-.0381	.0092	.0253
203	.0439	.0547	-.0177	-.0568
204	.0670	.1028	-.0301	-.0796
205	.1266	.1063	-.0258	-.0172
206	-.0034	.0003	.0007	-.0021
207	-.0033	.0003	.0007	-.0021
208	-.0032	.0002	.0006	-.0020
209	-.0030	.0002	.0005	-.0018
210	-.0026	.0003	.0004	-.0016
211	-.0020	.0004	.0003	-.0012
212	-.0015	.0004	.0002	-.0008
213	-.0010	.0004	.0001	-.0005
214	-.0006	.0004	.0000	-.0002
215	-.0003	.0003	.0000	-.0001
216	-.0003	.0002	-.0000	-.0000
217	-.0003	.0002	-.0000	-.0000
218	-.0005	.0001	-.0000	-.0001
219	-.0008	.0000	-.0000	-.0001
220	-.0012	.0000	-.0001	-.0000
221	-.0017	.0000	-.0001	.0001
222	-.0023	.0001	-.0001	.0003
223	-.0029	.0000	-.0002	.0003
224	.1463	.0864	-.0164	.0239
225	.1651	.0443	-.0001	.0860
226	.1591	-.0043	.0154	.1279
227	.1301	-.0499	.0270	.1419
228	.0843	-.0774	.0330	.1236

Table 11-6.—(Concluded)

ANTISYMMETRIC , LOW GROSS WEIGHT

ROW	MODE 17	MODE 18	MODE 19	MODE 20
229	.0341	-.0883	.0339	.0877
230	-.0073	-.0874	.0304	.0517
231	-.0346	-.0781	.0237	.0236
232	-.0446	-.0637	.0150	.0049
233	-.0409	-.0472	.0060	-.0078
234	-.0310	-.0257	-.0014	-.0168
235	-.0145	-.0139	-.0067	-.0187
236	.0062	-.0025	-.0093	-.0159
237	.0231	.0063	-.0106	-.0087
238	.0419	.0147	-.0106	.0056
239	.0643	.0209	-.0093	.0235
240	.0841	.0242	-.0084	.0401
241	.1380	.0107	-.0008	.0339
242	-.0035	-.0001	-.0001	.0004
243	-.0047	-.0003	-.0002	.0005
244	-.0057	-.0004	-.0002	.0007
245	-.0058	-.0004	-.0002	.0008
246	.2051	-.0132	.0124	.0092
247	.1450	-.0312	.0209	-.0285
248	-.0590	.0157	-.0053	.0041
249	-.4142	.0983	-.0549	.0820
250	-.0073	-.0005	-.0003	.0011
251	-.0032	.0005	-.0004	.0006
252	.2164	-.0338	.0244	-.0425
253	-.2430	.0477	-.0272	.0414
254	-.4932	-.0342	-.0182	.0726
255	-.0055	-.0004	-.0002	.0007
256	-.0020	.0003	-.0002	.0003
257	.4947	.0495	.0160	-.0696
258	.0992	.1147	-.0308	-.0541
259	.2100	-.0363	.0232	-.0193
260	-.0042	-.0002	-.0001	.0004

Table 11-7.—Preliminary Symmetric Vibration Mode Frequencies

High Gross Weight Condition

Mode	Wing structure		
	Initial design 6-kip/in. engine beams	Initial design with stiffened tip and aileron	
		9-kip/in. engine beams	27-kip/in. engine beams
1	1.00Hz	1.02Hz	1.03Hz
2	1.26	1.24	1.24
3	1.47	1.65	1.65
4	1.93	1.98	2.13
5	2.17	2.30 ^a	2.40
6	2.28	2.32	2.75
7	2.74	2.75	2.78 ^a
8	2.93	2.98	3.10
9	3.54 ^b	3.53	3.58
10	3.64	3.69	3.76
11	3.85	3.83	3.89
12	4.08	4.40	4.45
13	4.38	4.72	4.74
14	4.64	5.32	5.37
15	4.86	5.65	5.78
16	5.42	6.08	6.10
17	6.00	6.42	6.48
18	6.10	6.97	6.97

^aOutboard nacelle resonance.

^bLanding gear resonance.

Table 11-8.—Preliminary Symmetric Wing Flutter Results

M = 0.9—High Gross Weight Condition

Wing structure	Wing trailing edge condition			
	a Attached		b Detached	
	Flutter speed, KEAS	Frequency, Hz	Flutter speed KEAS	Frequency, Hz
Initial design	181.0 ^a	2.18	372.0	1.71
6-kips/in. engine beams	278.0	3.58	366.0	3.55
Initial design with stiffened tip and aileron, 9-kips/in. engine beams	217.0 ^c	2.29	401.0	1.75
	420.0	3.67	415.0	3.66
Initial design with stiffened tip and aileron, 27-kips/in. engine beams	436.0	1.90	426.0	1.90
	435.0	3.72	437.0	3.71

a "Attached" refers to the attachment of the wing trailing edge structure to the engine support beam, thus causing the trailing edge to follow the engine translation.

b "Detached" refers to the isolation of the wing trailing edge structure such that the trailing edge does not follow the engine translation.

c 20000-ft solution, Mach number not matched.
Clearance speed (1.2 V_D): 504 KEAS.
Bare wing flutter speed (no nacelles and fin): 413 KEAS, 5.7 Hz.

Table 1.9. - Energy Balance--Preliminary Low Frequency Symmetric Flutter
M = 0.9--High Gross Weight Condition

Relative contributions to energy balance (20 freedoms, neutral stability)													
436 KEAS, 1.91 Hz													
Flutter Vector r	θ	F rce		Pitch	Mode						Residue (other freedoms)		
		Velocity	Plunge		1	2	4	5	6	8		11	15
0.04	22°	Plunge	-0.051	-0.063	-0.238	0.050	0.020	0.158	0.016	0.008	0.043	0.048	0.009
0.13	157°	Pitch	-0.007	-0.048	-0.284	0.038	0.061	0.117	0.023	0.038	0.036	0.019	0.007
1.00	0°	Mode 1	-0.039	-0.027	-1.000	-0.500	0.439	0.340	0.083	0.272	0.110	0.196	0.117
0.47	10°	2	-0.027	0.040	-0.096	-0.347	0.063	0.076	0.003	0.079	0.003	0.148	0.058
0.50	165°	4	0.008	-0.010	0.060	0.060	0.153	0.119	-0.006	-0.014	0.034	-0.055	-0.043
0.13	117°	5	0.011	0.022	0.214	0.013	-0.070	-0.092	-0.018	-0.037	-0.042	-0.002	0.001
0.25	4°	6	0.000	0.001	0.039	0.023	0.018	-0.011	-0.010	-0.011	-0.004	-0.007	-0.002
0.24	18°	8	0.015	0.002	0.055	0.025	0.032	-0.053	0.015	-0.032	-0.016	-0.002	-0.041
0.04	40°	11	0.005	0.005	0.048	0.016	-0.012	-0.023	-0.001	-0.014	-0.011	-0.002	-0.011
0.03	129°	15	0.002	0.003	0.023	0.004	-0.011	-0.008	-0.001	0.000	-0.003	-0.003	-0.006
Σ other freedoms			0.007	0.002	0.077	0.070	0.014	-0.044	0.015	-0.020	-0.002	-0.020	-0.099
Net energy			-0.076	-0.073	-1.102	-0.548	0.365	0.588	0.119	0.269	0.148	0.320	-0.010

Table 11-10.—Strength Resized Wing Flutter With Initial Stiffness Constraints
Symmetric—High Gross Weight Condition

Stiffness design modification number	Strength resized wing inboard of fin ^a		Wing flutter speed ratio, (actual/goal) goal = 504 KEAS at M = 0.9			
			Flutter frequencies			
	Wing tip	Lowspeed controls (stiffened aileron)	1.9Hz	2.4Hz	3.4Hz	4.4Hz
2	Initial design	Locked	0.744	0.768	0.817	0.966
1	Stiffened	Locked	0.817	0.849	1.042	—
3	Stiffened	Unlocked	0.817	0.837	0.909	—

^a27-kip/in. engine beams
(4.5 x strength design)

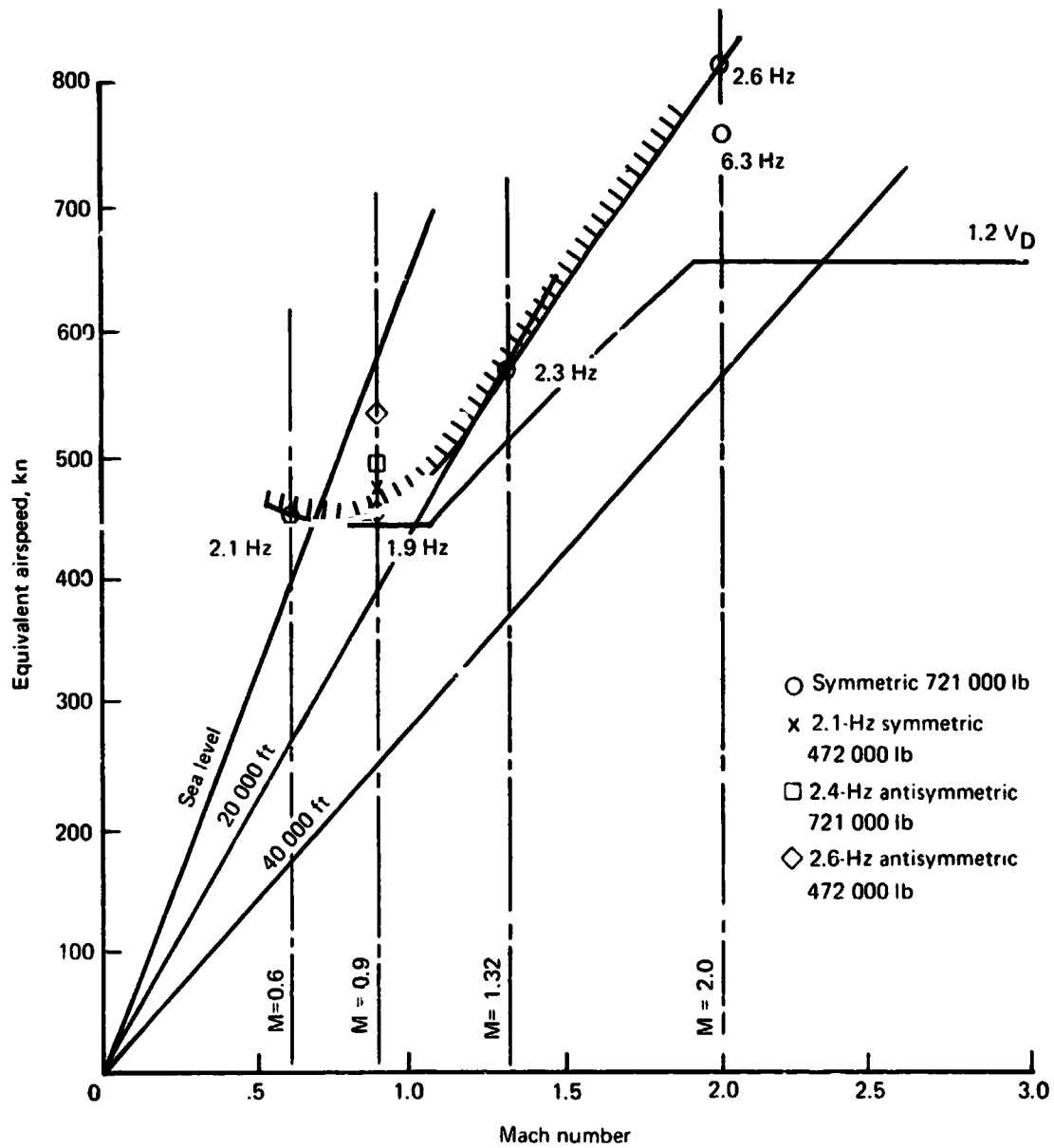


Figure 11-1.—Arrow Wing Flutter Boundary, 969-512B

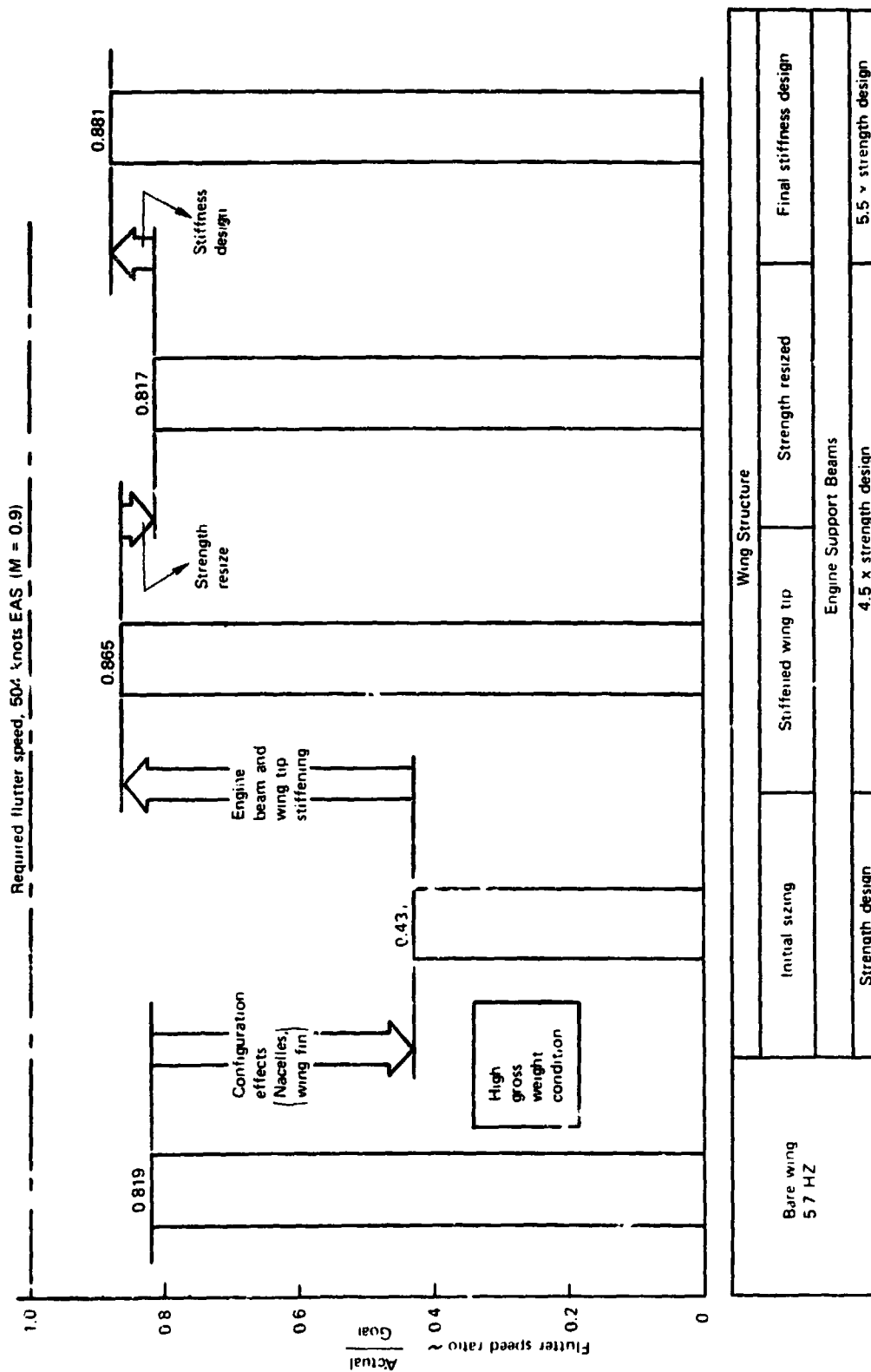


Figure 11 - 2. - Effect of Structural Changes on Critical Symmetric Flutter (1.9 HZ)

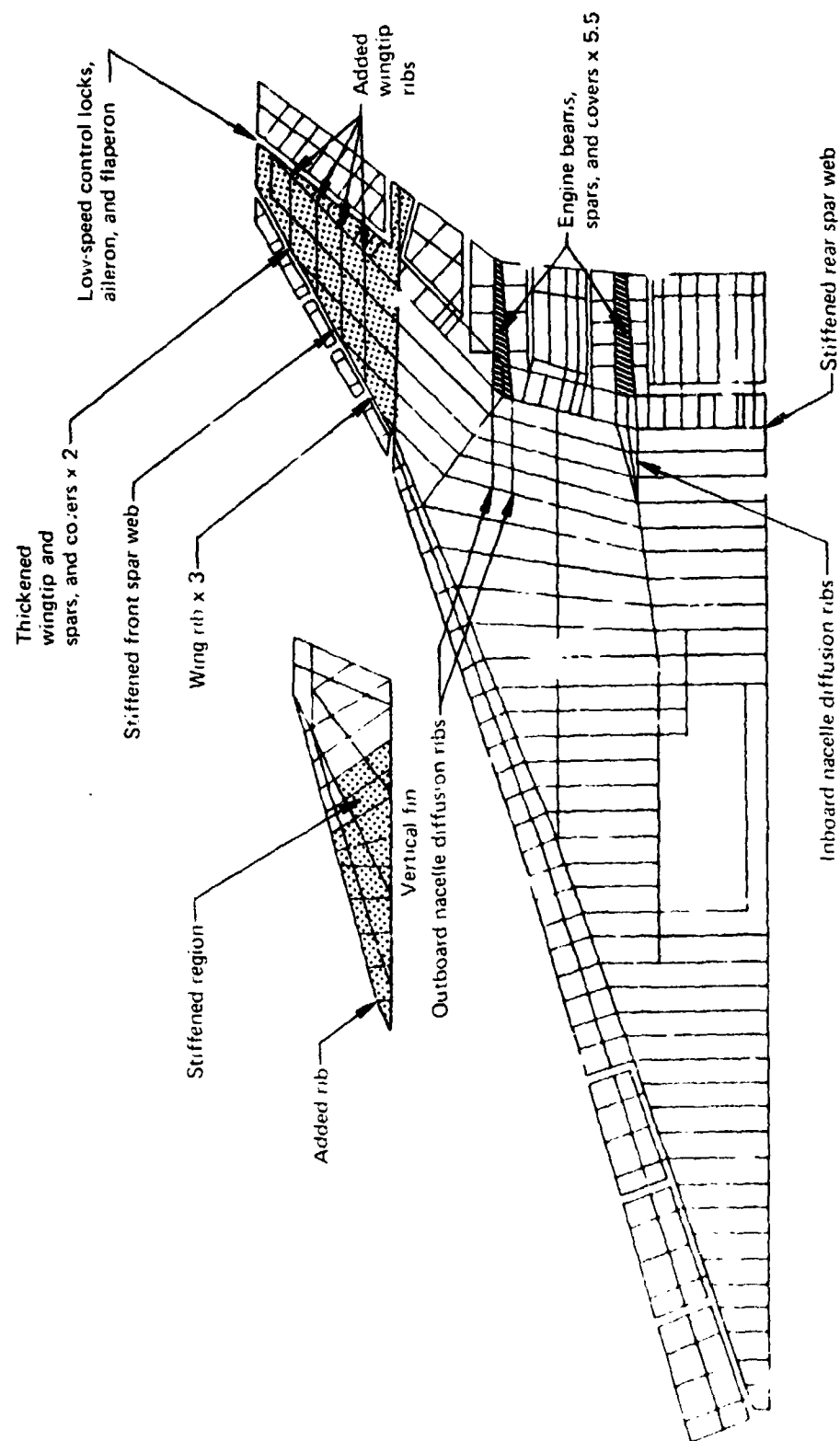


Figure 11-3. — Final Stiffness Design Modification 9

REPRODUCIBILITY OF THE
ORIGINAL PAGE IS POOR

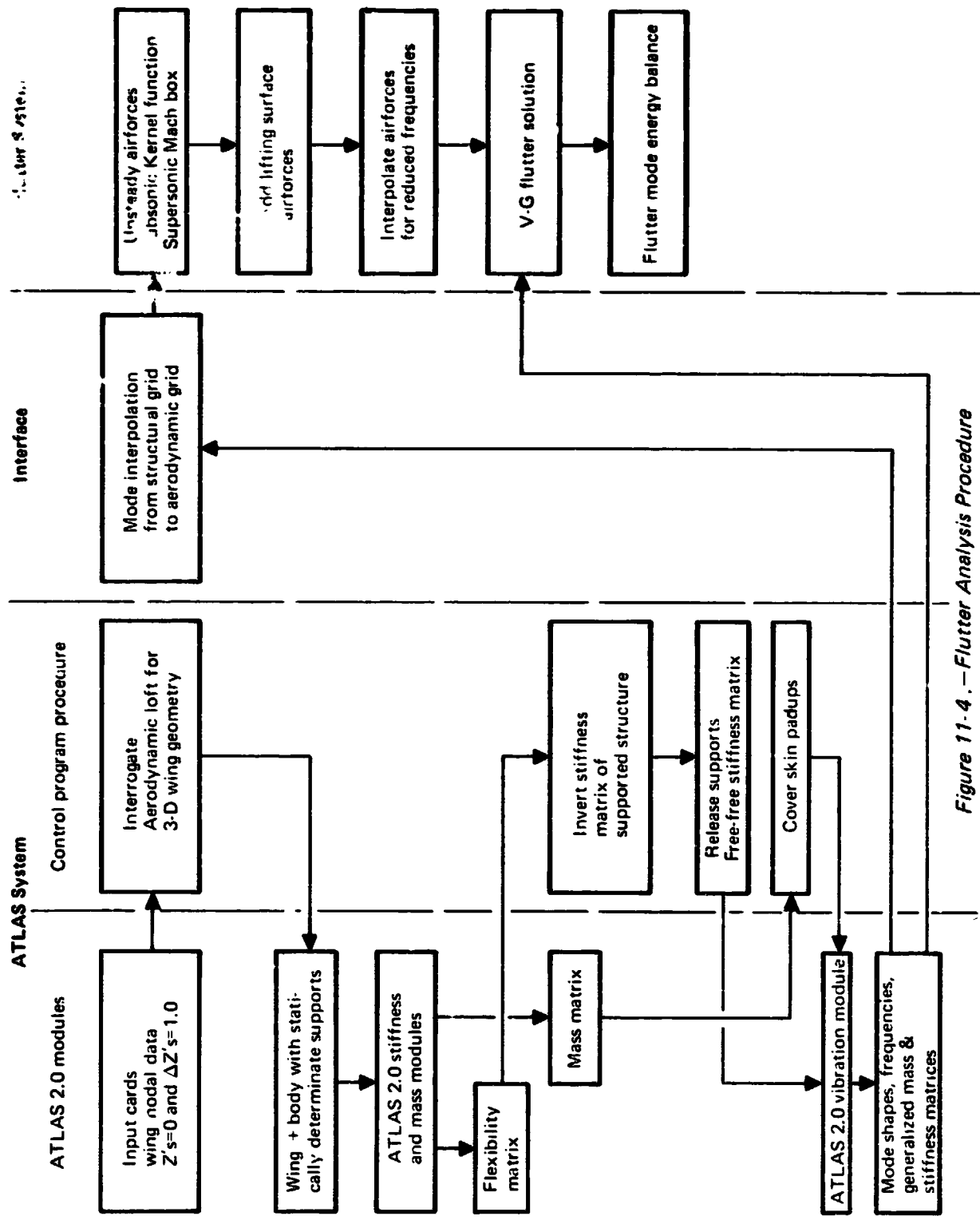


Figure 11-4. —Flutter Analysis Procedure

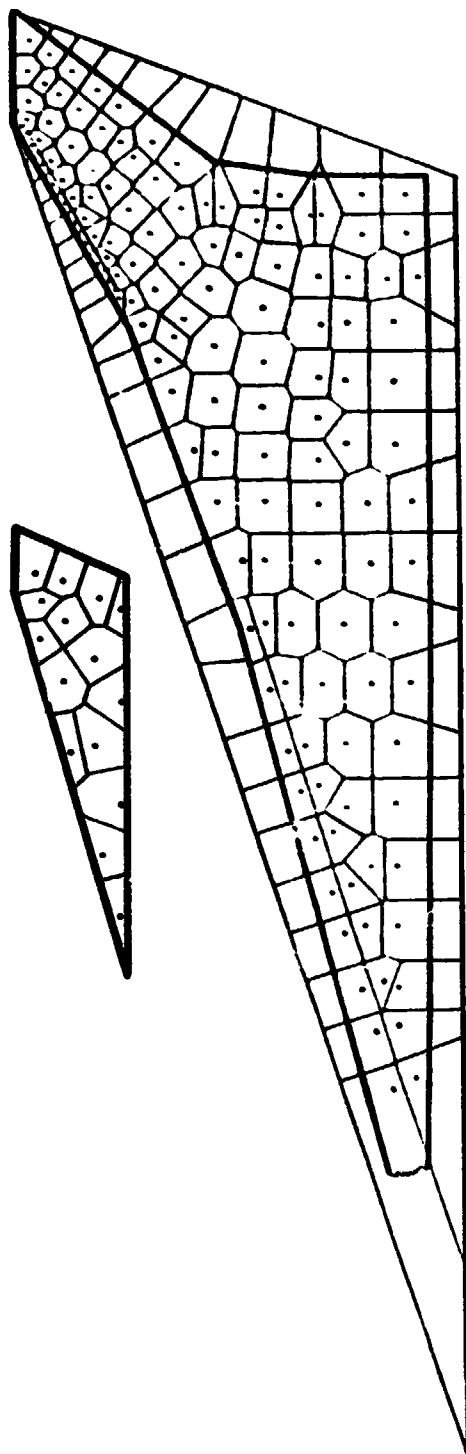


Figure 11-5.—Wing Mass Paneling for Flutter

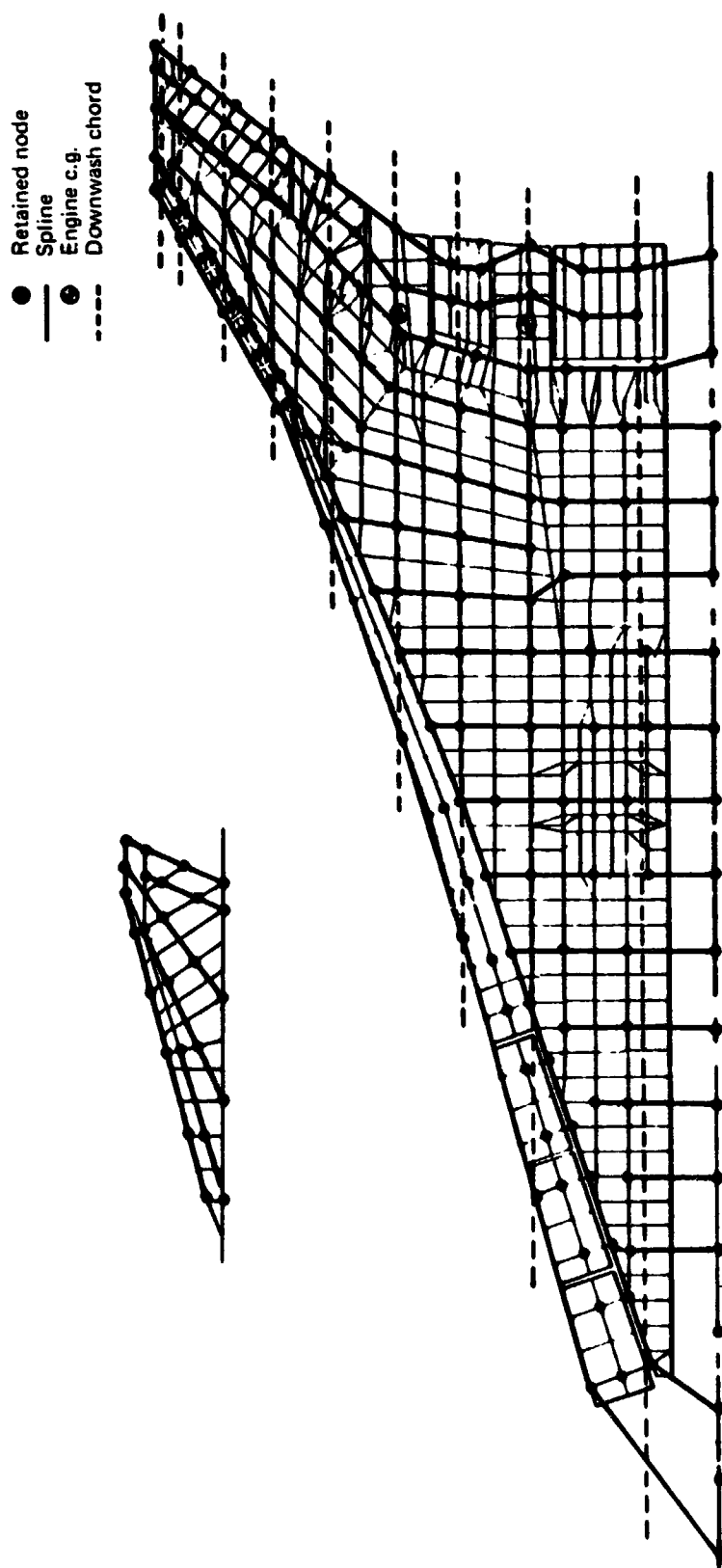


Figure 11-6. — Wing Retained Nodes and Mode Interpolation Beam Splines

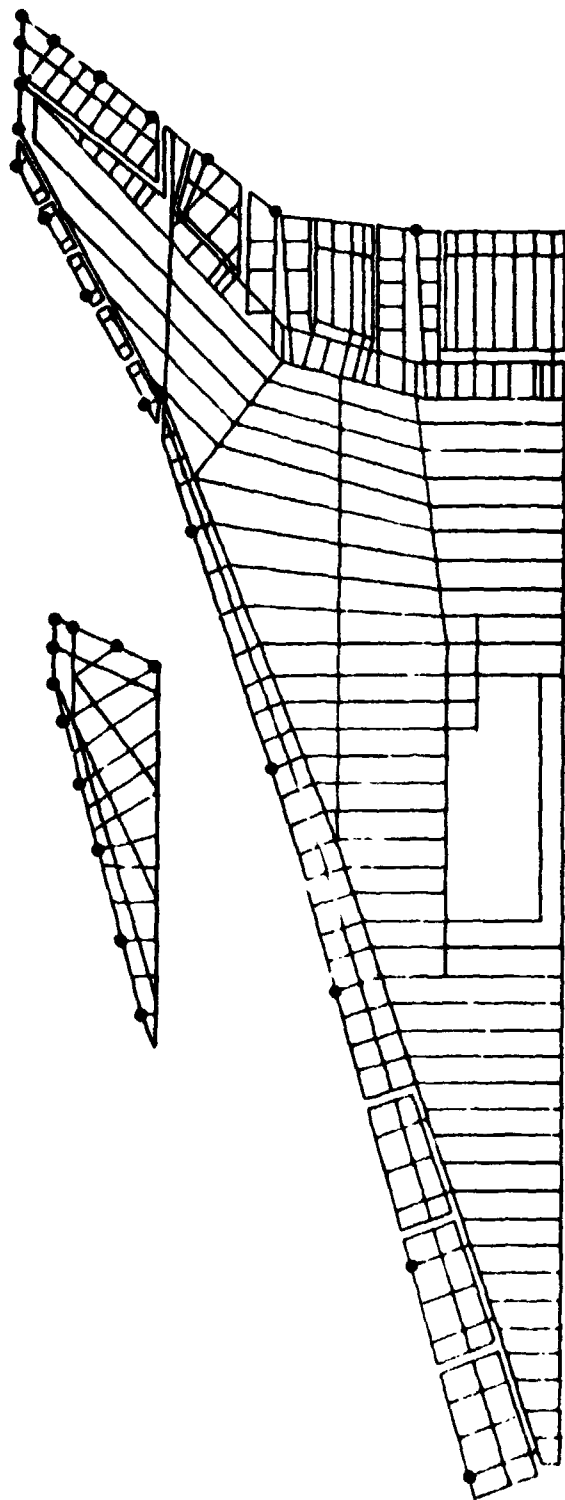


Figure 11-7.—Wing Edge Nodes for Vibration Mode Shapes

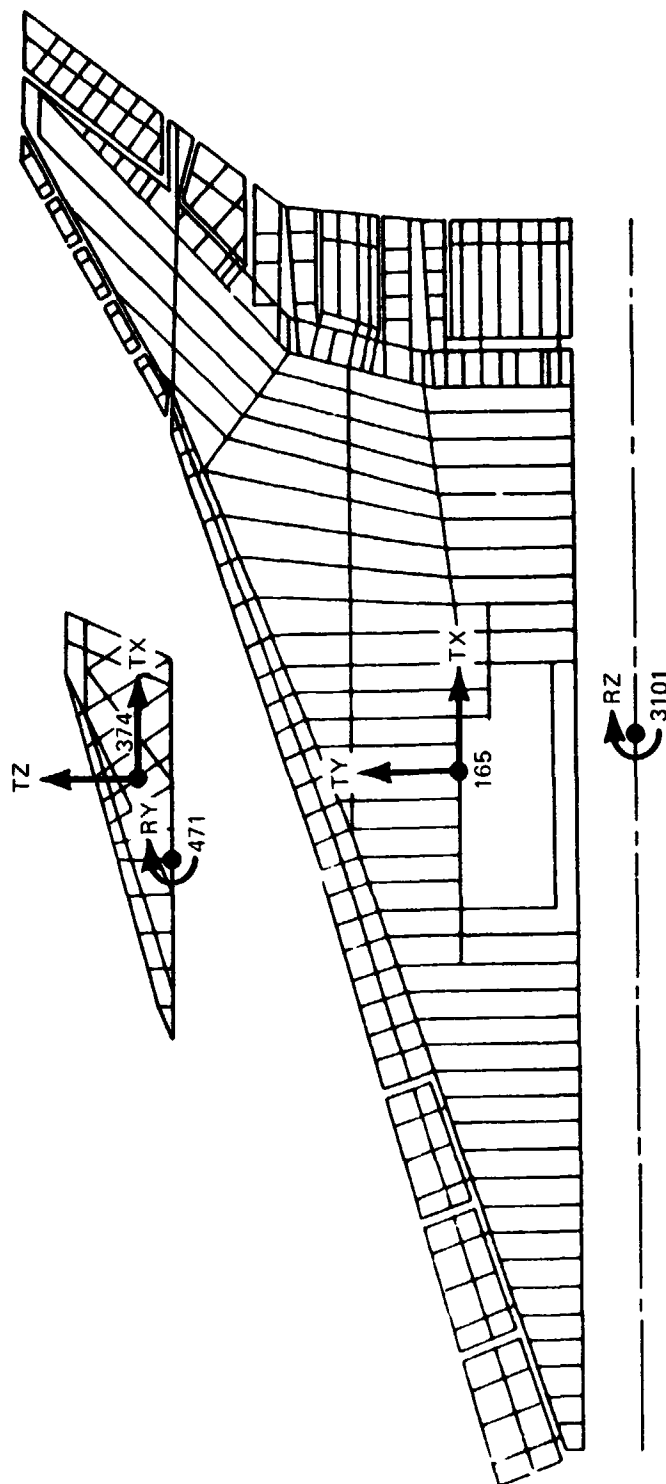


Figure 11-8.—Freedoms for Rigid In-Plane Motion of Vibration Modes

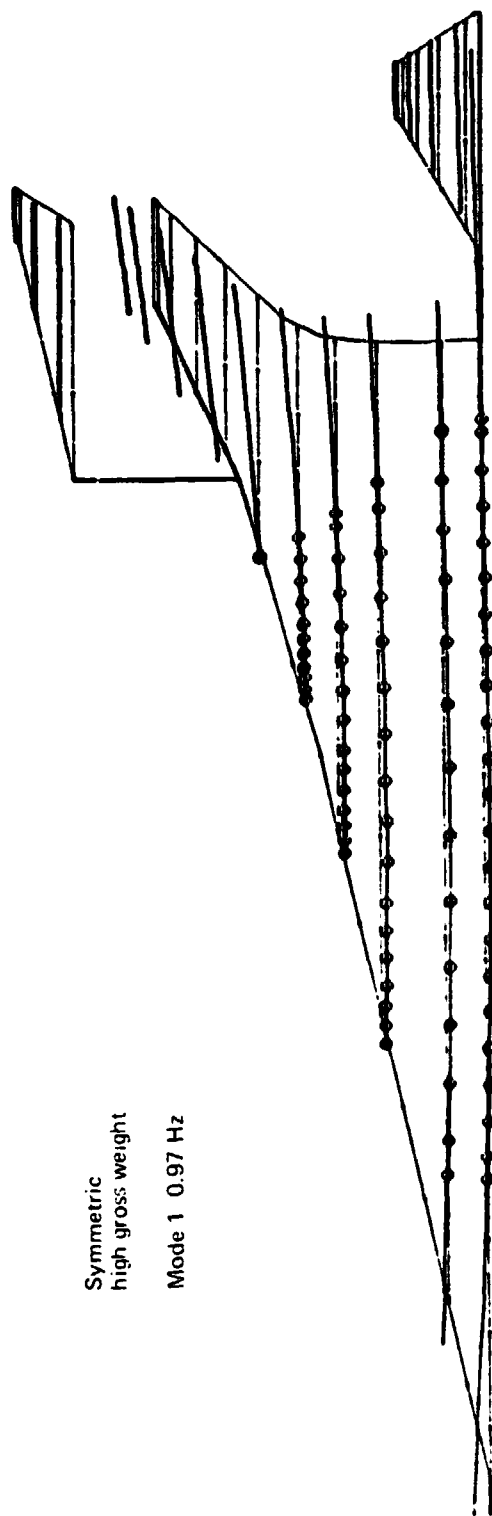


Figure 11-9.—Airplane Vibration Mode 1—Final Stiffness Design

Symmetric
high gross weight
Mode 2 1.18 Hz

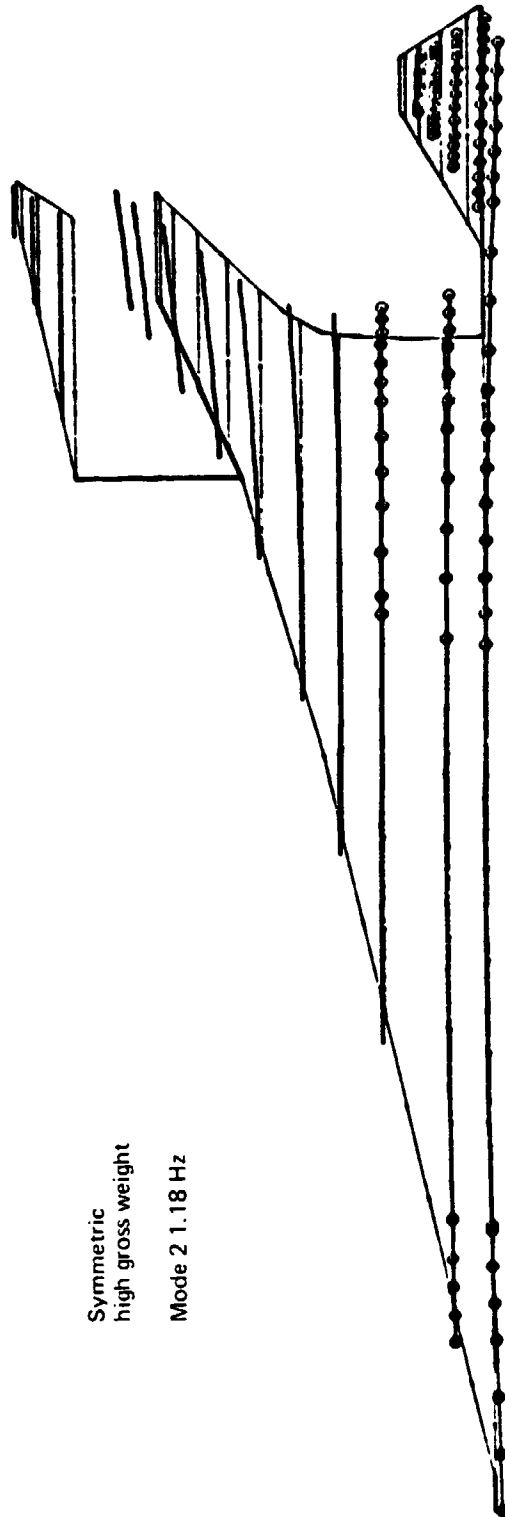


Figure 11-10.—Airplane Vibration Mode 2 -Final Stiffness Design

Symmetric
high gross weight
Mode 3 2.18 Hz

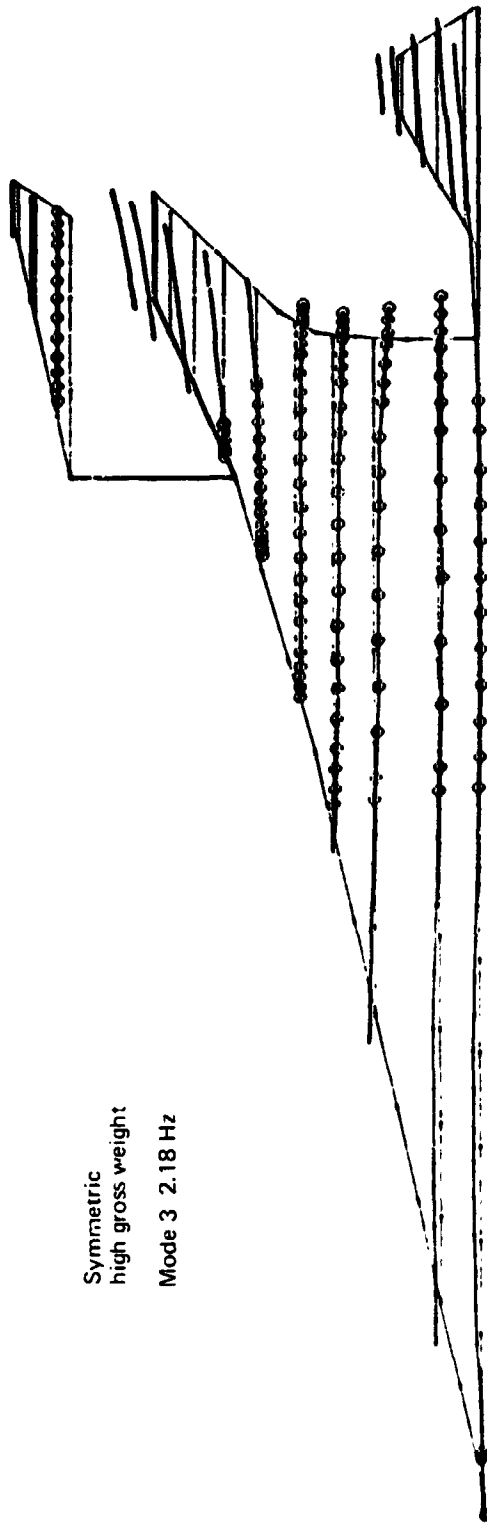


Figure 11-11. -Airplane Vibration Mode 3-Final Stiffness Design

Symmetric
high gross weight
Mode 4 2.43 Hz

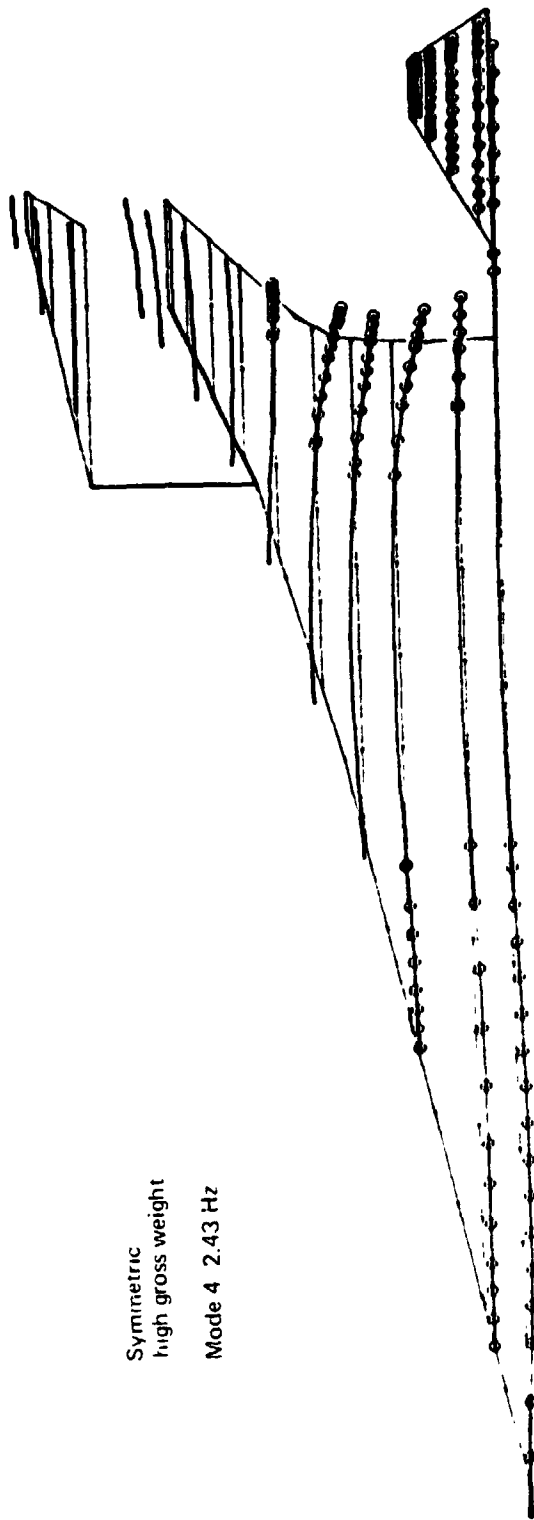


Figure 11-12. —Airplane Vibration Mode 4 —Final Stiffness Design

Symmetric
high gross weight
Mode 5 2.79 Hz

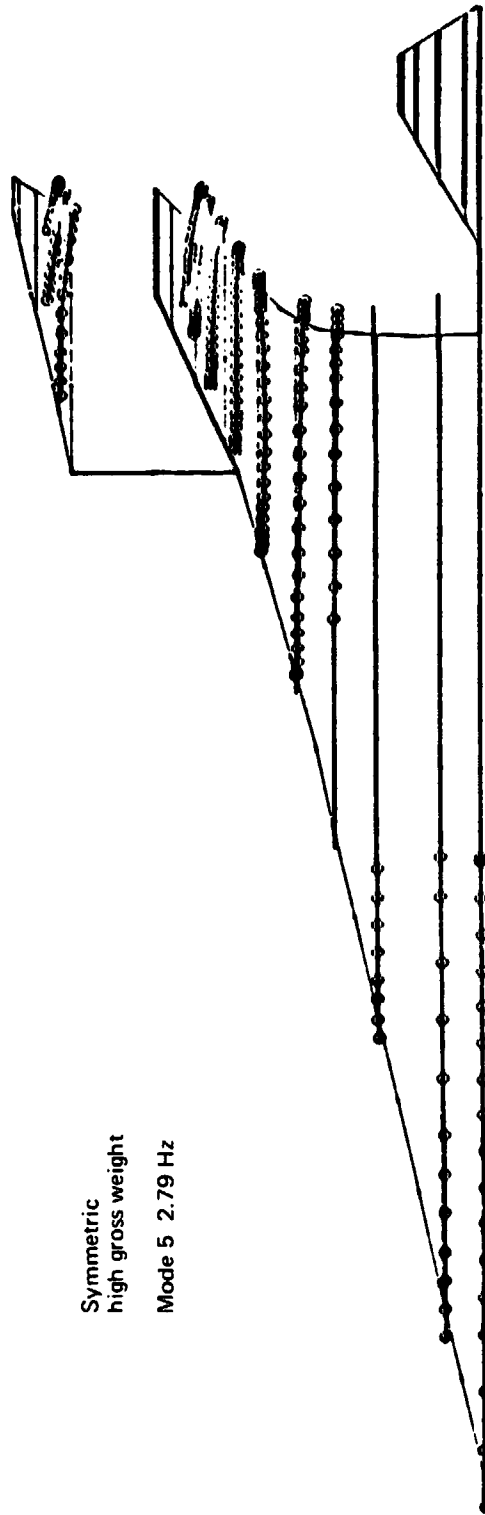


Figure 11-13. —Airplane Vibration Mode 5—Final Stiffness Design

Symmetric
high gross weight
Mode 6 3.00 Hz

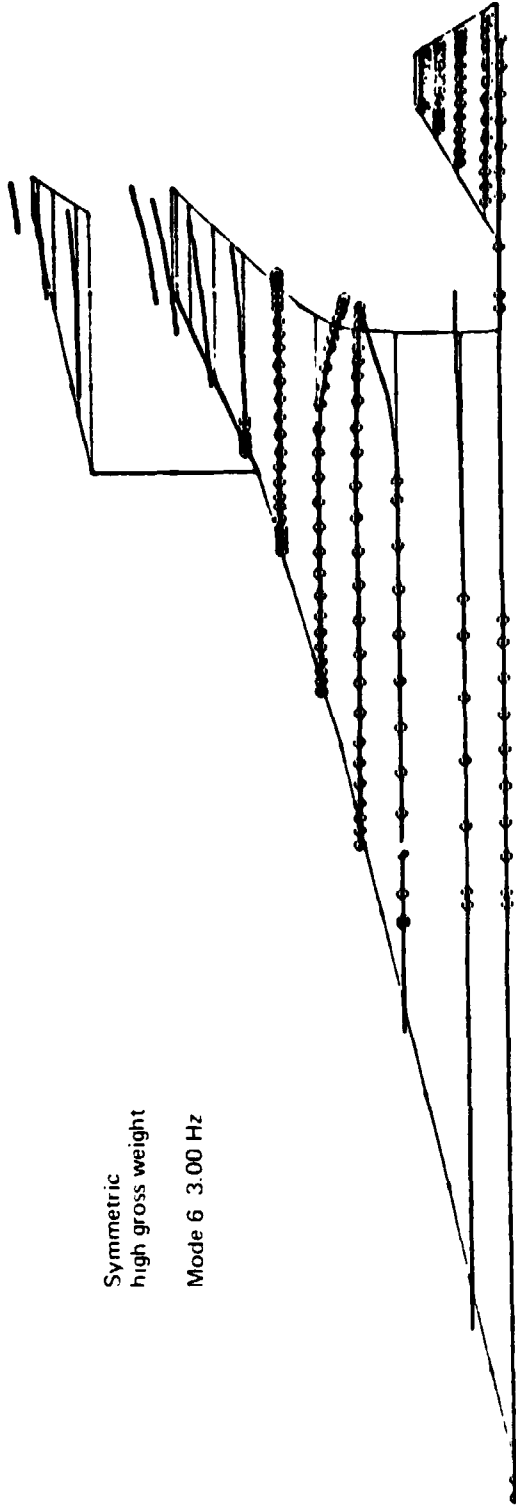
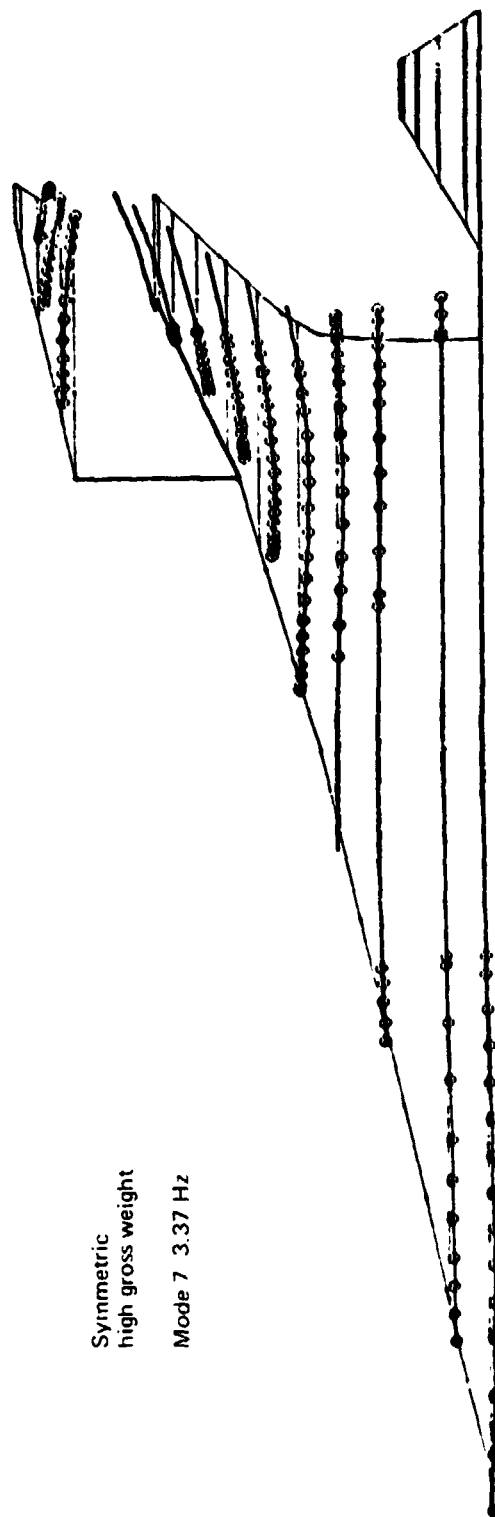


Figure 11 : 4 --Airplane Vibration Mode 6--Final Stiffness Design



Symmetric
high gross weight
Mode 7 3.37 Hz

Figure 11-15.—Airplane Vibration Mode 7—Final Stiffness Design

Symmetric
high gross weight
Mode 8 3.63 Hz

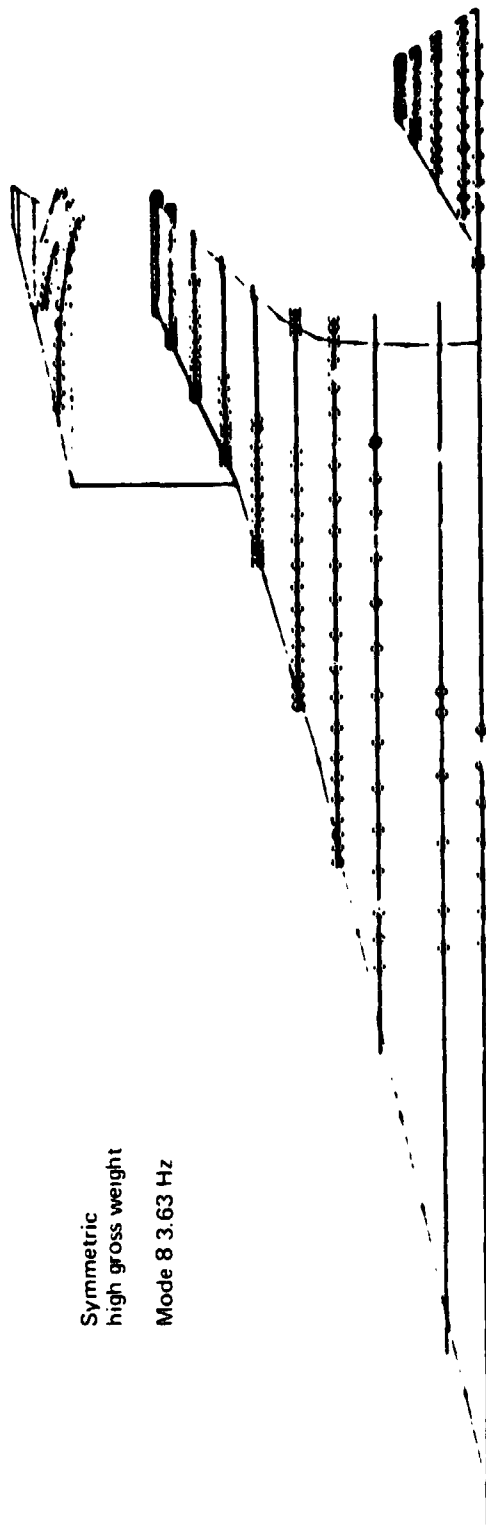


Figure 11-16. — Airplane Vibration Mode 8 — Final Stiffness Design

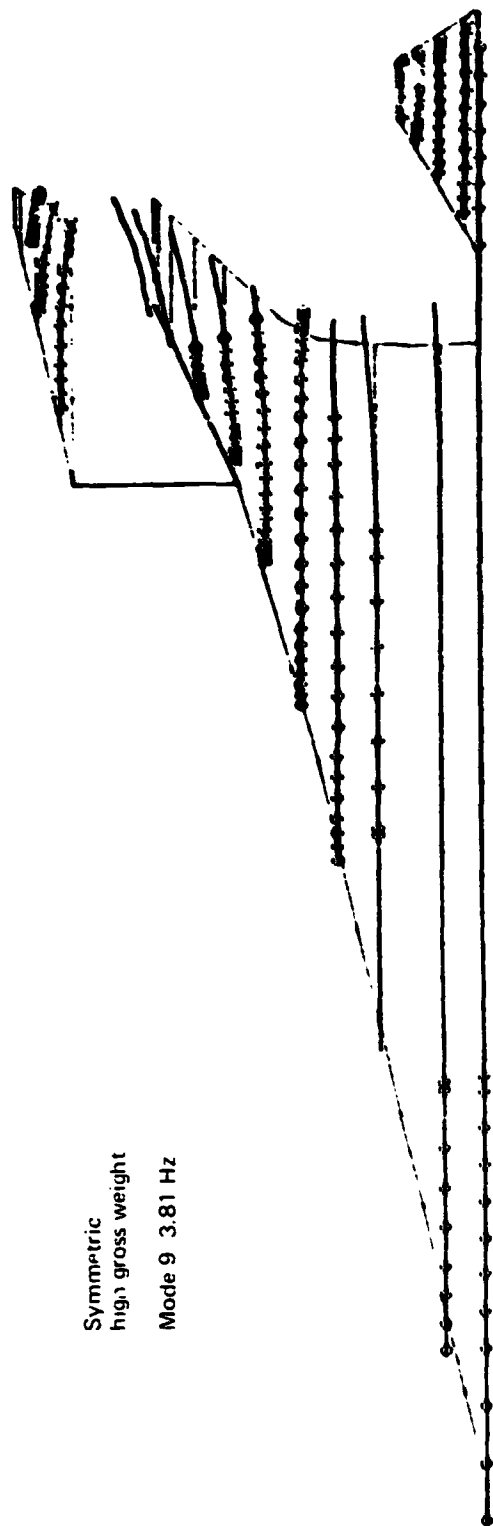


Figure 11-17.—Airplane Vibration Mode 9—Final Stiffness Design

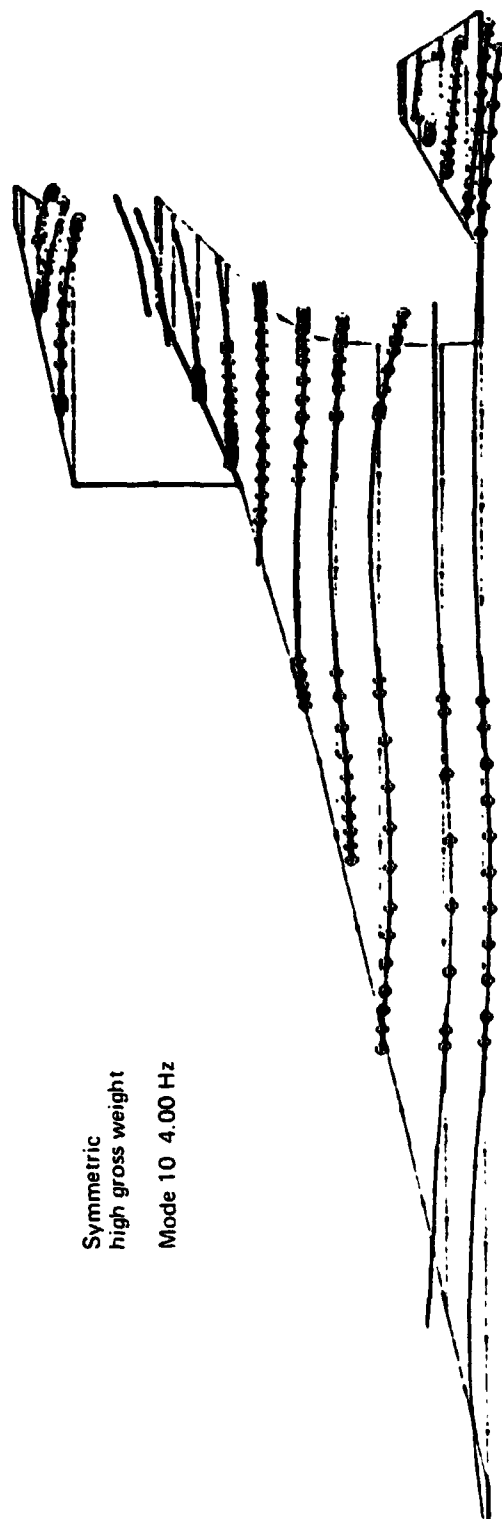


Figure 11-18.—Airplane Vibration Mode 10—Final Stiffness Design

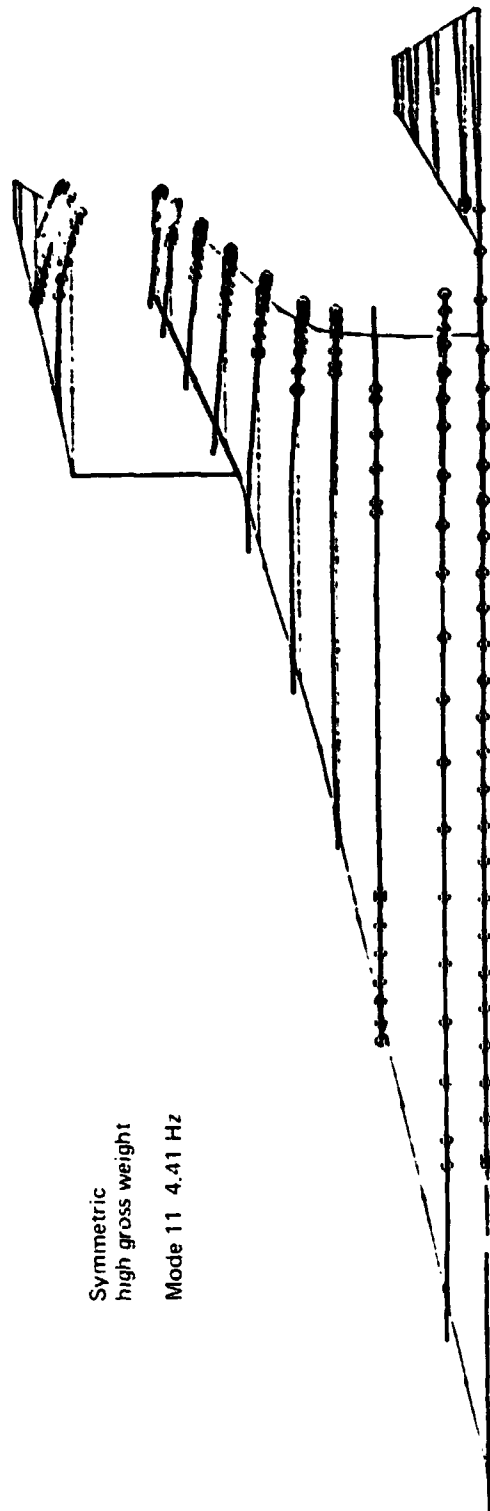


Figure 11-19.—Airplane Vibration Mode 11—Final Stiffness Design

Symmetric
high gross weight
Mode 12 4.68 Hz

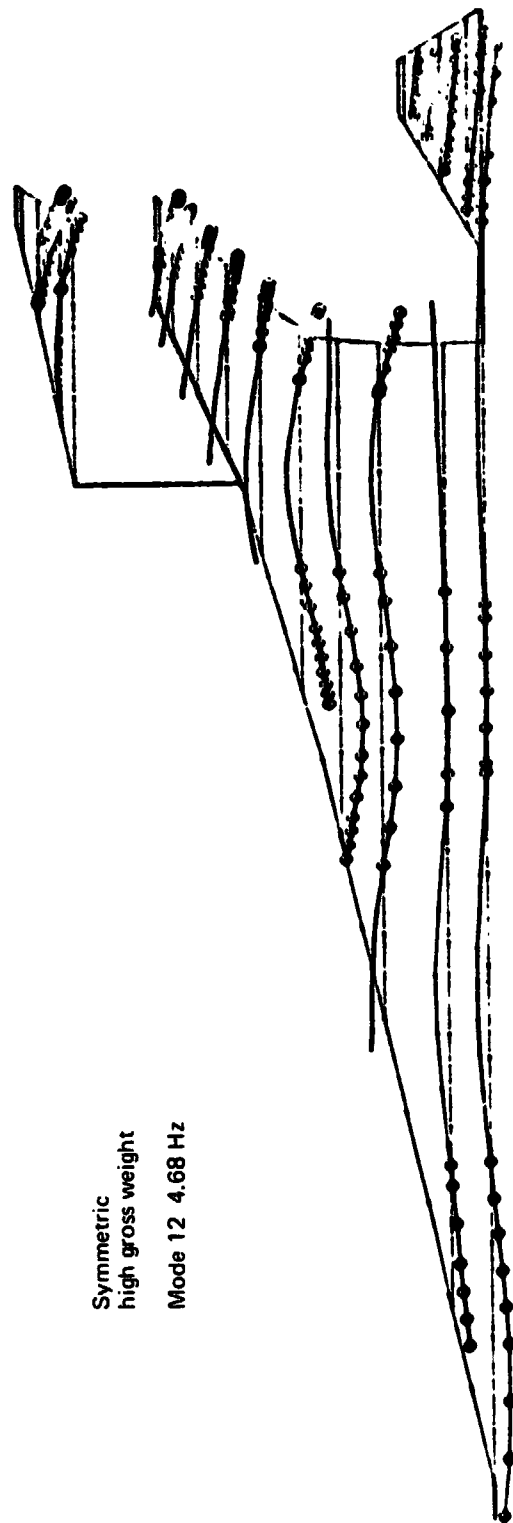
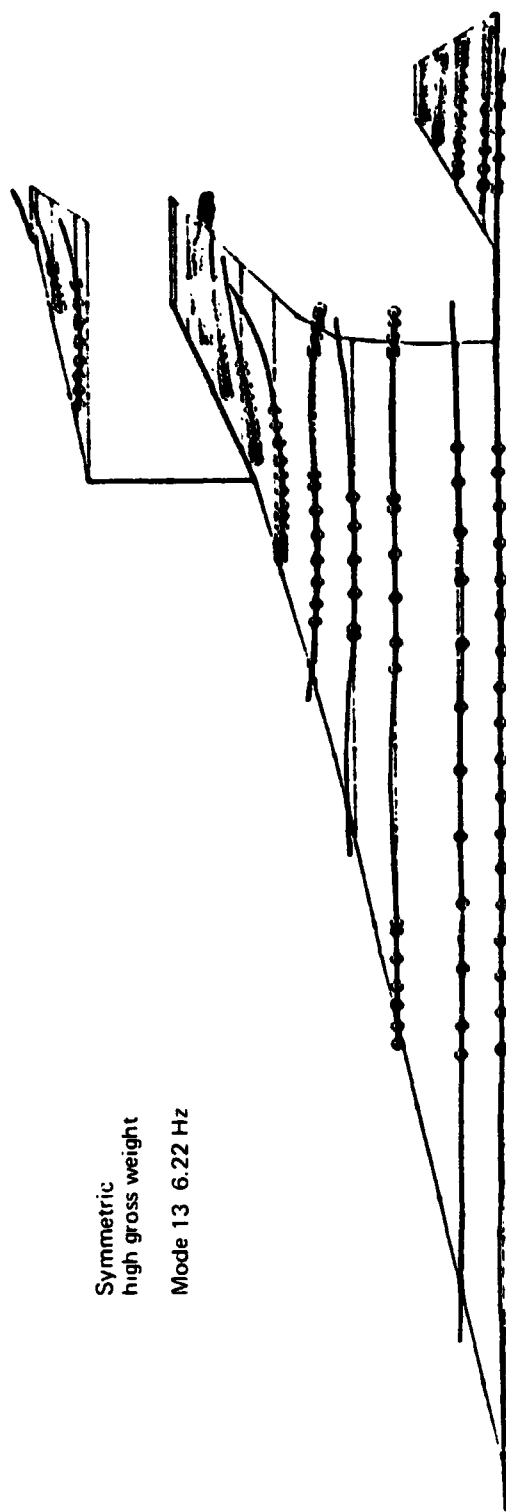


Figure 11-20.—Airframe Vibration Mode 12—Final Stiffness Design

REPRODUCIBILITY OF THE
ORIGINAL PAGE IS POOR



Symmetric
high gross weight
Mode 13 6.22 Hz

Figure 11-21.—Airplane Vibration Mode 13—Final Stiffness Design

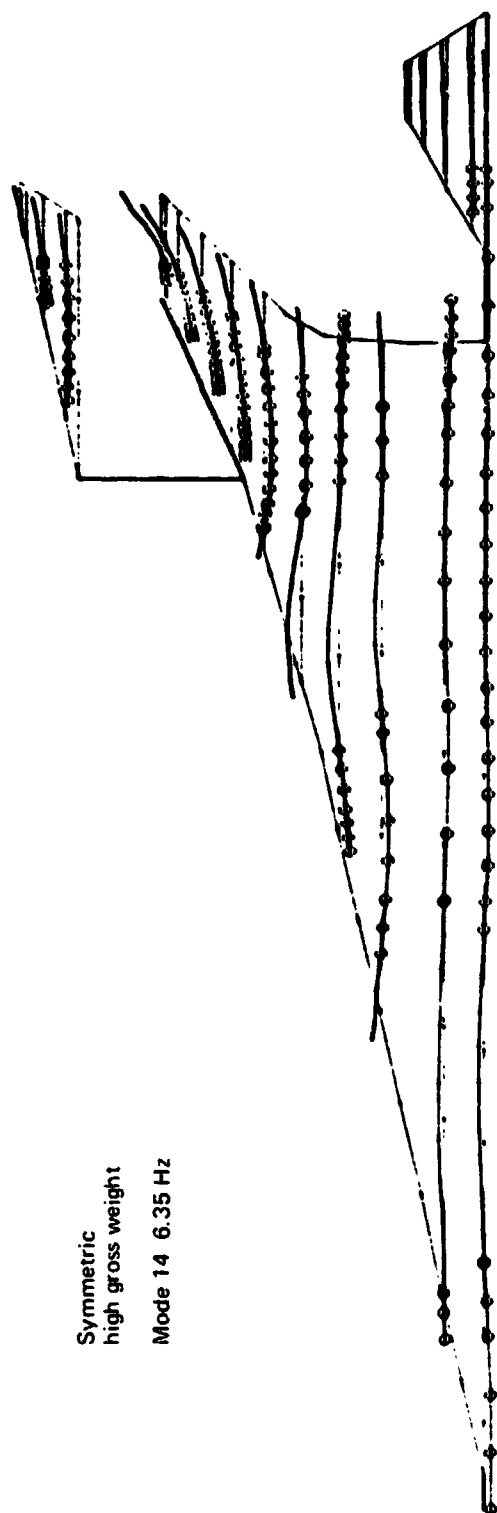


Figure 11-22.—Airplane Vibration Mode 14—Final Stiffness Design

Symmetric
high gross weight
Mode 15 6.75 Hz

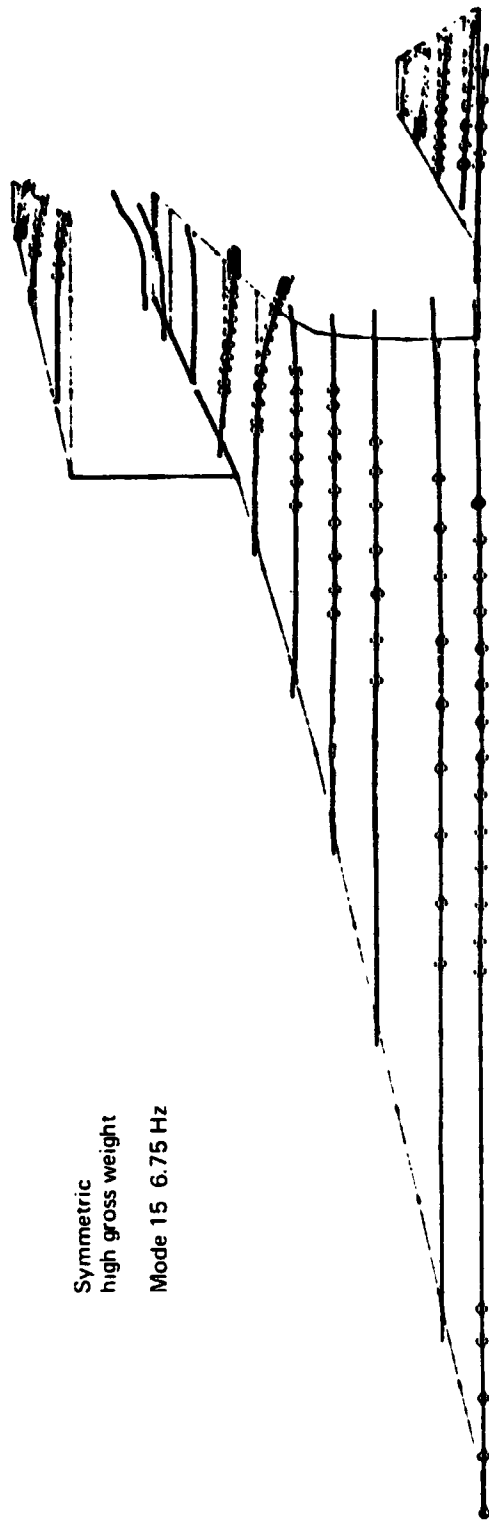


Figure 11-23. — Airplane Vibration Mode 15—Final Stiffness Design

Figure 11-24. – Airplane Vibration Mode 16—Final Stiffness Design

Symmetric
high gross weight
Mode 17 8.03 Hz

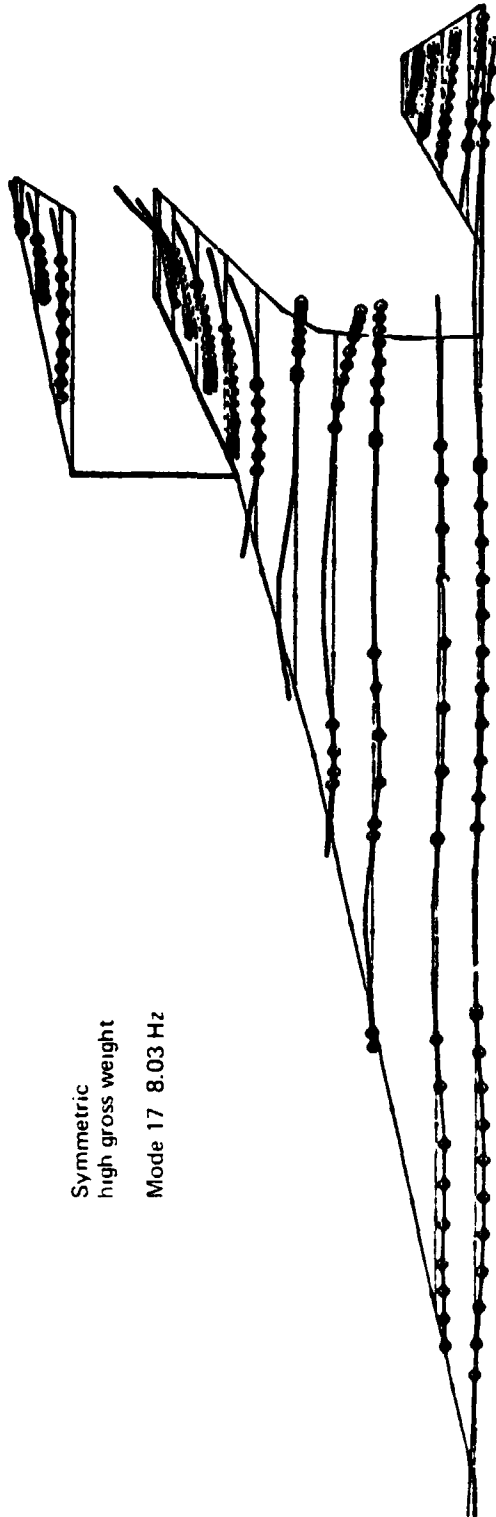


Figure 11-25. —Airplane Vibration Mode 17—Final Stiffness Design

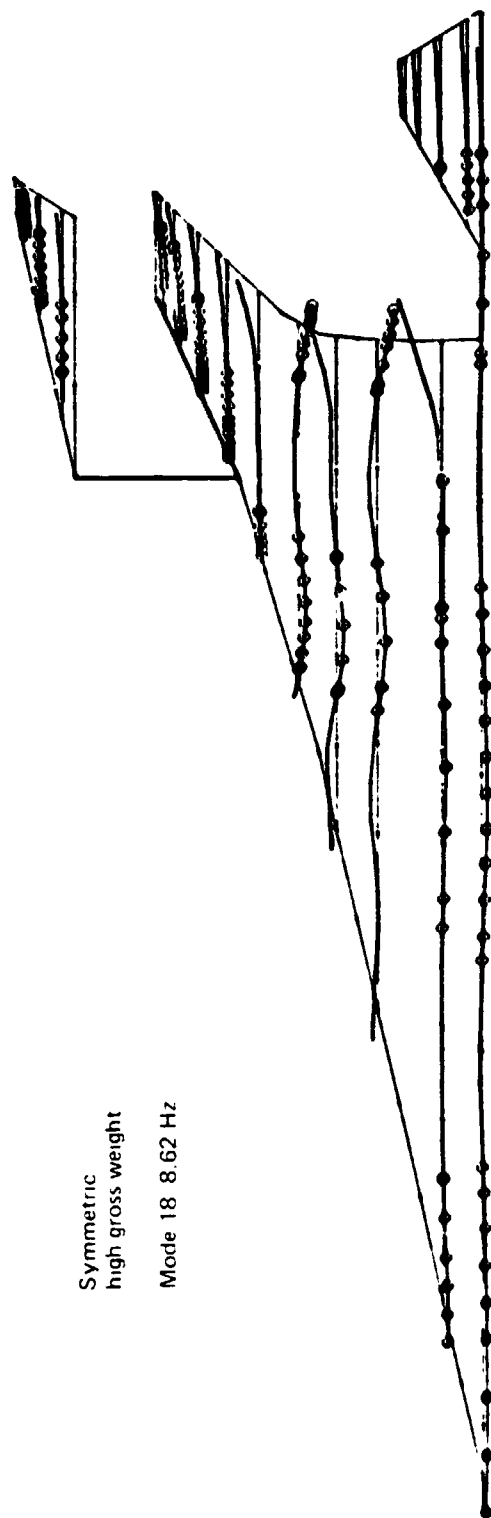


Figure 11-26.—Airplane Vibration Mode 18—Final Stiffness Design

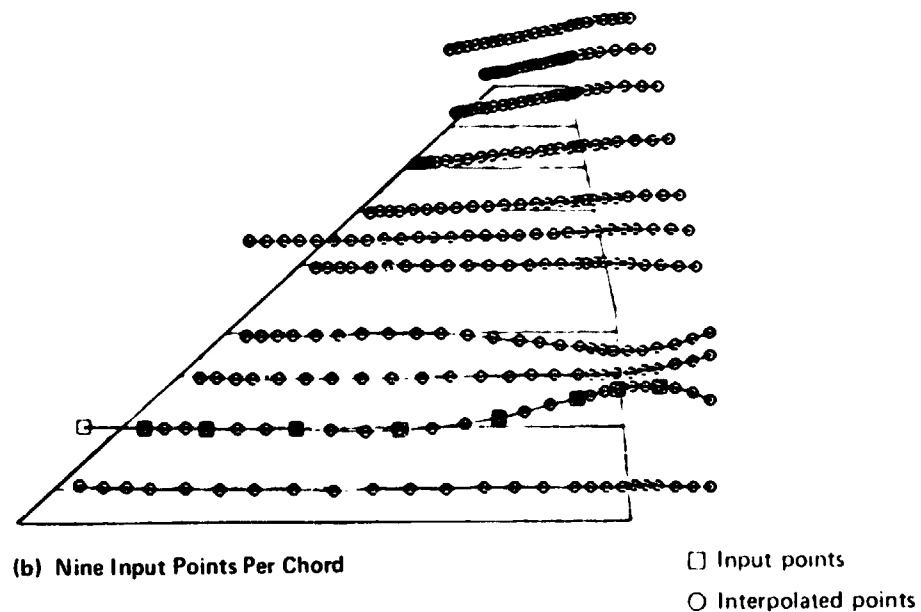
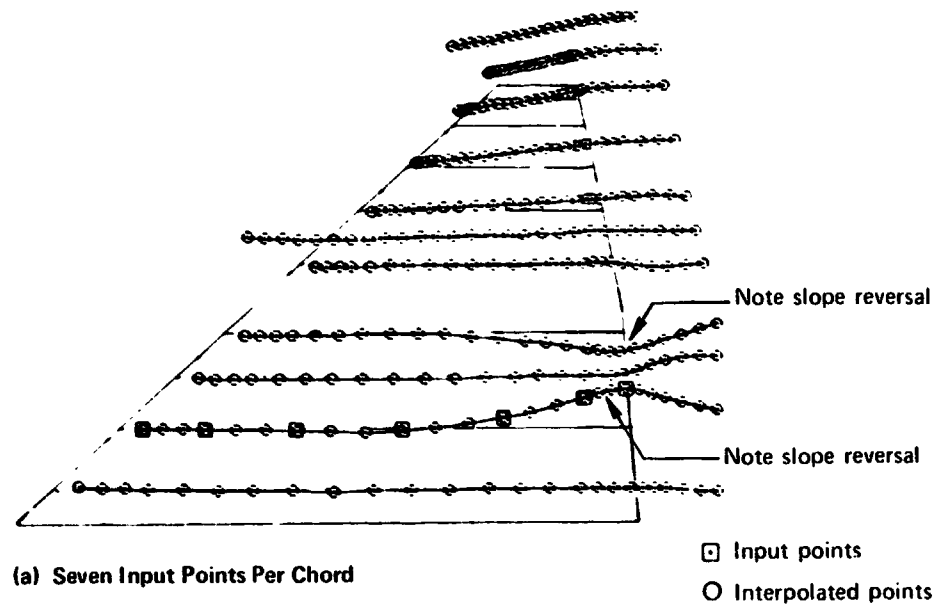


Figure 11-27.—Typical Surface Spline Interpolation

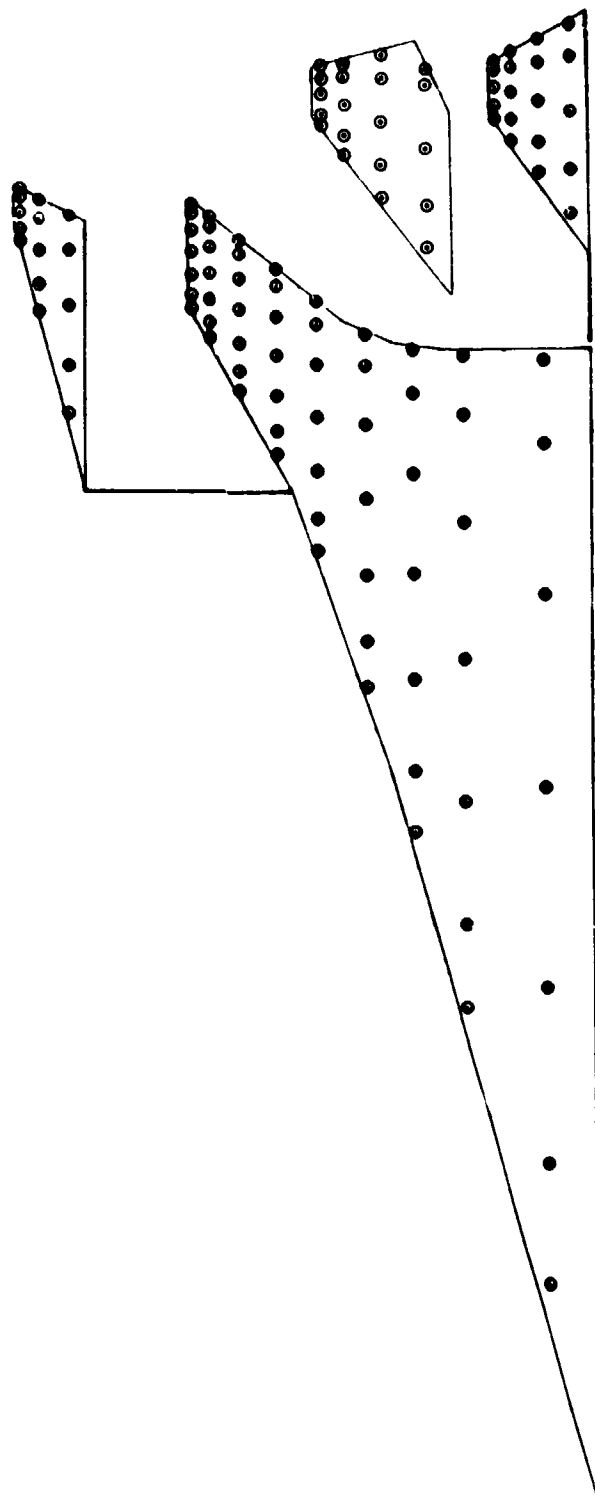


Figure 11-28.—Rho III Downwash Collocation Points

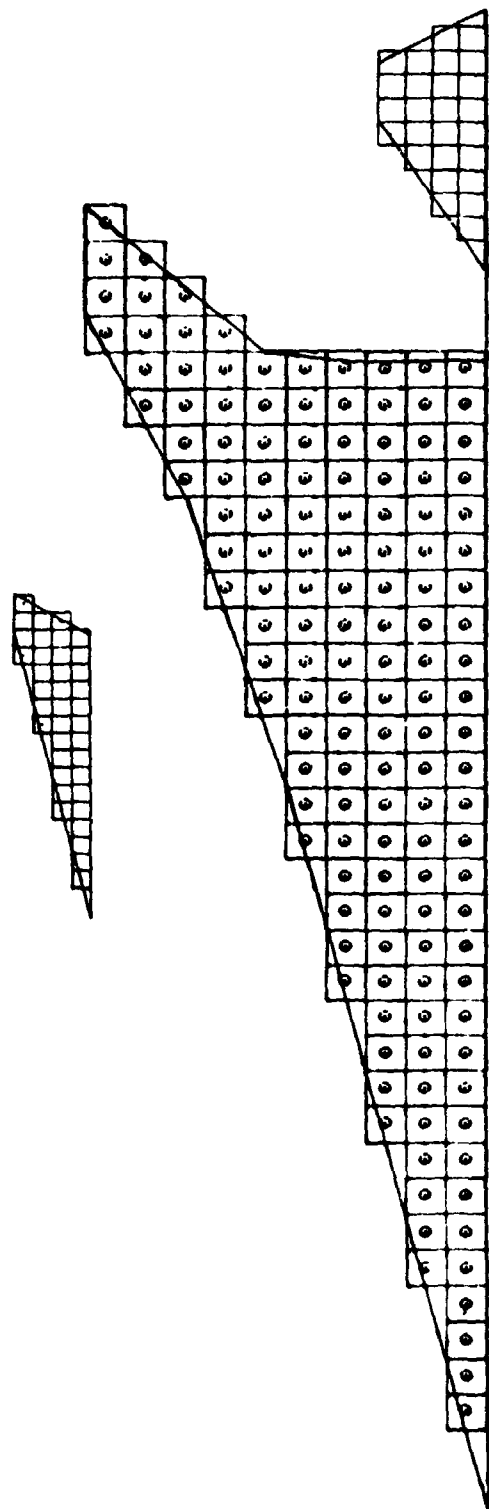


Figure 11-29. —Mach-Box Pattern—M = "

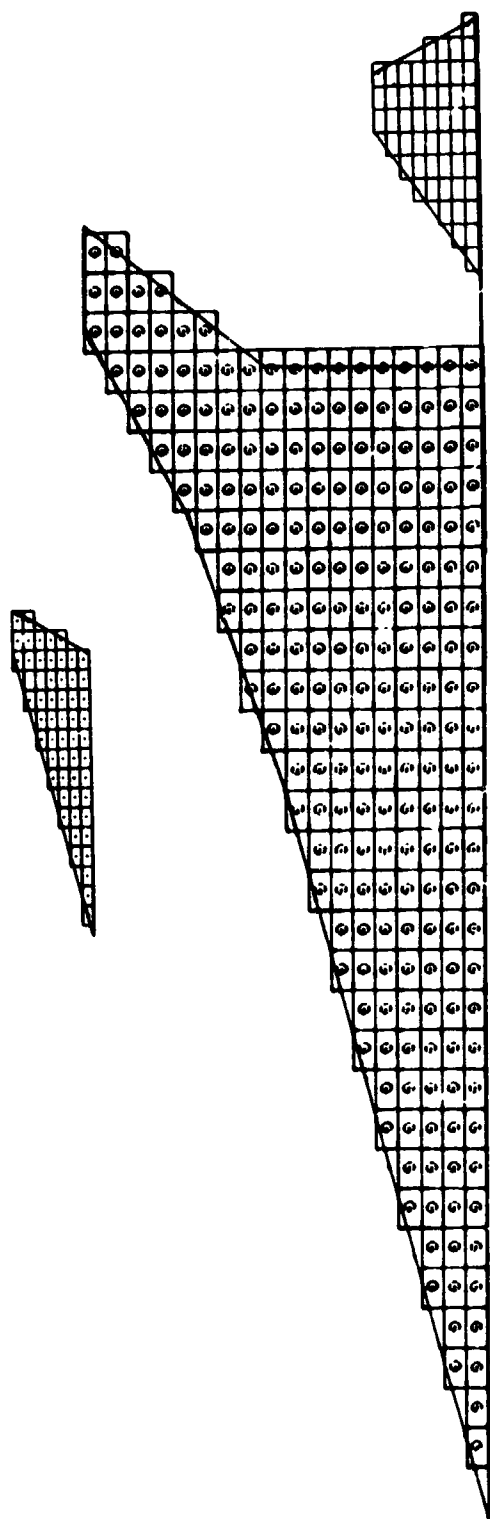


Figure 11-30. — Mach-Box Pattern— $M = 2.0$

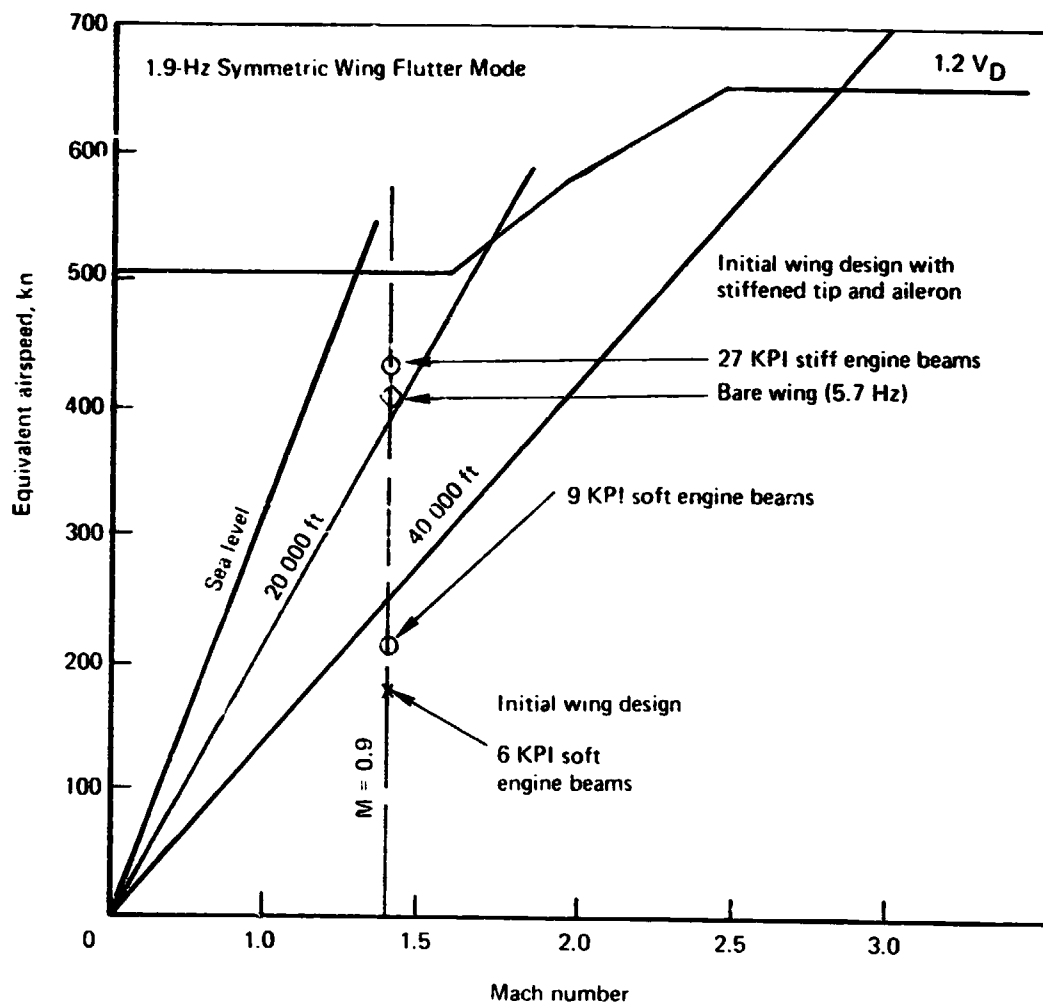
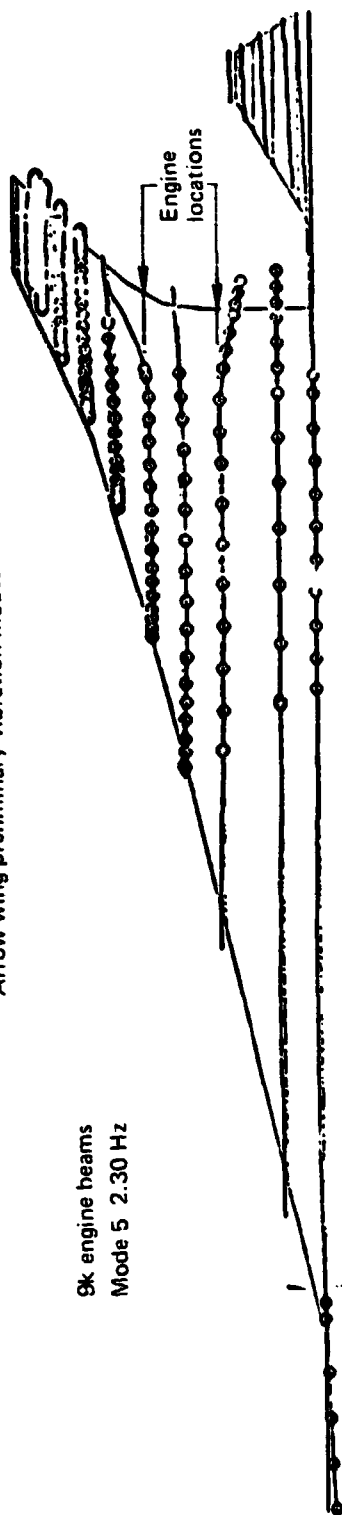


Figure 11-31.—Preliminary Flutter Speeds

Arrow wing preliminary vibration modes

8k engine beams
Mode 5 2.30 Hz



27k engine Beams
Mode 5 2.40 Hz



Figure 11.32a.—Effect of Nacelle Beam Stiffening on Modal Coupling

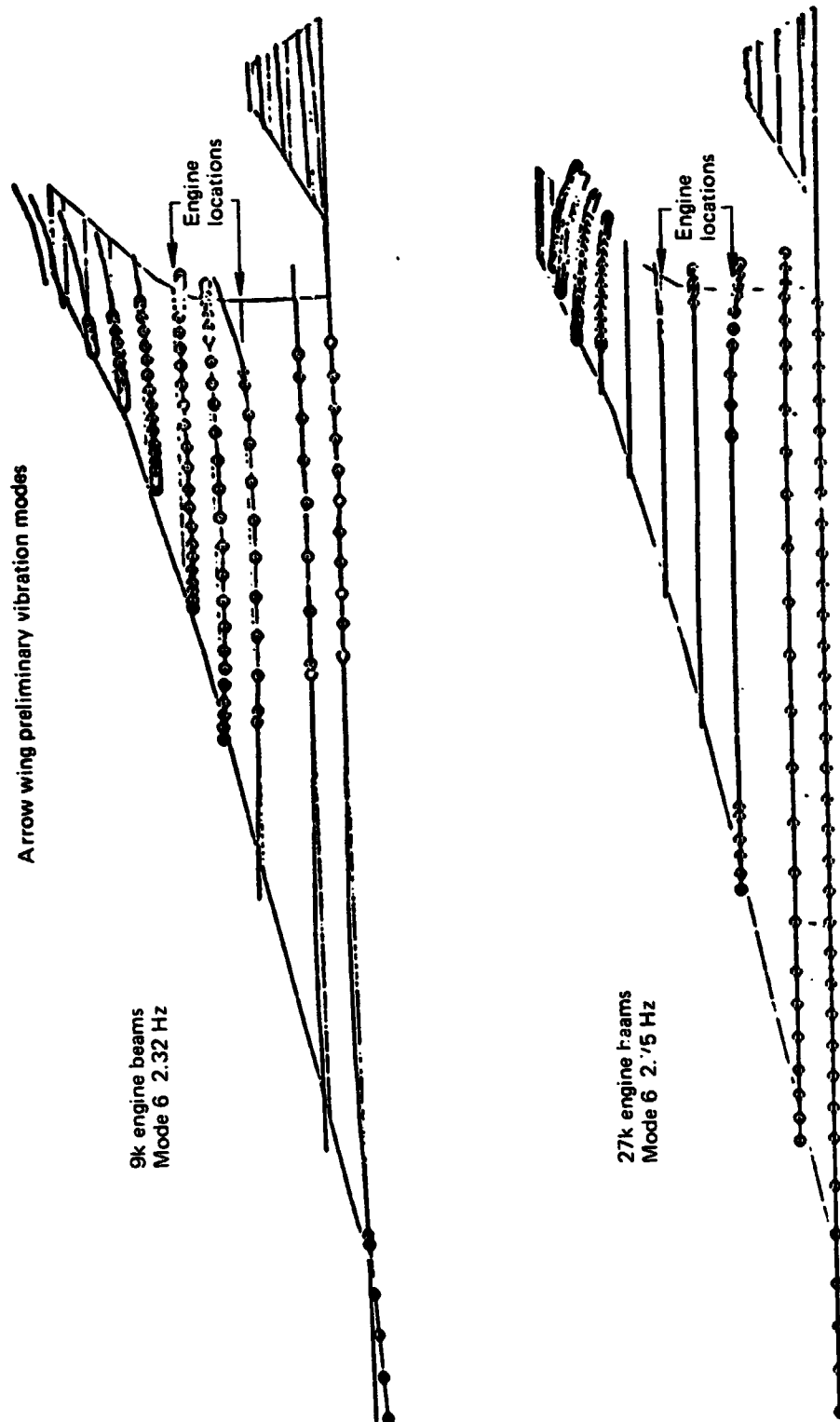


Figure 11-32b.—Effect of Nacelle Beam Stiffening on Modal Coupling

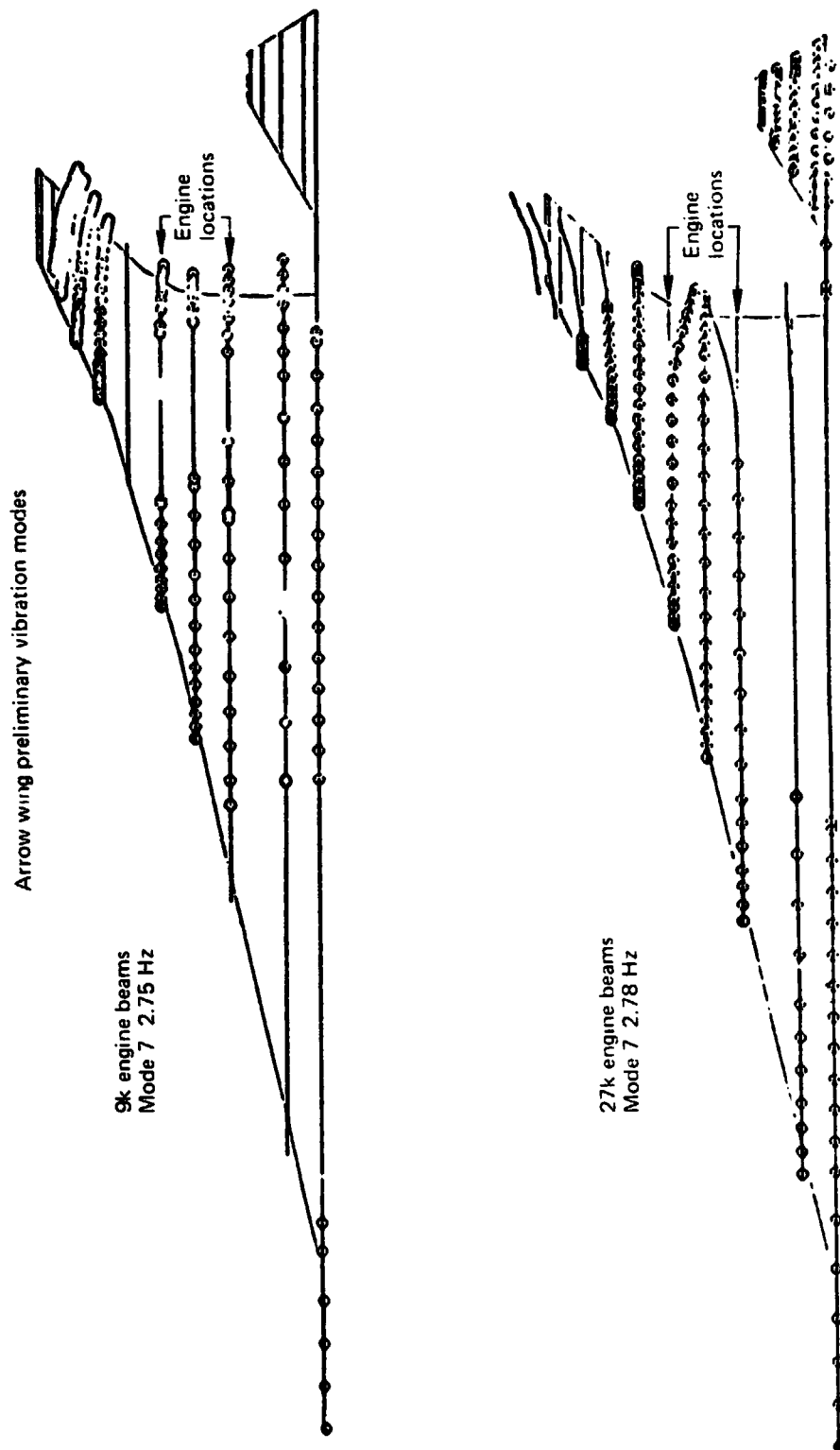
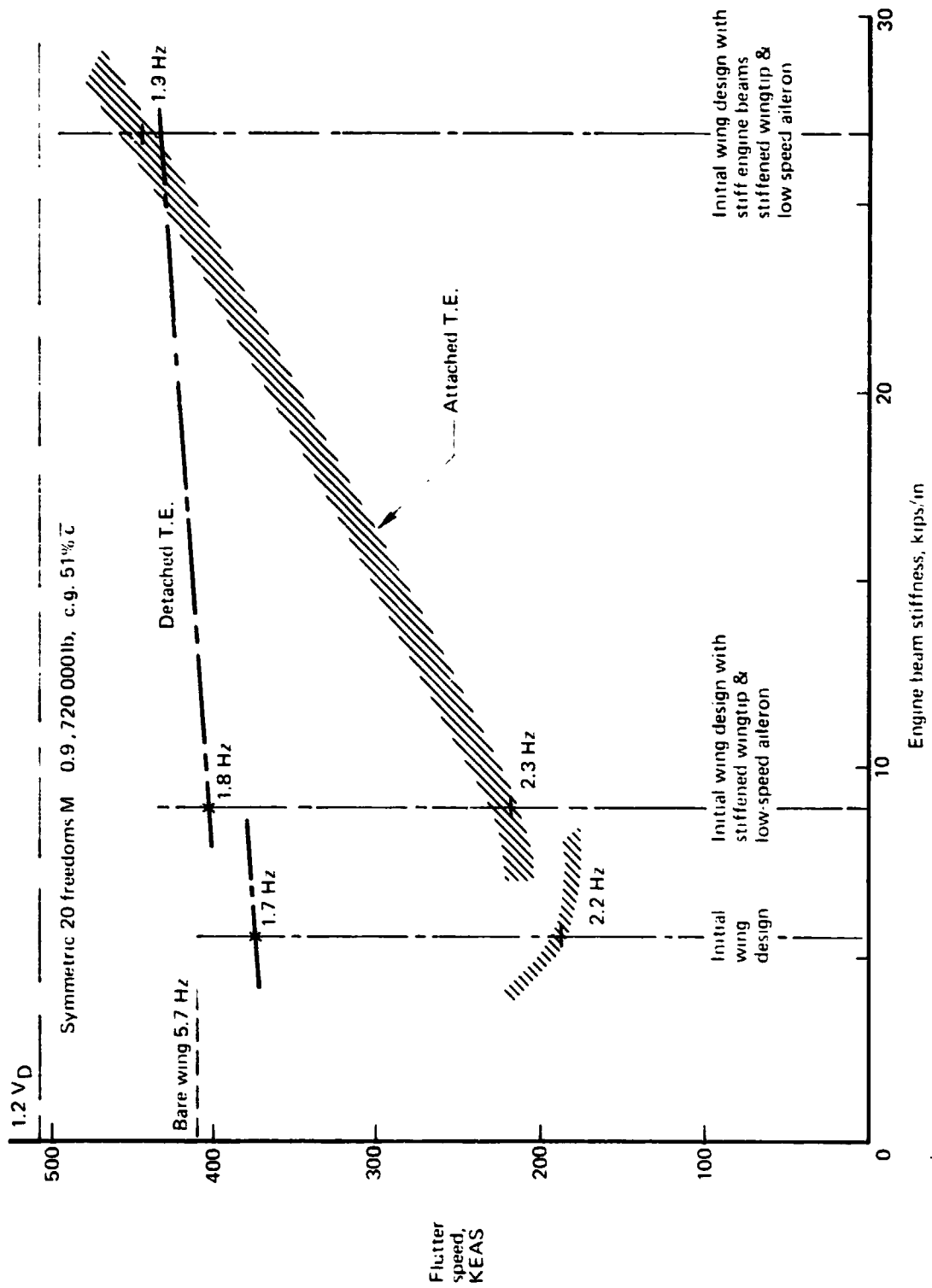


Figure 11-32 c. --Effect of Nacelle Beam Stiffening on Modal Coupling



+ 20 000-ft solution, Mach number not matched.

Figure 11-33.—Flutter Sensitivity to Engine Beam Stiffness

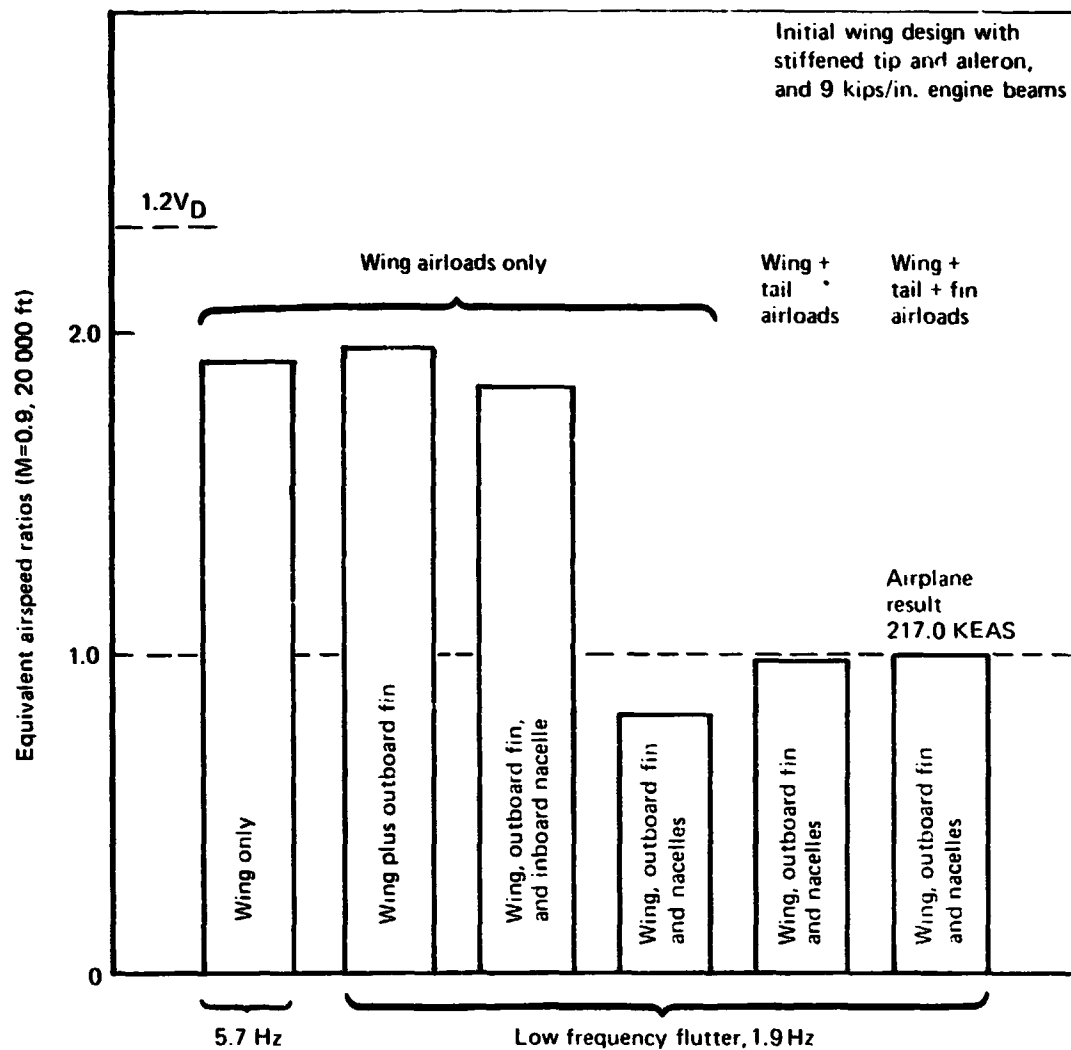


Figure 11-34.—Flutter Sensitivity to Airload and Structural Components

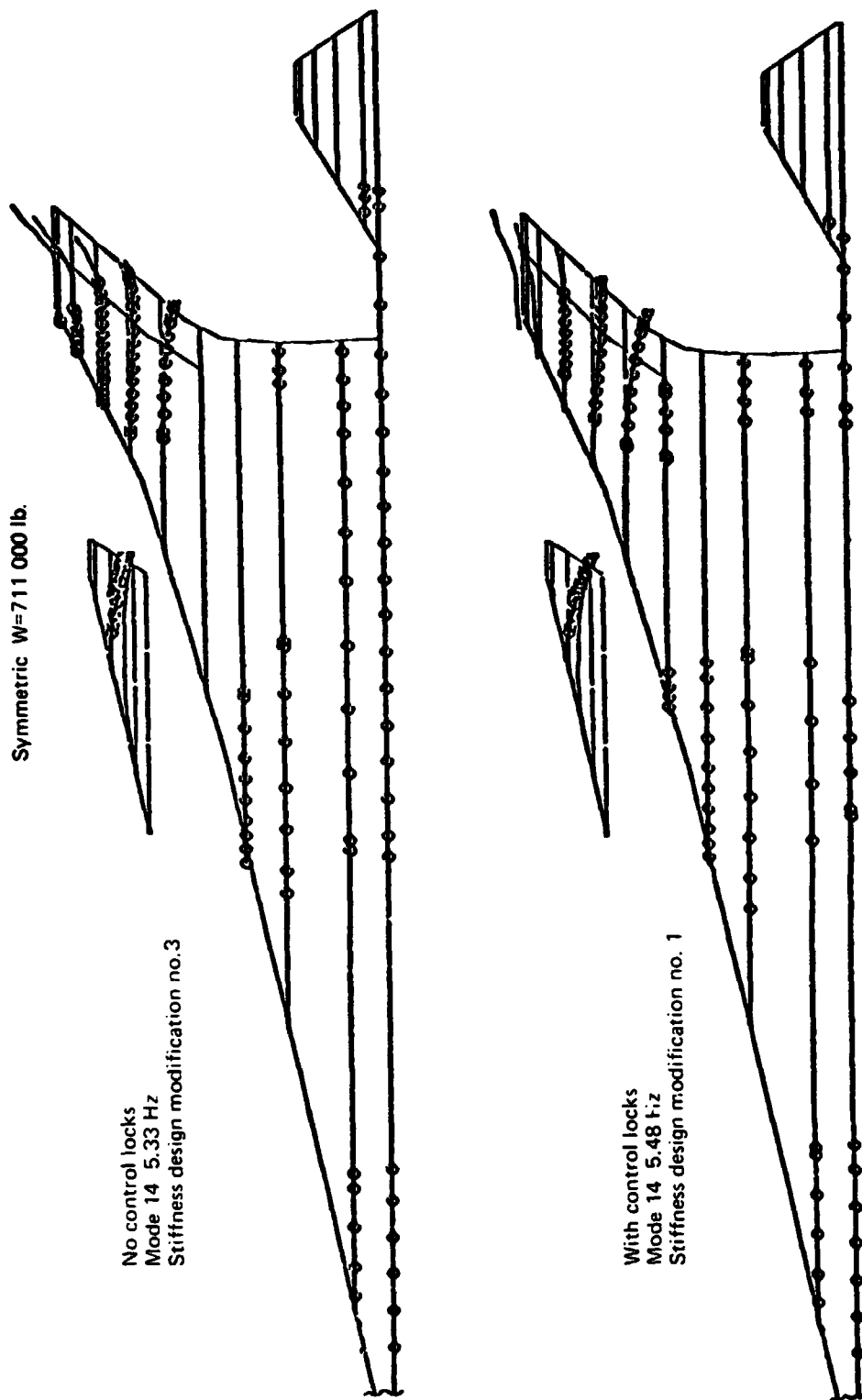


Figure 11-35.—Effect of Control Locks on a Vibration Mode

Symmetrical

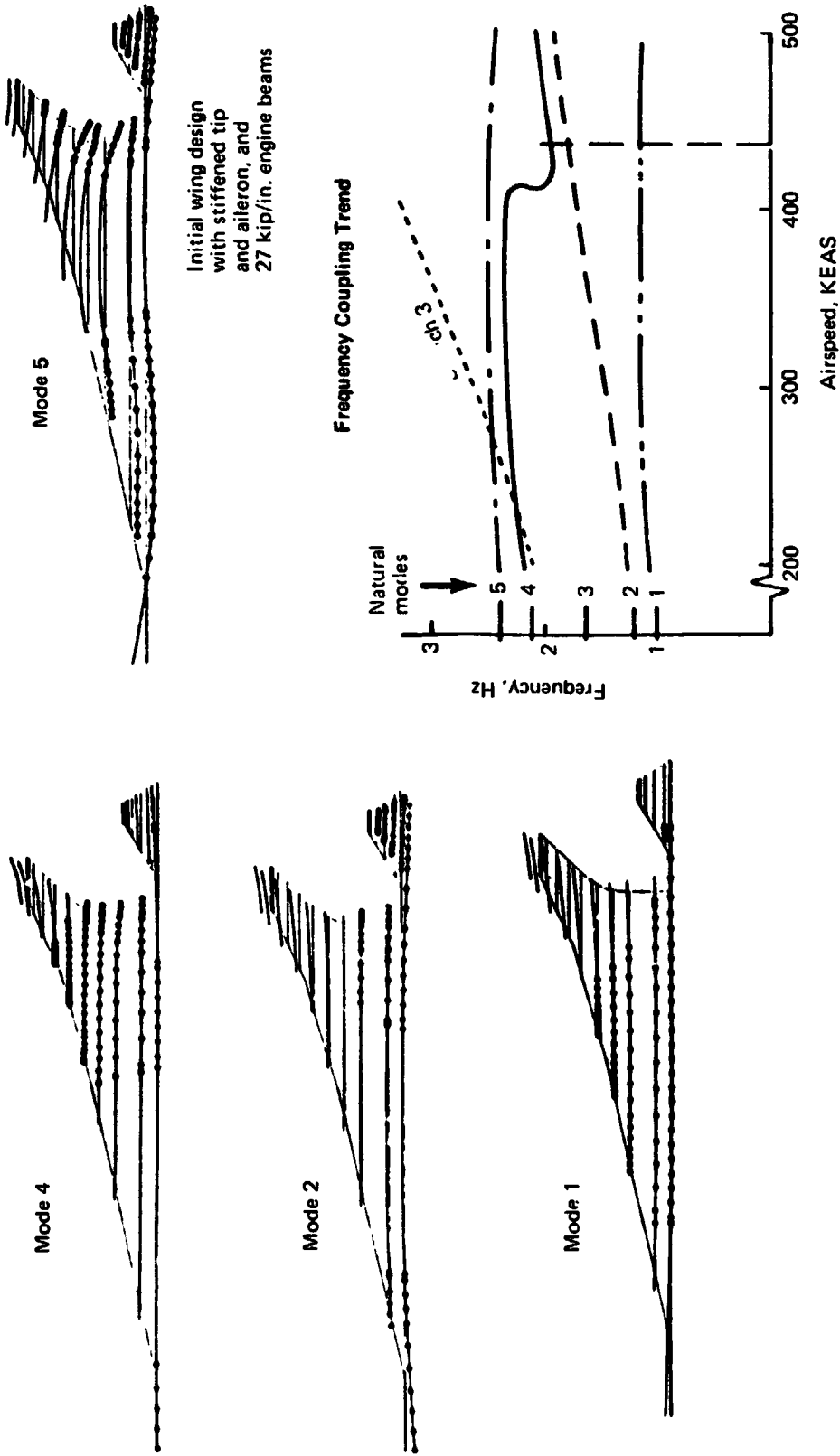


Figure 11-36—Low Frequency Flutter Mechanism

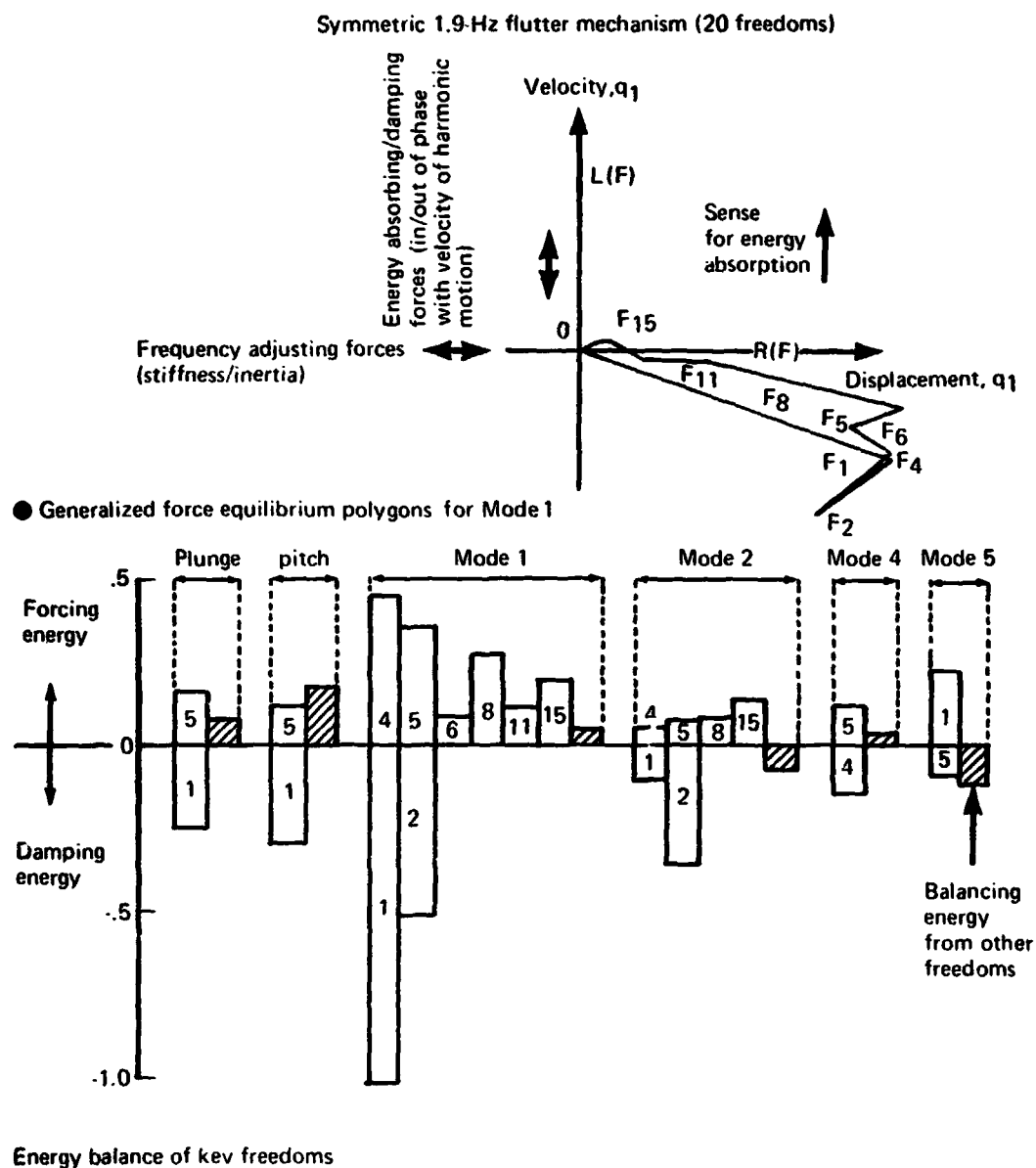
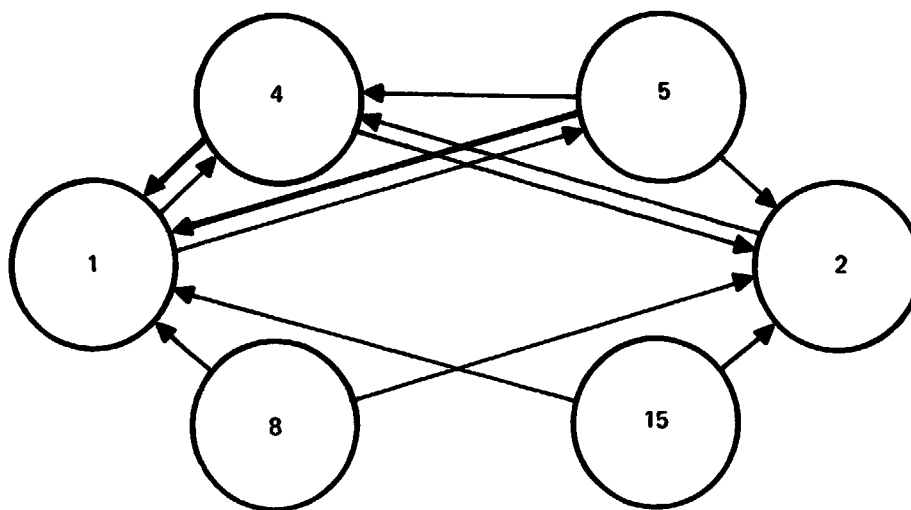
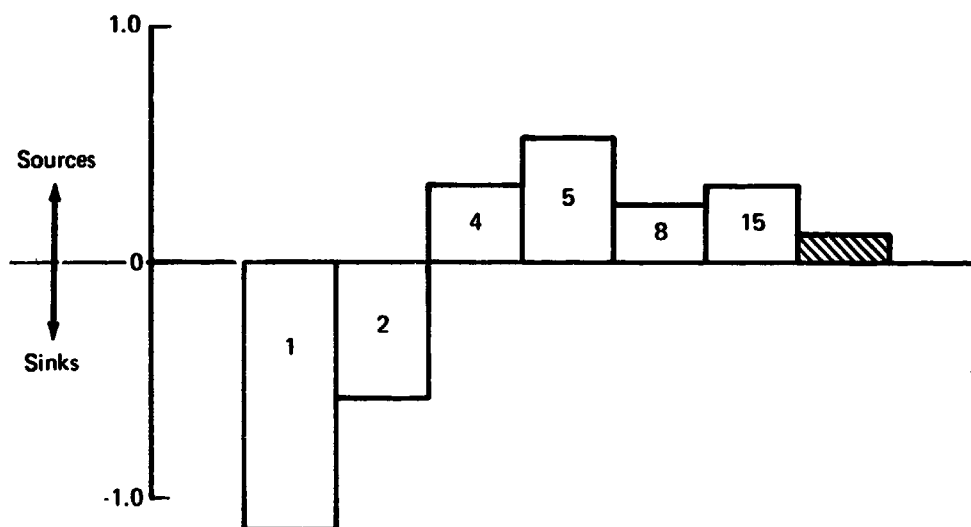


Figure 11-37.—Generalized Force Loops and Energy Balance

Symmetric 1.9-Hz flutter mechanism (20 freedoms)



Energy flux between key freedoms



Energy compatibility at neutral stability

Figure 11-38.—Energy Flux and Energy Compatibility

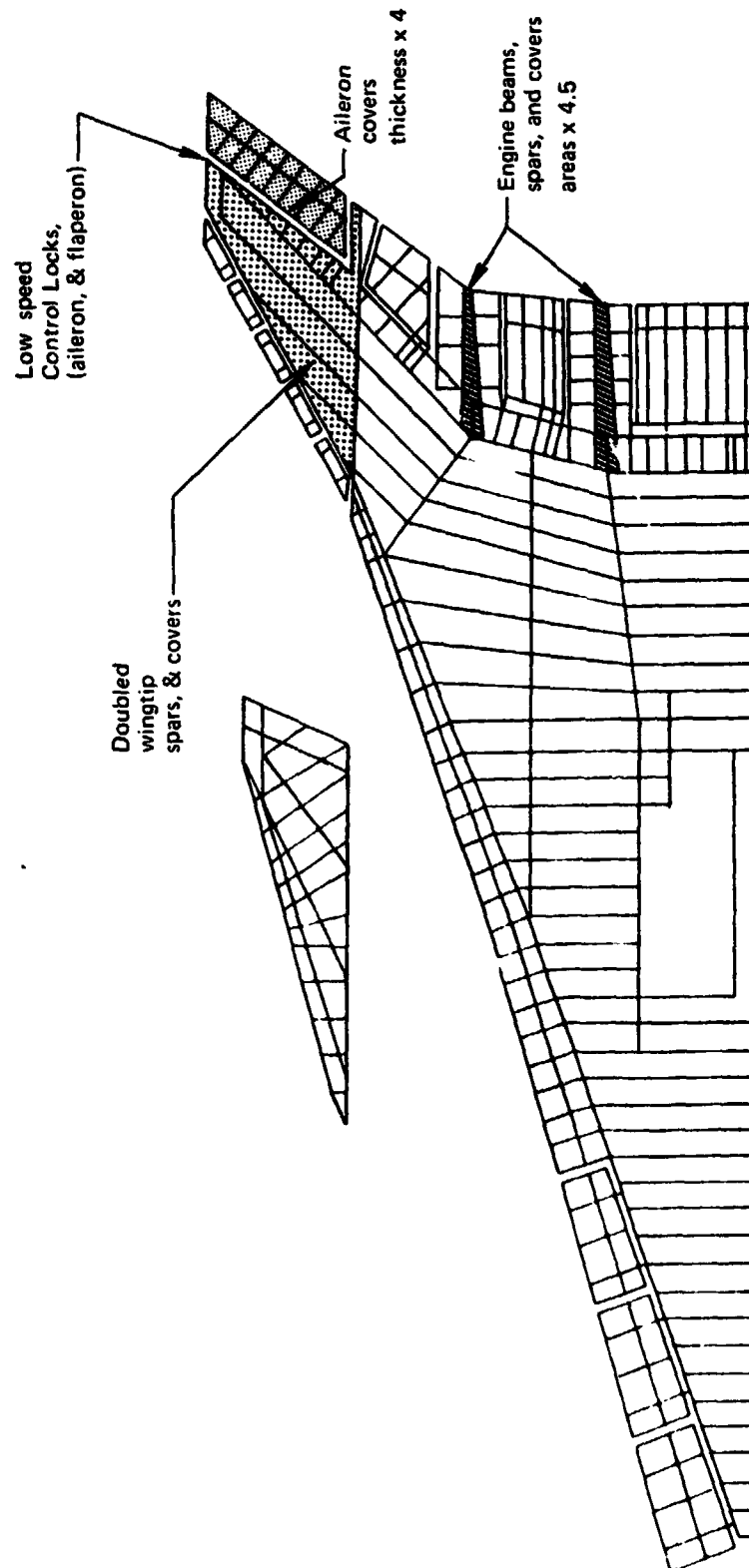


Figure 11-39.—Stiffness Design Modification 1

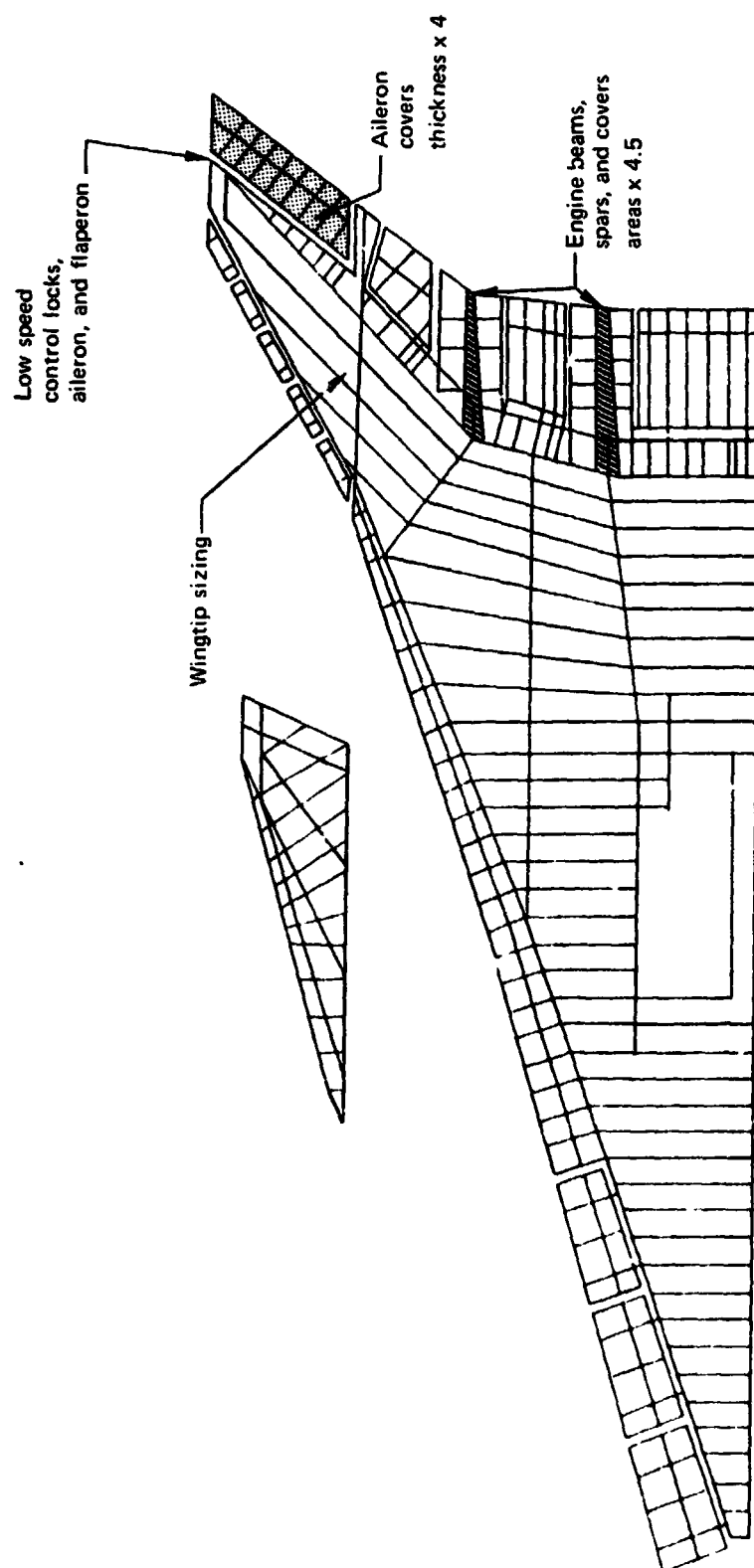


Figure 11-40.—Stiffness Design Modification 2

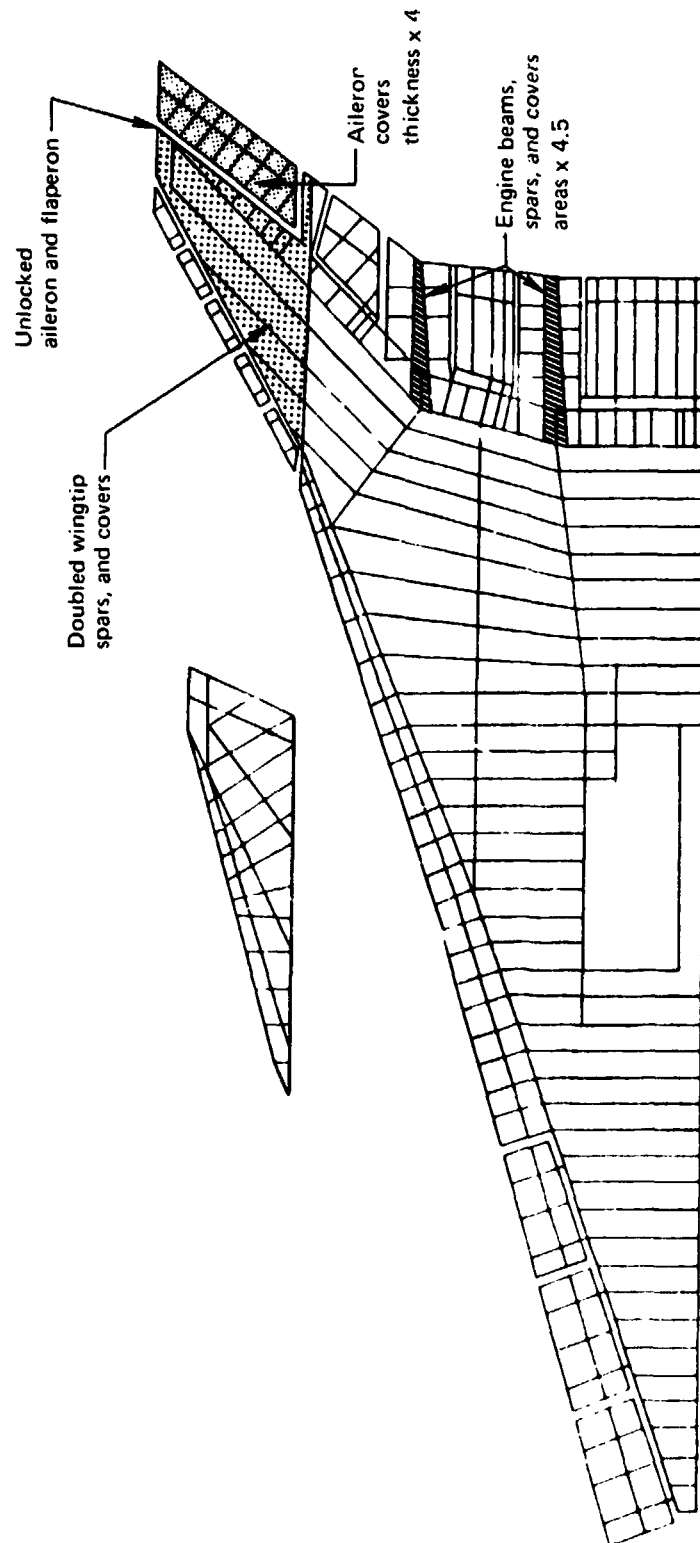


Figure 11-41.—Stiffness Design Modification 3

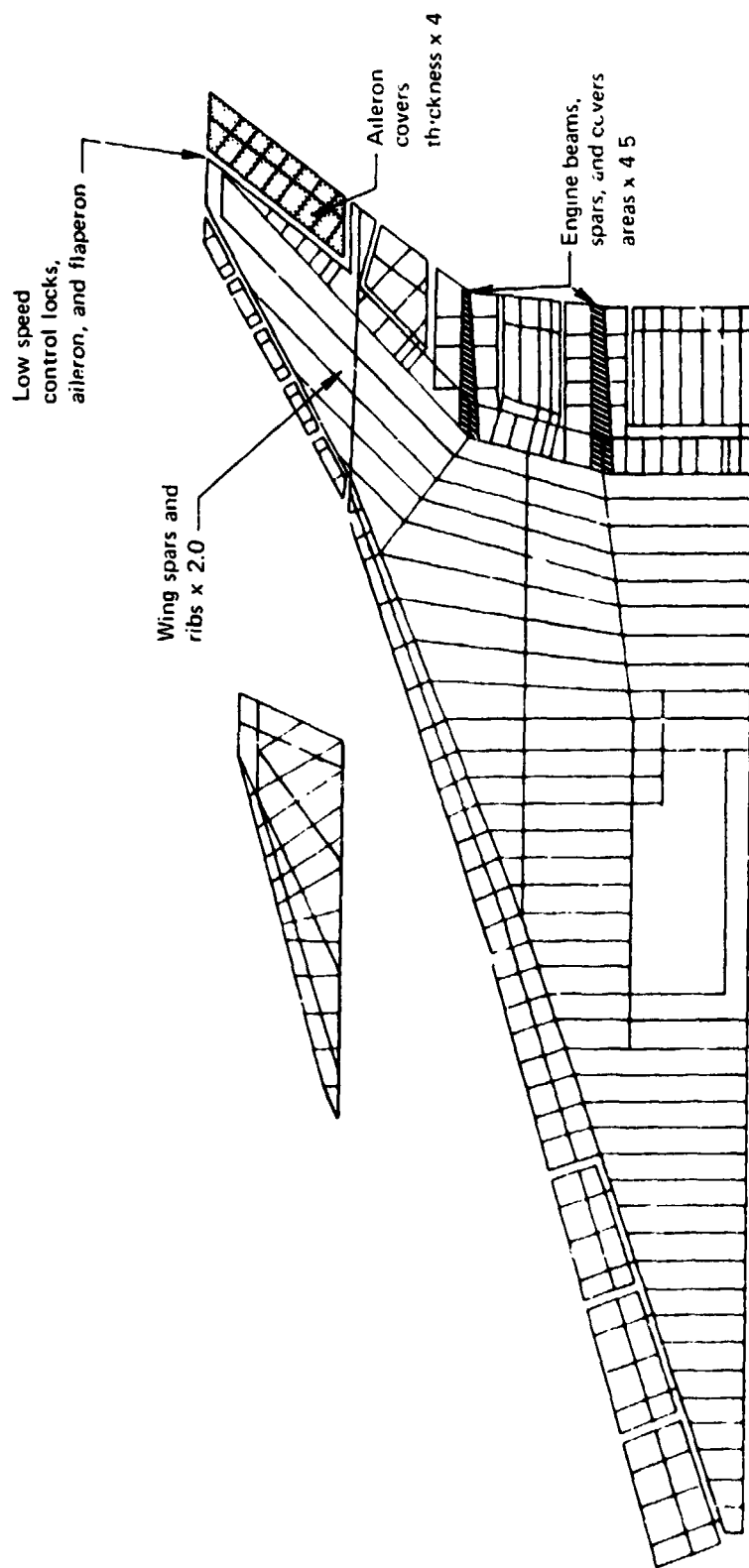


Figure 11-42.—Stiffness Design Modification 4

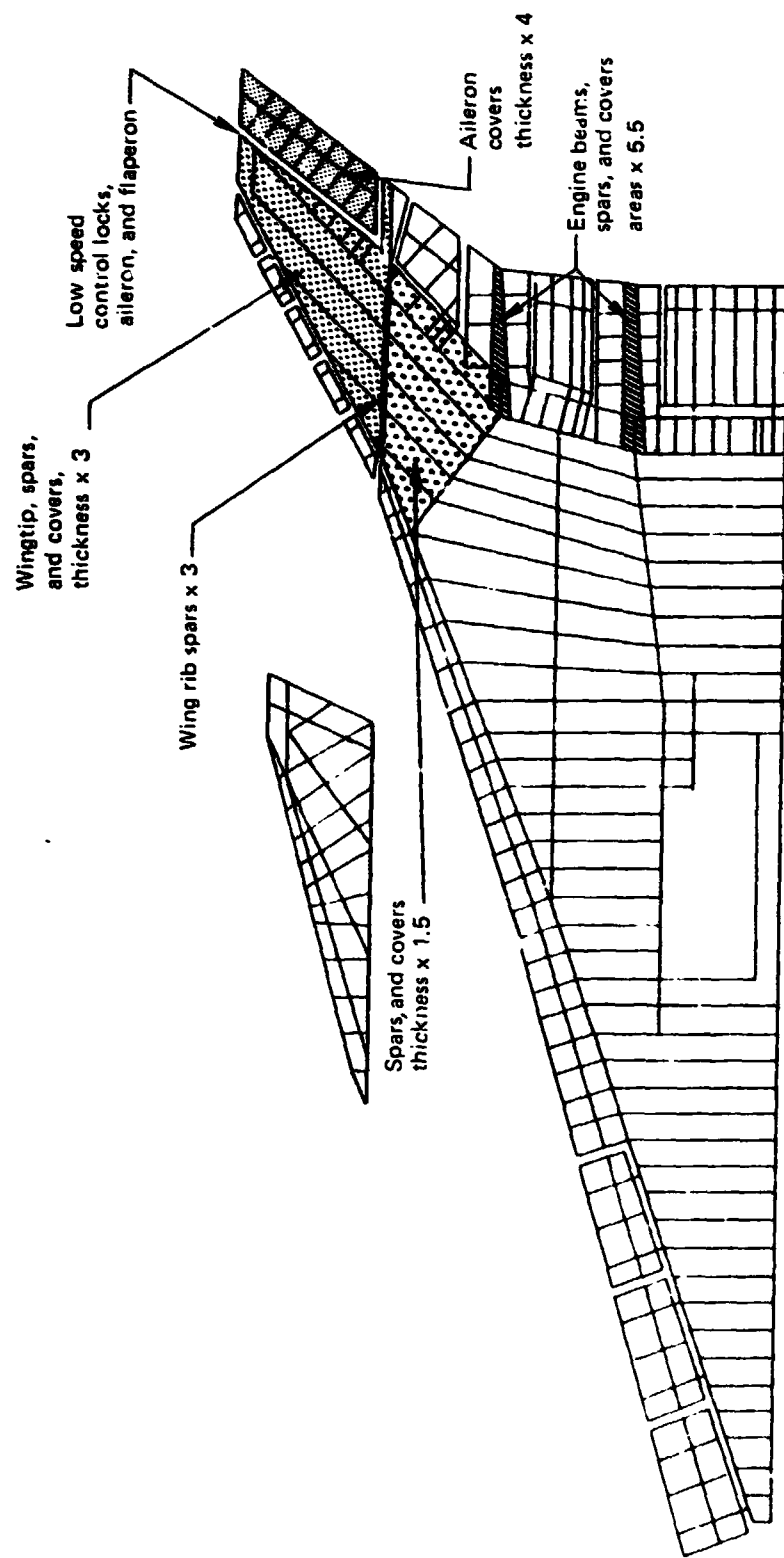


Figure 11-43.—Stiffness Design Modification 5

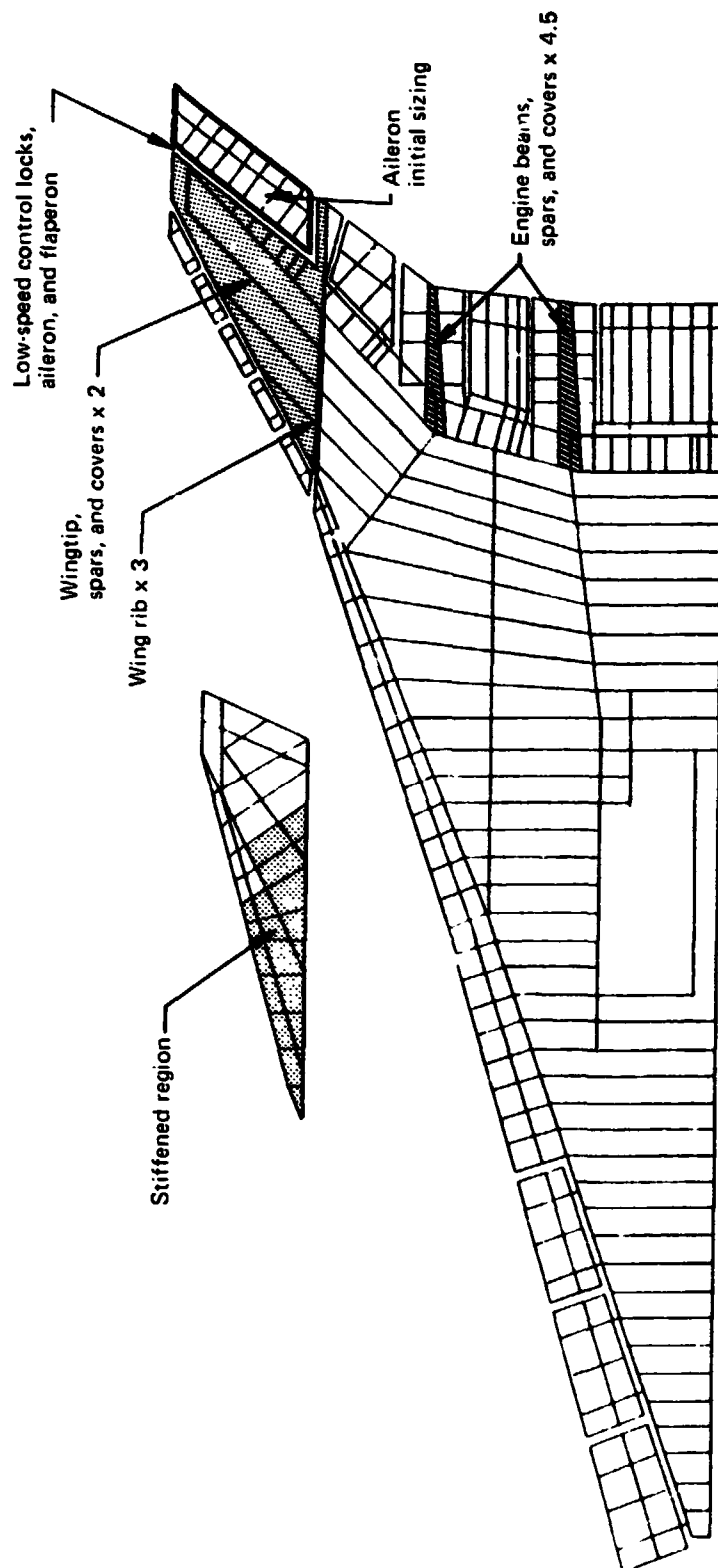


Figure 11-44. —Stiffness Design Modification 6

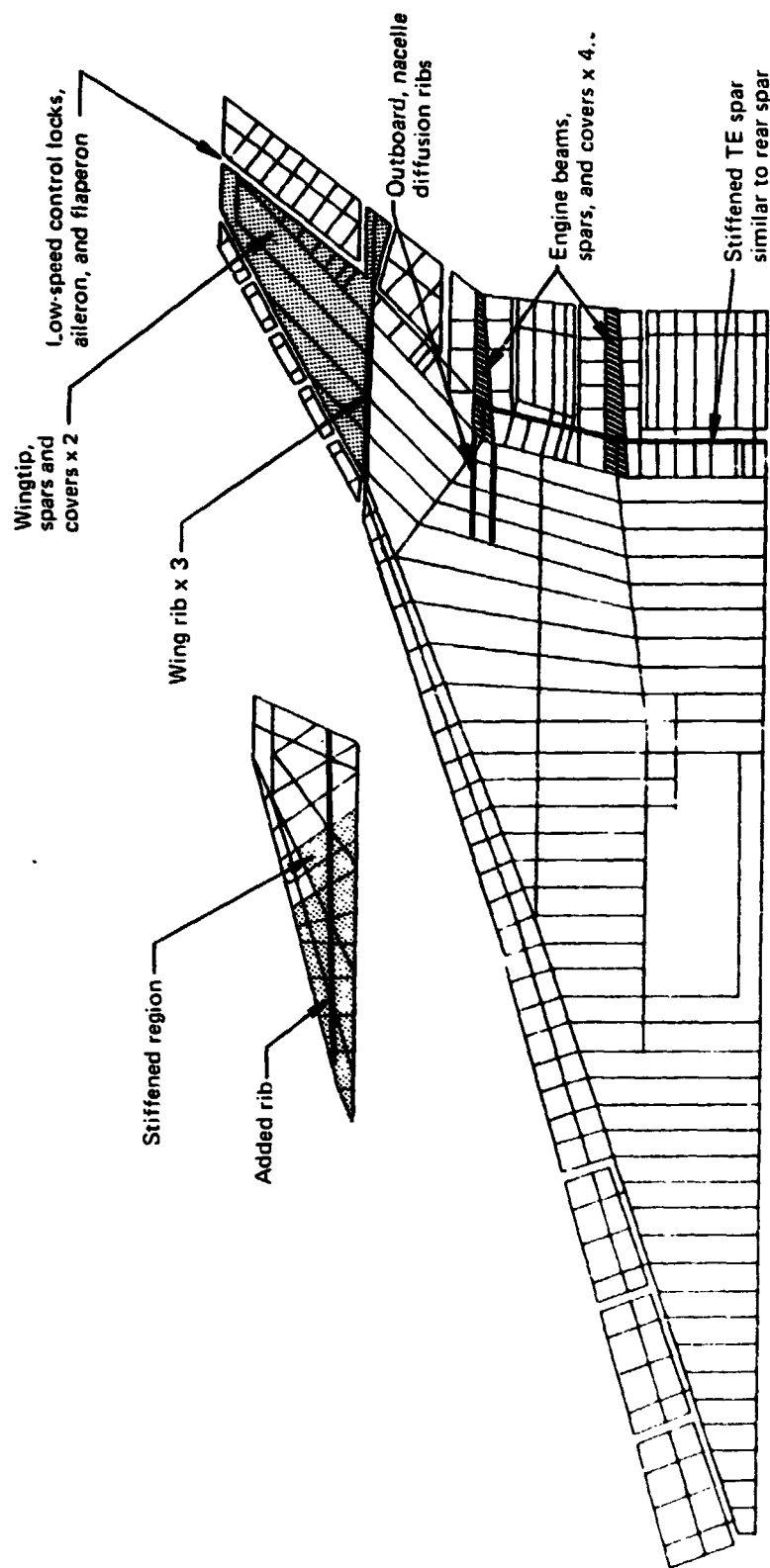


Figure 11-45. —Stiffness Design Modification 7

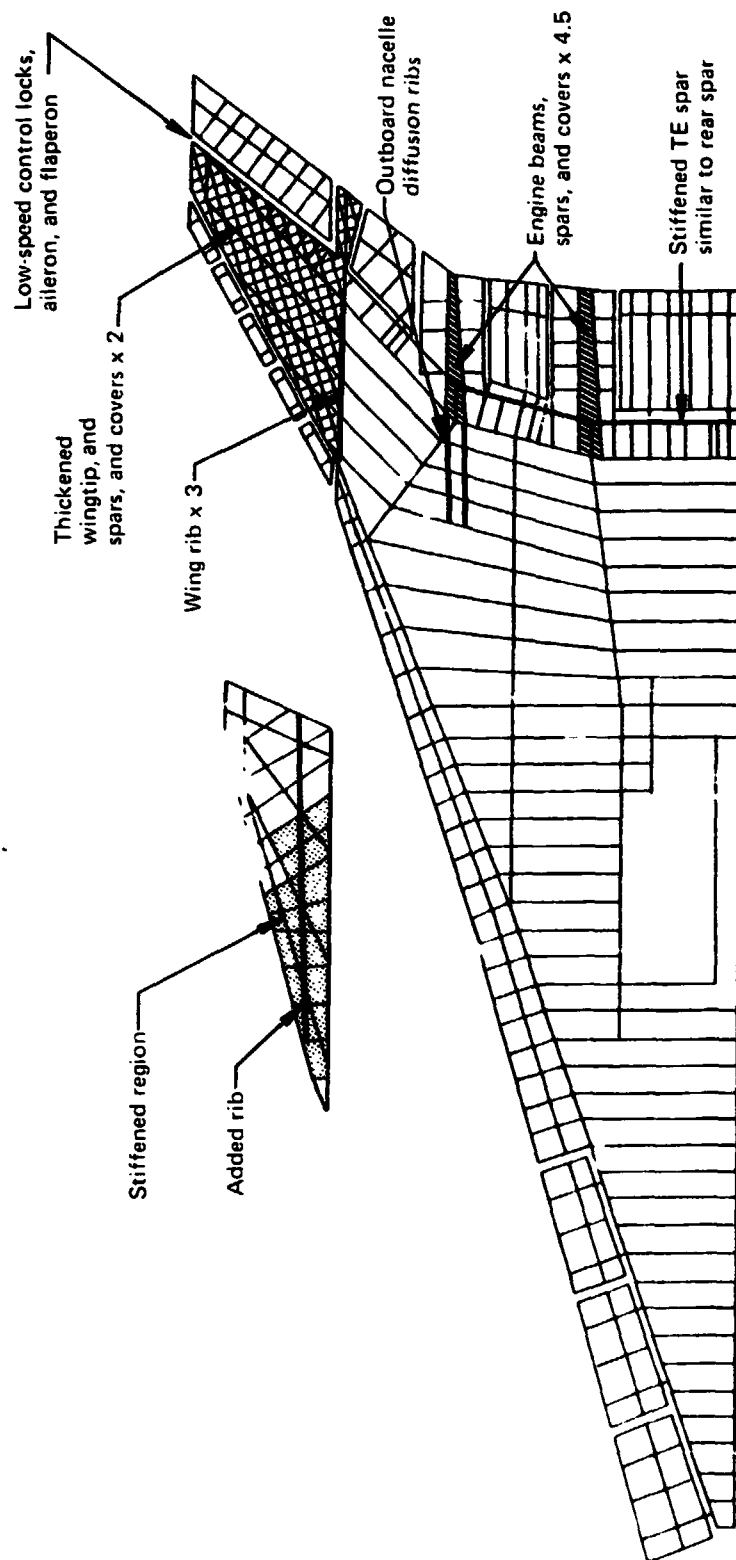


Figure 11-46.—Stiffness Design Modification 8

REPRODUCIBILITY OF THE
ORIGINAL PAGE IS POOR

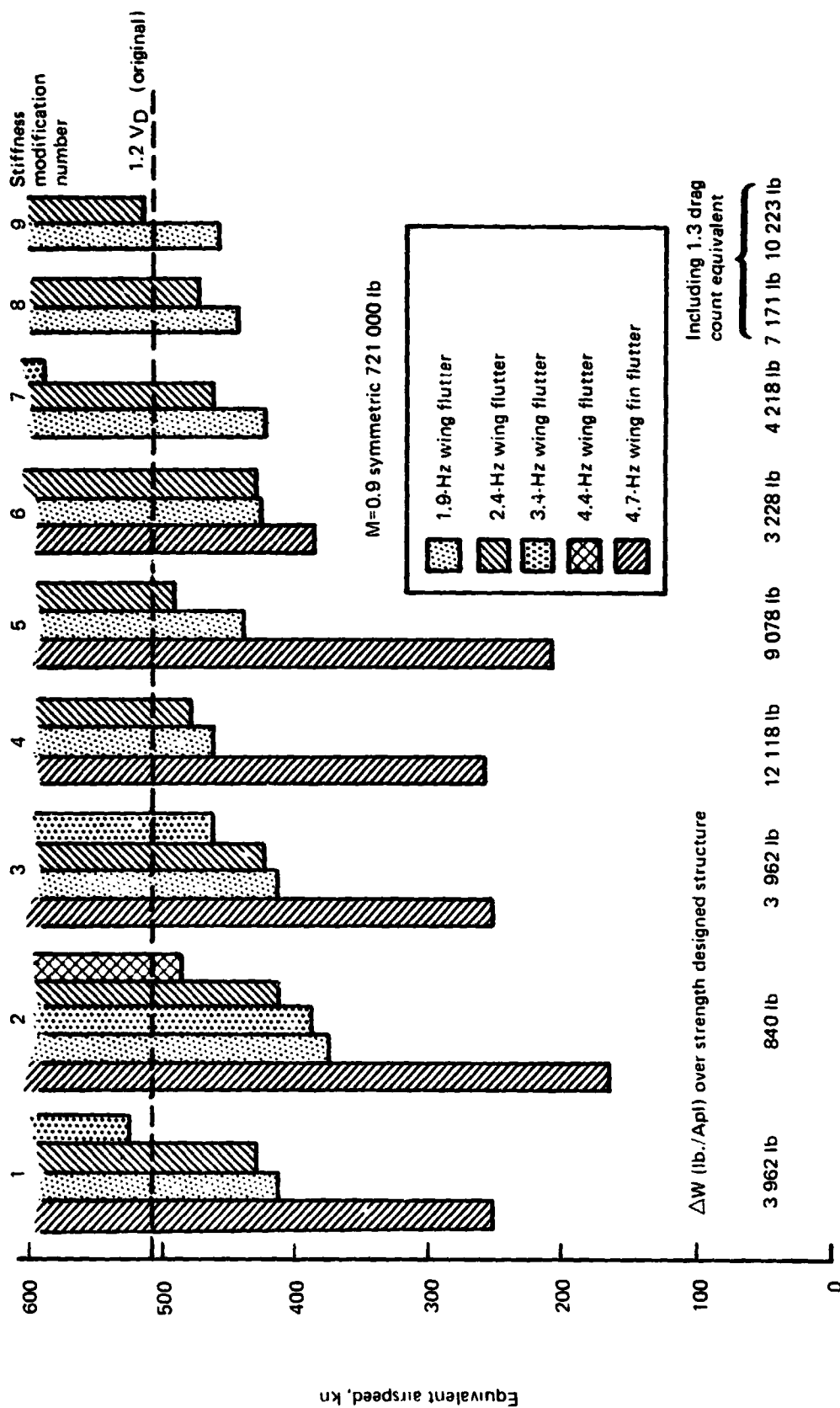


Figure 11-47.—Effect of Stiffness Design Changes on Flutter Speed

SECTION 12

WEIGHT ANALYSIS

by

K. J. DeBord
B. Giridharadas
M. D. Halvorsen

PRECEDING PAGE BLANK NOT FILMED

CONTENTS

	Page
WEIGHT ANALYSIS	723
Weight Distribution of Mass Models	723
Theoretical to Actual Factors	725
Weight Changes as a Result of Structural Analysis	726
Additional Weight Required for Stiffness	727
Group Weight Statement, Model 969-512B	728

TABLES

No.		Page
12-1	Wing Leading Edge and Trailing Edge Structure, Mass Input Elements ..	729
12-2	Wing Contents, Mass Input Elements	730
12-3	Aluminum Brazed Titanium Honeycomb Panels, Skin Weight and \bar{t}	731
12-4	Wing Structural Weight Change, Model 969-512B	732
12-5	Wing Mounted Fin Weight Comparison, Model 969-512B	733
12-6	Wing Stiffness Weight Change, Model 969-512B	734
12-7	Wing Stiffness Design Modifications, Model 969-512B	735
12-8	Group Weight and Balance Statement, Model 969-512B	736

FIGURES

No.		Page
12-1	Mass Distribution for Structural Analysis	737
12-2	Mass Components for Flutter Analysis	738
12-3	Wing Box Spar and Rib Elements	739
12-4	Wing Box Cover Elements	740
12-5	Wing Content Weight - Spanwise Distribution	741
12-6	Wing Content Weight - Chordwise Distribution	742
12-7	Wing Leading Edge, Mass Distribution	743
12-8	Wing Trailing Edge, Mass Distribution	744
12-9	Wing Leading Edge & Trailing Edge Structure, Mass Input Elements	745
12-10	Wing Contents, Mass Input Elements	746
12-11	Mass Paneling for Aeroelastic Loads Analysis, Output	747
12-12	Mass Paneling for Flutter Analysis, Output	748
12-13	Body Structure and Contents, Mass Distribution	749
12-14	Body Payload, Mass Distribution, Passenger Loading, Cargo Loading	750
12-15	Body Structure and Contents, Mass Input Elements	751
12-16	Wing Mounted Vertical Fin, Mass Input Elements	752
12-17	Body Mounted Vertical Tail, Mass Input Elements	753
12-18	Body Mounted Horizontal Tail, Mass Input Elements	754
12-19	Lumped Mass Items - Pounds/Side	755
12-20	Structural Weight Estimation	756
12-21	Non-Optimum Structural Definition, (Example)	757
12-22	Wing Box Sections, National SST	758
12-23	Aluminum Brazed Titanium Honeycomb Panels, Skin \bar{t} vs Skin Pad-Up	759
12-24	Structural Weight Estimation, Wing Box Cover Elements	760

**FIGURES
(CONCLUDED)**

No.		Page
12-25	Wing Box Weight Estimation	761
12-26	Wing Mounted Fin, Initial Sizing, Model 959-512B	762
12-27	Wing Mounted Fin, Skin Gages, Modification for Final Stiffness, Model 969-512B	763
12-28	Wing Mounted Fin, Spar & Rib Chord Areas, Modification for Final Stiffness, Model 969-512B	764
12-29	Wing Mounted Fin, Spar & Rib Web Gages, Modification for Final Stiffness, Model 969-512B	765

Symbols and Abbreviations

A	Area
FT	Feet
FWD	Forward
IBFLN-ACT	Inboard flaperon actuator
IBFLP-ACT	Inboard flap actuator
IN	Inches
IN²	Inches squared
K	1000 pounds
L.E.	Leading Edge
Lb, lb	Pounds
LEIF	Leading edge inboard flap
LEOF	Leading edge outboard flap
PPD	Prototype point design
PT	Prototype
REF	Reference
SECT	Section
SQ	Square
SRP	Structural reference plane
SST	Supersonic transport
t	Thickness
\bar{t}	Equivalent thickness
T.E.	Trailing edge
TEIF	Trailing edge inboard flap

Symbols (Concluded)

TEIFN	Trailing edge inboard flaperon
TEIS	Trailing edge inboard spoiler
TEOA	Trailing edge outboard aileron
TEOFN	Trailing edge outboard flaperon
TEOS	Trailing edge outboard spoiler
TES	Trailing edge spoiler
TESD	Trailing edge spoiler/slot deflector
TI	Titanium
WC	Wing contents
WL	Water line
WT	Weight
Δ	Delta-incremental
ρ	Density
ω	Unit weight
\mathcal{C}_L	Centerline
$^{\circ}\text{F}$	Degrees fahrenheit
#	Pounds
%	Percent

SECTION 12

WEIGHT ANALYSIS

WEIGHT DISTRIBUTION OF MASS MODELS

INTRODUCTION

Separate mass matrices are required for the integrated structural analysis as shown in figure 12-1: one for the aeroelastic loads analysis and the other for the flutter analysis. These are obtained from a preliminary weight and balance estimate of the airplane which is required before this mass distribution can begin. Except for those items outlined later, the Task I weight and balance estimate of the model 969-512B airplane shown in table 1-10 was used as input data for the Task II mass distribution in the integrated computer analysis. Figure 12-2 shows the method by which the various components of the operational empty weight, payload and fuel are distributed for the flutter analysis.

WING AND CONTENTS

The weight of the wing structure and contents is distributed into the mass model a number of ways. The wing box primary structure is built up as an assembly of spars, ribs and cover elements such as shown in figures 12-3 and 12-4. The weight of these structural elements is automatically calculated from the material density and volume required to satisfy the structural requirements.

To this must be added the nonoptimum structure consisting of pad-up, fasteners, fittings, etc., to arrive at a practical airframe weight. The theoretical-to-actual weight factor is input as a percentage of the cover material, spars, ribs and beams. The derivation and a more detailed explanation of the theoretical-to-actual factor is discussed in later paragraphs.

The surface panels, including honeycomb core and braze, and the main landing gear doors are entered in the program as plate mass elements and distributed as a uniform load over the area covered.

Some of the miscellaneous items in the wing box, such as fairing, fuel system provisions, aerodynamic fences and jacking provisions are treated as rods, plates or point masses, whichever is appropriate based on the shape similarity.

The wing box contents can be treated as a two-dimensional uniform load. The spanwise distribution is shown in figure 12-5. The chordwise distribution of the wing contents is plotted in a similar manner. Two sample span locations for chordwise distribution of the wing contents are shown in figure 12-6

Figure 12-7 shows the weight of the wing leading edge structure and contents as a function of the leading edge length. Similarly, figure 12-8 shows the wing trailing edge structure and contents.

The weight distributions given in figures 12-5 through 12-8 were determined from the Model 969-336C and are considered typical for an Arrow Wing configuration. These types of weight distributions, while not presently automated into the ATLAS program, were used as guides in distributing wing secondary structure and contents of the model 969-512B.

The weight of the leading and trailing edge structure and the wing contents are defined in terms of the mass panels shown in figures 12-9 and 12-10.

The mass panel definitions selected for the mass input into the ATLAS program are selected on a basis which most nearly represents the physical mass distribution. The ATLAS program has an internal capability to automatically lump these input distributions to provide a mass matrix consistent with the retained structural nodes for the aeroelastic loads and flutter analyses. Examples of the automatic relumping are shown in figures 12-11 and 12-12 for the aeroelastic load analysis and flutter analysis, respectively.

Tables 12-1 and 12-2 tabulate the wing mass distributions associated with the panels identified in figures 12-9 and 12-10. Inertia data are generated within the analysis module.

BODY AND CONTENTS

The body structure and contents are plotted as a one-dimensional running load in figure 12-13. The concentrated loads of galleys and contents at the galley doors are identified, as well as the build-up of the monocoque weight at the front spar. This plot does not include the wing-body intersection, passengers or cargo weights.

The wing-body intersection is included in the mass model as part of the body. This consists of the wing inboard of buttock line 55 and includes the wing carry through center section.

The passengers and cargo are shown as a one-dimensional load distribution in figure 12-14. The chart shows a full payload condition. This is modified for partial load conditions, such as forward and aft center of gravity conditions.

Figure 12-15 gives the body nodes associated with the mass panels used in the airplane modeling. The body structure and contents, wing-body intersection, passengers and cargo, are all modeled as point masses on these nodes for aeroelastic loads analysis and as concentrated loads for the flutter analysis. Required body inertia data is generated within the loads analysis; however, the flutter analysis requires roll inertia of the body structure and contents as input for the antisymmetric design conditions.

EMPENNAGE

The weight of the wing mounted vertical fin, the body mounted vertical tail, and the horizontal tail are all input as a set of concentrated masses in the mass model for the aeroelastic loads analysis. These data are shown in figures 12-16, 12-17 and 12-18. The corresponding inertia data is generated within the computer program.

The modeling of the empennage for the flutter analysis differs from the aeroelastic loads analysis in that the body mounted vertical tail and horizontal tail are each modeled as single lump masses with weight, center of gravity and three-axis inertia information. The wing mounted vertical fin is input as a set of concentrated masses similar to that on aeroelastic loads analysis.

NACELLES

The engine nacelles are input as a set of concentrated masses in the aeroelastic loads analysis and as single lump masses in the flutter model as shown in figure 12-19.

LANDING GEAR

For the aeroelastic load analysis, the nose gear is treated as two concentrated masses in the up position and as a single concentrated mass in the gear down position. The main gear is paneled as a single concentrated mass in both the gear up and down position. The landing gear is input as lumped masses along with inertia data for the flutter analysis.

FUEL

The fuel tank arrangement along with tank capacities for the model 969-512B are discussed in Section 1 and are shown in figure 1-29. A balance diagram with center of gravity limits and fuel management for the maximum gross weight condition is shown in figure 1-30, and discussed in section 1. The fuel distribution by tanks was calculated for each of the 27 design conditions while observing the center of gravity limits and fuel management sequence as outlined in section 1. These fuel quantities were translated into percentage of tank capacities and distributed into consistent mass panels as described previously. The body fuel is input as a set of point masses in the aerodynamic loads analysis and as concentrated masses in the flutter analysis.

THEORETICAL TO ACTUAL FACTORS

The finite element analysis produces the weight of the theoretically designed structural elements. To this primary structure must be added the weight of the nonoptimum structure to convert from the theoretical to the practical airframe weight as shown in figure 12-20. Figure 12-21 gives a descriptive example of these nonoptimum structural items in a honeycomb wing surface panel. These consist of: skin pad-ups along the panel edges and access doors, the basic honeycomb core, the dense core along the panel edges, the braze material and miscellaneous items such as access doors, fuel system provisions, fairings, etc.

The theoretical-to-actual structural factors used in the Arrow Wing program were derived from design details from the National SST program. The weight of the basic structural gages were compared with the calculated weight of the released structural drawings to arrive at the theoretical-to-actual factors. Figure 12-22 shows the sections of the National SST wing box which were used to develop the factors for the skin panels shown in the curves on figure 12-23. Table 12-3 gives a tabulation of total skin panel weight and the basic skin weight on which the theoretical-to-actual factors are based.

There are two sets of curves plotted in figure 12-23, one for the prototype airplane (PT) and the other for the prototype point design (PPD). The lower values of the PPD curve represents a production airplane and was used on the Model 969-512B in this study. The PT airplane, however, had more design detail and helped to substantiate the slope of the curve. These curves show that the lighter basic skin gage or thickness results in a greater theoretical-to-actual conversion factor. This is primarily due to the fastening complications and resulting pad-ups at the panel edges. The correction factor for the lower surface is larger than the upper surface because of the many cutouts in the lower surface. As can be seen on figure 12-23, outboard wing section 17 does not plot consistently with the remainder of the wing sections. It was found that this additional wing tip cover material was required to disperse concentrated loads from both the leading edge and trailing edge flaps accounting for the relatively high theoretical-to-actual conversion factor. The model 969-512B has a similar outboard wing tip section, but these higher factors were not considered appropriate as the basic gage of this area was doubled to help alleviate the flutter problem.

A review of the honeycomb core weights on the National SST Program showed that approximately 25 percent must be added to the upper surface and 30 percent to the lower surface basic core weight to account for the dense core around the panel edges and access holes. Similar percentages must be added to the basic braze weight to accommodate the dense core at the panel edges. Figure 12-24 gives a summary of the method of estimating the structural weight of the wing box cover elements, starting with the theoretical structure weight generated by ATLAS.

A study similar to that for the surface panels was made to determine the theoretical-to-actual conversion factors of the spars and ribs on the National SST Program wing. It was found that the average factor for all spars was 15% of the theoretical structural weight and 18% for all ribs.

Figure 12-25 summarizes the use of the theoretical-to-actual conversion factors in combination with the ATLAS structural weights to calculate a total structural wing box weight.

WEIGHT CHANGES AS A RESULT OF STRUCTURAL ANALYSIS

Table 12-4 shows three wing weights: (1) the Task I wing weight estimate, 94,160 pounds, (2) a re-estimate with preliminary stiffness, 101,820 pounds, and (3) a structurally resized wing with preliminary stiffness, 92,310 pounds.

Column (1) of table 12-4 shows the Task I preliminary wing weight. The weight was based on the model 969-336C with weight revisions added for changing material from stress skin to aluminum brazed titanium honeycomb, for changing the wing planform and flap configuration for Model 969-512B, for increasing the gross weight from 635,000 to 750,000 pounds and other miscellaneous design changes.

Column (2) is a revised estimate of Model 969-512B wing based on the ATLAS resized structural box, modified for preliminary stiffness increases. The preliminary stiffness increases consist of doubling the outboard wing tip spars and covers, quadrupling the outboard aileron cover material and stiffening the engine beams.

The breakdown of the 7,660 pound increment between Column (1) and (2) is as follows:

Outboard aileron stiffness increase	+ 840 lbs.
Outboard wing tip stiffness increase	+ 3,122 lbs.
Increase associated with initial sizing	+ 3,698 lbs.
	+ 7,660 lbs.

Column (3) is the weight of the wing as resized by ATLAS inboard of the wing mounted fin, while retaining the sizing for stiffness in the outboard aileron and wing tip region.

The distribution of 9,510 pound reduction is as follows:

Reduction of cover material	- 4,910 lbs.
Reduction of spar material	- 2,556 lbs.
Reduction of rib material	- 2,066 lbs.
Increase of beam material	+ 22 lbs.
	- 9,510 lbs.

Similarly, the wing mounted vertical fin weight was revised, based on the ATLAS structural resizing. The Task I fin weight estimate was 2,470 pounds per airplane. The Task II revision based on the resized elements was 2,850 pounds, or a 380 pound increase per airplane. Figure 12-26 shows the wing mounted fin with this initial structural sizing, and table 12-5 presents a detailed weight breakdown.

ADDITIONAL WEIGHT REQUIRED FOR STIFFNESS

The 92,310 pound strength designed wing with preliminary stiffness was not flutter free. Eight additional flutter analyses were completed with various stiffness design modifications. The final wing weighed 95,760 pounds and included 7,412 pounds of structural changes to satisfy the flutter criteria. These stiffness design modifications are outlined in more detail in section 11.

Table 12-4 tracks the Model 969-512B wing weight from Task I through the ATLAS resizing with preliminary stiffness. Table 12-6 tracks the wing weight changes through the wing "fixes" to satisfy the flutter criteria. Table 12-7 gives a tabulation of the flutter "fixes" and correlates them with the same nine stiffness design modification steps as shown in the wing weight tabulation in table 12-6.

Several revisions were also made to the wing mounted vertical fins to satisfy the flutter requirements. These modifications included increased skin gages, spars and ribs, as well as the addition of an intermediate horizontal rib. However, there was a decrease in the sizing of the base rib.

The Task II wing mounted fins with initial sizing weighed 2,850 pounds. Stiffness design modifications added another 470 pounds for a total of 3,320 pounds per airplane. Figures 12-27, 12-28 and 12-29 show the structural modifications for the final stiffness. Table 12-5 gives a detail weight comparison of the fin with initial sizing and the modifications for the final stiffness.

GROUP WEIGHT STATEMENT, MODEL 969-512B

Table 12-8 shows the Model 969-512B group weight statements for Task I and Task II and the weight increments.

The 1,600 pound increase in wing weight is the net weight change as a result of the ten cycles of analysis necessary for strength design and flutter prevention. This weight includes 1,812 pounds reduction due to structural resizing for strength, and 3,412 pounds increase for the final flutter stiffness modifications.

The 850 pound wing mounted vertical tail weight increase includes 380 pounds for strength design for Task II, and 470 pounds for the final stiffness modification for flutter.

A study was made to determine the fuel temperature rise during supersonic cruise on the Model 969-512B. The results showed a minimum requirement of 1,530 pounds of fuel tank insulation to keep the fuel below the 160° limit. This is 720 pounds over the 810 pounds allowed for in the Task I weight statement. This item is discussed further in section 13.

Table 12-1.--Wing Leading Edge and Trailing Edge Structure--Mass Input Elements

Leading edge structure	
Element number	Unit weight lb/in ²
LE-2	0.0762
LE-3	0.0762
LE-4	0.0650
LE-5	0.0650
LE-6	0.0428

Trailing edge structure	
Element number	Unit weight lb/in ²
TE-1	0.0402
TE-4	0.0402
TE-5	0.0402
TE-6	0.0402
TE-7	0.0402
TE-10	0.0402
TE-11	0.0402
TE-12	0.0402
TE-15	0.0402
TE-16	0.0402
TE-17	0.0402
TE-18	0.0402
TE-19	0.0402
TE-21	0.0402
TE-22	0.0402
TEIF	0.0235
TEIFN	0.0116
TEOFN	0.0201
TEOA	0.0275
TEIS-1	0.0521
TEIS-2	0.0521
TEOS-1	0.0521
TEOS-2	0.0521
TESD-1	0.0509

Table 12-2.—Wing Contents—Mass Input Elements

Leading edge	
Element number	Weight, lb
LEIF-1	317.0
LEIF-2	217.0
LEIF-3	233.0
LEOF-1	35.0
LEOF-2	35.0
LEOF-3	35.0
LEOF-4	35.0
LEOF-5	35.0

Trailing edge	
Element number	Weight, lb
TE-1	38.0
TE-4	557.5
TE-5	87.5
TE-6	124.5
TE-10	315.0
TE-11	87.5
TE-18	20.0
TES-1	236.0
TES-2	246.5
TES-3	330.5
TES-4	95.5
TES-5	123.5
IBFLP-ACT	198.25
IBFLP-ACT	198.25
IBFLN-ACT	133.8
IBFLN-ACT	133.8
IBFLN-ACT	133.8
OBFLN-ACT	107.0
OBFLN-ACT	107.0
OBFLN-ACT	107.0
OBAIL-ACT	118.3
OBAIL-ACT	118.3
OBAIL-ACT	118.3

Wing box	
Element number	Weight, lb
WC-17	263.8
WC-18	643.7
WC-19	597.6
WC-20	404.9
WC-21	86.5
WC-22	815.7
WC-23	1045.0
WC-30	67.7
WC-31	380.4
WC-32	396.1
WC-33	257.2
WC-34	374.7
WC-35	220.6
WC-36	446.9
WC-41	296.8
WC-42	183.4
WC-43	208.7
WC-44	409.7
WC-45	175.1
WC-46	658.3
WC-52	352.0
WC-53	175.7
WC-54	142.6
WC-55	224.2
WC-56	3.7
WC-59	31.0
WC-60	63.9
WC-61	51.9
WC-62	58.3
WC-63	55.1
WC-68	18.4
WC-69	49.1
WC-70	82.3
WC-71	82.9
WC-77	0
WC-78	0
WC-79	0.1
WC-80	53.6
WC-83	0
WC-84	0
WC-85	52.3
WC-90	0
WC-91	0

Table 12-3.—Aluminum Brazed Titanium Honeycomb Panels—Skin Weight and \bar{t}

Wing section	Total skin weight, inner plus outer, lb	Basic skin weight, inner plus outer, lb	Pad-up weight, lb	Pad-up percent of basic skin	Average \bar{t} , inner plus outer, lb
Section 11 outbd PPD upper	4968	4529	439	9.7	0.211
Section 11 outbd PPD lower	5266	4467	799	17.9	0.208
Section 11 center PPD upper	600	541	59	10.9	0.141
Section 11 center PPD lower	717	622	95	15.3	0.162
Section 12 PT upper	3519	3195	324	10.1	0.130
Section 12 PT lower	3972	3278	694	21.2	0.133
Section 13 PT upper	954	763	191	25.0	0.087
Section 14 PPD upper	791	547	244	44.6	0.034
Section 14 PPD lower	1000	675	360	53.3	0.043
Section 14 PT upper	812	547	265	48.4	0.034
Section 14 PT lower	1058	675	383	56.7	0.043
Section 15 PPD upper	253	171	82	48.0	0.027
Section 15 PPD lower	471	298	173	58.1	0.034
Section 15 PT upper	263	171	92	53.8	0.027
Section 15 PT lower	537	337	200	59.3	0.038
Section 17 outbd PT upper	1309	957	352	36.8	0.121
Section 17 outbd PT lower	1340	957	383	40.0	0.121

PPD = National SST prototype point design airplane

PT = National SST prototype airplane

Table 12.4.—Wing Structural Weight Change, Model 969-512B

	(1) Task 1 weight estimate, lb	(2) Reestimate with prelim. stiffness, lb	(3) Resize with prelim. stiffness, lb
Theoretical cover material		24 242	19 510
Nonoptimum cover material		5 188	5 010
Theoretical spars		16 068	13 844
Nonoptimum spar material		2 400	2 068
Theoretical ribs		4 152	2 396
Nonoptimum rib material		730	420
Theoretical beams		634	654
Nonoptimum beam material		96	98
Total structural element weight	46 690	53 510	44 000
Core	5 940	5 940	5 940
Brazes	3 210	3 210	3 210
Landing gear doors	4 100	4 100	4 100
Fairing, fence, and miscellaneous	960	960	960
Total wing box (less center section)	60 900	67 720	58 210
Wing center section	8 560	8 560	8 560
Wing leading edge	14 230	14 230	14 230
Wing trailing edge	10 470	11 310	11 310
Total wing structure, lb	94 160	101 820	92 310
<div style="display: flex; justify-content: space-around; align-items: center;"> <div style="text-align: center;"> <p>ΔWeight due to</p> <p>+ 1,030 lb Reestimate with preliminary stiffness</p> </div> <div style="text-align: center;"> <p>- 9510 lb Wing structural resizing</p> </div> </div>			

Table 12-5.—Wing Mounted Fin Weight Comparison, Model 969- 512B

	Task I lb	Task II	
		Initial sizing lb	Final stiffness lb
Structural box			
Honeycomb panels			
Skin		320.9	410.4
Core (3/4 in.)		145.9	145.9
Braze		83.5	83.5
Spars			
Chords		185.8	197.0
Webs		34.1	41.4
Base rib			
Chords		147.1	113.3
Web		34.3	28.7
Intermediate rib			
Chords			62.6
Web			18.5
Remaining ribs			
Chords		168.5	173.9
Webs		33.4	38.3
Leading edge			
Skin		58.9	76.9
Core (full depth)		42.7	42.7
Braze		24.2	24.2
Trailing edge			
Skin		19.3	19.3
Core (full depth)		29.5	29.5
Braze		15.4	15.4
Tip			
Skin		14.3	14.3
Core (full depth)		17.8	17.8
Braze		9.8	9.8
Miscellaneous (3%)		39.6	46.6
Total side	1235.0	1425.0	1610.0
Total/airplane	2470.0	2850.0	3320.0
ΔWeight		+380	+470

Table 12-6.—Wing Stiffness Weight Change, Model 969-512B

	Increase with present stiffness						Final stiffness		
	(1) lb	(2) lb	(3) lb	(4) lb	(5) lb	(6) lb	(7) lb	(8) lb	(9) lb
Theoretical cover material	19 510	22 820	24 520	24 132	27 670	24 518	24 518	24 514	24 547
Nonoptimum cover material	010								
Theoretical spars	13 844	14 718	15 912	23 434	17 655	15 909	15 904	16 031	16 317
Nonoptimum spar material	2 038								
Theoretical ribs	2 396	2 688	2 816	3 742	3 039	2 947	3 582	3 601	6 016
Nonoptimum rib material	420								
Theoretical beams	654	752	752	848	752	752	752	752	752
Nonoptimum beam material	98								
Total structural element weight	44 000	40 978	40 000	52 156	49 116	44 126	44 756	44 898	47 632
Core	5 940	5 940	5 940	5 940	5 940	5 940	5 940	5 940	5 940
Braze	3 210	3 210	3 210	3 210	3 210	3 210	3 210	3 210	3 210
Landing gear doors	4 100	4 100	4 100	4 100	4 100	4 100	4 100	4 100	4 100
Fairing, fence and miscellaneous	960	960	960	960	960	960	960	960	960
Total wing box (less center section)	58 210	55 188	58 210	66 366	63 326	58 336	58 966	59 108	61 842
Wing center section	8 560	8 560	8 560	8 560	8 560	8 560	8 560	8 560	8 560
Wing leading edge	14 230	14 230	14 230	14 230	14 230	14 230	14 230	14 230	14 230
Wing trailing edge	11 310	11 310	11 310	11 310	11 310	10 440	10 810	10 810	11 128
Total wing structure, lb	92 310	89 288	92 310	100 466	97 426	91 566	92 566	92 708	95 760

Table 12-7.—Wing Stiffness Design Modifications—Model 969-512B

Stiffness design modification	(1)	(2)	(3)	(4)	(5)	(6)	(7)	(8)	(9)
Double wing tip spars and covers	X		X			X	X	X	X
Quadruple outboard aileron covers	X	X	X	X	X				
Aileron control locks	X	X		X	X	X	X	X	X
Stiffened engine beams	X	X	X	X	X	X	X	X	X
Double all wing box spars and ribs				X					
Triple wing tip spars and covers					X				
Increase spars, ribs, and covers 50% between vertical fin and kink rib					X				
Triple fin support rib						X	X	X	X
Stiffen trailing edge spar							X	X	
Add outboard nacelle diffusion ribs							X	X	
Increase outboard wing box depth (refair)								X	X
Add four outboard wing tip ribs									X
Add outboard and inboard nacelle diffusion ribs									X
Increase front spar web gage to average skin gage outboard of wing fin									X
Increase total rear spar web gage to average skin gage									X

Table 12-8.—Group Weight and Balance Statement, Model 969-512B

Group	Task I		ΔWeight lb	Task II	
	Weight lb	Arm in.		Weight lb	Arm in.
Wing	94 160	2 604	+1 600	95 760	2 604
Horizontal tail	6 530	3 623		6 530	3 623
Vertical tail (body and wing mounted)	5 000	3 406	+850	5 850	3 406
Body	56 140	2 117		56 140	2 117
Main gear	37 320	2 548		37 320	2 548
Nose gear	3 760	1 178		3 760	1 178
Nacelle	19 080	2 949		19 080	2 949
Total structure	221 990	2 525.0	+2 450	224 440	2 528.9
Engine (incl T/R, S/S and nozzle)	45 200	3 076		45 200	3 076
Engine accessories	1 350	2 944		1 350	2 944
Engine controls	780	2 308		780	2 308
Starting system	300	2 919		300	2 919
Fuel system	8 390	2 495	+720	9 110	2 495
Total propulsion	56 020	2 974.3	+720	56 740	2 968.2
Instruments	1 865	1 710		1 865	1 710
Flight controls	14 700	2 679		14 700	2 679
Hydraulics	5 795	2 854		5 795	2 854
Electrical	5 160	2 092		5 160	2 092
Electronics	2 885	1 282		2 885	1 282
Furnishings	19 010	1 817		19 010	1 817
ECS	8 430	2 440		8 430	2 440
Anti-icing	135	558		135	558
APU	250	2 978		250	2 978
Insulation	2 900	1 913		2 900	1 913
Total systems and equipment	61 130	2 209.7		61 130	2 209.7
Options	2 500	2 491		2 500	2 491
Manufacturer's empty weight	341 640	2 542.0	+3 170	344 810	2 544.3
Standard items	8 200	2 193		8 200	2 193
Operational items	5 260	1 716		5 260	1 716
Operational empty weight	355 100	2 521.7	+ 3170	358 270	2 524.1
Payload	48 906	1 882		48 906	1 882
Zero fuel weight	404 006	2 444.3	+3 170	407 176	2 447.0

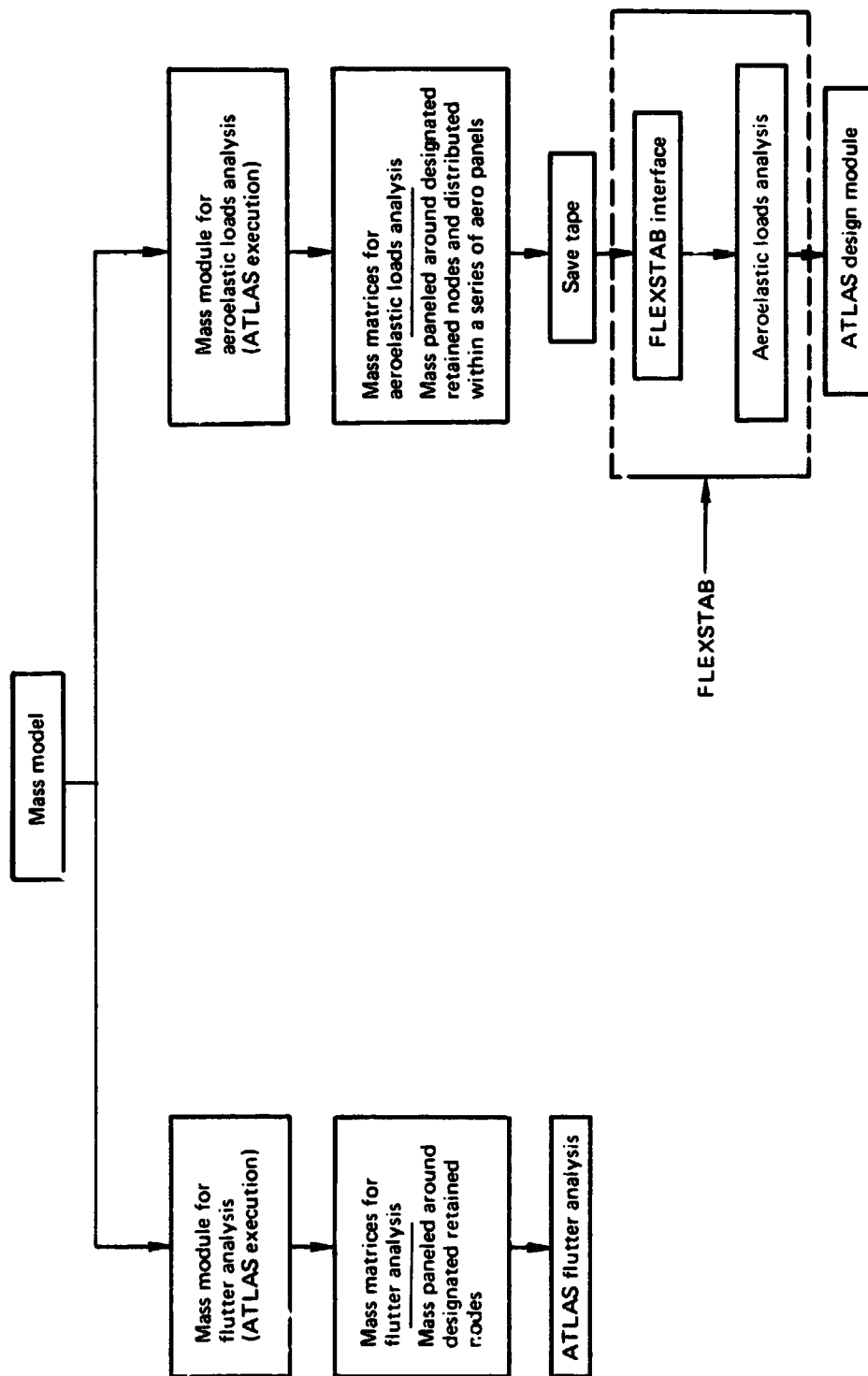


Figure 12-1.—Mass Distribution for Structural Analysis.

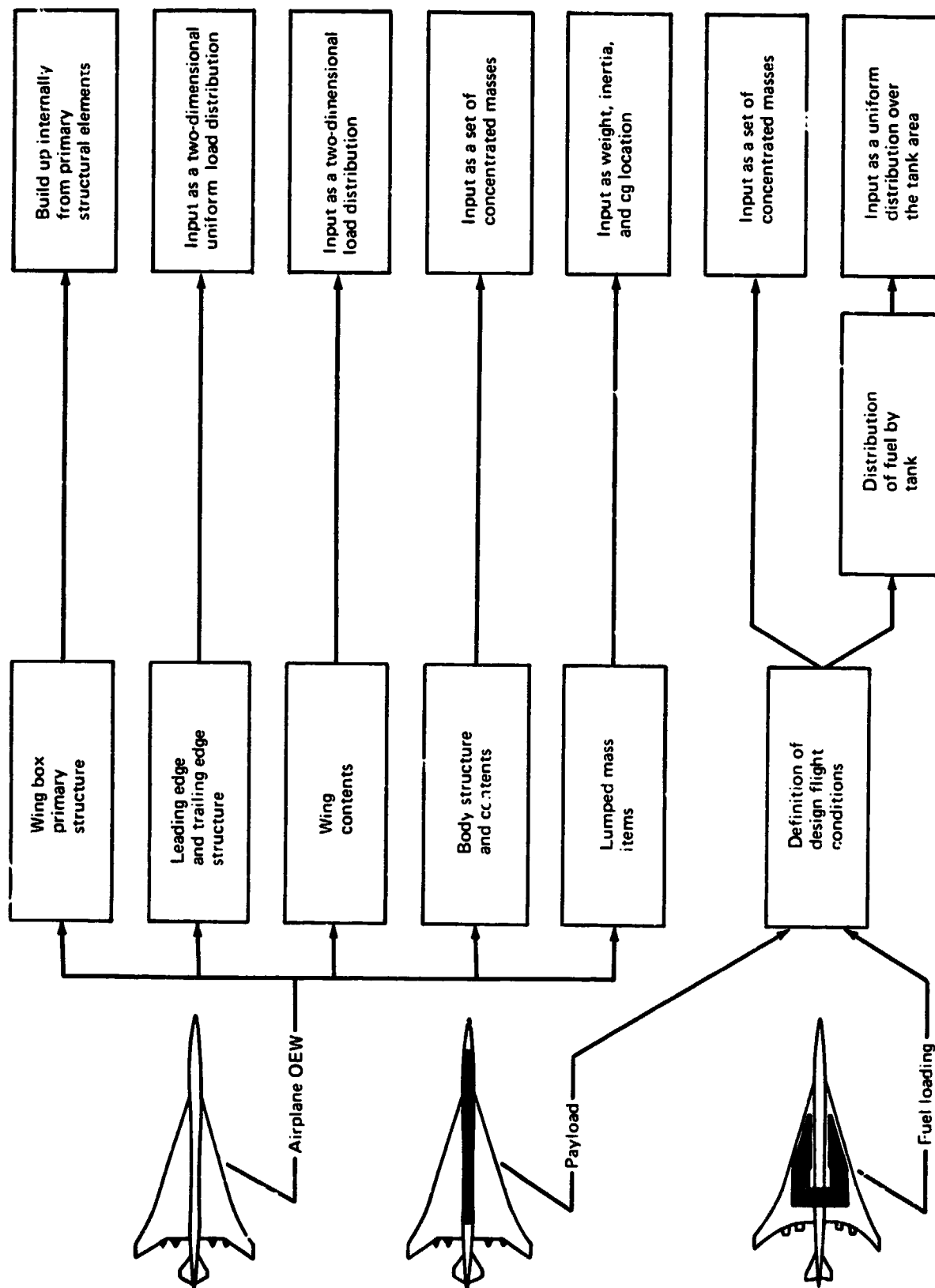


Figure 12-2.—Mass Components for Flutter Analysis

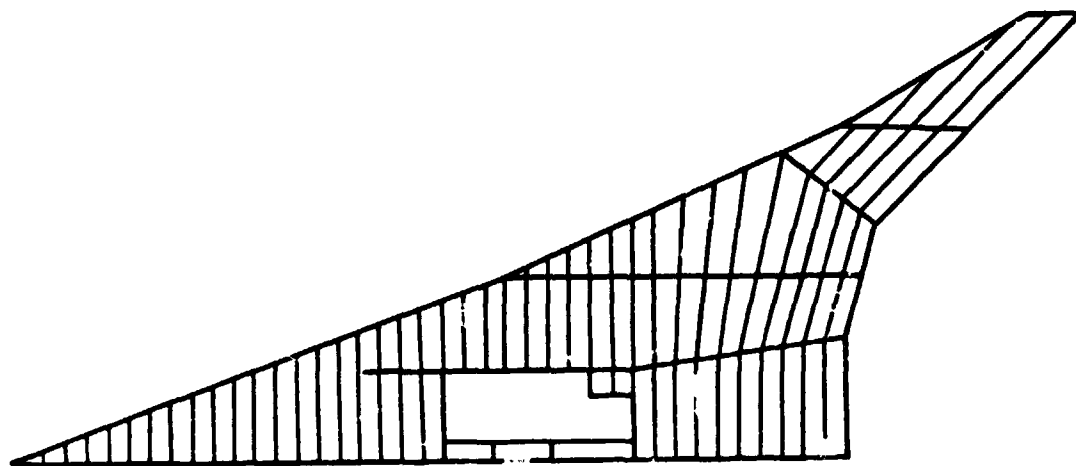


Figure 12-3.—Wing Box Spar and Rib Elements

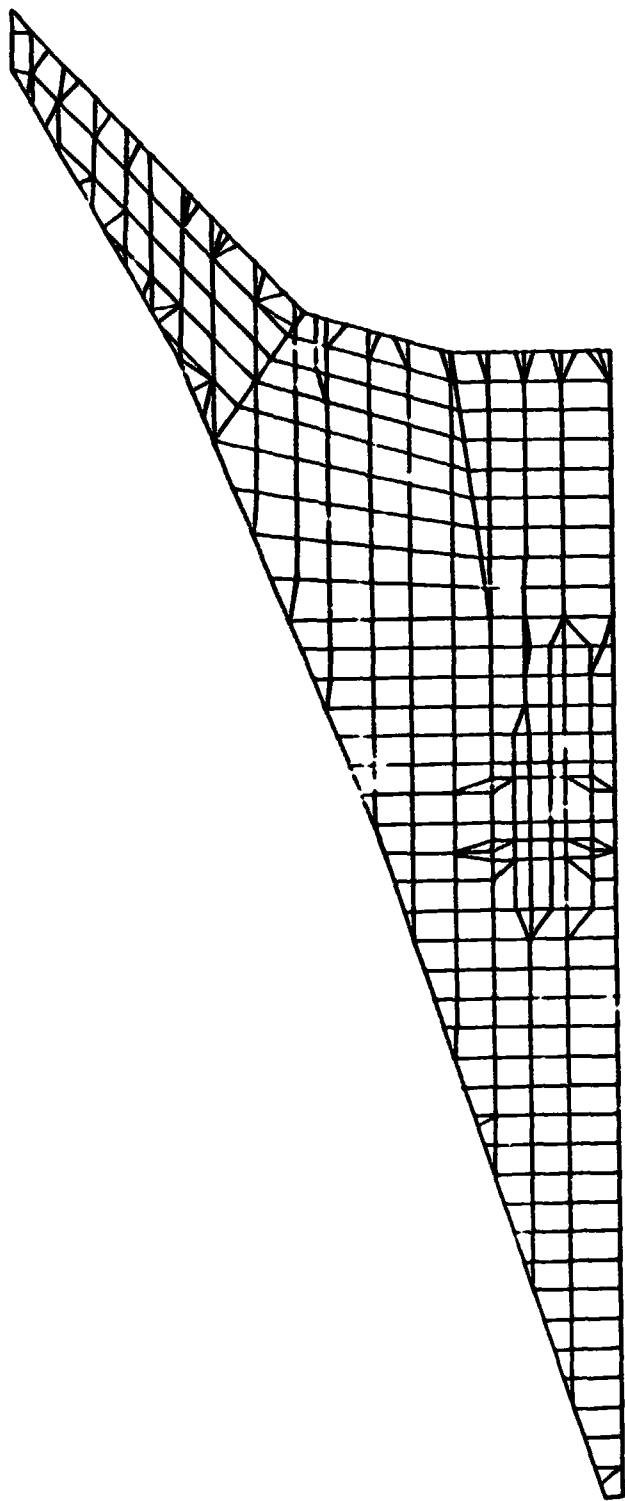


Figure 12-4.—Wing Box Cover Elements

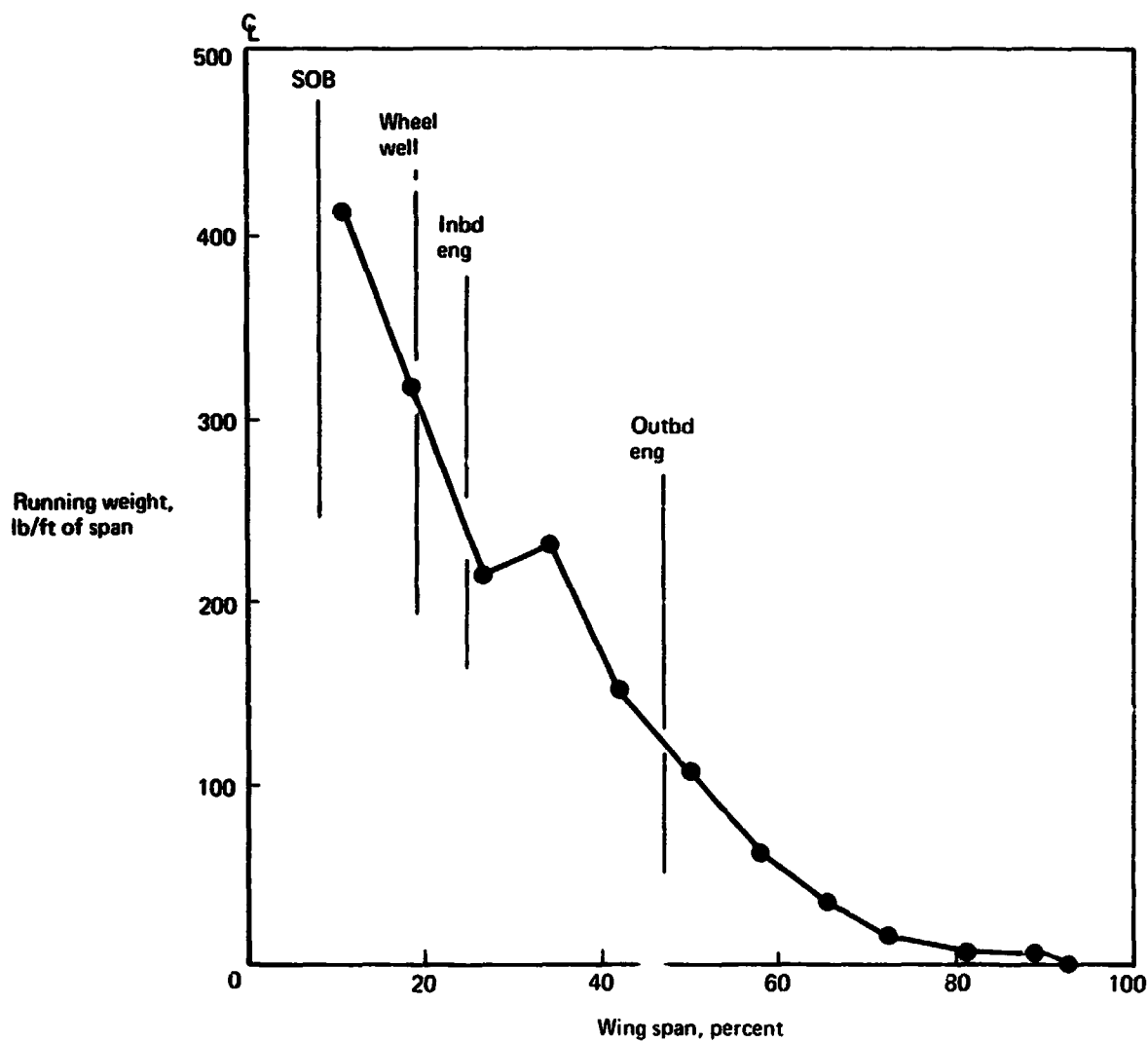


Figure 12-5.—Wing Content Weight—Spanwise Distribution

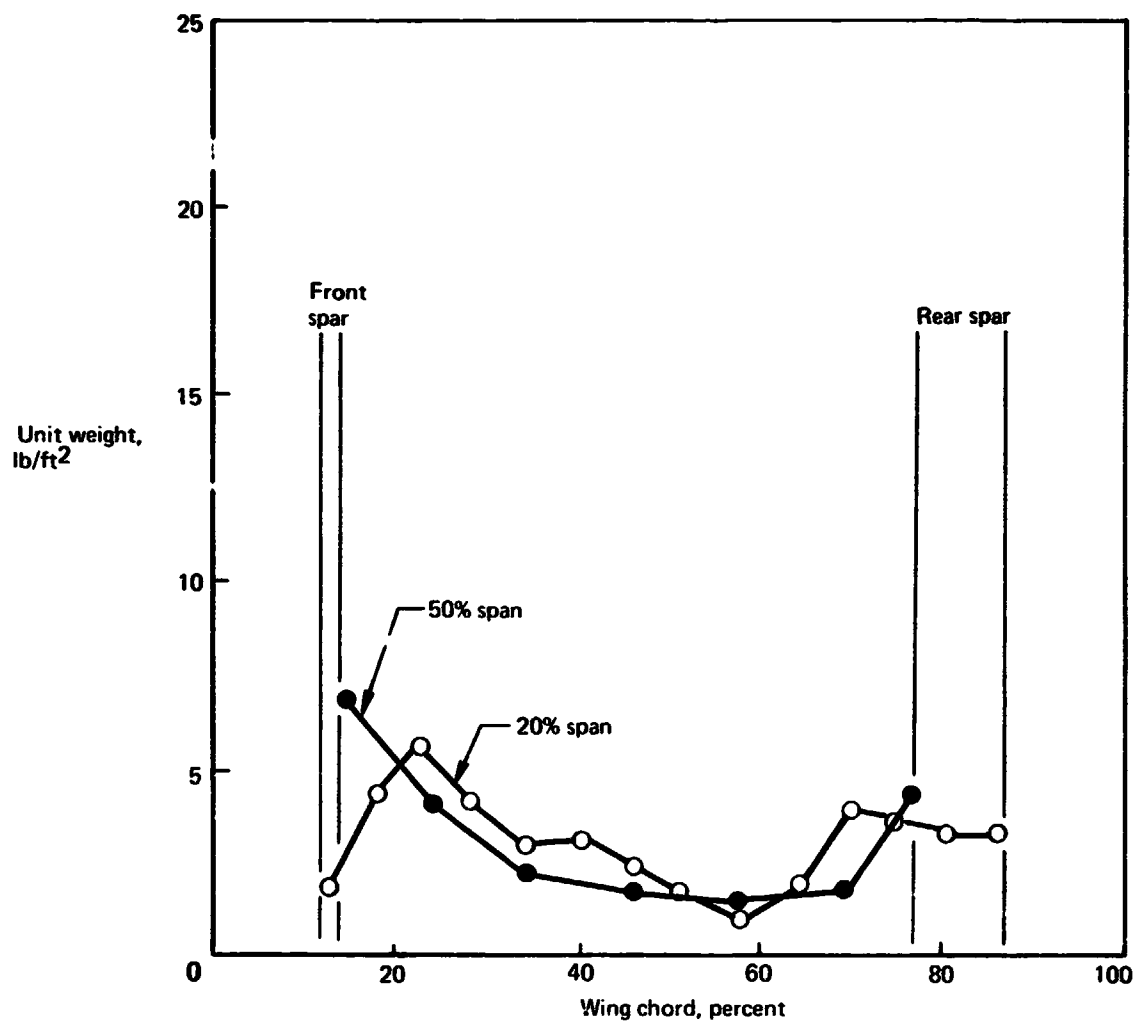


Figure 12-6.—Wing Content Weight—Chordwise Distribution

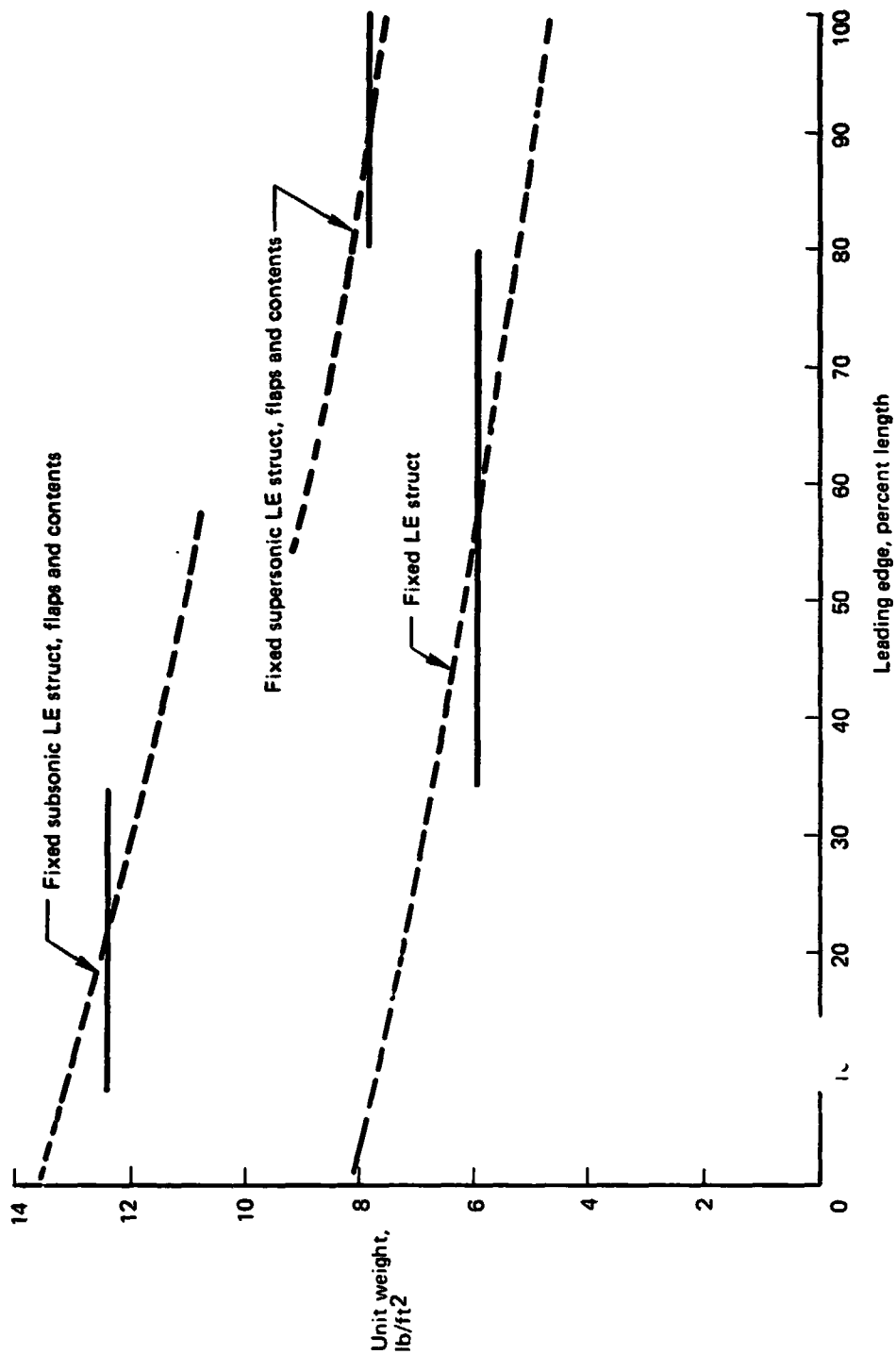


Figure 12.7.—Wing Leading Edge—Mass Distribution

REPRODUCIBILITY OF THE
ORIGINAL PAGE IS POOR

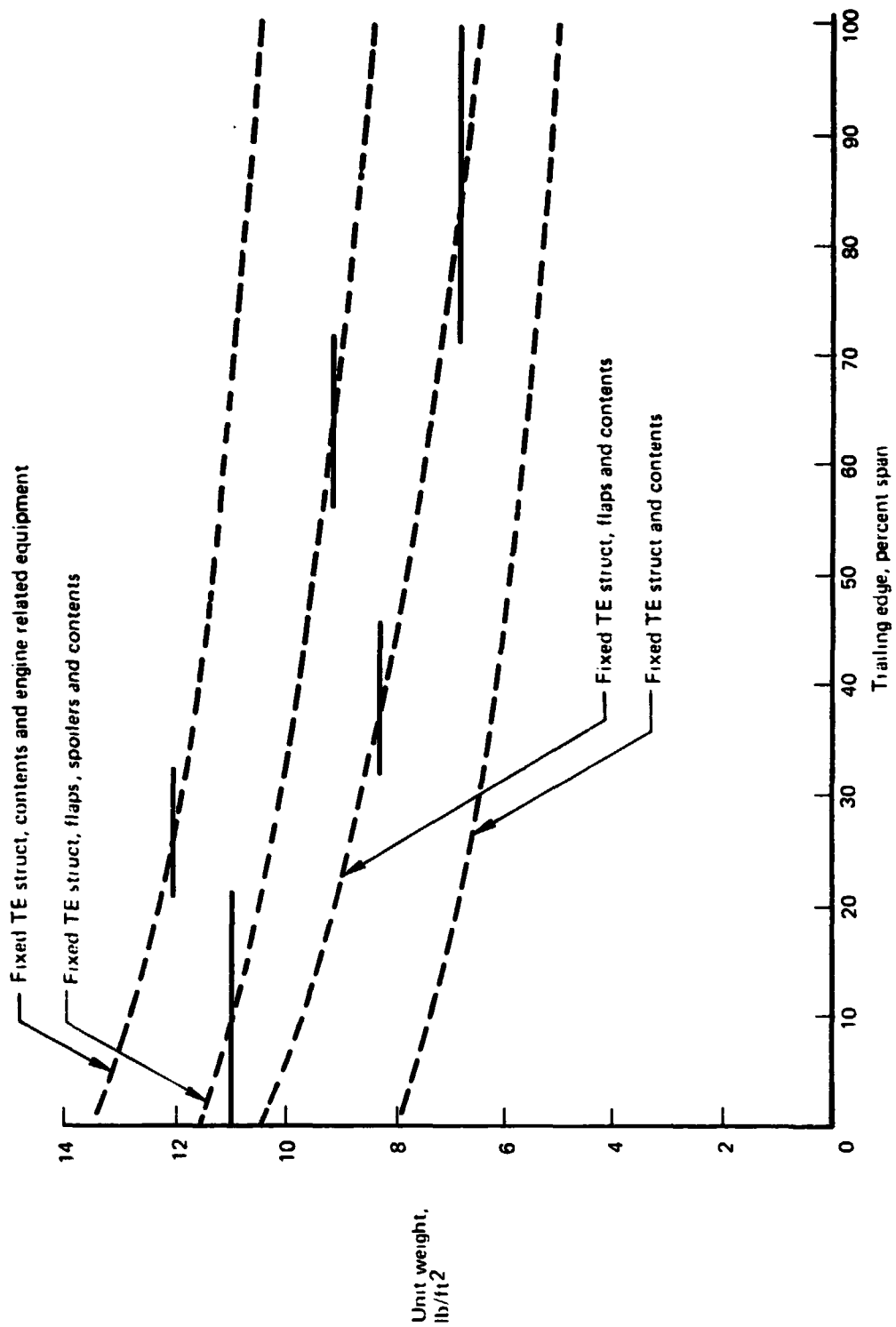


Figure 12-8. —Wing Trailing Edge - Mass Distribution

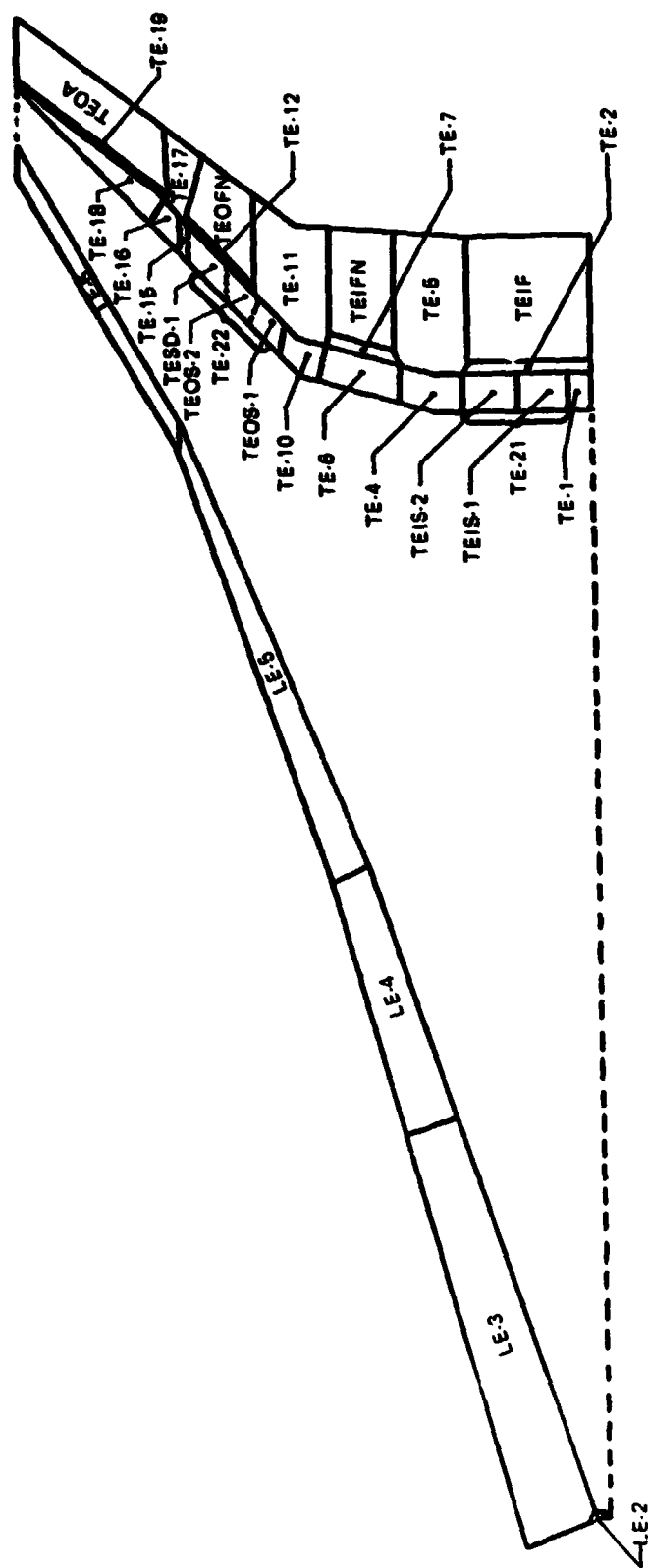


Figure 12-9.—Wing Leading Edge and Trailing Edge Structure—Mass Input Elements

Figure 12-10.—Wing Contents—Mass Input Elements

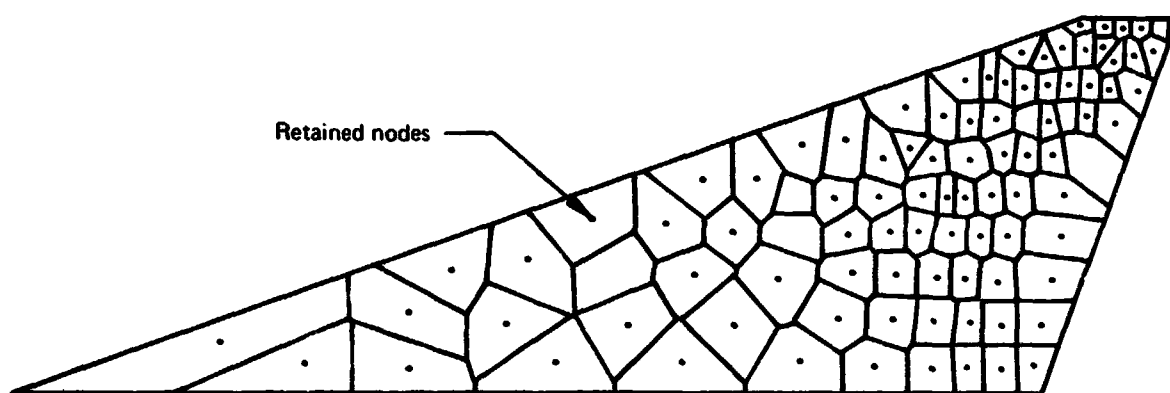


Figure 12-11.—Mass Paneling for Aeroelastic Loads Analysis—Output

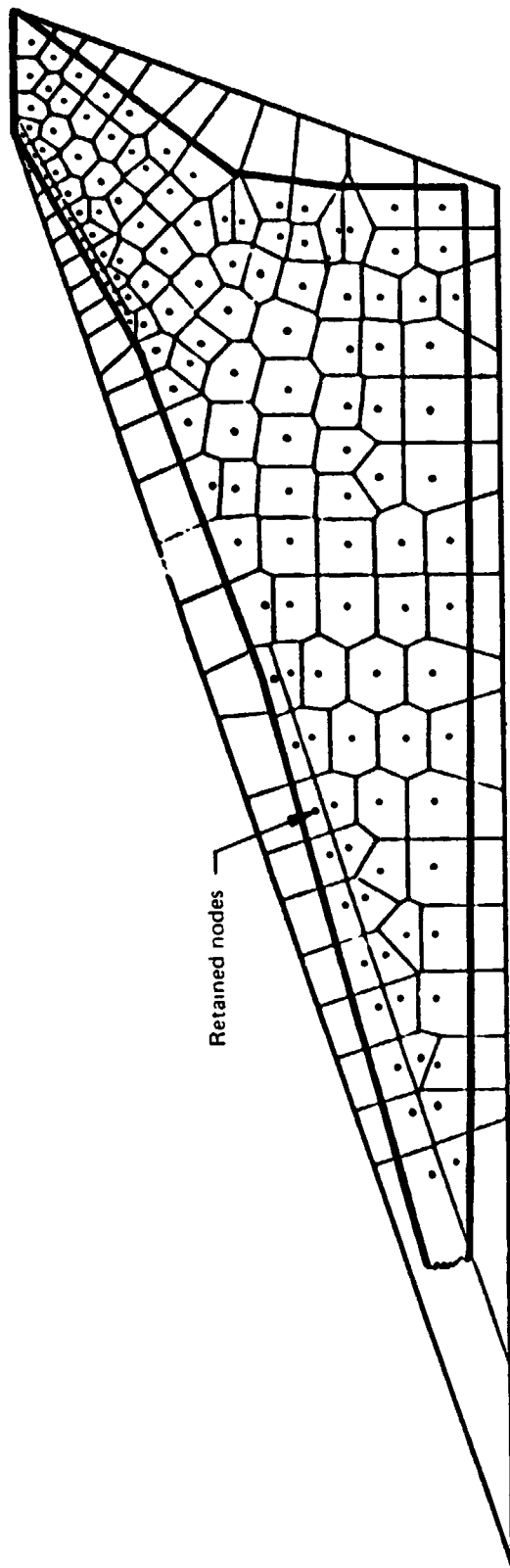


Figure 12.12. —Mass Paneling for Flutter Analysis—Output

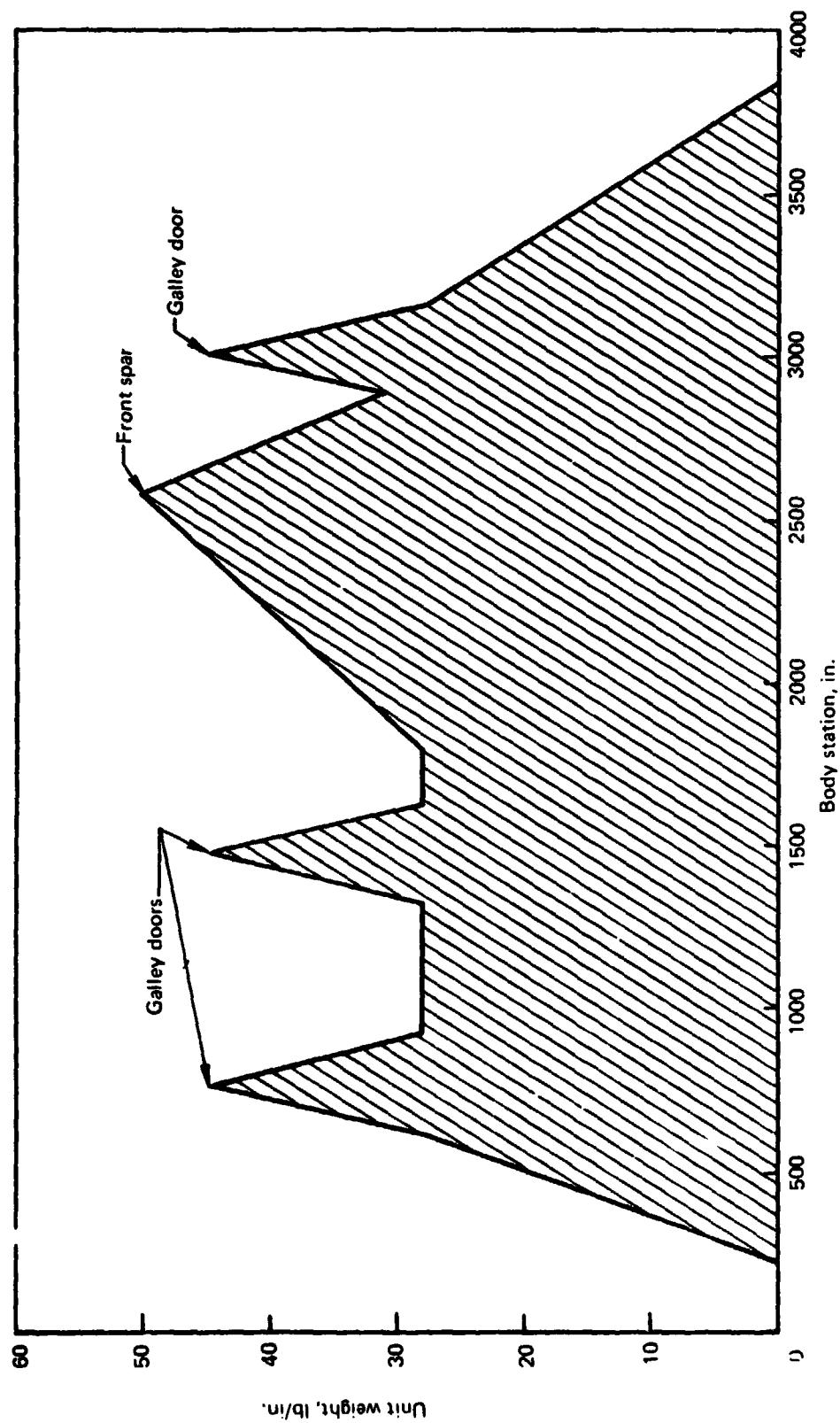


Figure 12-13. —Body Structure and Contents—Mass Distribution

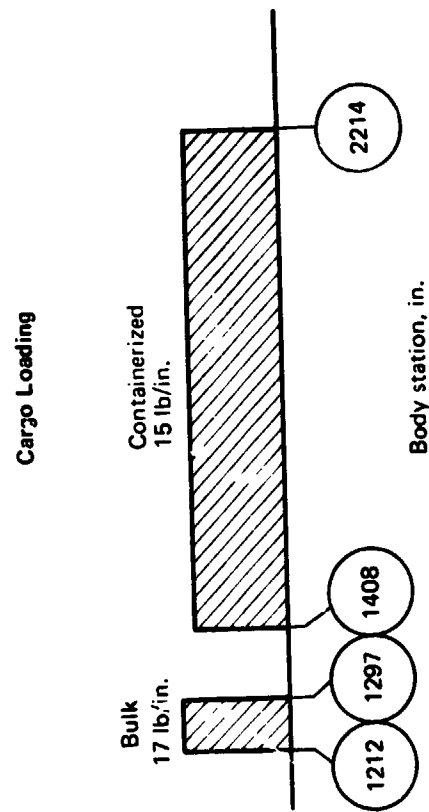
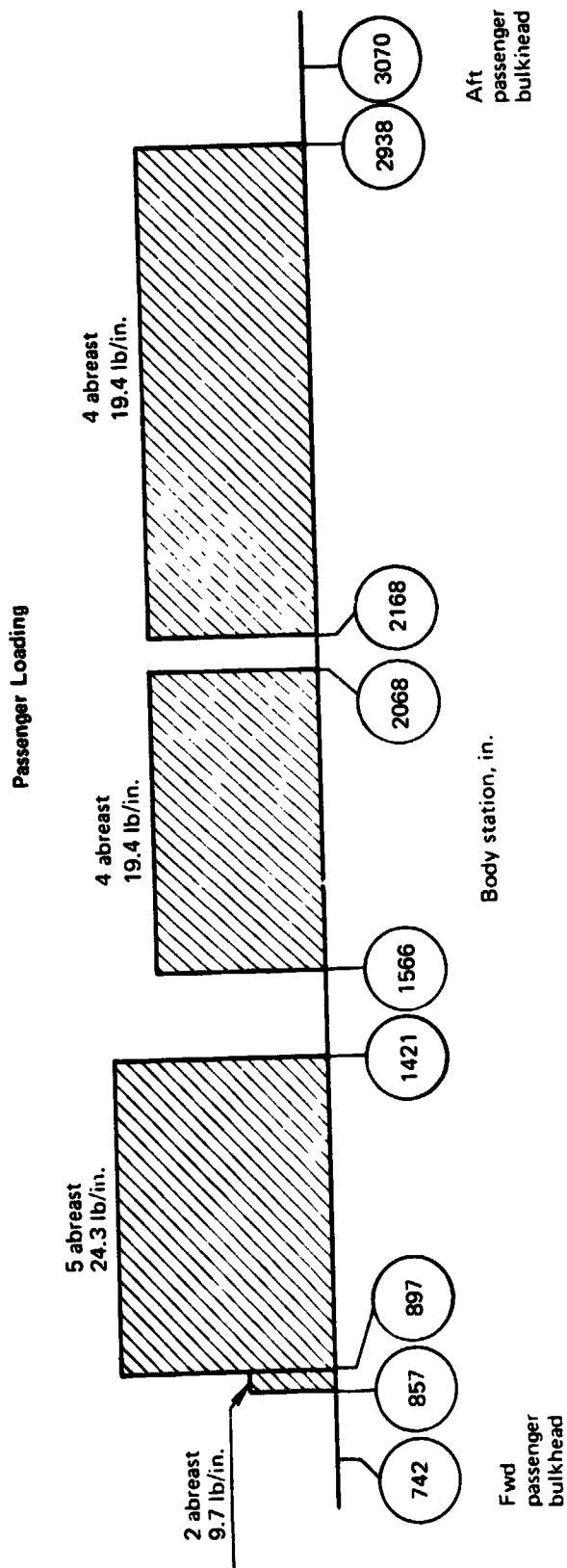


Figure 12-14. —Body Payload—Mass Distribution

Total less fuel, lb/side	Cargo lb/side	Passengers, lb/side	Wing/body intersection, lb/side	Body structure and contents, lb/side
1601.8				1601.8
1847.6				1847.6
3218.6		14.0		3204.6
2979.5		763.1		2216.4
3890.0		1930.0		1960.0
1639.9		761.4		878.5
3105.7	361.5	1274.2		1470.0
3294.6	361.0	1430.8		1502.8
3716.6	349.0	423.0		2944.6
3176.8	894.5	97.0	69.3	2116.0
3532.1	787.5	1062.0	171.2	1511.4
3447.7	787.5	1019.0	171.2	1470.0
3540.3	787.5	1019.0	171.2	1562.6
3859.5	787.5	1151.5	171.2	1749.3
3402.7	787.5	522.5	171.2	1921.5
3839.4	828.5	746.0	171.2	2093.7
3622.5	52.0	1097.5	207.1	2265.9
3700.6		1019.0	243.0	2438.6
3894.2		1019.0	243.0	2632.2
4220.6		1019.0	477.0	2724.6
4063.0		1019.0	711.0	2333.0
3607.2		1063.0	711.0	1833.2
3148.0		878.0	592.5	1677.5
2194.8				2194.8
2359.4				2359.4
1645.0				1645.0
1253.0				1253.0
952.0				952.0
473.0				473.0

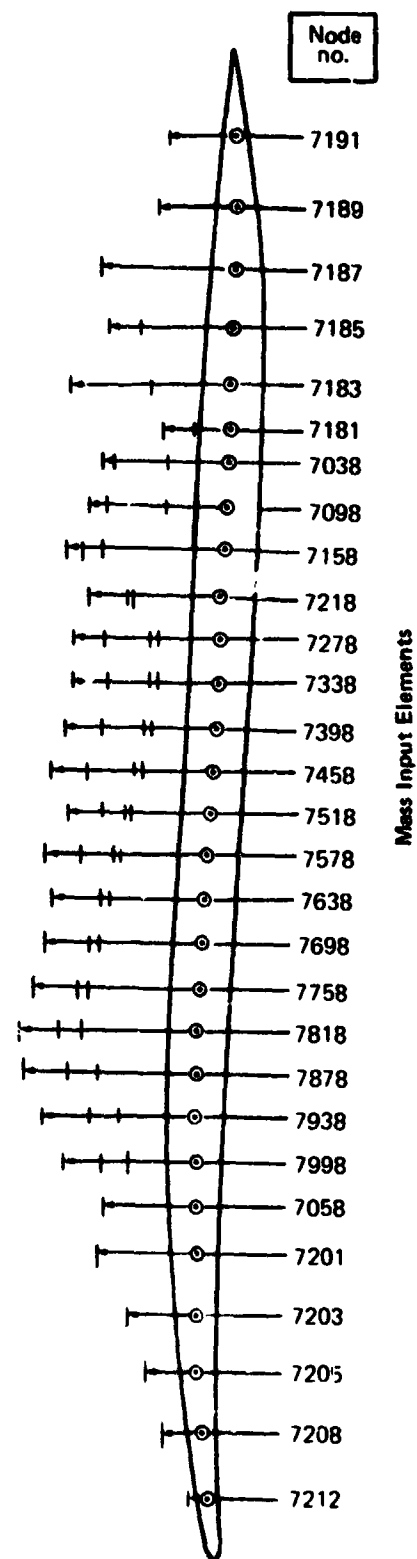


Figure 12-15.—Body Structure and Contents

Figure 12-16.—Wing Mounted Vertical Fin—Mass Input Elements

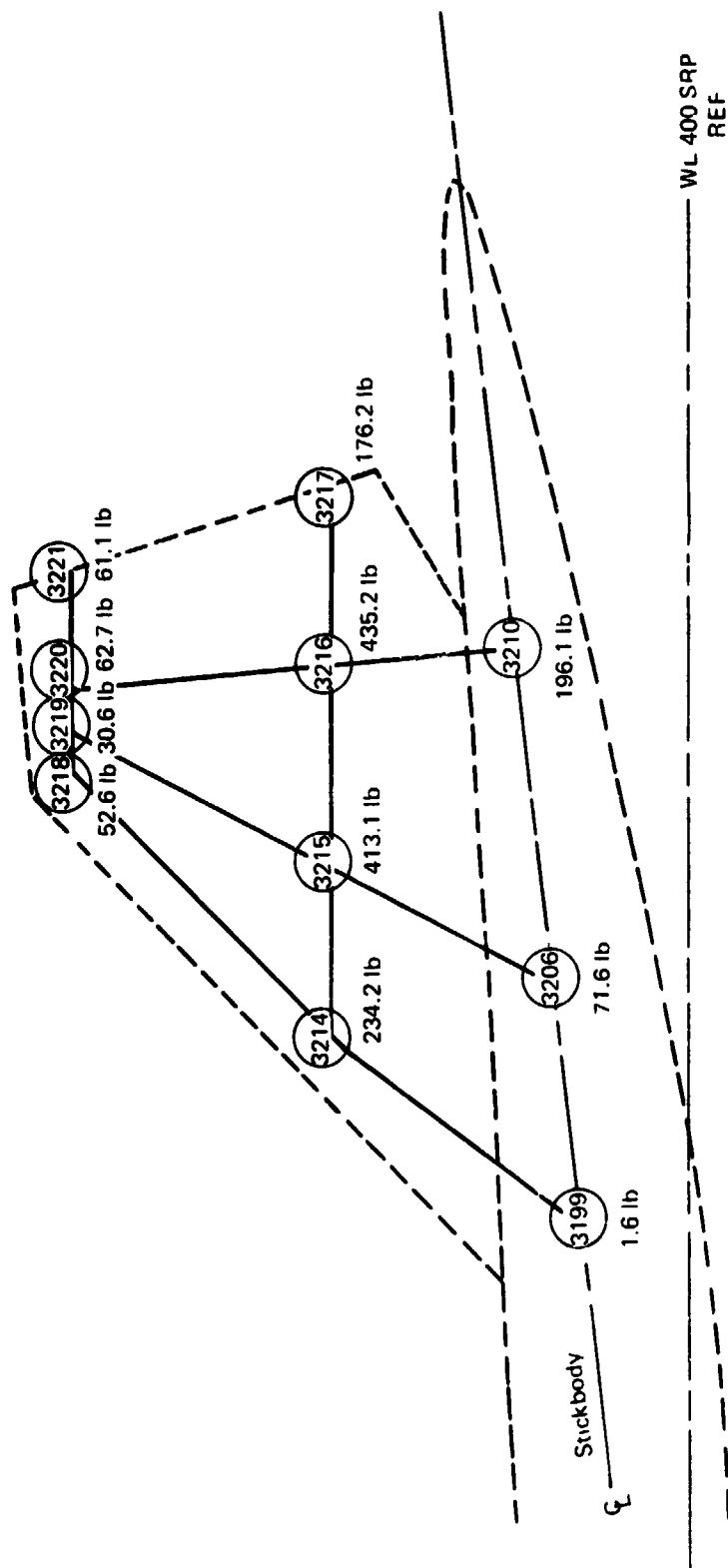


Figure 12-17.—Body Mounted Vertical Tail—Mass Input Elements

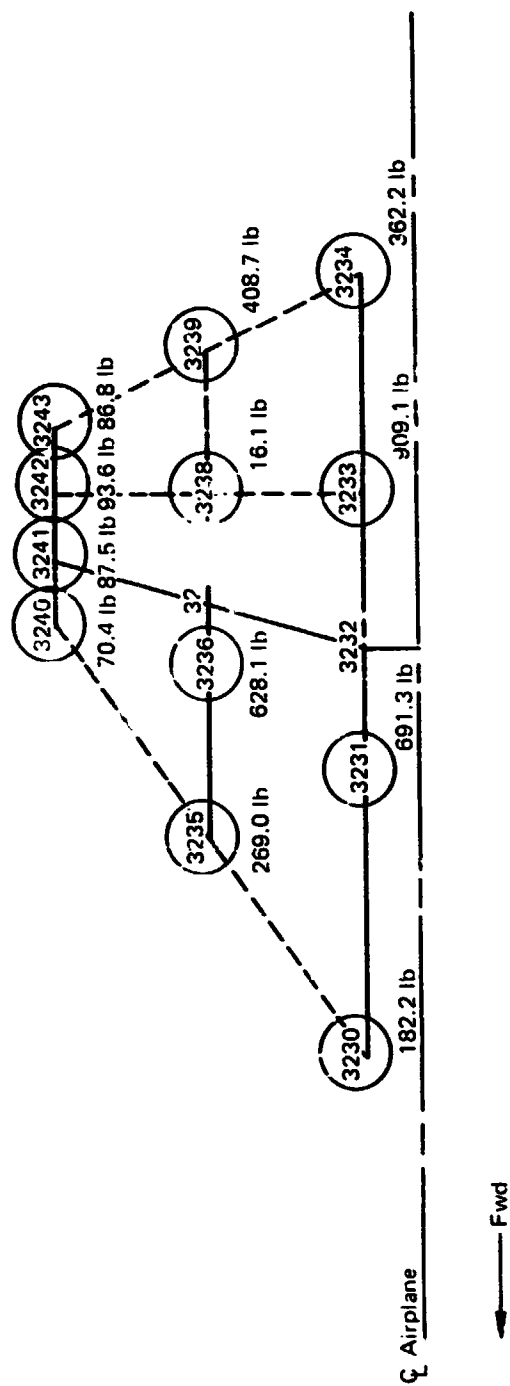


Figure 12-18.—Body Mounted Horizontal Tail—Mass Input Elements

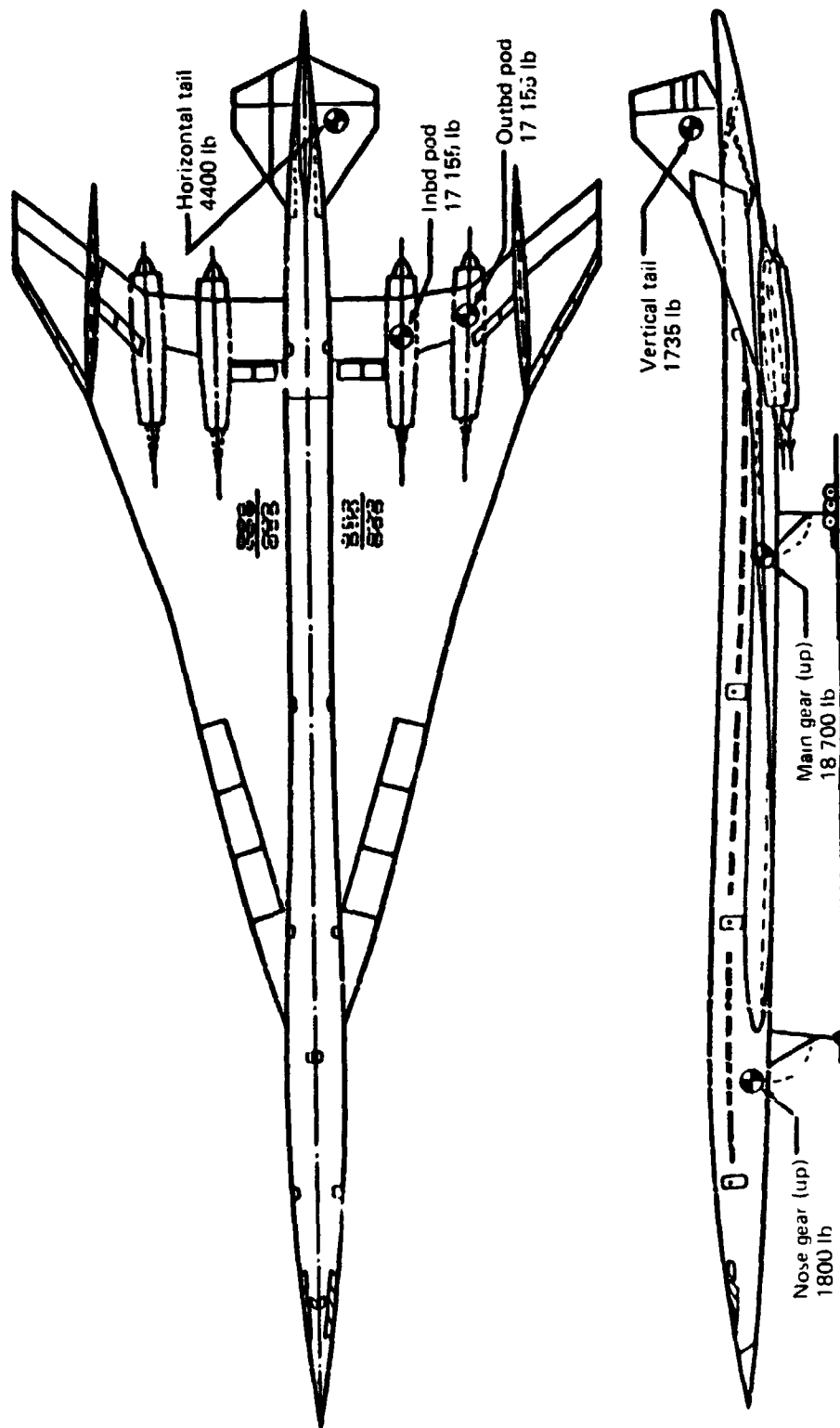


Figure 12.19. —Lumpei Mass Items—Pounds/Side

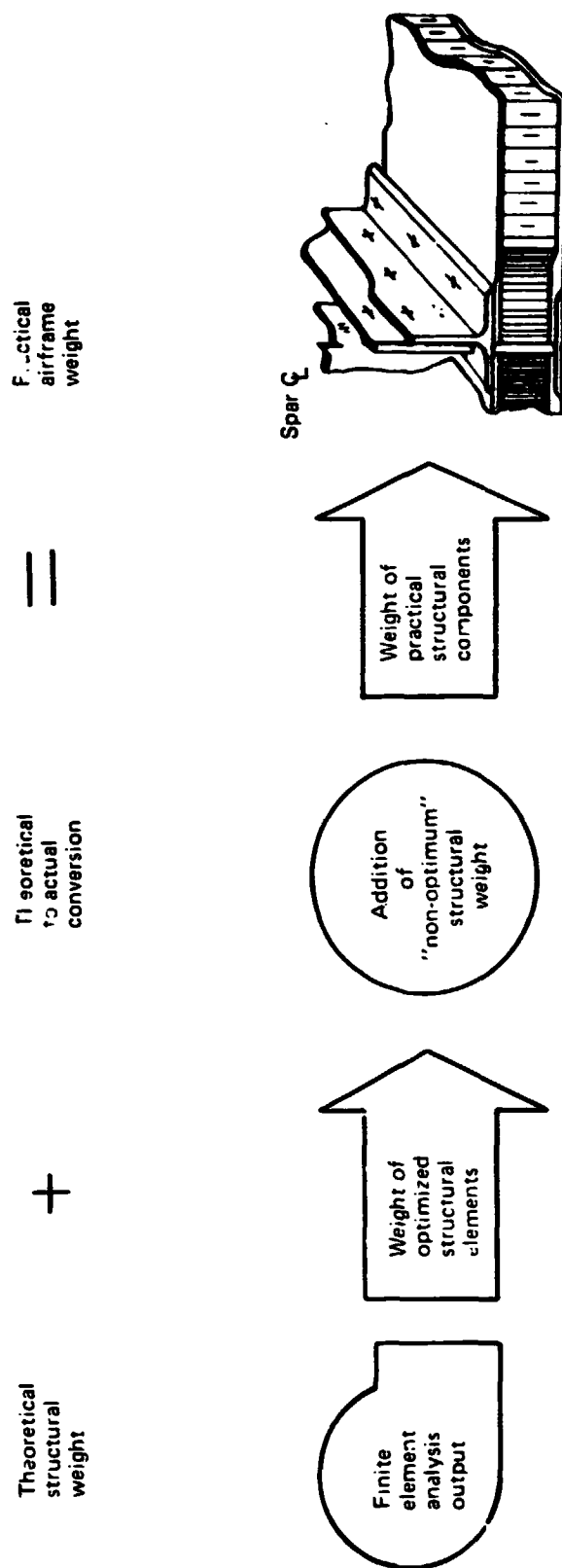


Figure 20.—Structural Weight Estimation

Cover Elements (Typical)

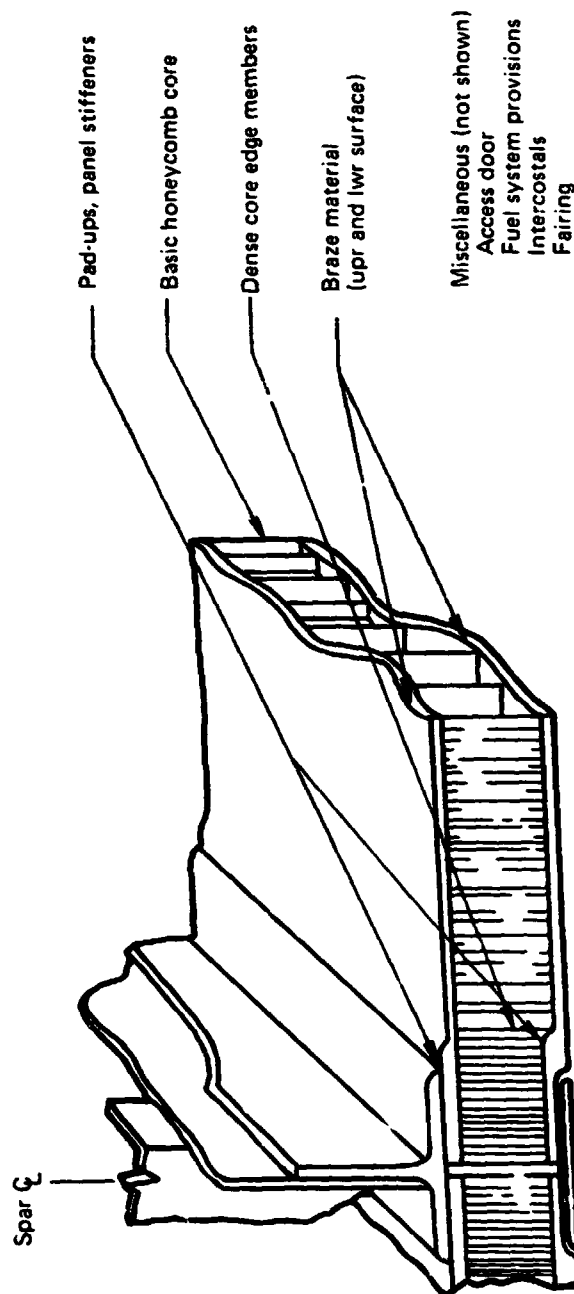


Figure 12-21.—Nonoptimum Structure Definition(Example)

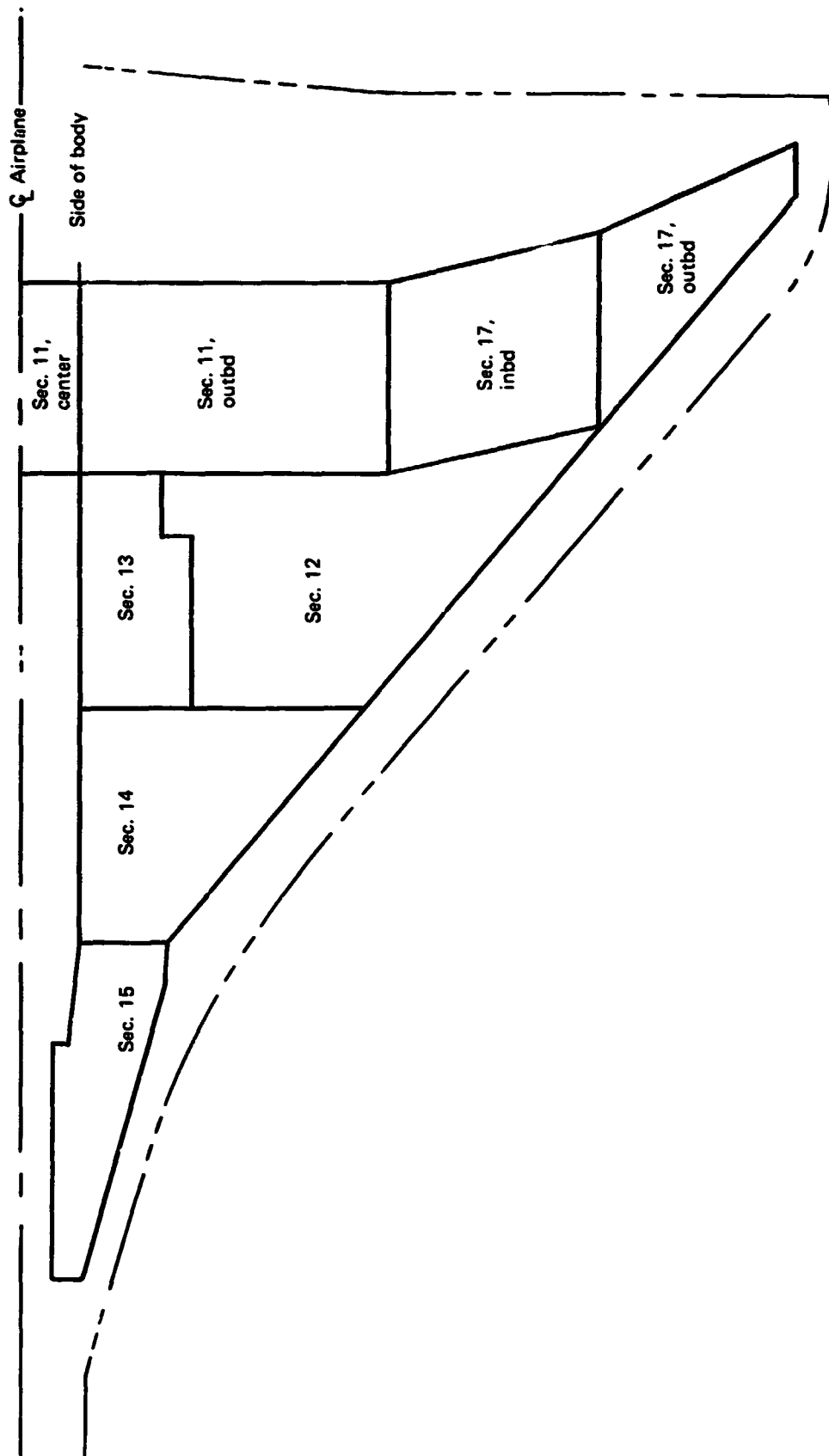


Figure 12-22.—Wing Box Sections, National SST

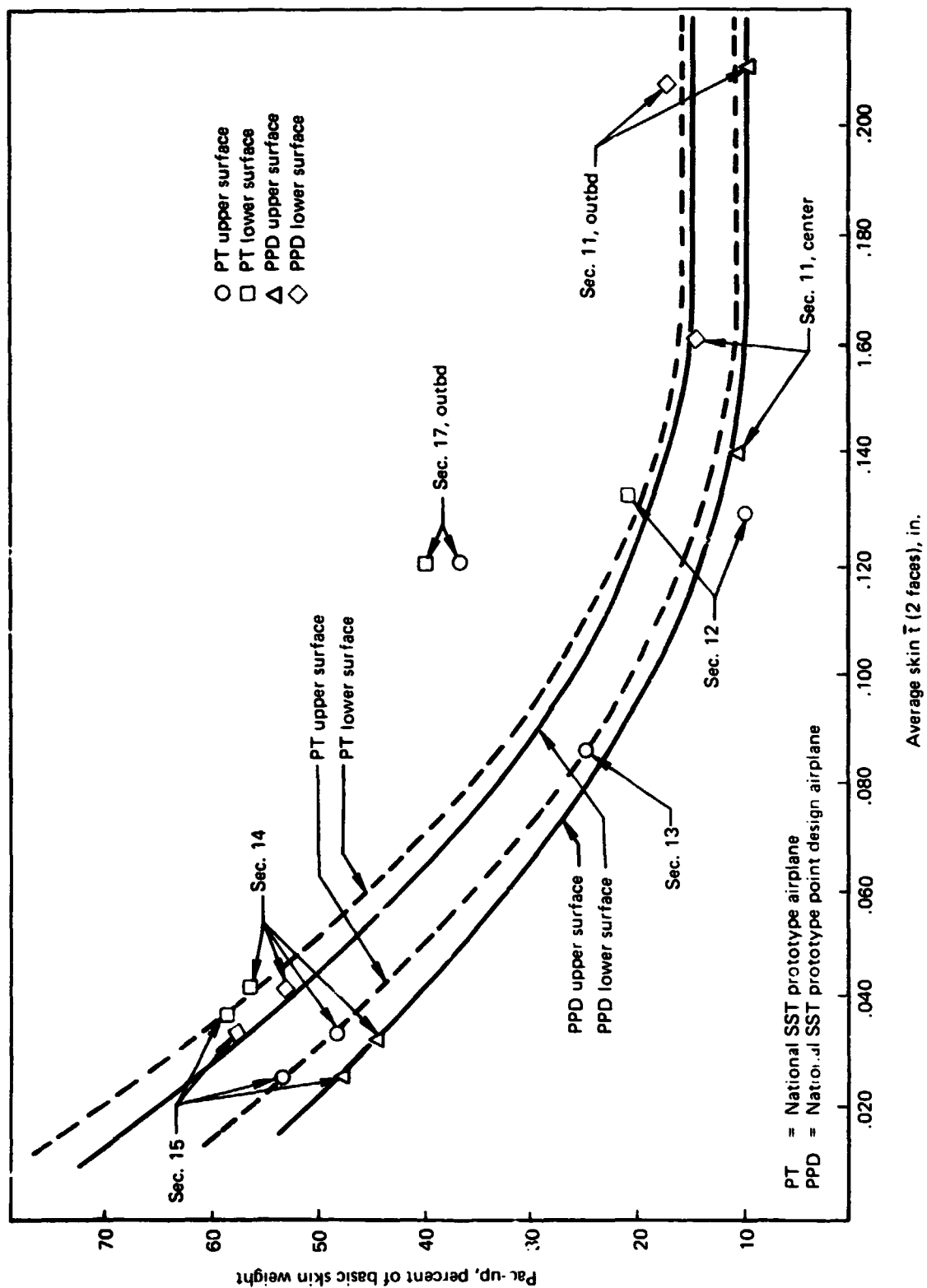
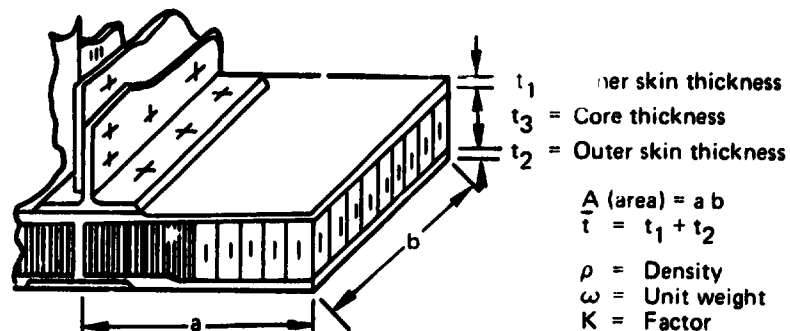


Figure 12-23.—Aluminum-Brazed Titanium Honeycomb Panels—Skin \bar{t} Vs Skin Pad-up

Spar ζ

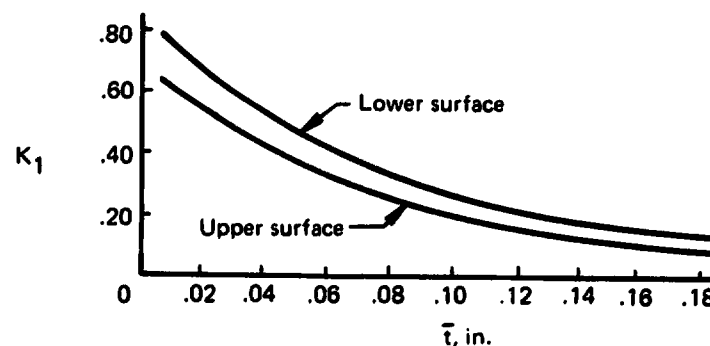


Theoretical structure + Theoretical to actual conversion = Wing box cover

● Inner and outer skin
= (finite element
analysis output)

● Pad-up weight = $A \bar{t} \rho_1 K_1$

$A \bar{t} \rho_1$



● Core weight = $A t_3 \rho_2 K_2$
($K_2 = 1.25$ for upper surface)
($K_2 = 1.30$ for lower surface)

● Braze weight = $A \omega K_3$
($K_3 = 1.25$ for upper surface)
($K_3 = 1.30$ for lower surface)

● Miscellaneous weight = K_4

Access doors Intercostals
Fuel system provisions Fairing

Figure 12-24.—Structural Weight Estimation, Wing Box Cover Elements

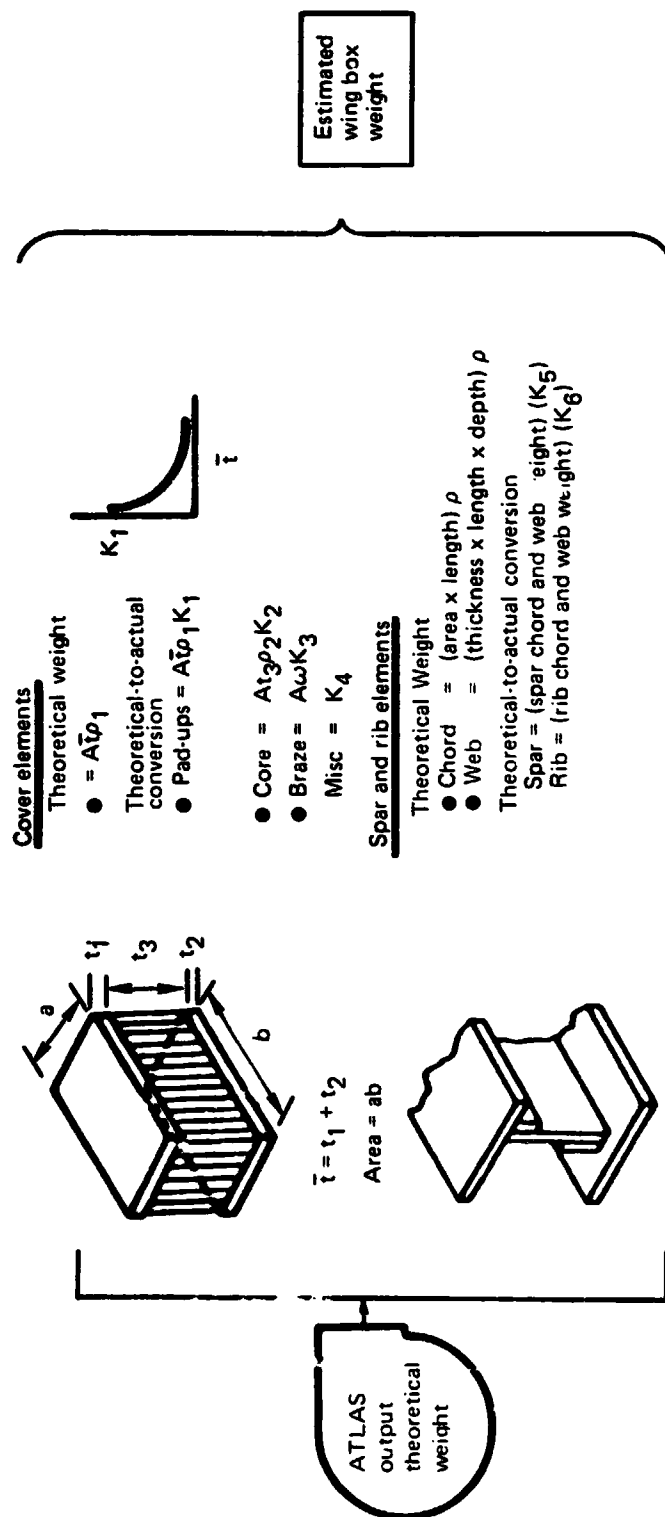


Figure 12-25.—Wing Box Weight Estimation

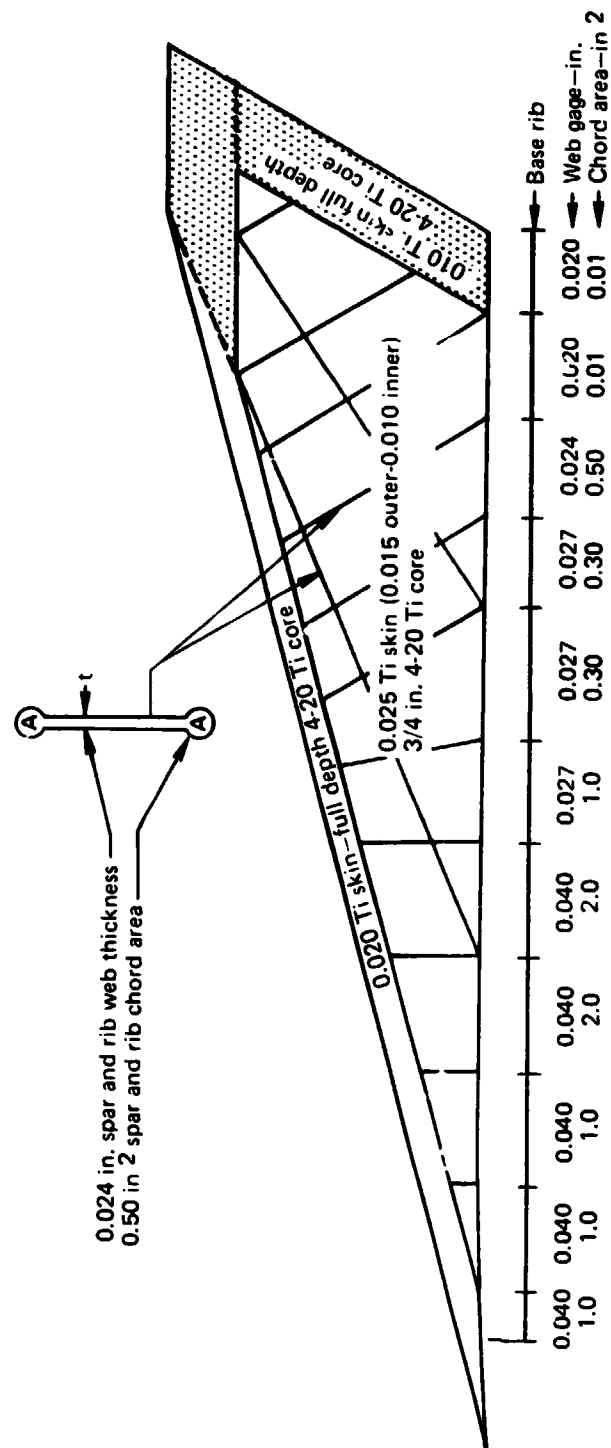
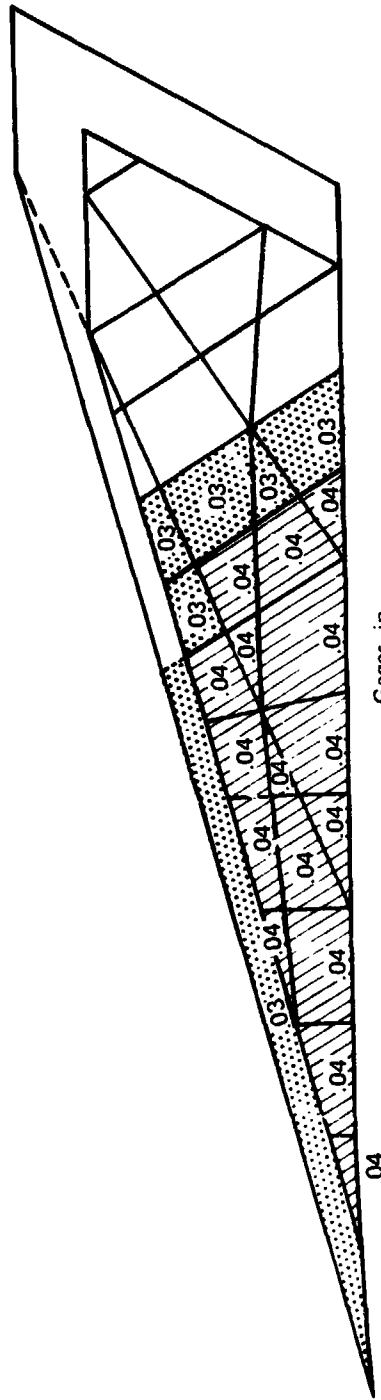
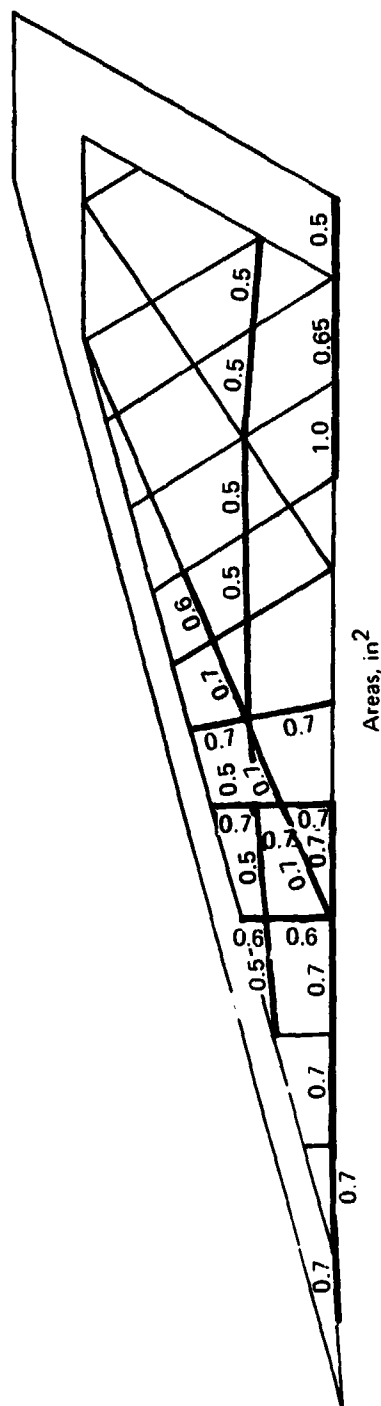


Figure 12-26.—Wing-Mounted Fin, Initial Sizing
Model 969-512B



Gages, in.

Figure 12-27.—Wing-Mounted Fin, Skin Gages
Modification for Final Stiffness
Model 969-512B



**Figure 12-28.—Wing-Mounted Fin, Spar and Rib Chord Areas
Modification for Fin's Stiffness
Model 969-512B**

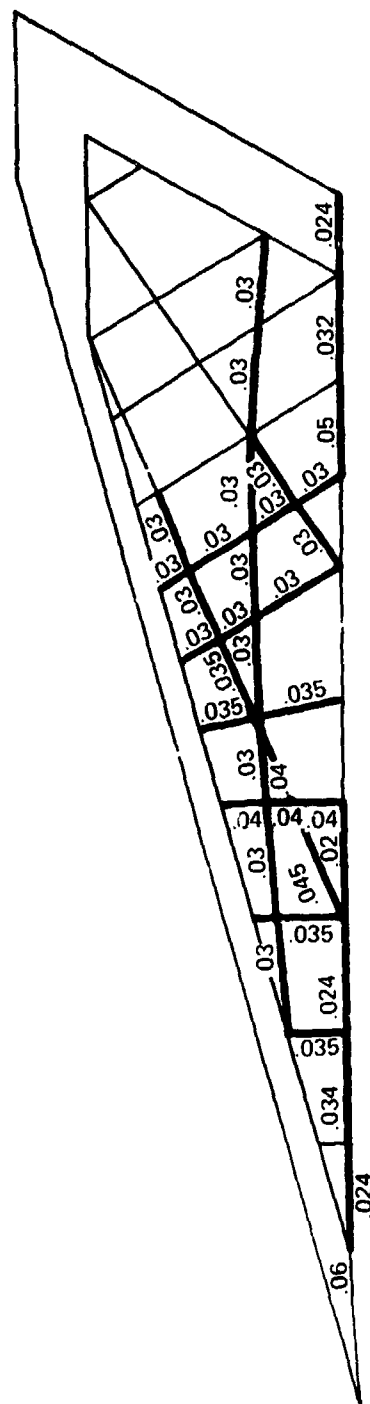


Figure 12-29. —Wing-Mounted Fin Spar and Rib Web Gages
Modification for Final Stiffness
Model 969-512B

SECTION 13

**IMPACT OF FUEL TEMPERATURE
ANALYSIS ON PERFORMANCE**

by

L. D. Richmond

PRECEDING PAGE BLANK NOT FILLED

CONTENTS

	Page
IMPACT OF FUEL TEMPERATURE ANALYSIS ON PERFORMANCE	770
Introduction	770
Fuel Temperature Analysis	770
Changes in Airplane Performance	776
REFERENCES	776

TABLES

No.		Page
13-1	Volume Versus Area for Fuel Tanks	777
13-2	Fuel Tank Conductance	779
13-3	Fuel Temperatures for Various Trip Conditions	780
13-4	Structural Design Impact on Mission Range	781
13-5	Structural Design Impact on Performance	782

FIGURES

No.		Page
13-1	Fuel Temperature Comparison	783
13-2	Typical Items Limiting Fuel Heat Sink Capacity With Respect to Temperature	784
13-3	Fuel Tank Volume Reduction Versus Tank Depth, M = 2.7 Airplane	785
13-4	Fuel Tank Layout - Model 969-512B	786
13-5	Fuel Management - Model 969-512B	787
13-6	Effect of Panel Thermal Conductance on Fuel Tank Thermal Conductance	788
13-7	Maximum Temperature of Fuel in Main Tanks at End of Supersonic Cruise	789
13-8	Temperature of Fuel in Rear Fuselage Auxiliary Tank (14A) at Start of Descent	790
13-9	Maximum Temperature of Fuel in Main Tanks at End of Supersonic Cruise - Compartmented Configuration	791
13-10	SST Performance Climb Placards	792

SECTION 13

IMPACT OF FUEL TEMPERATURE ANALYSIS ON PERFORMANCE

INTRODUCTION

This section addresses the impact of the results of the Task II wing structural and thermal analyses on the performance of the 969-512B configuration. These impacts will be expressed in terms of range increments and end of cruise fuel temperatures. The range increment reflects the change in airplane operating empty weight (OEW) as discussed in Section 12, the change in wing tip thickness and V_{MO} placard speeds all of which were necessary to satisfy structural design criteria. Weight penalties are estimated and included in the OEW to provide for fuel tank insulation to keep the end of cruise fuel temperatures from exceeding the 160° F limit.

FUEL TEMPERATURE ANALYSIS

SUMMARY

An analysis to determine the fuel temperature rise during an all supersonic mission was conducted for the 969-512B configuration. The results of this analysis were compared to an earlier analysis conducted on the 1968 Model 969-336C during Task III of NASA contract NAS1-11938, reference 1-5. As a result of the earlier analysis particular attention was given to the configuring of the 969-512B to locate the fuel tanks in areas of the wing and fuselage which offered the greatest depth thus minimizing the heating surface per unit of fuel volume and thus reducing the fuel temperature rise. As shown by figure 13-1, significant lowering of end of cruise fuel temperature resulted from the relocation of fuel tanks; however, the limit of 160° F is still exceeded by 10° F. Approximately 1530 pounds of fuel tank insulation of a foamed elastomeric fluoro silicone type would be required on the bottom, sides and lower surface skin stiffeners of auxiliary tank 14A and main tanks 1,2,3, and 4 to preclude the end of cruise fuel temperature from exceeding 160° F.

INTRODUCTION

The thermal analyses conducted during the National SST Program revealed the critical impact of aerodynamic heating during supersonic cruise on fuel temperatures and thermal management. The environmental control system (ECS) envisioned for the SST relies heavily upon the fuel as heat sink to maintain adequate cooling for the passenger cabin and flight deck; therefore, the control of the fuel temperature is a critical factor in the efficient operation of the ECS and the engine fuel system. Figure 13-2 shows the various items affected as the fuel temperature increases. The most critical item for this design is the 160° F limit for fuel boiling at altitude.

METHOD OF ANALYSIS, INPUTS, AND ASSUMPTIONS

The fuel temperatures during the 969-512B flight missions were calculated using a thermal analyzer computer program which was developed by Boeing during the National SST developmental program. A summary of the most important assumptions and inputs which were used in the application of this program is as follows:

Flight Profile

The 969-512B used the ATAT-1 (advanced technology afterburning turbojet) engine with an airflow sizing of 633 lb/sec as described in Section 1. The supersonic cruise mission subjected the airframe to approximately 106 minutes of Mach 2.7 cruise flight on a standard day using engine power setting 2 for climb. Significant points during the mission are as follows:

Condition	Time from start of taxi, (minutes)	Mach No.	Alt. (feet)	Airplane Wt. (lbs.)
Start of taxi-	0	0	0	750,000
Take off-	10.66	.32	35	740,437
Start of cruise-	35.68	2.7	60,973	651,792
End of cruise-	141.22	2.7	67,484	469,297
Start of descent-	142.54	2.4	67,484	468,853
Touchdown-	167.08	.22	0	461,503

Fuel Tank Configuration

An important input which influences fuel temperature rise is the amount of wetted area in each fuel tank for various volumes of fuel in the tank. To determine this wetted area/volume relationship, the wing and body surface coordinates and fuel tank boundaries were interrogated to determine both fuel volume and hot surface area of the fuel tanks including corrections for unusable fuel volume. The items contributing to unusable fuel volume and their impact on total tank volume are shown in figure 13-3. The resulting wetted area and volume relationships for the various tanks of the 969-512B are given in table 13-1. The values shown extend from the empty fuel to full fuel condition. The appropriate value is selected to agree with the airplane fuel loading at the analysis condition.

Fuel Loading and Management

The fuel loading and management used for the 969-512B are graphically displayed in figures 13-4 and 13-5 and discussed in Section 1. The initial temperature of the on-loaded fuel in all tanks for the first of the two consecutive flights, was taken as 90° F, based on reference 13-1 study which measured temperatures of fuel at various airports in the world. Onloaded fuel temperatures greater than 90° F were estimated to occur less than 2.5% of the time. For the second flight, the initial temperature in all the

auxiliary tanks which are refilled was 90° F, while in the main tanks the initial temperature was that resulting from mixing the hot fuel remaining from the previous flight with the required amount of 90° F unloaded fuel. This results in an initially high temperature in the main tanks which decreases as the depleted fuel is replaced by transfer from the auxiliary tanks during the climb segment. Transfer from the auxiliary tanks to the main tanks begins at Mach 0.9 during climb and continues until all auxiliary tanks except 14A are emptied. The sequence of transfer from the auxiliary tanks is 1A and 4A, 5A and 6A, and 2A, and 3A as shown in figure 13-5. Transfer from 14A is deferred until the end of cruise and carried out in the first few minutes of descent to provide for the necessary center of gravity shift.

Fuel Reserves

The fuel reserves were taken to be the same for each of the flights. For each pair of consecutive flights, it was assumed that fuel usage during the first flight corresponded to the nominal fuel usage given in the flight profiles and the airplane lands with all of the reserve fuel aboard. The fuel usage in the second flight was assumed to increase uniformly throughout the flight to reflect the use of the trip fuel allowance. This combination provides a worst case situation in that the greater amount of hot fuel left by not using the reserves in the first flight results in a higher initial fuel temperature in the main for the second flight, and during the second flight the use of reserve fuel leads to larger temperature rises in the main tanks at the end of cruise.

Heat Sources

In addition to the major transfer of aerodynamic heating to the fuel through contact with the tank walls, radiation to the fuel from dry areas of the tank walls was also included. Internal sources of heat which are included in the computations are heat rejection by fuel boost and transfer pumps, and heat transfer from hydraulic lines and other systems components located within the tanks. These internal sources combined, contribute from less than 1° F temperature rise in most of the auxiliary tanks to as much as 12° F in main tanks 2 and 3 for long range flights. The large contribution in main tanks 2 and 3 is mainly due to the location of the ECS heat exchangers in these tanks.

Fuel Recirculation

From the end of cruise to the start of approach (at 1500 feet altitude), fuel is recirculated through the airframe and engine heat exchangers and back to the tank to provide for adequate fuel heat sink. The recirculation rate is 250 pounds per minute per engine. The heat added to the recirculated fuel by these heat exchangers is also included in the tank fuel temperature computations. The heat loads in the airframe heat exchangers and the engine heat loads were based upon requirements for the 1971 version of the General Electric GE4 engine.

Engine Interface and Nozzle Temperatures

Temperatures at the airframe-engine interface and at the engine nozzles were also computed as a function of flight time for each flight. These were calculated from the tank temperatures and airframe and engine heat loads discussed above.

Recommended Fuel Temperature Limits

At the end of cruise the altitude is 67,500 feet. At this altitude the boiling temperature of maximum volatility kerosene is 175° F (ref. 13-2). A temperature margin of 15° F was selected to account for altitude variations, temperature stratification of the fuel in the tanks, and pump cavitation margins. Therefore, a bulk temperature of 160° F was established as the maximum allowable temperature of fuel remaining in any fuel tank, except at lower altitudes where the increasing tank pressure alleviates the fuel boiling problem.

During the AST studies (ref. 1-5) the engine companies were requested to provide their estimate of maximum engine/airframe interface fuel temperature and maximum burner nozzle fuel temperature. Pratt & Whitney responded with a recommendation that burner nozzle fuel temperature be limited to 300° F, and engine/airframe interface fuel temperature be limited to 200° F, except in configurations with a simplified control system, then 250° F would be permissible for the interface temperature. General Electric responded with a recommendation that burner nozzle temperature be less than 325° F except with special fuels, and engine/airframe interface temperatures be limited to 200° F to 225° F, unless engine electronics are to be supplied with another source of cooling. For an advanced technology SST, a reasonable recommendation is that engine/airframe interface fuel temperature be limited to 250° F (this assumes engine electronics will be cooled with another coolant), and that burner nozzle fuel temperatures be limited to 325°.

Fuel Tank Insulating Characteristics

The structural concept for the fuel tanks of 969-512B was aluminum brazed titanium honeycomb sandwich panels except for the rear fuselage auxiliary tank (14A) which was riveted sheet stiffener. For aluminum brazed titanium honeycomb sandwich panels the panel thermal conductance value was estimated to be 6 BTU/FT²,HR,°F. A previous analytical study estimated that additional heat shorts in fuel tank walls where panel edge members were joined resulted in tank conductances which were considerably higher than panel conductances, as illustrated in figure 13-6. Therefore, for a panel conductance value of 6 BTU/FT²,HR,°F, assuming no insulation, would result in an over all tank conductance of 11 BTU/FT²,HR,°F.

ANALYTICAL RESULTS

The maximum temperature of the fuel in the main tanks at the end of the supersonic cruise is shown as a function of fuel tank conductance in figure 13-7. For the purposes of this trade study, the conductance of all main and auxiliary tanks were considered equal. As indicated, tank conductances of about 4 BTU/FT²,HR,°F are required to keep the

rear main tank fuel temperature below the 160° F maximum, and conductances of about 6 BTU/FT²,HR,°F would be required for the forward main tanks. All auxiliary tanks except the rear fuselage auxiliary tank 14A are emptied early in the flight before much fuel heating can occur, and because the brazed aluminum honeycomb structure used in auxiliary tank walls provides reasonable insulation, it was determined that the fuel temperatures would be maintained below the 160° F maximum and that no insulation needed to be added to the auxiliary tanks (except 14A). Based upon the above study the tank conductances shown in table 13-2 were established as requirements and used in subsequent analysis. To attain this level of tank conductance it will require additional insulation in main tanks 1, 2, 3 and 4 and in auxiliary tank 14A.

As explained previously, the walls of the rear auxiliary fuel tank (14A) are of riveted sheet stiffener construction. This thin titanium wall provides almost no fuel tank wall insulation, (sheet stiffener wall conductance is estimated to be 600 BTU/FT²,HR,°F). Figure 13-8 shows the temperature of the fuel in the fully loaded tank (14A) just after the end of cruise when it normally would start to transfer to the main tanks. As shown, the temperature is almost within the 160° F limit without any tank insulation. However, fuel temperatures this hot leave no contingency margin and it is important that reasonably cool fuel be fed from tank (14A) during the descent, and possibly in some cases before the end of cruise, to keep main tank temperatures within the allowable limits. Therefore, until a more complete analysis is made it is recommended that tank 14A have a tank wall conductance of 11 BTU/FT²,HR,°F, which corresponds to the other auxiliary fuel tanks. This means that tank 14A will require insulation or that the tank walls must have a conductance equivalent to aluminum brazed titanium honeycomb sandwich structure.

The problem of excessive fuel temperatures is largely associated with flights which combine adverse thermal conditions such as high onloaded fuel temperatures, consecutive trips with hot reserve and/or ballast fuel remaining from the earlier trip combined with trips which used fuel reserves in an adverse manner. Table 13-3 shows the fuel temperatures at the end of cruise or start of descent (whichever is higher) in the main fuel tanks, and at the engine/airframe interface, and at the fuel nozzles for a series of conditions using the tank conductances listed in table 13-2. As can be seen for trip condition 1, on a first trip with onloaded fuel of 60° F, excessive fuel temperatures are no problem. When the onloaded fuel temperature is increased to 90° F, the end of mission fuel temperatures increase significantly but are still satisfactory. On a second consecutive trip with 90° F onloaded fuel, the main tank temperatures increase to above 160° F. If the second trip uses trip fuel reserve, the forward fuel tank temperature rises to over 165° F. In all cases the engine/airframe interface fuel temperature remains less than 250° F, and the engine nozzle temperature remains less than 325° F maximum.

The temperatures in table 13-3 were determined for the 969- 512B airplane which had a mission duration of 2.8 hours. A longer duration at supersonic cruise will tend to aggravate the fuel temperature problem. However increased mission range does not affect fuel temperature as adversely as might be expected, because the amount of onloaded fuel would have to be increased, which also increases the available fuel heat sink. Previous studies of the 969-336C airplane indicated that the fuel temperature rise with increasing range was a function of tank conductance, and for the conductances recommended herein would be about 1.5° F per 100 nautical mile range increase.

Potential Improvements

Two possible concepts to reduce fuel temperature in addition to adding tank insulation were investigated. The first of these was to compartmentize the main tanks such that the inboard portions of all main tanks would have a capacity of 30,000 lbs. fuel each, and the outboard portion would be converted into additional auxiliary tanks. The results of this concept are shown in figure 13-9. This compartmenting scheme, which may not necessarily be optimum, would reduce final fuel temperature about 8° F, but would introduce the additional weight of bulkheads, pumps, gages, etc. required for the additional auxiliary fuel tanks.

Another possibility is to start discharging the fuel from the rear fuselage auxiliary tank (14A) prior to the end of cruise. This is effective only when tank 14A has enough insulation to keep its fuel adequately cool. The results of this concept are shown in table 13-3, conditions 5 and 6. In both these cases the transfer from tank 14A started 15 minutes before the end of cruise. For condition 5 the transfer rate was 400 lbs/min per main tank (20 minutes discharge time), and for condition 6 the rate was 800 lbs/min per main tank (10 minute discharge time). As can be seen, this results in tank fuel temperature reductions of 5.5° F and 7.5° F respectively. The penalty for early discharge of tank 14A is that the c.g. moves forward during supersonic cruise, which would require an adequate forward c.g. limit, and would result in increased trim drag with the associated performance penalty. The magnitude of this performance penalty has not been established, nor has the increase in forward c.g. limit been identified.

CONCLUSIONS AND RECOMMENDATIONS

As discussed above, the tank conductances used in the analysis did not completely satisfy requirements for the most adverse condition. There are however possibilities to reduce the problem by tank compartmentation and/or earlier discharge of auxiliary tank 14A. Therefore, until additional studies are made, the tank conductances in table 13-2 are recommended. The above analysis was conducted assuming the same panel conductance on both the top and bottom of the tank. Previous studies have indicated that insulation of the top of the fuel tank was relatively ineffective in reducing fuel temperatures. The results showed that changing top tank wall conductance from 11 to 3 BTU/HR,FT²,°F would decrease fuel temperature rise about 1° F. Therefore, it is recommended that there should be no added tank insulation on the top of the fuel tanks.

Because of the importance of heat shorts through the spars and panel splices, it will be necessary to apply insulation to heat short areas of main tanks 1, 4, 2 and 3 to reduce the tank conductance to the values given in table 13-2. Because skin stiffener structure has very high conductance, auxiliary tank 14A, will need insulation to bring the conductance down to a value of 11 BTU/HR,FT²,°F. As a possible fuel tank insulation, the use of a foamed elastomeric fluorosilicone rubber insulation with a conductivity coefficient of $K = 0.4 \text{ BTU,IN/FT}^2\text{,HR,}^\circ\text{R}$, and a density of 40 LB,FT³ has been considered. Tests have not been made to assure that this would be practical material with adequate reliability, maintainability, and longevity in commercial use, but for purposes of estimating a weight penalty for added fuel tank insulation, this material was assumed to be appropriate. To obtain the tank conductivities on table 13-2 will

require insulation thickness of about .05 in. to cover the bottom surface and stiffeners in tank 14A. Main tanks 2 and 3 will require insulation thickness of about .15 in. on the bottom surface and stiffeners. Main tanks 1 and 4 will require about .05 in. thick insulation on the tank lower surface and on the lowest 2 in. of the spars. The weight of the above insulation is estimated to be 1530 lbs.

It is recommended that simplified experimental validation of the thermal analysis, particularly in the area of heat shorts, be conducted. Further development of insulation material and design installation concepts needs to be conducted to arrive at a practical means of insulating fuel tanks as the need arises.

CHANGES IN AIRPLANE PERFORMANCE

The mission performance of the "Arrow Wing", 969-512B configuration with the ATAT-1 engine has been updated to reflect the changes in weight, drag and climb placard which were necessary to satisfy strength sizing, flutter and thermal requirements. The total range decrement was 135 nmi and is itemized in table 13-4.

The changes in range due to increased OEW and drag were obtained from trades previously established and discussed in section 1 and shown in figure 1-19. The placard change from the original climb speed of 350 KEAS to 300 KEAS to provide for adequate flutter margin, illustrated in figure 13-10 by the dotted line, gave a range decrement of 24 miles, primarily due to reduced subsonic rate of climb at the reduced placard speed.

The updated performance is compared with the original 969- 512B in table 13-5. The take-off and approach data are unaltered by the updated changes.

REFERENCES

- 13-1 Swanson, R. L., "Hydrant Fuel Temperature Study," Coordination Sheet 6-2611-30-11A, August 28, 1968.
- 13-2 Hamamoto, M., "Fuel Tank Conductance-NASA Advanced Supersonic Transport Technology Task III," Coordination Sheet 6-8190-10-73-57, June 25, 1973.

Table 13-1.—Volume Versus Area for Fuel Tanks

Tank no	Volume, ft ³	Wetted Area, ft ²
Forward main tank 1 or 4	0.0	0.0
↓	37.4	68.4
	80.5	134.4
	125.6	216.7
	189.3	283.8
	265.8	314.3
	503.9	314.3
	784.7	331.2
	897.2	396.4
	956.2	511.7
	987.1	563.5
1 or 4	1000.6	627.7
Rear main tank 2 or 3	0.0	0.0
↓	9.7	78.7
	49.3	130.3
	192.7	211.9
	291.2	256.1
	357.3	300.8
	595.5	489.8
	850.9	680.5
	943.0	781.4
	985.2	864.5
	996.7	911.0
2 or 3	999.6	944.9
Auxiliary tank 1A or 4A	0.0	0.0
↓	4.9	31.6
	14.0	66.4
	28.2	91.5
	82.1	144.5
	184.7	172.2
	397.1	172.2
	537.7	206.2
	579.6	240.4
	608.3	277.9
1A or 4A	627.3	315.0
Auxiliary tank 2A or 3A	0.0	0.0
↓	12.4	52.2
	98.4	101.6
	220.3	153.0
	324.5	206.8
	416.2	271.4
	517.8	300.2
	586.5	320.8
	529.1	355.2
	646.8	377.1
	663.6	436.9
2A or 3A	670.5	481.7

Table 13-1.— (Concluded)

Tank no.	Volume, ft ³	Wetted Area, ft ²
Auxiliary tank 5A or 6A	0.0	0.0
↓	12.5	55.8
	25.2	111.4
	47.8	187.0
	114.5	279.9
	179.2	313.7
	379.8	313.7
	505.7	368.9
	551.5	446.9
	572.3	501.7
	602.3	569.4
5A or 6A	611.5	528.0
Rear fuselage auxiliary tank 14A	0.0	0.0
↓	17.8	26.1
	44.5	49.8
	71.2	70.5
	106.6	81.5
	117.9	91.0
	165.0	105.0
	231.5	113.0
	252.7	121.0
	275.8	132.0
↓	311.2	157.0
14A	331.0	174.5
Ballast tank	0.0	0.0
↓	5.2	17.4
	8.7	18.3
	15.1	32.9
	42.3	47.0
	50.6	56.4
	81.6	63.9
	206.1	74.4
	242.0	86.5
	260.9	100.0
↓	277.1	119.0
Ballast tank	289.5	150.2

Table 13-2.—Fuel Tank Conductance

Tanks	Tank conductance, Btu/hr, ft ² , ° F
Forward mains no. 1 and no. 4	5
Rear mains no. 2 and no. 3	3
Auxiliary 1A and 2A	11
Auxiliary 2A and 3A	11
Auxiliary 5A and 6A	11
Auxiliary 14A	11
Ballast	11

Table 13-3.—Fuel Temperatures for Various Trip Conditions

Trip condition	On loaded fuel temp, ° F	Maximum temperatures at end of cruise or start of descent (whichever is higher), ° F*			
		Forward main tanks no. 1 or no. 4	Rear main tanks no. 2 or no. 3	Engine/ airframe interface	Burner nozzle
1. Normal, first trip	60	130.3	129.9	217.4	285
2. Higher onloaded fuel temp, first trip	90	153.0	153.3	238.6	306
3. Same as 2, except second trip: reserve plus ballast fuel discharged to main tanks after first trip	90	159.8	161.1	246.4	315
4. Same as 3, except second trip used excess fuel (trip reserves) during trip	90	165.5	163.7	250.0	320
5. Same as 4, except with earlier discharge of rear auxiliary tank 14A at 400 lb/min per main tank (20 min)	90	160.2	157.5	246.0	307
6. Same as 5, except discharge of tank 14A at 800 lb/min per main tank (10 min)	90	158.2	156.0	244.0	308

* Conductances per table 13-2

Table 13-4.—Structural Des: Impact on Mission Range

Change	Equivalent weight, lb	Range, nmi
OEW	+3170	-59
$C_D = +0.00013$	+2811	-52
Placard	+1297	-24
Total	+7278	-135

Table 13-5.—Structural Design Impact on Performance

- Takeoff gross weight 340 194 kg (750 000 lb)
- Payload 22 183.8 kg (48 906 lb); 234 passengers, tourist
- Cruise M = 2.7, standard day

	969-512B. 1% LE rad + LE droop	969-512B update, 1% LE rad + LE droop
Propulsion <ul style="list-style-type: none"> • Type • Airflow, kg/s (lb/s) • Suppression 	ATAT-1 287 (633) Plug and chutes	ATAT-1 287 (633) Plug and chutes
Weights <ul style="list-style-type: none"> • OEW relative to 969-512B kg (lb) 	0	+1437 (+3170)
Range <ul style="list-style-type: none"> • Supersonic cruise, km (nmi) range relative to 969-512B • Supersonic cruise altitude, m (ft) 	0 19 507 (64 000)	-217 (-135) 19 507 (64 000)
Cruise performance <ul style="list-style-type: none"> • Supersonic range factor, km (nmi) at M = 2.7 • L/D (L/D_{max}) • SFC, kg/hr/kg (lb/hr/lb) 	15 268 (8239) 8.29/8.63 1.559	15 061 (8113) 8.22/8.53 1.566
Takeoff <ul style="list-style-type: none"> • FAR field length, m (ft) (Std + 15 K) • Lift-off speed, m/s (KEAS) • Sideline noise, EPNdB • Community noise, 6.49 km (3.5 nmi) from brake release EPNdB 	3780 (12 400) 101 (197) 117 108	3780 (12 400) 101 (197) 117 108
Approach <ul style="list-style-type: none"> • Approach speed, m/s (KEAS) • Wet FAR field length, m (ft) • L/D • Approach noise, 1.85 km (1 nmi) threshold, EPNdB 	84 (163.5) 3200.4 (10 500) 4.23 117.5	84 (163.5) 3200.4 (10 500) 4.23 117.5

Main tanks 2 and 3
 Tank wall thermal conductivity = 5 Btu/hr, ft², ° F
 90° onloaded fuel

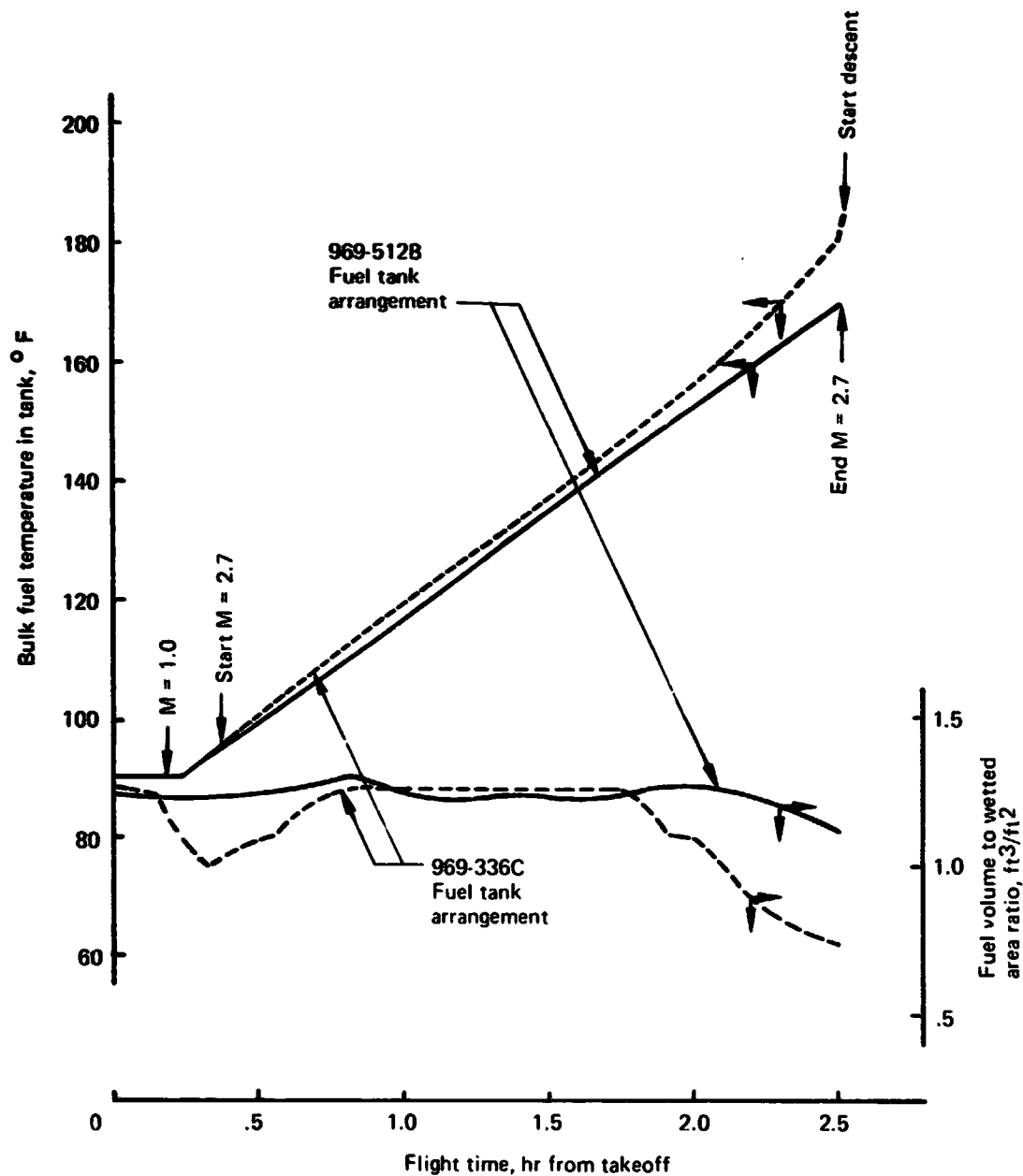


Figure 13-1.—Fuel Temperature Comparison

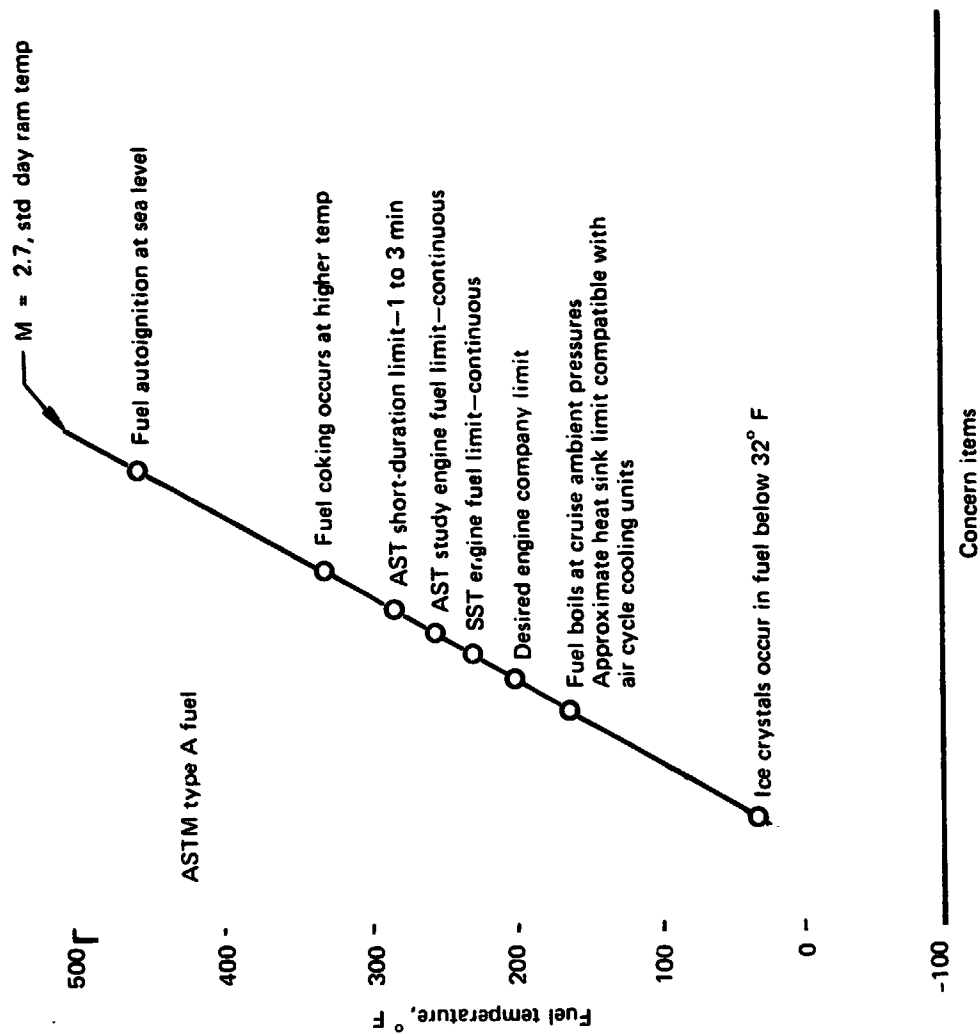


Figure 13-2.—Typical Items Limiting Fuel Heat Sink Capacity With Respect to Temperature

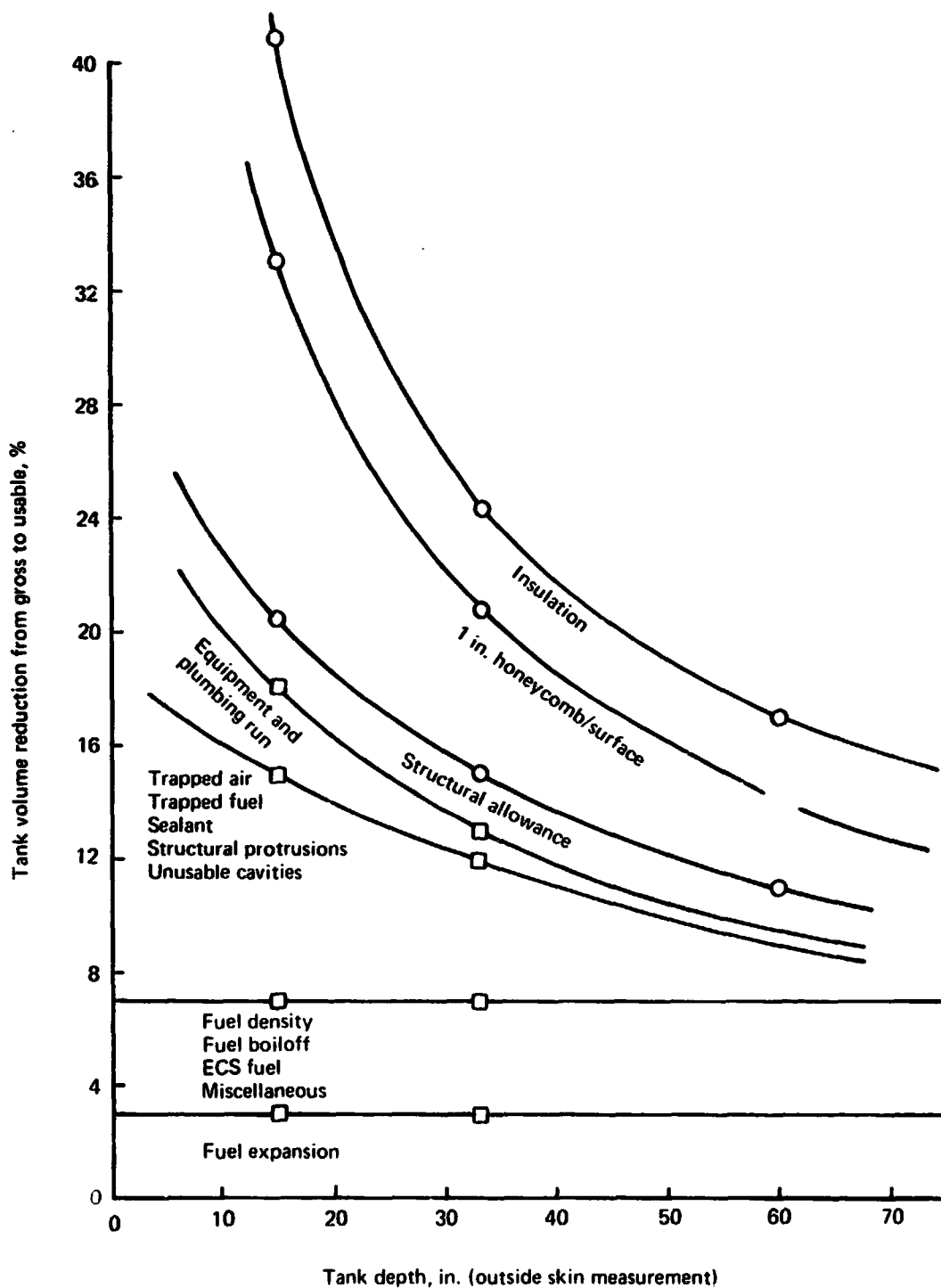
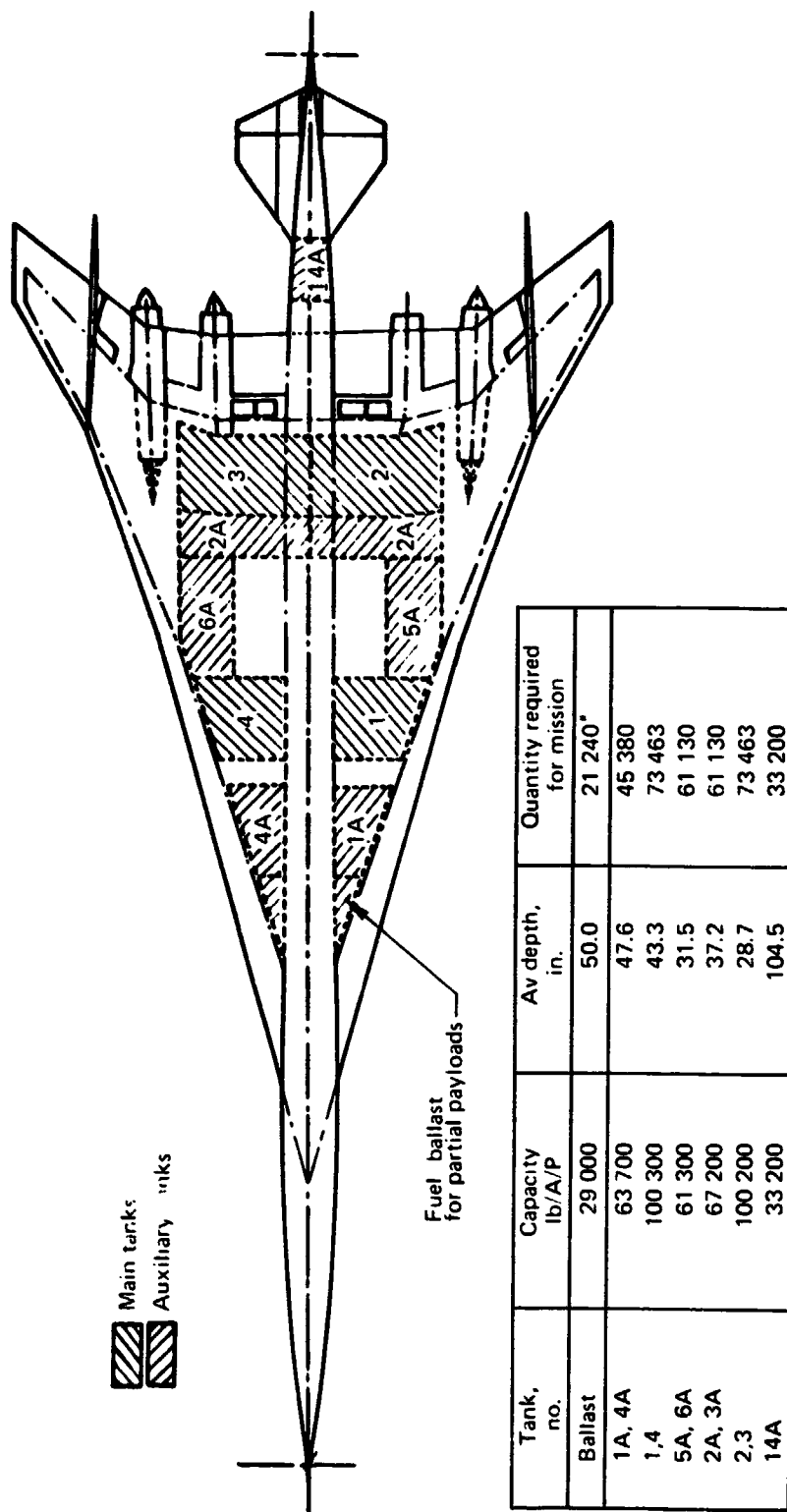


Figure 13-3.—Fuel Tank Volume Reduction Versus Tank Depth, $M = 2.7$ Airplane



Total capacity (excluding ballast), 425 900 lb/A/P

* Not required for a full payload mission, but included for these thermal studies because it is sometimes needed for partial payloads.

Figure 13-4.—Fuel Tank Layout—Model 969-512B

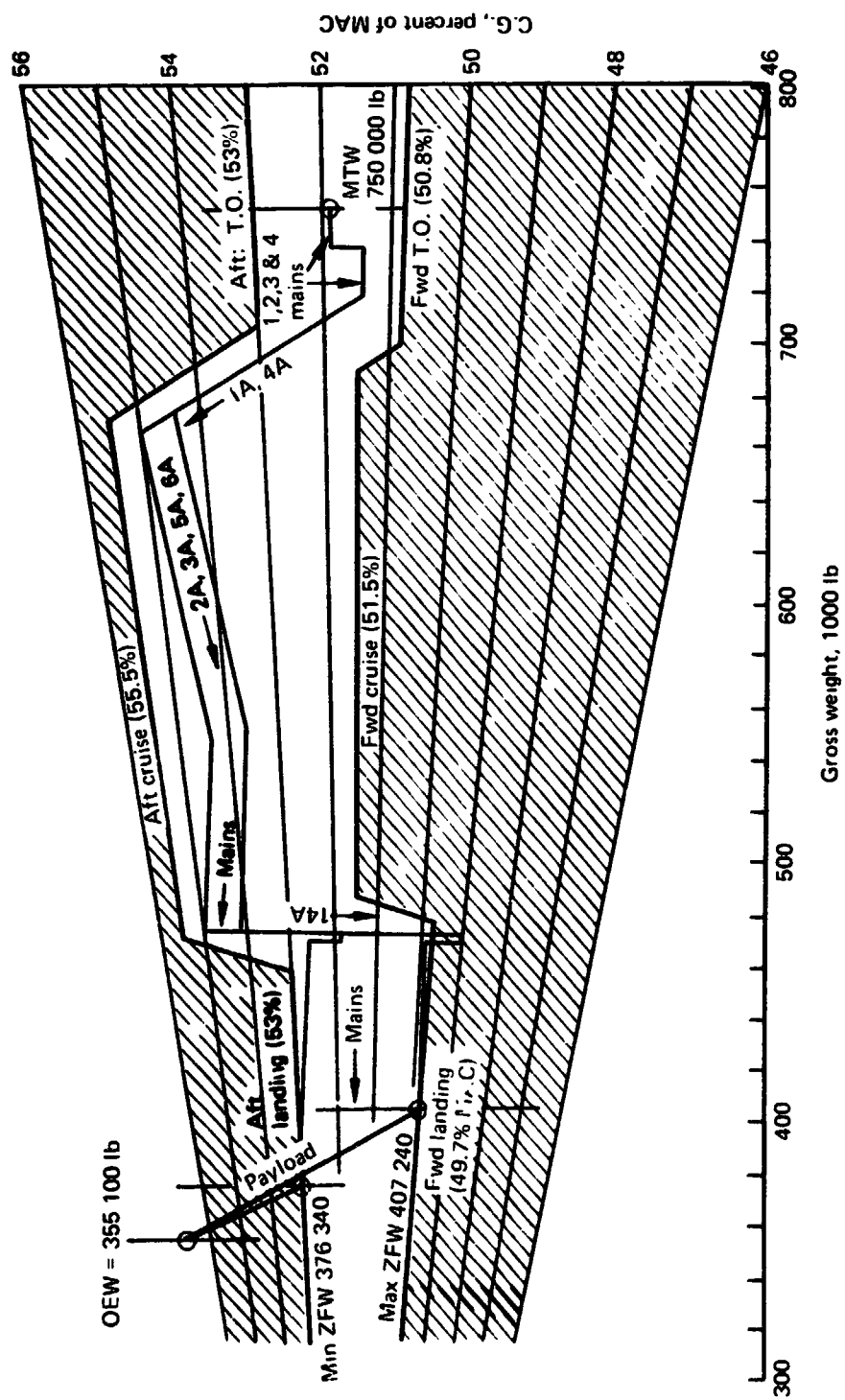


Figure 13-5.—Fuel Management—Model 969-512B

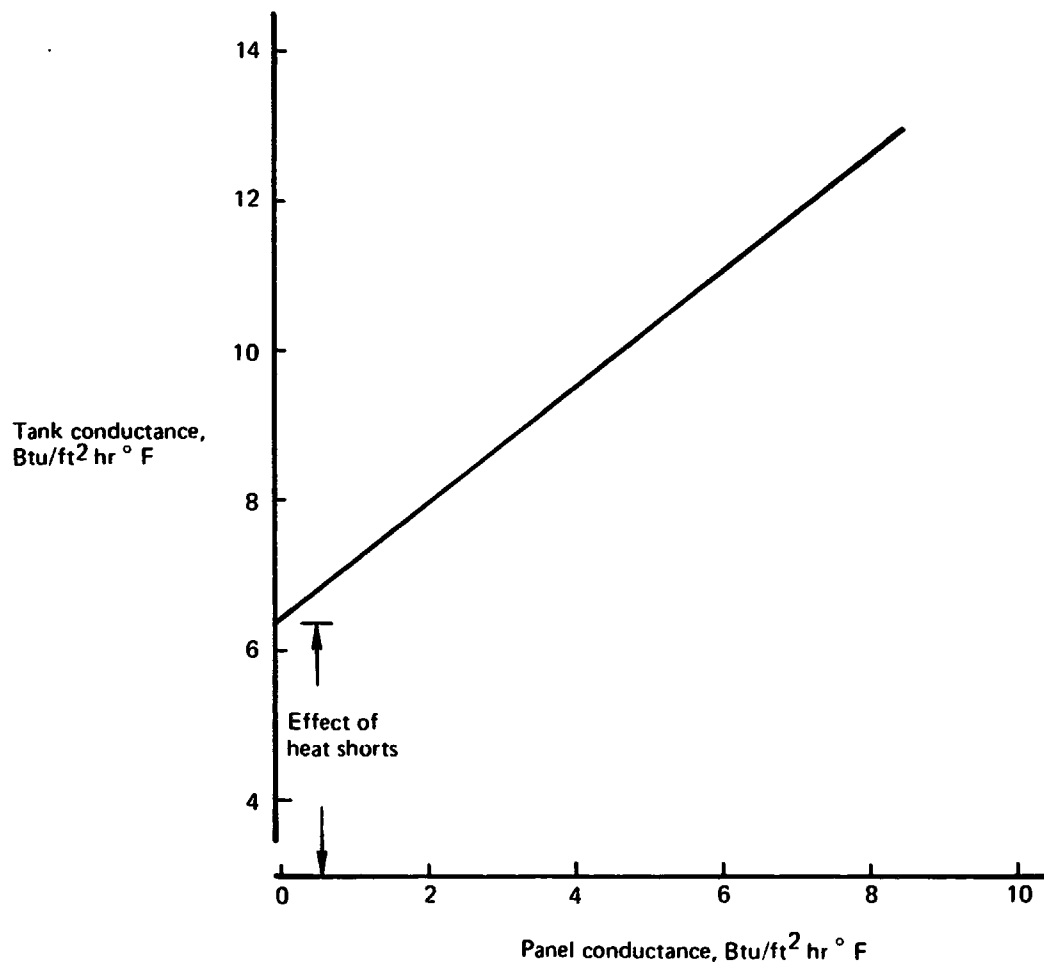


Figure 13-6.—Effect of Panel Thermal Conductance on Fuel Tank Thermal Conductance

969-512B Mission

969-512B baseline fuel tank arrangement,
all tanks have same conductance.

Note: Temperatures are for second trip;

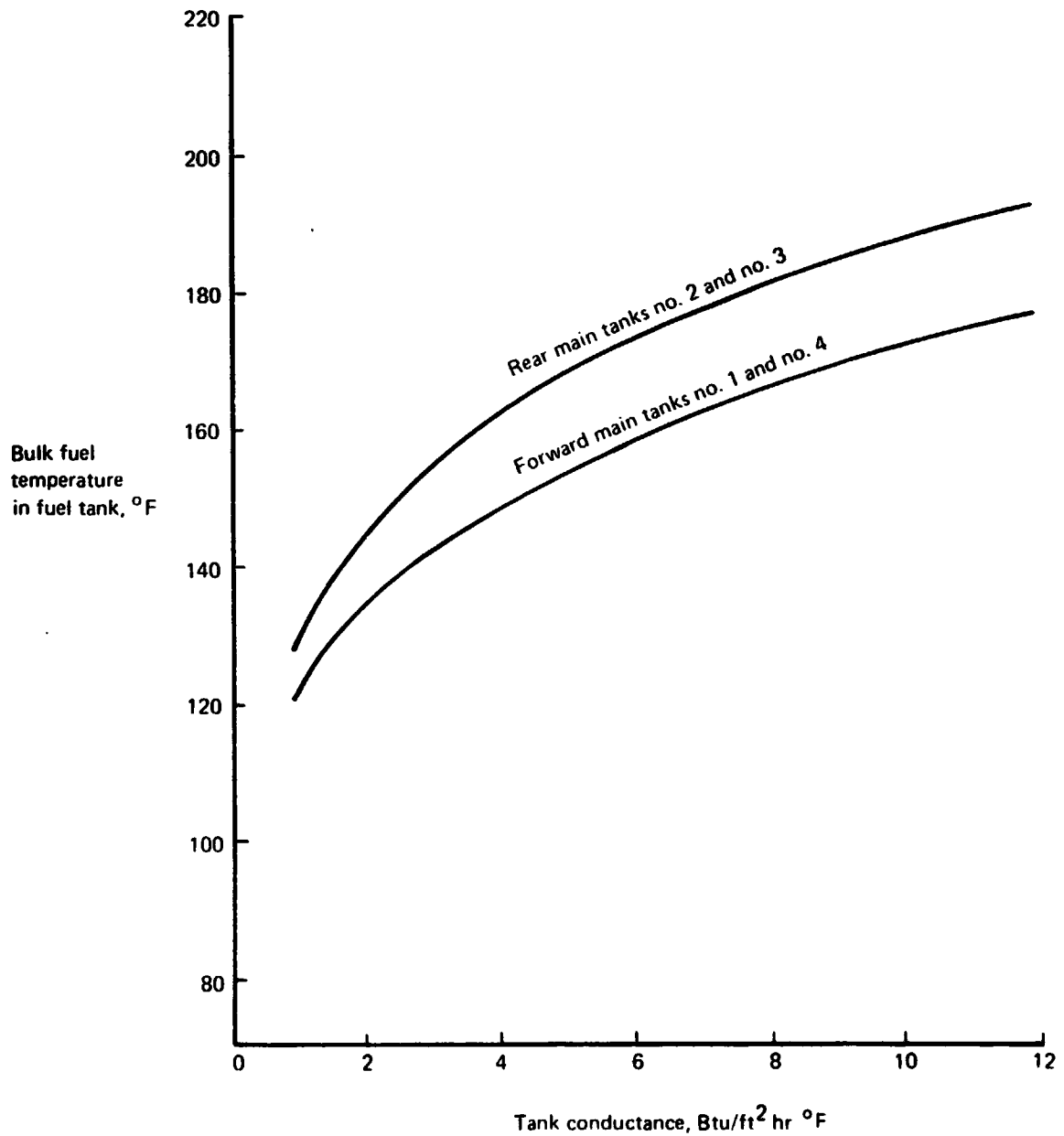


Figure 13-7.—Maximum Temperature of Fuel in Main Tanks at End of Supersonic Cruise

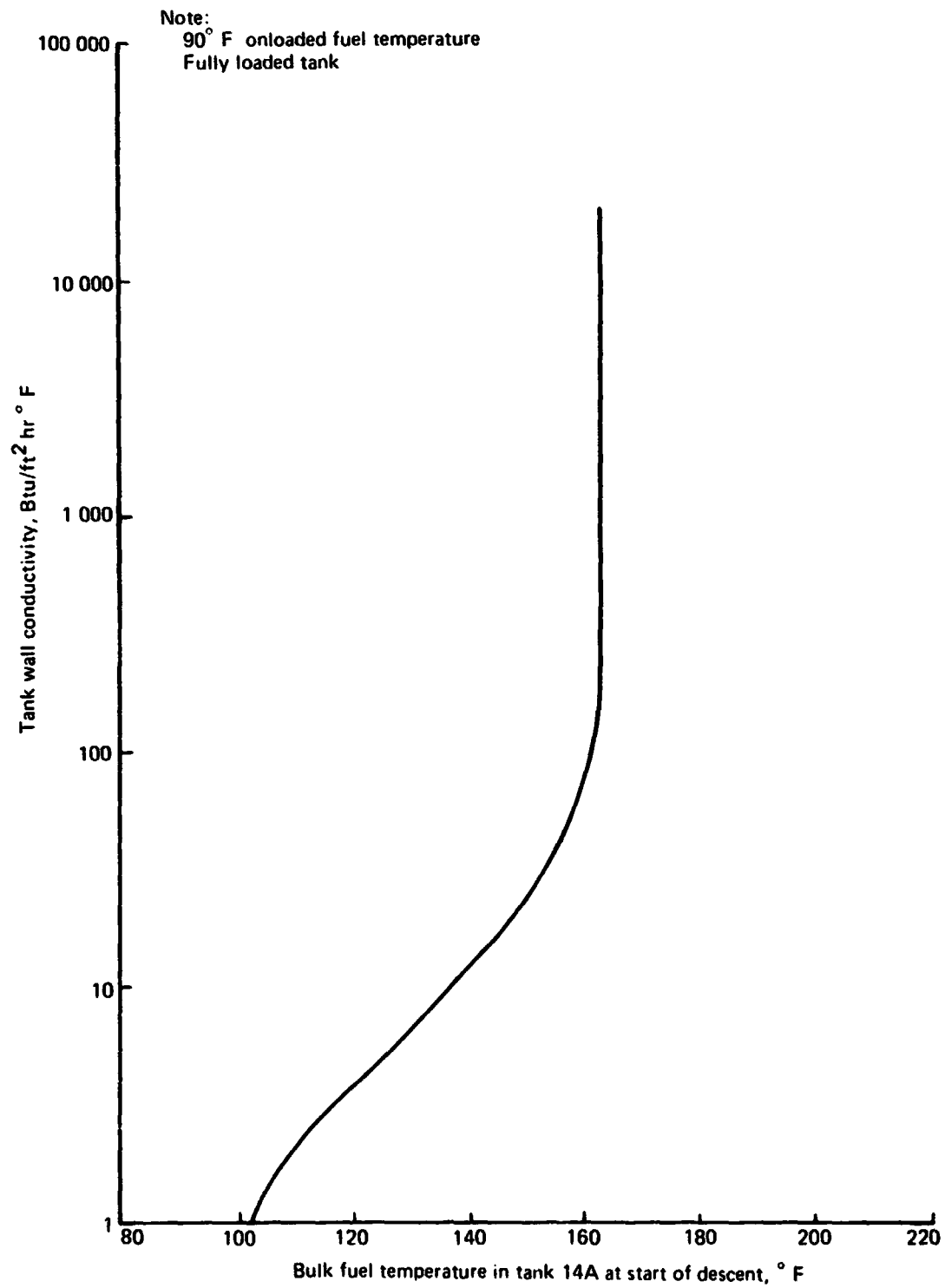


Figure 13-8.—Temperature of Fuel in Rear Fuselage Auxiliary Fuel Tank (14A) at Start of Descent

969-512B Mission

- 969-512B baseline fuel tank arrangement,
all tanks have same conductance.
- - - Same tank arrangement except main tanks
are compartmented. Inner portion with
30 000 lb capacity each are new main tanks.

Note: Temperatures are for second trip

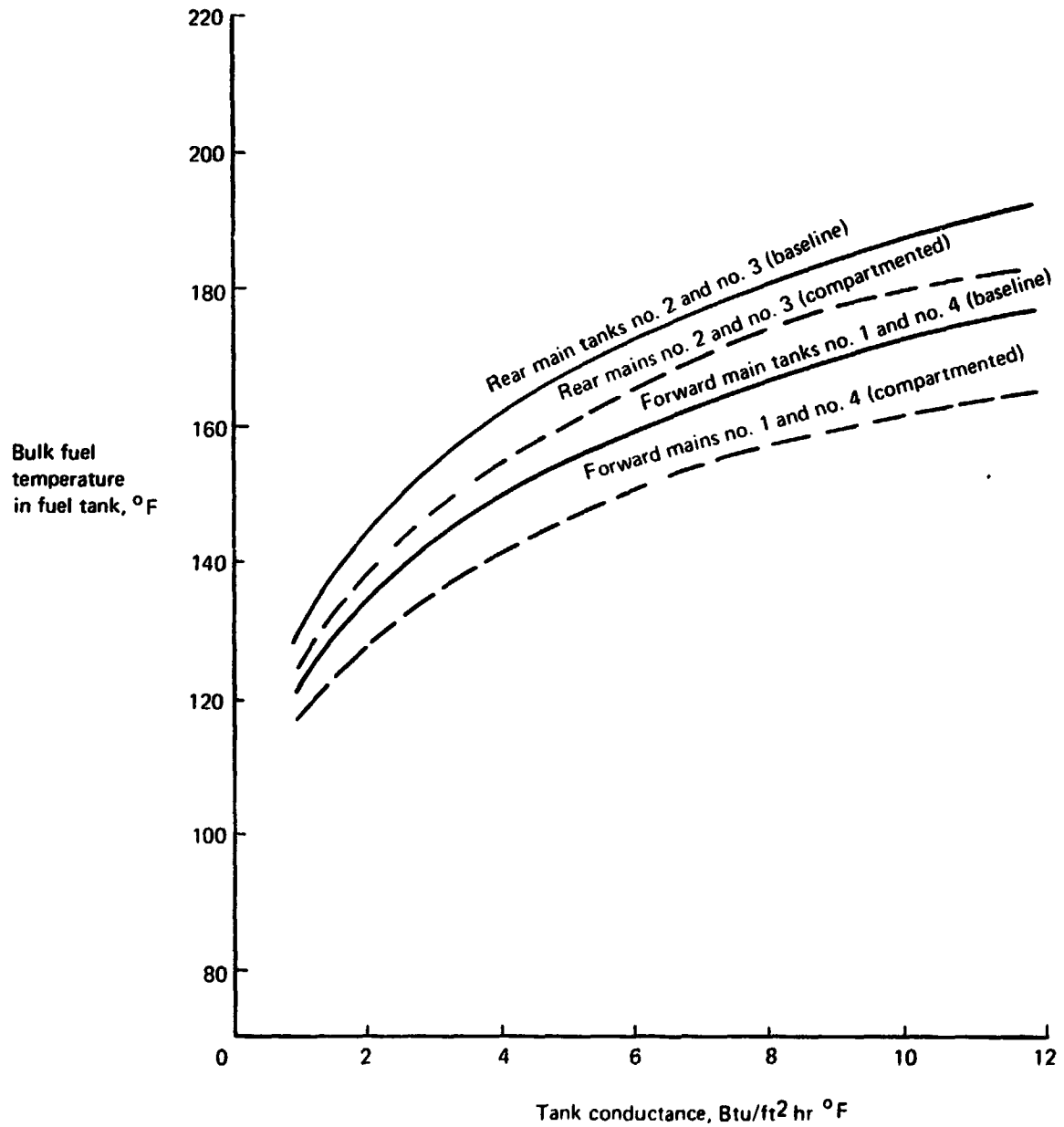


Figure 13-9.—Maximum Temperature of Fuel in Main Tanks at End of Supersonic Cruise (Compartmented Configuration)

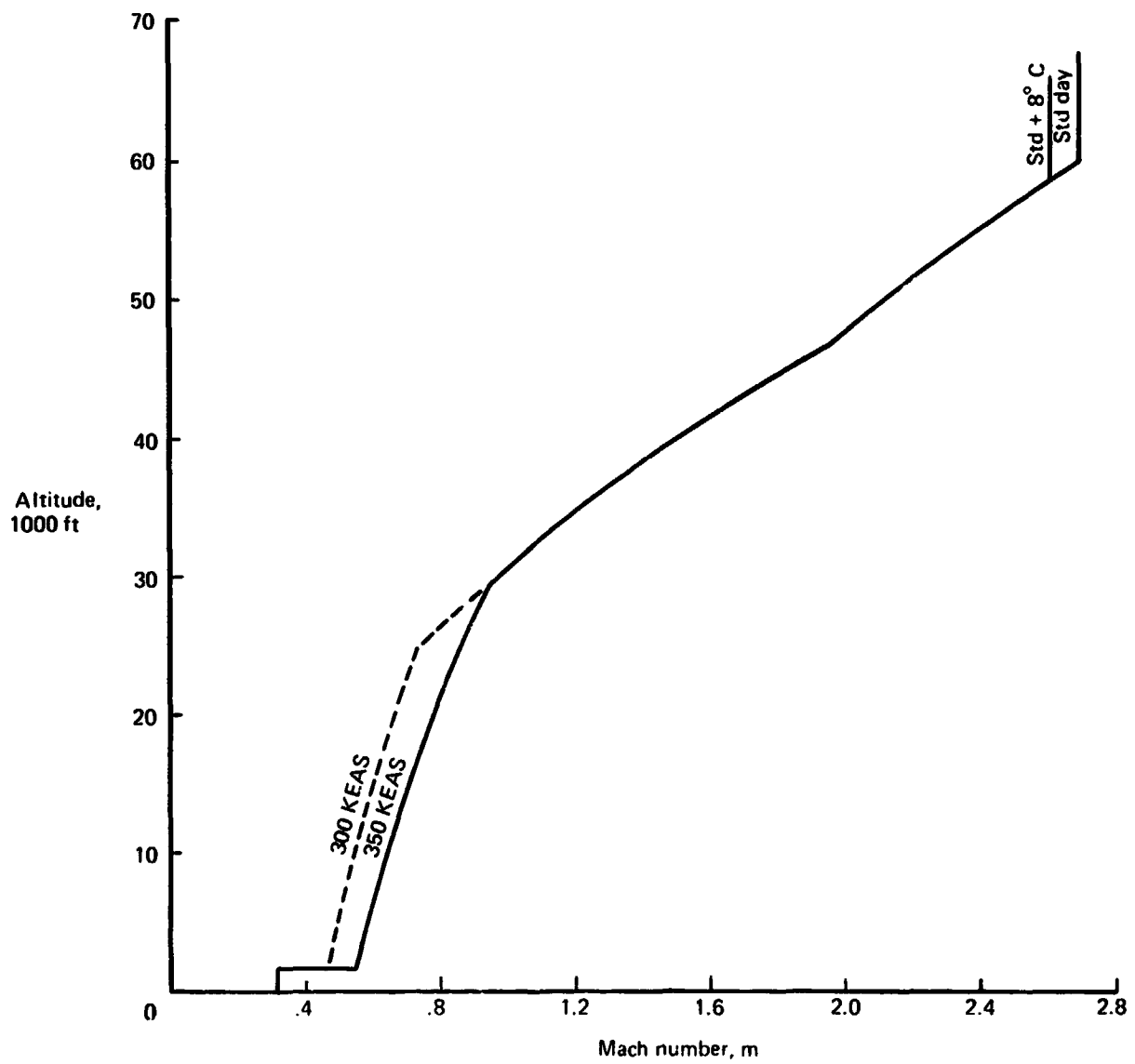


Figure 13-10.--SST Performance Climb Placards

SECTION 14

ADVANCED STRUCTURAL CONCEPTS

by

V. D. Bess
M. D. Halvorsen
H. M. Tomlinson

CONTENTS

	Page
ADVANCED STRUCTURAL CONCEPTS	798
Study Objectives	798
Study Approach	798
Summary	798
Material Selection and Structural Concepts	798
Sheet Stiffener Skin Panels-Borsic/Aluminum Skins and Uniaxially	
Reinforced Titanium Stiffeners	799
Stiffened Thin Honeycomb-Borsic/Aluminum Skin and Uniaxial	
Reinforced Titanium Stiffeners	800
Honeycomb Sandwich Skin Panels-Borsic/Aluminum Skin	801
Honeycomb Sandwich Panels-Organic Matrix Composite	803
Loads and Stress Analysis	804
Body	810
Weight Analysis	811
Body	811
Manufacturing Analysis	812
Material Costs	814
Structural Concept Evaluation and Selection	814
REFERENCE	815

TABLES

No.		Page
14-1	Control Point Loads	816
14-2	Weight Tabulation-Advanced Structural Concepts-Body	817
14-3	Weight Tabulation-Advanced Structural Concepts-Wing Upper Surface ..	818
14-4	Weight Tabulation-Advanced Structural Concepts-Wing Lower Surface ..	819
14-5	Manufacturing Producibility Rating, Body Skin	820
14-6	Manufacturing Producibility Rating, Wing	820
14-7	Cost Analysis of Structural Concepts	821
14-8	Location and Description of Structural Concepts	822
14-9	Structural Concepts Selection-Wing Panels Upper Surface	823
14-10	Structural Concept Selection-Wing Panels Lower Surface	824
14-11	Structural Concept Selection-Body Panels, Point 5	825
14-12	Structural Concept Recommendations	826

FIGURES

No.		Page
14-1	Wing and Body Control Points	827
14-2	Borsic/Aluminum Body Skin and Reinforced Titanium Stiffeners, 969-336C, M = 2.7 Cruise	829
14-3	Sheet Stiffener Panel Assembly, Borsic/Aluminum Skin- Borsic/Aluminum Reinforced Titanium Stiffeners	831
14-4	Borsic/Aluminum Body, Honeycomb Sandwich Skin and Titanium Stiffeners, 969-336C, M = 2.7 Cruise	833
14-5	Borsic/Aluminum Wing, Honeycomb Sandwich Skin and Titanium Stiffeners, 969-336C, M = 2.7	839
14-6	Borsic/Aluminum Body, Honeycomb Sandwich Skin, 969-336C, M = 2.7 ...	841
14-7	Brazed Honeycomb Panel Assembly, Borsic/Aluminum Skins, Titanium Core, 969-336C	842
14-8	Brazed Honeycomb Lower Surface Panel, Borsic/Aluminum Skins, Titanium Core, 969-336C	845
14-9	Graphite/PPQ Body, Honeycomb Sandwich, Skin 969-336C, M = 2.7	847
14-10	Bonded Wing, Honeycomb Panel, Graphite/PPQ Skins, 969-336C, M = 2.7	849
14-11	Projected Stress/Strain Curve for Bsc/Al 1980-1990 [0] and [90] Tension or Compression, Room Temperature	851
14-12	Projected Stress/Strain Curve for [±45] Bsc/Al 1980-1990 Tension or Compression, Room Temperature	852

FIGURES (CONTINUED)

No.	Page
14-13	Projected Shear Stress/Strain Curve for $[\pm 45]$ Bsc/Al 1980-1990, Room Temperature 853
14-14	Projected Shear Stress/Strain Curve for $[\pm 45]$ Bsc/Al 1980-1990, Room Temperature, NASA Langley Test 854
14-15	Projected Stress/Strain Curve for Bsc/Al 1980-1990, $[0]$ and $[90]$ Tension or Compression, 250° F 855
14-16	Projected Stress/Strain Curve for $[\pm 45]$ Bsc/Al, 1980-1990, Tension or Compression, 250° F 856
14-17	Projected Shear Stress/Strain Curve for $[\pm 45]$ Bsc/Al, 1980-1990, 250° F 857
14-18	Projected Shear Stress/Strain Curve for $[\pm 45]$ Bsc/Al, 1980-1990, 250° F, NASA Langley Test 858
14-19	Projected Stress/Strain Curve for Bsc/Al, 1980-1990, $[0]$ and $[90]$ Tension or Compression, 450° F 859
14-20	Projected Stress/Strain Curve for $[\pm 45]$ Bsc/Al, 1980-1990, Tension or Compression 450° F 860
14-21	Projected Shear Stress/Strain Curve for $[\pm 45]$ Bsc/Al, 1980-1990, 450° F 861
14-22	Projected Shear Stress/Strain Curve for $[\pm 45]$ Bsc/Al, 1980-1990, 450° F, NASA Langley Test 862
14-23	High Strength Graphite/PPQ Projected 1980-1990 Allowables $[0]$ Longitudinal and Transverse, Tension or Compression, Room Temperature 863
14-24	High Strength Graphite/PPQ Projected 1980-1990 Allowables $[\pm 45]$ Longitudinal and Transverse, Tension or Compression, Room Temperature 864
14-25	High Strength Graphite/PPQ Projected 1980-1990 Allowables $[\pm 45]$ Shear, Room Temperature 865
14-26	High Strength Graphite/PPQ Projected 1980-1990 Allowables $[0]$ Longitudinal and Transverse, Tension or Compression, 250° F 866
14-27	High Strength Graphite/PPQ Projected 1980-1990 Allowables $[\pm 45]$ Longitudinal and Transverse, Tension or Compression, 250° F 867
14-28	High Strength Graphite/PPQ Projected 1980-1990 Allowables $[\pm 45]$ Shear, 250° F 868
14-29	High Strength Graphite/PPQ Projected 1980-1990 Allowables $[0]$ Longitudinal and Transverse, Tension or Compression, 450° F 869
14-30	High Strength Graphite/PPQ Projected 1980-1990 Allowables $[\pm 45]$ Longitudinal and Transverse, Tension or Compression, 450° F 870

FIGURES (CONCLUDED)

No.		Page
14-31	High Strength Graphite/PPQ Projected 1980-1990 Allowables [± 45] Shear, 450° F	871
14-32	Weight Comparison - Advanced Structural Concepts - Body	872
14-33	Weight Comparison - Advanced Structural Concepts - Wing Upper Surface	873
14-34	Weight Comparison - Advanced Structural Concepts - Wing Lower Surface	874
14-35	Wing and Body Structural Selection	875
14-36	Initial Buckling of Flat Rectangular Panels	876

SECTION 14

ADVANCED STRUCTURAL CONCEPTS

STUDY OBJECTIVES

The Task II objective was to develop structural design concepts for a Mach 2.7 supersonic transport configuration using advanced technology materials and processes expected to be developed in the 1980-1990 time period. The design loads and environmental conditions used in Task I for sizing the 1975 technology concepts were also used in this study to permit a direct comparison between the two technology levels.

It was also desired to evaluate the manufacturing feasibility and weight advantage of various advanced structural concepts, and to define some analytical and manufacturing methods to be developed for the design and production of practical components made from advanced technology materials.

STUDY APPROACH

The study approach for Task II has been to select one body and one wing control point from those used in Task I. Only two control locations were chosen, so that each structural concept could be developed in sufficient detail to establish feasibility of designing practical airframe components of advanced composite materials.

Both metal matrix and organic polymer matrix material systems were investigated. The major effort was directed toward designs using metal matrix composite.

One of the structural configurations evaluated with a metal matrix at each control point was selected for design and evaluation using a high temperature polymer.

SUMMARY

The results of this study indicate that Borsic/Aluminum structural design concepts offer significant weight savings. Manufacturing complexities, however, are three to four times those of current materials, thus significantly increasing manufacturing costs. In general, weight savings are more significant for compression than for tension applications. In addition, Borsic/Aluminum shear allowables have a large effect on potential weight savings. The graphite/PPQ, full depth honeycomb skin panel concept investigated is potentially lighter, cheaper and easier to fabricate than Borsic/Aluminum. However the assumed material properties and manufacturing techniques need to be verified.

MATERIAL SELECTION AND STRUCTURAL CONCEPTS

Two families of advanced composites were selected for evaluation, namely a Borsic/Aluminum metal matrix and a high temperature polymer matrix. Polyphenylquinoxaline (PPQ), with high strength graphite filaments.

Three structural arrangements using Borsic/Aluminum composites were designed at body control point 5 and wing control point 269, shown in figure 14-1. These structural arrangements consist of the following:

- Stiffened Sheet-Skin Panel-Borsic/Aluminum Skins and Uniaxially Reinforced Titanium Stiffeners
- Stiffened Thin Honeycomb-Skin Panel-Borsic/Aluminum Skins-Titanium Core and Uniaxially Reinforced Titanium Stiffeners
- Honeycomb Skin Panels-Borsic Aluminum Skins-Titanium Core

From the evaluation of the metal matrix configurations, the full depth honeycomb skin panel arrangement was selected as the configuration for the PPQ matrix design study. This arrangement consisted of graphite/PPQ skins with titanium core.

Only a limited amount of development work has been done on high temperature polymers. The resulting high risk is offset by its highly attractive characteristics such as; low cost, relatively low density, high shear strength, and moderate manufacturing complexity compared to the metal matrix composites.

SHEET STIFFENER SKIN PANELS-BORSIC/ALUMINUM SKINS AND UNIAXIALY REINFORCED TITANIUM STIFFENERS

Body Skin Panel

The general arrangement of the Borsic/Aluminum skin concept is illustrated in figure 14-2. It consists of a $[0_2/\pm 45/90_3]$ layup with three additional pairs of $\pm 45^\circ$ plies located along the skin splices and body frames. The body pressure load is carried by the 90° skin plies with the majority of the body bending compression carried by the uniaxially reinforced titanium stiffeners. The body frame is of formed titanium sheet with a uniaxially reinforced circumferential flange adjacent to the skin. This skin flange makes maximum use of the available depth for frame bending as well as serving as a fail-safe strap. The stiffeners are of uniaxially reinforced titanium with symmetrical joggles over the frame skin chords. The uniaxial stiffener reinforcement is equal on both flanges and the stiffener joggle is symmetrical over the frame chord to prevent distortion of the stiffener by differential shrinkage during fabrication. The stiffeners are attached to the skin panel by spot brazing which reduces the number of fastener holes required through the panel. Preliminary tests shown in reference 14-1 have shown minimal degradation of borsic material properties by spot brazing.

The skin assembly is consolidated by applying heat and pressure to the Borsic/Aluminum skin plies. The titanium stringers are machined extrusions reinforced with uniaxial Borsic/Aluminum diffusion bonded to the stringer. Formed titanium body frames are chem-milled and installed by riveting. The skin panel is also installed by conventional rivets along the panel periphery.

Wing Skin Panel-Upper

The upper surface wing skin panel shown in figure 14-3 has been designed for the combined loads shown in table 14-1. Since the skin panel must carry chordwise (N_y) loads, the panel has been sized to be buckle-resistant at ultimate load. A stiffener spacing of 4.80 in. was selected as a compromise between compression buckling requirements and space requirements for installation of shear ties between stiffeners. The load transfer capability of the skin panels has been increased in the critical joint areas by the addition of eight titanium shims located between the Borsic/Aluminum plies. The titanium stiffeners are reinforced by uniaxial plies attached by diffusion bonding.

The wing panel fabrication is similar to that of the body. The Borsic/Aluminum skin panel is assembled by consolidation. The uniaxial Borsic/Aluminum reinforcement is attached to the stiffeners by diffusion bonding. The stiffeners are attached to the skin panel by spot brazing.

Wing Skin Panel-Lower

The lower wing skin panel, also shown in figure 14-3, is of similar structural configuration to the wing upper surface panel. The lower panel is critical for the tension condition. The stiffener spacing of 6.70 in. is determined by the reverse bending condition. The skin panel has been sized for two levels of material shear allowables. In each case, the tension and compression properties were the same for all designs. The fabrication and assembly of the lower surface tension panels is similar to the wing upper surface compression panel.

STIFFENED THIN HONEYCOMB-BORSIC/ALUMINUM SKIN AND UNIAXIAL REINFORCED TITANIUM STIFFENERS

Body Skin Panel

The stiffened thin honeycomb body skin panel is shown in figure 14-4. The honeycomb skin carries the pressure load in the 90° plies and shares the axial compression with the stiffeners. The thin honeycomb panel is buckle-resistant at ultimate load with a stiffener spacing of 8.00 in. Inner and outer face sheets consist of $[0_2/\pm 45/90]$ with added plies of Borsic/Aluminum used at the frame attach points and skin splices for increased load transfer capability. The formed titanium body frames use outer chord shear ties that splice through the stiffener flanges for load continuity. The machined titanium stiffeners are reinforced with ten plies of uniaxial Borsic/Aluminum on both inner and outer flanges.

The Borsic/Aluminum face sheets and the reinforced stiffeners are manufactured as separate sub-assemblies. The .188 in. titanium field core is spliced by spotwelding to the dense core used at panel edges. Fit up tolerances of the titanium core to the padded face sheets are critical for the brazing process. The stiffeners are spot brazed to the inner skin panel in sub-assembly and both the stiffener to face sheet, and face sheet to core attachments are made in the final braze cycle.

Wing Skin Panels

The stiffened thin honeycomb panels, designed of Borsic/Aluminum for the upper and lower wing surfaces, are shown in figure 14-5. The structural arrangements of both panels are similar, therefore the upper skin panel is described in detail with the exceptions noted for the lower surface panel.

The honeycomb panel is designed to be buckle-resistant at ultimate combined loads. This condition determined the selection of .30 in. core depth and 7.00 in. stiffener spacing. The reinforced stiffeners carry spanwise load. The Borsic/Aluminum face sheets for the upper wing panel are sized for two levels of material shear capability.

Both skins of the lower surface panel are $[0_2/\pm 45_6/90]$ and are critical for combined tension and shear. The lower surface honeycomb panel core depth is .152 in. It is thinner than the upper surface core because of reduced compression intensities.

The Borsic/Aluminum skins are reinforced by six metal shims in the areas of bolted skin joints. Dense titanium core, 28.1 pcf, is used to prevent core crushing in the joint fastener areas. Torque limited type fasteners are required to control the fastener crushing loads. The uniaxially reinforced stiffeners are spot brazed to the inner skin panel to reduce fastener hole penetrations. Separate machined titanium fittings are used to splice the stiffener loads at joints. The stiffener splice takes place through the padded titanium web to minimize fastener penetrations through the Borsic/Aluminum reinforcement.

The Borsic/Aluminum face sheets and reinforced stiffeners are fabricated as sub-assemblies. Core to face sheet fit-up tolerances must be controlled closely; however, there are fewer pad-ups requiring fit-up for the wing panels than for the body skin assemblies. The stiffener sub-assemblies are spot brazed to the inner skin followed by fit-up and subsequent brazing of the entire skin panel assembly.

HONEYCOMB SANDWICH SKIN PANELS-BORSIC/ALUMINUM SKINS

Body Skin Panels

The brazed Borsic/Aluminum honeycomb sandwich design shown in figure 14-6 carries the combined body pressure and bending loads, primarily in the panel face sheets. The 1.25 in. core depth is adequate to provide panel buckling stability with a 35.5 in. frame spacing. Panel width is limited by manufacturing capability.

Each body panel face sheet is consolidated of $[0_4/\pm 45/90]$ with six .009 in. titanium shims laminated between the Borsic/Aluminum plies along the circumferential splices. Dense titanium 6Al-4V core of 28.1 pcf (SS2-60) is used along the circumferential splices where .25 in. diameter bolts are used. At the longitudinal splices and body frame locations 14.1 pcf (SS2-30) titanium 6Al-4V honeycomb core is used with .187 in. diameter bolts. In the remaining field areas, 4.9 pcf honeycomb core of Ti 3Al-2.5V is used. The skin panels are recessed to accept flush circumferential body splice straps. The skin panels are full depth along the longitudinal splices with the external splice straps outside of contour.

The Borsic/Aluminum face sheets are consolidated as separate sub-assemblies. The core assembly is spotwelded and machined with the proper recesses to match the panel pad requirements. The panel assembly is completed by brazing the face sheets to the core assembly.

Wing Skin Panels

The honeycomb sandwich wing panel shown in figure 14-7 uses Borsic/Aluminum skins brazed to titanium honeycomb core. Both upper and lower wing surfaces are shown. The lower wing surface skins are sized for two levels of Borsic/Aluminum shear allowable. Since the structural configuration is similar for both upper and lower surface, the upper surface panel is described and the lower surface exceptions are noted. The upper wing surface is designed for combined spanwise and chordwise compression load as well as a significant shear load. The skin panels have been sized to carry these combined loads and be buckle resistant at ultimate load. The panel edges utilize laminated titanium shims for joint reinforcement. The 1.00 in. core is adequate to provide panel buckling stability for a 35 in. spar spacing. Panel joint splice loads are carried through flush splice plates attached to the panels by torque limited mechanical fasteners.

The upper wing panel utilizes an inner and outer Borsic/Aluminum skin, each consisting of $[0_4/\pm 45_3]$. The lower wing panel skins are $[0_4/\pm 45_6/90]$ and $[0_4/\pm 45_4/90]$ corresponding to the two levels of allowable shear. Four plies of .007 in. titanium shims are laminated between the Borsic/Aluminum plies to add additional capability at the mechanically fastened joints. Dense core of 28.1 pcf (SS 2-60) titanium 6Al-4V is used in the bolted areas and 4.9 pcf core is used for panel field core. Two rows of .250 in. diameter fasteners are used for chordwise splices and a single row for the spanwise splice.

The Borsic/Aluminum face sheets are made in sub-assembly by consolidation. The dense core and field core are joined by spotwelding and are machined to match the skin pad configuration. After proper fit-up, final assembly is made by brazing.

An alternate brazed honeycomb panel arrangement for lower surface application is shown in figure 14-8. This concept was investigated to evaluate the use of a uniaxial Borsic/Aluminum truss as an alternate means to $\pm 45^\circ$ plies for carrying the panel shear loads, the incentive being the significantly higher uniaxial material allowables for carrying panel shear compared to the $\pm 45^\circ$ shear allowables. This concept uses two trusses made up of uniaxial tapes with a multi-cycle wave pattern used to reduce the concentrated fastener loads occurring at the truss nodes. The truss loads at the nodes are reacted by laminating the truss plies between tabbed titanium edge members. The completed truss is then attached to the panel skins by consolidation. A truss was required for each skin to minimize the fastener size and keep a balanced joint load on both inner and outer skin. The outer skin truss is located inside the panel requiring recessing of the core locally over the buried shear truss, greatly complicating the manufacture of the panel.

The shear truss, sculptured edge members, and Borsic/Aluminum skins are consolidated together as a sub-assembly. The core assembly is spotwelded and machined to match the skin pad requirements. The assembly of the panel face sheets and core is completed with the final braze cycle.

HONEYCOMB SANDWICH PANELS-ORGANIC MATRIX COMPOSITE

The honeycomb sandwich concept was selected from the evaluation of the metal matrix configurations for further study with organic matrix composite. Polyphenolquinoxaline (PPQ) was the matrix selected for use with high strength graphite fibers.

Body Skin Panel

The graphite/PPQ body skin panel shown in figure 14-9 is of the same general configuration as that shown for the Borsic/Aluminum arrangement in figure 14-6. Both panels have been sized to the same loads and environmental conditions. Each skin layup for the graphite/PPQ panel is $[0_9/\pm 45_2/90_2]$ compared to $[0_4/\pm 45/90]$ for Borsic/Aluminum. This is due to a difference in ply thickness and material allowables. The single ply thickness used for graphite/PPQ is .0052 in. compared to .007 in. for Borsic/Aluminum. The core thickness is 1.00 in. Core densities and arrangement are the same as that used for the metal matrix configuration.

The graphite/PPQ panel is fabricated in a two stage bonding operation. Following the lay-up of each graphite/PPQ skin, the sub-assembly is completed by bonding. The titanium core components are assembled by spotwelding. The core assembly is then machined to fit the face sheet skin pads. The components are fitted and bonded to complete the assembly.

Wing Skin Panels

The graphite/PPQ wing skin panels shown in figure 14-10 are of similar structural arrangement to the Borsic/Aluminum brazed honeycomb arrangement shown in figure 14-7. Graphite/PPQ skins have replaced Borsic/Aluminum with the assembly being made by bonding as compared to brazing for the Borsic/Aluminum. Face sheet layup of the graphite/PPQ skins is $[0_8/\pm 45_5]$ for the upper surface panel and $[0_8/\pm 45_5]$ for the lower. The increase in upper panel core height to 1.25 in. for graphite/PPQ compared to 1.00 in. for Borsic/Aluminum is mainly a result of a reduction in effective modulus (E) when using high strength graphite rather than borsic filaments.

The lower surface panel core height of .75 in. was found satisfactory for both graphite and borsic configurations since it is critical in compression for only the lightly loaded negative bending condition.

The fabrication of the graphite/PPQ wing panel would be similar to that described for the graphite/PPQ body panel.

LOADS AND STRESS ANALYSIS

WING LOWER SURFACE

The critical design condition for the wing lower surface at control point 269 is combined biaxial tension and shear at room temperature, as shown in table 14-1.

Three structural concepts defined below were analyzed:

<u>Concept</u>	<u>Material</u>
Skin-Stringer	BSC/Aluminum (low shear)
	BSC/Aluminum (high shear)
Stiffened Honeycomb	BSC/Aluminum (low shear)
Honeycomb (2)	BSC/Aluminum (low shear)
	BSC/Aluminum (high shear)
	Graphite/PPQ

Failure mechanisms for combined loading on multi-directional layups of these materials are not well known. An attempt was made to establish a failure criteria for each material consistent with the allowable stress-strain curves adopted for [0], [90], and [± 45] layups.

Borsic/Aluminum With Low Shear Allowable

Material properties from reference 14-1 were used as a base. Tension and compression allowables were modified slightly to reflect assumed developments by the 1980-1990 time period. The modified data is shown in figures 14-11 and 14-12. The ultimate shear strength and shear stress-strain data presented in reference 14-1 is contradictory. The shear stress-strain data given in figure 1.2.1-55 of the reference indicates a failure at a shear stress of 35ksi and a shear strain of 7200 μ in/in. However, table 1.2.1 - XII, of the same reference, shows an allowable ultimate shear stress of 49ksi. Figure 14-13 shows what we used. It was an attempted compromise. The referenced stress strain curve was modified slightly and extended to the referenced 49ksi at an arbitrarily assumed failure strain (γ) of 16000 μ in/in.

Based on the assumed $\gamma_{crit} = 16000 \mu$ in/in for a [± 45] layup, it follows that the diagonal strain would be 8000 μ in/in, and that for a [0,90] layup loaded in equal biaxial tension-compression, the critical strain $\epsilon_{crit}^T = \epsilon_{crit}^C = 8000 \mu$ in/in. From figure 14-11, it was established that for a uniaxially loaded [0,90] layup is 6000 μ in/in. An effective (plastic) poissons ratio was established by

$$\frac{8000}{6000} - 1 = \nu_e = .33$$

It was next assumed that a [0,90] layup loaded in equal biaxial tension would be strain critical at

$$\frac{6000}{1 + M_e} = 4500 \mu \text{ in./in.}$$

From the foregoing assumptions, it follows for the skins that:

$$\frac{N_x}{E_x t} - \frac{N_y}{E_y t} \mu_e = \epsilon_x \quad (14-1)$$

and

$$\frac{N_y}{E_y t} - \frac{N_x}{E_x t} \mu_e = \epsilon_y \quad (14-2)$$

and

$$\epsilon_{x \text{ crit}} = \epsilon_{y \text{ crit}} = 4500 + \left(\frac{\epsilon_1 - \epsilon_2}{\epsilon_1} \right) 1500 \mu \text{ in./in.} \quad (14-3)$$

where ϵ_1 is the larger of

$$\frac{N_x}{E_x t} \text{ or } \frac{N_y}{E_y t}$$

Based on a critical diagonal strain of $8000 \mu \text{ in./in}$ when produced entirely by shear and $4500 \times 10^{-6} + (\epsilon_1 - \epsilon_2/\epsilon_1) 1500 \times 10^{-6}$ when produced entirely by biaxial tension, a diagonal strain limitation was established by requiring

$$\frac{\frac{N_{xy}}{2 G_{xy} t [\pm 45]}}{8000 \times 10^{-6}} + \frac{.5 (\epsilon_x + \epsilon_y)}{4500 \times 10^{-6} + \left(\frac{\epsilon_1 - \epsilon_2}{\epsilon_1} \right) 1500 \times 10^{-6}} \leq 1 \quad (14-4)$$

It was assumed that the [0,90] plies carried no shear, consequently, with non-linear shear stress-strain curves, it was important to establish shear stress by dividing N_{xy} by the thickness of [± 45] plies only. The shear modulus $G_{xy} = \tau/\gamma$ can be calculated using the shear stress, τ , as defined above, and shear strain, γ , values from figure 14-13.

Borsic/Aluminum with High Shear Allowables

Results of shear tests of [± 45] material at NASA Langley were available in May 1974. Extensive care had been exercised in setting up a shear test that was free of the typical problems inherent in this type of test. The resultant shear stress-strain curve was, as

expected, quite linear up to failure. The failure, however, was considered premature due to stress concentrations at the corners of the test panel. Figure 14-14 is a result of this test and figures 14-15 through 14-22 include projections to the 1980-1990 time period.

A more logical failure criteria could now be established with the introduction of the new and realistic shear stress-strain curve. Figures 14-11 and 14-12 were used along with figure 14-14. The latter figure shows $\gamma_{crit} = 12000 \mu \text{ in/in}$ and hence, the limiting diagonal strain was taken as $6000 \mu \text{ in/in}$. Figure 14-11 and 14-12 show limiting strains of $6000 \mu \text{ in/in}$. The resulting failure criteria, while simplified, emerged as simply limiting the strains in the 0° , $+45^\circ$, 90° , and -45° direction to $6000 \mu \text{ in/in}$ regardless of the forces that produced it. Poisson ratios were taken from reference 14-1, table 1.2.1-X for the $[0]$ and $[90]$ families, and table 1.2.1-XII for the $[\pm 45]$ family. Poisson ratios for the final layup were established by ratio in accordance with the number of plies of each of the families.

An iterative analysis was again necessary due to the non-linearity of the stress-strain curve.

For the honeycomb panels, all of the load was assumed carried by the skins and divided equally between them. Reasonable care was taken when analyzing splice details to insure equal strain across the joint for each skin. Axial loads carried by the splice plates were conservatively ignored.

The first step in the iterative process was to select a layup of the $[0, \pm 45_y, 90_z]$ family for trial. This selection was made by establishing the minimum number of plies in each direction required to carry the load in that direction. That is, $[0]$ for the N_x load, $[90]$ for the N_y load, $[\pm 45]$ for the shear load. A trial layup was established by a process of rounding to the next higher whole number and then adding plies, so that each skin could be laid up in a nearly symmetrical, balanced pattern.

The shear carried by the $[0]$ and $[90]$ plies was again assumed negligible and shear strain was established as discussed previously. The strains, ϵ_x' or ϵ_y' , produced by the N_x or N_y load, were estimated, stresses were established from figures 14-11 and 14-12. Loads calculated separately for each of the $[0]$, $[90]$ and $[\pm 45]$ families were summed. Strains were then re-estimated and the process repeated until the resultant load was equal to the design load.

Then

$$\epsilon_x = \epsilon_x' - \mu_{yx} \epsilon_y' \quad (14-5)$$

and

$$\epsilon_y = \epsilon_y' - \mu_{xy} \epsilon_x' \quad (14-6)$$

These strains were below the 6000 μ in/in limitation. The diagonal strain was then checked by

$$\epsilon_{\text{dia}}^t = .5 (\epsilon_x + \epsilon_y + \gamma) \quad (14-7)$$

If it exceeded 6000 μ in/in, plies were added and the process repeated until an adequate panel was established.

The adequacy of the panel was also verified by the modified Hill-von-Mises failure criteria:

$$\left(\frac{\sigma_1}{F_1}\right) + \left(\frac{\sigma_2}{F_2}\right) + \left(\frac{\sigma_1 - \sigma_2}{F_{1-2}}\right) - \left(\frac{\sigma_1 \sigma_2}{F_1 F_2}\right) \leq 1 \quad (14-8)$$

Analysis of the skins on the stiffened panels was conducted in the same general manner. However, the complexity increased because the N_x load was shared by the stiffeners and strain compatibility between the skin and stiffener had to be established at the assumed load distribution.

Lower surface wing down bending loads were assumed as 40% of the design loads. Panel stability was verified in accordance with the procedures outlined for the wing upper surface.

Graphite/PPQ

It is very probable that a high temperature organic matrix will exist by the 1980-1990 time period. The polyimide and the polyphenylquinoxaline families appear promising. High strength graphite was selected for the evaluation.

Very little information is available on the strength of either graphite/polyimide or graphite/PPQ at elevated temperatures, however, both are quite comparable to graphite/epoxy at room temperature. Allowables at 250° F and 450° F for graphite/PPQ were assumed equal to graphite epoxy allowables at 150° F and 250° F, respectively. The analysis was simplified by making the stress-strain curves linear.

Figure 14-23 shows a limitation of 4700 μ in/in transverse tension on [0]. This is matrix critical. The addition of at least one ply, in the load direction, was considered sufficient to make the composite fiber critical. Strain limitations were judged accordingly as 8600 μ in/in along any fiber.

Analyses were conducted with the same procedures outlined for the Borsic/Aluminum with high shear allowables.

WING UPPER SURFACE

The critical design condition for the wing upper surface at control panel 269, is combined biaxial compression and shear at 250° F. as shown in table 14-1.

Three structural concepts defined below were analyzed.

<u>Concept</u>	<u>Material</u>
Skin-Stringer	BSC/Aluminum (low shear)
Stiffened Honeycomb	BSC/Aluminum (low shear) BSC/Aluminum (high shear)
Honeycomb	BSC/Aluminum (low shear) Graphite/PPQ

Stress failure mechanisms assumed for the various materials were the same as outlined for the wing lower surface except for the changes in magnitudes due to temperature. See figures 14-15 through 14-18 for the Borsic/Aluminum and figures 14-23 through 14-31 for graphite/PPQ.

Negative bending loads were again assumed as 40% of the critical design loads. Chordwise (N_y) loads were of a small enough magnitude that the [90] plies could be eliminated from the skin layups. The [± 45] plies, required for shear strength and stability, provided more than sufficient chordwise strength.

Borsic/Aluminum with Low Shear Allowable

The sheet-stiffener and the stiffened honeycomb designs have titanium stiffeners reinforced with unidirectional Borsic/Aluminum. Crippling of these bimaterial elements was calculated by converting the cross section to equivalent titanium.

A generalized equation was established from crippling data of magnesium, aluminum, titanium and steel.

$$F_{cc} = 636 \times 10^{-15} E^{2.5} \left(\frac{b}{glt} \right)^{-0.88} \quad (14-9)$$

The above equation produces close agreement with all of the data. By holding all values of this equation constant, except E and t , it can be readily shown that

$$t_2 = t_1 \left(\frac{E_1}{E_2} \right)^{2.84} \quad (14-10)$$

The transverse modulus for the Borsic/Aluminum is used as the E value in this expression. The Borsic/Aluminum of each element was converted to titanium and added to the existing titanium. Crippling of the equivalent titanium cross-section was established either from titanium crippling curves or the generalized equation. The minimum F_{cc} of all of the elements in the cross-section was used as the crippling stress of the column. The limiting strain $\epsilon_l = F_{ccmin}/E$, where F_{cc} and E are titanium properties. If the ϵ_l is not in the linear range of the stress-strain curve for titanium, the process must be repeated using the secant E . The Borsic/Aluminum [0] layup is linear to failure.

Skins were analyzed using MIL Handbook 23A for the honeycomb and stiffened honeycomb configurations and using the following expression for the skin-stringer concept.

$$\bar{F}_{x_{cr}} = \frac{F_{x_{cr}}}{2} \left(\frac{F_{xy_{cr}}}{F_{x_{cr}}} \times \frac{F_x}{F_{xy}} \right)^2 \left[-1 + \sqrt{1 + 4 \left[\left(\frac{F_{x_{cr}}}{F_{xy_{cr}}} \right) \left(\frac{F_{xy}}{F_x} \right) \right]^2} \right] \quad (14-11)$$

where

F_x = applied compressive stress in x direction

F_y = applied compressive stress in y direction

F_{xy} = applied shear stress

$F_{x_{cr}}$ = allowable biaxial compressive buckling stress

$F_{xy_{cr}}$ = allowable shear buckling stress

$F_{x_{cr}}$ = allowable compressive buckling stress under the combined applied stresses

where

t = plate thickness

a = plate length

b = plate width

where

$$\theta = \frac{\sqrt{D_{11} D_{22}}}{D_{12} + 2D_{66}} < 1 \quad (14-12)$$

$$D_{11} = \frac{E_x t^3}{12 (1 - \mu_{xy} \mu_{yx})} \quad (14-13)$$

$$D_{22} = \frac{E_y t^3}{12 (1 - \mu_{xy} \mu_{yx})} \quad (14-14)$$

$$D_{12} = \frac{E_x \mu_{xy} t^3}{12 (1 - \mu_{xy} \mu_{yx})} \quad (14-15)$$

$$D_{66} = \frac{G_{xy} t^3}{12} \quad (14-16)$$

$$F_{xcr} = \frac{\pi^2}{tb^2} \left[\frac{D_{11} m^4 \left(\frac{b}{a}\right)^4 + 2(D_{12} + D_{66}) m^2 n^2 \left(\frac{b}{a}\right)^2 + D_{22} n^4}{m^2 \left(\frac{b}{a}\right)^2 + \left(\frac{F_y}{F_x}\right) n^2} \right]_{\min} \quad (14-17)$$

where

m = number of half sine waves in x direction

n = number of half sine waves in y direction

Buckling equation to be minimized with respect to m, n, = 3, 1, ----

The moduli were established by iteration from the stress strain curves. The strains were first estimated; the secant modulus was then determined for each family at that strain and ratioed by the number of plies of each family. The process was repeated until the estimated strain was equal to actual strain. The shear modulus of [0°] and [90°] plies was assumed as zero.

Borsic/Aluminum with High Shear Allowable

The only structural concept analyzed with these material allowables was the stiffened honeycomb. As with all stiffened concepts, the N_x load was shared between the skins and the stiffeners. This load distribution was again established by iteration because of the non-linear strain. As previously stated, the skins were sized in accordance with MIL Handbook 23 procedures. Skin buckling interaction was verified using figure 14-36.

Graphite/PPQ

The only graphite/PPQ structural concept analyzed was the honeycomb concept. Analysis methods have already been discussed.

BODY

The critical design condition for the body, at control point 5, occurs at the end of supersonic cruise when temperatures are at maximum, see table 14-1. The critical reverse bending condition occurs at sea level and room temperature, consequently, it does not contribute to the design.

Additional body design requirements are identical to those outlined in section 4.

Circumferential [90] plies are used to carry the ultimate design pressure. Although primary shear is not identifiable at the centerline of the lower crown, it does increase in magnitude as the panel extends circumferentially. Secondary shear will exist due to

differences in strain between skin frames or skin and stringers. For the above reasons, [± 45] plies are used. In addition, they provide improvements in "fail safety."

Borsic/Aluminum with Low Shear Allowable

Stiffeners were analyzed for crippling as explained for the wing upper surface. The honeycomb and the stiffened honeycomb configurations were not allowed to buckle.

The skin-stringer configuration was not allowed to buckle at the 1.1 x steady state cruise condition but the skin was permitted to buckle in compression at higher loads. There is some degree of risk in allowing the skin to buckle because of the brittle nature of the borsic fibers. The deformations are presumed to be small enough in this case to preclude fiber damage, however, testing may eventually be required to verify this assumption.

The honeycomb skin panels were analyzed per MIL Handbook 23. The skin of the skin-stringer configuration was shown stable at the cruise condition by the same procedure used in section 4, except that a pseudo-isotropic modulus was used. The values of E_x and E_y were reasonably close, so an $E_{equiv} = \sqrt{E_x E_y}$ was used.

Borsic/Aluminum with High Shear Allowable

Primary shear does not exist at the control point. For this reason, body concepts with the high shear strength Bsc/Al were not analyzed. The design would be the same as the low shear strength Bsc/Aluminum.

Graphite/PPQ

The only structural concept analyzed with graphite/PPQ was the honeycomb concept. Analysis methods have already been discussed.

WEIGHT ANALYSIS

The weights of the advanced structural concepts were calculated from the designated coupons from the body and wing panel drawings. While the weights are comparative for the selected control points, they should not be extrapolated to represent a total change in body or wing weights. Such items as window and door cutouts, bulkhead interface, tension, compression and shear panels, would have a different effect on the weight of the various body structural concepts. Similarly, door cutouts, rib interface and dispersion of leading and trailing edge concentrated loads would effect the wing panel weights differently from one wing structural concept to another. An example of this is shown by the 26.7% weight reduction for Borsic/Aluminum on the wing upper surface compression panel while only 8.4% reduction was realized on the lower surface tension panel.

BODY

The results of detail weight calculations of the body advanced structural concepts are shown in figure 14-32 and table 14-2.

The relative weight details show a significant reduction in the stringer and splice weights for the Borsic/Aluminum sheet stiffener and the stiffened thin sandwich structural concept compared to the baseline titanium sheet stiffener panel. The slightly heavier skin, core and braze weight on the full depth honeycomb panel is more than offset by its lack of stringers and lighter frame weight for comparable Borsic/Aluminum construction.

The full depth honeycomb with graphite/PPQ skin shows an additional weight reduction over the Borsic/Aluminum for a total of 43% reduction from the base skin and stiffener titanium panel.

WING UPPER SURFACE

Figure 14-33 and table 14-3 show the weight comparisons of the wing upper surface advanced structural concepts.

The full depth honeycomb construction with Borsic/Aluminum skin shows a 26.7% weight reduction from the titanium skin baseline upper surface wing panel. The graphite/PPQ skinned H/C panel is significantly lighter with a 43.9% reduction from the base panel.

None of the stiffened wing panels are as light as the advanced honeycomb panels except the Borsic/Aluminum thin honeycomb with reinforced titanium stiffeners evaluated with high shear allowables. This panel is 31.6% lighter than the baseline panel.

WING LOWER SURFACE

The wing lower surface weight calculations for the advanced structural concepts are shown in figure 14-34 and table 14-4.

Only three of the advanced structural concepts evaluated for the wing lower surface showed a weight reduction from the original baseline titanium skin and stringer construction. Weight reductions from the base panel were 7.6% for the Borsic/Aluminum skin with reinforced titanium stiffeners and 8.4% for the full depth honeycomb with Borsic/Aluminum skin respectively. Both of these panels were evaluated with high shear allowables.

The full depth honeycomb with graphite/PPQ skin showed a 30.9% weight reduction from the base panel.

MANUFACTURING ANALYSIS

The same manufacturing complexity evaluation approach has been used for the Task II advanced concept as for Task I. The "baseline" construction types for the wing and body used in Task I are retained so that all concepts in both Task I and Task II may be rated on the same scale of comparison. The baseline concepts have arbitrarily been rated at 100 with increasing complexity given an increasing number. For example, a structural

arrangement with a rating of 200 is considered twice as complex as the baseline to fabricate. The evaluation ground rules for advanced concepts were as follows:

- Assume a production program of (200) airplanes,
- Engineering go-ahead for the program is 1980.
- Capital facilities, plant equipment, raw materials, and manufacturing and inspection processes development requirements are excluded from the manufacturing producibility rating.
- The wing panels have gentle compound contours and are assumed to be 30" wide x 360" long.

BODY PANEL PRODUCIBILITY RATINGS-ADVANCED CONCEPTS

The producibility ratings for the body structural concepts are given in table 14-5 with the rivited titanium sheet stiffener baseline rated at 100. It is readily seen that the graphite/PPQ concepts assembled by bonding are considerably simpler to fabricate than Borsic/Aluminum concepts which are assembled by brazing. This is largely due to the less stringent fit-up tolerances, simpler process requirements, and less complex tooling facilities required for bonding as compared to brazing.

It is apparent that Borsic/Aluminum concepts as a group are significantly more complex to fabricate than the current structural arrangements. Not only is extensive manufacturing development required for handling, cleaning, and processing of the material but all of the assemblies investigated utilize some form of brazing in panel assembly. Brazing tends to minimize the quantity of fastener hole penetrations through the composite cover sheets, however, it is an exacting and expensive operation requiring a high degree of accuracy and specialized tooling.

A pattern can be observed to the complexity factors for the Borsic/Aluminum concepts. The sheet stiffener arrangement is rated least complex of the Borsic/Aluminum concepts. This concept allows more potential for sub-assembly and the build up of the structure in small steps rather than completing the entire assembly in a single step. The lower complexity rating for the sheet stiffener concept is dependent upon minimizing spotbrazing distortions.

The brazed honeycomb arrangement using conventional (0/±45/90) Borsic/Aluminum skins and titanium core is of intermediate complexity for the Borsic/Aluminum concepts considered. The consolidated skins are fabricated as a sub-assembly followed by panel brazing. The fit up tolerances and fixturing are more complicated for the honeycomb sandwich panel than the spotbrazed sheet stiffener concepts.

Relatively high manufacturing complexity ratings are given to the stiffened thin honeycomb sandwich configuration. This concept required not only the spotbrazing of the stiffeners to the inner skin, but also the brazing complexities required for the honeycomb sandwich concepts.

In summary, sheet stiffener concepts assembled by spotbrazing tend to be less complex than honeycomb concepts fabricated by brazing. The stiffened thin honeycomb structural arrangement has the complexities of both concepts.

WING PANEL PRODUCIBILITY RATINGS-ADVANCED CONCEPTS

Structural arrangements including sheet stiffener, honeycomb sandwich, and stiffened thin honeycomb were also evaluated for wing skin panels. The complexity ratings of these concepts are in the same relative order as for the comparable body arrangements. The actual quantitative values as seen in table 14-6 are different, however, because the structural baselines for comparison taken from the 969-336C for wing and body were different.

The alternate brazed honeycomb skin panel configuration utilizing the multicycle uniaxial truss in lieu of $\pm 45^\circ$ plies is rated considerably more complex to fabricate than the other concepts. New procedures would be required for the curved tape lay up required for the truss nodes. Extensive coordination is necessary to assure core fit up to match the shear truss located inside the panel assembly. These factors coupled with the complex edge consolidation of the truss nodes and titanium edge laminates all contribute to the high complexity factor of 700.

MATERIAL COSTS

A cost analysis was made to determine the impact on material costs of various processes used in the manufacture and fabrication of the structural concepts. The results of this analysis are shown in table 14-7. It is clear that the material costs/lb of the Borsic/Aluminum structural concepts are much greater than those constructed of titanium (see Section 4, Volume I). The lower material costs of the sheet stiffener and stiffened honeycomb concepts as compared to the honeycomb configuration is due to the fact that the stiffened designs contain greater quantities of titanium. The titanium material costs less and weighs more than Borsic/Aluminum, thereby reducing the material cost/lb.

The selection of the structural concepts for the 969-512B was influenced mainly by weight saving and manufacturing complexity with minimal consideration to material cost/lb. A more in-depth review of material cost would be necessary to justify a weight savings potential on final airplane design.

STRUCTURAL CONCEPT EVALUATION AND SELECTION

As a result of the Task II Study, some structural skin panel concepts have been selected and recommendations for future development were established. The concepts were selected using a screening process starting with selection of promising candidates, thence to concept design, evaluation and final recommendation.

CANDIDATE SELECTION

The initial screening of the structural concepts considered the following:

- A structural concept was not considered if it had a major defect preventing it from being competitive in all major requirements.
- Candidate structural types were selected based on previous SST evaluation experience of similar construction.

CONCEPT DESIGN

The design of structural concepts was conducted using the geometry and design conditions at wing control point 269 and body control point 5. The concepts were not explicitly designed for fatigue and failsafe requirements. The allowables (designated low shear allowables) used in the design were taken from the "Air Force Design Guide." Representative configurations at point 269 were redesigned using updated NASA-Langley allowables (designated high shear allowables) for comparative purposes.

The control point locations and structural concepts designed are shown in table 14-8.

CONCEPT EVALUATION

The evaluation of the structural concepts used a rating system which measures the characteristics of weight, manufacturing complexity, stiffness and material cost. No additional design work or studies were conducted on the characteristics of failsafety, fatigue, maintenance, repair and thermal conductivity, consequently, these items were not used in concept evaluation. As seen in tables 14-9 through 14-11, a rating factor (N) was selected for each characteristic from a range of 0 to 100 based on the concepts merit relative to a baseline which was arbitrarily given 50. Numbers greater than 50 indicate characteristics more desirable than the baseline.

Construction types were screened through several levels of evaluation. Each level of evaluation considered a different characteristic starting with the most important and continuing in a descending order of importance. From the initial screening level, the best candidates were evaluated through enough levels to establish a superior candidate. The symbols are for those concepts selected to carry through another level of evaluation until a superior candidate is established and noted by

STRUCTURAL RECOMMENDATIONS

The structural recommendations shown in table 14-12 are for the points 269 and 5 only and cannot be extrapolated to other areas of the wing and body. An analysis, using the loading conditions at various locations on the 969-512B, must be accomplished to determine overall wing and body structural recommendations.

REFERENCE

- 14-1 "Advanced Composite Design Guide," Los Angeles Division of North American Rockwell Corporation, Contract No. F 33615-71-6-1362, November 1971.

Table 14-1.—Control Point Loads

Body: control point 5 (lower body skin panel)

Design condition	
N_x	(11.92 kips/in.)
Pressure	(10.78 lb/in ²)
Temperature	(450° F)

Wing: control point 269

Component	Design condition	
Upper panel	N_x	-10.9 kips/in.
	N_y	- 1.48 kips/in.
	N_{xy}	6.32 kips/in.
	Temperature	250° F
Lower panel	N_x	11.82 kips/in.
	N_y	2.04 kips/in.
	N_{xy}	6.89 kips/in.
	Temperature	Room temperature

Table 14-2.—Weight Tabulation—Advanced Structural Concepts—Body

Concept	Figure no.	Skin, psf	Padups, psf	Stringers, and splices, psf	Clips, psf	Core, psf	Braze, psf	Frame, psf	Total, psf
Skin Stiffener	2-7	1.152	0.232	2.872	0.063	—	—	1.080	5.399
Bsc/Al Skin, Re- inforced Stiffener	14-2	0.691	0.136	2.523	0.093	—	0.036	0.861	4.340
Bsc/Al Sandwich, Ti Stiffener	14-4	0.988	0.359	1.816	0.063	0.104	0.219	0.737	4.286
Bsc/Al Sandwich	14-6	1.383	0.238	^a 0.405	0.063	0.681	0.348	0.491	3.609
Gr/PPQ Sandwich	14-9	1.258	0.056	^a 0.268	0.063	0.564	^b 0.380	0.491	3.080

^aSplices only

^bAdhesive bonding

Table 14.3.—Weight: Tabulation—Advanced Structural Concepts—Wing Upper Surface

Concept	Figure no.	Skin, psf	Padups, psf	Stiffeners/ reinforcement, psf	Clips, psf	Core, psf	Braze, psf	Support formers, psf	Total, psf
Al Brazed Ti	2-10 (baseline)	4.009	0.128	—	—	0.643	0.141	—	4.921
Bsc Sandwich	14-7	2.741	0.097	—	—	0.519	0.248	—	3.605
Gr/PPQ Sandwich	14-1U	1.496	0.237	—	—	0.652	^b 0.377	—	2.762
Bsc/Al Skin, Re- inforced Ti Stiff- ener	14-3	2.448	—	1.314	0.246	—	0.020	0.261	4.289
Bsc/Al Sandwich, Ti Stiffener	{ 14-5 14-5	2.350 1.762	0.290 0.290	0.571 0.571	0.163 0.163	0.143 0.143	0.176 0.176	0.261 0.261	3.954 ^a 3.366

^aHigh shear allowable^bAdhesive bonding

Table 14-4.—Weight Tabulation—Advanced Structural Concepts—Wing Lower Surface

Concept	Figure no.	Skin, psf	Padups, psf	Stiffeners/ reinforcement, psf	Clips, psf	Core, psf	Braze, psf	Support formers, psf	Total, psf
Internally Machined and Welded	2-13	2.881	—	0.597	—	—	—	0.261	3.739
B _{sc} /Al Akin, Re- inforced Ti Stiff- ener	{ 14-3	2.839	—	0.957	0.163	—	0.017	0.261	4.237
B _{sc} /Al Sandwich, Ti Stiffener	{ 14-3	2.056	—	0.957	0.163	—	0.017	0.261	^a 3.454
	14-5	2.937	0.290	0.571	0.163	0.056	0.124	0.261	4.402
	{ 14-7	3.328	0.097	—	—	0.384	0.202	—	4.011
BSC/AL Sandwich	{ 14-7	2.741	0.097	—	—	0.384	0.202	—	^a 3.424
	14-8	1.175	0.895	^c 1.094	—	0.457	0.381	—	4.002
Gr/PPQ Sandwich	14-10	1.579	0.245	—	—	0.381	^b 0.377	—	2.582

^aHigh shear allowable

^bAdhesive bonding

^cSkin reinforcement

Table 14-5.—Manufacturing Producibility Rating, Body Skin

Body skin arrangement	Rating
Riveted Ti sheet stiffener	100 ^a
Bonded H/C panel with PPQ/graphite skins	200
Consolidated Borsic-Al skins with spotbrazed Ti stiffeners	360
Brazed H/C panel with Borsic-Al skins and Ti core	400
Brazed H/C panel with Borsic-Al skins and Ti stiffeners	450

^aBaseline

Table 14-6.—Manufacturing Producibility Rating, Wing

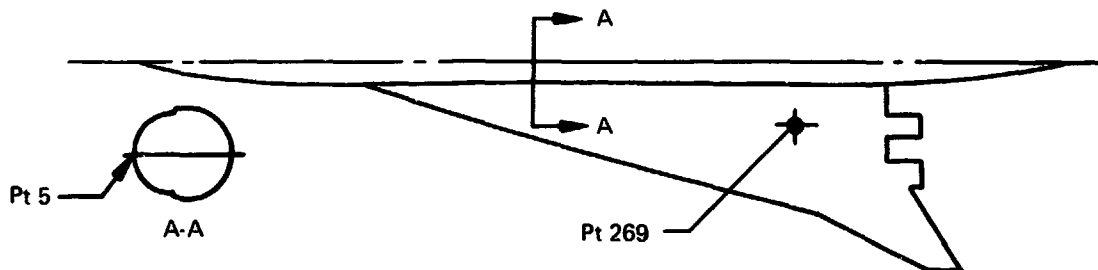
Wing structural arrangement	Rating
Spotwelded Ti corrugated core	100 ^a
Bonded H/C panel with PPQ/graphite skins	125
Borsic-Al skins with spotbrazed Ti stiffeners	300
Brazed H/C panel with Borsic-Al skins	350
Brazed H/C panel with Borsic-Al skins and Ti stiffeners	440
Brazed H/C panel with Borsic-Al skins, truss reinforced	700

^aBaseline for wing

Table 14-7.—Cost Analysis of Structural Concepts





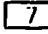


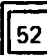
Location	Structural configuration	Cost, dollar/lb
Body panel, point 5	Sheet stiffener	364.00
	Stiffened H/C	341.00
	Full depth H/C	755.00
Wing panel, point 269	Sheet stiffener	587.00
	Stiffened H/C	693.00
	Full depth H/C	721.00



Table 14-8.—Location and Description of Structural Concepts



Component	Location	Concept
Wing skin panels	Pt 269 upr and lwr	Sheet stiffener Borsic-Al skin, uniaxial borsic reinforced Ti stiffeners (low shear allowable)
	Pt 269 lwr	Sheet stiffener Borsic-Al skin, uniaxial borsic reinforced Ti stiffeners (high shear allowable)
	Pt 269 upr and lwr	Stiffened thin H/C Borsic-Al skins, Ti core, uniaxial borsic reinforced Ti stiffeners (low shear allowable)
	Pt 269 upr	Stiffened thin H/C Borsic-Al skins, Ti core, uniaxial borsic reinforced Ti stiffeners (high shear allowable)
	Pt 269 upr and lwr	H/C (unstiffened) Borsic-Al skins, Ti core (low shear allowable)
	Pt 269 lwr	H/C (unstiffened) Borsic-Al skins, Ti core (high shear allowable)
	Pt 269 lwr	H/C (unstiffened) Borsic-Al truss skins, Ti core (low shear allowable)
Body skin panels	Pt 5	Sheet stiffener Borsic-Al skin, uniaxial borsic reinforced Ti stiffeners (low shear allowable)
	Pt 5	Stiffened thin H/C Borsic-Al skins, Ti core, uniaxial borsic reinforced Ti stiffeners (low shear allowable)
	Pt 5	H/C (unstiffened) Borsic-Al skins, Ti core (low shear allowable)

Table 14-9.—Structural Concept Selection—Wing Panels Upper Surface, Point 269

Item	Rating range	Baseline (braze Ti H/C)	Sheet stiffener	Stiffened H/C	H/C
	N 	N	N	N	N
Weight	0 to 100	50	63	 70	 77
Mfg complexity		50		 7	 19
Stiffness		50		52	 52
Material cost	0 to 100	50			

 Low shear allowable
 Rating factor:



 Carry-through to another level
 A superior candidate is established

Table 14-10.—Structural Concept Selection—Wing Panels Lower Surface, Point 269






Item	Rating range	Baseline (Ti integrally machined and welded sheet stiffener)	Sheet stiffener		Stiffened H/C		H/C		H/C (truss skin)	
			1	2	1	2	1	2	1	2
Weight	N 3	N	N	N	N	N	N	N	N	N
Mfg complexity										
Stiffness	0 to 100	50	37	58	33	52	42	59	42	42
Material cost										
		50		25		8		19		
		50		55						

1 Low: shear allowable
 2 High shear allowable
 3 Rating facto.
 4 Estimated from 1 values

□ Carry-through to another level

□ A superior candidate is established

Table 14-11.—Structural Concept Selection—Body Panels, Point 5

Item	Rating range	Baseline (Ti sheet stiffener)	Sheet stiffener	Stiffened H/C	H/C
	N 	N	N	N	N
Weight	0 to 100	50	62	 65	 81
Mfg complexity		50		21	 26
Material cost	0 to 100	50			

 Low shear allowable

 Rating factor

 Carry-through to another level

 A superior candidate is established

Table 14-12.—Structural Concept Recommendations

Component	Location	969-512B structural recommendation	Figure no.
Wing upr surface (at Pt 269)	See figure 14-1	Composite H/C	14-7
Wing lwr surface (at Pt 269)		Composite sheet stiffener	14-3
Body shell (at Pt 5)		Composite H/C	14-6

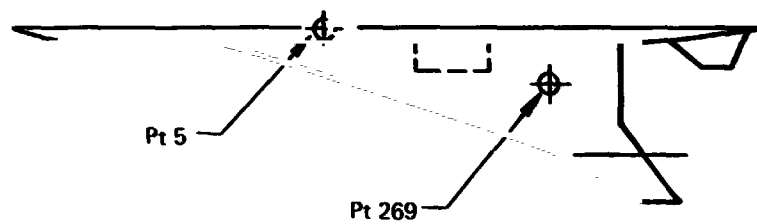
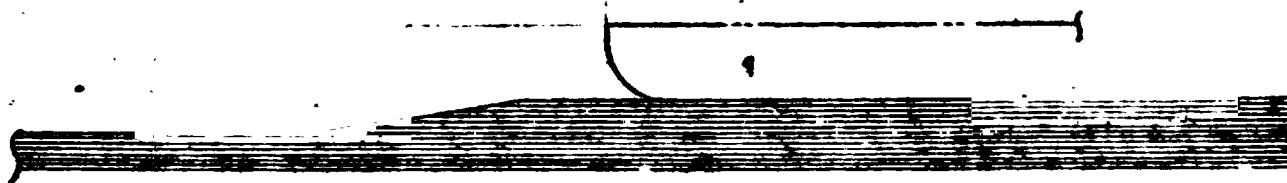
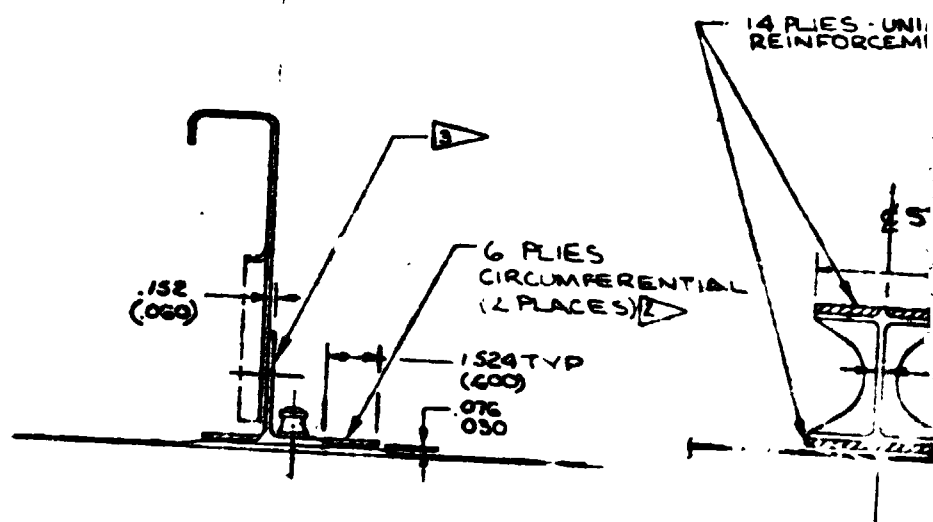


Figure 14-1.—Wing and Body Control Points



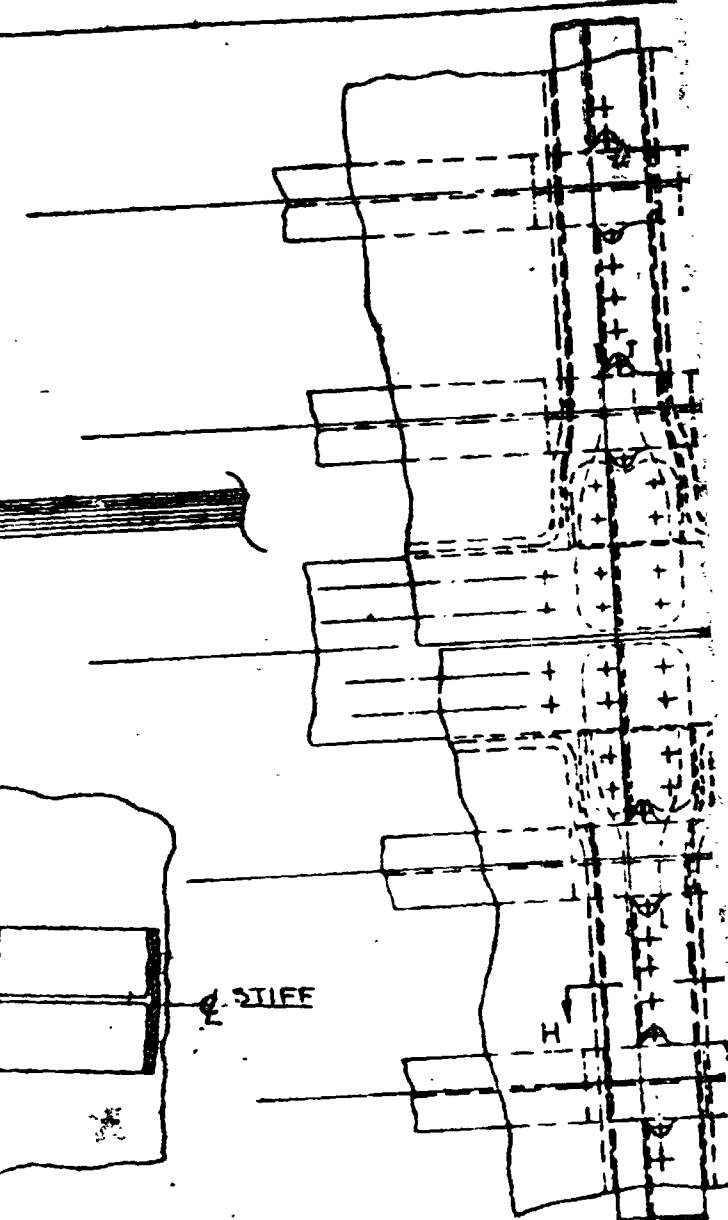
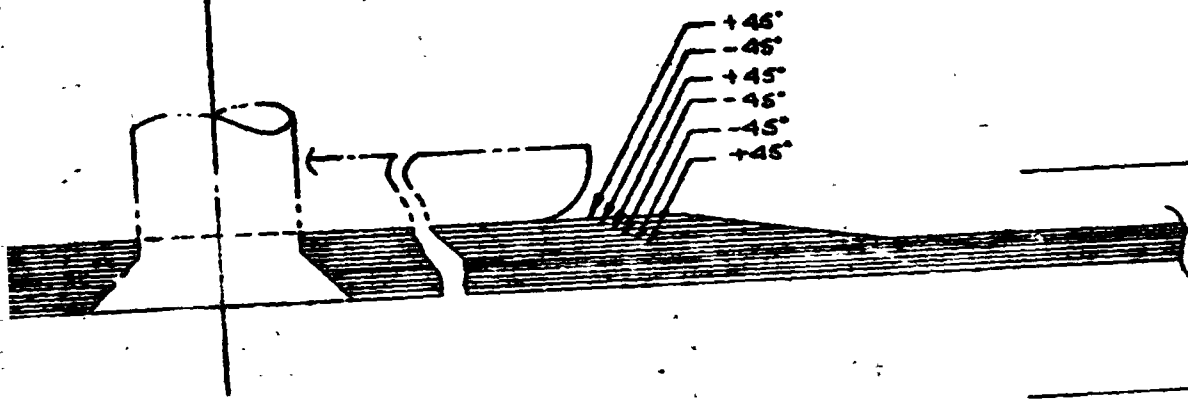
H-H
10/1
(SKIN DETAIL SH)



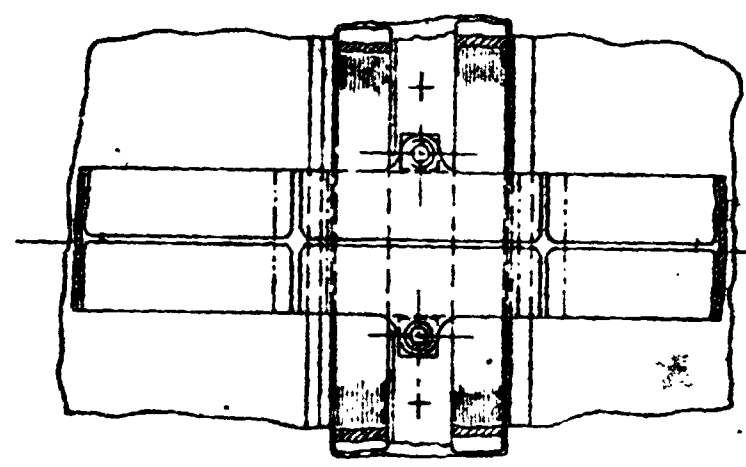
E-E
SCALE 1/1

F-F
SCALE

FOLDOUT FRAME



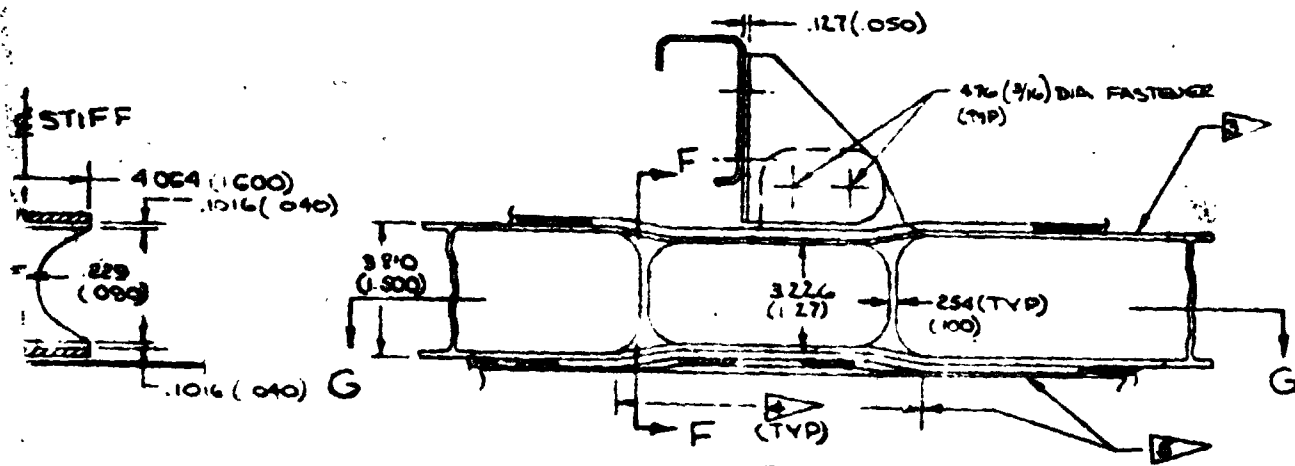
SHOWN ONLY)



STIFF

UNIAXIAL ELEMENT (2 PLACES)

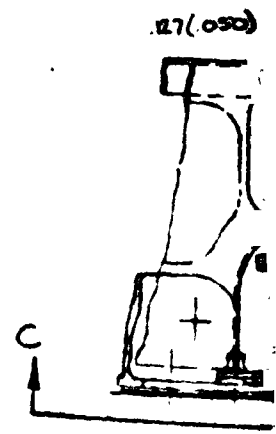
G-G
SCALE 1/1

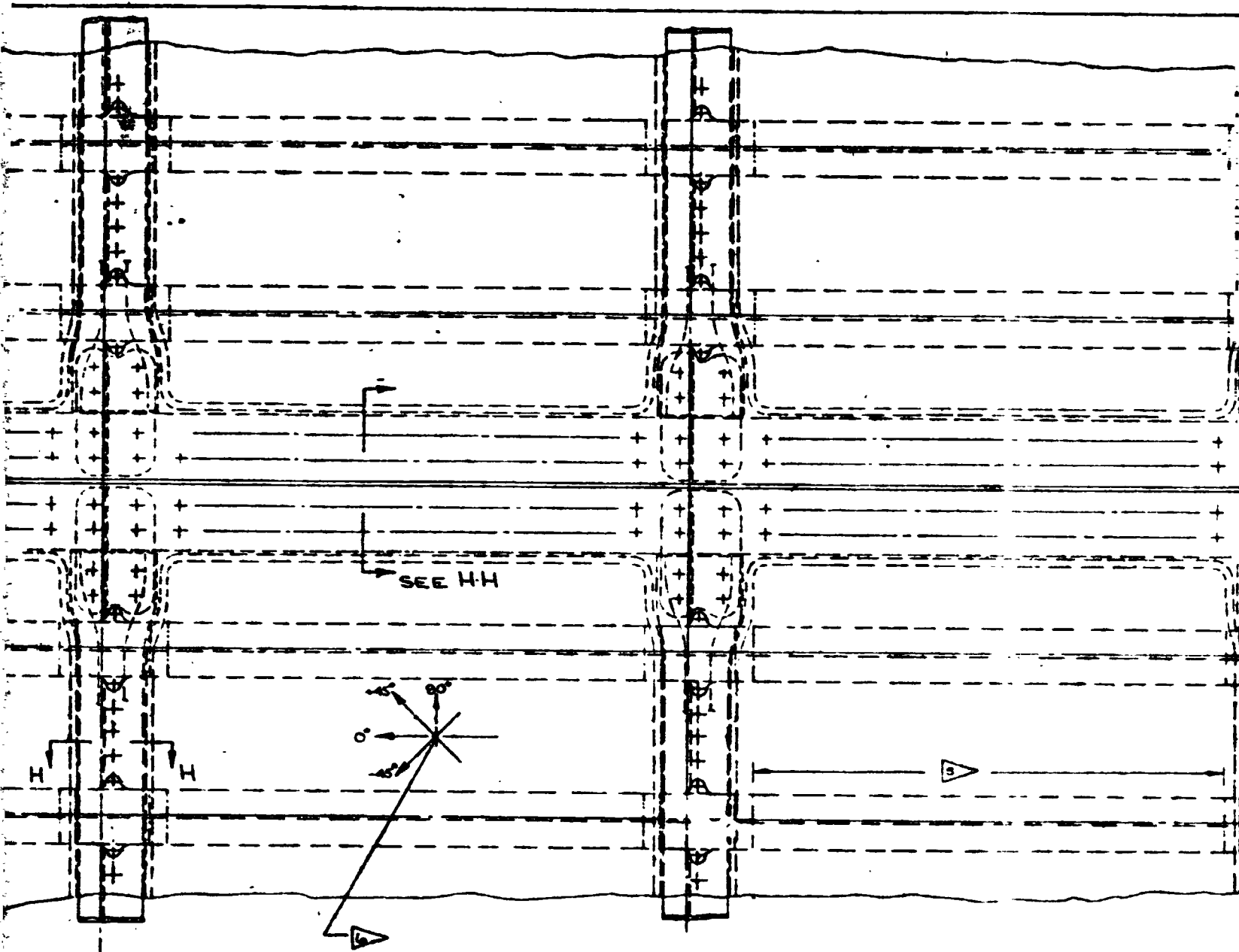


F
E 1/1

D-D
SCALE 1/1
FOLDOUT FRAME

REPRODUCIBILITY OF THE
ORIGINAL PAGE IS POOR



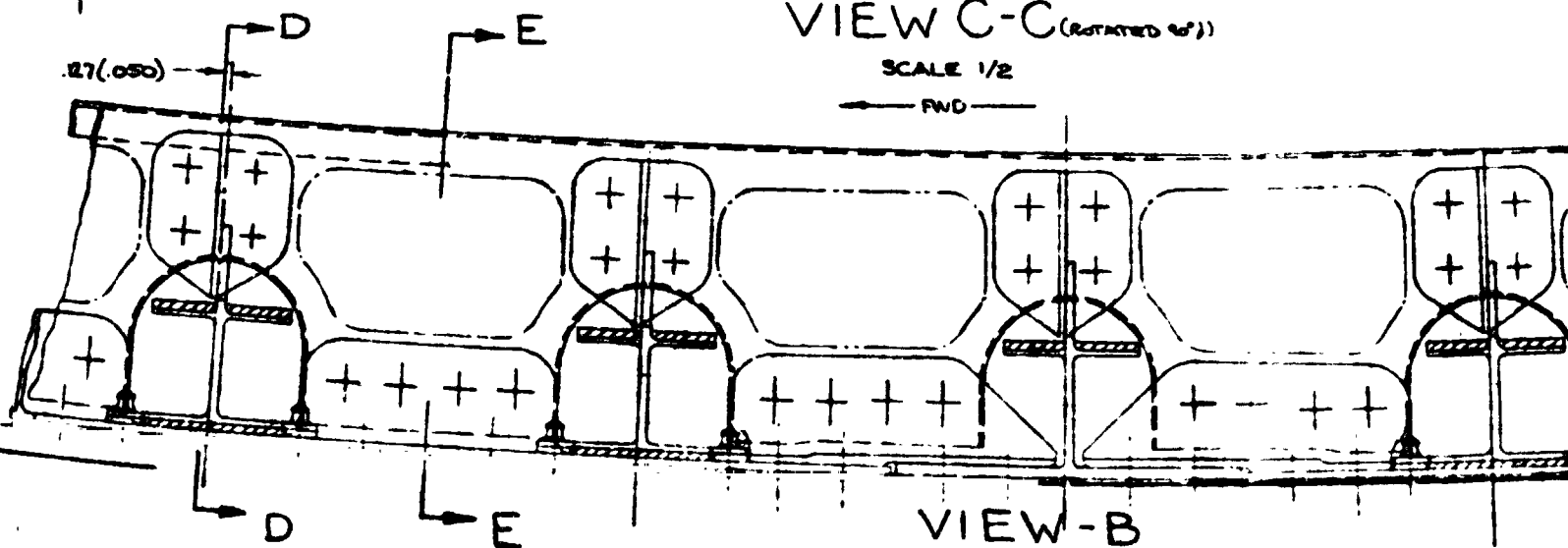


SEE H-H

VIEW C-C (ROTATED 90°)

SCALE 1/2

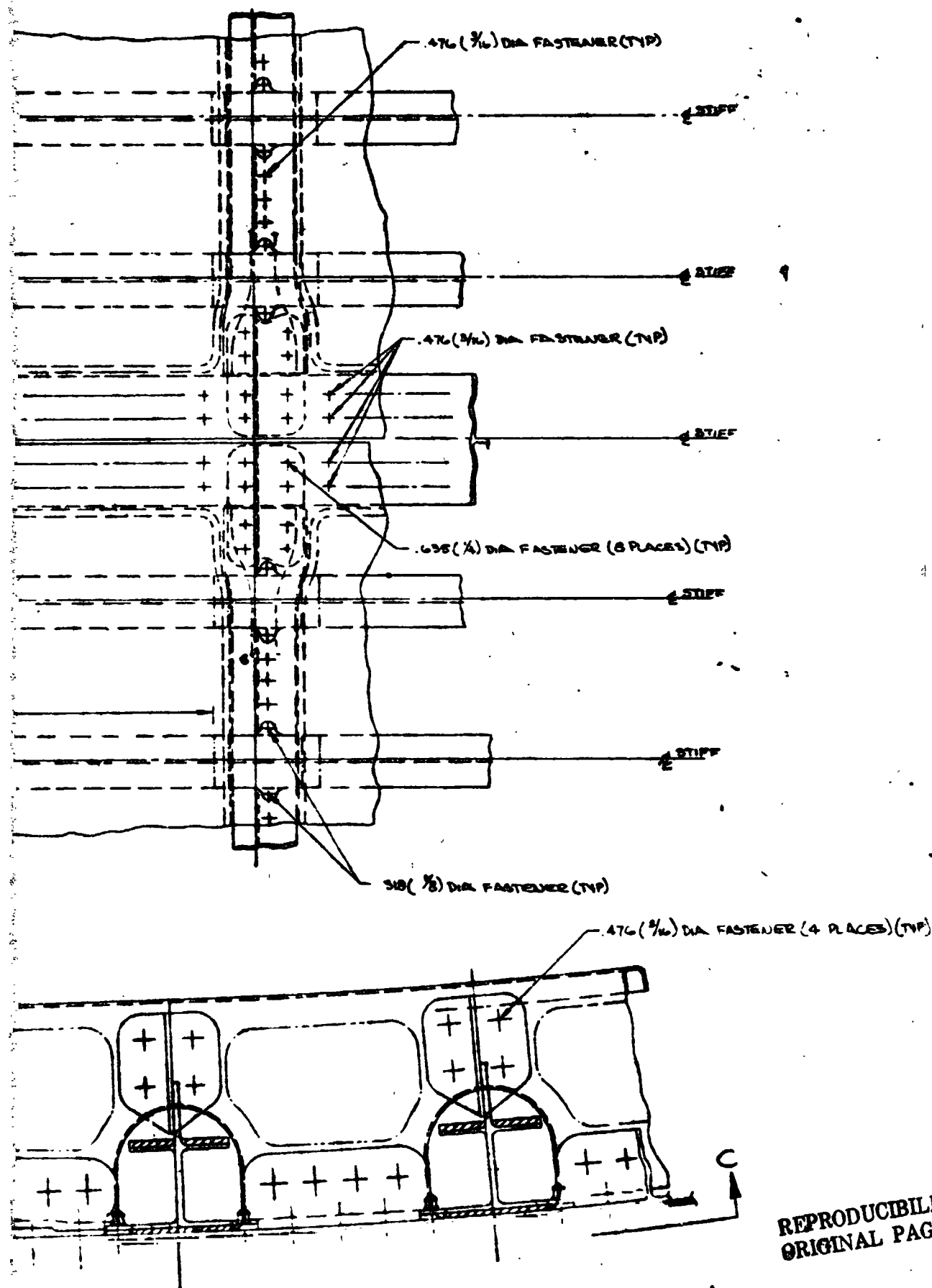
→ FWD →



VIEW-B

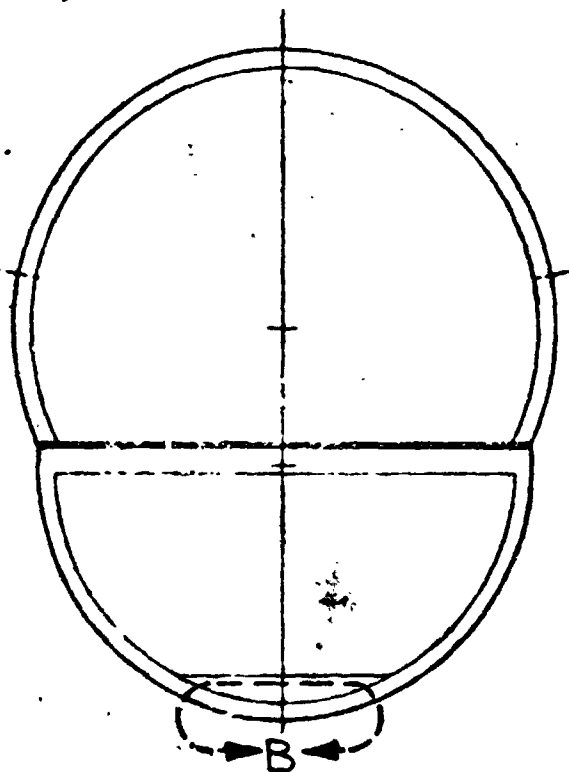
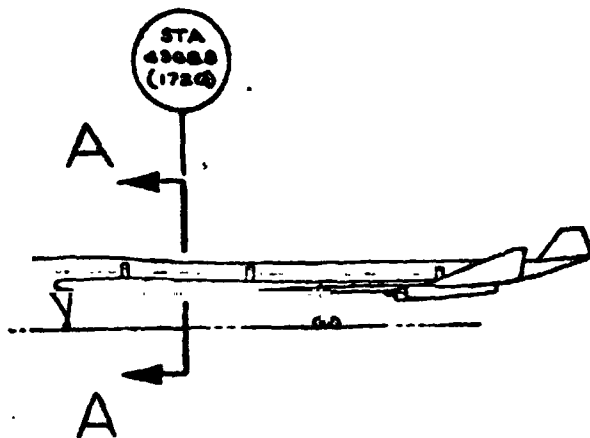
SCALE 1/1

FOLDOUT FRAME



REPRODUCIBILITY OF THE
ORIGINAL PAGE IS POOR

FOLDOUT FRAME 4



SECTION A-A

SCALE: 1/30

6 BORSIC ALUMINUM
SKIN - 7 PLIES:
(1) + 45°
PAD: 6 PLIES:
(3) + 45°

5 SPOT BRAZE S
(SPOTWELD SP)

4 DO NOT SPOT
IN THIS AREA

3 MACHINED TIT
CAL-4V PER

2 BORSIC ALUMINI
6 PLIES - 007 IN.

1 BORSIC ALUMI
14 PLIES PER

BASIC DIMENSION
() DIMENSIONS

REPRODUCIBILITY OF THE
ORIGINAL PAGE IS POOR

OF THE
POOR

FOLDOUT FRAME

USED ON
SHEET NO
CHG NO
GROUP ORG

- ▷ BORSIC ALUMINUM SKIN ASSY CONSOLIDATION
SKIN 7 PLYS - .007 IN./PLY MATERIAL (2) 0° PLYS,
(1) +45° PLY, (1) -45° PLY, (3) 0° PLYS
PAD. 6 PLYS - .007 IN./PLY MATERIAL
(3) +45° PLYS, (3) -45° PLYS
- ▷ SPOT BRAZE STIFFENERS TO FACE SHEET.
(SPOTWELD SPEC AND BRAZE TIME & TEMP CYCLE UNDEFINED)
- ▷ DO NOT SPOT BRAZE STIFFENER TO SKIN ASSY
IN THIS AREA.
- ▷ MACHINED TITANIUM EXTRUSION
6AL-4V PER BMS 7-44 CLASS B
- ▷ BORSIC ALUMINUM REINFORCEMENT CIRCUMFERENTIAL
6 PLYS - .007 IN./PLY MATL PER LOCATION
- ▷ BORSIC ALUMINUM UNIAXIAL REINFORCEMENT [0]
14 PLYS PER LOCATION .007 IN./PLY MATERIAL

FOLDOUT FRAME 6

BASIC DIMENSIONS - CENTIMETERS
() DIMENSIONS - INCHES

REPRODUCIBILITY OF THIS
ORIGINAL PAGE IS POOR


Figure 14-2.-

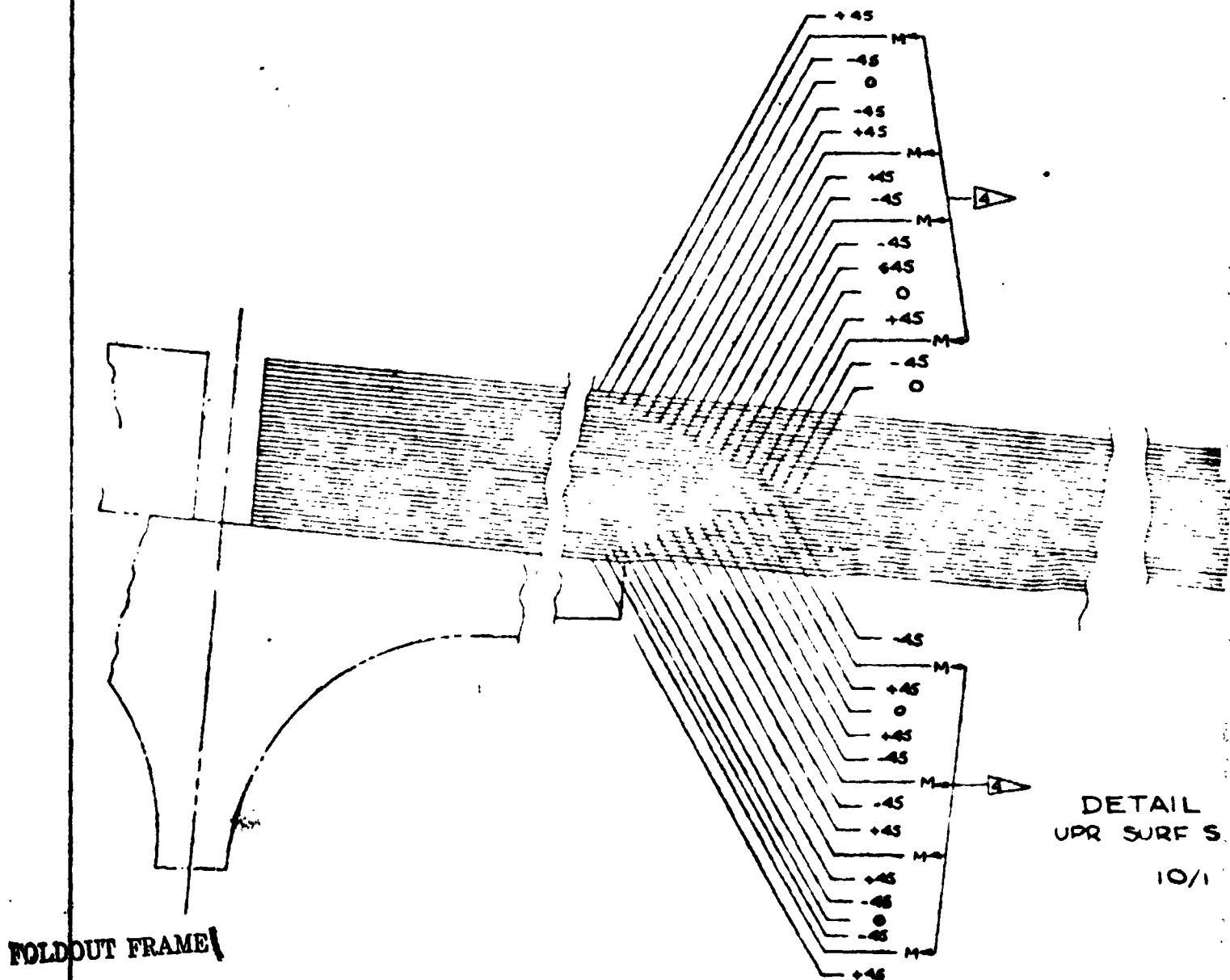
FOLDOUT FRAME 5

USED ON	DRAWN BY E. E. ROBINSON NO. 2-25-74	THE BORSIC COMPANY COMMERCIAL	UNCLASSIFIED EXCLUDED FROM AUTOMATIC DOWNGRADING AND DECLASSIFICATION
	CHECKED		
	STRESS		
SHEET NO	ENGR. E. E. ROBINSON U.S. AIR FORCE	2-25-74	
CHG NO	GROUP		
GROUP ORG	PROJ.		
		BORSIC/A BODY SKIN & REINFORCED TI STIFF 969-3360 27 CRUISE	
		JAWS-140	
		SCALE NOTED	

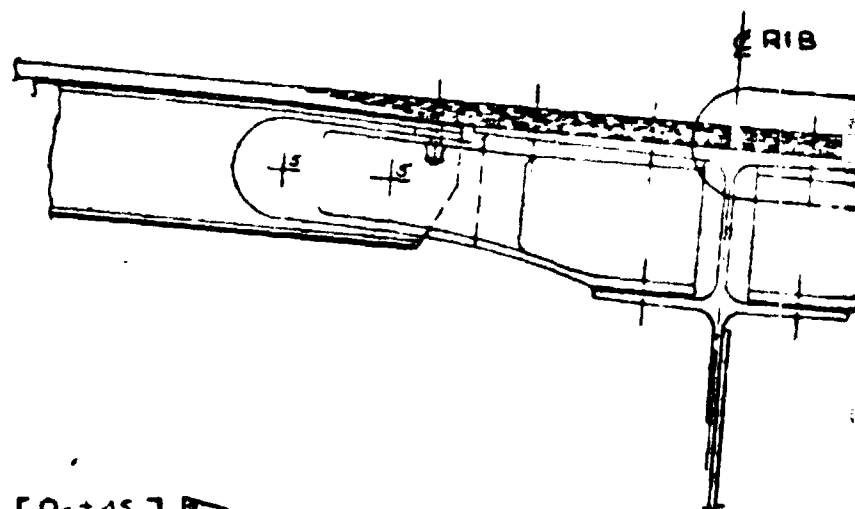
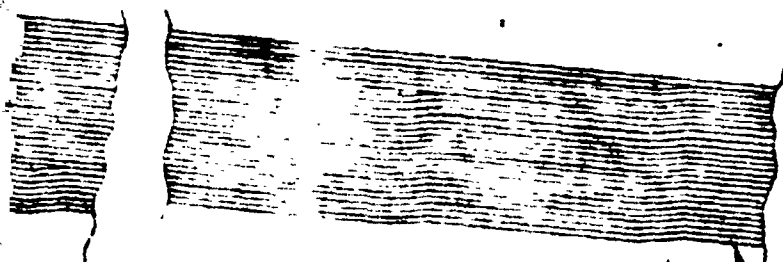
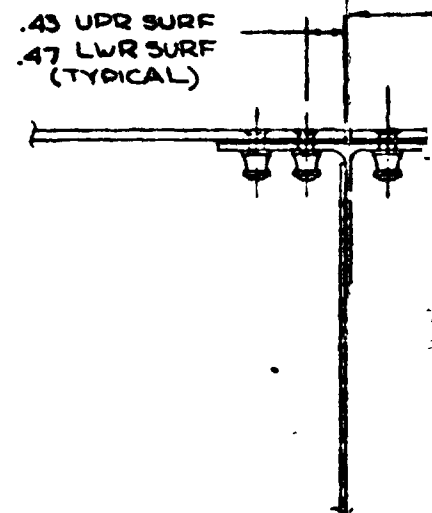
PRESENDING PAGE BLANK NOT FILE

AWA 041-2WA

	DIN			
	G	H	J	K
UPR SURF	3.81 (1.50)	.142 (.056)	.102 (.040)	.160 (.063)
LWR SURF 	3.81 (1.50)	.071 (.028)	.102 (.040)	.160 (.063)



DIMENSION					
J	K	L	M	N	
.102 (.040)	.160 (.063)	4.06 (1.60)	12.19 (4.80)	13.97 (5.50)	
102 (.040)	160 (.063)	4.06 (1.60)	17.02 (6.70)	18.92 (7.45)	



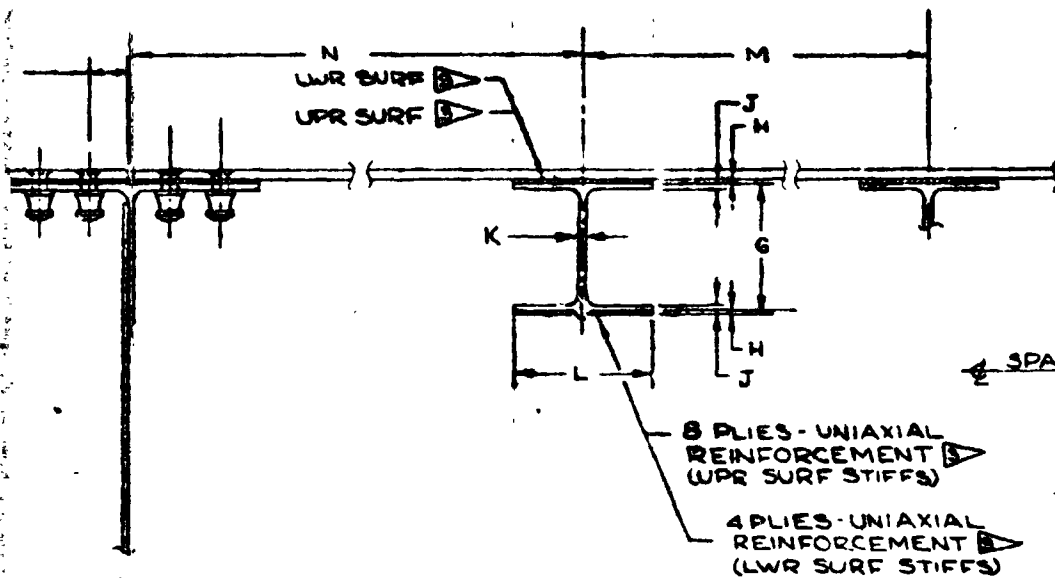
[0.5 ± 45°] ▸

DETAIL D
UPR SURF SHOWN

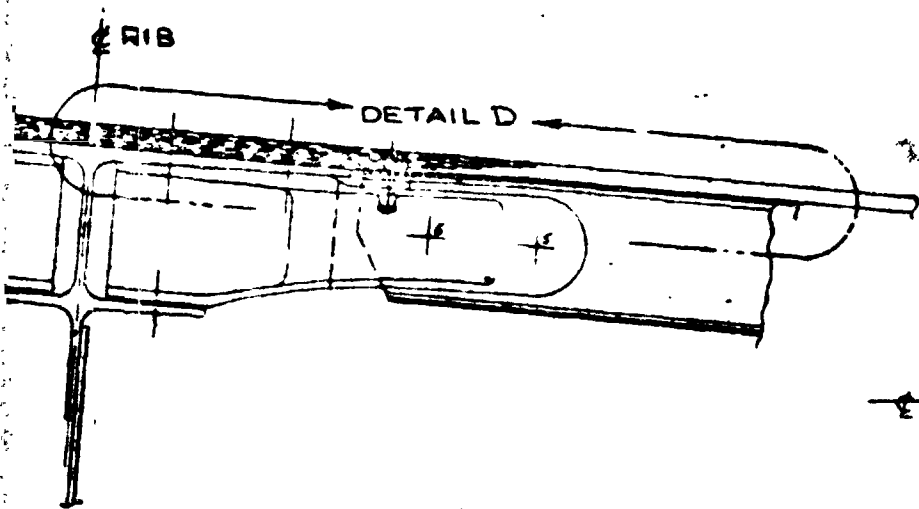
10/1

A-A
FULL SCALE

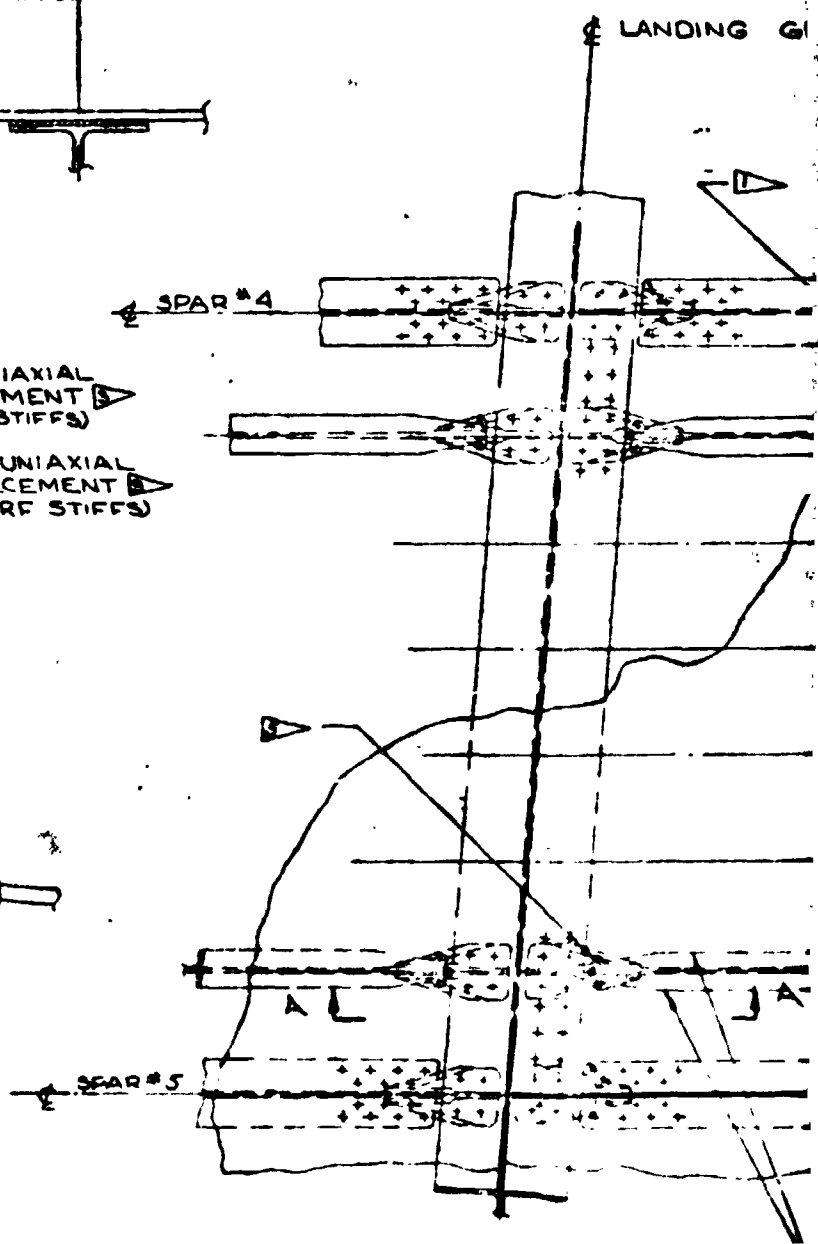
FOLDOUT FRAME 2

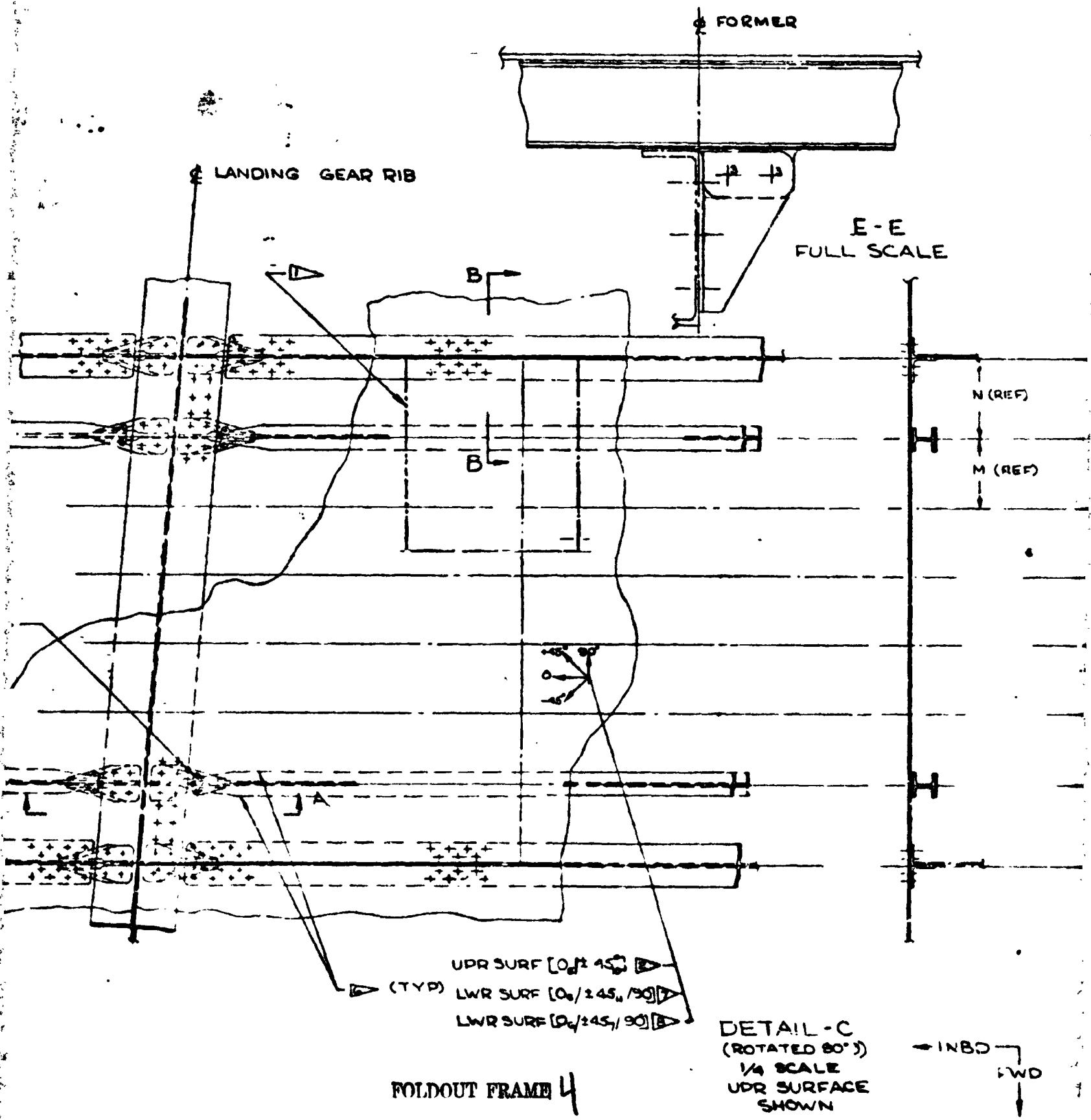


B-B
(ROTATED 90°)
FULL SCALE



A
SCALE





FORMER

E-E
FULL SCALE

N (REF)

M (REF)

PT 203
DETAIL-C

E L E

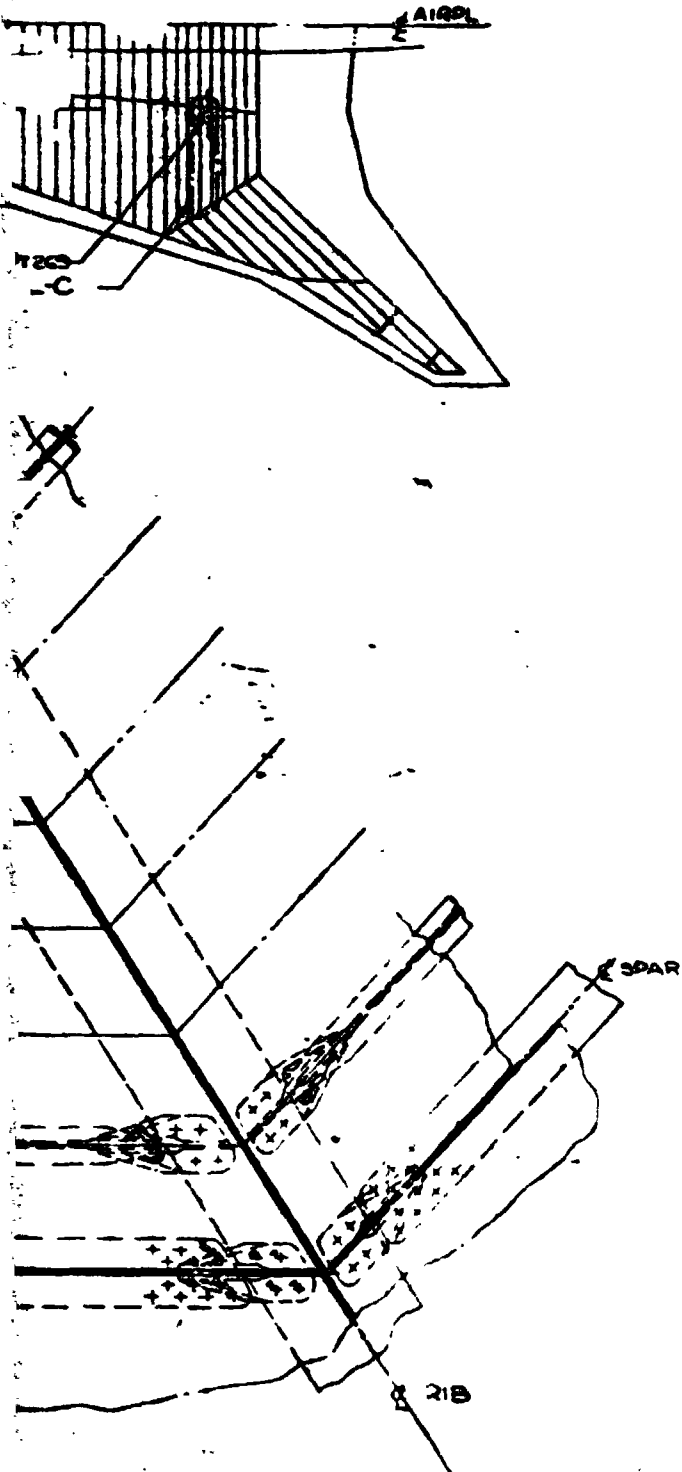
DETAIL-C
(ROTATED 90°)
1/4 SCALE
UPR SURFACE
SHOWN

← INBD
FWD ↓

∠ SUPPORT FORMER - 65.50
(2500) SPACING (TYP)

FOLDOUT FRAME

CHG	DESCRIPTION	DATE	APPRO
A	REVISED DWG TO ADD LWR WING SURFACE DESIGNS ADDED THEN	6/6/79	DEW JAW STW



- ▶ B₃/AL - UNIAXIAL REINFORCEMENT (4) - 0° PLIES PER LOCATION. .007 IN./PLY MATL - LWR SURFACE STIFFS (TYP)
- ▶ PER A.F. DESIGN GUIDE DATA EXCEPT FOR SHEAR PROJECTED FROM NASA-LANGLEY DATA WING UPR SURFACE B₃/AL SKIN ASSY CONSOLIDATED OF 21 PLIES OF .007 IN./PLY MATL (6) - 0° PLIES, (7) + 45° PLIES, (7) - 45° PLIES, (1) 90° PLY. SEE DETAIL D FOR REINFORCEMENT DETAIL.
- ▶ PER A.F. DESIGN GUIDE DATA. WING LOWER SURFACE B₃/AL SKIN ASSEMBLY CONSOLIDATED OF 29 PLIES OF .007 IN./PLY MATERIAL (6) - 0° PLIES, (11) + 45° PLIES (11) - 45° PLIES, (1) 90° PLY. SEE DETAIL D FOR REINFORCEMENT DETAIL.
- ▶ SPOTBRAZE STIFFENERS TO FACE SHEET (SPOT WELD SPEC AND BRAZE TIME & CYCLE UNDETERMINED)
- ▶ .032 IN DIA H. LOC FASTENERS TO PREVENT BRAZE PEELING
- ▶ .007 IN THICK TITANIUM SHIM - GAL-4V. 8 REQD UPR & LWR SURF (TYPICAL)
- ▶ BORSIC ALUMINUM - UNIAXIAL REINFORCEMENT (8) - 0° PLIES PER LOCATION .007 IN./PLY MATERIAL - UPR SURFACE STIFFS (TYP)
- ▶ WING UPPER SURFACE BORSIC ALUMINUM SKIN ASSY CONSOLIDATED OF 25 PLIES OF .007 IN./PLY MATERIAL (5) - 0° PLIES, (10) + 45° PLIES, (10) - 45° PLIES SEE DETAIL D FOR END REINFORCEMENT DETAILS
- ▶ JT 265 CONTROL POINT COUPON SIZE AND LOCATION SAME AS FOR TASK I

BASIC DIMENSIONS - CENTIMETERS
() DIMENSIONS - INCHES

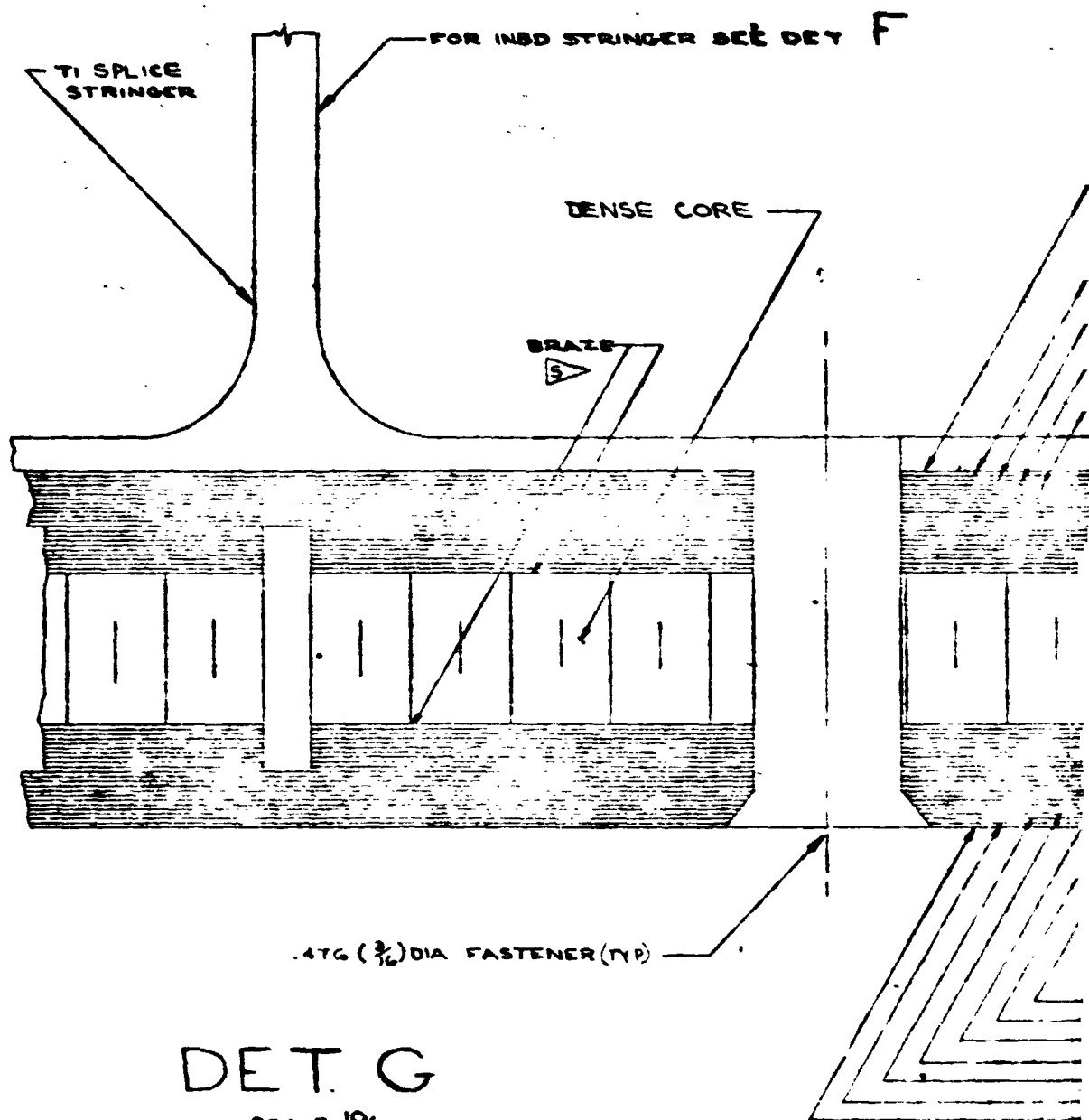
PRECEDING PAGE BLANK NOT FILLED

Figure 14.3 -

USED ON	DRAWN H. T. B. / J. B. W.	DATE 6/6/79	THE BOEING COMPANY COMMERCIAL AIRPLANE DIVISION, RENTON, WASH.	
ECT NO	CHECKED		SHEET STIFF PANEL ASSY BORSIC ALUM SKIN - B ₃ /AL REINFORCED TI STIFFS	
CHG NO	STRESS	6/22/79	CODE IDENT NO JAWS-143	
GROUP ORG	ENGR	6/22/79	SCALE NOTED	
	GROUP			
	PROJ			

FOLDOUT FRAME

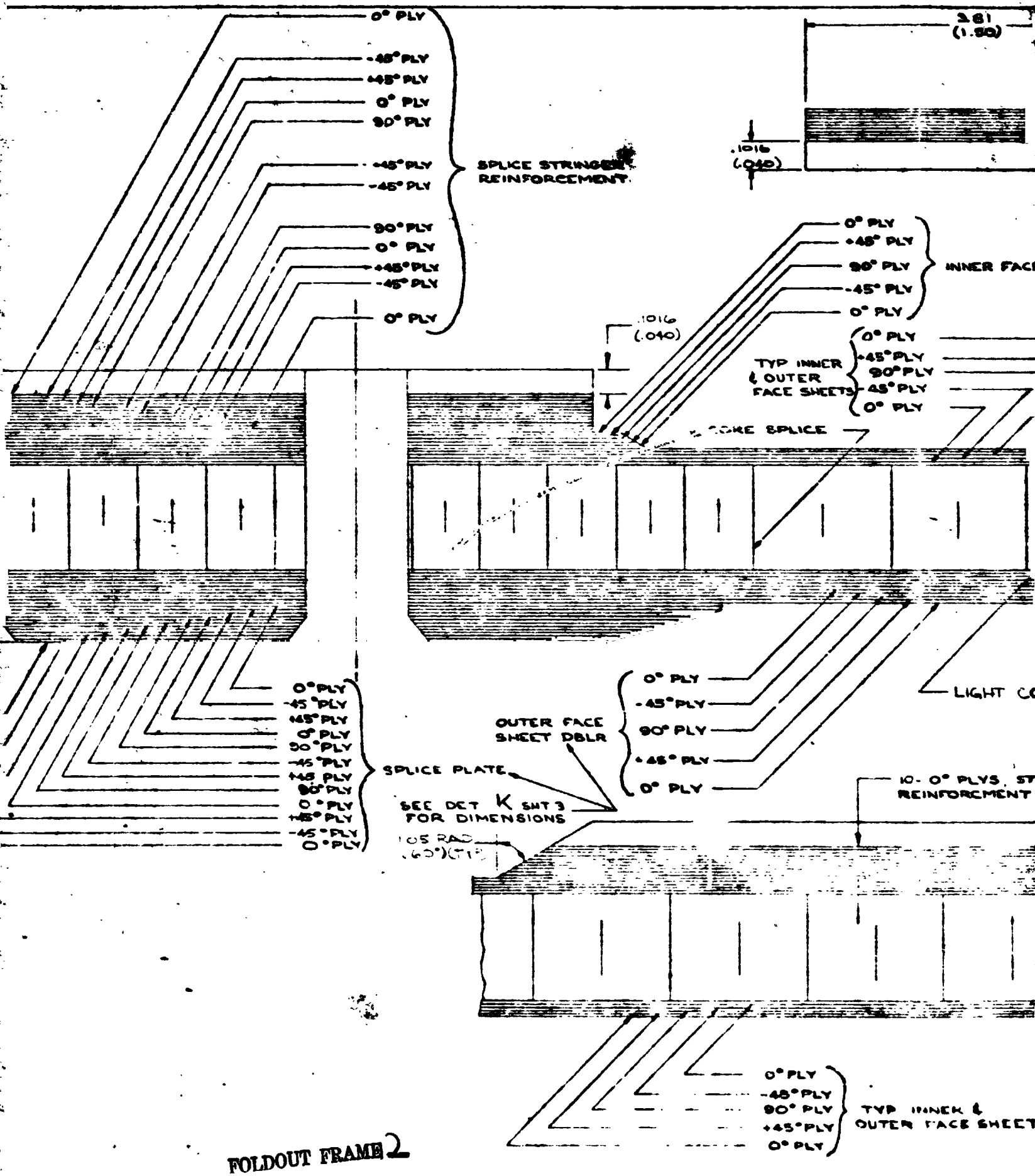
WING BAY 21 STIFF

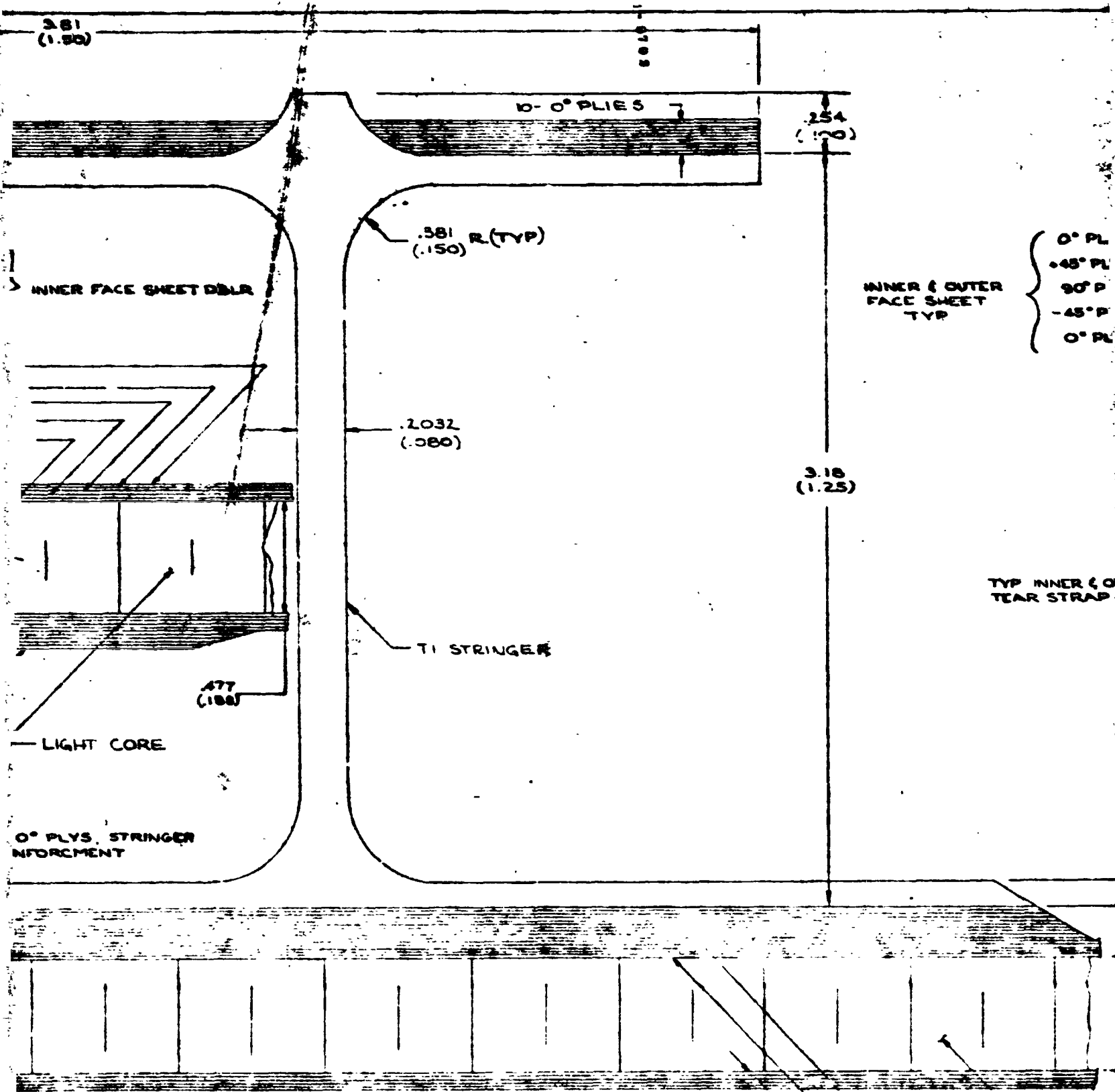


DET. G

SCALE 10X

FOLDOUT FRAME

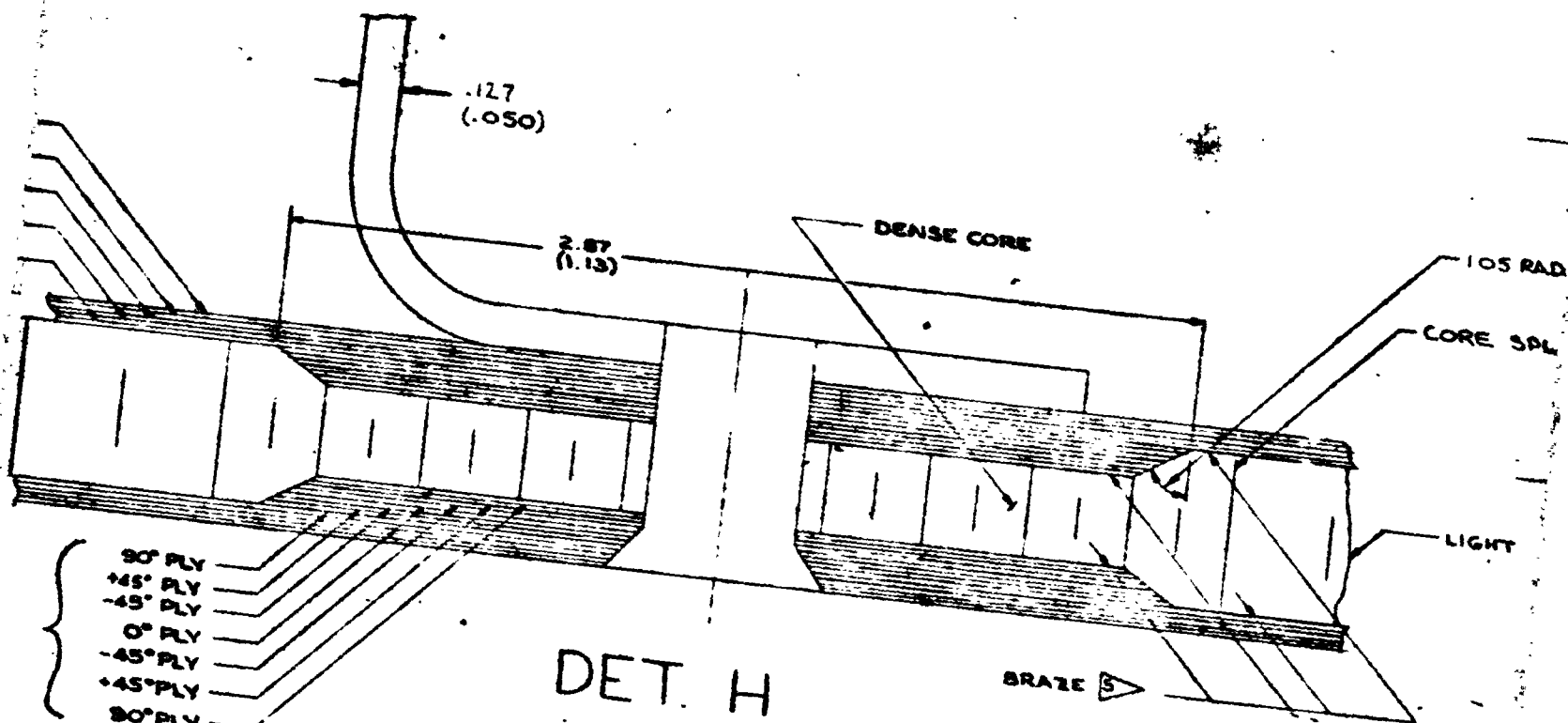




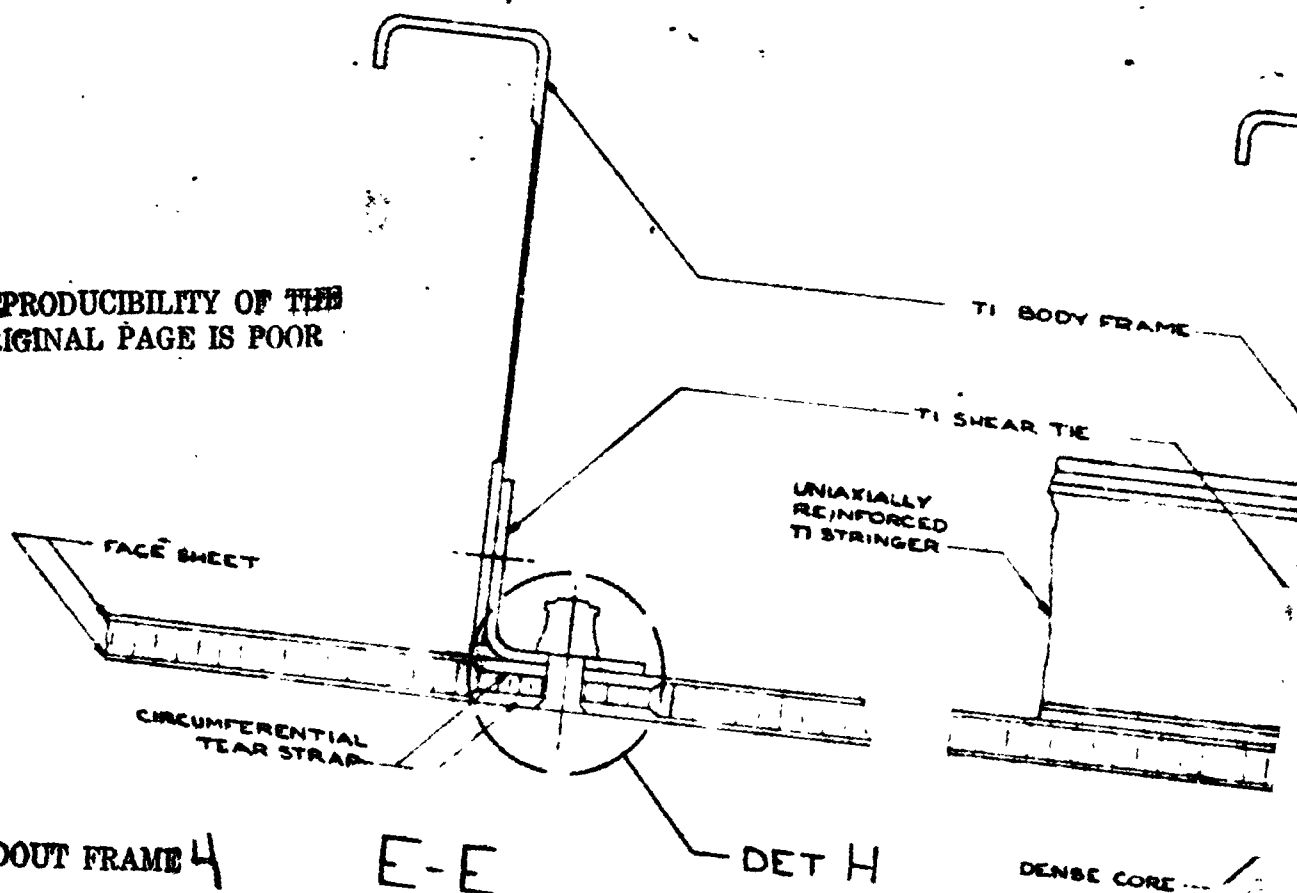
INNER & FACE SHEET

SCALE 1/4"

FOLDOUT FRAME 3



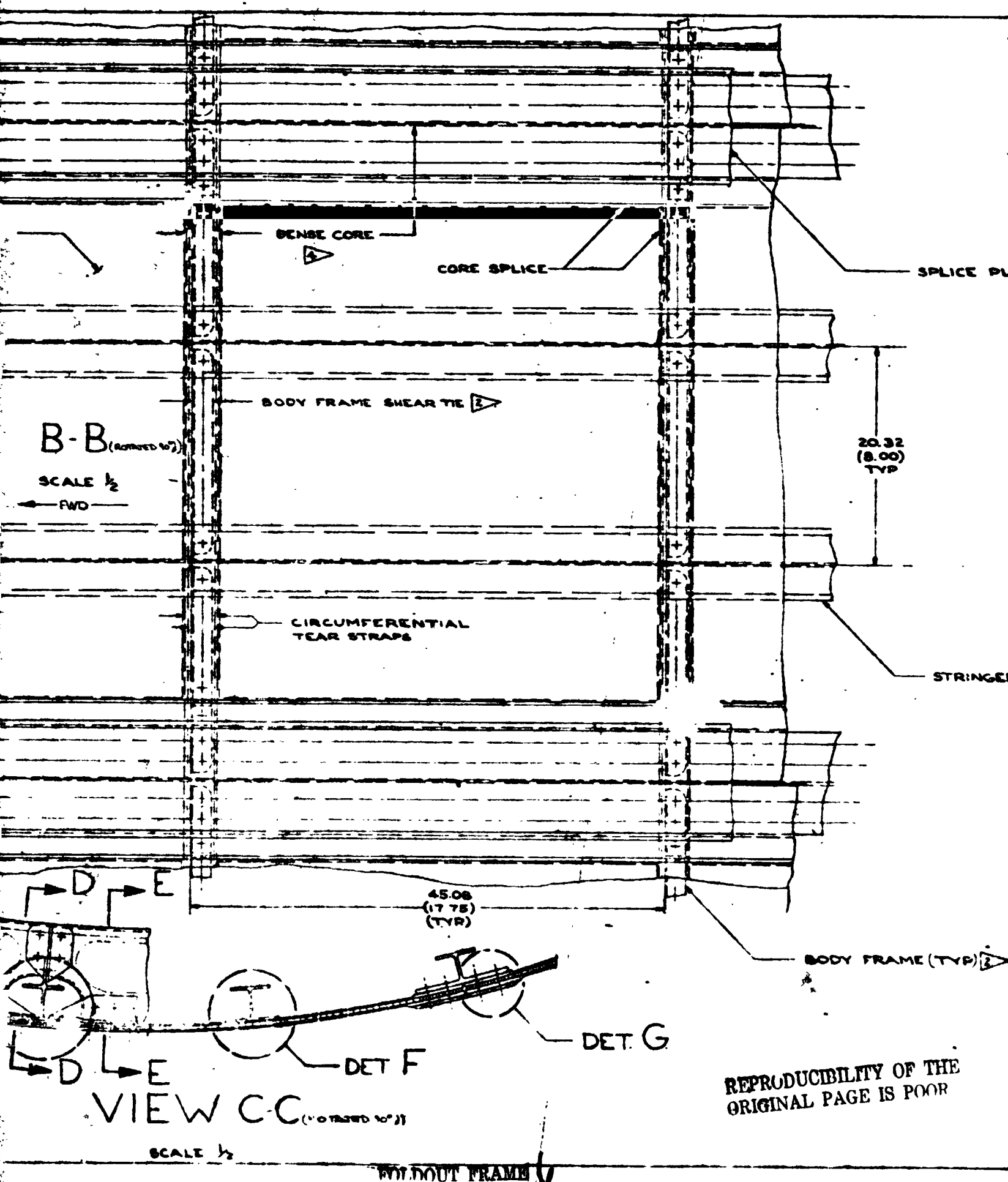
REPRODUCIBILITY OF THE
ORIGINAL PAGE IS POOR



FOLDOUT FRAME 4

E-E

FOLDOUT FRAME

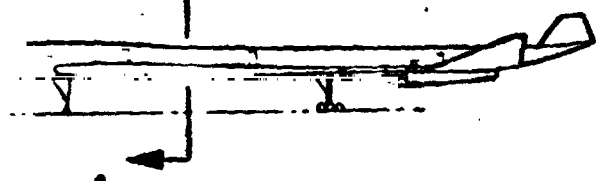


STA
43688
(1720)

A

A

PLATE (TYP)



- △ BASIC
DOT
- A) STI
A
- B) WAVE
TE
- C) OUT
TE
- D) OUT

△ ALUM
(BRA

△ 226 K
TI-

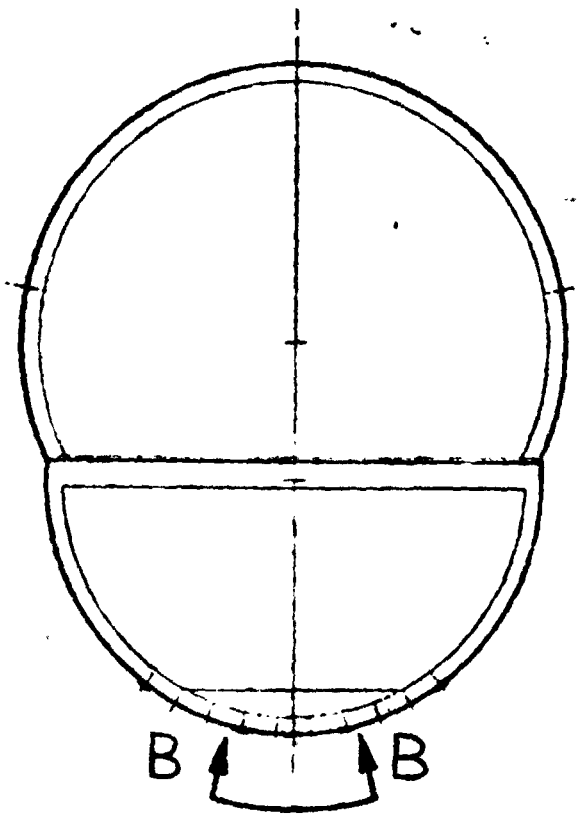
△ 78 K_g
TI-

△ TI-68

△ TI-6

BASIC DIA
() DIA

RINGER (TYP) △



B

B

VIEW A-A

SCALE 1/20

FOLDOUT FRAME 7

PRECEDING PAGE BLANK NOT FILLED

- ③ BASIC PLY ORIENTATION FOR ALL ASSY CONSOLIDATIONS
DOT IN/PLY MATERIAL
 - A) STIFFENER ASSY CONSOLIDATION: TITANIUM STRINGER AND FLANGE REINFORCEMENT
 - B) INNER FACE SHT ASSY CONSOLIDATION: FACE SHEET, TEAR STRAP AND DOUBLER
 - C) OUTER FACE SHT ASSY CONSOLIDATION: FACE SHEET, TEAR STRAP AND DOUBLER
 - D) OUTER SPLICE PLATE CONSOLIDATION
- ③ ALUMINUM BRAZE
(BRAZE TIME & TEMP CYCLE UNDEFINED)
- ③ 226 Kg/M^3 (141 Lb/FT^3) H/C CORE SS2-30
TI-6AL-4V
- ③ 78 Kg/M^3 (49 Lb/FT^3) H/C CORE SC4-20
TI-3AL-2.5V
- ③ TI-6AL-4V COND I
- ③ TI-6AL-4V EXTRUSION PER BMS 7-44 COND I

REPRODUCIBILITY OF THE ORIGINAL PAGE IS POOR

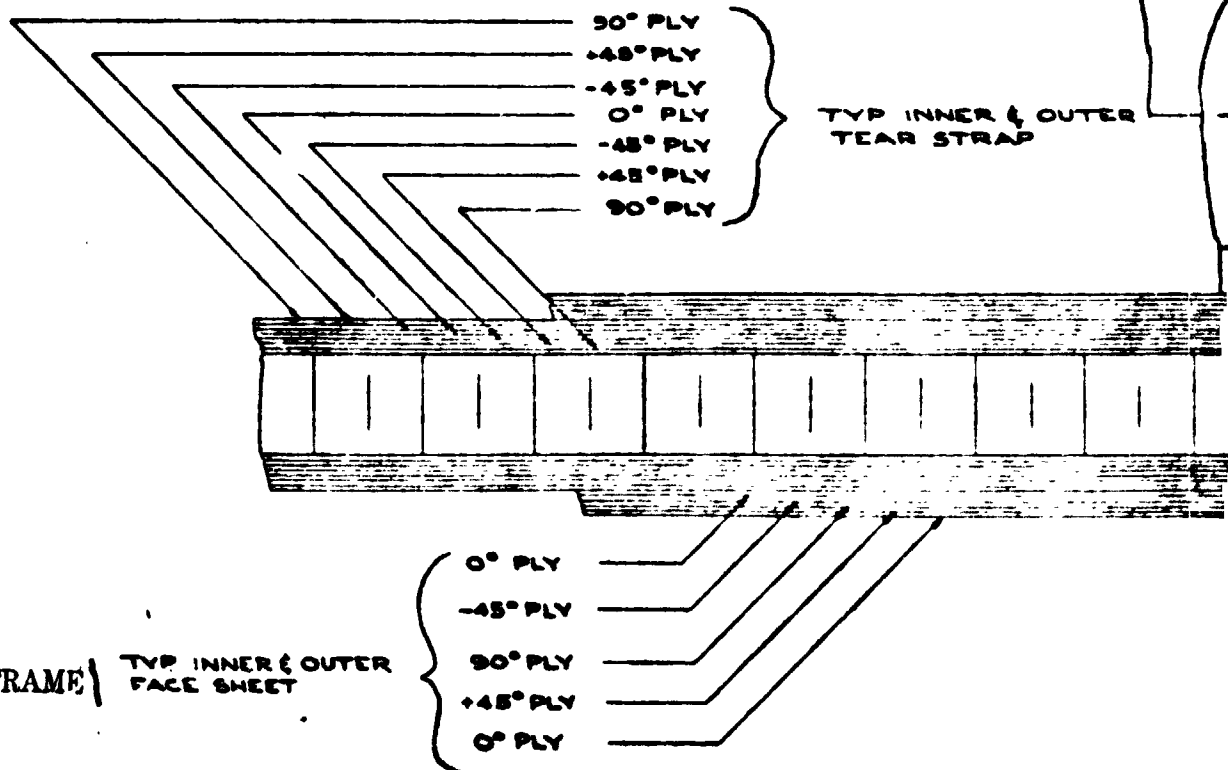
BASIC DIMENSIONS - CENTIMETERS
() DIMENSIONS - INCHES

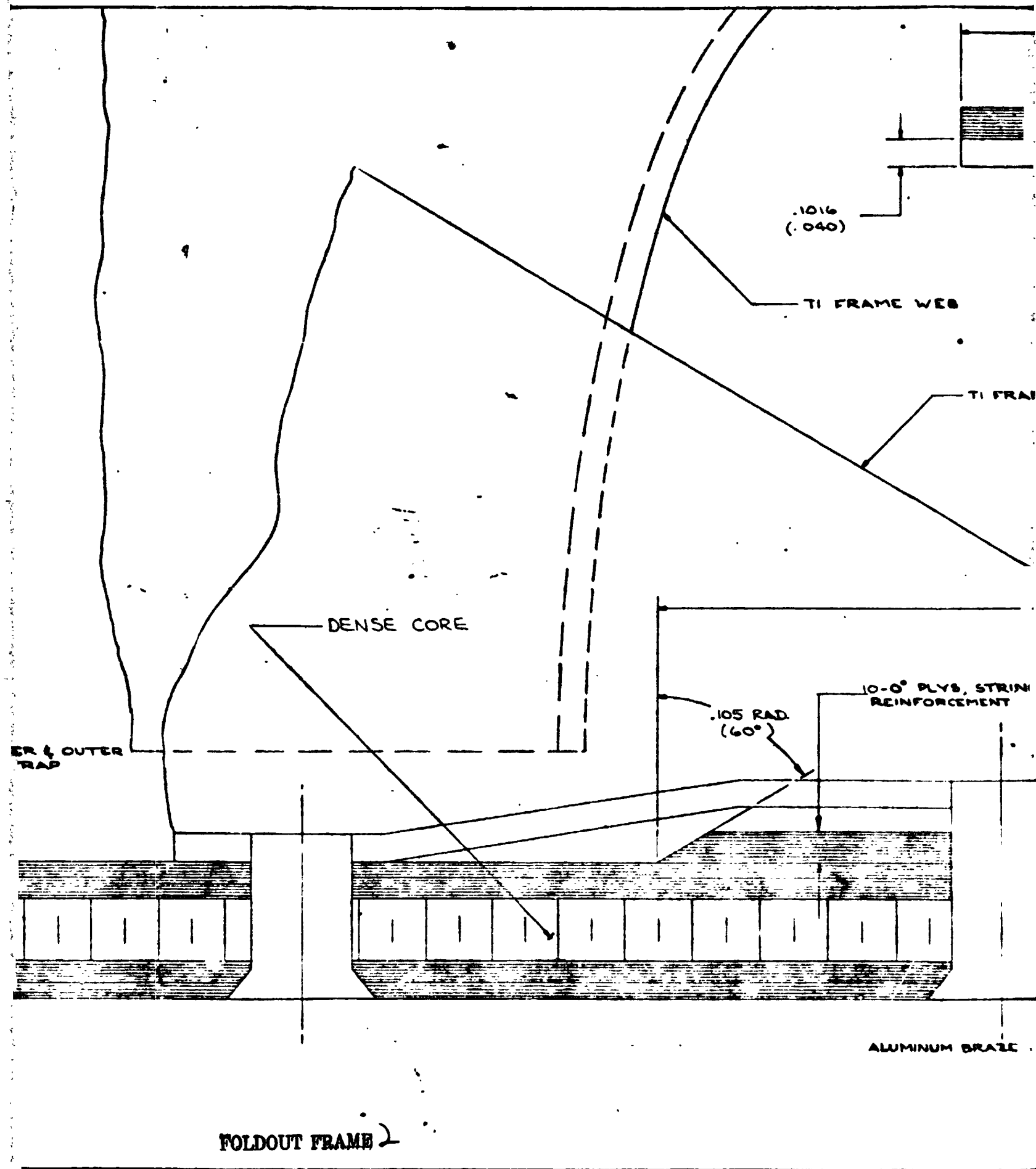
FOLDOUT FRAME 8

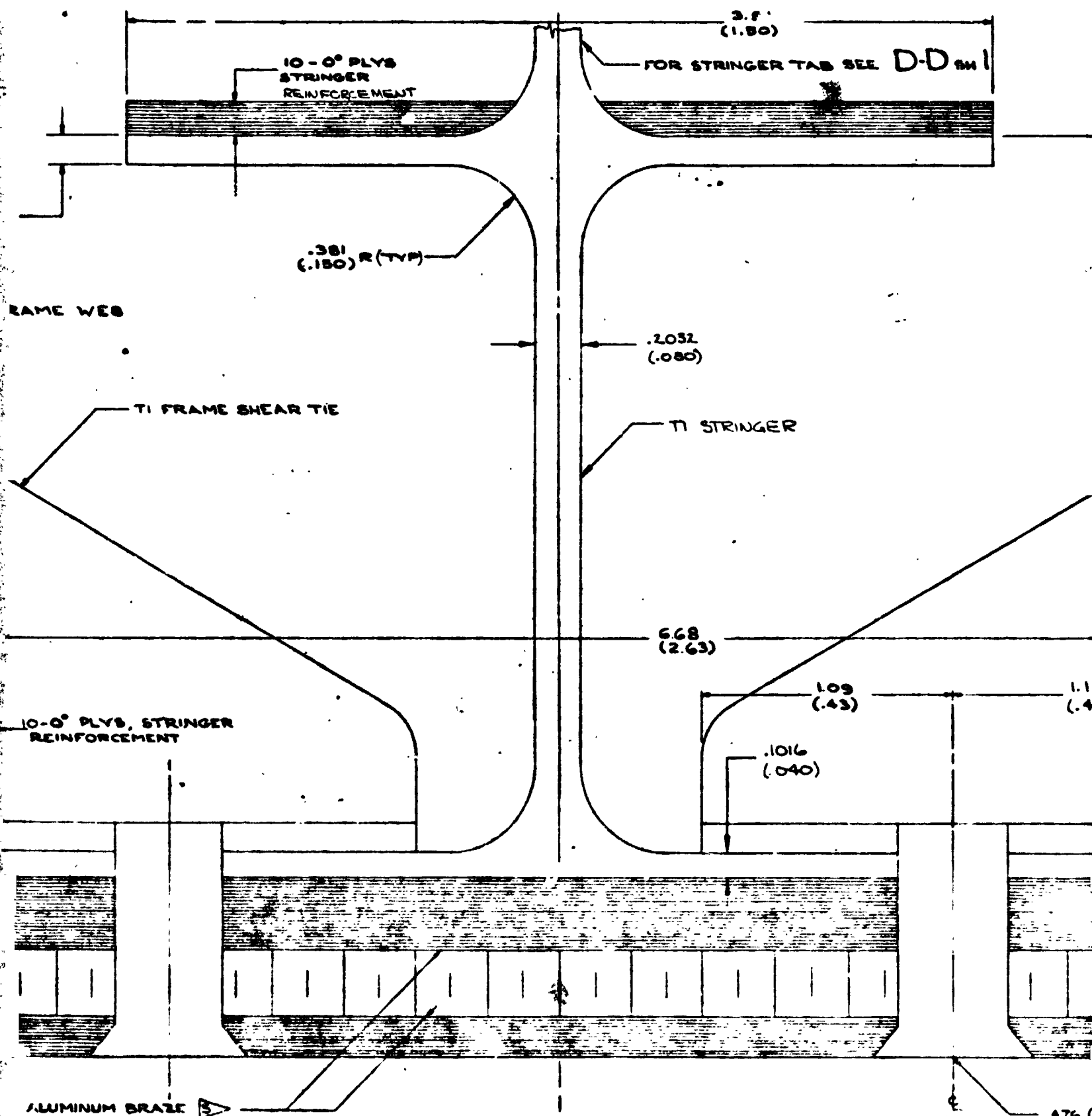
Figure 14-4. -

USED ON	DRAWN R E ROBINSON	DATE 12-2-73	THE BORG COMPANY AIRCRAFT DIVISION, RICHMOND, VA
	CHECKED		
SECT NO	STRESS		BORSIC/ALUMINUM BODY H/C SAND SKIN & TI SHIT
CHG NO	ENGR R E ROBINSON	12-2-73	969-336C M27CENIS
GROUP ORG	PROJ		CODE IDENT NO 81735
			SCALE NOTED
			SH 1

FOLDOUT FRAME 7







D-D 

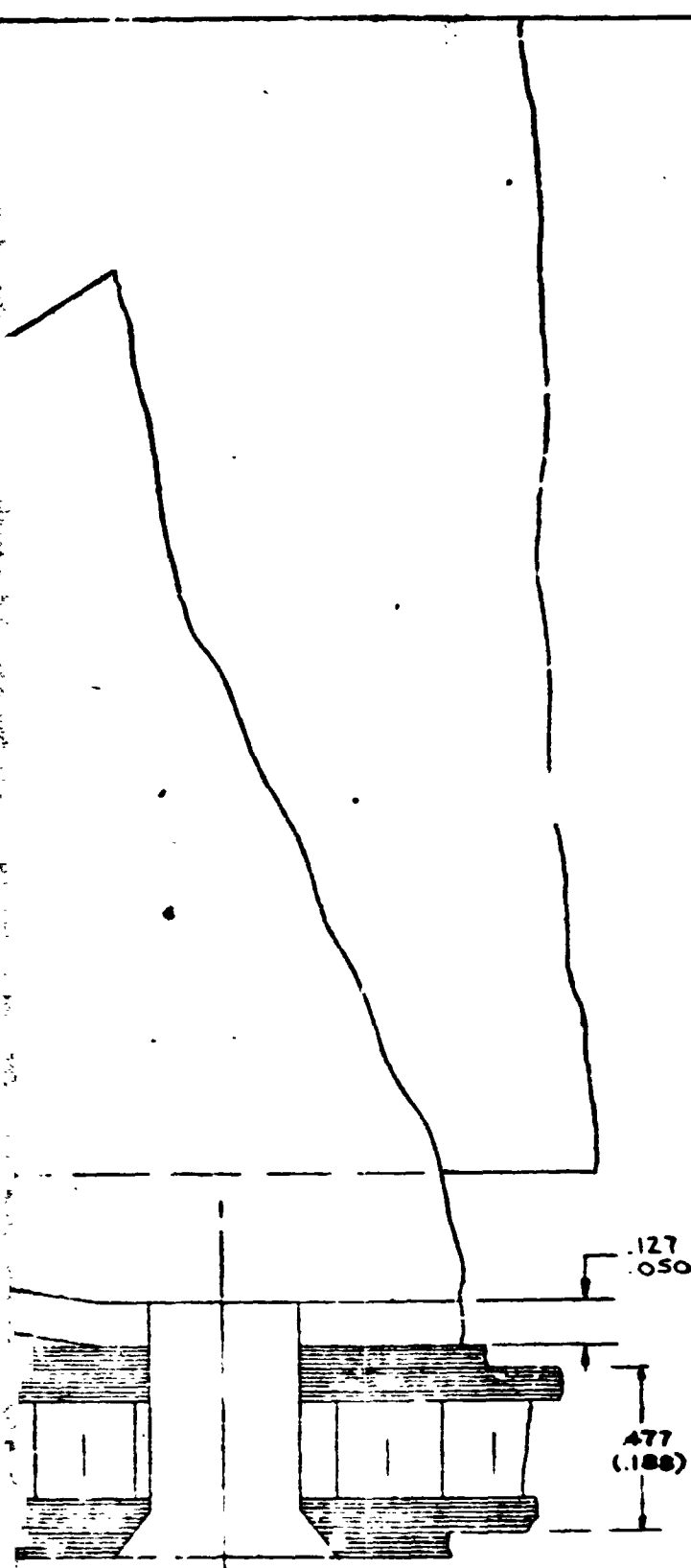
3.18
(1.25)

1.154
(.47)

SYM

.476 ($\frac{3}{16}$) DIA FASTENER (TYR)

DETAIL NAME 4



PRECEDING PAGE BLANK NOT FILLED

FOLDOUT FRAME

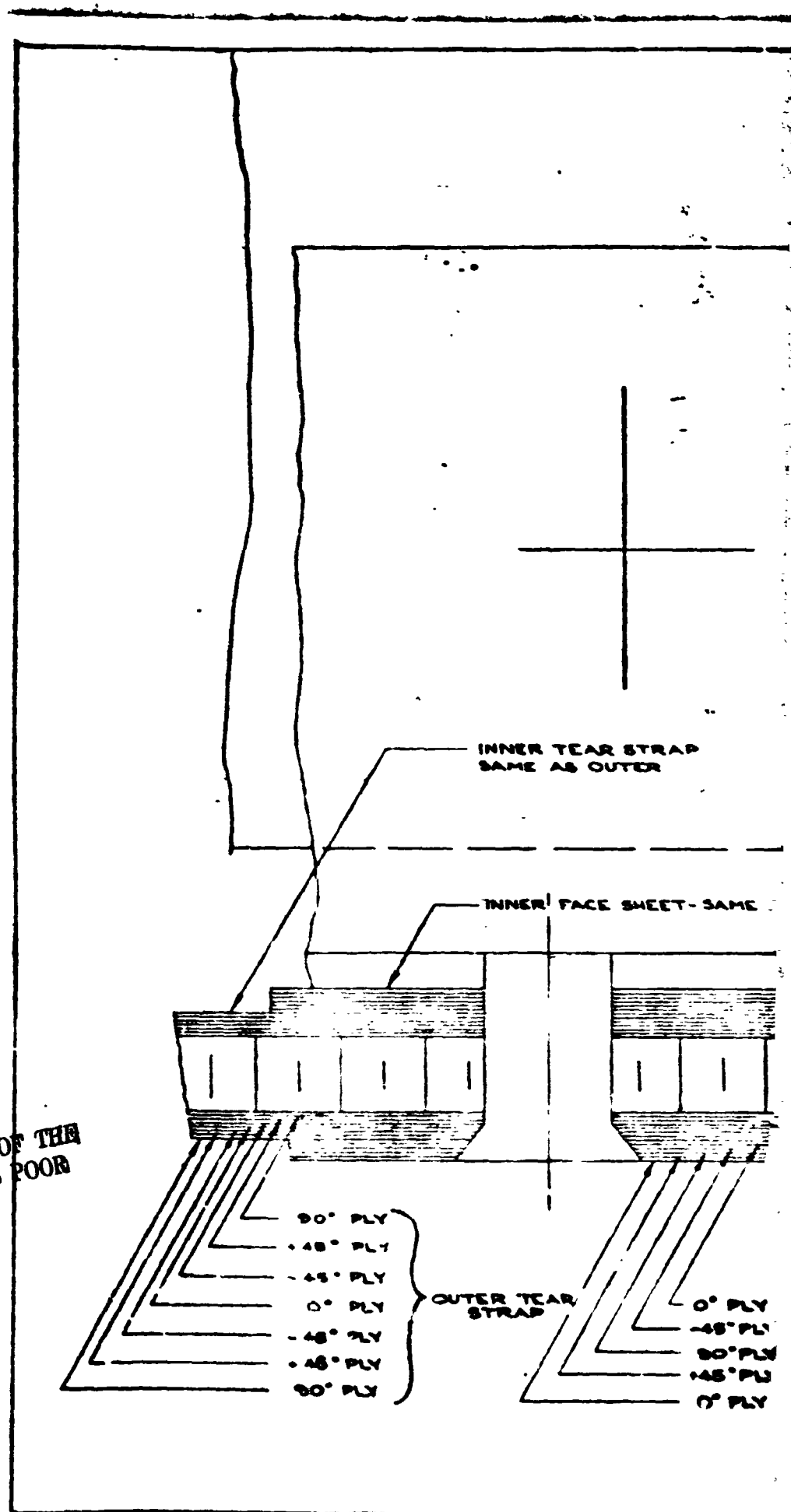
Figure 14.4. - (Continued)

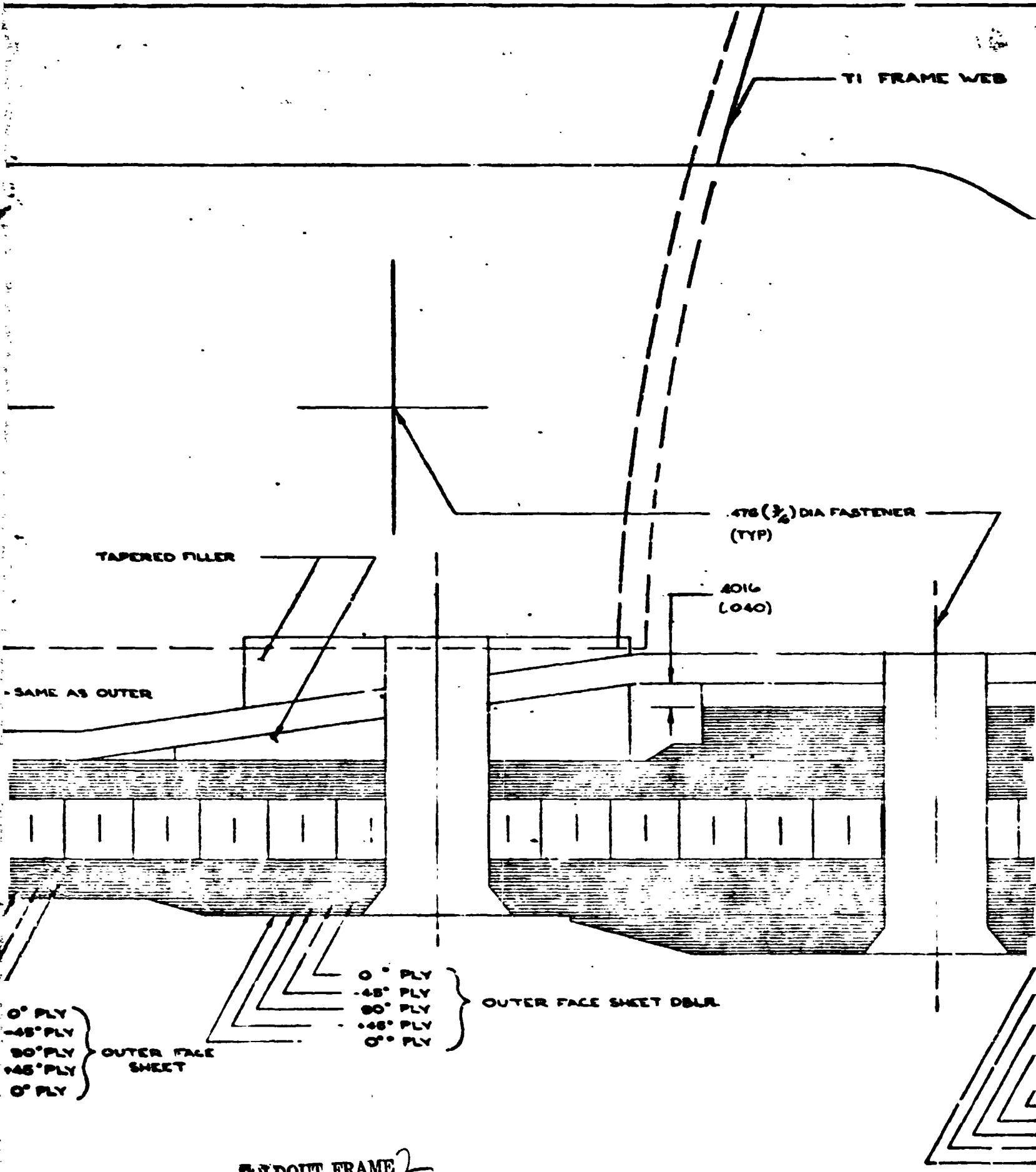
AME 4

USED ON	DRAWN R. K. ROBINSON	DATE 12-21-73	THE JENSEN COMPANY GENERAL PLANT, RENTON, WASH.	
	CHECKED		BASIC/ALUMINUM BODY H/C SAND SKIN & TI. STIFF	
SECT NO	STRESS		969-336C M27 CRUISE	
CHG NO	ENGR R. K. ROBINSON	12-21-73	CODE IDENT NO 8 205	
GROUP 020	GROUP		JAWS-139	
	PROJ		SCALE	
			TH 2	

REPRODUCIBILITY OF THE
ORIGINAL PAGE IS POOR

FOLDOUT FRAME





TI FRAME WEB

476 (3/4) DIA FASTENER
(TYP)

4016
(040)

TAPERED FILLER

- SAME AS OUTER

0° PLY
45° PLY
90° PLY
45° PLY
0° PLY
OUTER FACE
SHEET

0° PLY
45° PLY
90° PLY
45° PLY
0° PLY
OUTER FACE SHEET DBLR

FOLDOUT FRAME 2

TI FRAME WEB

TI FRAME SHEAR TIE

FOR WEB STRG DETAIL SEE DET FOR SHEET 1

REPRODUCIBILITY OF THE
ORIGINAL PAGE IS POOR

DENSE CORE

$\frac{3}{16}$ " DIA FASTENER

.127
(.050)

.1824
(.06)

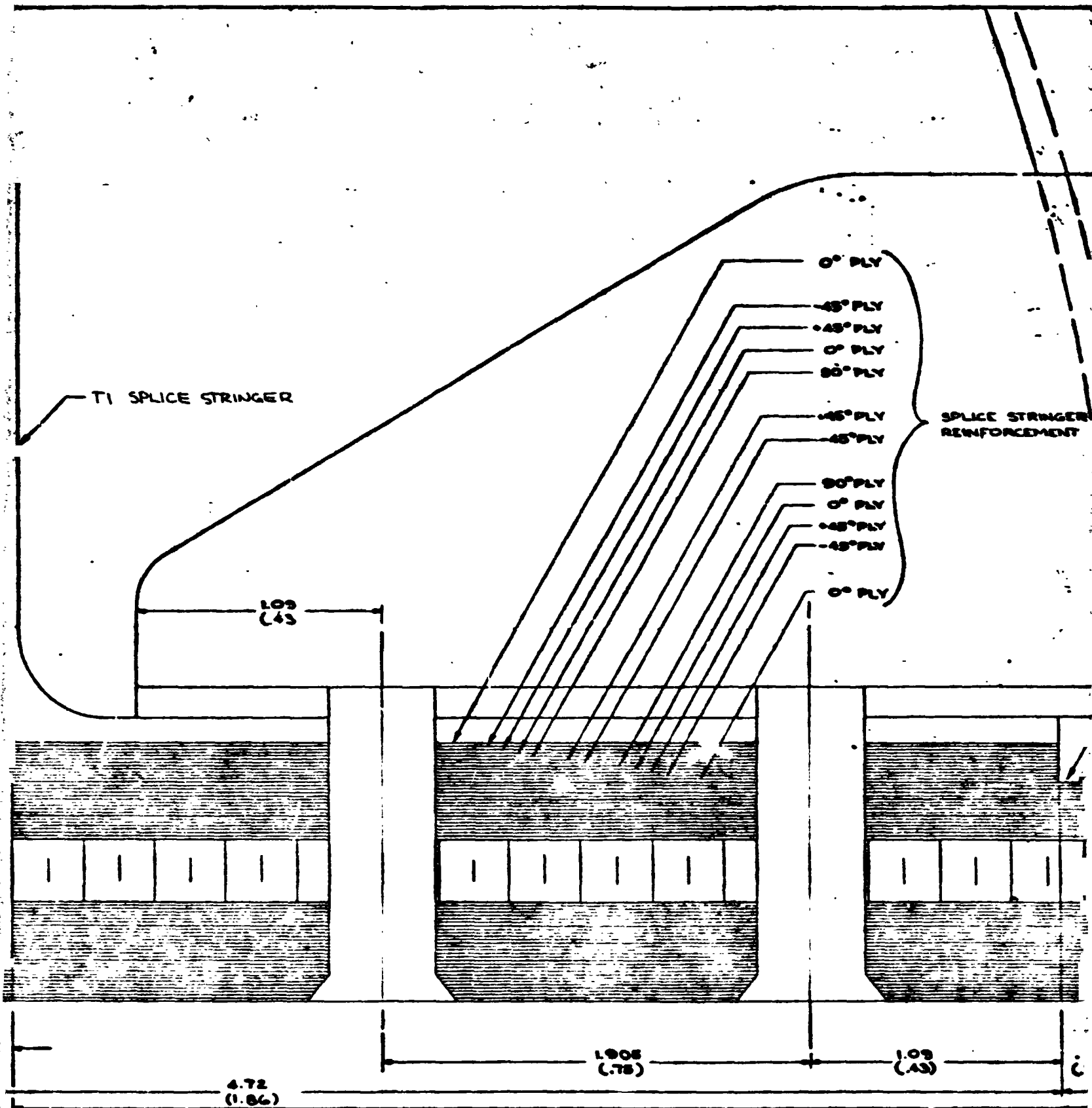
NOMINAL GAP

SYM. 2

SPRUE PLATE

FOLDOUT FRAME 3

0" PLY
-45° PLY
-45° PLY
0° PLY
90° PLY
-45° PLY
-45° PLY
90° PLY
0° PLY
-45° PLY
-45° PLY
0° PLY



STRINGER
REINFORCEMENT

0° PLY
+45° PLY
90° PLY
-45° PLY
0° PLY

INNER FACE SHEET DELR

477
(188)

BRACE

FOLDOUT FRAME 5

Figure 144.-(Concluded).

SEE SHEET 1 OR PL FOR LIST OF MATERIAL USAGE AND NOTES

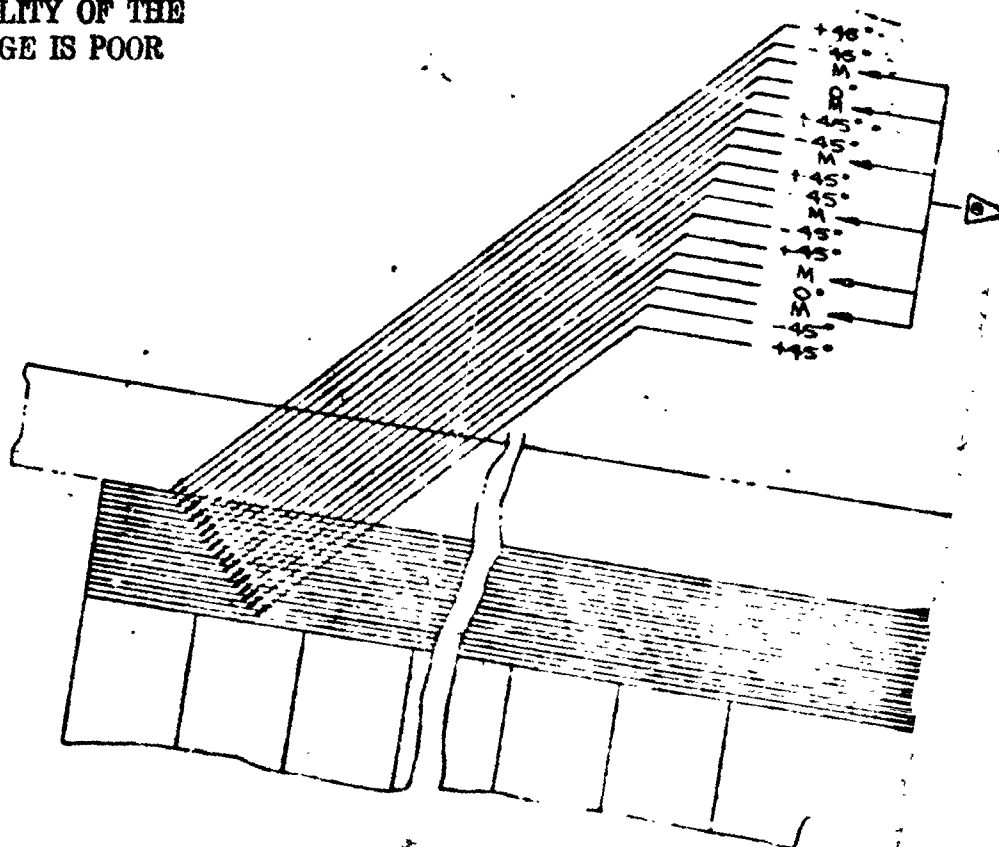
DRAWN R.K. ROBINSON		DATE 1-9-74	THE J. J. JENSEN COMPANY COMMERCIAL AIRPLANE DIV. WASH. D.C.	
CHECKED			BORSIC/ALUMINUM BODY H/C SAND SKIN & T.I. STIFF	
STRESS R.K. Robinson		3-27-74	969-336C M27 CRUISE	
GROUP		1-9-74	CODE IDENT NO 81205	
			J AWS-139	
			SCALE	

REPRODUCIBILITY OF THE
ORIGINAL PAGE IS POOR

AME 4

CH 2 221 2WA

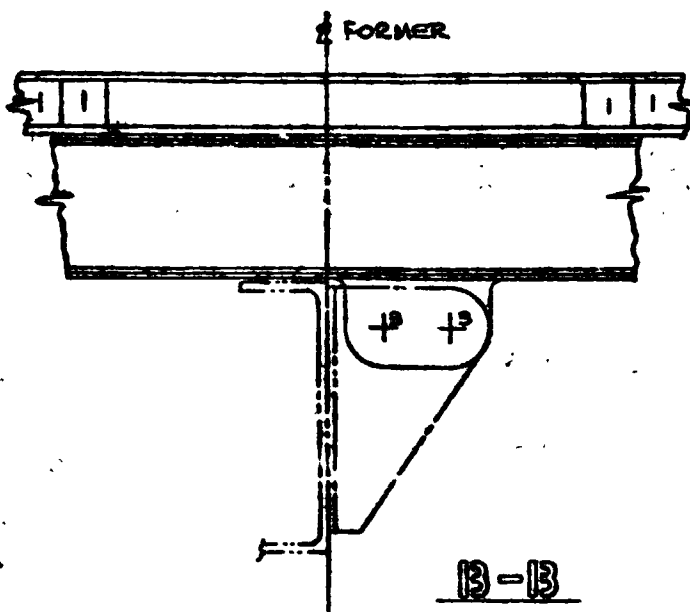
REPRODUCIBILITY OF THE
ORIGINAL PAGE IS POOR



MOLDOUT FRAME

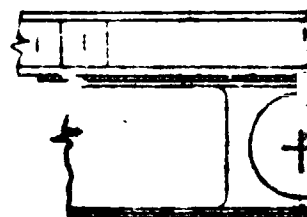
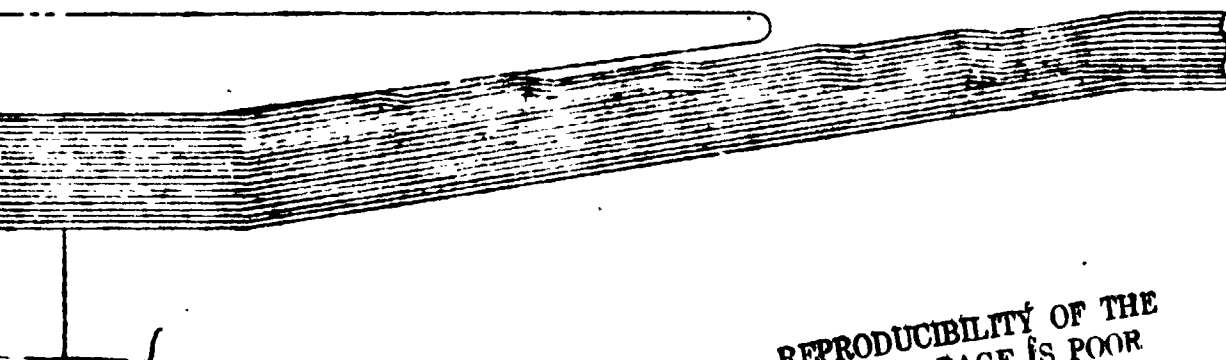
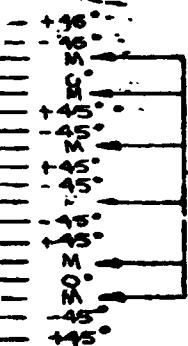
DETAIL - 1

(1/1 SCALE)
(UPPER SURFACE SHOWN ONLY)



B-B
(1/2 SC. 5)

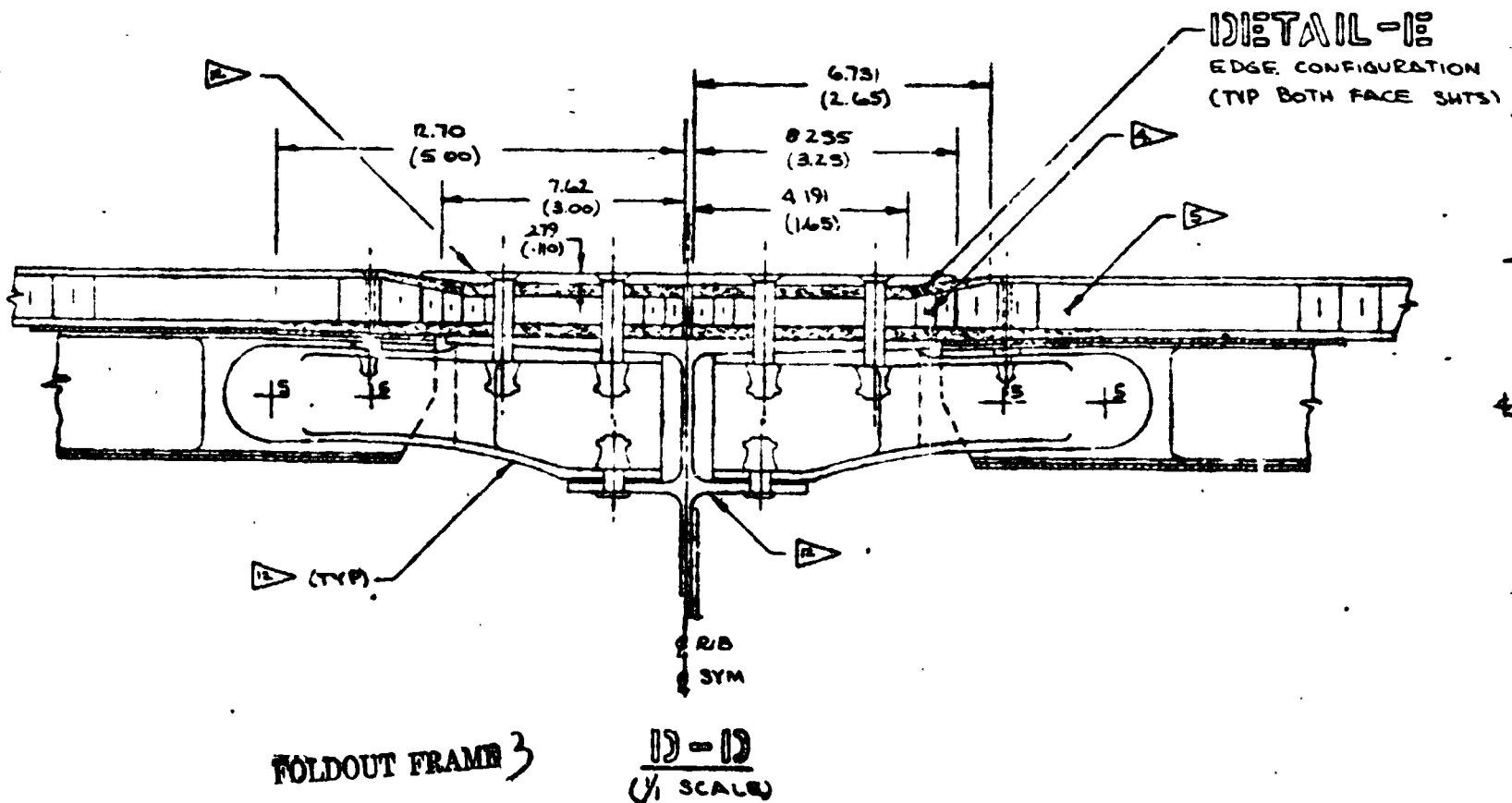
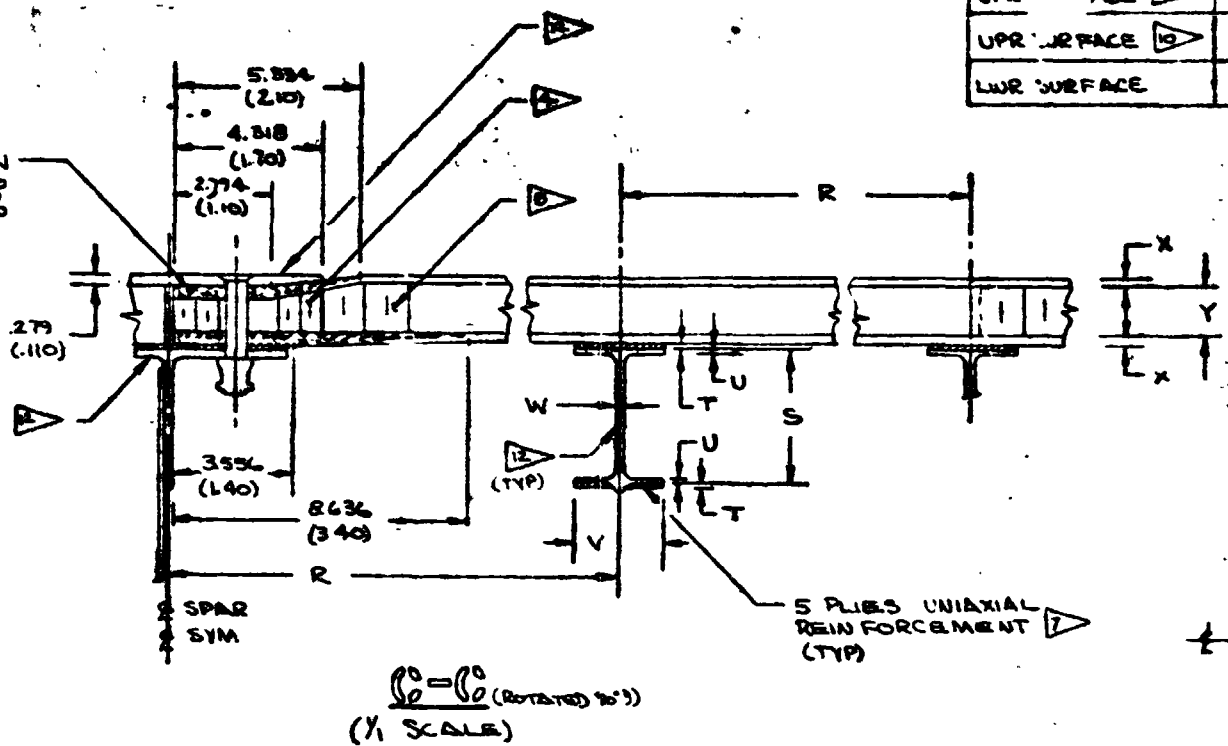
FOR EDGE CONFIG
SEE **DATA**
(TYP BOTH FACE)



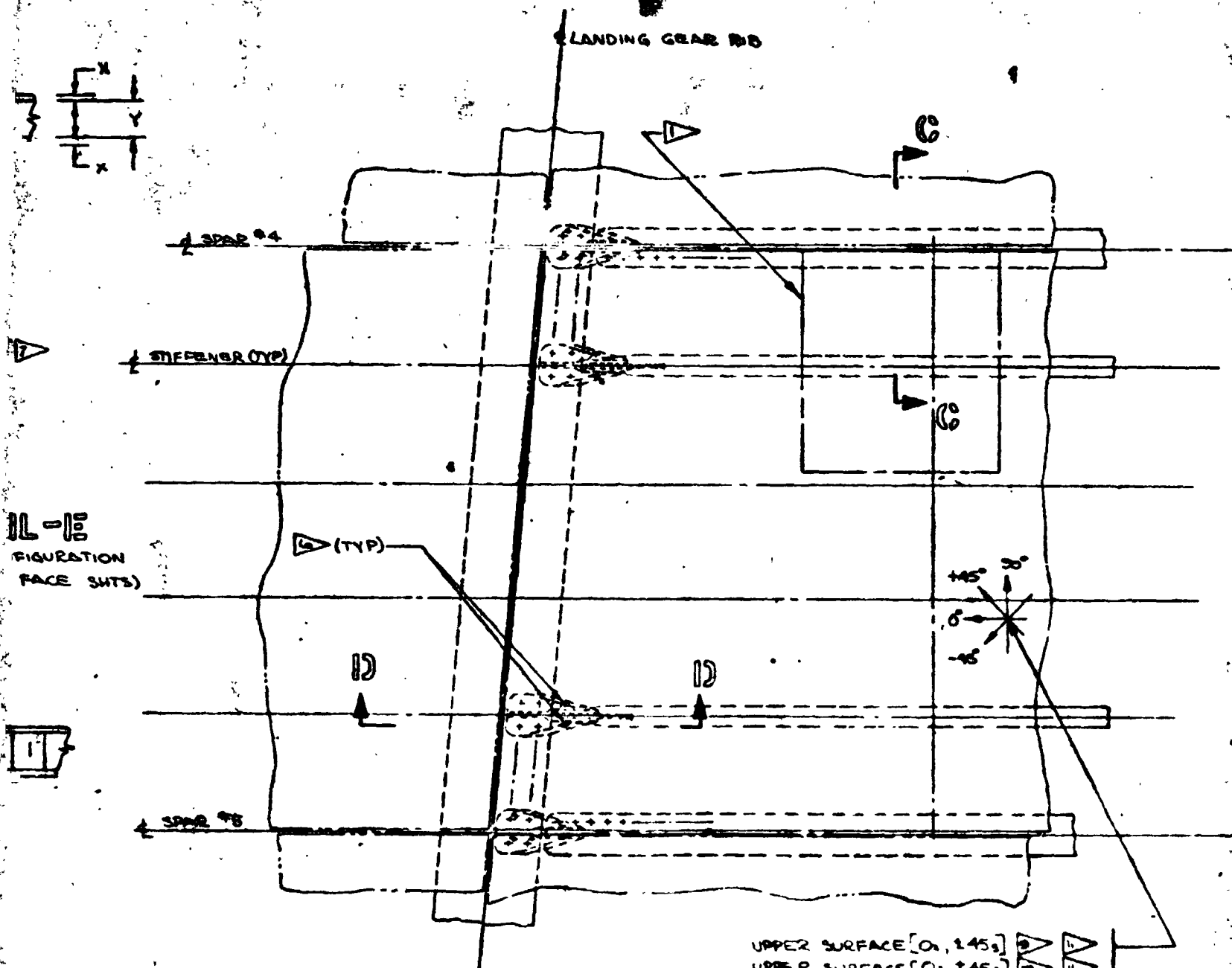
REPRODUCIBILITY OF THE
ORIGINAL PAGE IS POOR

FOLDOUT FRAME 2

FOR EDGE CONFIGURATION
SEE **DETAIL-E**
(TYP BOTH FACE SHTS)



		DIMENSION							
RFACE	▽	R	S	T	U	V	W	X	Y
RFACE	▽	17.78 (7.00)	3.81 (1.50)	.089 (.035)	.102 (.040)	2.54 (1.00)	.152 (.060)	.213 (.084)	.762 (.300)
RFACE	▽	17.78 (7.00)	3.81 (1.50)	.089 (.035)	.102 (.040)	2.54 (1.00)	.152 (.060)	.160 (.063)	.762 (.300)
RFACE		17.78 (7.00)	3.81 (1.50)	.089 (.035)	.102 (.040)	2.54 (1.00)	.152 (.060)	.267 (.105)	.886 (.353)

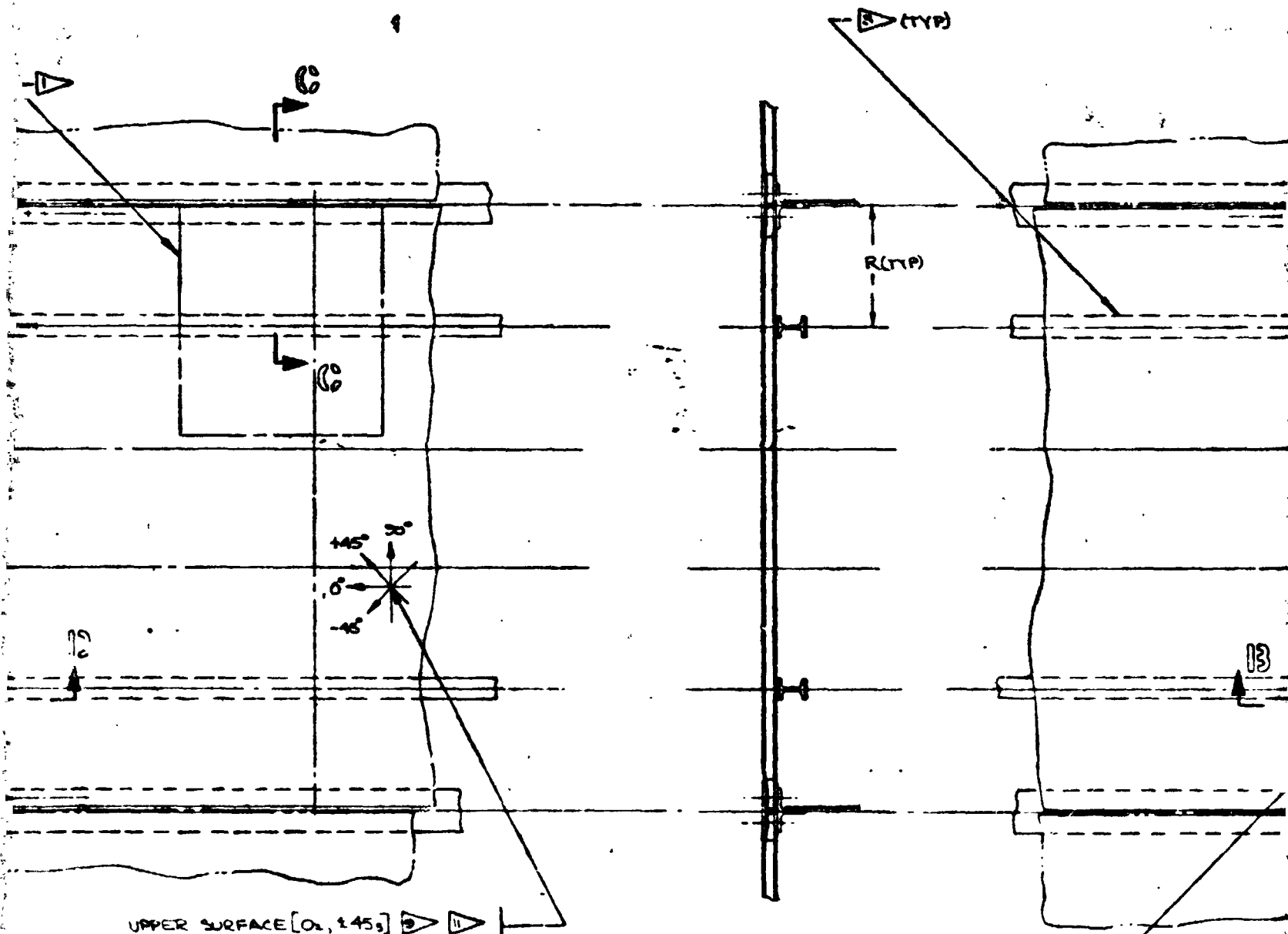


REPRODUCIBILITY OF THE
ORIGINAL PAGE IS PROVIDED

FOLDOUT FRAME 4

DIET
UPPER SURFACE
(X)

GEAR NO

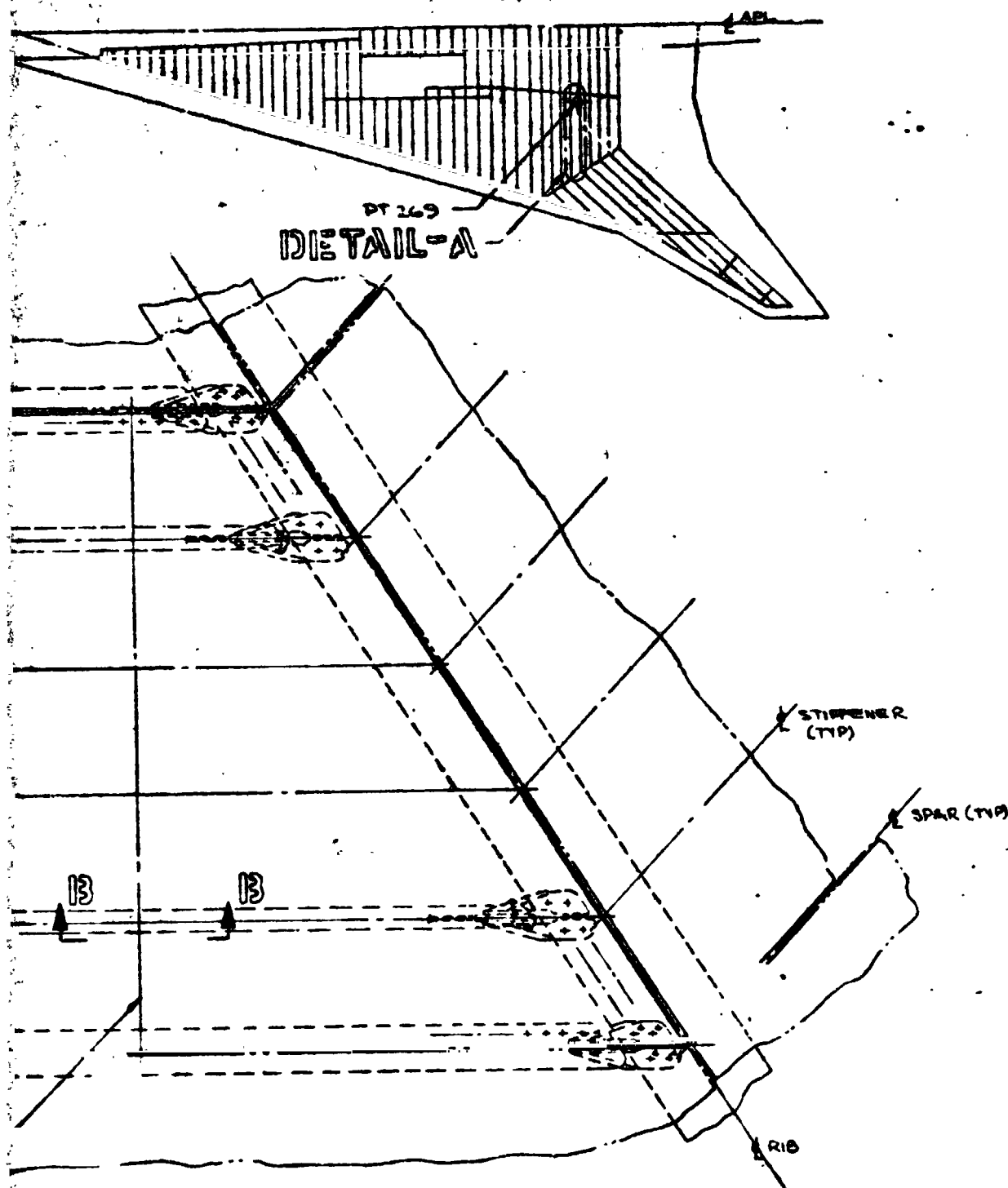


UPPER SURFACE [0, 145]
UPPER SURFACE [0, 145]
UPPER SURFACE [0, 145, 90]
ABILITY OF THIS PAGE IS PROVIDED

DETAIL-A (UPPER SURFACE SHOWN)
(1/4 SCALE)
← INDO
FWD
↓

FOLDOUT FRAME 5

← SUPPORT FOR



- ▶ TI-GAL-4V COND I
- ▶ TIP BOTH FACE THIS FAC
- ▶ PER AF DESIGN GUIDE DA (PROJECTED FROM NASA) BORSIC ALUMINUM SKIN A 3 PLYS OF .007 IN/PLY M (2) 0° PLYS, (1) +45° PLYS. SEE DETAIL E FOR E
- ▶ PER AF DESIGN GUIDE DA BORSIC ALUMINUM SKIN A OF .007 IN/PLY MATERIAL (2) 0° PLYS, (1) +45° PLYS. SEE DETAIL E FOR EN
- ▶ .007 IN THICK TITANIUM
- ▶ BORSIC ALUMINUM UN (2) 0° PLYS PER LOC MATERIAL
- ▶ 1/8 W DIA HI-LOC FASTEN BRAZE PEELING
- ▶ 785 KCM (4.9 RF) SE
- ▶ 450 KCM (28.1 RF) SE
- ▶ SPOT BRAZE STIFFEN (SPOTWELD SPEC & CYCLE UNDETERMIN
- ▶ BORSIC ALUMINUM SKIN A OF .007 IN/PLY MATERIAL (2) 0° PLYS, (1) +45° PLYS. SEE DETAIL E FOR E
- ▶ PT 269 CONTROL PO AND LOCATION SA

BASIC DIMENSIONAL CENT
() DIMENSION - INCH

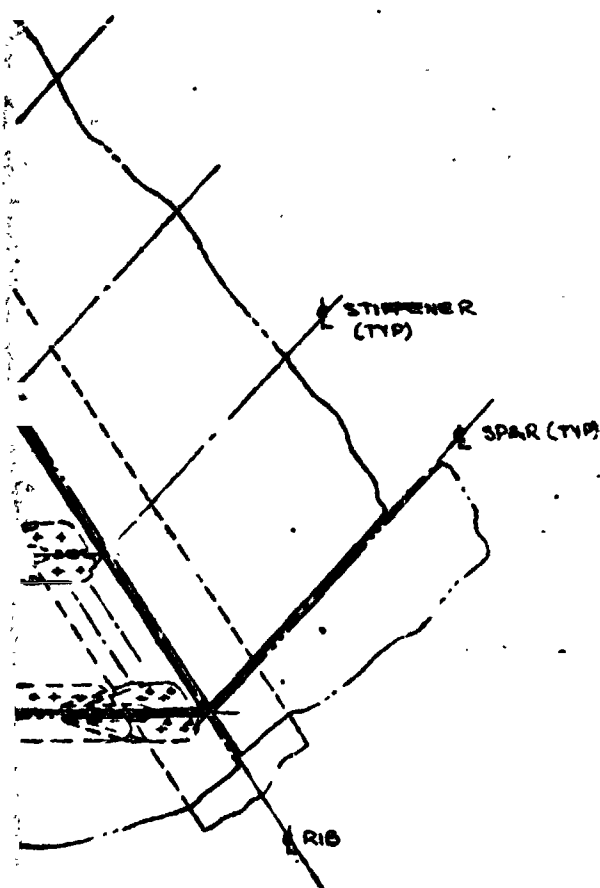
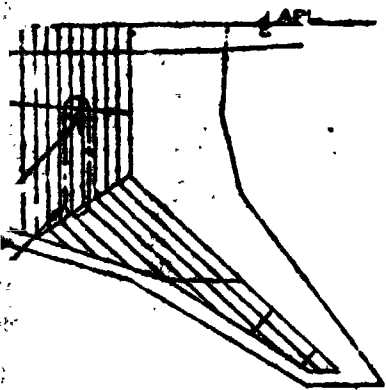
PRECEDING PAGE BL

Figure

JRT FORMER 69.50 (25.00) SPACING (TYP)

REPRODUCIBILITY OF THE
ORIGINAL PAGE IS POOR

US 7 ON	DRAWN: <i>Signature</i>	DATE: 5/10/64
	CHECKED	
SECT NO	STRESS	
CHG NO	ENGINEER & DRAWING	5/10/64
GROUP 000	GROUP	
	PROJ	



- 1. TI-6AL-4V COND I
- 2. TIP BOTH FACE SHEETS. FACE SHEETS SYM ABOUT $\frac{1}{2}$ OF CORE
- 3. PER AF DESIGN GUIDE DATA EXCEPT FOR SHEAR DATA (PROJECTED FROM NASA-LANGLEY DATA) UPPER SURFACE BORSIC ALUMINUM SKIN ASSY CONSOLIDATED OF 9 PLYS OF .007 IN/PLY MATERIAL
(2) 0° PLYS, (3) +45° PLYS, (3) -45° PLYS
SEE DETAIL E FOR END REINFORCEMENT
- 4. PER AF DESIGN GUIDE DATA. UPPER SURFACE BORSIC ALUMINUM SKIN ASSY CONSOLIDATED OF 12 PLYS OF .007 IN/PLY MATERIAL
(2) 0° PLYS, (5) +45° PLYS, (5) -45° PLYS
SEE DETAIL E FOR END REINFORCEMENT
- 5. .007 IN THICK TITANIUM SHIM TI-6AL-4V
- 6. BORSIC ALUMINUM UNIAXIAL REINFORCEMENT
(5) 0° PLYS PER LOCATION .007 IN/PLY MATERIAL
- 7. $\frac{1}{8}$ IN DIA HI-LOX FASTENER TO PREVENT BRAZE PEELING
- 8. 785 KCM (4.9 PCF) SC4-20 CORE TI-3AL-2.5V
- 9. 450 KCM (28.1 PCF) SS2-60 CORE TI-6AL-4V
- 10. SPOTBRAZE STIFFENERS TO FACE SHEET (SPOTWELD SPEC & BRAZE TIME & CYCLE UNDETERMINED)
- 11. BORSIC ALUMINUM SKIN ASSY CONSOLIDATED OF 15 PLYS OF .007 IN/PLY MATERIAL
(2) 0° PLYS, (6) +45° PLYS, (6) -45° PLYS, (1) 90° PLY
SEE DETAIL E FOR END REINFORCEMENT
- 12. PT 269 CONTROL POINT COUPON SIZE AND LOCATION SAME AS FOR TASK I

BASIC DIMENSIONS - CENTIMETERS
() DIMENSIONS - INCHES

PRECEDING PAGE BLANK NOT
FOLDOUT FRAME

Figure 14.5.-

USED ON	DRAWN <i>Santhwe</i>	DATE 5/10/74	BY <i>J. J. E.</i>	COMPANY
	CHECKED			
SECT NO	STRESS	5/10/74		
	ENGR <i>J. J. E.</i>			
ENG NO	GROUP			
	PROJ			
GROUP ORG				
			CODE IDENT NO 1 701	JAN 44
			SCALE	SM

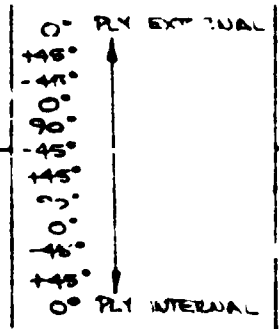
SPALE



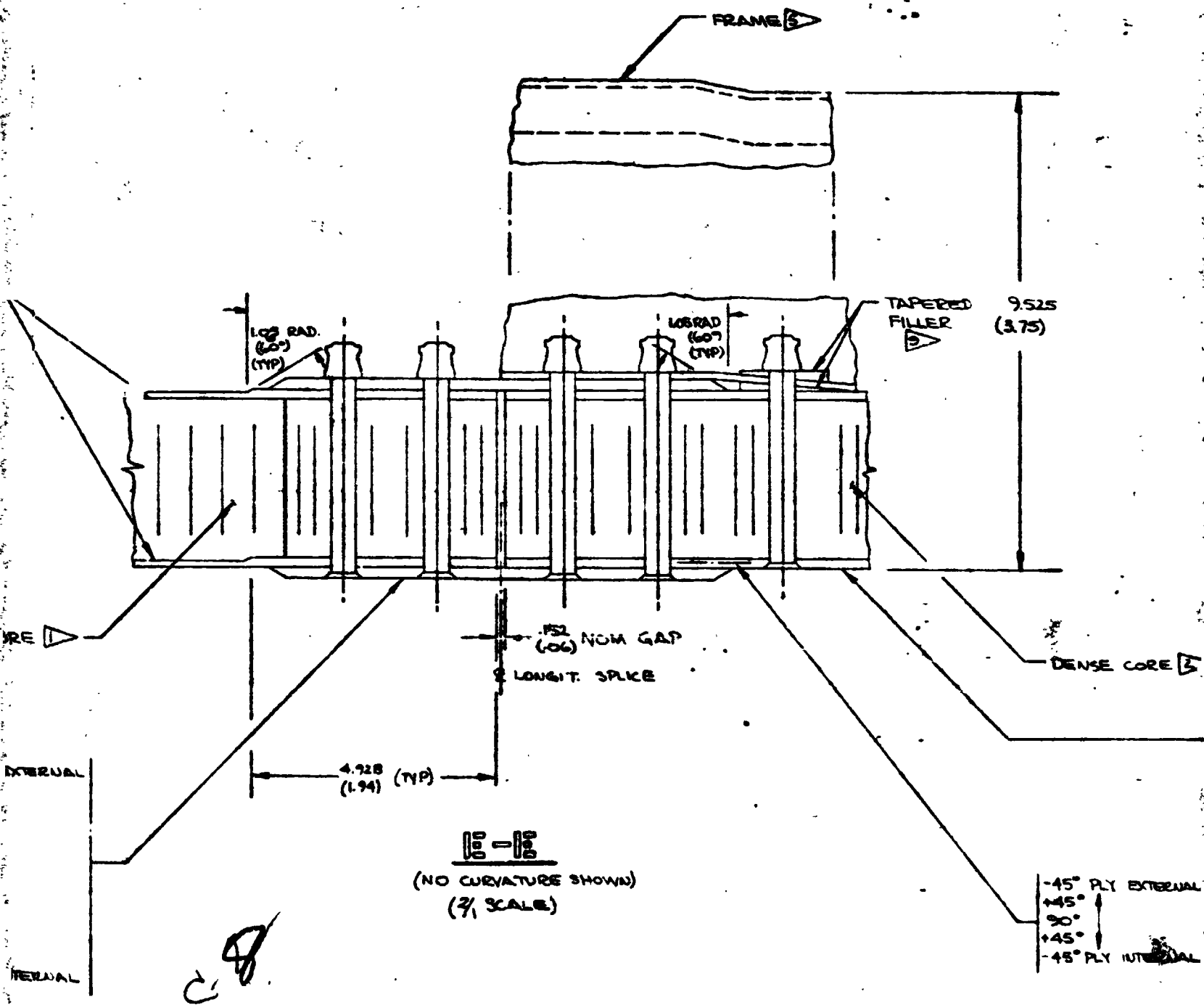
BASIC CORE



OUTER SPLICE PLATE
(INNER SPLICE PLATE TYP)



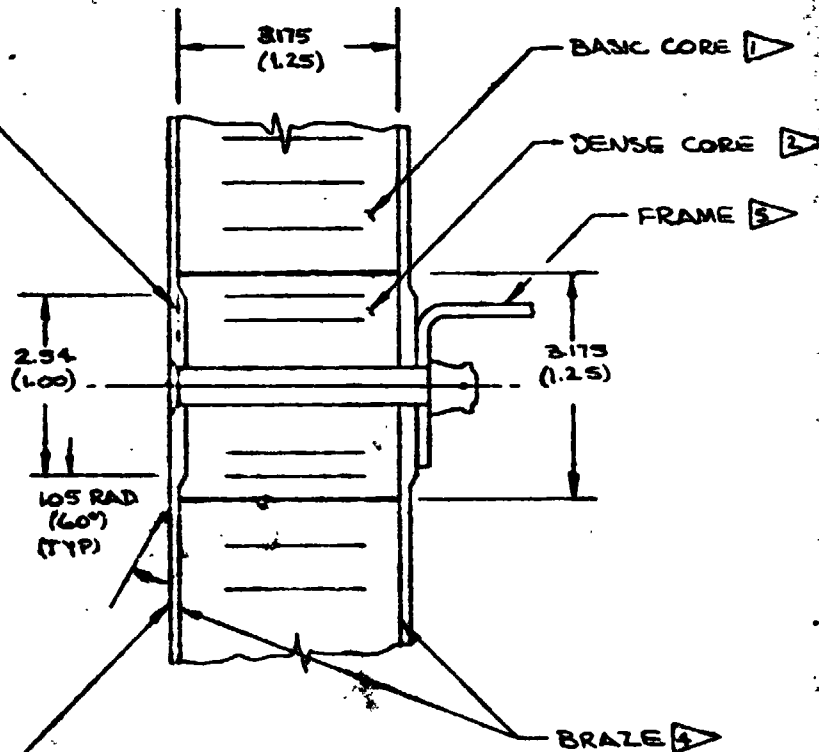
FOLDOUT FRAME



FOLDOUT FRAME 2

OUTER FACE SHT PAD-UP
(INNER FACE SHT PAD-UP TYP)

-45° PLY EXTERNAL
+45°
90°
+45°
-45° PLY INTERNAL



OUTER FACE SHT
(INNER FACE SHT TYP)

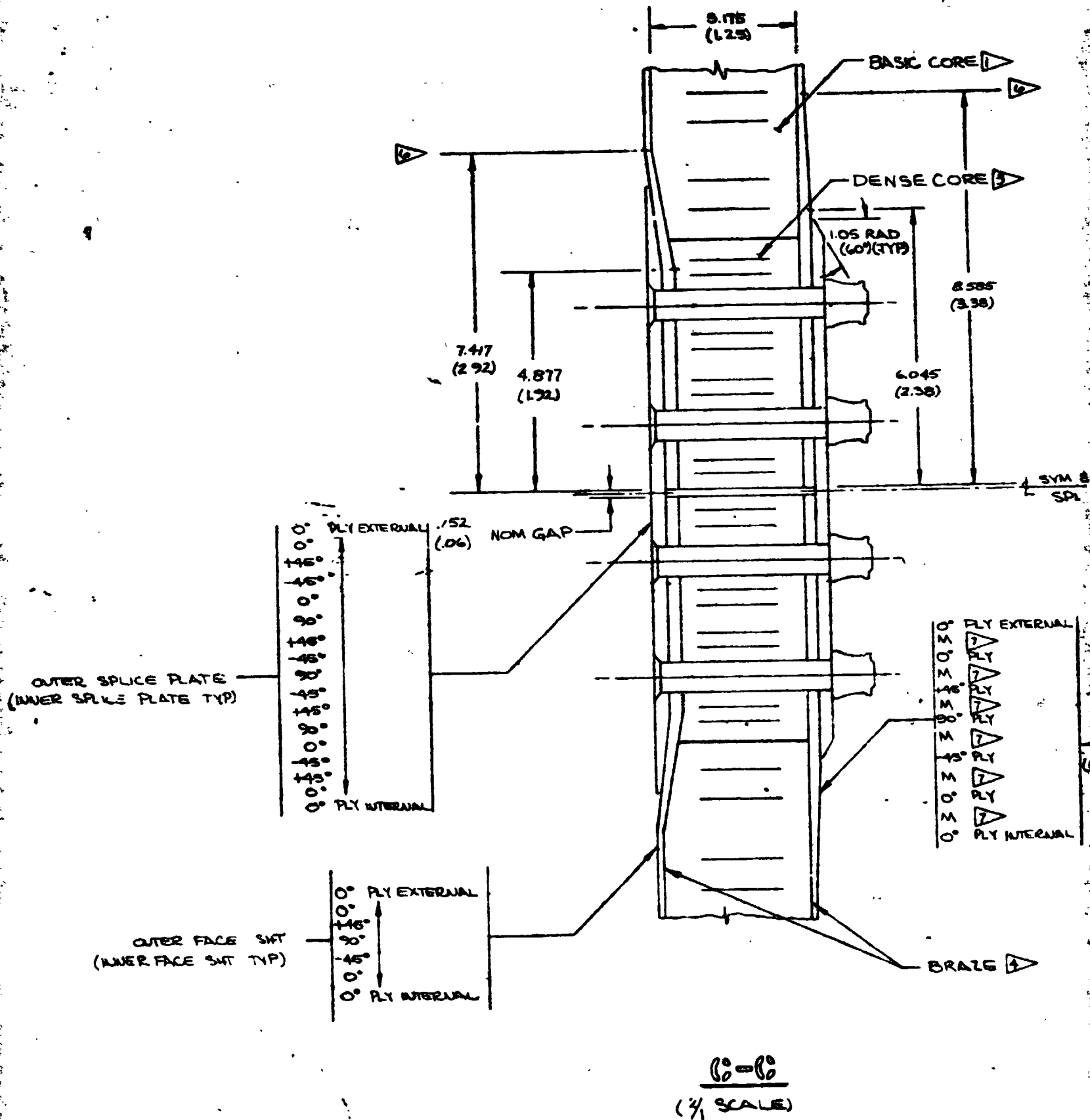
0° PLY EXTERNAL
0°
+45°
90°
-45°
0° PLY INTERNAL

13-13
(3/4 SCALE)

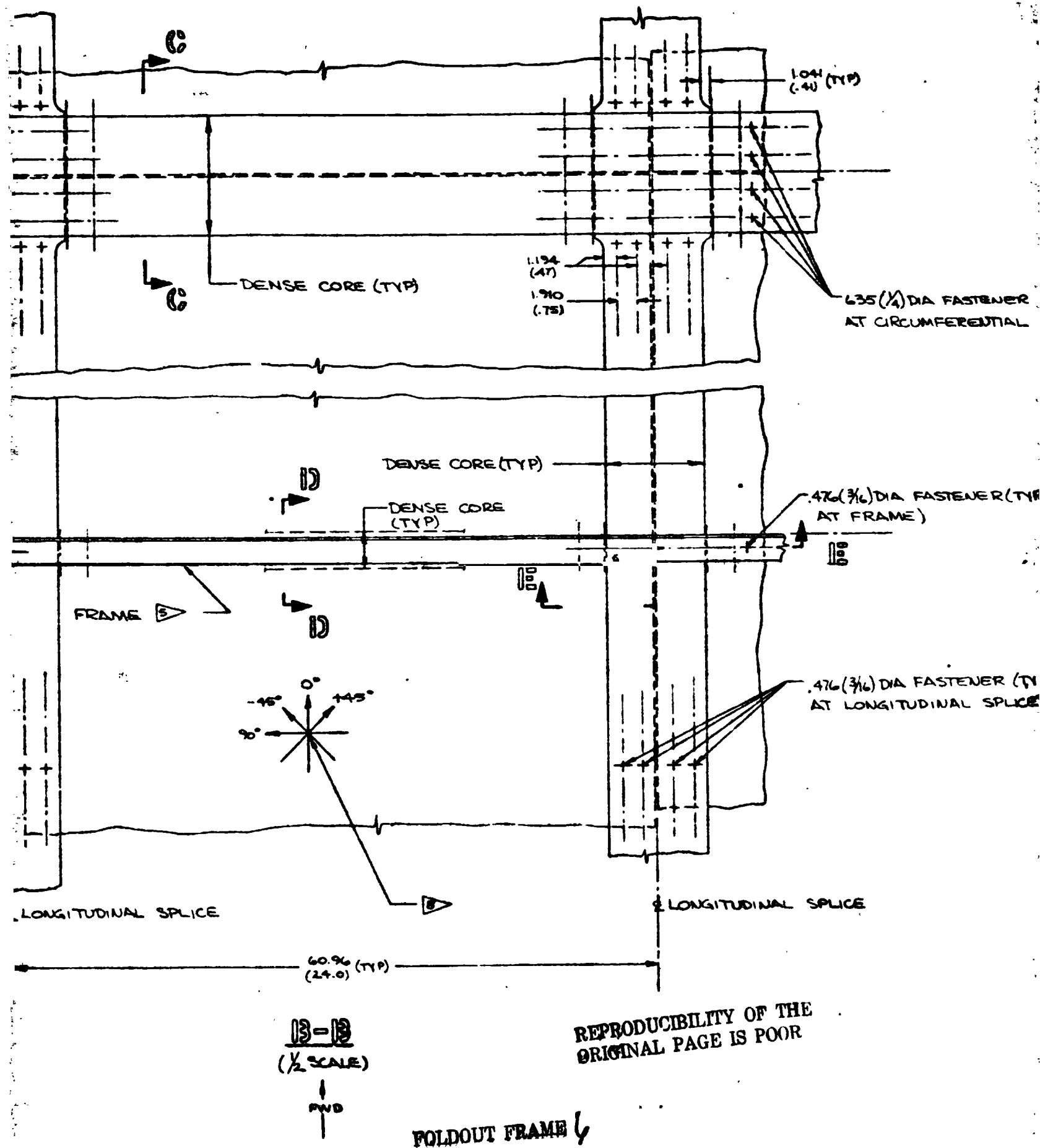
OUTER FACE SHT PAD-UP
(INNER FACE SHT PAD-UP TYP)

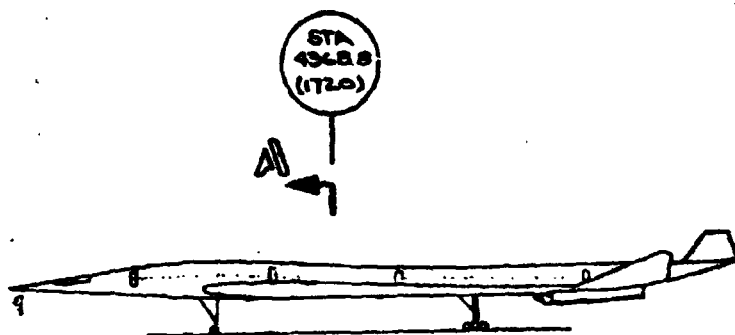
REPRODUCIBILITY OF THE
ORIGINAL PAGE IS POOR

WYLDOUT FRAME 3



FOLDOUT FRAME 4



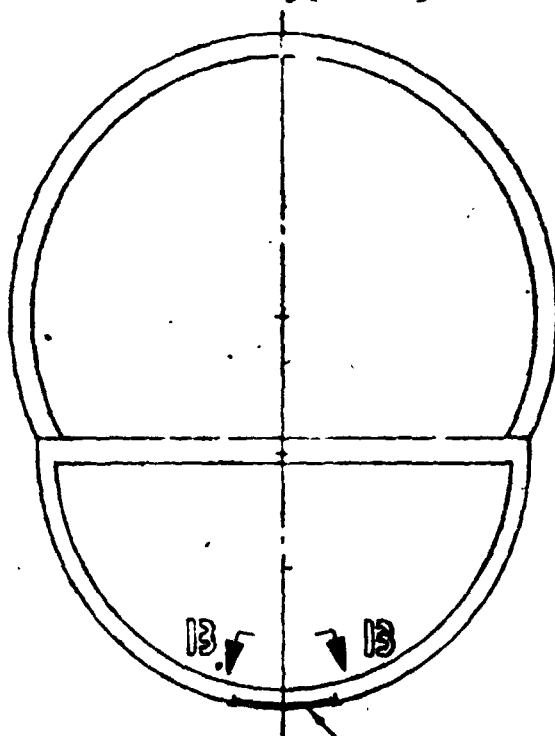


FASTENER (TYP
DIFFERENTIAL SPLICE)

(NO SCALE)

FASTENER (TYP
DIFFERENTIAL SPLICE)

FASTENER (TYP
DIFFERENTIAL SPLICE)



LWR BODY PANEL

A-A
(1/20 SCALE)

FOLDOUT FRAME

3 2024-T3 AL

4 BASIC PL
007 IN/P

A) INNER
FAC

B) INNER

7 .009 THICK

6 EDGE TT

5 TI-6AL-

4 ALUMINUM
(BRAZE)

3 450 Kg/M³
TI-6AL-4V

2 226 Kg/M³
TI-6AL-4V

1 78 Kg/M³
TI-3AL-

BASIC DIMEN
() DIMEN

USE
18
CM
2

3 2024-T3 ALUMINUM

4 BASIC PLY ORIENTATION FOR ALL ASSY CONSOLIDATIONS
OUT IN/PLY MATERIAL

A) INNER AND OUTER FACE SHT ASSY CONSOLIDATIONS:
FACE SHT AND PAD-UP

B) INNER AND OUTER SPLICE PLATE CONSOLIDATIONS

7 .009 THICK SHIM TI-6AL-4V COND I

6 EDGE TITANIUM SHIM

5 TI-6AL-4V COND I

4 ALUMINUM BRAZE
(BRAZE TIME & TEMP CYCLE UNDEFINED)

3 450 Kg/M³ (231 LB/FT³) H/C CORE SS2-60
TI-6AL-4V

2 226 Kg/M³ (141 LB/FT³) H/C CORE SS2-30
TI-6AL-4V

1 78 Kg/M³ (4.9 LB/FT³) H/C CORE SC4-20
TI-3AL-2.5V

BASIC DIMENSIONS - CENTIMETERS

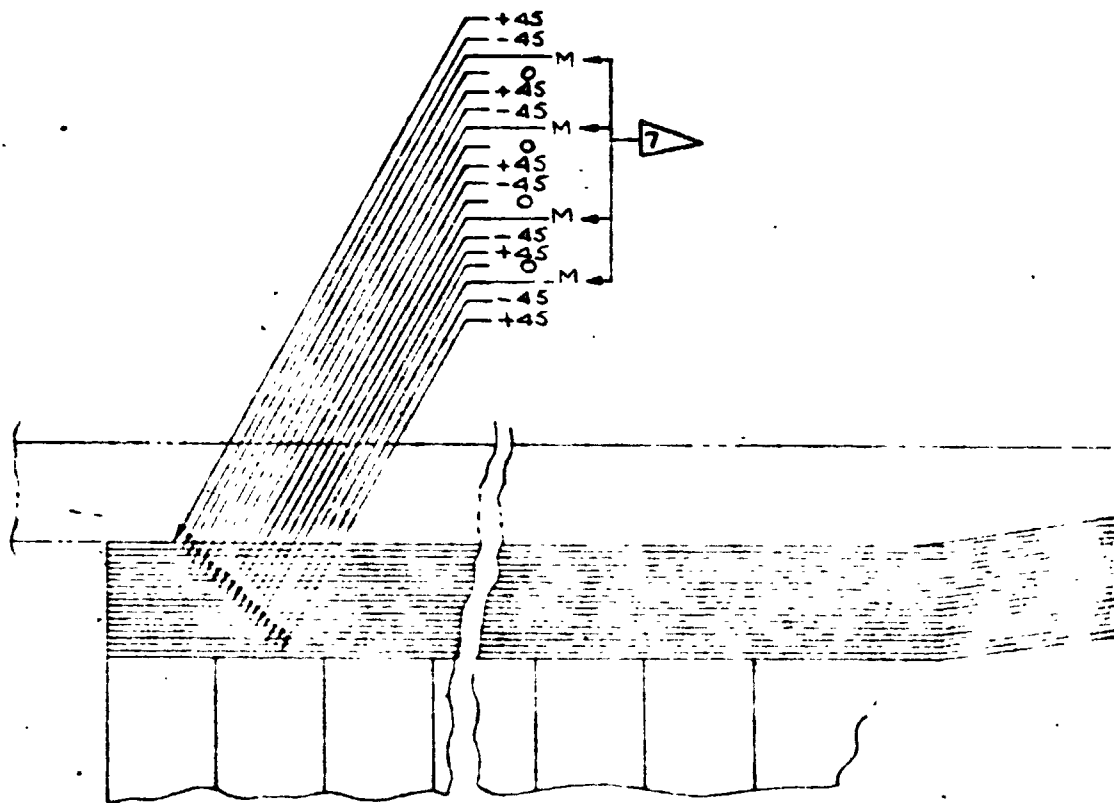
() DIMENSIONS - INCHES

Figure 14-6 -

SEE SHEET 1 FOR PLT FOR LIST OF MATERIAL USAGE AND NOTES

USED ON	DRAWN	DATE	THE BLISS COMPANY COMMERCIAL & PLASTIC REPAIR WASH
	CHECKED		
SECT NO	STRESS		BORSIC/ALUMINUM BODY H/C SANDWICH SKIN 969-336C M-27
	ENG		
CHG NO	GROUP		CODE IDENT NO 91708
	PROJ		
GROUP ORG			577 J AWS-141
SCALE NOTED			SM

FOLDOUT FRAME

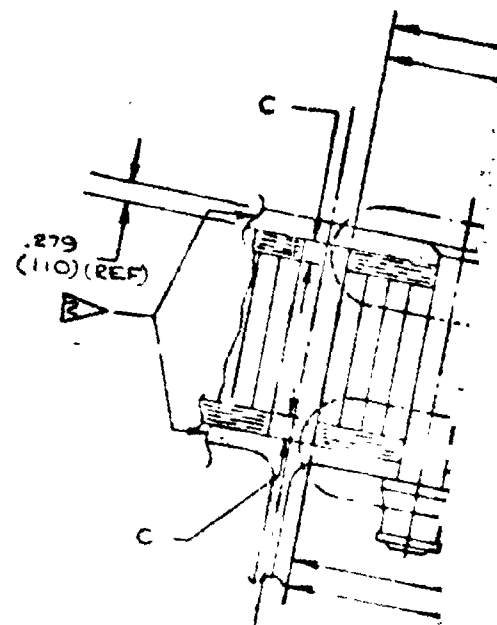


(UPPER SURFACE SHOWN ONLY)

DETAIL D

10/1

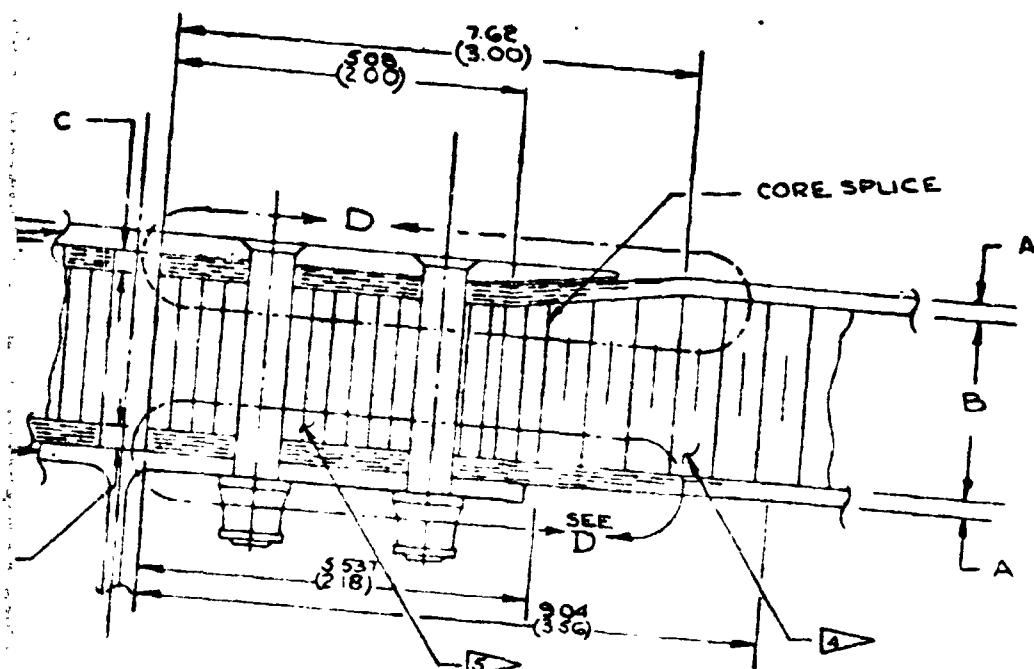
FOLDOUT FRAME |



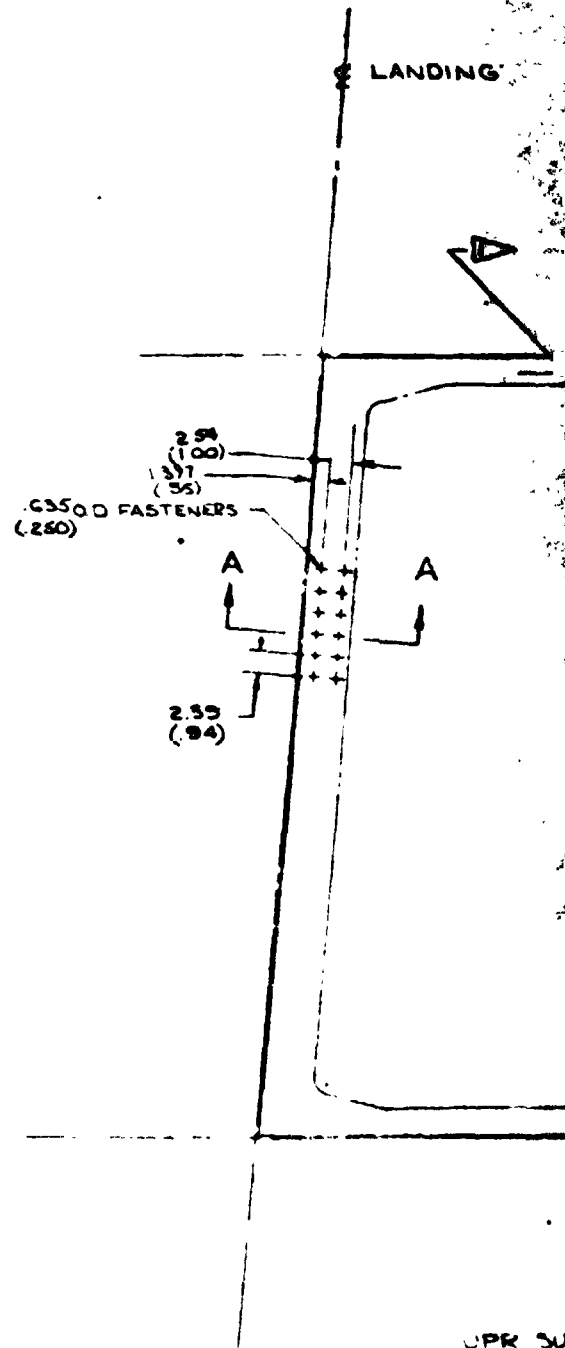
REPRODUCIBILITY OF THE
ORIGINAL PAGE IS POOR

LOCATION	A	
UPR SURFACE	248 (198)	2 (1)
LWR SURFACE	302 9	1 1
LWR SURFACE	249 (198)	1 1

FOLDOUT FRAME 2



SECT A-A
2/1



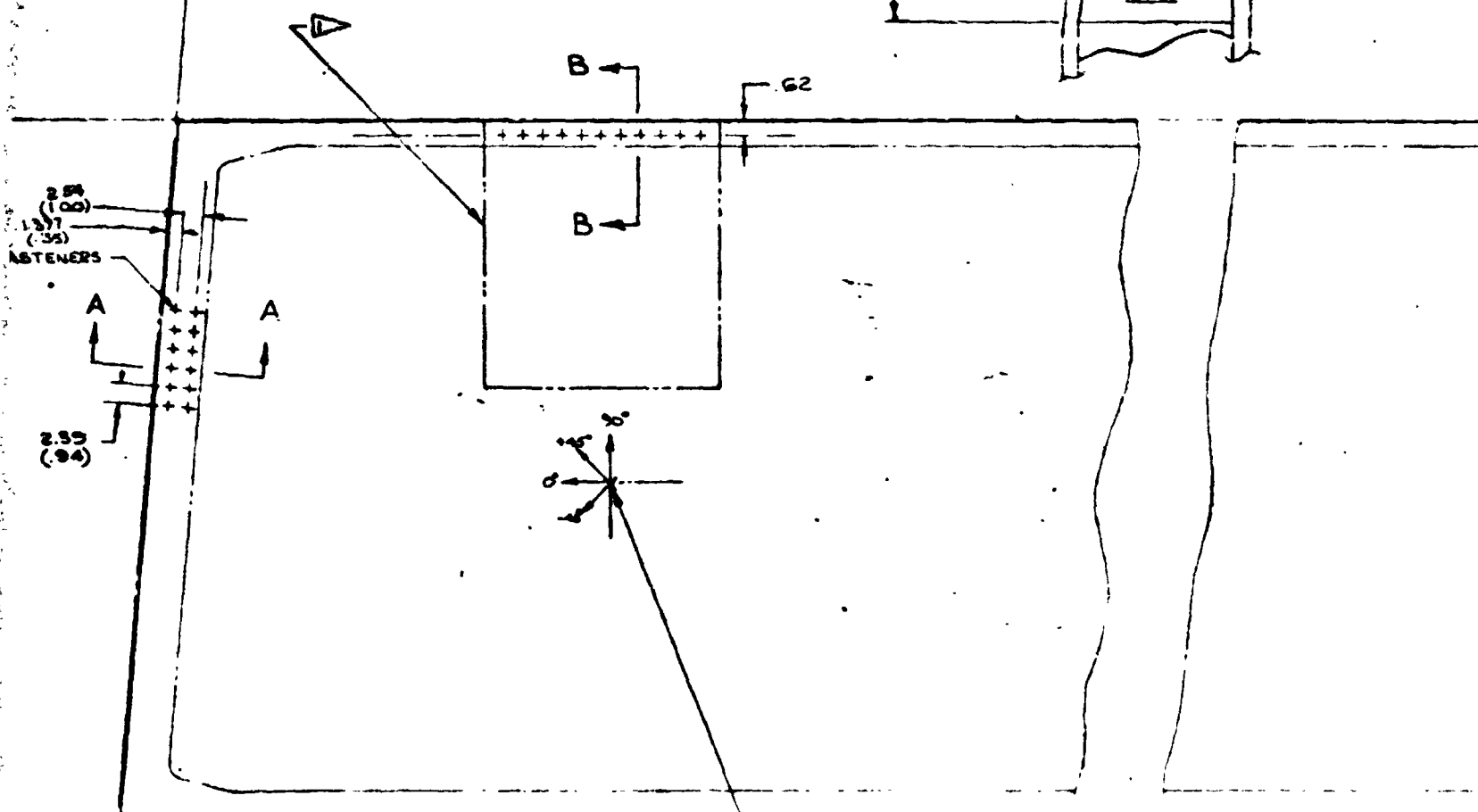
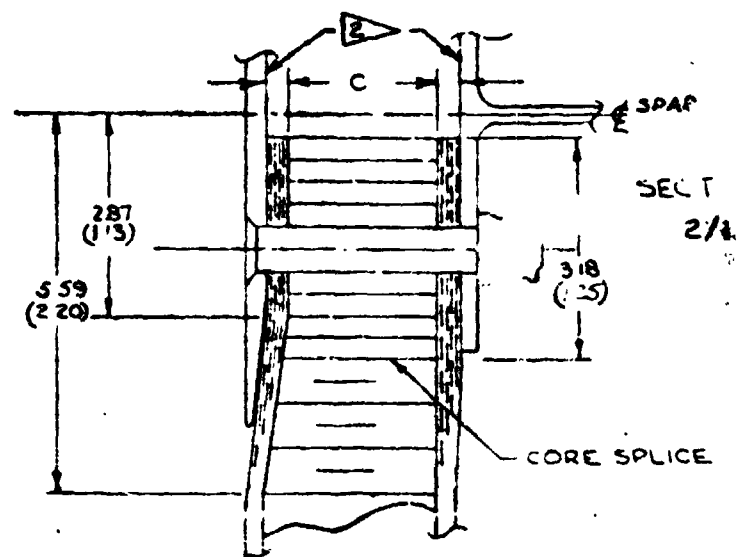
UPR SUR
LWR SUR
LWR SUR

	DIMENSION			
SECTION	A	B	C	
UPPER SURFACE	2.48 (.098)	2.54 (.100)	3.20 (.126)	
MIDDLE SURFACE	3.02 (.119)	1.91 (.075)	3.73 (.147)	
LOWER SURFACE	2.49 (.098)	1.91 (.075)	3.20 (.126)	

WITHOUT FRAME

LANDING GEAR RIB

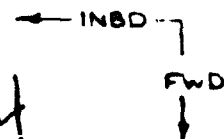
9



UPR SURFACE [C4, *45°]
 LWR SURFACE [C4, *45°]
 LWR SURFACE [C4, *45°]



DETAIL-C
 (ROTATED 90°)
 1/4 SCALE



FOLDOUT FRAME 4

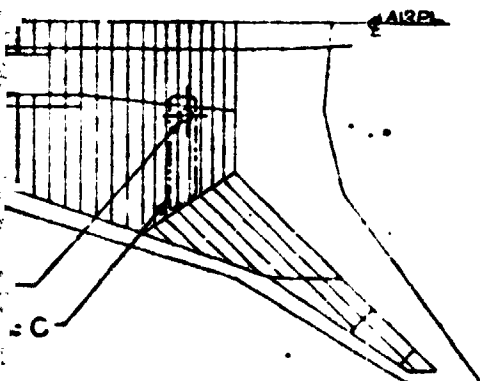


SE
BA
C

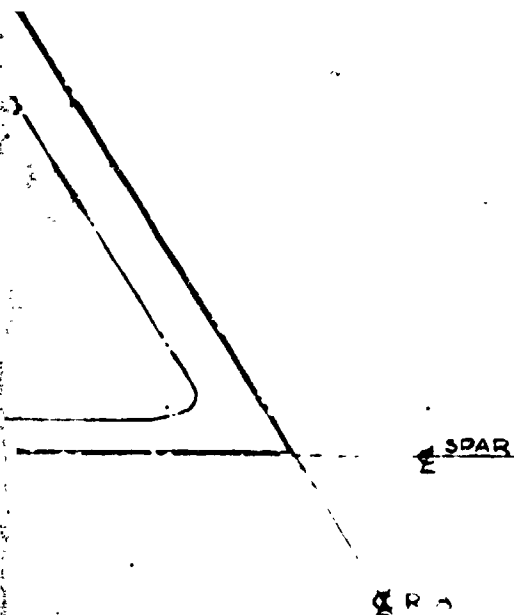
ME 5

100-100000
 100-100000
 100-100000
 100-100000

CHG	DESCRIPTION	DATE	APPRO
A	REVISED DWG TO REFLECT ONE UPR & TWO LWR SURFACE DESIGNS REVISED $\Delta \Delta \Delta$ ADDED $\Delta \Delta$ CHANGED TO SHT 1 OF 2	5-30-74	JOHN PETER STERN -BANK



SEE A A



- 1. PER AF DESIGN GUIDE DATA EXCEPT FOR SHEAR DATA (PROJECTED FROM NASA-LANGLEY DATA) LOWER SURFACE BORSIC/ALUM SKIN ASSY CONSOLIDATED OF 14 PLYS OF .007 IN/PLY MATERIAL
(5) 0° PLYS, (4) +45° PLYS, (4) -45° PLYS, (1) 90° PLY
- 2. PER AF DESIGN GUIDE DATA LWR SURFACE BORSIC/ALUM SKIN ASSY CONSOLIDATED OF 17 PLYS OF .007 IN/PLY MATERIAL
(4) 0° PLYS, (6) +45° PLYS, (6) -45° PLYS, (1) 90° PLY
- 3. TYP BOTH SKINS SKINS SYM ABOUT $\frac{1}{2}$ OF CORE
- 4. .007 THICK-TITANIUM SHIM GAL-4V COND I
4 METAL PLYS PER SKIN REQUIRED FOR BOTH UPPER AND LOWER PANEL ASSEMBLIES
- 5. BRAZE PANEL ASSEMBLY - (BRAZE CYCLE TIME & TEMPERATURE UNDETERMINED)
- 6. 450 KCM (28 PCF) SS2-60 CORE TIGAL-4V
- 7. 78.5 KCM (49 PCF) - SC4-10 CORE TI-3AL-26V
- 8. BORSIC ALUMINUM SKIN ASSY ABLY CONSOLIDATED OF 14 PLYS OF .007 IN/PLY MATERIAL
(4) 0° PLYS, (5) +45° PLYS, (5) -45° PLYS
- 9. TITANIUM GAL-4V COND I
- 10. PT 269 CONTROL POINT COUPON SIZE AND LOCATION SAME AS USED FOR TASK I

SEE AWS-100 FOR LOADS & ENVIRONMENTAL CONDITIONS

BASIC DIMENSIONS - CENTIMETERS

() DIMENSIONS - INCHES

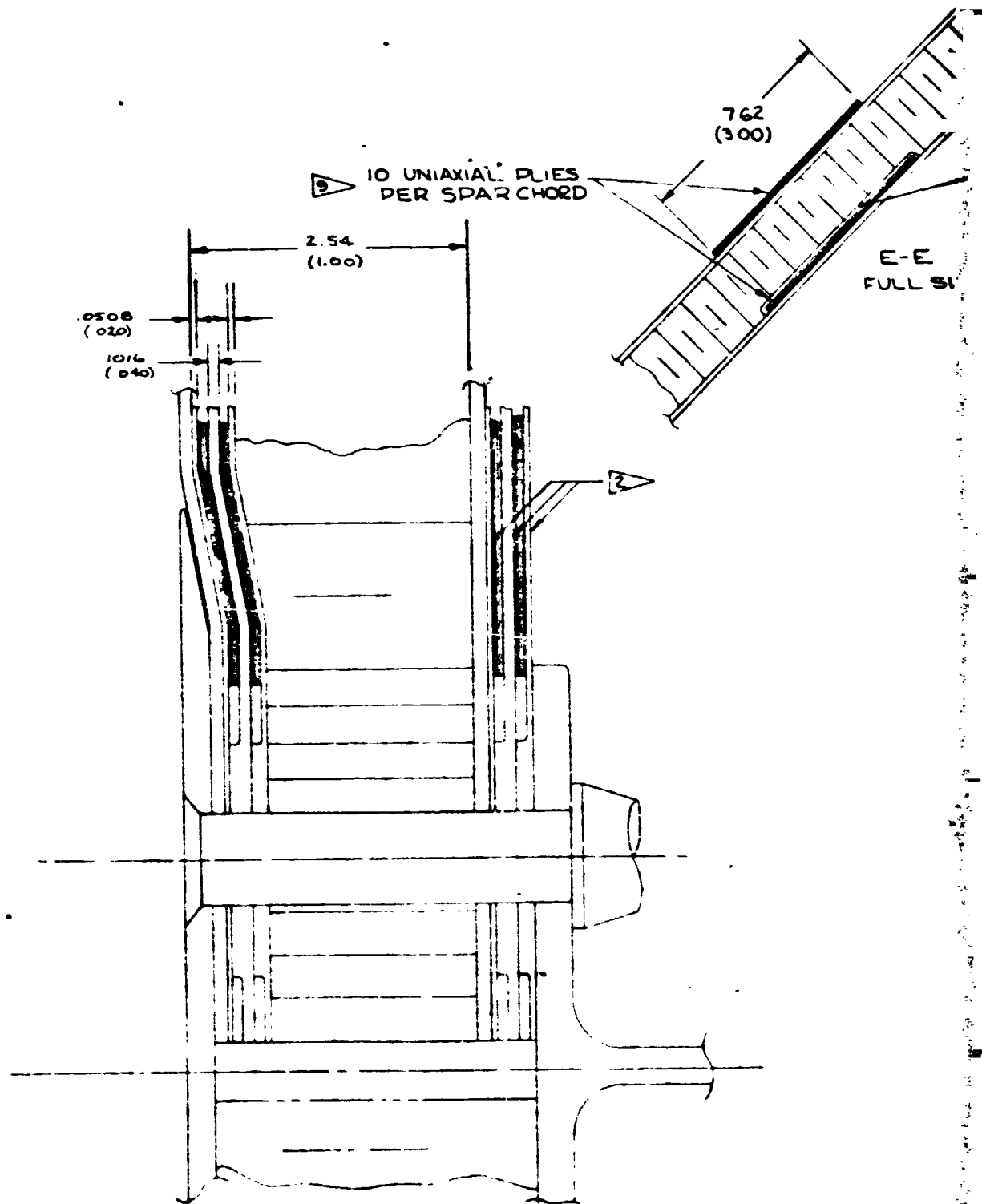
FOLDOUT FRAME

PRECEDING PAGE BLANK NOT FOLDED

Figure 14.7 -

USED ON	DATE	BY	APPROVED
SECT NO	DATE	BY	APPROVED
CHG NO	DATE	BY	APPROVED
GROUP ORG	DATE	BY	APPROVED

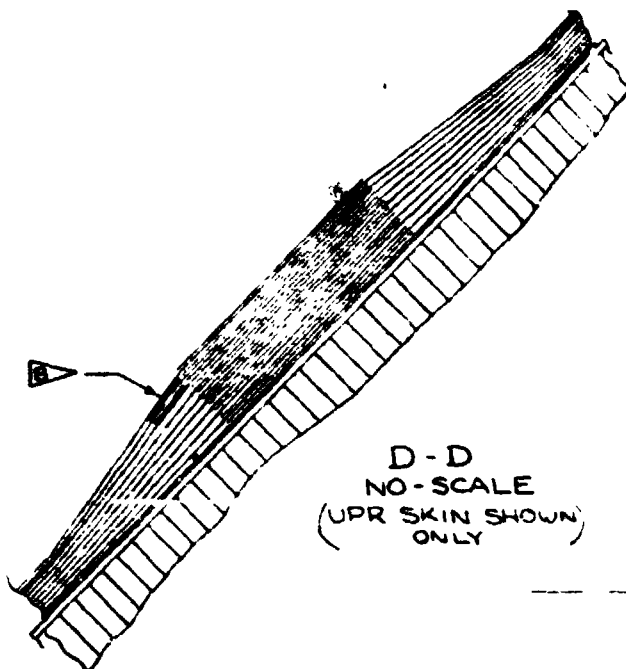
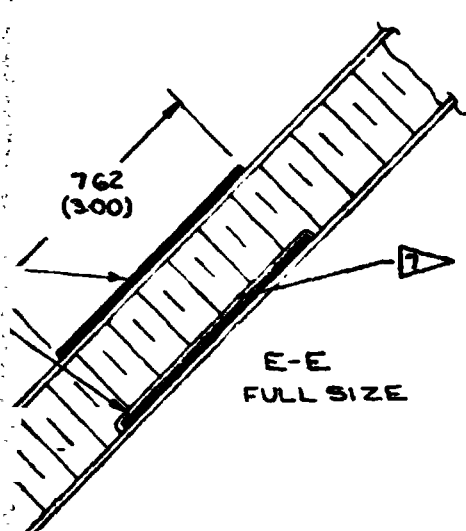
BRAZED TWO PANEL ASSY
BORSIC/ALUM SKIN ASSY
CORE 9.3336
AW 5-145



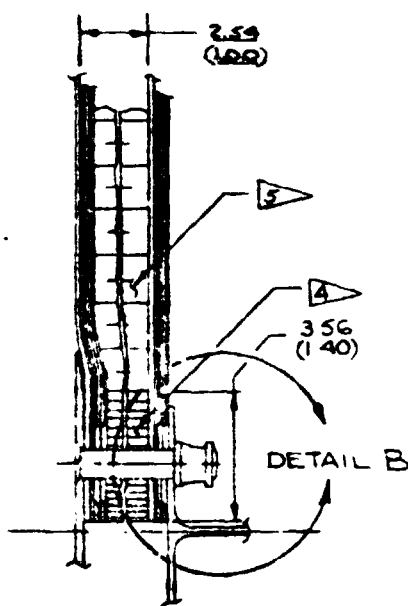
DETAIL-B
4/1 SCALE

FOLDOUT

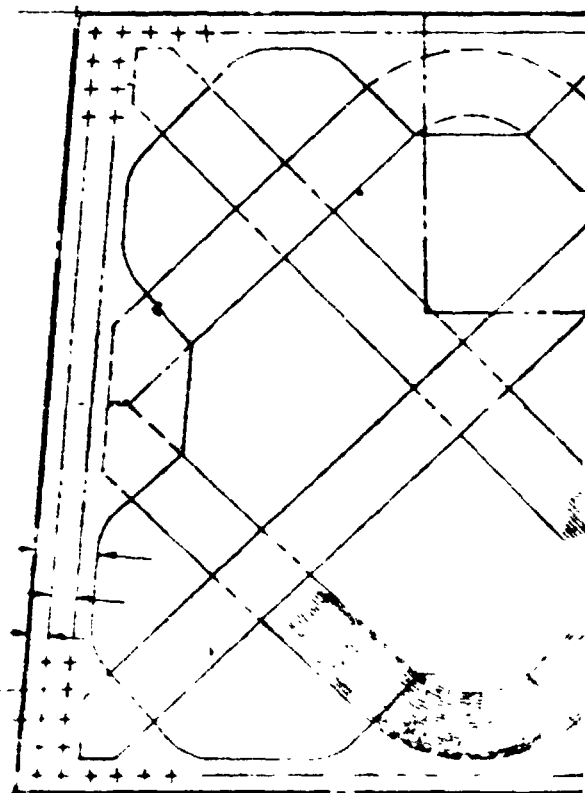
FOLDOUT FRAME



LANDING GEAR RIB



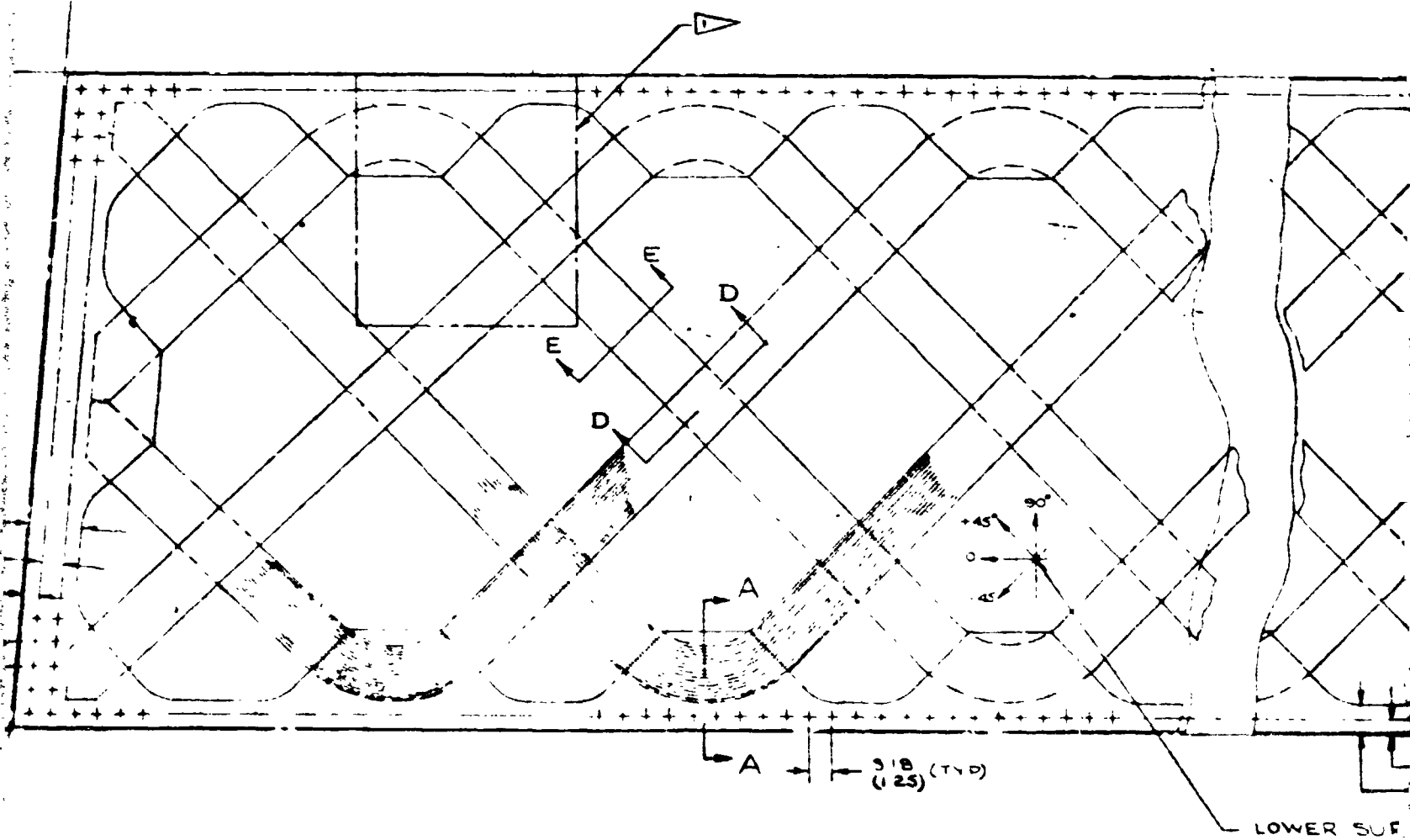
6.604 (260)
3.175 (125)
1.727 (68)
3.18 (125)



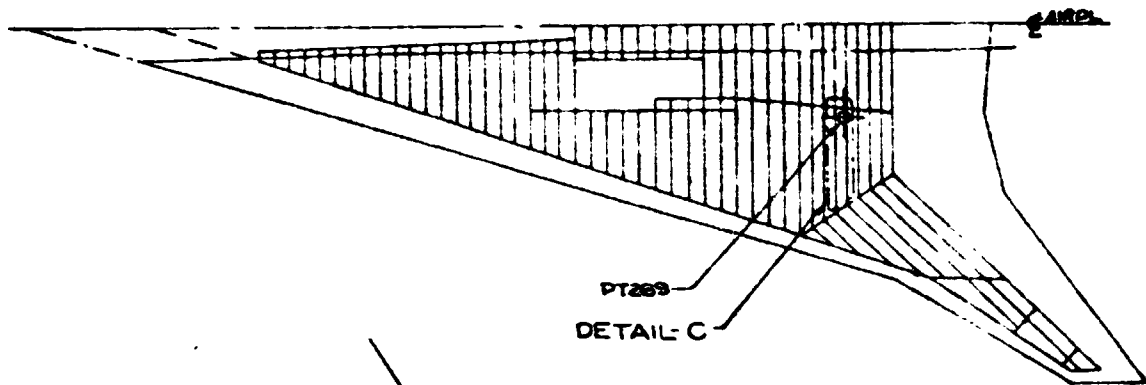
REPRODUCIBILITY OF THE
ORIGINAL PAGE IS POOR

FOLDOUT FRAME

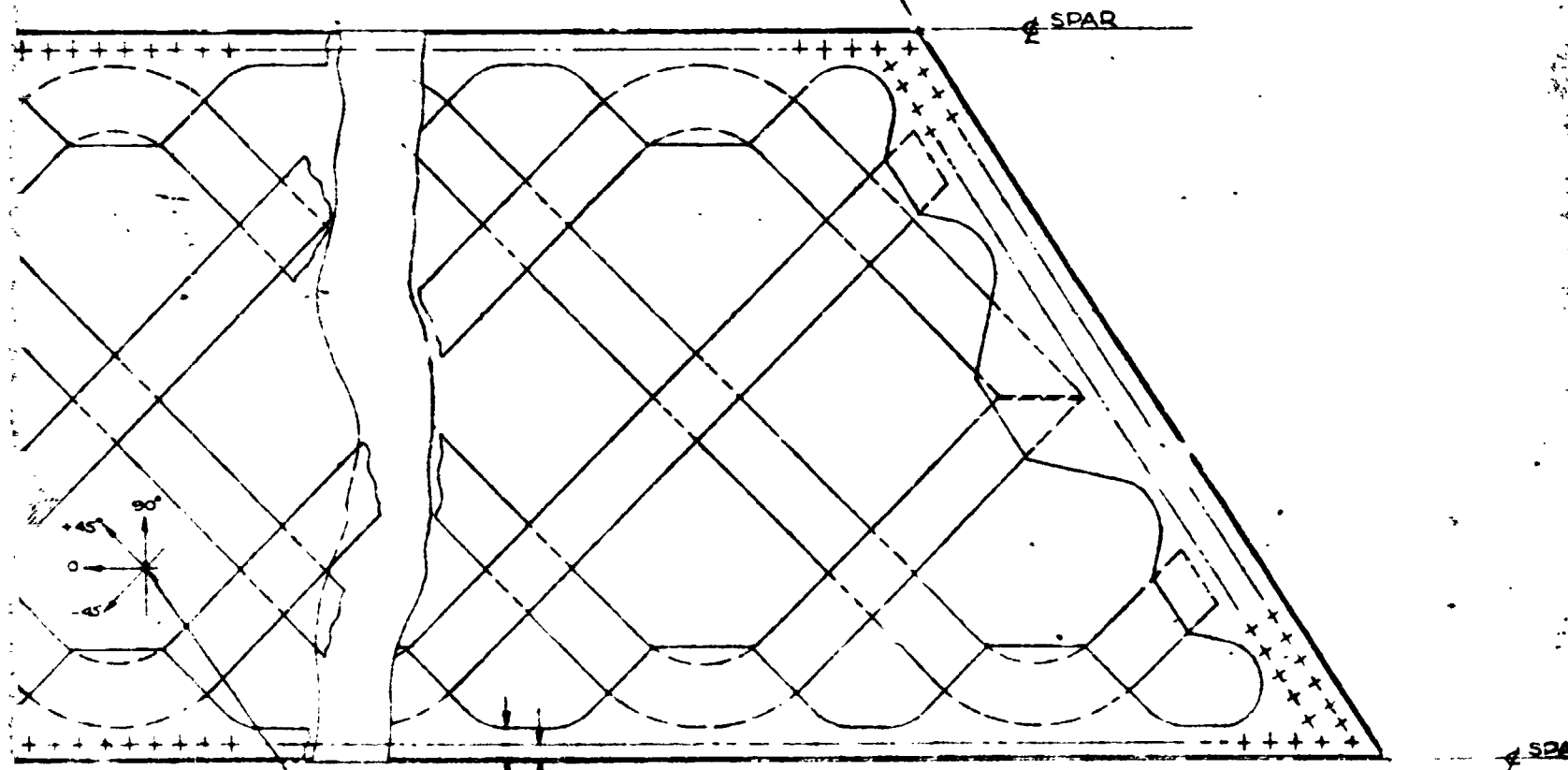
LANDING GEAR RIB



FOLDOUT FRAME



PT283
DETAIL C



SPAR

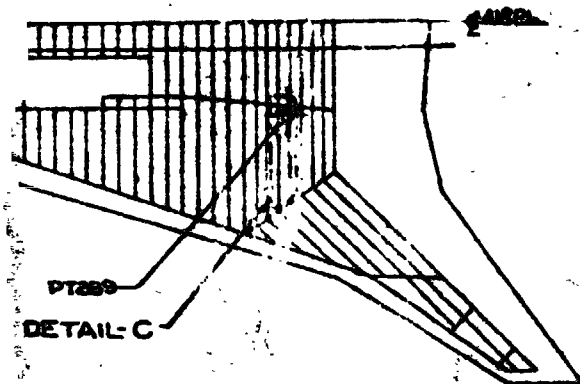
RIB

LOWER SURFACE $[0_2/90]_3$

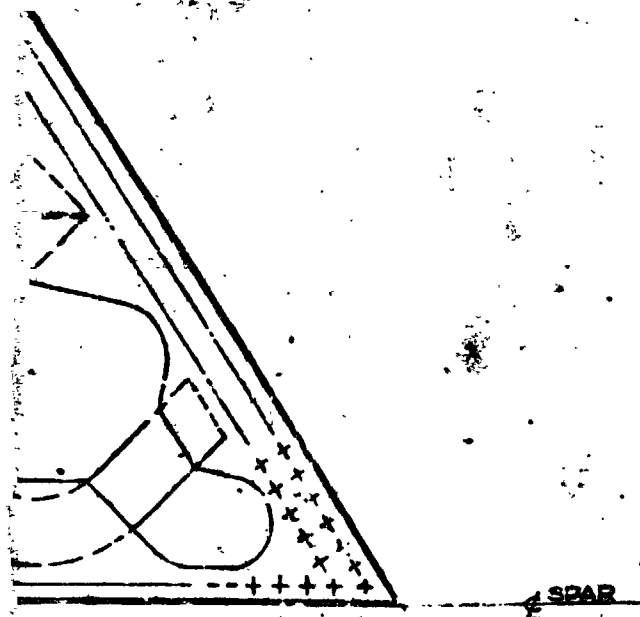
171
(68) 343
(135)

(T10)

FOYDOOT FRAME 4



SPAR



RIB

PREVIOUS PAGE BLANK NOT FIL

- ▷ BORSIC ALUMINUM CONSOLIDATED OF .007 IN./PLY MATERIAL. NUMBER OF PLYS AND ORIENTATION TO BE AS NOTED PER DWG
- ▷ LAMINATE TRANSITION TO BE FILLED BY DRESSED ALUMINUM ROD DURING CONSOLIDATION
- ▷ CORE RELIEF LOCALLY OVER SHEAR TRUSS EXCEPT AT PANEL EDGES
- ▷ BRAZE PANEL ASSEMBLY - (BRAZE CYCLE TIME & TEMPERATURE UNDETERMINED)
- ▷ 450 KCM (28.1 PCF) - SS2-60 CORE TIGAL-4V
- ▷ 78.5 KCM (4.9 PCF) - SC4-20 CORE TI-SAL-26V
- ▷ BORSIC ALUMINUM SKIN ASSEMBLY CONSOLIDATED OF 6 PLYS OF .007 IN./PLY MATERIAL (5) - 0° PLYS, (1) - 90° PLY
- ▷ TITANIUM 6AL-4V COND I
- ▷ PT 269 CONTROL POINT COUPON SIZE AND LOCATION SAME AS USED FOR TASK I

SEE AWS-100 FOR LOADS & ENVIRONMENTAL CONDITIONS

BASIC DIMENSIONS - CENTIMETERS

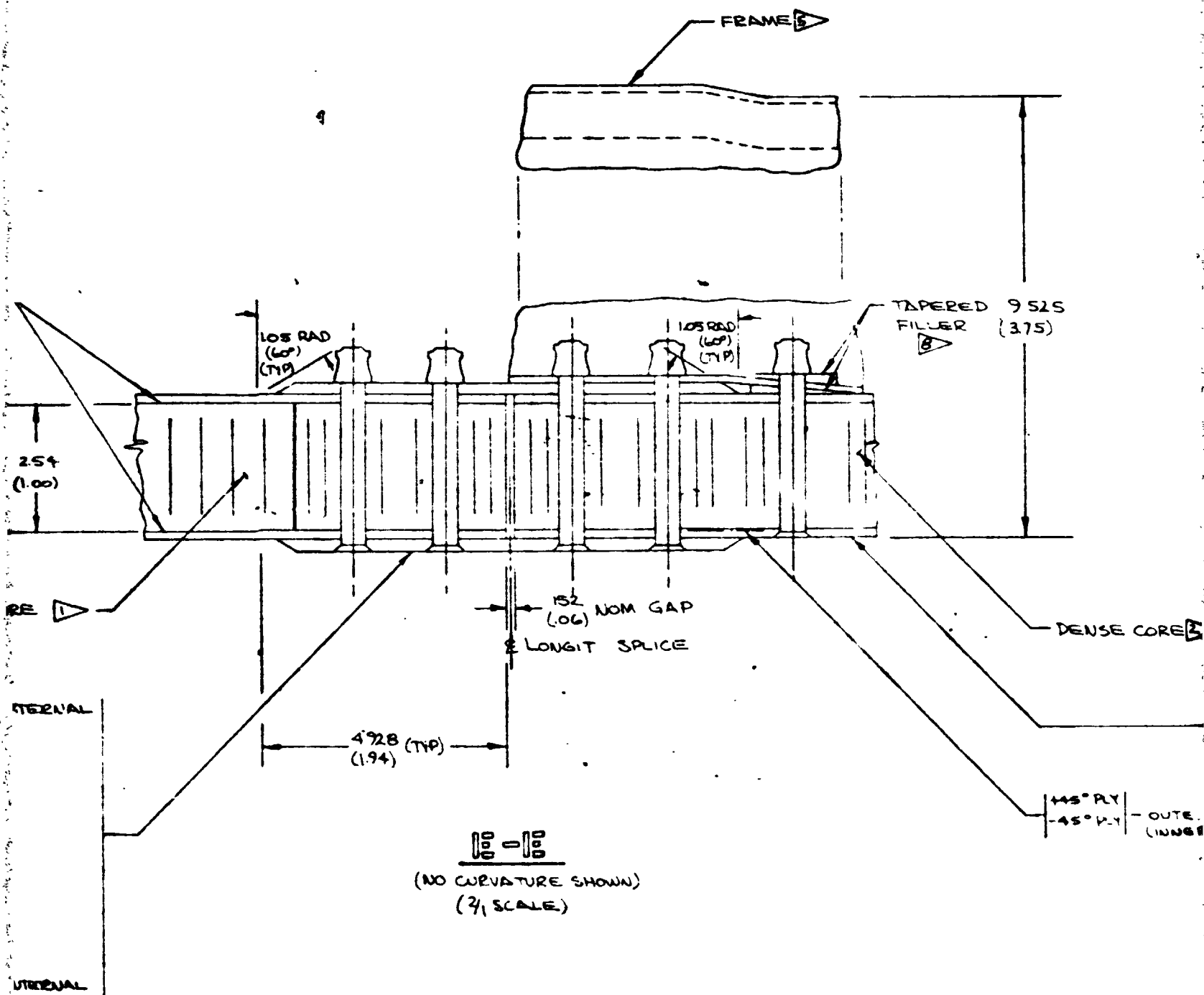
() DIMENSIONS - INCHES

REPRODUCIBILITY OF THE ORIGINAL PAGE IS POOR

Figure 14-8.-

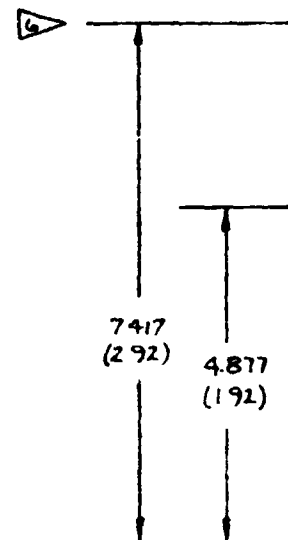
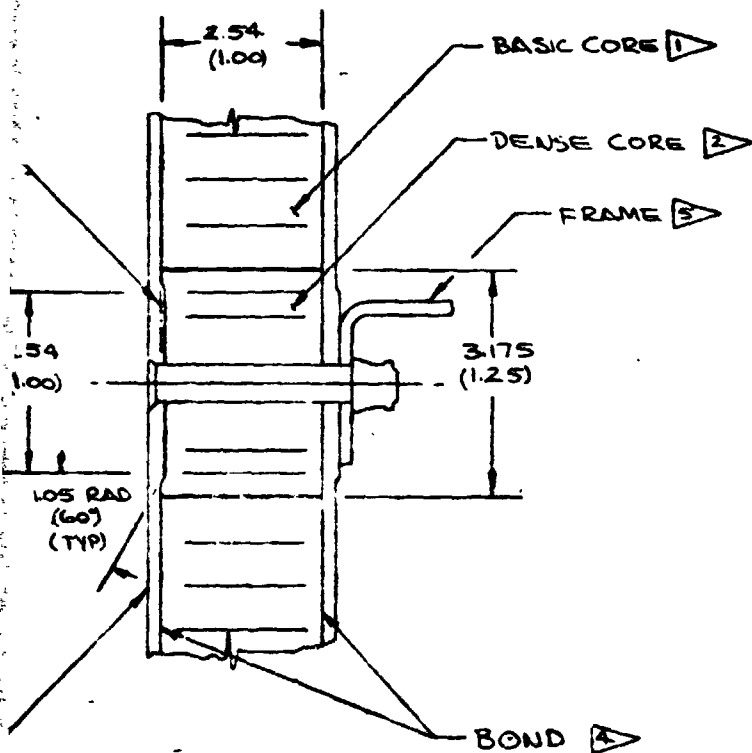
USED ON	DESIGN	DATE	THE JOE COMPANY COMMERCIAL AIRPLANE DIV. REAR WASH
	IN TOMLINSON	5/7/74	
	CHECKED		BRAZED HC LWR SURF PANEL BORSIC/ALUM SKINS TITANIUM-CORE 969-336C
	STRESS	5/7/74	
SECT NO	ENGR	5/7/74	IDENT NO 8125
	GROUP		
CHG NO	PROJ		J AWS-145
GROUP NO			
			SCALE NOTED

FOLDOUT FRAME

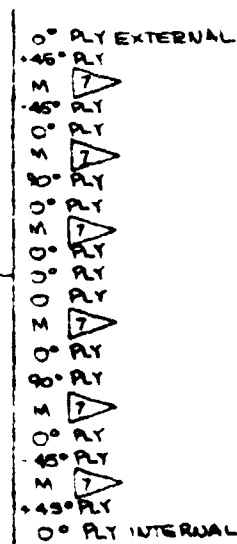


REPRODUCIBILITY OF THE
ORIGINAL PAGE IS POOR

FOLDOUT FRAME



OUTER SPLICE PLATE
(INNER SPLICE PLATE TIP)

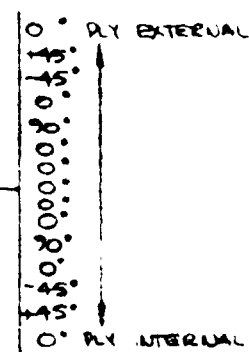


152
(06) NOM GAP

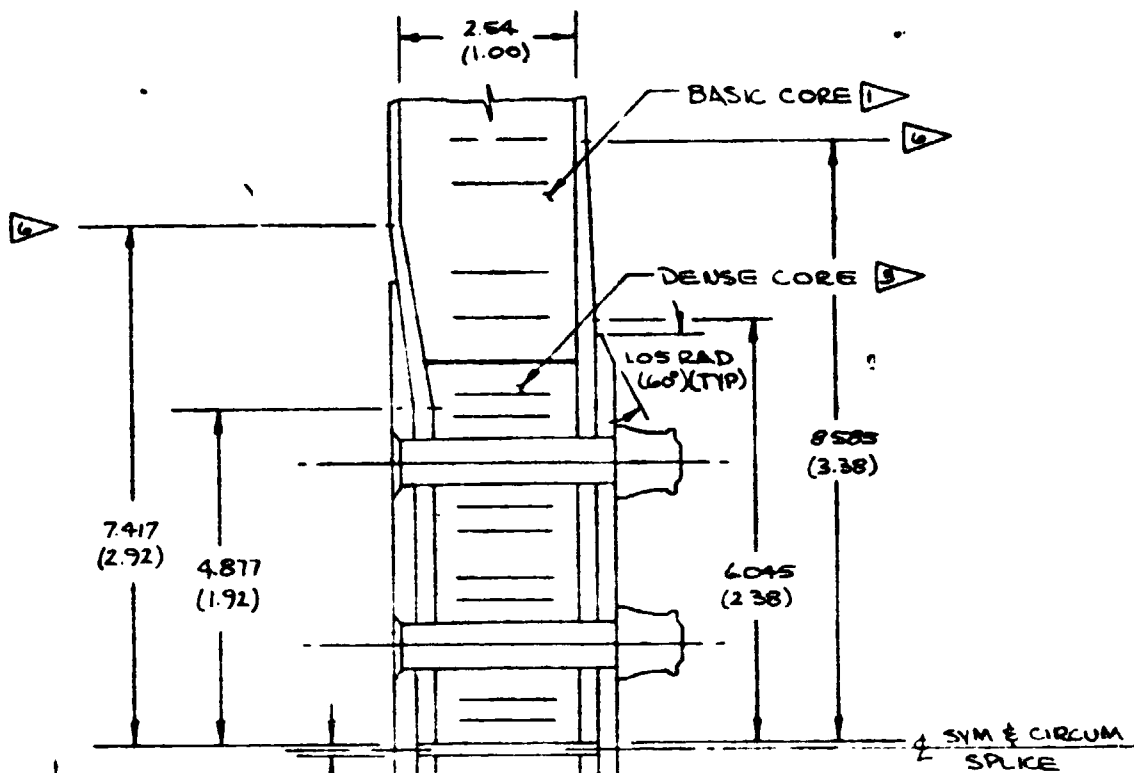
13-13
(2/ SCALE)

REPRODUCIBILITY OF THE
ORIGINAL PAGE IS POOR

OUTER FACE SHIT
(INNER FACE SHIT TIP)



FOLDOUT FRAME 4



PLY EXTERNAL
 0° 30° 45° 60° 75° 90° 105° 120° 135° 150° 165° 180°
 PLY INTERNAL

.152 (06) NOM GAP

PLY EXTERNAL
 0° 30° 45° 60° 75° 90° 105° 120° 135° 150° 165° 180°
 PLY INTERNAL

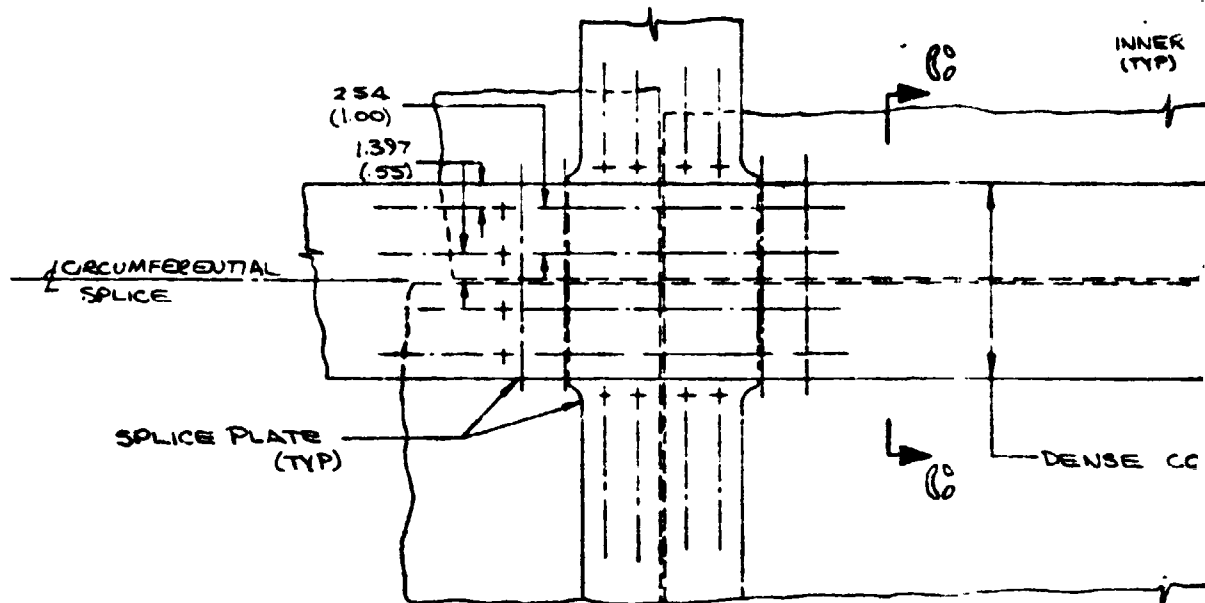
INNER FACE SMT EDGE RGTUF
 (OUTER FACE SMT TTP)

SMT TTP
 PLY EXTERNAL
 0° 30° 45° 60° 75° 90° 105° 120° 135° 150° 165° 180°
 PLY INTERNAL

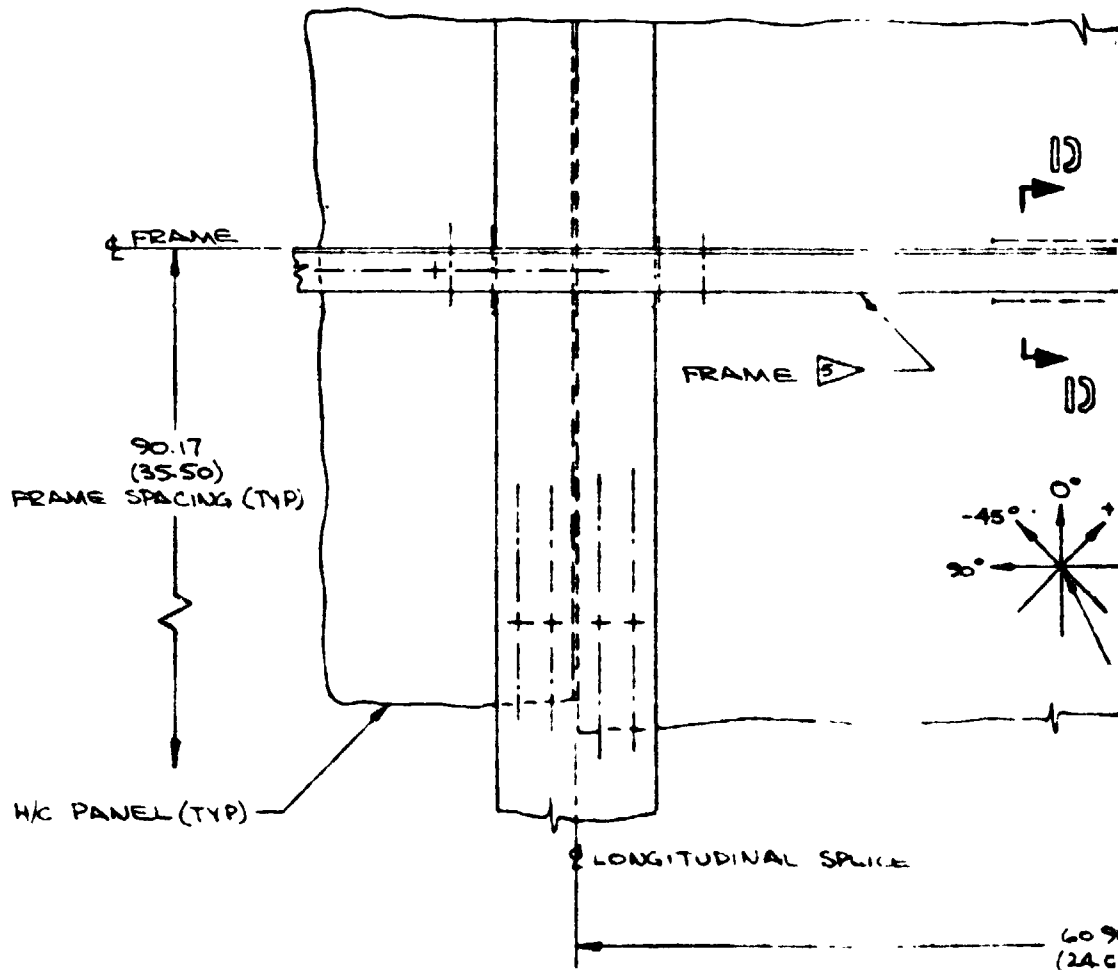
BOND

C-C
 (2/ SCALE)

FOLDOUT FRAME 5



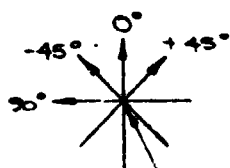
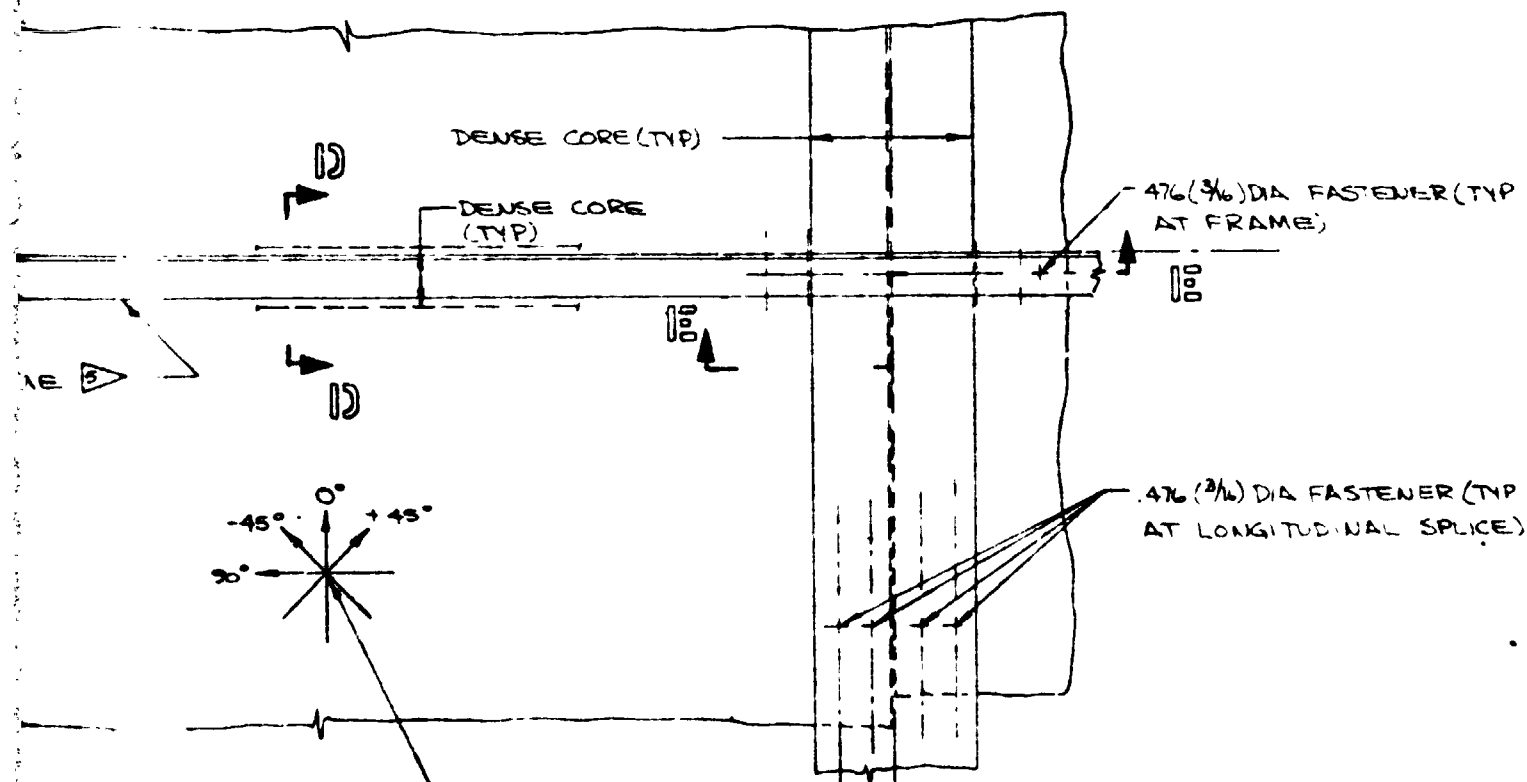
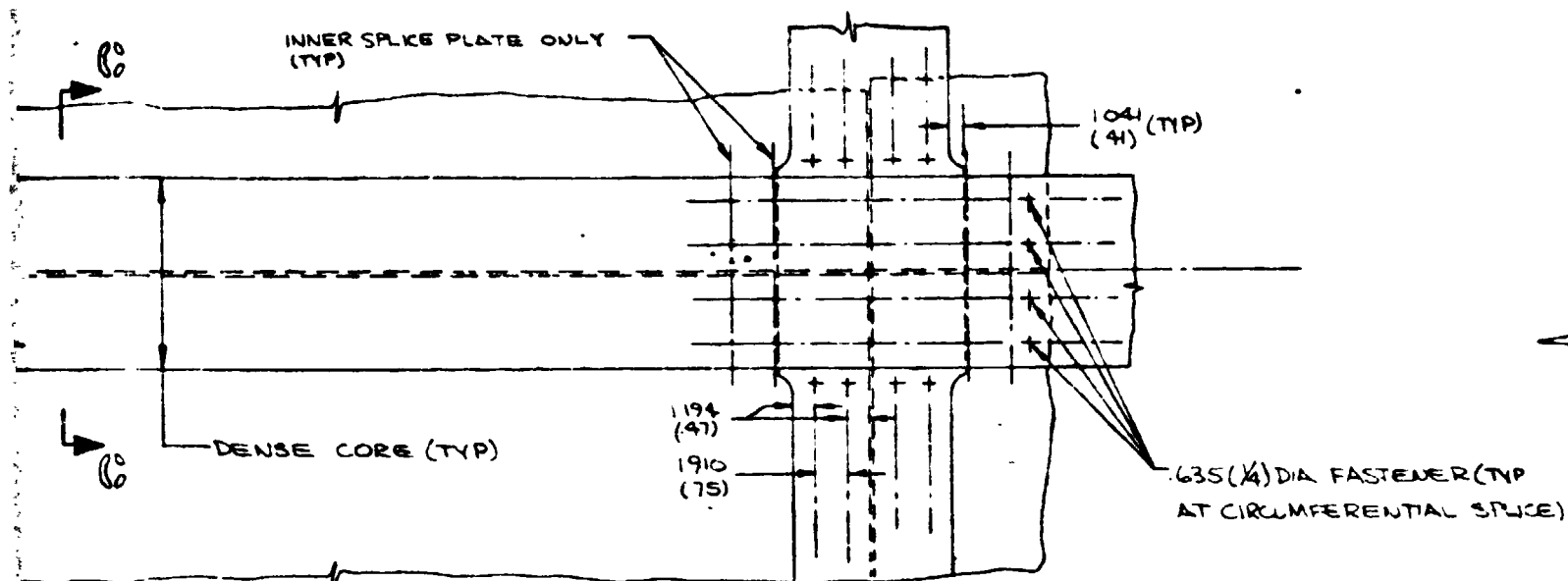
CIRCUM
-KE



INNER FACE SHT EDGE REINF
(OUTER FACE SHT TYP)

FOLDOUT FRAME 6

13-11
(1/2 SCA
FWC



AL SPLICE [0°, ±45°, 90°] (TYP & 4 FACE SHIT)

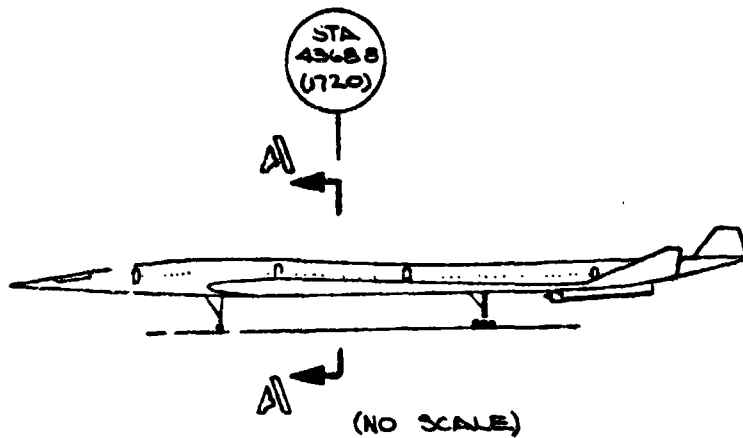
LONGITUDINAL SPLICE

60% (24.0) (TYP)

13-13
(1/2 SCALE)

FWD

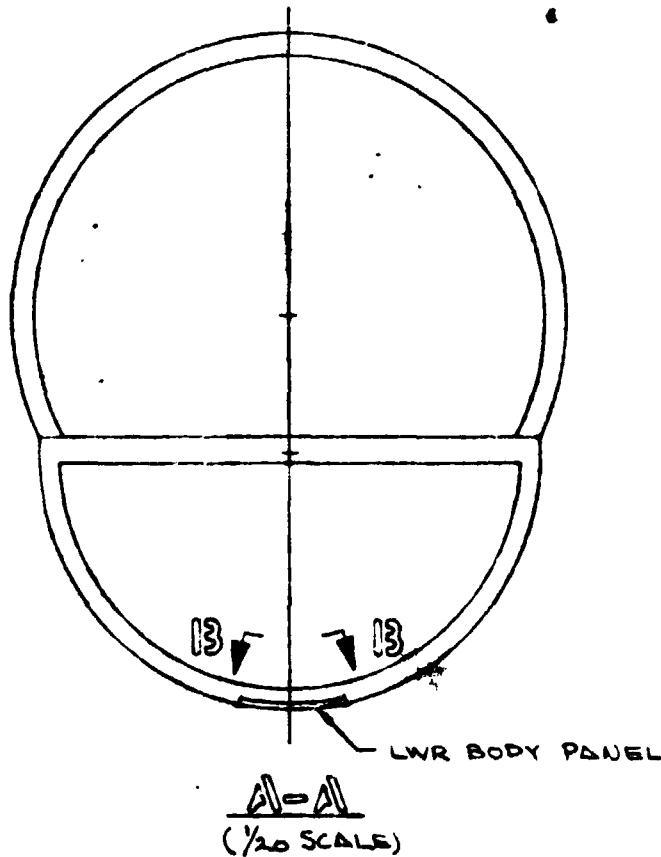
FOLDOUT FRAME 7



(1/4) DIA FASTENER (TYP
CIRCUMFERENTIAL SPLICE)

(1/4) DIA FASTENER (TYP
LONGITUDINAL SPLICE)

(1/4) DIA FASTENER (TYP
LONGITUDINAL SPLICE)



2 BASIC
081

A) 10N
B) 10N

2 2024

7 .007

4 EDG

5 7-

7 ADV
(ADV)

3 450
TI-

2 226
TI-

1 78N
TI-

BASIC DI
() DI

NO. 1017 FRAMPI 3

2 BASIC PL1 ORIENTATION FOR ALL ASSYS
0052 IN/PLY HIGH STRENGTH GRAPHITE/PPQ MATERIAL

A) INNER & OUTER FACE SHT ASSYS:
FACE SHT & PAD-UP

B) INNER & OUTER SPLICE PLATE ASSYS

8 2024-T3 ALUMINUM

7 .007 THICK SHIM TI-6AL-4V COND I

6 EDGE TITANIUM SHIM

5 TI-6AL-4V COND I

4 ADHESIVE BOND
(ADHESIVE & CURE CYCLE UNDEFINED)

3 450 Kg/M³ (281 Lb/FT³) H/C CORE SC2-60
TI-6AL-4V

2 226 Kg/M³ (141 Lb/FT³) H/C CORE SC2-30
TI-6AL-4V

1 78 Kg/M³ (49 Lb/FT³) H/C CORE SC4-20
TI-3AL-2.5V

PRECEDING PAGE BLANK NOT FIL

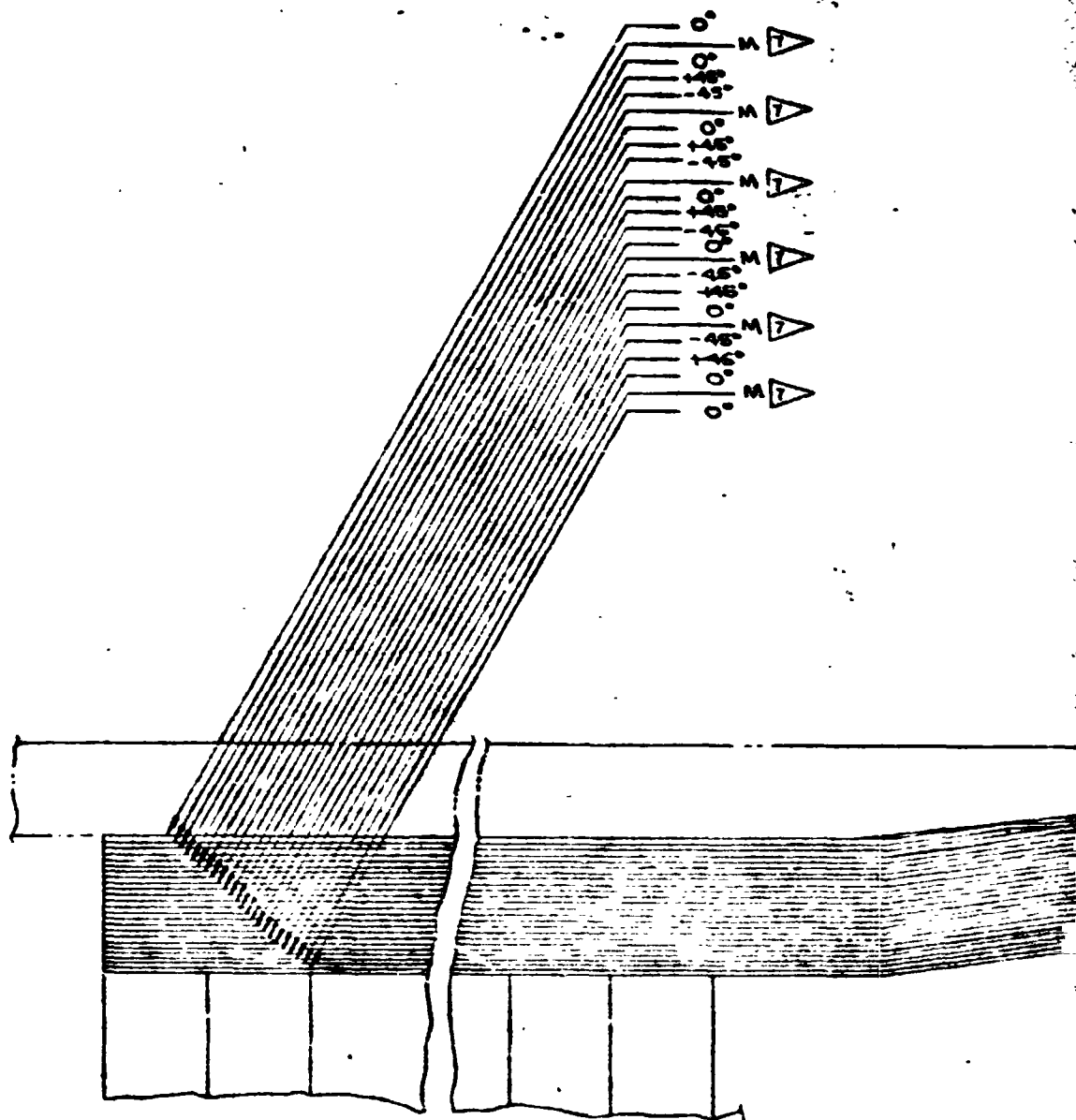
BASIC DIMENSIONS-CENTIMETERS

() DIMENSIONS-INCHES

Figure 14.9 -

USED ON	DRAWN BY	DATE	THE	COMPANY
	CHECKED		COMMERCIAL	Y. T. TON WA
SECT NO	STRESS		GRAPHITE/PPQ BODY	
	ENGR.		H/C SANDWICH SKIN	
CHG NO	GROUP		X, 1-336C M-2?	
GROUP ORG	PROJ		CODE	
			IDENT NO	
			81/05	J. V. S. - 142
			SCALE	

FOLDOUT FRAME



(TYP BOTH FACE SHTS)

DETAIL-13

10/1 SCALE

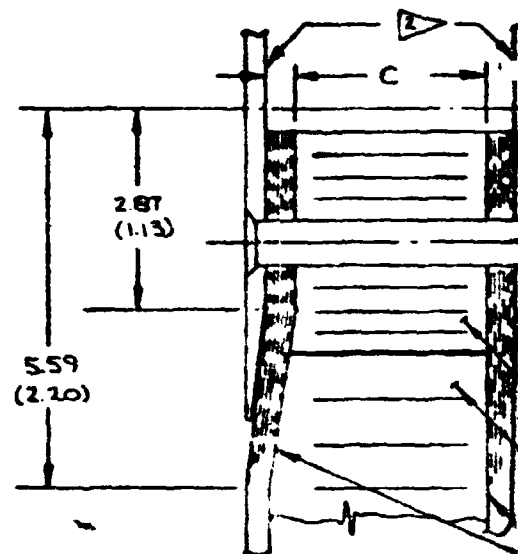
(UPPER SURFACE PANEL SHOWN, LWR SURFACE TYP)

FOLDOUT FRAME



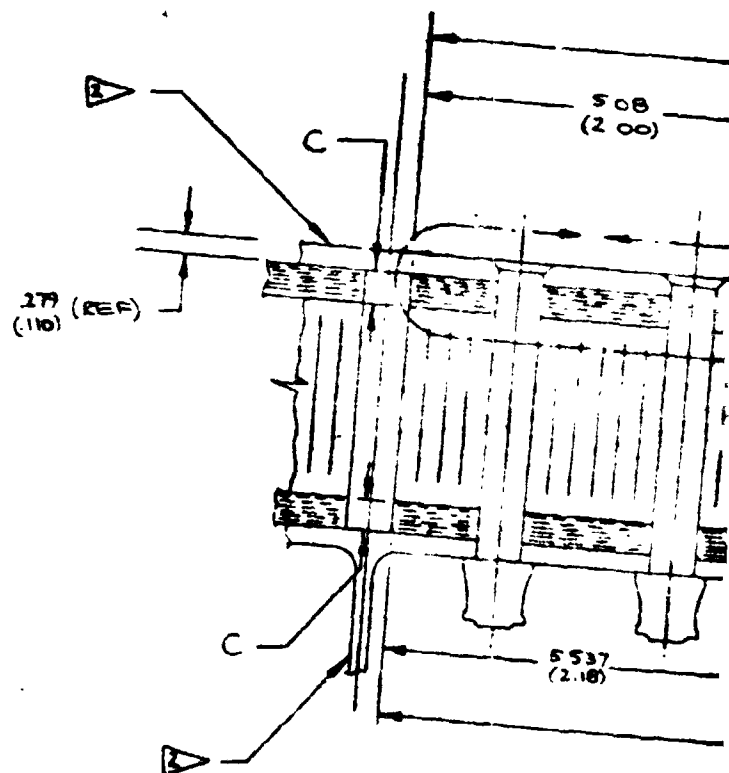
E		
LOCATION	A	
UPR SURFACE	2377 (0936)	3 (11)
LWR SURFACE	2509 (0988)	1 (6)

FOLDOUT FRAME 2



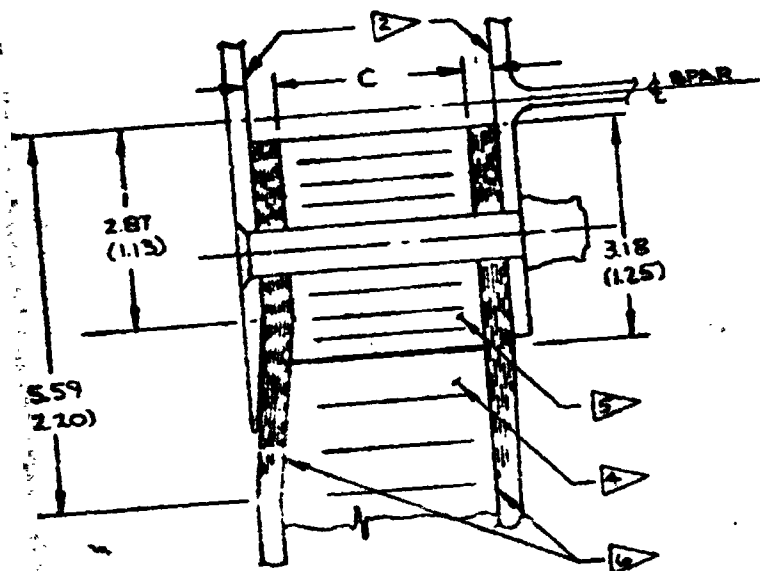
C-C
1/4 SCALE

LOCATION	DIMENSION				
	A	B	C		
UPR SURFACE	2377 (.0936)	3.175 (.125)	3444 (.1356)		
LWR SURFACE	2509 (.0988)	1905 (.75)	3876 (.1408)		

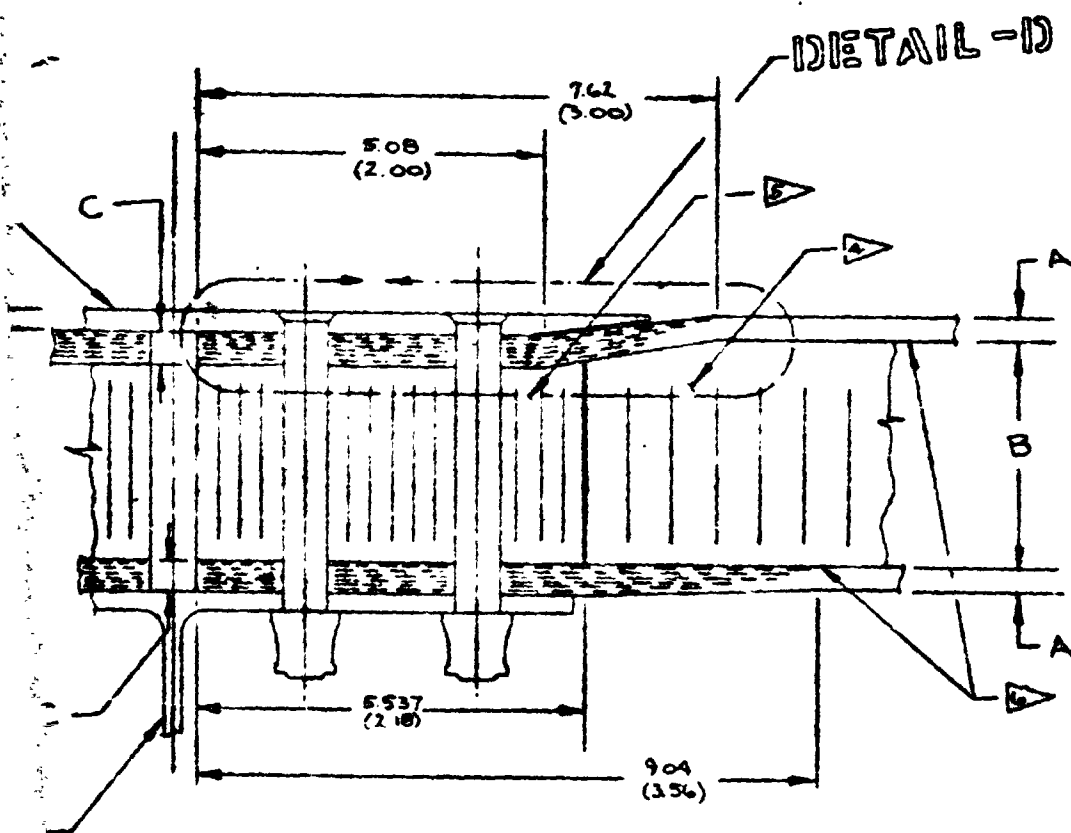


B-B
1/4 SCALE

FOLDAWAY FRAME 3



C-C
3/4 SCALE



13-13
3/4 SCALE

435 OD FASTENERS
(250) (TYP)

2.34
(.95)

13

2.34
(.95)

FOLDOUT FRAME 4

LANDING GEAR RIB

1397 UPR SURFACE PANEL
(65)
1575 LWR SURFACE PANEL
(62)

254
(100)

13

13

254
(100)



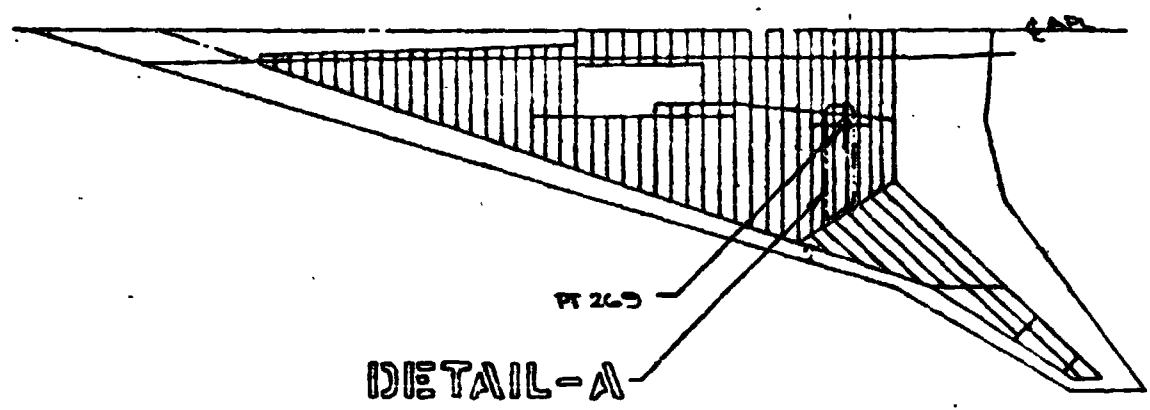
UPR SURFACE [08, ±45s] 3 8
LWR SURFACE [08, ±45s, 90] 3 8

DETAIL-A
(ROTATED 90°)
1/4 SCALE

← INBD
FWD
↓

FOLDOUT FRAME 5

CHG
A



DETAIL-A

PT 269

SPAR

SEE 13-13

9 HIGH STRENGTH
18 PLIES
(8) 0° PLIES

8 TYP BOTH

7 007 THICK
6 METAL

6 ADHESIVE
(ADHESIVE)

5 450 KCM

4 78.5 KCM

3 HIGH STRENGTH
18 PLIES
(8) 0° PLIES

2 TITANIUM

1 PT 269 C
SAME AS

SEE AWS-101

BASIC DIMENSIONS
() DIMENSIONS

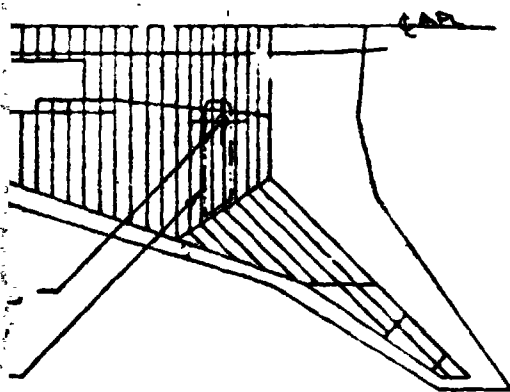
SPAR

RB

FORGET IT

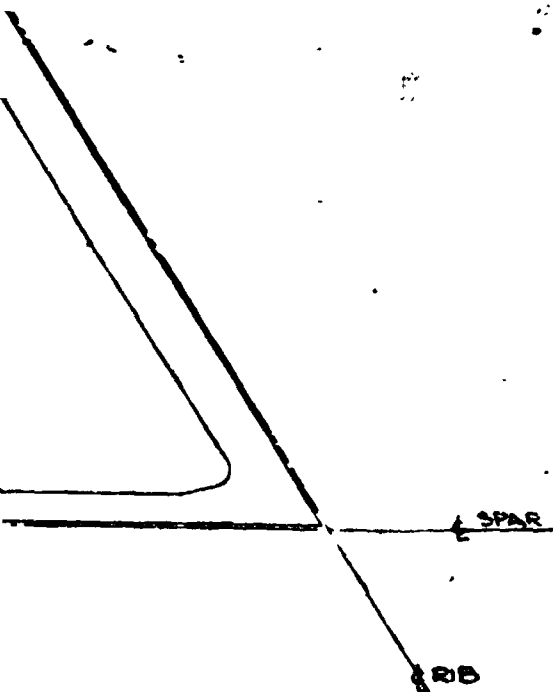
USED ON	DRAWN
	CHECK
SECT NO	STRESS
CHG NO	ENG
GROUP NO	GROUP
	PROJ

FOLD



SPAR

SEE 13-13



CHG	DESCRIPTION	DATE	APPD.
A	REVISED DWG TO ADD LWR WING SURFACE DESIGN ADDED 3	6/19/84	DESIGN: 725 STRESS: 725 MATERIAL: 725

3 HIGH STRENGTH GRAPHITE/PPQ SKIN ASSEMBLY
13 PLYS OF .0052 IN/PLY MATERIAL
(8) 0° PLYS, (5) +45° PLYS, (5) -45° PLYS, (1) 90° PLYS

3 TYP BOTH SKINS SKINS SYM ABOUT $\frac{1}{2}$ OF CORE

7 007 THICK-TITANIUM SHIM GAL-4V COND I
6 METAL PLYS PER SKIN REQUIRED

4 ADHESIVE BOND
(ADHESIVE & CURE CYCLE UNDEFINED)

3 450 KCM (281PCF) SS2-60 CORE TI-6AL-4V

4 78.5 KCM (49PCF) SC4-20 CORE TI-3AL-2.5V

3 HIGH STRENGTH GRAPHITE/PPQ SKIN ASSEMBLY
18 PLYS OF .0052 IN/PLY MATERIAL
(8) 0° PLYS, (5) +45° PLYS, (5) -45° PLYS

2 TITANIUM GAL-4V COND I

1 PT 269 CONTROL POINT COUPON SIZE & LOCATION
SAME AS USED FOR TASK I

SEE AWS-100 FOR LOADS & ENVIRONMENTAL CONDITIONS

BASIC DIMENSIONS - CENTIMETERS

() DIMENSIONS - INCHES

NOTHING PAGE BLANK NOT FILED

Figure 14.10.-

SEE SHEET 1 FOR PL FOR LIST OF MATERIAL USAGE AND NOTES

USED ON	DRAWN D. S. H. W. C.	DATE 6-19-84	THE T. C. H. G. COMPANY COMMERCIAL AIRCRAFT DIV. - RENTON WASH.
SECT NO	CHECKED		BONDED WING H/C PANEL GRAPHITE/PPQ SKINS 969-336C M-2.7
CHG NO	STRESS B. S. H. W. C.	6-19-84	CODE IDENT NO 81235
GROUP ORG	ENG D. S. H. W. C.		J AWS-146
	GROUP		SCALE NOTED
	PROJ		SM

FOLDOUT FRAME

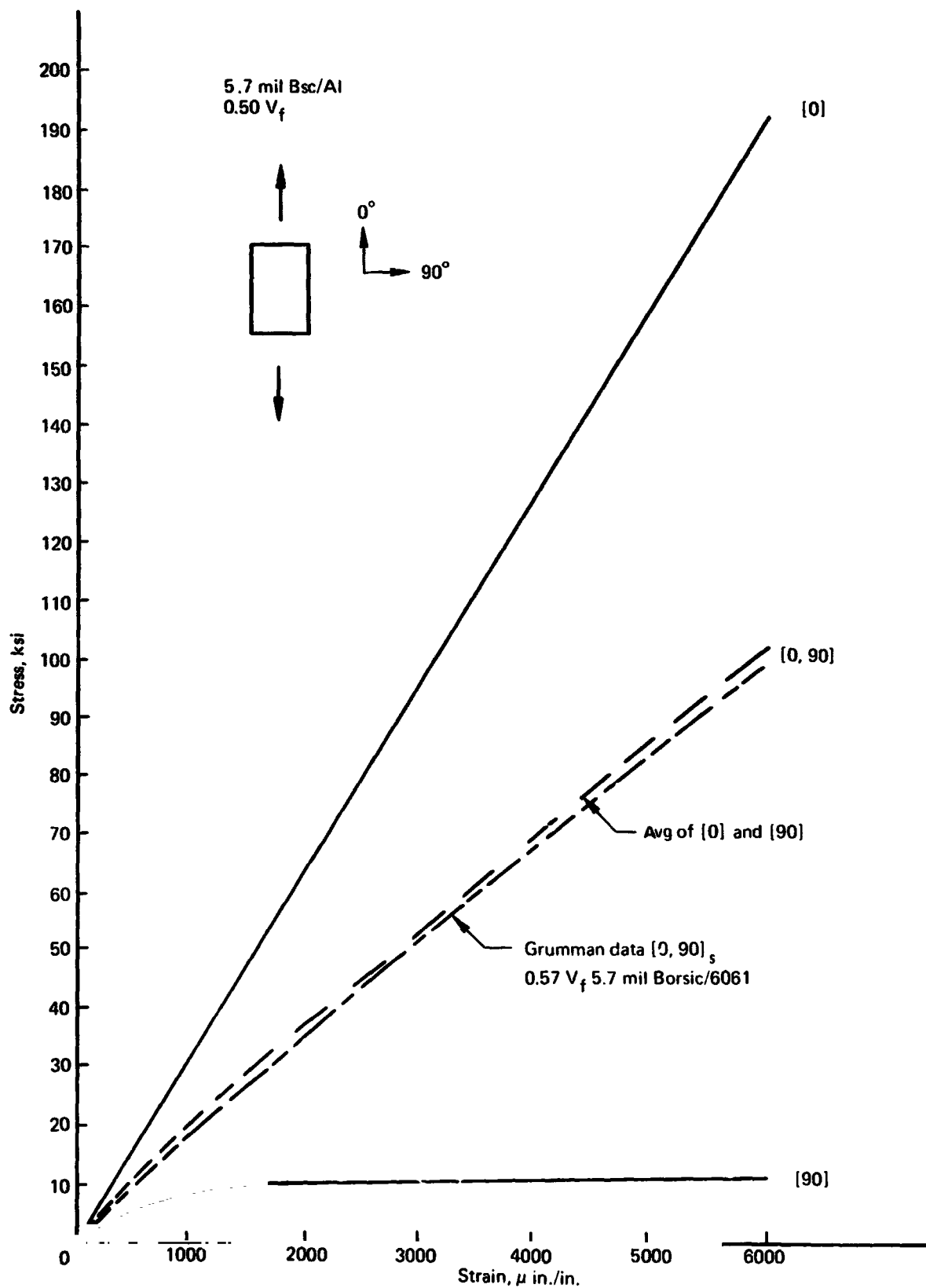


Figure 14-11.—Projected Stress/Strain Curve for Bsc/A! 1980-1990, [0] and [90] Tension or Compression, Room Temperature

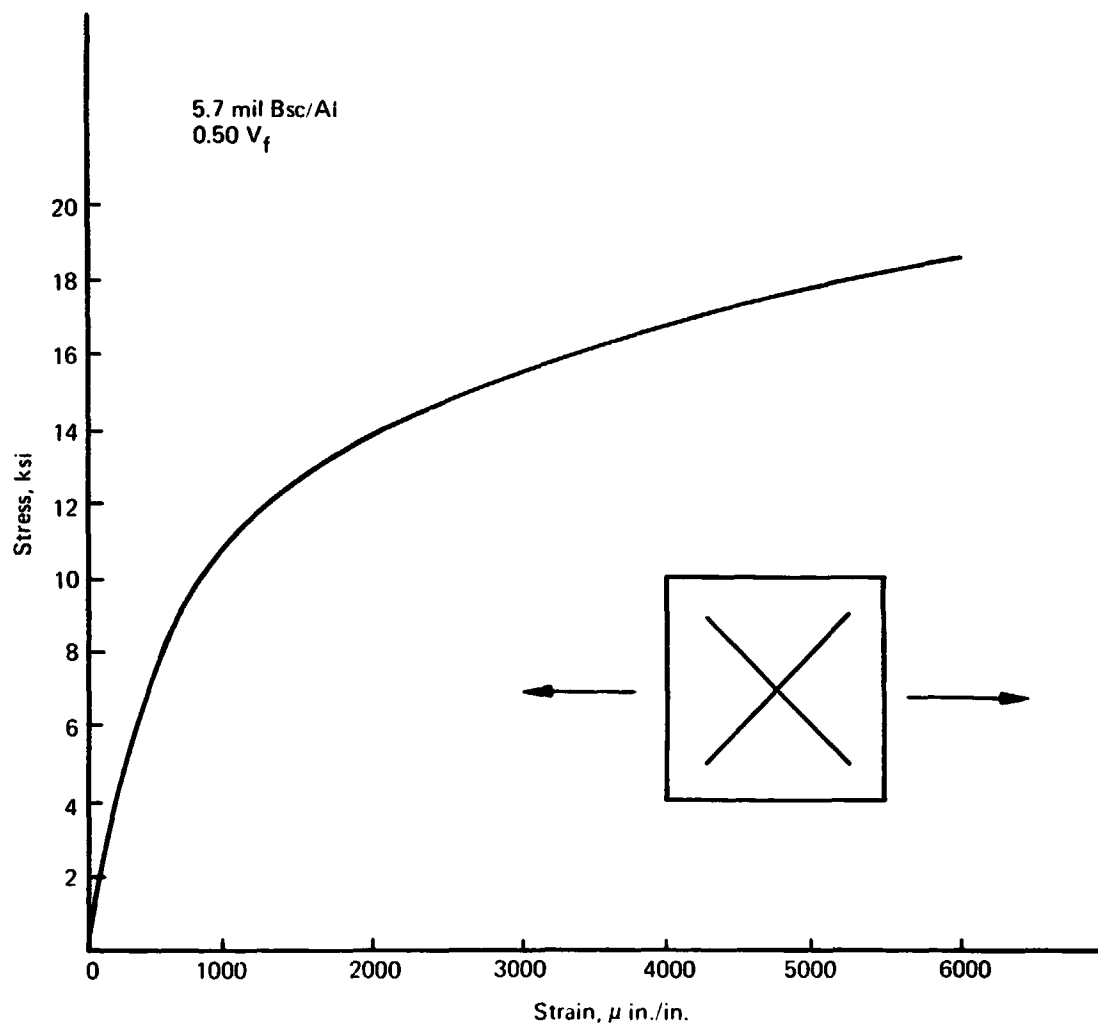


Figure 14-12.—Projected Stress/Strain Curve for $[\pm 45]$ Bsc/Al 1980-1990, Tension or Compression, Room Temperature

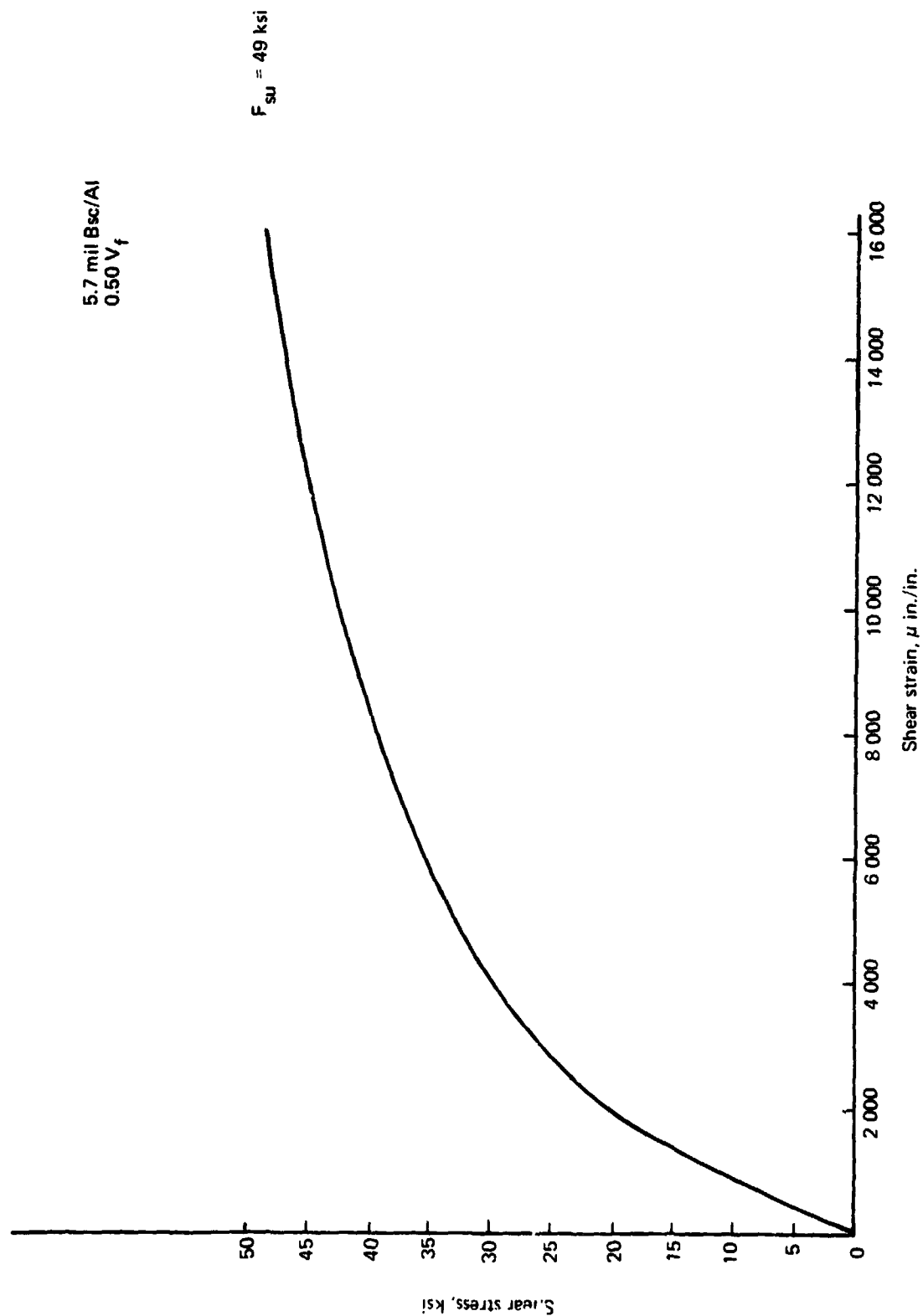


Figure 14-13 --Projected Shear Stress/Strain Curve for [± 45] Bsc/Al 1980-1990, Room Temperature

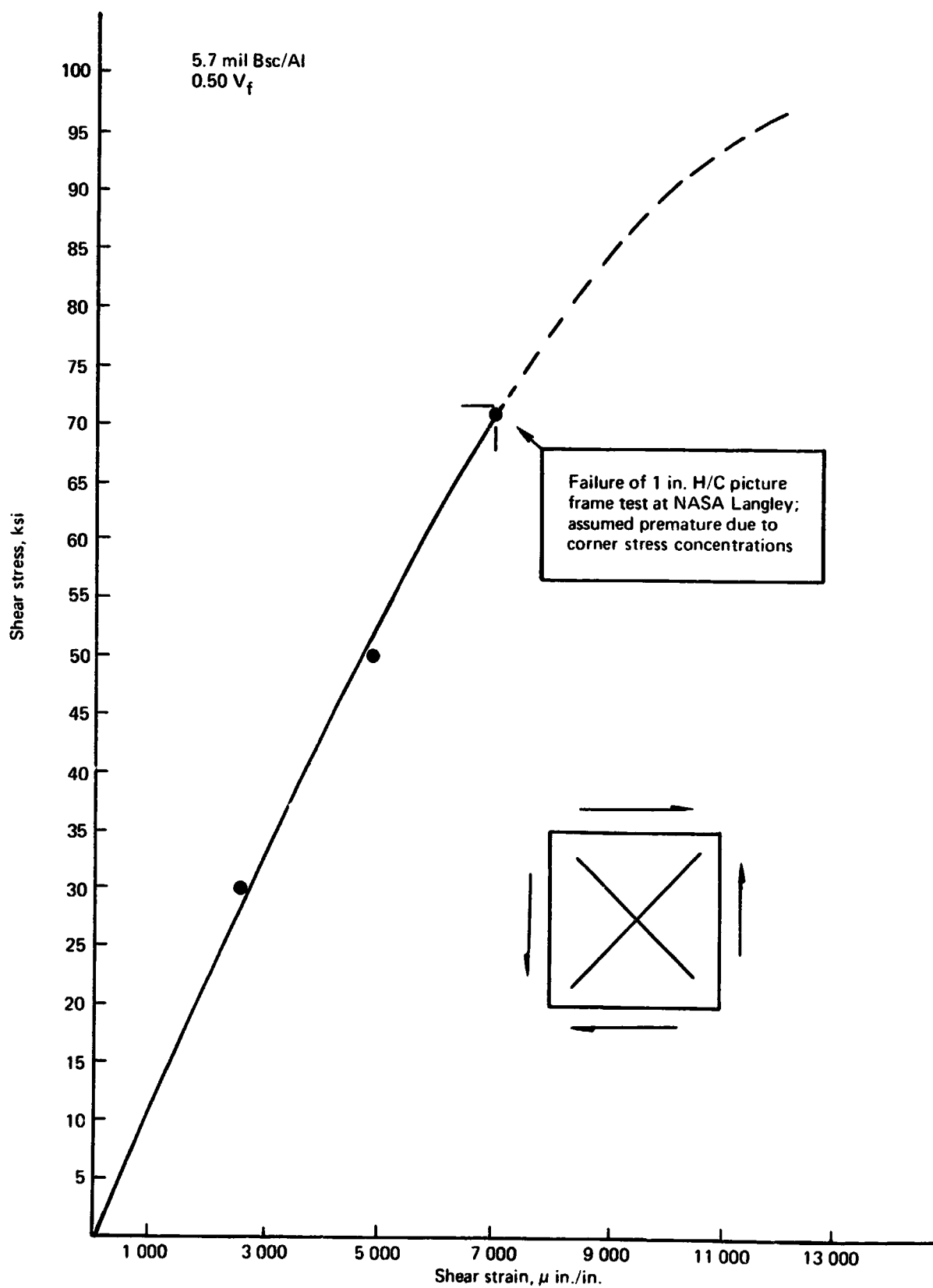


Figure 14-14.—Projected Shear Stress/Strain Curve for $[\pm 45]$ Bsc/Al 1980-1990, Room Temperature NASA Langley Test

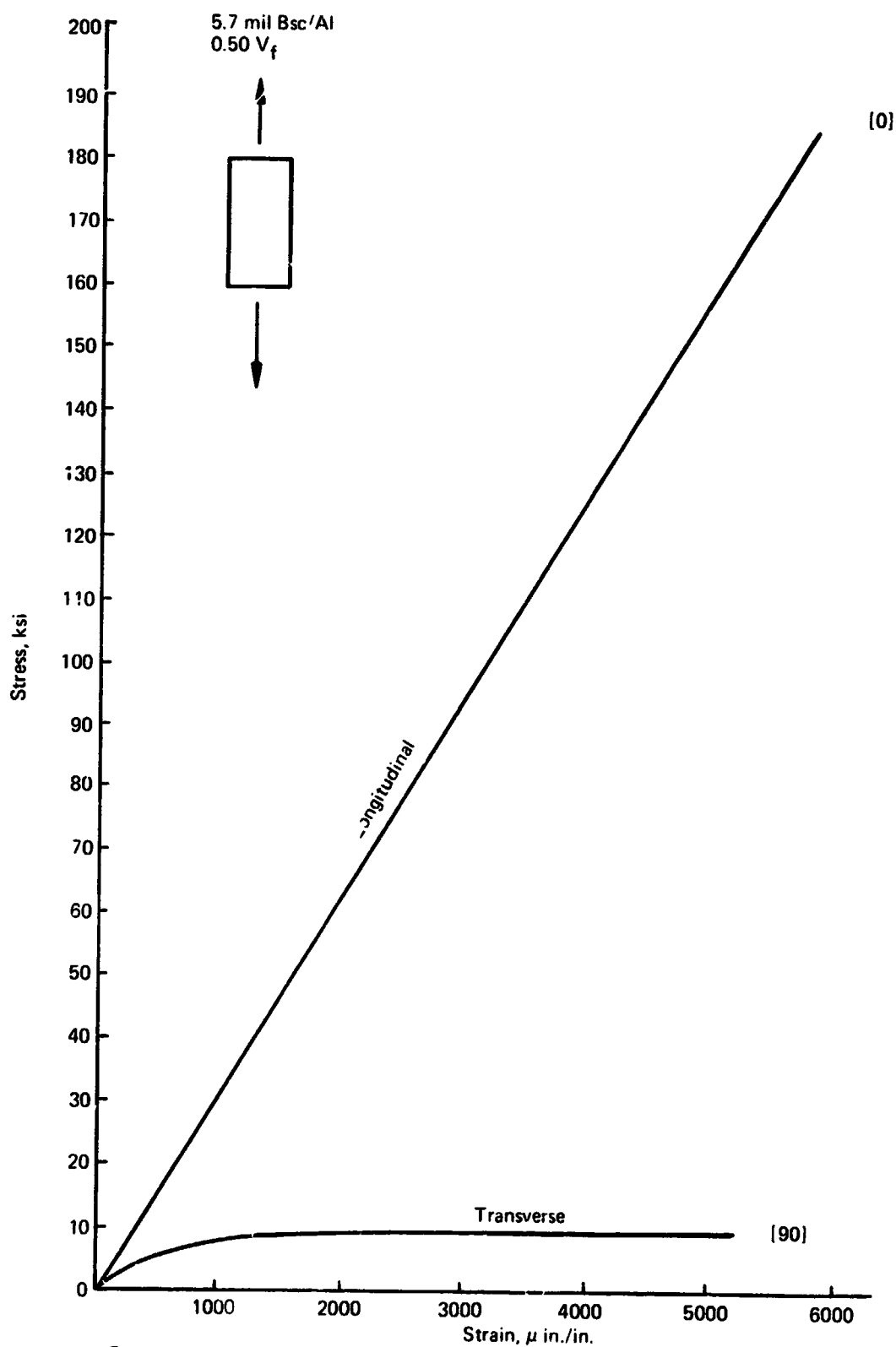


Figure 14-15.—Projected Stress/Strain Curve for Bsc/Al 1980-1990, [0] and [90] Tension or Compression, 250° F

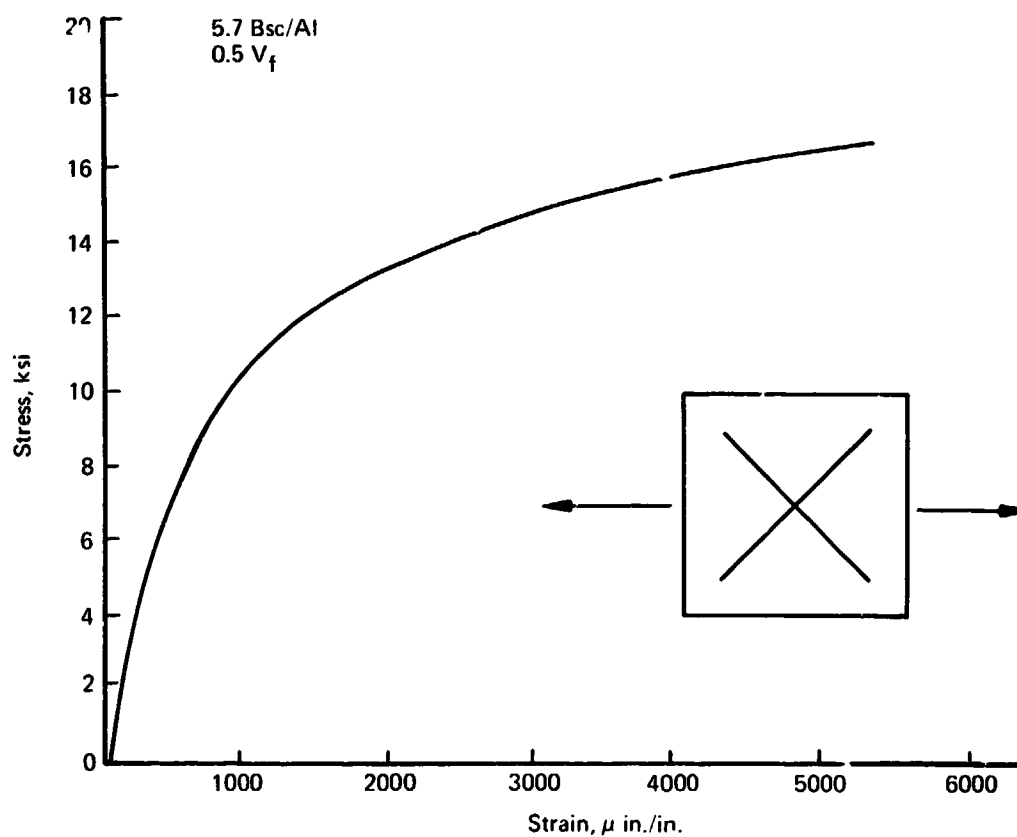


Figure 14-16.—Projected Stress/Strain Curve [± 45] for Bsc/Al 1980-1990, Tension or Compression, 250° F

5.7 m³ Bsc/Al
0.50 V_f

This curve is extended from Advanced
Composite Design Guide and hypothesized.

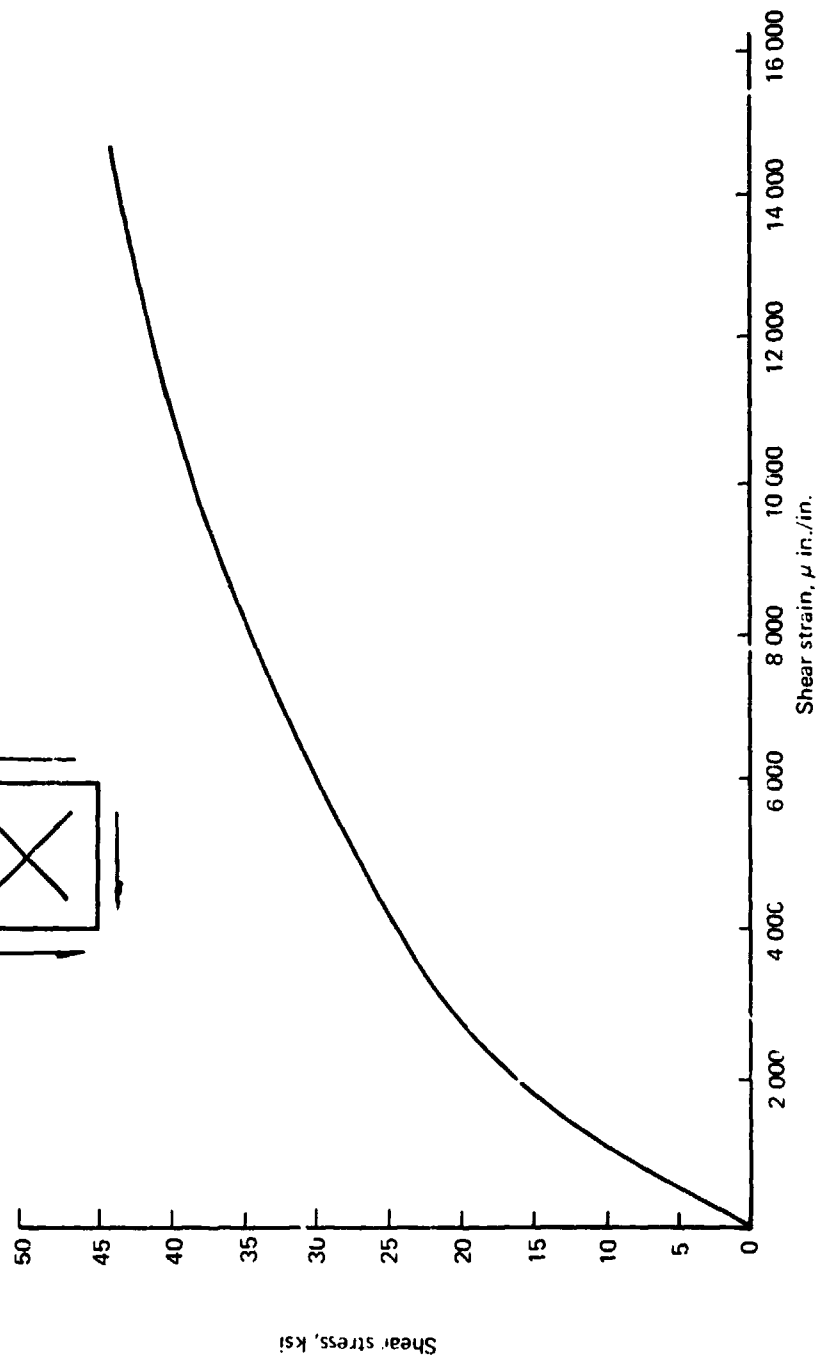
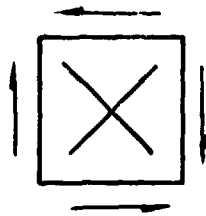


Figure 14-17.—Projected Shear Stress/Strain Curve for [± 45] Bsc/Al 1980-1990, 250° F

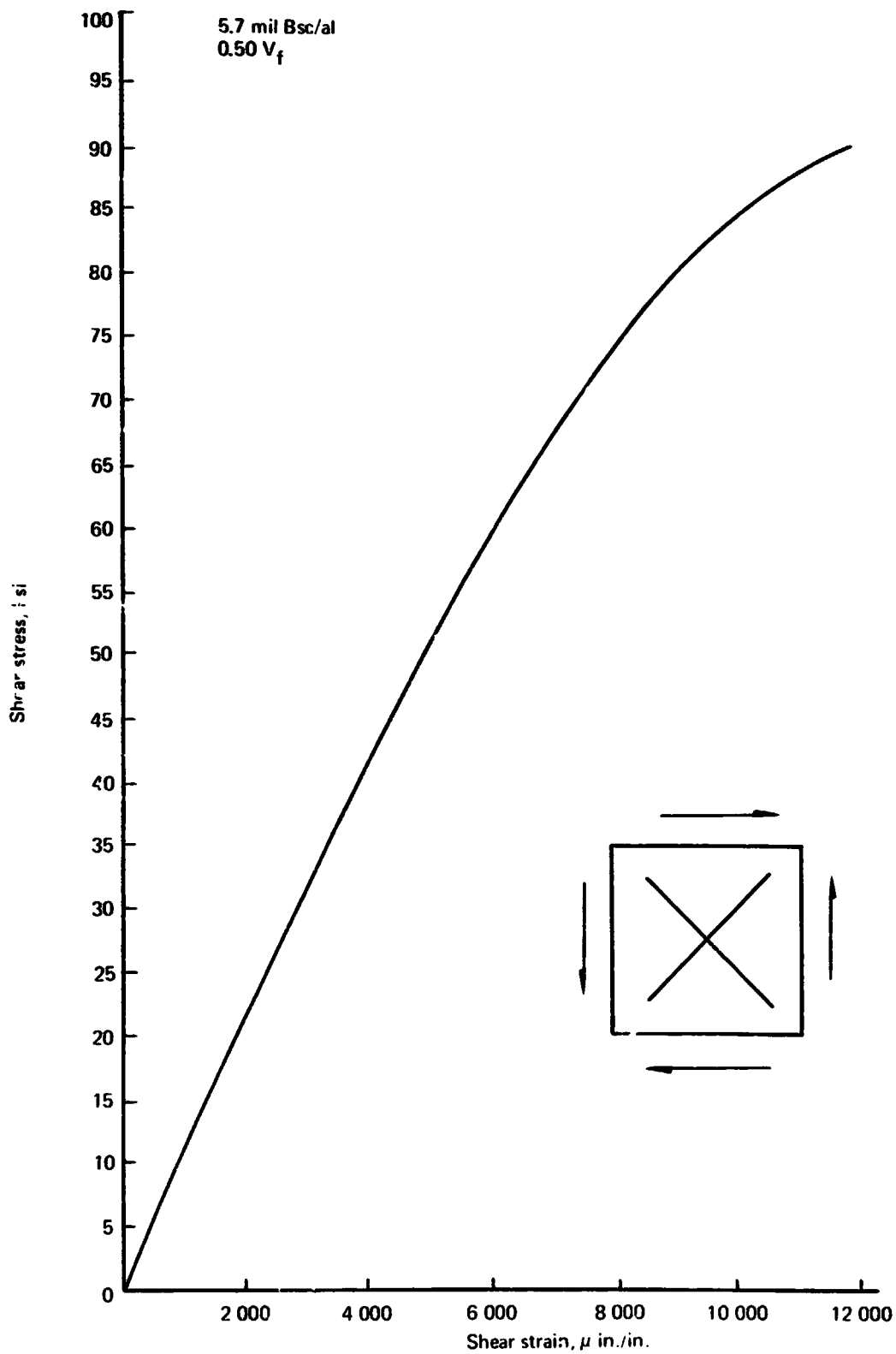


Figure 14-18.—Projected Shear Stress/Strain Curve for $[\pm 45]$ Bsc/Al 1980-1990, 250° F, NASA Langley Test

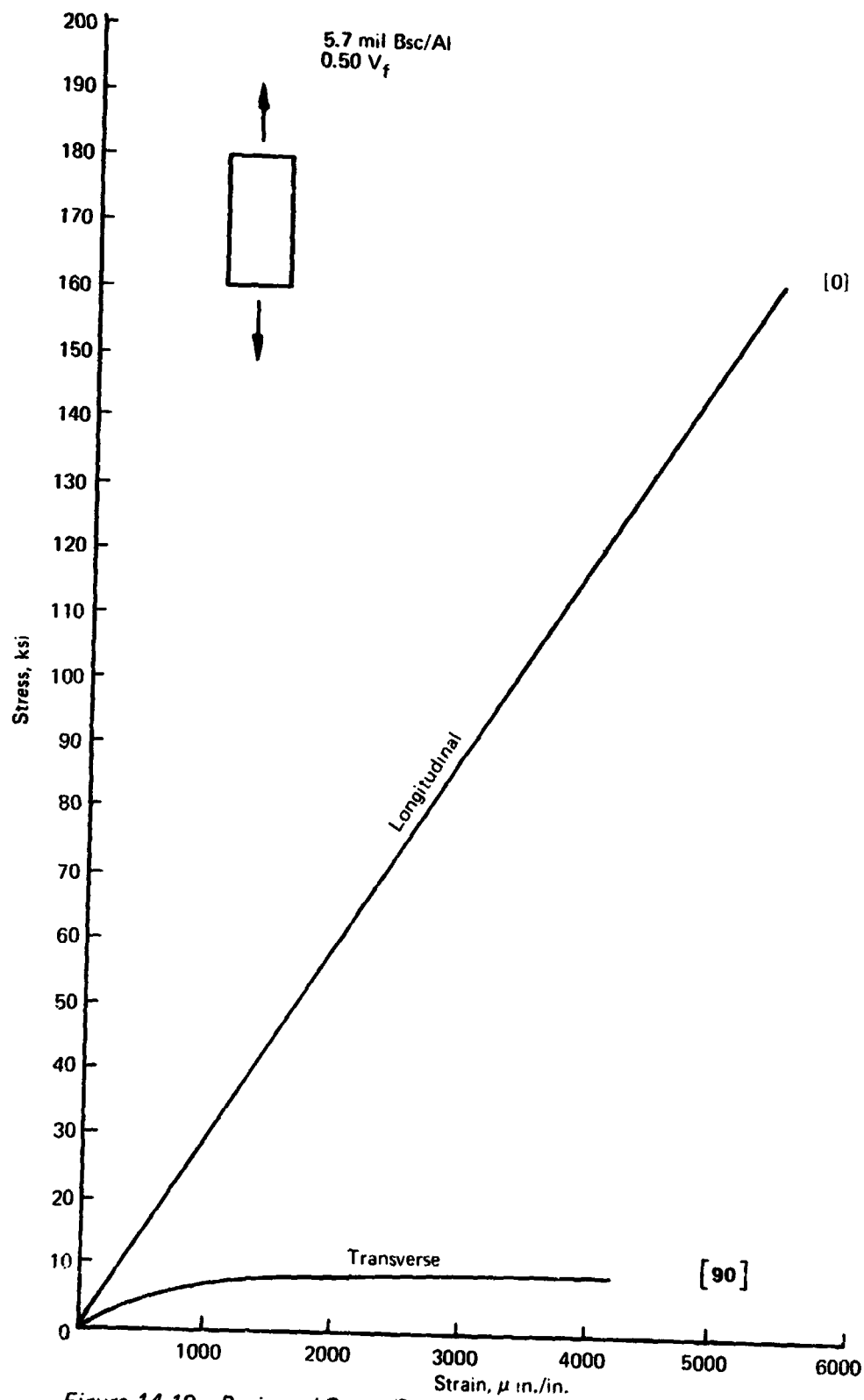


Figure 14-19.—Projected Stress/Strain Curve for Bsc/Al 1980-1990, [0] and [90] Tension or Compression, 450° F

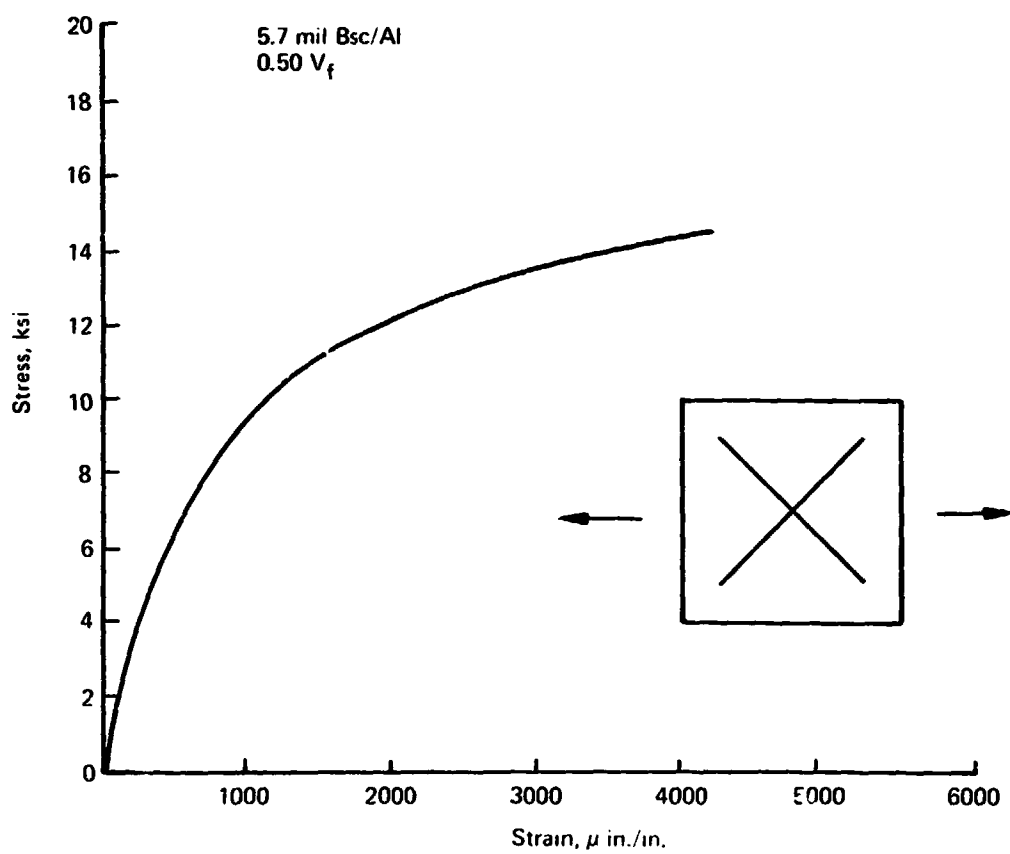


Figure 14-20.—Projected Stress/Strain Curve for $[\pm 45]$ Bsc/Al 1980-1990, Tension or Compression, 450° F

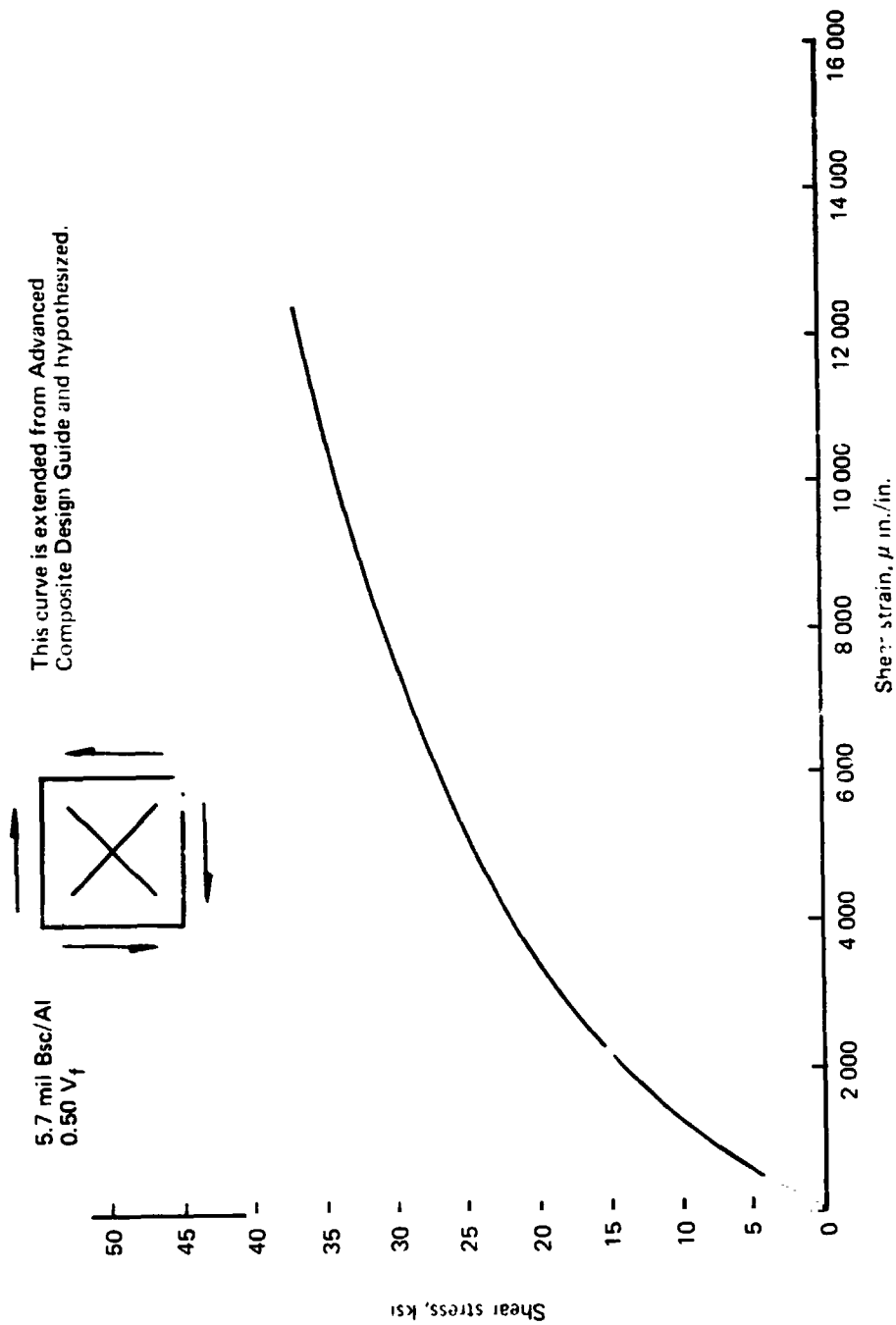


Figure 14-21.—Projected Shear Stress/Strain Curve for [± 45] Bsc/Al 1980-1990, 450° F

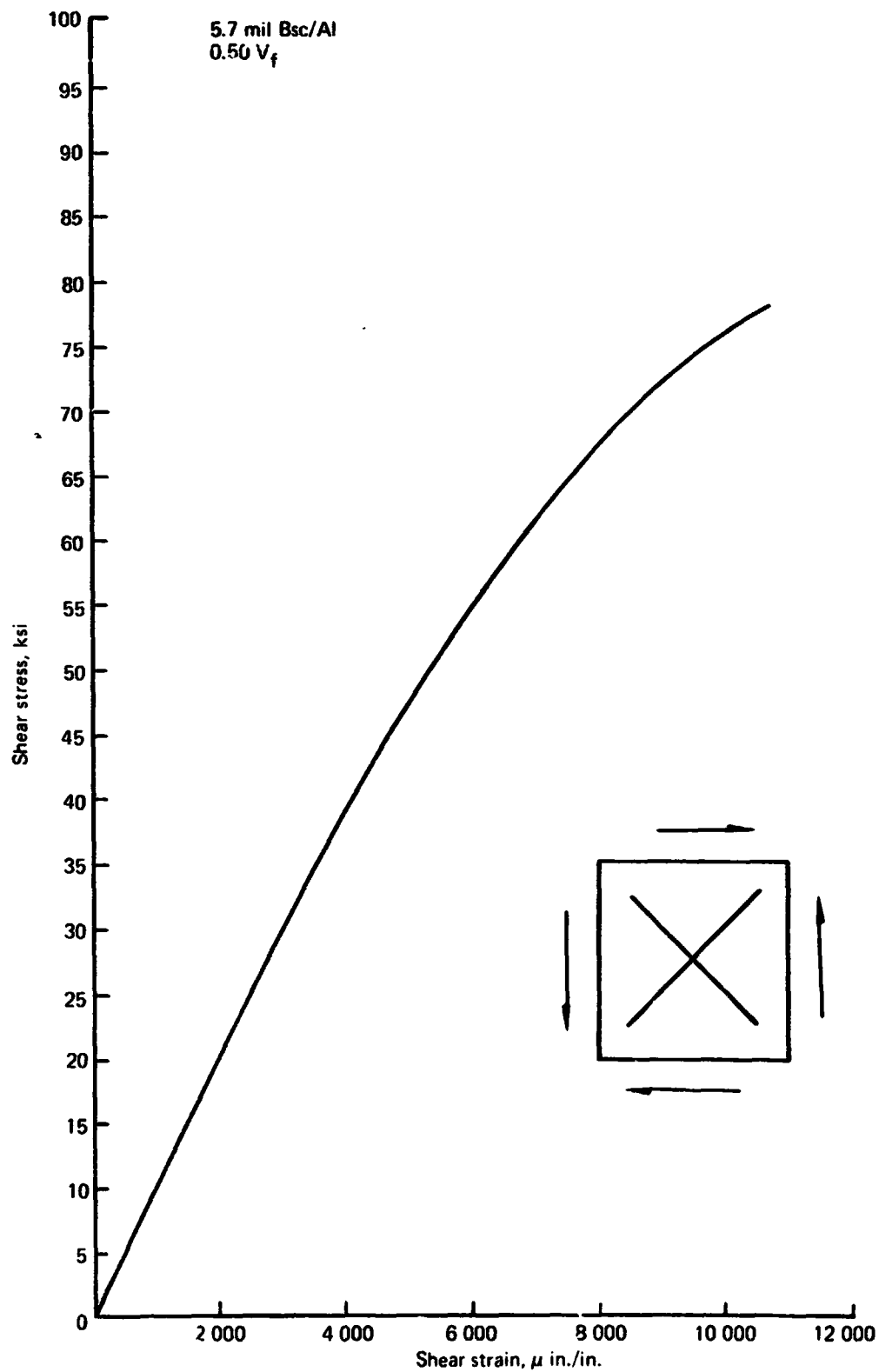


Figure 14-22.—Projected Shear Stress/Strain Curve for $[\pm 45]$ Bsc/Al 1980-1990, 450° F, NASA Langley Test

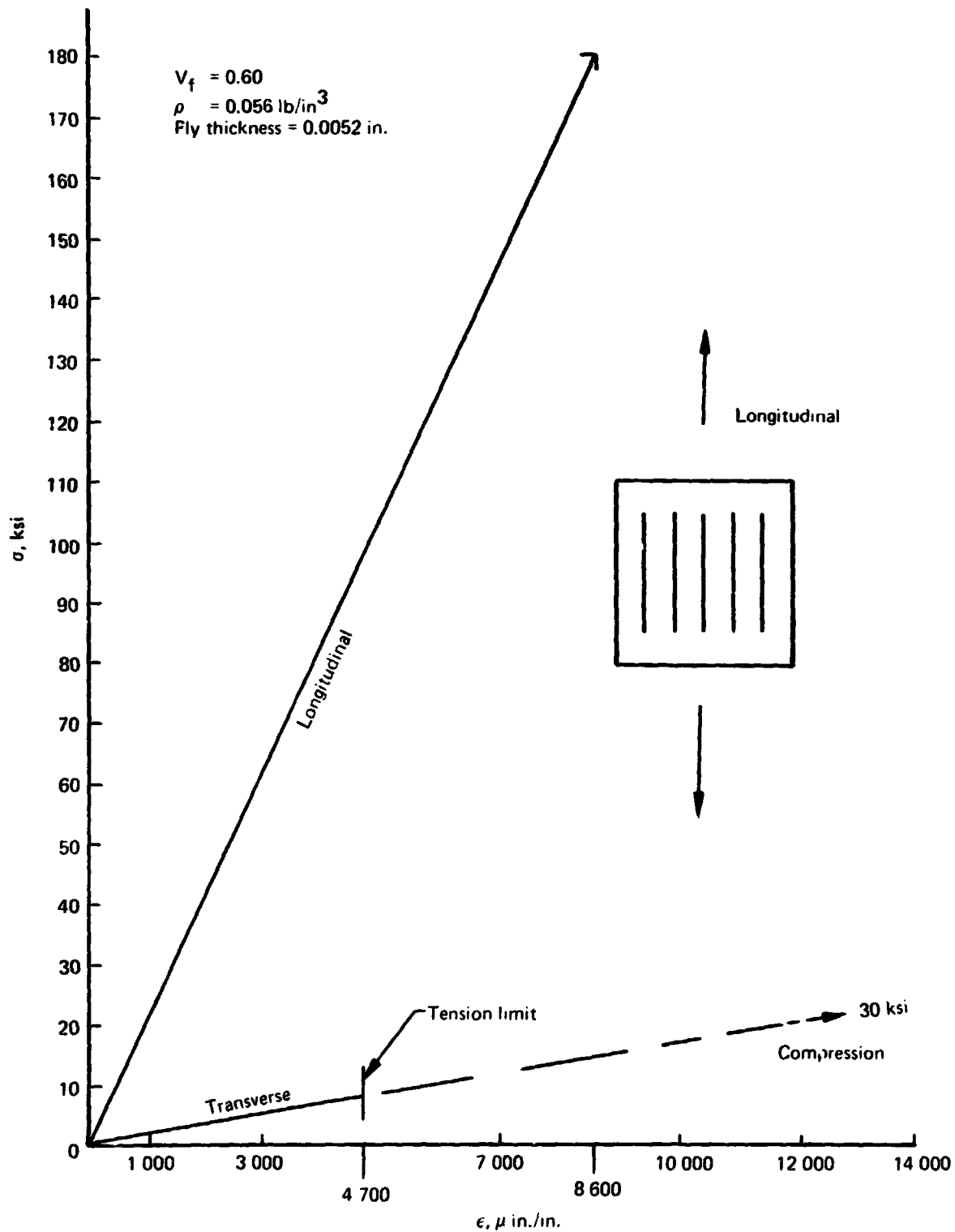


Figure 14-23.—High Strength Graphite/PPQ Projected 1980-1990 Allowables [0] Longitudinal and Transverse Tension or Compression, Room Temperature

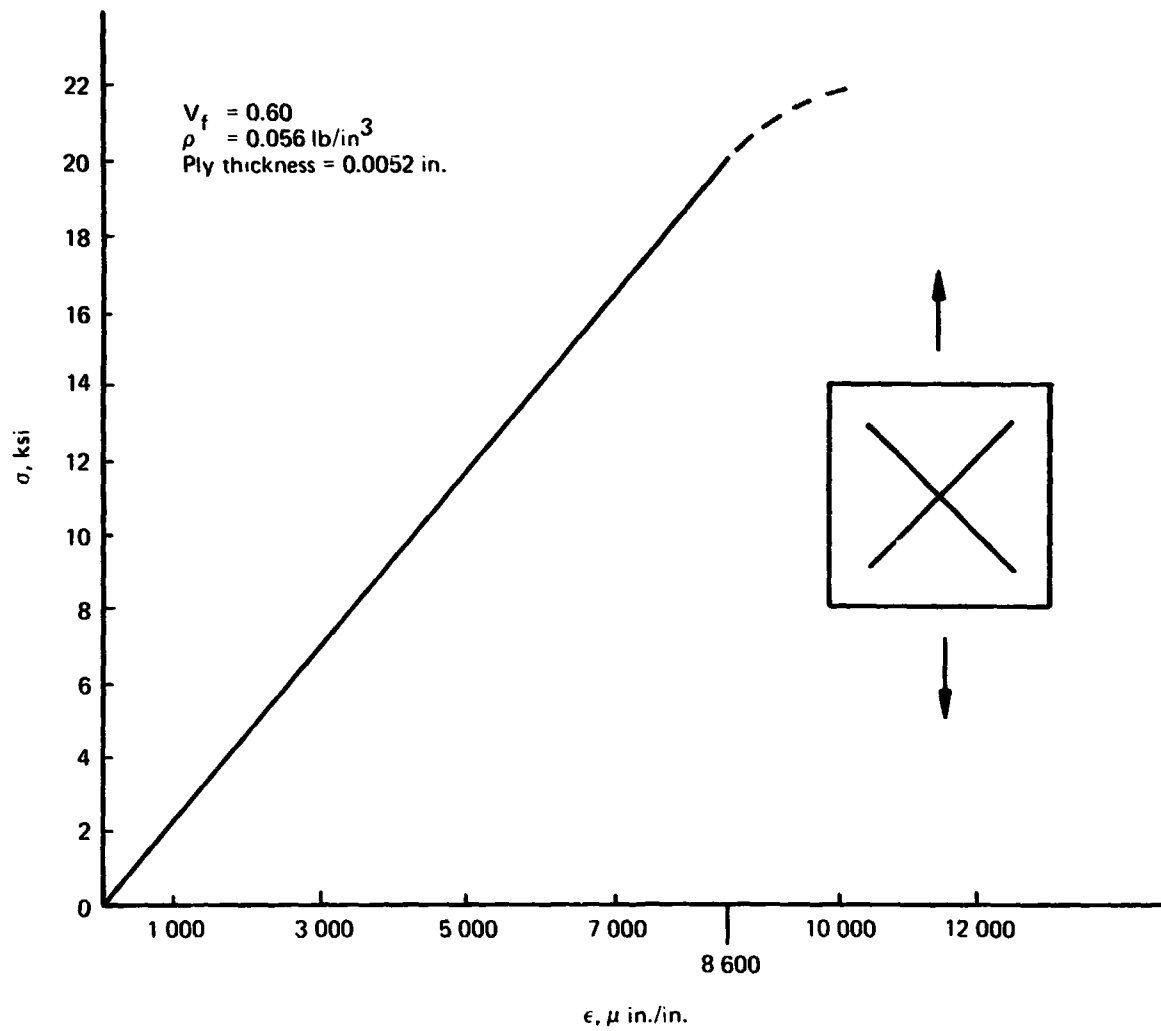


Figure 14-24.—High Strength Graphite/PPQ Projected 1980-1990 Allowables [± 45] Longitudinal or Transverse Tension or Compression, Room Temperature

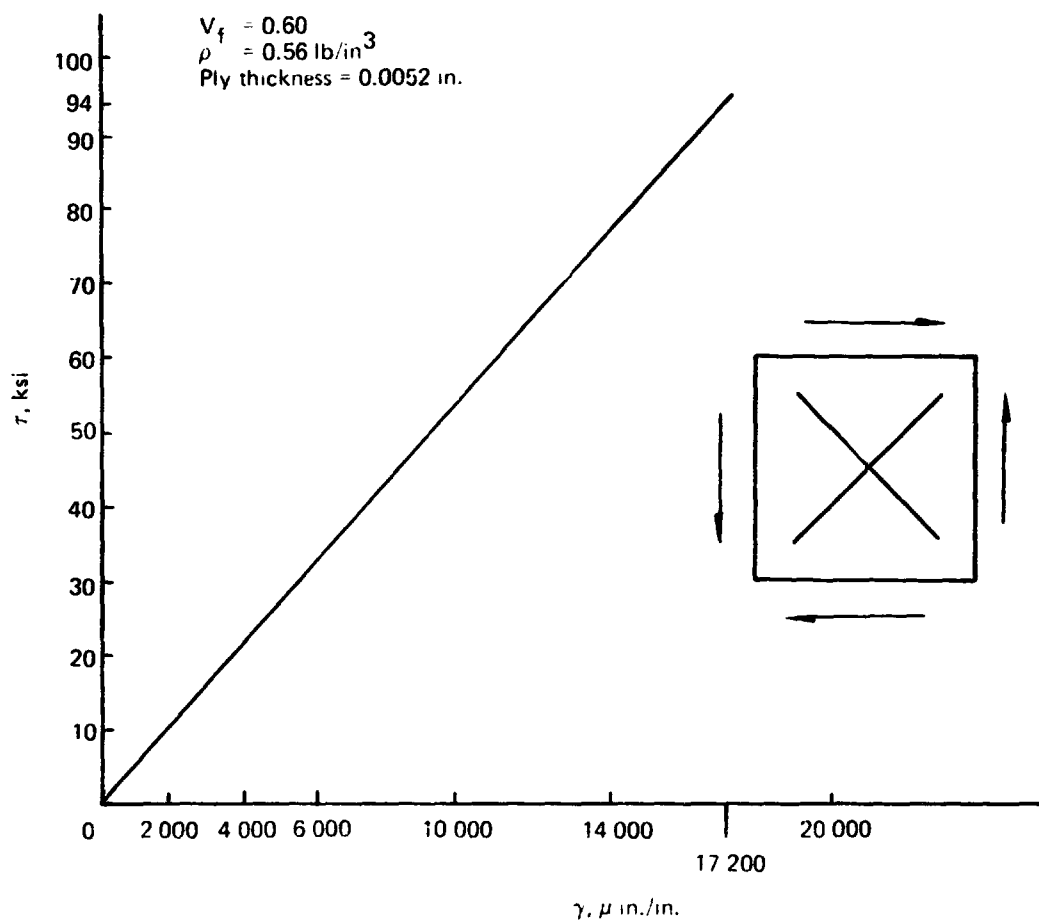


Figure 14-25. — High Strength Graphite/PPQ Projected 1980-1990 Allowables [$\pm 45^\circ$] Shear, Room Temperature

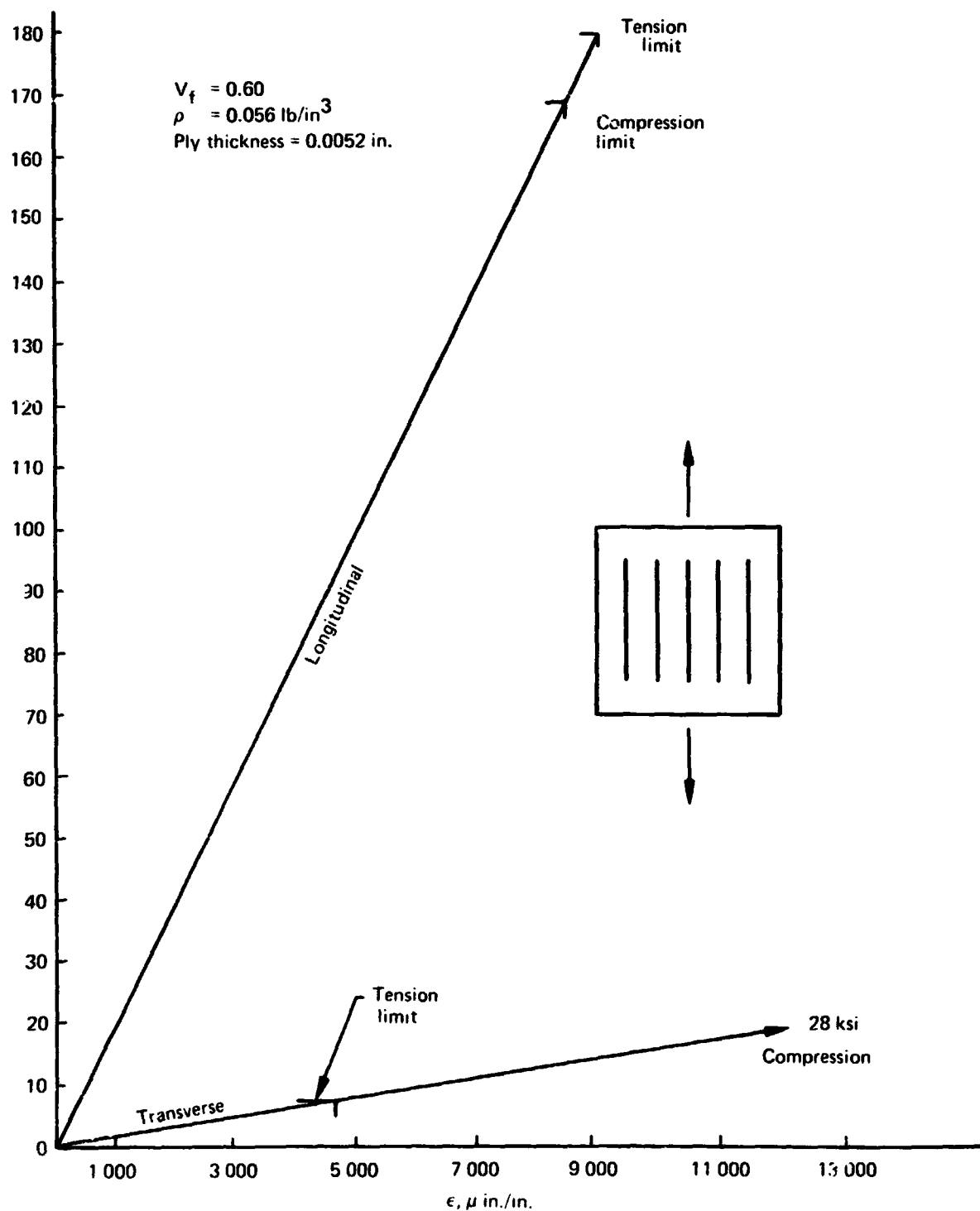


Figure 14-26.—High Strength Graphite/PPQ Projected 1980-1990 Allowables [0] Longitudinal and Transverse Tension or Compression, 250° F

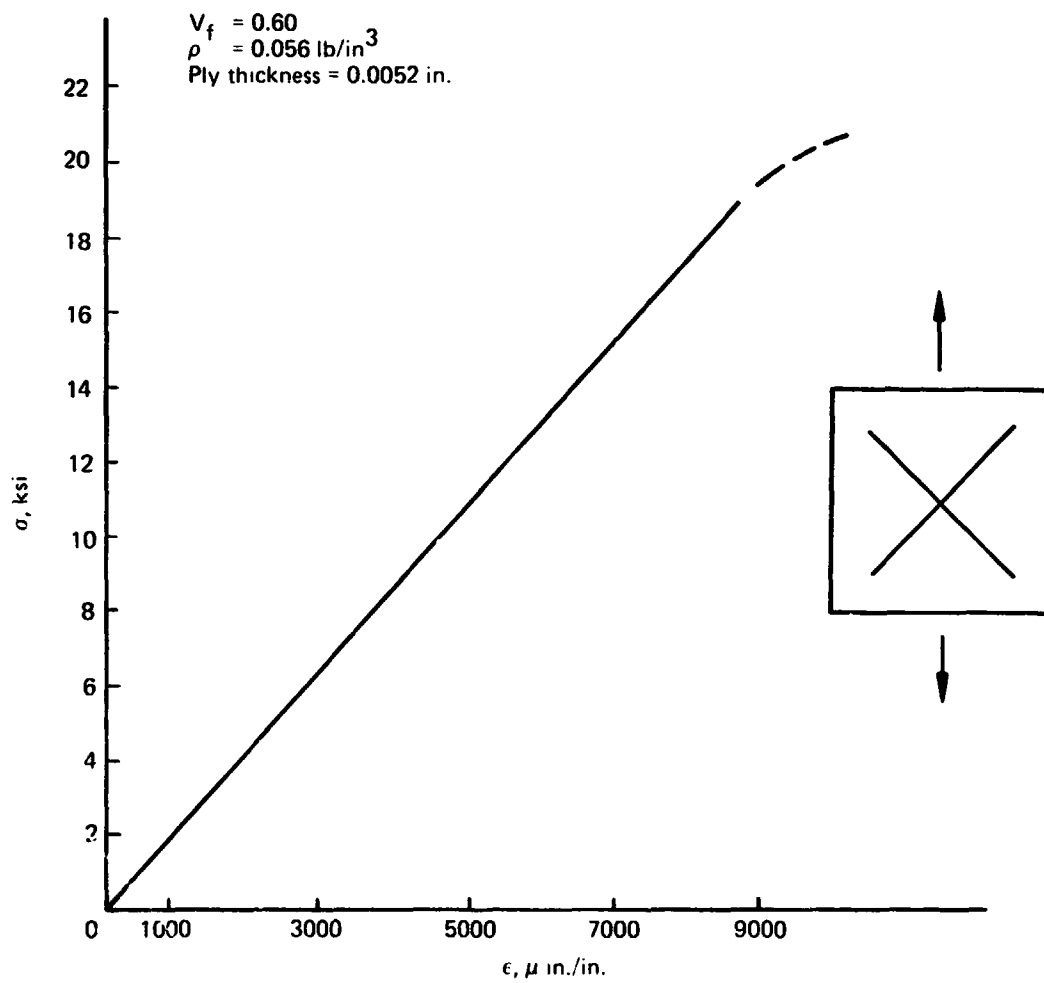


Figure 14-27.—High Strength Graphite/PPQ Projected 1980-1990 Allowables [± 45] Longitudinal and Transverse Tension or Compression, 250° F

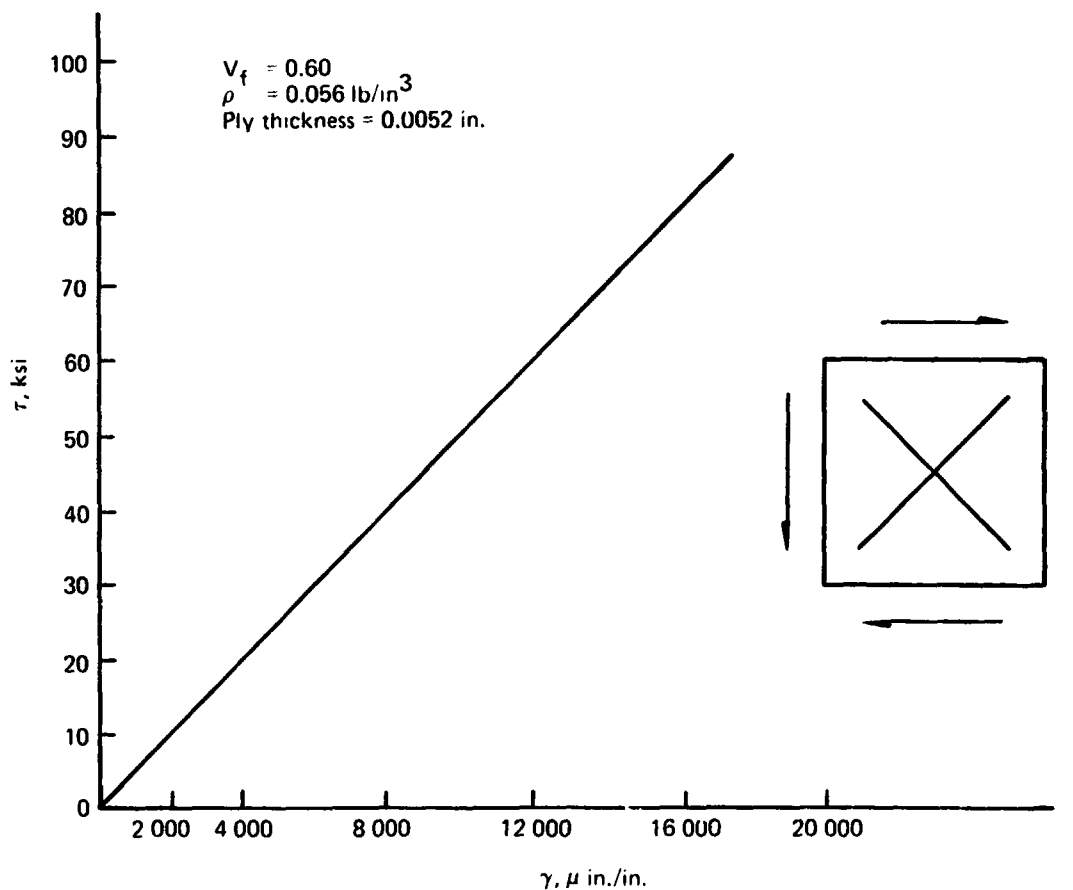


Figure 14-28.—High Strength Graphite/PPQ Projected 1980-1990 Allowables [± 45] Shear, 250° F

REPRODUCIBILITY OF THE
ORIGINAL PAGE IS POOR

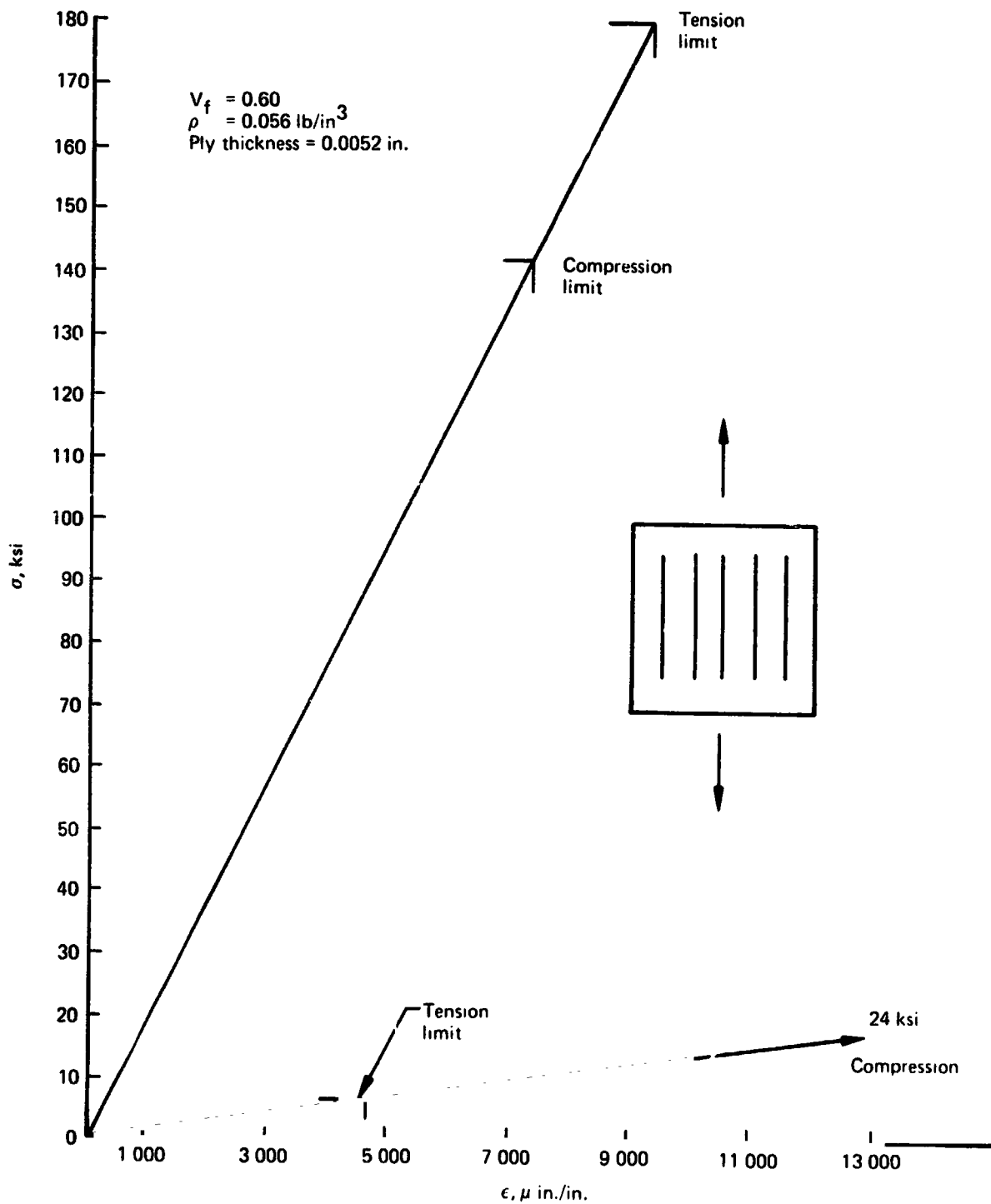


Figure 14-29.—High Strength Graphite/PPQ Projected 1980-1990 Allowables [0] Longitudinal and Transverse Tension or Compression, 450° F

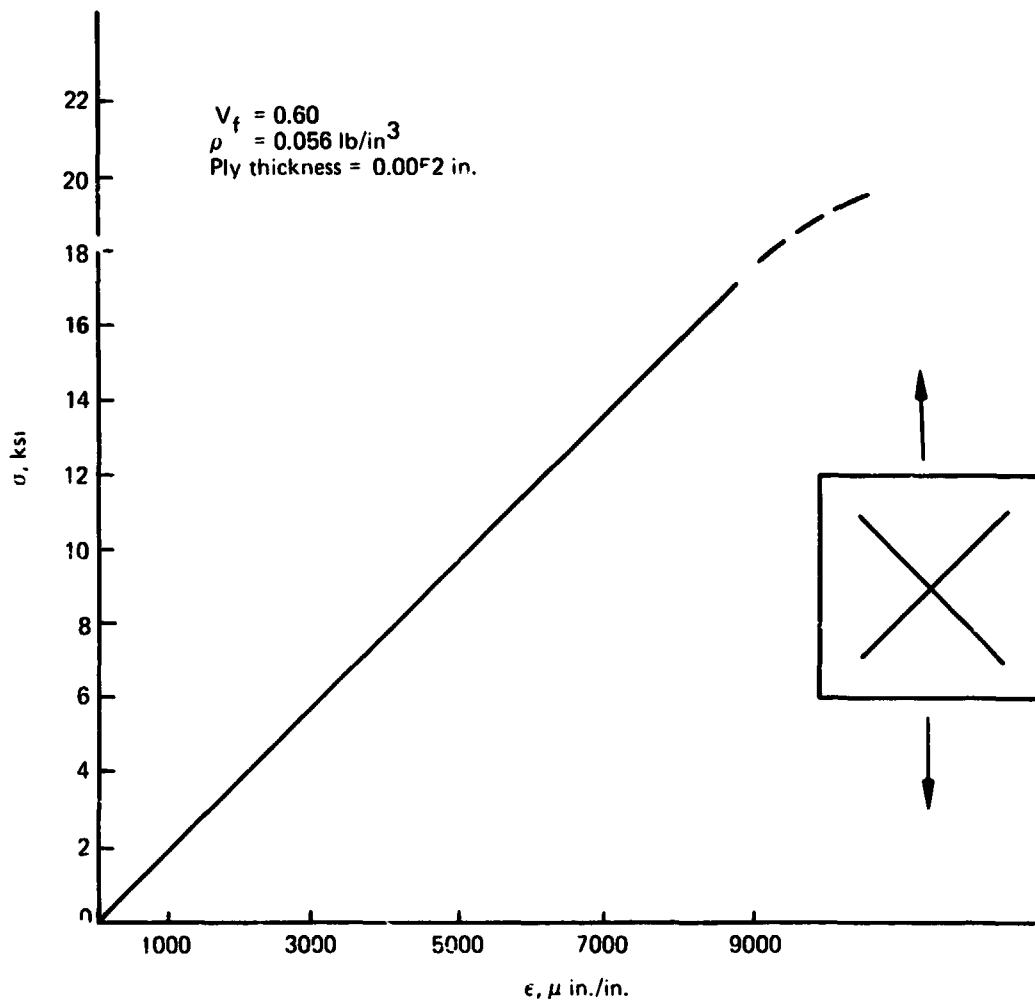


Figure 14-30.—High Strength Graphite/PPQ Projected 1980-1990 Allowables [± 45] Longitudinal and Transverse Tension or Compression, 450° F

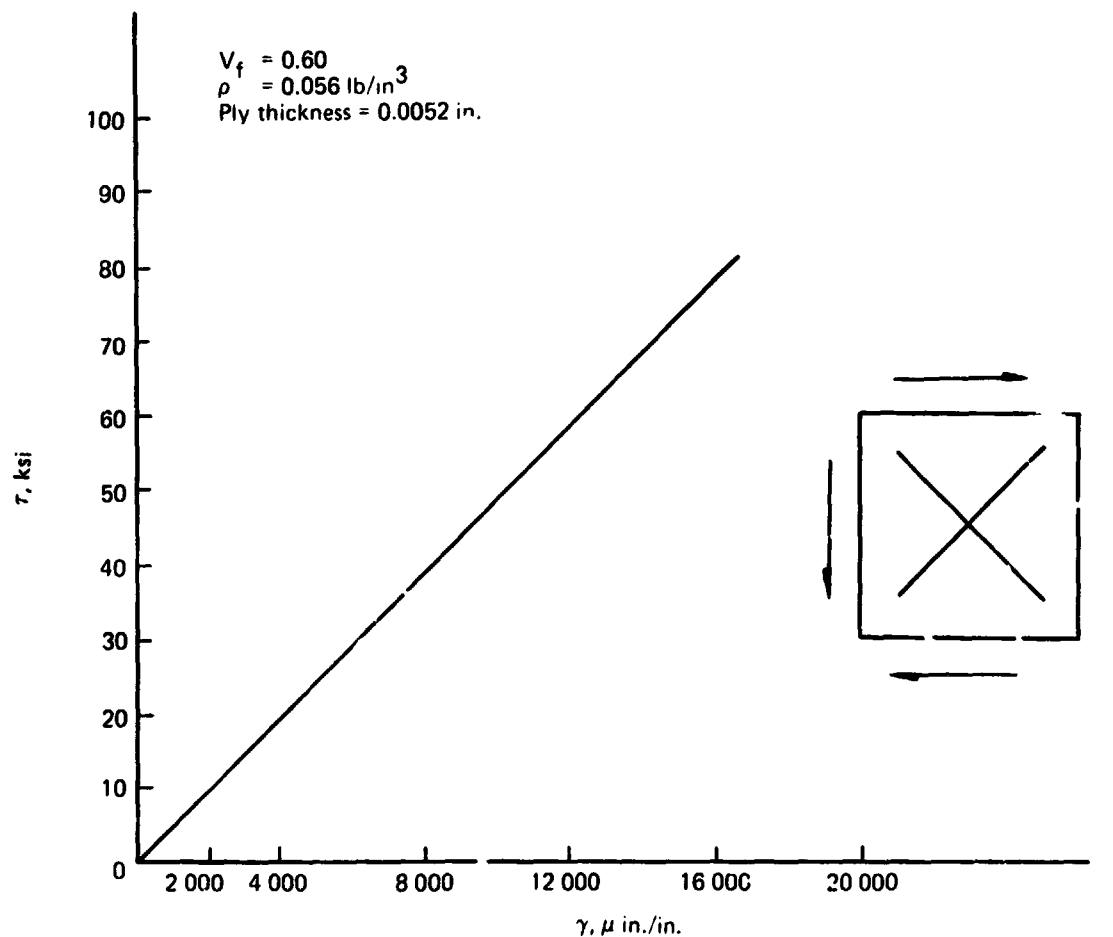


Figure 14-31.—High Strength Graphite/PPQ Projected 1980-1990 Allowables $[\pm 45]$ Shear, 450° F

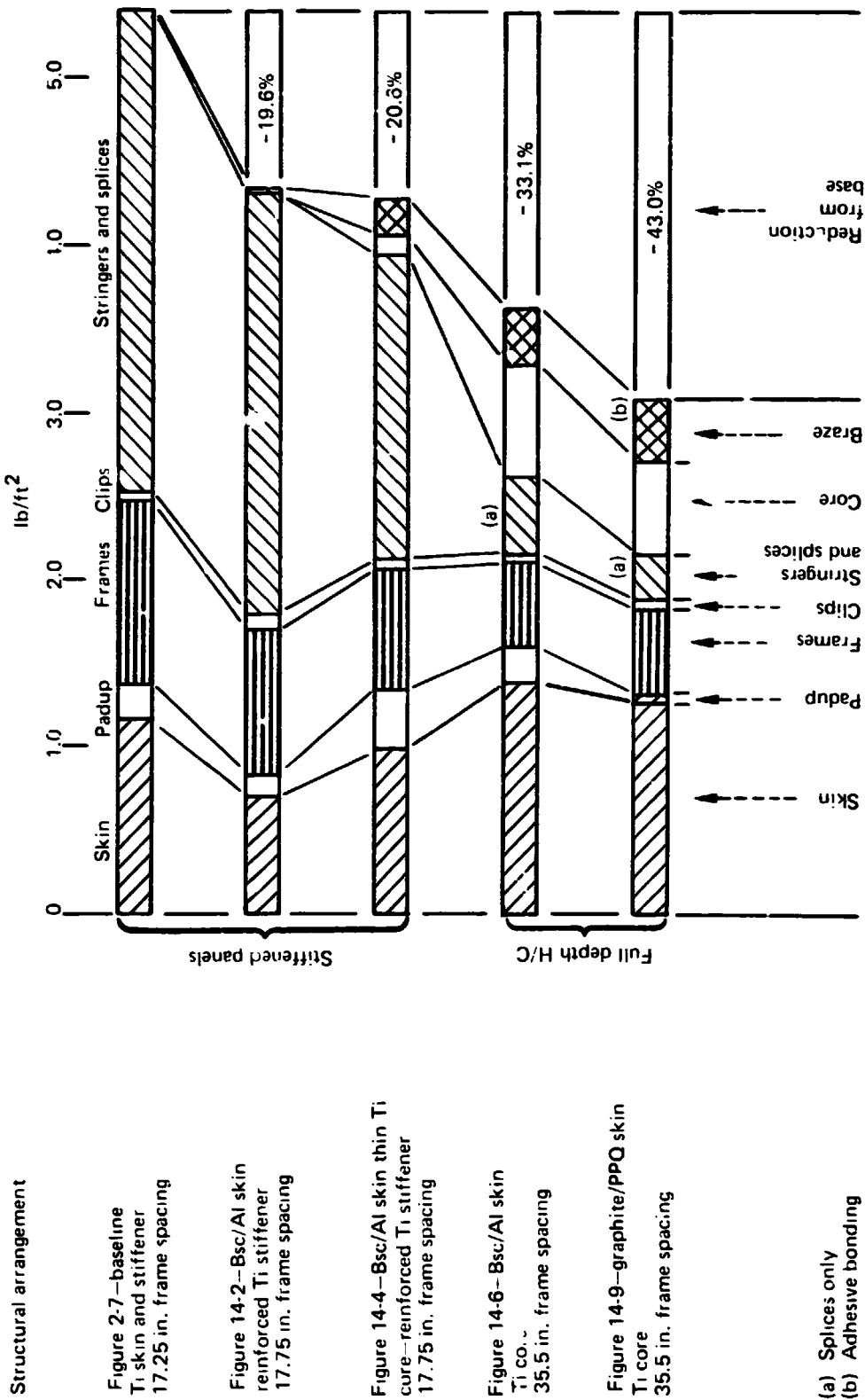


Figure 14-32.—Weight Comparison—Advanced Structural Concepts—Body

Figure 1 consists of two cross-sectional diagrams, (a) and (b), showing the layers of the test specimens. The vertical axis represents pressure in lb/ft², ranging from 0 to 5.0.

Diagram (a) shows the Stiffened panels. The layers from bottom to top are: Skin, Pads, Formers, Clips, Stiffener/reinforced, Core, Braze, and Reduction from base. The total thickness of the stiffened panels is indicated as -12.8%.

Diagram (b) shows the Full depth H/C. The layers from bottom to top are: Skin, Padup-core-braze, and Reduction from base. The total thickness of the full depth H/C is indicated as -43.9%.

Both diagrams include a vertical scale from 0 to 5.0 lb/ft².

Figure 14-33.—Weight Comparison—Advanced Structural Concepts—Wing Upper Surface

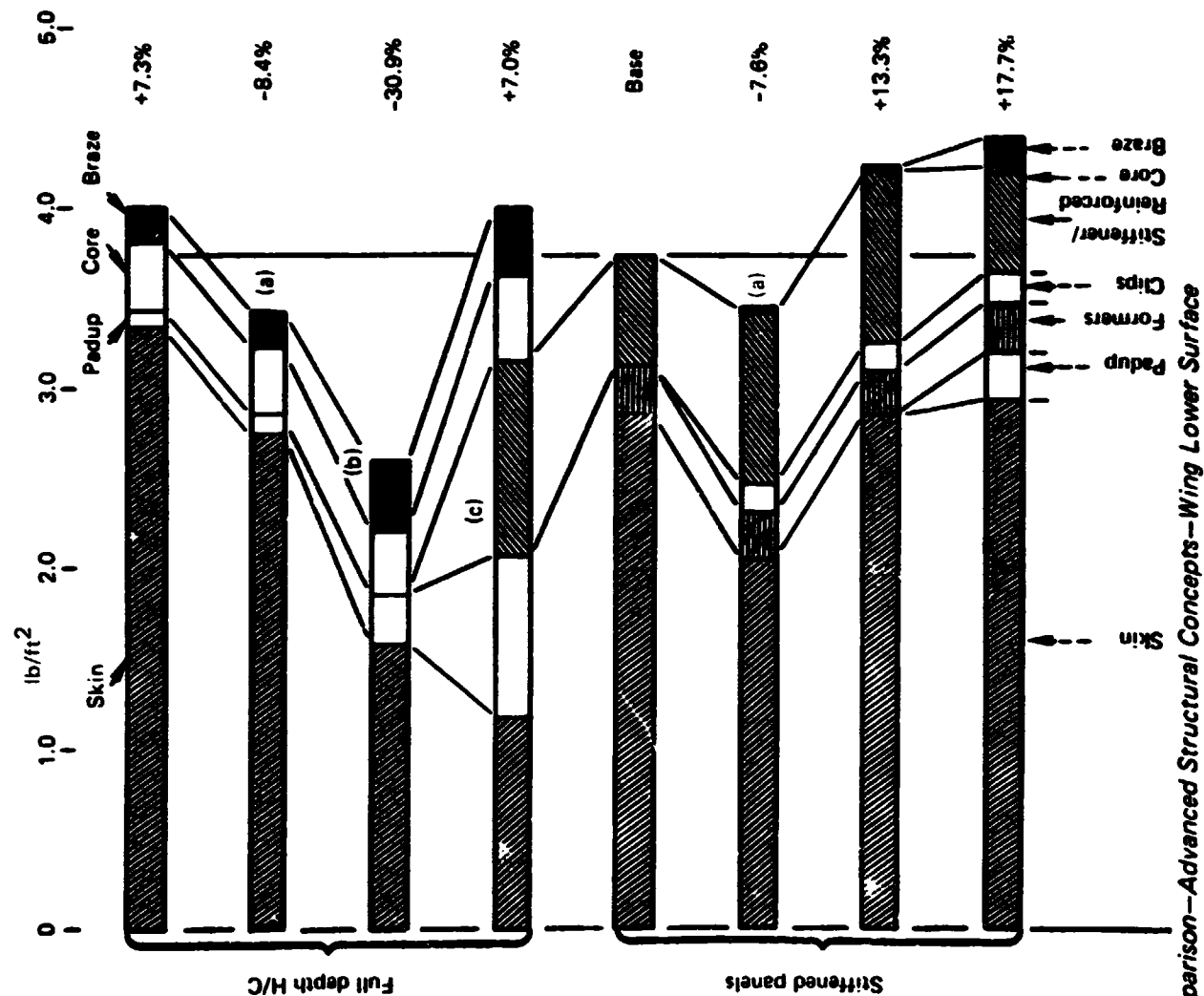


Figure 14-34.—Weight Comparison—Advanced Structural Concepts—Wing Lower Surface

Structural arrangement

Figure 14-7—Bsc/Al skin
Ti core
(2 to 17 ply skin assembly)

Figure 14-7—Bsc/Al skin
Ti core
(2 to 14 ply skin assembly)

Figure 14-10—graphite/PPQ skin
Ti core
(2 to 19 ply skin assembly)

Figure 14-8—Bsc/Al skin
Ti core
(2 to 6 ply and truss reinforced skin assembly)

Figure 2-13—baseline
integrally machined and
welded Ti skin and stiffener

Figure 14-3—Bsc/Al skin
reinforced Ti stiffener
(21 ply skin assembly)

Figure 14-3—Bsc/Al skin
reinforced Ti stiffener
(29 ply skin assembly)

Figure 14-5—Bsc/Al skin
thin Ti core—reinforced Ti stiffener
(2 to 15 ply skin assembly)
(a) High shear allowable
(b) Adhesive bonding
(c) Skin reinforcement

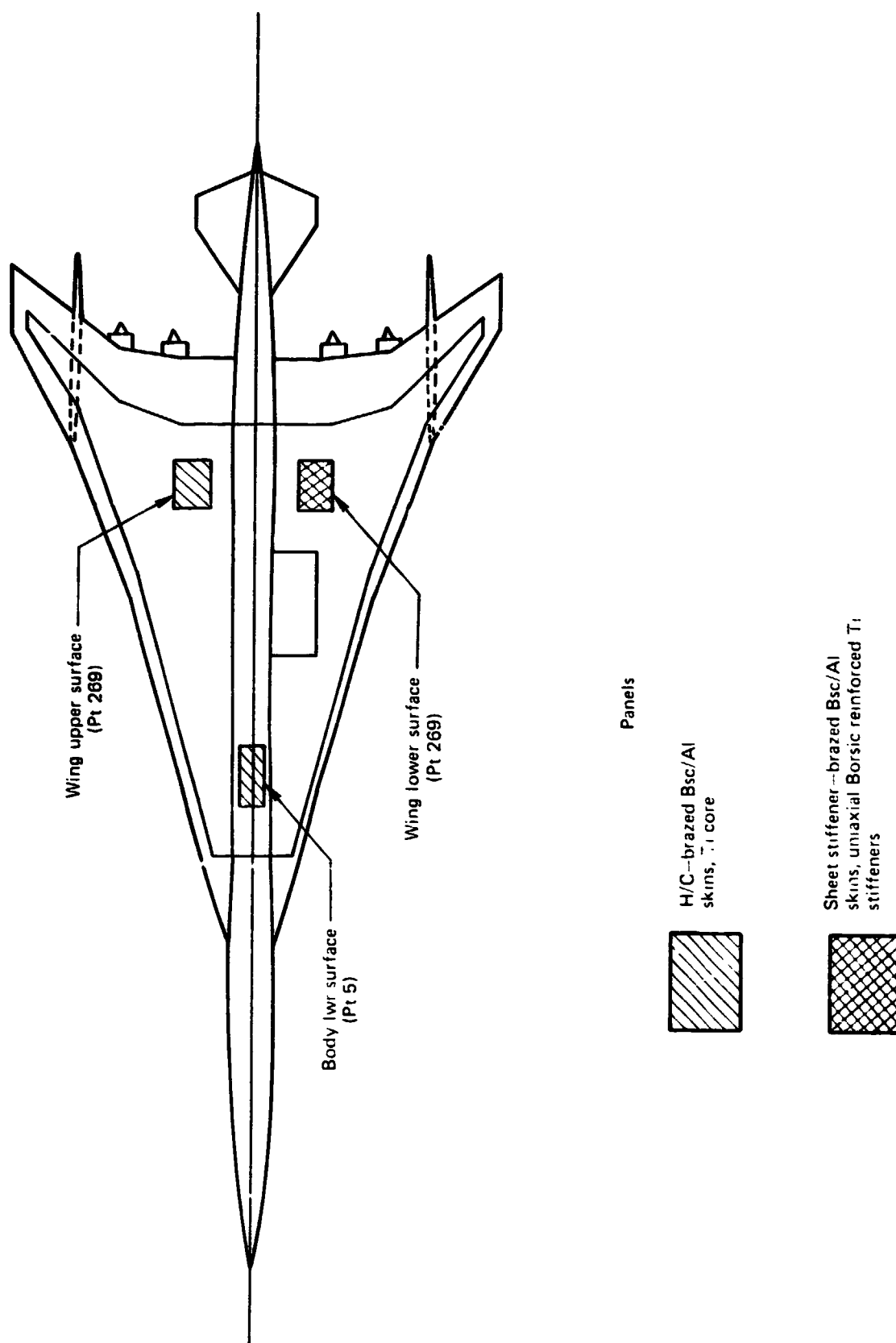


Figure 14-35. —Wing and Body Structural Selection

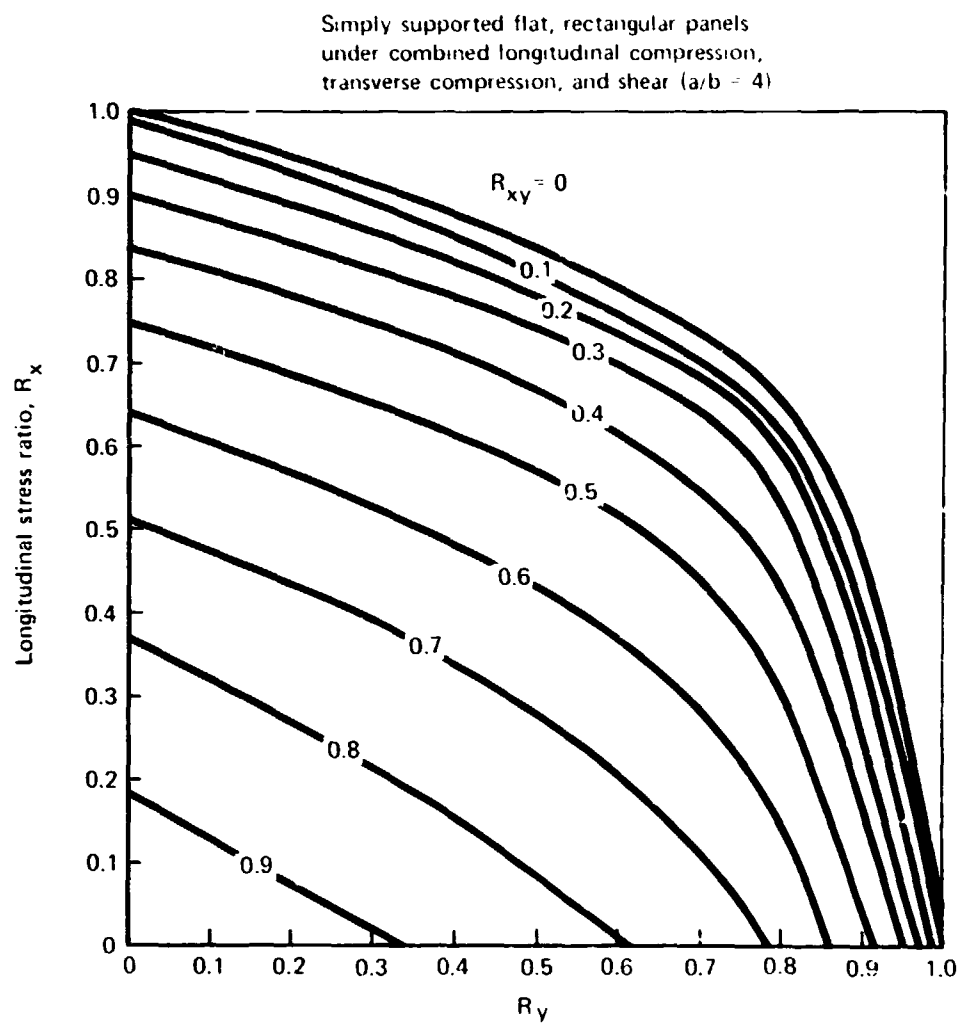


Figure 14-36.—Initial Buckling of Flat Rectangular Panels